GEOTECHNICAL, GEOLOGICAL AND EARTHQUAKE ENGINEERING

SEISMIC DESIGN, ASSESSMENT AND RETROFITTING OF CONCRETE BUILDINGS

based on EN-Eurocode 8

MICHAEL N. FARDIS

Springer

SEISMIC DESIGN, ASSESSMENT AND RETROFITTING OF CONCRETE BUILDINGS

GEOTECHNICAL, GEOLOGICAL AND EARTHQUAKE ENGINEERING

Volume 8

For other titles in this series, go to:
http://www.springer.com/series/6011

Seismic Design, Assessment and Retrofitting of Concrete Buildings

Based on EN-Eurocode8

by

MICHAEL N. FARDIS

Department of Civil Engineering, University of Patras, Greece

Springer

Michael N. Fardis
Department of Civil Engineering
University of Patras
P.O. Box 1424
26504 Patras
Greece
fardis@upatras.gr

ISBN 978-1-4020-9841-3 e-ISBN 978-1-4020-9842-0
DOI 10.1007/978-1-4020-9842-0
Springer Dordrecht Heidelberg London New York

Library of Congress Control Number: 2009926882

To Tonia and Nikos

Preface

The goal of the book is to present and explain the state of the art of design or retrofitting concrete buildings for earthquake resistance. To serve this goal, it also covers behaviour of concrete members under cyclic loading and seismic response of concrete buildings, as well as their modelling. Its main focus is the European Design Standard EN1998 – Eurocode 8: Design of structures for earthquake resistance, and in particular its Parts 1 and 3, dealing with seismic design of new buildings and with assessment and retrofitting of existing ones, respectively.

The book is addressed to practitioners of seismic design, assessment and retrofitting, to graduate and advanced undergraduate students in structural earthquake engineering and to researchers with interests in the field of earthquake resistant concrete structures. Certain familiarity of the reader with design of structural concrete and with structural analysis – including seismic analysis and structural dynamics – is presumed.

The book has been written in the course of my teaching activity for the MSc Degree in Earthquake Engineering and Engineering Seismology (MEEES), granted jointly by the Universities of Pavia and Patras and the J. Fourier University of Grenoble in the framework of the Erasmus Mundus programme of the European Commission. It has drawn from my involvement in the development of Eurocode 8 as a European Design Standard, and of its Parts 1 and 3 in particular. It has also drawn from my research at the University of Patras during the past 25 years and in particular from the joint work with my former doctoral students Dionysis E. Biskinis, Antonis J. Kosmopoulos and Telemachos B. Panagiotakos and my current colleague Stathis N. Bousias – as evident from the referencing throughout the book. I would also like to express my gratitude and appreciation to Eduardo C. Carvalho and Amr S. Elnashai for their very meticulous review and their comments for the book.

Patras, Greece — Michael N. Fardis

From the Reviews of the Book

The book is devoted to the seismic design of new buildings as well as to the assessment and retrofit of existing buildings, covering essentially the contents of Parts 1 and 3 of Eurocode 8. It must be stressed that its contents which refers to Assessment and Retrofit is a very important support tool to the application of Part 3 of Eurocode 8 which deals with Assessment and Retrofitting of Buildings and which in itself is a quite innovative document.

The book is organised in six chapters dealing sequentially with: the General Principles of Seismic Design; the Conceptual Design of Concrete Buildings for Earthquake Resistance; the Behaviour of Concrete Members under Cyclic Loading; the Analysis and Modelling for Seismic Design; the Detailing and Dimensioning and finally the Seismic Assessment and Retrofitting.

Summing up, the book is extremely valuable and represents a much updated state of the art in seismic design of concrete structures not only in Europe but also in other parts of the world. It is very carefully written with the clear intent to cover all aspects of seismic design and not leaving behind any aspect relevant for such. It shall be very useful and an authoritative source for the understanding and application of Eurocode 8 at several different levels, from the ordinary practitioner to the knowledgeable researcher passing by the software developer.

The book reflects the very solid knowledge of the author in earthquake engineering and his leading role in the recent developments of Eurocode 8, as well as the extreme care that was devoted to its planning and writing. No doubt, it shall become a reference in the field.

Eduardo C. Carvalho
Chairman of CEN/TC250/SC8
Lisbon, Portugal

The book starts with a Preamble that highlights a most important aspect of design, which is its interaction with construction, and emphasises the safety aspect of a well-designed structure that is difficult to build. The introductory notes set the scene for the subsequent detailed treatment of issues of seismic design of RC structures, a feature that is lacking in most design-oriented books in the earthquake engineering field. This leads naturally to Chapter 1, where the general principles of seismic design of RC structures are presented in a rational framework, which demonstrates the author's experience in conceptual and practical seismic design alike. Issues of single and multiple performance levels and their relationship with seismic hazard levels are succinctly explained. Covering both US and European practice, with emphasis on the latter, the author explains capacity design and the criteria used to establish a hierarchical dissipative and non-dissipative sequence of events. Capacity design is also applied in this chapter to typical systems, as well as to the flexure-shear problem.

Chapter 2 addresses conceptual design, guiding the reader through the steps postulated by the author for the selection of layout and preliminary sizing. The critical role of conceptual design in facilitating final and detailed design and reducing the number of iterations required is emphasised. A detailed treatment of regularity is given and examples are provided to demonstrate the adverse effects of irregularity on performance. Redundancy, continuity and mass minimisation are other features discussed in this chapter, with examples and practical guidance. The chapter concludes with examples of poorly conceived buildings that have been damaged in recent European earthquakes.

A most detailed and exhaustive treatment of the behaviour of RC members and connections is given in Chapter 3, with a wealth of behaviour-oriented expressions for deformation and strength. Examples from the literature are quoted and put into context to provide the reader with a comprehensive set of models for deformation and strength of members subjected to multi-axial stresses. This chapter is rather unique amongst recent seismic design books and on its own is worth reading carefully.

Another exhaustive treatment of modelling for design and assessment is given in Chapter 4, which also includes aspects of input motion. Elastic and inelastic analyses are addressed in detail, and examples and guidance on their applicability or otherwise are provided. Exceptionally insightful comments and guidance are given with regard to the intricate issue of modeling infill walls in frames. Three detailed examples are given in the closing part of the chapter where the guidance given throughout the chapter is applied to a test bed 3D frame structure, thus giving credence to the guidance.

Detailing and dimensioning requirement of Eurocode 8 are addressed in Chapter 5. Two worked examples that will prove invaluable to readers and potential users of the Eurocode are also given. The worked examples not only address the cases dealt with, but give clues as to how to apply Eurocode 8, as seen by the researcher who guided its final stages of development and implementation, to a wider range of design situations.

The last main chapter in the book, Chapter 6, deals with retrofitting of RC structures using Eurocode 8, with very considerable amounts of backup material from the research literature. The rules described in the chapter are then applied to two case studies, which are continuation of the "analysis" case studies, thus providing a thread through the various chapters. This thread will be valuable to readers because it establishes a clear link between design and analysis for assessment of the design, as well as retrofitting.

Amr S. Elnashai, FREng
Bill and Elaine Hall Endowed Professor
Director of the Mid-America Earthquake Center
Director of NEES@Illinois Earthquake Simulation Facility
Director of the Council on Global Engineering Initiatives
University of Illinois, Urbana, Illinois, USA

Preamble

The main activity of today's civil engineers is the production of structures. This activity has two phases:

- design, and
- construction – also termed "execution", as "construction" is also used for civil engineering works in general.

In the construction phase the civil engineer does not necessarily have the central role. In design, by contrast, his/her role is not just prime but almost exclusive.

With design being the 1st phase of the production process, many areas of the broader field of Earthquake Engineering ultimately serve design. For instance:

- a prime goal of Engineering Seismology and Geotechnical Earthquake Engineering is to determine the ground motion for the seismic design;
- a major role of Structural Dynamics – within the context of Earthquake Engineering – is the calculation of the response of the structure to a given seismic motion, either to verify that performance is satisfactory, or to provide the basis for the dimensioning of structural elements so that performance is indeed satisfactory.

There is strong interaction between design and construction of a structure. Design can be considered to govern production of a structure, as construction implements design drawings and specifications. However, design is influenced by, or depends on, construction as well. A structure is designed to be ultimately built; so the way it will be constructed should be a determining factor for its design. So, when designing the structure the engineer should have a clear and precise idea of how his/her design will be implemented with the human resources, equipment and materials available for that particular project. A design that seems excellent on paper but cannot be easily implemented with the available means and resources may in reality be poor or even unsafe, because bad implementation means poor quality. This point is very important for earthquake resistant concrete structures, as:

- Seismic performance depends heavily on the detailing of the reinforcement;
- In seismic regions a building's safety problem may remain hidden for long and show up only through its catastrophic consequences in the event of a strong earthquake. By contrast, in structures controlled by non-seismic actions, safety problems due to poor construction quality may become evident early on (e.g. upon striking off the formwork and falsework, or after all permanent loads are applied), before delivering the facility to the users.

The engineer should keep in mind that the earthquake will "see" the structure as it is built. The intentions of the designer, the assumptions made, the analysis methods used and the care exercised in its design, matter only to the extent they are indeed reflected in the as-built structure.

The seismic design process of a new concrete structure comprises four distinct phases:

(1) Conceptual design: the selection of the type and layout of the lateral-load-resisting system and of preliminary member sizes.
(2) Analysis: the calculation of the effects of the design actions, including the seismic one, in terms of internal forces and deformations in structural members.
(3) Detailed design: the verification of the adequacy of member dimensions and the dimensioning of the reinforcement on the basis of calculated action effects.
(4) Preparation of the end product of the design to be applied in the field: material specifications, construction drawings with detailing of the reinforcement, and any other information that may be necessary or helpful for the implementation of the design.

The design of the seismic retrofitting of an existing structure has the same four phases, but referring specifically to the retrofitting. In this case, however, we have two preliminary phases:

(–2) Collection of information on the history, geometry, reinforcement, materials, etc., of the as-built structure, as input for the subsequent phases.
(–1) Analysis and verification of the as-built structure, to confirm that retrofitting is indeed necessary and identify the deficiencies to be remedied.

The outcome of the design is just that of phase (4) and is often considered as the "design". The outcomes of phases (2) and (3) (and of (–2) and (–1) for existing structures) are just documentation of the "design". Stage (1) is the designer's personal business and is not documented anywhere.

Be it for a new building or for retrofitting an existing one, conceptual design is of utmost importance for the economy and the seismic performance of the structure. The choices and decisions made there are entirely based on the experience, judgment and ingenuity of the designer, even on his/her personal design philosophy and preferences. To some people design is just the conceptual design; all other phases being considered as "code checking".

During all design phases the engineer should use not just the scientific/technical tools at his/her disposal, but also judgment and experience, to produce a design that – to the best of his or her knowledge – cost-effectively fulfils the performance requirements. Experience is very important for the successful design of earthquake-resistant buildings. It provides ideas from previous, possibly similar, projects and helps avoiding poor choices, pitfalls or even design errors. Experience is also valuable to understand the "idiosyncrasy" of an existing building which is assessed for possible retrofitting.

The technology for earthquake resistance evolved essentially after 1970. Since then, scientific knowledge and technology in earthquake engineering and seismic design codes alike have seen a very rapid, and still ongoing, development. As a result, structures designed and constructed according to present generation codes enjoy a much higher safety level against earthquakes than older ones. The higher level of seismic safety comes at a higher cost (albeit less than proportional to the added safety). Moreover, the ultimate criterion for the success or not of current seismic codes and technology will be the performance of structures built with them in the event of an earthquake. Note that, owing to the short history of exposure of concrete construction to earthquakes (shorter than the time intervals between strong earthquakes, even in highly seismic regions) and the continuous evolution of seismic design codes during that history, we still lack sufficient feedback from the actual performance of concrete buildings. Finally, the short-term future will see further advances, as our knowledge and technology for earthquake resistance is in a state of continuous development. So, although we presently believe that our current know-how is satisfactory and produces safe structures, most likely in the medium-term seismic design will be quite different. Developments are expected mainly towards further rationalisation of seismic design, to achieve the same or better performance at lower cost. Empirical and prescriptive approaches will certainly give way to procedures based on more solid and rational grounds. The main vehicle for the transfer of such progress to engineering practice will be codes and standards for earthquake resistant design, notably those of the countries or regions most advanced in earthquake engineering (in alphabetical order, of the EU, Japan and the US). Practitioners of seismic design should follow the developments in codes and be prepared for changes to come. For those active in seismic assessment and retrofitting of existing buildings as well, certain knowledge of past codes and practice will help them identify and remedy their problems and deficiencies.

Chapter 2 of the book is devoted to conceptual design of new building structures for earthquake resistance. Chapter 1 provides an overview of the performance requirements for new building structures, of the philosophy of current seismic design codes for new earthquake-resistant buildings and of the main instruments for its implementation. Chapter 3 covers the behaviour under cyclic loading of the constituent materials and of concrete members of the type common in buildings, as well as the quantification of this behaviour. That chapter provides the background for Chapters 5 and 6. Chapter 4 is devoted to analysis and modelling issues, with emphasis on the analysis approaches commonly used within the context of codified seismic design or assessment (phase (2) of the design process). Chapter 5 deals with

dimensioning and detailing of new building structures for earthquake resistance and gives the background of some of the rules in Eurocode 8 on the basis of the material of Chapters 1 and 3. Chapter 6, on assessment and upgrading of the seismic performance of existing buildings, builds on Chapters 3 and 4, as well as on the general performance requirements set out in Chapter 1.

To a certain extent the book develops with reference to the European Standards for seismic design, assessment and retrofitting of buildings, Parts 1 and 3 of Eurocode 8. Some parts of Chapter 1 and 4 include references to Eurocode 8, but also to US seismic design standards. Chapters 5 and 6 are linked with Eurocode 8 – Chapter 5 very closely, but Chapter 6 less so.

In December 2004, Part 1 of Eurocode 8 (CEN 2004a) was published by the European Committee for Standardisation to become the first in history European Standard for seismic design of new buildings, complementary to the other EN-Eurocodes. It was followed in June 2005 by Part 3 of Eurocode 8 (CEN 2005a), for seismic assessment and retrofitting of existing buildings. The 31 member countries in CEN have since then published these European Standards as their own National Standards, together with their National Annexes. These Annexes state the national choices for the so-called "Nationally Determined Parameters", devised to provide the flexibility required for the application of Eurocode 8 in a whole continent with diverse engineering traditions and seismicity. Until March 2010 national design standards will be used in parallel with Eurocode 8, but by March 2010 national design standards that conflict in any aspect with any EN-Eurocode should be withdrawn.

In the USA seismic design of buildings follows a building design code that covers also non-structural aspects (architectural, mechanical, electrical, building equipment, etc.). Seismic design provisions for new buildings were traditionally developed either by the Building Seismic Safety Council (BSSC) and published as "NEHRP Recommended Provisions for the Development of Seismic Regulations for Buildings and Other Structures" (BSSC 2003), or by the Structural Engineers Association of California (SEAOC) and published as "SEAOC Recommended Lateral Force Requirements" (SEAOC 1999). With some time-lag the NEHRP provisions have traditionally been reflected in (but not fully adopted by) the "National Building Code", the "Standard Building Code" and more recently the "International Building Code" (ICC 2006). The SEAOC requirements have been in general reflected in the "Uniform Building Code", the last version of which was issued in 1997 (ICBO 1997). Local Authorities (States, counties, cities) formally adopt one of the three model codes after adaptation to local traditions/conditions. Recent years have seen a convergence of the seismic design provisions in the NEHRP and SEAOC documents, extending also to the main material codes referred to, or used as source documents by them, such as the ACI 318 code (ACI 2008), prepared by the American Concrete Institute. Moreover, in 1997 the "International Code Council" was formed and issued in 2000 the "International Building Code". Since then, the updated code (ICC 2006) is gradually adopted throughout the US.

Contents

Chapter 1
General Principles for the Design of Concrete Buildings for Earthquake Resistance

Chapter 1 presents the requirements posed by modern seismic codes and standards for the protection of life and property in new building designs and highlights the means provided for their fulfilment. The requirements and design rules provided in the European Standard for the seismic design of new buildings – EN 1998-1:2004, termed also Part 1 of Eurocode 8 – are given certain emphasis and compared to their US counterparts. These Eurocode 8 rules are elaborated further in Chapter 5 in the context of the process for the detailed design of new concrete buildings for earthquake resistance.

Chapter 1 gives also an overview of a new thinking towards more comprehensive coverage of the seismic performance needs of owners and occupants over the lifetime of the building. This thinking is currently penetrating newly emerging codes and standards for the seismic evaluation and upgrading of existing substandard buildings, including EN 1998-3:2005 (also known as Part 3 of Eurocode 8). The requirements and rules provided in this latter European Standard for the seismic assessment and retrofitting of existing buildings are further elaborated in Chapter 6.

1.1 Seismic Performance Requirements for Concrete Buildings

1.1.1 The Current Situation: Emphasis on Life Safety

Traditionally, introduction and enforcement of structural design codes and standards has been the responsibility of competent Authorities, with public safety as the overriding consideration. Accordingly, traditional seismic design codes or standards for buildings aim at protecting human life by preventing local or global collapse under a single level of earthquake. The no-(local-)collapse requirement normally refers to a rare seismic action, termed "design seismic action". In most present codes the "design seismic action" for ordinary structures is conventionally chosen as the one having a 10% probability to be exceeded in a conventional working life of 50 years, or 0.2% in a single year. This corresponds to a mean return period of 475 years for the "design seismic action".

M.N. Fardis, *Seismic Design, Assessment and Retrofitting of Concrete Buildings*, Geotechnical, Geological, and Earthquake Engineering 8, DOI 10.1007/978-1-4020-9842-0_1,

Within a single-tier design framework, enhanced safety of facilities that are essential or have large occupancy is normally achieved by modifying the hazard level (the mean return period) of the "design seismic action". The seismic action is multiplied times an "importance factor", γ_I. By definition, $\gamma_I = 1.0$ for structures of ordinary importance (buildings of "Importance Class" II in Eurocode 8). For buildings whose collapse may have unusually large social or economic consequences (large occupancy buildings, such as schools or public assembly halls, etc.) or for facilities housing institutions of cultural importance (e.g., museums), Eurocode 8 recommends a value $\gamma_I = 1.2$ (buildings of "Importance Class" III in Eurocode 8). It recommends $\gamma_I = 1.4$ for buildings which are essential for civil protection during the immediate post-earthquake period: hospitals, fire or police stations, power plants, etc. (categorised as "Importance Class" IV). For buildings of minor importance for public safety (i.e., belonging in "Importance Class" I, comprising agricultural and similar buildings) Eurocode 8 recommends a value $\gamma_I = 0.8$.

1.1.2 Performance-Based Requirements

Already in the 1960s the international earthquake engineering community was fully aware of the property loss that may be caused by frequent seismic events and their other economic consequences. Recognising that it is not feasible to avoid any damage under very strong earthquakes, the Structural Engineers Association of California (SEAOC) adopted in its 1968 recommendations the following requirements for seismic design:

"Structures should, in general, be able to:

- Resist a minor level of earthquake ground motion without damage.
- Resist a moderate level of earthquake ground motion without structural damage, but possibly experience some nonstructural damage.
- Resist a major level of earthquake ground motion having an intensity equal to the strongest either experienced or forecast for the building site, without collapse, but possibly with some structural as well as nonstructural damage."

Major earthquakes that hit developed countries in the second half of the 1980s and the first half of the 1990s caused relatively few casualties but very large damage to property and economic losses. In response to this, "Performance-based earthquake engineering" emerged in the SEAOC Vision 2000 document and developed into the single most important idea of recent years for seismic design or retrofitting of buildings (SEAOC 1995).

"Performance-based engineering" focuses on the ends, notably on the ability of the engineered facility to fulfil its intended purpose, taking into account the consequences of its failure to meet it. Conventional structural design codes, by contrast, are process-oriented, emphasising the means, namely the prescriptive, easy to apply, but often opaque rules that disguise the pursuit of satisfactory performance. These rules have been developed over time as a convenient means to provide safe-sided,

yet economical solutions for common combinations of building layout, dimensions and materials. They leave limited room for the designer to exercise judgement and creativity and do not provide a rational basis for innovative designs that benefit from recent advances in technology and structural materials.

"Performance-based earthquake engineering" in particular tries to maximise the utility from the use of a facility by minimising its expected total cost, including the short-term cost of the work and the expected value of the loss in future earthquakes (in terms of casualties, cost of repair or replacement, loss of use, etc.). One would like to take into account all possible future seismic events with their annual probability and carry out a convolution with the corresponding consequences during the design working life of the facility. However, this is not practical. Therefore, at present "performance-based earthquake engineering" advocates just replacing the traditional single-tier design against collapse and its prescriptive rules, with a transparent multi-tier seismic design, meeting more than one discrete "performance levels", each one under a different seismic event, identified through its annual probability of exceedance and termed "seismic hazard level". Pairing off all "performance levels" considered for a particular case with the associated "seismic hazard levels" is termed, in performance-based earthquake engineering, "performance objective".

Each "performance level" is normally identified with a physical condition of the facility, well-described together with its possible consequences: likely casualties, injuries and property loss, continued functionality, cost and feasibility of repair, expected length of disruption of use, cost of relocation of occupants, etc. Commonly four "performance levels" are identified:

(i) "Operational"
(ii) "Immediate occupancy"
(iii) "Life-safety" and
(iv) "Near collapse".

The definition of these "performance levels" is roughly as follows:

"Operational": The facility has suffered practically no structural or non-structural damage and can continue serving the original intention of its design with little disruption of use for repairs. Continuous operation is supported either by undamaged lifelines or by back-up systems. Any repair that is necessary can take place in future without disruption of occupancy or use.

"Immediate occupancy": The facility can return to full use, as soon as utility systems are back in operation and cleanup is complete. The structure itself is very lightly damaged: some yielding of reinforcement may have taken place and concrete cracking may be visible, but there are no residual drifts or other permanent structural deformations. The risk to life is negligible. The structure retains fully its pre-earthquake strength and stiffness. Its ability to withstand future earthquakes, including aftershocks, is not diminished. Non-structural components and systems may have minor damage (e.g. distributed cracking in infill walls) that can be easily and economically repaired at a later stage.

"Life-safety": The structure, or any parts of it, do not collapse, retaining integrity and residual load capacity after the earthquake. The structure is significantly

damaged and may have moderate permanent drifts, but retains its full vertical load-bearing capacity and sufficient residual lateral strength and stiffness to protect life even during strong aftershocks. Non-structural components are damaged, but do not block evacuation routes or cause life-threatening injuries by falling. Sometimes reparability is economically questionable and demolition may be preferable.

"Near collapse": The structure is heavily damaged, at the verge of collapse of several gravity load-carrying elements in a storey, or even of total collapse. It may have large permanent drifts and retains little residual strength and stiffness against lateral loads, but its vertical elements can still carry the (quasi-)permanent gravity loads. Most non-structural elements (e.g. infill walls) have collapsed. There is substantial, but not full, life safety, as falling hazards may cause life-threatening injury. The building is unsafe for use, as it may collapse in a strong aftershock. Repair may not be technically feasible and certainly is not economically sensible.

Sometimes, reference is made to two more performance levels: "Damage onset", as a performance level before "Operational" associated with absolutely no structural or non-structural damage; and "Reparable", as a performance level between "Immediate occupancy" and "Life-safety", associated with structural or non-structural damage that is not only technically, but also economically, reparable.

Different performance criteria are also defined for the verification of structural or non-structural elements under the various performance levels. Criteria for structural or non-structural damage are normally expressed in terms of deformation limits. For example, performance level (i) ("Operational") may be identified with "yielding" of structural members, while performance level (iv) ("Near collapse") is often associated with near exhaustion of member "ultimate" deformation, signalling loss of lateral load capacity. Damage limitation criteria for non-structural cladding or partitions that follow the deformations of the structural frame are normally expressed in terms of interstorey drift limits. For equipment mounted or supported on the structure, limits relevant to damage may be expressed in terms of response accelerations at the support points of the equipment.

The discrete hazard levels normally paired off with the four main performance levels listed under (i)–(iv) above for the design of ordinary (i.e., standard occupancy) new buildings, are:

1. a "frequent" earthquake, expected to take place during the conventional working life of the building, having therefore a mean return period much shorter than 50 years (e.g., around 25 years);
2. an "occasional" earthquake, not expected during the conventional working life of the building, with a mean return period between 75 and 200 years;
3. a "rare" earthquake, with a mean return period of about 500 years; and
4. a "very rare" or "maximum considered" earthquake, with quoted values of the mean return period in the order of 1000–2500 years.

According to this idea, the "performance objective" for structures of ordinary importance is to meet performance level (i) under hazard level (1), (ii) under (2), etc.

If higher performance is desired, or for critical facilities, an "enhanced objective" may be selected – e.g. performance level (ii), or even (iii), under hazard level (1), etc.

Note that, depending on the slope of the seismic hazard curve, at any given site certain aspects of the design may be governed by the fulfilment of one performance level under the corresponding hazard level. The other performance levels will be met then automatically at the associated hazard levels. If this applies in general to all types of buildings at a given geographic location or region, then a four-tier performance-based seismic design may degenerate there into a fewer-tier (e.g., a two-tier) one.

Performance-based seismic design serves better the interests and objectives of owners, by allowing more rational decision-making, with explicit verification of performance levels related to property loss and operation of the facility under frequent or occasional earthquakes. It may also provide more flexibility in conceptual design, as collapse prevention under very rare events is explicitly verified, instead of indirectly designed against by explicit verification only at the "life safety" level and using capacity design as a safeguard against collapse under much stronger earthquakes (see Section 1.3). On the other hand, a full-fledged performance-based design process may be arduous and complex. Besides, there is a liability issue to be resolved: the designer is protected to a certain extent against liability claims or other charges for property loss, casualties, etc., in an unforeseeable future event, if he or she has strictly adhered to all rules of a current-generation prescriptive code, which is opaque about the intended performance objective. This may not be the case anymore in a performance-based design context, with explicit and transparent performance objectives which the owner or the courts may interpret as guaranteed. For all these reasons, there is still a long way to go before seismic design codes for new buildings adopt a full-fledged performance-based approach. Such an approach has been adopted, though, in guidelines and standards for the seismic assessment and retrofitting of existing buildings, as it is there that the inherent flexibility of the approach can best bear fruits to accommodate the specific interests, objectives and means of owners. Moreover, buildings not designed to modern-day seismic codes normally do not possess structural features serving as safeguards against collapse under very strong earthquakes (e.g., a layout and a hierarchy of strengths that prevent concentration of deformation demands in a small part of the structural system). Therefore, older buildings require explicit verification against such an outcome.

1.1.3 Performance-Based Seismic Design, Assessment or Retrofitting According to Eurocode 8

In Europe performance levels in seismic design, assessment or retrofitting are associated to, or identified with, Limit States of the structure. The Limit State concept appeared in Europe in the 1960s, to define states of unfitness of the structure for its intended purpose (CEB 1970, Rowe 1970). Limit States concerning the safety of people or of the structure are termed Ultimate Limit States. Those concerning the

normal function and use of the structure, the comfort of its occupants, or damage to property (mainly to finishes and non-structural elements) are called Serviceability Limit States. Intermediate Limit States may also be considered (CEB 1988b). According to the Eurocode "Basis of Structural Design" (CEN 2002) the Limit States approach is the backbone of structural design for any type of action, including the seismic one.

Part 1 of Eurocode 8 (CEN 2004a) provides for a two-tier seismic design of new buildings, with the following explicit performance levels ("Limit States"):

1. No-(local-)collapse, which is considered as the Ultimate Limit State against which the structure should be designed according to the Eurocode "Basis of Structural Design" (CEN 2002). It entails protection of life under a rare seismic action, through prevention of collapse of any structural member and retention of structural integrity and residual load capacity after the event.
2. Damage limitation, which plays the role of the Serviceability Limit State against which the structure should be designed according to CEN (2002). The aim is mitigation of property loss in frequent earthquakes, through limitation of structural and non-structural damage. After such an earthquake structural elements are supposed to have no permanent deformation, retain their full strength and stiffness and need no repair. Non-structural elements may suffer some damage, which can be easily and economically repaired at a later time.

The no-(local-)collapse performance level is achieved by dimensioning and detailing structural elements for a combination of strength and ductility that provides a safety factor (in the order of 1.5–2) against substantial loss of lateral load resistance.

The damage limitation performance level is achieved by limiting the overall deformations (lateral displacements) of the building to levels acceptable for the integrity of all its parts (including non-structural ones). More specifically, interstorey drift ratios (defined as the difference between the mean lateral displacements of adjacent storeys divided by the interstorey height) are limited to the following values:

(i) 0.5%, if the storey has brittle non-structural elements attached to the structure (notably, ordinary masonry infills);
(ii) 0.75%, if the storey's non-structural elements are ductile; or
(iii) 1%; when there are no non-structural elements that follow the deformations of the structural system.

The two explicit performance levels – (local-)collapse prevention and damage limitation – are pursued under two different seismic actions. The seismic action under which (local) collapse should be prevented is the "design seismic action". The one for which damage limitation is pursued is called the "damage limitation seismic action". Within the Eurocode philosophy of national competence on issues

of safety and economy, the hazard levels for these two seismic actions are left to national determination. For structures of ordinary importance, Part 1 of Eurocode 8 recommends:

1. a "design seismic action" having 10% probability of being exceeded in 50 years (a mean return period of 475 years); and
2. a "damage limitation seismic action" with 10% exceedance probability in 10 years (mean return period: 95 years).

Although not explicit, an additional performance objective in buildings designed to provide earthquake resistance by dissipating energy is to prevent global collapse during a very strong and rare earthquake (performance level (iv) in Section 1.1.2 under hazard level (4)). This implicit performance objective is pursued via systematic and across-the-board application of capacity design, which imposes a hierarchy of strengths that permits full control of the inelastic response mechanism (see Section 1.3).

Following the example of the US standard for seismic rehabilitation (ASCE 2007) and its draft predecessors, Part 3 of Eurocode 8 for assessment and retrofitting of buildings (CEN 2005a) has fully adopted the "performance-based" approach. It provides for three different performance levels (termed Limit States):

1. "Damage Limitation" (DL), corresponding to "Immediate Occupancy": The structure has no permanent drifts; its elements have no permanent deformations, retain fully their strength and stiffness and do not need repair. Members are verified to remain elastic.
2. "Significant Damage" (SD), corresponding to "Life safety" and to the (local-)collapse prevention performance level to which new buildings are designed according to Part 1 of Eurocode 8. The structure is significantly damaged, may have moderate permanent drifts, but retains some residual lateral strength and stiffness and its full vertical load-bearing capacity. Repair may be uneconomic. The verifications should provide a margin against member ultimate capacities.
3. "Near Collapse" (NC), similar to "Collapse prevention" in the US: The structure is heavily damaged, may have large permanent drifts, retains little residual lateral strength or stiffness, but vertical elements can still carry the gravity loads. In the verifications, a member may approach its ultimate force or deformation capacity.

The "Seismic Hazard" levels for which the three Limit States should be met are chosen either nationally through the National Annex to this part of Eurocode 8, or by the owner if the country leaves the choice open. The Eurocode itself gives no recommendation, but mentions that the performance objective recommended as suitable for ordinary new buildings is a 225 year earthquake (20% probability of exceedance in 50 years), a 475 year event (10% probability in 50 years), or a 2475 year one (2% probability of being exceeded in 50 years), for the DL, the SD or

the NC "Limit State", respectively. Countries (or the owners, if the country lets the choice to them) have the authority to decide whether all three Limit States will be verified, or whether checking one or two of them at the corresponding seismic hazard level suffices.

1.1.4 Performance-Based Design Aspects of Current US Codes

In the NEHRP provisions (BSSC 2003) seismic design of new buildings is for a single level of ground motion, namely for two-thirds of the Maximum Considered Earthquake (MCE). This is the "design seismic action" in the US. The MCE is given by the USGS Seismic Hazard Maps from the USGS/BSSC 97 project (Frankel et al. 1996, 1997). These maps are also used by almost all recent nationally applicable US documents. They map the values of the 5%-damped elastic response spectral acceleration in the acceleration-controlled region, S_{as} (which is equal to 2.5 times the effective peak acceleration, *EPA*) and at a period of 1 s (S_{a1}, from which the velocity-controlled spectral region is derived). National and regional maps (at a scale of 1:500.000–1:5.000.000) are given for the MCE, which is defined for this purpose as 1.5 times the characteristic event produced by well known active faults every few hundred years. Where no major active faults can be identified, the values of S_{as} and S_{a1} with 2% probability of being exceeded in 50 years (i.e., with mean return period of 2500 years) is used. Factors are given for the conversion of the values of S_{as} and S_{a1} over firm rock to other types of ground.

For structures of ordinary importance the Life Safety performance level is required under the design seismic action of two-thirds of MCE. If this performance objective is fulfilled, it is deemed that collapse prevention is indirectly achieved under the 1.5-times stronger MCE and that immediate occupancy is expected under a frequent event with 50% probability of being exceeded in 50 years (mean return period of 72 years). Facilities which are essential for post-earthquake recovery or contain hazardous substances are designed for 1.5-times higher forces (through a 1.5-times smaller force reduction factor), implying Life Safety performance under the MCE. Such structures are claimed to indirectly achieve the Immediate Occupancy performance level under frequent earthquakes. Structures with increased public hazard, owing to large occupancy or limited ability of occupants to evacuate (medical or daycare facilities, schools, jails), are designed for 25% higher forces than ordinary ones and believed to fulfill intermediate performance objectives.

The performance objectives achieved by other than ordinary structures through the SEAOC '99 recommendations are less clear: they provide just for 25% increased design forces for essential or hazardous facilities.

Note that the importance of the structure is taken into account only in the performance under the single level of design action considered and does not affect the design seismic action. This is also evident from the fact that the importance factor does not enter in the calculation of storey drifts – calculated and checked under the design seismic action for life protection and not under a more frequent event for damage limitation.

1.2 Force-Based Seismic Design

1.2.1 Force-Based Design for Energy-Dissipation and Ductility

For the no-(local-)collapse requirement to be met for the "design seismic action" the structure does not need to remain elastic under this action. That would have required a lateral force resistance close to 50% of the building's weight. Although technically feasible, this is economically prohibitive. It is also completely unnecessary, as the earthquake is a dynamic action and imparts to the structure a certain total energy input and certain displacement and deformation demands, but not a demand to sustain specific forces. So, current codes for earthquake-resistant design allow structures to develop significant inelastic deformations under the design seismic action, provided that the integrity of individual members and of the structure as a whole is not impaired. The design approach for this is still based on forces, but its real aim is to impart to the structure capacity for energy dissipation and ductility.

Force-based seismic design is against physical reality. It is the deformation that causes a structural member to lose its lateral load resistance. It is lateral displacements (and not lateral forces) that cause structures to collapse under their own weight during the earthquake. However, force-based seismic design is well-established in current seismic design codes, because:

- structural engineers are familiar with force-based design for other types of actions (such as gravity and wind loads),
- static equilibrium for a set of prescribed external loads is a robust basis for the analysis, and
- tools for the direct verification of structures for seismic deformations are not considered yet as fully developed for practical application.

The last bullet point refers both to nonlinear analysis methods for the calculation of deformation demands and to the estimation of deformation capacities of structural members.

For all these reasons, it seems that in the foreseeable future force-based seismic design for energy dissipation and ductility will not disappear from design codes and practice.

Force-based seismic design for ductility is based on the inelastic response spectrum of a single-degree-of-freedom (SDOF) system with elastic-perfectly plastic force-displacement curve, F-δ, in monotonic loading. For a fixed value of viscous damping (the value $\zeta = 5\%$ is commonly adopted by convention), the inelastic spectrum relates:

- the period, T, of the SDOF system;
- the ratio $q = F_{\mathrm{el}}/F_{\mathrm{y}}$ of the peak force, F_{el}, that would had developed if the SDOF system were linear-elastic, to the yield force of the system, F_{y}, (q is called "behaviour factor" in Europe, while the term "force reduction factor" or "response modification factor" and the symbol R are used in the US for it) and

– the maximum displacement demand of the inelastic SDOF system, δ_{max}, expressed as a ratio to the yield displacement, δ_y (i.e. as the displacement ductility factor, $\mu_\delta = \delta_{max}/\delta_y$).

Eurocode 8 has adopted the inelastic spectra proposed in (Vidic et al. 1994):

$$\mu_\delta = q, \qquad \text{if } T \geq T_C \tag{1.1}$$

$$\mu_\delta = 1 + (q-1)\frac{T_C}{T}, \quad q = 1 + (\mu_\delta - 1)\frac{T}{T_C} \quad \text{if } T < T_C \tag{1.2}$$

where T_C is the "transition" or "corner" period of the elastic spectrum between the constant spectral pseudo-acceleration and the constant spectral pseudovelocity ranges (see Fig. 1.1, for inelastic spectra normalised to peak ground acceleration of 1 g, with $T_C = 0.6$ s).

The reduction in force response due to ductility bears certain similarities with the effect of higher viscous damping on an elastic SDOF system. The underlying mechanism is similar: energy dissipation; viscous in the case of the elastic SDOF, of hysteretic nature for the elastic-perfectly plastic one. Equation (1.1), applicable in the intermediate-to-long period range, expresses Newmark's well known "equal displacement rule", i.e. the empirical observation that in the constant spectral pseudovelocity range the peak displacement response of the inelastic and of the elastic SDOF systems are approximately the same. The underlying physical reason is that inertia tends to keep the mass of a flexible SDOF system at the same absolute position while the ground moves underneath, no matter whether the spring of the system yields or not. Equation (1.2) suggests that a very high ductility is needed to appreciably reduce the peak force in a very stiff system (i.e., one with $T << T_C$): for the hysteretic energy dissipation to significantly reduce the force response, the system has to undergo large displacements, which, when divided by the low yield displacement, δ_y, of the very stiff system are translated to very high ductility demands.

The "behaviour factor" q (as well as the "force reduction" or "response modification" factor R) is applied as a global reduction factor of the internal forces that would

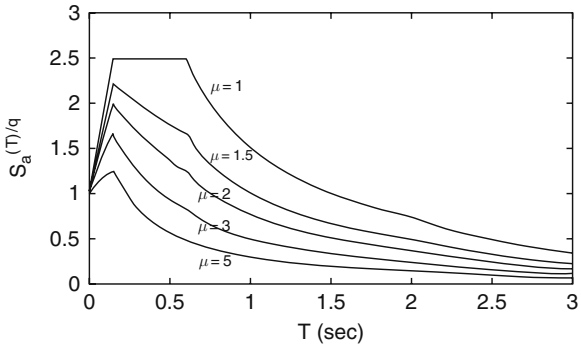

Fig. 1.1 Inelastic spectra from Eqs. (1.1) and (1.2) normalised to peak ground acceleration

develop in the fictitious representation of the structure as elastic with 5% damping (equivalently, on the seismic inertia forces that would develop in the hypothetical elastic structure and induce the seismic internal forces). In this way the seismic internal forces for which the members of the structure are dimensioned can be calculated through linear elastic analysis. A set of prescriptive rules are used, then, to provide the structure with the real aim of the design, namely the capacity to withstand a peak global displacement at least equal to its global yield displacement times the displacement ductility factor, μ_δ, corresponding to the value of q applied for the reduction of elastic force demands (cf. Eqs. (1.1) and (1.2)). The so designed and detailed structure is considered to have "ductility" or "energy-dissipation" capacity – a more general term often used in Europe and in Eurocode 8, as ductility during cyclic response implies that the members and the structure as a whole dissipate a major part of the seismic energy input through hysteresis.

1.2.2 Force-Based Dimensioning of Ductile "Dissipative Zones" and of Other Regions of Members

Not every member or location in a structure is capable of developing ductile behaviour and hysteretic energy dissipation. Typical force-deformation relations (e.g., of moment (M) to curvature (ϕ), or of Force (F) to deflection (δ), etc.) of "ductile" members, regions or mechanisms of load transfer are as those shown in Fig. 1.2(a) for shear span ratio $L_s/h = 2.5$ for monotonic loading or in Fig. 1.2(c) for cyclic loading. It is such members, regions etc., that are entrusted through "capacity design" for inelastic deformations and energy dissipation. Elements, regions or mechanisms of force transfer with force-deformation behaviour as shown for $L_s/h = 1.9$ in Fig. 1.2(a) for monotonic loading or in Fig. 1.2(b) for cyclic loading are "brittle" (or "non-ductile"). They are the ones shielded through "capacity design" from the inelastic action they are incapable of.

Once it yields, a ductile element, etc., can undergo large (sometimes limitless) inelastic deformations at no additional resistance. In concrete, this type of behaviour is characteristic of pure flexure (i.e. without axial load) and of flexural deformations (curvatures, chord rotations, etc.), resembling the behaviour of hinges that allow limitless rotation under zero moment. For this reason regions exhibiting after yielding the behaviour depicted in Fig. 1.2(c) are termed "plastic hinges". They are finite length regions of prismatic concrete members (beams, columns, slender walls) where phenomena like wide cracking, spalling of concrete and yielding and buckling of longitudinal bars are concentrated and where the behaviour accompanying or signaling ultimate conditions (fracture of longitudinal bars, disintegration of concrete, etc.) take place.

The black-and-white distinction of members as "ductile" and "brittle" is convenient. However, the behaviour of the different types of concrete members covers a very broad range from absolute "brittleness" to limitless "ductility". A convenient measure of "ductility" is the available value of the displacement ductility factor of

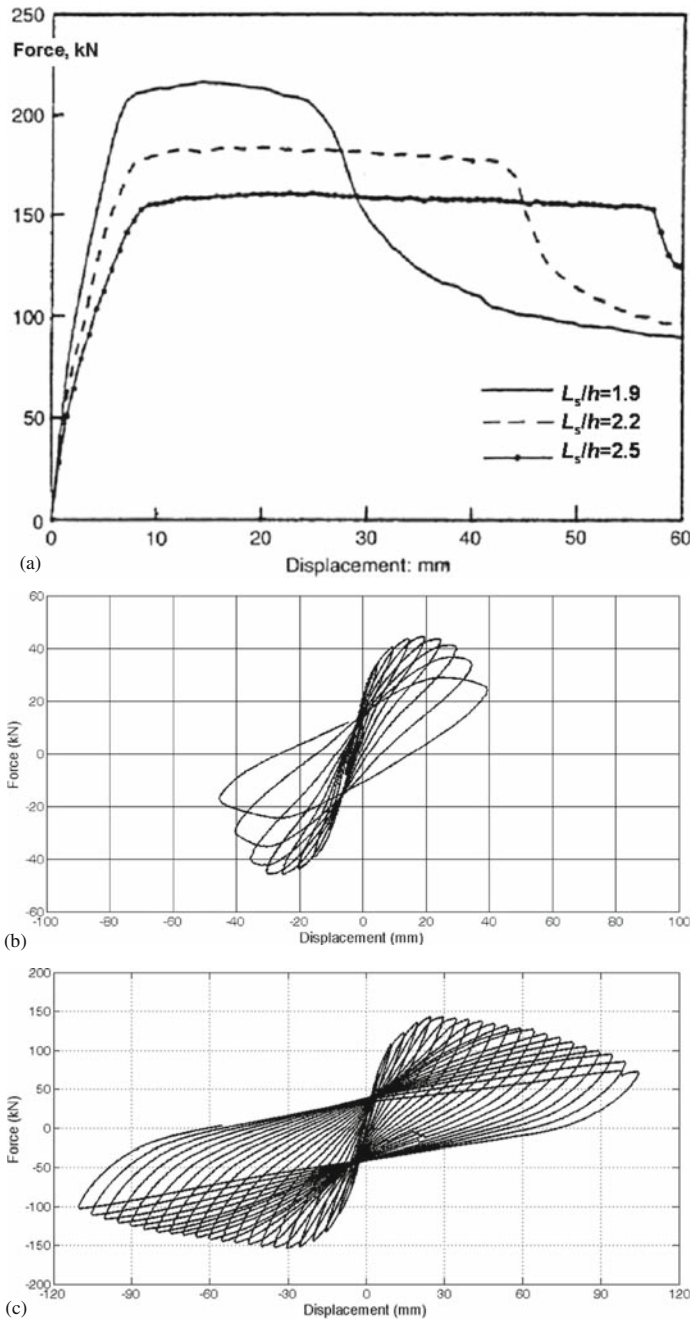

Fig. 1.2 Force-displacement curves for typical: (**a**) ductile behaviour for shear span ratio $L_s/h = 2.5$ to semi-brittle for $L_s/h = 1.9$ in monotonic loading (adapted from Garstka 1993); (**b**), brittle behaviour in cyclic loading (Bousias et al. 2007a); (**c**) ductile behaviour in cyclic loading (Bousias et al. 2007b)

the member, μ_δ (defined as the ratio of its ultimate deflection to the deflection at the corner of a bilinear approximation of the member's force-deflection curve up to ultimate deformation ("yield" deflection)). A conventional limit $\mu_\delta = 2.5$ often distinguishes ductile from brittle behaviour.

To limit occurrence of inelastic deformations only to those members, regions and mechanisms capable of ductile behaviour and hysteretic energy dissipation, while the rest of the structure stays in the elastic range, seismic design codes use a special instrument of seismic design called "Capacity design" and described in detail in Section 1.3. With this instrument a hierarchy of strengths between adjacent structural members or regions, and between different mechanisms of load transfer in the same member is achieved, so that members, regions and mechanisms capable of ductile behaviour and hysteretic energy dissipation are the first ones to develop inelastic deformations. More important, they do so in a way that precludes forever the development of inelastic deformations in any member, region or mechanism deemed incapable of ductile behaviour and hysteretic energy dissipation. Among all current seismic design codes, Eurocode 8 makes the most systematic and extensive use of capacity design to control the inelastic response mechanism (see Section 1.3 for details). Eurocode 8 calls the regions of members which are entrusted for hysteretic energy dissipation "dissipative zones". These regions are designed and detailed to provide the required ductility and energy-dissipation capacity. In concrete, an equivalent term is a "plastic hinge" region or zone, as concrete members can develop hysteretic energy dissipation and ductility only in flexure.

Before designing and detailing a "dissipative zone" for the necessary ductility and energy dissipation capacity, the designer should first dimension it for a force resistance, R_d, at least equal to the action effect, E_d, computed from the elastic analysis for the design seismic action plus the concurrent gravity loads:

$$E_\mathrm{d} \leq R_\mathrm{d} \tag{1.3}$$

The value of E_d in Eq. (1.3) is due to the "design seismic action" (as defined in Sections 1.1.1, 1.1.3 and 1.1.4) and to the quasi-permanent value of the other actions expected to act concurrently. The Eurocode "Basis of Structural Design" (CEN 2002) calls this combination of actions "seismic design situation" (this is the reason for subscript "d" in E_d) and defines the quasi-permanent value of the other actions as the nominal value of permanent loads plus the arbitrary-point-in-time expected value ("quasi-permanent") of gravity loads due to imposed (i.e., live) loads or snow. Normally E_d is calculated through linear analysis. Then the value of E_d may be found by superposition of the seismic action effects from an analysis for the seismic action alone, to the action effects from the analysis for the other actions in the seismic design situation. Second-order effects should be taken into account in the calculation of E_d.

All regions and mechanisms not designated as "dissipative zones" are designed to provide a design value of force resistance, R_d, at least equal to an action effect, E_d, obtained not from the analysis but through "capacity design", as explained in detail in Section 1.3.

The value of force resistance in Eq. (1.3) incorporates one or more safety factors that reduce the nominal value of resistance (i.e., the one calculated using the nominal dimensions of the member and the nominal properties of the materials). In the Eurocodes this is called design value of resistance (hence subscript "d" in R_d). For concrete members the Eurocodes (CEN 2002, 2004b) compute the value of R_d using design values of material strengths: the characteristic or nominal values, f_k (i.e., the nominal yield stress of the reinforcement, f_{yk}, the characteristic 28-day cylindrical compressive strength of concrete, f_{ck}), divided by the corresponding partial factors γ_M for materials. As the γ_Ms are safety elements, they are Nationally Determined Parameters with values specified in the National Annexes to the Eurocodes. Eurocode 8 itself does not recommend the values of γ_M to be used for seismic design. It just mentions in notes the following options:

1. To use the same values of γ_M as in design against monotonic, non-seismic actions (e.g. for the "persistent and transient design situation" in CEN (2002), i.e. the combination of factored permanent actions and factored imposed actions – i.e. live loads – or wind). This option is very convenient for the designer, as he/she may then dimension the dissipative zone to provide a design value of force resistance, R_d, at least equal to the largest among the two action effect due to the "persistent and transient design situation" and that in the "seismic design situation". As for all Nationally Determined Parameters, values of γ_M are specified in the National Annex, in this case that to Eurocode 2. Eurocode 2 itself (CEN 2004b) recommends in a note the following values of γ_M for the "persistent and transient design situation": $\gamma_s = 1.15$ for the strength of the reinforcement, $\gamma_c = 1.5$ for any strength property of concrete.
2. To use the values $\gamma_M = 1$ applicable for design against accidental actions. This is sensible for regions of low to very low seismicity, where knowledge of historical seismicity is not sufficient to support statistical association of the "design seismic action" with a probability of being exceeded in 50 years (or a mean return period). In such cases the "design seismic action" may be conventionally chosen based more on judgement than on a probabilistic hazard analysis. It may have less than 10% probability of being exceeded in 50 years (i.e., mean return period longer than 475 years) and qualify for characterisation as an accidental action. In that case dissipative zones will be dimensioned separately for the action effect due to the persistent and transient design situation, computing the design value of force resistance, R_d, in Eq. (1.3) with $\gamma_M > 1$, and separately for the action effect of the "seismic design situation", using $\gamma_M = 1$ in the calculation of R_d.

Note that the more safe-sided approach 1 above implicitly accounts for some reduction in force resistance due to inelastic cyclic loading (low cycle fatigue). If the actual reduction is large and the value of R_d against monotonic, non-seismic actions is grossly inadequate, a special rule, applicable for inelastic cyclic loading, should be provided by the seismic design code.

1.3 Control of Inelastic Seismic Response Through Capacity Design

1.3.1 The Rationale of Capacity Design

As pointed out in Section 1.2, the horizontal displacement at the point of application of the resultant lateral force due to the design seismic action is known in good approximation, if the fundamental period, T, of the SDOF system is given. Moreover, the maximum energy to be converted to potential (i.e. deformation) energy is also approximately known: the maximum kinetic energy during the response, to be converted to potential energy during the following quarter-cycle, is roughly equal to one-half the total mass times the square of the spectral pseudovelocity, S_v, which for $T \geq T_C$ (cf Eq. (1.1)) is roughly independent of the value of T.

The seismic design of the building determines how the (roughly) given peak global displacement and peak kinetic energy are distributed to the various elements of the building. To distribute them just to those elements best suited to withstand these demands, current seismic design codes use "capacity design" as the main instrument. In the detailed design phase "capacity design" works with and on the strengths of individual elements to ensure that all-along the load path of inertia forces, from the masses to the foundation, the strength of the structural system is governed by the ductile elements. Although capacity design is used during detailed design, its effectiveness depends strongly on the layout and sizing chosen early on, during conceptual design.

The elements to which the peak global displacement and deformation energy demands are channeled by capacity design are selected on the basis of the following criteria:

1. The elements' "ductility", i.e., their capacity to develop large inelastic deformations and dissipate energy under cyclic loading, without substantial loss of force-resistance.
2. The importance of the element for the stability of other elements and for the integrity of the whole. Vertical elements are more important than horizontal ones and their importance increases from the roof to the foundation, as their failure may precipitate loss of support for all overlying elements.
3. The accessibility of the element and the difficulty to inspect and repair any damage.

On the basis of the criteria above, a hierarchy of the various elements and regions of the structure can be established, determining the order in which they are allowed to enter the inelastic range during the seismic response. "Capacity design" is used, then, to ensure that this order is indeed respected. As we will see in more detail later in this section, "Capacity design" works as follows:

Once the elements or regions which are more important for the system, or more difficult to inspect/repair, or inherently less "ductile" are identified, "capacity design" determines their required force resistance on the basis of the available

force capacities of neighbouring elements or regions which have been ranked as less important, easier to inspect/repair, or inherently more "ductile". The required force resistances of the former elements or regions are determined, so that the latter ones exhaust their force resistances (i.e. yield) before the former and in a way that shields them from yielding. "Capacity design" is based on equilibrium alone, resembling in this respect the static method of plastic design, which gives a lower-bound type of solution.

1.3.2 The Importance of a Stiff and Strong Vertical Spine in a Building

In structures which have horizontal elements at various levels, forming "storeys" (as in multistorey buildings), the spreading of the inelastic deformation demands throughout the structure implies that inelastic action develops in every single storey. For this to be kinematically possible in a concrete building, the beam-column nodes along any column (or any vertical element, in general) should stay on the same line during the seismic response. This implies that vertical elements should:

- stay in the elastic range throughout their height, from the base to the roof, and
- rotate at the base, either by developing a plastic hinge just above the connection to the foundation system, or by rigid-body rotation of their individual foundation element with respect to the ground.

Under these conditions, large horizontal displacements of the storeys are kinematically possible only if plastic hinges form at both ends of every single horizontal member in the system. Such a pattern of plastic hinges and deformations corresponds to the widest possible spreading of the global displacement demand and energy dissipation throughout the entire structural system. It gives, therefore, the smallest possible local deformation and energy dissipation demand on individual members or locations.

In the building of Fig. 1.3(b)–(e) rotations take place at plastic hinges at both beam ends, as well as at plastic hinges at the base of the vertical elements (in Fig. 1.3(b) and (d)) or at the interface between the foundation element and the ground (in Fig. 1.3(c) and (e)). In all these cases, if the intended pattern of distributed plastic hinges forms simultaneously throughout the structure, the maximum chord rotation demand at beam ends or at the base of vertical elements[1] is about equal to the roof displacement, δ, divided by the total building height, H_{tot} (i.e. to the average drift ratio of the building, δ/H_{tot}). Moreover, the demand value of the chord rotation ductility factor at member ends (i.e. the peak chord rotation demand

[1]The chord rotation at a member end is the angle between the normal to the member section there and the chord connecting the two member ends, see Fig. 1.4. If a plastic hinge forms at an end, the plastic part of the chord rotation there is about equal to the plastic hinge rotation.

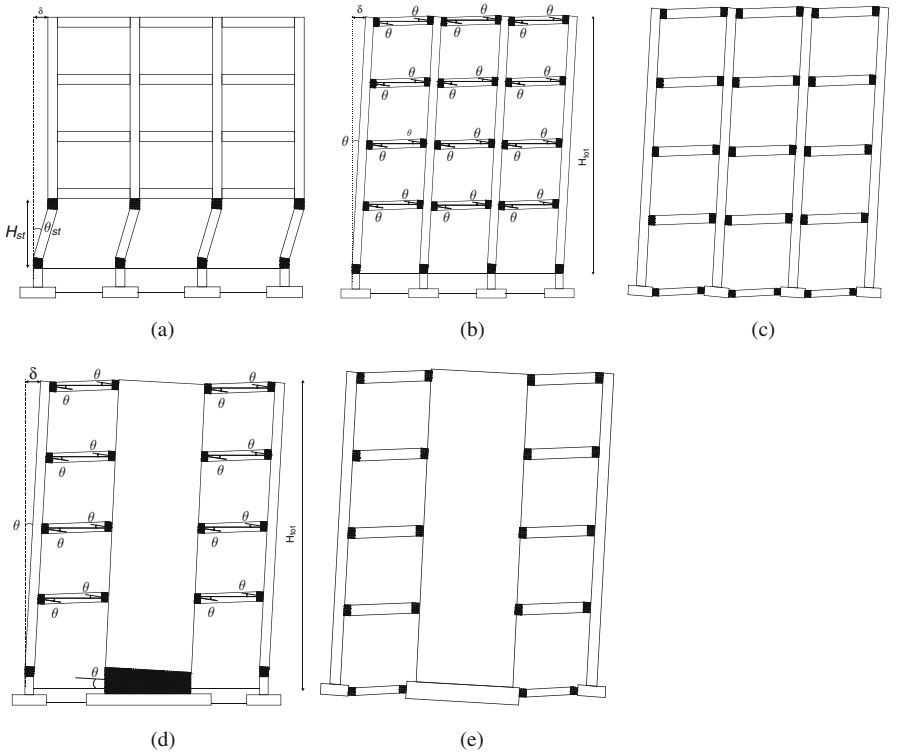

Fig. 1.3 Plastic mechanisms in frame and wall systems: (**a**) soft-storey mechanism in weak column/strong beam frame; (**b**), (**c**) beam-sway mechanisms in strong column/weak beam frame; (**d**), (**e**) beam-sway mechanisms in wall system

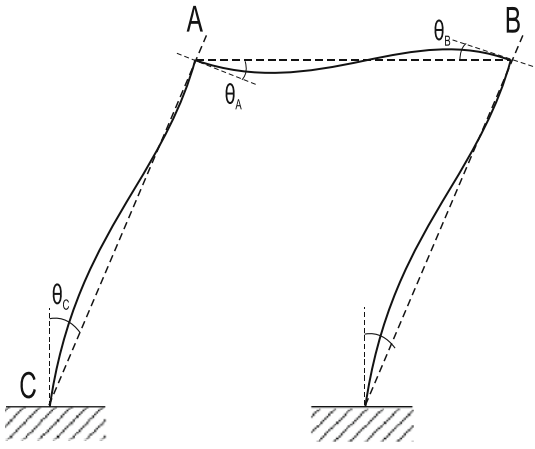

Fig. 1.4 Definition of chord rotation at member ends

during the response, divided by the chord rotation at that end at yielding of the element there) is roughly equal to the demand values of the top displacement ductility factor, μ_δ.[2] According to Eqs. (1.1) and (1.2), μ_δ is about equal to q and assumes relatively low values, well within the capacities of concrete members with appropriately detailed end regions. So, the seismic design of buildings that develop the "beam-sway" mechanisms of Fig. 1.3(b)–(e) is very cost-effective, in the sense that fairly high q-factor values can be relatively easily achieved.

The other extreme is shown in Fig. 1.3(a), where all inelastic deformations take place in a single storey. This is kinematically possible only if all vertical elements in the storey develop plastic hinges at both ends and in opposite bending (i.e. with the same sense of action of bending moments at the two ends). If such a "soft-storey" or "storey-sway" mechanism develops, the chord rotation demand at the ends of the vertical elements of the "soft-storey" are about equal to the roof displacement demand, δ, divided by the height of the soft-storey, h_i. For given value of δ such rotation demands are about equal to those developing in a "beam-sway" mechanism times H_{tot}/h_i. By the same token the chord rotation ductility ratio demand in the soft-storey columns is about equal to H_{tot}/h_i times the global displacement ductility factor, μ_δ, derived from the q-factor value used in the design according to Eqs. (1.1) and (1.2). The chord rotation capacities required to meet these demands in medium- or high-rise buildings with $H_{tot} >> h_i$ are not reliably attainable, even with special detailing for very high ductility and energy dissipation capacity. Therefore, it is not feasible to design and detail a building other than a low-rise one or for low-seismicity to develop a "soft-storey" or "storey-sway" mechanism of the type of Fig. 1.3(a).

The best way to spread the global inelastic deformation and energy dissipation demand to the entire structural system and prevent its concentration to a "soft-storey" is by providing a strong and stiff spine consisting of vertical elements that are forced by design to stay elastic above their base. This is achieved by overdesigning these vertical elements relative to the horizontal ones and/or to the internal force demands from the analysis, without any overdesign of the horizontal elements and of the region of the vertical elements at their connection to the foundation. Sections 1.3.4 and 1.3.5 describe how this is pursued through "capacity design" of the columns or walls, respectively.

So far the importance of strong vertical elements for spreading the total deformation and energy dissipation demand to the entire system has been emphasised. Capacity-designing the vertical elements to be strong enough to achieve this end is consistent with the concept of "capacity design" as enforcement of an inelastic response mechanism that does not entail plastic hinging in vertical elements, as these elements are:

---

[2] In reality plastic hinges form sequentially, starting at the lower part of the building and never extending throughout their full intended pattern. So the maximum chord rotation and chord rotation ductility factor at any member end will be about double the ideal values of δ/H_{tot} and μ_δ, respectively.

1. inherently less "ductile" than the beams, due to the adverse effect of axial compression on ductility;
2. more important than the beams, as far as stability and integrity of the whole is concerned.

Modern seismic design codes, such as Eurocode 8, promote development of beam-sway mechanisms in multi-storey buildings thanks to a stiff and strong vertical spine. This is pursued through:

– choices in the structural layout, and
– rules for the dimensioning of vertical members, so that they stay elastic above the base during the response.

More specifically for concrete buildings:

a) Wall systems (or wall-equivalent dual systems according to the definition in Eurocode 8 given in Section 1.4.3.1) are promoted and their walls are (capacity-) designed in flexure and shear to remain elastic above the base.
b) In frame systems and in frame-equivalent dual systems (see Section 1.4.3.1 for the definition of such systems in Eurocode 8) strong columns are directly promoted, through the capacity design of columns in flexure described in Section 1.3.4, so that plastic hinging in columns is prevented. Moreover, in codes that adopt a two-tier seismic design, such as Eurocode 8, strong columns are indirectly promoted by strict interstorey drift limits for the damage limitation seismic action. Unless the columns are large, frame systems cannot easily meet the interstorey drift limits of Eurocode 8 – especially as the cracked stiffness of concrete members is used in the analysis.

1.3.3 Overview of Capacity-Design-Based Seismic Design Procedure

In force-based seismic design using linear analysis with the q-factor, the general seismic design procedure for control of the inelastic response through capacity design is the following:

– Inherently ductile mechanisms of force transfer in "dissipative zones" are dimensioned so that their design resistance, R_d, and the design value of the corresponding action effect from the analysis for the combination of the design seismic action and the concurrent gravity actions, E_d, satisfy Eq. (1.3). In concrete buildings, this phase is normally limited to dimensioning of the end sections of beams in flexure and of the base section of vertical elements (at the connection to the foundation).
– Non-ductile mechanisms of force transfer within or outside the dissipative zones are dimensioned to remain elastic until and beyond yielding of the ductile mechanism(s) of the dissipative zones, through overdesign with respect to the

corresponding action effects from the analysis, E_d. This overdesign is normally accomplished through "capacity design", where the already dimensioned ductile mechanisms of force transfer are assumed to develop overstrength capacities, $\gamma_{Rd} R_d$, and the action effects in the non-ductile mechanisms of force transfer are computed from equilibrium alone.

- Dissipative zones are detailed to provide the deformation and ductility capacity that is consistent with the demands placed on them by the design of the structure for the chosen q-factor value.
- The foundation to the ground is capacity-designed on the basis of the overstrength of ductile mechanisms of force transfer in dissipative zones of the superstructure. Foundation elements are normally capacity-designed as well to stay elastic beyond yielding in dissipative zones of the superstructure. The designer may also use the option to dimension and detail them for energy dissipation and ductility as in the superstructure, despite the difficulty to repair them.

1.3.4 Capacity Design of Columns in Flexure

The objective of current seismic design codes is to force plastic hinges out of the columns of frame systems and into the beams, so that a beam-sway mechanism develops and a soft-storey is prevented. To this end, at beam-column nodes columns are (capacity-)designed to be stronger than the beams, with an overstrength factor of γ_{Rd} applied on the design values of the moment resistances of beams:

$$\Sigma M_{Rc} \geq \gamma_{Rd} \Sigma M_{Rb} \tag{1.4}$$

In Eq. (1.4) M_{Rc} or M_{Rb} denote the moment resistances of columns or beams, respectively. The summation at the left-hand-side extends over the column sections above and below the joint, while the one at the right-hand-side is over all beam ends framing into the joint (Fig. 1.5). Eurocode 8 adopts $\gamma_{Rd} = 1.3$ for the overstrength factor, while US codes (BSSC 2003, SEAOC 1999, ICBO 1997, ACI 2008) use $\gamma_{Rd} = 1.2$.

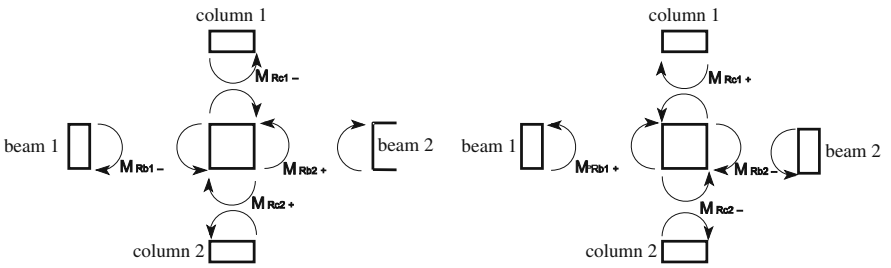

Fig. 1.5 Beam and column moment resistances at a joint, for the implementation of the "Capacity-Design" rule, Eq. (1.4)

Equation (1.4) is verified separately in each one of the two main horizontal directions of the building in plan. For a beam framing into a joint at an angle α to the horizontal direction in which Eq. (1.4) is checked, its M_{Rb}-value enters Eq. (1.4) multiplied times $\cos\alpha$. Equation (1.4) is checked in each horizontal direction, first with both column moment resistances acting on the joint in the positive (clockwise) sense about the normal to that horizontal direction (the direction of the frame) and then in the negative (counterclockwise) sense. Beam moment resistances are always taken to act on the joint in the opposite sense with respect to the column capacities (Fig. 1.5).

Equation (1.4) should normally be checked at the centre of the joint (at the theoretical node at the intersection of the beam and column centrelines), because equilibrium of moments on the joint refers to that point. This would entail transferring the moment resistances from the faces of the joint to the theoretical node: by multiplying the sum of the column moment resistances times $(1 + h_{\mathrm{b}}/H_{\mathrm{cl}})$ and that of the beams times $(1 + h_{\mathrm{c}}/L_{\mathrm{cl}})$, where h_{b}, h_{c} denote the cross-sectional depth of the beam and the column, respectively, in the vertical plane within which Eq. (1.4) is checked, and L_{cl}, H_{cl} are the average clear span of the beams on either side of the joint, or the average clear storey height above and below the joint, respectively. Both Eurocode 8 and the US codes allow using instead in Eq. (1.4) as M_{Rc} and M_{Rb} the moment resistance of the columns and the beams at the face of the joint, respectively. This simplification is normally on the safe side, because in general we have $h_{\mathrm{b}}/H_{\mathrm{cl}} \geq h_{\mathrm{c}}/L_{\mathrm{cl}}$.

US codes require that the nominal values of M_{Rb} and M_{Rc} (those resulting from the characteristic or nominal values of material strengths, f_{ck}, f_{yk}, instead of the design values, f_{cd}, f_{yd}) be used in Eq. (1.4). For simplification, Eurocode 8 allows using instead the design values of the member moment resistances, $M_{\mathrm{Rd,b}}$ and $M_{\mathrm{Rd,c}}$ for M_{Rb} and M_{Rc}, respectively. Note that, if the values of material partial factors, γ_{M}, applicable for non-seismic actions are adopted also for seismic design (option 1 in Section 1.2), the difference between M_{Rd} and the value of M_{R} for nominal material strengths is larger in the columns than for beams. So, compared to the use of M_{Rc} and M_{Rb} for nominal strengths on both sides of Eq. (1.4), the Eurocode 8 approach gives more safe-sided results for the columns (however, less so than the US approach).

With these differences and the higher value of γ_{Rd} (1.3 versus 1.2), the application of Eq. (1.4) in Eurocode 8 seems to be more safe-sided than in US codes. However, this difference may be overshadowed by how the code accounts for the contribution of slab bars parallel to the beam to the value of M_{Rb} in negative (hogging) bending. There is ample experimental and field evidence that, when the beam is driven past flexural yielding in negative bending and into strain hardening, such reinforcing bars in the slab are fully activated as tension reinforcement of the beam, even when they are at a significant distance from the web. For T-beams (ACI 2008) specifies the total width of the slab effective in tension as 25% of the span, but not larger than 16 times the slab thickness, h_{f}, plus the web width. For L-beams (ACI 2008) considers that the width of the slab beyond the web which is effective in tension is one-twelfth of the span, but not more than $6h_{\mathrm{f}}$. Eurocode 8 specifies

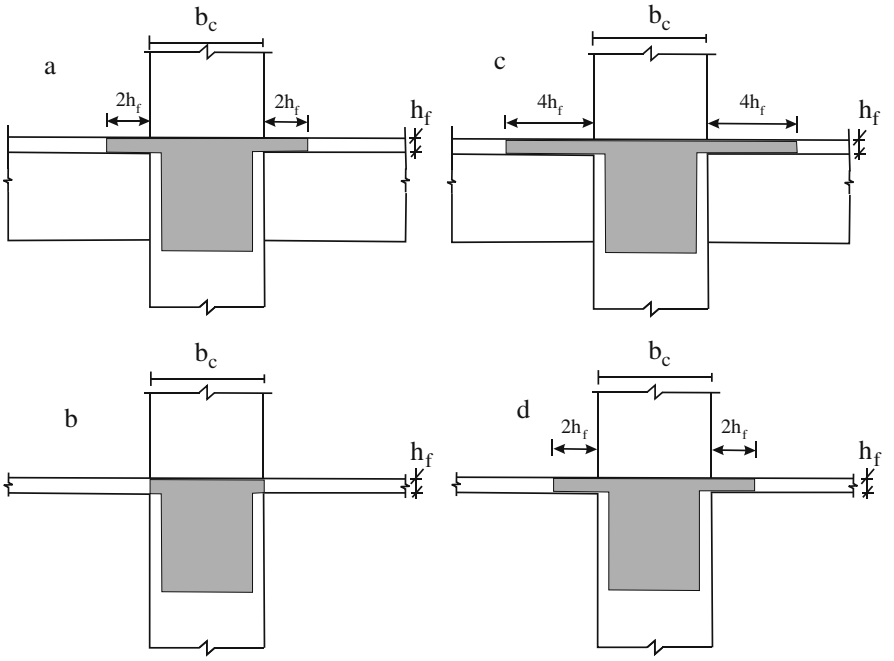

Fig. 1.6 Width of the slab effective as tension flange of beams at the support on a column, according to Eurocode 8 (**a**, **b**: at exterior column; **c**, **d**: at interior column)

as effective in tension a much smaller slab width from the side of the column into which the beam frames, as shown in Fig. 1.6:

- at joints with interior columns within the plane of the frame where Eq. (1.4) is checked:
  - $4h_f$, if a transverse beam of similar size frames into the joint on the side in question, or
  - $2h_f$, if there is no such transverse beam;
- at the two exterior columns within the plane of the frame where Eq. (1.4) is checked:
  - $2h_f$, if a transverse beam of similar size frames into the joint on the side in question, or
  - zero, if there is no such transverse beam.

These effective slab widths are specified in Eurocode 8 for the ULS dimensioning of beams at the supports to columns against the negative (hogging) bending moment from the analysis for the design seismic action combined with the concurrent gravity loads. Slab bars which are parallel to the beam and well anchored within the joint or beyond may count as top beam reinforcement, to reduce the tension reinforcement to be placed within the width of the web. In that context, the effective in tension

width of the slab on each side of the web has been chosen in Eurocode 8 lower than the values of about 25% of the beam span suggested by field and experimental evidence, to be safe-sided for the dimensioning of beam top bars. However, this leads to underestimation of $M_{\mathrm{Rd,b}}$ for negative bending and hence is on the unsafe side as far as prevention of column hinging through fulfillment of Eq. (1.4) is concerned (see e.g., (Panagiotakos and Fardis 1998)).

Yielding in opposite bending and plastic hinging at both the top and bottom sections of a concrete wall in a storey is extremely unlikely, even for walls with minimum dimensions (e.g. just 0.2 m by 0.8 m). So, when walls provide most of the lateral force resistance (i.e., in wall systems and in wall-equivalent dual systems according to the Eurocode 8 classification of systems, see Section 1.4.3.1) in a horizontal direction of the building, they can normally be trusted for the prevention of a soft-storey mechanism in that direction. So, Eurocode 8 exempts the columns of wall systems or wall-equivalent dual systems from fulfilling Eq. (1.4) in that horizontal direction. Besides, Eurocode 8 does not require meeting Eq. (1.4) in the following cases of columns of frame systems or of frame-equivalent dual systems (see Section 1.4.3.1 for the definition of these systems):

- Around the joints of the top floor. As a matter of fact, it does not make any difference for the plastic mechanism whether the plastic hinge forms at the top of the top storey column or at the ends of the top floor beams. Moreover, columns of the top floor have low axial load, hence good ductility, and are less critical for the stability of the whole than the columns of lower floors. After all, it is difficult to satisfy Eq. (1.4) there, as only one column contributes to the left-hand-side.
- In two-storey buildings, provided that in none of the ground storey columns the axial load in any of the combinations of the design seismic action with the simultaneous gravity loads exceeds 30% of the cross-sectional area times the design value of the concrete compressive strength, f_{cd}. Columns with such a low axial load ratio have good ductility and develop low 2nd-order (P-Δ) effects. So, if a soft-storey mechanism develops at the ground storey of a two-storey building these columns can withstand a displacement ductility demand of about twice the displacement ductility factor, μ_δ, corresponding to the value of q used in design.
- One-out-of-four columns of plane frames with columns of similar size. The designer may choose to skip fulfilment of Eq. (1.4) at an interior column rather than at an exterior one, as only one beam frames into exterior joints and it is easier to satisfy Eq. (1.4) there.

At all column ends where Eq. (1.4) is not checked owing to the exemptions above (including the columns of wall systems or wall-equivalent dual ones), as well as at the base of columns where a plastic hinge will form anyway, the Eurocode 8 detailing rules provide a column ductility supply sufficient for development of a plastic hinge there.

US standards require meeting Eq. (1.4) at every column of frames of the high ductility class, termed “Special Moment Frames”. If Eq. (1.4) is not satisfied at a single level of a column of such a frame, the contribution of that column to the frame’s lateral strength and stiffness is neglected and the column is dimensioned

for gravity loads alone. However, all the requirements for minimum longitudinal and transverse reinforcement of "Special Moment Frames" should be fulfilled all along that column, to sustain the ductility demands imposed on the column by the lateral-force-resisting system, whose lateral displacements it shares.

Fulfillment of Eq. (1.4) just ensures that the column cross-sections above and below the joint will not yield at the same time under uniaxial bending moments having the same sense of action on the joint. Note that, as vertical reinforcement of a column continues into the storey above and covers the column sections both above and below the joint, these sections have about the same moment resistance if they have the same size. Then $M_{\mathrm{Rc}} \approx 0.5\gamma_{\mathrm{Rd}}\Sigma M_{\mathrm{Rb}}$. However, the bending moments that develop above and below the joint during the dynamic response, may have quite different magnitude $M_{\mathrm{E1}} \neq M_{\mathrm{E2}}$. Therefore, the largest of them, e.g. M_{E1}, may possibly reach the corresponding moment resistance, $M_{\mathrm{Rc1}} \approx 0.5\gamma_{\mathrm{Rd}}\Sigma M_{\mathrm{Rb}}$, and cause column yielding. If this happens simultaneously at both top and bottom of all columns in a storey, then a "soft-storey" may develop there momentarily. If Eq. (1.4) is fulfilled, this event will be of very short duration. Although this possibility cannot be ruled out, the inelastic deformations it induces to the storey columns will not be of such magnitude to jeopardise the stability of the whole (Panagiotakos and Fardis 1998).

In closing this general presentation of capacity design of columns in flexure, it is worth noting, again, that Eq. (1.4) is based on equilibrium and the "static method" of plastic design. The relative stiffness of members is not considered, although its impact on the effectiveness of Eq. (1.4) may sometimes be important. More specifically, as the effective stiffness of concrete members is roughly proportional to their moment resistance, columns whose strength is increased relative to the beams to satisfy Eq. (1.4) in all likelihood will also be stiffer than the beams. They will tend to behave then more as vertical cantilevers – i.e. as walls – rather than as columns of a frame. Wall-like columns may develop bending moments with the same sign (i.e. opposite sense of action on the joint) above and below a joint (cf. the bending moment of diagram typical of walls in Fig. 1.7). Then one of the column sections above or below the joint works with the beams against the other section (instead of with it, against the beams) and might force it to yield. Even in such an unlikely event, a "soft-storey" will not develop, because it requires simultaneous yielding at the top and bottom of the vertical elements of the same storey, which is not physically possible if the bending moment diagram has the same sign within the storey, as in Fig. 1.7. Therefore, although the collateral effects of Eq. (1.4) on member stiffness may render Eq. (1.4) meaningless, the end result is the same: no soft-storey can physically develop.

1.3.5 Design of Ductile Walls in Flexure

What essentially distinguishes walls from columns is that walls have much larger stiffness than the beams they may be connected to. As a result, the beams work with the walls mainly as part of the horizontal diaphragms transferring lateral forces to

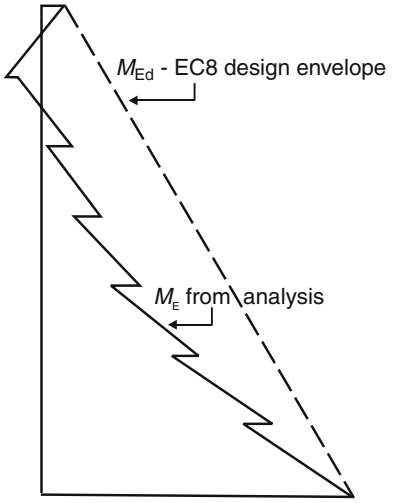

Fig. 1.7 Typical bending moment diagram in a ductile RC wall from the analysis and linear envelope for its design according to Eurocode 8

the walls, rather than as horizontal elements of a frame. Therefore bending moment diagrams that develop during the seismic response in the walls resemble that of a vertical cantilever under horizontal loading (see Fig. 1.7). Notably, the sign of bending moment does not change within a storey (with the possible exception of one or more storeys near the top), while moments decrease considerably from the base to the top of the wall (much more than shear forces do). Moreover, the bending moment at the wall section right above a floor level is normally larger than just below it. As these two sections are crossed by the same vertical bars and an increase in axial compression increases the wall moment resistance, a plastic hinge can conceivably form only at one of these two sections, namely above the floor level. Multiple plastic hinging along the height of the wall may well develop, if the flexural resistance of wall sections at floor levels and at the base (i.e. at the connection to the foundation) are tailored to the elastic seismic moment demands. Even then, a soft-storey mechanism cannot form, as it requires plastic hinging in opposite bending at two different locations along the height of the wall.

To ensure that a wall works as a strong and stiff vertical spine, mobilising all beams into inelastic action and minimising local rotation and ductility demands for given global displacement demand, Eurocode 8 takes measures to localise wall inelastic deformations at its base. A so-designed wall is called “ductile wall”. It is designed and detailed to dissipate energy in a flexural plastic hinge only at the base and remain elastic throughout the rest of its height, in order to promote – or even enforce – a beam-sway mechanism. For a flexural plastic hinge with high ductility and dissipation capacity to develop at its base, a “ductile wall” should be fixed there to prevent relative rotation of the base with respect to the rest of the structural system. Besides, just above its base a ductile wall should be free of openings or large perforations that might jeopardise the ductility of the plastic hinge. To force

the wall to stay elastic above the plastic hinge region, Eurocode 8 (but not US standards) requires dimensioning in bending of the rest of the wall height for a linear envelope of the positive and negative wall moments from the analysis for the design seismic action (Fig. 1.7). The envelope intends to cover also a potential increase in bending moments above the base due to higher mode inelastic response after development of the plastic hinge at the base. The rest of the wall does not need to be detailed for high flexural ductility and the design of the wall may be simpler and possibly more economical. Moreover, the rest of the wall above the plastic hinge at the base may be dimensioned in shear disregarding the degradation of cyclic shear resistance in regions that have already yielded in flexure (cf. Section 3.2.4).

US standards (BSSC 2003, SEAOC 1999, ICBO 1997, ACI 2008) do not require designing a wall above the base for flexural overstrength with respect to the demands from the analysis. They rely only on the wall large stiffness and on the fulfilment of Eq. (1.4) by the columns of the system for the prevention of a soft-storey mechanism.

Section 5.6 describes an alternative to "ductile walls", termed "(systems of) large lightly reinforced walls", provided by Eurocode 8 alone among all international seismic design codes. In them flexural overstrength over the seismic demands of the analysis is intentionally avoided anywhere along the height of the wall. This promotes development of plastic hinges in the wall at as many floor levels above the base as physically possible. In this way a given global displacement demand is spread to rotation demands at several locations up the height of the wall. The inelastic deformation demands that need to be resisted by a single location, e.g., at the wall base, are then reduced, facilitating therefore detailing of that location for ductility.

1.3.6 Capacity Design of Members Against Pre-emptive Shear Failure

1.3.6.1 The Principle

Among the two constituents materials of RC members, reinforcing steel is inherently ductile – and as a matter of fact only in tension, as bars in compression may buckle, shedding their compressive force and risking fracture. Concrete is brittle, unless its lateral expansion is well restrained by confinement.

Flexure is the only mechanism of force transfer that allows using to advantage and reliably the fundamental ductility of tension reinforcement and effectively enhancing the ductility of concrete and of the compression steel through lateral restraint. Even under cyclic loading, flexure creates stresses and strains in a single and well-defined direction (parallel to the member axis) and therefore lends itself to the effective use of the reinforcing bars, both to take up directly the tension, as well as to restrain concrete and compression steel (against buckling) transverse to their compressive stresses.

An inelastic stress field dominated by shear is two-dimensional. It induces principal stresses and strains in any inclined direction (especially for cyclic loading)

and does not lend itself to effective inelastic action in the reinforcement for the control of the extent of cracking (which, if not effectively controlled, may extend into the compression zone and completely destroy it) and for confinement of concrete. Moreover, after tensile yielding of the transverse bars shear deformations are associated with slippage along wide-open inclined cracks and dissipate very little energy. Last but not least, large reversals of the shear force may accumulate inelastic strains in the same transverse bars crossing both sets of diagonal cracks, leading to uncontrolled crack opening. So, unlike steel members where shear is a ductile force transfer mechanism (as the ductility of steel is always available along the rotating direction of principal strains), in concrete shear is considered brittle and is constrained by design in the elastic range of behaviour. Energy dissipation and cyclic ductility is entrusted only to flexure, in the "plastic hinges" that develop at member ends where seismic bending moments attain their maximum values. The plastic hinge regions are then detailed for the inelastic deformation demands expected to develop there under the design seismic action.

In concrete members the mechanisms of force transfer by shear or by flexure act in series, as both of them have to transfer the same force and ultimate strength is controlled by the weakest of the two mechanisms. So, the shear force transfer mechanism can be constrained to the elastic range through "capacity design". Namely, by dimensioning a concrete member in shear not for the force demand from the analysis but for the maximum shear force that may physically develop in it, as controlled by attainment of the force resistance in flexure. The maximum value of the shear force is computed by:

- expressing (through equilibrium) the shear force in terms of the bending moments at the nearest sections where plastic hinges may form, and
- setting these bending moments equal to the corresponding moment resistances.

Because the bending moment in a plastic hinge cannot physically exceed its moment capacity – including the effect of strain hardening – the so-computed shear force is the maximum possible. Once dimensioned for this design force, a member will remain elastic in shear until and after development of plastic hinges at the sections that affect the value of the shear force.

1.3.6.2 Capacity Design Shear of Beams

The basic concept behind capacity design of beams is presented with reference to Fig. 1.8. If the sense of internal forces at beam ends in that figure is considered as positive, equilibrium of moments about one end gives the value of the moment at the other end:

$$V_1 = V_{g+\psi q,1} + \frac{M_2 + M_1}{L_{cl}} \tag{1.5}$$

$$V_2 = V_{g+\psi q,2} - \frac{M_1 + M_2}{L_{cl}} \tag{1.6}$$

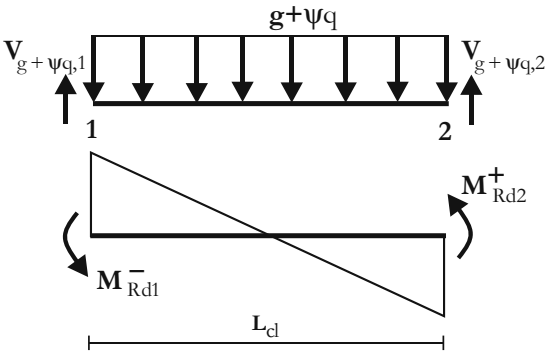

Fig. 1.8 Equilibrium of forces and moments on a beam

where $V_{g+\psi q,1}$ and $V_{g+\psi q,2}$ are moments of the transverse load acting between the two ends with respect to 2 or 1, respectively, divided by the clear span of the beam, L_{cl} (i.e., they are the reactions to this load when the beam is simply supported).

The maximum value of V_1 develops when the sum $M_2 + M_1$ is maximum, i.e. when both M_1 and M_2 attain their maximum possible positive value. When M_2 and M_1 attain their absolutely maximum possible negative values V_2 reaches its maximum possible value.

If the beam frames at both ends into stronger columns that satisfy there Eq. (1.4) with $\gamma_{Rd} = 1$ the maximum possible positive values of M_1 and M_2 are equal to the corresponding moment resistances. For convenience, these capacities may be taken equal to their design values, M_{Rd}, times an overstrength factor, $\gamma_{Rd} \geq 1.0$. Accordingly, in Eq. (1.5) we may take $M_2 = \gamma_{Rd} M^{+}_{Rd,b2}$, $M_1 = \gamma_{Rd} M^{-}_{Rd,b1}$, while in Eq. (1.6) we have $M_1 = -\gamma_{Rd} M^{+}_{Rd,b1}$, $M_2 = -\gamma_{Rd} M^{-}_{Rd,b2}$. This gives finally the maximum possible ("capacity design") shear forces at the two ends:

$$V_{CD,1} = V_{g+\psi q,1} + \gamma_{Rd} \frac{M^{-}_{Rd,b1} + M^{+}_{Rd,b2}}{l_{cl}} \tag{1.7}$$

$$V_{CD,2} = V_{g+\psi q,2} + \gamma_{Rd} \frac{M^{+}_{Rd,b1} + M^{-}_{Rd,b2}}{l_{cl}} \tag{1.8}$$

Strong beams framing into weak columns (i.e. not satisfying Eq. (1.4) with $\gamma_{Rd} = 1$) are unlikely to develop first plastic hinges at the ends, before the columns do. Assuming that at end i (= 1 or 2) of the beam in question the beam moment is negative and the sum of beam design moment resistances around the joint exceeds that of the columns in the sense associated with negative beam moment at that end (i.e. if $(\Sigma M_{Rd,b})_{i-} > (\Sigma M_{Rd,c})_{i-}$, where subscripts denote the end of the beam and the sign of beam moment there), $M^{-}_{Rd,bi}$ in Eq. (1.6) should be replaced with the beam moment at hinging of the column both above and below the joint at end i . Assuming that the moment input from the yielding columns to the elastic beams is shared by the two beams framing into the joint in proportion to their own moment

resistance, the beam moment at end i at the time the columns yield can be assumed equal to the design value of the moment resistance of the beam at that end, $M^{-}_{\mathrm{Rd,bi}}$, times $[\Sigma M_{\mathrm{Rd,c}}/\Sigma M_{\mathrm{Rd,b}}]_{\mathrm{i}}$, where $\Sigma M_{\mathrm{Rd,b}}$ refers to the sections of the beam across the joint at end i and $\Sigma M_{\mathrm{Rd,c}}$ to those of the column above and below it. Similarly for the positive sense of bending of the beam at end i. So, a rational generalisation of Eqs. (1.7) and (1.8) for the design value of the maximum shear at a section x in the part of the beam closer to end i is (see Fig. 1.9):

$$\max V_{i,d}(x) = \frac{\gamma_{Rd}\left[M^{-}_{Rd,bi}\min\left(1;\dfrac{\Sigma M_{Rd,c}}{\Sigma M_{Rd,b}}\right)_i + M^{+}_{Rd,bj}\min\left(1;\dfrac{\Sigma M_{Rd,c}}{\Sigma M_{Rd,b}}\right)_j\right]}{L_{cl}} + V_{g+\psi q,o}(x) \tag{1.9a}$$

In Eq. (1.9a) j denotes the other end of the beam (i.e. if $i = 1$, then $j = 2$). All moments and shears in Eq. (1.9a) have positive sign. The sense of action of $(\Sigma M_{\mathrm{Rd,b}})_{\mathrm{i}}$ on the joint is the same as that of $M_{\mathrm{Rd,bi}}$, while that of $(\Sigma M_{\mathrm{Rd,c}})_{\mathrm{i}}$ is opposite. $V_{\mathrm{g}+\psi\mathrm{q,o}}(x)$ is the shear force at cross-section x due to the quasi-permanent gravity loads, $g + \psi q$, concurrent with the design seismic action, with the beam considered as simply supported (index: o). The value of $V_{\mathrm{g}+\psi\mathrm{q,o}}(x)$ may be conveniently computed (especially if the loads $g + \psi q$ are not uniformly distributed along the length of the beam) from the results of the analysis of the structure for the gravity load $g + \psi q$ alone: $V_{\mathrm{g}+\psi\mathrm{q,o}}(x)$ may be taken equal to the shear force $V_{\mathrm{g}+\psi\mathrm{q}}(x)$ at cross-section x in the full structure, corrected for the shear force $(M_{\mathrm{g}+\psi\mathrm{q},1} - M_{\mathrm{g}+\psi\mathrm{q},2})/L_{\mathrm{cl}}$ due to the bending moments $M_{\mathrm{g}+\psi\mathrm{q},1}$ and $M_{\mathrm{g}+\psi\mathrm{q},2}$ at the end sections 1 and 2 of the beam in the full structure.

Eurocode 8 adopts Eq. (1.9a) for the capacity design shear of beams, with factor γ_{Rd} accounting for possible overstrength due to steel strain hardening and taken equal to $\gamma_{\mathrm{Rd}} = 1.2$ for beams of Ductility Class High and to $\gamma_{\mathrm{Rd}} = 1$ for those of Ductility Class Medium (see Section 1.4.2.1 for the definition of these Ductility

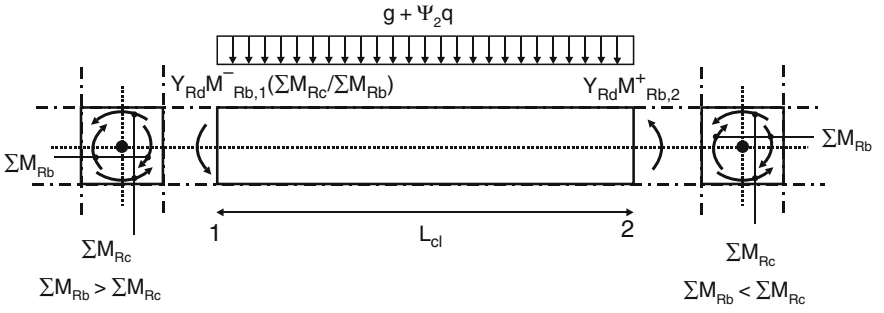

Fig. 1.9 Derivation of the capacity-design shear force in beams according to Eurocode 8

Classes). US codes (BSSC 2003, SEAOC 1999, ICBO 1997, ACI 2008) discount the possibility of column hinging and compute the first term of Eq. (1.9a) with the terms min(...) taken equal to 1.0. They use $\gamma_{\mathrm{Rd}} = 1/0.9 = 1.11$ for the beams of "Intermediate Moment Frames" and $\gamma_{\mathrm{Rd}} = 1.25/0.9 = 1.39$ for those of "Special Moment Frames". For "Intermediate Moment Frames" they allow capping the 1st term in Eq. (1.9a) at twice the shear force at x due to the design seismic action from linear analysis, $V_{\mathrm{E}}(\mathrm{x})$.

With $V_{\mathrm{g}+\psi\mathrm{q,o}}(x)$ taken positive at sections x in the part of the beam closer to end i, the minimum shear in that section is:

$$\min V_{i,d}(x) = -\frac{\gamma_{Rd}\left[M^{+}_{Rd,bi}\min\left(1;\frac{\Sigma M_{Rd,c}}{\Sigma M_{Rd,b}}\right)_i + M^{-}_{Rd,bj}\min\left(1;\frac{\Sigma M_{Rd,c}}{\Sigma M_{Rd,b}}\right)_j\right]}{L_{cl}} + V_{g+\psi q,o}(x) \tag{1.9b}$$

The moments and shears at the right-hand-side of Eq. (1.9b) being positive, its outcome may be positive or negative. If it is positive, the shear at section x will not change sense of action at any time during the seismic response. If it is negative, the shear force does change sense. As described in Section 5.5.2, the ratio:

$$\zeta_i = \frac{\min V_{\mathrm{i,d}}(x_i)}{\max V_{\mathrm{i,d}}(x_i)} \tag{1.10}$$

is used by Eurocode 8 as a measure of the reversal of the shear force at end i, for the dimensioning of the shear reinforcement of beams in buildings of the High Ductility Class (similarly at end j).

The values of $\Sigma M_{\mathrm{Rd,ci}}$ and $\Sigma M_{\mathrm{Rd,cj}}$ to be used in Eqs. (1.9) should be the ones giving the largest absolute value of the capacity design shear in Eq. (1.9a) and the algebraically minimum value of the ζ-ratio in Eq. (1.10). These are the maximum values of $\Sigma M_{\mathrm{Rd,ci}}$ and $\Sigma M_{\mathrm{Rd,cj}}$ within the range of fluctuation of the column axial load from the analysis for the combination of quasi-permanent gravity loads and of the design seismic action. More detailed guidance is given in Section 5.7.3.5.

A positive plastic hinge may develop not at end j of the beam but elsewhere along its span, namely at the point where the available moment resistance in positive bending is first exhausted by the demand seismic moment under the combination of (a) the quasi-permanent gravity loads, $g + \psi q$, and (b) the seismic action that causes beam or column yielding – whichever occurs first – around the joint at end i of the beam. Although the distance between these two likely plastic hinge locations is less than the clear span L_{cl} of the beam, a lower shear force will normally result then near end i of the beam than the value from Eq. (1.9a).

1.3.6.3 Capacity-Design Shear of Columns

The simplest way to derive the capacity design shear of a column is to assume that its ends, 1 and 2, both develop plastic hinges in opposite bending (+ or –) and compute the resulting shear force from equilibrium. Normally no intermediate transverse loads act on columns. So, the capacity design shear is constant throughout the column height and equal to:

$$V_{CD}^{-} = \gamma_{Rd} \frac{M_{Rd,c1}^{-} + M_{Rd,c2}^{+}}{H_{cl}} \tag{1.11a}$$

$$V_{CD}^{+} = \gamma_{Rd} \frac{M_{Rd,c1}^{+} + M_{Rd,c2}^{-}}{H_{cl}} \tag{1.11b}$$

Factor γ_{Rd} in Eqs. (1.11) accounts again for possible overstrength due to steel strain hardening; H_{cl} is the clear height of the column within the plane of bending (in general equal to the distance between the top of the beam or slab at the base of the column and the soffit of the beam at the top).

Normally the column shear capacity is independent of the direction of the shear force. Then only the maximum of the shear forces V_{CD}^{-} and V_{CD}^{+} in Eqs. (1.11) matters. Moreover, usually the column cross-section is symmetric and $M_{\mathrm{Rd,ci}}^{+}$ and $M_{\mathrm{Rd,ci}}^{-}$ at end i (= 1, 2) are equal. Then Eqs. (1.11a) and (1.11b) give the same outcome.

As shown in Fig. 1.10, a column may not develop plastic hinges at end i ($i = 1$, 2), if plastic hinges develop there first in the beams framing into the same joint at end i (as is normally the case in columns fulfilling Eq. (1.4)). If that happens, the sum of column moments above and below the joint is equal to the total moment resistance of the beam across that joint, $\Sigma M_{\mathrm{Rd,b}}$. It may be assumed that this sum is shared by the two column sections above and below the joint in proportion to their own moment resistance. Then, the bending moment at end section i ($i = 1$, 2) of the column may be taken equal to the design value of the moment resistance of the column at that end, $M_{\mathrm{Rd,ci}}$, times $(\Sigma M_{\mathrm{Rd,b}}/\Sigma M_{\mathrm{Rd,c}})_{\mathrm{i}}$, where $\Sigma M_{\mathrm{Rd,b}}$ refers to the sections of the beam on opposite sides of the joint at end i and $\Sigma M_{\mathrm{Rd,c}}$ to the sections of the column above and below it. The sense of action of $\Sigma M_{\mathrm{Rd,c}}$ on the joint is the same as that of $M_{\mathrm{Rd,ci}}$, while that of $\Sigma M_{\mathrm{Rd,b}}$ is opposite. So, a rational generalisation of Eqs. (1.11) for the design value of the maximum shear of the column is:

$$V_{CD,c} = \frac{\gamma_{Rd}\left[M_{Rd,c1}\min\left(1;\left.\frac{\Sigma M_{Rd,b}}{\Sigma M_{Rd,c}}\right)_1\right. + M_{Rd,c2}\min\left(1;\left.\frac{\Sigma M_{Rd,b}}{\Sigma M_{Rd,c}}\right)_2\right.\right]}{H_{cl}} \tag{1.12}$$

Equation (1.12) is the form of capacity design shear of columns adopted in Eurocode 8, with factor γ_{Rd} taken equal to $\gamma_{\mathrm{Rd}} = 1.3$ for columns of buildings of Ductility Class High and to $\gamma_{\mathrm{Rd}} = 1.1$ for those of Ductility Class Medium (see Section 1.4.2.1 for the definition of these Ductility Classes).

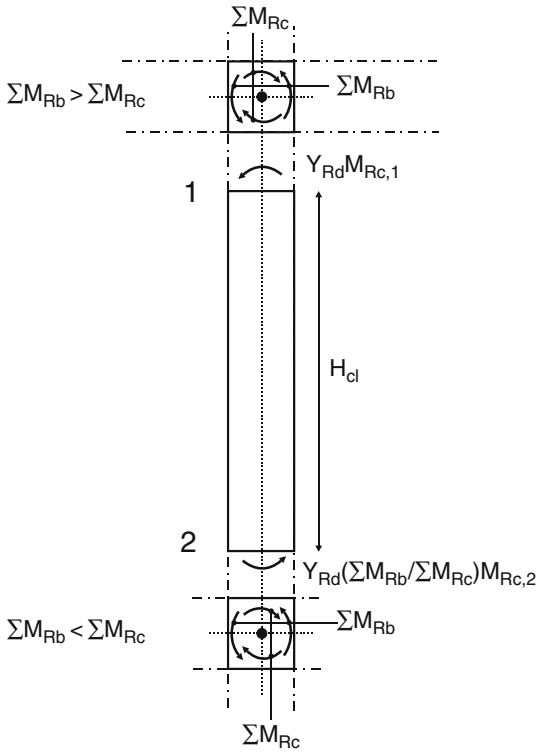

Fig. 1.10 Derivation of the capacity-design shear force in columns according to Eurocode 8

ACI (2008) adopts a format similar to Eq. (1.12) for columns of "Special Moment Frames":

$$V_{CD} = \gamma_{Rd} \frac{\left[\min(M_{Rd,c};\ \frac{\min(\Sigma M_{Rd,c},\ \Sigma M_{Rd,b})}{\Sigma\,|M_{Ec}|}|M_{Ec}|\right]_1 + \left[\min(M_{Rd,c};\ \frac{\min(\Sigma M_{Rd,c},\ \Sigma M_{Rd,b})}{\Sigma\,|M_{Ec}|}|M_{Ec}|\right]_2}{H_{cl}} \tag{1.13}$$

In Eq. (1.13) the moment input from the yielding elements around the joint at end i (= 1, 2) is shared by the two columns framing into that joint in proportion to their end moments from the analysis for the design seismic action, M_{Ec}; factor γ_{Rd} is taken equal to $\gamma_{\mathrm{Rd}} = 1.25/0.7 = 1.79$. For the columns of "Intermediate Moment RC Frames" (ACI 2008) does not take into account the possibility of beam hinging and uses the simpler version, Eqs. (1.11) with $\gamma_{\mathrm{Rd}} = 1/0.7 = 1.43$. It also caps the value of the capacity design shear to twice the shear force due to the design seismic action from linear analysis, V_{E}.

The values of $M_{\mathrm{Rd,c1}}$ and $M_{\mathrm{Rd,c2}}$ to be used in Eqs. (1.11), (1.12) and (1.13) should be the most adverse ones within the range of fluctuation of the column axial force under the combination of quasi-permanent gravity loads and the design seismic action. If the dependence of the column shear capacity on axial force is taken into account (in fact shear capacity increases with increasing axial compression), more than one possible axial force values should be considered for the calculation of $M_{\mathrm{Rd,ci}}$ ($i = 1, 2$) in Eqs. (1.11), (1.12) and (1.13), in search of the most critical condition for the shear verification of the column and the dimensioning of its transverse reinforcement. If the shear capacity of the column is taken independent of its axial force, then the values of $M_{\mathrm{Rd,c1}}$ and $M_{\mathrm{Rd,c2}}$ should be the maximum ones within the range of fluctuation of the column axial load from the analysis for the combination of the design seismic action and the concurrent gravity loads. More detailed guidance is provided in Section 5.7.3.5.

1.3.6.4 Capacity-Design Shear of "Ductile Walls"

US standards do not require designing walls for overstrength in shear relative to the demands from the analysis or over the seismic action that induces plastic hinging. In Eurocode 8, by contrast, "ductile walls" are designed to develop a plastic hinge only at the base section and to stay elastic throughout the rest of their height. The value of the moment resistance at the base section of the wall, M_{Rdo}, and equilibrium alone are not sufficient for the derivation of the maximum seismic shears that can develop at various levels of the wall. The reason is that, unlike in the members of Figs. 1.8, 1.9 and 1.10, the (horizontal) forces applied on the wall from the floors are not constant but change during the seismic response. In the face of this difficulty, a first assumption made is that, if M_{Rdo} exceeds the bending moment at the base from the elastic analysis for the design seismic action, M_{Edo}, seismic shears at any level of the wall exceed those from the same elastic analysis in proportion to ($M_{\mathrm{Rdo}}/M_{\mathrm{Edo}}$). So, the shear force from the elastic analysis for the design seismic action, V'_{Ed}, should be multiplied by a capacity-design magnification factor ε proportional to $M_{\mathrm{Rdo}}/M_{\mathrm{Edo}}$.

$$\varepsilon = \frac{V_{Ed}}{V'_{Ed}} = \gamma_{Rd}\left(\frac{M_{Rdo}}{M_{Edo}}\right) \leq q \tag{1.14}$$

Factor γ_{Rd} in Eq. (1.14) is meant to capture the overstrength at the base over the design value of the moment resistance there, M_{Rdo}, e.g. owing to strain hardening of the vertical steel.

Section 1.3.5, dealing with flexural design of ductile walls, has already mentioned the possibility of higher mode response after formation of a plastic hinge at the base, i.e., of the response of a structure with little rotational restraint at plastic hinges that have already formed and are loading along the ascending post-yield branch of their moment-rotation relation. This response may increase also the wall shear forces at the base and higher up, to values well beyond those corresponding to plastic hinging at the base according to the predictions of elastic analysis.

The taller and more slender the wall, the more pronounced are such effects, being almost absent in "squat" walls.

To cover both capacity design in shear, expressed by Eq. (1.14), as well as any inelastic higher mode effects, Eurocode 8 has adopted the following expression for walls with ratio of height to horizontal dimension, $h_w/l_w > 2$ ("slender" walls) of Ductility Class High:

$$\varepsilon = \frac{V_{Ed}}{V'_{Ed}} = \sqrt{\left(\gamma_{Rd}\frac{M_{Rdo}}{M_{Edo}}\right)^2 + 0.1\left(q\frac{S_a(T_C)}{S_a(T_1)}\right)^2} \leq q \tag{1.15}$$

where:

- the overstrength factor γ_{Rd} is taken equal to $\gamma_{Rd} = 1.2$;
- $S_a(T_1)$ is the value of the elastic spectral acceleration at the period of the fundamental mode in the horizontal direction closest to that of the wall shear force[3] (see Eqs. (4.2) in Section 4.2.1.2), and
- $S_a(T_C)$ is the spectral acceleration at the corner period, T_C, of the elastic spectrum.

The 2nd term under the square root of Eq. (1.15) has been proposed in Eibl and Keintzel (1988) and Keintzel (1990) to capture the increase of shear forces over the elastic overstrength value represented by the 1st term, owing to higher mode effects in the elastic and the inelastic regime of the response. In modes higher than the first one the ratio of shear force to the bending moment at the base exceeds the corresponding value at the fundamental mode, which is considered to be primarily (if not exclusively) reflected by the results of the elastic analysis. The longer the period T_1 of the fundamental mode with respect to the corner period, T_C, of the elastic spectrum (e.g., for flexible frame-wall systems on stiff soil), the higher is the value of ε, reflecting the more significant influence of higher modes on shears. Note that the correction factor in Eq. (1.15) has been proposed in Eibl and Keintzel (1988) and Keintzel (1990) just for the shear force results of the "lateral force" (equivalent static) procedure of elastic analysis for the design seismic action. "Modal response spectrum" elastic analysis fully captures the effects of higher modes on elastic seismic shears, but fails to do so for the inelastic ones, after formation of a plastic hinge at the base.

The 1st term under the square root of Eq. (1.15) assumes a different value for different individual walls of the building (even for coupled ones), but the 2nd term is the same for all walls in the building, regardless of size and contribution to lateral force resistance. Note also that, by including the behaviour factor q, this 2nd term removes part of the reduction of the elastic response spectrum by q, reflecting the smaller influence of inelasticity on the higher mode response of wall structures.

[3] Strictly speaking, T_1 is the period of the mode with the largest modal mass in the direction closest to that of the wall shear force.

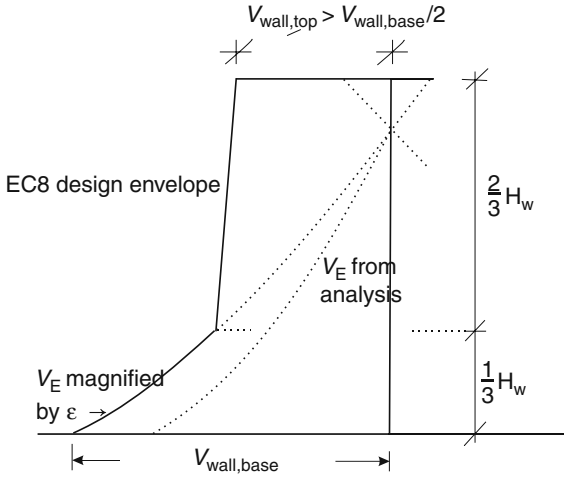

Fig. 1.11 Design envelope of shear forces in "ductile walls" of dual (frame-wall) systems according to Eurocode 8

Equation (1.15) gives safe-sided results, especially when used together with the further increase of shear forces imposed by Eurocode 8 over the upper two-thirds of the height of walls in frame-wall structural systems (see last paragraph of this section and Fig. 1.11).

In walls with ratio of height to horizontal dimension, $h_w/l_w \leq 2$ ("squat" walls) of Ductility Class High Eurocode 8 uses just Eq. (1.14) with $\gamma_{Rd} = 1.2$.

Note that, if the axial force in the wall from the analysis for the design seismic action is high (as, e.g., in slender walls near the corner of high-rise buildings, or in piers of coupled walls), the difference between the algebraically maximum and minimum axial force of the wall in the various combinations of the design seismic action with the concurrent acting gravity loads will be large. The vertical reinforcement at the base of the wall will be governed by the combination of the bending moment from the analysis, M_{Edo}, with the algebraically minimum axial force there (for compression taken as positive), while, under the algebraically maximum axial force the moment resistance, M_{Rdo}, will be much larger than M_{Edo}. Then the value of ε from Eqs. (1.14) and (1.15) may be so high, that the verification of the wall in shear (especially against failure by diagonal compression) may be unfeasible. This may be particularly the case for the piers of coupled walls.

For simplicity, in walls of buildings of Ductility Class Medium Eurocode 8 adopts the following shear magnification factor:

$$\varepsilon = \frac{V_{Ed}}{V'_{Ed}} = 1.5 \tag{1.16}$$

Compared with Eq. (1.15), Eq. (1.16) is much easier to use and gives more economical wall designs in shear. However, this simplicity and economy may be at the

detriment of performance, as Eq. (1.16) provides a very low safety margin (if any at all) against flexural overstrength at the base and inelastic higher mode effects.

In walls of Ductility Class High the value of ε from Eqs. (1.14) and (1.15) does not need to be taken greater than the value of the q-factor, so that the final design shear, V_{Ed}, does not exceed the value qV'_{Ed} corresponding to fully elastic response. Of course, ε may not be taken less than the value of 1.5 specified for Ductility Class Medium.

Higher mode effects on inelastic shears are larger at the upper storeys of the wall, and indeed more so in frame-wall structural systems. The frames of such systems restrain the walls in the upper storeys, so that the shear forces at the top storey of the walls obtained from the "lateral force procedure" of elastic analysis are opposite to the total applied seismic shear, turning to positive one or two storeys below the top. Multiplication of these very low storey shears by the factor ε of Eqs. (1.14), (1.15) and (1.16) will not bring their magnitude anywhere close to the relatively high values that may develop there owing to higher modes (cf. dotted curves representing the shear forces from the analysis and their magnified by ε version in Fig. 1.11). Eurocode 8 deals with this question by requiring the minimum design shear at the top of ductile walls of frame-wall systems be at least equal to half the magnified shear at the base, increasing linearly to the magnified value of the shear, $\varepsilon V'_{\mathrm{Ed}}$, at one third of the wall height from the base (Fig. 1.11).

1.4 The Options of Strength or Ductility in Earthquake-Resistant Design

1.4.1 Ductility as an Alternative to Strength

Equations (1.1) and (1.2) show that design seismic forces are about inversely proportional to the demand value of the global displacement ductility factor, μ_δ. So, there is an apparent economic advantage in increasing the available global ductility, to reduce the internal forces for which structural members are dimensioned. Besides the economic one, there are a number of other advantages of ductility as a substitute for strength in earthquake-resistant design:

- If the lateral force resistance of the structure is reduced by dividing the elastic lateral force demands by a high q-factor value, verification of the foundation soil, which by necessity is based on strength rather than on deformation capacity, is much easier.
- A cap on the magnitude of lateral forces that can develop in the structure reduces response accelerations and protects better the contents of the building (including valuable equipment and artefacts), as well as non-structural parts which are sensitive to acceleration (e.g. infill panels in the out-of-plane direction). Note that non-structural elements that are sensitive to deformations (such as infill panels in the in-plane direction) are not adversely affected by inelastic action in

the structural system. The reason is that, according to the "equal displacement rule" expressed by Eq. (1.1) and applying in good approximation for most buildings, lateral displacements and interstorey drifts are equal to those in the elastic structure.

– A structure with ample ductility supply is more resilient to earthquakes much stronger than the design seismic action and less sensitive to the details of the ground motion (i.e., to its frequency content and duration). So, in view of the large uncertainty associated with the extreme earthquake demand in the lifetime of a building, such a structure can be considered as a better earthquake-resistant design. Moreover, it can put its robustness into use against other actions of accidental nature, such as extreme natural or man-made hazards, for which structures are normally not designed.

There are also strong arguments in favour of less ductility and dissipation capacity and more lateral force resistance in seismic design:

– A RC structure that uses its high ductility in a strong earthquake will survive the event, but with large residual deformations, i.e., with significant structural damage, often difficult to repair. In the light of performance-based design and of protection of property as one of its prime motivations, the higher the lateral strength of a structure, the smaller will be the structural damage, not only during more frequent, moderate earthquakes, but also due to the design seismic action and beyond.
– From the construction point of view, detailing of members for ductility normally entails fixing the reinforcement in the form of cages of closely-spaced ties engaging practically every single longitudinal bar, and placing and compacting concrete within and through such cages. So, it is sometimes doubtful that the desired quality of the end product is achieved, even when workmanship is of high level and on-site supervision strict. By contrast, detailing of members just for strength is much easier and simpler.
– Many buildings designed for earthquake resistance possess anyway significant lateral strength, thanks to their force-based design against non-seismic actions. So, they may have significant resistance to earthquake forces, without even been designed for them. Examples include: low-to-medium-rise buildings in low-to-moderate seismicity regions, with gravity loads controlling their design; tall, flexible buildings dominated by wind, etc. In such cases it makes sense to benefit from the available margin of lateral strength, in order to avoid complex and expensive detailing of members for ductility.
– Often the layout of the structural system is unusually complex and irregular and falls outside the framework of the ordinary structural layouts mainly addressed by seismic design standards. In that case the designer may feel more confident for his/her design if he/she narrows the distance between the results of the linear elastic analysis used for dimensioning the members – and the nonlinear seismic response to the design seismic action. This can be achieved through a lower value of the behaviour factor q, implying lower global and local ductility demands.

If the global ductility demand is reduced at the expense of increased lateral strength, application of capacity design may be drastically relaxed, or even omitted. Capacity design rules for columns in bending and beams or columns in shear aim at avoiding overstrength in the ductile modes of behaviour and member failure – e.g., of beams in flexure – with respect to the more brittle ones, notably of all elements in shear. Such overstrengths may occur if the resistance of the more ductile modes is controlled by gravity loads or by minimum reinforcement, while that of more brittle ones is governed by the design seismic action. In structures of low ductility design seismic internal forces are in the order of about two-thirds of those resulting from purely elastic response to the design ground motion. For so high design seismic forces, it is expected that the seismic action will control dimensioning of every single member against all failure modes and there will not be any undesirable overstrengths. Accordingly, capacity design requirements can be waived to simplify the entire design process. Moreover, member ductility demands associated with the low global displacement ductility factor of low ductility structures, are relatively low, even though inelastic deformation demands may not be uniformly distributed throughout the system. Such low local ductility demands can be easily accommodated with detailing for non-earthquake resistant members, which is easier to design for and implement in-situ. So, the selection of a higher or lower ductility level for a structure has very important implications on the design and construction effort. A designer who opts for higher ductility, should have at his/her disposal more advanced design tools along with the experience and expertise necessary for their use, as well as confidence in the construction crews for the implementation of demanding member detailing.

1.4.2 The Trade-Off Between Strength and Ductility – Ductility Classification in Seismic Design Codes

Most modern seismic codes provide more than one combinations of strength and ductility. Some of them let the designer choose the strength-ductility combination, depending on the particular features of the project. Others specify which combination is appropriate, depending on the seismicity of the site, the importance and occupancy of the building and other design parameters.

European or US standards provide a few “discrete” strength-ductility combinations, each one with its own well-defined rules for member dimensioning and detailing. They are, therefore, most convenient for computational implementation and routine application, although they limit significantly the choices available to the designer.

1.4.2.1 Eurocode 8

Eurocode 8 allows trading ductility for strength through the provision of three alternative Ductility Classes (DCs):

- Ductility Class Low (DC L),
- Ductility Class Medium (DC M), or
- Ductility High (DC H).

Buildings of DC L are not designed for any ductility but only for strength. Except certain minimum conditions for the ductility of reinforcing steel, such buildings have to follow only the dimensioning and detailing rules specified in Eurocode 2 (CEN 2004b) for non-seismic actions. They are designed against the earthquake exactly as against other lateral actions, e.g. wind. Although they are expected to respond elastically to the combination of its design seismic action with the concurrent gravity loads, they are entitled to a behaviour factor value of $q = 1.5$ (instead of $q = 1.0$), attributed only to member overstrength over the seismic internal forces they are dimensioned for. The sources of overstrength are:

- The systematic difference between the expected strength of steel or in-situ concrete from the corresponding design values: the mean strength is considered to exceed normally the characteristic value by 8 MPa for concrete, or by about 15% for reinforcing steel. Moreover, in dimensioning the characteristic strengths are divided by the partial factors for materials to arrive at their design values.
- The fact that often the reinforcement is controlled by non-seismic actions and/or minimum reinforcement requirements, etc.
- The use of the same reinforcement at the two cross-sections of a beam or column across a joint, as determined by the maximum required steel area at these two sections.
- The rounding-up of the number and/or diameter of reinforcing bars.

In regions of moderate or high seismicity DC L buildings are, in general, not cost-effective. Moreover, as they do not have any engineered ductility, they may not have a reliable safety margin against an earthquake significantly stronger than the design seismic action. So, they are not considered as suitable for such regions. Eurocode 8 itself recommends using DC L only for "low seismicity cases", for which it is expected to be more economic and easier to apply. It is up to National Authorities, however, to follow this recommendation or not. The definition of what is a "low seismicity case" has also been left to National Authorities. Eurocode 8 recommends that a "low seismicity case" be one where the design ground acceleration on rock, a_g, (including the importance factor of the building, γ_I), does not exceed 0.08 g, or that at the ground surface the site, $a_g S$ is not more than 0.1 g (see Section 4.2.1 for the definitions of a_g and S).

Design of buildings for DC L is allowed by Eurocode 8 in cases beyond those of "low seismicity" when in the horizontal direction considered the value of the seismic design base shear (at the level of the foundation or of the top of a rigid basement) calculated with a behaviour factor of $q = 1.5$ is less than the base shear due to the design wind action, or any other lateral action for which the building is designed using linear elastic analysis.

Design for strength alone without engineered ductility is an extreme, only for special cases. Within the fundamental case of seismic design, namely that of design for ductility and energy dissipation, Eurocode 8 normally gives the option to design for more strength and less ductility or vice-versa, by choosing between Ductility Class Medium (DC M) or High (DC H).

Buildings of DC M or H have q-factors higher than the value of 1.5 considered available thanks to overstrength alone. DC H buildings are entitled higher values of q than DC M ones (see Section 1.4.3.1). They also have to meet more stringent detailing requirements for members (see Tables 5.1, 5.2 and 5.3) and provide higher safety margins in capacity design in shear (see Sections 1.3.6.2 and 1.3.6.3 for the differences in the γ_{Rd} values for the capacity design shear force of DC M and DC H beams or columns, and Section 1.3.6.4 for differences in the shear magnification factor ε for ductile walls). Fardis and Panagiotakos (1997a) have reported on the detailed design of 26 concrete buildings – frame or frame-wall systems – according to the pre-standard version of Eurocode 8 and (Panagiotakos and Fardis 2003, 2004) on the design of nine regular RC frame buildings to the EN-Eurocode 8. The conclusion of both studies was that, although the total quantity of steel and concrete is essentially independent of the Ductility Class adopted for the design, the higher the DC, the larger is the share of transverse reinforcement and of the reinforcement of vertical members in the total quantity of steel. Moreover, DC M and DC H are roughly equivalent in terms of achieved performance under the design seismic action. DC M is slightly easier to design for and implement in-situ and may provide better performance in moderate earthquakes. DC H seems to provide larger safety margins than DC M against local or global collapse under earthquakes (much) stronger than the design seismic action. In high seismicity regions DC H may hold some economic advantage. Its use there will be facilitated by the existing tradition and expertise in seismic design and on-site implementation of complex detailing for ductility.

Eurocode 8 itself does not link selection between the two higher ductility classes to seismicity of the site or importance of the structure, nor puts any limit to their application. It is up to countries to choose for the various parts of its territory and types of construction therein, or – preferably – to leave the choice to the designer, depending on the particular design project.

1.4.2.2 US Standards

US standards (BSSC 2003, ICC 2006) specify the combination of strength and ductility depending on the seismicity of the site, the type of occupancy and the importance of the building. To this end, they introduce "Seismic Design Categories" A–F. A building is classified as A, if the (effective) peak ground acceleration (*EPA*) and the 5%-damped elastic spectral acceleration at 1 s period, S_{a1}, are both below 0.067 g. The next threshold level for *EPA* or S_{a1} is 0.133 g, below which a building is classified as B – or C if it houses an essential or hazardous facility. The next threshold level is 0.2 g, below which a building is classified as C – or D for essential or hazardous facilities. For *EPA* or S_{a1} above 0.2 g of a building is classified

as D. If the value of S_{a1} for the MCE (Maximum Considered Earthquake) over firm rock exceeds 0.75 g, a building is classified as F if it houses essential or hazardous facilities, or as E otherwise.

Buildings of "Seismic Design Category" A are only required to have a complete tied-together lateral load resisting system designed for a lateral force of 1% of total weight. "Seismic Design Category" B buildings may just be designed for the seismic internal forces from linear analysis without special detailing, i.e., as "Ordinary Moment Frames" (ACI 2008). "Seismic Design Category" C buildings are subject to mild detailing requirements; concrete frames – but not walls – should satisfy the (ACI 2008) requirements for "Intermediate Moment Frames". Buildings in "Seismic Design Categories" D, E or F should be detailed for high ductility, with "Special Moment Frames" or walls of "special" ductility, entitled to larger force reduction or response modification factors, R, than "Intermediate Moment Frames".

According to ACI (2008), "Ordinary Moment Frames" are not subject to ductility requirements. "Special Moment Frames" have very good global ductility, thanks to the application of capacity design of columns in bending (see Section 1.3.4) and of beams and columns in shear (see Section 1.3.6). They also have high local ductility, thanks to the application of stringent detailing rules for the longitudinal and transverse reinforcement of all types of members. "Intermediate Moment Frames" do not have to satisfy the capacity design rule of columns in bending, Eq. (1.4), may follow less demanding capacity design of beams and columns in shear (see Section 1.3.6.2) and are subject to less stringent requirements for the longitudinal reinforcement of beams and the transverse bars of columns.

1.4.3 Behaviour Factor q *of Concrete Buildings Designed for Energy Dissipation*

For building structures designed for energy dissipation and ductility, the value of the behaviour factor q, by which the elastic spectrum used in linear analysis is divided, depends:

- on the ductility class selected for the design,
- on the type of lateral-force-resisting-system, and
- (in Eurocode 8) on the regularity of the structural system in elevation.

The value of the q-factor is linked, indirectly (through the ductility classification) or directly (as in Eurocode 8, see Chapter 5), to the local ductility demands in members and hence to the corresponding detailing requirements.

1.4.3.1 Eurocode 8

The overstrength of materials and elements is presumed to correspond to a q-factor value of 1.5, which is assigned to DC L buildings without any association to

ductility. This value is also incorporated in the q-factors of buildings of DC M or H. Besides, overstrength of the structural system due to redundancy is explicitly included in the q-factor, through a multiplicative factor α_u/α_1. This is the ratio of the seismic action that causes development of a full plastic mechanism, to the seismic action at formation of the first plastic hinge in the system – both in the presence of the gravity loads considered concurrent with the design seismic action. If α_1 is taken as a multiplicative factor on seismic action effects from the elastic analysis for the design seismic action, its value may be computed as the lowest value of the ratio $(M_{Rd}–M_V)/M_E$ over all member ends in the structure. M_{Rd} in this case is the design value of the moment capacity at the member end; M_E and M_V are the bending moments there from the elastic analysis for the design seismic action and for the concurrent gravity loads, respectively. The value of α_u may be found as the ratio of the base shear at development of a full plastic mechanism according to a nonlinear static ("pushover") analysis (with the gravity loads concurrent with the seismic action maintained constant in the course of the analysis, while lateral forces monotonically increase, according to Section 4.6.1), to the base shear due to the design seismic action (Fig. 1.12). For consistency with the calculation of α_1, the moment capacities at member ends in the pushover analysis should be the design values, M_{Rd}. If the mean values of moment capacities are used instead, as customary in pushover analysis, the same values should also be used for the calculation of α_1.

In most cases the designer will not consider worth doing iterations of pushover analyses and design based on elastic analysis, just for the sake of computing the ratio α_u/α_1 for the q-factor. For this reason, Eurocode 8 provides default values of this ratio. For buildings regular in plan, the default values are:

- $\alpha_u/\alpha_1 = 1.0$ for wall systems with just two uncoupled walls per horizontal direction;
- $\alpha_u/\alpha_1 = 1.1$ for:
  - one-storey systems and frame-equivalent dual (i.e., frame-wall) ones, and
  - wall systems with more than two uncoupled walls in the horizontal direction considered.

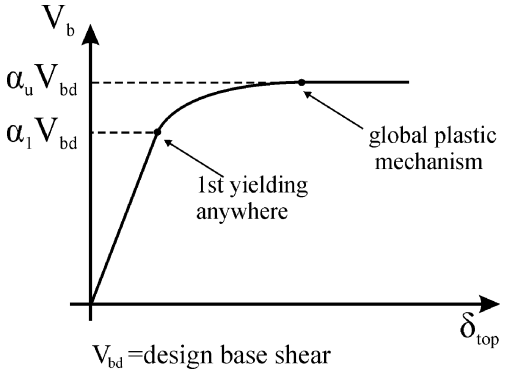

Fig. 1.12 Definition of factors α_u and α_1 on the basis of base shear v top displacement diagram from pushover analysis

– $\alpha_u/\alpha_1 = 1.2$ for:
  - one-bay multi-storey frame systems and frame-equivalent dual ones,
  - wall-equivalent dual systems, and
  - coupled wall systems.
– $\alpha_u/\alpha_1 = 1.3$ for multi-storey multi-bay frames or frame-equivalent dual systems.

In buildings which are irregular in plan according to the classification criteria of Eurocode 8 presented in Sections 2.1.5 and 2.1.6, the default value of α_u/α_1 is the average of:

– 1.0, and
– the default values given above for buildings regular in plan.

Values higher than the default ones may be used for α_u/α_1, up to a maximum of 1.5, provided that the higher value is confirmed through a pushover analysis, after design with the resulting q-factor.

The various types of structural systems that appear in the definition of the above default values of α_u/α_1 are defined in Eurocode 8 as follows:

In a "frame system" or in a "wall system" the seismic base shear taken, according to the analysis, by frames of beams and columns, or by walls, respectively, designed and detailed for earthquake resistance is at least 65% of the total. In-between "frame" and "wall" systems are the "dual systems". These are classified as "wall-equivalent dual" or as "frame-equivalent dual", if the fraction of the base shear resisted by walls is more, or less, than 50%, respectively. A wall system is considered as a "coupled wall system", if more than 50% of the total wall resistance is provided by coupled walls. According to Eurocode 8, two walls are considered as coupled, if they are connected together (normally at each floor level) through regularly spaced beams that meet special ductility conditions ("coupling beams") and this coupling reduces by at least 25% the sum of the bending moments at the base of the individual walls (the "piers"), compared to that of the two "piers" working separately.

For concrete buildings which are characterised as regular in elevation according to criteria 1–6 in Section 2.1.7, Eurocode 8 specifies the values of the q-factor given in Table 1.1.

Table 1.1 Basic value, q_o, of behaviour factor for heightwise regular concrete buildings in Eurocode 8

Lateral-load resisting structural system	DC M	DC H
Inverted pendulum system	1.5	2
Torsionally flexible structural system	2	3
Uncoupled wall system, not belonging in one of the two categories above	3	$4\alpha_u/\alpha_1$
Any structural system other than those above	$3\alpha_u/\alpha_1$	$4.5\alpha_u/\alpha_1$

"Inverted pendulum systems" are defined as those with at least 50% of their total mass in the upper third of the height, or with energy dissipation at the base of a single element. One-storey frame systems with all columns connected at the top (via beams) in both horizontal directions and maximum value of normalised axial load ν_d in the combination(s) of the design seismic action with the concurrent gravity loads not greater than 0.3 are excluded. "Inverted pendulum systems" are entitled very low q-factors (the q-factor for those of DC M does not exceed the value of 1.5 available thanks to overstrength alone, without design for ductility), because of concerns for potentially large P-Δ effects or overturning moments and reduced redundancy. However, inverted pendulum buildings seem unduly penalised, in view of the q-factors of 3.5 assigned by Eurocode 8 to bridges with concrete (single-)piers and more than 50% of the mass at the level of the deck. To alleviate this penalty, Eurocode 8 permits increasing the value of q_o for inverted pendulum systems that are shown capable of energy dissipation in their potential plastic hinges higher than normal for their chosen Ductility Class.

A system is defined in Eurocode 8 as "torsionally flexible", if at any floor the radius of gyration of the floor mass exceeds the torsional radius in one or both of the two main directions of the building in plan. As emphasised in Section 2.1.6, such systems are sensitive to torsional response about a vertical axis.

The values of q in Table 1.1 are called basic values, q_o, of the q-factor. They are the ones linked to ductility demands and member detailing (see Chapter 5). For the calculation of the seismic action effects from linear analysis, the value of q is reduced with respect to q_o in the following cases:

- In buildings which are irregular in elevation according to the classification criteria of Eurocode 8 presented in Section 2.1.7, the q-factor value is reduced by 20%.
- In wall, wall-equivalent dual or "torsionally flexible" systems, the value of q is the basic value q_o (reduced by 20% if there is irregularity in elevation), multiplied by a factor equal to $(1 + \alpha_o)/3$, but with values between 0.5 and 1, where α_o is the (mean) aspect ratio of the walls in the system (sum of wall heights, h_{wi}, divided by the sum of wall cross-sectional lengths, l_{wi}). This factor reflects the adverse effect of a low shear span ratio on the ductility of walls. It is less than 1 if α_o is less than 2, which corresponds to a mean shear span ratio of the walls in the system less than 1.33 (squat, typically non-ductile walls).

The above reductions of q notwithstanding, DC M and H buildings are entitled to a final q-factor value of 1.5, considered to be always available owing to overstrength alone.

A building that is not characterised as an "inverted pendulum" or a "torsionally flexible system" can have different q-factors in the two main horizontal directions, depending on the structural system and its vertical regularity classification in these two directions, but not due to ductility class, which is the same for the entire building.

1.4.3.2 US Standards

The force reduction or response modification factor R depends on the structural system and its ductility. The force reduction factors R specified by US standards (BSSC 2003, SEAOC 1999, ICBO 1997, ACI 2008) are considered to be composed of the following factors:

- One factor due to system ductility, equal to the ratio of the total lateral force for elastic response, to the actual lateral force resistance at full yielding of the system.
- Another factor due to overstrength, denoted by Ω_o, and equal to the ratio of the actual resistance at full yielding to the prescribed design forces. This factor is the counterpart of the product $1.5\alpha_u/\alpha_1$ representing overstrength of materials, elements and the structural system in Eurocode 8.

The NEHRP provisions (BSSC 2003) set $\Omega_o = 3$ in frames and $\Omega_o = 2.5$ in those dual systems where the frame provides at least 25% of the lateral force resistance and in systems that carry gravity loads through a space frame and lateral loads via concrete walls ("building frame systems"). Inverted pendulum systems have $\Omega_o = 2.0$. The overstrength factor Ω_o is also used to calculate the design shear force using an alternative to capacity-design, namely as Ω_o times the value from linear analysis. This amounts to calculating the seismic moments from the composite R factor and the seismic shears from the part of the R factor which is due to system ductility alone. In (SEAOC 1999) $\Omega_o = 2.8$, except in inverted pendulum systems, where $\Omega_o = 2.0$.

The composite R factor depends on the structural system. Values quoted below for concrete buildings are according to BSSC (2003), with the (SEAOC 1999) values given in parenthesis:

- The highest value of $R = 8$ (8.5) is for "Special Moment Frames".
- "Intermediate Moment Frames" have $R = 5$ (5.5).
- "Ordinary Moment Frames" have $R = 3$, due to overstrength alone ($R = \Omega_o$).
- Systems where gravity loads are taken by a 3D frame ("building frame") and the full lateral resistance is provided by concrete walls have $R = 6$ (5.5) if the walls are of "special" ductility, or $R = 5$ if they are of "ordinary".
- Systems where gravity loads are taken by walls ("bearing walls") and the full lateral resistance is provided by the same or other concrete walls have $R = 5$ (4.5) for walls of "special" ductility or $R = 4$, for "ordinary".
- Dual systems where "Special Moment Frames" provide at least 25% of the lateral force resistance (with the rest provided by walls) have $R = 8$ (8.5) if the walls are of "special" ductility (coupled walls included), or $R = 6$ if they are of "ordinary".
- Dual systems where "Intermediate Moment Frames" provide at least 25% of the lateral force resistance (the rest being provided by walls) have $R = 6.5$ (6.5) for walls of "special" ductility (coupled walls included) or $R = 5.5$ for "ordinary".
- Inverted pendulum systems have $R = 2.5$ (2.2) if their columns are of "special" ductility, or $R = 1.25$ if the columns are "ordinary".

Recent efforts to rationalize the R factor of US codes through system ductility and overstrength notwithstanding, the R values are still based on performance in past earthquakes and economic considerations. The R-factor values above were developed mostly on the basis of past performance of frames with multiple bays and with all their connections moment resisting. For reasons of economy and functionality, recent years have seen wider application of frames with fewer bays, supporting large floor areas. To counter the reduced redundancy of such systems, in buildings of "Seismic Design Category" D, E or F the R factor is reduced by a redundancy factor ρ, taking values between 1.0 and 1.3 (BSSC 2003) or 1.5 (SEAOC 1999). In (SEAOC 1999) ρ is the largest calculated in all storeys within the lower two-thirds of the building. Its value increases with increasing floor area and with the maximum (over all storeys for a given horizontal direction) fraction, $r_{\max}$, of a storey shear resisted by a single component (see Section 2.1.9 and Eqs. (2.3) and (2.4) for details). In dual systems with at least 25% of the lateral force resisted by the frame (SEAOC 1999) reduces the so-computed ρ-value by 20%. In (BSSC 2003) ρ is equal to 1.0, unless any storey where the storey shear exceeds 35% of the base shear depends on a single wall or pier of a coupled wall (including their connection to the rest of the lateral load resisting system) or on (both ends of) a single beam, for more than one-third of the storey's shear resistance or for the storey's torsional regularity (with a regular storey defined as one where the interstorey displacement at any point on the perimeter does not exceed by 40% or more the average in the storey). In these other cases ρ is taken equal to 1.3 (BSSC 2003).

Chapter 2
Conceptual Design of Concrete Buildings for Earthquake Resistance

Like Chapter 5, this chapter is devoted exclusively to the seismic design of new buildings. It emphasises the importance of the layout of the structural system for the building's seismic performance and highlights the principles to be followed and the pitfalls to be avoided during the initial stage of the design process, notably during conceptual design. Examples of unsatisfactory performance of concrete buildings with poor structural layout are amply given.

The three main types of structural systems used in concrete buildings for lateral-load resistance:

- frames of beams and columns,
- structural walls, and
- their combination in a "dual" system

are presented, along with their advantages and disadvantages and with guidance for the preliminary sizing of the components of these systems during conceptual design.

The importance of the layout of the foundation system for the seismic performance and the design of the superstructure is emphasised, the pros and cons of the available options of shallow foundation systems are highlighted and general rules for the seismic design of the foundation system are presented.

As in Chapter 1, certain emphasis is given to the relevant provisions of the European Standard for the seismic design of new buildings (CEN 2004a), with their US counterparts presented also for comparison.

2.1 Principles and Rules for the Conceptual Design of Building Structures

2.1.1 The Importance of Conceptual Design for Earthquake Resistance

Unlike the two other main phases of design, namely analysis and detailed design, which are now fully governed by the use of the computer, conceptual design has not been penetrated yet by computers, and in all likelihood it never will. So, conceptual

M.N. Fardis, *Seismic Design, Assessment and Retrofitting of Concrete Buildings*, Geotechnical, Geological, and Earthquake Engineering 8, DOI 10.1007/978-1-4020-9842-0_2,

design is *the* phase where the designer can make best use of his/her creativity, imagination, resourcefulness, capability for innovation and experience, without any competition from the new "master" of the design office, the computer.

In conceptual design of a structure:

- the structural materials are chosen,
- the type and layout of the structural system is selected,
- preliminary sizing of structural members – at least of important ones – takes place, and
- the method of construction is (implicitly or explicitly) specified.

In this phase of the design process, the structural engineer uses judgement and creativity and profits from his/her experience to examine alternative options and assess their cost-effectiveness for the fulfillment of the structure's performance requirements for:

- safety,
- serviceability, and
- durability

within the limits of the design constraints posed by:

- the architectural layout and functionality considerations,
- site and soil conditions,
- the available budget,
- considerations of construction time and scheduling,
- the available materials, workmanship and equipment,
- etc., including special requirements of the owner.

If the building is to be earthquake-resistant, then the choice of structural layout and structural materials in conceptual design should aim at reducing the uncertainty of its seismic response, promoting its satisfactory seismic performance and facilitating its eventual detailed design in a cost-effective way.

The governing consideration in the conceptual design of structures not controlled by the seismic action is the maximisation of their cost-effectiveness, within the limitations posed by the performance requirements and the design constraints. Safety is seldom an overriding concern in the conceptual design of non-earthquake-resistant structures, as it is essentially ensured by the subsequent design phases, notably by the application of State-of-the-Art analysis methods and member dimensioning and detailing in accordance with design codes. By contrast, if the design is governed by earthquake resistance, the structural layout is the key factor that determines the seismic performance or vulnerability of the building. Damage in strong earthquakes shows that, all other design conditions being the same (design code, computational methods and tools, professional skill and design effort), irregular and geometrically complex structures perform on average worse than simple and regular ones. So earthquake resistance should be a compelling consideration in the conceptual

design from the very beginning. The designer should never configure first the structural system for resistance to gravity loads and then try to add features for earthquake resistance as a follow up.

It is impossible (or prohibitively expensive) to fully make up for inappropriate conceptual design choices during the subsequent design stages, e.g. through sophisticated analysis, extraordinary attention to detailing, larger member sizes and more reinforcement, etc. Faulty decisions made at the conceptual design stage can be corrected later only by revisiting and reversing them. Otherwise, the subsequent design stages can only mitigate the adverse consequences of these decisions, always at a high cost and at the expense of seismic performance. So, the designer would better make sure that his/her first steps during design are in the right direction.

It is normally hard to achieve a proper structural layout, if the structural designer's task starts after the architectural design is finished. A good conceptual design can more easily be achieved if the structural engineer communicates and interacts with the architect from the early stages of architectural design. Sometimes a minor and painless change in the architectural layout greatly facilitates the task of the structural designer.

In the Preamble conceptual design of earthquake-resistant buildings has been set within the context of the overall structural design for earthquake resistance. Its connection to the subsequent phases of the design procedure was pointed out. Chapter 1 emphasised that control of the inelastic seismic response is a prime aim of the design for earthquake resistance and that capacity design is the major instrument of detailed design for the achievement of that aim. In this connection, Chapter 2 focuses on what the designer should pursue or avoid beforehand, in the conceptual design phase, to enhance the effectiveness of capacity design and of other codified design rules aiming at controlling the inelastic seismic response.

The rules of current seismic design codes have been developed mainly for fairly simple and regular structural layouts. The more complex and irregular the structural layout, the further is the structure from the limits of applicability of present day design methods and codes. In particular, a simple and regular structural layout reduces the deviation of the actual and strongly inelastic response to the design seismic action from the presumed response calculated by simplified elastic analysis and used as the basis of member dimensioning. It is reminded in this respect that in current force-based codified seismic design the design seismic action is – about – q-times stronger than that causing purely elastic response. So it induces significant inelastic deformations in most, if not all, structural members. The performance of the structure under the design seismic action will be satisfactory, if the deformation capacity of these members – as determined by their detailing – exceeds the corresponding inelastic deformation demands. These demands are not explicitly computed during the design process. They are assumed instead to be – roughly – proportional to those elastically computed under the design seismic action reduced by the q-factor (the proportionality constant being equal to q). This assumption is not far from reality, provided that the structural layout is fairly simple and regular, as has been presumed during the development of present-day seismic design codes. If it isn't, the global response may be completely different from what is predicted by

elastic analysis, with inelastic deformation demands possibly concentrated in certain elements or parts of the structure and leading to local failures. So, if the designer wishes to design a cost-effective earthquake-resistant structure profiting from the relatively high q-factor values allowed by codes – in the order of 5 or more – then he/she should select a simple and clear structural system. Otherwise, he/she would better opt for a lower value of q, so that the seismic response under the design earthquake is within the elastic range and within the limits of applicability of elastic analysis.

Note that the widespread use of reliable computer codes for the elastic analysis of structures in 3D has made some designers overconfident of their ability to produce a safe seismic design, even for very complex and irregular structural layouts. Such confidence is warranted only for well-defined loadings (e.g., for gravity loads) and provided that the designer has the experience and skills necessary for the construction of a mathematical model representing well the complexities of the real structure.

2.1.2 Fundamental Attributes of a Good Structural Layout

By-and-large conceptual design is subjective and personal. It significantly depends on the designer's experience, creativity and judgment. There are, however, certain fundamental principles to be taken into account in order to arrive at a structural concept that is considered sound for earthquake resistance. Accordingly, important features of a good layout of a building structure are:

- Clarity of the lateral-load-resisting system.
- Simplicity and uniformity.
- Symmetry and regularity in plan.
- Large torsional stiffness about the vertical.
- Heightwise regularity of geometry, mass and lateral stiffness.
- Regularity of lateral resistance in elevation.
- Redundancy of the lateral-load-resisting system.
- Continuity of the force paths, without local concentrations of force or deformation demands.
- Effective horizontal connection of vertical elements at all floor levels.
- Minimal total mass.
- Minimal adverse effects of elements not considered as part of the lateral-load resisting system and of masonry infills in particular.

These features are elaborated in the following Sections 2.1.3–2.1.13.

2.1.3 Clear Lateral-Load-Resisting System

The structural system resisting the seismic action should be crystal clear, not only to whom that chose it but to any competent designer as well. For a concrete building, a clear lateral-load-resisting system is one consisting of certain plane frames and/or

structural walls arranged in two orthogonal horizontal directions. Any single plane frame should be continuous from one side of the building plan to the opposite, without interruptions (i.e. with beams connecting adjacent columns of the frame at all floors) or offsets, or indirect supports of some beams on others. Note that indirectly supported beams are much less effective as frame members and introduce significant uncertainty regarding interaction with the supporting beam through torsion.

The cross-sectional shape and dimensions of walls should be consistent with their modelling and dimensioning as prismatic members. Complex composite cross-sections and openings – staggered or not – in the wall should be avoided.

The layout of the structural system that supports the gravity loads is usually dictated by architectural design. Sometimes this layout does not lend itself to building a clear system for earthquake resistance (for instance, when the arrangement of columns in plan is very irregular). In such cases the system supporting the gravity loads should have low lateral stiffness: e.g., with small column sections, or without beams between irregularly arranged columns (as in a flat slab). A clear lateral-load-resisting system should be provided instead, having lateral stiffness and resistance sufficient to resist 100% of the design seismic action. Such a system may consist of certain appropriately arranged structural walls. Strong perimeter frames is another option.[1] The designer may use to advantage the facility of primary versus secondary elements provided by modern seismic design codes (including Eurocode 8, as highlighted in Section 4.12), to resist the full seismic action by a proper lateral-force resisting system, without relying at all on structural members or combinations thereof that are not appropriate for earthquake resistance.

The expected inelastic response mechanism, i.e. the location of plastic hinges, should also be crystal clear. Plastic hinges should be limited to the ends of beams and to the lower-most cross-section of vertical elements.[2] The rules of modern seismic codes for capacity design of columns at their connections with the beams (see Section 1.3.4) and of walls in all sections above the base (see Section 1.3.5) are meant to ensure that plastic hinges will indeed form in beams. Nevertheless, the designer should not rely too much on the mechanistic application of these rules: he/she should promote formation of plastic hinges at the desired locations by avoiding (significant) reduction of the cross-sectional dimensions of vertical elements from one storey to the next and by selecting from the very beginning large column sizes. It is reminded that certain design codes (including Eurocode 8) allow plastic hinging above the base of certain columns: e.g. in columns of dual systems dominated by the structural walls, or in a few interior columns of multiple-column frames. Such columns and the location of plastic hinges in them should be clearly identified in the conceptual design phase.

---

[1] The beams of such frames may be hard to dimension and detail for the large alternating shear forces that may develop from the combination of the low shear forces due to gravity and the large shears due to the seismic action.

[2] If the flexural capacity of tie-beams or foundation beams is small with respect to that of the vertical element they are connected to, plastic hinges may develop in them, and – depending on the resistance of the foundation soil against rotation – may prevent plastic hinging at the base of the vertical element.

2.1.4 Simplicity and Uniformity in the Geometry of the Lateral-Load-Resisting System

Simplicity and uniformity goes hand-in-hand with clarity (see Section 2.1.3) and regularity (see Sections 2.1.5 and 2.1.7). If, in each one of the two orthogonal principal horizontal directions, the lateral-load-resisting system consists of a few identical and regularly arranged structural walls, then seismic force and deformation demands at every storey will be uniformly distributed to all walls, without undue concentration of deformation demands to a single location or wall and consequent early failure. Lateral-load-resisting systems consisting of identical and regularly spaced plane frames, with all bays having the same length and member cross-sections, will also have uniformly distributed seismic demands. As a matter of fact, if the two exterior columns of such a frame have about half the effective cross-sectional stiffness and moment resistance of the interior columns, seismic demands (bending moments and chord rotations) will be the same at all beam ends of a storey. Note that such a choice is consistent with the requirement on the moment resistances of exterior columns to exceed that of a single beam according to Section 1.3.4 and Eq. (1.4), instead of that of two beams as for interior columns.

The price to pay for complete uniformity is reduced (or no) redundancy. Plastic hinges will develop almost simultaneously wherever they are expected to form. The system will have limited overstrength after formation of the first plastic hinge and little opportunity to redistribute forces from certain locations to others. This is against the aims advanced in Section 2.1.9.

2.1.5 Symmetry and Regularity in Plan

One of the Eurocode 8 (CEN 2004a) criteria for building regularity in plan is approximate symmetry of lateral stiffness and mass with respect to two orthogonal horizontal axes.

If at every storey the structural system and the mass distribution in plan are fully symmetric with respect to two orthogonal horizontal axes, then the response to the translational horizontal components of the seismic action will not involve torsion about a vertical axis. A rotational component of the ground motion about such an axis, possibly arising from differences of the translational component between opposite sides of the building foundation, may induce, though, such a torsional response.

The more torsional the response, the larger is the difference in seismic displacements between opposite sides of the building and the larger the local deformation demands on the side that develops the larger displacement (called “flexible side”). Unless sufficiently designed against these larger seismic demands, the side of the building experiencing them may yield earlier than the opposite (“stiff”) side. The resulting reduction of the instantaneous effective stiffness of the “flexible side” may exacerbate the imbalance in stiffness and increase further the torsional response, possibly leading to early failure of certain elements of the “flexible” side. Figure 2.1

Fig. 2.1 Collapse of a building due to torsional response about a stiff shaft at the corner, Athens (1999) earthquake

shows the example of a 3-storey building (plus penthouse) that had lateral stiffness and resistance concentrated near one of the corners owing to a staircase and elevator shaft. The rest of the floor had a large open area. The response to the 1999 Athens earthquake was strongly torsional about the "stiff" and "strong" corner. The vertical elements on the other sides (the "flexible" ones) experienced large deformation demands and failed.

The lack of symmetry in plan is often measured in terms of the "static eccentricity" between the "centre of mass" of a storey (centroid of overlying masses, denoted by CM) and the "centre of rigidity" (CR) or the "centre of resistance" (CV). The "centre of rigidity" is important during the elastic response, while the "centre of resistance" may become important when the building responds well in the inelastic range.

A useful guide for what constitutes an acceptable magnitude of the "static" eccentricity, e, derives from one of the Eurocode 8 (CEN 2004a) criteria for regularity in plan. According to that criterion, for a building to be considered as regular in plan, the "static" eccentricity, e, between the floor centre of mass and the storey centre of lateral stiffness should not exceed 30% of the torsional radius, r, of the corresponding storey in each of the two orthogonal horizontal directions, X and Y, of near-symmetry:

$$e_x \leq 0.3\, r_x; \qquad e_y \leq 0.3\, r_y \tag{2.1}$$

The "torsional radius" r_x in Eq. (2.1) is defined as the square root of the ratio of:

- the torsional stiffness of the storey with respect to the centre of lateral stiffness, to
- the storey lateral stiffness in the Y direction (orthogonal to X)

For r_y the storey lateral stiffness in the X direction (orthogonal to Y) is used in the denominator.

The centre of lateral rigidity (CR) is defined as the point in plan through which application to the elastic structure of lateral forces produces only translation of the

individual floors, without twisting of any floor. It can be determined from separate analyses in the two orthogonal horizontal directions of the building, with all nodal displacements at each floor constrained to be the same in the direction of the applied lateral loads and zero in the orthogonal direction. Then the centre of lateral rigidity is determined at each floor as in (Cheung and Tso 1986, Tso 1990), namely as the point of application of the resultant of the forces applied on the floor in the direction of the applied lateral loads by the members above and below. Conversely, any set of storey torques (i.e. of moments with respect to the vertical axis, Z) produces only rotation of the floors about the vertical axis that passes through the centre of lateral stiffness, without translation of that point in X and Y at any floor. If such a point exists and is independent of the heightwise distribution of the storey lateral forces, the torsional radius is unique and well-defined. It can be computed by applying to the building separately:

- a set of storey torques, T_i, and
- a set of storey forces in the horizontal direction of interest but through the (unique) centre of lateral stiffness, with magnitudes proportional to those of the corresponding storey torques: $F_i = T_i/c$, and an arbitrary choice of the lever of arm, c.

The torsional stiffness is then defined as the ratio of:

- the storey torsional moment (sum of all storey torques applied above and at storey i), to
- the corresponding storey twist with respect to the base of the building.

Similarly, the lateral stiffness is defined as the ratio of:

- the storey shear, to
- the corresponding horizontal displacement of the storey with respect to the base.

If the centre of lateral rigidity is independent of the heightwise distribution of the storey lateral forces, the so-computed value of r is also invariant and unique, irrespective of the heightwise pattern of the storey torques, T_i, and of the storey forces, $F_i = T_i/c$.

Unfortunately, the centre of lateral rigidity, CR, as defined above, and the torsional radius, r, are unique and independent of the lateral loading only in single-storey buildings. In buildings with more storeys the centre of lateral rigidity depends on the distribution of lateral loading with height. This is especially so if the structural system consists of sub-systems that develop different patterns of storey horizontal displacements under the same set of storey forces.[3] Neglecting the dependence of CR on the heightwise distribution of lateral loading, this distribution is commonly chosen the same as that of (equivalent) lateral forces in the lateral force method of analysis (i.e. proportional to the product of storey mass, m_i, times its elevation from

[3] As pointed out in Section 2.2.3, under lateral loading frames exhibit a shear-beam-type of lateral displacements, while walls behave more like vertical cantilevers.

the base, z_i, see Section 4.3.3). Even then, in buildings that are strongly irregular in elevation and/or have a dual (frame-wall) structural system, the planwise location of the storey CR may not vary smoothly along the height of the building. It may be very different at adjacent storeys and sometimes even fall outside the perimeter of the framing plan (Kosmopoulos and Fardis 2008). Section 2.4.2 (and Fig. 2.22) exemplifies erratic variations of the storey CR, denoted there as CR-effective.

A convenient approximation of the centre of lateral rigidity may be obtained as follows. A first analysis of the elastic structure is carried out under a set of storey torques proportional to the product of storey mass, m_i, times elevation from the base, z_i (as for the storey lateral forces, F_i, in the lateral force method of analysis).The centre of twist (CT) of each floor due to these storey torques T_i is geometrically determined. The (horizontal projection of the) centre of twist at elevation z from the base about equal to 80% of the total building height, H, from this analysis may be taken as the centre of lateral stiffness of the building, because a set of horizontal forces, F_i, proportional to $m_i z_i$ and applied at floor levels through that point produces translation of the individual storeys with minimum (in a least-squares sense) twist about the vertical. Once the centre of twist at $z = 0.8H$ due to these storey torques is determined, another elastic analysis is carried out for each one of the two orthogonal horizontal directions, this time under a set of storey horizontal forces, F_i, in that direction, numerically equal to T_i of the first analysis and applied to the storey masses. Then, for the calculation of the torsional radius, r:

- the torsional stiffness at the numerator is computed as the ratio of the total applied torque, $\sum_i T_i = \sum_i F_i$, to the resulting rotation $\theta_{0.8H}$ at z=0.8H from the 1st elastic analysis, and
- the lateral stiffness in the denominator is computed as the ratio of total applied shear, $\sum_i F_i$, to the displacement $\delta_{0.8H}$ at z=0.8H in the horizontal direction of the forces F_i, from the 2nd elastic analysis.

For length units taken as for the unit ratio of $\sum_i T_i = \sum_i F_i$, r is equal to $r = \sqrt{(\delta_{0.8H}/\theta_{0.8H})}$.

Section 4.10.5.2 and Fig. 4.14 exemplify the centre of twist (CT) in a heightwise regular building consisting of sub-systems that develop similar patterns of storey horizontal displacements under storey horizontal forces F_i proportional to $m_i z_i$. In that case CT is close to the centre of lateral rigidity determined rigorously as outlined above and denoted in Fig. 4.14 as CR-effective. In that case, as well as in the heightwise strongly irregular buildings of Sections 2.4.2 (Fig. 2.22) and 4.10.5.3 (Fig. 4.19), composed of sub-systems with dissimilar patterns of storey horizontal displacements under storey forces F_i proportional to $m_i z_i$ (walls and frames), point CT varies smoothly from storey to storey, although the rigorous centre of rigidity, CR-effective, does not.

For single-storey buildings, where the centre of lateral rigidity, CR, and the torsional radius are independent of the loading pattern, they may be established in

approximation from the moments of inertia of the cross-sections of the vertical elements, neglecting the effect of beams, as:

$$x_{\mathrm{CR}} = \frac{\sum \left(x E I_y\right)}{\sum \left(E I_y\right)}; \qquad y_{\mathrm{CR}} = \frac{\sum \left(y E I_x\right)}{\sum \left(E I_x\right)} \tag{2.2}$$

$$r_x = \sqrt{\frac{\sum \left[(x - x_{\mathrm{CR}})^2 E I_y + (y - y_{\mathrm{CR}})^2 E I_x\right]}{\sum \left(E I_y\right)}}; \qquad r_y = \sqrt{\frac{\sum \left[(x - x_{\mathrm{CR}})^2 E I_y + (y - y_{\mathrm{CR}})^2 E I_x\right]}{\sum \left(E I_x\right)}} \tag{2.3}$$

In Eqs. (2.2) and (2.3) EI_{y} and EI_{x} denote the section rigidities for bending within a vertical plane parallel to horizontal directions X or Y, respectively (i.e. about an axis parallel to axis Y or X, respectively).

Equations (2.2) and (2.3) may be used to determine the centre of lateral rigidity and the torsional radius also in multi-storey buildings, provided that their structural system consists of sub-systems that develop similar patterns of storey horizontal displacements under storey horizontal forces F_{i} proportional to $m_{\mathrm{i}} z_{\mathrm{i}}$: namely only moment frames (exhibiting a shear-beam type of horizontal displacement pattern), or only walls (deflecting like vertical cantilevers). For wall systems, in which shear deformations are also significant in addition to the flexural ones, an equivalent rigidity of the section should be used in Eqs. (2.2) and (2.3). Unlike the general and more accurate methods outlined in the previous paragraphs, which yield a single pair of r_{x} and r_{y} for the entire building, whenever the cross-section of vertical elements changes from storey to storey the approximation of Eqs. (2.2) and (2.3) gives different pairs of r_{x} and r_{y} at different storeys.

US codes base the definition of irregularity in plan on the planwise-variation of floor displacements from the analysis, due to the torsional component of the response:

- A building is considered as "irregular in plan", if, at any point of a floor, the floor displacement exceeds by 20% or more the mean floor displacement.
- The building is considered as "extremely irregular in plan" if, at any point of a floor, the displacement exceeds by 40% or more the mean floor displacement.

These criteria are not useful for conceptual design, as they require carrying out full-fledged elastic analyses. By contrast, the Eurocode 8 (CEN 2004a) criteria, Eqs. (2.1), used together with the approximation in Eqs. (2.2) and (2.3), can be easily checked at the conceptual design stage.

In buildings with masses and structural system perfectly symmetric in plan, the centres of mass, rigidity and resistance coincide. If such coincidence is not due to full actual symmetry of the structural system and of the masses but to other – "coincidental" – reasons, it may be "accidentally" disturbed if the actual distributions of

mass and/or stiffness or resistance of the members deviate from the ones considered in the design calculations. Seismic design codes postulate an "accidental eccentricity" of the storey masses in plan from their nominal location, to be combined with the systematic "static" eccentricity in the most adverse way. For example, Eurocode 8 (CEN 2004a) and US codes, normally set the accidental eccentricity at 5% of the parallel building dimension in plan (see Section 4.8). If the "static" eccentricity is large, the effect of the "accidental eccentricity" on the calculated seismic response is minor.

In most cases in practice full symmetry in plan of the structural system and of the masses is not feasible. Fortunately, the elastic analysis in 3D which is required by modern seismic design codes for asymmetric and irregular in plan buildings captures sufficiently the inelastic torsional seismic response (Kosmopoulos and Fardis 2007) and provides a reliable basis for seismic design against its effects.

If the building plan is far from rectangular, then the seismic response may not be sufficiently predictable, even though the storey centres of mass may coincide with those of rigidity and/or resistance. Eurocode 8 (CEN 2004a) sets another criterion for the building to be considered as regular in plan, besides Eq. (2.1) above and Eq. (2.4) in Section 2.1.6: that the outline of the structure in plan (as defined by the outermost vertical elements) has a compact layout, delimited by a convex polygonal line. Any single re-entrant corner of the perimeter should not leave an area between the perimeter and the convex polygonal line enveloping it which is more than 5% of the area inside the outline.[4] L-, C-, H-, I- or X-shaped plans should respect this condition, for the structure to be considered as regular in plan according to Eurocode 8 (CEN 2004a).

In seismic design practice floor diaphragms are commonly assumed to be rigid. If this assumption is far from real, an element of uncertainty of the response is introduced. Floors with T-, U-, H-, or L-shaped plan may not behave as rigid diaphragms but deform within their horizontal plane, allowing flexible wings of the building to oscillate separately. Moreover, significant in-plane tension may develop at re-entrant corners of non-rectangular diaphragms, causing early cracking and tensile failure of the diaphragm there and reducing its effectiveness in tying at floor levels the vertical members into an integral system (see also Section 2.1.11). Sections 2.4.2 and 2.4.4 present two real cases of multi-storey buildings with L-shaped floor plan, where the weakness of the floor diaphragm contributed to the collapse of one of the two wings of the building.

If the building plan consists of more than one (approximately) rectangular parts with significant plan dimensions, the problems and uncertainties associated with the shape of the diaphragm may be avoided if the building is separated into two or more independent structural systems of rectangular plan (e.g. in two such parts for buildings with L- or T- shaped plan, or in three for U-, H- or Z- shaped plans,

[4]For a rectangular plan with a single re-entrant corner or edge recess, the limit is equivalent to, e.g., a recess of 20% of the outer floor dimension in one direction and of 25% of that in the other. If there are four such re-entrant corners or edge recesses, the limit is equivalent, to, e.g., a recess of 25% of the outer floor dimension in both directions.

etc.). The (seismic) joint between individual independent structural systems should be sufficiently wide to prevent pounding under the design seismic action, or, in the event that such pounding occurs, limit its consequences. The seismic joint may be filled, locally or fully, with a soft non-structural material. Eurocode 8 (CEN 2004a) prescribes the necessary width of the seismic joint as outlined below:

The maximum horizontal displacements of both independent structural units at right angles to the joint between them are calculated as follows for the design seismic action. If the analysis uses the design response spectrum (i.e. the elastic spectrum with 5% damping, divided by the behaviour factor q), then the floor displacement due to the design seismic action is taken as that from the analysis times the behaviour factor q adopted in the horizontal direction at right angles to the joint. If the analysis is nonlinear, the floor displacements are determined directly from the analysis for the design seismic action. Unless the analysis is of the response-history type, it only gives the peak values of floor displacements during the response. To account for non-concurrence of these peaks, the width of the seismic joint is taken as the square root of the sum of the squares (SRSS) of the peak horizontal displacements of the two units at the corresponding level. Eurocode 8 allows reducing the so-calculated width of the joint by 30%, if at every storey the floors of the two adjacent independent structural units overlap in elevation, so that there is no danger of one ramming vertical elements of the other within their clear height.

2.1.6 Torsional Stiffness About a Vertical Axis

If the building has a natural mode that is purely or primarily torsional about the vertical and has natural period longer than the lowest (purely or predominantly) translational mode, then accidental reasons may trigger twisting about the vertical, with transfer of vibration energy from the response in the lowest translational mode to the torsional one. The torsional response may induce significant and unforeseen horizontal displacements along the perimeter of the building, possibly driving some of the elements there to ultimate deformation.

Such situations should be prevented by proper conceptual design, notably by selecting a structural system whose predominantly torsional natural period is (much) shorter than the lowest translational period is each one of two orthogonal horizontal directions.

The relevant Eurocode 8 criterion for regularity in plan (supplementing those given in Section 2.1.5) is: The torsional radius of the storey in each of the two orthogonal horizontal directions, X and Y, of near-symmetry is not less than the radius of gyration of the floor mass:

$$r_x \geq l_s; \qquad r_y \geq l_s \tag{2.4}$$

The radius of gyration of the floor mass in plan, l_s, is defined as the square root of the ratio of:

– the polar moment of inertia in plan of the overlying masses with respect to the centre of mass of the floor, to
– the total overlying mass.

If the mass is uniformly distributed over the area of rectangular floors with dimensions l and b (including the floor area outside the outline of the vertical elements of the structural system), then $l_s = \sqrt{(l^2 + b^2)/12}$.

Fulfilment of Eq. (2.4) ensures that the period of the fundamental (primarily) translational mode in each of the two horizontal directions, X and Y, is not shorter than that of the lowest (primarily) torsional mode about the vertical axis Z. It prevents also strong coupling of the torsional and translational response, which is considered as uncontrollable and potentially very dangerous. As a matter of fact, as l_s is defined with respect to the centre of mass of the floor in plan, the "torsional radii" r_x and r_y that should be used in Eq. (2.4) for the desirable ranking of the three modes to be ensured are those with respect to the storey centre of mass, r_{mx} and r_{my}. These are related to the "torsional radii" r_x, r_y with respect to the storey centre of lateral stiffness as: $r_{mx} = \sqrt{r_x{}^2 + e_x{}^2}$, $r_{my} = \sqrt{r_y{}^2 + e_y{}^2}$.

If the elements of the lateral-load-resisting system are distributed in plan as uniformly as the mass, then Eq. (2.4) is satisfied at the margin. To meet Eq. (2.4), important lateral-load-resisting elements close to the centre in plan (e.g., strong walls around a service core housing elevators, stairways, vertical piping, etc.), should be balanced with perimeter elements (walls or frames) at least twice as stiff as those at the centre. Structural walls near the middle of all four sides of the plan, as in Fig. 2.2(a), is a recommended means to achieve this goal. If placed near the corners – where their effectiveness against torsional response may be significantly enhanced by giving them an L-shaped cross-section as in Fig. 2.2(b) – the walls restrain the shrinkage and may cause cracking of the floors. Moreover, it is difficult to provide fixity of corner walls at the foundation. Just three large walls at the perimeter as in Fig. 2.2(c) may be effective from the point of view of torsional stiffness about the vertical, but are less redundant against yielding or failure of just one wall. If the early-yielding wall is one of the two parallel ones, torsional stiffness may be significantly reduced. If it is the single wall in its direction, the lateral stiffness and strength in that direction may decrease very much.

Fig. 2.2 Arrangement of walls in plan: (**a**) preferable; (**b**) restraining the floors and difficult to provide foundation at the corners; (**c**) vulnerable in case of failure of an individual wall

2.1.7 Geometry, Mass and Lateral Stiffness Regular in Elevation

If the storey mass, or the horizontal dimensions, or the storey lateral stiffness of the building change significantly from storey to storey, then the shape of the fundamental mode in the two orthogonal horizontal directions may significantly differ from the heightwise linear one underlying the distribution of lateral forces to the individual floors postulated by most seismic design codes in the framework of the "equivalent static" or "lateral force" method of linear seismic analysis. So, most seismic design codes, including Eurocode 8 (CEN 2004a), do not allow using this procedure for heightwise irregular buildings.

Examples of significant heightwise variation of storey lateral stiffness are the following:

- A significant reduction in the cross-section (or even an interruption) of one or more important vertical elements from one storey to the next.
- A storey height significantly shorter than in the rest of the building (e.g., a "service" storey).
- A floor not extending throughout the building plan at a certain level (e.g., at a mezzanine).
- A storey significantly taller than the others (e.g., the ground storey, if the street level use, for retail, parking, etc. is completely different from the standard storeys above).

Figure 2.3 shows collapses of the upper floors in buildings with significant setbacks and Fig. 2.4 collapses at intermediate floors where the stiffness or strength of vertical elements was abruptly reduced.

Concentration of inelastic deformation demands at the level(s) where a drastic change in mass, geometry or storey stiffness takes place cannot be prevented solely through the choice of the method for linear analysis. Extreme irregularities in elevation, such as an increase in plan dimensions from the ground to the roof, or a large reduction in the cross-section (or even interruption) of important vertical elements from the upper storeys to the lower ones, should be avoided early on at the

Fig. 2.3 Collapse of upper storeys with reduced plan dimensions (*left*): Kalamata (GR) 1986; (*right*): Kocaeli (TR) 1999

Fig. 2.4 Middle-storey collapses due to abrupt changes in stiffness or resistance of vertical elements (Kobe 1995)

conceptual design stage, as their adverse consequences cannot meaningfully be prevented in subsequent stages of the design.

Very good guidance for the conceptual design of regular in elevation buildings are the relevant code criteria. Particularly useful are the criteria of Eurocode 8 (CEN 2004a), as they are qualitative and hence easy to apply at the conceptual design stage. According to them, a building is characterised as regular in elevation, if it meets all of the following criteria:

1. The storey mass and lateral stiffness are either constant in all storeys, or decrease gradually and smoothly from the base to the roof.
2. All lateral-load-resisting sub-systems (frames, walls, etc.) continue from the foundation to the top of the corresponding part of the building.
3. Individual setbacks of each side of the building do not exceed 10% of the parallel dimension of the storey below (see Fig. 2.5).
4. If setbacks are not symmetric at opposite sides of the building, the total setback of the roof at each side with respect to the base does not exceed 30% of the parallel dimension at the building base (Fig. 2.5).
5. If there is a single setback within the lowest 15% of the total height of the building, it does not exceed 50% of the parallel dimension at the base of the building. In that particular case, there should be no over-reliance on the enlargement of

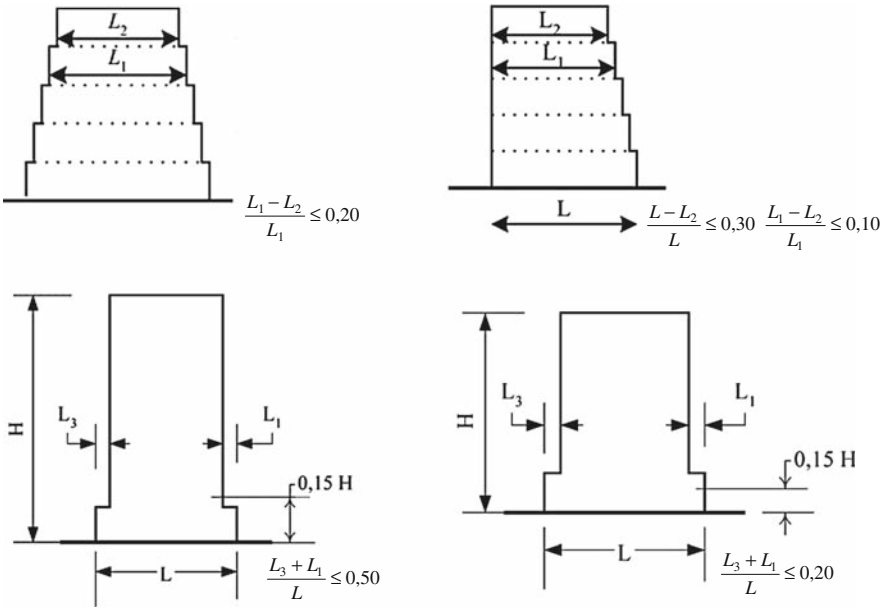

Fig. 2.5 Eurocode 8 criteria for regularity in elevation of buildings with setbacks

the structure plan at the base (the "podium") for the transfer to the ground of the seismic shears that develop in the overlying tower. These shears should be transferred mainly through the continuation of the framing of the tower to the ground; the "podium" should transfer to the ground mainly its own seismic shear (see Fig. 2.5).

6. In frame buildings, there is no abrupt variation of the overstrength of individual storeys, including the contribution of masonry infills to the storey shear strength, (see Section 2.1.13.3) with respect to the design storey shear. If the lateral-load-resisting system meets criteria no. 1 and 2 above, the storey overstrength criterion may be considered as fulfilled, unless there are abrupt variations of infills from storey to storey. In that latter case the storey shear force capacity will need to be determined. Normally, it may be computed by summing up over all vertical elements the ratio of moment capacity at the storey bottom to the corresponding shear span (half of clear storey height for columns, or about half the distance from the storey bottom to the top of the building for walls) and the shear strength of all infill walls (about equal to the minimum horizontal section area of the wall, times the shear strength of bed joints). However, the moment resistance of vertical elements is not known at the time the designer needs to characterise the building as regular in elevation or not. At that stage it may be presumed that the subsequent detailed design of the vertical elements of the lateral-load-resisting system will provide them with a total storey force resistance equal to the design seismic shear in the corresponding horizontal direction. Then, the value of η

in a storey with reduced infills, given by Eq. (2.7) in Section 2.1.13.3, may be conveniently used for the characterisation of the frame building as regular or not in elevation on the basis of the storey overstrength. If it does not exceed 1.1, the storey overstrength in the building may be considered as regular in elevation.

Criterion 1 refers to the storey mass and lateral stiffness and not to the storey dimensions of the framing in plan. On the other hand, criteria 4 and 5 refer specifically to reductions of a storey plan dimension with respect to the underlying storey. According to the letter of these criteria, buildings with storey overhangs are not necessarily considered as heightwise irregular. However, in essence they are. So, a sound conceptual design will avoid overhangs in the structural system.

The criteria of US codes (BSSC 2003, SEAOC 1999) for regularity in elevation are quantitative, based on the variation of mass, lateral stiffness and strength from storey to storey. According to these criteria a building is considered as irregular in elevation, if:

- the mass of any storey exceeds by 50% that of an adjacent storey; or
- the horizontal dimension of the lateral-load-resisting system exceeds by at least 30% the parallel dimension of an adjacent storey; or
- the stiffness of any storey is less than 70% of that of the overlying storey, or less than 80% of the average stiffness of the three storeys above.

An "extreme soft storey" is one with stiffness less than 60% of the stiffness of the storey above, or 60% of the average stiffness of the three overlying storeys.

Although quantitative, the US criteria are easy to check and apply at the conceptual design stage, because, for the purposes of the last bullet point or of the identification of an "extreme soft storey", the storey lateral stiffness may be evaluated on the basis of the sum of the ratios, EI/h, of vertical elements. At subsequent design stages it is preferable to evaluate changes in the storey lateral stiffness on the basis of the ratio of storey shear to interstorey drift from linear analysis (be it according to the "lateral force" or "equivalent static" method). If the results of such an analysis are available, US seismic design codes allow considering a building as heightwise regular irrespective of the criteria in the three bullet points above, provided that at any storey other than the two uppermost ones the interstorey drift ratio does not exceed 130% of the interstorey drift ratio in the overlying storey.

2.1.8 Lateral Resistance Characterised by Regularity in Elevation

Heightwise irregularities of the ratio of storey lateral strength to the corresponding seismic demand may have much more adverse consequences than those of storey mass, stiffness or even dimensions in plan. Reasons are not limited to the inability of elastic analysis – be it of the multimodal response spectrum type – to capture the effects of such irregularities. The prime reason is that, unless the distribution of available resistance follows the seismic force demands, the fundamental objective

of earthquake-resistant design, namely the control of inelastic seismic response and of the plastic mechanism by spreading the inelastic deformation demands over the full height of the building (cf. Section 1.3.2) cannot be met. Inelastic deformation demands may be concentrated in storeys where the available lateral strength is closest to the seismic demand. In a worst case scenario, a soft storey may ensue, leading to collapse.

An undesirable type of overstrength is that of beam moment resistances with respect to the corresponding seismic demands. It may show up in beams of the upper storeys with the minimum longitudinal reinforcement of the design code. Beam cross-sectional dimensions should be as small as reasonably feasible, so that their longitudinal reinforcement is controlled by the corresponding seismic action effects and not by minimum requirements. The ideal beam size is the one for which at each beam end the following design moments are equal:

- the moment due to the factored gravity loads (in the "persistent and transient" design situation in Eurocode terminology), which is practically independent of the beam depth, and
- the moment due to the design seismic action together with the quasi-permanent gravity loads (the "seismic design situation" of the Eurocodes), which increases with increasing beam depth.

The most dangerous overstrength is one that may cause a storey-sway plastic mechanism at a certain storey before a beam-sway mechanism over the full height of the structure above ("soft storey", see Fig. 1.3(a)). This may happen in frames where the capacity design condition applied over all joints of the frame as: $\Sigma(\Sigma M_{\mathrm{Rb}}) < \Sigma(\Sigma M_{\mathrm{Rc}})$ is not met at certain storeys. To avoid such situations, at the conceptual design stage cross-sections should be selected much smaller in beams than in columns.

Seismic design codes emphasise the importance of avoiding irregularity of overstrength in elevation for the prevention of "soft-storeys". US codes consider the risk of soft-storey development as "significant" or "very large", if the storey strength (in terms of the storey shear) is less than 80% or 65%, respectively, of the storey above. In cases of "very large" risk of soft-storey development, the building is limited to two storeys or to a height of 9 m.

An important and common source of irregularity in storey overstrength is the heightwise irregularity of masonry infills, shortly mentioned in Section 2.1.7 under criterion no. 6 of Eurocode 8 for irregularity in elevation, but addressed in detail in Section 2.1.13.3.

2.1.9 Redundancy of the Lateral Load Resisting System

Architectural functionality, pressures on budgets or construction time, as well as the application of higher grades of steel and concrete, have promoted in recent years a trend towards increased column spacing and the use of only few, but strong walls in

a building. So modern buildings may rely for earthquake resistance on fewer vertical elements per unit floor area than those of the past, may have less back-up capacity and may be more vulnerable in case a single element fails early.

The importance of system redundancy and of multiple force paths can be appreciated with reference to Fig. 2.2 (especially to (c)), in case the walls shown there are indeed the only means of earthquake resistance in the corresponding horizontal direction. This is not prudent.

Redundant structural systems with many lateral-load-resisting elements and alternative paths for earthquake resistance have also a significant overstrength margin between the value of the seismic base shear corresponding to first yielding anywhere in the structural system, V_1, and the base shear that turns the system into a plastic mechanism, V_u. Recall that force-based seismic design, with lateral forces obtained from an elastic response spectrum divided by the behaviour factor q, is founded on the dependence of the q-factor on the displacement ductility factor, μ_δ, (cf. Eqs. (1.1) and (1.2)) of a SDOF system with elastic-perfectly plastic dependence of the base shear, V_b, on a representative lateral displacement, e.g. at the top. So, for the quantification of the behaviour factor, q, the relationship between V_b and the top displacement, δ_{top}, of the building – as obtained, e.g., from pushover analysis – should be idealised as elastic-perfectly-plastic. The perfectly plastic branch of such an idealisation is at a base shear $V_b = V_u$. However, the seismic action for force-based design using the reduced (by q) elastic spectrum corresponds to the base shear V_1 at first yielding anywhere in the system, in the sense that member dimensioning for the ULS in flexure on the basis of the seismic action effects from the elastic analysis corresponds to yielding of the section(s) dimensioned. Therefore, the ratio $\alpha_u/\alpha_1 = V_u/V_1$ expresses the overstrength margin between the base shear at first attainment of the aim of dimensioning for the design seismic action, V_1, and the ultimate strength of the elastic-perfectly plastic system for which q is defined. It is for this reason that Eurocode 8 (CEN 2004a) gives the q-factor of concrete buildings as the product of a value characterising the inherent ductility of the structural system and of its detailing, times the factor $\alpha_u/\alpha_1 = V_u/V_1$ (see Fig. 1.12 and Section 1.4.3.1). This factor expresses the overstrength of the structural system due to redundancy and ability to redistribute internal forces after first yielding. As it is not very convenient for the design to use the exact value of α_u/α_1 from a pushover analysis of the structure after its detailed design is complete, Eurocode 8 provides default values that express the inherent redundancy of the structural system. These values range from 1.0 in buildings with just the minimum number of two uncoupled walls per direction (as in Fig. 2.2), to 1.3 in the more common case of multi-storey multi-bay frames (cf. Section 1.4.3.1).

Instead of providing a bonus to the q-factor value due to enhanced redundancy, US codes penalise the R-factor value for lack of redundancy. This is accomplished through an empirical factor ρ which multiplies the storey design seismic forces (and effectively divides the R-factor value used for the storey). The rules in (BSSC 2003) for the determination of the value of ρ are simpler and have been summarised at the end of Section 1.4.3.2. Those in (SEAOC 1999) are further elaborated here, as a guide for the choice of a redundant system:

According to (SEAOC 1999) ρ cannot be taken greater than 1.5. Its value depends:

- on the ratio of the maximum seismic shear in any one among all vertical elements in a storey, to the total storey shear V_{storey}, and
- on a characteristic plan dimension L_{plan}, equal to the square root of the floor plan A.

For purely frame systems (SEAOC 1999) gives:

$$\rho_{\text{frame}} = 2\left(1 - \frac{V_{\text{storey}}}{V_{\text{max,col}}}\frac{L_{\text{o}}}{L_{\text{plan}}(m)}\right) \tag{2.5}$$

In Eq. (2.5) $V_{\text{max,col}}$ is the largest sum in the storey of the seismic shear forces among any two adjacent columns, with the seismic shear of interior columns multiplied by 0.7, and $L_{\text{o}}. = 3$ m (more precisely $L_{\text{o}}. = 10$ ft, i.e. 3.05 m). A minimum number of columns should be provided in "Special Moment Frames" such that $\rho_{\text{frame}} < 1.25$, which corresponds to $V_{\text{max,col}}/V_{\text{storey}} < 8/L_{\text{plan}}$ (m). The optimum number of columns in the storey is the one that gives $V_{\text{max,col}}/V_{\text{storey}} < 2L_{\text{o}}/L_{\text{plan}}$, for which $\rho_{\text{frame}} = 1$.

For purely wall systems (SEAOC 1999) gives:

$$\rho_{\text{wall}} = 2\left(1 - \frac{V_{\text{storey}}}{V_{\text{max,wall}}}\frac{\max\left(L_{\text{o}}; l_{\text{w}}\right)}{L_{\text{plan}}}\right) \tag{2.6}$$

where $V_{\text{max,wall}}$ and l_{w} are the seismic shear and the horizontal dimension – length – of the wall with the largest seismic shear in the storey. If $V_{\text{max,wall}}/V_{\text{storey}} < 2\max(L_{\text{o}}; l_{\text{w}})/L_{\text{plan}}$ (giving $\max(L_{\text{o}}; l_{\text{w}}) > L_{\text{plan}}/4$ in the extreme case of $V_{\text{max,wall}} = 0.5V_{\text{storey}}$), then ρ=1 and there is no penalty on the design. If $V_{\text{max,wall}}/V_{\text{storey}} > 4\max(L_{\text{o}}; l_{\text{w}})/L_{\text{plan}}$ (e.g. if $\max(L_{\text{o}}; l_{\text{w}}) < L_{\text{plan}}/8$ for $V_{\text{max,wall}} = 0.5V_{\text{storey}}$), then we have the heaviest penalty, i.e. $\rho = 1.5$.

Dual systems consisting of concrete frames – that are inherently flexible – and structural walls – which are inherently stiff – are considered to have higher overstrength and larger reserves in the event of premature failure of one or few elements. So, provided that the frame can stand-alone sustain at least 25% of the seismic base (SEAOC 1999) allows taking the value of ρ for a dual system as 80% of the largest among the values given by Eqs. (2.5) and (2.6) for the frames or the walls of the system, respectively. In the lower storeys, where the walls resist most of the design storey shear, there is no penalty (i.e. $\rho = 1$) if $V_{\text{max,wall}}/V_{\text{storey}} < 8l_{\text{w}}/(3L_{\text{plan}})$. The penalty is maximum possible ($\rho = 1.5$) at the lower storeys, if there $V_{\text{max,wall}}/V_{\text{storey}} > 16l_{\text{w}}/L_{\text{plan}}$. Near the top, it is the frame that resists most of the storey seismic shear. Then there the maximum and the minimum penalty ($\rho = 1.5$ and $\rho = 1$, respectively) correspond to $V_{\text{max,col}}/V_{\text{storey}} > 16L_{\text{o}}/L_{\text{plan}}$ and to $V_{\text{max,col}}/V_{\text{storey}} < 8L_{\text{o}}/(3L_{\text{plan}})$, respectively.

The above rules and bounds of the SEAOC recommendations can be used to advantage during conceptual design as guides against over-reliance of earthquake resistance on few strong elements.

2.1.10 *Continuity of the Force Path, Without Local Concentrations of Stresses and Deformation Demands*

Inertia forces should find their way to the foundation via a smooth and continuous path in the structural system. From this point of view, cast-in-situ reinforced concrete is the ideal structural material for earthquake resistant construction, compared to prefabricated elements – be it of timber, steel or precast concrete – assembled on site. The joints between such elements are inherently points of discontinuity in the flow of forces. Speaking of prefabricated concrete buildings, the joints between different elements may fail, either by failure of the joining element itself, or because of damage of the concrete around the fastenings of this element.

The prime implication of the requirement for continuity of the force path in buildings of cast-in-situ concrete is that floor diaphragms should have sufficient strength for the transfer of inertia forces to the lateral load resisting system and from one element to the other and should be adequately tied into it. Ordinary cast-in-situ concrete slabs generally have the necessary in-plane strength and stiffness, provided that they have the minimum reinforcement for crack control in both horizontal directions. The same cannot be said for floors consisting of precast concrete segments joined together and with the structural system via a lightly reinforced, few-cm-thick cast-in-situ topping, or for waffle slabs with a thin and lightly reinforced top slab. Figure 2.6 shows typical building collapses in the Spitak (Armenia) earthquake of 1988, due to insufficient connection of the precast floors to the load-bearing concrete walls. Many parking garage structures built of precast concrete in the Los Angeles area collapsed also in the Northridge (1994) earthquake. Large openings in floor slabs, for interior atriums and patios or for large elevator shafts or stairways, etc.,

Fig. 2.6 Collapse of buildings with precast floors inadequately connected to the walls (Spitak, Armenia, 1988)

may also disrupt the continuity of the force path, especially if they are next to large structural walls near the perimeter of the building plan. Section 2.4.4 presents a real case of a multi-storey building with L-shaped floor plan, where floor diaphragms with large openings at critical locations contributed to the collapse of one of the two wings. In Section 2.4.2 the tearing of the floor diaphragms during the collapse of one of the two wings of another 6-storey buildings with L-shaped floor plan is attributed to the complete lack of secondary reinforcement in one-way floor slabs.

Continuity of the force path should not be limited to the floor diaphragms that transfer inertia forces from their source to the lateral load resisting system and from one element of that system to the other. The load path should be continuous within the lateral-load resisting system itself. Points or cases where the continuity of the structural system may be disrupted, include:

- strongly eccentric connections of beams to columns,
- beams supported indirectly on other beams or girders (instead of framing into beam-column joints),
- an offset of a beam with respect to those of adjacent span(s),
- column axes offset with respect to those of the adjacent storey,
- "floating" columns or walls, supported by a beam or girder and not continuing to the ground,
- walls that are supported by a pair of columns (instead of continuing to the foundation).

The current State-of-the-Art is not sufficiently advanced to describe with much confidence the behaviour under cyclic loading of regions of discontinuity like the ones above.

Regarding connections, our present knowledge of their cyclic behaviour is limited to concentric ones of simple geometry. Because connections are crucial for the seismic performance of the system, the designer should choose for them a geometry that ensures a smooth and continuous load path. Simplicity and clarity is at least as important at the microlevel (i.e., at the connections) as at the macrolevel (for the structural system). Complex structural layouts can be analysed with certain degree of confidence using sophisticated models and techniques. This cannot be claimed, by contrast, of geometrically complex connection details.

For the reasons above Eurocode 8 (CEN 2004a) limits the eccentricity between the axes of the beam and the column at connections of ductile frames (of Ductility Classes M or H) to 25% of the column width, which is considered sufficient for the smooth flow of forces from one element to the other.

2.1.11 Effective Horizontal Connection of Vertical Elements by Floor Diaphragms at All Floor Levels

Floor diaphragms and beams should tie together the vertical elements of the lateral-force-resisting system at all horizontal levels where significant masses are

Fig. 2.7 Collapse of precast concrete buildings: (**a**)–(**c**) in Athens 1999; (**d**) in Spitak (Armenia) 1988

concentrated, as well as at the foundation level. This is essential for the effective transfer of inertia forces from the masses – mainly concentrated at the floors – to the lateral load resisting system and for the integration of this system as a whole. Figure 2.7 shows collapsed buildings consisting of precast concrete elements with the tops of columns not connected at roof level, floor diaphragms poorly tied to floor beams and floor beams with insufficient seating.

In the analysis for the seismic action floor diaphragms are commonly modelled as rigid. A rigid diaphragm over any horizontal level where significant masses are concentrated is convenient from the modelling point of view, enhancing the clarity of the global dynamic response of the system. In this respect, diaphragms that indeed act as rigid serve a fundamental objective of conceptual seismic design, namely the reduction of uncertainty about the expected seismic response and performance. To illustrate the point, consider the long building of Fig. 2.8, with the diaphragm spanning over the large distance of the two end frames, where walls resist practically the full transverse seismic action. To transfer the floor inertia loads to the end frames floor diaphragms may flex like horizontal deep beams simply supported at the two ends. In low-rise buildings with thin diaphragms the in-plane deflection of the long diaphragm between the end frames may be significant. If so, the distribution of seismic shears between the middle and the end frames may differ from the one intended with the diaphragms considered rigid. The middle frames may be overloaded

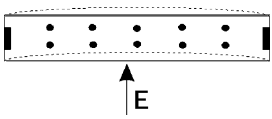

Fig. 2.8 In-plane bending of diaphragm in building with large aspect ratio in plan and strong walls just at the end frames

compared to the predictions obtained from the rigid diaphragm hypothesis and may yield earlier than expected. They may even fail prematurely, if, for instance, they have been designed only for gravity loads and have not been detailed to sustain large inelastic deformations (i.e., as secondary seismic elements, see Section 4.12).

To fulfill their role, diaphragms should have not only sufficient in-plane stiffness to act as rigid, but also sufficient strength to remain elastic and – if practicable – uncracked during the inelastic seismic response of the structural system. Solid concrete slabs having thickness at least 120 mm and at least the minimum reinforcement for crack control at top and bottom surface and in both horizontal directions are sufficient, provided that:

- all storeys have similar planwise distribution of lateral stiffness,
- the slab is at the same horizontal level throughout every storey, and
- the slab continuity in plan is not seriously impaired by large openings.

Demands on the diaphragms are increased, if important elements of the lateral-force-resisting system are discontinued vertically. In such cases the diaphragm has to transfer horizontally not only the inertia loads of the storey but also shear forces from certain location(s) in plan to others. As an example, if the lowermost storey – sometimes serving as a basement – has a concrete wall all along its perimeter, the diaphragm at the top of that storey has to transfer very large shear forces from all interior vertical elements to the perimeter wall. Dual structural systems are another example, as in the lower storeys the walls restrain the frames, while by contrast at the upper ones the frames restrain the walls, always through transfer shears in the diaphragms. The transfer of floor inertial loads to the vertical elements, or that of seismic shears from certain vertical elements to others, induces significant shear stresses in the diaphragm. To withstand them, concrete diaphragms should have two-way reinforcement, preferably at both surfaces (top and bottom). Shear stresses are normally larger at the interior than at the perimeter.

Diaphragms spanning a distance between strong and stiff vertical elements much longer than their transverse dimension in plan develop significant in-plane bending (see Fig. 2.8). In-plane flexural deformations and stresses are significant also in rectangular diaphragms with large aspect ratio, or in L-, T-, U- or H-shaped diaphragms without seismic joints between the individual rectangular parts. Similarly in diaphragms with large openings for patios, elevator shafts, staircases, etc. Flexural stresses are normally larger at the edge of the diaphragm, especially at recesses and re-entrant corners. To resist these stresses without excessive cracking, continuous longitudinal reinforcement should be provided along the edges. The

seismic action induces significant flexural stresses only along the edges that are at right angle to its direction, while it does not fully stress perimeter beams along these edges. So, part of the (top and bottom) longitudinal reinforcement of these beams is available to resist the peak flexural stresses in the diaphragm. There is no problem if the edge of the diaphragm cantilevers beyond the exterior beams, especially if it has the minimum secondary reinforcement parallel to the edge. Any cracks that may develop there at right angle to the edge will stop at the beam. If there is no beam near an edge of the diaphragm – e.g., along the perimeter of large recesses or openings in plan, for patios, etc. – diaphragm stresses there should be resisted by an edge band of reinforcement with sufficient anchorage length, especially at re-entrant corners.

An effective horizontal connection of the vertical elements at the level of the foundation reduces significantly the uncertainty of the response. Although the seismic action is commonly perceived as a system of inertia forces that develops in the superstructure and needs to be safely transferred to the ground, in reality it is a dynamic displacement imposed to the base of the structure. Therefore, foundation elements may move separately, unless they are tied horizontally into an integral system moving together as a whole. The seismic response of the superstructure is not easily predicted if foundation elements can move separately. Section 2.3 treats the conceptual design of the foundation system.

2.1.12 Minimal Total Mass

The maximum elastic base shear and the peak top displacement, elastic or inelastic, due to a horizontal component of the design seismic action depend on the value of the fundamental translational period in that horizontal direction, T. In concrete buildings the value of T that determines the peak elastic force and inelastic displacement demands corresponds to members that are fully cracked and at incipient yielding of the end section(s). Its value is either within the constant spectral pseudoacceleration range of the elastic response spectrum, or, more often, in the constant spectral pseudovelocity range. In the first case, the peak elastic base shear and the maximum elastic or inelastic displacement demand are proportional to the total mass of the building, M. In the second case they are proportional to $\sqrt{M}$. Any reduction of M that is feasible, reduces therefore the peak seismic response.

The lateral force resisting system itself does not contribute significantly to the total mass of the building. Therefore, the type of the structural system and the sizes of its members should be chosen on the basis of their stiffness, strength and deformation capacity, without any mass considerations. A reduction of the total mass of a building with a concrete structural system should be pursued by:

- avoiding heavy finishings, claddings and veneers;
- reducing the thickness of concrete slabs to the minimum required for serviceability, durability, fire rating and strength under gravity loads and for their role as diaphragms under seismic loading;

– using relatively lightweight partitions and exterior walls, but not to so flimsy that they will suffer heavy damage under frequent or occasional earthquakes;
– avoiding a massive roof or unnecessarily heavy pieces of equipment (which are also unfavourable from the point of view of mass regularity in elevation).

2.1.13 Absence of Adverse Effects of Elements Not Considered As Part of the Lateral-Load Resisting System and of Masonry Infills in Particular

2.1.13.1 Overview of Potential Adverse Effects – The Position of Eurocode 8 on Masonry Infills

In addition to the vertical elements (walls and columns) and the beams framing into them, which form the system charged with the task of resisting the seismic action, some elements may have secondary role in, and contribution to earthquake resistance – or considered so by the designer, for convenience. If these elements are of structural concrete, they fall in the category of "secondary members"; which are designed for non-seismic (e.g., gravity) actions as normal structural members, but – at least for the design of new buildings – are not relied upon for lateral load resistance and are subject to special verification rules. Section 4.12 deals at length with the design of such structural elements in new buildings and their modeling for the purposes of seismic analysis. It also gives – be it indirectly – certain conceptual guidance for them.

A special case of structural members normally discounted for lateral load resistance and neglected in seismic design (or at most considered as "secondary members") are the concrete stairs. Specific guidance on how a staircase may be included in the model is given in Section 4.9.6 for a linear seismic response analysis and in Section 4.10.5 for a nonlinear one. Besides, in Section 4.10.5.3 staircases are modelled and verified in two case studies of nonlinear seismic response analysis. However, staircases are not specifically dealt with in Section 4.12. So, their potential adverse effects on (local or global) seismic performance are addressed here, while some guidance for conceptual design is given in Section 2.1.13.5.

Non-structural elements, notably masonry infills, may also interfere in the seismic response with means other than their mass. Non-structural masonry is commonly used around the world, especially in seismic-prone southern Europe, to infill the structural framing of concrete buildings. The masonry is built after casting the surrounding frame and in contact to it, but without positive attachment. At least for concrete buildings, masonry infills are still the most cost-effective means for partition and sound insulation between different compartments of the same storey and as external cladding with good insulation (thermal and for sound) and waterproofing properties.

Field experience and analytical and experimental research (Fardis and Panagiotakos 1997b, Fardis 2000) have demonstrated their overall beneficial effect on seismic performance, especially when the building structure itself has poor engineered

earthquake resistance. Infill panels that are effectively confined by the surrounding frame:

- impart lateral stiffness to the building, reducing seismic deformation demands on storeys and members,
- increase, through their in-plane shear strength, the storey lateral force resistance and
- contribute, with their hysteresis, to the global energy dissipation capacity.

In buildings designed for earthquake resistance non-structural masonry infills normally constitute a second line of defence and a cost-effective source of significant overstrength. This is how Eurocode 8 (CEN 2004a) sees infills. It does not encourage the designer to reduce the seismic action effects for which the structure is designed thanks to the overall beneficial effect of infills. At the same time, acknowledging this overall beneficial effect, Eurocode 8 does not penalise the design seismic action effects of the structure for the presence of infills, as some national codes do. For the same reason, and to avoid the special detailing needed for waterproofing and out-of-plane stability of infills separated from the surrounding structural frame, it does not adopt the position of few seismic design codes (e.g., those of New Zealand and Russia) to isolate the infills from the frame through appropriate joints.[5]

If the contribution of masonry infills to the lateral strength and stiffness of the building is large relative to the strength and stiffness of the structure itself, the infills may override the seismic design of the structure and undermine the efforts of the designer and the intention of design codes to control the inelastic response by spreading the inelastic deformation demands throughout the structure. In particular:

- loss of integrity of the infills in the ground storey may produce a soft storey and trigger global collapse;
- if infills are non-uniformly distributed in plan or in elevation, inelastic deformation demands will concentrate in the part of the building which has more sparse infills (i.e., at the "flexible" side of a building asymmetrically infilled in plan, or at the "weak" or "soft" storey of the infilled frame);
- local effects of infills may cause pre-emptive brittle failure of frame members, notably columns.

Eurocode 8 (CEN 2004a) stands out among the major seismic design codes for new concrete buildings, in providing specific guidance to the designer, or even mandatory rules, as safeguards against local or global detrimental effects of masonry infills, without explicitly accounting for the individual infill panels in the model

[5] As a matter of fact, to avoid contact of the infill and the columns under the interstorey drifts induced in a bare frame by the design seismic action, a joint between them would need to have a width of several centimetres.

for the seismic analysis. Any Eurocode 8 rules presented in Sections 2.1.13.2 and 2.1.13.3 are mandatory, if the structure itself is designed for relatively low lateral stiffness and strength and high ductility and deformation capacity. This is the case of frame systems and of frame-equivalent dual ones (where at least 50% of the seismic base shear is resisted by frames) of Ductility Class High (DC H). Concrete buildings of the lower Ductility Classes (L or M) are considered as designed for sufficient lateral strength to overshadow the infill walls. Wall systems and wall-equivalent dual ones (where at least 50% of the seismic base shear is resisted by walls) are also considered as sufficiently stiff, not to be affected by the presence of masonry infills. For such systems of any Ductility Class, and for Ductility Class L or M frames and frame-equivalent dual systems the safeguards in Eurocode 8 against the negative effects of infills presented in Sections 2.1.13.2 and 2.1.13.3 are not mandatory. However, Eurocode 8 advises designers to take them into account even for such systems, as guidance for good practice.

The Eurocode 8 provisions against the adverse effects of infills do not apply if there is positive structural connection between the masonry and the surrounding frame, through shear connectors, or other ties, belts or posts. In that case, Eurocode 8 considers the structure as a confined masonry building, rather than as a concrete structure with masonry infills.

The rest of Section 2.1.13 highlights the potential global or local detrimental effects of masonry infills and the design measures specified or recommended by Eurocode 8 for their mitigation. We should keep in mind, though, that the best solution to any potential problem is to avoid the problem altogether. It is the architectural design that sets out the layout of infills in plan and elevation, as well as the size and location of openings next to or between columns. It is there that appropriate decisions should be made, or design modifications implemented. If this is not feasible, the structural designer should consider changes in the lateral-load-resisting system, to mitigate certain global or local adverse effects of the infills. It is only when such conceptual design measures are not sufficient, that recourse to the specific relevant rules of Eurocode 8 should be pursued.

2.1.13.2 Irregular Layout of Infills in Plan

An asymmetric layout of the infills in plan may cause torsional response to the translational horizontal components of the seismic action. Owing to the torsional component of the response, structural members on the sides of the plan which have fewer infills (“flexible” sides) will be subjected to larger deformation demands than those on the opposite, heavier infilled, side(s). It is not prudent to counteract an asymmetric layout of the infills with a reversely asymmetric layout of the lateral-load-resisting system. This will create problems in the calculation of the static eccentricities and their checks (e.g., through Eq. (2.1)), as well as in the seismic analysis, all of which, according to the seismic design code, should be based on the lateral-load-resisting system alone neglecting the infills. Fortunately, analytical and experimental research (Fardis et al. 1999a) has shown that the adverse consequences

of an asymmetric layout of infills in plan are not so serious. The increase in lateral strength and stiffness due to the infills makes up for the uneven distribution of inter-storey drift demands over the plan. In other words, when infilling is asymmetric, the maximum lateral displacements at a certain point of the structural system do not exceed (at least appreciably) the maximum demands at that point in a similar un-infilled structure. However, as local member deformation demands might exceed those estimated from an analysis neglecting the infills, Eurocode 8 (CEN 2004a) requires doubling the accidental eccentricity (see Sections 2.1.5 and 4.8.1) in the analysis of structural systems with planwise irregular infills that are not included in the analysis model. This requirement does not unduly penalise the design procedure or the structural system. It is also effective, especially when the structural system is almost fully symmetric and regular in plan. In that case the results of a seismic response analysis without accidental eccentricity have no torsional features.

A strongly asymmetric layout of infills may cause severe irregularity in plan. If buildings are practically in contact with each other in the city blocks, the corner ones have solid infills along the two adjacent sides of the perimeter to the inside of the block, while the ones on the street sides have either no infills at all, or large openings in them. As a matter of fact, corner buildings seem to have larger incidence of severe damage or collapse in earthquakes, although sometimes this is attributed to pounding or to the lower subsoil strength on the street side because of smaller overburden. Eurocode 8 does not consider doubling the accidental eccentricity sufficient for such cases of severely irregular in plan infilling. It requires instead analysis of a 3D structural model explicitly including the infills. Moreover, given the uncertainty about the properties, the modelling and even the future layout of the infills and their openings, Eurocode 8 requires also a sensitivity analysis of the effect of the stiffness and the position of the infills. It mentions as (a main) part of such a sensitivity analysis disregarding one out of three or four infill panels per planar frame, especially on the more flexible sides. Unfortunately, other than stating that infill panels with two or more significant openings should not be included in the model, Eurocode 8 does not provide any guidance for modelling infill panels.

For buildings with asymmetric layout of infills in plan Eurocode 8 draws the attention of the designer to the verification of structural elements furthest away from the side where the infills are concentrated ("flexible side") for the torsional response due to the infills. If there are stiff and strong infills along two adjacent sides of the perimeter, the response to the horizontal components of the seismic action is nearly torsional about the common corner of these two sides. It turns out that in vertical elements close to that corner the peak deformation and internal force demands computed for separate action of these two components on the system without the infills take place simultaneously (Fardis 2000, Fardis et al. 1999a). So, regardless of whether the infills are taken into account or not in a 3D structural model, the seismic action effects in these vertical structural elements due to the two horizontal components would better be taken to occur simultaneously, instead of combined in accordance with Section 4.7.

2.1.13.3 Irregular Distribution of Infills in Elevation

A soft and weak storey may develop wherever along the height of a multistorey building the infills are reduced compared to the overlying storey. The consequences on the global seismic performance are most critical in buildings with an (almost) open ground storey. Owing to commercial use or parking facilities at street level, unfortunately this seems to be the most common case of infill irregularity in elevation.

A reduction of the infills in a storey relative to the ones above increases the inelastic deformation demands on the columns of that storey, owing to:

- concentration of the global lateral drift demands to that storey (soft/weak storey effect); and
- the near-fixity conditions of the columns of that storey at floor levels, as the infill panels of neighbouring storeys restrain the drift there (and hence the flexural deformations of the beam as well).

The second of these reasons is explained as follows, with reference to Fig. 2.9 and to the definition of chord rotation at the end of a member in Fig. 1.4 of Section 1.3.2. The interstorey drift ratio of the frame (i.e. the relative horizontal displacement of the two floors, divided by the storey height) is equal to the sum of:

- the chord rotation of the columns of the storey (average chord rotation at the top and bottom joints over all columns of the storey), plus

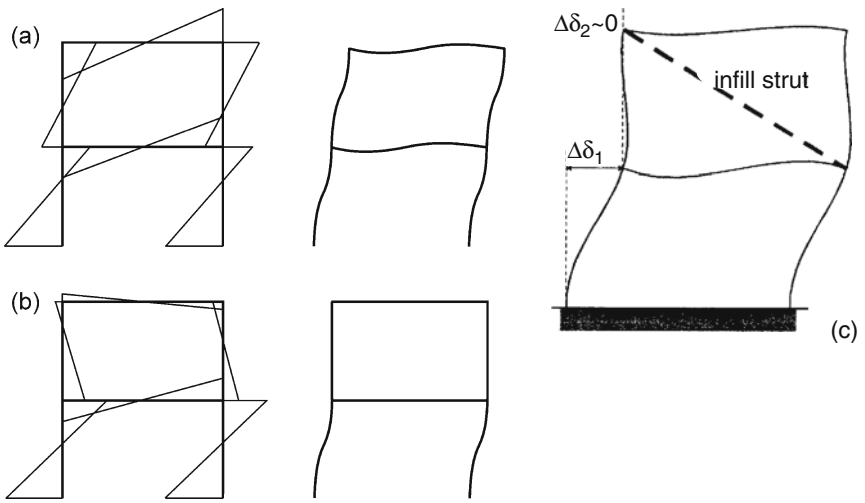

Fig. 2.9 Two-storey frame: (**a**) bending moments and deformation of frame without infills; (**b**), (**c**) bending moments and deformation of frame with stiff infills in 2nd storey

– the chord rotation of the floor beams above and below (average chord rotation at the two ends over all beams of the two floors above and below the storey columns).

Owing to the contribution of infills to their lateral stiffness, the storeys above and below the one with the reduced infills develop low interstorey drift ratio(s). So, the floor beams just above and below the less infilled storey develop small chord rotations demands and hence are protected from damage. The (large) interstorey drift ratio demand in this storey develops almost exclusively through chord rotations at the top and bottom ends of its columns, which explains their higher damage and vulnerability. Moreover, these columns cannot be effectively protected from plastic hinging through application of the capacity design rule, Eq. (1.4). The reason is the following (Fardis et al. 1999b): As the storeys above and below that with less infills develop low interstorey drift ratios, chord rotations at the ends of their columns will also be very low. As a matter of fact, if the infills of these storeys are very stiff and strong, chord rotations there may have opposite sign in the columns and in the beams, so that their algebraic sum gives indeed a low interstorey drift ratio. This is the case at the 2nd storey of the frame in Fig. 2.9(b) and (c). Because the moments at column ends have magnitude directly related to that of chord rotations there, the ends of columns in the less infilled storey will receive very little help from the other column section across the joint to resist the sum of beam flexural capacities, ΣM_{Rb}, around the joint, without yielding (Fardis 2000, Fardis et al. 1999b). The end result is that, fulfilment of Eq. (1.4) at the joints of the frame notwithstanding, plastic hinges may develop in the columns of the storey with the less infills (see Fig. 3.27(a) and (b) for two examples). Chord rotation demands at these plastic hinges may be large enough to exhaust their capacities. The end result may well be storey collapse. This is often the case when the ground storey is open, while the overlying ones are fully or partially infilled (see Fig. 2.10 for examples).

To prevent plastic hinging at top and bottom and collapse of columns in a storey where infills are less than in the overlying one, Eurocode 8 (CEN 2004a) requires designing these columns to remain elastic until and after the infills of the overlying storey attain their ultimate force resistance. To achieve this, the deficit in infill shear strength in a storey should be compensated by an increase in the resistance of the frame (vertical) members there. More specifically, the seismic internal forces in the columns (bending moments, axial forces, shears) from the analysis for the design seismic action are multiplied by the factor η:

$$\eta = (1 + \Delta V_{Rw}/\Sigma V_{Ed}) \leq q \tag{2.7}$$

where ΔV_{Rw} is the total reduction of resistance of masonry infills in the storey concerned compared to the overlying storey and ΣV_{Ed} is the sum of the seismic shear forces in all vertical primary members of the storey (i.e., the design seismic shear of the storey). As shown in (Fardis and Panagiotakos 1997b), application of the η factor on the seismic internal forces of the beams adjoining the less infilled

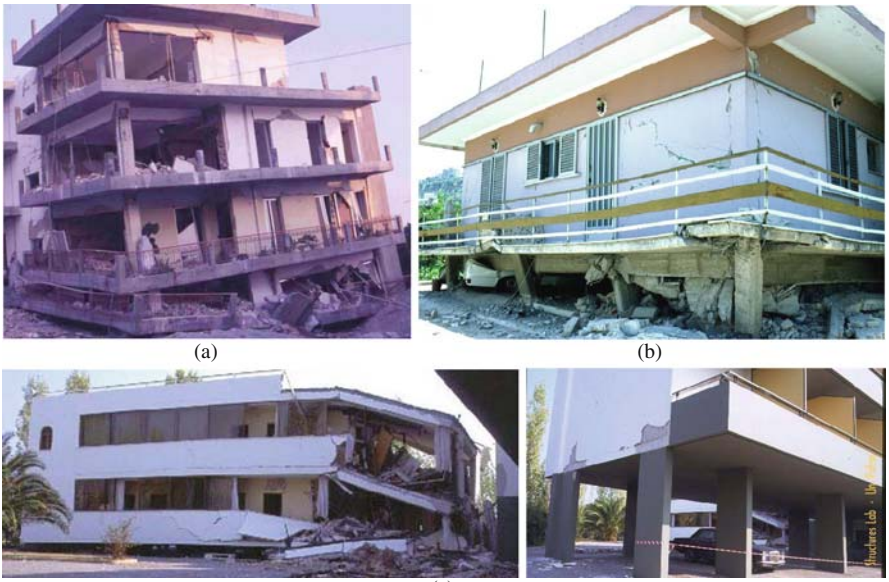

Fig. 2.10 Open ground storey collapses: (**a**) Kalamata, Greece, 1986; (**b**) Aegio, Greece, 1995; (**c**) Athens, 1999 (*Left*: collapsed unit; *Right*: spared similar unit, at right angles to that on the left). (See also Colour Plate 1 on page 717)

storey is counter-productive for the columns of the storey, as it increases further seismic demands in them.

If the value of η is not more than 1.1, Eurocode 8 (CEN 2004a) allows omitting the magnification of seismic action effects with η.

It is reminded that Eurocode 8 penalises frame buildings of DC M and H having abrupt heightwise variations in storey overstrength – including the contribution of infills – with a reduction of their q-factor by 20% (cf. criterion no. 6 for irregularity in elevation in Section 2.1.7). As Eurocode 8 itself does not specify a quantitative criterion for what is an abrupt heightwise variation of storey overstrength, it is proposed here to use for this purpose the factor η in a storey with reduced infills from Eq. (2.7). Should its value exceed 1.1, not only are the column seismic internal forces from the analysis for the design seismic action multiplied in that storey by η, but the q-factor of the entire building is reduced by 20%. Of course, this penalty should be imposed only to the types of systems to which application of Eq. (2.7) refers, namely to frame systems and frame-equivalent dual ones of Ductility Class H.

A warning is in order at this point. Large values of η from Eq. (2.7) cannot be implemented in the design of the columns of the storey with less infills, without significantly increasing the size of the columns in just that storey (Fardis and Panagiotakos 1997b, Fardis 2000). So, if the storey deficit in infill strength is large, the designer would better solve the problem in the conceptual design stage, through a structural system with lateral stiffness and strength sufficient to overshadow the

infills. The best way is with walls that collectively resist most of the seismic base shear (as in wall systems and in wall-equivalent dual ones). For DC H buildings with such walls Eurocode 8 waives the requirement to apply the factor of Eq. (2.7) for the design of the columns of storeys with less infills. For Ductility Class M or L, this requirement does not apply anyway.

2.1.13.4 Potential Local Adverse Effects of Infills

In addition to the potential detrimental effect of infills on global response, there may also be local adverse effects. These are mainly two:

1. Stiff and strong infills may shear-off weak columns, especially for imbalanced (i.e., one-sided) contact. Figure 2.11 shows two examples.
2. A column in contact with infills over a fraction of its full height is laterally restrained along that length ("captive" column). This localises the development of the entire interstorey displacement within the column free length. Therefore, the chord rotation demands at its two ends are larger than those that would had developed should the column were unrestrained, by a factor equal to the ratio of the full-to-the-free-height of the column. Moreover, owing to the short shear span (moment-to-shear ratio) of the "captive" column, its shear ratio (shear span over column depth within the plane of the infill) is low, making the column liable to a combined flexure-shear failure, or to pure shear failure dominated by diagonal compression. Figure 2.12 shows examples of failure of captive columns.

Rules in Eurocode 8 for the protection of concrete buildings from these two types of adverse local effects apply to buildings designed for DC H or M (but not L), no matter the structural system (wall or frame).

Regarding adverse local effect no. 1 above, failure or heavy damage of an infill panel may dislodge part of it, exerting a concentrated force on the adjacent column. The stronger the infill, the larger is the magnitude of this force and the higher the likelihood of column shear failure. Infill panels are more likely to fail or suffer heavy damage at the ground storey, as there the shear force demand is largest. For this reason, in buildings with masonry or concrete infills Eurocode 8 imposes

Fig. 2.11 Examples of shear failure of weak columns interacting with strong infills. (See also Colour Plate 2 on page 771)

the special detailing and confinement requirements for column critical regions over the full clear height of the columns of the ground storey, to help them withstand local overloading due to dislodgement of the infill at any point along their height. Eurocode 8 subjects also the entire length of columns that are in contact with infills on one side only per vertical plane to the special detailing and confinement requirements applying to critical regions. Column failure due to imbalanced contact with infills may take place in columns which are exterior in the plane of the frame (see Fig. 2.11-right for an example).

Buildings may have captive columns for purely architectural reasons. Openings with small height between the beam soffit and the sill often extend from column to column, to provide natural lighting and ventilation according to building regulations together with function and working space over the height of the wall under the sill, while preventing visibility through the opening. Such openings are very common for toilettes, classrooms, industrial spaces, warehouses, storage rooms, partially buried basements, etc. Captive columns are also created by parapet walls along open corridors.

Failure of captive columns (adverse local effect no. 1 above) is very common in earthquakes (see Fig. 2.12 for examples), especially if the column is weak and fails before it crushes the adjoining infill over the contact area.

Captive columns have such a high failure rate in earthquakes, that architectural design should avoid them altogether. Possible architectural ways out of the problem include:

- offsetting the infill with respect to the column, so that there is no contact between them in the plane of the infill; or
- reducing the horizontal dimension of the opening so that it does not extend up to the column, but stops at a distance from it such that it does not intercept the diagonal strut from one corner of the infill panel to the diagonally opposite one (see Fig. 4.4 in Section 4.9.8 and Fig. 5.7 in Section 5.7.3.6).

Measures for the captive column problem can, and should, be pursued also during conceptual structural design. The most effective one is to provide structural walls with strength and stiffness sufficient to overshadow those of columns (e.g., walls resisting at least 50% of the seismic base shear in the horizontal direction of those infills that keep the columns captive). Another option just for those columns that are in partial-height contact with infills is to select a large cross-section depth within the plane of the infill, so that the column is sufficiently strong and stiff not be “disturbed” (or even “notice”) the infill and its opening. Before reaching its ULS resistance in shear, such a strong column will crush the adjoining infill over the contact area. In this connection, it is worth mentioning that in Japan it is common practice to add “wing walls” to captive columns within the plane of the infill, with the same thickness as the infill. The width of the “wing walls” in the plane of the infill panel is (often several times) larger than the cross-sectional dimension of the column normal to the infill. This has proven to be an effective solution in practice. However, dimensioning and detailing a column with T- or L-section composed of a wide flange (the “wing walls”) and a small web (the column) is neither straightforward, nor supported by a large volume of cyclic test results.

Fig. 2.12 Examples of captive column failures. (See also Colour Plate 3 on page 718)

If there is no architectural or conceptual design solution for the captive columns, we are left with dimensioning and detailing them for the adverse effect of the infill (as described in Section 5.7.3.6 for Eurocode 8).

2.1.13.5 Avoiding Adverse Effects of Staircases

By connecting adjacent floors of a building, concrete stairs which are integral with floors act as bracing elements contributing to the storey lateral stiffness and strength. For instance, the shear failure in Fig. 2.13(a) shows that the flight connecting the mid-storey landing to the floor above works in the strong direction of its cross-section as a wall element inclined to the horizontal. The global effect of that staircase was beneficial: together with the masonry infills around it, it helped the 3-storey building survive the Aegio (GR) 1995 earthquake, while an identical (except for the staircase) adjoining building collapsed. Examples of adverse local and global effects are shown in Fig. 2.13(b) and (c). The stair itself rammed the column supporting it at mid-storey (Fig. 2.13(b)). More important, the torsional response of the flexible, open ground storey building due to the staircase at one corner in plan exceeded the deformation capacity at the tops of the columns near the diagonally opposite corner (Fig. 2.13(c)). Witness also in Fig. 3.35 (at the bottom left corner) a column that failed in shear after been made short by the inclined edge beam of a stair it supports.

The location and sometimes the shape of the staircase in plan are normally conditioned by architectural and functional considerations or even by regulations. So, there is little a structural designer can do to prevent a strongly eccentric in plan staircase. However, he/she normally has full control of the way the stair is connected to the rest of the structural system for vertical support and can use it to minimise the contribution of the staircase to the global lateral stiffness and avoid its adverse local effects in an earthquake. There are two options to this end:

1. The first is to support the stair vertically all the way by a large structural wall, which by itself provides a major contribution to the lateral stiffness and resis-

(a) (b) (c)

Fig. 2.13 (**a**) Stair flight failing in shear as an inclined wall element in its strong direction; (**b**) corner stair in an open ground floor causes damage to the column it is connected to at mid-storey; and (**c**) columns at the diagonally opposite corner of the building failed during torsional response due to the stair in (**b**) – shown near bottom right at the back. (See also Plate 4 in the Colour Plate Section on page 719)

tance of the building. For instance, a U-shaped wall may run around a staircase of similar shape, or a long rectangular one may run all-along a (mostly) straight in plan stair. The stair will then be built integral with the wall, cantilevering from it at right angles to the stair's axis. It will serve as an inclined rib of the wall, but it will be safe-sided and simpler to neglect the increase in the wall strength and stiffness that this entails. If the building depends for its lateral force resistance on structural walls, this is the option of choice. Moreover, if these walls are anyway very stiff, the staircase may be placed elsewhere in plan and supported independently (but not by columns at midstorey): seismic interstorey drifts will be too low to mobilise a noteworthy part of its lateral force resistance.

2. If the building does not have walls large enough to support the stair or fully overshadow its lateral stiffness, there are two things that the designer should do to minimise the contribution of the stair to the (anyway low in this case) lateral stiffness of the building and its local and global adverse effects:

   a Avoid at any cost connecting the stair to a column at mid-storey. If the column is slender, it may be rammed by the stair and fail in flexure (see Fig. 2.13(b) for an example). If it is not, it may turn into a squat column on one or both sides of the connection and fail in shear (see an example at the bottom left corner of Fig. 3.35), etc. Besides, such a connection increases the interstorey lateral stiffness of the column and hence its seismic force demands. It will also increase the lateral stiffness of the stair-column system, increasing its impact on the rest of the structural system and possibly inducing stiffness and strength eccentricities (see Fig. 2.13(c)).
   b The stair – supported according to (a) only at floor levels – should make a turn in plan of at least 180°, preferably 270° or more. In that way it will present a relatively low interstorey lateral stiffness, working as part of a spiral.

   Option (b) requires special attention to be paid to the (non-trivial) design of the stair for gravity loads, as well as to its integrity under the design seismic action. To this end, the staircase should be designed/verified as a "secondary member". Section 4.9.6 provides modeling guidelines for the calculation of the seismic action effects for which this "secondary member" will be verified.

2.2 Frame, Wall or Dual Systems for Concrete Buildings

2.2.1 Seismic Behaviour and Conceptual Design of Frame Systems

2.2.1.1 Features of the Seismic Behaviour of Frames

A frame resists the seismic storey shears through bending moments in its columns. The algebraic difference between the bending moments at top and bottom of each column produces the column's contribution to the seismic shear of the storey. The seismic overturning moment of the building is resisted by axial forces in the columns, tensile at one side of the plan and compressive at the opposite one.

Therefore, the seismic behaviour of frames is governed by flexure, or strictly speaking by normal action effects, i.e., by combination of bending moment(s) and axial force.

In ordinary regular plane frames the column inflection points are close to the storey midheight. Therefore, at the column end with the maximum bending moment the shear span is normally between one-half and two-thirds of the column clear height. So, the most crucial components of a frame, its columns, normally have shear span ratios greater than 2.5. In beams, most critical is the end which is in hogging (negative) bending. The shear span ratio there is normally in the order of 3. For such values of the shear span ratio the inelastic behaviour and the ultimate deformation of frame members are governed by flexure and are inherently ductile (provided, of course, that all members are dimensioned not to fail in shear before their ends yield in flexure).

2.2.1.2 Advantages and Disadvantages of Frames for Earthquake Resistance

The main advantage of frames for earthquake resistance is that, provided that they are capacity-designed for plastic hinging in the beams and against pre-emptive shear failure of any member, their flexural behaviour lends itself to the development of large global ductility and deformation capacity. Moreover, if there are several plane frames in the building, each one with several bays, the lateral-force-resisting system has high redundancy and offers multiple load paths.Therefore, with appropriate detailing of the end regions of their members, frames can be easily designed to resist strong earthquakes through global ductility, rather than thanks to strength. For this reason, they are the structural system of choice in high seismicity regions, such as the Western US and Japan. However, one can fully trust only fairly regular frames, having concentric beam-column connections. Strongly irregular frames and eccentric connections may have poor seismic performance. Moreover, they are not sufficiently covered by present State-of-the-Art.

Although the seismic behaviour of beams, columns and frames has been studied experimentally and analytically much more thoroughly than those of walls or wall systems, there are still significant uncertainties and gaps of knowledge about it. A prime uncertainty is about the width of the slab which is effective as flange of the beam, especially in tension. Within this effective flange width, slab bars parallel to the beam increase the beam flexural capacity for hogging (negative) moment, M_{Rb}. This moment resistance controls negative plastic hinging in the beam and enters into the capacity design check at beam-column connections, Eq. (1.4), as well as in the calculation of capacity design shears, Eqs. (1.7), (1.8) and (1.9), (1.12) and (1.13). As noted in Section 1.3.4, the Eurocode 8 rules for the effective flange width of beams target the dimensioning of beam top reinforcement for the ULS in bending under the design bending moment. As such, they tend to be safe-sided for the beam top reinforcement, i.e., to underestimate the flange width and, therefore, the actual beam flexural capacity, M_{Rb}, as well. This is unsafe, not only for the design of columns against plastic hinging, but also for the capacity design shears of the beams and the columns.

The flange width of beams effective in tension increases with increasing deformation demand at the beam end, especially after that end yields and its top reinforcement enters the strain-hardening range, exhibiting large elongations that spread in the slab next to the beam. If the slab has two-way reinforcement, a realistic estimate of the slab width that is effective as tension flange of the beam after plastic hinging is about 25% of the clear beam span on each side of the web, but not exceeding the mid-distance to the next parallel beam (cf. relevant US code provisions, outlined in Section 1.3.4). The magnitude of the slab width that is effective as compression flange under a sagging (positive) moment at the beam end is of little practical significance, as it affects very little the magnitude of the corresponding flexural capacity, M^{+}_{Rb}, which is governed by the beam bottom reinforcement. Moreover, it is the ultimate deformation of the beam in hogging bending that normally governs beam failure, as it is associated with a large amount of tension reinforcement at the top (including the slab reinforcement within the effective flange width) and a narrow compression zone at the bottom with much less reinforcement.

Note that, at the connection of a beam with an exterior column the tension or compression force in the effective flange width of the slab is applied to the transverse perimeter beam at an eccentricity with respect to its axis, producing a torque loading on the beam. The torsional moment that develops in the transverse beam due to this torque attains its maximum value near the face of the column at the joint and often causes spiral cracking of that beam. The cracking often extends to the exterior face of the joint. These phenomena are complex and their possible effects are, at present, rather unclear.

The advantages of frames for earthquake resistance may be summarised as follows:

1. The members of frames are inherently ductile.
2. Two-way frame systems, consisting of several plane frames in each horizontal direction with several bays each, have very high redundancy and multiple load paths.
3. Frames place few constraints on the architectural design, especially of the façade.
4. Provided that the frame has concentric connections and regular geometry, there is little uncertainty about its seismic response, because:
   - the seismic performance of frames and frame members is well known and understood, on the basis of thorough experimental and analytical studies;
   - frames are fairly easy to model and analyse for design.
5. Certain features make frames attractive and cost-effective for earthquake resistance:
   - beams and columns are needed in buildings anyway to support the gravity loads; so, why not use them for earthquake resistance as well?
   - columns have strength and lateral stiffness against both horizontal components of seismic action;
   - it is easy to design the foundation of smaller vertical elements (notably, columns) than of larger ones (walls), with each foundation element transferring to the ground a small fraction of the seismic base shear.

Frames have also disadvantages for earthquake resistant design:

1. Frames are inherently flexible and the size of their members is often governed by the interstorey drift limits (e.g., those listed in Section 1.1.3 under (i)–(iii) for Eurocode 8).
2. Column counter-flexure within the same storey lends itself to soft-storey mechanisms and a "pancake" type of collapse.
3. Detailing of frames for ductility requires high quality workmanship and strict supervision on site (especially for fixing the dense reinforcement and placing and compacting concrete through joints of two-way frames).
4. There are certain elements of uncertainty about the seismic response and performance of frames:
   - The effects of eccentric connections or strongly irregular layouts in 3D are not sufficiently known.
   - There is considerable uncertainty about the effective slab width in tension, which affects the likelihood of plastic hinging in the columns.
   - The behaviour of columns of 3D frames under the complex loading conditions (cyclic biaxial bending with varying axial force) to which they are subjected during real earthquakes is poorly known.
   - In 3D frames subjected to real earthquakes, columns that have been capacity-designed on the basis of Eq. (1.4) against plastic hinging, may well form plastic hinges owing to the biaxial moment demands from beams connected to them in the two horizontal directions.

2.2.1.3 General Guidance for the Conceptual Design of Frames

The location of frames in plan, the span lengths and often the depth of beams, are normally controlled – sometimes even dictated – by architectural and functional considerations, as well as by design for gravity loads. However, the structural designer is normally left with considerable latitude for decisions and choices on the basis of seismic design considerations alone.

In a regular plane frame having:

– constant span length in all bays,
– beams and interior columns with constant cross-section in each storey, and
– (effective) rigidity of the two exterior columns 50% of that of interior ones,

the elastic seismic bending moments at the ends of all beams in the storey will be the same, while those in the two exterior columns will be just half of the bending moments in interior ones. In the elastic range the seismic overturning moment will be resisted by axial forces in the exterior columns alone, approximately equal to the ratio of the seismic overturning moment at storey mid-height to the distance between the axes of these columns. If members are dimensioned for the elastic seismic moments, all beam ends in a storey will be subjected to about the same inelastic

chord rotation demand; all columns, interior or exterior, will also develop about the same inelastic chord rotation demand at the storey bottom. The same at column tops.

Provided that the seismic base shear of the building stays the same, an increase or reduction of the cross-section of a certain column or beam will increase or decrease the elastic seismic moments in that element, respectively, along with those of the beams or columns it is connected to. The seismic moments in other members of the frame will also change, but by less and maybe in the reverse direction. Therefore, if during dimensioning the cross-section of a certain frame member turns out to be insufficient, it may not be enough to increase just its cross-sectional dimension(s), because its seismic moments will increase almost proportionally. It may be necessary to increase the cross-sectional dimensions of other members as well. In certain cases it may be more effective to reduce cross-sectional dimensions, instead. For example, in a frame structure composed of several parallel frames, a reduction of the depth of all beams or columns of a single frame will reduce its share in the seismic storey shears, at the expense of those of other frames.

Because frames are inherently flexible, the size of their members is normally governed by damage limitation requirements under the corresponding seismic action (e.g., in Eurocode 8 by the interstorey drift limits listed in Section 1.1.3 as (i)–(iii))). In frames sized for damage limitation, P-Δ (2nd-order) effects are unimportant. The interstorey drift, $\Delta\delta_i$, from mid-height of storey i to midheight of storey i+1 of the frame may be approximately estimated on the basis of the Virtual Work Principle as:

$$\Delta\delta_i = \frac{H_{\mathrm{cl},i}^3}{24}\left[\frac{V_{\mathrm{Ec},i+1}}{(EI)_{\mathrm{c},i+1}} + \frac{V_{\mathrm{Ec},i}}{(EI)_{\mathrm{c},i}}\right] \times \left(1 + 1.5\frac{h_{\mathrm{b},i}}{H_{\mathrm{cl},i}}\right) + \frac{L_{\mathrm{cl},i}^3}{24}\left(\frac{H_i}{L_i}\right)^2\left[\frac{V_{\mathrm{Ec},i+1} + V_{\mathrm{Ec},i}}{(EI)_{\mathrm{b},i}}\right]\left(1 + 1.5\frac{h_{\mathrm{c},i}}{L_{\mathrm{cl},i}}\right) \tag{2.8}$$

where:

$V_{\mathrm{Ec},i}$: average column seismic shear in storey i (equal to the storey seismic shear divided by the number of columns in the storey, with a weight of 0.5 on exterior columns),
$(EI)_{\mathrm{c},i}$: average (effective) rigidity of the columns in storey i (with a weight of 0.5 on exterior columns),
$(EI)_{\mathrm{b},i}$: average (effective) rigidity of the beams in storey i,
$h_{\mathrm{b},i}$: average beam depth in storey i,
$h_{\mathrm{c},i}$: average column depth in storey i, within the plane of the frame,
H_i: average height of storeys i and i+1,
$H_{\mathrm{cl},i} = H_i – h_{\mathrm{b},i}$: average clear column height in storeys i and i+1,
L_i: average beam span in storey i,
$L_{\mathrm{cl},i} = L_i – h_{\mathrm{c},i}$: average beam clear span in storey i,

If the columns of storey i and i+1 have the same cross-section, $(EI)_{\mathrm{c},i} = (EI)_{\mathrm{c},i+1}$, Eq. (2.8) is simplified to:

$$\Delta\delta_i = \frac{V_{\mathrm{Ec},i+1} + V_{\mathrm{Ec},i}}{24}\left[\frac{H_{\mathrm{cl},i}^3}{(EI)_{\mathrm{c},i}}\left(1+1.5\frac{h_{\mathrm{b},i}}{H_{\mathrm{cl},i}}\right)+\frac{L_{\mathrm{cl},i}^3}{(EI)_{\mathrm{b},i}}\left(\frac{H_i}{L_i}\right)^2\left(1+1.5\frac{h_{\mathrm{c},i}}{L_{\mathrm{cl},i}}\right)\right] \tag{2.8a}$$

Equations (2.8) and (2.8a) suggest that interstorey drift is governed by that element, beam or column, which is on average shorter than the other (normally the columns).

The designer should avoid too short or too long bay lengths, either throughout a plane frame or in one or several bays. If the span is very long, the beam top reinforcement over the supports may be governed by factored gravity loads (the "persistent and transient design situation" in Eurocode terminology), rather than by the design seismic action together with the quasi-permanent gravity loads (termed in Eurocodes "seismic design situation"). This penalises capacity design moments of columns at the joints (cf. Eq. (1.4)), as well as the capacity design shears of beams and columns. It produces also flexural overstrengths in beams with respect to the corresponding seismic demands and creates uncertainty about the inelastic response and the plastic mechanism. If plastic hinges do indeed form in a long beam, they may exhibit large deformation capacity; not only owing to the high shear span ratio at the location of plastic hinges, but also because the large negative (hogging) moment at the ends due to the quasi-permanent gravity loads may prevent reversal of the inelastic flexural deformations there. Yielding in positive (sagging) bending and a positive plastic hinge will take place at some distance from the end section. The deformation capacities under monotonic loading will then apply both at the negative and the positive plastic hinge. These capacities are significantly larger than in cyclic loading (see Eqs. (3.78) in Section 3.2.3.5). Although the primary effect of non-reversal of inelastic flexural deformations is positive, there is a collateral negative one: as exemplified in Figs. 3.6 and 3.7, inelastic elongations accumulate in the reinforcement and the beam gradually becomes longer, pushing out its supporting columns and possibly forcing exterior ones to separate from the exterior beams which are at right angles to the elongating one(s) (see also Section 3.2.3.6). Finally, according to Eq. (2.8a) and the remark that follows it, if the average beam clear span in the storey is much longer than the storey clear height, the cross-section of the beam may have to be increased too much, for the storey to meet the drift limits for damage control.

The other extreme of very short beam spans gives very high seismic shears in the beams, both from the analysis for the design seismic action and from capacity design of the beam in shear. If the span is not short in all bays, but only in few, then the high seismic shears in the short beams give a large variation of the axial force in the adjoining columns upon reversal of the direction (sign) of the seismic action. This reversal will also cause an almost full reversal of the sign of shear at the ends of the short beam(s), because quasi-permanent gravity loads produce insignificant shear forces in short beams, especially as these beams usually support the secondary direction of floor slabs (cf. Eqs. (1.9) and (1.10)). A full reversal of high shears may exhaust the shear capacity in both diagonal directions (at $\pm 45^\circ$) or cause sliding shear failure along through-depth cracks at the end section(s) of

the beam. Design against such shear effects may require diagonal reinforcement in the beam or shear reinforcement at ±45° to the beam axis (see Section 5.5.2). Last but not least, short beams have low shear span ratio (often below 2.5) and hence, unless they are diagonally reinforced, their deformation capacity is low (possibly controlled by shear).

For the most common storey heights and for ordinary gravity loads, the optimum beam span in earthquake resistant buildings is between 4 and 5 m. Span lengths should be as uniform as possible within each frame.

2.2.1.4 Sizing of Beams

The size of the cross-section and the moment resistance at the end sections of beams normally govern many aspects of the design of the frame:

1. the column depth at right angles to the frame, which ideally should exceed the width of the beam by at least 100 mm, to allow the beam longitudinal bars to pass through the confined core of the column section, between its outermost bars;
2. the column depth within the plane of the frame, on the basis of bond considerations for the beam longitudinal bars inside the joint (see Sections 3.3.2 and 5.4.1);
3. the column moment resistances above and below the joint, to meet the weak beam-strong column capacity design condition, Eq. (1.4);
4. the size and horizontal reinforcement of beam-column joints (see Section 5.4.2);
5. the capacity design shears of the beams themselves (see Eqs. (1.9) in Section 1.3.6.2) and of columns (see Eqs. (1.11) in Section 1.3.6.3).

So, sizing of the beams and a preliminary estimation of their longitudinal reinforcement is needed, not only for a preliminary check of the adequacy of the beams, the columns and the joints in shear in 4 and 5 above, but also to ensure at an early stage that the very restrictive condition of the beam maximum reinforcement ratio (see Section 5.3.2) will be met, without revisiting beam sizes during detailed design. Needless to say, the cross-section of the beam should remain the same in all bays of the same frame. Moreover, if the number of different beam sections in the storey and, if feasible, in the building is kept to a minimum, the formwork will be simplified and the risk of errors during construction will be reduced.

Equations (2.8) and (2.8a) may be used as the basis for rough calculations (manually or with spreadsheets) to size beams and columns in conceptual design. More specifically, the lateral stiffness of a frame may be estimated as the ratio $(V_{\mathrm{Ec},i} + V_{\mathrm{Ec},i})/\Delta\delta_{\mathrm{i}}$ and used to distribute (a first estimate of) the storey seismic shear to the frames of that storey. The frame seismic shear may then be distributed to its columns in proportion to their $(EI)_{\mathrm{c},i}$-value with a weight of 0.5 on exterior columns, and used to estimate the column moments at the face of the joint as: $M_{\mathrm{Ec},i+1} = \pm V_{\mathrm{Ec},i+1} H_{\mathrm{cl},i+1}/2$ just above the joint and $M_{\mathrm{Ec},i} = \pm V_{\mathrm{Ec},i} H_{\mathrm{cl},i}/2$ just below, where $V_{\mathrm{Ec},i}$ and $H_{\mathrm{cl},i}$ are not the average column shear in storey i and the average height of storeys i and i+1 (as in Eqs. (2.8) and (2.8a)), but the actual ones in that column and

storey (similarly for $V_{Ec,i+1}$ and $H_{cl,i+1}$). The sum ($M_{Ec,i}$+$M_{Ec,i+1}$) may then be distributed to the ends of the beams framing into the joint, in inverse proportion to their actual span, L. The so-estimated beam seismic moments should then be reduced to the face of the joint, by multiplying them by (1–0.5h_c/L), where h_c is the depth of the column at that joint, and L pertains to the particular beam. If the resulting seismic moment at the face of the joint is denoted as M_{Eb}, the top and bottom reinforcement there may be estimated from the ULS verification for the moments:

$$M_t = \max[M_{\gamma gG+\gamma qQ}; M_{Eb} + M_{G+\psi 2Q}]; \qquad M_b = M_{Eb} - M_{G+\psi 2Q} \tag{2.9}$$

respectively.

If the quasi-permanent loads which are concurrent with the design seismic action, G+ψ_2Q, amount to an "equivalent uniform" line load on the beam,[6] $q_{G+\psi 2Q}$ (kN/m), they produce moments $M_{G+\psi 2Q}$ for Eq. (2.9):

– At the support on an exterior column:

$$M_{G+\psi 2Q} \approx \frac{7+12k}{7+24k+16k^2}\frac{q_{G+\psi 2Q}L^2}{12} \tag{2.10a}$$

– At the support on an interior column:

$$M_{G+\psi 2Q} \approx \frac{7+30k+24k^2}{7+24k+16k^2}\frac{q_{G+\psi 2Q}L^2}{12} \tag{2.10b}$$

In Eqs. (2.10):

$$k = (I_b/I_c)(H/L) \tag{2.11}$$

where H is the storey height, L the (average) beam span and I_b, I_c denote the moments of inertia of the beam and of the interior columns, respectively (the moment of inertia of the exterior column considered to be about equal to 0.5I_c).

If the factored gravity loads ("persistent and transient design situation" in the Eurocodes), γ_gG + γ_qQ, amount to an "equivalent uniform" line load on the beam, $q_d = \gamma_g g + \gamma_q q$ (kN/m), where g is the "equivalent uniform" line load due to nominal permanent ("dead") loads and q that due to nominal imposed ("live") loads, they produce moments $M_{\gamma gG+\gamma qQ}$ for Eq. (2.9):

[6] A triangularly distributed load on the beam with maximum value q_m at midspan gives an "equivalent uniform" load: q= (5/8)q_m. A load with a trapezoidal distribution, rising linearly from each end to a value q_a at a distance a from that end and staying constant in a central part of the beam with length L–2a, gives an "equivalent uniform" load: q=$\{1-(a/L)^2[2-(a/L)]\}q_a$.

– At the support on an exterior column:

$$M_{\gamma gG+\gamma qQ} \approx \frac{7+12k}{7+24k+16k^2}\frac{(q_d+g)L^2}{24} + \frac{7+6k}{7+12k+4k^2}\frac{(q_d-g)L^2}{24} \tag{2.12a}$$

– At the support on an interior column:

$$M_{\gamma gG+\gamma qQ} \approx \frac{7+30k+24k^2}{7+24k+16k^2}\frac{(q_d+g)L^2}{24} + \frac{7+6k}{7+12k+4k^2}\frac{(q_d+g)L^2}{24} \tag{2.12b}$$

Redistribution of the so-estimated beam moments according to Section 5.7.2.2 is not just allowed, but strongly encouraged. The targets of the redistribution should be:

1. To equalise beam design moments across the joint, so that both beam sections at the faces of the column across the joint can be covered by the same longitudinal bars.
2. To reduce hogging design moments and increase sagging ones at each support, so that the amounts of top and bottom reinforcement of the beam come out as close to each other as possible, especially over that beam support where the hogging design moment, $M_t = \max[M_{\gamma gG+\gamma qQ}, M_{G+\psi 2Q} + M_{Eb}]$, is the maximum over the storey in the frame.

The ultimate objective of target no. 2 is to enhance the critical deformation capacity at beam ends, which occurs under hogging moments and increases when the difference (or ratio) between the top and bottom reinforcement area decreases. The practical benefit from the convergence of the top and bottom reinforcement areas is that codes normally let the beam maximum allowable top reinforcement ratio increase, if the bottom reinforcement increases as well (see Section 5.3.2 for the case of Eurocode 8 (CEN 2004a)).

Note that the two beam ends across a joint will be subjected to the same chord rotation demand (equal to the rotation angle of the joint), while their chord rotation capacities increase with increasing shear span ratio of the beam, L_s/h, and with decreasing top-to-bottom-reinforcement-ratio (see Eqs. (3.78) in Section 3.2.3.5). So, if we want to balance the chord rotation capacities across a joint between two unequal beam spans, the beam end section towards the longer span should have lower top-to-bottom-reinforcement-ratio. This is consistent with the relative magnitude of the elastic design moments at these sections, $M_t = \max[M_{\gamma gG+\gamma qQ}, M_{G+\psi 2Q} + M_{Eb}]$, $M_b = M_{Eb} - M_{G+\psi 2Q}$, because as the beam span increases, the $M_{\gamma gG+\gamma qQ}$ and $M_{G+\psi 2Q}$ increase while M_{Eb} decreases. Therefore, target no. 1 above, aiming at serving both beam sections across the joint with the same longitudinal bars, as well as target no. 2, aiming at increasing the absolute magnitude of the deformation

capacity of beams, run against balancing the deformation capacities of unequal adjacent beam spans.

The beam top and bottom reinforcement areas over the supports are estimated from the beam design moments (after redistribution) divided by the product of the design yield strength of the reinforcement, f_{yd}, times the beam internal lever arm, $z_b \approx 0.9d_b$. The beam effective depth, d_b, in this estimation is obtained from the initial choice of beam depth, h_b, used in the calculation of the average (effective) rigidity of beams, $(EI)_b$, and of their uniform line loads, q_d and $q_{G+\psi 2Q}$. Then the initial choice of the width of the web of the beam, which affects much less than h_b the value of $(EI)_b$, is confirmed or revised, so that the beam maximum allowable top reinforcement ratio is respected at the beam end section where the difference between the top and the bottom reinforcement area is maximum.

Once a first estimate of the area of top reinforcement required over the supports is available, it is a good idea to translate it into a specific number and diameter of longitudinal bars. The maximum diameter of these bars controls their bond within the core of the joint (see Section 5.4.1) and determines the minimum depth of the supporting column within the plane of the frame.

2.2.1.5 Sizing the Columns

Architectural considerations sometimes require the column to be flush with, or protrude laterally from, the beam. Structural considerations suggest a column protruding from the beam(s) by at least 50 mm on each side, to allow the beam longitudinal bars to pass through the confined core of the column.

Columns should be sized during conceptual design so that, under the design seismic action and the concurrent gravity loads, the following criteria are met:

1. the bond requirements along beam bars passing through the joint or anchored there (Eqs. (5.10) in Section 5.4.1) are met using a reasonable (i.e., not too small) maximum bar diameter;
2. the column axial load ratio, $\nu_d = N_d/(A_c f_{cd})$ (defined as the ratio of the column axial load to the product of its cross-sectional area, A_c, and the design value of the concrete compressive strength, f_{cd}) is kept low, to the benefit of the flexural ductility of the column (see Section 3.2.2.8 and Eqs. (3.78) in Section 3.2.3.5, as well as Table 5.2 for the upper limits to the maximum value of ν_d in Eurocode 8 depending on the Ductility Class of the building).

The minimum and the maximum value of the column axial load under the design seismic action and concurrent gravity loads, N_d, to be used in the check of criteria 1 and 2, respectively, may be estimated in conceptual design without any analysis, as (see Fig. 2.14):

$$\max N_d \approx \sum_{\text{floors}} (A_{tr}(g + \psi_2 q) + \Delta V_E); \quad \min N_d \approx \sum_{\text{floors}} (A_{tr}(g + \psi_2 q) - \Delta V_E) \tag{2.13}$$

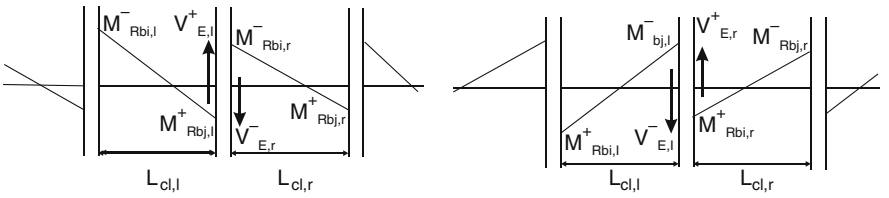

Fig. 2.14 Extreme values of seismic shears in beams producing extreme seismic axial force values in columns

$$\Delta V_E = \sum_{\text{adj. spans}} \max \left[\left(\frac{M^+_{Rbi} + M^-_{Rbj}}{L_{cl}} \right)_{\text{r}} - \left(\frac{M^+_{Rbi} + M^-_{Rbj}}{L_{cl}} \right)_{\text{l}} ; \left(\frac{M^-_{Rbi} + M^+_{Rbj}}{L_{cl}} \right)_{\text{l}} - \left(\frac{M^-_{Rbi} + M^+_{Rbj}}{L_{cl}} \right)_{\text{r}} \right] \tag{2.14}$$

In Eq. (2.13) the summation extends over the overlying floors and A_{tr} is the tributary floor area of the column in plan, bounded by lines along column mid-spans. The uniformly distributed quasi-permanent floor load, $g + \psi_2 q$, should be estimated from the thickness of the slab and the finishing and use of the floor; a value of 8 kN/m^2 is quite representative of ordinary concrete buildings. Equation (2.14) gives the maximum difference of seismic shear forces, ΔV_{E}, that develop in the beams framing into the column from the right (subscript r) or from the left (subscript l), discounting the possibility of plastic hinging in the columns. The moment resistances, M_{Rb}, hogging (–) or sagging (+), at the ends i and j of the beams adjacent to the column may be taken with their design values, $M_{\text{Rb,d}}$. Note that, in rectangular in plan buildings, with continuous frames from one side of the plan to the opposite, each frame with about uniform spans, the difference in beam seismic shears, ΔV_{E}, may be neglected for interior columns. Exterior columns may be assumed to share the total seismic axial force in the row of exterior columns in proportion to their cross-sectional area. The total seismic axial force in the row of exterior columns may be taken equal to the total seismic overturning moment at storey mid-height, divided by the plan dimension parallel to the horizontal direction of the seismic action. In a building with a total height H_{tot} and storeys with the same mass and storey height, H_{st}, each, the total seismic overturning moment at mid-height of the ground storey may be taken as the base shear times $(2/3)H_{\text{tot}} - H_{\text{st}}/6$.

The procedure above should be applied to estimate the minimum cross-section that meets criterion 1 at the most critical storey (normally the top one, but at exterior columns of medium- or high-rise buildings sometimes the lowermost storey) and at the base of columns for criterion 2. As the seismic bending moments and the total axial force in the columns decrease from the base to the roof, the designer might be tempted to reduce the column section towards the upper storeys, of course by a

small amount from one storey to the next.[7] However, there is strong evidence from field experience and large- or full-scale tests that abrupt changes in the strength of vertical elements at an intermediate storey may trigger its collapse, especially in high-rise buildings where higher mode effects (inducing significant shears at intermediate storeys) are dominant. Figure 2.4 shows examples of such failures, while Section 2.4.2 presents a real case of a multi-storey building in which collapse of one wing appears to have started from the upper floors where column cross-sections had been reduced to a small fraction of their size at the lower storeys.

If the column cross-section changes from one storey to the next, passage of vertical bars through the joint is tricky and difficult to depict in drawings or implement on site. Remember also that, for the same reinforcement ratio and cross-sectional dimensions, the column moment resistance decreases from the ground storey to the top owing to the reduction in column axial compression. So, if column cross-sectional dimensions are significantly reduced towards the top, more vertical reinforcement may by needed in upper storeys, especially at the top storey where bending moments due to gravity loads are much larger than in the underlying ones. Finally, keeping the cross-section of each column constant over the full height of the building simplifies the formwork. So, this is the recommended practice from every point of view.

Elastic analysis uses the nominal value of column rigidity, (EI), producing elastic predictions of seismic moments in the columns that are proportional to bh^3 (with a weight of 0.5 on exterior columns). Therefore, the dimensioning of the vertical reinforcement in the columns will be based on non-dimensional moments $\mu \equiv M/(bh^2 f_{cd})$ proportional to h. Therefore, if the columns have different sections in a storey, the larger ones will end up with higher vertical reinforcement ratios than the smaller. More important, the chord rotation capacity of the column decreases with decreasing shear span ratio, L_s/h, (see Eqs. (3.78) in Section 3.2.3.5), while the chord rotation demand in all columns of a frame, being controlled by the frame's interstorey drift ratio, is about the same. So, at the base of the building where plastic hinges do form, the larger columns are expected to fail first, as confirmed by observations from earthquakes. Therefore, it is more cost-effective to choose as uniform a size of the columns in the frame system as practically feasible.

2.2.2 Seismic Behaviour and Conceptual Design of Wall Systems

2.2.2.1 Definition of What is a Wall

Design codes define a concrete wall as a concrete vertical element with an elongated cross-section. A limit of 4.0 for the aspect ratio (long-to-short dimension) of a rectangular cross-section is conventionally adopted by most design codes to distinguish

[7] Note that, if the reinforcement ratio is kept the same, a reduction of the cross-sectional dimensions by a certain percentage causes an about three times larger percentage reduction of moment resistance.

walls from columns. If the cross-section consists of rectangular parts, one of which has aspect ratio greater than 4, the element is also classified as a wall. With this definition on the basis of the cross-sectional shape alone, a wall differs from a column in that:

- it resists lateral forces mainly in one direction, notably parallel to the long side of the section, and
- it can be designed for such a unidirectional resistance by assigning flexural resistance to the two far ends of the section ("flanges", or "tension and compression chords") and shear resistance to the "web" in-between them, as in beams.

So, for the purposes of flexural resistance and deformation capacity one may concentrate the vertical reinforcement and provide concrete confinement only at the two ends of the section. Note that, if the cross-section is not elongated, the vertical element is called upon to develop significant lateral force resistance in both horizontal directions. Then it is meaningless to distinguish between "flanges" on one hand, where vertical bars are concentrated and concrete is confined, and "web" on the other, where they are not.

The above definition of "walls" is consistent with concrete design codes and appropriate for dimensioning and detailing at the level of the cross-section. It is not very meaningful, though, in view of the intended role of "walls" in the structural system and of their design, dimensioning and detailing as an entire element and not just at the cross-sectional level. As noted in Section 1.3.4, seismic design often relies on walls for prevention of a storey-mechanism in their long direction, without any verification that plastic hinges form in beams rather than in columns (Eq. (1.4)). Nevertheless, walls can enforce a beam-sway mechanism only if they act as vertical cantilevers (i.e. if their bending moment diagram does not change sign within at least the lower storeys, see Fig. 1.7) and if they develop a plastic hinge only at the base (at the connection to the foundation). As a matter of fact, unless the wall bending moment attains two values of large magnitude but of opposite sign within the full height of the wall (let alone within the same storey), the wall cannot develop two plastic hinges in opposite bending (positive and negative) along its height and a storey mechanism between them. Whether a "wall", as defined above, will indeed act as a vertical cantilever and form a plastic hinge only at its base, depends not so much on the aspect ratio of its section, but primarily on how stiff and strong the wall is relative to the beams it is connected to at storey levels. For concrete walls to play their intended role, the length dimension of their cross-section, l_w, should be large, not just relative to its thickness, b_w, but in absolute terms. To this end, and for the beam sizes commonly found in buildings, a value of at least 1.5 m for low-rise buildings or 2 m for medium- or high-rise ones is recommended here for l_w.

Obviously vertical elements with cross-sectional aspect ratio less than 4.0 (i.e. defined conventionally as "columns") can work as vertical cantilevers and form a plastic hinge only at the base, if they are connected at storey levels with very flexible beams or with no beams at all (as in flat slab systems). However, normally the moment resistance at the base of vertical elements with non-elongated section is

relatively small, so that, given their long shear span (moment-to-shear ratio) there, such vertical elements cannot contribute significantly to the base shear of the building. Moreover, their lateral stiffness is also rather low. So, they are ineffective for reduction of interstorey drifts for damage limitation and sensitive to P-Δ (2nd-order) effects. At the other extreme, vertical elements with cross-section sufficiently elongated to be classified as walls but connected at storey levels with very stiff and strong beams, may act as frame columns rather than as vertical cantilevers.

2.2.2.2 Optimal Length of Walls

We will stick with the definition of a wall as a vertical element with a bending moment diagram similar to that of a vertical cantilever (Fig. 1.7), forming a plastic hinge only at the base. If the lateral-force-resisting system comprises only such elements, the full seismic overturning moment at the base of the building is resisted directly by the (sum of) bending moments at the base of the walls, instead of indirectly by their axial forces. So, at the base of a wall the bending moment is large and the shear span (M/V ratio), L_s, long. If the beams are very flexible compared to the walls, each wall works as a vertical cantilever subjected only to horizontal forces at storey levels. Then L_s is about equal to 2/3 of the total wall height, H_{tot}. For the usual beam sizes, L_s is about equal to 50% of H_{tot} if the length l_w of the wall section is fairly large, or about equal to 1.5 times the storey height if l_w is relatively short (near the limit $l_w = 4b_w$).

The shear strength of a concrete element is roughly proportional to its cross-sectional depth, h. Therefore, lumping the shear resistance to a few vertical elements with large values of h, instead of distributing it to many small-sized ones, does not save materials. On the other hand, the rigidity of RC members, nominal or "effective", is roughly proportional to h^3. So, lumping the lateral stiffness into few vertical elements, rather than spreading it to many small ones, is quite cost-effective. Using a few walls with large cross-section is also cost-effective from the point of view of moment resistance and vertical reinforcement, according to the considerations of the following paragraph.

By dividing both sides of $M = L_s V$ by $bh^2 f_c$ we get: Non-dimensional moment $\mu \equiv M/(bh^2 f_c) = (L_s/h) \cdot (V/(bhf_c))$. For given base shear, V, and concrete volume per linear meter of building height, bh, i.e. for given value of $V/(bhf_c)$, reduction of the shear span ratio, L_s/h, reduces μ and, therefore, the total vertical reinforcement ratio necessary to resist μ, as well. As explained in the previous paragraph, for a wall with a fairly large value of $h = l_w$, the shear span, L_s, is roughly a fixed fraction of the building height. Therefore, μ can be reduced by increasing h as much as reasonably feasible, i.e. by lumping the vertical elements into a few large walls. The optimum value of h is one that gives values of L_s/h in the range between 2.5 and 3.0, below which the cyclic behaviour of the wall and its ultimate deformation may be adversely affected by shear. For the typical value $L_s \approx 0.5H_{tot}$, a shear span ratio equal to $L_s/h = 3.0$ gives $l_w = h \approx H_{tot}/6$, i.e $l_w \approx n_{storey}/2$ for a typical storey height of 3 m. Note also that the closing remark of Section 2.2.1.5 about the cost-effectiveness of a uniform choice for the size of all vertical elements in the system

applies also for walls. Remember, though, that too few large walls provide fewer alternative load paths and less redundancy (especially if they are of the same size), which is against the recommendations of Section 2.1.9.

2.2.2.3 Foundation of Walls

The base section of large and strong walls has a large moment resistance. It is difficult to transfer this large moment capacity to the ground through isolated footings (pads). The maximum bending moment that an isolated footing can transfer to the ground is slightly less than the moment causing the footing to overturn, which is equal to $0.5NB$, where N is the vertical force and B the dimension of the footing in the direction of bending. If the wall section is long, the parallel dimension of its footing is not much longer than the wall length $h = l_w$. So, the maximum value of the non-dimensional base moment in the wall, $\mu \equiv M/(bh^2 f_c)$, that can be transferred by an isolated footing is $\mu \leq 0.5\nu$, where $\nu \equiv N/(bhf_c)$ is the non-dimensional axial load at the base of the wall. Because walls have relatively low values of ν (in the order of $\nu \approx 0.05$), the maximum value of μ that can transferred to the ground through an isolated footing is also very low, in the order of the non-dimensional moment at cracking of the wall base section (as the tensile strength of concrete is typically around 10% of f_c). Therefore, in order to develop its moment resistance at the base, a strong wall:

- should be provided with a very large isolated footing, which is not cost-effective and introduces significant uncertainty about the seismic response (it will uplift, following a nonlinear relation between bending moment and uplift rotation which is hard to quantify, at least within everyday design practice – see Section 4.10.3), or
- should be fixed at the top of a box-type foundation provided for the building as a whole.

As we will see in Section 2.3.3.3, a box-type foundation for the entire building consists of:

1. Wall-like deep foundation beams along the entire perimeter of the foundation, possibly supplemented with interior ones across the full length of the foundation system. These deep beams are the main foundation elements transferring the seismic action effects to the ground. In buildings with a basement, the perimeter foundation beams may also serve as basement perimeter walls.
2. A concrete slab at the level of the top flange of the perimeter foundation beams (as the roof of the basement, if there is one), acting as a rigid diaphragm.
3. A foundation slab, or a grillage of tie-beams or foundation beams, at the level of the bottom of the perimeter foundation beams.

Such a foundation system fixes all walls at their base and maximises their effectiveness.

An isolated footing will uplift from the ground when the moment at its bottom exceeds the value corresponding to decompression at its edge (cf. Eqs. (4.102) and (4.102a) in Section 4.10.3). Then it starts rocking, with the value of the moment at its base approaching but never reaching the overturning moment of the footing, $0.5NB$, where B is the dimension of the footing in the vertical plane where rocking takes place. The wall and its footing will rock as a rigid body. As the seismic action is not static but dynamic, rocking is a very stable mode of response for the wall, provided that:

- the angle of rocking θ does not exceed the value $\phi = \arctan(B/H_{\text{tot}})$ which corresponds to overturning under the weight of the wall alone, where the total height of the wall, H_{tot}, is measured from the bottom of the footing (see Fig. 2.15); and
- the concentrated force at the edge of the footing does not bring about bearing capacity failure of the foundation soil.

The peak rotation angle of a rocking rigid wall may be roughly estimated assuming that the kinetic energy at the beginning of a half-cycle of rocking (when the footing is still horizontal) is converted not into deformation energy (that may involve inelastic deformation and damage) but into potential energy, by lifting the centre of gravity of the wall (and of the footing). More specifically, if the rocking wall is considered as a SDOF system, the maximum kinetic energy during its response is about equal to $MS_{\text{v}}{}^2/2$, where S_{v} is the spectral pseudo-velocity. Equating the difference in potential energy due to an angle of rotation θ, i.e., $(Mg)\theta/2$, to the peak kinetic energy gives: $\theta = S_{\text{v}}{}^2/g$. As a matter of fact, the effective period of rocking generally lies within the constant spectral pseudo-velocity range of the response spectrum. So, the peak value of θ turns out to be roughly independent of this effective period.

The relationship between the lateral force and the horizontal displacement during rocking under cyclic loading is non-linear but nearly elastic, following an approximately bilinear envelope and recentring to approximately zero displacement for zero force. Therefore, rocking of a wall on an isolated footing may be considered as a ductile mode of seismic response, almost as ductile as that of a fixed wall with a flexural hinge at the base. For this reason some international standard-like documents (ATC 1998, JBDPA 1977) acknowledge for rocking a q-factor value of

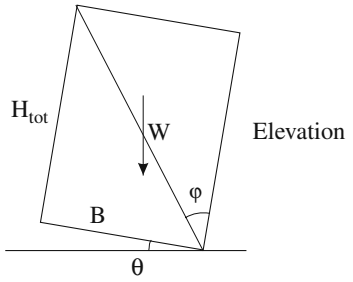

Fig. 2.15 Rocking wall

the same order as that applying to ductile structural response. However, there is so much uncertainty about rocking – notably about its implications for the seismic action affects within the superstructure – that it cannot be reliably quantified and modelled in the context of earthquake-resistant design of wall systems.

2.2.2.4 Special Features of the Seismic Response of Large Walls

Walls with large cross-sectional length fixed at the base exhibit certain features in their seismic response which remind rocking of walls with isolated footings. This is because of the proximity of the neutral axis of the cracked (or yielded) base section to the edge of the section (owing to the small magnitude of the wall axial force) and its large distance from the centroid of the wall gross section. Therefore, flexure of the wall significantly lifts the centroid of the gross section and, with it, the tributary mass of the building supported on the wall. So, part of the kinetic energy is – be it temporarily – harmlessly transformed to potential energy of these tributary masses, in lieu of damaging deformation energy of the wall itself. Furthermore, the end of any beams framing into the part of the wall section outside the compression zone is also lifted (see Fig. 2.16). So long as the other end of these beams does not uplift by the same amount, their shear forces have a stabilising effect. They act downwards on the wall, increasing its axial compression to the benefit of the instantaneous wall strength, stiffness and stability, while reducing the resultant moment on the section.

The above beneficial aspects of the behaviour are due to the large horizontal dimension of the wall, combined with the no-tension feature of cracked concrete (similar to the interface between a footing and the ground) that causes the flexural rotation to take place about a pivot near the edge of the wall section. These phenomena being of purely geometric origin (due to coupling of the rotations with the vertical displacement at the centroid of the wall section), they are neglected in ordinary geometrically linear analyses of the response, even when the analysis accounts for material nonlinearities. Therefore, they are unaccounted-for sources of good performance of structural systems consisting of large walls.

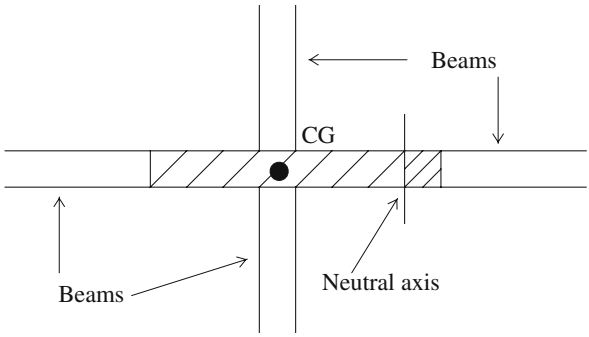

Fig. 2.16 Plan view of beams framing into a wall

Walls with large horizontal dimension compared to their height cannot be designed effectively for energy dissipation through plastic hinging at the base, as they cannot be easily fixed there against rotation with respect to the rest of the structural system. Design of such walls for plastic hinging at the base is even more difficult, if the wall is monolithically connected with one or more transverse walls which are also large enough that they cannot be considered merely as "flange(s)" or "rib(s)" of the first wall. Walls with large horizontal dimensions will most likely develop limited cracking and inelastic behaviour under the design seismic action. Cracking will be mainly horizontal, at construction joints at floor levels. Flexural yielding, if it occurs, will also take place mainly there. Then the lateral deflections of large walls, acting as vertical cantilevers, will be produced by a combination of:

- a rotation of the foundation element of the wall with respect to the ground, most often with uplifting; and
- similar rotations at sections of horizontal cracking and (possibly) flexural yielding at one or more floor levels, with the wall swaying as a stack of rigid-blocks.

Owing to the rather low axial load level in large walls, all these rotations will take place about a "neutral axis" very close to the compressed tip of the foundation element, or to the compressed edge of the wall section at locations of cracking and (possibly) yielding. As already noted, such rotations induce significant uplift of the centroid of the sections, raising the floor masses tributary to the wall and the ends of beams framing into it, to the benefit of the global response and stability of the system. Moreover, rigid-body rocking of the wall with its footing promotes radiation damping, which is particularly effective in reducing the high-frequency components of the input motion.

Eurocode 8 (CEN 2004a) recognises the ability of large walls to withstand large seismic demands through their geometry, rather than via strength and hysteretic dissipation derived from vertical reinforcement. It defines a "large lightly reinforced wall" as a wall with horizontal dimension, l_w, at least equal to 4.0 m or to two-thirds of its height, h_w (whichever is less) and gives it a special role. It also provides special design and detailing rules for such walls, allowing much less reinforcement than in "ductile walls", under the condition that they belong in a lateral-force-resisting system consisting mainly of such walls. The provisions of Eurocode 8 for "Systems of large lightly reinforced walls" are highlighted in Section 5.6.

2.2.2.5 Behaviour Factors of Wall Systems

Most present codes for the design of concrete buildings for earthquake resistance assign lower q-factor values to wall systems than to frame systems (cf. Section 1.4.3). The reasons are the following:

- Walls with large cross-sectional length, l_w, have generally lower shear span ratios than the beams and columns of frames. Therefore, shear plays a greater role for their cyclic behaviour and deformation capacity.

– The State-of-the-Art on the cyclic behaviour of walls and wall systems is less advanced than for frames, because experimental studies on walls is practically difficult and numerical/analytical research is more demanding. So, design codes tend to be safe-sided for them.

However, in view of the beneficial features of the seismic behaviour of walls described in the previous sections and of the very favourable experience of their performance in very strong earthquakes (e.g. in Chile, 1985 and in Kocaeli, Turkey, 1999), there is presently a tendency towards convergence of the q-factor values for frame and wall systems. This tendency is more evident in Europe and South America, but grows stronger in the USA as well, which was traditionally the most fervent proponent of frame systems for concrete buildings. One of the prime arguments of the pro-wall school of thought is that, through their stiffness, walls are best suited for protection from non-structural damage in frequent moderate earthquakes. The strength of this argument has grown with the recent emergence of performance-based seismic design as a means to reduce the economic consequences of earthquakes over the whole range of their potential intensity (see Section 1.1.2).

2.2.2.6 Walls with Non-Rectangular Section or With Openings

Most of what has been said so far in Section 2.2.2, as well as practically everything we know today about the cyclic behaviour of concrete walls, is about walls with rectangular or quasi-rectangular (barbelled) doubly-symmetric section.[8] Such walls are modelled and dimensioned as prismatic elements with axis through the centroid of their section. Lacking a better alternative, the same practice is applied when a rectangular wall runs into or crosses another wall at right angles, to form a wall with a composite cross-section of more than one rectangular parts, each with aspect ratio greater than 4 (L-, T-, U-, H-, Z-shaped walls, etc). Such walls have high stiffness and strength in both horizontal directions. So, they are subjected to biaxial bending and bi-directional shears during the earthquake. They appear to be more cost-effective than the combination of their constituent parts as individual rectangular walls – and indeed they are. We should not forget, however, that our knowledge of their behaviour under cyclic biaxial bending and shear is very limited, and that the rules used for their dimensioning and detailing still lack a sound basis. Moreover, their detailing for ductility is complex and difficult to implement on site. For this reason, it is strongly recommended to make limited use of such walls in practical design. Designers choosing to use non-rectangular walls should opt for fairly simple geometries (e.g. symmetric U- or doubly-symmetric H-sections).

Large openings should be avoided in ductile walls, especially near the base, where a plastic hinge will form. If they are necessary for functional reasons (e.g.

[8] Defined as rectangular walls with a rectangular or square "column" or a compact flange (with aspect ratio less than 4) added to the ends of the cross-section, to enhance its moment resistance and prevent lateral instability of the compression zone.

for doors or windows), openings should be arranged at every floor at a very regular pattern, turning the wall into a coupled one, with the lintels between the openings serving and designed as coupling beams.

2.2.2.7 Advantages and Disadvantages of Walls for Earthquake Resistance

On the basis of what has been said so far in Section 2.2.2 and elsewhere in this chapter, the advantages of walls systems for earthquake-resistant design may be summarised as follows:

1. Walls are inherently stiff, so:
   - they are insensitive to the presence and to the adverse global or local effects of infills;
   - they prevent or limit damage in frequent or occasional earthquakes.
2. Walls offer excellent protection against collapse, as the lack of wall counter-flexure within a storey makes a soft-storey mechanism physically impossible.
3. The seismic behaviour and performance of individual walls is less sensitive than that of frames to lower quality design or poor workmanship on site.
4. Geometric effects and phenomena in large walls are favourable for the seismic response and performance.
5. All things considered, walls are more cost-effective for earthquake-resistance than frames.

Wall systems have also disadvantages for earthquake resistant design:

1. Walls are inherently less ductile than beams or columns, more sensitive to shear effects and harder to detail for ductility.
2. Wall systems offer limited redundancy and few alternative load paths.
3. Walls limit the freedom of the architectural layout, especially at the façade.
4. It is not cost-effective to use walls alone to support the gravity loads of the building; some beams and columns are needed anyway for that purpose.
5. To avoid large eccentricities or low torsional stiffness of the storeys, walls with large contribution to lateral stiffness and strength (e.g., those around service cores housing elevators, stairways, vertical piping, etc., close to the centre in plan, or large perimeter walls), require balancing in plan by other elements with similar lateral stiffness and strength.
6. It is difficult to provide an effective foundation to a wall, especially with isolated footings.
7. There is large uncertainty about the seismic response of wall systems:
   - the cyclic behaviour and seismic performance of walls and wall systems are less well known than those of frames, because experimental research is more difficult to carry out and analytical models need to be more advanced and sophisticated;

- the effects of rocking or of the rotations about the neutral axis of the wall cannot be accounted for reliably in practical design;
- walls are more complex to model, analyse, dimension and detail in practical design (especially those with non-rectangular section).

2.2.3 Dual Systems of Frames and Walls

Walls and frames, each has its advantages and disadvantages as lateral-load-resisting systems (see Sections 2.2.2.7 and 2.2.1.2, respectively). Although walls seem to have a better balance of advantages v disadvantages, we should keep in mind that there are almost always beams and columns in a building to carry gravity loads to the ground. It is a waste not to use them at all for earthquake resistance. So, it is cost-effective for earthquake resistance to combine within the same structural system frames and walls.

Dual systems of frames and walls combine the high strength and stiffness and insensitivity to soft-storey effects of wall systems (advantages no. 1 and 2 of walls in Section 2.2.2.7) with the large ductility, deformation capacity and redundancy of frames (advantages no. 1 and 2 of frames in Section 2.2.1.2). The walls offer protection from nonstructural damage in frequent, moderate earthquakes and help meeting the code's interstorey drift limits (e.g., those listed in Section 1.1.3 under (i)–(iii) for Eurocode 8). The frames may act as a second line of defense in very strong earthquakes, in case the deformation capacity of the inherently less ductile walls is exhausted and some walls lose a significant part of their strength and stiffness. In view of this potential back-up role of frames, US codes require the frames of dual systems to be designed for at least 25% of the design seismic action, no matter the relative stiffness of the walls and the frames in the system. If this condition is met, US codes entitle dual systems of high ductility frames and walls with as high a value of the force reduction factor, R, as in frame systems. Eurocode 8 (CEN 2004a) assigns also the same q-factor value to frames and to dual systems having frames resisting at least 35% of the design base shear.

Frames subjected to lateral loading have shear-beam-type lateral displacements, with the floors sliding horizontally with respect to each other. Interstorey drifts follow the heightwise pattern of storey seismic shears: they decrease from the base to the roof (see Eq. (2.8a)). By contrast, walls fixed at the base deflect laterally like vertical cantilevers, i.e. their interstorey drifts increase from the base to the roof. If frames and walls are combined in the same structural system, floor diaphragms impose on them roughly common floor displacements. As a result, the walls restrain the frames at lower floors, undertaking there the full inertia loads of the floor. Near the top of the building the frame is called upon, not only to resist the full floor inertia loads, but also to hold back the wall, which – if acting alone – would have developed a very large deflection at the top. It is often stated that in dual systems the walls may be considered to be subjected to (cf. Section 5.8.2):

- the full inertia loads of all floors, and
- a concentrated force at the roof level, in the reverse direction with respect to the peak seismic response and the floor inertia loads.

The magnitude of the concentrated force at the top exceeds that of the resultant inertia loads in the upper floors (i.e., of the storey seismic shear there). Consequently, in the upper storeys the walls are often under reverse bending and shear with respect to the storeys below. The frame may be considered to be subjected to just a concentrated force at the top, equal and opposite to the one applied there to the wall(s) and in the same sense as the floor inertia loads. Then the frame has roughly constant seismic shear in all storeys and hence about the same bending moments in all of them. As a result, even when the cross-sectional dimensions of frame members are kept the same in all storeys, their reinforcement requirements for the seismic action do not increase from the top to ground level. As a matter of fact, column reinforcement requirements may even decrease in lower storeys, thanks to the favourable effect of the increased axial force on flexural strength. Therefore, in dual systems column size should not decrease toward the roof.

Dual systems are geometrically more complex than frame or wall systems and have more complicated seismic response than either one of them. Therefore, there is larger uncertainty about their seismic behaviour and performance. This uncertainty is the main (if not only) inherent drawback of dual, against pure frame or wall systems. Their conceptual design should aim at reducing this uncertainty. For instance, as the diaphragms of dual systems are called upon to impose common floor displacements to the two systems by transferring horizontal forces from the frame to the wall or vice-versa, they should be thicker and stronger within their plane than what is required in pure frame systems. Another uncertainty arises from any rocking of the wall(s) at the base. Such rocking shifts part of the storey shears from the wall(s) to the frame. It is reminded that rocking of wall footings with uplift is an intrinsically complex phenomenon, that cannot be reliably modelled in the framework of seismic design practice. Underestimation of such rocking leads to unsafe design of the frames, while overestimation is unsafe for the wall(s). So, a prudent design would eliminate rocking in dual systems, by providing full fixity of the walls at the foundation.

Note that in a system consisting only of walls, the distribution of seismic shear between them will be practically unaffected by the rotation of all the walls at the foundation level. The rotation will only increase the absolute magnitude of storey drifts. The effect of rotations of foundation elements will be even less in purely frame systems. Any rotation of the footing of a frame column has practically no consequences beyond the ground storey. Moreover, such a rotation will be much smaller than in a wall footing, because the higher axial load of the column resists uplift. More important, the smaller the cross-section of a vertical element compared to the plan dimensions of its footing, the smaller is its rotation. So, it is the design of systems that combine the two types of elements, walls and columns, that suffers from increased uncertainty owing to the rotations of footings with respect to the ground.

Tall buildings often have a dual system comprising a strong wall near the centre in plan (around a service core housing elevators, stairways, vertical piping, etc.) and stiff and strong perimeter frames. In such a system outrigger beams may be used to advantage, increasing the global lateral stiffness and strength of the system and mobilising the perimeter frames in resisting the seismic overturning moment.

2.2.4 The Special Case of Flat-Slab Frames

Beamless slabs ("flat slabs", called "flat plates" in North America if they are supported on columns directly without drop panels or column capitals) provide larger clear storey height, unobstructed passage of services under the slab and freedom for irregular layouts of the column grid and for potential modifications of the layout of partitions. Moreover, if labour is expensive, they may be cost-effective for residential or office buildings. Most common are solid cast-in-place slabs, sometimes post-tensioned with bonded or unbonded tendons. Waffle slabs with drop panels around the columns are also common. "Lift slabs" are all precast at ground level around the columns and lifted to their final position.

In flat slab frames subjected to lateral loading strips of the flat slab between the columns act and behave as beams. The effective width of such strips increases with increasing seismic demands, as measured, e.g., by interstorey drift, but is quite uncertain. Irrespective of this uncertainty, the stiffness and flexural capacity of these strips is relatively low compared to those of the columns, conducive to a beam mechanism with column plastic hinging only at the base, as in a strong-column-weak-beam design. Note that, owing to the flexibility of the flat slab, flat slab frames may develop large 2nd-order (P-Δ) effects. There is also large uncertainty about the behaviour of the region of the slab around the column under inelastic cyclic loading, and especially about its capacity to transfer to the column the floor gravity loads through vertical shear stresses, along with the slab moment due to the cyclic lateral loading. A compilation of past experimental work on slab-column connections subjected to large amplitude cyclic deformations suggests that, when the vertical shear force transferred from the slab to the column through the connection increases from zero to about 45% of the capacity of the connection in concentric punching shear, the overall displacement ductility ratio of the slab-column system at failure of the slab decreases from an average value of around 3.5 to about 1.0 (i.e. to brittle failure), while the ultimate interstorey drift ratio of the system decreases from an average value of above 4% to about 2% (Moehle et al. 1988, Pan and Moehle 1989, Moehle 1996). Given that yielding of the slab-column system takes place at an interstorey drift ratio of around 1.5% on average, slab-column connections having a large safety margin against punching shear failure seem able to sustain significant cyclic deformation demands.

According to current conventional wisdom, beamless frames of columns and flat slabs ("flat slab frames") are not considered suitable for earthquake resistance owing to questions about their lateral displacement capacity. Indeed, buildings with "flat

slab frame" systems suffered heavy damage in the Northridge (1994) earthquake. However, in all earthquakes that have inflicted heavy damage to urban centres in Greece in the 1980s and 1990s (Kalamata 1986, Aegio 1995, Athens 1999), such buildings either performed surprisingly well, despite the lack of proper design and detailing for earthquake resistance, or were damaged only in the vertical elements supporting the flat slab and not at the connection (see Fig. 2.10(c) for an example). So, there is no conclusive evidence that "flat slab frames" are condemned in a strong earthquake.

The provisions of Eurocode 8 do not cover flat slab frames used as part of the lateral-load-resisting system (i.e. as "primary seismic" elements). Eurocode 2 (CEN 2004b) includes special rules for the detailing of flat slabs for non-seismic actions. For Ductility Class M or H buildings, flat slab frames cannot be considered as part of the lateral-load-resisting system (i.e., they are considered as "secondary seismic" elements) and the relevant Eurocode 2 rules alone apply to the flat slabs and to the columns supporting them. The Eurocode 2 rules apply also to flat slab frames of Ductility Class L buildings designed as part of the lateral load resisting system (i.e., as "primary seismic" elements), with a value of the behaviour factor q for the entire building not larger than 1.5. It is reminded, though, that Ductility Class L buildings are recommended by Eurocode 8 only for low seismicity regions.

The 1987 Mexico City code has provisions for closed stirrups in flat slabs, as well as for the effective slab width. However, the use of flat slab frames over Mexico City soft soils is practically limited by lateral stiffness requirements and by increased lateral forces, to low-rise buildings. US codes (ACI 2008) include rules for the design and detailing of flat slabs for gravity loads and special rules for their design and detailing as part of an "Intermediate Moment Frame", excluding them from use in "Special Moment Frames". These rules, as well as those applicable for the design and detailing of flat slabs for gravity loads, were developed in the late 1980s (ACI-ASCE Committee 352, 1988). They have not been updated since then, despite the significant volume of research conducted in the mean time on slab-column connections subjected to large amplitude cyclic deformations, or on entire flat slab frame buildings under lateral actions simulating earthquakes.

A prime example of the second type of research mentioned above is a 3-storey, full-size waffle slab frame with one-bay in each direction depicted in Fig. 2.17. The four slab-column connections encompass a corner and an interior one, as well as two edge connections, with the edge either parallel or at right angles to the direction of lateral loading. The waffle slab had a total depth of 0.29 m. In addition to drop panels next to the columns, it had solid column strips between them; in the direction of testing the edge strip was 0.45 m wide and the interior one 0.525 m wide. The building was subjected to pseudodynamic testing at the ELSA laboratory of the JRC of the European Commission in Ispra (Zaharia et al. 2004). The damage pattern in Fig. 2.17 is after a test that has driven the frame to a top drift ratio of 4.3%, corresponding to interstorey drift ratios varying from 5% at the ground floor to 3.75% at the top floor. At these peak drifts the corner connection and the one along the edge at right angles to the direction of loading were subjected to negative (hogging) moments in the slab (inducing upwards shear stresses near the free edge

Fig. 2.17 Flat slab frame after pseudodynamic test at the ELSA laboratory of the JRC: (**a**) side parallel to loading; (**b**) hinge in slab in positive (sagging) bending and plastic hinges at column base; (**c**) side at right angles to loading, with slab damage around connections; (**d**) edge slab-column connection, 1st floor; (**e**) edge slab-column connection, 2nd floor; (**f**) edge slab-column connection, 3rd floor (pictures (**d**)–(**f**) courtesy F. Taucer, JRC). (See also Colour Plate 5 on page 719)

in Fig. 2.17(c) and to downwards shear due to the overturning moment). These peak drifts had been preceded by interstorey drift ratios in the opposite direction ranging from 1.5 to 2%. Column plastic hinges formed only at the base (Fig. 2.17(b)). Plastic hinges (or rather yield lines) in positive (sagging) bending formed next to the transition from a solid slab to a ribbed section (Fig. 2.17(b). The cleavage failures at all six connections on the free edge in Fig. 2.17(c)–(f) are due to the transfer of part of the strongly eccentric shear from the slab to the faces of the column that are parallel to the direction of loading via torsion in the column strip which is transverse to the direction of loading. The termination of the straight ends of column bars within the roof slab was a factor for the location and the pattern of damage in Fig. 2.17(f). The cleavage failures prominent in Fig. 2.17(c) (with two of them shown in detail in Figs. 2.17(e) and (f)) took place at the phase when the peak negative (hogging) moments in the slab induced upwards shear stresses near the free edge. The exception is the edge connection at the 1st floor slab (Fig. 2.17(d)), which suffered the largest damage in the preceding half-cycle of the response when the peak positive (sagging) moments in the slab induced downwards shear stresses near the free edge and the overturning moment an upwards seismic shear on the connection.

Studies like (Zaharia et al. 2004) may shed more light into the seismic response and performance of flat slab frames and contribute to the prompt development of

rules for their seismic design. The cost-effectiveness and seismic performance of earthquake resistant concrete buildings will benefit from the rational use of flat slab frames as part of the lateral-load-resisting system (i.e., as what is called in Eurocode 8 "primary seismic elements").

2.3 Conceptual Design of Shallow (Spread) Foundation Systems for Earthquake-Resistance

2.3.1 Introduction

This section presents the principles for the conceptual design of systems of shallow foundations in earthquake resistant buildings. The "term shallow foundations" covers systems of isolated footings (pads) and tie-beams, foundation-beams and rafts. The same types of foundations are often called (e.g. in Eurocode 7) "spread" foundations. Deep foundations, through piles, are not commonly used for buildings and are not treated at all in this book.

Seismic design of buildings should pay due attention to the foundation, for the following reasons:

- The foundation should be protected from seismic damage, because it is difficult and costly to access and inspect after an earthquake, repair any damage to it, or remedy any deficiency by retrofitting.
- The superstructure will be adversely affected by any damage in the foundation – normally manifested as excessive deformations, felt by the superstructure as differential settlements of its supports – but not the other way around.

Eurocode 8 is one of the few seismic design codes that pays due attention to the design of foundations. The whole of Part 5 of Eurocode 8 (CEN 2004c) is devoted to foundations and other geotechnical aspects, while Part 1 (CEN 2004a) pays significant attention to the design of foundation systems and elements.

Despite its importance, the foundation receives little attention in design practice. Its conceptual design is often done last and its layout follows the choices in the conceptual design of the superstructure.

Under-rating the foundation in seismic design codes and practice may not only be because foundation failures pose limited threat to life, but also because of their low incidence in past earthquakes. There are on record many cases of liquefaction or landsliding, but they are of purely geotechnical interest and have little to do with the presence of a building. There are widely quoted cases of building settlements in Mexico City during the 1985 earthquake due to bearing capacity failure (Fig. 2.18(a)). A few similar cases took place over very soft soils in Adapazari (TR) during the 1999 Kocaeli earthquake (Fig. 2.18(b)) and several corner buildings there toppled, most likely owing to one-sided bearing capacity failure and cyclic accumulation of permanent deformations under the street side part of the building due to smaller overburden there (Fig. 2.18(c)–(f)) (Gazetas and Anastasopoulos 2007).

Fig. 2.18 Bearing capacity failures at: (**a**) in Mexico City (1985) (**b**)–(**f**) Adapazari (TR) in the 1999 Kocaeli earthquake (courtesy G. Gazetas, NTUA). (See also Colour Plate 6 on page 720)

There are no widely known cases of damage or collapse in the superstructure itself due to influences of, or problems in the foundation.

The scarcity of failures or serious problems in foundations during earthquakes could be due to the traditionally very high safety factors against bearing capacity

failure of the ground under gravity or seismic loads and to the oversized foundation elements. In other words, inadequacies of the conceptual design of the foundation or the lack of a meaningful design of it against seismic actions may be overshadowed by the oversizing of the foundation. Clearly this is not a rational and cost-effective design practice. There is, therefore, wide scope for improvement of the cost-effectiveness and rationality of the seismic design of the foundation, without any loss of the safety level it provides.

2.3.2 Foundation of the Entire Building at the Same Level

It has been emphasised in Section 2.1.11 that all foundation elements should be tied together horizontally, into a system that introduces to the base of the structure the same ground motion throughout the plan. This implies that all foundation elements should be essentially at the same horizontal level.

Foundation of the entire building at the same level not only promotes integration of all foundation elements into a single entity, but also facilitates modelling of the support conditions of the building for the seismic response analysis. Figure 2.19 illustrates the case for a building on sloping ground. The most common modelling of the support conditions to the ground employs vertical springs under the foundation elements, simulating the vertical compliance of the soil. Such springs are essential for realistic calculation of the effects on foundation elements and the superstructure, not only of the seismic action but also of gravity (including the action effects of the "persistent and transient design situation"). Given the high static indeterminacy of a typical building structure, there is no way to calculate the internal forces induced in tie-beams, foundation beams, rafts or the superstructure by differential settlements or rotations between different points of the foundation, unless compliance of the ground under bearing stresses is realistically modeled.

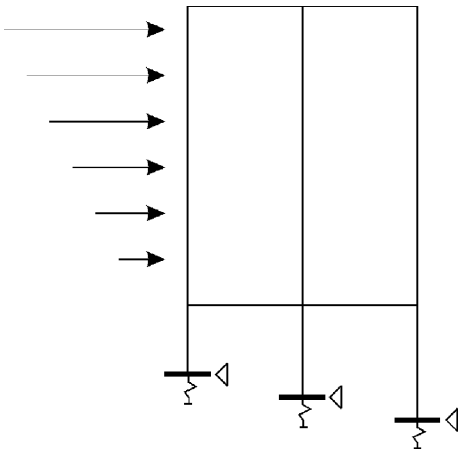

Fig. 2.19 Common (but erroneous) modelling of support conditions in a building with foundation elements at different levels

It is also common modelling practice to constrain horizontally all nodes at the interface of the foundation and the ground, instead of using horizontal springs there for the horizontal compliance of the ground. The reason for this practice is three-fold:

- There is almost no loss of accuracy in the calculation of action effects in the structure, if the compliance of the soil in the horizontal direction is neglected in the model, especially when all elements of the foundation are connected horizontally.
- There is much higher uncertainty about the horizontal than the vertical compliance of the ground. This is not only owing to modelling reasons, but also because it depends on relatively unknown or poorly controlled factors, such as the embedment depth, the presence of and interaction with adjacent structures, etc.
- (Most important:) If included in the model, the horizontal soil compliance will strongly affect the calculated dynamic characteristics of the structure. The fundamental mode and the corresponding period in each horizontal direction will most likely be that of translation of the structure as a rigid body on horizontally deformable ground. It is feasible, but not trivial, to isolate any spurious effects from the results of analyses that consider the horizontal soil compliance. The end result for the superstructure will be close to that obtained neglecting the horizontal soil compliance.

If the common modelling approach described above is adopted and all horizontal displacement constraints are at the same horizontal level, the seismic overturning moment will be (correctly) reflected by the analysis results in the form of reactions in the vertical springs that vary from one side in plan to the opposite. If the horizontal displacement constraints are not all at the same horizontal level, the full seismic overturning moment will be taken by a couple of horizontal reactions developed between horizontal constraints at different levels. So, it will not affect at all the distribution of vertical soil reactions under the foundation. Regarding the seismic action effects in the superstructure, the seismic overturning moment will produce differences in the column shear forces – corresponding to the horizontal reactions due to the overturning moment – instead of axial forces in the columns. These are spurious results and the modelling that leads to them should be avoided.

Introducing horizontal constraints only to nodes of the foundation that are all at the same horizontal level, while letting all others free in the horizontal direction, is obviously not the proper way out of the problem, as the vertical elements connected to the second set of nodes will develop no seismic shears, which is also a spurious result. The only ways out are:

- either to arrange all foundation elements at the same horizontal level, or
- to provide a rigid horizontal connection between all foundation elements that are at different levels, so that they effectively work as if they were all at the same horizontal level.

2.3.3 The Options for Shallow Foundation Systems

2.3.3.1 Isolated Footings with Tie-Beams

Isolated footings cannot be effectively designed for the large eccentricity normally produced by the combination of the moment(s) and of the vertical reaction force due to the design seismic action acting along with the concurrent (quasi-permanent) gravity loads. To reduce this eccentricity, stiff tie-beams should connect every footing with the adjacent ones in both horizontal directions. The bending moments and shears in tie-beams always have a sense of action that leads to reduced moment reaction of the ground at the underside of the footing. So, for given moments and forces applied at the top of the footing by the vertical element, the larger the stiffness of the tie-beams, the smaller is this moment reaction at the base of the footing. Tie-beams should be connected directly to the body of the footing in order to:

- avoid creating a squat column between the soffit of the beam and the top of the footing;
- increase the effectiveness of tie-beams, by increasing their stiffness, EI/L_{cl}, through the reduction of the clear length, L_{cl}.

If we want to calculate the action effects in tie-beams and the ground reactions, it is essential to model realistically the ground compliance for rotation of the footing (Sections 4.9.9.4 and 4.10.3).

2.3.3.2 Two-Way Systems of Foundation Beams

A system of foundations beams, arranged in both horizontal directions throughout the plan of the foundation to support all vertical elements of the building, is much more effective for earthquake resistance than a combination of footings with two-way tie-beams. It is also often more cost-effective.

In order to impart to the building a large torsional stiffness about the vertical, end frames are often made stiffer than interior ones, sometimes by including walls. So, they resist a larger share of the seismic action, while, owing to their smaller tributary area, supporting a smaller fraction of the quasi-permanent gravity loads. So their foundation may be more challenging than for interior vertical elements. If there is a basement, the perimeter foundation beams can extend up to the floor slab at its top, at least along most of each side of the perimeter. In that case, the building can be provided with the most effective foundation system for earthquake resistance, namely the box system outlined in Section 2.2.2.3. Section 2.3.3.3 is devoted to this system.

It is essential to model the soil compliance under the foundation beams, even for their design for gravity loads. The approach commonly used to that end is that of the subgrade reaction modulus (also known as Winkler foundation spring). Libraries of commercial software for analysis and design of buildings for seismic or non-seismic actions often include a special linear-elastic beam-on-elastic-foundation element,

with the soil subgrade-reaction-modulus among its parameters. A single element of this type can be conveniently used to model the full length of a foundation beam between adjacent vertical elements. Uplift between the underside of the foundation beam and the ground cannot be modelled with this linear approach. Anyway, neither the extent nor the consequences of partial uplift are significant in a two-way system of stiff foundation beams. To take into account uplift, soil compliance may be modelled with discrete no-tension vertical springs at regular spacing along the underside of each foundation beam. A linear-elastic version of such modelling may be applied, if the computer code used does not include in its library a special beam-on-elastic-foundation element.

2.3.3.3 Box Type Foundation Systems

The ideal shallow foundation for earthquake-resistant buildings is the box-system already described in Section 2.2.2.3. Such a system suits well buildings with basement, even when that basement is only partially embedded and has some openings along the perimeter. However, for the system to be fully effective, any openings between the top of the perimeter foundation beam and the soffit of the beam supporting the basement roof should be limited to a small fraction of the corresponding side of the perimeter.

It is not essential to have a raft, or a two-way system of foundation beams connecting the bottoms of the perimeter deep foundation beams. Interior vertical elements may be founded, instead, on individual footings, provided that these footings are connected to the bottom of the perimeter foundation beams through a diaphragm consisting of two-way tie-beams or a slab (possibly serving also as the basement floor). As the transfer of the full seismic action from the ground to the superstructure (or vise-versa) takes place through the perimeter beams, the foundation of interior elements and the above-mentioned diaphragm may be at a level slightly above the bottom of the perimeter beams.

Owing to its large rigidity and strength, a box-type foundation works as a rigid body. Thus, it minimises uncertainties about the distribution of seismic action effects over the interface between the ground and the foundation system and imposes the same rotation of all vertical elements at the level of their connection with this system, so that they may be considered as fixed there against rotation. Plastic hinges in walls and columns will develop just above the top of the box-type foundation. Fixity of interior vertical elements at the top of the foundation system is achieved through a couple of horizontal forces that develop at the levels of the top and bottom of this system. The main role of the diaphragm at the bottom of the perimeter foundation beams is to provide the bottom horizontal force for the fixity of vertical elements at the top of the foundation box.

Because of the large rigidity and strength of a box-type foundation system, no inelasticity is expected to take place under the design seismic action in the interior vertical elements within the box (apart from potential plastic hinges at their tops underneath the roof of the basement) or in any beam of the foundation system (including those at the roof of the basement).

The seismic bending moment at the connection of interior vertical elements with their foundation element is small, and a footing (subjected in this case to essentially concentric compression) is sufficient for each one of them. The free height of the interior vertical element will be subjected to a seismic shear approximately equal to the moment resistance of the element at the level of the roof of the box, divided by the free height of the vertical element within the box (see Fig. 2.20 for a wall).

The top slab of a box-type foundation transfers the seismic shears from the interior vertical elements to the perimeter wall-type foundation beams. It should have sufficient in-plane stiffness (i.e. thickness) and strength (two-way reinforcement) and should be free of large interior openings. The restraint of shrinkage of this slab by the stiff perimeter elements may induce through-thickness cracking (cf. Section 2.1.6). Two-way reinforcement at both surfaces of the slab will reduce the consequences of such cracking on its in-plane stiffness. If the slab is cast shortly after the perimeter elements of the box to minimise their differential shrinkage, cracking due to restraint of drying shrinkage is less likely. Another option is to lap-splice all slab reinforcement in each direction of the slab along a strip all the way from one side of the perimeter to the opposite and defer for a few days casting of the concrete in that strip and striking of the formwork of the entire slab. In this way the early (and largest) part of the ultimate drying shrinkage of the parts of the slab cast first takes place without any restraint.

A box-type foundation offers additional advantages, which are not captured by a conventional analysis of the seismic response:

– An integral rigid foundation for the whole building filters out differences in the seismic input between different points of the base, due to arrival there of the seismic waves with a time-lag (be it short) and other minor differences. So, it introduces in the superstructure a single seismic excitation, which at any given point in time is the average of the ground motion over the entire interface (horizontal and vertical) between the foundation system and the ground. This smoothing of the input motion removes its high-frequency components. The larger the interface

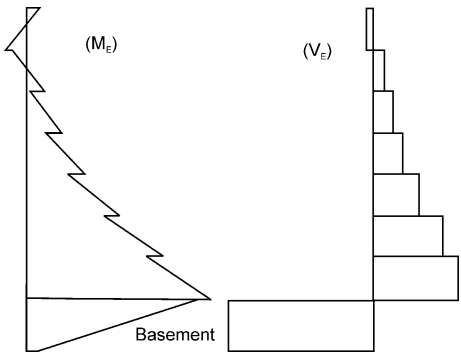

Fig. 2.20 Seismic moments and shears in an interior wall of a building with box-type foundation

between the ground and an integral foundation (e.g. in buildings with a raft at the bottom or with deep embedment due to more than one basement storeys), the more extensive is the smoothing of the input motion.

– If the system of the foundation and the superstructure is stiff relative to the underlying soil stratum (more specifically, if its fundamental period is shorter than that of the soil deposit) and, moreover, there is an integral and rigid foundation system for the entire building, some of the input energy is radiated back into the ground, instead of being trapped within the building. This phenomenon, termed "radiation damping" reduces the seismic forces and deformations in the superstructure.
– It is extremely rare, but not inconceivable, to have surface faulting through the foundation (as happened at Awaji island in Kobe (1995) and at the Bolu viaduct in the Ducze (TR) 1999 earthquake). An integral and rigid foundation may straddle the fault without collapse or severe damage in the superstructure due to the fault displacements – horizontal or vertical.

2.3.4 Capacity Design of the Foundation

The foundation is of paramount importance for the integrity of the whole. It is also difficult to access for inspection of seismic damage and even more difficult to repair or retrofit. So, it is ranked at the top of the hierarchy of strengths in the entire structural system and should be designed to remain elastic, with inelastic deformations and hysteretic energy dissipation limited to the superstructure it supports. To this end, the verification of the foundation of buildings designed for energy dissipation should be based on seismic action effects derived from capacity design calculations, on the basis of the overstrength capacity of the yielding elements of the superstructure. Eurocode 8 applies this capacity design concept for the verification of the foundation soil and, in general, for the dimensioning of the foundation elements. US codes (BSSC 2003, SEAOC 1999), by contrast, reduce the overturning moment at the base from the analysis, by 25% for "equivalent" static (lateral force) analysis, or by 10% for a multimodal response spectrum one. This is to account for uplift and (for the "equivalent" static analysis) for the different contribution of higher modes to the overturning moment than to the base shear.

For individually founded vertical elements (i.e., essentially for individual footings) seismic action effects from capacity design may be calculated assuming that the corresponding action effects from the elastic analysis increase proportionally until the dissipative zone or element that controls the seismic action effect of interest reaches the design value of its force capacity, R_{di}, times an overstrength factor, γ_{Rd}. This can be achieved by multiplying all seismic action effects from the analysis by:

– for individual footings: $$a_{\mathrm{CD}} = \gamma_{\mathrm{Rd}}\Omega = \gamma_{\mathrm{Rd}}(R_{\mathrm{di}}/E_{\mathrm{di}}) \qquad (2.15)$$

where E_{di} is the seismic action effect from the elastic analysis in the dissipative zone or element controlling the seismic action effect of interest. Implicit is the assumption

that the action effect of gravity loads concurrent with the design seismic action is negligible compared to R_{di} and E_{di}. Eurocode 8 specifies $\gamma_{\mathrm{Rd}} = 1.2$ if the q-factor value used in the design of the superstructure exceeds 3, or $\gamma_{\mathrm{Rd}} = 1.0$ if it doesn't.

For individual footings of walls or columns Ω is the minimum value of $M_{\mathrm{Rd}}/M_{\mathrm{Ed}}$ in the two orthogonal directions, y, z, of the sides of the element (even for L-, T- or U-section) at its lowest cross-section where a plastic hinge can form, as it is in that direction that the element will first develop its force resistance:

– for individual footings of columns or walls

$$a_{\mathrm{CD}} = \gamma_{\mathrm{Rd}} \min[(M_{\mathrm{Rd,y}}/M_{\mathrm{Ed,y}});\ (M_{\mathrm{Rd,z}}/M_{\mathrm{Ed,z}})] \tag{2.15a}$$

The moment resistances M_{Rd} in Eq. (2.15a) should be determined for a value of the axial force in that section of the vertical element from the analysis, $N_{\mathrm{Ed,}}$ using the same combination rule of the effects of the two horizontal seismic action components as for $M_{\mathrm{Ed,y}}$, $M_{\mathrm{Ed,z}}$. As we will see in Section 4.7.2, depending on the method of analysis (linear static or modal response spectrum analysis) and on how the effects of the seismic action components are combined, we may have 4 or even 16 such combinations of $M_{\mathrm{Ed,y}}$, $M_{\mathrm{Ed,z}}$, N_{Ed}. The value of a_{CD} computed for each one of these combinations multiplies the seismic action effects applied from the ground to the footing as reactions (biaxial moments and horizontal forces, vertical reaction), as well as those applied on the footing from the vertical element and all tie-beams framing in it. It multiplies also the seismic action effects in the tie-beam, up to the tributary length of the footing, i.e., normally up to tie-beam mid-span. (The value of a_{CD} from the column at the other footing to which the tie-beam is connected applies over the rest of the tie-beam). The seismic action effects multiplied by a_{CD} pertain to the same combination from which the value of a_{CD} has been computed. All these 4 or 16 combinations should normally be considered, as different ones may be critical for different verifications. For example, the bearing capacity of the soil, to be compared with the vertical reaction, decreases with increasing biaxial horizontal force reactions (which are the seismic ones from the analysis times a_{CD} for the same combination of seismic action effects) but decreases more with increasing biaxial eccentricities of the vertical reaction with respect to the centre of the underside of the footing. For the same (absolute) values of $M_{\mathrm{Ed,y}}$, $M_{\mathrm{Ed,z}}$ in Eq. (2.15a), the value of a_{CD} is largest when $M_{\mathrm{Rd,y}}$, $M_{\mathrm{Rd,z}}$ are largest, i.e., when the seismic axial force in the column or wall is compressive. The same holds for the vertical reaction (the seismic one from the analysis times a_{CD}, plus that due to the concurrent gravity loads) and the biaxial moment and horizontal force reactions (all proportional to a_{CD}), with the increase of which the bearing capacity decreases. However, the bearing capacity is very sensitive to the values of the eccentricities, which, being ratios of moment reactions to the vertical reaction, are largest when the vertical seismic reaction (the one from the analysis times a_{CD}) is tensile (uplifting). So, the bearing capacity verification may be more critical when the seismic axial force in the column or wall is tensile than when it is compressive (especially under exterior columns of tall frame systems), despite the lower value of a_{CD}. For sure, all verifications of the tie-beams

framing into the footing will be more critical when a_{CD} is largest, i.e., when the seismic axial force in the column or wall is compressive.

For common foundations of more than one vertical elements (e.g. in a box-type foundation, a raft, foundation beam, etc.) the value of Ω should be derived from the vertical element that develops the largest seismic shear for that particular direction and sense of the horizontal component of the seismic action. Eurocode 8 allows, as an alternative, to take the value of $\gamma_{Rd}\Omega$ equal to:

– for common foundations of two or more members: $a_{CD} = 1.4$ (2.16)

and multiply the seismic action effects from the analysis by 1.4, without capacity design calculations. The intention is not to fully cover the potential overstrength of all jointly-founded vertical elements, because plastic hinging of all these elements at the same instant in the seismic response is considered unlikely.

According to Eurocode 8, wherever in the foundation or its elements the seismic action effects from an analysis for the design seismic action with $q = 1.0$ is less than the result of capacity design calculations, this smaller value from the analysis may be taken as seismic demand in the verifications. This applies to parts of the foundation and to individual foundation elements. Eurocode 8 allows also calculating the seismic action effects for the entire foundation system from the analysis for the design seismic action using $q = 1.5$ and omit capacity design calculations. This option is consistent with the way seismic action effects are calculated in buildings designed for strength alone and not for ductility, (Ductility Class L, see Section 1.4.2.1). This is not a feasible alternative in high seismicity regions, especially for medium- or high-rise buildings, as the seismic action effects resulting from $q = 1.5$ for the entire foundation system may be prohibitively high for the verification of certain parts of that system.

Foundation elements dimensioned for seismic action effects derived from the above capacity design approach are expected to stay elastic under the design seismic action. So, Eurocode 8 allows applying to them the simpler dimensioning and detailing rules appropriate for seismic design for strength alone, in lieu of ductility. It also allows this simplification whenever the seismic action effects for the foundation element(s) are derived from an analysis with $q = 1.5$.

The foundation ground should always be verified for capacity design effects (or, as an alternative allowed by Eurocode 8 (CEN 2004a), with seismic action effects from the analysis for the design seismic action with $q = 1.5$). However, as far as the foundation elements themselves, in certain cases it makes more sense to dimension and detail them for ductility and energy dissipation, as in the superstructure. In that option, allowed by Eurocode 8, foundation elements are dimensioned in bending for seismic action effects derived from the analysis for the design seismic action using the q-factor of the superstructure. They are also dimensioned and detailed according to all relevant special rules pertaining to the corresponding ductility class and applying to elements of the superstructure. For example, tie-beams and foundation beams should be dimensioned in shear for a shear force derived from capacity design calculations (according to Section 1.3.6.2) and should follow all the special detailing

rules for the longitudinal and transverse reinforcement that aim at enhanced local ductility.

As pointed out in Section 2.3.3.3, owing to the large rigidity and strength of a box-type foundation, interior vertical elements in the box as well as all beams in this foundation system (including those at the roof of the foundation box) are expected to stay elastic under the design seismic action (except potential plastic hinging at the top of interior vertical elements underneath the roof of the basement). They can be designed and detailed following the simpler rules for seismic design for strength alone without ductility.

The connection between a foundation beam and a concrete column or wall is essential for the transfer of the seismic action effects from one element to the other. This connection is an inverted-T or a knee "beam-column joint" and should be dimensioned and detailed according to the rules applicable to such joints. This normally implies, among others, that the transverse reinforcement of the critical region at the base of the column or the wall should also be placed within its entire connection region with the foundation beam or wall (see Section 5.4). In buildings of DC H the connection region of a foundation beam with a concrete column or wall should also be explicitly verified in shear (see Section 5.4.2). The value of the design horizontal shear force to be used in this verification, V_{jhd}, may be obtained as follows:

- If the foundation beam is dimensioned on the basis of seismic action effects from capacity design calculations (i.e., in the simplification allowed by Eurocode 8, for 1.4 times the seismic action effects from the analysis for the design seismic action), then V_{jhd} may be determined from the analysis for the design seismic action. However, that analysis does not provide directly seismic action effects for the joints. So, V_{jhd} may be conservatively estimated as the design moment resistance at the base section of the column or wall, M_{Rd}, divided by the depth of the foundation beam, h_{b}.
- If the foundation beam is dimensioned for seismic action effects from the analysis for the design seismic action, V_{jhd} itself may be conservatively determined via capacity design calculations, on the basis of the areas of the top and bottom reinforcement of the foundation beam (see Sections 3.3.3.1 and 5.4.2).

2.3.5 A Look into the Future for the Seismic Design of Foundations

All modern seismic codes, including Eurocode 8 (CEN 2004a), consider the structure and the ground as uncoupled. Soil-structure interaction is taken into account to a limited extent, only in special cases and always considering the ground and its interaction with the structure and its foundation system as linear. Soil-structure interaction aspects covered in Eurocode 8 are limited to isolated issues, such as those of dynamic impedance of foundations, of material or geometric/radiation damping in the soil, etc. What is really needed in future is to consider in seismic design (a) the structure, (b) its foundation and (c) the soil, coupled into a single system and not

as isolated components. This includes consideration of the effects on the superstructure of (important) phenomena in the soil (large deformations and nonlinearities), or at its interface with the structure (e.g. sliding and/or uplift/rocking). Taking the structure, its foundation and the soil as a coupled system may lead to alternative cost-effective seismic design concepts that will allow – under certain conditions – concentration of nonlinearity and energy dissipation in the soil or in the foundation, with the soil and/or the foundation (possibly modified with the use of geo-textiles, or other structural inclusions) engineered into an isolation system of the superstructure. It may also change the global ductility demands in the superstructure, leading to inelastic spectra that relate the behaviour factor, q, of the superstructure not only to the period, T, and the displacement ductility factor, μ_δ, of the SDOF system, but also to important parameters of the foundation and the soil (e.g., uplift, embedment, resistance to combined shear and vertical force, etc.).

The concept of considering the soil and the structure as a system in seismic design is also very important for structures developing large interaction with the surrounding ground, such buildings with deep embedment, or underground facilities (including underground rail or metro stations, tunnels, buried storage facilities, etc.), which are currently outside the scope of Eurocode 8.

2.4 Examples of Seismic Performance of Buildings with Poor Structural Layout

2.4.1 Introductory Remarks

This section gives three examples of buildings that suffered partial collapse during earthquakes that hit Greek cities in the 1990s. All three buildings had been designed and built in the 1970s with very little engineered earthquake resistance. Their structural framing had been conceived with gravity loads as the main, if not sole, consideration.

The author has been involved in studies of the mechanisms that led to the collapses. Technical views expressed in the following are his own.

2.4.2 Collapse of Wing of Apartment Building in the Athens 1999 Earthquake

Figure 2.21 shows the framing plans of an L-shaped 5-storey apartment building (plus penthouse at the top, shown at the bottom row, right-hand side) in Athens. The 1st storey (top row, left-hand side) is essentially a mezzanine running along the middle of the L in plan, with its floor suspended via RC ties from the floor above (top row, right-hand side). Storeys 3–5 (bottom row, left-hand side) are very similar to each other, except that most columns decrease in size, sometimes from 400 or 600 mm at the ground floor to 200 mm at the top storey. There is a U-shaped wall

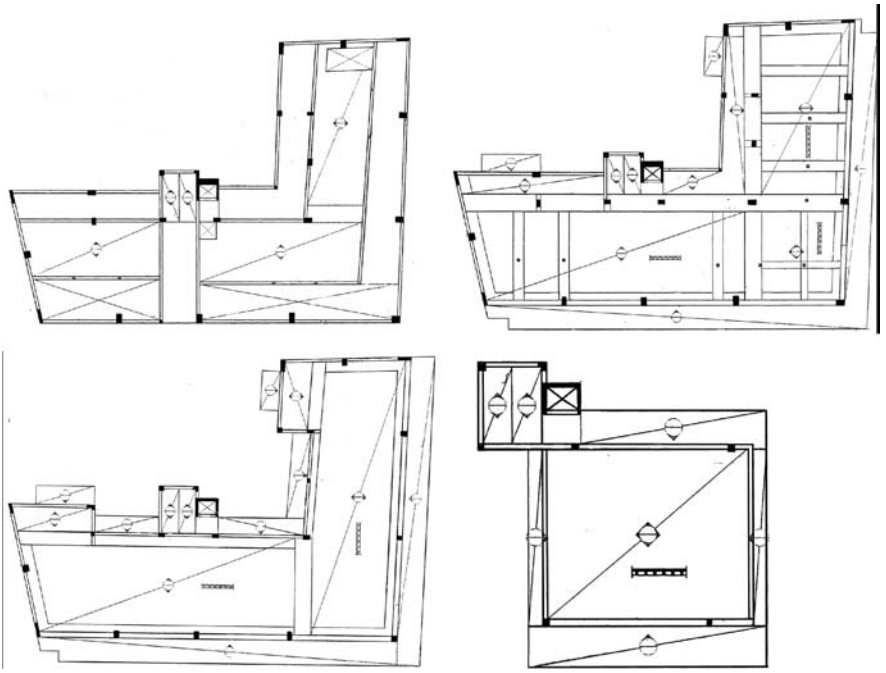

Fig. 2.21 Framing plans of partially collapsed apartment building in Athens (1999) earthquake

around the elevator shaft and a staircase right to the left of it, both very loosely connected to the rest of the framing (essentially, via a single beam per storey with a 200 × 400 mm cross-section). Floors have one-way ribbed slabs, with ribs and reinforcement essentially only along the short dimension of the L in plan. In floors 2–5 a 1.3 m-wide beam, with depth equal to that of the ribbed slab, is the only interior beam, running from the re-entrant corner to the opposite side in plan. Its intended purpose was to provide support to the one-way ribbed slab. The 2nd storey floor slab (top row, right-hand side) has several wide beams (with the same depth as the ribbed slab) to suspend the RC ties holding the 1st floor slab. Infills were rather uniformly distributed in plan and elevation and had many openings, except at the ends of the legs of the L, where the building – being a corner one – was in contact with the property line and adjacent buildings.

Figure 2.22 shows the location of the centre of overlying masses in each storey, CM, vis-à-vis those of:

- the centroid of the gross-section rigidity of storey vertical members, CR-uncracked, from Eqs. (2.2) in Section 2.1.5;
- the centre of rigidity of storey vertical members, CR-col, determined from Eqs. (2.2) but using the stiffness to yield-point, $(EI)_{\text{eff}}$, of storey vertical members (at both ends in skew-symmetric bending for columns, at the base section of the storey for walls) from Eq. (3.68) in Section 3.2.3.3;

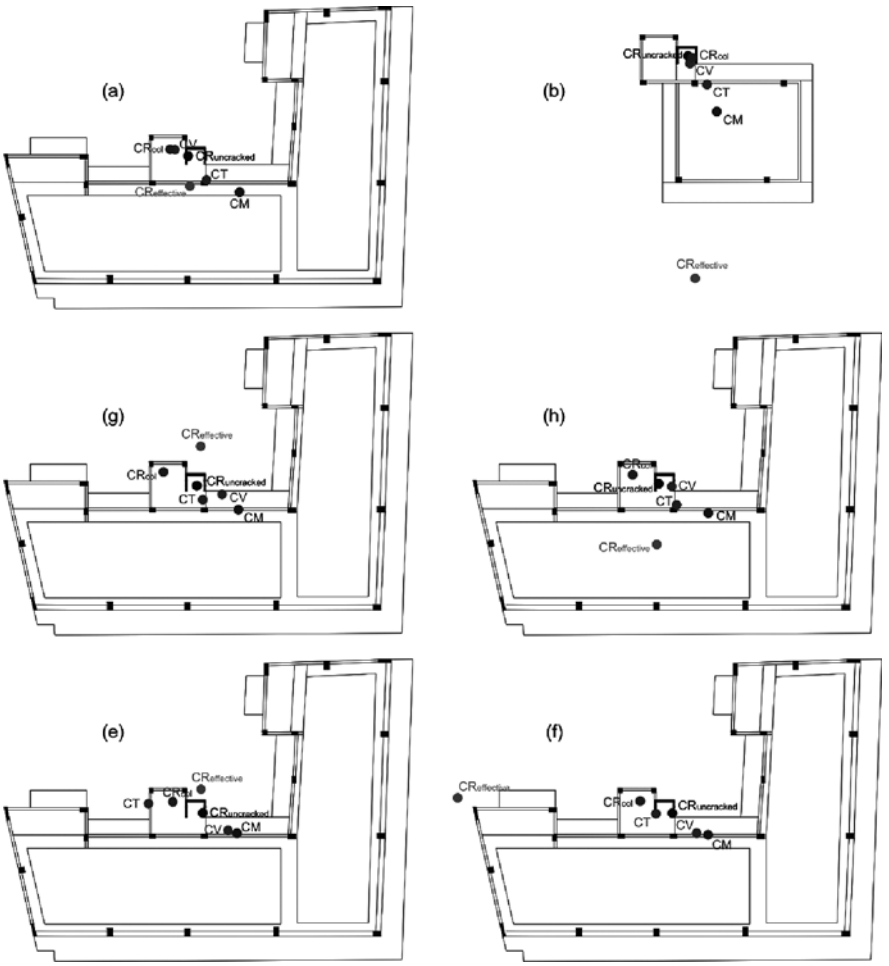

Fig. 2.22 Centres of mass (CM), rigidity (CR), strength (CV) and twist (CT) of 1st to 5th storey and of penthouse in the partially collapsed apartment building in Athens (Kosmopoulos and Fardis 2006)

- the storey centre of rigidity, CR-effective, defined and determined as in (Cheung and Tso 1986, Tso 1990) according to Section 2.1.5;
- the storey centre of twist, CT, determined as the pivot of the floor from elastic analysis with member stiffness equal to their stiffness to yield-point under storey torques with inverted triangular heightwise pattern (see Section 2.1.5); and
- the storey centre of resistance, CV, determined as the centroid of the lateral force resistance of storey vertical members, as controlled by shear or flexure – whichever is most critical.

As shown in Fig. 2.23(a), the wing of the building to the right of the elevator shaft and of the column on the opposite side in plan collapsed in the Athens 1999

(a)

(b)

Fig. 2.23 Apartment building in Athens: (**a**) wing that did not collapse; (**b**) detail of (**a**) showing the side of the 1st storey beam along the line where floor diaphragms were torn apart

earthquake. Witness in Fig. 2.23(b) the lack of any connection of the side of the beam with the secondary direction of the collapsed ribbed slab, along the line where floor diaphragms were torn apart.

The unusually large irregularity of the building in plan and elevation, the lack of a clear and simple lateral-load-resisting system, as well as the vulnerability of its diaphragms, are evident from Figs. 2.21 and 2.22. The eccentricities in Fig. 2.22 between the centre of overlying masses, CM, and the storey centre of twist, CT, representing the elastic storey rigidity, or the storey centre of resistance, CV, which is most pertinent for the inelastic range, suggest a torsional component of the response that would induce larger lateral displacements in the right-hand wing of the building.

Section 4.10.5.3 presents the conclusions of an in-depth study of the response of the building on the basis of a series of nonlinear response-history analyses. Most critical seem to be the penthouse above the 5th floor and several columns in the upper storeys of the right-hand wing. A very likely scenario is that collapse was triggered by shear failures of columns at the penthouse and in the upper storeys of the part of the building to the right of the elevator shaft. Very crucial turned out to be the large reduction of the cross section of many columns from the ground floor to the top storey, which in some cases may allow diagonal cracks that do not engage a single tie of the column. Floor diaphragms, being essentially unreinforced in the secondary direction, had indeed torn off along a line that starts next to the shaft and extends to the opposite side in plan. So, the part to the left of the elevator shaft did not follow the rest of the building to collapse, although it sustained heavy damage.

2.4.3 *Collapse of Four-Storey Hotel Building in the Aegio (GR) 1995 Earthquake*

A sea-side hotel building was located in between the city of Aegio (GR) and the epicentre of the 1995 earthquake. One of its three (structurally independent) four-storey buildings, shown in Fig. 2.24, collapsed during the earthquake. The framing plan of the standard floor of that building is shown in Fig. 2.24(a). There was a staircase near the upper left-hand corner in plan, with straight flights between landings at floor levels and in-between floors. The standard storeys from the 2nd to the 4th had one row of rooms along each long side in plan, separated by an internal corridor.

The short sides of the perimeter were fully infilled with 200 mm-thick masonry block-work in all storeys, except for certain openings at the ends of the corridor between the rooms at storeys 2–4 and for the right-hand side of the ground floor, which was open. The ground floor had a few 100 mm-thick solid interior partitions in the vicinity of the staircase and a similar one between the restaurant and the cooking facilities, all along one of the two interior longitudinal frames. It also had an exterior infill wall along the façade opposite to the one in Fig. 2.24(b), with an opening over its upper part creating a series of captive columns above the sill. In

Fig. 2.24 Collapsed hotel in Aegio (GR): (**a**) framing plan of standard floor; (**b**) façade frame intact; (**c**) collapsed part with the frame surrounding the staircase shown at the far-right

the overlying storeys, solid interior partitions with a thickness of 100 mm infilled the bays between columns in the direction of the short sides and, given that these columns had that direction as their strong one in bending, made up for the lack of interior beams and framing action along the short side in plan. At the 2nd to the 4th storeys the exterior infills of the two long façades, as well as the 100 mm-thick interior partitions between the rooms and the interior corridor, had many large openings and imparted very little lateral strength and stiffness to the frame. Overall, the ground floor had much fewer infills than the overlying ones. The slabs were one-way, with almost no secondary reinforcement.

The collapse of the building left the staircase and its surrounding frame almost intact, as well as the entire exterior frames on the side bordering the staircase and on the façade of Fig. 2.24(b). In all likelihood the collapse was triggered by shear failures of captive columns at the ground floor of the façade frame opposite to that of Fig. 2.24(b). The imbalance of infills between the ground floor and the overlying ones played a prime role. The survival of the staircase and of the surrounding frame may give the impression that the eccentricity they induced played an important role. However, torsional response was partially restrained by the almost full contact of the building with the adjacent stronger and stiffer one all along the side opposite to the staircase. The lack of interior beams and framing action along the short side in plan was also not a prime factor for the collapse, as the solid masonry panels between columns in that direction in the 2nd to the 4th storey made up for it (even for the ground floor, by limiting the column chord rotation at the level of the 1st floor).The lack of slab secondary reinforcement did not allow the diaphragm to redistribute forces from the distressed vertical elements whose collapse was imminent to the others and contributed to the partial collapse of the building.

2.4.4 Collapse of Six-Storey Apartment Building in the Aegio (GR) 1995 Earthquake

A six-storey (plus basement) corner building, with framing plans shown in Fig. 2.25, was standing at the top of a ridge in Aegio (GR) during the 1995 earthquake.

Due to the sloping ground, the wing of the L-shaped plan to the right of the staircase/elevator shaft was founded (through isolated footings without any tie-beams, as shown at the top right of Fig. 2.25) one storey-level above the other wing (that had the basement).

The far-right and the uppermost sides in plan were on the property line and were fully infilled in all storeys with stiff and strong 200 mm-thick masonry block-work. Infill panels on the two façades adjoining the external corner of the building and the two opposite ones (adjoining the re-entrant corner) had many large openings and imparted very little lateral strength and stiffness to the frame. Interior partitions were of 100 mm thick masonry block-work. The ones with solid panels were oriented mainly at right angles to the streets: i.e., parallel to the 200 mm-thick solid infills on the property line of the corresponding wing.

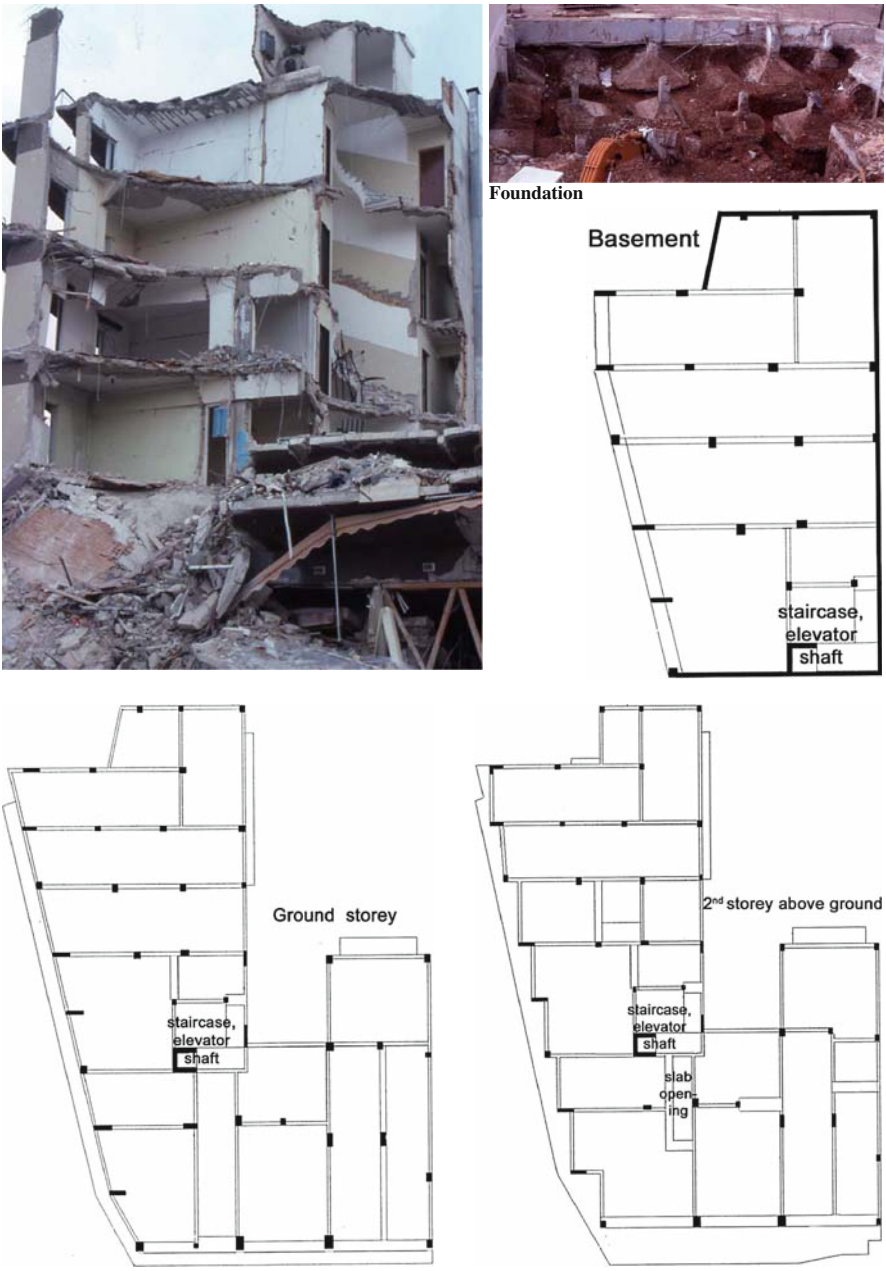

Fig. 2.25 Framing plans of collapsed apartment building in Aegio (GR) and pictures after removal of debris

Fig. 2.25 (continued)

At the ground storey and at the 2nd storey above ground level, a wide but shallow beam has replaced a proper beam along the full length of the façade frame shown at the bottom of each part of Fig. 2.25, probably to enhance lighting and the unobstructed view through the windows of the façade. A 800 mm wide strip of slab, with more reinforcement than the rest, plays the role of a beam at the level of the partly embedded basement in the frame of the façade to the left of that part of Fig. 2.25. In other cases such heavily reinforced strips of slab have replaced missing beams along part of the perimeter of two-way slabs (e.g., on two sides of the elongated slab open-

ing near the re-entrant corner of the L-shaped plan). At the upper right-hand side of the 4th storey above ground a heavily reinforced strip of the slab is used to support three one-storey "floating" structural walls, starting at that level owing to a setback of the 5th storey.

Witness the limited lateral strength and stiffness of the wing of the L-shaped plan to the right of the staircase/elevator shaft in its longitudinal direction (the horizontal one in Fig. 2.25):

- interior frames in that direction are not continuous throughout this part of the plan;
- columns there have their strong direction of bending in the transverse one of the wing;
- the beams of the three-bay façade frame at the bottom of each part of Fig. 2.25 are shallow and wide at the ground storey and the storey above, or eccentric with respect to the columns at the 3rd and 4th storeys above ground level;
- all infill panels on the two façade along the street and along the back side, as well as the 100 mm thick interior partitions in the same direction have many large openings.

The same wing has, by contrast, larger lateral strength and stiffness in its transverse direction, owing to, among others, the 200 mm-thick solid infills at the far-right side on the property line.

There is a relative surplus and a relative deficit in lateral strength and stiffness in the other wing of the L-shaped plan, but they are at right angles with respect to those of the former wing. Witness:

- the several structural walls at the façade to the left of each part of Fig. 2.25, with their strong direction of bending almost at right angles to the façade;
- the several continuous interior frames in the transverse direction of the wing;
- the two thick rectangular walls of the elevator shaft in the transverse direction of the wing, vs. the single thin one in its longitudinal direction
- the 200 mm-thick solid infills on the property line at the uppermost side in plan and several 100 mm thick solid interior partitions parallel to it and at right angles to the façade facing the street to the left.

Normally, a relative surplus in the lateral strength and stiffness of one of the two wings can make up for a deficit in the same direction in the other wing, provided that the diaphragms are strong enough to transfer large in-plane seismic shears from one wing to the other. In the present case, however, a large opening in the diaphragm starts at the very critical re-entrant corner of the perimeter, with another major opening next to it for natural lighting of interior spaces. The very narrow strip between that opening and the corner of the two façade frames is what is left of a diaphragm.

The strength and stiffness in the longitudinal direction of the wing to the right of the staircase/elevator shaft was apparently insufficient to withstand the seismic demands, probably increased in that direction (at right angles to the ridge) by topographic amplification of the ground motion (see Section 4.2.1). The wing could had mustered support in the direction of its distress from the surplus of lateral strength

and stiffness of its presumed partner on the left of the staircase/elevator shaft, had the narrow available strip of diaphragm the ability to deliver the support. The strip was torn apart, letting the wing to the right suffer the only collapse of a concrete building in the city itself, with many casualties.

After removal of the debris, the surviving wing of the building stood next to the line of separation as shown at the top left in Fig. 2.25.

Chapter 3
Concrete Members Under Cyclic Loading

This chapter presents the mechanical behaviour:

- of the constituent materials of concrete members, namely concrete and reinforcing steel, as well as of their interaction; and
- of concrete members typical of buildings,

under cyclic loading of the type induced by strong earthquake shaking. This behaviour determines how concrete and reinforcing steel are used in concrete elements (notably, the shape and dimensions of concrete members and the shape, amount and layout of their reinforcement), for satisfactory seismic performance of the members and the structural system as a whole.

Some of the material in this chapter provides the background for detailing rules specified in Part 1 of Eurocode 8 for ductile members in new earthquake resistant buildings. These rules are derived in Chapter 5. Besides, the rules and expressions given in Part 3 of Eurocode 8 for the deformations of concrete members at yielding and at ultimate conditions are also presented here, along with their background and justification. This material is used and developed further in Chapter 4 for the modelling of concrete members in seismic response analysis and in Chapter 6 for the assessment and retrofitting of existing concrete members.

3.1 The Materials and Their Interaction

3.1.1 Reinforcing Steel

3.1.1.1 Stress-Strain Behaviour Under Cyclic Uniaxial Loading

Owing to their one-dimensional geometry, reinforcing bars are essentially subjected to uniaxial tension or compression. So, we are interested in the uniaxial σ-ε behaviour of reinforcing steel. The fundamental features of this behaviour are shown in Fig. 3.1. Yielding at the yield stress f_y is followed by the yield plateau, which is relatively short, at least in the reinforcing steels currently used in most of the world.

M.N. Fardis, *Seismic Design, Assessment and Retrofitting of Concrete Buildings*, Geotechnical, Geological, and Earthquake Engineering 8, DOI 10.1007/978-1-4020-9842-0_3,

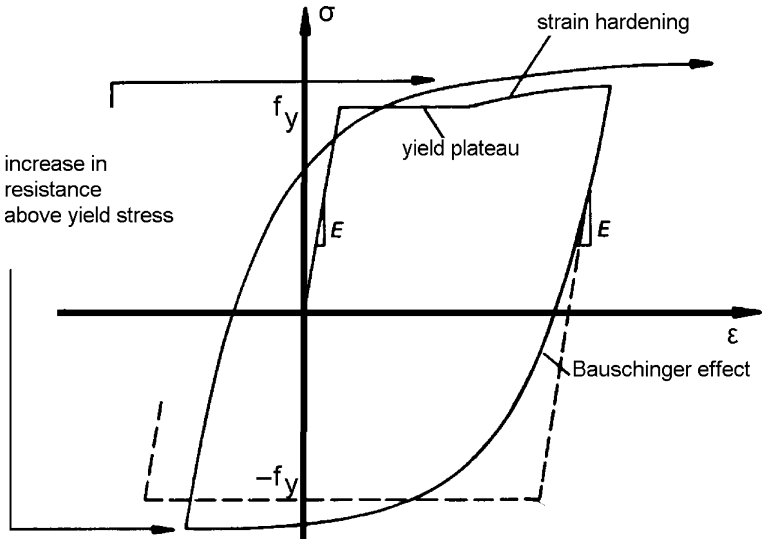

Fig. 3.1 Features of the cyclic σ-ε behaviour of reinforcing bars

Strain-hardening follows. Under monotonic loading strain-hardening leads to the maximum stress, f_t, termed tensile strength, that takes place at strain ε_{su}, which is called strain at maximum stress (or uniform elongation at failure) and is taken as the nominal ultimate strain of steel under monotonic loading.

Unloading from the yield plateau or from the strain-hardening region is initially elastic, but it gradually deviates from linearity before reaching the yield stress in monotonic compression, $-f_y$, as if the steel yielded prematurely. This is termed "Bauschinger effect". Because of it the tangent modulus of elasticity decreases from the elastic value, $E_s = 200$ GPa, to zero; but it does so gradually, not abruptly as when steel first yields in monotonic loading.

If the steel has yielded first in tension, then unloading does not lead to a yield plateau in compression. The Bauschinger effect leads to a stress that exceeds the yield stress in compression, $-f_y$. If there is a reversal of stress and strain (i.e., unloading from compression and reloading towards the original direction of loading, i.e. to tension), it leads to a σ-ε branch similar to that of the previous unloading from tension to compression. The reloading branch exceeds the yield stress f_y in first (virgin) loading and heads towards the point from where the previous reversal from tension to compression had started (previous peak stress and strain point in the current direction of loading). If loading continues past that point, it follows the σ-ε curve in monotonic loading till rupture of the bar, unless a new reversal of loading takes place towards compression.

In the unlikely case (for a bar in a concrete member) that before it yields in tension the bar yields in compression without buckling, the yield plateau takes place in compression alone (see Fig. 3.2(a)). The rest of the σ-ε behaviour is similar to the one described above, with the roles of compression and tension interchanged.

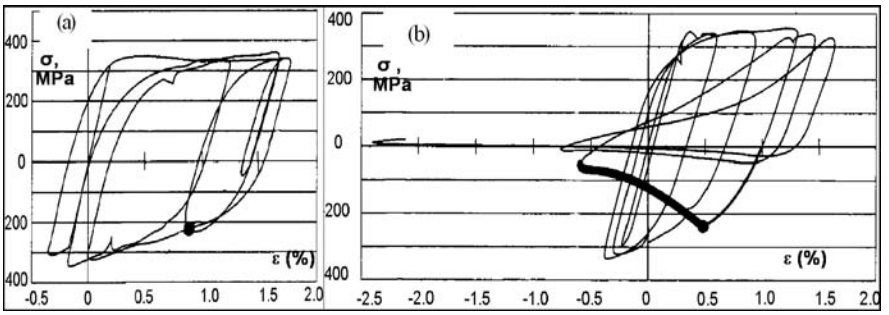

Fig. 3.2 σ-ε loops of bar that buckles in a concrete member under cyclic loading: (**a**) stress σ v real strain ε along the axis of the buckled bar; (**b**) stress v apparent strain in the original direction of the bar axis (adapted from Suda et al. (1996)). Buckling is displayed as (•)

An unloading branch from tension to compression (or vice-versa) and the following reverse branch of reloading in the opposite direction towards the point from where the first branch started, constitutes a hysteresis loop. If the second reversal (from compression to tension) occurs at a stress and strain equal and opposite to those at the first reversal (from tension to compression), the hysteresis loop is symmetric (see Fig. 3.3(a)).

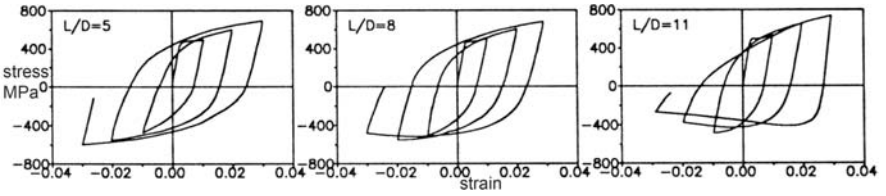

Fig. 3.3 Loops of stress vs apparent strain of bar subjected to cyclic loading with full reversal, as a function of the ratio of free bar length to diameter, *L*/*D* (Monti and Nuti 1991)

3.1.1.2 Buckling of Longitudinal Reinforcing Bars in Concrete Members Subjected to Cyclic Flexure and Its Consequences

Unless well restrained laterally – by a thick shell of sound concrete cover and/or engagement by closely spaced transverse reinforcement – a longitudinal bar in a flexural plastic hinge of a concrete member may buckle. Outward lateral pressures exerted on the bar from the bulging concrete core accelerate buckling.

As buckling entails lateral deflection of the bar, the distance between the two ends of the buckled length, *L*, shortens without any real axial shortening of the bar itself. The experimental σ-ε values in Fig. 3.2(a) show that right after buckling the mean axial strain of the bar increases algebraically: the bar axis unloads (its mean compressive stress decreases) following the σ-ε law of the material. As bending of the bar axis due to buckling shortens the distance between the ends of its buckled

length, the apparent strain of the bar along its original axis (i.e., the relative displacement of the two ends along the original axis, divided by their original distance L) decreases algebraically. Remember that what matters for the macroscopic behaviour of the member, in whose compression zone the bar belongs, is the force in the bar as a function of the average strain of the surrounding concrete, i.e. of the apparent strain of the buckled bar, not of the real one. The stress-apparent strain behaviour of a buckling bar is as shown in Fig. 3.2(b) and in Fig. 3.3(b) and (c) for bars with unrestrained length 8- or 11-times the diameter, respectively.

A longitudinal bar in a flexural plastic hinge will not buckle, unless the adjacent concrete has already disintegrated or the concrete cover is thin and weak, providing little lateral restraint. Real lateral restraint against buckling is provided only by closed ties. The effective buckling length depends on the conditions of engagement of the bar by, and the spacing and diameter of the ties. Under ideal conditions, the effective buckling length is equal to 50% of the tie spacing or of the distance of the first tie engaging the bar from the end section where the member connects to another one or to the foundation. In reality, the deflection of the bar upon buckling will extend beyond the ties engaging it and the effective buckling length will exceed the ideal value above. Ties with small diameter compared to the longitudinal bar may stretch and let the effective buckling length extend over several tie spacings (see Fig. 3.4(b)).

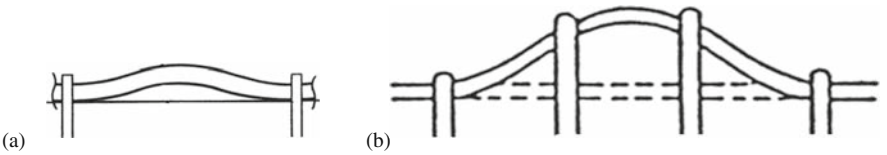

Fig. 3.4 Bar buckling over: (**a**) one; or (**b**) several tie spacings

The stress at which the bar may buckle is proportional to its Modulus and to the square of the ratio of the bar diameter to the effective buckling length. Regarding the Modulus, note that bars in concrete members subjected to seismic loading normally yield in tension before they do so in compression (see Figs. 3.5, 3.6 and 3.7 for typical seismic σ-ε histories of bars in various types of concrete members). Buckling usually takes place during a σ-ε branch of unloading from tension to compression

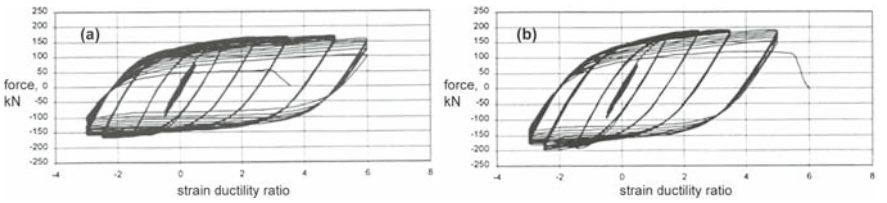

Fig. 3.5 σ-ε histories of the type induced by seismic action to column bars: (**a**) for grade S400 steel; (**b**) for S500 steel (Carvalho and Coelho 1997)

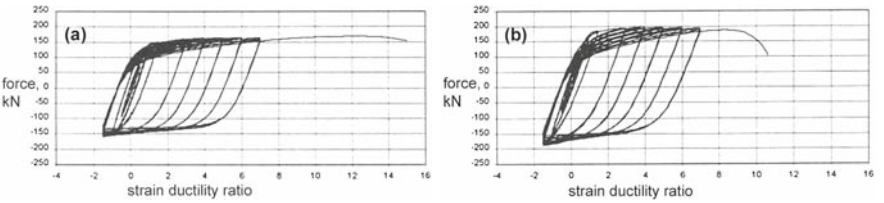

Fig. 3.6 σ-ε histories of the type induced by seismic action to bottom bars of beams: (**a**) for grade S400 steel; (**b**) for S500 steel (Carvalho and Coelho 1997)

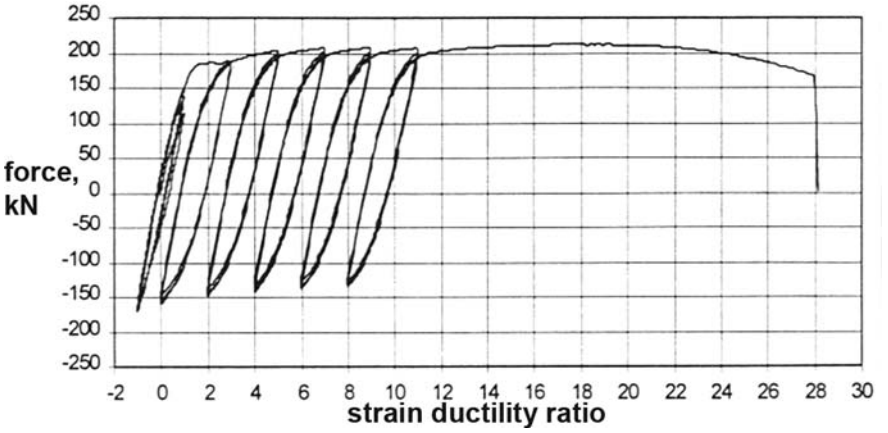

Fig. 3.7 σ-ε history of the type induced by seismic action to S500 top bars in beams (Carvalho and Coelho 1997)

that exhibits the Bauschinger effect, or in the hardening branch that follows it. So, it is not the Elastic Modulus, $E_s = 200$ GPa, that applies for the critical buckling load of the bar, but a much lower value. If bending due to buckling is considered to cause one side of the bar cross-section to unload elastically while the opposite side continues loading, then Engesser's "Reduced Modulus" or "Double Modulus" applies, which has a value between E_s and the tangent Modulus, E_t. For buckling of round bars in the strain hardening range the "Reduced Modulus" is about double the strain hardening modulus (Pantazopoulou 1998). In Shanley's alternative model for inelastic buckling the axial force in the bar is considered to keep increasing while buckling commences (as if the full bar section continues loading). So the tangent Modulus (which is much lower than Engesser's "Reduced Modulus") is considered to apply. No matter which one of the two approaches is adopted, the reduction in Modulus is such that an individual bar is predicted to buckle at a load much lower than Euler's critical load for elastic buckling.

The buckling behaviour of an individual bar compressed under force-control is different from that of a longitudinal bar in the compression zone of a flexural plastic hinge (Pantazopoulou 1998), as the latter is just one component in a highly

redundant parallel system encompassing the entire compression zone and comprising concrete and several longitudinal bars. Occurrence of buckling is very sensitive to minor differences in the lateral restraint conditions of the bar and to the pressure exerted on it by the bulging concrete. So, the longitudinal bars of the compression zone will not buckle all at the same time. Buckling of a bar takes place under conditions of deformation control and allows force redistribution to the rest of the parallel system. So, it does not have the immediate catastrophic consequences that we see, e.g., when a strut in a statically determined steel truss buckles. Normally the member will survive buckling of one or more longitudinal bars.

The immediate consequence of buckling of a compression bar in a concrete member is a drop in the lateral force resistance of the member, due to the following reasons:

- Unless it has already taken place, spalling of the shell of concrete cover will be triggered by bar buckling, as, without prior disintegration of the concrete core inside the cage of reinforcing bars, bars can buckle only outwards.
- Redistribution of the compressive force of the buckled bar brings the surrounding concrete closer to exhaustion of its compressive strength.
- A buckled bar does not contribute anymore to the confinement of the concrete core, particularly if its buckled length extends over several tie spacings. In this latter case the lateral bar deflection due to buckling stretches all ties that lie within the buckled length and reduces their own effectiveness in confining the concrete inside.

Note that in a concrete member subjected to bending the compression zone is on the concave side. So, its longitudinal bars, having their convex side inwards, would tend to buckle inwards against the concrete core. Buckling outwards would be much easier, as the concrete shell may have already spalled off, or if it hasn't, it can spall upon bar buckling. For the bar to buckle outwards, it has to overcome and reverse its inwards pre-curvature, which is unlikely. So, it is the corner bars that normally buckle first, and, as a matter of fact, they do so outwards almost at right angles to the plane of bending of the member and of the bar. For an intermediate bar to buckle, the concrete core in its immediate vicinity should be in (imminent) disintegration.

The interplay between the tendency of a compression bar in a concrete member to buckle over one or more tie spacings, the lateral pressures exerted on it by the confined concrete core and the restraint provided by the ties both against bar buckling and bulging of the confined concrete, is very complex even for monotonic loading (Pantazopoulou 1998). The phenomena are much more complex under cyclic loading, as described in the following paragraphs.

In a concrete member subjected to cyclic bending, the tension is taken exclusively by the tensile reinforcement, while the compression reinforcement shares the compressive force with the surrounding concrete. As a result, if the member is subjected to no axial load or to low axial compression, symmetric load cycles (i.e. cycles between equal and opposite values of moment M, or curvature, φ) induce in longitudinal bars asymmetric σ-ε cycles, with peak tensile strains significantly

exceeding the peak compressive ones and permanent tensile strains accumulating in the reinforcement of both sides. The σ-ε histories in Figs. 3.5, 3.6 and 3.7 are typical of what happens in concrete members subjected to cycles of constant moment amplitude but increasing deformation amplitude:

- in Fig. 3.5, for the bars of a column with symmetric reinforcement and relatively low axial load ratio, $\nu = N/A_c f_c$;
- in Fig. 3.6, for the bottom bars of an asymmetrically reinforced beam, that yield in compression in order for the crack to close at the bottom under positive (sagging) moments;
- in Fig. 3.7, in the beam's top reinforcement, which normally has larger cross-sectional area than the bottom one and never yields in compression.

In the σ-ε histories of Fig. 3.5 bar buckling may take place under conditions of tensile strain but of compressive stress in the bar. These bars, having unrestrained length six-times their diameter, indeed buckled during the last compressive half-cycle and ruptured in the following tensile half-cycle. The bars of Fig. 3.6(a) and (b) have the same geometry and mechanical properties as those of Fig. 3.5(a) and (b), respectively, but didn't buckle. They eventually broke in tension, at a strain at maximum stress not much lower than the uniform elongation, ε_{su}, of the steel in monotonic loading. Note the superior ductility of grade S400 steel over S500 in Figs. 3.5 and 3.6.

Bars seem very vulnerable to buckling during that phase of unloading-reloading when the crack is open throughout the depth of the section, owing to cyclic accumulation of tensile strains in the reinforcement of both sides, exhibited by all bars in Figs. 3.5, 3.6 and 3.7 (see also point 3 in Section 3.2.2.6). During that phase the reinforcement alone resists the compression force of the section and, in the absence of the stabilising effect of concrete, the bars of the compression zone may be considered as liable to buckling all at the same time. Fortunately, the crack may be open throughout the depth only at about the time the bending moment of the section changes sign. The likelihood of buckling during that stage is reduced by the low magnitude of compression stresses in the reinforcing bars and of the lateral pressure exerted on them by the concrete inside. Buckling may start shortly thereafter, before the surrounding concrete is fully mobilised in compression but after the bending moment increases sufficiently to build up the stress in the bar and reduce its tangent Modulus to the level necessary for buckling (see, e.g., the point where buckling occurs in Fig. 3.2(a)). It may start even later, after the outward pressure exerted on the bar and its restraining ties by the bulging concrete builds up as well.

Sometimes, but not often, bar buckling entails an immediate drop in the lateral force resistance of the member, large enough to be considered as ultimate failure.[1]

[1] A member is conventionally considered to have reached its ultimate deformation, if its (lateral) force resistance cannot increase above 80% of the maximum ever force resistance (defined as the force capacity of the member) by increasing the member's deformation, see Section 3.2.2.7.

Even when it is not, buckling of longitudinal bars in members subjected to cyclic loading may precipitate ultimate failure afterwards, by rupture in tension of the buckled bar during a subsequent half-cycle of loading, according to the following mechanism: Buckling induces in the bar additional flexural strains, positive (tensile) on one side and negative (compressive) on the other. These strains are superimposed on the axial strain of the axis of the bar (the one on the horizontal axis of Fig. 3.2(a)). The shorter the length, L, over which the bar buckles, the larger are the additional flexural strains. In all likelihood, the mean bar strain on which the flexural strains are superimposed is tensile, due to the yielding of the bar in tension before and the permanent extension it entails (cf. Fig. 3.2(a)). So, the total (mean plus flexural) strain of the extreme tensile fibres of the bar may approach, or even exceed, the uniform elongation, ε_{su}, of steel. Note that, exceedance of the rupture strain at the bar surface upon buckling is more likely in the Tempcore steels currently dominating the European market. These bars owe their superior yield and tensile strengths to quenching and tempering of their surface, which increases very much the strength of the skin but reduces its elongation at failure.[2] So, a crack may develop at the surface of the buckled bar. After reversal of the loading of the member, the bar that has buckled straightens up and – depending on the magnitude of the new half-cycle – may go into the inelastic range in tension. Then the pre-existing crack may extend through the entire cross-section, causing complete loss of the bar. If the loss of the tensile capacity of the bar causes a drop in the peak force resistance exceeding 20% of the maximum ever force resistance (see footnote 1 above), we will conventionally call this failure (or ultimate deformation) of the member.

Should the compression zone lose a large fraction of its compressive strength owing to abrupt or gradual disintegration of the concrete during load cycling, its longitudinal bars will buckle, unless they have done so already.

3.1.1.3 Time Effects on the Mechanical Behaviour of Steel

The fundamental quantities characterising a reinforcing steel, notably the yield stress, f_y, the tensile strength, f_t and the uniform elongation at rupture, ε_{su}, are measured in the lab under strain rates which are very slow compared to those induced by an earthquake. For the types of steel normally used in earthquake resistant design, namely steel grades S400–S500, it may be considered that the values of the aforementioned σ-ε parameters under monotonic loading increase with strain rate, $\dot{\varepsilon}$, by $c\ln(\dot{\varepsilon}/\ 5 \times 10^{-5})$ above those measured in the lab under quasi-static loading with $\dot{\varepsilon} = 5 \times 10^{-5}\ \mathrm{s}^{-1}$, where (CEB 1988a):

$c = 6$ MPa for f_y,
$c = 7$ MPa for f_t and
$c = 0.3\%$ for ε_{su}.

[2] Whatever effect, internal or external, increases the strength of steel, typically reduces its ductility and elongation at failure.

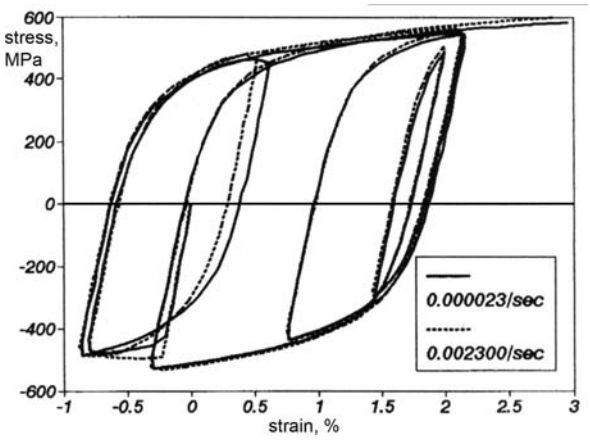

Fig. 3.8 Effect of strain rate on hysteresis loops of reinforcing steel (adapted from Restrepo-Posada et al. (1993))

Cold worked reinforcing steels, that are normally not used in earthquake resistant structures, exhibit a smaller effect of strain rate on the values of f_y and f_t than the more ductile types of steel, like those of grade S400–S500. The effect on their – anyway low – ultimate elongation is more pronounced.

Everything that has been said so far refers to monotonic loading. Figure 3.8 suggests that under cyclic loading the strain rate affects only the yield stress, leaving the subsequent σ-ε behaviour (notably the peaks of hysteresis loops) unaffected.

The strain rate is not constant during seismic loading. It is zero at peaks of the deformation, positive or negative, and attains a maximum value in-between these peaks (normally, at zero stress). The increase in strength relative to the quasi-static value is not derived from the mean strain rate during the half-cycle of the response, but from a lower value, about 15% of the peak strain rate during the response (i.e. of the strain rate attained at practically zero stress), or about 30% of the average strain rate.

3.1.1.4 Requirements on the Reinforcing Steel Used in Earthquake Resistant Construction

The steel parameters which are of prime importance for the seismic performance of concrete members are:

- the strain at maximum stress (uniform elongation at failure), ε_{su}, and
- the ratio of tensile strength to yield stress, f_t/f_y ("hardening ratio"),

of reinforcing bars. The yield stress, f_y, per se is important just for the onset of yielding of structural members, to the extent it matters for the Operational or the Immediate Occupancy performance levels and for the member stiffness to the yield point.

The importance of ε_{su} for the failure of reinforcing bars, possibly after buckling, has been noted in Sections 3.1.1.1 and 3.1.1.2. The impact of ε_{su} on the ultimate deformation of a RC member is elucidated by the relationship between the ultimate

curvature of a concrete section, φ_{su}, as controlled by rupture of the tension reinforcement, and the value of ε_{su}:

$$\varphi_{su} = \frac{\varepsilon_{su}}{(1 - \xi_{su})\, d} \tag{3.1}$$

where d is the effective depth of the section and ξ_{su} the neutral axis depth at steel rupture, normalised to d.

The hardening ratio f_t/f_y is important for several reasons. First, the higher its value, the greater is the tangent modulus of the steel bar in its strain-hardening range and the later buckling will take place. More important is the role of f_t/f_y for the control of the value of the maximum moment at the end of a member and, through it, of the extent of plastification near that end. This extent may be defined as the length of the member over which the bending moment exceeds the yield moment, M_y. If we assume that after yielding the internal lever arm at the end section stays approximately constant, then the bending moment at the end section is equal to $M = (\sigma_s/f_y)M_y$, where σ_s is the stress of the tension reinforcement there. If failure of the end section takes place due to rupture of the tension bars, at that section we have $\sigma_s = f_t$. If the bending moment diagram is approximately linear in the vicinity of the end section over a length L_s (which is equal to the moment-to-shear ratio at the end section, i.e., to the shear span), then member plastification at failure due to steel rupture extends over a length of:

$$l_{pl} = L_s \left(1 - \frac{M_y}{M_u}\right) = L_s \left(1 - \frac{f_y}{f_t}\right) \tag{3.2}$$

Therefore, the higher the value of f_t/f_y, the longer is the zone of plastification as a fraction of the shear span L_s. In turn, the longer the length of plastification, l_{pl}, the larger is the value of the chord rotation at flexure-controlled failure of the shear span (see footnote 1 in Chapter 1 and Fig. 1.4 for the definition of the chord rotation at a member end). As a matter of fact, if we assume that along the shear span, L_s, only flexural deformations take place, the ultimate chord rotation at the end of the shear span, θ_u, is derived from Fig. 3.9 as:

$$\theta_u = \varphi_y \frac{L_s}{3} + \frac{l_{pl}}{3}\left[\varphi_u \left(1 + \frac{f_y}{2f_t}\right) - \varphi_y \left(\frac{1}{2} + \frac{f_t}{f_y}\right)\right] \tag{3.3}$$

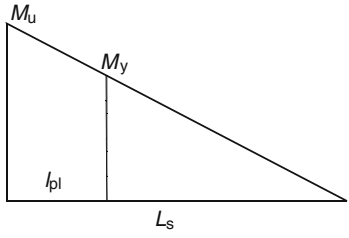

Fig. 3.9 Extent of plastification of member when the end section reaches its ultimate moment

where φ_y is the curvature at yielding of the end section and φ_u the ultimate curvature there (see Sections 3.2.2.2 and 3.2.2.4). For increasing f_t/f_y ratio, the value of the expression in brackets decreases, but not sufficiently to override the ensuing large increase in the value of l_{pl}. So, overall, the larger the hardening ratio, f_t/f_y, the greater is the flexure-controlled ultimate chord rotation at the end of the member where inelasticity takes place. As a matter of fact, if the value of f_t/f_y is close to 1.0, that of l_{pl} approaches zero and the flexure-controlled ultimate chord rotation is very low as well. For this reason, Eurocode 8 sets a lower limit to the value of the hardening ratio, f_t/f_y, of the steel to be used in ductile structures.

As emphasised in Section 1.3, current seismic design codes pursue the control of the inelastic seismic response through capacity design. The required force resistance of those regions or mechanisms intended to remain elastic is computed from equilibrium and the force capacities of the adjacent ductile regions or force-transfer mechanisms considered capable of developing large inelastic deformations. The only mechanism of force transfer entrusted to develop inelastic deformations under cyclic loading is flexure – provided that the yield moment is controlled by the tensile reinforcement and its nominal yield stress, f_{yk}. If the tensile strength of steel is much higher than its yield stress, soon after the ductile members yield their force resistance may increase well beyond the value used in the capacity design calculations. This increase may upset the balance between the force resistances of ductile and brittle mechanisms achieved through capacity design and cause the brittle mechanisms to exceed their force resistance and start developing inelastic deformations that they are not capable of. For this reason, Eurocode 8 sets an upper bound on the value of f_t/f_y of reinforcing steel to be used in ductile structures. For similar reasons, and, in addition, to ensure that the steel of any section or region will indeed yield before the concrete crushes, Eurocode 8 sets an upper limit on the ratio of the actual yield stress of the steel to the nominal value, f_{yk}.

Recognising that deformation and ductility capacity depends not only on the detailing of members, but on the inherent ductility of their materials as well, Eurocode 8 increases the ductility requirements on the steel in "critical regions" (i.e., those where inelastic deformations may take place under the design seismic action, see Section 5.1.1) of the elements of the lateral-load-resisting system (the "primary seismic" ones, see Section 4.12) with the Ductility Class, DC, as shown in Table 3.1. The limits on the hardening ratio, f_t/f_y, and the strain at maximum stress (uniform elongation at failure), ε_{su}, refer to lower 10% fractiles. The lower bound on ε_{su} is for ensuring a minimum curvature ductility and flexural deformation capacity, by preventing bar fracture prior to concrete crushing, or simply delaying it until a target flexural deformation is reached. The lower limit on f_t/f_y aims at ensuring a minimum length of the flexural plastic hinge according to Eq. (3.2). The ceiling on the values of f_t/f_y and $f_{yk,0.95}/f_{yk}$ is to limit flexural overstrength, and hence shear force demands on members and joints, as controlled by flexural yielding at the end of members, as well as the moment input from beams to columns.

Steels of class B or C according to Eurocode 2 (CEN 2004b) fulfil the conditions for the steel in DC L or M buildings. The conditions on ε_{su} and f_t/f_y of steel in DC H buildings are met only by steels of class C according to Eurocode 2.

Table 3.1 Requirements of Eurocode 8 for reinforcing steel in elements of the lateral-load-resisting system of new buildings

Ductility Class	DC L or M	DC H
5%-fractile yield strength f_{yk}	400–600 (MPa)	
95%-fractile actual yield strength $f_{yk,0.95}/f_{yk}$	–	$\leq$1.25
$(f_t/f_y)_{k,0.10}$	$\geq$1.08	$\geq$1.15
		$\leq$1.35
10%-fractile strain at maximum stress, $\varepsilon_{su,k,0.10}$	$\geq$5%	$\geq$7.5%

Strictly speaking, for buildings belonging in DC M the Eurocode 8 requirement for the use of steel of at least class B applies only to the "critical regions" at the ends of "primary seismic" elements. As in DC L buildings "critical regions" are not defined, the requirement for the use of steel of at least class B applies throughout the length of their elements. As DC M or H buildings should not in any respect be inferior in local ductility to DC L ones, the whole length of "primary seismic" elements of DC M and H buildings should have reinforcing steel of at least class B. The additional requirements on the steel of the "critical regions" of DC H buildings essentially apply:

- thoughout the entire height of "primary seismic" columns,
- in the "critical region" at the base of "primary seismic" walls, and
- in the "critical regions" near the supports of "primary seismic" beams on columns or walls (including the slab bars which are parallel to the beam and fall within the effective flange width in tension).

In practice, the Eurocode 8 requirements on reinforcing steel of "critical regions" are expected to be applied over the entire primary seismic element, including the slab it may be working with.

Thanks to its lower cost-to-strength ratio, weldability and fairly good ductility, weldable tempcore steel of type S500s has become the reinforcing steel of choice in the more seismic prone European countries since the mid-1990s. It is a surface-hardened low carbon steel with nominal yield strength of 500 MPa. It easily fulfils all Eurocode 8 requirements for DC L or M buildings, but it meets those for DC H ones (notably the lower limit on f_t/f_y) only when produced for application in moderate- or high-seismicity regions. The small quantity of S400 steel still on the market of these countries has higher strain at maximum stress, ε_{su}, and hardening ratio, f_t/f_y, both meeting easier the limit values for DC H buildings. However, the value of $f_{yk,0.95}/f_{yk}$ may exceed the maximum limit permitted for DC H. The main reason is that steels produced as S500 but failing to meet the minimum criteria on f_{yk}, are sometimes re-classified and marketed as S400.

The widest available survey of ductile steels of the type used in the seismic regions of Europe has been carried out in the early 1990s (Carvalho and Coelho 1997, Carvalho 1995, Pipa and Carvalho 1994), drawing several thousands of data from nine different European countries (Carvalho and Pipa 1994, Plumier and

Table 3.2 Outcome of surveys of steel used in seismic regions of Europe

Country of production	Spain, Portugal	Italy	Belgium, France, Germany, Italy, Luxembourg, Netherlands, Portugal, Spain	UK	Various
nominal yield strength, f_{yk} (MPa)	400	430	500	500	460
mean yield strength, f_{ym} (MPa)	496	478	571	552	530
95%-fractile of actual yield strength, $f_{yk,0.95}/f_{yk}$	*1.335*	1.19	1.23	1.165	*1.27*
mean tensile strength, f_{tm} (MPa)	598	733	663	653	618
$(f_t/f_y)_{k,0.10}$	1.15	1.44	*1.10*	*1.13*	–
$(f_t/f_y)_{k,0.90}$	1.27	*1.62*	1.23	1.23	–
mean strain at maximum stress, $\varepsilon_{su,m}$ (%)	11.8	11.6	10.4	11.7	11.1
10%-fractile of strain at max. stress, $\varepsilon_{su,k,0.10}$ (%)	9.6	9.7	8.6	9.7	–

Vangelatou 1995, Stanescu and Plumier 1993, Elnashai 1994, Calvi et al. 1994). That survey paved the way for the revision of the requirements of ENV 1998-1-3:1993 (the prestandard version of Part 1 of Eurocode 8) toward the limits in Table 3.1. The statistical outcome of that survey is compiled in Table 3.2, columns 1–5, in the form of average statistics of those steel parameters which are of interest to Eurocode 8. The last column of Table 3.2 gives also statistics of steel properties provided by the UK certification agency (Cairns 2006). All values listed in Table 3.2 meet the requirements of EN-Eurocode 8 for the reinforcement of DC L or M buildings. However, the values in italics in Table 3.2 violate the corresponding limit for the steel of DC H buildings. So, not a single one among the types of steel in Table 3.2 conformed fully to the limits placed on the steel of DC H buildings. Nevertheless, since then the steel industry in at least some European countries has developed and marketed cost-effective products that meet all Eurocode 8 limits for the steel of DC H buildings.

3.1.2 The Concrete

3.1.2.1 Concrete Under Cyclic Uniaxial Compression

Unlike reinforcing bars, which by geometry develop essentially only uniaxial stress conditions, concrete may be subjected also to biaxial or triaxial stresses. Because of its low tensile strength, concrete normally cracks at right angles to any significant tensile stresses. As a result, these stresses drop to zero. Even when there is no cracking tensile stresses are low anyway. The compressive strength and stiffness

of concrete decreases with increasing tensile stress in the transverse direction. This reduction is taken into account where relevant (see Eqs. (3.96) in Section 3.2.4.2 under *The Variable Strut Inclination Truss of the CEB/FIP Model Code 90 and Eurocode 2*). Compressive stresses in one of the three principal stress directions increase the compressive strength and stiffness in the orthogonal directions, but if the lowest of the three principal stresses is much smaller than the other two (regardless of its sign) the increase is negligible.

The prime case where multiaxiality of stresses has a major effect on the behaviour in the direction of the predominant compressive stress is when the stresses in both orthogonal directions are compressive and significant in magnitude. This is the case of confinement, Except for that case (dealt with at length in Section 3.1.2.2) and the strength reduction due to transverse tension (Eqs. (3.96) in Section 3.2.4.2 under *The Variable Strut Inclination Truss of the CEB/FIP Model Code 90 and Eurocode 2*), the multiaxiality of the stress field is neglected and the behaviour in the direction of the predominant compressive stress is considered, as if we had uniaxial compression.

The σ-ε behaviour depicted in Fig. 3.10 is typical of concrete under cyclic uniaxial compression. The energy dissipated by the material (i.e. the area enclosed by unloading-reloading hysteresis loops) is small, compared to either the deformation energy stored in the concrete at the peak of a loading cycle, or to the energy dissipated by steel under cyclic loading. Reloading σ-ε branches are directed toward the σ-ε curve in monotonic loading and follow it if reloading continues past the maximum ever previous strain value. Therefore, the monotonic σ-ε curve is the envelope and the skeleton curve of σ-ε loops under cyclic loading.

If unloading-reloading from and to a constant maximum stress equal to a large fraction of the uniaxial compressive strength, f_c, is repeated indefinitely, permanent compressive strains accumulate and the falling branch of the monotonic σ-ε envelope will ultimately be reached, signaling failure. In Fig. 3.10(b) 19 cycles at a peak stress of $0.9f_c$ suffice to reach the monotonic σ-ε curve. If the peak stress is at $0.85f_c$, 200 cycles are required for this to happen (Karsan 1968). This behaviour is characteristic of low-cycle fatigue. If the peak stress level is lower, the loading–unloading loops stabilise and the falling branch of the monotonic σ-ε curve is never reached.

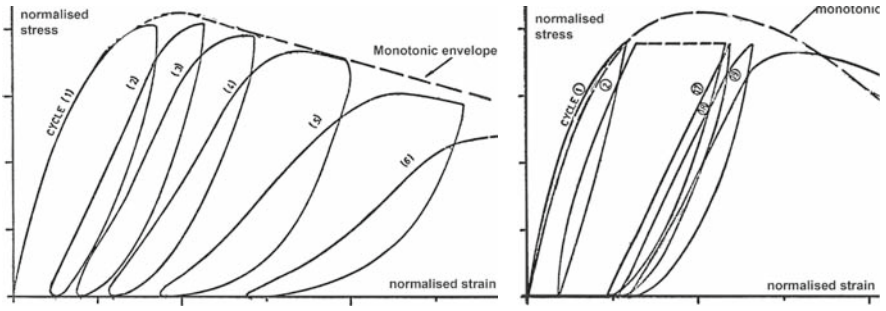

Fig. 3.10 σ-ε behaviour of concrete under cyclic uniaxial compression (adapted from Karsan (1968))

The number of stress cycles approaching the uniaxial compressive strength, f_c, in an earthquake is roughly equal to the duration of strong ground shaking divided by the predominant period of the structure. For a concrete building this number would normally be expected to be not more than 10, which means that low-cycle fatigue effects will not be important. Then, only the monotonic σ-ε behaviour of concrete in uniaxial compression is of interest.

Until a uniaxial stress of about $0.95f_c$ the Poisson ratio of concrete is approximately constant and close to 0.20. Above that stress level it increases fast, reaching a secant value of about 0.4 at ultimate strength. The underlying physical reason is that, as failure approaches, pre-existing microcracks at the interface of aggregates with the hardened cement paste extend into the latter in a direction parallel to that of the applied uniaxial compression stress and tend to join up as macro-cracks in that direction. The opening up of these macro-cracks soon leads to ultimate strength, manifesting itself as a precipitous increase in the apparent lateral strain. The volumetric contraction, which so far had been continuously increasing, starts decreasing. Right after ultimate strength it gives way to volumetric expansion (dilation). This mechanism has important implications for the enhancement of concrete strength through confinement.

3.1.2.2 Effects of Confinement on σ-ε Behaviour in Compression – Modelling

The case of prime interest in earthquake resistant design is that of concrete under the following conditions of triaxial compression:

- the stress in one principal direction, let's say direction 1, is compressive and rather high;
- the two other principal stresses, in directions 2 and 3, are compressive and about equal in magnitude, but smaller than σ_1: $\sigma_2 \approx \sigma_3 < \sigma_1$.

Such triaxial stress conditions are found in the compression zone when the concrete approaches its ultimate strength, provided that the lateral expansion that precedes its failure is restrained (Pantazopoulou 1995). Lateral restraint may come from various sources:

- tests have demonstrated that the restraint of the dilation of the compression zone of the end section of a member framing into another (a beam into a column, a column into a floor slab or a foundation element, etc.) by the volume of the surrounding concrete of the latter produces a triaxial stress condition, greatly enhancing the local strength and deformation capacity of the concrete (Takiguchi et al. 1997, Imai et al. 2005);
- closely spaced hoops or ties as transverse reinforcement restrain the lateral dilation of the concrete inside the cage of stirrups and longitudinal reinforcement (the "concrete core");
- Fibre-Reinforce Polymers (FRPs) wrapped around the member have a similar effect on the enclosed volume of concrete.

The restraint of the lateral dilation of concrete by such means is termed "confinement", and the volume of concrete affected is considered as "confined".

By opposing the large Poisson expansion arising from the opening up of internal macro-cracks parallel to the predominant compressive stress σ_1 when concrete is close to ultimate strength, a uniform pressure, $\sigma_2 = \sigma_3 = p$, at right angles to σ_1 and to these macro-cracks, increases the compressive strength in the direction of σ_1 from f_c to $f_c{}^*$ and the strain at the peak of the σ_1–ε_1 curve from $\varepsilon_{co} \approx 0.2\%$ to $\varepsilon_{co}{}^*$. The larger the lateral pressure, the greater is the enhancement of ultimate strength and of the corresponding strain. Moreover, the falling branch of the σ_1–ε_1 diagram after the peak at $f_c{}^*$, $\varepsilon_{co}{}^*$ becomes flatter with increasing value of p (i.e., confined concrete strain-softens slower). The monotonic σ_1–ε_1 curve for $p > 0$ is the envelope of the hysteresis loops under cycling loading with $p > 0$.

Several models have been proposed over the past decades for the σ-ε behaviour of confined concrete. A few of them are described here, notably those that are – for some reason or another – widely used, as well as simple models that fit well available experimental results.

The available test results for concentric compression show that the compressive strength in the direction of $\sigma_1 > \sigma_2 = \sigma_3$ increases with p as:

$$f_c^* = f_c(1 + K) \tag{3.4}$$

Eurocode 8 Part 3 (CEN 2005a) has adopted the value of K proposed in (Newman and Newman 1971).

$$K \approx 3.7 \left(\frac{p}{f_c} \right)^{0.86} \tag{3.5}$$

As shown in Fig. 3.11(a), Eq. (3.5) gives about the same result as the more complex expression fitted to data by (Elwi and Murray 1979):

$$K = 2.254 \left[\sqrt{1 + 7.94 \frac{p}{f_c}} - 1 \right] - \frac{2p}{f_c} \tag{3.6}$$

After its adoption by Mander et al. (1988), Eq. (3.6) is widely quoted and used today.

One of the earliest confinement models is the one proposed in Sheikh and Uzumeri (1982), still used in the US. It referred directly to confinement by ties. That model, gives:

$$K = a \left(7 \frac{\sqrt{2p}}{f_c} \right) \quad (p \text{ and } f_c \text{ in MPa}) \tag{3.7}$$

where a is the "confinement effectiveness factor" of the ties, given by Eqs. (3.24), (3.20), (3.21) and (3.22) in Section 3.1.2.3. The lateral pressure may be taken equal

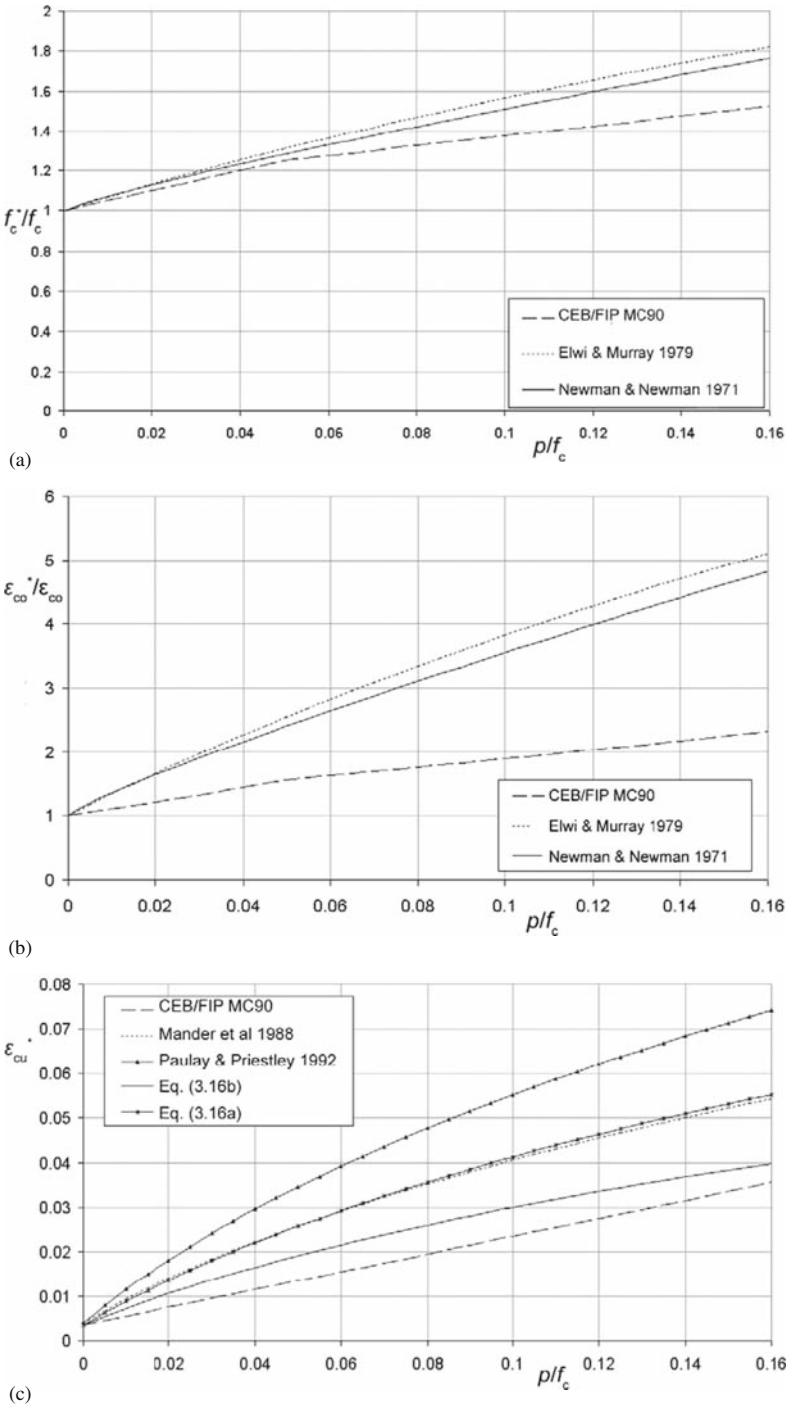

Fig. 3.11 Comparison of the predictions of various confinement models for the enhancement of concrete: (**a**) strength; (**b**) strain at maximum strength; and (**c**) ultimate strain

to $p = 0.5\rho_w f_{yw}$, where f_{yw} is the yield stress of the ties and ρ_w their volumetric ratio (ratio of the volume of stirrups to the volume of the confined core of the concrete, measured to the centreline of the perimeter stirrup) (cf. Eqs. (3.19) and (3.23)).

In Europe, the model in Model Code 90 of CEB/FIP (CEB 1991) is still in use, although it gives, in general, less enhancement of the key properties of concrete with confinement (see Fig. 3.11(a)). In that sense it is safe-sided for design. It is used mainly thanks to its adoption by Eurocode 2 (CEN 2004b). In that model the enhancement of ultimate strength and of the corresponding strain are given as:

$$f^* = \beta f_c = \min\left(1 + 5\frac{p}{f_c}; 1.125 + 2.5\frac{p}{f_c}\right) f_c \tag{3.8}$$

$$\varepsilon_{co}{}^* = \varepsilon_{co}\beta^2 \tag{3.9}$$

where β in Eq. (3.9) is the strength amplification factor in Eq. (3.8), standing for the factor (1+K) of Eq. (3.4).

If the two transverse stresses are not equal ($\sigma_2 > \sigma_3$) the value $p \approx (\sigma_2 + 4\sigma_3)/5$ may be used in Eqs. (3.5), (3.6) and (3.8). The smaller of the two transverse stresses controls confinement, implying that detailing of concrete members for earthquake resistance should aim at providing (about) the same restraint of lateral expansion in both transverse directions of the member.

Larger than the enhancement of maximum strength with confinement is the increase in the strain at maximum strength. According to Richart et al. (1928) the following expression applies (adopted also in Eurocode 8, Part 3 (CEN 2005a)):

$$\varepsilon_{co}{}^* \approx \varepsilon_{co}(1 + 5\,K) \tag{3.10}$$

Equation (3.10) gives much higher enhancement of the strain at maximum strength than Eq. (3.9) in Model Code 90 (CEB 1991) and Eurocode 2 (see Fig. 3.11(b)).

Confinement starts affecting the σ_1–ε_1 diagram only when the value of σ_1 approaches the uniaxial compressive strength of unconfined concrete, f_c. Until then, neither the tangent, nor the secant value of the elastic modulus of concrete are affected much by confinement. Note that the secant modulus from the origin to the peak of the σ_1–ε_1 diagram, i.e. the value of $f_c{}^*/\varepsilon_{co}{}^*$, drops, as the confining pressure increases. Note also that, if the ascending branch of the σ_1–ε_1 diagram is modelled as a parabolic curve (a common practice for uniaxial compression), then the initial tangent modulus is equal to $2f_c{}^*/\varepsilon_{co}{}^*$ and decreases with increasing value of p. This anomaly can be avoided by adopting – instead of the commonly used parabolic diagram – the σ_1–ε_1 relation proposed by Eurocode 2 (CEN 2004b) for use in nonlinear analysis of concrete structures. The generalised form of that relation is:

$$\frac{\sigma}{f_c^*} = \frac{\dfrac{\varepsilon}{\varepsilon_{co}^*}\left(k - \dfrac{\varepsilon}{\varepsilon_{co}^*}\right)}{1 + (k-2)\dfrac{\varepsilon}{\varepsilon_{co}^*}} \tag{3.11}$$

where:

$$k = 1.05 E_c \varepsilon_{co}{}^* / f_c^* \tag{3.12}$$

with E_c denoting the secant modulus of elasticity from the origin to a stress σ_1=0.4f_c, which is equal to $E_c = 11000 f_c{}^{0.3}$ (for E_c and f_c in MPa) according to Eurocode 2 (CEN 2004b). Equation (3.11) reduces into the simple parabolic σ_1–ε_1 diagram if k is taken equal to 2. By extension from the uniaxial compression for which it has been adopted in Eurocode 2, Eq. (3.11) may be considered to apply also along the softening branch beyond the peak at $f_c{}^*$ and ε_{co}.

In seismic design, more than the strength of concrete matters its ultimate strain – i.e. the strain beyond which concrete is considered to shed all its resistance to load and disintegrate – denoted as ε_{cu} (or $\varepsilon_{cu}{}^*$ for confined concrete). The ultimate deformation of a member (i.e. "failure") is conventionally identified with attainment of ε_{cu} at the extreme compression fibre of that section where the bending moment is largest (typically at the end section for seismic action), or of $\varepsilon_{cu}{}^*$ at the extreme fibres of the confined core. ε_{cu} is also conventionally defined as the strain at the point on the softening branch of the σ_1–ε_1 diagram where the stress, σ_1, has dropped to 0.85f_c (or to 0.85$f_c{}^*$, for $\varepsilon_{cu}{}^*$ in confined concrete). Recall that in design the flexural resistance of concrete sections is conveniently calculated assuming that the σ_1–ε_1 diagram is parabolic up to the peak stress and horizontal thereafter, until the value of ε_{cu}. The implication is that the value of ε_{cu} should be such that the softening branch of the σ_1–ε_1 diagram contributes to the maximum possible force that can develop in the compression zone with a force of $f_c b x(\varepsilon_{cu}$–$\varepsilon_{co})/\varepsilon_{cu}$, or of $f_c{}^* b^* x^* (\varepsilon_{cu}{}^* - \varepsilon_{co}{}^*)/\varepsilon_{cu}{}^*$ for confined concrete, where b and x are the width and depth of the compression zone, if rectangular, and b^*, x^* their counterparts in the confined core.

The Model Code 90 CEB/FIP model (CEB 1991), adopted by Eurocode 2 (CEN 2004b) for the design of new buildings, gives the following ultimate strain of confined concrete:

$$\varepsilon_{cu}{}^* = 0.0035 + 0.2 p / f_c \tag{3.13}$$

On the basis of test results showing that concrete confined by stirrups and subjected to concentric compression ultimately fails when concrete dilation causes the stirrups to exhaust their uniform elongation at failure, $\varepsilon_{su,w}$ and rupture, Mander et al. (1988) proposed that when the ultimate strain of confined concrete is reached, the total deformation energy stored in the stirrups until they rupture at strain $\varepsilon_{su,w}$ is equal to the gain in the total deformation energy of the confined concrete core. Assuming, for convenience, that the σ-ε diagram of the stirrup steel is horizontal (i.e. rigid-plastic) at a stress equal to f_{yw} until the failure strain of $\varepsilon_{su,w}$, the idea in Mander et al. (1988) gives: $\rho_w f_{yw} \varepsilon_{su,w} \approx f_c{}^* (\varepsilon_{cu}{}^* - \varepsilon_{cu})$, i.e.:

$$\varepsilon_{cu}{}^{*} \approx \varepsilon_{cu} + 2\varepsilon_{su,w}\frac{p}{f_c^*} \tag{3.14}$$

where the confining pressure p is taken equal to $p = 0.5\rho_w f_{yw}$, according to the discussion right after Eq. (3.7) and to Eqs. (3.19) and (3.23).

Paulay and Priestley (1992) proposed a modified form of Eq. (3.14), on the basis of test results for concentric compression (again with $p = 0.5\rho_w f_{yw}$):

$$\varepsilon_{cu}{}^{*} \approx 0.004 + 2.8\varepsilon_{su,w}\frac{p}{f_c^*} \tag{3.15}$$

Whatever has been said so far has been developed for concentrically compressed concrete and, strictly speaking, applies only there. What matters, though, for earthquake resistance is the behaviour of the extreme fibres in the confined concrete core of members subjected to cyclic bending, with or without axial load. Apart from the strain gradient (i.e. the fact that the strain is maximum at the extreme fibres, decreasing to zero towards the neutral axis), what is different from concentric compression is the target, which is the flexure-controlled ultimate deformation of the member.[3] Test results, especially in cyclic loading, show that by the time the ultimate curvature is reached, stirrups very rarely exhaust their elongation capacity and snap. Therefore, the value of $\varepsilon_{su,w}$ is not of prime importance for the confined concrete core.

If we adopt the analysis in Section 3.2.2.4 for the calculation of the ultimate curvature, φ_u, on the basis of first principles and use Eqs. (3.4), (3.5) and (3.10) for the confined concrete strength, $f_c{}^{*}$, and for the associated strain, $\varepsilon_{co}{}^{*}$, good average fitting to available experimental results on φ_u of cross-sections with rectangular compression zone and confined concrete core is achieved (with acceptable scatter) if the following expressions are used for $\varepsilon_{cu}{}^{*}$ (Biskinis 2007):

– for monotonic loading:

$$\varepsilon_{cu}{}^{*} = 0.0035 + \left(\frac{10}{h_c}\right)^2 + 0.57\frac{p}{f_c^*} \tag{3.16a}$$

– for cyclic loading:

$$\varepsilon_{cu}{}^{*} = 0.0035 + \left(\frac{10}{h_c}\right)^2 + 0.4\frac{p}{f_c^*} \tag{3.16b}$$

or, alternatively:

– for monotonic or cyclic loading:

$$\varepsilon_{cu}{}^{*} = 0.0035 + \left(\frac{1}{x_c}\right)^{3/2} + \frac{1}{3}\frac{p}{f_c^*} \tag{3.17}$$

[3] See footnote 1 in Section 3.1.1.2 for the definition of ultimate deformation (see also Sections 3.2.2.4 and 3.2.2.7).

where:

- h_c is the depth of the confined concrete core within the plane of bending (in mm);
- x_c is the neutral axis depth in the confined concrete core within the plane of bending (mm);
- the confining pressure, p, is related to the geometric ratio and to the arrangement of the confining medium (the transverse reinforcement), differently for Eqs. (3.16) or for Eq. (3.17) as specified in Section 3.1.2.3;
- the confined compressive strength, f_c^*, is given from Eqs. (3.4) and (3.5).

The "ultimate strain" of the extreme compression fibres of the unspalled section at its ultimate curvature (i.e. when the moment resistance of the unspalled section drops below 80% of the maximum previous moment resistance, see footnotes 1 and 3 of this chapter) may be determined from Eqs. (3.16) and (3.17) with $p = 0$ and the full section depth in the plane of bending, h, or the neutral axis depth x in the full concrete section, instead of h_c or x_c, respectively.

The 2nd terms in Eqs. (3.16) and (3.17) imply a size-effect, as in Bigaj and Walraven (1993) and Bosco and Debernardi (1993). Although this is a controversial issue (e.g., Alca et al. 1997), a size effect on ε_{cu} is rationalised on the basis of stability considerations of the compression zone (cf. the definition of ε_{cu} as the terminal strain of a parabolic-rectangular σ-ε diagram that reproduces the maximum possible resisting force of the compression zone).

Part 3 of Eurocode 8 (CEN 2005a) proposes the following for the ultimate strain at the extreme fibres of the confined concrete core in members under cyclic bending:

$$\varepsilon_{cu}^* = 0.004 + 0.5\frac{p}{f_c^*} \tag{3.18}$$

Equation (3.18) is meant to be used with Eqs. (3.4), (3.5) and (3.10) for f_c^* and ε_{co}^* in a package considered by Part 3 of Eurocode 8 as more accurate and representative than the confinement model of Eurocode 2, consisting of Eqs. (3.8), (3.9) and (3.13).

Figure 3.11(c) compares the outcome of Eqs. (3.16) to those of Eqs. (3.13), (3.14) and (3.15). For the purposes of this comparison, the value of $\varepsilon_{su,w}$ used in Eqs. (3.14) and (3.15) is the average in the tests to which Eqs. (3.16) have been fitted. The predictions of Eq. (3.15) are on the high side, while Eq. (3.14) seems to agree well with Eq. (3.16a) – and hence with the underlying monotonic data – but to be on the unsafe side compared to Eq. (3.16b) – and to the underlying cyclic data. The predictions of Eq. (3.18) – not shown in Fig. 3.11(c) – are half-way between those of Eqs. (3.16a) and (3.16b). Being design-oriented, Eq. (3.13) gives safe-sided estimates of the ultimate strain, but not overly so, and hence is an acceptable alternative to Eq. (3.16b) for cyclic loading.

Sections 3.2.2.4 and 3.2.2.10 elaborate further the context of Eqs. (3.16) and (3.17), notably the expressions for the ultimate curvature φ_u in which the value of ε_{cu}^* is to be used.

Note that all expressions given in the present section, except Eqs. (3.16), (3.17) and (3.18), have been fitted to concentric compression test results. The reader should be cautioned, then, for the fact that all confinement models are applied throughout the compression zone of sections subjected to bending with or without axial load, and especially to its extreme fibres. The implicit assumption there is that every point in the compression zone is laterally restrained by the surrounding volume of concrete in the same way that the perimeter stirrup and any intermediate ones restrain a section under concentric compression. Being under smaller strains than the extreme fibres, the ones immediately inwards have a lower tendency to dilate and do indeed restrain the inward dilation of the extreme fibres. However, it is rather arbitrary to assume that this restraint depends on the diameter, layout and spacing of stirrups, in exactly the same way as the outward restraint does (see next Section 3.1.2.3). Indeed, the available experimental evidence suggests they don't.

3.1.2.3 Confinement by Transverse Reinforcement

The confinement of the end section of a member by the surrounding concrete beyond the member end – i.e. by a larger column for a beam, or a large foundation element for the base of a vertical element – is neglected in design, as it refers to a single section. However, confinement of the concrete core inside the reinforcement cage by closely spaced transverse reinforcement is a key point in the detailing of concrete members for earthquake resistance.

The yield strain of reinforcing steel is about 2.5-times the lateral strain of concrete at uniaxial ultimate strength. When the uniaxial stress approaches f_c the confining steel is activated and, if in sufficient quantity, reaches its yield stress, f_{yw}, while the – by now triaxially compressed – concrete attains its enhanced ultimate strength.

Circular hoops or spirals provide the most efficient confinement. Hoops or spirals with small spacing or pitch, respectively, compared to the centreline diameter of the hoop or spiral, $D_o = 2R_o$, may be considered as a tube of thickness $t = A_{sw}/s$, where A_{sw} is the cross-section of the tie or spiral and s its spacing or pitch. (Strictly speaking, the equivalent thickness is equal to $a_s t$, where a_s is the confinement effectiveness factor given by Eqs. (3.20a) and (3.20b) and which is close to 1.0 if s/D_o is small). Reacting to the tendency of the enclosed concrete core to dilate when it approaches its ultimate strength under axial compression, the hoop or spiral will develop a tensile stress σ_s and exert on the concrete core a radial (confining) pressure, p, related to σ_s as: $p = t\sigma_s/R_o$. The confining steel reaches its yield stress, f_{yw}, while the triaxially compressed concrete attains its enhanced ultimate strength. After yielding of the confining steel, $\sigma_s = f_{yw}$, the lateral pressure p remains constant. On this basis, confinement models, like those in Section 3.1.2.2, fitted to triaxial compression tests under constant value of p are considered to apply when the lateral pressure derives from transverse reinforcement. If this reinforcement is idealised as a tube of thickness t, the value of p (normalised to the unconfined concrete strength) to be used in these confinement models is:

$$\frac{p}{f_c} = 0.5\rho_w \frac{f_{yw}}{f_c} = 0.5\omega_w \tag{3.19}$$

Where $\omega_w = \rho_w f_{yw}/f_c$ is the mechanical volumetric ratio of the confining reinforcement, defined with respect to the volume of the concrete core to the centreline of the confining hoop or spiral: $\rho_w = (2\pi R_o)A_{sw}/(\pi {R_o}^2 s) = 2A_{sw}/sR_o = 2t/R_o$.

A circular hoop or spiral exerts its confining action on the concrete it surrounds not as a uniform pressure $p = t\sigma_s/R_o$, but as a radial force per unit length of the perimeter, $2\pi R_o$. The effect of this force is dispersed within the volume of the concrete core inside the hoop or the spiral. A convenient assumption for the dispersal of the confinement force was initially proposed by Sheikh and Uzumeri (1982) and extended by Mander et al. (1988). According to this assumption, the confinement force is dispersed following parabolic arcs defined within planes through the member axis (meridional planes) and spanning from one hoop (or intersection of the spiral with the meridional plane) to the next with tangents there at $\pm 45^\circ$ to the plane of the cross-section (see Fig. 3.12(a)). Any concrete outside these parabolic arcs is assumed as unconfined, like the concrete cover outside the hoop or spiral. The entire concrete volume inside these arcs is considered as uniformly confined.

For circular hoops, the minimum confined cross-sectional area along the member is mid-way between consecutive hoops. The apex of a parabolic arc is at a distance from the chord connecting its two ends equal to $0.5(s/2)\tan\alpha$, where α is the angle of the tangent to the parabola at each end with respect to the chord of the parabolic arc. For the assumptions in Sheikh and Uzumeri (1982) and Mander et al. (1988), $\alpha = 45^\circ$. The minimum confined cross-section has a diameter equal to $2(R_o - s/4) =$

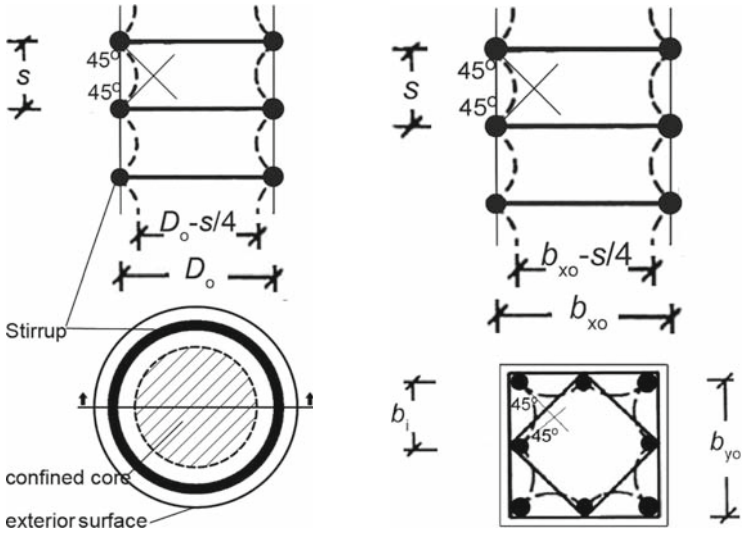

Fig. 3.12 Confined and unconfined parts over the cross-section and along a member with: (**a**) circular section and circular hoops; or (**b**) square section and multiple ties

D_o–$s/2$ and a cross-sectional area of $\pi(D_o–s/2)^2/4$, i.e. to the following fraction of the confined core defined by the centreline of the hoop:

$$a_s = \left(1 - \frac{s}{2D_o}\right)^2 \tag{3.20a}$$

If confinement is provided by a spiral, the model in Sheikh and Uzumeri (1982) and Mander et al. (1988) gives a constant confined cross-sectional area along the member. This area is circular with the ends of its diameter defined as follows:

- One end is at the apex of the parabolic arc extending between consecutive points of intersection of a meridional plane with the spiral.
- The other end is at the intersection of the same meridional plane with the spiral itself.

Then the diameter of the confined area is equal to $D_o–s/4$, where s is now the pitch of the spiral. Therefore, the confined area is equal to the following fraction of the cross-sectional area inside the centreline of the spiral:

$$a_s = \left(1 - \frac{s}{4D_o}\right)^2 \approx 1 - \frac{s}{2D_o} \tag{3.20b}$$

In rectangular sections confinement is normally provided by rectangular ties. If the centreline dimensions of the tie are b_{xo} and b_{yo} (Fig. 3.12(b)) the same reasoning gives a minimum confined cross-sectional area mid-way between consecutive ties with area equal to the following fraction of the cross-section area inside the tie centreline:

$$a_s = \left(1 - \frac{s}{2b_{xo}}\right)\left(1 - \frac{s}{2b_{yo}}\right) \tag{3.20c}$$

Circular hoops or spirals exert radial confining forces all along the perimeter. By contrast, straight stirrup legs along the perimeter do not develop any confining action, because the tendency of concrete to dilate when its stress approaches its ultimate strength causes these legs to bend outwards. The confining force exerted by a unit length of a stirrup bent to a radius of curvature equal to R is $A_{sw}\sigma_s/R$, where A_{sw} is the stirrup cross-section area and σ_s its tensile stress. This force is negligible, until eventually outwards bending of the straight stirrup leg reduces its radius of curvature, R, to a value of the order of the cross-sectional dimensions. But then it may be too late for the concrete. So, rectangular or polygonal stirrups are considered to exert concentrated confining forces on the concrete inside, only:

- at the corners, and
- wherever outwards bending of their straight legs is prevented by the hook of a cross-tie, well anchored within the concrete volume (the end hooks of intermediate single-legged cross-ties normally engage opposite sides of a perimeter tie).

Normally every stirrup corner or any intermediate point of the perimeter tie laterally restrained by a cross-tie hook engages also a longitudinal bar with much larger diameter than the stirrup itself. This bar plays an important role for the dipersal of the confining force concentrated there to the volume of the concrete core. The dispersal model in Sheikh and Uzumeri (1982) and Mander et al. (1988) is used also to separate the unconfined from the fully confined part inside the cross-section where the stirrup lies. The unconfined part is the one outside parabolic arcs connecting consecutive stirrup corners or points laterally restrained by a cross-tie hook, and the fully confined part is that inside these arcs. The apex of each parabolic arc is at a distance $b_i \tan\alpha/4$ from the chord connecting its two ends, where b_i is the length of this chord along the perimeter and α the angle between the chord and the tangent of the arc at each end, taken as $\alpha = 45^\circ$ according to Sheikh and Uzumeri (1982) and Mander et al. (1988). The area enclosed by the arc and its chord of length b_i is equal to their distance at the apex times $2b_i/3$, i.e. to ${b_i}^2/6$. So, the confined part of the cross-section at the level of a rectangular stirrup with centreline dimensions b_{xo} and b_{yo} is equal to the following fraction of the area enclosed by the centreline of the stirrup:

$$a_n = 1 - \frac{\sum {b_i}^2/6}{b_{xo} b_{yo}} \tag{3.21}$$

Circular hoops or spirals provide confinement all along their perimeter, so the counterpart of Eq. (3.21) is:

$$a_n = 1 \tag{3.22}$$

Rectangular columns or beams have a closed perimeter stirrup providing confinement only at its corners. Columns of earthquake resistant buildings designed for ductility are required by codes to have intermediate longitudinal bars engaged by a stirrup corner or cross-tie hook not further apart than a specified maximum spacing (of the order of 150–250 mm, see Table 5.2 in Chapter 5 for Eurocode 8). As a matter of fact, for buildings of Ductility Class M or H Eurocode 8 requires (for other reasons) a least one intermediate bar between adjacent corners of a column section, but does not impose engaging such bars with a cross-tie hook. Lateral restraint of intermediate bars is provided by cross-ties engaging two intermediate bars at opposite sides of the cross-section, or, more commonly in large cross-sections, by intermediate closed stirrups engaging one bar at each stirrup corner. A tensile stress $\sigma_s = f_{yw}$ in all stirrup legs and cross-ties parallel to transverse direction x (or 2) that opposes the dilatation of a concrete that approaches its ultimate strength, produces an average compressive stress σ_2 in the concrete, computed from equilibrium as: $\sigma_2 b_{yo} = (\Sigma A_{swx}/s) f_y$, i.e. $\sigma_2/f_c = \rho_x f_{yw}/f_c$, where $(\Sigma A_{swx}/s)$ is the total cross-sectional area of all stirrup legs or cross-ties per unit length of the member parallel to transverse direction x, and $\rho_x = \Sigma A_{swx}/(s b_{yo})$ the geometric ratio of transverse reinforcement in that direction. Similarly in the other transverse direction y (or 3): $\sigma_3/f_c = \rho_y f_{yw}/f_c$. If $\rho_x > \rho_y$ it is the value $p \approx (\sigma_2 + 4\sigma_3)/5$ that counts. It is simpler and safe-sided to consider that essentially the minimum of the two transverse reinforcement ratios controls confinement:

$$p/f_c \approx \min(\rho_x, \rho_y) f_{yw}/f_c = 0.5\omega_w \tag{3.19a}$$

where the volumetric ratio of confining reinforcement, ρ_w, referring to the volume of the confined concrete core inside the centreline of the perimeter stirrup, is not the real one, but that defined as:

$$\rho_w = 2\min(\rho_x, \rho_y) = 2\min(\Sigma A_{swx}/b_{yo}, \Sigma A_{swy}/b_{xo})/s \tag{3.23}$$

The mechanical volumetric ratio of confining reinforcement in Eq. (3.19a), $\omega_w = \rho_w f_{yw}/f_c$, derives from the fictitious volumetric ratio of confining reinforcement, ρ_w, given by Eq. (3.23).

Equations (3.19a) and (3.23) are similar to the one for confinement by circular hoops or spirals, Eq. (3.19), but applies only to cross-sections with stirrup legs or cross-ties parallel to the section sides. In (nearly) square columns (with $b_x \approx b_y$) with just one intermediate bar to be laterally restrained along each side, all four intermediate bars can be conveniently restrained at the same time by a diamond-shaped interior tie (Fig. 3.13 (a)). That tie enters in the calculation of ρ_x and ρ_y with its cross-sectional area A_{sw}, times $\sqrt{2}$. In that special case the value of ρ_w

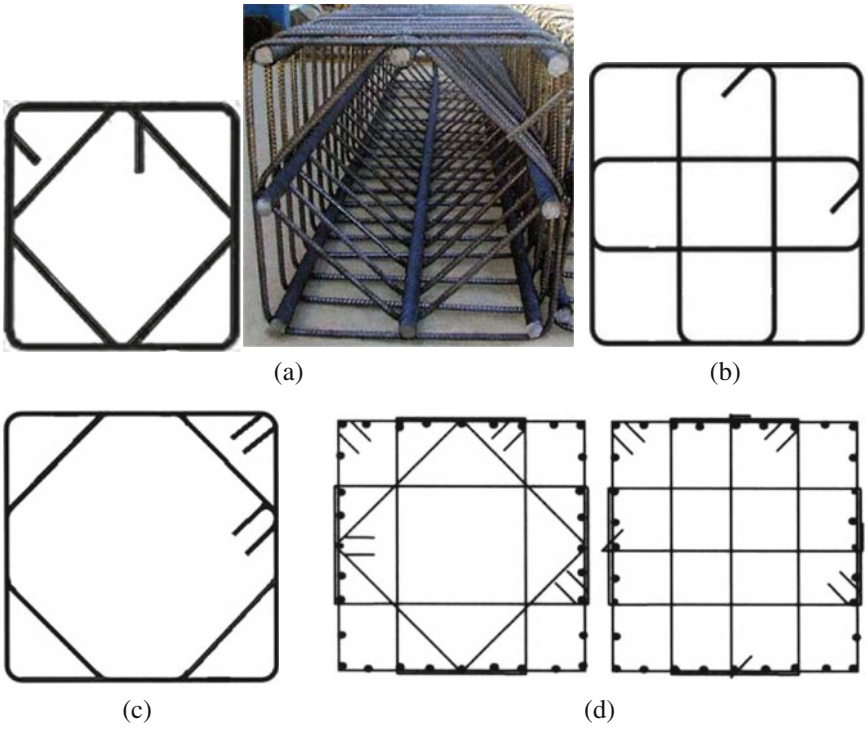

Fig. 3.13 Ties in square column engaging the four corner bars and (**a**) four mid-side bars; (**b**), (**c**) two intermediate bars per side; (**d**) three intermediate bars per side

coincides with the real volumetric ratio of confining reinforcement (volume of all tie legs, divided by the volume of confined core to the centreline of the perimeter tie). In a (nearly) square section with two intermediate bars that need lateral restraint along each side, it is cost-effective and convenient to employ a single octagonal interior tie engaging all eight intermediate bars (Fig. 3.13(c)), instead of two interior rectangular ties each engaging two pairs of intermediate bars at opposite sides of the section (Fig. 3.13(b)). The octagonal tie enters in the calculation of ρ_x and ρ_y with its cross-sectional area, A_{sw}, times $\sqrt{2}$ so, the volumetric ratio from Eq. (3.23) is slightly less than the real volumetric ratio of confining reinforcement. If all intermediate bars in a square column are laterally restrained by single-leg cross-ties, the outcome of Eq. (3.23) coincides with the real volumetric ratio of confining reinforcement. This is not the case anymore if interior rectangular ties engage each two pairs of intermediate bars at opposite sides of the section (Fig. 3.13(b) and (d)), because the legs of an interior tie on the perimeter do not count in Eq. (3.23).

Equations (3.21) and (3.22) express the confined fraction of the cross-section at the level of an individual stirrup, as a fraction of the area enclosed by the centreline of the perimeter stirrup. Equations (3.20) give the minimum confined area along the length of the member as a fraction of the confined area at the level of individual stirrups. Factors a_s and a_n may be considered as coefficients of confinement effectiveness along the member, or over the cross-section, respectively. The combined confinement effectiveness factor is the product:

$$a = a_n a_s \tag{3.24}$$

which gives the minimum confined cross-sectional area anywhere along the member, as a fraction of the area enclosed by the centreline of the perimeter stirrup or spiral (Fig. 3.12(b)).

Early work about the effect of confinement on the behaviour of concrete focused on the ultimate strength of columns under concentric compression. Under such loading the compression strength of the column is equal to that of its least confined cross section. If unconfined concrete does not exhaust its ultimate strain, ε_{cu}, before the confined concrete reaches its compressive strength, f_c^*, the ultimate compressive force of the column may be taken to be approximately equal to $(A_c + aKA_o)f_c$, where A_c is the area of the gross concrete section, A_o is the cross-sectional area enclosed by the centreline of the perimeter stirrup or spiral, a is the confinement effectiveness factor of Eq. (3.24) and K the strength enhancement factor in Eq. (3.4). It is often considered that just the concrete cover spalls-off before the confined concrete reaches its ultimate strength, f_c^*. Then the ultimate compressive load may be estimated as $aA_o f_c^*$, computed from Eq. (3.4) with the value of K multiplied times the confinement effectiveness factor of Eq. (3.24). As a matter of fact (Sheikh and Uzumeri 1982), that first introduced the concept of a confinement effectiveness factor essentially in the form of Eqs. (3.20), (3.21), (3.22) and (3.24), incorporates it in K as a multiplicative factor in Eq. (3.7).

If K is proportional to the confining pressure p (as, e.g., in the 1st term of the model of Eq. (3.8)), which in turn is proportional to the mechanical volumetric ratio of transverse reinforcement (see Eqs. (3.19) and (3.19a)), then a may multiply directly ω_w. However, this practice has been common even in models where K is nonlinear in p. In the Mander et al. (1988) model factors a_n and a_s multiply the transverse stresses σ_2 and σ_3. More specifically, for circular hoops or spirals a_s multiplies ω_w in Eq. (3.18); for rectangular ties a from Eq. (3.24) multiplies the mechanical stirrup ratios in the two transverse directions, $\omega_x = \rho_x f_{yw}/f_c$ and $\omega_y = \rho_y f_{yw}/f_c$, for the calculation of $\sigma_2/f_c = a\omega_x$, $\sigma_3/f_c = a\omega_y$. A similar approximation is common in the use of Eq. (3.5), which is also nonlinear in p. Unfortunately, this practice is carried over to the calculation of $\varepsilon_{co}{}^*$ through Eq. (3.10) and of $\varepsilon_{cu}{}^*$ through Eqs. (3.13) and (3.18). So, the common practice is to apply Eqs. (3.5), (3.6), (3.8), (3.13) and (3.18) with a value of p/f_c from Eqs. (3.19) or (3.19a) multiplied by a (which is equivalent to multiplying ω_w at the right-hand-side of Eqs. (3.19) and (3.19a) by a):

$$\frac{p}{f_c} = 0.5a\rho_w \frac{f_{yw}}{f_c} = 0.5a\omega_w \tag{3.25}$$

The same for Eqs. (3.16) and (3.17), but not for Eqs. (3.14) and (3.15).

The so resulting value of K is used then in Eqs. (3.4) and (3.10).

In earthquake resistant structures confinement is primarily of interest for the compression zone of members subjected to bending with or without axial force. A more meaningful measure of the effectiveness of confinement for a member with rectangular section subjected to bending in a plane parallel to side b_x, would involve a value of a modified as follows (see Fig. 3.14):

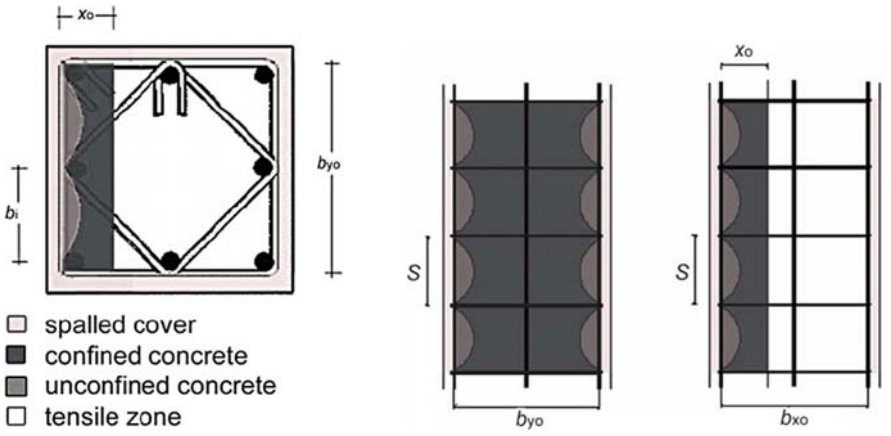

Fig. 3.14 Calculation of confinement effectiveness in the compression zone of the confined core of a member in flexure

- instead of the depth of the confined concrete core, $h_c = b_{xo}$, its neutral axis depth from the centreline of the perimeter stirrup, x_o, is used, calculated from the normalised neutral axis depth at ultimate conditions of the confined concrete core, ξ_{cu}, computed according to Section 3.2.2.4 under *Ultimate Curvature of the Confined Core, After Spalling of the Cover* and Flow Chart 3.2;
- the summation $\Sigma_i b_i^2$ in the numerator of the 2nd term of Eq. (3.21) extends over the external perimeter of the confined compression zone – i.e. from one intersection of the neutral axis with the centreline of the perimeter stirrup to the other intersection on the opposite side, excluding the neutral axis itself between these two intersection points;
- the 1st parenthesis at the right-hand-side of Eq. (3.20c) is replaced by $1–0.25s/x_o$, where s is the stirrup spacing.

The end result is a factor for the effectiveness of confinement of the compression zone:

$$a_x = \left(1 - \frac{s}{2b_{xo}}\right)\left(1 - \frac{s}{4x_o}\right)\left(1 - \frac{\sum b_i^2}{6x_o b_{yo}}\right) \tag{3.24a}$$

replacing a in Eq. (3.24).

The strong interaction between confinement of concrete and buckling of longitudinal bars, already noted in Section 3.1.1.2, is worth re-emphasising:

- Thanks to their flexural stiffness, longitudinal bars contribute to the confinement of the adjacent concrete, no matter that the model in Sheikh and Uzumeri (1982) and Mander et al. (1988) and Eqs. (3.20) and (3.21) derived from it discount this contribution. The confined concrete in turn exerts on these bars outwards pressures driving them toward buckling.
- Once they buckle outwards, longitudinal bars contribute little to confinement and to axial force resistance. Moreover, they may buckle over several tie spacings (see Fig. 3.4(b)), stretching the ties and diminishing their role for confinement. So, bar buckling may precipitate disintegration of the confined concrete core.

3.1.2.4 Confinement by FRP Wrapping

The columns of existing substandard buildings normally have widely spaced and/or poorly closed stirrups. Such stirrups provide little confinement, if at all. Confinement can be very conveniently provided a-posteriori by wrapping the end regions of columns where plastic hinges may form in Fibre-Reinforced-Polymers (FRPs) with fibres oriented (primarily) in the hoop direction of the section (see Section 6.8.3).

The lateral stress-axial strain response for the two most common Fibre-Reinforced-Polymers, notably carbon FRP (CFRP) and glass FRP (GFRP), is contrasted in Fig. 3.15(a) to that for confinement by steel. Being essentially linear-elastic, once activated by concrete that dilates after its unconfined ultimate strength

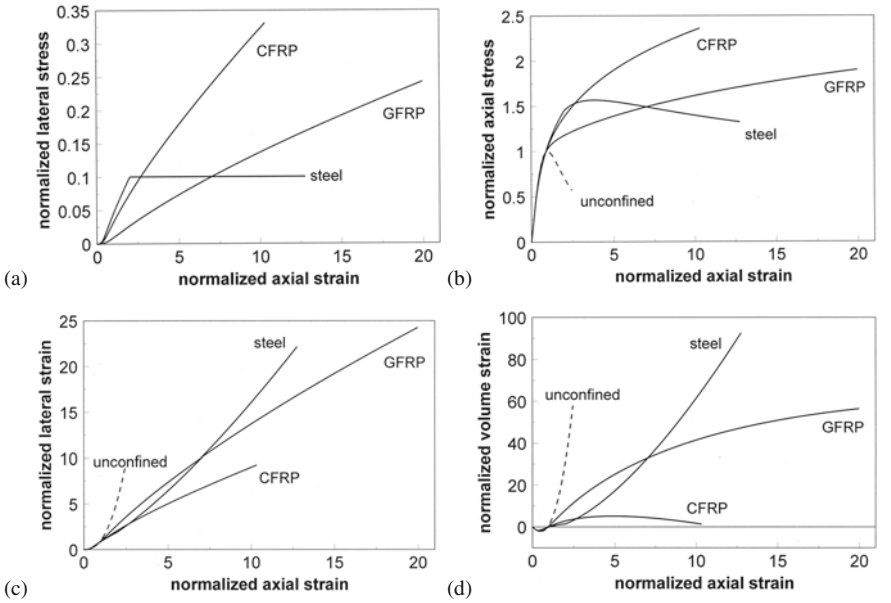

Fig. 3.15 Schematic behaviour of concrete confined with steel, CFRP or GFRP: (**a**) σ-ε curves of confining material, normalised to the yield stress and strain of steel; (**b**) axial σ-ε curves of confined concrete, normalised to the strength and the corresponding strain of unconfined concrete; (**c**) (**d**) lateral or volumetric strain v axial strain of confined concrete, normalised to the corresponding strains of unconfined concrete at ultimate strength (adapted from *fib* 2006)

is attained, the FRP provides an ever increasing confining pressure until it fractures in tension. So, unlike the σ-ε curve of concrete confined by ties which exhibits softening after the ultimate strength, those of FRP-wrapped concrete continue hardening until the FRP breaks (Fig. 3.15(b)). As shown in Fig. 3.15(c) and (d), after they yield steel ties lose effectiveness compared to CFRP, and later on to GFRP as well, in restraining the lateral and volumetric strains of concrete. As a matter of fact, as shown in Fig. 3.15(d), after the unconfined ultimate strength of concrete is exceeded, the restraint of its dilation by the large confining stiffness of CFRP can soon turn dilation into contraction (Teng and Lam 2004). Of course, for the σ-ε curve of confined concrete to be continuously ascending until rupture of the FRP, the FRP wrapping should have a minimum of tensile strength, $f_{\mathrm{fu}}t_{\mathrm{f}}$, and extensional stiffness, $E_{\mathrm{f}}t_{\mathrm{f}}$, with f_{fu} and E_{f} denoting the ultimate strength and Modulus of the FRP material and t_{f} the thickness of the FRP jacket (see Fig. 3.16 for FRP wrapping with large values of $f_{\mathrm{fu}}t_{\mathrm{f}}$ and $E_{\mathrm{f}}t_{\mathrm{f}}$). Otherwise, the confined concrete will soften after ultimate strength, as shown schematically in Fig. 3.16(b) for concrete wrapped with FRP having low values of $f_{\mathrm{fu}}t_{\mathrm{f}}$ and $E_{\mathrm{f}}t_{\mathrm{f}}$. According to Yan and Pantelides (2006, 2007), the transition from hardening to softening takes place when the value of $f_{\mathrm{fu}}t_{\mathrm{f}}/R$ drops below $0.2f_{\mathrm{c}}$.

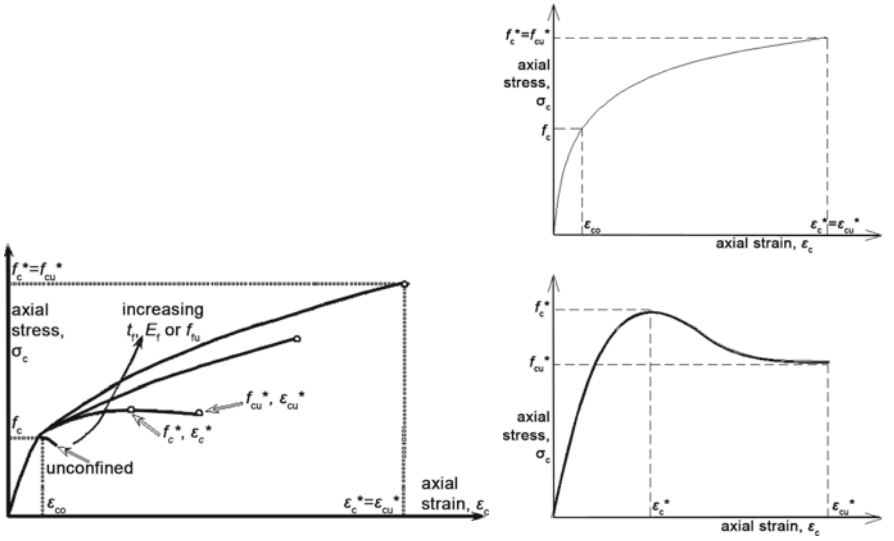

Fig. 3.16 Schematic axial σ-ε response of FRP-confined concrete (**a**) for increasing FRP strength, $f_{fu}t_f$, and stiffness, $E_f t_f$, (**b**) hardening (*top*) or softening (*bottom*) behaviour, for $f_{fu}t_f/R > 0.2f_c$ or $f_{fu}t_f/R < 0.2f_c$, respectively (adapted from Yan and Pantelides 2007)

The difference between the passive confinement offered by an elastic material, such as FRP, and an active one by a constant lateral pressure p was not recognised at the beginning. So, in the first publications that proposed and investigated the use of FRP to confine the concrete (Fardis and Khalili 1981, 1982), Eqs. (3.4) and (3.5) have been applied for the enhancement of the concrete strength. Equations (3.4), (3.7) and (3.10) were adopted for the same purpose when the subject was first revisited (Saadatmanesh et al. 1994) and later adopted in ACI Committee 440 (2002) too. All subsequent work avoided blind adoption of models of active confinement by a constant lateral pressure, p, such as those presented in Section 3.1.2.2 for concrete confined by steel ties. Models were custom-fitted, instead, to the stress-strain behaviour and the strength of FRP-confined concrete.

Research on the experimental behaviour of FRP-confined concrete under concentric compression and its modelling has been intense since the mid-1990s and will continue at least till the end of the first decade of the 20th century. In the absence of agreement within the research community about the models to be used in practice, the present section covers the subject at a greater length than warranted by its importance. Hopefully, the dust will soon settle and some of the following material will become redundant.

The ultimate strength and strain of confined concrete under concentric compression are controlled by the failure strain of the FRP in the hoop direction. It has recently emerged that the value of the effective ultimate hoop strain of the FRP, ε_{fu}, is a much more important factor for stress-strain and strength models

of FRP-confined concrete than the model itself. There is indeed strong experimental evidence that the full elongation at rupture of the FRP material, as measured in coupon tests, cannot be utilised for confinement. The FRP that confines concentrically compressed concrete fails when its hoop strain reaches a fraction of the ultimate elongation of tension coupons. In ACI Committee 440 (2002) this fraction is called efficiency factor and is given a value of 0.75 for rectangular members subjected to bending and shear (but with the value of the effective ultimate strain of FRP not to exceed 0.004), or of 1.0 for circular sections. In the light of current knowledge the values in ACI Committee 440 (2002) are high: values of the efficiency factor around 0.5 (Yan and Pantelides 2007, Toutanji et al. 2007, Fujikake et al. 2004), 0.6 (Lam and Teng 2003a,b, Tamužs et al. 2007, Tabbara and Karam 2007), or 0.85 just for AFRP (Lam and Teng 2003a,b) are more consistent with test results. It has also been found in Tabbara and Karam (2007) that models of active confinement by a constant lateral pressure, p, such as those presented in Section 3.1.2.2 for concrete confined by steel ties, can describe well the ultimate strength of FRP-confined concrete under concentric compression, provided that p is derived from the FRP geometric ratio $\rho_f = 2t_f/D$ as $p = \rho_f f_{fu}$, with the effective ultimate strength of FRP taken as $f_{fu} = E_f \varepsilon_{fu}$, where ε_{fu} is the effective, reduced ultimate hoop strain of the FRP and not the ultimate elongation of tension coupons. Finally, it has been demonstrated in Teng and Lam (2004) that σ-ε models for confined concrete agree much better to test results if they employ the measured ultimate hoop strain of the FRP, instead of a default value or the ultimate elongation of tension coupons. So, the reader should consider the statement in the second sentence of the present paragraph as well substantiated and should keep it in mind while going through the rest of this section.

The Spoelstra and Monti model in Spoelstra and Monti (1999):

$$\frac{f_c^*}{f_c} = 0.2 + 3\sqrt{\rho_f \frac{f_{fu}}{f_c}} \tag{3.26a}$$

$$\frac{\varepsilon_{cu}^*}{\varepsilon_{co}} = 2 + 1.25 \frac{E_c}{f_c} \varepsilon_{fu} \sqrt{\rho_f \frac{f_{fu}}{f_c}} \tag{3.26b}$$

applies to circular sections with diameter D, wrapped with FRP having a geometric ratio $\rho_f = 2t_f/D$ and effective ultimate strain ε_{fu}, giving an effective ultimate FRP strength $f_{fu} = E_f \varepsilon_{fu}$. Although widely quoted – notably *in fib* (2001, 2003) – the model has been recently found (Vintzileou and Panagiotidou 2007, Yan and Pantelides 2006, Tamužs et al. 2007, De Lorenzis and Tepfers 2001) to overestimate on average by about 5% the strength of confined concrete cylinders (via Eq. (3.26a)) and much more (by more than half) their ultimate strain (via Eq. (3.26b)). Moreover, it predicts that a very low level of confinement (with $\rho_f f_{fu}/f_c < 0.07$) reduces the strength below the unconfined value.

Among the widely known proposals so far, the model in Lam and Teng (2003a,b) has emerged from an independent comparison with the largest known database of FRP-confined concrete under concentric compression (Vintzileou and Panagiotidou

2007) as the most unbiased for ultimate strength and strain (with median value of experimental-to-predicted or predicted-to-experimental ratio within a few percent from 1.00), with acceptable overall scatter. Moreover, it is fairly complete: it provides the full hardening σ-ε law of circular or rectangular FRP-confined sections, giving at the limit the one of unconfined concrete. The σ-ε curve consists of a parabolic ascending branch followed by a linear one that intercepts (if extended) the stress axis at the unconfined concrete strength, f_c, and terminates to the following ultimate strength and strain point:

$$\frac{f_c^*}{f_c} = 1 + 3.3\left(\frac{b}{h}\right)^2 a_n \frac{\rho_f f_{fu}}{f_c} \tag{3.27a}$$

$$\frac{\varepsilon_{cu}^*}{\varepsilon_{co}} = 1.75 + 12\sqrt{\frac{h}{b}} a_n \frac{\rho_f f_{fu}}{f_c} \left(\frac{\varepsilon_{fu}}{\varepsilon_{co}}\right)^{0.45} \tag{3.27b}$$

The parabolic first branch merges into the linear one at the same slope $E_2 = (f_c^* - f_c)/\varepsilon_{cu}^*$ and at a strain equal to $2f_c/(E_c - E_2)$.

In Eqs. (3.27) b and h are the shorter and the longer of the two sides of the section ($b = h$ for circular sections). The confinement effectiveness factor, a_n, is given by Eq. (3.22) for circular sections and by Eq. (3.28) below for rectangular ones. On the basis of the measured hoop strains at failure of the FRP and the specimen, Lam and Teng (2003a,b) have concluded that the effective FRP ultimate strength, $f_{u,f}$, is equal to $f_{u,f} = E_f \varepsilon_{fu}$, where ε_{fu} is on average about equal to 60% of the failure strain of tensile coupons for CFRP and GFRP, or about 85% of the coupon failure strain for AFRP (for GFRP or AFRP these percentages were estimated from very limited data).

According to Lam and Teng (2003a,b), if $\rho_f f_{fu}/f_c < 0.07$, the strength enhancement in Eq. (3.27a) is neglected. However, this departure from Eq. (3.27a) may not be sufficient for the realistic description of the behaviour of concrete for low levels of FRP-confinement. In the model in Yan and Pantelides (2006, 2007) the expressions for ultimate strength and strain under hardening behaviour (i.e., for $f_{fu} t_f/R > 0.2 f_c$) are supplemented with rules for softening behaviour (with $f_{fu} t_f/R < 0.2 f_c$), namely with expressions giving both the ultimate strain point in Fig. 3.16, f_{cu}^*, ε_{cu}^*, and the peak or ultimate strength one, f_c^*, ε_c^*. That σ-ε model is more complete in this respect, but it has been fitted to limited data of tests carried out by its very proposers. So, till an independent assessment of its performance for a wider database of test results, the reader is referred to Yan and Pantelides (2006, 2007) for details.

An FRP jacket provides continuous confinement all along the length of its application around the member. So, the confinement effectiveness factor in that direction is $a_s = 1$ (cf. Eqs. (3.20) for confinement by steel ties).

Regarding the effectiveness of confinement by FRP within the section, for circular members the FRP jacket is fully effective all along the perimeter. So, the confinement effectiveness factor within the section is $a_n = 1$, as in circular steel hoops or spirals (cf. Eq. (3.22) for confinement by steel ties).

If the section is rectangular, the FRP jacket exerts confining forces only at the corners and not at all in-between (similar to a perimeter tie). Primarily to enhance the confinement effectiveness of the FRP jacket, but also to reduce stress concentrations in it at the corner that may cause premature rupture, the corner of the section is rounded into a quarter-circle of radius R before applying the FRP. Note that, when a sheet of fibre-reinforced fabric of thickness t is applied around such a corner, a strain of $\varepsilon = 0.5t/R$ is locked in at the expense of the ultimate strain capacity of the FRP. From this point of view, to achieve a target value of total tensile strength of the FRP in the circumferential direction of a rectangular section, a larger number of thin individual fibre-reinforced sheets – each with thickness t not more than a fraction of a millimetre – is preferable to fewer but thicker sheets.

In rectangular sections, confinement by the FRP jacket is fully effective right inside the rounded corners of the section. In-between the corners the parabolic arc model in Sheikh and Uzumeri (1982) and Mander et al. (1988) may be applied as in Fig. 3.17, giving in the end the following fraction of the original rectangular section as confined (CEN 2005a, *fib* 2001, 2003):

$$a_n = 1 - \frac{(b_x - 2R)^2 + (b_y - 2R)^2}{3b_x b_y} \tag{3.28}$$

The long exposé above refers exclusively to concentric compression. Strictly speaking it applies only in that case. It has been emphasised in Sections 3.1.2.2 and 3.1.2.3 that what matters for earthquake resistance is the compression zone of members subjected to cyclic flexure with or without axial load and notably the flexure-controlled ultimate deformation of the member,[4] conveniently expressed by the ultimate curvature of the section. By analogy to the development of Eqs. (3.16) and (3.17) in Section 3.1.2.2, the ultimate curvature, φ_u, is calculated from first principles according to the analysis in Section 3.2.2.4 modified to accept a parabolic-trapezoidal σ-ε curve for the confined concrete, instead of the parabolic-rectangular one used for unconfined concrete. In addition, the σ-ε model in Lam and Teng

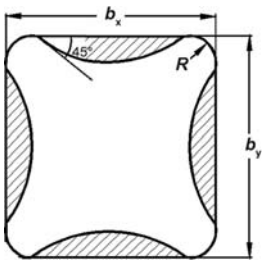

Fig. 3.17 Confinement of rectangular section by FRP jacket

[4]See footnote no. 1 in Section 3.1.1.2 for the definition of ultimate deformation (see also Section 3.2.2.7).

(2003a,b) is adopted, except that the ultimate strain, $\varepsilon_{cu}{}^*$, is determined for optimal fitting of available experimental results on φ_u of FRP-confined sections. It has been found that such a fitting is unbiased (i.e., good on average) and associated with acceptable scatter, if for cyclic loading Eq. (3.16b) is modified as follows for confinement by FRP (Biskinis and Fardis 2009):

$$\varepsilon_{cu}{}^* = 0.0035 + \left(\frac{10}{h}\right)^2 + 0.4a_n \min\left[0.5;\ \frac{\rho_f f_{u,f}}{f_c^*}\right] a_{eff\,,j} \tag{3.29}$$

where:

- h is the full section depth in the plane of bending, in mm;
- a_n is the confinement effectiveness factor of the FRP, equal to $a_n = 1$ for circular sections or given by Eq. (3.28) for rectangular ones;
- $\rho_f = 2t_f/b$ is the geometric ratio of the FRP in the direction of bending;
- $f_{fu} = E_f \varepsilon_{fu}$, with ε_{fu} as in Lam and Teng (2003a,b), i.e. about equal to 60% of the failure strain of tensile coupons; note that in Lam and Teng (2003a,b) this percentage value has been proposed only for CFRP or GFRP, while 85% was given for AFRP, but on the basis of limited test results;
- $a_{eff,j}$ is an additional effectiveness factor for the FRP jacket, expressing that its effectiveness is not proportional to the geometric ratio and stiffness of the FRP:

  - $$a_{eff,j} = 0.5\left(1 - \min\left[0.5;\ \frac{\rho_f f_{u,f}}{f_c^*}\right]\right) \quad \text{for CFRP, GFRP,} \tag{3.30a}$$
  - $$a_{eff\,,j} = 0.3\left(1 - \min\left[0.5;\ \frac{\rho_f f_{u,f}}{f_c^*}\right]\right) \quad \text{for AFRP} \tag{3.30b}$$

Section 3.2.3.10 under *Members with Continuous Bars* gives details about the outcome of the application of Eqs. (3.28), (3.29) and (3.30) for the estimation of the ultimate flexural deformation of FRP-wrapped members.

Note that, if the FRP provides relatively light confinement compared to the transverse reinforcement, the end section may survive rupture of the FRP jacket and reach subsequently a larger ultimate curvature controlled by the confined concrete core inside the stirrups, for which Section 3.1.2.2 applies.

3.1.2.5 Concrete Strength Requirements for Earthquake Resistant Buildings

Because the effect of concrete strength on member ductility and energy dissipation capacity seems to be beneficial in practically every respect (from the increase of bond and shear resistance, to the direct enhancement of deformation capacity), Eurocode 8 (CEN 2004a) sets a lower limit on the nominal cylindrical concrete strength in primary seismic elements, equal to 16 MPa (concrete class C16/20) in buildings of DC M, or 20 MPa (concrete class C20/25) in those of DC H. No upper bound is set on concrete strength, as there is no experimental evidence that the

lower apparent ductility of high strength concrete (due to which the values specified in Eurocode 2 for ε_{co} and ε_{cu} converge, from $\varepsilon_{co} = 0.002$ and $\varepsilon_{cu} = 0.0035$ for concrete class C50/60, to a single value of 0.0026 at C90/100) has any adverse effect on member ductility and energy dissipation capacity. The above lower limits on nominal concrete strength are consistent with the lowest concrete strengths currently used in buildings of the more seismic prone European countries.

3.1.3 Interaction Between Reinforcing Bars and Concrete

3.1.3.1 Cyclic Shear Transfer Along Cracks Crossed by Reinforcement

Cracks in concrete take place at right angles to the direction of a principal tensile stress. So, the crack plane is initially free of shear stresses. Owing to the change in the stress field during cyclic loading, shear stresses later develop along the crack plane. Due to such shear stresses one of the two faces of the crack tends to slip with respect to the other. Unless the shear is accompanied by stresses normal to the crack, slippage along the crack would be restrained only in the presence of reinforcing bars crossing the crack – at right angles or at an inclination. The magnitude of the slippage induced by a given shear stress (i.e., the effect of the crack on shear stiffness) and the maximum shear force that can be transferred along the crack (the shear resistance) depend on the diameter, spacing and inclination of the bars crossing the crack and the tensile stress already in them due to other reasons (i.e. at zero shear stress along the crack).

Rough cracks crossed by reinforcing bars can transfer shear by friction. In this "interface shear transfer" or "aggregate interlock" mechanism, the clamping force needed for the development of friction is provided by the reinforcing bars that cross the crack and depends on their total cross-sectional area, inclination with respect to the crack and tensile stress due to other reasons. These bars connect also the two faces of the crack as "dowels". Their effectiveness in this respect depends on their diameter (more than on their cross-sectional area) and on the minimum concrete cover in the direction of the shear stress on either side of the crack (or, if this cover is small, by the engagement of the bar acting as dowel by transverse reinforcement close to and almost parallel to the crack).

Significant shear forces can be transferred by aggregate interlock and dowel action under monotonic loading (see virgin loading branches in Figs. 3.18 and 3.19). However, both mechanisms are very sensitive to the cycling of the shear force and of the associated slip along the crack. Cycling of the slip polishes the crack faces and reduces the effectiveness of aggregate interlock. Bearing stresses under a bar acting as dowel may crush locally the concrete and open a "gap" that may need to be closed, for the bar to be re-engaged as a dowel in a subsequent load cycle. This is evident from the cyclic shear force (or stress) v slip behaviour depicted in Fig. 3.18 for aggregate interlock and in Fig. 3.19 for dowel action. In both cases (but especially for aggregate interlock) unloading-reloading loops have an inverted-S shape, with initially steep unloading and steep final reloading in the opposite direction.

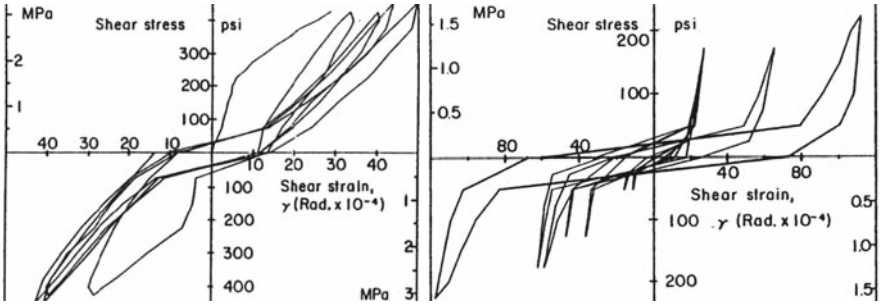

Fig. 3.18 Increase of slip in aggregate interlock for cycles of about constant shear stress amplitude, with the clamping reinforcement normal to the crack initially at: (**a**) zero tensile stress; or (**b**) 90% of yield stress (Perdikaris 1980)

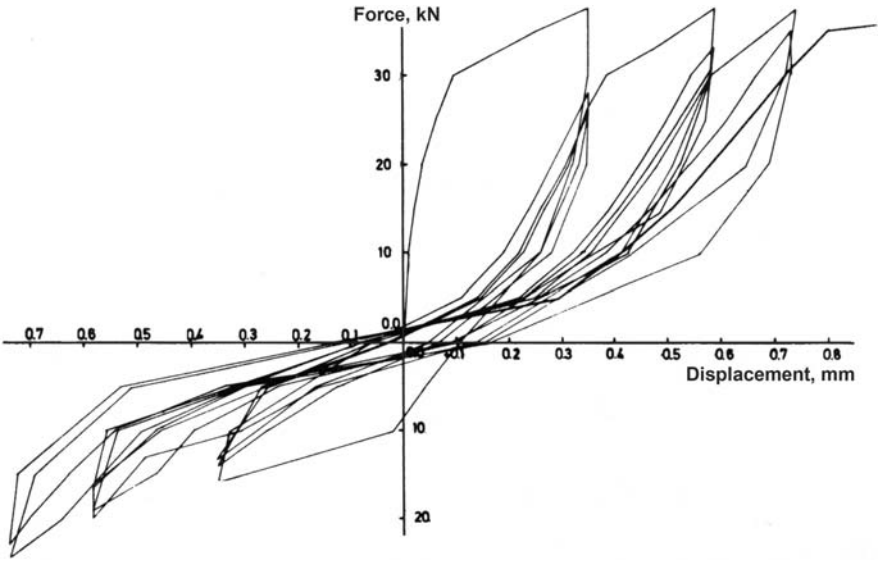

Fig. 3.19 Dowel force v slip loops for asymmetric cover of the dowel (adapted from Vintzeleou 1984)

In-between there is an intermediate phase of nearly unrestrained slippage, until hard contact of the two polished faces of the cracks resumes in the cases of Fig. 3.18, or till the bar bears against sound concrete again in that of Fig 3.18. Hysteresis loops are narrow (especially for aggregate interlock), dissipating very little energy.

Note that not only dowel action, but also shear transfer by aggregate interlock is a mechanism of concrete-steel interaction: the shear transfer by aggregate interlock is essentially a friction mechanism (Fardis and Buyukozturk 1979). For slippage to take place along a rough crack, asperities of one face have to ride over those on the opposite face. So the crack opens-up, stretching the reinforcement that crosses it.

The clamping force necessary for the friction is provided by compressive contact forces that develop between asperities of the crack faces as reaction to the tension that builds up in the reinforcement owing to the sliding and opening-up of the crack. Witness in Fig. 3.18(b) the detrimental effect of high initial tension in the clamping reinforcement on the cyclic resistance and stiffness of the aggregate interlock mechanism. Bars under high initial tension provide little clamping effect. Once they yield, almost unrestrained slippage takes place along the crack. Similar is the detrimental effect of a high tensile stress in a bar that acts as a dowel: the combination of this stress with the direct shear and bending stress due to dowel action precipitates generalised yielding of the bar in the vicinity of the crack, diminishing its resistance against further slippage. Therefore, the longitudinal bars in a plastic hinge of a concrete element, which are expected to yield during the seismic response, cannot contribute to interface shear transfer on the side.

The overall conclusion is that, under cyclic conditions the shear resistance and stiffness along cracks crossed by reinforcement degrades fast and offers practically no energy dissipation. So, one cannot rely on it for earthquake resistance.

3.1.3.2 Bond of Reinforcing Bars to Concrete

Smooth (plain) reinforcing bars were quite common until the mid-1960s (in the US) to the mid-1980s (in some European countries). Nowadays only ribbed (deformed) bars are used in concrete structures. Such bars are bonded to the surrounding concrete by bearing of their ribs against it. A characteristic parameter for the bond properties of a ribbed bar is its relative rib area, which is defined as the ratio of the projected area of the ribs on a plane normal to the bar axis to the lateral surface area of the bar – both per unit length of the bar – and is roughly equal to the rib height-to-distance ratio. A relative rib area value typical of turn-of-the-century European production is around 0.06. Doubling it to 0.12 improves the bond by just 10% (Cairns 2006). For such values of the relative rib area, bond failure along bars or laps having clear cover or clear mid-distance to the nearest anchored bar or lap less than about three bar-diameters normally is in the form of concrete splitting along planes through the axis of the bar(s), as in Figs. 3.20 and 3.21. Splitting is caused by the circumferential tensile stress that develops in the concrete due to the bursting action of the radial component of the bearing forces exerted by the ribs on the concrete. For typical configurations of the surface of the ribs, the bursting radial component is in the order of 25% of the longitudinal one (i.e., of the bond force).

Bond resistance drops rather rapidly after splitting, as the slip of the bar with respect to the surrounding concrete increases. Transverse reinforcement intercepting the potential splitting crack(s), and/or transverse pressure on the bar – be it active, due to external forces, or passive, thanks to confinement – delay splitting and reduce the drop in bond resistance it entails; they can even prevent splitting. Splitting can also be prevented if the clear cover and the clear mid-distance to the nearest anchored bar or lap are fairly large (at least three bar-diameters, for no transverse reinforcement or pressure). If in such cases bond failure ultimately takes place, it

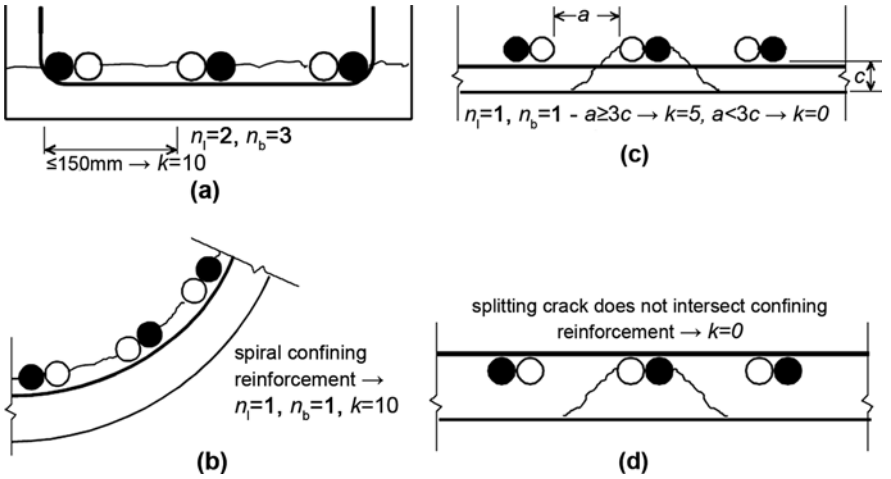

Fig. 3.20 Splitting failures of lapped bars, with definition of *k*-factor in Eq. (3.31) and of the number of bars or stirrup legs in Eq. (3.32) (adapted from Eligehausen and Lettow 2007)

has the form of bar pull-out (or -through) by shearing of the concrete around the bar or the lap, all along a surface through the tops of the ribs. This failure mode is far less brittle than by splitting: bond resistance is almost fully maintained until the bar travels nearly the full clear distance between successive ribs – about 80% of the bar diameter (Cairns 2006) – fully crushing the concrete between them.

Design codes consider bond as a uniform shear stress over the lateral surface of the bar. To determine the minimum required length of anchorages or lap splices they specify the design value of the ultimate bond stress, f_{bd}, considering it as a material property.[5] In Eurocode 2 (CEN 2004b) and hence in Eurocode 8 (CEN 2004a) as well, f_{bd} is taken as 2.25 times the design value of concrete tensile strength, $f_{ctd} = f_{ctk,0.05}/\gamma_c = 0.7 f_{ctm}/\gamma_c$, where γ_c is the partial factor for concrete and indices k, 0.05 and m to f_{ct} denote the lower characteristic and the mean value, respectively. These Eurocode 2 values of f_{bd} apply for "good" bond conditions, i.e. if the bar:

- is at an angle more than 45° to the horizontal; or
- is not more than 250 mm from the bottom of the concrete layer cast; or
- is at least 300 mm from the top surface of the concrete layer cast.

For all other positions of the bar during casting, bond conditions are considered as "poor", owing to the effects of laitance and consolidation of concrete during

[5] As we will see shortly, the concept of bond strength as a property of the concrete for given relative rib area and position of the bar with respect to casting, albeit convenient, is not representative of reality.

Fig. 3.21 Splitting cracks along corner bars due to bond

compaction. The Eurocode 2 value of f_{bd} for "poor" bond conditions is 70% of that applying under "good" conditions (CEN 2004b). So, f_{bd} is finally equal to $0.315{f_{ck}}^{2/3}$ for "good" bond conditions, or to $0.22{f_{ck}}^{2/3}$ for "poor" conditions (with f_{ck} in MPa) and for the recommended value of the partial factor for concrete $\gamma_c = 1.5$. For f_{ck} between 16 and 30 MPa, the value of f_{bd} is from 2 to 4.3 MPa under "good" bond conditions and from 1.4 to 3 MPa for "poor" conditions.

The code-specified value of f_{bd} is meant to correspond not to the real ultimate bond stress, but to the monotonic bond stress causing a slip between the bar and the surrounding concrete about equal to 0.1 mm. According to the CEB/FIP Model Code 90 (CEB 1991), the real ultimate monotonic bond stress of ribbed bars

corresponds to a slip of $s = 0.6$ mm. In unconfined concrete the ultimate bond stress in CEB (1991) is about equal to $2\sqrt{f_c}$ (units: in MPa) for "good" bond conditions, or to $\sqrt{f_c}$ for "poor" (not incorporating the partial factor γ_c). For f_c from 16 to 50, the CEB/FIP Model Code 90 ultimate bond stress ranges from 8 to 14 MPa in the former case, or from 4 to 7 MPa in the later. According to more recent results (Huang et al. 1996, Oh and Kim 2007) the ultimate monotonic bond stress along elastic ribbed bars occurs at a bond slip of about 1 mm and is higher than the CEB/FIP Model Code 90 value. In Huang et al. (1996) it was found equal to $0.45f_c$ for "good" bond conditions (i.e., between 7.2 and 22.5 MPa, for f_c from 16 to 50 MPa) and to half that value ($0.225f_c$) for "poor" conditions. In Oh and Kim (2007) the ultimate monotonic bond stress (in MPa) was found equal to $2.5{f_c}^{0.6}$ (f_c in MPa) for "good" bond conditions (i.e., between 13 and 26 MPa, for f_c from 16 to 50 MPa).

Once the bar yields, the ultimate bond stress drops by about 80%, giving in the end values of the ultimate monotonic bond stress in the range of those specified by Eurocodes 2 and 8 and incorporating a partial factor $\gamma_c = 1.5$.

Bond stress reduces gradually with increasing slip, after the real ultimate value is reached, ending up at a very low residual value of about 15% of the ultimate stress, or even less if there is little confinement.

The values quoted above for the bond resistance in unconfined concrete are for splitting failure. For bond failure by pull-out (or -through) it is considered that the above quoted ultimate stress values increase by at least 25% and the residual strength to about 40% of the ultimate stress. As noted at the beginning of this section, the slip for which the ultimate stress is retained before residual strength is reached is of the order of the bar diameter.

The slip that accompanies bond stresses is irreversible, because it is due to local micro-crushing of concrete against which the ribs of the bar bear. So, the residual slip after unloading to zero bond stress is about equal to the peak slip attained. Repeated loading, with the bond stress cycling without reversal between zero and a peak value (as in bridges due to traffic loads) produces a gradual increase in slip, similar to the accumulation of concrete strains in the right-hand part of Fig. 3.10. However, unless the cumulative slip exceeds the value of (about) 1 mm associated with the peak stress of the monotonic bond-slip curve, the ultimate monotonic bond stress is not adversely affected by any previous cycles at lower bond stress levels and is available in case of subsequent loading up to ultimate stress (Oh and Kim 2007).

The apparent conclusion from the above is that the value of the design bond stress used for the design of anchorages and splices is but a small fraction of the real ultimate stress. It is indeed about equal to the residual bond strength attained well beyond the ultimate bond strength. However, what appears under monotonic or repeated loading as a wide safety margin, is necessary in earthquake resistant structures, because reversal and full cycling of the bond stress causes a large drop in the effective bond strength and stiffness (Balázs 1991). This is evident from the test results in Fig. 3.22, showing that for constant amplitude cycling of bond stress the slip gradually increases. Hysteresis loops are narrow and pinched, dissipating very little energy. The inverted-S shape of the loops is due to:

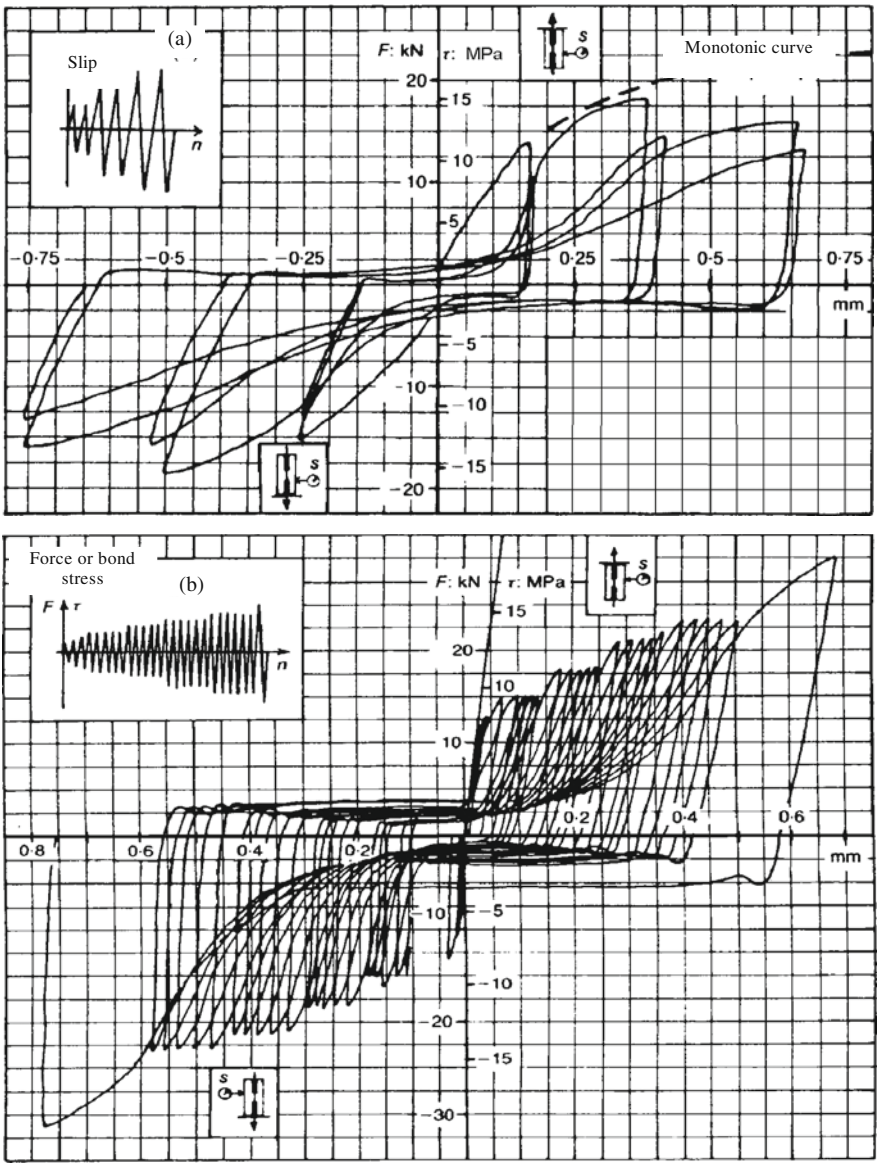

Fig. 3.22 Bond stress v slip behaviour under cyclic loading in concrete with $f_c = 25$ MPa (adapted from Balázs 1989)

- the abrupt release of the bond stress upon reversal, with no recovery of the slip;
- the almost unstrained slippage of the bar until hard contact of the ribs with sound concrete beyond the locally crushed volume of concrete, and
- the resistance of the newly contacted concrete to deformation.

Such a shape of hysteresis loops suggests that the behaviour is controlled by friction and sliding, as in aggregate interlock. The underlying mechanism is the gradual disintegration of the volume of concrete on which the ribs bear. Microcracks starting from the area of contact extend and join up with those that have formed during loading in the opposite direction.

If sufficient anchorage or lap splice length is provided, the peak bond stress demand is low and accumulation of slip as in Fig. 3.22 is limited. Moreover, seismic loading does not cause full reversals of bond stress at bar anchorages or lap splices. During the half-cycle that induces compression in the anchored or spliced bar the bond demand is reduced, as the bar shares the compressive force with the concrete around it and transfers part of its own share through bearing of its end. In buildings designed for earthquake resistance it is generally easy to keep the peak bond stress demand low, except along the length of the bar within beam-column joints. Bond stress along that length reverses fully during seismic loading, while the joint size is normally insufficient for the full anchorage length to develop (see Section 3.3.2). Moreover, the top bars of the beams framing into a joint may have yielded at its face and developed already significant inelastic deformations (see Fig. 3.7). Just inside the face of the joint tensile stresses and strains in the bar are lower, but still rather high and most likely beyond yielding. As bar slippage with respect to the surrounding concrete is equal to the integral of the steel strains along the bar (minus the normally negligible tensile strains in any still uncracked concrete), large tensile strains in the bar imply also large slippage. This in turn means that the bond stress conditions at that point of the bar will be at the tail of the monotonic bond-slip relation, where bond resistance has dropped to low values. As a result, relatively high bond stresses can develop only well inside the joint, where the concrete around the bars is well confined and can sustain high bond stress with very little slippage of the bar. So, anchorage takes place only in the core of the joint which is confined by the stirrups. Outside this core the bond is not sufficient for the reduction of the tensile stress in the bar below the yield value. For this reason, the outermost length of bars within joints, in the order of a few bar diameters, is called "yield penetration depth" (see Section 3.2.2.9 and Eqs. (3.63) there).

Implicit in the concept of ultimate bond stress as a concrete property (for given relative rib area and position of the bar with respect to casting) is the notion that the maximum force that can be transferred by bond from a bar to the surrounding concrete is equal to the ultimate bond stress times the lateral surface area of the bar within the length, l_b, available for force transfer by bond (i.e., l_b times the perimeter of the bar, πd_b). So, this force, and hence the maximum tensile stress in the bar that can be transferred by bond, are taken as proportional to l_b. Moreover, design codes consider that force transfer by bond through the concrete from the straight end of a bar to that of a nearby parallel one for lap-splicing is one-sided and hence less effective than the force transfer from the straight end of a terminating bar to the concrete. In Eurocode 2 (CEN 2004b) the loss in effectiveness ranges from 0 to 50%, if the lap-splicing of less than 25% to more than 50%, respectively, of the total cross-sectional area of the bars overlaps along the member.

In the context of the conventional wisdom above (Darwin et al. 2002a,b) overviewed several empirical expressions developed in the USA – ACI Committee 408 (2001) included – for the minimum length l_b required for full anchorage or lap-splicing of straight ribbed bars. They evaluated also these expressions on the basis of available test results on bond and anchorage. The bias (deviation in the mean) for 325 tests ranges from 12 to 24% and the coefficient of variation about the biased mean from 13 to 29%.

Against this background (Eligehausen and Lettow 2007) departed from the conventional wisdom of a maximum bar tensile stress that can be transferred by bond which is proportional to l_b and fitted a model to the largest available experimental database, comprising more than 800 tests for anchorage or lap-splicing of straight ribbed bars. According to this most complete and accurate model in the current State-of-the-Art, in "good" bond conditions the maximum possible tensile stress that such a bar can develop, f_{sm}, at a straight distance l_b from its end is about the same, no matter whether the bar is anchored or lap-spliced with a parallel bar (for clear distance of the two bars not more than $4d_b$). Its expected value is equal to:

$$f_{sm}(MPa) = 51.2 \left(\frac{l_b}{d_b}\right)^{0.55} \left(\frac{f_c(MPa)}{20}\right)^{0.25} \left(\frac{20}{\max(d_b; 20\,mm)}\right)^{0.2} \left[\left(\frac{c_d}{d_b}\right)^{1/3} \left(\frac{c_{\max}}{c_d}\right)^{0.1} + kK_{tr} + 0.2p(MPa)\right] \leq f_y \tag{3.31}$$

where:

- d_b: bar diameter;
- $c_d = \min$ [min$c$; a/2], limited in the range of d_b/2–3d_b (see Fig. 3.23),
- $c_{\max} = \max$ [max$c$; a/2], with an upper limit of $5c_d$, where:
  - min$c$ and max$c$ are the minimum and the maximum, respectively, clear cover of the anchored or lap-spliced bars (see Fig. 3.23), and
  - a is the clear distance between anchored bars or pairs of lapped bars (see Fig. 3.23);

$$K_{tr} = \frac{1}{n_b d_b} \frac{n_l A_{sh}}{s_h} \leq 0.04 \tag{3.32}$$

is the total cross-sectional area of reinforcement placed within the length l_b transverse to the axis of the anchored or lap-spliced bars and crossing the potential splitting crack, divided by $n_b d_b l_b$; in Eq. (3.32):

- n_b: number of anchored bars or pairs of lapped bars on the plane of the potential splitting crack that reaches the concrete surface;
- $n_l A_{sh}/s_h$: total cross-sectional area of legs of transverse reinforcement crossing the splitting crack, per unit length of the lapped or anchored bar;

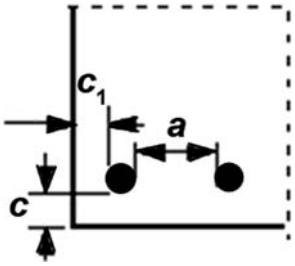

Fig. 3.23 Definition of bar distances for Eq. (3.31) ($c_d = \min[a/2; c_1; c] \geq d_b$, $c_d \leq 3d_b$, $c_{max} = \max[a/2; c_1; c] \leq 5d_b$)

Figure 3.20 shows examples of n_b and n_l from Cairns (2006).

– k = effectiveness factor, with the following values:

  - $k = 10$, if the legs of transverse reinforcement are at right angles to the splitting plane (provided that the clear distance of all anchored bars or pairs of lapped bars from the point where a leg of transverse reinforcement intersects a splitting crack is less than 150 mm, see Fig. 3.20(a)), or in circular sections with a circular perimeter tie or spiral reinforcement, where the splitting crack may either extend from the bar at right angles to the surface or develop between the bars parallel to the perimeter (Fig. 3.20(b));
  - $k = 5$, if the potential splitting extends from the bar to the surface and is crossed by a straight leg of transverse reinforcement placed within the cover, provided that the clear distance between anchored bars or pairs of lapped bars is not less than three-times the cover (Fig. 3.20(c));
  - $k = 0$, in all other cases (Fig. 3.20(c) and (d));

– p = "active" confining pressure normal to the axis of the anchored or lapped bars due to external actions (e.g., a load applied to the surface of the member) or their effects (e.g., the axial load of a column); the mean value of p across the section of the member in the plane of the bar is used.

Implicit in Eq. (3.32) is a tensile stress in the transverse reinforcement equal to the tensile strength of concrete, f_{ct}, times the ratio of Moduli, E_s/E_c. This is because the role of this reinforcement is to prevent cracking, not to make up for it. If splitting failure nonetheless does occur, the yield stress of transverse reinforcement may be mobilised to the benefit of the post-ultimate residual strength.

Equation (3.31) refers to splitting failure of bond along ribbed straight bars in tension. Its applicability is defined by the range of parameters in the tests to which it has been fitted in Eligehausen and Lettow (2007): f_c from 10 to 117 MPa, relative rib area between 0.05 and 0.07, l_b not less than $12d_b$, minimum clear cover at least $0.5d_b$ but not more than $3d_b$ and clear distance between anchored bars or pairs of lapped bars at least d_b. The coefficient of variation of the fitting is about 15%. The data show that, for given values of the parameters at the right-hand side of Eq. (3.31), the experimental value of f_{sm} is on average about 5% larger for anchored bars than for lap-splices, irrespective of the number of bars anchored or lapped at the same

location. The difference may be neglected as statistically insignificant (Eligehausen and Lettow 2007).

For the pull-out (or -through) mode of failure, Eq. (3.31) may still be applied, with the confinement terms (1st and 2nd one in the last, bracketed term) replaced by an upper limit value of 2.0.

If anchorage or lapping of ribbed bars in tension is supplemented with a hook, a bend or an anchor plate at the end, or by welding to a transverse bar, then the anchor force developed by these additional means, divided by the bar cross-sectional area is added to the right-hand-side of Eq. (3.31).

Anchorage or lapping of ribbed straight bars in compression is assisted by bar end bearing. Provided that the cover of the end in the direction of the bar axis is at least $2d_b$, the contribution of end bearing may be taken into account by adding to the right-hand-side of Eq. (3.31) the product of $3f_c$ and of the confinement term (the last, bracketed one in Eq. (3.31)) (Cairns 2006). That term can be taken equal to 2, if the bar end bears against a volume of very well confined concrete (e.g., at the tip of a column bar bearing on the top surface of the floor slab).

FRP wrapping of the member over at least the full length l_b contributes to confinement. In that case the following value of kK_{tr} may be used in Eq. (3.31) (Biskinis and Fardis 2007, 2008):

$$kK_{tr} = \frac{1}{n_b d_b}\left(\frac{k_s n_l A_{sh}}{s_h} + \frac{k_f n_f t_f E_f}{E_s}\right) \tag{3.32a}$$

where t_f: total thickness of fibre sheets in the wrapping; E_f: Modulus of the fibre material; k_s: effectiveness factor of transverse steel (the k of Eq. (3.31) and Fig. 3.20); n_f: number of FRP wraps intersected by a potential splitting crack to the surface and k_f: their effectiveness factor. For example, if the members in Fig. 3.20 are wrapped with FRP, then: for Fig. 3.20(a) $n_f = 2$, $k_f = 10$; for Fig. 3.20(b) $n_f = 1$, $k_f = 10$; for Fig. 3.20(c) and (d) $n_f = 1$ with $k_f = 5$ if $a \geq 3c$ or $k_f = 0$ if $a < 3c$.

3.1.4 Concluding Remarks on the Behaviour of Concrete Materials and Their Interaction Under Cyclic Loading

As pointed out in Section 1.3.6.1, of the two constituent materials of structural concrete, only steel is inherently ductile, with stable hysteresis loops and considerable energy dissipation capacity up to very large deformations. And that only in tension, as reinforcing bars may buckle in compression, shedding their force resistance and risking subsequent fracture. Concrete is fairly brittle, but when it is well confined it can sustain cycles of large compressive strains without appreciable drop in resistance. Confined concrete, however, cannot dissipate significant energy by itself in compressive stress cycles.

Under cyclic loading, the transfer of shear along cracks and the bond between reinforcing bars and concrete are characterised by rapid degradation of resistance

with cycling and little energy dissipation. The first of these mechanisms should not be relied upon at all, whereas bond should be kept in the elastic range, possibly through confinement.

The only way to dissipate significant energy during large amplitude deformation cycles is by combining:

- reinforcing steel in the direction where tensile internal forces and stresses are expected to develop; and
- concrete and reinforcement in the direction of compressive internal forces and stresses, provided that closely spaced ties confine the concrete and restrain the bars against buckling.

It is clear that this is feasible wherever in the member inelastic stresses and strains invariably develop in the directions where reinforcement can be conveniently placed. In essentially one-dimensional members, such as beams, columns and slender walls, it is convenient to place the reinforcement in the longitudinal and the (two) transverse direction(s). So concrete members can be designed to develop large inelastic deformations and reliably dissipate significant energy, only in their regions dominated by flexure (with or without axial load). These regions lend themselves to effective use of reinforcing bars to take up directly the tension and to restrain concrete and compression steel exactly at right angles to their compression stresses. Even there energy dissipation takes place primarily – essentially only – in the reinforcement and not in the confined concrete.

3.2 Concrete Members

This part of Chapter 3 deals with the behaviour of individual members subjected to cyclic flexure and shear of the type induced by seismic actions. Member types considered are those commonly used in earthquake resistant concrete buildings, notably prismatic members with rectangular, L- or T-section. Connections between such members are addressed at the end of the chapter.

3.2.1 The Mechanisms of Force Transfer in Concrete Members: Flexure, Shear and Bond

In prismatic concrete members, such as beams or columns, it is convenient to work with the centroidal member axis, x, and with cross-sections normal to it, and with the resultant force and moments of the normal stresses acting on the section (normal force N, bending moments M_y, M_z with respect to the centroidal principal axes y and z of the cross section, respectively) and of the shear stresses acting on it (shear forces V_y, V_z parallel to axes y, z, respectively, torsional moment T with respect to axis x). It is then convenient to distinguish the "flexural" deformations as those attributed

mainly to N, M_y and M_z and computed on the basis of the Navier-Bernoulli hypothesis of plane sections remaining plane and normal to the x axis. Shear forces cause additional ("shear") deformations, which can be computed by relaxing the Navier-Bernoulli assumption to allow cross-sections not to remain normal to the axis, while they still remain plane. Interaction effects, i.e. the influence of shear forces on flexural deformations and that of normal stress resultants on shear deformations, are important in general and cannot be neglected, especially for inelastic cyclic loading. However, if the bending moment is relatively high and the shear force low, flexural deformations not only dominate, but can also be computed in good approximation neglecting the influence of shear forces. The controlling factor is the shear span ratio, M/Vh, defined as the ratio of the shear span, $L_s = M/V$, at the end of the member where flexural yielding is expected, to the depth h of the cross-section within the plane of bending. Indeed, even within the framework of linear elasticity, the ratio of the maximum normal stress parallel to the member axis, $\sigma_{x,max} = M/W$, to the maximum value of the shear stress, $\tau_{xy,max} = 1.5V/A$, in a rectangular cross-section under uniaxial bending and shear, is equal to: $\frac{\sigma_{x,max}}{\tau_{xy,max}} = 4\frac{M}{Vh}$. So, even in the context of linear elasticity, the lower the shear span ratio, L_s/h, the more important are the shear stresses vis-à-vis the normal ones.

Beams, columns and slender walls commonly have values of shear span ratio above (about) 2.5. For such values of L_s/h the mechanisms of force transfer by flexure (i.e. through forces and stresses parallel to the member axis) or shear (i.e. via forces or stresses at right angles to the member axis) may be considered as practically uncoupled and independent. If L_s/h is less than (about) 2.5, as in squat walls or columns and in short beams, these two mechanisms of force transfer tend to merge, as the shear span itself becomes a two-dimensional element. If the member is still considered for convenience as one-dimensional, the merger of the two force transfer mechanisms is reflected in a reduction of the moment resistance due to the high shear force and of the shear capacity due to the bending moment.

In members with L_s/h above (about) 2.5, the two practically independent mechanisms of force transfer may be considered to act in series along the shear span, L_s, in the sense that:

- internal forces need to be safely transferred by both mechanisms and failure of one of the two precipitates failure of the member; and
- the overall deformations of the member are the sum of the individual (elastic or inelastic) deformations of the two mechanisms.

As a matter of fact, capacity design of members in shear (see Section 1.3.6) is based on the concept that these two mechanisms act in series, so that the overall inelastic deformations and the deformation capacity of the member can be engineered to come from the ductile flexural mechanism alone.

To the extent that the above mechanisms of force transfer require development of (tensile) stresses in reinforcing bars, they require also transfer of forces from the bars to the concrete and vice-versa through bond. Force transfer by bond is normally considered as part of the afore-mentioned two main force transfer mechanisms,

if it takes place within the shear span. It should be taken, though, as a separate force transfer mechanism in series with the other two, if it takes place along that part of the longitudinal bars extending beyond the ends of the shear span (notably into the joints with other elements). So, for the shear span of a member, L_s, a series system of the following force transfer mechanisms may be considered to develop:

i. the flexural mechanism within the shear span
ii. the shear mechanism, again within the shear span; and
iii. the development of the (mainly tensile) forces in the longitudinal reinforcement through bond beyond the end of the shear span.

The overall force capacity of the member is governed by the weakest of these three mechanisms, while the overall deformation is the sum of those of the individual ones.

In members with L_s/h below (about) 2.5, it is understood that mechanisms (i) and (ii) merge into one.

The concluding remarks of Section 3.1.4 imply that the design of a member and the detailing of its reinforcement within the member and beyond (i.e., in its anchorage zone outside the shear span), should ensure that mechanisms (ii) and (iii) will work in their elastic range, by designing mechanism (i) to have lower force capacity than the other two.

3.2.2 Flexural Behaviour at the Cross-Sectional Level

3.2.2.1 Physical Meaning and Importance of Curvature in Concrete Members

There is experimental evidence that the Navier-Bernoulli plane section hypothesis can be applied as a rough approximation to slender concrete members during practically all ranges of flexural behaviour: till and beyond concrete cracking, towards yielding of the reinforcement and even further, almost up to the ultimate deformation of the member. The plane-section hypothesis lends itself to a very convenient description of the flexural behaviour at the cross-sectional level through the relation of moment (M) to curvature (φ). It allows relating the normal strain ε to the distance y from the neutral axis as $\varepsilon = \varphi y$. Therefore, the strain of the extreme compression fibres is: $\varepsilon_c = \varphi x$, where $x = \xi d$ is the neutral axis depth; the strain of the tension reinforcement is equal to $\varepsilon_{s1} = \varphi(d–x) = \varphi(1–\xi)d$, while that of the compression reinforcement at distance d_1 from the extreme compression fibres is $\varepsilon_{s2} = \varphi(x–d_1) = \varphi(\xi–d_1/d)d$. Note that the curvature φ is the conjugate of the moment M, in the sense that the integral of $M\mathrm{d}\varphi$ gives the flexural deformation energy per unit length of the member.

The flexural behaviour of concrete members is commonly described in M–φ terms, because for monotonic loading with constant axial force N the M–φ curve can be easily established by calculation, even up to ultimate deformation. For given

geometry of the cross-section and amount and layout of the longitudinal reinforcement and for known material σ-ε laws, this is done in a stepwise manner:

- For a value of φ, the value of the neutral axis depth x is assumed, the strain distribution across the section is derived as $\varepsilon = \varphi y$ (with y measured from the trial location of the neutral axis) and the corresponding stress distribution is derived from the material σ-ε laws. Force equilibrium in the axial direction, $N = \int \sigma \, dA$, is checked and the value of x is revised, with calculations repeated until force equilibrium is satisfied.
- The value of M corresponding to this value of φ (and N) is computed from moment equilibrium: $M = \int \sigma y_{cg} dA$, where y_{cg} is the distance from the centroid of the section to which the value of M refers.
- For the next value of φ the calculations are repeated, starting the iterations with a trial value of x equal to the one for which convergence to the value of N has been achieved in the previous step.

This approach can be used to construct cyclic M–φ relations for a given history of imposed curvatures, provided that the complete cyclic σ-ε relations of the materials are known, including the rules applying after reversal of loading from any (σ, ε) point.

Owing to its computational convenience, curvature is an appealing and very popular measure of flexural deformations. However, in concrete members loaded beyond cracking, the curvature loses its physical meaning. The reason is that concrete cracking, and later on cover spalling, bar buckling and concrete crushing, are all of discrete nature. For this reason, in concrete members curvature is commonly defined – and experimentally measured – as the relative angle of rotation $\Delta\theta$ of two neighbouring sections, divided by their distance, Δx. This distance is not infinitesimal but finite and should be of the order of:

- the typical distance of two adjacent flexural cracks, if the behaviour prior to yielding is of interest, or
- the length over which concrete is expected to spall or crush and reinforcing bars may buckle or even break.

The resulting value of $\varphi = \Delta\theta/\Delta x$ is a mean curvature that corresponds to the mean moment within Δx. In experiments, values of Δx in the range of $h/2$–h are commonly selected.

3.2.2.2 Moment-Curvature Relation up to Yielding Under Uniaxial Bending with Axial Force

Cross-Sections with Rectangular Compression Zone

Until concrete cracks the M–φ relation is linear, with slope M/φ equal to the rigidity, $E_c I_t$, of the uncracked transformed section, i.e. of a concrete section in which any reinforcing bar of cross-sectional area $A_{s,i}$ has been replaced by an equiv-

alent concrete area, $\alpha A_{s,i}$, where $\alpha = E_s/E_c$ is the ratio of Moduli of the two materials. A flexural crack forms at the cracking moment M_{cr} (which is equal to $M_{cr} = (f_{ctm}+N/A_t)I_t/y_t$, where N is the axial force – positive for compression – A_t is the cross-sectional area of the transformed section and y_t the distance of the extreme tension fibres from the centroid). The rigidity of the cross-section drops abruptly then, remaining practically constant until the section finally yields.

The members of concrete buildings typically have rectangular, T-, L-, H- or U-section (in beams monolithically connected with the slab, or in walls or columns with non-rectangular section). If the compression zone of a non-rectangular section falls within a single rectangular part of the section, the compression zone is rectangular. This is the case considered here. The next section addresses cases with a T-, L- or U-shaped compression zone.

If section yielding is identified with yielding of the tension steel, the yield curvature is:

$$\varphi_y = \frac{f_{yL}}{E_s\left(1-\xi_y\right)d} \tag{3.33a}$$

with f_{yL} denoting the yield stress of the longitudinal bars and ξ_y the neutral axis depth at yielding (normalised to the section effective depth, d), given by:

$$\xi_y = \left(\alpha^2 A^2 + 2\alpha B\right)^{1/2} - \alpha A \tag{3.34}$$

in which $\alpha = E_s/E_c$ denotes the ratio of elastic moduli (steel-to-concrete) and A, B are given from Eqs. (3.35a) (Panagiotakos and Fardis 2001a):

$$A = \rho_1 + \rho_2 + \rho_v + \frac{N}{bdf_y}, \quad B = \rho_1 + \rho_2\delta_1 + \frac{\rho_v\left(1+\delta_1\right)}{2} + \frac{N}{bdf_y} \tag{3.35a}$$

where ρ_1 and ρ_2 are the ratios of the tension and compression reinforcement and ρ_v is the ratio of "web" reinforcement (i.e. of the reinforcement which is – almost – uniformly distributed between the tension and the compression steel). The area of any diagonal bars, times the cosine of their angle with respect to the member axis, is added to the reinforcement area included in ρ_1 and ρ_2. All steel ratios are normalised to bd. Further in Eq. (3.35a), b is the width of the compression zone, N the axial load (with compression taken as positive) and $\delta_1 = d_1/d$, where d_1 is the distance of the centre of the compression reinforcement from the extreme compression fibres.

Sometimes members with high axial load ratio, $\nu = N/A_c f_c$, exhibit apparent yielding as a distinct downwards curving of the moment-curvature diagram of the end section, owing to significant nonlinearity of the concrete in compression before the tension steel yields. A simple way to treat such apparent yielding is by identifying it with exceedance of a certain strain at the extreme compression fibres, while still considering both steel and concrete as linear-elastic till that point. The test results on members yielding under high axial load ratio suggest the following value for this "elastic strain limit" (Panagiotakos and Fardis 2001a):

$$\varepsilon_c \approx \frac{1.8 f_c}{E_c} \tag{3.36}$$

Then apparent yielding of the member takes place at a curvature:

$$\varphi_y = \frac{\varepsilon_c}{\xi_y d} \approx \frac{1.8 f_c}{E_c \xi_y d} \tag{3.33b}$$

where the neutral axis depth at yielding, ξ_y (again normalised to the section effective depth, d), is still given by Eq. (3.34), but this time with A, B from Eqs. (3.35b):

$$A = \rho_1 + \rho_2 + \rho_v - \frac{N}{\varepsilon_c E_s b d} \approx \rho_1 + \rho_2 + \rho_v - \frac{N}{1.8\alpha\, b d f_c}, \quad B = \rho_1 + \rho_2 \delta_1 + \frac{\rho_v (1 + \delta_1)}{2} \tag{3.35b}$$

The lower of the two φ_y values from Eqs. (3.33a) or (3.33b) is the yield curvature. Then the yield moment, M_y, can be computed from equilibrium of the (plane) section as:

$$\frac{M_y}{b d^3} = \varphi_y \left\{ E_c \frac{\xi_y^2}{2} \left(\frac{1 + \delta_1}{2} - \frac{\xi_y}{3} \right) + \frac{E_s (1 - \delta_1)}{2} \left[\left(1 - \xi_y\right) \rho_1 + \left(\xi_y - \delta_1\right) \rho_2 + \frac{\rho_v}{6} (1 - \delta_1) \right] \right\} \tag{3.37}$$

It is noted that, by the time a strong earthquake shakes a building, practically every end section of its beams, columns or walls are already cracked, owing to the gravity loads combined with stresses due to the restrained shrinkage or thermal strains or other imposed deformations. Normally such previous stresses are not sufficient to cause cracking of columns and walls having significant axial load. However, the construction joint at the base of these members in each storey and often at the top as well (at the beam soffit) have little cohesion and will readily open in an earthquake. So, concrete members may be considered as already cracked at the time of the earthquake and their M –φ diagram may be taken as linear up to yielding.

Sections with T Compression Zone

T-, L-, H-, U- or hollow rectangular sections are considered here to have a compression flange with constant width and thickness, b and t, respectively, and total thickness of the webs b_w. The bending moment is about an axis parallel to the flange and induces compression in it. Equations (3.34) and (3.35) may still be applied, but if the outcome of Eq. (3.34) (significantly) exceeds the ratio of the flange thickness to the effective depth: $\xi_y > t/d$, the neutral axis falls in the web and the compression zone has T-, L- or U-shape. The neutral axis depth and the moment at yielding

may then be obtained from an extension of the analysis in the previous sub-section *Cross-Sections with Rectangular Compression Zone*, under the same assumptions and yield criteria. The tension, the compression and the web reinforcement are again normalised to bd, to give ratios ρ_1, ρ_2 and ρ_v, respectively. The counterparts of Eqs. (3.35) are (Biskinis 2007, Biskinis and Fardis 2007):

– For section yielding because of yielding of the tension steel:

$$\begin{aligned} A &= \frac{b}{b_w}\left(\rho_1+\rho_2+\rho_v+\frac{N}{bdf_y}\right)+\frac{1}{\alpha}\frac{t}{d}\left(\frac{b}{b_w}-1\right), \\ B &= \frac{b}{b_w}\left(\rho_1+\rho_2\delta_1+0.5\rho_v\left(1+\delta_1\right)+\frac{N}{bdf_y}\right)+\frac{1}{2\alpha}\left(\frac{t}{d}\right)^2\left(\frac{b}{b_w}-1\right) \end{aligned} \tag{3.38a}$$

– For section yielding when the strain limit of Eq. (3.36) is reached at the extreme compression fibres:

$$\begin{aligned} A &= \frac{b}{b_w}\left(\rho_1+\rho_2+\rho_v-\frac{N}{\varepsilon_c E_s bd}\right)+\frac{1}{\alpha}\frac{t}{d}\left(\frac{b}{b_w}-1\right), \\ B &= \frac{b}{b_w}\left(\rho_1+\rho_2\delta_1+0.5\rho_v\left(1+\delta_1\right)\right)+\frac{1}{2\alpha}\left(\frac{t}{d}\right)^2\left(\frac{b}{b_w}-1\right) \end{aligned} \tag{3.38b}$$

Equations (3.33) and (3.34) still apply, but the yield moment should be computed from the following counterpart of Eq. (3.37) (Biskinis 2007, Biskinis and Fardis 2007):

$$\frac{M_y}{bd^3}=\varphi_y\left\{\begin{array}{l} E_c\left[\frac{\xi_y^2}{2}\left(\frac{1+\delta_1}{2}-\frac{\xi_y}{3}\right)\frac{b_w}{b}+\left(1-\frac{b_w}{b}\right)\left(\xi_y-\frac{t}{2d}\right)\left(1-\frac{t}{2d}\right)\frac{t}{2d}\right]+ \\ \frac{E_s\left(1-\delta_1\right)}{2}\left[\left(1-\xi_y\right)\rho_1+\left(\xi_y-\delta_1\right)\rho_2+\frac{\rho_V}{6}\left(1-\delta_1\right)\right] \end{array}\right\} \tag{3.39}$$

Note that Eqs. (3.38) and (3.39) degenerate into Eqs. (3.35) and (3.37) respectively, if b_w equals b.

Comparison with Experimental Results and Empirical Expressions for the Curvature

The outcome of Eqs. (3.37) and (3.39), with φ_y computed according to the two sub-sections above: *Cross-Sections with Rectangular Compression Zone* or *Sections with T Compression Zone*, has been compared in Biskinis (2007) to the "experimental yield moment", estimated as the moment at the corner of a bilinear M–θ (moment-chord rotation) curve fitted to the envelope of the measured M–θ

hysteresis loops, taking into account P–Δ effects. The data come from tests of about 2050 beam/columns, 125 rectangular walls or 155 members with T-, H-, U- or hollow rectangular section, all with shear span ratio and reinforcement such that there were no flexure-shear interaction effects (see Section 3.2.5). The "experimental yield moment" exceeds the prediction of Eqs. (3.37) and (3.39) by an average factor of: 1.025, 1.015 or 1.075 for beams/columns, rectangular walls or members with T-, U- or hollow rectangular section, respectively (Biskinis 2007). The reason for the difference is that the corner of a bilinear M–θ curve that envelops the measured hysteresis loops expresses global yielding of the member and hence is slightly past the point where the extreme tension steel or compression fibres of the end section "yield". The factor of 1.025, 1.015 or 1.075 should be applied, as correction factor, also to the value of φ_y obtained from Eqs. (3.33) for beams/columns, rectangular walls or members with T-, U- or hollow rectangular section, respectively. The coefficient of variation of the test-to-prediction ratio for M_y is equal to 16.3, 14.8 and 12.6% for beams/columns, rectangular walls or members with T-, U- or hollow rectangular section, respectively (Biskinis 2007). Test-to-test variability and natural scatter of material properties (e.g., of the yield stress of specimen rebars with respect to reported values from few coupons, or of the concrete strength relative to the reported mean values from test cylinders or cubes, etc.) or of geometric parameters (e.g., of the effective depth to the tension or compression reinforcement, etc.) correspond to a coefficient of variation of experimental-to-predicted M_y values of about 5% (Biskinis 2007). The rest of the scatter is due to model uncertainty. Assuming statistical independence, the corresponding coefficient of variation of the test-to-prediction ratio for M_y is about equal to the values quoted above reduced by just 1%.

The comparison above refers to members with ribbed bars. Bond along smooth (plain) bars may not be sufficient for full mobilisation of their yield strength at "apparent yielding" at the section of maximum moment. This may explain why the mean and median of the test-to-prediction ratio in about 40 tests of beam/columns with such bars is about 0.95.

The literature contains also experimental data on the yield curvature, φ_y, "measured" as relative rotation between the section of maximum moment and a nearby one, divided by the distance between the two sections. In some of them measured relative rotations include also the effect of reinforcement pull-out from its anchorage zone beyond the section of maximum moment. Because:

- the "experimental yield moment", $M_{y,exp}$, is established more accurately in a test than the "measured" yield curvature, and
- the relation between φ_y and M_y, Eqs. (3.37) and (3.39), is well established, as based on equilibrium and plane section analysis,

it is preferable to consider as "experimental yield curvature", $\varphi_{y,exp}$, the value derived from the "experimental yield moment", $M_{y,exp}$, by inverting Eq. (3.37) or (3.39). The theoretical yield curvature from Eqs. (3.33), (3.34), (3.35) and (3.38), times the correction factor of 1.025, 1.015, or 1.075 for beams/columns, rectangular

walls or members with T-, U- or hollow rectangular section, respectively, may be considered to predict the $\varphi_{y,exp}$ with a median test-to-prediction ratio of 1.0 and a coefficient of variation equal to that of the test-to-prediction ratio for M_y, i.e. 12.5–16%.

The following expressions have also been fitted to $\varphi_{y,exp}$ (Biskinis 2007):

– for beams or columns:

$$\varphi_y \approx \frac{1.54 f_{yL}}{E_s d} \tag{3.40a}$$

– for rectangular walls:

$$\varphi_y \approx \frac{1.34 f_{yL}}{E_s d} \tag{3.40b}$$

– for T-, U- or hollow rectangular sections:

$$\varphi_y \approx \frac{1.47 f_{yL}}{E_s d} \tag{3.40c}$$

or alternatively:

– for beams or columns:

$$\varphi_y \approx \frac{1.75 f_{yL}}{E_s h} \tag{3.41a}$$

– for rectangular walls:

$$\varphi_y \approx \frac{1.44 f_{yL}}{E_s h} \tag{3.41b}$$

– for T-, U- or hollow rectangular sections:

$$\varphi_y \approx \frac{1.57 f_{yL}}{E_s h} \tag{3.41c}$$

Being empirical, Eqs. (3.40) and (3.41) predict $\varphi_{y,exp}$ without any bias (i.e., with median value of 1.0 for the ratio test-to-prediction). However, as important parameters (e.g., the axial load level and the ratios and layout of longitudinal reinforcement) are neglected, these expressions give a larger coefficient of variation of the test-to-prediction ratio than Eqs. (3.33) (3.34), (3.35) and (3.38): 17.5, 18.4 and 16.2% for Eqs. (3.40a), (3.40b) and (3.40c), respectively, or 29.2, 17.9 and 17.9% for Eqs. (3.41a), (3.41b) and (3.41c) (Biskinis 2007).

3.2.2.3 Fixed-End Rotation Due to Bar Pull-Out from the Anchorage Zone Beyond the Section of Maximum Moment – Value at Yielding

If there is complete symmetry of the member and its loading with respect to the section of maximum moment (as at mid-span of a beam subjected to symmetric loading), or if the longitudinal reinforcement is anchored by welding right next to this cross-section, there is no slippage (pull-out) of the longitudinal reinforcement from the region beyond the section of maximum moment. However, such slippage takes place from the anchorage of longitudinal bars within a joint or footing where the member frames, contributing to the transverse deflections of the entire shear span by a rigid-body rotation, θ_{slip}. The effect of this rotation is included in the measurement of transverse deflections and of chord-rotations of a test specimen with respect to the base or the joint into which it frames.

If s denotes the slippage of the tension reinforcement from its anchorage beyond the section of maximum moment, θ_{slip} is equal to $\theta_{slip} = s/(1–\xi)d$, where ξ is the neutral axis depth, normalised to the effective depth, d. The value of s is equal to the sum of:

- the slip of the bar with respect to the surrounding concrete at the far end of its straight embedment length (which is non-zero only if there is a hook, bend or anchor plate at that end, in which case the slip there is equal to the local deformation of the concrete due to the contact pressure under the hook, bend or anchor plate); plus
- the elongation of the bar between the far end of its straight embedment length and the section of maximum moment of the member.

Note that the value of M at the section of maximum moment is roughly proportional to the force in the tension reinforcement and that this force is the resultant of bond stresses along the anchorage length. So, the $M–\theta_{slip}$ relation reflects the bond-slip behaviour with its strongly pinched shape of the hysteresis loops. To the extent that the total chord-rotation θ is due to θ_{slip}, the apparent flexibility of the member increases and the shape of the overall $M–\theta$ loops includes certain pinching.

Fixed-end rotation due to bar pull-out equals the slip from the anchorage zone divided by the depth of the tension zone, $(1–\xi)d$ (Fig. 3.24). Assuming that bond stresses are uniform over a length l_b of the tension bars beyond the end section, the stress increases linearly along l_b from zero at the end of the bar to the bar elastic steel stress at the end section of the member, σ_s. Bar slippage from its anchorage equals $0.5\sigma_s l_b/E_s$. The ratio σ_s/E_s to $(1–\xi)d$ is the curvature, φ. The length l_b is proportional to the force in the bar, $A_s\sigma_s$, divided by its perimeter, πd_b (i.e. to $d_{bL}\sigma_s/4$ where d_{bL} is the mean tension bar diameter) and inversely proportional to bond strength, i.e., in good approximation, to $\sqrt{f_c}$. Setting at yielding of the end section: $\varphi = \varphi_y$, taking the mean bond stress in MPa along l_b equal to f_c(MPa) (which is about 50% or 40% of the bond stress corresponding to a slip equal to $s = 0.6$ mm of about $2\sqrt{f_c}$ in unconfined or confined concrete, respectively, for "good" bond conditions according

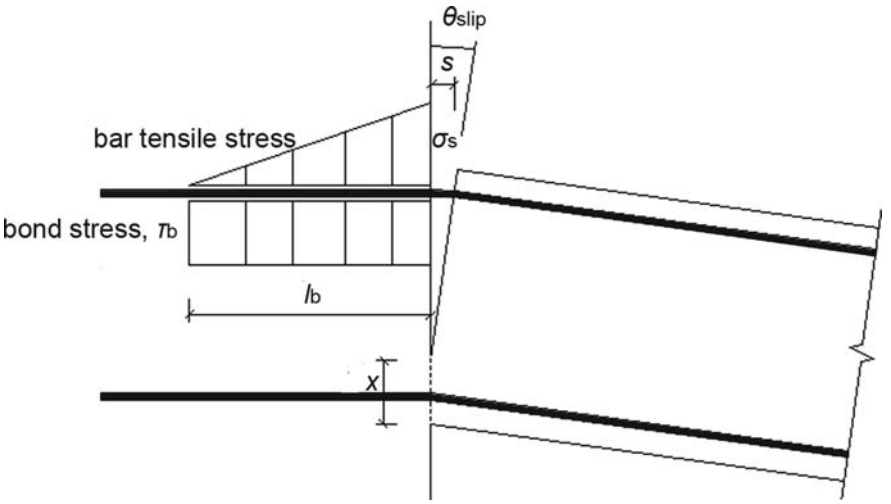

Fig. 3.24 Fixed-end rotation, θ_{slip}, due to slippage of longitudinal bars from their anchorage within a joint in which the member frames

to CEB (1991)) and setting for simplicity $\sigma_s = f_{yL}$ (even when φ_y is obtained from Eq. (3.33b)), the "fixed-end rotation" of the end section at yielding is:

$$\theta_{y,slip} = \frac{\varphi_y d_{bL} f_{yL}}{8\sqrt{f_c}} \qquad (f_{yL} \text{ and } f_c \text{ in MPa}) \tag{3.42}$$

Equation (3.42) has been calibrated to about 160 cases in the literature where curvature was measured as relative rotation between the section of maximum moment and a nearby one, divided by the distance between the two sections, including the effect of reinforcement pull-out from its anchorage zone beyond the section of maximum moment (including a few cases where the rigid-body rotation due to bar pull-out, θ_{slip}, was directly measured). The ratio of the (experimental) yield curvature from the measured relative rotations including the effect of pull-out from the specimen base, to the theoretical one from Eqs. (3.33) (3.34), (3.35) and (3.38) times the correction factor of 1.025, 1.015 or 1.075, plus the value from Eq. (3.42) divided by the gauge length over which relative rotations are measured, does not exhibit any systematic effect of the gauge length in these 160 cases and has a median value of 1.00 and a coefficient of variation of 33.9% (Biskinis 2007).

3.2.2.4 Ultimate Curvature of Sections with Rectangular Compression Zone Under Uniaxial Bending with Axial Force

Definitions and Assumptions

The ultimate curvature φ_u of a section is commonly (and conventionally) identified with a distinct change in the pattern of the moment-curvature response:

– In monotonic loading, with a noticeable drop of the moment resistance after the peak (at least 20% of the maximum resistance).
– In cycling loading, with an abrupt and distinct reduction of the reloading slope, or of the area of the hysteresis loops, or of the peak moment of the cycle, compared to those of the preceding cycle(s). Such abrupt degradation phenomena are typically associated with a drop in the maximum possible resisting moment of at least 20% of the maximum ever resisting moment. Whenever such abrupt and distinct degradation phenomena cannot be identified, the conventional rule of a maximum possible resisting moment less than 80% of the maximum ever moment resistance is used to define the ultimate deformation. Section 3.2.2.7 discusses in more detail this conventional definition of ultimate deformation.

The calculation of φ_u can be based on a plane section analysis but with nonlinear σ-ε laws, described below under (i) and (ii).

A section will reach its ultimate condition under increasing deformations when one of the following takes place:

a. The tension reinforcement reaches its ultimate elongation, ε_{su}, and ruptures. This gives an ultimate curvature equal to:

$$\varphi_{su} = \frac{\varepsilon_{su}}{(1 - \xi_{su})\, d} \tag{3.43}$$

where ξ_{su} is the neutral axis depth (normalised to d) when the ultimate curvature of the section is attained due to steel rupture.[6] This case is the subject of the sub-section below titled *Failure of the Full Section Due to Rupture of Tension Reinforcement Before Spalling of the Concrete Cover*.

b. The compression zone disintegrates and sheds (most of) its compressive force. This takes place when the concrete of the extreme compression fibres reaches its ultimate strain, ε_{cu}, giving an ultimate curvature of:

$$\varphi_{cu} = \frac{\varepsilon_{cu}}{\xi_{cu} d} \tag{3.44}$$

This case is dealt with in the sub-section below on *Curvature at Spalling of the Concrete Cover*.

Depending on:

– the value of the axial load on the section,
– the amount and location of longitudinal bars, and
– the confinement of the compression zone by transverse reinforcement, etc.,
– failure mode (a) or (b) may take place either:

[6] Equation (3.43) has already appeared in Section 3.1.1.4 as Eq. (3.1).

1. before, or at spalling of the unconfined concrete cover, i.e. at the level of the full section (sub-sections *Failure of the Full Section Due to Rupture of Tension Reinforcement Before Spalling of the Concrete Cover* and *Curvature at Spalling of the Concrete Cover*), or
2. in the confined core, after spalling of the unconfined concrete cover (sub-section *Ultimate Curvature of the Confined Core, After Spalling of the Cover*); then Eqs. (3.43) and (3.44) are applied with: the effective depth of the full section, d, replaced by that of the confined core, d_c; the neutral axis depth, ξ, referring to the confined core and normalised to d_c; and the ultimate strain of confined concrete, $\varepsilon_{cu}{}^*$, used in Eq. (3.44) in lieu of ε_{cu}.

The following σ-ε laws of the materials are adopted here:

1. Unconfined concrete has a parabolic σ-ε law up to the ultimate strength of f_c and the corresponding strain, ε_{co}. Beyond that point the σ-ε law is horizontal until a strain $\varepsilon_c \leq \varepsilon_{cu.}$[7] Then the compression zone contributes to the axial compressive force with a force equal to $\xi(bdf_c)(1-\varepsilon_{co}/3\varepsilon_c)$.
2. The σ-ε law of reinforcing steel is elastic-perfectly plastic at relatively low strains, as those at section ultimate conditions due to crushing of the concrete (failure mode (b) above). At the large steel strains accompanying section failure due to steel rupture (failure mode (a)), the steel is considered to strain-harden after the yield plateau at the yield stress f_y. Strain-hardening is linear, starting from the yield stress f_y at a strain ε_{sh}, till the ultimate strength f_t of steel at an elongation of ε_{su}. The σ-ε parameters (f_y, $\varepsilon_y = f_y/E_s$, ε_{sh}, f_t, ε_{su}) of tension, compression and web reinforcement are indexed by 1, 2 or v, respectively.

The ultimate curvature of sections with rectangular compression zone is computed according to the multi-step procedure of sub-sections *Failure of the Full Section Due to Rupture of Tension Reinforcement Before Spalling of the Concrete Cover, Curvature at Spalling of the Concrete Cover*, *Ultimate Curvature of the Confined Core, After Spalling of the Cover* and Flow Charts 3.1 and 3.2. Symbols used in the analysis are:

- $\nu = N/bdf_c$: axial load ratio, positive for compression;
- $\omega_1 = \rho_1 f_{y1}/f_c$, $\omega_2 = \rho_2 f_{y2}/f_c$, $\omega_v = \rho_v f_{yv}/f_c$: mechanical reinforcement ratios of tension, compression and web reinforcement, respectively, with ρ_1, ρ_2, ρ_v normalised to bd;
- $\delta_1 = d_1/d$: the distance of compression reinforcement from the extreme compression fibres, (normalised to d).

[7] This is the σ-ε law used in CEN (2004b) and CEB (1991) for the calculation of the resistance of cross-sections.

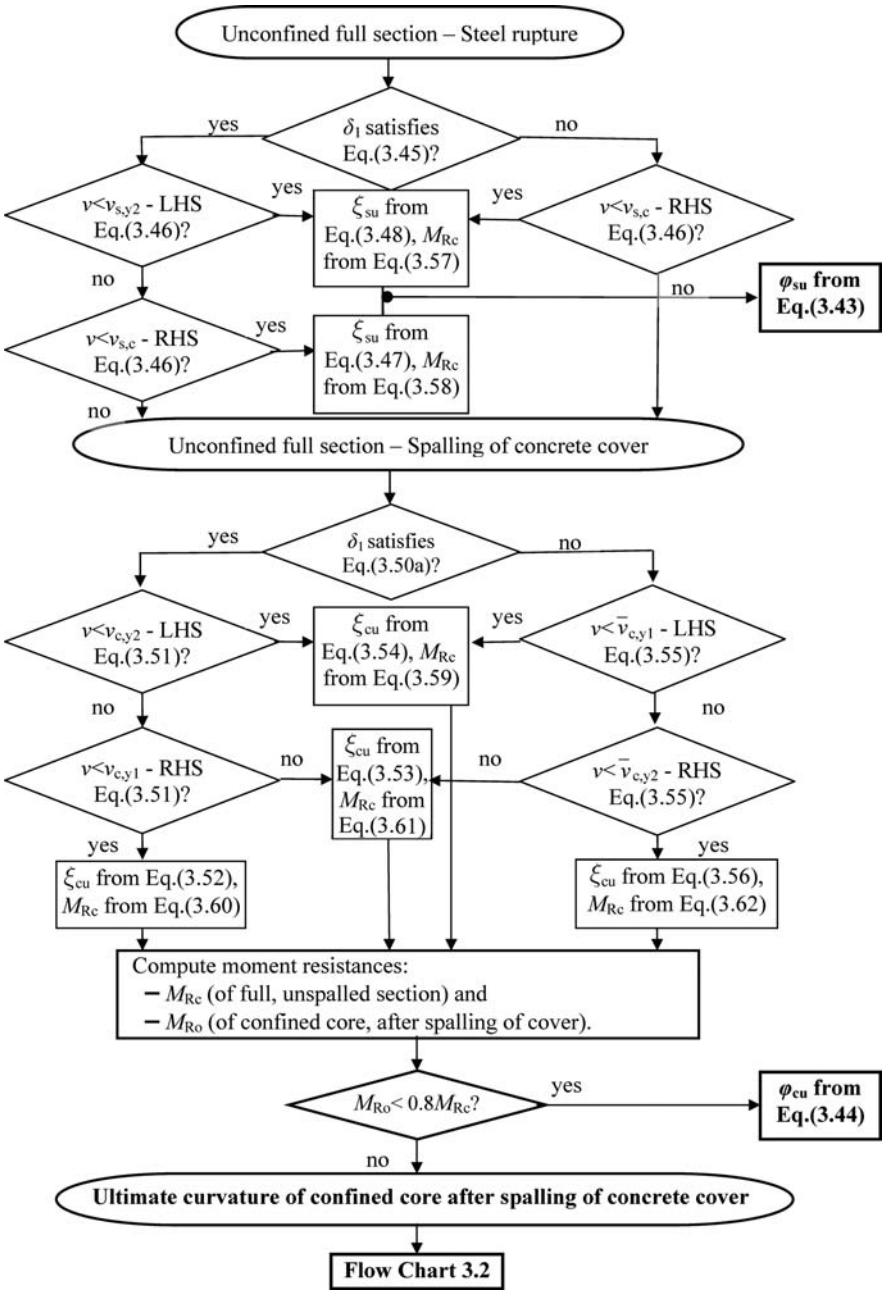

Flow Chart 3.1 Calculation of ultimate curvature for the full section before spalling of the concrete cover (LHS: left-hand-side, RHS: right-hand-side)

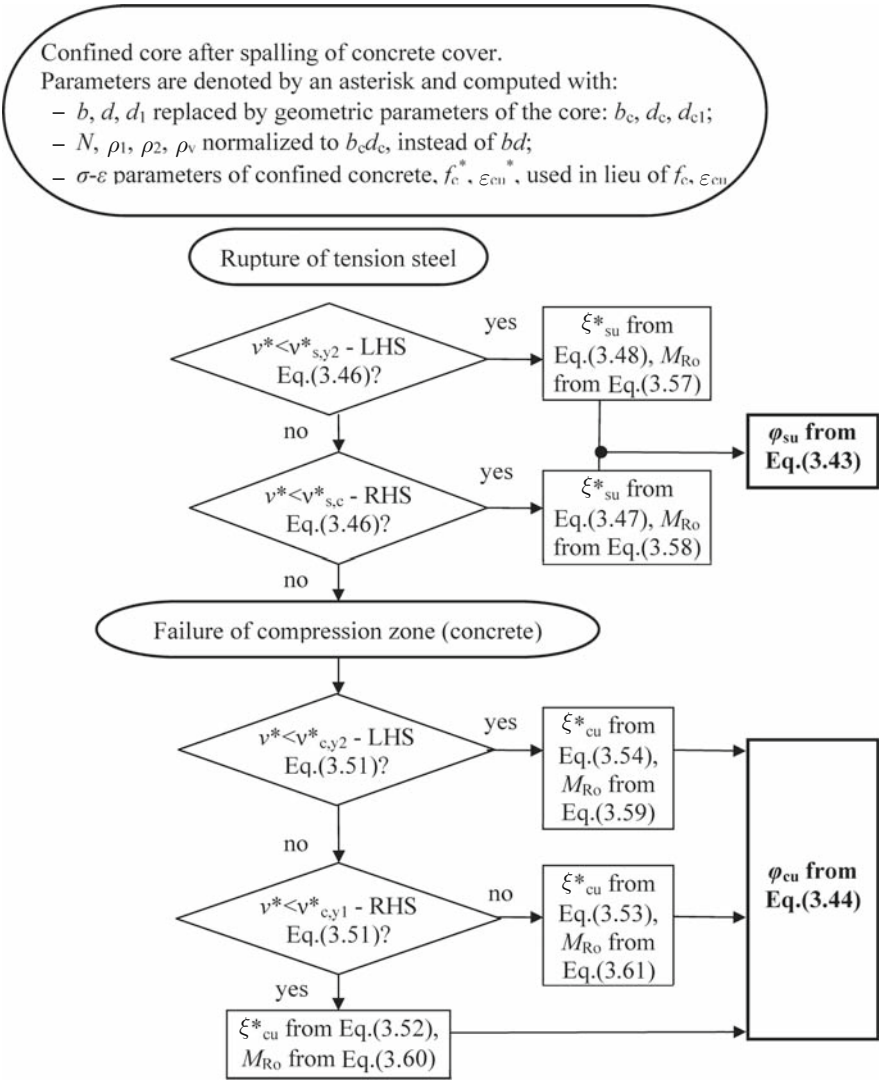

Flow Chart 3.2 Calculation of ultimate curvature for the confined core of the section after spalling of the concrete cover

Section 3.2.2.4 applies also to sections with more than one rectangular parts in two orthogonal directions, with the width b taken as that of the section at the extreme compression fibres, provided that the so-computed depth $x = \xi d$ of the compression zone does not exceed the other dimension (depth) of the rectangular part to which b belongs.

Failure of the Full Section Due to Rupture of Tension Reinforcement Before Spalling of the Concrete Cover

Failure of the full section by rupture of the tension reinforcement at an elongation of ε_{su} takes place before the extreme fibres of the concrete cover reach the crushing strain of unconfined concrete, ε_{cu}, if the neutral axis depth (normalised to d) ξ is: $\xi < \varepsilon_{cu}/(\varepsilon_{cu}+\varepsilon_{su})$. Such a failure may also occur before yielding of the compression reinforcement, if ξ satisfies the inequality: $\xi < (\varepsilon_{y2}+\varepsilon_{su}\delta_1)/(\varepsilon_{y2}+\varepsilon_{su})$. So, the full section may fail by steel rupture after yielding of the compression reinforcement, if the distance of the compression reinforcement from the extreme compression fibres, $\delta_1 = d_1/d$ (normalised to d), meets the condition:

$$\delta_1 \leq \frac{\varepsilon_{cu} - \varepsilon_{y2}}{\varepsilon_{cu} + \varepsilon_{su}} \tag{3.45}$$

If Eq. (3.45) is satisfied and the axial load ratio, ν, fulfills the inequality:

$$\begin{aligned} &\frac{\delta_1\varepsilon_{su} + \varepsilon_{y2} - (1-\delta_1)\frac{\varepsilon_{co}}{3}}{\varepsilon_{su1} + \varepsilon_{y2}} + \omega_2 - \omega_1\frac{f_{t1}}{f_{y1}} - \frac{\omega_v}{\varepsilon_{su1} + \varepsilon_{y2}} \\ &\left[\varepsilon_{su1} - \varepsilon_{y2} + \frac{1}{2}(\varepsilon_{su1} - \varepsilon_{shv})\left(1 + \frac{f_{tv}}{f_{yv}}\right)\right] \equiv \nu_{s,y2} \leq \nu \leq \\ &\nu_{s,c} \equiv \frac{\varepsilon_{cu} - \frac{\varepsilon_{co}}{3}}{\varepsilon_{cu} + \varepsilon_{su1}} + \omega_2 - \omega_1\frac{f_{t1}}{f_{y1}} - \frac{\omega_v}{(1-\delta_1)(\varepsilon_{su1} + \varepsilon_{cu})} \\ &\left[\delta_1(\varepsilon_{su1} + \varepsilon_{cu}) - (\varepsilon_{su1} - \varepsilon_{cu}) + \frac{1}{2}(\varepsilon_{su1} - \varepsilon_{shv})\left(1 + \frac{f_{tv}}{f_{yv}}\right)\right] \end{aligned} \tag{3.46}$$

failure of the full section by rupture of the tension reinforcement takes place with the compression reinforcement already beyond yielding. Then, plane-sections analysis gives the following value of ξ_{su} to be used in Eq. (3.43):

$$\xi_{su} \approx \frac{(1-\delta_1)\left(\nu + \omega_1\frac{f_{t1}}{f_{y1}} - \omega_2 + \frac{\varepsilon_{co}}{3\varepsilon_{su}}\right) + \left(1 + \delta_1 + \frac{1}{2}\left(1 - \frac{\varepsilon_{shv}}{\varepsilon_{su1}}\right)\left(1 + \frac{f_{tv}}{f_{yv}}\right)\right)\omega_v}{(1-\delta_1)\left(1 + \frac{\varepsilon_{co}}{3\varepsilon_{su1}}\right) + \left(2 + \frac{1}{2}\left(1 - \frac{\varepsilon_{shv}}{\varepsilon_{su1}}\right)\left(1 + \frac{f_{tv}}{f_{yv}}\right)\right)\omega_v} \tag{3.47}$$

If the condition of Eq. (3.45) is met, but the axial load ratio, ν, is less than the limit value $\nu_{s,y2}$ defined at the left-hand-side (LHS) of Eq. (3.46), then the full section fails by steel rupture not only before spalling of the concrete cover but also before the compression reinforcement yields. In that case, the value of ξ_{su} for use in Eq. (3.43) is the positive root of the equation:

$$\left[1+\frac{\varepsilon_{co}}{3\varepsilon_{su}}+\frac{\omega_v}{2(1-\delta_1)}\left(1+\frac{f_{tv}}{f_{yv}}\left(1-\frac{\varepsilon_{shv}}{\varepsilon_{su1}}\right)+\frac{\varepsilon_{shv}-3\varepsilon_{yv}}{\varepsilon_{su1}}-\frac{\varepsilon_{su1}}{\varepsilon_{yv}}\right)\right]\xi^2$$
$$-\left[1+\nu+\frac{2\varepsilon_{co}}{3\varepsilon_{su}}+\omega_1\frac{f_{t1}}{f_{y1}}+\omega_2\frac{\varepsilon_{su1}}{\varepsilon_{y2}}+\frac{\omega_v}{(1-\delta_1)}\left(1+\frac{f_{tv}}{f_{yv}}\left(1-\frac{\varepsilon_{shv}}{\varepsilon_{su1}}\right)\right.\right.$$
$$\left.\left.+\frac{\varepsilon_{shv}-3\varepsilon_{yv}}{\varepsilon_{su1}}-\delta_1\frac{\varepsilon_{su1}}{\varepsilon_{yv}}\right)\right]\xi+\left[\nu+\frac{\varepsilon_{co}}{3\varepsilon_{su}}+\omega_1\frac{f_{tv}}{f_{yv}}+\omega_2\delta_1\frac{\varepsilon_{su}}{\varepsilon_{y2}}\right.$$
$$\left.+\frac{\omega_v}{2(1-\delta_1)}\left(1+\frac{f_{tv}}{f_{yv}}\left(1-\frac{\varepsilon_{shv}}{\varepsilon_{su1}}\right)+\frac{\varepsilon_{shv}-3\varepsilon_{yv}}{\varepsilon_{su1}}-\delta_1^2\frac{\varepsilon_{su1}}{\varepsilon_{yv}}\right)\right]=0 \tag{3.48}$$

If Eq. (3.45) is met and the axial load ratio, ν, exceeds the limit value $\nu_{s,c}$ defined at the right-hand-side (RHS) of Eq. (3.46), spalling of the concrete cover when its outermost fibres reach the crushing strain of unconfined concrete, ε_{cu}, will precede rupture of the tension reinforcement, but will take place with the compression reinforcement already beyond yielding. Then the procedure in sub-section *Curvature at Spalling of the Concrete Cover* should be followed.

If the condition of Eq. (3.45) is not met, the limit value $\nu_{s,y2}$ defined at the left-hand-side of Eq. (3.46) is greater than the limit value $\nu_{s,c}$ given by the right-hand-side of that inequality. The implication is that the compression reinforcement will already have yielded, when the tension reinforcement ruptures before spalling of the concrete cover. Then, if the axial load ratio, ν, is less than the limit value $\nu_{s,c}$ at the left-hand-side of Eq. (3.46), the value of ξ_{su} to be used in Eq. (3.43) is still the positive root of Eq. (3.48). If, by contrast, the axial load ratio, ν, exceeds the limit value $\nu_{s,c}$, the concrete cover will spall before the tension reinforcement ruptures, but with the compression reinforcement already beyond yielding. The procedure in sub-section *Curvature at Spalling of the Concrete Cover* should be followed in that case.

Curvature at Spalling of the Concrete Cover

When the outermost fibres reach the crushing strain of unconfined concrete, ε_{cu}, and the concrete cover spalls, the moment resistance of the section drops – be it temporarily. To see what happens after cover spalling, the following moment resistances should be computed:

- the moment resistance of the full unspalled section, neglecting any effect of confinement on the concrete properties, M_{Rc},
- the moment resistance of the confined core of the section (conventionally defined to the centreline of the perimeter stirrup), after spalling of the concrete cover, M_{Ro}.

The moment capacity of the confined core, M_{Ro}, is determined on the basis of the strength f_c^* and ultimate strain ε_{cu}^* of confined concrete and of the dimensions b_c, d_c, d_{c1} of the confined core; d_c and d_{c1} are obtained by subtracting from d or d_1, respectively, the sum of the cover and of half the diameter of transverse reinforcement; b_c is obtained by subtracting twice this sum from b.

$$\text{If}: \quad M_{\text{Ro}} \leq 0.8 M_{\text{Rc}} \tag{3.49a}$$

spalling of the concrete cover can be taken as the ultimate condition of the section. Then, the ultimate curvature is given by Eq. (3.44), where the value of the neutral axis depth, ξ_{cu} (normalised to d), may be determined from Eqs. (3.52), (3.53), (3.54) or (3.56).

If $\xi < \varepsilon_{\text{cu}}/(\varepsilon_{\text{cu}}+\varepsilon_{\text{y1}})$, then the tension steel has already yielded by the time the extreme compression fibres reach the crushing strain of unconfined concrete ε_{cu}.

When ε_{cu} is reached at the outermost compression fibres, the compression steel will still be elastic if $\xi < \delta_1 \varepsilon_{\text{cu}}/(\varepsilon_{\text{cu}}-\varepsilon_{\text{y2}})$. By contrast, if $\xi > \delta_1 \varepsilon_{\text{cu}}/(\varepsilon_{\text{cu}}-\varepsilon_{\text{y2}})$ the compression steel will be beyond yielding at crushing of the extreme compression fibres. It follows from this and the previous paragraph that a range of ξ values exists for which both the tension and the compression reinforcement have yielded before ε_{cu} is reached at the extreme compression fibres, provided that $\varepsilon_{\text{cu}}/(\varepsilon_{\text{cu}}+\varepsilon_{\text{y1}}) > \delta_1 \varepsilon_{\text{cu}}/(\varepsilon_{\text{cu}}-\varepsilon_{\text{y2}})$, i.e. if:

$$\delta_1 \leq \frac{\varepsilon_{cu} - \varepsilon_{y2}}{\varepsilon_{cu} + \varepsilon_{y1}} \tag{3.50a}$$

If Eq. (3.50a) is not met, there can never be a range of ξ values for which both the tension and the compression reinforcement yield before the crushing strain of concrete is reached at the outermost compression fibres. Instead, a range of ξ values exists where both the tension and the compression reinforcement will still be elastic when the extreme compression fibres reach a strain of ε_{cu}. This latter situation does not lend itself to ductile behaviour of the cross section. In the sequel, two distinct cases are considered:

i. Equation (3.50a) is satisfied, or
ii. The following condition is fulfilled instead:

$$\delta_1 > \frac{\varepsilon_{cu} - \varepsilon_{y2}}{\varepsilon_{cu} + \varepsilon_{y1}} \tag{3.50b}$$

Case i is considered first, as more common in practice (and more desirable too).

Values of ξ between $\varepsilon_{\text{cu}}/(\varepsilon_{\text{cu}}+\varepsilon_{\text{y1}})$ and $\delta_1 \varepsilon_{\text{cu}}/(\varepsilon_{\text{cu}}-\varepsilon_{\text{y2}})$ correspond to the following range of values for the axial load ratio, ν:

$$\begin{aligned} &\omega_2 - \omega_1 + \frac{\omega_v}{1-\delta_1}\left(\delta_1 \frac{\varepsilon_{cu} + \varepsilon_{y2}}{\varepsilon_{cu} - \varepsilon_{y2}} - 1\right) + \delta_1 \frac{\varepsilon_{cu} - \frac{\varepsilon_{co}}{3}}{\varepsilon_{cu} - \varepsilon_{y2}} \equiv \nu_{c,y2} \leq \nu < \\ &\nu_{c,y1} \equiv \omega_2 - \omega_1 + \frac{\omega_v}{1-\delta_1}\left(\frac{\varepsilon_{cu} - \varepsilon_{y1}}{\varepsilon_{cu} + \varepsilon_{y1}} - \delta_1\right) + \frac{\varepsilon_{cu} - \frac{\varepsilon_{co}}{3}}{\varepsilon_{cu} + \varepsilon_{y1}} \end{aligned} \tag{3.51}$$

Within this range the value of ξ_{cu} to be used in Eq. (3.44) is:

$$\xi_{cu} = \frac{(1-\delta_1)(\nu+\omega_1-\omega_2)+(1+\delta_1)\omega_v}{(1-\delta_1)\left(1-\frac{\varepsilon_{co}}{3\varepsilon_{cu}}\right)+2\omega_v} \tag{3.52}$$

For values of ν greater than the limit value $\nu_{\mathrm{c,y1}}$ defined at the right-hand-side of Eq. (3.51) the extreme compression fibres reach the crushing strain of concrete, $\varepsilon_{\mathrm{cu}}$, after yielding of the compression reinforcement, but with the tension reinforcement elastic. Then the value of ξ_{cu} to be used in Eq. (3.44) is the positive root of the equation:

$$\left[1-\frac{\varepsilon_{co}}{3\varepsilon_{cu}}-\frac{\omega_v}{2(1-\delta_1)}\frac{\left(\varepsilon_{cu}-\varepsilon_{yv}\right)^2}{\varepsilon_{cu}\varepsilon_{yv}}\right]\xi^2+\left[\omega_2+\omega_1\frac{\varepsilon_{cu}}{\varepsilon_{y1}}-\nu+\frac{\omega_v}{1-\delta_1}\left(\frac{\varepsilon_{cu}}{\varepsilon_{yv}}-\delta_1\right)\right]\xi$$
$$-\left[\frac{\omega_1}{\varepsilon_{y1}}+\frac{\omega_v}{2\,(1-\delta_1)\,\varepsilon_{yv}}\right]\varepsilon_{cu}=0 \tag{3.53}$$

Finally, if ν is less than the limit value $\nu_{\mathrm{c,y2}}$ defined at the left-hand-side of Eq. (3.51), the outermost compression fibres reach the strain $\varepsilon_{\mathrm{cu}}$ after the tension reinforcement yields, but with the compression reinforcement still elastic. In that case the value of ξ_{cu} to be used in Eq. (3.44) is the positive root of the equation:

$$\left[1-\frac{\varepsilon_{co}}{3\varepsilon_{cu}}+\frac{\omega_v}{2(1-\delta_1)}\frac{\left(\varepsilon_{cu}+\varepsilon_{yv}\right)^2}{\varepsilon_{cu}\varepsilon_{yv}}\right]\xi^2-\left[\nu+\omega_1-\omega_2\frac{\varepsilon_{cu}}{\varepsilon_{y2}}+\frac{\omega_v}{1-\delta_1}\left(1+\frac{\varepsilon_{cu}\delta_1}{\varepsilon_{yv}}\right)\right]\xi$$
$$-\left[\frac{\omega_2}{\varepsilon_{y2}}-\frac{\omega_v\delta_1}{2\,(1-\delta_1)\,\varepsilon_{yv}}\right]\varepsilon_{cu}\delta_1=0 \tag{3.54}$$

Case ii, where Eq. (3.50b) is fulfilled, is not so desirable. Fortunately it is rare in practice, as the right-hand-side of Eqs. (3.48) is in the order of 0.15–0.2, implying that the compression steel is at a distance to the extreme compression fibres of over 15–20% of the section depth, which is uncommon. At any rate, if Eq. (3.50b) is met, for values of the axial load ratio between $\overline{\nu}_{\mathrm{c,y1}}$ and $\overline{\nu}_{\mathrm{c,y2}}$, in Eq. (3.55), both the tension and the compression reinforcement are still elastic by the time the extreme compression fibres reach the crushing strain of concrete:

$$\frac{\omega_2}{\varepsilon_{y2}}\left((1-\delta_1)\varepsilon_{cu}-\delta_1\varepsilon_{y1}\right)-\omega_1+\frac{\omega_v}{2\varepsilon_{yv}}\left(\varepsilon_{cu}-\frac{1+\delta_1}{1-\delta_1}\right)+\frac{\varepsilon_{cu}-\frac{\varepsilon_{co}}{3}}{\varepsilon_{cu}+\varepsilon_{y1}}\equiv\overline{\nu}_{c,y1}\le\nu<$$
$$\overline{\nu}_{c,y2}\equiv\omega_2-\frac{\omega_1}{\varepsilon_{y1}}\frac{(1-\delta_1)\varepsilon_{cu}-\varepsilon_{y2}}{\delta_1}+\frac{\omega_v}{\delta_1\varepsilon_{yv}}\left(\frac{1+\delta_1}{1-\delta_1}\varepsilon_{y2}-\varepsilon_{cu}\right)+\delta_1\frac{\varepsilon_{cu}-\frac{\varepsilon_{co}}{3}}{\varepsilon_{cu}-\varepsilon_{y2}} \tag{3.55}$$

Within this range of ν the value of ξ_{cu} to be used in Eq. (3.44) is the positive root of:

$$\left[1-\frac{\varepsilon_{co}}{3\varepsilon_{cu}}\right]\xi^2-\left[\nu-\left(\frac{\omega_1}{\varepsilon_{y1}}+\frac{\omega_2}{\varepsilon_{y2}}+\frac{\omega_v}{(1-\delta_1)\varepsilon_{yv}}\right)\varepsilon_{cu}\right]\xi \\ -\left(\frac{\omega_1}{\varepsilon_{y1}}+\frac{\delta_1\omega_2}{\varepsilon_{y2}}+\frac{\omega_v(1+\delta_1)}{2(1-\delta_1)\varepsilon_{yv}}\right)\varepsilon_{cu}=0 \tag{3.56}$$

For values of ν greater than the limit value $\overline{\nu}_{c,y2}$ defined at the right-hand-side of Eq. (3.55) the extreme compression fibres reach the crushing strain of concrete after yielding of the compression reinforcement, but with the tension reinforcement still elastic. The value of ξ_{cu} to be used in Eq. (3.44) is the positive root of Eq. (3.53) above. If, by contrast, ν is less than the limit value $\overline{\nu}_{c,y1}$ defined at the left-hand-side of Eq. (3.55), the extreme compression fibres reach a strain of ε_{cu} after yielding of the tension reinforcement, but with the compression reinforcement still elastic. In that case the value of ξ_{cu} to be used in Eq. (3.44) is the positive root of Eq. (3.54).

The expressions above for ξ (i.e., Eqs. (3.47), (3.48), (3.52), (3.53), (3.54) and (3.56)) are derived from the equivalence of the normal stress resultant on the section to the axial force N. The plane sections hypothesis and the nonlinear σ-ε laws outlined in points (i) and (ii) at the end of sub-section *Definitions and Assumptions* are also used. Equation (3.52) is derived below for illustration, with the tension reinforcement not considered to go into strain-hardening.

Because the tension and the compression reinforcement are both past yielding, their joint contribution to the axial compressive force is equal to $(A_{s2}–A_{s1})f_y=(\omega_2–\omega_1)bdf_c$. For a neutral axis depth equal to ξd the web reinforcement, taken as uniformly distributed over a length $(1–\delta_1)d$ between the compression and tension steel, contributes to the axial compression with a force of $[(\omega_v bdf_c)/(1–\delta_1)][(\xi–\delta_1)–(1–\xi)]=(\omega_v bdf_c)(2\xi–1–\delta_1)/(1–\delta_1)$. Equilibrium gives: $\nu=\frac{N}{bdf_c}=\omega_2-\omega_1+\frac{\omega_v(2\xi-1-\delta_1)}{1-\delta_1}+\left(1-\frac{\varepsilon_{co}}{3\varepsilon_{cu}}\right)\xi$, from which Eq. (3.52) is derived.

Ultimate Curvature of the Confined Core, After Spalling of the Cover

If

$$M_{Ro}>0.8M_{Rc} \tag{3.49b}$$

then the confined core of the section recovers from spalling of the concrete shell around it. It ultimately fails either by rupture of the tension reinforcement or by disintegration of the extreme compression fibres of the core itself.

The analysis in sub-sections *Definitions and Assumptions*, *Failure of the Full Section Due to Rupture of Tension Reinforcement Before Spalling of the Concrete Cover* and *Curvature at Spalling of the Concrete Cover* applies for the calculation of the ultimate curvature of the confined core after spalling of the cover, provided that:

- dimensions b, d and d_1 are replaced by b_c (equal to b minus the diameter of transverse reinforcement and twice the cover), d_c (equal to d minus the cover and half the diameter of transverse reinforcement) and d_{c1} (equal to half the diameter of transverse reinforcement plus half that of longitudinal bars), respectively;
- N, ρ_1, ρ_2, ρ_v are normalised to $b_c d_c$, instead of bd, and
- the σ-ε parameters of confined concrete, f_c^*, ε_{cu}^*, are used, in lieu of f_c, ε_{cu}.

Note that d_{c1} is small compared to d_1 above. So, the conditions of Eqs. (3.45) and (3.50a) are always met in the confined core. Then, only Eqs. (3.46), (3.47), (3.48), (3.51), (3.52), (3.53) and (3.54) in sub-sections *Failure of the Full Section Due to Rupture of Tension Reinforcement Before Spalling of the Concrete Cover* and *Curvature at Spalling of the Concrete Cover* are meaningful for the ultimate curvature of the confined core.

3.2.2.5 Moment Resistance of Concrete Sections with Rectangular Compression Zone

The moment resistance of the confined core and of the unspalled section, M_{Ro}, M_{Rc}, respectively, for use in Eqs. (3.49), may be estimated as uniaxial moment resistances of concrete sections with rectangular compression zone, through dimensioning tools (tables, diagrams, analytical expressions or computer codes) available for the Ultimate Limit State of such sections under uniaxial bending with axial force. When such design tools are utilised, the actual (or expected) value of material strengths should be used, instead of the design values:

- for reinforcing steel, use f_{ym} or f_y in lieu of $f_{yd}=f_{yk}/\gamma_s$;
- for concrete, instead of $f_{cd}=f_{ck}/\gamma_c$, the value f_{cm} or f_c should be used before spalling and the value f_{cm}^* or f_c^* for the confined concrete core after spalling (for M_{Ro}); if the design tools used include a reduction factor on f_{cd} due to long term or other effects, e.g. a reduction factor of 0.85, this factor should be removed by using the value $f_c/0.85$ or $f_c^*/0.85$ for f_{cd}.
- for the moment corresponding to rupture of the tension reinforcement at the full section before spalling (and to the ultimate curvature φ_{su}), or at the confined core afterwards (and to φ_{su}^*), the cross-sectional area of tension reinforcement should be taken equal to $A_{s1}f_t/f_y$ (i.e., ω_1 should be multiplied by f_t/f_y).

As an alternative, the flexural resistance may be calculated analytically, as described below for M_{Rc} (see also Flow Charts 3.1 and 3.2). The value of M_{Ro} can be calculated similarly, using the geometric and strength parameters of the confined core.

For failure of the section due to rupture of the tension steel (i.e., when the axial load ratio, ν, is less than the minimum of the limit values $\nu_{s,y2}$, $\nu_{s,c}$ defined in Eq. (3.46) of sub-section *Failure of the Full Section Due to Rupture of Tension Reinforcement Before Spalling of the Concrete Cover*), we consider first the usual

case when Eq. (3.45) is met. Then, for ν less than the limit value $\nu_{s,y2}$ defined at the left-hand-side of Eq. (3.46), the compression reinforcement is elastic while the tension reinforcement is at ultimate strength. With ξ given by Eq. (3.48), the moment resistance of the section is:

$$\begin{aligned}\frac{M_{Rc}}{bd^2 f_c} &= (1-\xi)\left[\frac{\xi}{2} - \frac{\varepsilon_{co}}{3\varepsilon_{su1}}\left(\frac{1}{2} - \xi + \frac{\varepsilon_{co}}{4\varepsilon_{su1}}(1-\xi)\right)\right] \\ &+ \frac{(1-\delta_1)}{2}\left(\omega_1 \frac{f_{t1}}{f_{y1}} + \omega_2 \frac{\xi - \delta_1}{1-\xi}\frac{\varepsilon_{su1}}{\varepsilon_{y2}}\right) \\ &+ \frac{\omega_v}{6(1-\delta_1)}\left\{\left[1 - \delta_1 + \xi\left(1 - \frac{\varepsilon_{yv}}{\varepsilon_{su1}}\right)\right]\left[1 + \frac{\varepsilon_{su1}}{\varepsilon_{yv}}\left(\frac{\xi - \delta_1}{1-\xi}\right)\right]\right. \\ &\left[\frac{1-\delta_1}{2} - (1-\xi)\frac{\varepsilon_{yv}}{\varepsilon_{su1}}\right] + \left[\frac{2(1-\delta_1)}{3} - \left(1 - \frac{\varepsilon_{shv}}{\varepsilon_{su1}}\right)(1-\xi)\right] \\ &\left.\left(1 - \frac{\varepsilon_{shv}}{\varepsilon_{su1}}\right)\left(\frac{f_{tv}}{f_{yv}} - 1\right)(1-\xi)\right\}\end{aligned} \tag{3.57}$$

If, by contrast, ν satisfies Eq. (3.46), the compression reinforcement is beyond yielding but not yet in strain-hardening. Then, with ξ from Eq. (3.47), the section moment resistance is:

$$\begin{aligned}\frac{M_{Rc}}{bd^2 f_c} &= (1-\xi)\left[\frac{\xi}{2} - \frac{\varepsilon_{co}}{3\varepsilon_{su1}}\left(\frac{1}{2} - \xi + \frac{\varepsilon_{co}}{4\varepsilon_{su1}}(1-\xi)\right)\right] \\ &+ \frac{(1-\delta_1)}{2}\left(\omega_1 \frac{f_{t1}}{f_{y1}} + \omega_2\right) + \frac{\omega_v}{1-\delta_1}\left\{(\xi - \delta_1)(1-\xi) - \frac{1}{3}\left(\frac{(1-\xi)\,\varepsilon_{yv}}{\varepsilon_{su1}}\right)^2\right. \\ &\left.+ \left[\frac{(1-\delta_1)}{4} - \left(1 - \frac{\varepsilon_{shv}}{\varepsilon_{su1}}\right)\frac{1-\xi}{6}\right]\left(1 - \frac{\varepsilon_{shv}}{\varepsilon_{su1}}\right)\left(\frac{f_{t1}}{f_{y1}} - 1\right)(1-\xi)\right\}\end{aligned} \tag{3.58}$$

If Eq. (3.45) is not met, but the axial load ratio, ν, is still less than the limit value $\nu_{s,c}$ defined at the right-hand-side of Eq. (3.46), the compression reinforcement is still elastic while the tension reinforcement is at ultimate strength. Then the moment resistance of the section is again given by Eq. (3.57), with ξ from Eq. (3.48).

For section failure due to concrete crushing (i.e., for axial load ratio, ν, greater than the minimum of the limit values $\nu_{c,y2}$, $\overline{\nu}_{c,y1}$ defined at the left-hand-side of Eqs. (3.51) and (3.55), respectively, in sub-section *Curvature at Spalling of the Concrete Cover*), we consider first the case of Eq. (3.50a) being met. Then, if ν is less than the limit value $\nu_{c,y2}$ at the left-hand-side of Eq. (3.51), the compression reinforcement is elastic while the tension reinforcement is beyond yielding but not yet in strain-hardening. With ξ given by Eq. (3.54), the moment resistance of the section is:

$$\frac{M_{Rc}}{bd^2 f_c} = \xi\left[\frac{1-\xi}{2} - \frac{\varepsilon_{co}}{3\varepsilon_{cu}}\left(\frac{1}{2} - \xi + \frac{\varepsilon_{co}}{4\varepsilon_{cu}}\xi\right)\right] + \frac{(1-\delta_1)}{2}\left(\omega_1 + \omega_2\frac{\xi-\delta_1}{\xi}\frac{\varepsilon_{cu}}{\varepsilon_{y2}}\right) + \frac{\omega_v}{4(1-\delta_1)}\left[\xi\left(1+\frac{\varepsilon_{yv}}{\varepsilon_{cu}}\right) - \delta_1\right]\left[1+\frac{\varepsilon_{cu}}{\varepsilon_{yv}}\left(\frac{\xi-\delta_1}{\xi}\right)\right]\left[1-\frac{\delta_1}{3} - \frac{2}{3}\xi\left(1+\frac{\varepsilon_{yv}}{\varepsilon_{cu}}\right)\right] \tag{3.59}$$

If ν satisfies Eq. (3.51), the tension and the compression reinforcement are both beyond yielding but not in strain-hardening. The moment resistance of the section is then:

$$\frac{M_{Rc}}{bd^2 f_c} = \xi\left[\frac{1-\xi}{2} - \frac{\varepsilon_{co}}{3\varepsilon_{cu}}\left(\frac{1}{2} - \xi + \frac{\varepsilon_{co}}{4\varepsilon_{cu}}\xi\right)\right] + \frac{(1-\delta_1)(\omega_1+\omega_2)}{2} + \frac{\omega_v}{1-\delta_1}\left[(\xi-\delta_1)(1-\xi) - \frac{1}{3}\left(\frac{\xi\varepsilon_{yv}}{\varepsilon_{cu}}\right)^2\right] \tag{3.60}$$

with ξ given by Eq. (3.52). If, by contrast, ν exceeds the limit value $\nu_{c,y1}$ at the right-hand-side of Eq. (3.51), the tension reinforcement is elastic while the compression reinforcement is beyond yielding but not in strain-hardening. With ξ from Eq. (3.53) the moment resistance is:

$$\frac{M_{Rc}}{bd^2 f_c} = \xi\left[\frac{1-\xi}{2} - \frac{\varepsilon_{co}}{3\varepsilon_{cu}}\left(\frac{1}{2} - \xi + \frac{\varepsilon_{co}}{4\varepsilon_{cu}}\xi\right)\right] + \frac{(1-\delta_1)}{2}\left(\omega_1\frac{1-\xi}{\xi}\frac{\varepsilon_{cu}}{\varepsilon_{y1}} + \omega_2\right) + \frac{\omega_v}{4(1-\delta_1)}\left[1-\xi\left(1-\frac{\varepsilon_{yv}}{\varepsilon_{cu}}\right)\right]\left[1+\frac{\varepsilon_{cu}}{\varepsilon_{yv}}\left(\frac{1-\xi}{\xi}\right)\right]\left[\frac{1}{3} - \delta_1 + \frac{2}{3}\xi\left(1-\frac{\varepsilon_{yv}}{\varepsilon_{cu}}\right)\right] \tag{3.61}$$

We consider next the rare case when Eq. (3.50b) is met. If ν is less than the limit value $\overline{\nu}_{c,y1}$ at the left-hand-side of Eq. (3.55), the compression reinforcement is elastic and the tension reinforcement is beyond yielding but not strain-hardening yet. The moment resistance of the section is given by Eq. (3.59), with ξ from Eq. (3.54). If ν satisfies Eq. (3.55), the entire reinforcement of the section is elastic and the moment resistance is:

$$\frac{M_{Rc}}{bd^2 f_c} = \xi\left[\frac{1-\xi}{2} - \frac{\varepsilon_{co}}{3\varepsilon_{cu}}\left(\frac{1}{2} - \xi + \frac{\varepsilon_{co}}{4\varepsilon_{cu}}\xi\right)\right] + \frac{(1-\delta_1)\varepsilon_{cu}}{2\xi}\left((1-\xi)\frac{\omega_1}{\varepsilon_{y1}} + (\xi-\delta_1)\frac{\omega_2}{\varepsilon_{y2}}\right) + \frac{\omega_v(1-\delta_1)^2}{12\xi}\frac{\varepsilon_{cu}}{\varepsilon_{yv}} \tag{3.62}$$

with ξ from Eq. (3.56). If ν exceeds the limit value $\overline{\nu}_{c,y2}$ defined at the right-hand-side of Eq. (3.55), the tension reinforcement is elastic and the compression

reinforcement is beyond yielding but not in strain-hardening. The moment resistance of the section is given by Eq. (3.61), with ξ from Eq. (3.53).

Equations (3.57), (3.58), (3.59), (3.60), (3.61) and (3.62) are derived from moment equilibrium of the normal stresses acting on the section with respect to its centroid, taken to be at mid-distance between the tension and the compression reinforcement. The plane section hypothesis and the nonlinear σ-ε laws outlined in points (i) and (ii) at the end of sub-section *Definitions and Assumptions* are used also. As an illustration, the derivation of Eq. (3.60) is given below, with the tension reinforcement not considered to be in strain-hardening.

The tension and compression longitudinal reinforcement, with mechanical ratios ω_1 and ω_2, each at a distance $h/2–d_1=(d–d_1)/2$ to the centroid of the section, contribute to its moment resistance a moment of $(\omega_1+\omega_2)bd^2f_c(1–\delta_1)/2$. When the strain of the outermost compression fibres is equal to ε_{cu}, the "web" reinforcement, distributed between ω_1 and ω_2 and having mechanical ratio ω_v, contributes to the flexural resistance a moment about the centroid of the section equal to $\omega_v bd^2f_c/(1–\delta_1)[(\xi–\delta_1)(1–\xi)–(\xi f_y/E_s\varepsilon_{cu})^2/3]$. With respect to the same point and for a parabolic-rectangular σ-ε diagram, the compression zone contributes a moment equal to $bd^2f_c\xi[(1–\xi)/2–(1/2–\xi+\xi\varepsilon_{co}/4\varepsilon_{cu})(\varepsilon_{co}/3\varepsilon_{cu})]$. Adding all three contributions, Eq. (3.60) is obtained.

3.2.2.6 Flexural Behaviour Until Failure Under Cyclic Loading

Let's consider the following load history, which is quite commonly part of the load history applied in experimental studies of the cyclic behaviour of concrete members:

- reversal of loading into unloading at a value of curvature φ_r past flexural yielding;
- continuation of unloading into reloading in the opposite direction, up to a curvature of about $-\varphi_r$[8];
- new unloading from $-\varphi_r$ towards the original direction of loading, until and past the peak curvature reached in the previous cycle, φ_r;
- new unloading from a peak curvature greater than φ_r.
- The experimental behaviour is shown in:
- Fig. 3.25 for a rectangular section with symmetric reinforcement and zero axial load;
- Fig. 3.26 for a rectangular beam with less reinforcement at the bottom (corresponding in Fig. 3.26 to negative moment) than at the top and zero axial load.

Measured curvatures in these two figures do not include the effect of bar pull-out from the anchorage zone beyond the end section. Figure 3.26 is typical of a frame beam, which at the face of the column usually has greater top reinforcement than

[8]Symmetric deflection cycles, i.e. from a deflection δ_r to $-\delta_r$; as commonly applied on test specimens, produce almost but not quite symmetric curvature cycles at the member end where yielding takes place.

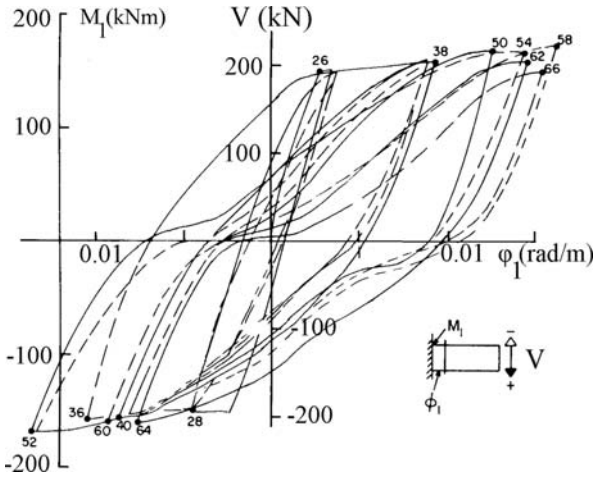

Fig. 3.25 Experimental M-(mean) φ curves of symmetrically reinforced member in cyclic bending (Ma et al. 1976)

at the bottom. In an actual beam the cross-section is not rectangular, but T or L, with different effective flange width in tension or compression. As pointed out in Sections 1.3.4 and 2.2.1, in beams integral with the slab the effective flange width increases with increasing end moment and deformation, especially after the yielding of the longitudinal bars placed within the width of the web mobilises the strength and stiffness of the flange and spreads the nonlinearity into the slab further away from the web.

In both cases the cyclic behaviour exhibits the following features:

1. In the monotonic branch before any unloading (i.e., during primary or virgin loading) flexural cracking is followed by a gradual softening of the response. If the reinforcement is concentrated near the extreme tension and compression fibres of the section, yielding of the tension bars shows up as a rather abrupt softening of the overall moment-curvature response. After yielding the resisting moment keeps increasing, initially because the reduction of the neutral axis depth due to the large post-yield elongation of the tension reinforcement increases the internal lever arm, and then because strain hardening of the tension bars starts. When the concrete cover spalls at a compressive strain equal to the ε_{cu}-value of unconfined concrete, the resisting moment drops momentarily. Depending on the magnitude of its strains, the compression steel will most likely yield at that point and may not contribute further to the increase of the resisting moment. These effects are usually more than offset by the increase of the strength and stiffness of the core concrete effected by the mobilisation of confinement.
2. During unloading from the post-yield branch of the primary loading curve, the unloading stiffness is initially high, about equal to the ”elastic” (post-cracking) stiffness. The unloading branch gradually softens, especially as the applied

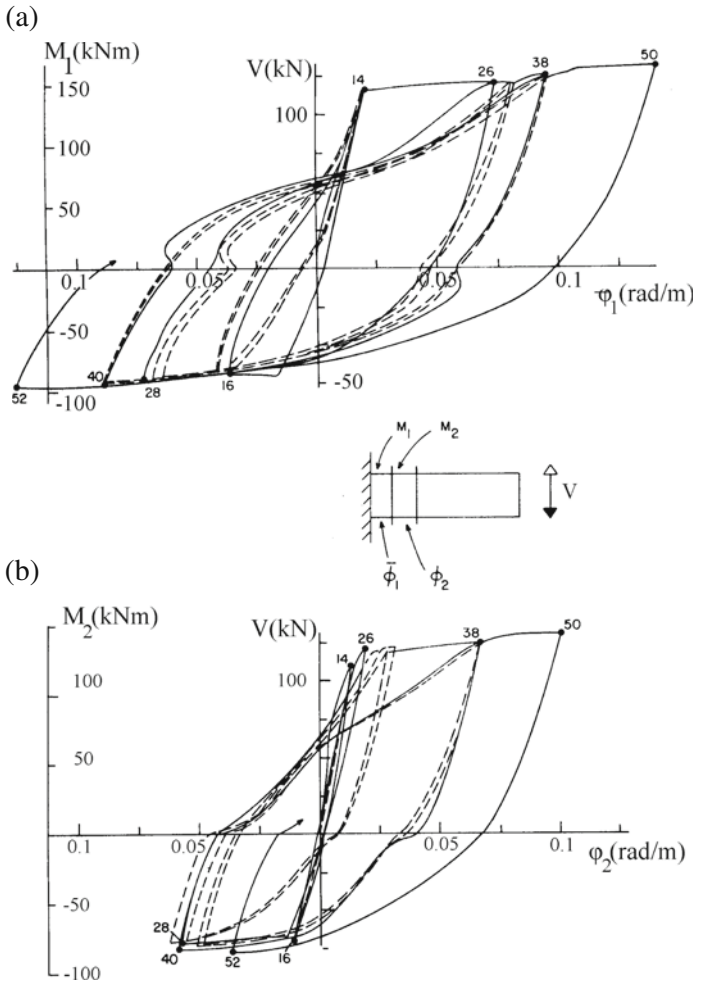

Fig. 3.26 Experimental M–(mean) φ curves of asymmetrically reinforced member in cyclic bending: (**a**) next to the member end; (**b**) a short distance from the member end (Ma et al. 1976)

moment approaches zero. Overall, and throughout the unloading branch until the horizontal axis, $M = 0$, the unloading slope is less than the "elastic" secant stiffness to the yield-point, M_y/φ_y and decreases with increasing value of the peak curvature where unloading started, φ_r. This reduction is part of the so-called "stiffness degradation", which is a characteristic feature of the cyclic flexural behaviour of concrete members. When the applied moment becomes zero, there is a significant residual deformation, mainly due to the permanent inelastic strains locked in the tension bars and to the residual slip between the bars and the concrete. Owing to this residual slip, at zero applied moment the cracks remain open.

3. Right after the applied moment changes sign, the slope ("stiffness") of the branch of loading in the opposite direction ("reloading") considerably decreases. The reduction in stiffness is due to the fact that, when the applied moment changes sign, the crack is open throughout the depth of the section, including the (new) compression side. The reason is that the bars of that side – now in compression – have previously yielded in tension and have a certain plastic elongation locked-in. So, the applied moment is resisted only by the force couple of the tension and compression reinforcement. So long as the steel couple alone resists the moment, the M–φ diagram resembles that of the σ-ε diagram of steel in cyclic loading, including the Bauschinger effect for yielding in the opposite direction (cf. Fig. 3.1 in Section 3.1.1.1). Moreover, the slope (tangent stiffness) of the M–φ diagram is considerably less than the slope of unloading to the horizontal axis. For the crack to close at the (newly) compressed side and for the concrete to be activated again there, the compression reinforcement needs to develop compressive stresses sufficiently large to suppress its (plastic) tensile strains (or to buckle). Once this takes place, the crack closes and the slope (tangent stiffness) of the reloading branch increases again, tending to a roughly constant value, which is maintained until the previous maximum curvature, φ_r, in the current direction of (re)loading is reached. As a result, the unloading-reloading branch has an inverted-S shape. If the section is symmetrically reinforced with all the reinforcement concentrated at the two ends of the section,[9] the shape of unloading-reloading branches resembles an inverted-S for both directions of loading (cf. Fig. 3.25) The inverted-S shape of one or both unloading-reloading branches produces hysteresis loops that are "pinched" at the middle. In sections with asymmetric reinforcement, i.e. with $\rho_1+\rho_v > \rho_2$ as in Fig. 3.26, the unloading-reloading branch exhibits a clear pinching only when reloading takes place from a state with the less reinforced side (that with ratio ρ_2) in tension towards one with this reinforcement in compression. Being less than that of the other side, this reinforcement yields soon in compression, allowing the crack to close at the compression side. For reloading in the reverse direction, with the more heavily reinforced side (that with ratio ρ_1) going from tension to compression, the reinforcement of the opposite side (with ratio ρ_2) is not sufficient to drive the reinforcement with the large ratio (ρ_1) to yielding in compression. This delays closure of the through-depth crack. As shown in Fig. 3.7, at the more heavily reinforced side of the section compressive strains are relatively low and the concrete is not heavily stressed, because the reinforcement there can resist the full compression force even without yielding. So, in asymmetrically reinforced sections, unloading-reloading branches have the shape of an inverted-S only when reloading takes place in the direction towards the larger

[9] If a large fraction of the reinforcement is distributed between the top and the bottom of the section, e.g., along the two sides that are parallel to the plane of bending, as in large columns or walls, most, if not all, of this reinforcement is normally in tension, because the compression zone is limited to (much) less than half of the effective section depth. So, the tension reinforcement is always more than the compression reinforcement and can easily drive it to yielding and beyond.

moment resistance. Reloading in the reverse direction always takes place at a lower stiffness, namely that developed by the steel couple alone. This stiffness is the same as the initial reloading stiffness in the reverse direction, before the concrete is engaged in compression and the tangent stiffness increases. An external compressive force on the section helps close the crack on the compression side and reduces the length of the branch exhibiting low stiffness. Large axial compression does not let the crack remain open throughout the depth. Then the stiffness along the unloading-reloading branch decreases steadily and smoothly.

If the continuation of unloading into (re)loading in the reverse direction happens to be a first-time post-elastic loading in that direction, it may be considered as virgin loading. The softening that follows the stiffening at the end of the pinching (due to yielding of the bars at the side currently in tension) is more gradual than during first loading in the original direction, because the bars now yielding in tension have in all likelihood yielded in compression previously and exhibit the Bauschinger effect. The same effect causes the bars on the compression side, that have previously yielded in tension, to start yielding early and gradually, contributing to the gradual softening of reloading. After the yielding of both the tension and the compression bars is complete, the moment-curvature response in further loading is like primary post-elastic loading in the current loading direction, as affected by possible spalling of the concrete cover on the newly compressed side and by strain-hardening of the steel bars on the side newly in tension.

4. In addition to the degradation of resistance with increasing lateral displacements, which is due to the increased deformations imposed on concrete and steel, cycling of the deformations per se even at constant amplitude normally causes degradation of strength with respect to the envelope provided by the primary loading curve. The sources of this ”strength degradation” are many. First, alternating opening and closing of cracks causes degradation of strength and stiffness of the concrete in compression, because small shear sliding, flaking off or debris accumulation along a crack prevents its faces from returning to even and full contact. Second, cyclic deterioration of the bond-slip behaviour along the bars (cf. Fig. 3.22) gradually increases the crack width and reduces the tension-stiffening effect (i.e. the activation of the concrete in tension around the bar). Third, apart from the gradual deterioration with cycling of the shear behaviour per se (i.e., of aggregate interlock, dowel action, etc.), the transfer of the shear force by dowel action along open full-depth cracks when the steel couple alone resists the applied moment, causes concrete splitting along the longitudinal bars (the “dowels”) and subsequent further bond deterioration and stiffness degradation, or even spalling of the concrete cover and deterioration of both flexural strength and stiffness. Well designed and detailed members exhibit little degradation of strength with cycling. Moreover, for constant amplitude cycling of either force or deflection, the deterioration is noticeable between the 1st and the 2nd cycle but diminishes almost to zero thereafter, leading to very stable hysteretic behaviour. Lack of such stabilisation is a sign of imminent failure under

cyclic loading. Increasing the transverse steel reduces strength degradation with cycling, as it enhances confinement. However, increasing the longitudinal steel seems to increase also the degradation of strength and stiffness with cycling, because the concrete, which is the main source of the degradation, becomes more critical.

Besides the absence of strong pinching in reloading towards the direction of the lower moment resistance, the prime difference of the cyclic flexural behaviour between the cases of symmetric (Fig. 3.25) and asymmetric cross-section and reinforcement (Fig. 3.26) is in the stiffness and strength exhibited by the envelope (and primary loading) curve in the two directions of bending, positive or negative.

3.2.2.7 Failure of Members Under Cyclic Flexure

Flexural damage is physically concentrated in the end region of the member and entails one or more of the following (see Fig. 3.27 for examples):

- spalling of the concrete cover, often extending to disintegration of the concrete core inside the reinforcement cage;
- buckling of reinforcing bars (especially of the corner ones);
- rupture of one or more reinforcing bars.

Members detailed for earthquake resistance normally do not fail abruptly under cyclic loading. Their failure in flexure is typically gradual, governed by the progressive deterioration of the compression zone. Damage starts with spalling of the cover concrete and normally continues with buckling of the bars that lose their lateral support and finally with disintegration of the core concrete. Lightly reinforced members may fail suddenly by fracture of one or more tension bars. Such a fracture often takes place at a minute crack in the bar caused by buckling during the previous half-cycle. The reduction in moment resistance caused by a bar fracture shows up in the moment-curvature response as an abrupt drop in the moment, often considered as failure. When there are no such clear signals of failure, the member may be considered to have failed if, from a certain point on, the pattern of the response changes. For example, when, during constant amplitude cycling the peak force drops disproportionately from one cycle to the next ("strength decay"), compared to previous cycles at the same or smaller deformation amplitude. Another example is an entire hysteresis loop that tilts or shrinks relative to the previous ones. The column in Fig. 1.2(b) exhibits both these features during the last cycles of the response. Such changes in the macroscopic behaviour signify a marked loss of stiffness, strength or energy dissipation capacity and may be taken to signal failure. Examples in this chapter include Fig. 3.5(a) and (b) (for reinforcing bars), the shear failures of specimens No. 1, 3 and 4 in Fig. 3.36(a), the ductile shear failure in Fig. 3.38(c) and (f) and the subassembly failure in Fig. 3.46(c).

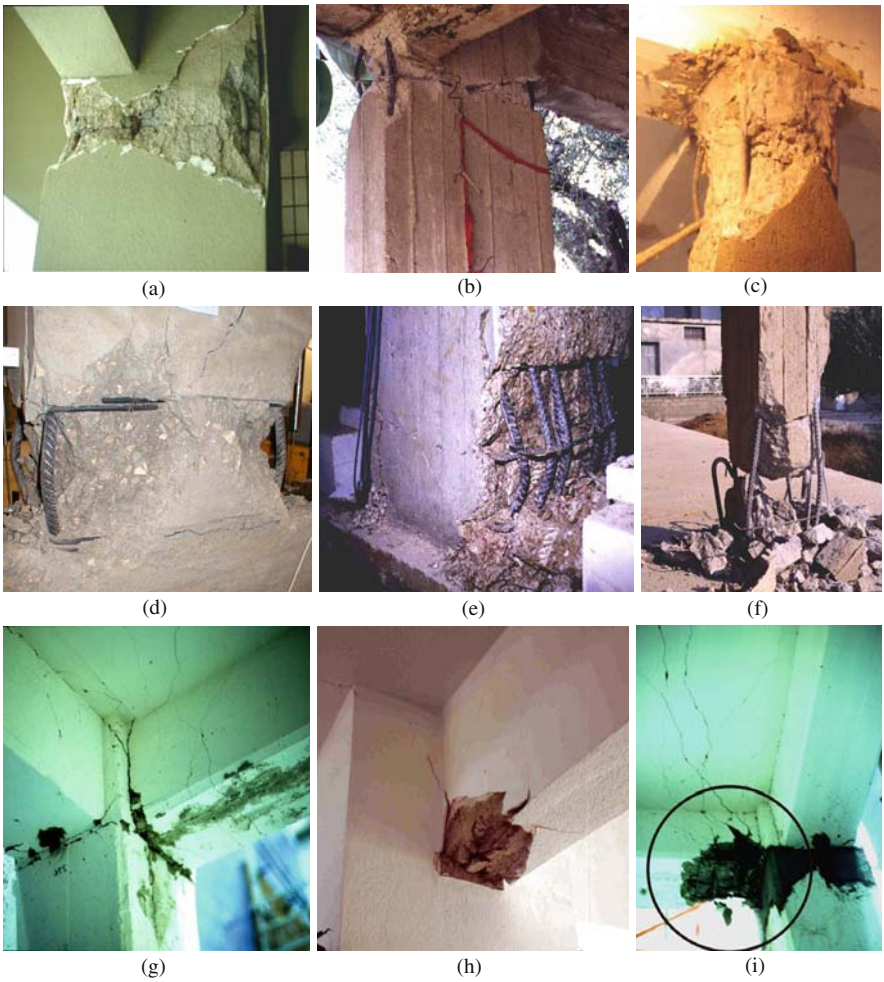

Fig. 3.27 Examples of flexural damage or failure in the lab or in the field: (**a**), (**b**) horizontal crack at column top, concrete spalling at the corners, buckling of corner bars; (**c**) complete loss of cover, partial disintegration of concrete and buckling of bars in horizontal zone near the column top; (**d**) full loss of cover, partial disintegration of concrete and buckling of bars in horizontal zone just above column base; (**e**) loss of cover, partial disintegration of concrete core and bar buckling, with tie opening-up on one side of a column above the base; (**f**) full disintegration of concrete and buckling of bars in a lapping region at floor level; (**g**) through-depth cracking near the support of a T-beam with extension of the cracks into the slab at the top flange; (**h**) local crushing of concrete and bar buckling at the bottom of a T-beam; (**i**) disintegration of concrete and bar buckling at the bottom of a T-beam, with through-depth flexural cracks extending into the slab at the top flange (See also Colour Plate 7 on page 721)

No matter whether the loss of strength, stiffness or energy dissipation capacity is abrupt or gradual, a conventional definition of member failure under cyclic loading is necessary. A definition covering both the abrupt and the gradual change in the force-deformation response has been proposed in French and Schultz (1991) and Saatcioglou (1991). According to it, failure is taken to occur when it is not possible to increase the force resistance above 80% of the maximum resistance attained during the test, even though the imposed deformation keeps increasing. In the examples of Figs. 1.2(b), 3.5(a) and (b), 3.36 (no. 1, 3 and 4), 3.38(c) and (f) and 3.46(c), the conventional identification of failure with a 20%-drop in post-ultimate resistance coincides with a rather abrupt change in the cyclic force-deformation response. By contrast, the column of Fig. 1.2(c), the material behaviour in Figs. 3.3(right), 3.6(b) and 3.10 and the subassembly in Fig. 3.46(b), exhibit a very gradual deterioration of peak resistance with cycling and failure can be defined only conventionally (as the 20% drop in post-ultimate resistance).

If the qualitative definition of failure as a change in the hitherto pattern of behaviour is applied to monotonic loading, then failure may be identified with the peak force resistance (ultimate strength, see Fig. 1.2(a) and monotonic conclusion of the tests in Figs. 3.6(a) and (b), 3.7 and 3.36(b) (specimen No. 8)). On the other hand, identification of failure with inability to increase the force resistance above 80% of its hitherto peak value, coincides with the frequently used convention of identifying failure under monotonic loading with a force point on the falling branch of the force-deformation response at 80% of the ultimate strength. In Figs. 1.2(a), 3.6(b) and 3.7, the drop in post-peak resistance by at least 20% is clearly meaningful as failure.

If the section and the reinforcement are symmetric, flexural damage (in a cyclic test or in the field during an earthquake) is also nearly symmetric at the two sides of the section. In an asymmetric cross-section the two sides may experience different failure modes under cyclic loading. Failure with the stronger side in tension is typically gradual, with progressive disintegration of the weaker compression side and crushing of the concrete there. Failure with the weaker side in tension may be abrupt, owing to fracture of the steel bars there, possibly after buckling in a previous half-cycle. Often steel fracture on the weaker side is preceded by a significant drop in strength (called, conventionally or not, failure) during a half-cycle with the stronger side in tension. So, under displacement-controlled cyclic load histories, failure of asymmetric sections typically occurs with the stronger side under tension.

3.2.2.8 Effect of Axial Force on the Cyclic Flexural Behaviour

If the axial load ratio, $\nu = N/A_c f_c$, is low, zero or negative (tensile) and the compression zone is well confined, repetition of a full cycle between equal and opposite values of peak curvature produces fairly stable hysteresis loops, with no degradation of the peak resistance from cycle to cycle.

Some axial compression on the cross-section helps close the cracks in the final phase of unloading and the first stage of reloading in the reverse direction, by promoting yielding in compression of the bars that have previously yielded in tension

and now go into compression. As a result, never during the loading cycle are the cracks open through the section depth or is the applied moment carried by the steel couple alone. So, the moment-curvature behaviour does not exhibit strong pinching of the loops. However, high axial compression has adverse effects on the behaviour, especially if the normalised axial force, ν, approaches the value at balance load (which coincides with $\nu_{c,y1}$, defined at the right-hand-side of Eq. (3.51) if the condition of Eq. (3.50a) is met, or with $\overline{\nu}_{c,y1}$, defined at the left-hand-side of Eq. (3.55), if it is not). For high axial compression the compression zone may disintegrate with cycling and the peak resistance may drop from cycle to cycle, giving shallower and narrower hysteresis loops. Failure then may be abrupt, unless the concrete core is very well confined.

The axial load in frame columns does not always stay constant during the seismic response. The seismic overturning moment produces an axial force (mainly) in the exterior columns, compressive on the "leeward" side of the building, tensile on the "windward" one (see Eq. (2.13) in Section 2.2.1.5). Seismic axial forces are largest at the bottom storey. The variation of axial compression during the cyclic response may significantly affect the column inelastic behaviour, so long as the column stays below its balance load,[10] as described below.

An increase in the axial compression increases the yield and ultimate moments (cf. Eqs. (3.37), (3.39), (3.57), (3.58), (3.59), (3.60), (3.61) and (3.62)), the ordinates of the envelope curve of the hysteresis loops under cyclic loading, and the stiffness in virgin loading, unloading and reloading, as the larger neutral axis depth increases the contribution of concrete to the flexural resistance and stiffness. By contrast, when the axial compression decreases, all its strength and stiffness properties decrease. So, a history of symmetric displacement cycles with variation of the axial force during the cycle produces asymmetric hysteresis loops, with strength and stiffness distinctly higher in the direction of increasing axial compression (that of negative moments in Fig. 3.28) than in the opposite one (for positive moments in Fig. 3.28). Therefore, during the seismic response the "leeward" exterior columns exhibit an increase in stiffness (increasing momentarily their share in the seismic shear) and yield moment. The "windward" exterior columns exhibit the reverse effects.

So long as the response is elastic, the seismic axial force in the columns varies in proportion both to the column moment and to the column deformation. This proportionality does not apply anymore, once plastic hinging and inelastic response start developing in the frame. So long as the column end section of interest is still in the elastic range, its seismic axial force will vary less than proportionally to the column moment and deformation. In the post-yield range of the column end section, and provided that the mechanism developing in the frame is closer to the beam-sway type (cf. Fig. 1.3(b)–(e)), the column's seismic axial force will keep varying with the column deformation (not the moment) but again less than proportionally to it. If a soft-storey type of mechanism tends to form (as in Fig. 1.3(a)), the column's

[10] If the value of the axial force varies around the column balance load, there is no clear-cut effect of this variation on the column flexural behaviour.

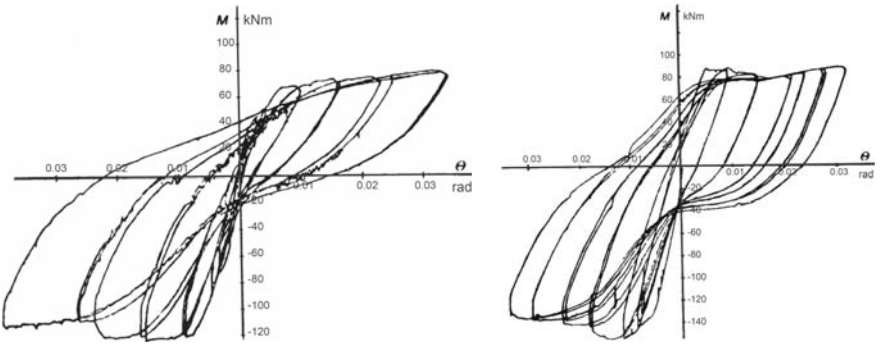

Fig. 3.28 Moment-chord rotation response of column with axial force varying in proportion: (**a**) to the moment; (**b**) to the deformation (adapted from CEB 1996a)

seismic axial force will stay essentially constant during post-yield primary loading but vary again with the column moment during unloading or reloading.

Tests on columns with the axial load varying about its mean value in proportion to the moment (Abrams 1987) demonstrate (Fig. 3.28(a)) that the effect of axial load on post-elastic stiffness in virgin loading or reloading shows up gradually, accelerating the softening in that direction of loading in which the axial compression decreases with increasing moment (i.e., for positive moments in Fig. 3.28(a)) but reducing it for loading in the opposite direction (toward negative moments in Fig. 3.28(a)), even to the point of producing an overall stiffening effect. An axial force that varies with the applied moment will remain essentially constant after column yielding. The different final values of axial force for the two directions of loading just cause different yield moments in these directions. The post-yield behaviour follows closely the envelope associated with the corresponding constant axial force value.

If the axial load varies about its average value in proportion to the deformations (Fig. 3.28(b)), yielding in the direction of decreasing axial force (i.e., for positive moments in Fig. 3.28(b)) is followed by a drop in the moment resistance, as this decreases with decreasing axial load (Abrams 1987). In the other direction of loading (towards negative moments in Fig. 3.28(b)), the increase of axial load with the post-yield deformation increases the yield moment further, showing up initially as an apparent but significant increase in the post yield stiffness. However, this post yield stiffening is soon followed by a strength decay, which may eventually lead to failure.

No matter whether the axial force varies with the moment or with the deformation, failure by rupture of the tension steel (Section 3.2.2.4 under *Failure of the Full Section Due to Rupture of Tension Reinforcement Before Spalling of the Concrete Cover*) is reached sooner for decreasing axial compression, while that by concrete crushing (Section 3.2.2.4 under *Curvature at Spalling of the Concrete Cover*) happens earlier for increasing axial load. As the ultimate curvature is much lower for the latter failure mode than for the former, the "leeward" exterior columns typically fail before the "windward" ones.

3.2.2.9 Fixed End-Rotation at Member Ultimate Curvature, Due to Bar Pull-Out from the Anchorage Zone Beyond the Section of Maximum Moment

If the anchorage of the longitudinal bars beyond the member end is insufficient, it will fail, normally by pull-out. Such a failure may well pre-empt yielding of these bars and flexural yielding of the member's end section. It will certainly prevent that section from developing its full moment resistance, Eqs. (3.57), (3.58), (3.59), (3.60), (3.61) and (3.62). Figure 3.29 shows examples of wide residual cracks at the ends of beams with short bar anchorage in corner joints, suggesting very large fixed-end rotations there during the response. In concrete buildings with well designed and detailed members, anchorage failures of this type do not take place. Instead, the fixed-end rotation due to bar pull-out from the anchorage zone will keep increasing from its value at yielding of the end section, Eq. (3.42), while the member heads towards its ultimate flexural deformation.

Strain hardening of the tension bars at the section of maximum moment does not increase markedly the bond stress demand along their anchorage past that section. The increase of the fixed-end rotation from yielding till the ultimate flexural deformation is due to penetration of inelastic strains into the initial part of the anchorage length of these bars (see Section 3.1.3.2). Bar anchorage beyond this "yield penetration length", $l_{y,p}$, remains intact and the fixed-end rotation produced by bar pull-out from the anchorage zone is still given by Eq. (3.42). However, steel elongation along the "yield penetration length" shows up as additional slippage of the tension bars at the section of maximum moment. If these bars are perfectly-plastic along the yield

Fig. 3.29 Pull-out of beam bars from short anchorage in corner joint has produced fixed-end rotation during the response and wide residual cracks (See also Colour Plate 8 on page 722)

penetration length, their strain is practically constant along that length and equal to the steel strain, ε_s, at the section of maximum moment. It produces then an additional slippage of $\varepsilon_s l_{y,p}$ and an additional fixed-end-rotation, $\Delta\theta_{u,slip} = \varphi_u l_{y,p}$, by the time of the ultimate curvature, φ_u, of the end section. If the tension bars are considered as linearly strain-hardening all along the yield penetration length, their strain may be taken to increase linearly along that length from the yield strain, ε_y, to the value ε_s at the section of maximum moment. In that case we have: $\Delta\theta_{u,slip} = (\varphi_y+\varphi_u)l_{y,p}/2$.

Biskinis (2007) used about 465 measurements of relative rotations near the end of the member at the time of member ultimate deformation, 120 of which included the fixed-end rotation due to reinforcement pull-out. On the basis of these tests the additional fixed-end rotation between yielding and ultimate curvature can be inferred as equal to:

– for cyclic loading:

$$\Delta\theta_{u,slip} = 5.5 d_{bL} \varphi_u \tag{3.63a}$$

– for monotonic loading:

$$\Delta\theta_{u,slip} = 9.5 d_{bL} \varphi_u \tag{3.63b}$$

or

– for cyclic loading:

$$\Delta\theta_{u,slip} = 10 d_{bL} \left(\varphi_y + \varphi_u\right)/2 \tag{3.63c}$$

– for monotonic loading:

$$\Delta\theta_{u,slip} = 16 d_{bL} \left(\varphi_y + \varphi_u\right)/2 \tag{3.63d}$$

A slightly better fit to the data is achieved with Eqs. (3.63c) and (3.63d) than with Eqs. (3.63a) and (3.63b): the coefficient-of-variation is 45.5% v 47.5%.

Note, in this connection, that according to Eurocode 8 (CEN 2004a) the anchorage length of beam or column bars in beam-column joints of DC H buildings should be measured starting 5-bar-diameters inside the joint for reasons of yield penetration. This length is quite consistent with Eq. (3.63a).

The value of φ_u in Eqs. (3.63) is calculated according to Section 3.4.4.2, using Eqs. (3.4), (3.5), (3.10), (3.16) or (3.17), (3.20), (3.21), (3.22), (3.23), (3.24) and (3.25) for the properties of concrete, including the confined core, as well as Eqs. (3.64) of Section 3.2.2.10 for the strain at which the tension bars rupture.

3.2.2.10 Experimental Ultimate Curvatures and Comparison with Predictions for Various Confinement Models

The most important parameters in the approach of Section 3.2.2.4 for the calculation of ultimate curvature, φ_u, are the ultimate strain of concrete, confined or not, and the available elongation of the tension reinforcement.

Equations (3.16) or (3.17) in Section 3.1.2.2 give the ultimate strain of concrete, confined or not, to be used together with Eqs. (3.4), (3.5), (3.10), (3.20), (3.21), (3.22), (3.23), (3.24) and (3.25) for the prediction of ultimate curvature. Biskinis (2007) has developed Eqs. (3.16) and (3.17) on the basis of about 465 measurements of relative rotations near the end of the member at the time of member ultimate deformation. About 120 of these measurements included fixed-end rotation due to reinforcement pull-out and were corrected for its effect using Eqs. (3.63). The first two terms of Eqs. (3.16) and (3.17) have been derived from 65 cases with almost no confinement, where the ultimate curvature had been reached at spalling of the concrete cover. The resulting predictions for φ_u give a test-to-prediction ratio with a median of 0.925 and a coefficient-of-variation of 55.5%. The 3rd term in Eqs. (3.16) and (3.17) has been derived from 105 monotonic and about 80 cyclic tests that reached ultimate curvature by crushing of the confined concrete core. The resulting φ_u-values give a test-to-prediction ratio with median of 1.02 or 0.99 and a coefficient-of-variation of 51.9% or 52.6%, for these monotonic or cyclic tests, respectively. Finally, about 115 monotonic and 100 cyclic tests, reported or inferred to have reached ultimate curvature by rupture of the tension reinforcement, lead to the conclusion that the available elongation of tension reinforcement at ultimate curvature is on average equal to the following fraction of the nominal bar strain at maximum stress, $\varepsilon_{su,nominal}$, as obtained from coupon tests of the bars (Biskinis 2007, Biskinis and Fardis 2009):

– for monotonic loading:

$$\varepsilon_{su,mon} = (7/12)\varepsilon_{su,nominal} \tag{3.64a}$$

– for cyclic loading:

$$\varepsilon_{su,cy} = (3/8)\varepsilon_{su,nominal} \tag{3.64b}$$

The adverse effect of cyclic loading on steel bars (e.g., surface cracking upon buckling, etc.) is the main reason for the large difference of $\varepsilon_{su,cy}$ from $\varepsilon_{su,nominal}$, in Eq. (3.64b). By contrast, the prime reason for the (smaller, albeit significant) difference of $\varepsilon_{su,mon}$ from $\varepsilon_{su,nominal}$ in Eq. (3.64a) is not mechanical but statistical, similar to the well known statistical size effect that decreases strength with increasing specimen size. The 115 monotonic tests that reached ultimate curvature by rupture of the tension reinforcement had from 1 to 20 tension bars (on average 5). Unlike the cyclic test results, which do not exhibit a statistically significant effect of the number of bars on $\varepsilon_{su,cy}$, the monotonic ones show clearly that when the number of

bars increases, the actually available elongation of tension reinforcement, $\varepsilon_{su,mon}$, decreases. This is consistent with control of failure by the minimum value of ε_{su} among the bars. Normally, the probability distribution of the minimum value of ε_{su} among N bars is taken to follow a Type I extreme value distribution of the smallest values. The parameters of that probability distribution depend on the functional dependence of the lower tail of the underlying distribution of the value of ε_{su} of the individual bars, on ε_{su}. A reasonable form of dependence is an exponential of the negative of an increasing function of the deviation of ε_{su} from its mean value, taken as $\varepsilon_{su,nominal}$ (Benjamin and Cornell 1970). If that function is taken proportional to $(\varepsilon_{su}-\varepsilon_{su,nominal})^2$, the mode (i.e., most likely value) of the minimum value of ε_{su} among N bars is a linear function of $\sqrt{lnN}$ (Benjamin and Cornell 1970). Then, as Eq. (3.64a) corresponds to an average of 5 tension bars in the 115 monotonic tests with rupture of tension reinforcement, it can be generalised as follows:

– For monotonic loading:

$$\varepsilon_{su,mon} = \left(1 - \frac{1}{3}\sqrt{\ln N_{b,tension}}\right)\varepsilon_{su,nominal} \tag{3.64c}$$

where $N_{b,tension}$ is the number of bars in the tension zone. Equation (3.64c) gives $\varepsilon_{su,mon} = \varepsilon_{su,nominal}$ if $N_{b,tension} = 1$ and $\varepsilon_{su,mon} \approx (7/12)\varepsilon_{su,nominal}$ for the average value of $N_{b,tension} = 5$ in the tests. When Eqs. (3.64c) and (3.64b) are used, the test-to-prediction ratio for φ_u has a median of 1.00 or 1.01 and a coefficient-of-variation of 44.8% or 34.7%, for these monotonic or cyclic tests, respectively.

Overall, in about 465 ultimate curvature values derived from measurements of relative rotation, the test-to-prediction ratio for φ_u has a median of 0.995 and a coefficient-of-variation of 49.8% (or 1.01 and 0.985, and 53.2 and 44.6% separately for monotonic and cyclic loading, respectively) (Biskinis 2007). Natural and test-to-test variability contributes to the scatter a coefficient of variation of about 18.5% in practically identical specimens. After subtracting this source of the scatter, model uncertainty corresponds to a coefficient of variation equal to the values quoted above, reduced by 3.3% for the larger values to 5.2% for the smaller ones. The overall statistics, as well as those for the individual failure modes, are slightly worse if the ultimate concrete strain is given by a single expression, Eq. (3.17), both for monotonic and cyclic loading, instead of the two different ones of Eqs. (3.16).

After correcting the "experimental" value of φ_u for any fixed-end rotation due to reinforcement pull-out from its anchorage beyond the section of maximum moment according to Eqs. (3.63), its magnitude does not exhibit any systematic effect of the gauge length over which the relative rotation had been measured (Biskinis 2007).

Notwithstanding the large scatter, the above statistics demonstrate that φ_u-values based on Eqs. (3.4), (3.5), (3.10), (3.16), (3.17) and (3.64) agree much better with test results than the φ_u-values obtained from alternative well known or widely used models, namely:

a. From the model in informative Annex A of Part 3 of Eurocode 8 (CEN 2005a). According to it, the ultimate strain of longitudinal reinforcement, ε_{su}, to be used for cyclic loading can be taken equal to the following values, higher than those of Eq. (3.64b):

   - the lower limit values specified in Eurocode 2 (CEN 2004b) for the 10%-fractile strain at maximum force, ε_{uk}, if the steel class is A or B (for class B, this is the minimum value for DC L or M in Table 3.1 of Section 3.1.1.4); and
   - 6% for steel class C (i.e., steel meeting the requirements for DC H in Table 3.1 of Section 3.1.1.4).

   According to CEN (2005a), the parameters of confined concrete, including the effect of confinement, may be obtained either:

   i. from Eqs. (3.4), (3.5), (3.10) and (3.18), or
   ii. from Eqs. (3.8), (3.9) and (3.13) (i.e., according to CEN (2004b) and CEB (1991)).

   For confinement model (i) the test-to-prediction ratio of φ_u has a median of 1.04 or 0.94 and coefficient-of-variation of 67.2% or 47.3% for monotonic or cyclic loading, respectively. Overall (for monotonic and cyclic loading) the median is 0.985 and the coefficient-of-variation 62.9%.
   For confinement model (ii) the median and the coefficient-of-variation of the test-to-prediction ratio of φ_u is 1.37 or 1.3, and 70.6% or 51.3% for monotonic or cyclic loading, respectively, and overall (monotonic and cyclic) 1.33 and 65.6% (Biskinis 2007). If the ultimate strain of steel, ε_{su}, is taken from Eqs. (3.64) instead, the median improves to 1.39, 1.14 and 1.27, for monotonic, cyclic loading and overall (monotonic and cyclic), respectively, without a significant increase of the scatter.

b. From Mander et al. (1988) and Paulay and Priestley (1992) regarding confinement, i.e., from Eqs. (3.4), (3.6) and (3.10) and either Eq. (3.14) (Mander et al. 1988), or Eq. (3.15) (Paulay and Priestley 1992) for the ultimate strain of confined concrete.
   Best average agreement of these models with tests is obtained if the ultimate strain of longitudinal reinforcement, ε_{su}, is taken according to Part 3 of Eurocode 8 (CEN 2005a). Then the ultimate strain model of Eq. (3.14) (Mander et al. 1988) gives a median of 1.015 or 1.155 for the test-to-prediction ratio of φ_u and a coefficient-of-variation of 71.5% or 52.4%, for monotonic or cyclic loading, respectively, and overall a median ratio of 1.035 and a coefficient-of-variation of 64.5%. If the ultimate strain model of Eq. (3.15) (Paulay and Priestley 1992) is used instead, the test-to-prediction ratio of φ_u has a median of 0.95 or 0.89 and a coefficient-of-variation of 74.5% or 53% for monotonic or cyclic loading, respectively. Overall the median is 0.925 and the coefficient-of-variation 68.4%.
   When the ultimate strain of longitudinal reinforcement, ε_{su}, is taken from Eqs. (3.64), the ultimate strain model of Eq. (3.14) (Mander et al. 1988) gives

for the test-to-prediction ratio of φ_u a median equal to 0.895 or 0.945, and a coefficient-of-variation of 78.3% or 44.2%, for monotonic or cyclic loading, respectively, and a median of 0.92 and a a coefficient-of-variation of 68.3% overall. If the ultimate strain model of Eq. (3.15) (Paulay and Priestley 1992) is used instead, the test-to-prediction ratio of φ_u has a median of 0.87 or 0.835 and a coefficient-of-variation of 84.2% or 47.1%, for monotonic or cyclic loading, respectively. Overall the median is 0.835 and the coefficient-of-variation 75.1%.

3.2.2.11 Curvature Ductility Factor

Equations (1.1) and (1.2) in Section 1.2 relate:

- the behaviour factor q by which the elastic force demand on the structure as a whole is divided, in order to obtain the design force (base shear) that the system should be designed to resist at the ULS, to
- the global (lateral) displacement ductility factor, μ_δ, of the system, defined as ratio of the displacement demand at the top or at the point of application of the resultant lateral force, to the displacement at the same point at global yielding (i.e., at the corner of an elastoplastic curve fitted to the force displacement response)

The importance of μ_δ arises from its relation with q through Eqs. (1.1) and (1.2).

As noted in Section 1.3 with reference to Fig. 1.3, if the plastic mechanism of the response is known, member deformation demands (conveniently expressed as chord rotation demands at member ends, see Figs. 1.3 and 1.4) can be related to the global displacement demand on the building and evaluated from it. Accordingly, these member deformation demands are also normalised to the corresponding value at yielding of the member (i.e., to θ_y, if the chord rotation θ is used), i.e. as member deformation (e.g. chord rotation) ductility factors (e.g. $\mu_\theta = \theta/\theta_y$). This practice is extended to the curvature of sections, for which the curvature ductility factor is defined as $\mu_\varphi = \varphi/\varphi_y$.

There is always a demand value for any ductility factor, deriving from the seismic action, and a supply value, characterising the corresponding deformation capacity (at ultimate deformation) of the section, member or system. The demand value of the curvature ductility factor is:

$$\mu_\varphi = \frac{\varphi}{\varphi_y} \tag{3.65a}$$

and its supply (or available) value is:

$$\mu_{\varphi u} = \frac{\varphi_u}{\varphi_y} \tag{3.65b}$$

where φ_y can be obtained according to Section 3.2.2.2 and φ_u from Section 3.2.2.4, using Eqs. (3.16) or (3.17) in Section 3.1.2.2 for the ultimate strain of concrete, confined or not, together with Eqs. (3.4), (3.5), (3.10), (3.20), (3.21), (3.22), (3.23), (3.24) and (3.25), as well as Eq. (3.64) for the available elongation of the tension reinforcement

The importance of μ_φ derives mainly from the possible link of its available value from Eq. (3.65b) to a supply value of the member chord rotation ductility factor, μ_θ. The link is via Eq. (3.71) in Section 3.2.3.4 and certain approximations. In the end it relates μ_φ to μ_δ and hence to q through Eqs. (1.1) and (1.2) (see Section 5.1, Eqs. (5.1) and (5.2)).

3.2.3 Flexural Behaviour at the Member Level

3.2.3.1 Chord Rotations from Member Tests

The chord rotation at a member end has been introduced in Section 1.3 with reference to Figs. 1.3 and 1.4. The chord rotations $\theta_A = \int_{x_A}^{x_B} \varphi(x)(x_B - x)dx / (x_B - x_A)$, $\theta_B = \int_{x_A}^{x_B} \varphi(x)(x_A - x)dx / (x_B - x_A)$ at the two ends A and B of a member are the angles between the chord connecting the ends in the deformed configuration of the member and the normal to the cross-section at A and B, respectively. The relative rotation θ_{AB} of these two sections is: $\theta_{AB} = \int_{x_A}^{x_B} \varphi(x)dx = \theta_A - \theta_B$.

The chord rotation at a member's end is the most important and convenient deformation measure for concrete members, for the following reasons:

- Both in the elastic and inelastic range, chord rotations at member ends are equal to the nodal rotations there, after subtracting the rigid-body displacements of the member axis. Therefore, it is in terms of them that the stiffness or flexibility relation of the member is formulated in member-type models (see Sections 4.10.1.2 and 4.10.1.4). For example, in the elastic range the moments at ends A and B are derived from the chord rotations there as: $M_A = (2EI/L)(2\theta_A+\theta_B)$, $M_B = (2EI/L)(2\theta_B+\theta_A)$. The chord rotations due to flexure determine the distribution of bending moments along the full length of the member.
- Unlike curvatures, which lack physical meaning and are hard to measure experimentally, deflections are reliably measured or controlled. So, test results, mostly from single- or double-cantilever specimens, are typically presented as a lateral force-deflection diagram, F–δ, at the point of application of the lateral load and reflect the overall load-displacement response of the specimen. Normally the deflection δ is at the end B of the shear span, $L_s = M/V$, and is measured with respect to the original axis of the specimen, which coincides with the normal to the section A of maximum moment. The F–δ diagram can be translated into an end moment-chord rotation (or "drift") diagram, M–θ, of the member, by multiplying the shear force by L_s and dividing δ by L_s. Such a diagram refers to the

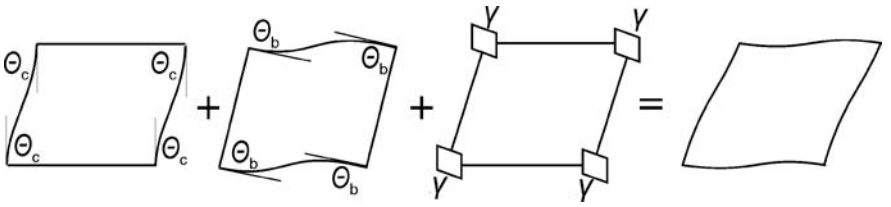

Fig. 3.30 Contribution of chord rotations of columns and beams to the angular distortion of a frame bay

entire shear span and is closely linked to its length. Note that it is the deflection at point B (where the load is applied) with respect to the tangent at the section A of maximum moment, that gives the chord-rotation at A, θ_A.

– The angular distortion of a frame bay with beams and columns in skew symmetric bending ($\theta_A = \theta_B$) is equal to the sum, $\theta_c + \theta_b$, of the chord rotations of a column and a beam around the bay, plus the (average) shear distortion of the joint panel, γ (Fig. 3.30). In design for earthquake or wind, damage to non-structural elements filling the frame panel, such as partition walls, etc., is limited by limiting this angular distortion, usually termed drift angle or drift ratio. The term "drift" is also used for the chord rotation in single- or double-cantilever member tests.

Tests are the main source of information for the cyclic behaviour of concrete members up to failure. Recall that energy dissipation and inelastic action should take place mostly in the beams, which should be weaker than the columns they frame into. In buildings beams are normally subjected to uniaxial bending with practically zero normal force, whereas columns, in general, may be subjected to biaxial bending with axial force. So, most of the experimental research on the cyclic behaviour of reinforced concrete members has addressed the simplest case of uniaxial flexure without axial force. However, although in practice only beams are subjected to uniaxial bending and zero axial force, in most tests the specimen has rectangular cross-section and symmetric reinforcement, as in columns. There are few tests on specimens with T-section and asymmetric reinforcement. But even in them another source of asymmetric behaviour is missing: the shear span is maintained constant during testing, whereas in a beam carrying gravity loads and belonging in a frame subjected to seismic loading the shear span varies during the response. It is minimum, and hence the effect of shear on behaviour is greatest, when the moment and the shear due to the seismic loading act in the same sense as those due to gravity loads (i.e., introducing tension to the top flange).

In the most common test setup the specimen cantilevers from a large concrete base and is subjected to a cyclic lateral force at the tip under displacement control. Then the shear span is the distance of the point of application of the force to the top of the base. In another setup, more representative of frame members (especially of columns), the specimen is fixed against rotation at both ends and subjected to skew symmetric counter-flexure. Then the shear span is half the specimen

length. In both setups there is slippage (partial pull-out) of the longitudinal bars from their anchorage in the concrete block(s) at the end(s) of the specimen, that macroscopically shows up as "fixed-end rotation" of the member's end section(s) (see Sections 3.2.2.3 and 3.2.2.9). In yet another setup the specimen is a simply supported beam subjected to cyclic deflections at mid-span. The symmetry with respect to the section of maximum moment in principle prevents slippage of the reinforcement towards either side of that section. This is essentially a test of two specimens simultaneously, namely of the two halves. From a certain point on during the test symmetry is destroyed by unavoidable differences in the behaviour of the two halves (with one of them reaching ultimate strength or deformation before the other), the mid-span section rotates and deflection measurements there become difficult to use and interpret.

3.2.3.2 Member Chord Rotation at Flexural Yielding of the End Section in Uniaxial Loading

Of interest is the drift ratio of the shear span of a member, L_s, at yielding of the end section of the shear span. This is the chord rotation at the yielding end, θ_y.

"Tension stiffening", i.e., the contribution of the concrete in tension between cracks to stiffness, is relatively small in members with longitudinal reinforcement ratios as high as those typical of members designed for earthquake resistance. Moreover, this contribution depends heavily on the bond along the bars between the cracks, which degrades with cyclic loading. So, as the member has normally been subjected to one or more elastic load cycles by the time its end section yields, the (anyway small) effect of concrete in tension on the overall flexural deformations of the member at yielding is negligible. Therefore, the part of the chord rotation at yielding which is due to purely flexural deformations is: $\theta_y = \varphi_y L_s/3$.

Inclined cracking and shear deformations along the shear span increase the magnitude of θ_y. Diagonal cracking near the yielding end of the member spreads yielding of the tension bars up to the point where the first diagonal crack from the end section intersects them (Fig. 3.31). This is the "shift rule" in dimensioning of the tension reinforcement for the Ultimate Limit State in bending with axial force. According to it the value of the force in the tension reinforcement is shifted from the section to which it corresponds on the basis of the moment and axial force diagrams, to one where the moment is lower (i.e. further away from the member end). The shift is due to diagonal cracking and its magnitude depends on the inclination of the diagonal cracks to the member axis and on the amount of transverse reinforcement. However, usually a default value is taken for the shift equal to the internal lever arm, z. Such a shift increases the value of θ_y which is theoretically due to flexural deformations, from $\varphi_y L_s/3$ to about $\varphi_y(L_s+z)/3$.[11] Of course, such an increase would not take place

[11] Strictly speaking the increase is to a value of $\varphi_y[(L_s-z)(1-z/L_s)(1+0.5z/L_s)/3+z(1-0.5z/L_s)]$, but the difference from $\varphi_y(L_s+z)/3$ is practically insignificant.

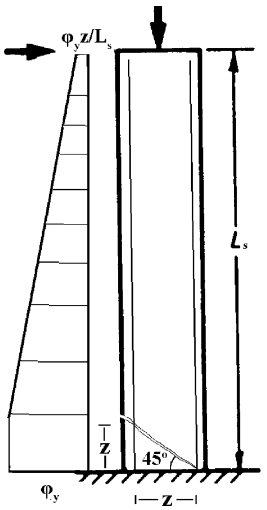

Fig. 3.31 Shift of yielding of tension reinforcement along the member due to diagonal cracking (Biskinis 2007)

unless diagonal cracking precedes flexural yielding at the end section. So, the term z should be added to L_s only if the shear force that causes diagonal cracking, V_{Rc}, is less than the shear force at flexural yielding of the end section, $V_{My} = M_y/L_s$.

Any fixed-end rotation due to reinforcement pull-out from its anchorage zone beyond the yielding end contributes to θ_y with the fixed-end-rotation, $\theta_{y,slip}$, from Eq. (3.42). However, the sum of $\varphi_y L_s/3$ (or $\varphi_y(L_s+z)/3$ if there is diagonal cracking) and of the fixed-end-rotation (if any) from Eq. (3.42) on average falls short of the "experimental" chord rotation at flexural yielding, taken at the corner of a bilinear M–θ curve fitted to the envelope of the experimental M–θ hysteresis loops, including P–Δ effects (cf. Section 3.2.2.2 under *Comparison with Experimental Results and Empirical Expressions for the Curvature*). The shortfall can be empirically corrected via the 2nd term of Eqs. (3.66), fitted to "experimental" chord rotations at flexural yielding of members with shear span ratio and reinforcement such that there are no flexure-shear interaction effects on yielding (see Section 3.2.5) (Biskinis 2007, Biskinis and Fardis 2004):

– For beam/columns with rectangular section (about 1560 tests):

$$\theta_y = \varphi_y \frac{L_s + a_V z}{3} + 0.0014\left(1 + 1.5\frac{h}{L_s}\right) + a_{sl}\frac{\varphi_y d_{bL} f_y}{8\sqrt{f_c}} \tag{3.66a}$$

– For walls (rectangular or not) and hollow rectangular members (about 250 tests):

$$\theta_y = \varphi_y \frac{L_s + a_V z}{3} + 0.0013 + a_{sl}\frac{\varphi_y d_{bL} f_y}{8\sqrt{f_c}} \tag{3.66b}$$

where:

- φ_y in the 1st term is the "theoretical" yield curvature from Eqs. (3.33), (3.34), (3.35) and (3.38) times the correction factor of 1.025, 1.015 or 1.075, for beams/columns, rectangular walls, or members with T-, U-, H- or hollow rectangular section, respectively;
- a_v is a zero-one variable:
  - $a_v = 0$, if $V_{Rc} > V_{My} = M_y/L_s$, with V_{Rc} taken here from Eurocode 2 (CEN 2004b), Eq. (3.67);
  - $a_v = 1$, if $V_{Rc} \leq V_{My} = M_y/L_s$;
- z is the length of the internal lever arm, taken as:
  - $z = d–d_1$ in beams, columns, or members with T-, H-, U- or hollow rectangular section, and:
  - $z = 0.8h$ in walls with rectangular section.
- a_{sl} is a zero-one variable:
  - $a_{sl} = 1$ if slippage of longitudinal bars from the anchorage zone beyond the end section is possible, or
  - $a_{sl} = 0$ if slippage is not possible.
- as in Eq. (3.42), f_y and f_c in the last term are in MPa.

The shear force at diagonal cracking of the member, V_{Rc}, is taken here equal to the shear resistance of members without shear reinforcement, given in Eurocode 2 (CEN 2004b) as:

$$V_{R,c} = \left\{ \max \left[180\,(100\rho_1)^{1/3}\,,\ 35\sqrt{1+\sqrt{\frac{0.2}{d}}}\,f_c^{1/6} \right] \left(1+\sqrt{\frac{0.2}{d}}\right) f_c^{1/3} + 0.15\frac{N}{A_c} \right\} b_w d \tag{3.67}$$

With ρ_1 denoting the tension reinforcement ratio and the axial load N taken positive for compression (but if N is tensile, then $V_{R,c} = 0$), Eq. (3.67) gives the value of $V_{R,c}$ in kN when b_w (width of the web) and d are in m, f_c is in MPa and N in kN.

Annex A of Part 3 of Eurocode 8 (CEN 2005a) has adopted an earlier version of Eqs. (3.66a) and (3.66b) (Biskinis and Fardis 2004) with a coefficient of 0.13 instead of 1/8 = 0.125 in the 3rd term and with Eq. (3.66b) applicable only to walls and its 2nd term replaced by $0.002[1–0.125L_s/h]$. It has also adopted an alternative form of these expressions where the pullout of tensile reinforcement at the yielding end section, $0.5f_y l_b/E_s$, has been translated to fixed-end rotation by dividing it by the distance between the tension and the compression bars in the section, $(d–d_1)$, instead of the depth of the tension zone at yielding, $(1–\xi_y)d$ (Biskinis 2007, Biskinis and Fardis 2004). The 3rd term of the alternative expressions uses $\varepsilon_y d_{bL} f_y/[6(d–d_1)\sqrt{f_c}]$ (with $\varepsilon_y = f_y/E_s$ being the yield strain of longitudinal bars) instead of $\varphi_y d_{bL} f_y/(8\sqrt{f_c})$. This

alternative fits the data almost as well as Eqs. (3.66), but is probably easier to apply in that the 3rd term is independent of φ_y, whose calculation is harder and more prone to errors.

Equations (3.66) give a median of 1.01 or 0.995 for the test-to-prediction ratio of θ_y, and a coefficient-of-variation of 32.1% or 33.7%, for beams/columns or walls/hollow rectangular members, respectively. Natural and test-to-test variability contributes to the scatter a coefficient of variation of about 10% in practically identical specimens. The rest of the scatter is mainly due to model uncertainty and corresponds to coefficients of variation equal to the values above reduced by about 1.5%. The variants of Eqs. (3.66a) and (3.66b) adopted in Part 3 of Eurocode 8 (CEN 2005a) (with the value 0.13 used in the 3rd term instead of 1/8) give as good or even slightly better fit to the data.

The comparison above refers to tests with ribbed bars. In about 20 tests of beam/columns with smooth (plain) bars the mean or the median of the test-to-prediction ratio are about 0.98. So, the poorer bond along such bars does not seem to increase member deformations at yielding.

A prime use of the prediction of θ_y from Eqs. (3.66) is for the calculation of the effective member stiffness at incipient yielding from Eq. (3.68) in Section 3.2.3.3. So, the fitting of Eqs. (3.66) to the experimental values of θ_y aims at accuracy in the median, as much for θ_y, as for the effective stiffness at yielding from Eq. (3.68) in Section 3.2.3.3. So, any mismatch in the median between the experimental and the predicted values of θ_y should not be seen independently of the median agreement or mismatch between the effective stiffness from Eq. (3.68) and the test values.

3.2.3.3 Effective Stiffness of Members at Incipient Yielding: Importance and Estimation

A fundamental simplification underlying the provisions of force-based seismic design using elastic forces reduced by the behaviour factor q is that the global inelastic response of the structure to monotonic lateral forces is bilinear, close to elastic-perfectly-plastic. Then, the stiffness used in the elastic analysis should correspond to the stiffness of the elastic branch of such a bilinear global force-deformation response. So, the full elastic stiffness of uncracked concrete in the analysis is not the proper value to use. Eurocode 8 (like US codes) requires concrete buildings be designed using in the seismic analysis stiffness values for members that take into account the effect of cracking and correspond to the initiation of yielding of the reinforcement (secant stiffness to the yield-point). Unless more accurate modelling is used, Eurocode 8 follows US codes in allowing to derive that stiffness from 50% of the uncracked gross section rigidity, $E_c I_c$, neglecting the effect of reinforcement.

Within the force- and strength-based seismic design philosophy of current seismic design codes, a high estimate of the effective stiffness gives safe-sided results, as it increases the period(s) and therefore the corresponding spectral acceleration(s) and design forces. The use of $0.5E_cI_c$ serves exactly that purpose, as the experimental secant stiffness of concrete members at incipient yielding is generally much

lower. Only the lateral drifts and the P–Δ effects computed from these overly high stiffness values may be (seriously) underestimated. As a matter of fact, Eurocode 2 (CEN 2004b) specifies as follows the effective stiffness for the calculation of 2nd-order effects in concrete structures:

- as equal to the stiffness $E_s I_s$ of the section reinforcement with respect to the centroid of the section, plus the minimum of $0.2E_c I_c$ and $0.3\nu E_c I_c$ (where $\nu = N/A_c f_c$ is the axial load ratio),
- $0.3E_c I_c$ if the reinforcement ratio exceeds 1% (although its exact value is not known in this stage of the design).

Clause 10.11.1 of ACI (2008) specifies the effective stiffness for the magnification of moments in compression members and frames due to 2nd-order effects as follows:

- $0.35E_c I_c$ for beams and cracked walls,
- $0.70E_c I_c$ for columns and uncracked walls,
- $0.25E_c I_c$ for flat plates or slabs.

Clause 10.12.3 of ACI (2008), by contrast, gives the following effective stiffness for the calculation of moment magnification due to 2nd-order effects in non-sway frames:

- the stiffness $E_s I_s$ of the reinforcement with respect to the centroid of the section, plus $0.2E_c I_c$ (i.e., as in the Eurocode 2 rule, except that the fraction of $E_c I_c$ is not taken as $0.3\nu = 0.3N/A_c f_c$, if this value is smaller than 0.2); or
- $0.2E_c I_c$, as a simpler approximation.

Note that, using in the analysis a low-side estimate of effective stiffness increases 2nd-order effects, which is safe-sided in the context of design for non-seismic actions, as with Eurocode 2 or Clause 10 of the ACI 318 code.

As elaborated in Chapter 6, seismic assessment and retrofitting of existing buildings is nowdays fully displacement-based, with direct or indirect verification of member deformation capacities against the inelastic deformation demands. So it needs a relatively accurate estimation of inelastic deformation demands throughout the structure, which in turn requires realistic values of the effective cracked stiffness of concrete members at yielding. The use of a member stiffness of $0.5E_c I_c$ for displacement-based seismic assessment and retrofitting of existing structures is unsafe: member seismic deformation demands will be seriously underestimated.

The most realistic estimate of the effective elastic stiffness of the shear span, $L_s = M/V$, in a bilinear force-deformation model of a concrete member under monotonic loading, is the secant stiffness of the shear span to the member yield-point:

$$EI_{eff} = \frac{M_y L_s}{3\theta_y} \tag{3.68}$$

where M_y is the yield moment in the bilinear M–θ model of the shear span and θ_y the chord rotation at the yielding end, both by calculation (from Sections 3.2.2.2 and 3.2.3.2, respectively).

The "experimental effective stiffness" at member yielding is obtained by using experimental values of M_y and θ_y in Eq. (3.68). Its ratio to the value obtained from Eq. (3.68), using the M_y and θ_y values from Sections 3.2.2.2 and 3.2.3.2, respectively, has a median of 1.01 or 0.99 and a coefficient of variation of 32.3% or 47.1% for beams/columns, or walls/hollow rectangular members, respectively. Natural and test-to-test variability contributes to the scatter with a coefficient of variation of about 10% in practically identical specimens. If Eqs. (3.66a) and (3.66b) are replaced by their variants in Part 3 of Eurocode 8 (CEN 2005a) for the calculation of θ_y, the agreement with the data is almost the same (Biskinis 2007, Biskinis and Fardis 2004). These comparisons refer to tests with ribbed bars. In about 20 tests of beam/columns with smooth (plain) bars the mean test-to-prediction ratio of the secant stiffness to yield point is about 1.03, implying that the poorer bond along these bars does not seem to adversely affect the member stiffness.

The specimens in the large database used for the calibration of the expressions for M_y and θ_y in Sections 3.2.2.2 and 3.2.3.2, have "experimental effective stiffness" at member yielding on average equal to 22% or 15% of the stiffness of the uncracked gross section, $E_c I_c$, for beams/columns, or walls and members with hollow rectangular section, respectively. The coefficients of variation of the experimental effective stiffness with respect to this average are about twice the values from the application of Eq. (3.68).

For Eq. (3.68) to be applied using the values of M_y and θ_y, the amount and layout of the longitudinal reinforcement should be known. In displacement-based seismic assessment of existing buildings this information is available before the analysis. If it is not, as in displacement-based seismic design of new structures, a purely "empirical effective stiffness" would be more convenient, if it is expressed in terms of geometric, etc., characteristics of the member known before dimensioning its reinforcement. The following expression has been fitted in Biskinis (2007) to the "experimental effective stiffness" at member yielding:

$$\frac{\mathrm{EI_{eff}}}{\mathrm{E_c I_c}} = a\left(0.8 + \ln\left[\max\left(\frac{L_s}{h};\, 0.6\right)\right]\right)\left(1 + 0.048\ \min\left(50\,MPa;\, \frac{N}{A_c}\right)\right) \tag{3.69}$$

where N/A_c is in MPa, and

- $a = 0.081$ for columns;
- $a = 0.10$ for beams;
- $a = 0.115$ for rectangular walls; and
- $a = 0.09$ for members with T-, U-, H- or hollow rectangular section.

Equation (3.69) refers to the – common in practice – case where slip of the longitudinal bars from their anchorage beyond the member's end section is physically possible ($a_{sl} = 1$ in Eqs. (3.66)). If it isn't (i.e., if $a_{sl} = 0$ in Eqs. (3.66)), the effective stiffness increases by one-third, i.e. the values above should be multiplied by 4/3.

Being purely empirical, Eq. (3.69) achieves a median of 1.00 for the test-to-prediction ratio. However, neglecting the dependence of effective stiffness on the amount and layout of longitudinal reinforcement increases the scatter: the coefficient of variation of the test-to-prediction ratio is 37.6, 58.7 and 42.6%, for beams/columns, rectangular walls and members with T-, U-, H- or hollow rectangular section, respectively. More serious than the larger scatter is the lack-of-fit of Eq. (3.69) with respect to the amount of longitudinal reinforcement. Equation (3.69) has been fitted to a database of mainly seismically detailed members, with total reinforcement ratio between 0.1 and 7% (2% on average) and tension reinforcement ratio between 0.1 and 4.8% (on average 0.9%). So it overpredicts the experimental value by 10% on average for members with reinforcement ratio at the lower end of the range and underpredicts it by 40% on average at the upper end.

One would expect the empirical effective stiffness to be a decreasing function of $d_{bL}f_y/(h\sqrt{f_c})$, which is proportional to the last term in Eqs. (3.66) and is known before dimensioning of the longitudinal reinforcement if its diameter has been chosen. However, the increase of the "experimental effective stiffness" with the tension reinforcement ratio – which does not appear in Eq. (3.69) and is proportional to the square of d_{bL}/h– fully masks its dependence on $d_{bL}f_y/(h\sqrt{f_c})$ in the cases when slip from the anchorage beyond the member's end takes place.

3.2.3.4 Flexure-Controlled Ultimate Chord Rotation Under Uniaxial Loading: Calculation from Curvatures and the Plastic Hinge Length

The ultimate condition in terms of deformations is commonly defined conventionally, as described in Sections 3.2.2.4 and 3.2.2.7 for the ultimate curvature. The ultimate chord rotation occurs at the same time as the ultimate curvature and is defined similarly.

The most common model for the ultimate chord rotation at the member end (let's say A) where the moment is maximum (Fig. 3.32) uses the yield and ultimate curvatures at section A and assumes that at ultimate conditions the plastic part of the curvature is constant and equal to $\varphi_u - \varphi_y$ over a length L_{pl} next to the end section at A. This means that the real distribution of plastic curvatures, which is nearly triangular over the length of plastification l_{pl}, is replaced by a uniform plastic curvature over a shorter length $L_{pl} \approx 0.5l_{pl}$. L_{pl} is called "plastic hinge length" and is a conventional quantity. The plastic rotation that has developed in the plastic hinge length by the time the ultimate condition is reached is equal to $\theta_{pl,u} = (\varphi_u - \varphi_y)L_{pl}$. It takes place with respect to the centre of the plastic hinge length and produces a plastic part of the deflection at the end B of the shear span equal to $\theta_{pl}(L_s - L_{pl}/2)$. If the entire deflection at B is attributed to flexure, its elastic part is equal to $\varphi_y {L_s}^2/3$. Therefore, the ultimate chord rotation at end A is equal to $\theta_A = \delta_B/L_s$, i.e. to:

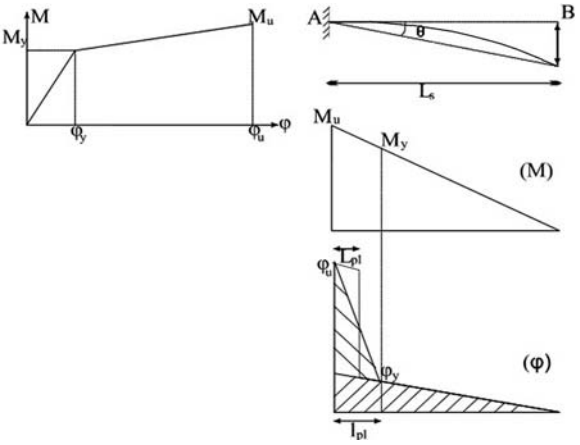

Fig. 3.32 Actual plastification length, l_{pl} and plastic hinge length L_{pl} in the shear span

$$\theta_u = \varphi_y \frac{L_s}{3} + \left(\varphi_u - \varphi_y\right) L_{pl} \left(1 - \frac{L_{pl}}{2L_s}\right) \tag{3.70a}$$

A variant of Eq. (3.70a) may give the chord rotation at end A, θ, when the curvature φ at A is between yielding and ultimate:

$$\theta = \varphi_y \frac{L_s}{3} + \left(\varphi - \varphi_y\right) L_{pl} \left(1 - \frac{L_{pl}}{2L_s}\right) \tag{3.70b}$$

If the behaviour is postulated to be purely flexural, the chord rotation at yielding equals $\theta_y = \varphi_y L_s/3$. So, the chord rotation ductility factor, $\mu_\theta = \theta/\theta_y$, is linked to the curvature ductility factor of the end section of the shear span, $\mu_\varphi = \varphi/\varphi_y$, as:

$$\mu_\theta = 1 + \left(\mu_\phi - 1\right) \frac{3L_{pl}}{L_s} \left(1 - \frac{L_{pl}}{2L_s}\right) \approx \frac{3L_{pl}}{L_s} \mu_\phi \tag{3.71}$$

The formulation in Eqs. (3.70) and (3.71) offers the following advantages:

- it represents a mechanical and physical model (inelasticity is considered as lumped in the plastic hinge and uniformly spread within the plastic-hinge length), and
- φ_y and φ_u can be expressed through plane section analysis in terms of cross-section and material properties, as in Sections 3.2.2.2 and 3.2.2.4, respectively.

This formulation normally deals indirectly with any effects of shear, bond-slip, etc., through L_{pl}, which is not a physical but a conventional quantity, such that Eq. (3.70a) is satisfied when the ultimate deformation is attained.

Notwithstanding its mechanical and physical appeal, the real criterion for the value of Eq. (3.70a) is its ability to predict the experimental ultimate drift ratio or chord rotation, θ_u. Empirical expressions for L_{pl} needed to this end cannot be developed independently of the models used for the other variables in Eq. (3.70a), notably for φ_u and φ_y. To maintain the apparent rationality of Eq. (3.70a), priority should be given to models based on rational mechanics. A natural choice for φ_y is the model in Section 3.2.2.2, based on first principles and calibrated for good average agreement with test results. Regarding φ_u, a good choice is the model in Section 3.2.2.4 (also based on first principles) in conjunction with the proposals developed/calibrated in Section 3.2.2.10 on the basis of a large volume of test data. Those proposals include the use of the confinement model of Eqs. (3.4), (3.5), (3.10), (3.16) or (3.17) and of the ultimate steel strain, ε_{su}, from Eqs. (3.64).

A better overall fit of Eq. (3.70a) to the data on θ_u is possible, if the chord at yielding, θ_y, from Eqs. (3.66) in Section 3.2.3.2 is used in lieu of the flexural term, $\varphi_y L_s/3$, alone. Besides, to recognise the contribution of the fixed-end rotation due to bar pull-out from the anchorage zone beyond the end of the member where failure takes place, we should add to the right-hand-side of Eq. (3.70a) the fixed-end rotation that takes place between yielding and ultimate curvature of the end section, from Eqs. (3.63) in Section 3.2.2.9. The final expression is:

$$\theta_u = \theta_y + a_{sl}\,\Delta\theta_{u,slip} + (\varphi_u - \varphi_y) L_{pl} \left(1 - \frac{L_{pl}}{2L_s}\right) \tag{3.72}$$

The 1st term in Eq. (3.72) is the chord rotation at yielding from Eqs. (3.66). The 2nd one is the fixed-end rotation from yielding to ultimate due to bar slippage from the anchorage zone beyond the member end where flexural failure takes place. It may be calculated from Eqs. (3.63), with $a_{sl} = 0$ if bar slippage from the anchorage zone beyond the member end is not physically possible, or with $a_{sl} = 1$ if it is (cf. 3rd term in Eqs. (3.66)). The 3rd term is the plastic deformation of the flexural plastic hinge.

The same empirical expression for L_{pl} cannot fit both the monotonic and the cyclic data. Best among the possible simple expressions for L_{pl} seem to be a linear combination of the shear span, L_s, and of the section depth, h. Under the conditions outlined above for the calculation of φ_y, φ_u, θ_y, the following expressions provide optimal overall fit to θ_u at flexural failure of rectangular beams, columns and walls and for members with T-, H-, U- or hollow rectangular section, in monotonic or cyclic loading (about 300 or 1050 tests, respectively):

– if the ultimate concrete strain is given by the two separate expressions of Eqs. (3.16) for monotonic and cyclic loading (Biskinis 2007):

  • for monotonic loading, regardless of detailing for earthquake resistance:

$$L_{pl,mon} = h\left(1.1 + 0.04 \min\left(9; \frac{L_s}{h}\right)\right) \tag{3.73a}$$

- for cyclic loading, but with member detailing for earthquake resistance:

$$L_{pl,cy} = 0.2\,h\left(1 + \frac{1}{3}\min\left(9; \frac{L_s}{h}\right)\right) \tag{3.73b}$$

– if the ultimate concrete strain is given by the same expression for monotonic and cyclic loading, Eq. (3.17):

- for monotonic loading, regardless of detailing for earthquake resistance:

$$L_{pl,mon} = h\left(1.2 + 0.04\min\left(9; \frac{L_s}{h}\right)\right) \tag{3.74a}$$

- for cyclic loading, but with member detailing for earthquake resistance:

$$L_{pl,cy} = 0.2\,h\left(1 + \frac{3}{8}\min\left(9; \frac{L_s}{h}\right)\right) \tag{3.74b}$$

If Eqs. (3.16) and (3.73) are used, the test-to-prediction ratio of Eq. (3.72) has a median of 1.00 and coefficient of variation of 66.8, 44.8 and 51.7%, for monotonic, cyclic loading and overall (monotonic and cyclic), respectively. Better overall agreement is achieved if Eqs. (3.17) and (3.74) are used instead of Eqs. (3.16) and (3.73): the median of the test-to-prediction ratio is also 1.00 and the coefficient of variation 65.6, 43.5 and 50.5%, for monotonic, cyclic loading and overall (monotonic and cyclic), respectively. Besides, the median is 1.07 and 1.03 for the sub-groups of rectangular walls and members with T-, H-, U- or hollow rectangular section, compared to medians of 1.08 and 1.05 for these two sub-groups if Eqs. (3.16) and (3.73) are used. Natural and test-to-test variability contributes to the scatter a coefficient of variation of about 18% in practically identical specimens. After subtracting this source of scatter, the coefficient of variation due to model uncertainty is equal to the values quoted above, reduced by 2.5% for the larger of these values to 3.5% for the smaller ones. But even after this reduction, the variance of the cyclic data with respect to Eq. (3.72) is still about 80% of their total variance if Eqs. (3.16) and (3.73b) are used, or about 75% of its value if Eqs. (3.17) and (3.74b) are applied. The picture is only slightly better for the monotonic data.

Well known or widely used alternatives for the plastic hinge length can be evaluated on the basis of the data used for the fitting of Eqs. (3.73) and (3.74). Each expression for L_{pl} is applied here as proposed in its source, i.e., with its accompanying models for the calculation of φ_{u} and Eq. (3.70a) (or variations thereof) instead of Eq. (3.72), as slippage of reinforcement from its anchorage zone is reflected by a separate term in these expressions for L_{pl}, in lieu of the 2nd term at the right-hand-side of Eq. (3.72).

I. The first two expressions evaluated here are those given in Annex A of Part 3 of Eurocode 8 (CEN 2005a) for cyclic loading of members detailed for earthquake

resistance. According to CEN (2005a) these expressions are meant to be used in Eq. (3.70a), but with the full expression for θ_y from Eqs. (3.66) instead of the flexure-only yield term, $\varphi_y L_s/3$. The ultimate steel strain values specified in CEN (2005a) for the calculation of φ_u have been given at the end of Section 3.2.2.10 under point (a). A different expression is given in CEN (2005a) for L_{pl}, for each one of the two alternative concrete confinement models in CEN (2005a):

i for the model of Eqs. (3.4), (3.5), (3.10) and (3.18):

$$L_{pl} = \frac{L_s}{30} + 0.2\,h + a_{sl}\frac{0.11 d_{bL} f_{yL}}{\sqrt{f_c}} \qquad (f_{yL} \text{ and } f_c \text{ in MPa}) \qquad (3.75)$$

ii. for the model of Eqs. (3.8), (3.9) and (3.13) (i.e., according to CEN (2004b), CEB (1991)):

$$L_{pl} = 0.1 L_s + 0.17\,h + a_{sl}\frac{0.24 d_{bL} f_{yL}}{\sqrt{f_c}} \qquad (f_{yL} \text{ and } f_c \text{ in MPa}) \qquad (3.76)$$

Options (i) and (ii) produce a median test-to-prediction ratio for θ_u in over 1000 cyclic tests of rectangular beams, columns, walls and members with T-, H-, U- or hollow rectangular section under cyclic loading equal to 0.90 and 0.79, respectively. The corresponding coefficients of variation are 52.5 and 62.1% (Biskinis 2007). The poorer performance of option (ii) (which includes also a certain lack of fit for high experimental values of θ_u) is mainly due to its serious handicap in the prediction of ultimate curvature (see Section 3.2.2.10, point (a)).

II. The other model evaluated here is the widely used and quoted expression (Paulay and Priestley 1992):

$$L_{pl} = 0.08 L_s + a_{sl}(0.22 d_{bL} f_{yL}) \qquad (f_{yL} \text{ in MPa}) \qquad (3.77)$$

It is used in Eq. (3.70a), along with the σ-ε models and parameters for the calculation of φ_u outlined at the end of Section 3.2.2.10 under point (b), namely:

- the two concrete confinement models in Mander et al. (1988) and Paulay and Priestley (1992) and
- the two ultimate steel strain options for which the ultimate curvature predictions resulting from the above confinement models have been evaluated at the end of Section 3.2.2.10 under point (b), namely:

  a. the ultimate steel strain in Annex A of Part 3 of Eurocode 8 (CEN 2005a) and described in Section 3.2.2.10, point (a); this is the strain used in the evaluation above pertaining to Part 3 of Eurocode 8 (CEN 2005a), for both options (i) and (ii); or
  b. the values from Eqs. (3.64) in Section 3.2.2.10; used also above in the calculation of θ_u from Eq. (3.72) together with Eqs. (3.73) and (3.74) and the concrete ultimate strain models of Eqs. (3.16) and (3.17), respectively.

The confinement model in Mander et al. (1988) combined with options (a) or (b) for steel give a median test-to-prediction ratio for θ_u in over 1000 cyclic tests of rectangular beams, columns, walls or members with T-, H-, U- or hollow rectangular section equal to 0.96 or 1.14, respectively. The corresponding coefficient of variation is 74.9% or 65.5% (Biskinis 2007). The median and the coefficient of variation of the test-to-prediction ratio for the confinement model in Paulay and Priestley (1992) used with options (a) or (b) for steel are 0.83 or 1.035 and 83.6% or 70.9%, respectively (Biskinis 2007). These four options give a median test-to-prediction ratio for the approximately 300 monotonic tests between 1.7 and 1.85.

Note that, for all options considered in I and II above the variance of the cyclic data with respect to Eq. (3.72) is not less than their total variance, even after removing the contribution of natural and test-to-test variability from the scatter. So, none of these options seems to be of much value for the prediction θ_u.

3.2.3.5 Flexure-Controlled Ultimate Chord Rotation Under Uniaxial Loading: Empirical Calculation

The scatter of the predictions of Eq. (3.72), used together with Eqs. (3.73) and (3.74) and the corresponding ultimate concrete strains, Eqs. (3.16) and (3.17), respectively, is significant. Even larger is that of Eq. (3.70a), used together with Eqs. (3.75), (3.76) and (3.77) and the corresponding concrete confinement and steel ultimate strain models. In view of this, purely empirical expressions for the chord rotation at flexural failure, θ_u, have been developed in Panagiotakos and Fardis (2001a). That work has shown:

- that θ_u depends on whether loading to failure is monotonic or fully-reversed (cyclic), but is rather insensitive to the number of major deflection cycles preceding failure;
- that monotonic test data should be distinguished from the cyclic, but used together in regressions for θ_u, as complementary: monotonic tests in the literature cover many members with asymmetric reinforcement and/or less ductile steel, but few walls or members with T-, H-, U- or hollow rectangular section and no diagonally reinforced elements; the reverse applies for the available cyclic tests;

As a follow up and improvement over (Panagiotakos and Fardis 2001a), a larger databank of test results has been used in Biskinis (2007) and Biskinis and Fardis (2004, 2007) to develop three alternative – and almost equivalent – expressions for the chord rotation at flexure-controlled failure, θ_u, of members with rectangular compression zone and detailing for earthquake resistance (including the use of continuous ribbed bars for the longitudinal reinforcement). The first one, Eq. (3.78a), is for the total ultimate chord rotation, θ_u. Equations (3.78b) and (3.78c) by contrast separate θ_u into its elastic component, θ_y, given by Eqs. (3.66), and the plastic one, $\theta_u{}^{pl} = \theta_u - \theta_y$.

$$\theta_u = a_{st}(1 - 0.43a_{cy})\left(1 + \frac{a_{sl}}{2}\right)(1 - 0.42a_{w,r})\left(1 - \frac{2}{7}a_{w,nr}\right)(0.3^{\nu})$$
$$\left[\frac{\max\,(0.01;\,\omega_2)}{\max\,(0.01;\,\omega_1)}f_c\right]^{0.225}\left[\min\left(9;\,\frac{L_s}{h}\right)\right]^{0.35}25^{\left(\frac{a\rho_s f_{yw}}{f_c}\right)}1.25^{100\rho_d} \tag{3.78a}$$

$$\theta_u = \theta_y + \theta_u^{pl} = \theta_y + a_{st}^{pl}(1 - 0.52a_{cy})$$
$$\left(1 + \frac{a_{sl}}{1.6}\right)(1 - 0.44a_{w,r})\left(1 - \frac{a_{w,nr}}{4}\right)(0.25)^{\nu}\left(\frac{\max(0.01;\,\omega_2)}{\max(0.01;\,\omega_1)}\right)^{0.3}$$
$$f_c^{0.2}\left[\min\left(9;\,\frac{L_s}{h}\right)\right]^{0.35}25^{\left(\frac{a\rho_s f_{yw}}{f_c}\right)}1.275^{100\rho_d} \tag{3.78b}$$

$$\theta_u = \theta_y + \theta_u^{pl} = \theta_y + a_{st}^{hbw}(1 - 0.525a_{cy})$$
$$(1 + 0.6a_{sl})\left(1 - 0.052\max\left(1.5;\min\left(10,\,\frac{h}{b_w}\right)\right)\right)(0.2)^{\nu}$$
$$\left[\frac{\max(0.01;\,\omega_2)}{\max(0.01;\,\omega_1)}\min\left(9;\,\frac{L_s}{h}\right)\right]^{\frac{1}{3}}f_c^{0.2}25^{\left(\frac{a\rho_s f_{yw}}{f_c}\right)}1.225^{100\rho_d} \tag{3.78c}$$

where:

a_{st}, $a^{pl}{}_{st}$, $a^{hbw}{}_{st}$: coefficients for the steel type: $a_{st} = a^{pl}{}_{st} = 0.0185$ and $a^{hbw}{}_{st} = 0.022$ for ductile hot-rolled or heat-treated (Tempcore) steel; $a_{st} = 0.0115$, $a^{pl}{}_{st} = 0.009$ and $a^{hbw}{}_{st} = 0.0095$ for cold-worked steel;

a_{cy}: zero-one variable for the type of loading, equal to $a_{cy} = 0$ for monotonic loading and to $a_{cy} = 1$ for cyclic loading;

a_{sl}: zero-one variable for slip, equal to $a_{sl} = 1$ if there is slip of the longitudinal bars from their anchorage beyond the section of maximum moment, or to $a_{sl} = 0$ if there is not (cf. Eqs. (3.66) and (3.72));

$a_{w,r}$: zero-one variable for rectangular walls, $a_{w,r} = 1$ for rectangular walls, $a_{w,,r} = 0$ otherwise;

$a_{w,nr}$: zero-one variable for non-rectangular walls, $a_{w,nr} = 1$ for walls with T-, H-, U- or hollow rectangular section and $a_{w,nr} = 0$ for other members;

$\nu = N/bhf_c$, with b = width of compression zone, N = axial force, positive for compression;

$\omega_1 = (\rho_1+\rho_v)f_{yL}/f_c$: mechanical reinforcement ratio of tension and "web" longitudinal reinforcement;

$\omega_2 = \rho_2 f_{yL}/f_c$: mechanical reinforcement ratio of compression longitudinal reinforcement;

f_c: uniaxial (cylindrical) concrete strength (MPa);

$L_s/h = M/Vh$: shear span ratio at the section of maximum moment;
$\rho_s = A_{sh}/b_w s_h$: ratio of transverse steel parallel to the loading direction;
f_{yw}: yield stress of transverse steel;
a: effectiveness factor for confinement by transverse reinforcement from Eq. (3.24) (using Eqs. (3.20c) and (3.21));
ρ_d: steel ratio of diagonal reinforcement in each diagonal direction.
b_w: width of one web, even in cross-sections with one or more parallel webs (for Eq. (3.78c) which distinguishes walls and members with T-, H-, U- or hollow rectangular section only through the aspect ratio, h/b_w, of each web).

Annex A of Eurocode 8, Part 3 (CEN 2005a) has adopted the special case of Eqs. (3.78a) and (3.78b) for cyclic loading ($a_{cy} = 1$) and slippage of the longitudinal bars from their anchorage beyond the section of maximum moment ($a_{sl} = 1$), but with a different value of the coefficient multiplying $a_{w,r}$ for walls: 0.40, in lieu of 0.42 or 0.44.

The dependence of θ_u on h/b_w according to Eq. (3.78c) suggests that the lower ultimate deformation of non-rectangular walls and mainly of rectangular ones, compared to beams or columns with more compact section, may be due to lateral instability.

Equations (3.78b) and (3.78c) can be extended more easily than Eq. (3.78a) to variations of the standard case of unretrofitted members with continuous longitudinal bars. Lap-splicing of longitudinal bars within the plastic hinge region (see Section 3.2.3.9) and/or wrapping of the end region with an FRP jacket (see Section 3.2.3.10) affect differently the elastic and the plastic part of the ultimate chord rotation and should be accounted for accordingly.

For the subsets of 300 monotonic and 1040 cyclic tests available, as well as overall, each one of Eqs. (3.78) give a median test-to-prediction ratio for θ_u of (effectively) 1.00. The coefficient of variation of the test-to-prediction ratio in the monotonic tests is 53.3%. In the 1040 cyclic tests the corresponding values are 37.4, 37.3 and 38%. For the overall 1340 monotonic or cyclic tests the coefficient of variation of the test-to-prediction ratio is 42.4%. For the subgroup of 62 rectangular walls, Eq. (3.78a), (3.78b) or (3.78c) give a median test-to-prediction ratio of 1.00 and a coefficient of variation of 33.6, 33.1 and 37.5%. For 55 members with T-, H-, U- or hollow rectangular section, either Eq. (3.78a) or (3.78b) give a median test-to-prediction ratio of 1.00 and coefficients of variation of 33 and 31.5%, while Eq. (3.78c) gives a median of 1.07 and a coefficient of variation of 28.6%.

Although Eqs. (3.78) give a fairly uniform scatter throughout the full range of all independent variables, they underpredict high values of θ_u, especially for monotonic loading, and overpredict low ones. They share this lack of fit with any model in Section 3.2.3.4 based on curvatures and the plastic hinge length. In all cases Eqs. (3.78) give a less biased and more accurate estimate of θ_u than anyone of the models in Section 3.2.3.4. The scatter of the test-to-prediction ratio is much less, notably not much larger than that of Eqs. (3.66) for the chord rotation at yielding, and not unduly large compared to the contribution of the natural or test-to-test variability, which gives a coefficient of variation of about 18% for θ_u of practically

identical specimens. After subtracting this source of scatter, the coefficient of variation due to model uncertainty is equal to the values quoted above, reduced by about 3% for the larger of these values to 5% for the smaller ones. After this reduction, the variance of the cyclic data with respect to Eqs. (3.78a), (3.78b) or (3.78c) is 36.5%, 41.5% or 41%, respectively of their total variance. The corresponding variances of the monotonic data values are 43, 44.5 and 46%, respectively. So, Eqs. (3.78) perform better than any of the models in Section 3.2.3.4.

The few data for members without detailing for earthquake resistance (e.g., not closed stirrups), but with continuous ribbed (deformed) longitudinal bars, show that their chord rotation at flexure-controlled failure may be obtained by the following modification of Eqs. (3.78) (Biskinis 2007):

$$\theta_{u,old} = \theta_{u,Eq.(3.78a)} / 1.2, \text{ or} \tag{3.79a}$$

$$\theta_{u,old} = \theta_y + \theta^{pl}_{u,Eq.(3.78b) \text{ or } Eq.(3.78c)} / 1.2 \tag{3.79b}$$

Annex A of Eurocode 8, Part 3 (CEN 2005a) has adopted a version of Eqs. (3.79) with factor $1/1.2 = 0.833$ replaced by 0.825.

For about 50 cyclic tests of members without detailing for earthquake resistance but with continuous ribbed longitudinal bars, Eq. (3.79a) and (3.79b) (the latter with $\theta_u{}^{pl}$ from Eq. (3.78c)) give a median of 1.00 for the test-to-prediction ratio and a coefficient of variation of 30.8%. The corresponding values for Eq. (3.79b) with $\theta_u{}^{pl}$ from Eq. (3.78b) are 0.99 and 32.2% (Biskinis 2007). The Eurocode 8-Part 3 versions give medians higher than the above by 0.01.

Few (about 30) available cyclic tests of members without detailing for earthquake resistance and continuous smooth (plain) longitudinal bars suggest the following expression for the chord rotation at flexure-controlled failure, giving a median of 1.00 and a coefficient of variation of 32.7% for the test-to-prediction ratio:

$$\theta_{u,smooth} = 0.95\,\theta_{u,Eq.(3.79)} \tag{3.80}$$

3.2.3.6 Member Axial Deformations Due to the Flexural Response

When the curvature increases from zero to φ, the axial strain at mid-depth of a section changes by:

$$\Delta\varepsilon_o = |\varphi|(0.5 - \xi)d \tag{3.81}$$

If the axial load on the cross-section is zero or low (as in beams or in walls, respectively), the neutral axis depth, normalised to the effective depth d as ξ, is less than 0.5. It may even become negative during the phase of the response when the cracks are open through the depth and the steel couple alone resists the applied moment. Because ξ increases with increasing axial force ratio, ν, the higher the value of ν, the lower is the additional elongation (as a comparison between

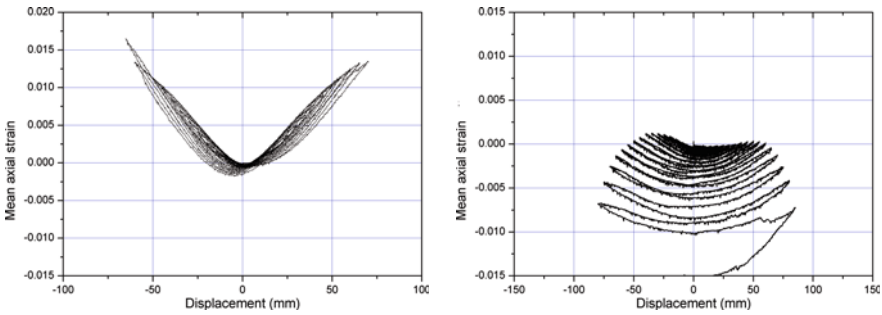

Fig. 3.33 Axial strain at section mid-depth due to cycling of the lateral displacement: (**a**) column with low axial force that does not fail; (**b**) column with high axial load ultimately failing in bending

Fig. 3.33(a) and (b) shows). If ν exceeds the balance load, the value of ξ exceeds 0.5 and the axial strain at mid-depth of the cross-section turns into shortening.

At each displacement cycle an axial *extension* normally accompanies the development of curvature, regardless of the sign of curvature. Except during the phase when cracks are open through the depth, the value of ξ is approximately constant along the member and the total additional axial displacement between two sections A and B of the member is equal to:

$$\Delta\delta_x = \int_l \Delta\varepsilon_o \, dx = (0.5 - \xi)d \int_l |\varphi| dx = (0.5 - \xi)\theta_{AB} d \tag{3.82}$$

where θ_{AB} is the relative rotation of sections A and B.[12] Equation (3.82) shows that the maximum additional axial extension takes place when relative rotation attains its peak value and is proportional to it.

The axial extension given by Eqs. (3.81) and (3.82) is additional to any axial deformation that may exist during the "neutral" part of the loading cycle, i.e. when the section curvature, φ, is (about) zero. At that stage through-depth cracks may be open and the total axial strain at mid-depth of the section, ε_o, is the average of the permanent strains locked in the tension and the compression reinforcement. These permanent strains are normally tensile (see the values of strain in Figs. 3.5, 3.6 and 3.7 at zero stress, after several load cycles). In beams, or in columns and walls with low axial load, the tensile strain at mid-depth of the section may be significant in magnitude and increase in a ratcheting manner during cycling of the deflection (see evolution of axial displacements at the bottom left diagram of Fig. 3.34). In columns, after the cover spalls, the concrete core partially disintegrates and/or vertical bars buckle, the mean compressive stress of the concrete increases and normally turns the axial strain, ε_o, at section mid-depth during the "neutral" part of the loading cycle from extension to shortening. Axial shortening accelerates as failure due to cyclic

[12] If moments and curvatures change sign between sections A and B, θ_{AB} is not the angle between the tangent to the member axis at these two sections, but the sum of the absolute values of relative rotations between section A and the point of inflection and between the point of inflection and section B.

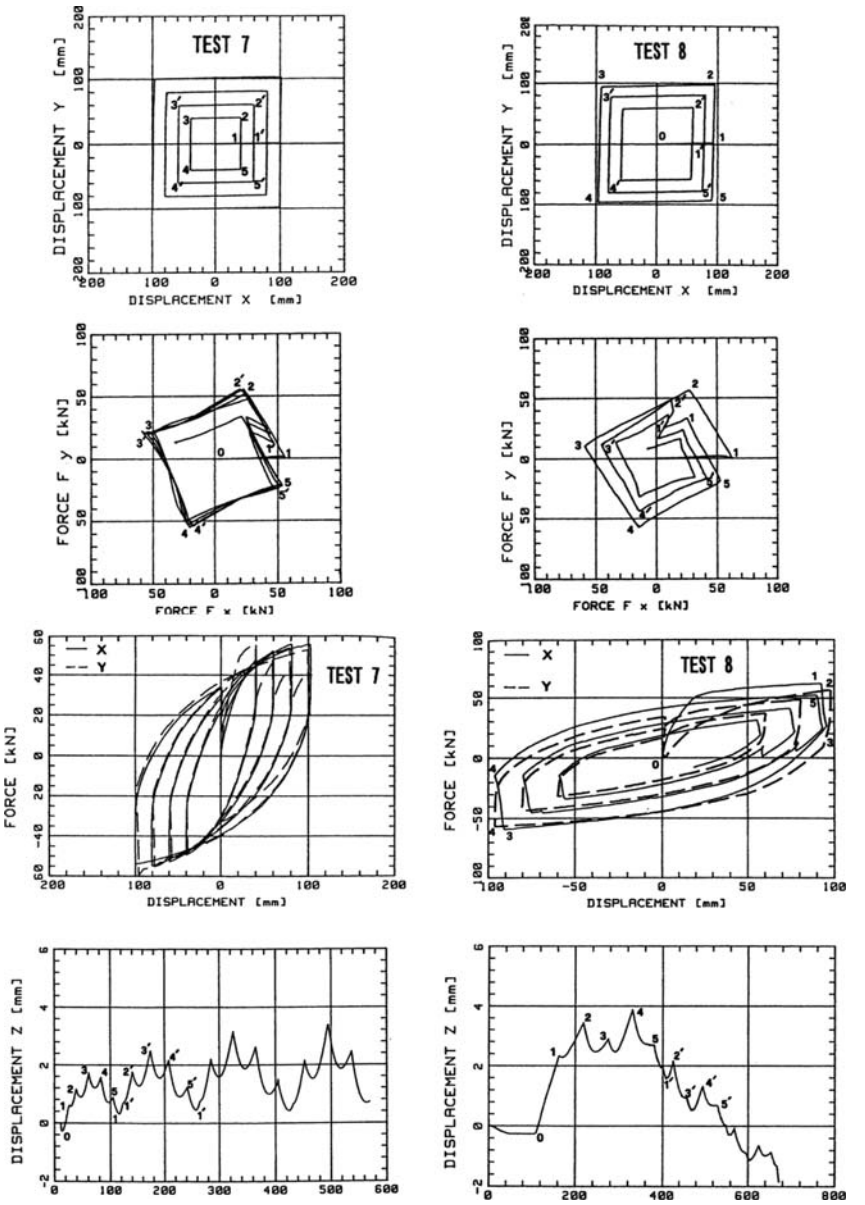

Fig. 3.34 Column biaxial deflection paths (**a**), (**b**), resulting biaxial force paths (**c**), (**d**), force-deflection loops in the two lateral directions (**e**), (**f**), evolution of axial displacement (**g**), (**h**) (Bousias 1993)

loading approaches (Fig. 3.33(b)). So, what has started as accumulation of tensile axial strains at the axis of the column may at the end of the cyclic load history revert into net shortening (see evolution of axial displacements at the bottom right diagram of Fig. 3.34). Moreover, if the axial load ratio ν has intermediate values (e.g., above 0.2), from the very beginning of the cyclic loading the ratcheting axial strain at mid-depth of the column section, ε_o, during the "neutral" part of the loading cycle is shortening instead of elongation (Fig. 3.33(b)).

Unlike the axial strain of Eq. (3.81) that may refer to the full length and produces a net axial elongation at the peak of the lateral displacement cycle according to Eq. (3.82), ratcheting axial strains that develop during the "neutral" (low-displacement) part of the load cycle according to the previous paragraph take place only within the plastic hinge. Therefore, their overall effect on the length of the member is normally smaller than the additional net elongation of Eq. (3.82) at the peaks of the cyclic lateral displacement history.

There is another facet of the coupling between flexural and axial behaviour, notably the effect of the variation of axial force on flexural deformations: for constant moment, the reduction of flexural deformation due to an increase in the axial compression is less than its increase due to an axial force reduction by the same amount. So, cycling of the axial force causes a ratcheting increase of flexural deformations. Their cumulative magnitude is significant in comparison to the residual flexural deformations due to cycling of the moment itself (Bousias et al. 1992, 1995). The build-up of flexural deformations due to an axial force that varies concurrently with the bending moments amounts to a gradual, albeit significant, apparent degradation of flexural stiffness.

According to Eq. (3.82) walls with large effective depth, d, develop large net elongation at the centroid of the section concurrently with the peaks of their lateral displacements response. We have seen in Section 2.2.2.4 that the effects of such elongation on the response and performance of wall or wall-equivalent dual systems are beneficial.

Compared to walls, columns have much shorter effective depth, d, and larger values of ξ. So, the peaks of their lateral displacement response are accompanied by small additional elongation according to Eq. (3.82). This additional elongation brings about an increase in the axial compression of those columns that have larger size (effective depth, d), smaller ξ-value (i.e., lower axial load ratio, ν) and/or larger deformation response (relative rotation between sections, θ_{AB}) than the other columns, especially their neighbouring ones. The increase in axial compression of these columns will be counterbalanced by a reduction in the others, effected through shear forces in the beams connecting the columns in the 3D frame structural system. Although small, the increase in axial compression is detrimental for the performance of large, lightly loaded columns with the larger deformation response, as it reduces their ultimate flexural deformation. By contrast, the net shortening of the columns with fairly heavy axial load (with axial load ratio well above 0.2), or of any column that approaches its ultimate deformation capacity, has a beneficial effect, as it causes part of the axial load to be transferred – via shear forces in the beams – to other columns of the system.

Beams have about the same effective depth, d, as columns but much smaller ξ-values. So, the additional net elongation according to Eq. (3.82) accompanying the peaks of their flexural response is larger. The columns into which a beam frames restrain this axial extension through shear forces translated into a compressive axial force in the beam. This compressive force will not only tend to reduce its axial extension, but will also affect its flexural behaviour, increasing its stiffness and strength, etc.

The three paragraphs above have pointed out the coupling between the flexural and the axial behaviour of the members of real frames or dual structural systems. This coupling is not taken into account explicitly in practical seismic design. To account for it in a nonlinear seismic response analysis, a member model should capture not only the flexural behaviour, but also the axial one, including its coupling with the flexural response. Fibre models, described in Section 4.10.1.2, have this capability.

3.2.3.7 Flexural Behaviour Under Cyclic Biaxial Loading

The behaviour of axially loaded concrete members under biaxial moment histories is important, as in general the seismic response of columns in concrete frames is in three dimensions (3D). Biaxial flexure reduces the moment resistance in any of the two principal directions of bending and increases cyclic strength degradation compared to uniaxial loading. By contrast, the beams of 3D frame systems are subjected to uniaxial flexure and do not suffer from the adverse effects of biaxial loading. So, biaxial column moments and the 3D response work against strong-column/weak-beam behaviour and reduce the effectiveness of the relevant criterion, Eq. (1.4), applied separately in two orthogonal horizontal directions in 3D frames.

Test results on axially loaded members under biaxial bending moment histories are limited. So, as the manner in which the histories of bending moments in the two orthogonal directions are combined adds considerably to the complexity of the problem, current knowledge of the inelastic behaviour of columns under biaxial cyclic moments is well behind our understanding of their behaviour in uniaxial cyclic flexure with axial load.

The available test results point to the conclusion that after flexural yielding there is strong coupling of the behaviour in the two orthogonal directions of bending. The M–φ and M–θ response in one of these directions is affected by the magnitude and the history of the moment and/or deformation in the orthogonal direction. The main effects of this coupling on the M–φ and M–θ behaviour in each of the two orthogonal directions of bending are the following:

1. The apparent resistance and stiffness in each individual direction decrease, owing to a concurrent deformation in the orthogonal direction. So, the moment component required to maintain a given deformation in the same direction drops (Fig. 3.34). Similarly, the moment increment necessary for an increment in deformation decreases. Ratcheting flexural deformations in the direction of a moment

component that is maintained constant are induced by cycling of the deformation in the orthogonal direction (Bousias 1993, Bousias et al. 1992, 1995).

2. The hysteretic energy dissipation increases, as hysteresis loops in each individual direction become broader (e.g., when the peak resistance in a cycle drops under constant deformation in its own direction, owing to an increase in moment and deformation in the orthogonal direction, Fig. 3.34). If the response is described in terms of a path in the 2D space of the two components of bending moment and the concurrent path in the 2D space of the two deformation components, the deformation vector always trails the moment vector by a "phase lag", ψ (Fig. 3.34). The increase in hysteretic energy dissipation due to the coupling of the two components can be expressed as an equivalent viscous damping ratio equal to $\sin\psi$ (Bousias et al. 1992, 1995). The "phase lag", ψ, increases with inelasticity, i.e. with the magnitude of the post-yield excursion, especially when column failure is imminent.
3. The deformation capacity in each individual direction decreases. When a flexure-controlled ultimate deformation is reached (i.e., when the resultant of the two moment components cannot increase above 80% of the peak moment resultant reached so far during the biaxial response) the individual deformation components are lower than they would had been, if flexure-controlled ultimate deformation were attained by uniaxial loading in the corresponding lateral direction.

Effects no. 1 and 3 are adverse, but effect no. 2 is beneficial.

The additional axial extension accompanying biaxial flexural deformations roughly follows Eqs. (3.81) and (3.82) in Section 3.2.3.6 and is independent of the direction of the lateral displacement. The same applies for the ratcheting axial strains (extension for low values of axial load ratio, shortening for medium or high ones) that accumulate due to cycling of the deflections. The axial displacements at the bottom of Fig. 3.34 increase in a ratcheting manner during cycling of the lateral displacement. At the diagram on the right the axial extension turns at the end of the load history to shortening as failure due to cyclic loading approaches.

Loading along the diagonal of the cross-section may be considered as simultaneous equal biaxial loading parallel to the sides of the section. When presented in terms of moment and deformation components along the sides of the cross-section, the behaviour appears to give a reduced (by about $\sqrt{2}$) strength and stiffness compared to uniaxial loading and accordingly reduced energy dissipation. If presented, however, in terms of the resultant moment and deformation along the single direction of loading, hysteresis loops are similar to those in uniaxial loading, with about the same or even sometimes enhanced strength and energy dissipation capacity. This applies in general for any loading in a single transverse direction oblique to the sides of the section.

Except when the axial load varies near the balance load, the variation of the axial force with both components of the biaxial moment/deformation affects the flexural response in both lateral directions as in the uniaxial case. When the axial compression increases, the instantaneous resistance and stiffness increase, strength decay with cycling accelerates and deformation capacity is reduced. Reduction of the

axial compression has the opposite effects. Variation of the axial load only with one component of the moment/deformation affects the resistance, stiffness and cyclic strength decay, mainly in the corresponding lateral direction.

3.2.3.8 Flexural Yielding and Flexure-Controlled Ultimate Chord Rotation Under Cyclic Biaxial Loading

Test results of columns under cyclic biaxial bending with axial force are sparse, owing to the practical difficulties of such testing. Yielding in such tests may be identified with the corner of a bilinear M–θ envelope of the experimental monotonic M–θ curve or of the M–θ hysteresis loops, separately for each one of the two directions of bending, y and z. The so-determined components, $M_{\mathrm{yy,exp}}$ and $M_{\mathrm{yz,exp}}$, of the experimental yield moment in 35 flexure-dominated biaxial tests in which yielding had taken place under biaxial loading, have been compared with the components of the biaxial moment resistance. These components have been computed from plane-section analysis, using an elastic-perfectly plastic σ-ε law for the reinforcing bars (at their exact location in the section) and a parabolic-rectangular one for the concrete, up to a compressive strain of 0.0045 at one corner of the cross-section.[13] Both of the so-computed components of moment resistance gave a mean test-to-prediction ratio of 1.0, which is better than what has been achieved for uniaxial bending in Section 3.2.2.2, where section yielding was identified with yielding of the extreme tension bars or with a fixed concrete strain at the extreme compression fibres for linear-elastic concrete in compression. This confirms that the corner of a bilinear M–θ envelop of the measured hysteresis loops, expressing overall section yielding is slightly past yielding of the extreme corner bar or compression fibre.

The uniaxial chord rotations in the two directions of bending, $\theta_{\mathrm{yy,uni}}$, $\theta_{\mathrm{yz,uni}}$, have also been computed from Eqs. (3.66) for these 35 biaxial tests. The experimental values at section yielding, $\theta_{\mathrm{yy,exp}}$, $\theta_{\mathrm{yz,exp}}$, give ratios $\theta_{\mathrm{yy,exp}}/\theta_{\mathrm{yy,uni}}$ and $\theta_{\mathrm{yz,exp}}/\theta_{\mathrm{yz,uni}}$ that on average exceed by a little more than 10% a circular interaction diagram of the form:

$$\left(\frac{\theta_{yy,\mathrm{exp}}}{\theta_{yy,uni}}\right)^2 + \left(\frac{\theta_{yz,\mathrm{exp}}}{\theta_{yz,uni}}\right)^2 = 1 \tag{3.83}$$

The prime role of θ_{y} is for the calculation of the effective stiffness to yield point via Eq. (3.68). Using the values of $M_{\mathrm{yy,exp}}$, $\theta_{\mathrm{yy,exp}}$, and $M_{\mathrm{yz,exp}}$, $\theta_{\mathrm{yz,exp}}$ at the corner of a bilinear envelope M–θ of the experimental monotonic M–θ curve or of the M–θ hysteresis loops, 35 pairs of the "experimental" effective stiffness have been

[13] Except for the value of the terminal strain, these assumptions are the same as those made for the calculation of the uniaxial moment resistance in Section 3.2.2.5. The computed components of the biaxial moment resistance were found to be fairly insensitive to the precise value of this limit strain.

computed from Eq. (3.68), separately in each direction of bending, y or z. They have been compared to:

i. the corresponding effective stiffness computed from Eq. (3.68) separately from $M_{yy,uni}$, $\theta_{yy,uni}$ and $M_{yz,uni}$, $\theta_{yz,uni}$, using the uniaxial yield moment from Section 3.2.2.2 and the chord rotation at yielding from Eq. (3.66), and
ii. the "empirical" effective stiffness from Eq. (3.69),

in the transverse direction, y or z, of interest (Biskinis 2007). The test-to-prediction ratios suggest that the "experimental" effective elastic stiffness in each one of the two directions is about 10% less, on average, than the uniaxial theoretical effective stiffness calculated in (i), i.e. theoretically from Eq. (3.68). By contrast, it exceeds by about 7% the "empirical effective stiffness" in (ii). These trends are opposite and hence inconclusive. However, as the theoretical effective stiffness is more reliable and unbiased than the "empirical" one, the limited test results may be considered to suggest that biaxial loading reduces slightly the effective elastic stiffness in each one of the two directions of loading.

Biaxial tests carried to flexure-controlled failure are also few (about 35). The components of chord rotation along the sides of the section at ultimate in these tests, $\theta_{uy,exp}$ and $\theta_{uz,exp}$, may be normalised to the corresponding ultimate chord rotations in uniaxial loading from:

(a) the semi-empirical procedure of Section 3.2.3.4 (i.e. Eqs. (3.72) and (3.73), together with curvatures according to Sections 3.2.2.4 and 3.2.2.10); and
(b) the purely empirical procedure of Section 3.2.3.5 and Eqs. (3.78).

The test-to-prediction ratio exceeds, on average, the circular interaction diagram:

$$\left(\frac{\theta_{uy,\mathrm{exp}}}{\theta_{uy,uni}}\right)^2 + \left(\frac{\theta_{uz,\mathrm{exp}}}{\theta_{uz,uni}}\right)^2 = 1 \tag{3.84}$$

by about 5% if the uniaxial ultimate chord rotations are calculated according to Eqs. (3.72) and (3.73), etc. or by about 16% if Eqs. (3.78) in Section 3.2.3.5 are used instead (Biskinis 2007, Bousias et al. 2002). Therefore, Eq. (3.84) is safe-sided for the verification of the ultimate chord rotations under biaxial bending, with uniaxial ultimate chord rotations estimated according to Sections 3.2.3.4 or 3.2.3.5.

3.2.3.9 Members with Ribbed Longitudinal Bars Lap-Spliced in the Plastic Hinge Region

Effect of Lap-Splicing on the Yield Properties

It is still common in many parts of the world – including Europe – to lap-splice all vertical bars of columns or walls at floor levels, for convenience of bar fixing.

The seismic parts of the US follow nowadays the good practice of splicing longitudinal bars of vertical elements outside their end regions where plastic hinges may develop. But even there, short lap splices at floor levels are typical of vertical members in existing substandard construction, adversely affecting their resistance and cyclic deformation capacity.

Provided that the lap length is sufficient (i.e., greater than the value giving $f_{sm} = f_y$ in Eq. (3.31) of Section 3.1.3.2, or greater than the limit value in Eq. (3.85) below), the yield moment and the moment resistance of columns with ribbed (deformed) longitudinal bars lapped starting at the column base is clearly higher than in similar members with continuous longitudinal bars (Biskinis and Fardis 2004, Fardis et al. 2005, Bousias et al. 2005a,b). This is thanks to end bearing of a compression bar stopping at the base section against the very well confined concrete beyond (i.e., the concrete at the top of a footing or at the face of 3D joint, etc.), which seems sufficient for the build-up of a compressive stress in that bar almost as high as in its companion bar in the lap that continues beyond the end section. Compatibility of longitudinal strains between these two bars and the concrete surrounding them near the member's end section contributes to this effect. The measured yield moment of such columns compares better with the outcome of Eq. (3.37) in Section 3.2.2.2 under *Cross-Sections with Rectangular Compression Zone* (after correction with the calibration factors given in Section 3.2.2.2 under *Comparison with Experimental Results and Empirical Expressions for the Curvature*), if in the calculation of M_y both bars in any pair of lapped compression bars count towards the compression reinforcement ratio within the lap splice.

The measured secant stiffness to the yield-point is also higher than in a similar member with continuous longitudinal bars. It compares better with the outcome of Eq. (3.68) in Section 3.2.3.3, if in Eq. (3.68):

i. the value of M_y is based on the yield curvature, φ_y, calculated from Eqs. (3.33), (3.34), (3.35) and (3.36) in Section 3.2.2.2 under *Cross-Sections with Rectangular Compression Zone*, including in the compression reinforcement ratio both bars of any pair of lapped bars in the compression zone, and
ii. θ_y is calculated from Eqs. (3.66) with the 1st and 3rd terms there based on the value of φ_y in (i) above and with the 2nd term multiplied by the ratio of the yield moment M_y modified for the lap splicing, to the value of M_y outside the lap splice; moreover, to determine whether $a_V = 1$ in the 1st term of Eqs. (3.66), $L_s V_{Rc}$ is compared to the value of M_y accounting for the effect of lapping.

The recommendations above, adopted also in Part 3 of Eurocode 8 (CEN 2005a), refer to lapped bars in compression. Regarding the lapped tension bars, Eqs. (3.31) and (3.32) in Section 3.1.3.2 may be applied for their maximum possible stress to be used in the calculation of M_y and φ_y. If this is done for over 100 tests on members with rectangular or hollow rectangular section and ribbed bars lapped starting at the section of maximum moment, the test-to-prediction ratio for the yield moment has a median of 0.995 and a coefficient of variation of 11.7% (Biskinis and Fardis 2007). Equations (3.66) may also be applied for the chord rotation at yielding according

to rule (ii) of the previous paragraph. Then, the test-to-prediction ratio of the chord rotation at yielding in over 80 tests has a median of 1.04 and a coefficient of variation of 20.5%. The corresponding statistics for the secant stiffness to the yield-point are 0.935 and 25.4%.

A simpler rule has been proposed in Biskinis and Fardis (2004, 2007) for the maximum possible stress of lapped tension bars and adopted in Part 3 of Eurocode 8 (CEN 2005a). According to it, if the straight lap length, l_o, is less than a minimum value of lap length, $l_{oy,min}$, required for the full transfer of the yield stress of a lapped bar in tension to the continuing one, M_y and φ_y should be calculated with the yield stress of the tension bars, f_{yL}, multiplied by $l_o/l_{oy,min}$. The value of $l_{oy,min}$ is given by the following expression (Biskinis and Fardis 2004, 2007, CEN 2005a):

$$l_{oy,\min} = \frac{0.3 d_{bL} f_{yL}}{\sqrt{f_c}} \qquad (f_{yL} \text{ and } f_c \text{ in MPa}) \tag{3.85}$$

where d_{bL} and f_{yL} are the mean diameter and the yield stress of longitudinal bars, respectively. Again, Eqs. (3.66) are applied for the chord rotation at yielding according to rule (ii) above (Biskinis and Fardis 2004, 2007, CEN 2005a). The test-to-prediction ratio for the so-computed yield moment has a median of 1.00 and a coefficient of variation of 11.6%, that for the chord rotation at yielding a median of 1.05 and a coefficient of variation of 19.9% and the one of the secant stiffness to the yield-point a median of 0.935 and a coefficient of variation of 25.6%. Note that, if $l_o \geq l_{oy,min}$, the value of M_y from Eq. (3.37) and of the secant stiffness to the yield-point from Eq. (3.68) increase owing to the lapping. If $l_o < l_{oy,min}$, both M_y and the secant stiffness to the yield-point decrease with decreasing l_o.

There is very little experimental information about members with short anchorage of the longitudinal bars beyond the end section. Section 3.1.3.2 has pointed out, though, that Eq. (3.31) applies equally well either to a single ribbed bar with straight anchorage length l_b or to two bars lap-spliced over the same length. On this basis, M_y, φ_y and θ_y at an end section with insufficient anchorage length l_b of its longitudinal bars beyond the end section may be estimated applying the rules above for the calculation of the tensile stress in the tension bars, using l_b instead of l_o.

Effect of Lap-Splicing on the Flexure-Controlled Ultimate Deformation

A column with ribbed vertical bars lapped starting at its base exhibits higher flexure-controlled ultimate deformation than a similar one with continuous vertical bars, provided that the lapping is at least equal to a certain minimum lap length, $l_{ou,min}$, given by the following expression (Biskinis and Fardis 2004, 2007), adopted also in Part 3 of Eurocode 8 (CEN 2005a):

$$l_{ou,\min} = \frac{d_{bL} f_{yL}}{\left(1.05 + 14.5 a_{l,s} \frac{\rho_s f_{yw}}{f_c}\right) \sqrt{f_c}} \qquad (f_{yL},\ f_{yw},\ f_c \text{ in MPa}) \tag{3.86}$$

where:

– ρ_s is the ratio of the transverse steel parallel to the plane of bending, and

$$a_{l,s} = (1 - 0.5s_h/b_o)(1 - 0.5s_h/h_o)n_{restr}/n_{not}, \tag{3.87}$$

with

- s_h: stirrup spacing,
- b_o, h_o: dimensions of the confined concrete core to the hoop centreline,
- n_{tot}: total number of lapped longitudinal bars along the perimeter of the section and
- n_{restr}: number of lapped bars which are engaged by a stirrup corner or a cross-tie.

To reflect this finding, the ultimate curvature or chord rotation, monotonic or cyclic, calculated according to the pertinent models in Sections 3.2.2.4, 3.2.3.4 and 3.2.3.5, should include in the compression reinforcement ratio both bars of any pair of lapped bars in the compression zone.

Tests to flexural failure of rectangular members with ribbed longitudinal bars lap-spliced starting at the section of maximum moment suggest that the flexure-controlled ultimate deformation decreases with decreasing lap length, l_o, if $l_o < l_{ou,min}$. With the effect of lapping on the chord rotation at yielding, θ_y, quantified according to the sub-section above on the *Effect of Lap-Splicing on the Yield Properties*, it is convenient to compute the ultimate chord rotation as the sum of the so-modified value of θ_y plus a plastic part, ${\theta_u}^{pl}$, appropriately reduced owing to the short lapping, $l_o < l_{ou,min}$. There are two approaches for the estimation of the reduced value of ${\theta_u}^{pl}$:

(i) The empirical approach of Section 3.2.3.5. The available test results suggest that ${\theta_u}^{pl}$ decreases linearly with l_o, if $l_o < l_{ou,min}$; ${\theta_u}^{pl}$ may be taken equal to the last term at the right-hand-side of Eqs. (3.78b) or (3.78c) times $l_o/l_{ou,min} \leq 1$, with $l_{ou,min}$ from Eq. (3.86) (Biskinis and Fardis 2004, 2007, CEN 2005a). In about 75 tests to flexure-controlled ultimate deformation the test-to-prediction ratio of the so-computed ultimate chord rotation, θ_u, has a median of 1.065 and a coefficient of variation of 36.4% if the un-reduced value of ${\theta_u}^{pl}$ is taken from Eq. (3.78b), or a median of 1.045 and a coefficient of variation of 35.9% if Eq. (3.78c) is used instead.

(ii) The approach of Section 3.2.3.4, based on curvatures and the plastic hinge length. In that case, the yield curvature, φ_y, entering the calculation may be modified according to the sub-section above on the *Effect of Lap-Splicing on the Yield Properties* for the effect of lap-splicing. The only other modification is in the calculation of φ_u. There, in addition to including in the compression reinforcement ratio both lapped compression bars in any pair, if the lap length, l_o, is shorter than the value of $l_{ou,min}$ from Eq. (3.86), the maximum elongation

of the extreme tension bars at ultimate conditions due to steel rupture should be reduced to:

$$\varepsilon_{su,l} = \left(1.2\frac{l_o}{l_{ou,\min}} - 0.2\right)\varepsilon_{su} \geq \frac{l_o}{l_{oy,\min}}\frac{f_{yL}}{E_s} \tag{3.88}$$

where ε_{su} is given by Eq. (3.64c) or (3.64b) for monotonic or cyclic loading, respectively, and $l_{oy,min}$, $l_{ou,min}$ are given by Eqs. (3.85) and (3.86), respectively. In about 75 tests to flexure-controlled ultimate deformation the test-to-prediction ratio of the so-computed ultimate chord rotation, θ_u, has a median of 1.005 and a coefficient of variation of 35.2%, i.e., better than in approach (i) above.

There are very few cyclic tests of columns without detailing for earthquake resistance and smooth (plain) hooked bars lapped starting at the base (just 7 tests to the author's knowledge, all with $l_o \geq 15d_{bL}$). They suggest the following modification of Eq. (3.80) for the chord rotation at flexure-controlled failure:

$$\theta_{u,\text{smooth-lapped}} = \frac{10 + \min\left(\frac{l_o}{d_{bL}}; 40\right)}{50}\theta_{u,Eq.(3.80)} \tag{3.80a}$$

giving a median of 1.0 and a coefficient of variation of 28% for the test-to-prediction ratio.

3.2.3.10 Effect of FRP Wrapping of the Plastic Hinge Region on Flexural Behaviour

Members with Continuous Bars

Flexural yielding of the member's end section is normally associated with yielding of the tension reinforcement and is insensitive to what happens at the compression zone unless the axial load is high. The experimental yield moment of members having the plastic hinge region wrapped with FRP nonetheless exceeds on average the value calculated according to Section 3.2.2.2. This exceedance is not fully redressed when the confined concrete strength, f_c^*, estimated from Eq. (3.27a) in Section 3.1.2.4, is used instead of the unconfined value, f_c: the test-to-prediction ratio of the so-estimated yield moment in 180 FRP-wrapped members has a median of 1.065 (in lieu of 1.025 for beams or columns without FRP wrapping, see Section 3.2.2.2 under *Comparison with Experimental Results and Empirical Expressions for the Curvature*) and a coefficient of variation of 19.6% (Biskinis and Fardis 2009). So, a calibration factor of 1.065 should be applied on the values of the yield moment and curvature, M_y, φ_y, obtained from 1st principles according to Section 3.2.2.2 using the confined concrete strength, f_c^*, in lieu of f_c. The correction factor of 1.065 should be applied also on the 1st (flexural) term of Eqs. (3.66) for the chord rotation at apparent yielding, θ_y, of members with FRP-wrapped ends. By doing so,

the test-to-prediction ratio of θ_y in about 135 FRP-wrapped members has a median of 0.995 and a coefficient of variation of 37.8% (Biskinis and Fardis 2009). If the so-computed values of M_y and θ_y are used in Eq. (3.68), the test-to-prediction ratio of the secant stiffness to the yield-point of these FRP-wrapped test specimens has a median of 1.055 and a coefficient of variation of 28.7% (Biskinis and Fardis 2009).

FRP-wrapping is often applied to retrofit members that have suffered serious damage during an earthquake (ranging from yielding to ultimate deformation), of course after repair of the damage. Repair followed by FRP-wrapping fully re-instate the yield moment of the damaged member: the mean and the median of the test-to-prediction ratio of the yield moment of 20 FRP-wrapped pre-damaged columns do not deviate significantly from those of the undamaged ones. By contrast, repair and FRP-wrapping cannot redress the effect of previous damage on the effective flexural stiffness to yielding (as controlled by the chord rotation at yielding, θ_y): the result of Eq. (3.68) has been found to exceed the secant stiffness to the yield-point of 20 FRP-wrapped pre-damaged columns by about 30% on average (Biskinis and Fardis 2009).

If the plastic hinge region is wrapped with FRP its ultimate flexural deformation is enhanced, primarily thanks to the confinement of the compression zone and the increase of the concrete ultimate strain there. As a matter of fact, Eqs. (3.29) and (3.30) in Section 3.1.2.4 for the ultimate strain of concrete under cyclic loading have been fitted to ultimate curvature data in about 35 tests of rectangular FRP-wrapped columns (Biskinis and Fardis 2009). In that case the ultimate curvature, φ_u, is calculated from first principles according to the analysis in Section 3.2.2.4, modified to accept a parabolic-trapezoidal σ-ε curve for the confined concrete – as in Lam and Teng (2003a,b) – instead of the parabolic-rectangular one of unconfined concrete. Equations (3.29) and (3.30) used together with the (Lam and Teng 2003a,b) confined strength model, Eq. (3.27a), give an average test-to-prediction ratio of 1.01 for φ_u with a coefficient of variation of 27.5%.[14] If the so-computed ultimate curvature, φ_u, is used in Eq. (3.72) of Section 3.2.3.4 together with the value of L_{pl} from Eq. (3.73) (fitted to members without FRP wrapping under cyclic loading), the test-to-prediction ratio of θ_u in about 95 tests of members with FRP wrapping has a median of 0.995 and a coefficient of variation of 34.6% (Biskinis and Fardis 2009). In another 18 members that had suffered certain damage by testing before been repaired, FRP-wrapped and re-tested, Eqs. (3.72) and (3.73) give a median test-to-prediction ratio of 0.985 and a coefficient of variation of 23.1%. If the columns that had been FRP-wrapped after been damaged and repaired are put together with the virgin ones, the overall median of the test-to-prediction ratio is 0.995 and the coefficient of variation 33.4%.

---

[14] If the Lam and Teng Eq. (3.27b) is used for $\varepsilon_{cu}{}^*$ instead of Eqs. (3.29) and (3.30), the ultimate curvature of the FRP-wrapped member is underpredicted by a factor of about 2.3. So, notwithstanding any adverse effect of the cycling, the FRP that confines the extreme compression fibres seems to be put under lower demands by cyclic bending than by the condition of monotonic concentric compression for which Eq. (3.27b) has been developed, a condition inducing a uniformly large strain to the FRP all around the section.

It has been proposed in Biskinis and Fardis (2004) and adopted by Eurocode 8, Part 3 (CEN 2005a) to extend to members with FRP wrapping the purely empirical model for θ_u, Eqs. (3.78) in Section 3.2.3.5, by adding the term $a_f \rho_f f_{f,e}/f_c$ to the exponent of the 2nd term from the end to include the effect of confinement by the FRP, where:

- $\rho_f = 2t_f/b_w$ is the geometric ratio of the FRP parallel to the loading direction,
- a_f is the confinement effectiveness factor of the section by the FRP, given by Eq. (3.28) where it is denoted by a_n, and
- $f_{f,e}$, is the effective stress of the FRP:

$$f_{f,e} = \min\left(f_{fu,nom};\ \varepsilon_{u,f} E_f\right)\left(1 - \min\left[0.5;\ 0.7\min\left(f_{fu,nom};\ \varepsilon_{u,f} E_f\right)\frac{\rho_f}{f_c}\right]\right) \tag{3.89}$$

with $f_{fu,nom}$ and E_f denoting the nominal strength and the Elastic modulus of the FRP and $\varepsilon_{u,f}$ being a limit strain, equal to:

- $\varepsilon_{u,f} = 0.015$ for CFRP or AFRP; and
- $\varepsilon_{u,f} = 0.02$ for GFRP.

With this modification Eqs. (3.78) give a median for the test-to-prediction ratio in about 95 tests of FRP-wrapped members equal to 1.10 and a coefficient of variation of 31.8%. In 18 members that had been FRP-wrapped and re-tested after been pre-damaged by testing and repaired, the modification of Eqs. (3.78) on the basis of Eq. (3.89) gives a median test-to-prediction ratio of 0.925 and a coefficient of variation of 24%. If all FRP-wrapped columns, virgin and pre-damaged/repaired are lumped together, the overall median of the test-to-prediction ratio is 1.09 and the coefficient of variation is 31.5%.

The proposal above has been improved as follows (Biskinis and Fardis 2009): the term added to the exponent of the 2nd term from the end of Eqs. (3.78) to reflect effective confinement by the FRP is:

$$\left(a\frac{\rho f_u}{f_c}\right)_{f,eff} = a_f \min\left[1.0;\ \min\left(f_{fu,nom};\ \varepsilon_{u,f} E_f\right)\frac{\rho_f}{f_c}\right] \left(1 - 0.4\min\left[1.0;\ \min\left(f_{fu,nom};\ \varepsilon_{u,f} E_f\right)\frac{\rho_f}{f_c}\right]\right) \tag{3.90}$$

where the limit strain is always equal to $\varepsilon_{u,f} = 0.015$. With this modification Eqs. (3.78) give a median test-to-prediction ratio in about 95 tests of FRP-wrapped virgin members equal to 1.06 and a coefficient of variation of 31.3%.

An even better fit to those tests is achieved (median test-to-prediction ratio of 1.035 and coefficient of variation of 31.2%) if the FRP-confinement term added to the exponent of the 2nd term from the end of Eqs. (3.78) is based on the effective FRP strength of the model in Lam and Teng (2003a,b): $f_{fu,L\&T} = E_f \varepsilon_{fu}$, with ε_{fu} about

equal to 60% of the failure strain of tensile coupons.[15] The resulting alternative to Eq. (3.90) is:

$$\left(a\frac{\rho f_u}{f_c}\right)_{f,eff} = a_f c_f \min\left[0.4;\ \frac{\rho_f f_{fu,L\&T}}{f_c}\right]\left(1 - 0.5\min\left[0.4;\ \frac{\rho_f f_{fu,L\&T}}{f_c}\right]\right) \tag{3.91}$$

where $c_f = 1.8$ for CFRP and $c_f = 0.8$ for GFRP or AFRP.

In the 18 members that were FRP-wrapped and re-tested after been pre-damaged by testing and repaired, Eqs. (3.78) modified on the basis of Eqs. (3.90) or (3.91) give a median test-to-prediction ratio of 0.925 or 0.945, and a coefficient of variation of 24% or 26%, respectively. If all FRP-wrapped columns, virgin and pre-damaged/repaired are lumped together, the overall median of the test-to-prediction ratio of Eqs. (3.78) modified on the basis of Eqs. (3.90) or (3.91) is 1.045 or 1.03, respectively, and the coefficient of variation is about 31%.

Note that the last term in each one of Eqs. (3.89), (3.90) and (3.91) reflects the experimentally documented reduced effectiveness of FRP-wrapping when larger amounts of FRP are used.

It has been suggested above that previous damage does not have a statistically significant effect on the ultimate chord rotation of FRP-wrapped members predicted from Eqs. (3.72), (3.73) and (3.74) and using in Eq. (3.72) an ultimate curvature, φ_u, from:

- first principles, according to the analysis in Section 3.2.2.4 modified to use a parabolic-trapezoidal σ-ε curve for confined concrete – as in the (Lam and Teng 2003a,b) model for confinement by FRP – instead of a parabolic-rectangular one,
- the (Lam and Teng 2003a,b) model for the confined strength, Eq. (3.27a), and
- Equations (3.29) and (3.30) for the ultimate strain of FRP-confined concrete under cyclic loading.

That conclusion is not corroborated by the comparisons of the predictions of Eqs. (3.78), modified with the help of Eqs. (3.89), (3.90) and (3.91). Although the data are not sufficient for a statistically meaningful conclusion, previous damage seems to reduce by 10–15% the ultimate chord rotation predicted by Eqs. (3.78) as modified on the basis of Eqs. (3.89), (3.90) or (3.91). The predictions are on the safe side for members that are intact when wrapped with FRP and slightly on the unsafe side for previously damaged ones.

Members with Lap-Spliced Ribbed Bars

What has been said in the sub-section above on *Effect of Lap-Splicing on the Yield Properties* regarding the effect of lap-splicing on the yield moment and the member

[15] As noted in Section 3.1.2.4, in Lam and Teng (2003a,b) this percentage value is proposed only for CFRP or GFRP, and 85% is given for AFRP, but on the basis of few test results.

secant stiffness to the yield-point still applies if the end region(s) of the member is wrapped with FRP. The only difference is in the calculation of the maximum possible stress of lapped tension bars, where the effect of the FRP wrapping should be taken into account. Provided that the wrapping extends over at least the full length of the lap, M_y and φ_y may be calculated with the maximum possible stress of the lapped tension bars from Eq. (3.31), using there Eq. (3.32a) (see Section 3.1.3.2). In about 30 tests on members of rectangular section, having their ribbed bars lapped and FRP wrapping applied starting at the section of maximum moment, the test-to-prediction ratio for the so-computed yield moment is on average equal to 1.13 and its coefficient of variation is 8.8%. The corresponding statistics for the chord rotation at yielding are 1.17 and 18% and for the member secant stiffness to the yield-point 1.00 and 18.8%, respectively.

Section 3.2.3.9 under *Effect of Lap-Splicing on the Yield Properties* has presented a simpler alternative to the use of Eq. (3.31) to account for the effect of lapping of ribbed bars on the yield properties of members without FRP wrapping. In that alternative the yield stress of lapped tension bars, f_{yL}, is multiplied by $l_o/l_{oy,min} \leq 1$ (Biskinis 2007, Biskinis and Fardis 2004, 2007, CEN 2005a). The extension of that rule to members with FRP wrapping all along the length of the lap splice entails just a reduction by one-third of the minimum length given by Eq. (3.85):

For FRP wrapping:

$$l_{oy,\min} = \frac{0.2 d_{bL} f_{yL}}{\sqrt{f_c}} \qquad (f_{yL} \text{ and } f_c \text{ in MPa}) \tag{3.85a}$$

This simplification, proposed in (Biskinis 2007, Biskinis and Fardis 2004, 2007) and adopted in Part 3 of Eurocode 8 (CEN 2005a), gives for the test-to-prediction ratio of the yield moment in about 30 tests an average of 1.06 and a coefficient of variation of 11.4% (Biskinis and Fardis 2009). The corresponding statistics for the chord rotation at yielding are 1.085 and 16.6% and for the member secant stiffness to the yield-point 1.005 and 18.2%, respectively.

The approach of Section 3.2.3.9 under *Effect of Lap-Splicing on the Flexure-Controlled Ultimate Deformation* for the effect of lap-splicing of ribbed longitudinal bars on the member's flexure-controlled ultimate deformation can be extended to members with FRP wrapping all along the lap-splicing. In a way similar to that approach, the ultimate chord rotation, θ_u, is expressed as the sum of the chord rotation at yielding, θ_y, plus a plastic part, $\theta_u{}^{pl}$. The effect of FRP-wrapping on θ_y is estimated according to the paragraph above. Regarding the effect on $\theta_u{}^{pl}$, approach (i) in Section 3.2.3.9 under *Effect of Lap-Splicing on the Flexure-Controlled Ultimate Deformation*, based on the empirical ultimate chord rotation of Section 3.2.3.5, takes $\theta_u{}^{pl}$ as equal to the last term at the right-hand-side of Eqs. (3.78b) or (3.78c) times $l_o/l_{ou,min} \leq 1$, with $l_{ou,min}$ from Eq. (3.86) (Biskinis 2007, Biskinis and Fardis 2007, CEN 2005a). For the extension of that approach to members with FRP wrapping all along the region with the lap-splice, recall the three approaches presented in the sub-section above on *Members with Continuous Bars* for the empirical estimation of $\theta_u{}^{pl}$ of members with continuous bars and FRP wrapping:

1. The one proposed in (Biskinis 2007, Biskinis and Fardis 2004, 2007) and adopted in Eurocode 8, Part 3 (CEN 2005a), uses Eq. (3.89) in the calculation of the effect of confinement by the FRP. Its natural extension, also proposed in (Biskinis 2007, Biskinis and Fardis 2007) and adopted in CEN (2005a), is to calculate $l_{ou,\min}$ via the following modification of Eqs. (3.86) and (3.87):

$$l_{ou,\min} = \frac{d_{bL} f_{yL}}{\left(1.05 + 14.5 \frac{4}{n_{tot}} a_f \frac{\rho_f f_{f,e}}{f_c}\right) \sqrt{f_c}} \qquad (f_{yL},\ f_{f,e},\ f_c \text{ in MPa}) \qquad (3.92)$$

where $f_{f,e}$ comes from Eq. (3.89) and n_{tot} denotes the total number of lapped longitudinal bars along the perimeter of the section, out of which only the four corner ones are confined by the FRP ($n_{restr} = 4$ in Eq. (3.87)). Note that, θ_u^{pl} before its reduction due to the lap splice is calculated from Eqs. (3.78b) or (3.78c) with the exponent of the 2nd term from the end reflecting confinement by the steel ties as well as by the FRP (i.e., the term $a_f \rho_f f_{f,e}/f_c$ is added). By contrast, confinement of lapped bars by the FRP alone and not by the steel ties is taken into account in Eq. (3.92). Thirty members with lap-spliced ribbed bars and FRP-wrapping cyclically tested to flexure-controlled ultimate deformation have mean test-to-prediction ratio for the so-computed ultimate chord rotation, θ_u, equal to 0.965 or 0.95, and a coefficient of variation of that ratio of 26.6% or 27.2%, if the un-reduced value of θ_u^{pl} is taken from Eq. (3.78b) or (3.78c), respectively (Biskinis and Fardis 2009).
2. The improvement of the approach in (Biskinis 2007, Biskinis and Fardis 2004, 2007, CEN 2005a) as proposed in Biskinis and Fardis (2009), namely the use of Eq. (3.90) for the FRP-confinement term. The natural extension of that approach, also presented in Biskinis and Fardis (2009), is to modify Eqs. (3.86) and (3.87) for $l_{ou,\min}$ as follows:

$$l_{ou,\min} = \frac{d_{bL} f_{yL}}{\left(1.05 + 14.5 \frac{4}{n_{tot}} \left(a \frac{\rho f_u}{f_c}\right)_{f,eff}\right) \sqrt{f_c}} \qquad (f_{yL},\ f_{f,u},\ E_f,\ f_c \text{ in MPa}) \qquad (3.93)$$

with $(a\rho f_u/f_c)_{f,eff}$ from Eq. (3.90). Again the value of θ_u^{pl} before the reduction due to the lap splice is calculated from Eq. (3.78b) or (3.78c) accounting for confinement by the steel ties and by the FRP through the exponent of the 2nd term from the end (i.e., adding there the term $(a\rho f_u/f_c)_{f,eff}$ from Eq. (3.90)), while Eq. (3.93) accounts only for confinement of lapped bars by the FRP but not by the steel ties. In 30 cyclic tests of members with lap-spliced ribbed bars and FRP-wrapping the test-to-prediction ratio of the so-computed ultimate chord rotation, θ_u, is on average equal to 0.925 or 0.91, and has a coefficient of variation of 28.4% or 28.9%, if the un-reduced value of θ_u^{pl} is taken from Eq. (3.78b) or (3.78c), respectively (Biskinis and Fardis 2009).
3. The further modification of the approach, in order to use in the FRP-confinement term the effective FRP strength of the Lam and Teng (2003a,b) model: $f_{fu,L\&T} = E_f \varepsilon_{fu}$, with ε_{fu} about equal to 60% of the failure strain of tensile coupons. This

modification uses Eq. (3.90) for the FRP-confinement term in the calculation of θ_u^{pl} for members with continuous bars and FRP wrapping. It is extended to members with lap-spliced bars by using in Eq. (3.93) the value of $(a\rho f_u/f_c)_{f,eff}$ from Eq. (3.91). The test-to-prediction ratio of the so-computed value of θ_u in 30 cyclic tests of members with lap-spliced ribbed bars and FRP-wrapping is on average equal to 0.98 or 0.965, if the un-reduced value of θ_u^{pl} is taken from Eq. (3.78b) or (3.78c), respectively, and has a coefficient of variation of 30.6% (Biskinis and Fardis 2009).

So, although with the approach in (Biskinis 2007, Biskinis and Fardis 2004, 2007, CEN 2005a) modified as in 2 and 3 above the accuracy of the predictions of θ_u improves for members with continuous bars and FRP wrapping, it deteriorates if the bars inside the wrapping are lap-spliced.

In approach (ii) of Section 3.2.3.9 under *Effect of Lap-Splicing on the Flexure-Controlled Ultimate Deformation* the limit strain of steel for the calculation of the ultimate curvature of members without FRP wrapping (used in the estimation of the ultimate chord rotation from the plastic hinge length according to Section 3.2.3.4) is corrected for the effect of lap-splicing according to Eq. (3.88). On the other hand, the ultimate curvature of FRP-wrapped members with continuous bars may be calculated according to the 3rd paragraph of the sub-section above on *Members with Continuous Bars*: from (a) the analysis in Section 3.2.2.4 modified to use a parabolic-trapezoidal σ-ε curve for the confined concrete (as in the (Lam and Teng 2003a,b) model), instead of the parabolic-rectangular one of unconfined concrete, (b) the (Lam and Teng 2003a,b) confined strength model and (c) the ultimate strain of FRP-confined concrete under cyclic loading given by Eqs. (3.29) and (3.30) in Section 3.1.2.4. If the tension bars are lapped inside the FRP wrapping their limit strain may be taken from Eq. (3.88), but using there the value of $l_{ou,min}$ for FRP-wrapped members from Eq. (3.93). In that expression the value of $(a\rho f_u/f_c)_{f,eff}$ should be the one from Eq. (3.91), consistent with the (Lam and Teng 2003a,b) model applied for the FRP-confined concrete in the calculation of φ_u. If this is done, the test-to-prediction ratio of θ_u in 30 cyclic tests of members with lap-spliced ribbed bars and FRP-wrapping is on average equal to 1.42 and has a coefficient of variation of 25.7%. Therefore, if the more "fundamental" approach for the ultimate chord rotation is extended to FRP-wrapped members with lapped bars, it gives worse predictions than the versions 1–3 of the empirical approach presented in the paragraphs above.

3.2.3.11 Effect of Bonded Prestressing Tendons on the Cyclic Flexural Behaviour

Prestressing of long span beams or girders can be used to advantage in concrete buildings. However, the scope of current seismic design codes, including Eurocode 8 (CEN 2004a), does not include prestressed elements that are part of the lateral-load-resisting system ("primary seismic" elements in Eurocode 8, see Section 4.12). The exclusion is implicit. It comes from the fact that code rules on design and detailing

for ductility of beam ends where plastic hinges are expected to form apply only to reinforced concrete beams. A notable exception is the CEB Seismic Model Code (CEB 1985) that includes a few clauses warning against the use of unbonded tendons in "primary" members (except in partially prestressed beams with 80% of their flexural resistance coming from ordinary reinforcement and with prestressing tendons placed only within the mid-third of the section depth) and against placing tendon anchorages in beam-column joints next to potential plastic hinges. CEB (1985) also limits the neutral axis depth in potential plastic hinges of prestressed beams at the moment resistance to less than 20% of the section depth (to avoid brittle failure of the compression zone) and asks for a 25% margin between cracking and ultimate moments of any prestressed section.

Concrete buildings designed for energy dissipation according to current codes may include prestressed girders, provided that they, as well as the columns connected to them, are not taken to be part of the lateral-load-resisting system, i.e., they are considered and designed as "secondary seismic" elements in the Eurocode 8 terminology (see Section 4.12). According to Eurocode 8 (CEN 2004a) this implies that the total lateral stiffness of all frames in the building that include prestressed girders does not exceed 15% of the lateral stiffness of the system of "primary seismic" elements. As a matter of fact, it is sensible to consider the columns supporting prestressed girders as "secondary seismic", because normally the weak-beam/strong-column capacity design rule of Eq. (1.4) cannot force plastic hinging in girders with size typical of prestressed ones. Another option is to design concrete buildings having prestressed girders for Ductility Class L and a value of the behaviour factor q not higher than 1.5 (as recommended in Eurocode 8 only for low seismicity regions).

Note that, at least in buildings, prestressing is primarily – if not exclusively – used in long span horizontal elements for resistance against gravity loads. So tendons are placed eccentric in the member section, on the side where gravity moments induce tension. Eccentric tendons normally do not enhance the ductility and deformation capacity of plastic hinges, particularly at beam supports under hogging moments that induce tension to the top flange, where the tendons are located. Under such moments the beam section at the face of the column soon reaches its deformation capacity, owing either to the low ultimate strain of prestressing steel (compared to ordinary reinforcement) or to crushing of the concrete at the narrow bottom flange. So, a less eccentric placement of tendons at beam supports and a larger quantity of ductile ordinary reinforcement at both flanges may be appropriate, for the plastic hinges at the ends of prestressed beams to develop significant ductility and deformation capacity.

Conventional wisdom in seismic design and codification is against prestressing members expected to develop plastic hinges, because compression due to prestressing is thought to place additional demands on the compression zone, reducing the flexural deformation capacity. Recent tests, however, have demonstrated the beneficial effect of prestressing on the cyclic behaviour of bridge piers: ultimate deformation increases with prestressing and residual displacements decrease (Sakai et al. 2006, Inoue and Tanabe 2006).

So, prestressing of bridge piers has received considerable attention in the draft code of the Japan Prestressed Concrete Engineering Association for performance-based seismic design of prestressed concrete bridges (JPCEA 2002).

The international literature contains very few cyclic tests on prestressed members, mainly with square section and concentric prestressing. Their results are compared below to the predictions of the models proposed in previous sections, after appropriate modifications.

In the application of the model in Section 3.2.2.2 for the calculation of the yield moment and curvature of prestressed members with rectangular compression zone, any bonded tendons that are near the extreme tension fibres are included in the ratio of tension reinforcement, ρ_1, after weighing the cross-sectional areas of any reinforcement near the outermost tension fibres by the corresponding yield stress. The same weighing is applied for the determination of the centroid of the tension reinforcement. Bonded tendons and non-prestressed reinforcement in the compression zone and the web are elastic at yielding of the section. So, their cross-sectional areas may be added without any weighing by the yield stress.

There are two alternatives for considering the effect of prestressing:

1. Prestress is considered as part of the actions, as in Serviceability Limit States:

   – the action effects due to prestress are taken from the elastic analysis; in isostatic (statically determinate) systems prestressing induces an axial force equal to the total prestressing force, P (positive for compression) and a bending moment equal to P times the eccentricity of the mean tendon, and
   – bonded tendons are considered as an integral part of the section, working elastically up to their available yield stress, which is equal to their full yield stress, $f_{0.01}$, minus the initial stress in the tendon, σ_p.

2. The prestress is considered as part of the resistance: This is how bonded tendons that yield are normally considered at the Ultimate Limit States:

   – bonded tendons that yield are taken to contribute to the resistance as an integral part of the section, working in the plastic range with their full yield stress, $f_{0.01}$;
   – bonded tendons that have not yielded are considered as in case (1) above, i.e.:

     • they are taken to induce in the section an axial force and a bending moment equal to the force and moment resultant of their prestressing, and
     • they are considered to work elastically as an integral part of the section up to their available yield stress, $f_{0.01}$–σ_p.

For either one of the two alternative considerations (1) and (2) above, the model in Section 3.2.2.2 underestimates by 13.5% on average the yield moment, M_y, of concentrically prestressed members. More important, Eq. (3.66) overestimates the chord rotation at yielding, by 11% on average when prestress is taken as part of the actions and by almost 50% when it is considered as part of the resistance. The scatter of the predictions for chord rotations at yielding is large. These differences are

carried over to the calculation of the secant stiffness to the yield-point through Eq. (3.68). Its average test-to-prediction ratio is 1.50 if prestress is taken as part of the actions and about 2.0 when it is considered as part of the resistance! The empirical secant stiffness to the yield-point from Eq. (3.69) does not improve the predictions.

In view of the very small sample size, the magnitude of underestimation of the yield moment of concentrically prestressed members by the models for non-prestressed members is considered as acceptable. The same could be said for the overestimation of the chord rotation at yielding, but only when prestress is taken as part of the actions. These deviations, however, accumulate into a more significant underestimation of the secant stiffness to the yield-point through Eq. (3.68), which borders the unacceptable. It seems that the effects of the suppression of cracking by the prestress along part of the member is not fully captured by considering an axial force equal to the total prestressing force, P. Taking the prestress as part of the resistance, or using the empirical secant stiffness to the yield-point, Eq. (3.69), give very poor predictions both for the chord rotation at yielding and for the secant stiffness to it.

The three versions of Eqs. (3.78) underestimate the flexure-controlled cyclic ultimate chord rotation, θ_u, of five concentrically prestressed specimens by 7.5–8.5% on average (with a coefficient of variation of the test-to-prediction ratio from 8.5 to 12.5%). The concentrically prestressed specimens may have exceeded the expecations of a formula fitted to conventionally reinforced members, because their tendons are always in tension and do not buckle under cyclic loading. For this reason, it seems appropriate to apply Eq. (3.72), based on the ultimate curvature, φ_u, from Sections 3.2.2.4 and 3.2.2.10 and the plastic hinge length from Eq. (3.73b), with the limit strain of tendons taken from Eq. (3.64a), for monotonic loading that does not cause buckling of the tendons. However, the cyclic ultimate chord rotation in the five tests is still underestimated by 9% on average (and with a coefficient of variation of the test-to-prediction ratio of 35.5%).

Note that bending moments nowhere enter in the application of Eqs. (3.78) and (3.72). So, if the prestress is taken as part of the resistance, there is no way to take into account the bending moment induced by the bonded tendons that have not yielded. Therefore, in the calculations of θ_u the prestress has been taken as part of the action, even though bonded tendons close to the extreme tension fibres had yielded before the ultimate flexural failure.

The very limited available test data suggest that concentric prestressing is beneficial for the flexure-controlled cyclic ultimate chord rotation, θ_u. Moreover, the recentring effect of concentric prestressing reduces the residual deformations, and therefore damage, no matter whether the conventionally defined flexure-controlled chord rotation capacity, θ_u, has been exceeded or not. If this capacity is not exceeded, a member without any ordinary non-prestressed reinforcement and with only concentric prestressing returns to about zero residual deformations. If there is a combination of non-prestressed and prestressed reinforcement, the residual deformation may be considered to decrease in proportion to the contribution of prestressing (in percent) to the yield moment of the section, i.e. to the ratio $M_y(A_p=0)/M_y$, where $M_y(A_p=0)$ is the yield moment for presumed zero cross-sectional area of prestressed reinforcement in the section.

3.2.4 Behaviour of Members Under Cyclic Shear

3.2.4.1 Introduction: Brittle vs. Ductile Shear Behaviour

If it precedes flexural yielding, ultimate failure of concrete members in shear occurs at relatively low deformations and is associated with a large drop in lateral load resistance. So, it is considered as a "brittle" failure mode. Figure 3.35 depicts characteristic shear failures of columns or walls in past earthquakes. A shear failure of a stair flight acting as an inclined wall has been shown in Fig. 2.13(a).

Often concrete members that first yield in flexure may, under cyclic loading, ultimately fail in a mode showing strong and clear effects of shear: diagonal cracks are prominent and their width and extent increase during cycling, despite the gradual drop of peak force resistance with cycling of the load. At the same time, phenomena which are associated with flexure (e.g., a single wide crack at right angles to the member axis at the section of maximum moment, disintegration of the compression zone and/or buckling of longitudinal bars next to that section) may not be so pronounced in such cases. By contrast, these phenomena (often including rupture of a longitudinal bar) grow in magnitude when flexure-controlled ultimate deformation approaches, while any diagonal cracks that may have formed initially decrease in width and may even disappear owing to the drop of the force resistance with load cycling after the flexure-controlled ultimate strength. Failure in shear under cyclic loading after initial flexural yielding is termed "ductile shear" failure (Kowalsky and Priestley 2000). It occurs only under cyclic loading, because shear strength degrades faster with load cycling than flexural strength. It is normally associated with diagonal tension and yielding of the web reinforcement, rather than with web crushing by diagonal compression.

The left-hand-side of Fig. 3.36 (Yoshimura et al. 2004) shows force-drift hysteresis loops of three columns with high longitudinal reinforcement ratio, ρ_{tot}, and low transverse steel ratio, ρ_w, failing in brittle shear before yielding in flexure. Their right-hand-side companions have sufficiently low values of ρ_{tot} to first yield in flexure and then fail in "ductile shear" (the upper two columns) or in flexure (that at the lower right corner).

Dimensioning of concrete members against brittle shear failure is a familiar subject, covered in current codes and standards for the design of concrete structures under non-seismic action effects that increase monotonically until ultimate strength. Relevant models are reviewed in the Section 3.2.4.2. Shear design of members in new earthquake-resistant concrete buildings and seismic evaluation of existing elements in substandard ones should also consider the reduction of shear resistance with cyclic loading below the monotonic value.

Several mechanisms may explain the degradation of shear strength during cyclic loading:

1. The degradation of dowel action with cycling of the shear (see Section 3.1.3.1) and with the accumulation of inelastic strains in the longitudinal bars.
2. The development of flexural cracks through the depth of the member and the ensuing decreased contribution of the compression zone to shear resistance.

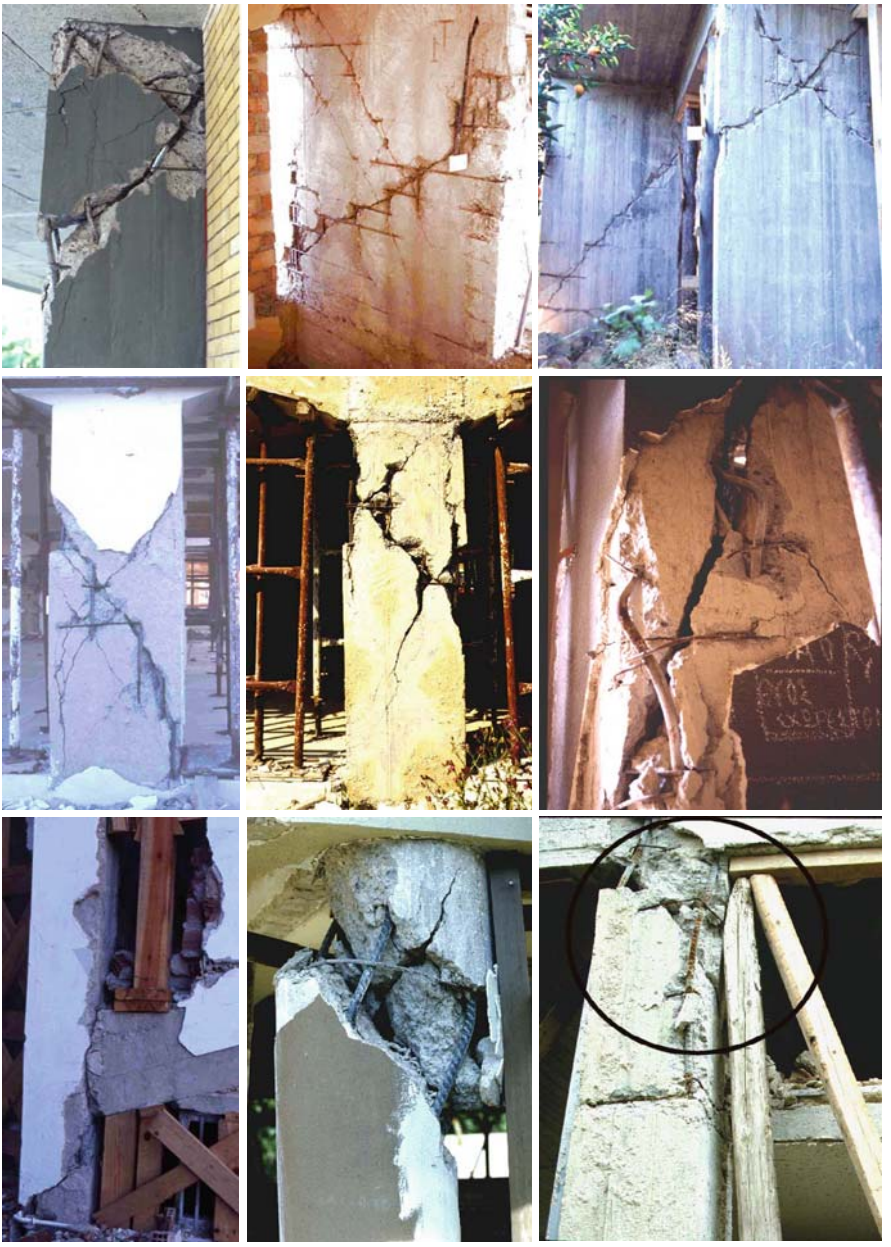

Fig. 3.35 Shear failures of columns or walls (See also Colour Plate 9 on page 723)

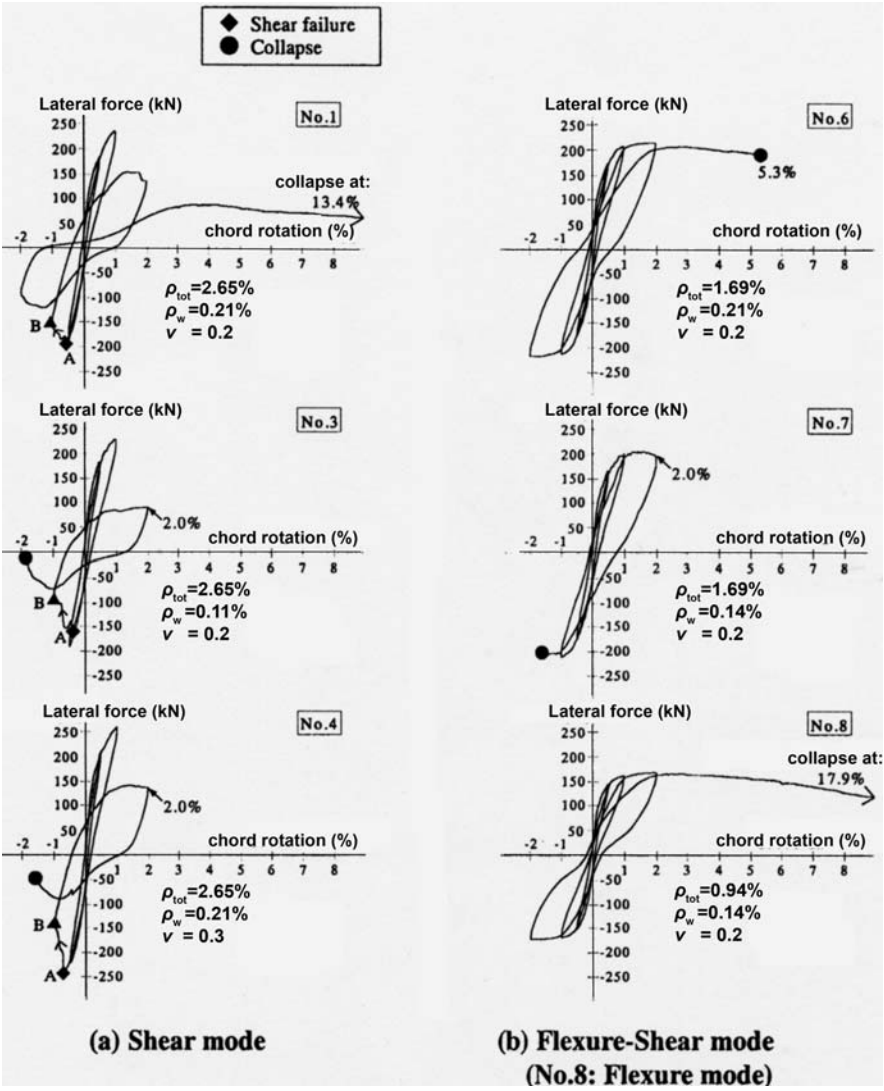

Fig. 3.36 Shear force-chord rotation behaviour for: (**a**) brittle shear; and (**b**) "ductile shear" or flexural behaviour (adapted after Yoshimura et al. 2004)

3. The reduction of aggregate interlock along diagonal cracks, as their interfaces are ground and become smoother with cycling; in addition, the cracks open up owing to bond slippage and accumulation of inelastic strains in the stirrups crossing the cracks.
4. The softening of concrete in diagonal compression due to accumulation of transverse tensile strains.

The degradation of shear strength during cyclic loading is normally associated with diagonal tension and yielding of the web reinforcement, rather than with diagonal compression failure in the web. It has by now prevailed to quantify this failure mode in terms of a shear resistance, V_R, (as this is governed by web reinforcement according to the well-established Mörsch-Ritter truss analogy) that decreases with increasing (displacement) ductility ratio under cyclic loading (Kowalsky and Priestley 2000, Moehle et al. 2001, Ascheim and Moehle 1992). The contributions to shear strength decay listed above as 1–3 have to do with the contribution of concrete to shear resistance, i.e. with the term V_c normally added to the contribution of transverse steel according to a 45°-truss analogy, V_w. Degradation mechanisms no. 3 and 4 involve also, be it indirectly, the contribution of transverse steel to shear resistance, reflected in V_w.

Naturally the cyclic degradation of shear resistance is larger within flexural plastic hinges, as it is there that:

- flexural cracks extend into wide and intersecting diagonal cracks,
- the compression zone suffers more damage and decreases in size,
- longitudinal bars develop inelastic strains, or even buckle, and lose most of their effectiveness in dowel action, and
- (at the end section) the compression zone supports the diagonal strut of the truss mechanism of shear resistance.

Consequently, the decay of shear strength with cycling takes place mainly in concrete members that develop flexural plastic hinges before exhausting their shear resistance. Therefore, the phenomenon is normally expressed quantitatively as a reduction of shear strength with cyclic inelastic deformations, until the so-reduced shear strength, V_R, becomes less than the shear force corresponding to flexural yielding, $V_y = M_y/L_s$. The member deformation where this takes place may be considered as its deformation capacity, as governed by shear.

An alternative way to describe the phenomenon might be to consider that the member develops a relatively ductile failure mode in shear after initially yielding in flexure, but that its ultimate cyclic deformation capacity is less than in an – otherwise similar – member with higher shear resistance but ultimately failing in flexure. Such an approach might allow direct quantification of member cyclic deformation capacity as governed by shear without recourse to a force-based criterion. However, owing to:

- the lack of rational models for the ultimate deformation of concrete elements as controlled by “ductile shear” failure, and
- the scarcity of sufficient data for the development of purely empirical alternatives,

the models proposed so far for the description of ultimate shear failure due to cyclic deformations beyond flexural yielding use force-based criteria as outlined in the previous paragraph and described in detail in Section 3.2.4.3. These criteria

employ empirical corrections of the truss analogy model of shear resistance, to incorporate the effect of cyclic degradation.

The experimental results in Fig. 3.37 (Ma et al. 1976) are typical of the evolution of shear phenomena under cyclic loading. They refer to a T-beam with $L_s/h = 3.9$ subjected to symmetric cycles of tip deflection in sets of three cycles of the same amplitude. Figure 3.37(a) displays the moment-(mean) curvature loops measured over a length of $d/2$ next to the beam end section. Figure 3.37(b) presents the corresponding loops of shear force v mean shear strain up to a distance $0.3d$ from the end section. Diagonal cracking occurred at a shear force of 50 kN (point A in Fig. 3.37(c)). It is only after that stage that the stirrups were activated and shear strains started developing. After flexural yielding of the end section, shear strains grew rapidly with deflection cycles, although the peak force of the cycles remained almost the same. As a matter of fact, shear strains increased from the 1st to the 3rd cycle of each set of three cycles, while the corresponding peak curvatures of the cycle decreased (cf Fig. 3.37(a) and (b)). The gradual increase of shear strains during cycling accelerated the activation of the stirrups, driving the one monitored in Fig. 3.37(c) to yielding. Witness the small stress of that particular stirrup (about 25% of its yield stress) at the time the end section first yielded.

Similar is the behaviour of the 3-storey barbelled wall in Fig. 3.38 (Wang et al. 1975). It is reminded that walls are considered to resist flexure with the two well-confined and heavily reinforced section edges, while the web in-between resists the shear. The vertical bars in the web play of course a role for the behaviour and resistance of the wall in flexure (see term ρ_v in Eqs. (3.35), (3.37), (3.38) and (3.39) and ω_v in Eqs. (3.57), (3.58), (3.59), (3.60), (3.61) and (3.62)). Moreover, if the shear capacity provided by the web reinforcement is exhausted, the boundary elements at the two ends of the section may contribute to shear resistance via the dowel action of their large diameter bars, or, even, by acting themselves as big dowels. Notwithstanding the presumed distinct and uncoupled roles of the web and of the two boundary elements, flexural yielding at the base of the wall's 1st or 2nd storey (see Fig. 3.38(a), or (b), respectively) triggers the onset of significant inelastic shear deformations over the entire 1st or 2nd storey, respectively (see Fig. 3.38(c) and (d)). Ultimate failure of that wall took place in shear at the 1st storey, while the moment-curvature response in the 1st and 2nd storeys was very stable (see Fig. 3.38(a) and (b)). Besides the gradual degradation of shear resistance due to inelastic cyclic deformations, Figs. 3.37(b) and 3.38(c), (d) display the shape of force-deformation loops typical of shear behaviour. Unlike the ones in flexure in Figs. 3.25, 3.26, 3.28, 3.34, 3.37(a), 3.38(a) and (b), the loops in Figs. 3.37(b) and 3.38(c), (d), become almost flat upon unloading to zero force and remain so until a steep but late increase in stiffness while the wall reloads in the reverse direction. The end result is a narrow and inverted-S V-γ loop, with very little energy dissipation.

The inverted- S shape of the V-γ loop derives from the following mechanism: Because of dislodgement of aggregates along the diagonal cracks and of inelastic strains in stirrups that have yielded in tension, diagonal cracks do not close immediately after reversal of the shear force. Significant reverse shear deformation needs

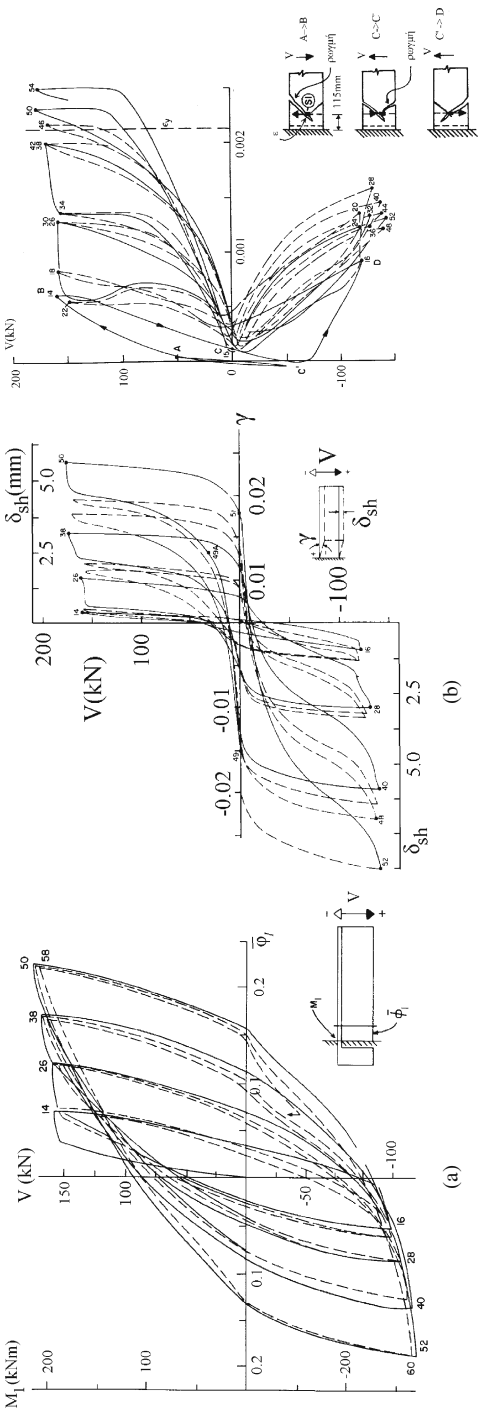

Fig. 3.37 T-beam under cyclic loading: (**a**) M-φ loops next to the end section; (**b**) V-γ loops in plastic hinge region; (**c**) loops of shear force V vs stirrup strain (adapted from Ma et al. 1976)

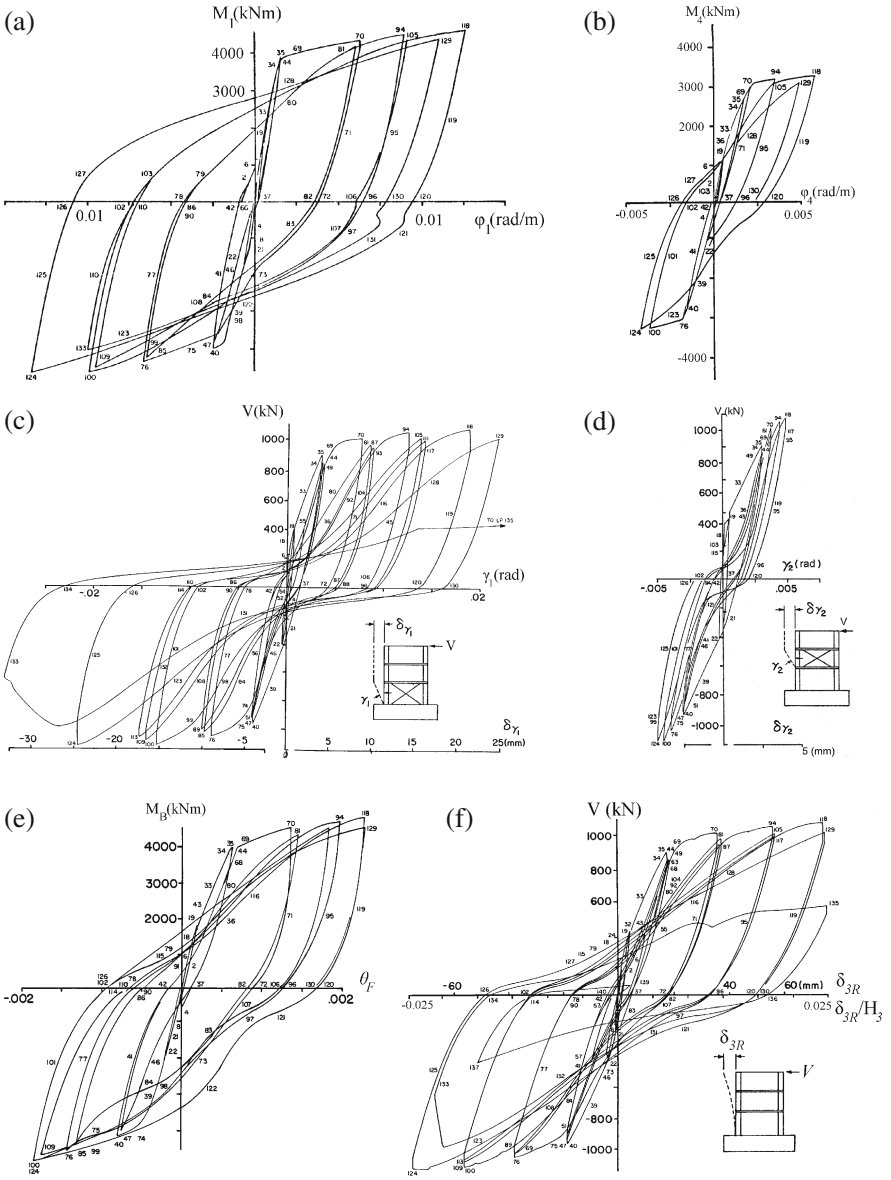

Fig. 3.38 3-storey wall (adapted from Wang et al. 1975): (**a**), (**b**): *M*-φ loops next to the base of 1st and 2nd storey; (**c**), (**d**): *V*-γ loops over 1st and 2nd storey; (**e**) loops of base moment vs fixed-end rotation due to bar pull-out from the anchorage in the footing; (**f**) base shear vs. top deflection

to be applied, to suppress the inelastic tensile strains in the stirrups and force the cracks to fully close and develop compressive stresses normal to their face. Especially when their geometric ratio, ρ_w, is low, stirrups present little stiffness until the crack closes. When that happens, a steep increase in stiffness takes place.

The small energy dissipation capacity of the shear mechanism of force transfer in cyclic loading and the steady accumulation of inelastic shear deformations in constant-amplitude cycling of the shear force suggest that the behaviour in shear does not possess the stability and dissipation capacity required for ductile behaviour under cyclic loading. Moreover, ultimate failure in shear takes place either by propagation of diagonal cracks into the compression zone, causing its disintegration, or by diagonal web crushing in compression. In both cases failure is abrupt and catastrophic and cannot be prevented or mitigated by confinement. For all these reasons, shear should be confined in the elastic region. Capacity design rules in shear aim at exactly that. For the same reason, what is primarily of interest for concrete members in shear is their cyclic shear resistance and not their (anyway small) inelastic shear deformations.

3.2.4.2 Fundamental Models for Shear Resistance in Monotonic Loading

The Variable Strut Inclination Truss of the CEB/FIP Model Code 90 and Eurocode 2

CEB/FIP Model Code 90 (CEB 1991) and Eurocode 2 (CEN 2004b) have adopted for shear resistance the variable strut inclination truss model – strictly speaking, a model with variable angle of inclination, δ,[16] of the compression stress field in the web with respect to the member axis. According to this model (Walraven 2002), a concrete member with:

- longitudinal reinforcement, typically concentrated at two "chords" at the ends of the section, and
- reinforcement transverse to the axis, with geometric ratio ρ_w

equilibrates a shear force V through a statically determinate "truss" mechanism comprising:

1. a compressive stress field in the concrete, at an angle δ to the member axis; equilibrium gives the compression stress in the concrete as: $\sigma_c = 2V/(b_w z \sin 2\delta)$;
2. a tensile stress in the transverse reinforcement equal to $V\tan\delta/(\rho_w b_w z)$, where b_w is the width of the web and z is the internal lever arm between the two "chords"; this stress amounts to a tension force per unit length of the member equal to $V\tan\delta/z$;
3. a tension force of $V\cot\delta$ in the longitudinal reinforcement.

Diagonal cracking first takes place at about 45° to the member axis. At that time the compression stress field is parallel to the cracks and at an angle to the member axis $\delta \approx 45°$. So long as the web has sufficient strength to resist the compres-

[16] The symbol δ is used here instead of the symbol θ normally used for the angle of inclination, to avoid confusion with chord rotations.

sive stress field, the member can sustain yielding of the transverse reinforcement at its yield stress, f_{yw}, and develop a further increased shear resistance at a steadily decreasing inclination of the new cracks and of the compression field, δ, with respect to the member axis:

$$V_{R,s} = \rho_w b_w z f_{yw} \cot\delta \tag{3.94}$$

Shear resistance increases with the rotation of the compression field, until either one of the following possibilities takes place:

i. The tension chord yields, as its tensile force increases owing both to the increase of the loading and the decrease of the inclination δ. If the member is also subjected to a bending moment, M, and an axial force N (positive for compression), and the longitudinal reinforcement is concentrated at two "chords" at the ends of the section, the force in the tension chord is: $M/z + 0.5(V\cot\delta - N)$. The shear force at yielding of a tension chord with cross-sectional area A_{s1} and yield stress f_{yL} is:

$$V_{R,L} = 2\left(A_{sl} f_{yL} - M/z + N/2\right)\tan\delta \tag{3.95}$$

ii. The web concrete fails in diagonal compression, as the compressive stresses in the web also increase owing both to the reduction of δ and the increase of V. Note that the compressive strength of concrete at an angle δ to the member axis is less than its uniaxial compressive strength, f_c, because of the tensile stresses and strains in the orthogonal direction (namely those associated with yielding of the transverse reinforcement and the tensile stresses in the concrete between adjacent diagonal cracks). The reduced strength of concrete is taken equal to nf_c,[17] with:

$$n = 0.6\left(1 - \frac{f_c(MPa)}{250}\right) \quad \text{in Eurocode 2 (CEN 2004b) or Model Code 90 (CEB 1991)} \tag{3.96a}$$

$$n = 0.7\left(1 - \frac{f_c(MPa)}{200}\right) \quad \text{in the AIJ Guidelines (AIJ 1994)} \tag{3.96b}$$

So, the shear resistance at diagonal compression failure of the web is:

$$V_{R,\max} = 0.5 b_w z (n f_c) \sin 2\delta \tag{3.97}$$

According to Eq. (3.94), a low value of δ gives less transverse reinforcement, as the shallower crack intersects and activates more stirrups. According to Eq. (3.95),

[17] The symbol n is used here instead of the symbol v used in both Eurocode 2 and CEB/FIP Model Code 90, to avoid confusion with the normalised axial force $v = N/A_c f_c$.

however, it is more demanding for the chords in tension and, according to Eq. (3.97), for the inclined compression stress field as well.

The shear resistance normally attains its maximum value when the web concrete fails in diagonal compression, while the transverse reinforcement has already yielded (case ii above). The condition $V_{\mathrm{R,s}} = V_{\mathrm{R,max}}$ gives the following lower limit for the inclination angle, δ (Walraven 2002):

$$\sin\delta = \sqrt{\frac{\omega_w}{n}},\ \tan\delta = \sqrt{\frac{\frac{\omega_w}{n}}{1-\frac{\omega_w}{n}}} \tag{3.98}$$

where $\omega_{\mathrm{w}} \equiv \rho_{\mathrm{w}} f_{\mathrm{yw}}/f_{\mathrm{c}}$ is the mechanical ratio of transverse reinforcement. At this limit value of δ the dimensionless shear resistance is:

$$\upsilon_R = \frac{V_R}{b_w z f_c} = \sqrt{\omega_w(n-\omega_w)} \tag{3.99}$$

Although less common than case ii, case i above may also lead to shear failure. The condition $V_{\mathrm{R,s}} = V_{\mathrm{R,L}}$ gives the following limit value of δ:

$$\tan\delta = \sqrt{\frac{\omega_w}{2(\omega_1-\mu)+\nu}} \tag{3.100}$$

where $\omega_1 \equiv A_{\mathrm{s1}} f_{\mathrm{yL}}/(b_{\mathrm{w}} z f_{\mathrm{c}})$ is the mechanical ratio of tension reinforcement and $\mu \equiv M/(b_{\mathrm{w}} z^2 f_{\mathrm{c}})$, $\nu \equiv N/(b_{\mathrm{w}} z f_{\mathrm{c}})$ are the dimensionless bending moment and axial force, respectively (using in all normalisations the internal lever arm, z, in lieu of the effective depth). At this value of δ the dimensionless shear resistance is:

$$\upsilon_R = \frac{V_R}{b_w z f_c} = \sqrt{\omega_w(2(\omega_1-\mu)+\nu)} \tag{3.101}$$

Even less common is a failure mode where the tension chord yields first, followed by diagonal compression failure of the web concrete while the transverse reinforcement stays elastic. The condition $V_{\mathrm{R,max}} = V_{\mathrm{R,L}}$ gives the following upper limit for δ:

$$\cos\delta = \sqrt{\frac{2(\omega_1-\mu)+\nu}{n}},\ \tan\delta = \sqrt{\frac{n-2(\omega_1-\mu)-\nu}{2(\omega_1-\mu)+\nu}} \tag{3.102}$$

and a dimensionless shear resistance of:

$$\upsilon_R = \frac{V_R}{b_w z f_c} = \sqrt{(n-2(\omega_1-\mu)-\nu)(2(\omega_1-\mu)+\nu)} \tag{3.103}$$

The variable strut inclination truss model is rational, transparent and consistent with the strut-and-tie approach for the Ultimate Limit State (ULS) design of

two-dimensional concrete regions (including discontinuities of geometry, supports and regions with concentrated forces). So there is smooth transition between such regions and adjacent prismatic ones. Accordingly, in Europe it is the basis of the provisions for calculation of shear resistance of concrete members at the ULS. The designer is allowed to choose the value of δ in the range:

– in Eurocode 2 (CEN 2004b):

$$0.4 \leq \tan\delta \leq 1 \,(22^\circ \leq \delta \leq 45^\circ); \tag{3.104a}$$

– in the CEB/FIP Model Code 90 (CEB 1991):

$$1/3 \leq \tan\delta \leq 1 (18^\circ \leq \delta \leq 45^\circ) \tag{3.104b}$$

Eurocode 2 and CEB/FIP Model Code 90 consider that a compressive axial force, N, contributes to shear resistance according to the following mechanism. Shear force goes together with bending moments. In the common case of a column in counter-flexure, the axial force N will be equilibrated at the two end sections by concrete compressive stress blocks that develop at opposite ends of these two sections.[18] The axial force N is transferred, therefore, from the compressive stress block at one end section to that at the other end via a diagonal compression strut (Fig. 3.39(a), left). The component of the strut force parallel to the column axis is equal to N, while the component transverse to the axis is equal to $V_N = N(z_1+z_2+d_1-d)/L$ where z_1 and z_2 are the internal lever arms at the two end sections, $d_1 = h-d$ and L is the clear column length. This internal force is in the opposite sense with respect to the acting (external) shear force. So, it can be considered as the contribution of the diagonal compression strut to the shear resistance of the column. In the common case that the two ends have about the same acting moment and cross section reinforcement, this contribution is: $V_N = N(h-x)/L$ where x is the neutral axis depth of the end sections at flexural yielding (computed as $x = \xi_y d$, with ξ_y from Section 3.2.2.2). The rest of the shear force, $V-V_N$, is resisted by the internal truss mechanism with a (variable) strut inclination δ (Fig. 3.39(a), right). The normal stress component $\sigma = N/b_w(h-x)$ in the strut acts together with the compression field of the truss, which is equal to $2(V-V_N)/(b_w z \sin 2\delta)$ and is at an angle δ to the column axis.

As shown in Fig. 3.40, for monotonic loading the variable strut inclination truss model gives a safe-side bound of test results on beams failing by diagonal compression of the web after yielding of the transverse reinforcement (Walraven 2002). In Fig. 3.40(b) the beneficial effect of the (compressive) prestressing force on shear resistance is taken into account at the same time as the adverse effect of the superposition of the normal stress component in the strut due to prestress with the

[18] Being symmetrically reinforced, each end section will resist the bending moments there through approximately equal and opposite forces in the two "chords", that produce no net contribution to N.

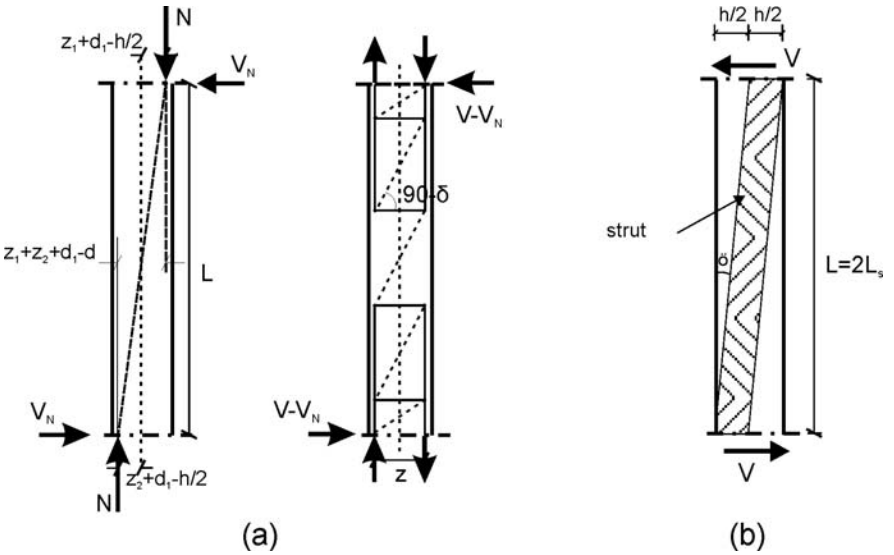

Fig. 3.39 Shear resistance model: (**a**) according to (CEB 1991); (**b**) according to (AIJ 1994)

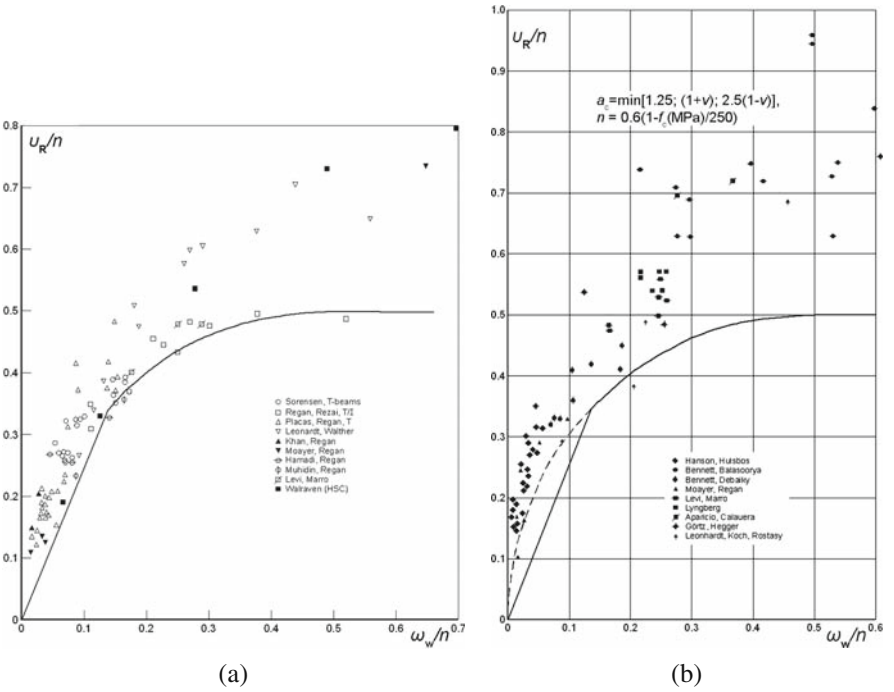

Fig. 3.40 Comparison of Eq. (3.99), subject to the limits of Eq. (3.104a), to monotonic shear resistance data: (**a**) reinforced beams with rectangular or T-section; (**b**) prestressed T- or I-beams (Walraven 2002)

compression field of the truss, by multiplying the shear resistance at diagonal compression failure in the web by the following empirical factor given in Eurocode 2:

$$a_c = \min[1.25;\ (1 + \nu);\ 2.5(1 - \nu)] \tag{3.105}$$

where ν is the normalised axial compression, in this case due to the prestress: $\nu = P/A_c f_c$.

The variable strut inclination approach is a generalisation of the classical Mörsch-Ritter truss, where $\delta = 45^\circ$. The 45°-truss is still the basis for shear design in the US (ACI 2008). In such an approach, transverse reinforcement is dimensioned to take a tensile force per unit length along the member axis equal to $(V–V_c)/z$, instead of the value $V\tan\delta/z$ of the variable strut inclination truss model. The V_c term replaces the increase in the contribution of stirrups to shear strength, $V_{R,s}$, according to Eq. (3.94) as the strut inclination decreases from $\delta = 45^\circ$ to a lower value. It is considered as the "concrete contribution to shear resistance". Its physical basis is claimed to be the contributions to the truss model of shear resistance of:

- the uncracked compressive zone;
- aggregate interlock along open diagonal cracks (considered at an angle $\delta = 45^\circ$);
- dowel action of the longitudinal bars; and
- the tensile strength of concrete between diagonal cracks.

As it is not feasible to quantify the contribution of each one of the above four mechanisms in terms of the corresponding parameters, the V_c term is just the difference between:

- the experimentally measured shear resistance, and
- the contribution of transverse reinforcement calculated from Eq. (3.94) with $\delta = 45^\circ$, plus any contribution of the axial force N.

So the value of V_c is commonly given by empirical or semi-empirical expressions in terms of all other parameters that seem to significantly affect shear resistance. Recall in this connection the Eurocode 2 empirical expression, Eq. (3.67), for the shear resistance of concrete members without shear reinforcement, V_{Rc}.

The Truss Plus Diagonal Strut Model of the AIJ Guidelines

The approach of the Guidelines of the Architectural Institute of Japan (AIJ 1994) for the shear resistance of concrete members under cyclic loading is the most fundamental in all codes or standards for earthquake-resistant design of concrete structures. In this approach shear resistance is taken as the sum of contributions from two mechanisms:

- a "variable strut inclination" truss, as in Eurocode 2 (CEN 2004b) and Model Code 90 (CEB 1991); and

– a diagonal strut between the two end sections of the member, considered in skew symmetric bending (i.e. with length L twice the shear span L_s).

The contribution of the truss mechanism to shear resistance is considered to be controlled by the transverse reinforcement according to Eq. (3.94). A compression field at an angle δ to the member axis equal to: $\sigma_c = 2V_w/(b_w z \sin 2\delta) = \rho_w f_{yw}/\sin^2\delta$ is necessary, to support this contribution to shear resistance. The stress σ_c uses up part of the reduced diagonal concrete strength, nf_c (see Eqs. (3.96) for the reduction factor n). Neglecting the different orientations of the diagonal strut and of the compression field of the truss mechanism, the effective compressive strength available to the diagonal strut is $nf_c - \rho_w f_{yw}/\sin^2\delta$. The AIJ Guidelines assume the diagonal strut to take up half of the cross-sectional depth h in the direction of the shear force, no matter the width of the compression zone due to flexure. The strut inclination with respect to the member axis, ϕ, is such that:

$$\tan\phi = \sqrt{\left(\frac{2L_s}{h}\right)^2 + 1} - \frac{2L_s}{h} \approx h/4L_s. \tag{3.106}$$

In the end the maximum compressive force that the diagonal strut can develop has a component transverse to the member axis equal to $0.5 b_w h(nf_c - \rho_w f_{yw}/\sin^2\delta)\tan\phi$, which is the strut contribution to shear resistance. Therefore, the total shear resistance is:

$$V_R = \rho_w f_{yw} b_w z \cot\delta + 0.5 b_w h[nf_c - \rho_w f_{yw}(1 + \cot^2\delta)]\tan\phi \tag{3.107}$$

An upper limit is set for the value of $\cot\delta$, equal to the smallest of the three values:

– $\cot\delta \le 2\ (\delta \ge 26.5)^\circ$ (3.108a)

for a positive term in brackets in Eq. (3.107):

– $\cot\delta \le \sqrt{(nf_c/\rho_w f_{yw} - 1)}$ (3.108b)

– $\cot\delta \le z(h\tan\phi) \approx 4\zeta L_s/h$ (3.108c)

(with $\zeta = z/h$), which gives the maximum possible shear resistance from Eq. (3.107).

The effect of inelastic cyclic deformations on the shear strength of plastic hinge regions is taken into account:

– by replacing the limit of Eq. (3.108a) with:

$$\cot\delta \le \max(1;\ 2 - 50\theta_{pl}) \tag{3.108d}$$

– by reducing the value of n from Eq. (3.96b) to:

$$n = 0.7\left(1 - \frac{f_c(MPa)}{200}\right)\max\left(0.25;\ 1 - 15\theta_{pl}\right) \tag{3.109}$$

where θ_{pl} is the plastic hinge rotation: $\theta_{\mathrm{pl}} = (\mu_\theta - 1)\theta_{\mathrm{y}}$, with μ_θ denoting the demand value of the displacement or chord rotation ductility factor.

3.2.4.3 Models of Cyclic Resistance in Diagonal Tension After Flexural Yielding

At pointed out in Section 3.2.4.1, after flexural yielding the shear strength degrades in the plastic hinge with increasing cyclic inelastic deformations. It has also been noted that this phenomenon is normally expressed quantitatively as a reduction of shear strength with cyclic inelastic deformations, until the so-reduced shear strength, V_{R}, drops below the value of shear force corresponding to flexural yielding, $V_{\mathrm{y}} = M_{\mathrm{y}}/L_{\mathrm{s}}$.

Several models have been proposed for the cyclic decay of the strength of concrete members for diagonal tension failure (Kowalsky and Priestley 2000, Moehle et al. 2001, Ascheim and Moehle 1992, Biskinis et al. 2004). They all recognise a contribution of transverse reinforcement to shear resistance, V_{Rs}, and a separate concrete contribution, V_{c}.

The "Revised UCSD model" model in Kowalsky and Priestley (2000) has been developed on the basis of 18 circular columns that failed in shear after yielding in flexure. Predictions also compare well to the strength of 20 circular columns yielding and failing in shear and are compatible with the strength of 9 circular columns failing in flexure.

As in the CEB/FIP Model Code 90, the model in Kowalsky and Priestley (2000) includes the contribution of the column axial force to shear resistance as a distinct mechanism, giving a shear resistance:

$$V_R = N\frac{h-x}{2L_s} + \sqrt{f_c}k\left(\mu_\theta\right)\min\left(1.5,\ \max\left(1;\ 3 - \frac{L_s}{h}\right)\right) \\ \min\left(1;\ 0.5 + 20\rho_{tot}\right)(0.8A_c) + V_{Rs}\ \text{(units: MN, m)} \tag{3.110}$$

where:

– ρ_{tot} is the total ratio of longitudinal steel, reflecting in this case dowel action,
– A_{c} is taken equal to $\pi {D_{\mathrm{c}}}^2/4$ (with D_{c}: diameter of concrete core inside the hoops),
– h is the depth of the cross-section (equal to the diameter D in circular sections),
– N is the axial load (positive for compression),
– x is the neutral axis depth at flexural yielding ($x = \xi_{\mathrm{y}} d$, with ξ_{y} from Section 3.2.2.2), and
– $L_{\mathrm{s}}/h = M/Vh$ is the shear span ratio at the member end, reflecting the arch mechanism of shear resistance.

Shear strength degradation due to cyclic deformations of the shear span up to a chord rotation ductility ratio μ_θ[19] is taken into account through the coefficient $k(\mu_\theta)$ in the concrete term V_c:

$$k(\mu_\theta) = \frac{1.07 - 0.115\mu_\theta}{3} \quad , 0.05 \le k(\mu_\theta) \le 0.28 \tag{3.111}$$

Equations (3.110) and (3.111) have been developed for circular columns with the contribution of transverse steel, V_{Rs}, taken as:

$$V_{Rs} = \frac{\pi}{2}\frac{A_{sw}}{s_h} f_{yw}(D - x - c)\cot\delta \tag{3.112}$$

where A_{sw} denotes the cross-sectional area of a circular hoop, s_h its spacing and c its concrete cover. In the "revised UCSD model" the truss inclination is taken as: $\delta = 30^\circ$.

Although originally developed for columns with circular section, Eqs. (3.110) and (3.111) are often applied to rectangular sections as well, using for V_{Rs} Eq. (3.94) with $z = d–x$, $\delta = 30^\circ$, and replacing the term $0.8A_c$ by $b_w d$ (where b_w is the width of the web and d the effective depth). In that case it overestimates the shear resistance of rectangular columns by about 20%, of rectangular walls by about 10% and of non-rectangular walls or hollow rectangular piers by about 30% (Biskinis 2007, Biskinis et al. 2004).

In the most recent one of the family of models by Moehle and co-workers for rectangular columns (Moehle et al. 2001), the contribution of axial compression to shear resistance is accounted for in the V_c term and not as a separate mechanism (cf. 1st term in Eq. (3.110)). More important, the reduction of shear strength with cyclic deformation is considered to affect both the V_{Rs} and the V_c terms, which are multiplied by the same coefficient $k(\mu_\theta)$ (Moehle et al. 2001):

$$V_R = k(\mu_\theta)(V_c + V_{Rs}) \; ; \quad V_c = 0.5\sqrt{f_c}\left(\sqrt{1 + \frac{N}{0.5\sqrt{f_c}A_c}}\right)A_c\frac{d}{L_s} \quad \text{(units: MN, m)} \tag{3.113a}$$

$$k(\mu_\theta) = 1.15 - 0.075\mu_\theta, \; 0.7 \le k(\mu_\theta) \le 1.0 \tag{3.113b}$$

where $A_c = b_w d$, for cross-sections with rectangular web of width b_w and effective depth d. The part of the V_c term multiplied by d/L_s in Eq. (3.113a) is the product of the gross section area and the principal tensile stress at diagonal cracking, computed on the basis of a postulated concrete tensile strength of $0.5\sqrt{f_c}$. For beams, rectangular columns, rectangular walls or barbelled, T-, H- or hollow rectangular sections the contribution of transverse reinforcement, V_{Rs}, is taken from Eq. (3.94), with

[19] In members the chord rotation ductility factor, μ_θ, is the same as the displacement ductility factor.

$\delta = 45^\circ$, as in the classical Ritter-Mörsch truss analogy. In circular columns $V_{R,s}$ may in this case be taken from Eq. (3.112), but with $\delta = 45^\circ$ and (D–x–c) replaced by (D–2c).

Equations (3.113) agree well, on average, with the experimental results on rectangular columns, but underestimate the shear resistance of circular ones by almost 20% and of rectangular walls by about 10%, while it overestimates that of non-rectangular walls or hollow rectangular piers by about 15% (Biskinis 2007, Biskinis et al. 2004).

Note that in Eqs. (3.110) and (3.111) the V_c term is constant and equal to 18% of its value for zero ductility demand, when the value of μ_θ exceeds 8. According to Eq. (3.113b), it is for values of μ_θ above 6 that the entire shear resistance V_R attains its minimum value of 70% of that for zero ductility demand. The difference in the limiting value may be attributed to:

- the reduction of the entire shear resistance with increasing μ_θ in Eq. (3.113a), whereas only one term out of three is taken to decrease with increasing μ_θ in Eqs. (3.110) and (3.111); and
- the relative small magnitude of the only term that decreases with μ_θ in Eq. (3.110), owing to the adoption of a value $\delta = 30^\circ$ for the truss inclination δ in Eqs. (3.94) and (3.112).

In both models above, μ_θ is derived from the experimental θ_y, which is not known a-priori in practical applications. This may be considered as a weakness.

The models proposed in (Biskinis et al. 2004, Biskinis and Fardis 2004, Biskinis 2007) and adopted in Part 3 of Eurocode 8 (CEN 2005a) are based on the largest database of cyclic tests of members failing by diagonal tension after yielding in flexure: 70 circular columns, 192 rectangular beams/columns, 12 rectangular walls and 26 hollow rectangular piers or non-recangular walls. The range of important parameters in these tests are:

- $\nu = N/A_c f_c$: –0.01–0.85;
- L_s/h: 0.5–6;
- ρ_{tot}: 0.55–5.5%;
- f_c: 13–113 MPa;
- μ_θ: 1.0–9.5.

In these models the resistance in diagonal tension, V_R, is taken a function of $\mu_\theta^{pl} = (\mu_\theta – 1)$, computed as the ratio of the plastic part of the chord rotation at ductile shear failure (: total chord rotation minus experimental yield value) to the yield chord rotation, θ_y, from Eqs. (3.66), instead of the experimental θ_y. In this way μ_θ^{pl} is not affected by the flexibility of the base of some test specimens, which increases the measured pre-yield deflection but affects very little the post-elastic deformations of the specimen itself. Similar to Eq. (3.110) of Kowalsky and Priestley (2000), the axial compression N is taken to affect shear resistance according to the CEB/FIP Model Code 90 (CEB 1991), but the effect of axial tension is neglected. As in Eqs.

(3.110) and (3.113a), $\sqrt{f_c}$ appears in the V_c term, reflecting the tensile strength of concrete.

In the first one of two models only the V_c term is taken to degrade with inelastic cyclic displacements (cf. Eq. (3.110)). With units: MN, m, this model is:

$$V_R = \frac{h-x}{2L_s} \min\left(N;\ 0.55A_c f_c\right) + 0.16\left(1 - 0.095\min\left(5;\ \mu_\theta^{pl}\right)\right) \max(0.5,\ 100\rho_{tot})\left(1 - 0.16\min\left(5;\ \frac{L_s}{h}\right)\right)\sqrt{f_c}A_c + V_{Rs} \tag{3.114a}$$

In the other model both V_c and the contribution of V_{Rs} degrade with cyclic μ_θ :

$$V_R = \frac{h-x}{2L_s} \min\left(N;\ 0.55A_c f_c\right) + \left(1 - 0.05\min\left(5;\ \mu_\theta^{pl}\right)\right) \left[0.16\max(0.5;\ 100\rho_{tot})\left(1 - 0.16\min\left(5;\ \frac{L_s}{h}\right)\right)\sqrt{f_c}A_c + V_{Rs}\right] \tag{3.114b}$$

V_{Rs} is taken with $\delta = 45^\circ$ and as for Moehle et al. (2001): in circular columns from Eq. (3.112) with (D–x–c) replaced by (D–2c) and for all other sections from Eq. (3.94).

Both Eqs. (3.114a) and (3.114b) agree very well with the data and are practically equivalent as far as scatter is concerned. Their test-to-prediction ratio in 300 cyclic tests to diagonal tension failure has median of 0.995 and coefficients of variation of 15.5% or 14.6%, respectively. For comparison, the median test-to-prediction ratio for Eqs. (3.110) or (3.113) is 0.83 or 1.015, respectively, and the coefficient of variation of both is about 25%.

Equations (3.114) are also in good agreement with three cyclic tests on prestressed specimens, failing by diagonal tension after flexural yielding. In this calculation the prestress can only be taken as part of the actions, even though bonded tendons near the extreme tension fibres may yield, when the member's end section yields before ultimate failure in shear. The prestress cannot be taken as part of the resistance, because bending moments nowhere enter in this calculation and hence the bending moment induced by the bonded tendons that have not yielded cannot be taken into account.

According to Eqs. (3.114), beyond $\mu_\theta = 6$ there is no further decay of shear strength. For $\mu_\theta > 6$ the V_c term in Eq. (3.114a) assumes a constant value equal to 52.5% of that at $\mu_\theta = 1$. In Eq. (3.114b) for $\mu_\theta > 6$ the sum of V_c and V_{Rs} attains a constant value of 75% that at $\mu_\theta = 1$.

Equations (3.110), (3.111), (3.112), (3.113) and (3.114) can be conveniently used to assess whether a member that initially yields in flexure may ultimately fail in shear by diagonal tension at a cyclic deformation less than that at failure by flexure. In principle, they can also be inverted to estimate the cyclic deformation capacity of members failing by diagonal tension after flexural yielding: by setting the shear resistance V_R equal to the shear force, M_y/L_s, at flexural yielding, solving for μ_θ

and estimating the shear-controlled chord rotation capacity as μ_θ times θ_y, from Eqs. (3.66). However, the sensitivity of V_R to μ_θ is not sufficiently large to allow using this force-based criterion to predict the deformation capacity as controlled by shear. So, the predictive capability of the inverted procedure is poor (Biskinis 2007, Biskinis et al. 2004).

3.2.4.4 Inclination of Compression Stress Field at Ductile Shear Failure Under Cyclic Loading

The method of choice in Eurocode 2 (CEN 2004b) for the design of concrete elements in shear is the "variable strut inclination" model, Eqs. (3.94), (3.95) and (3.97), along with Eqs. (3.96a) and (3.104a). Eurocode 8, conforms to the Eurocode 2 framework and uses Eq. (3.94), that includes a term proportional to cotδ but no V_c term. According to Eurocode 8, columns and walls of DC H (High) buildings, as well as any member of a DC Medium (M) building, may be dimensioned for an angle δ of the compression diagonals as low as $\delta = 22^\circ$ (cot $\delta = 2.5$).The beams of DC H buildings should be dimensioned in shear for $\delta = 45^\circ$ (i.e. with a classical 45° truss and no V_c term).

The data used for the fitting of Eqs. (3.114) have also been utilised in (Biskinis 2007, Biskinis et al. 2004) to compute the value of δ at which the sum of $N(h-x)/2L_s$ and V_{Rs} from Eq. (3.94) is equal to the experimental shear resistance. The outcome for the 300 tests is depicted in Fig. 3.41 as a function of the chord rotation ductility factor, μ, at failure. Figure 3.41 shows a tendency of the angle δ to

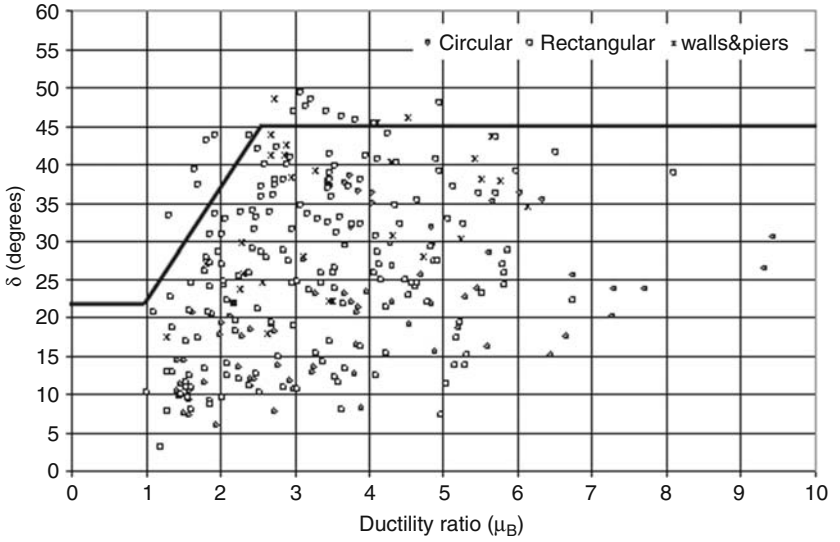

Fig. 3.41 Experimental data on the dependence of the strut inclination δ on chord rotation ductility ratio, for cyclic loading after flexural yielding (Biskinis 2007, Biskinis et al. 2004)

increase on average with increasing μ, from a value well below the Eurocode 2 lower limit of $\delta = 22^\circ$ for $\mu = 1$. However, as important parameters reflected in the V_c term of Eqs. (3.110), (3.113) and (3.114) are missing, the scatter is very large. So, any attempt to fit the angle δ as a function of μ_θ is meaningless. An approximate 5%-fractile line is drawn in Fig. 3.41, extending from the Eurocode 2 lower limit of $\delta = 22^\circ$ for $\mu = 1$, to $\delta = 45^\circ$ for $\mu = 2.5$. This line may be considered to give a very safe-sided estimate of shear strength for design purposes. So, despite the merits of the "variable strut inclination" method for shear design against monotonic loads, a classical 45°-truss model with a V_c term that depends on displacement ductility demand, seems to be a better means for the design of concrete members against diagonal tension failure under cyclic loading after flexural yielding.

3.2.4.5 Degradation with Cyclic Loading of the Diagonal Compression Strength of Walls

Squat shear walls subjected to cyclic loading in the lab or in the field may fail in shear by diagonal compression, often after flexural yielding. Over 50 wall or hollow rectangular piers (all with shear span ratio, L_s/h, less or equal to 2.5) have been found in the literature as having failed by shear compression under cyclic loading (Biskinis 2007, Biskinis et al. 2004). Most of them failed in shear after they had yielded in flexure, but a total of 18 specimens (walls with barbelled or T-section or hollow rectangular piers) failed before flexural yielding. Figure 3.42 shows that the cyclic shear resistance of these walls decreases when their inelastic deformations increase.

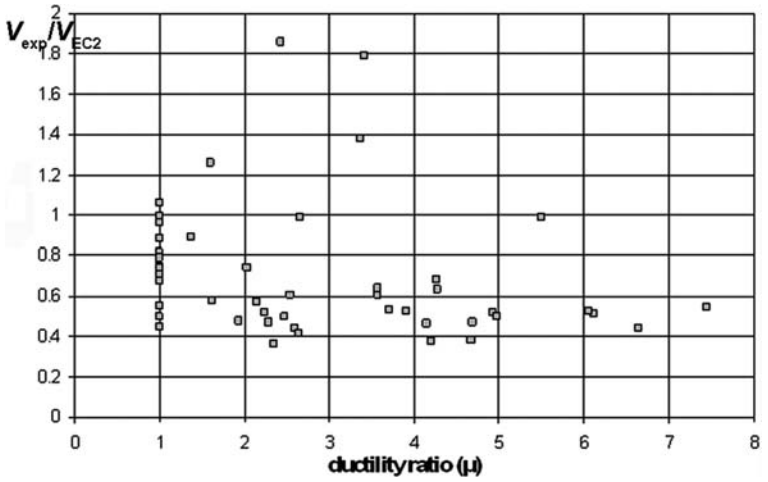

Fig. 3.42 Experimental shear resistance of squat walls for web diagonal compression, as a fraction of the shear resistance from Eqs. (3.97), (3.98) and (3.99), using the concrete strength reduction factor of Eurocode 2 and Model Code 90, Eq. (3.96a)

More important, it is generally much less than the shear resistance of walls in diagonal compression of the web for monotonic, non-seismic actions from Eqs. (3.97), (3.98), (3.99) and (3.96a) (CEN 2004b, CEB 1991). The cyclic shear resistance of these walls is less than the monotonic value in (CEN 2004b, CEB 1991), even when shear failure occurs before flexural yielding ($\mu_\theta = 1$ in Fig. 3.42). It seems therefore, that the Eurocode 2 design rules are not safe for shear compression failure of squat walls under cyclic loading. For this reason in Part 1 of Eurocode 8 the value of $V_{\mathrm{R,max}}$ of ductile walls in DC H buildings is just 40% of the value in Eurocode 2, Eqs. (3.96a) and (3.97). As shown in Fig. 3.42, that value is a 5%-fractile.

A purely empirical model for the cyclic degradation of the shear strength in diagonal compression has been fitted in (Biskinis 2007, Biskinis et al. 2004) to the data that have been used in Fig. 3.42. In addition to ${\mu_\theta}^{\mathrm{pl}} = \mu_\theta - 1$, expressing the effect of inelastic cyclic displacements, statistically significant parameters for the shear strength in cyclic diagonal compression are those included in the V_{c} term of Eqs. (3.114) plus the axial force. Most specimens in the database failed around the value of δ that maximises $V_{\mathrm{R,max}}$ in Eq. (3.97): $\delta = 45^\circ$. So, the model is based on the classical 45° truss. For units MN, m, it gives the cyclic decay of diagonal compression strength as (Biskinis 2007, Biskinis et al. 2004):

$$\begin{aligned} V_{R,\max} = {} & 0.85\left(1 - 0.06\min\left(5;\ \mu_\theta^{pl}\right)\right)\left(1 + 1.8\min\left(0.15;\ \frac{N}{A_c f_c}\right)\right) \\ & (1 + 0.25\max(1.75;\ 100\rho_{tot}))\left(1 - 0.2\min\left(2;\ \frac{L_s}{h}\right)\right) \\ & \sqrt{\min(f_c;\ 100)}\, b_w z \end{aligned} \tag{3.115}$$

The internal lever arm z is taken as $z = 0.8 l_{\mathrm{w}}$ for rectangular walls and $z = d - d_1$ for walls with barbelled or T-section and in hollow rectangular piers.

Equation (3.115) fits the data with a median test-to-prediction ratio of 1.01 and a coefficient of variation of 17.6% (Biskinis 2007). The data fitted include the 18 cyclically loaded walls with barbelled or T-section or hollow rectangular piers failing in shear compression prior to yielding in flexure. Therefore, it may be considered to hold also (with ${\mu_\theta}^{\mathrm{pl}} = 0$) for failure in cyclic shear before flexural yielding.

Equation (3.115) has been adopted in Part 3 of Eurocode 8 (CEN 2005a). Being fully empirical, it applies strictly within the range of parameter values in the fitting:

- L_{s}/h from 0.5 to 2.4 (squat walls),
- $N/A_{\mathrm{c}}f_{\mathrm{c}}$ from 0 to 0.18,
- ρ_{tot} from 0.5 to 3%,
- f_{c} from 16.5 to 137 MPa,
- μ_θ from 1 to 7.5.

3.2.5 Cyclic Behaviour of Squat Members, Controlled by Flexure-Shear Interaction

3.2.5.1 Introduction

Short columns (including captive ones, see Section 2.1.13.4), deep beams and squat walls have low shear span ratio, M/Vh. During earthquakes short columns develop nearly equal and opposite bending moments at their ends. The same holds in short beams, because their end moments due to gravity loads are normally very small. So, the shear span ratio of short columns or beams is equal to $0.5L/h$, where L is the clear length and h the depth of their section. The bending moment diagram of squat walls is affected little by any beams framing into them. So their shear span ratio at the base is between $0.5H_w/l_w$ and $2/3(H_w/l_w)$, where H_w is the total height of the wall.

For given cross-sectional dimensions and longitudinal reinforcement, hence for given moment resistance, the shear force increases with decreasing shear span ratio. Moreover, low shear span ratio elements have a two-dimensional geometry. So it is not possible to distinguish between their end regions, governed by flexure, and the rest of their length, where (the constant) shear force controls the resistance and the behaviour. As a matter of fact, if we ignore that the short length of the member – compared to its depth – invalidates the simple models applicable to prismatic elements, we may be surprised at first sight by some conclusionst. For example, if the usual fan pattern of cracking and of the compression field near the member's end regions extends up to mid-length, $x = L/2$, then, if the corresponding value of the inclination of the compression field at $x = L/2$: $\cot\delta = L/z$ is used for the forces in the chords: $F_t(x) = M(x)/z + 0.5V\cot\delta$ (see Section 3.2.4.2 under *The Variable Strut Inclination Truss of the CEB/FIP Model Code 90 and Eurocode 2*), we get:

- at the mid-section, $x = L/2$: a tensile force in both chords equal to that at the end sections: $F_t = M(x{=}0)/z$,
- at the end sections $x = 0$ and $x = L$: zero force in one chord, instead of the compressive force $F_t = -M(x = L)/z$ expected there on the basis of flexure alone.

So, the stress in the tension longitudinal reinforcement should drop from $\sigma_s = f_y$ at $x = L/2$, to $\sigma_s = 0$ at $x = L$, inducing very high bond demands on the length of the bars between these two sections. Unless another failure mode develops first, splitting cracks may form all-along the corner bars of short concrete members subjected to cycling loading.

Figure 1.2(a) in Section 1.3.1 shows the load-deformation response of an element with $L_s/h = 1.9$ under monotonic loading. Soon after the monotonic ultimate strength is reached, resistance drops drastically. In cyclic loading, hysteresis loops are narrow and have inverted-S shape, with a tendency to tilt and shrink further with cycling. The ultimate deformation is low and the displacement ductility factor

at member failure is not much larger than 1.0. The behaviour is not ductile and is strongly affected (or even governed) by shear.

3.2.5.2 Monotonic Lateral Force Resistance of Squat Members with Flexure-Shear Interaction

As pointed out in Section 3.2.1, if the shear span ratio is low the mechanisms of force transfer by shear or flexure essentially merge into a single one. Diagonal compression in the concrete plays a prime role in this joint mechanism. A good starting point for the understanding of the mechanism of force transfer and of ultimate failure of low shear span ratio elements is the shear resistance model in AIJ (1994), outlined in Section 3.2.4.2 under *The Truss Plus Diagonal Strut Model of the AIJ Guidelines*. That model, though, has certain limitations:

1. the assumption that the diagonal compression strut takes up one-half of the member depth, h, is arbitrary;
2. the effect of axial load is ignored;
3. concrete stresses in the diagonal strut are directly added to those in the compression field of the truss mechanism, although they do not act in the same direction, but at angles ϕ and δ to the member axis, respectively.

An important feature of the AIJ model is that the diagonal compression strut acting between the compression zones at the two end sections resists, via its force component that is transverse to the member axis, a certain part of the shear force (cf. term $N(h–x)/2L_s$ in Eqs. (3.110) and (3.114)). The rest of the shear force is resisted through the familiar truss mechanism comprising:

– the two parallel chords,
– the stirrups, and
– the concrete compression field at an inclination δ to the member axis.

The AIJ model for shear resistance of relatively slender elements without effect of the axial force (Section 3.2.4.2 under *The Truss Plus Diagonal Strut Model of the AIJ Guidelines*) is extended below to squat elements with axial compression:

(a) by taking into account the contribution of the axial load, N, and
(b) by considering that at the two end sections the diagonal strut extends over the neutral axis depth there at flexural yielding (i.e., it is equal to: $x = \xi_y d$, with ξ_y from Section 3.2.2.2 under *Cross-Sections with Rectangular Compression Zone*), in lieu of $0.5h$.

Owing to (b), the strut inclination to the member axis is $\phi = \arctan[(h-x)/2L_s]$. Its width normal to the strut axis is $x \cos\phi$.

As in the AIJ (1994) model, the member is considered to fail in diagonal compression under the action of:

- the normal stress in the diagonal strut, assumed uniform over its width, $x \cos \phi$, even at the end section of the member;
- the inclined compression field of the truss mechanism, considered uniform over the internal lever arm $z = \zeta h$ between the chords and acting at an angle δ to the member axis.

Also as in the AIJ shear model, the difference in the orientation of these two compression fields is neglected. So, their stress magnitudes are added up and the sum is set equal to a fraction n of the uniaxial compressive strength of concrete, f_c (see Eqs. (3.96)).

The assumptions and approximations above give the following, as generalisation of the procedure in Shohara and Kato (1981) – where the truss was a classical Mörsch-Ritter one with $\delta = 45^\circ$ and $n = 1$ – (see Fig. 3.43(a), where $\nu = N/bhf_c$, $\upsilon = V/bhf_c$, $\lambda = L/h = 2L_s/h$, $\zeta = z/h$ and ω_s is the total mechanical longitudinal reinforcement ratio, denoted here as ω_{tot}).

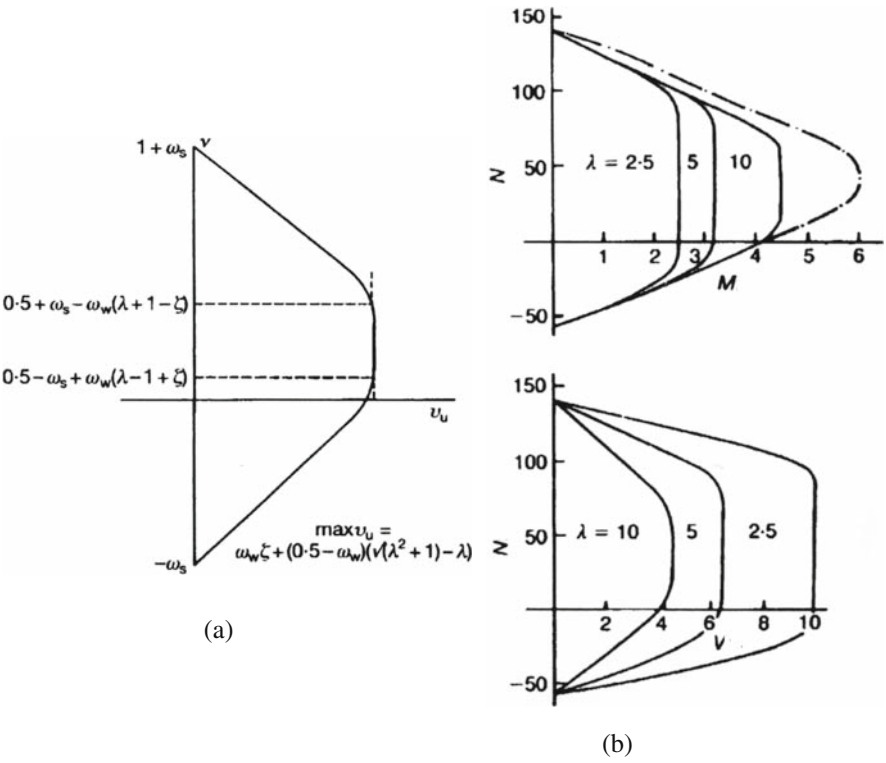

Fig. 3.43 (**a**) Schematic interaction diagram in dimensionless *V-N* space (CEB 1996a); (**b**) application for dimensional *M-N* and *V-N* diagrams of 200 mm square column with four 16 mm bars (CEB 1996a)

1. In the following range of axial forces N (positive for compression):

$$\begin{aligned} N_1 = {} & 0.5bhnf_{\mathrm{c}} - A_{\mathrm{s,tot}} f_{\mathrm{y}} + \rho_{\mathrm{w}} b_{\mathrm{w}} f_{\mathrm{yw}} [\cot\delta(2L_{\mathrm{s}} + (z - 0.5\,h)\cot\delta) - 0.5\,h] \\ & \le N \le N_2 = 0.5bhnf_{\mathrm{c}} + A_{\mathrm{s,tot}} f_{\mathrm{y}} - \rho_{\mathrm{w}} b_{\mathrm{w}} f_{\mathrm{yw}} \\ & [\cot\delta(2L_{\mathrm{s}} - (z - 0.5\,h)\cot\delta) + 0.5\,h] \end{aligned} \tag{3.116}$$

   failure is brittle, taking place by yielding of transverse reinforcement and diagonal concrete crushing, while all the longitudinal reinforcement is still in the elastic range. The shear resistance is independent of the exact value of N between N_1 and N_2 and of the total cross-sectional area of longitudinal reinforcement, $A_{\mathrm{s,tot}}$. It is obtained from Eq. (3.107) using there the value of tan ϕ from Eq. (3.106).
2. In the range of N-values:

$$N_1 \ge N \ge -A_{\mathrm{s,tot}} f_{\mathrm{y}} \tag{3.117}$$

   failure is by diagonal concrete crushing, but it is less brittle than in case 1, as not only the transverse steel but also the tension reinforcement have already yielded. The shear resistance is:

$$V_R = (N + A_{s,tot} f_y)\tan\phi + \rho_w f_{yw} b_w \cot\delta\,(z - (2L_s + z\cot\delta)\tan\phi) \tag{3.118}$$

   where:

$$\tan\phi = \min\left(\sqrt{\left(\frac{L_s}{\eta h}\right)^2 + \frac{1-\eta}{\eta}} - \frac{L_s}{\eta h},\ \frac{h}{2L_s}\right) \tag{3.119}$$

   and

$$\eta = \frac{N + A_{s,tot} f_y - \rho_w f_{yw} b_w (2L_s + z\,\cot\delta)\cot\delta}{b_w h\left(nf_c - \rho_w f_{yw}\left(1 + \cot^2\delta\right)\right)} \tag{3.120}$$

3. In the remaining range of N-values, i.e. for

$$nf_{\mathrm{c}} b_{\mathrm{w}} h + A_{\mathrm{s,tot}} f_{\mathrm{y}} \ge N \ge N_2 \tag{3.121}$$

   failure is again by diagonal concrete crushing with the transverse steel at yielding, but in this case with the compression reinforcement yielding as well. So, it is again less brittle than in case 1. The shear resistance is:

$$V_R = (N - A_{s,tot} f_y)\tan\phi + \rho_w f_{yw} b_w \cot\delta\,(z + (2L_s - z\cot\delta)\tan\phi) \tag{3.122}$$

   The value of tan ϕ is still given by Eq. (3.119), but with the following value of η:

$$\eta = \frac{\left(N - A_{s,tot} f_y\right) + \rho_w f_{yw} b_w \left(2L_s - z \cot\delta\right) \cot\delta}{b_w h \left(n f_c - \rho_w f_{yw} \left(1 + \cot^2\delta\right)\right)} \tag{3.123}$$

The upper limit of $\cot\delta$ is still given by Eq. (3.108b). An inclination of the compression field close to the cracking pattern is: $\cot\delta = L_s/h$.

Case 1 above, of brittle failure and of shear resistance independent of N exists only if $N_2 > N_1$, i.e. only if:

$$\cot\delta \leq \frac{\omega_{tot}}{\omega_w} \frac{h}{2L_s} \tag{3.124}$$

Equations (3.116), (3.117), (3.118), (3.119), (3.120), (3.121), (3.122) and (3.123), supplemented with Eqs. (3.106) and (3.107) where relevant, are essentially analytical expressions of the monotonic ULS resistance of squat columns under skew-symmetric bending, as governed by moment, shear and axial force. In other words, they give the reduction of flexural resistance due to high shear.

Using the relationship $M = VL_s$, Eqs. (3.116), (3.117), (3.118), (3.119), (3.120), (3.121), (3.122) and (3.123) can be converted into interaction diagrams relating the dimensionless moment $\mu = M/bh^2 f_c = (V/bhf_c)(L_s/h)$ to the dimensionless axial force $\nu = N/bhf_c$. When the shear span ratio, L_s/h, increases, such μ–ν interaction diagrams tend asymptotically to the simple bilinear diagram:

$$\mu = 0.5\zeta(\nu + \omega_{\text{tot}}) \qquad \text{for } 0.5n > \nu \geq -\omega_{\text{tot}} \tag{3.125a}$$

$$\mu = 0.5\zeta(n + \omega_{\text{tot}} - \nu) \qquad \text{for } n + \omega_{\text{tot}} \geq \nu \geq 0.5n \tag{3.125b}$$

Equations (3.125) can be derived as interaction relations between dimensionless moment and axial force of a single section at the ULS in bending, assuming:

- for Eq. (3.125a), that the resultant force of the concrete stresses in the compression zone is applied at the location of the compression reinforcement and
- for Eq. (3.125b), that the entire cross-section is under a compressive stress of nf_c.[20]

Figure 3.43(b) presents interaction diagrams derived from the above procedure with $n = 1$ and $\delta = 45^\circ$ (Shohara and Kato 1981).

3.2.5.3 Under What Conditions Does Shear Reduce the Moment Resistance?

The conventional criterion for the characterisation of an element as squat and prone to reduction of its moment resistance owing to shear, is its slenderness, $\lambda = L/h$, or – preferably – its shear span ratio, $M/Vh = L_s/h$. A more rational criterion can

[20] Normally we take $n = 1$ for flexure with axial load without shear.

be based on Eq. (3.124), which is the condition for the existence of the axial-load-range where failure is brittle, Eq. (3.116). Equation (3.124) has been generalised in Biskinis (2007) to members with not just tension and compression reinforcement, but also with "web" reinforcement in-between. Taking for simplicity $\delta = 45^\circ$ as in Shohara and Kato (1981), the generalised criterion is:

$$2\frac{L_s}{h} \leq \frac{\omega_{tot}}{\omega_w} \tag{3.124a}$$

The yield moment of rectangular beams or columns with relatively low shear span ratio, L_s/h, has been compared in Biskinis (2007) with the value calculated from Section 3.2.2.2.[21] Over 300 such members were identified to exhibit reduction of the yield moment owing to shear and low slenderness. Calculation according to Section 3.2.2.2 gives for them a median test-to-prediction ratio of 0.86, distinctly lower than the median test-to-prediction ratio of 1.025 for about 2050 beams or columns that do not exhibit effects of shear on their yield moment (see Section 3.2.2.2 under *Comparison with Experimental Results and Empirical Expressions for the Curvature*). Scrutiny of the experimental results has led to proposed new criteria for members whose moment resistance is reduced by shear:

i. If $2.0 < L_s/h < 3.0$: the axial force N is between the bounds of Eq. (3.116).
ii. If $L_s/h < 2.0$: Eq. (3.124a) is met.

If the member does not satisfy one of these two criteria, its yield moment may be calculated according to Section 3.2.2.2.

The yield moment of the over 300 members found to meet one of these two criteria is slightly underpredicted by the procedure of Section 3.2.5.2, even when applied with $n = 1$ and $\delta = 45^\circ$, i.e. as in Shohara and Kato (1981). The test-to-prediction ratio has a median of 1.085 and a coefficient of variation of 29.1%, to be contrasted with the median of 1.025 and the coefficient of variation of 16.3% of the about 2050 beams/columns without effects of shear (Biskinis 2007).

A more sophisticated alternative to the analysis in Section 3.2.5.2 has also been considered in Biskinis (2007), where:

- the difference in the orientation of the truss (at an angle δ to the member axis) and of the stress in the diagonal strut is taken into account; the principal compressive stress of the combined field is set equal to nf_c
- plane-sections analysis is carried out at the end sections.

It has further been found in Biskinis (2007) that:

(a) If the principal compressive stress of the combined stress field reaches the limit value of nf_c together with yielding of the stirrups but before attainment of the

[21] In squat members whose moment resistance is reduced owing to shear, the yield moment is essentially equal to the moment resistance.

moment resistance of the end section(s) with exceedance of ε_{cu} at the extreme compression fibres, the more sophisticated alternative gives predictions closer to the experimental yield moment than the procedure in Section 3.2.5.2 with $n = 1$ and $\delta = 45^\circ$. In those cases the test-to-prediction ratio of the yield moment has a median of 0.99 and a coefficient of variation of 23.7%.

(b) When the moment resistance of the end section(s) is not attained before failure of the concrete in diagonal compression and yielding of the stirrups, the procedure of Section 3.2.5.2 with $n = 1$ and $\delta = 45^\circ$ gives better prediction: a median of 1.035 for the test-to-prediction ratio and a coefficient of variation of 31.3%.

Among those members meeting criteria (i) and (ii) for dependence of their moment resistance on shear, alternative (a) above has been found to approximately correspond to one of the following two conditions (Biskinis 2007):

$$\nu \geq 0.4; \tag{3.126a}$$

$$\frac{\omega_{tot}}{\omega_w} \leq 2\frac{L_s}{h}\max(2;\ 10\nu) \tag{3.126b}$$

If none of these two conditions is met, the procedure of Section 3.2.5.2 gives better predictions.

3.2.5.4 Degradation with Cyclic Loading of the Resistance of Squat Columns to Shear Compression Failure, After Flexural Yielding

The main problem of squat columns is that, after reaching their shear-dependent flexural capacity (see Section 3.2.5.2), they may fail in shear at relatively low values of the chord rotation, θ. Most often shear failure of squat columns takes place by compression along the diagonal of the element between opposite ends of its end sections.

Close to 40 columns from the literature with shear span ratio, L_s/h, less or equal to 2, have failed under cyclic loading by shear compression after flexural yielding (Biskinis et al. 2004). A purely empirical model for the cyclic degradation of shear strength in members failing by diagonal compression has been fitted to those data. Based on the experimental observations, compression failure is taken to occur along the column diagonal in elevation. Inelastic cyclic displacements are expressed through $\mu_\theta{}^{pl} = \mu_\theta - 1$. For units: MN, m, the cyclic shear resistance is (Biskinis et al. 2004):

$$V_{R,\max} = \frac{4}{7}\left(1 - 0.02\min\left(5;\ \mu_\theta^{pl}\right)\right)\left(1 + 1.35\frac{N}{A_c f_c}\right)(1 + 0.45\cdot 100\rho_{tot})\sqrt{\min(f_c;\ 40)}\ b_w z \sin 2\delta \tag{3.127}$$

where δ is the angle between the diagonal and the axis of the column ($\tan\delta = h/2L_s$). The internal lever arm z is taken as $z = d - d_1$.

Equation (3.127) fits the test results with a median value of the test-to-prediction ratio equal to 1.005 and coefficient of variation of 8.9%. Being almost fully empirical, it applies only in the range of parameter values in the relevant database:

- L_s/h from 1 to 2,
- $N/A_c f_c$ from –0.1 to 0.7,
- ρ_{tot} from 0.7 to 4%,
- f_c from 14.5 to 61 MPa,
- μ_θ from 1.4 to 7.

Equation (3.127) has been adopted for squat columns in Part 3 of Eurocode 8 (CEN 2005a).

3.2.5.5 Diagonal Reinforcement in Squat Columns or Deep Beams

It has been pointed out already that elements with low shear span ratio are nearly two-dimensional. Design of two-dimensional concrete elements for monotonic loads is normally based on Strut-and-Tie Models (STMs). In the STM approach, the internal stress field is idealised as a statically determined truss. Bands of compressive stresses identified with concrete struts are verified in compression. Reinforcement is placed along tensile stress bands considered as ties of the STM.

Let's consider a squat column or a deep beam in skew-symmetric bending, i.e. with equal and opposite design moments at its ends: $M_d = V_{Ed}L/2 = V_{Ed}L_s$ where L and L_s are the total clear length and the shear span, respectively, and V_{Ed} is the design shear associated with M_d. The simplest STM of the member consists of;

- a concrete strut along its diagonal in elevation, connecting the compression zones of its two end sections, and
- a (steel) tie along its other diagonal.

Dimensioning of the diagonal steel tie would give a cross-sectional area, A_{sd}, such that:

$$V_{Ed} = 2A_{sd} f_{yd} \sin\delta \tag{3.128a}$$

$$M_d = zA_{sd} f_{yd} \cos\delta \tag{3.128b}$$

where:

- z is the internal lever arm at the end section(s) and
- δ is the angle between the diagonal reinforcement and the axis of the member:

$$\delta = \arctan(z/L) = \arctan(0.5z/L_s) \tag{3.129}$$

If the loading is cyclic, the strut and the tie would alternate between the two diagonals and the member should be reinforced along both, with a steel tie having cross-sectional area, A_{sd}, satisfying Eqs. (3.128) and (3.129). When the diagonal tie is in compression, it could resist (if effectively restrained laterally against buckling) the full compressive force along the diagonal. The surrounding concrete would be protected from diagonal crushing.

Reinforcement placed along both diagonals of the element in sufficient quantity to prevent shear failure before or after flexural yielding of the end sections greatly enhances the flexure-controlled deformation capacity of the element, no matter whether it is sufficient to take the full design action effects according to Eqs. (3.128). The last term in Eqs. (3.78) shows that, all other parameters being the same, a diagonal reinforcement ratio of 1% increases, on average, by 25% the ultimate chord rotation capacity or by 27.5% its plastic part. The enhancement increases more than proportionally for larger diagonal reinforcement ratios. Moreover, the hysteresis loops of the diagonally reinforced element resemble those of steel in uniaxial tension-compression, i.e. they are broad and stable.

Diagonal reinforcement can easily be placed in deep beams, like coupling beams between coupled walls. It may even be placed fairly easily in squat walls (although there it crosses the base section at mid-length, its main purpose being to prevent sliding shear failure, and it does not enhance much the wall moment resistance). As a matter of fact, in deep coupling beams diagonal reinforcement should preferably be arranged in square column-like elements with dense hoops around them, to prevent buckling of the longitudinal bars and confine the concrete inside (Fig. 3.44). In such cases, only nominal (e.g. the minimum) longitudinal and transverse reinforcement needs to be placed in the coupling beam, as the diagonal one is dimensioned to resist the full design action effects according to Eqs. (3.128).

It is very difficult to place diagonal reinforcement in squat columns, while providing at the same time transverse reinforcement at the density and with a pattern normally necessary for confinement of the concrete core and anti-buckling action. Note that, if the column is squat in both horizontal directions, diagonal reinforce-

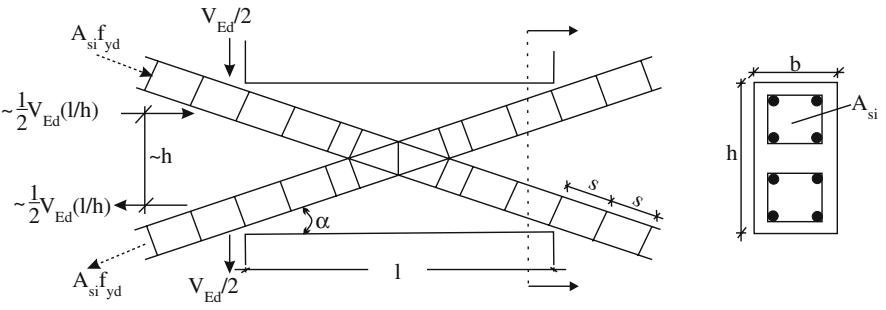

Fig. 3.44 Diagonally reinforced coupling beam (CEN 2004a)

ment should normally be placed along both. This is impracticable. It might be feasible, though, to place diagonal reinforcement in a column which is effectively squat only in one direction (e.g., if beams frame into it at short vertical spacing only within one vertical plane, or if its squatness is due to a concrete or masonry infill in contact with the column, see Fig. 2.12 in Chapter 2).

3.3 Joints in Frames

3.3.1 Force Transfer Mechanisms in Concrete Joints: Bond and Shear

Bending moments in beams due to gravity loading normally have the same sign at opposite faces of their joint with a vertical member. By contrast, beam bending moments due to seismic loading have opposite sign at opposite faces of the joint. Therefore, seismic shear forces are very high in the joint itself. Figure 3.45(a) illustrates the reason for the magnitude of this shear:

- With the joint considered as part of the beam, the change in the beam moment from a (high) negative value to a positive one across the joint produces a vertical shear force, $V_{\mathrm{jv}} = \Sigma M_{\mathrm{b}}/h_{\mathrm{c}} = \Sigma V_{\mathrm{b}} L_{\mathrm{cl}}/2h_{\mathrm{c}}$, where M_{b} and V_{b} denote the beam seismic moments and shears at the face of the joint, L_{cl} the beam clear span and h_{c} the depth of the column.
- With the joint considered as part of the column, the change of the column bending moment from a high value just above the joint to an equally high value with opposite sign just below, produces a horizontal shear force, $V_{\mathrm{jh}} = \Sigma M_{\mathrm{c}}/h_{\mathrm{b}} = \Sigma V_{\mathrm{c}} H_{\mathrm{cl}}/2h_{\mathrm{b}}$, where M_{c} and V_{c} denote column seismic moments and shears above or below the joint, H_{cl} the clear storey height and h_{b} the beam depth.

The joint shear forces produce a nominal shear stress in the concrete of the joint: $v_{\mathrm{j}} = \Sigma M_{\mathrm{c}}/(h_{\mathrm{c}} h_{\mathrm{b}} b_{\mathrm{j}}) = \Sigma M_{\mathrm{b}}/(h_{\mathrm{c}} h_{\mathrm{b}} b_{\mathrm{j}})$, where $(h_{\mathrm{c}} h_{\mathrm{b}} b_{\mathrm{j}})$ is the volume of the joint, with b_{j} its effective width normal to the plane of bending, conventionally taken by seismic design codes (CEN 2004a) as:

$$\text{if } b_{\mathrm{c}} > b_{\mathrm{w}}: \qquad b_j = \min\{b_c; (b_w + 0.5h_c)\}; \tag{3.130a}$$

$$\text{if } b_{\mathrm{c}} \le b_{\mathrm{w}}: \qquad b_j = \min\{b_w; (b_c + 0.5h_c)\} \tag{3.130b}$$

where b_{c} and b_{w} denote the width of the column and the beam, respectively, at right angles to the plane of bending.

Shear stresses are introduced in a joint mainly by bond along the bars of the beam and the column (or wall) around the core of the joint. Because the nominal shear stress in the concrete of the joint is the same, no matter whether it is computed

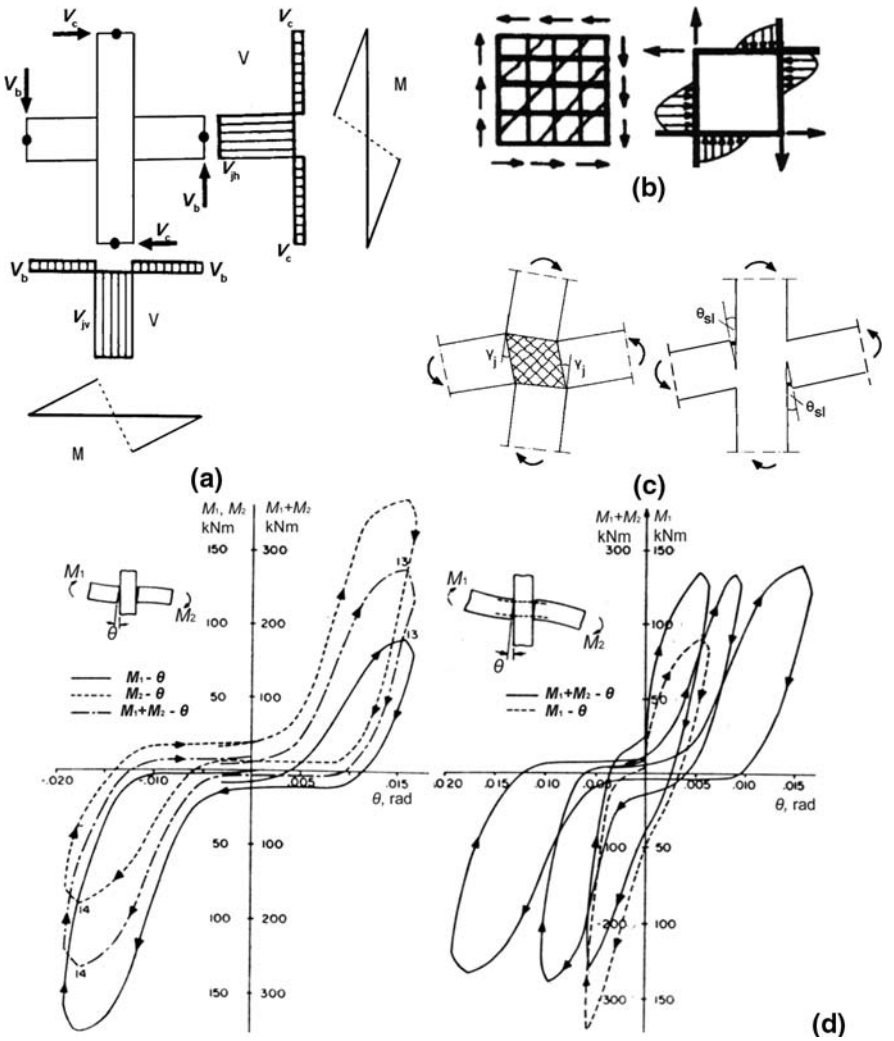

Fig. 3.45 Interior beam-column joint: (**a**) shear forces within the joint; (**b**) shear resistance mechanisms; (**c**) joint deformation; (**d**) experimental loops of moment on joint v fixed-end rotation due to bar slippage within/through joint (adapted from Viwathanatepa et al. 1979)

from the horizontal or the vertical shear force, V_{jh} or V_{jv}, it is more convenient to compute it from the horizontal shear, V_{jh}, which is based on the forces transferred via bond stresses along the top bars of the beam. Note that, even when Eq. (1.4) is not fulfilled, the beams framing into a joint normally yield before the column or the wall. If they don't, the horizontal joint shear is overestimated if computed from the top bars of the beam, and hence is on the safe side for the joint.

So, the joint may be considered as a series system of two (independent) mechanisms of force transfer:

- from the beam and column (or wall) longitudinal bars to the core of the joint, by bond;
- from each side of the joint core to the opposite, through shear (see Fig. 3.45(b)).

This implies that:

- if one of the two force transfer mechanisms fails, the joint fails as well; and
- the overall (shear) deformation of the joint is the sum of the individual deformations of the two mechanisms (see Fig. 3.45(c)).

Force transfer to the joint core by bond along the longitudinal bars passing through the joint or anchored in it causes slippage along these bars. Slippage shows up as fixed-end rotation, θ_{sl}, of the end of the member where the longitudinal bars belong (see Fig. 3.45(c) and (d)). Force transfer through the joint by shear causes an angular distortion (shear strain) of the joint core, γ_j (Fig. 3.45(c)). The total deformation of the joint is an apparent shear deformation, equal to the sum of γ_j and of the fixed-end rotations, θ_{sl}, at the ends of all (four, in an interior joint) members framing into the joint (unless such a fixed-end rotation is incorporated in the chord rotation of the member, see discussion in Section 3.3.2). As shown in Fig. 3.30, the total shear deformation of a frame panel made up of two beams and two columns is equal to the sum of:

- the average apparent shear deformation of the four joints at the corners of the panel; plus
- the average chord rotation at the (four) column ends on either side of the panel, θ_c; plus
- the average chord rotations at the (four) beam ends above and below the panel, θ_b.

It is interesting that, although it adds to $\theta_c + \theta_b$, the angular distortion (shear deformation) of the joint core, γ_j, takes place in the opposite sense with respect to the sum of $\theta_c + \theta_b$ (see Fig. 3.45(c)): the joint diagonal that shortens is the one parallel to the panel diagonal that gets longer during the deformation of the panel. This is consistent with the opposite sign of the joint shears, V_{jv}, and V_{jh}, with respect to those in the members themselves (see Fig. 3.45(a)).

3.3.2 The Bond Mechanism of Force Transfer in Joints

Beams normally yield before the columns. Moreover, compressive stresses in the vertical bars of columns are normally below yield (as cracks at column ends normally are not open through the column depth and the concrete participates fully in

resisting the force of the compressive zone). Therefore, bond stresses are normally higher along the longitudinal bars of beams passing through a joint, than along the column bars. So, the transfer of forces into the joint is normally controlled by the longitudinal bars of the beam.

As the (unusual) example in Fig. 3.21 shows, bond failure along longitudinal bars of beams or columns within the very length of the element manifests itself as a splitting crack along the bar, especially if it is a corner one. Bond failure along the length of the bar within the joint normally manifests itself through partial pull-out of the bar through the joint. The high static indeterminacy of the system of the joint and of the members framing in it limits the magnitude of any pull-out of member longitudinal bars from the joint. Such pull-out manifests itself as a large fixed-end rotation, θ_{sl}, of the end of that member to which the longitudinal bars belong. Witness the resemblance of the end moment-fixed end rotation loops in Fig. 3.45(d) (Viwathanatepa et al. 1979) to the bond-slip loops in Fig. 3.22. They are narrow, have inverted-S shape and degrade with cycling.

The fixed-end rotation, θ_{sl}, at a member end due to partial pull-out of the member's bars from the joint is normally added to the chord rotation of the member itself at that end (see Fig. 3.24 and Eq. (3.42) in Section 3.2.2.3 and 3rd term in Eqs. (3.66) in Section 3.2.3.2) increasing its apparent flexibility (through Eq. (3.68), Section 3.2.3.3). It also increases its apparent deformation capacity (see 2nd term in Eq. (3.72) in Section 3.2.3.4 and terms with a_{sl} in Eqs. (3.78) in Section 3.2.3.5). At the extreme, bond failure along the member's longitudinal bars within the joint may prevent the full yield moment from developing at the end section of the member (see Fig. 3.29 in Section 3.2.2.3 for two field cases).

The problem of bond is more acute at interior joints, where beam longitudinal bars continue into the adjacent span, rather than at exterior ones, where beam bars are anchored with a 90° bend at the far end of the joint. As a matter of fact, taking into account that bond stresses along the part of the beam bars outside the confined joint core are negligible because:

- yielding penetrates into the initial length of the bar into the joint while confinement there is poor, and
- horizontal cracking of the column may take place at the plane of the beam longitudinal bars,

and taking the width of the joint confined core along the depth h_c of the column as: $h_{co} \approx 0.8h_c$, the average bond stress along a beam bar is:

- $\sim d_{bL}f_y/4h_{co} \approx 0.3d_{bL}f_y/h_c$, if the bar reaches its yield stress in tension at one face of the joint and has zero compressive stress at the opposite face,
- $\sim d_{bL}f_y/2h_{co} \approx 0.6d_{bL}f_y/h_c$, if the bar reaches its yield stress in tension at one face of the joint and in compression at the opposite one. This may happen if the crack at the beam section at the face of the column stays open at the top under positive moments (see Fig. 3.7 in Section 3.1.1.1 and point 3 in Section 3.2.2.6). In that case the top bars of the beam bear the full force of the compression zone.

At exterior joints, the average bond stress along beam bars bent by 90° at the far end of the joint is lower: $\sim 0.2 d_{\mathrm{bL}} f_{\mathrm{y}} / h_{\mathrm{c}}$.

For common values of d_{bL} and h_{c} the level of bond stresses estimated above ranges from 5 to 15 MPa, often exceeding the ultimate bond stress under cyclic loading. Test results show, however, that cyclic bond stresses of that magnitude can develop in joints, without causing unduly large pull-through slippage of the beam bars (thanks primarily to lateral confinement at the level of the beam top bars by the transverse beams and the slab, but also to enhancement of bond by compression normal to the bar surface due to the column axial load).

Figure 3.46 demonstrates the effect of the column depth, h_{c}, on the hysteresis loops of shear force v overall deformation of a cross-shaped beam-column subassembly (Kaku and Asakusa 1991). If the column size is small, namely $h_{\mathrm{c}} = 18.8 d_{\mathrm{bL}}$, the overall force-displacement loops are controlled by bond slip within the joint and their shape resembles the loops in Fig. 3.22. However, the system's peak force resistance does not degrade with cycling. Only the reloading stiffness is greatly reduced, giving lower energy dissipation and certain growth of the overall lateral displacements with cycling. For larger column sizes bond slip in the joint does not govern and the overall force-displacement loops are controlled by the flexural behaviour of the beam.

If l (: left) and r (: right) index the two vertical faces of the joint, σ_{s} denotes the stress in the beam bars and h_{co} is the width of the confined core of the joint along the depth h_{c} of the column, the average bond stress along these beam bars is:

$$\tau_b = \frac{\pi d_{bL}^2}{4} \frac{|\sigma_{sl} - \sigma_{sr}|}{\pi d_{bL} h_{co}} = \frac{d_{bL}}{4} \frac{|\sigma_{sl} - \sigma_{sr}|}{h_{co}} \tag{3.131}$$

Bond stresses along the length of the bars outside the confined core are negligible. Plastic hinges are assumed to develop in the beam at both sides of the joint. Let's consider the top flange to be in tension on the left of the joint and in compression on the right (as in Fig. 3.45(a), (b) and (c)). The top flange is normally much stronger than the bottom one, both in tension and in compression and, therefore, its yield force cannot be balanced by the bottom flange unless the bottom bars yield. So, the stresses of the bottom bars are: $\sigma_{\mathrm{s,l}} = -f_{\mathrm{y}}$, $\sigma_{\mathrm{s,r}} = f_{\mathrm{y}}$ and the average bond stress along them at beam plastic hinging is: $\tau_{\mathrm{b}} = 0.5 d_{\mathrm{bL}} f_{\mathrm{y}} / h_{\mathrm{co}}$. Regarding now the top bars, they yield at the plastic hinge of the left beam: $\sigma_{\mathrm{s,l}} = f_{\mathrm{y}}$. At the opposite face of the joint these bars have a compressive stress, $\sigma_{\mathrm{s,r}}$, such that, acting together with the force of the concrete at the top flange, $F_{\mathrm{c,r}}$ (taken negative for compression), they balance the tension force of the bottom bars. These latter bars are forced by the stronger top flange to yield. So, if $A_{\mathrm{s,r1}}$ and $A_{\mathrm{s,r2}}$ denote the cross-sectional area of the top and bottom beam bars on the right of the joint, the compressive stress of the top bars there is:

$$\sigma_{s,r} = -\frac{A_{s,r2}}{A_{s,r1}} f_y - \frac{F_{c,r}}{A_{s,r1}} = -\frac{\rho_2}{\rho_1} f_y \left(1 - \frac{\xi_{eff}}{\omega}\right) \tag{3.132}$$

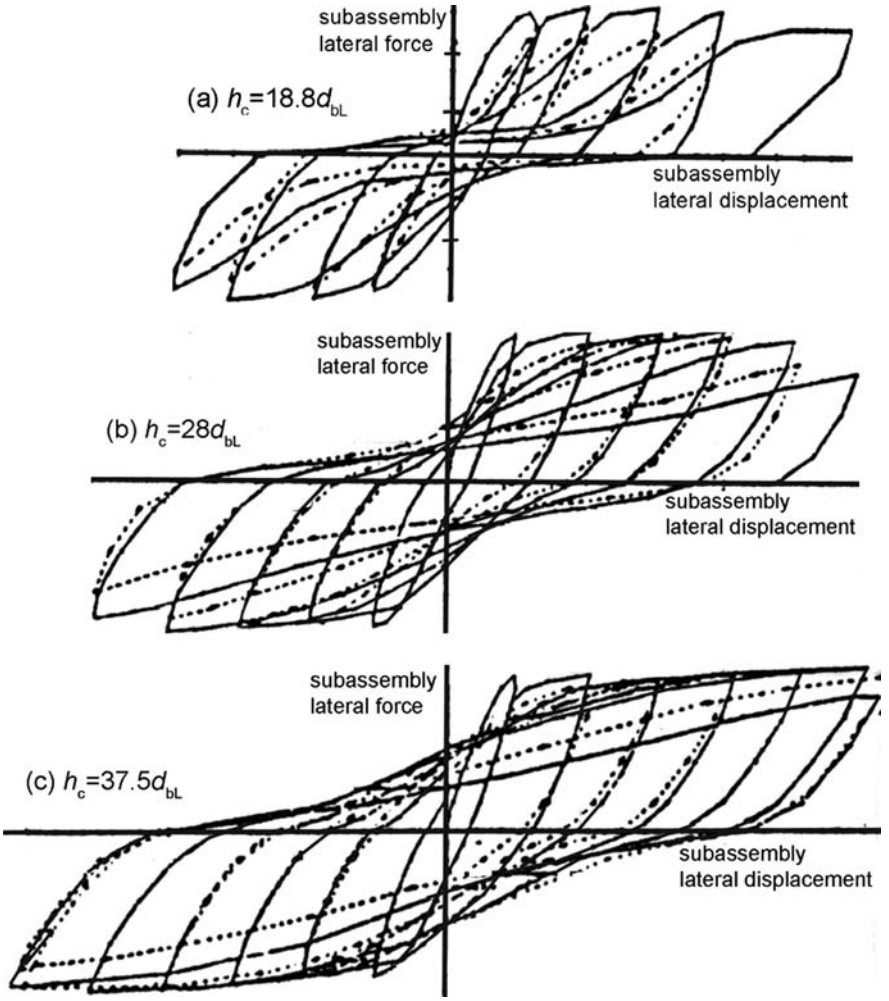

Fig. 3.46 Effect of bond-slip in the joint, as controlled by column size, on overall force-displacement loops of a beam-column subassembly (adapted from Kaku and Asakusa 1991)

where ρ_1 and ρ_2 are the ratios of top and bottom reinforcement at the right of the joint, normalised to the product bd of the beam, ω is: $\omega = \rho_1 f_y / f_c$ and ξ_{eff} is the depth of a fictitious compression zone (normalised to d), such that $F_{c,r} = -bd\xi_{\text{eff}} f_c$. Therefore the average bond stress along the top bars at beam plastic hinging is:

$$\tau_b = \frac{d_{bL}}{4} \frac{f_y}{h_{co}} \left(1 + \frac{\rho_2}{\rho_1} \left(1 - \frac{\xi_{eff}}{\omega}\right)\right) \tag{3.133}$$

and is less than the average bond stress along bottom bars with the same diameter, d_{bL}. However, the bond problem is more acute along the top bars, because bond stresses are not uniform around a bar but are concentrated more on the side facing the joint core. This is the underside of the top bars, where bond conditions are considered "poor" owing to laitance and consolidation of concrete during compaction. All around the bottom bars bond conditions are considered as "good" (see Section 3.1.3.2).

The bond stress demand given by Eq. (3.133) is capped at the ultimate bond stress along these bars. Bond outside the confined joint core is normally neglected, but its enhancement inside the joint core due to confinement by the joint stirrups, the top bars of the transverse beam and all the surrounding concrete is taken into account. It has been pointed out in Section 3.1.3.2 that the maximum steel stress at pull-out (or -through) bond failure may be obtained from Eq. (3.31) with the 1st and 2nd terms inside the bracketed last term replaced by the upper limit value of 2.0. Bond strength is further enhanced by the 3rd term inside the brackets, $0.2p$ (in MPa), owing to the mean normal stress across the horizontal plane of the bar due to the axial load of the column: $p = N/A_c = \nu f_c$ (f_c in MPa). In Section 5.4.1 these considerations are used with Eq. (3.133) to justify the lower limit on the h_c/d_{bL} ratio imposed by Eurocode 8 on beam bars passing through, or anchored at joints.

Notwithstanding the shortfall within the joint of the full anchorage of the yield stress of (top) beam bars in tension at one face of the joint and in compression at the opposite one, there is a real problem only for low h_c/d_{bL} values. The solution is a large column size and/or a small bar diameter. Needless to say, bars of small diameter are more susceptible to buckling and may require very dense stirrups at the end of the beam for its prevention. Fortunately, compressive stresses are lower in beam top bars than in the bottom ones (cf. histories of bar strains in Figs. 3.6 and 3.7) and the slab next to the beam prevents top bar buckling in a horizontal plane.

3.3.3 Force Transfer Within Joints Through the Shear Mechanism

3.3.3.1 Shear Force Demand in Joints

As already pointed out in Section 3.3.1, if there is no pull-out (or -through) of the beam or column bars around the joint core, shear stresses develop within the joint core with a nominal value equal to the ratio of $\Sigma M_c = \Sigma M_b$ to the volume of the joint, $h_c h_b b_j$. Shear failure of the joint, as in the examples of Fig. 3.47, is far more brittle than any failure of plastic hinges around the joint, even in the columns. So, it should be prevented through design and detailing of the joint. To this end, the maximum possible shear force that can develop in the joint is established from capacity design calculations, on the basis of the capacity of the beams or the columns framing into the joint (whichever is weaker) to deliver shear through bond along the outermost beam or column bars passing through the joint.

If the sum of moment resistances of the beams framing into a joint, $\sum M_{Rb}$, is less than that of the columns, $\sum M_{Rc}$, ($\sum M_{Rb} < \sum M_{Rc}$), the shear input in the joint

(a) (b) (c)

Fig. 3.47 Shear failure of exterior joints. (**a**) reinforced joint; (**b**), (**c**): unreinforced joints (See also Colour Plate 10 on page 724)

is governed by the beams. If pull-out (or -through) of the beam top bars does not take place, the maximum possible value of the horizontal shear force in an interior joint, V_{jh}, can be computed as:

- the maximum possible tensile force in the top bars at one face of the joint, $A_{\mathrm{sb1}} f_{\mathrm{y}}$,
- plus the maximum possible compressive force in the top flange at the opposite face,
- minus the shear force V_{c} in the column above the joint.

No matter how it is shared by the concrete and the top reinforcement, the maximum possible compression force in the top flange will be governed by the bottom reinforcement. It will be equal to its maximum possible tensile force, $A_{\mathrm{sb2}} f_{\mathrm{y}}$. So, the horizontal shear force in the joint is (Fardis et al. 2003):

If $\sum M_{\mathrm{Rb}} < \sum M_{\mathrm{Rc}}$:

$$\begin{aligned} V_{jh} &= (A_{sb1} + A_{sb2})\, f_y - V_c = (A_{sb1} + A_{sb2})\, f_y - \frac{\sum M_{Rb}}{H} \frac{L}{L_{cl}} \\ &= \sum M_{Rb} \left(\frac{1}{z_b} - \frac{1}{H} \frac{L}{L_{cl}} \right) \approx (A_{sb1} + A_{sb2})\, f_y \left(1 - \frac{z_b}{H} \frac{L}{L_{cl}} \right) \end{aligned} \tag{3.134}$$

where:

- A_{sb1}, A_{sb2}: cross-sectional area of the beam top reinforcement at one face of the joint and of its bottom reinforcement at the opposite face, respectively;
- V_{c}: column shear at beam plastic hinging;
- H: storey height;
- L, L_{cl}: theoretical and clear beam span, respectively; and
- z_{b} ($\approx h_{\mathrm{jb}}$) = d–d_1: beam internal lever arm.

The larger of the two sums $A_{sb1}+A_{sb2}$ diagonally across the joint should be used in Eq. (3.134). Normally, no such distinction needs to be made at interior joints, as the steel area is the same at both sides. At exterior joints one term in $A_{sb1}+A_{sb2}$ is zero.

The shear force is translated into a nominal shear stress, considered uniform within the joint core:

$$v_j = \frac{V_{jh}}{b_j h_{jc}} \tag{3.135}$$

where:

- h_{jc}: horizontal distance between the outermost layers of column reinforcement in the direction of the horizontal joint shear force, and
- b_j: joint width in the orthogonal horizontal direction, conventionally taken from Eqs. (3.130).

If $\sum M_{Rb} > \sum M_{Rc}$, it is the columns that govern the shear input in the joint. Let's $A_{sc,top}$ and $A_{sc,bot}$ denote the cross-sectional area of vertical bars on one side of the column above or below the joint, respectively.[22] Then the vertical shear force in the joint core is (Fardis et al. 2003):

$$V_{jv} = f_y(A_{sc,top} + A_{sc,bot}) + N_{top} - V_{b,\min}, \tag{3.136}$$

where:

- N_{top}: axial force in the column above; and
- $V_{b,min}$: algebraically minimum (and possibly negative) beam shear force on either side of the joint:

$$V_{b,\min} \approx \frac{\sum M_{Rc}}{L}\frac{H}{H_{cl}} - \max\left(\left[V_{g+\psi q,b}\right]_l ; \left[V_{g+\psi q,b}\right]_r\right) \tag{3.137}$$

where:

- H and H_{cl} are the theoretical and the clear storey height and
- $V_{g+\psi q,b}$ is the shear force at the beam end on the left (index: l) or on the right (index: r) face of the joint, due to the gravity loads acting on the beam concurrently with the seismic action.

$$\sum M_{Rc} \approx f_y(A_{sc,top} + A_{sc,bot})z_c + 0.5h_c\left(N_{top}\left(1-\nu_{top}\right) + N_{bot}\left(1-\nu_{bot}\right)\right) \tag{3.138}$$

[22] Normally column vertical bars are the same above and below the joint: $A_{sc,top} = A_{sc,bot}$, except at the joints of the top floor where $A_{sc,top} = 0$.

with z_c ($\approx h_{jc}$) $\approx 0.9d \approx 0.8h_c$ denoting the internal lever arm of the column and $\nu = N/A_c f_c$.

So, Eq. (3.136) finally gives: If $\sum M_{Rb} > \sum M_{Rc}$:

$$V_{jv} \approx \sum M_{Rc} \left(\frac{1}{z_c} - \frac{1}{L} \frac{H}{H_{cl}} \right) + \frac{1}{2} \left| \left[V_{g+\psi q,b} \right]_l - \left[V_{g+\psi q,b} \right]_r \right| \tag{3.139}$$

The shear stress in the joint core is computed as:

$$v_j = \frac{V_{jv}}{b_j h_{bj}} \tag{3.140}$$

where h_{bj} is the clear depth of the beam between its top and bottom reinforcement.

3.3.3.2 Joint Shear Strength

Diagonal tension cracking of the joint core takes place when the principal tensile stress under the combination of the shear stress, v_j, and of the mean vertical compressive stress in the joint, $v_{top} f_c$, exceeds the tensile strength of concrete, f_{ct}, i.e. when:

$$v_j \geq v_{cr} = f_{ct} \sqrt{1 + \frac{v_{top} f_c}{f_{ct}}} \tag{3.141}$$

According to Priestley (1997) confinement by beam bars bent vertically towards the core of exterior joints increases the shear stress at joint diagonal cracking by 50% over the value in Eq. (3.141).

Diagonal cracking of the joint core seldom has grave consequences, especially if the joint is reinforced with horizontal hoops and/or beams of significant cross-section frame into all four sides of the joint. After cracking, the joint core is called to resist the shear without reaching its ultimate stress in cyclic loading, v_{ju}.

The seismic behaviour of joints has been studied experimentally and analytically since the 1960s. Nevertheless, there is still no universally accepted rational model for the mechanism through which a joint resists cyclic shears. Variations of a rational physical model in Park and Paulay (1975) are still used in certain seismic design codes. According to it a joint resists shear via a combination of two mechanisms (Fig. 3.45(b)):

1. A diagonal concrete strut between the compressive zones of the beams and columns at opposite corners of the joint, contributing to the resistance against the horizontal shear force in the joint, V_{jh}, with the horizontal component of its diagonal force.
2. A truss extending over the entire core of the joint, comprising:

- (any) horizontal hoops in the joint;
- (any) intermediate vertical bars between the column corner bars in planes parallel to that of bending (including column bars contributing to the column moment resistance above and below the joint as distributed "web" reinforcement, ω_v);
- a diagonal compression field in the concrete.

The force in the strut under (1) above is assumed to develop from:

- the concrete forces in the compression zones of the beam and the column at the two ends of the strut, and
- the bond stresses transferred to the joint over the length of the beam bars within the width of the strut itself.

The truss under (2) above takes the rest of the joint shear force, V_{jh}, not resisted by the horizontal component of the strut diagonal force. So, for safe-sided dimensioning of the horizontal joint reinforcement, the horizontal component of the strut force should not be overestimated.

Unless there is bond failure along the beam bars, pushing their compressed end into the joint, the neutral axis depth of the beam is significantly reduced by cycling of the beam moment, as the crack may not fully close (especially at the top flange) owing to accumulation of plastic strains in the reinforcement. Then the compression zone of the beam does not deliver a horizontal force to the diagonal concrete strut, but only a compressive force to the beam reinforcement. The sum of this force and of the tension force at the opposite face of the joint is transferred to the truss and the strut in proportion to their share in the joint width at the level of the beam top reinforcement. So, the width of the diagonal strut is defined by the neutral axis depth of the column at the faces of the joint. According to this reasoning, the force input into the strut directly from the compression zones of the members is reduced during cycling of the moments. By contrast, the force input into the strut by bond increases, as the degradation of bond with cycling pushes the force transfer by bond mainly to that length of the bar within the joint core where bond is enhanced by transverse compression, i.e. the bar length within the strut width. Therefore, despite the deterioration of bond along most of the bar length within the joint core, the strut mechanism remains intact.

Paulay and Priestley (1992) make the assumption that at the face of the joint where the beam is under sagging moment (tension at the bottom) the crack cannot close at the top flange, owing to accumulation of plastic strains in the top reinforcement. This means: $\xi_{eff} = 0$ in Eq. (3.133). Then the horizontal width of the strut at that level is equal to the neutral axis depth of the column above the joint, x_c. So, the beam compression chord does not contribute to the force of the diagonal concrete strut and the horizontal component of the strut diagonal force is equal to:

- the force transferred by bond along the bar length within the strut width, minus
- the column shear force, V_c (appearing also in Eq. (3.134) for V_{jh} and considered to be applied directly to the strut through the compression zone of the column above and affect only its horizontal shear force and not that of the truss).

Moreover, Paulay and Priestley (1992) assume – for simplicity – that the transfer of the total force $(A_{sb1}+A_{sb2})f_y$ by bond takes place uniformly along the total length of the top bars within the joint, h_c. So, the fraction of this force going to the horizontal force of the strut is equal to x_c/h_c. The rest, equal to $(1–x_c/h_c)$, goes to the truss. Therefore, as the truss extends over the full vertical face of the joint, the total area of the horizontal legs of hoops within the joint, A_{sh}, should be dimensioned for a force equal to $(1–x_c/h_c)(A_{sb1}+A_{sb2})f_y$. The value of $\xi_c = x_c/h_c$ may be obtained from Eq. (3.52) in Section 3.2.2.4 under *Curvature at Spalling of the Concrete Cover*, using there: $\omega_1 = \omega_2$, $\omega_v = 0$ (for convenience), $\varepsilon_{co} = 0.002$ and $\varepsilon_{cu} = 0.004$ (for spalling of the extreme concrete fibres at the end section of the column). Then $\xi_c \approx (6/5)\nu$, with both ν and ξ_c normalised to h_c. So the following total area of horizontal hoops should be provided according to this version of the Park and Paulay model.

– At interior joints:

$$A_{sh} f_{yw} \geq (A_{sb1} + A_{sb2})\, f_y \left(1 - \frac{6}{5}\nu\right) \tag{3.142a}$$

where the normalised axial force, ν, is the minimum value in the column above the joint for any combination of the design seismic action with the concurrent gravity loads.

The reinforcement required in exterior joints cannot be obtained by setting $A_{sb2} = 0$ in Eq. (3.142a), because the beam top reinforcement is bent down at the far face of the joint. Then, when the bar is in tension, the bend delivers to the diagonal strut starting there the full diagonal compression force of the strut. The horizontal component of that force is about equal to $f_y A_{sb1} – V_c$. So, very little force is transferred by bond along the part of the top bars outside the strut, to be resisted as horizontal shear by the part of the truss falling between the strut and the face of the joint towards the beam. The horizontal shear force of the truss is governed by the force transferred by bond along the part of the bottom bars outside the strut.[23] The compression zone at the bottom flange of the beam delivers to the lower end of the strut a horizontal force equal to the compression force in the concrete, i.e. to the tension force in the top reinforcement, $A_{sb1}f_y$, minus the force, $A_{sb2}f_y$, in the bottom reinforcement that yields in compression. The difference between:

– the horizontal component of the strut force at its top end, $A_{sb1}f_y – V_c$, and
– the horizontal forces delivered
  - to the lower end of the strut by the beam and the column below: $(A_{sb1}–A_{sb2})f_y – V_c$, and
  - by bond within the strut width at the level of the bottom reinforcement: $(1–x_c/h_c)A_{sb2}f_y$,

[23]The upward bend of the bottom bars at the far face of the joint does not deliver forces to the joint core when these bars are in compression.

is the force transferred by bond along the length of the bottom bars outside the strut width. This force is a horizontal shear force to be resisted by the part of the truss falling between the strut and the exterior face of the joint. This gives:

– At exterior joints:

$$A_{sh} f_{yw} \geq A_{sb2} f_y \left(1 - \frac{6}{5}\nu\right) \tag{3.142b}$$

where now ν is the minimum value of the normalised axial force in the column below the joint, for any combination of the design seismic action with the concurrent gravity loads.

Test results on interior joints have been collected and compiled in Kitayama et al. (1991) as in Fig. 3.48. Figure 3.48 suggests that the joint ultimate shear strength, expressed in terms of the shear stress, v_j, of Eqs. (3.135) and (3.140), increases about linearly with the ratio of horizontal reinforcement within the joint, ρ_{jh}, from a minimum value $v_{ju} \approx 0.15 f_c$ at $\rho_{jh} = 0$ (unreinforced joint) to an upper limit value in the range of $0.24 f_c$–$0.4 f_c$ (with mean value: $v_{ju} \approx 0.32 f_c$) at $\rho_{jh} = 0.4\%$. Above that value of the steel ratio and up to $\rho_{jh} = 2.4\%$, the joint ultimate strength seems to be attained always by diagonal compression in the concrete and to be practically independent of the value of ρ_{jh} and of the axial load ratio in the column, $\nu = N/f_c A_c$ (Kitayama et al. 1991).

The experimental results in Fig. 3.48, along with careful and detailed measurements of the evolution of strains in the horizontal hoops within the joint during the history of cyclic displacements (Kitayama et al. 1991), lead to the following conclusions:

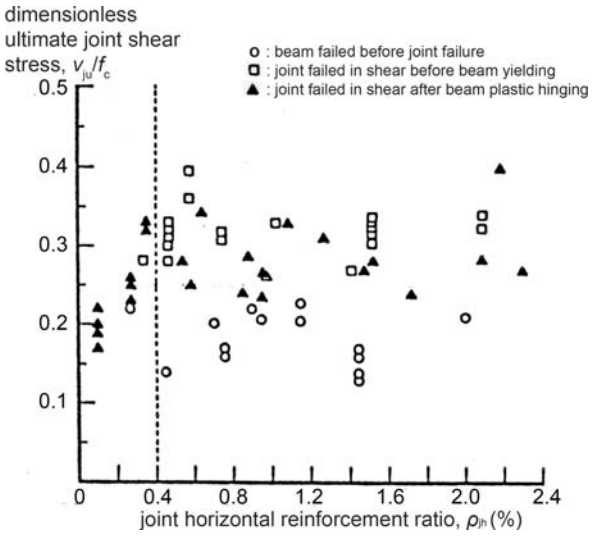

Fig. 3.48 Effect of horizontal reinforcement ratio in interior joint, ρ_{jh}, on joint strength (adapted from Kitayama et al. 1991)

- Cycling of applied loads and displacements causes a gradual degradation of bond along the length of a bar within the joint closer to its end which is in tension, and a concentration of most of the bond transfer near the opposite end of the bar within the joint, where the bar is in compression (the part falling within the strut width).
- The breakdown of bond along the length of the beam bar falling outside the strut width may cause drastic reduction of the contribution of the truss mechanism to the shear resistance of the joint. When this happens the horizontal component of the strut diagonal force resists almost the full horizontal joint shear, V_{jh}. This force is delivered to the strut partly by bond along the length of the beam bars falling within the strut and partly by the compression zone of the beam.
- The joint shear that the strut can resist is governed by the compressive strength of the concrete in its diagonal direction. Any horizontal hoops in the joint affect the contribution of the strut to shear resistance only to the extent they enhance this diagonal compressive strength through confinement. So, attainment of the joint ultimate strength activates not only the hoop legs parallel to the applied shear (i.e. in the plane of bending), considered in the truss mechanism to resist part of the joint shear, but also (and to the same extent) the orthogonal hoop legs (at right angles to the plane of bending). The top and bottom reinforcement of any beams framing into the joint at right angles to the plane of bending play a role similar to these orthogonal hoop legs, confining the core of the joint.
- Yielding of the horizontal reinforcement in the joint caps the confinement of the concrete core and increases tensile strains in the direction(s) normal to the diagonal strut, reducing further the diagonal compressive strength.
- The column axial force level, measured through $\nu = N/A_c f_c$, does not seem to be important, neither for the bond-slip performance of the beam bars, nor for the joint ultimate shear stress, v_{ju}.

Test results in Fig. 3.49 (Kitayama et al. 1991) suggest that confinement on both sides of the joint by a slab at the level of the beam top and/or by a transverse beam significantly increases the joint ultimate shear strength, v_{ju} (to values close to $0.4f_c$). This may explain the scarcity of shear failures at interior joints – even unreinforced ones – in the field in strong earthquakes.

In view of the test results of Figs. 3.48 and 3.49 and the conclusions above that cast doubts about the validity of the truss-and-strut physical model, alternative simple plane stress models have emerged for the shear strength of beam-column joints. For example, the model adopted in Eurocode 8 (CEN 2004a) as alternative to the truss-and-strut model and to Eqs. (3.142) for the calculation of joint horizontal reinforcement assumes a homogeneous stress field in the body of the joint, comprising:

1. the shear stress, v_j, from Eqs. (3.135) or (3.140),
2. the vertical normal stress from the column, $N/A_c = \nu f_c$ (positive for compression), and
3. a smeared horizontal normal stress, such that the concrete core and the joint horizontal reinforcement balance together the zero external horizontal force applied

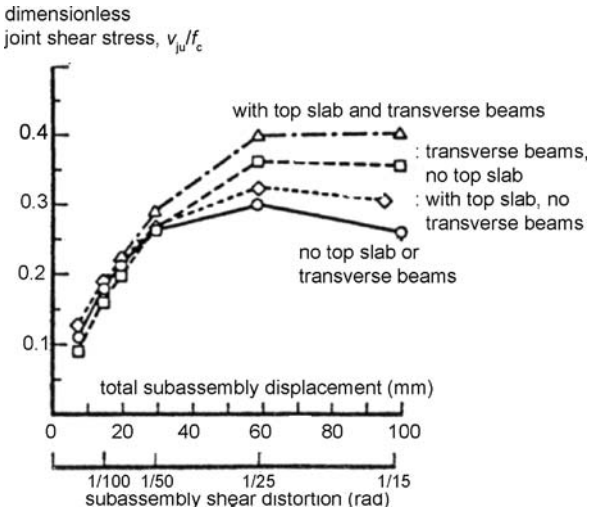

Fig. 3.49 Effect of top slab and/or transverse beam on both sides on the ultimate shear strength of interior joints (adapted from Kitayama et al. 1991)

on the joint by the beams; this normal stress has a limit value of $-\rho_{jh} f_{yw}$ (compression), when the joint horizontal reinforcement is driven to yielding by the dilatancy of the concrete core at imminent failure.

Joint strength criteria in Eurocode 8 are based on the principal stresses, in tension, σ_I, and compression, σ_{II}, under the above system of stresses, 1–3. The joint shear stress at diagonal cracking ($\sigma_I = f_{ct}$) in the presence of horizontal reinforcement is (CEN 2004a):

$$\frac{v_j}{f_c} = \sqrt{\left(\frac{f_{ct}}{f_c} + \nu_{top}\right)\left(\frac{f_{ct}}{f_c} + \frac{\rho_{jh} f_{yw}}{f_c}\right)} \tag{3.143}$$

where ν_{top} is computed from the minimum value of the axial force of the column above the joint under any combination of the design seismic action with the concurrent gravity loads, including the effect of overturning moment on exterior joints. Note that, for $\rho_{jh} = 0$ and ν_{top} between 0 and 0.3, Eq. (3.143) gives values of v_j from $0.1 f_c$ to $0.2 f_c$, in good agreement with the average value of $v_j \approx 0.15 f_c$ suggested for $\rho_{jh} = 0$ by the test results in Fig. 3.48 (Kitayama et al. 1991).

The real threat to the joint is crushing of its core by the diagonal compression. According to the simple plane stress model above, this may take place if σ_{II} reaches the concrete compressive strength, as this is reduced due to the tensile stresses and/or strains in the transverse direction (i.e. that of σ_I). The reduction factor on f_c may be taken the same as factor n from Eq. (3.96a) for diagonal compression in concrete members due to shear. Eurocode 8 (CEN 2004a) neglects for simplicity the – adverse – effect of the horizontal normal stress, $-\rho_{jh} f_{yw}$, on the magnitude of σ_{II}, as well as its (more important) favourable effect on the compressive strength in the

diagonal direction through confinement. So the condition: $\sigma_{II} = -nf_c$ gives (CEN 2004a):

$$\frac{v_{ju}}{f_c} = n\sqrt{1 - \frac{v_{bottom}}{n}} \tag{3.144}$$

where ν is computed from the maximum axial force of the column below the joint under any combination of the design seismic action with the concurren gravity loads.

For common values of ν ($\sim$0.25) Eq. (3.144) gives an ultimate shear stress, v_{ju}, close to $0.4f_c$, at the upper strength limit of interior joints in Figs. 3.48 and 3.49. It does not seem to provide a safety margin against diagonal compression failure, unless the design value $f_{cd} = f_{ck}/\gamma_c$ is used for f_c, with a partial factor for concrete, γ_c, (significantly) higher than 1.0.

An alternative plane stress approach is to apply the variable strut inclination truss model of Section 3.2.4.2 under *The Variable Strut Inclination Truss of the CEB/FIP Model Code 90 and Eurocode 2* to the joint that is already cracked diagonally, owing to a shear stress above the limit of Eq. (3.143). In this analogy the counterpart of the transverse direction of the concrete element of Section 3.2.4.2 under *The Variable Strut Inclination Truss of the CEB/FIP Model Code 90 and Eurocode 2* is the horizontal direction of the joint. Its transverse reinforcement ratio, ρ_w, corresponds to the joint horizontal reinforcement ratio, ρ_{jh}. The counterpart of the vertical direction of the joint is the longitudinal one of the concrete element, but with $M = 0$, $\omega_1 = 0$ and N equal to the axial force of the column (positive for compression). The inclination δ is the angle of the centreline of the diagonal strut in the joint to the vertical direction.

According to the variable strut inclination truss analogy, the shear stress in the joint at yielding of the horizontal reinforcement before failure of the concrete in the diagonal direction may be obtained from Eq. (3.101), adapted as follows to the conditions of the joint:

$$\frac{v_j}{f_c} = \sqrt{v_{top}\frac{\rho_{jh} f_{yw}}{f_c}} \tag{3.145}$$

which coincides with Eq. (3.143) for $f_{ct} = 0$.

Adapted to the conditions of the joint, Eq. (3.99) gives the shear strength of the joint for diagonal concrete failure after yielding of the joint horizontal reinforcement:

$$\frac{v_{ju}}{f_c} = \sqrt{\frac{\rho_{jh} f_{yw}}{f_c}\left(n - \frac{\rho_{jh} f_{yw}}{f_c}\right)} \tag{3.146}$$

The counterpart of Eq. (3.97) for the joint shear at diagonal compression failure is:

$$\frac{v_{ju}}{f_c} = 0.5n \sin 2\delta \tag{3.147}$$

If the amount of horizontal reinforcement is large, namely if $\rho_{\mathrm{jh}} f_{\mathrm{yw}} > 0.5nf_{\mathrm{c}}$, diagonal compression failure will take place before yielding of the joint reinforcement, at the upper limit value of both Eqs. (3.146) and (3.147): $v_{\mathrm{ju}} = 0.5nf_{\mathrm{c}}$. With this value of v_{ju} for $\rho_{\mathrm{jh}} f_{\mathrm{yw}} > 0.5nf_{\mathrm{c}}$, Eq. (3.146) gives a variation of the joint ultimate shear with the strength of the horizontal reinforcement similar to the parabola-cum-horizontal line given for Eq. (3.99) in Fig. 3.40. The mean upper limit: $v_{\mathrm{ju}} \approx 0.32 f_{\mathrm{c}}$ in Fig. 3.48 agrees well with the theoretical upper limit of: $v_{\mathrm{ju}} = 0.5nf_{\mathrm{c}}$. However, although the data in Fig. 3.48 might suggest a parabolic variation up to $\rho_{\mathrm{jh}} = 0.4\%$, the value $\rho_{\mathrm{jh}} = 0.4\%$ is much lower than the theoretical one of $0.5nf_{\mathrm{c}}/f_{\mathrm{yw}}$ giving the peak value of v_{ju} according to Eq. (3.146).

Equation (3.103), adapted to the conditions of the joint gives an ultimate shear stress of:

$$\frac{v_{ju}}{f_c} = \sqrt{v_{top}\left(1 - \frac{v_{top}}{n}\right)} \tag{3.148}$$

which is not supported at all by the experimental data.

The shear strain in the joint core, γ_{ju}, at the ultimate shear stress, v_{ju}, is in the order of 0.005 rad (0.5%), i.e., very small compared to the total shear distortion of a system of ductile beams and columns at failure of the joint.

Chapter 4
Analysis and Modelling for Seismic Design or Assessment of Concrete Buildings

As pointed out in the Preamble, analysis carried out within the framework of seismic design or assessment determines by calculation the effects of the design actions (including the seismic action) in terms of internal forces and deformations, for the purpose of dimensioning or assessing structural members. For concrete members, design action effects are used to verify the sizes of members and to dimension or assess the amount of reinforcement.

Chapter 4 does not pretend to be a treatise on seismic analysis methods. Its scope is limited to the essentials for the application of well-established analysis methods in the design or assessment of buildings for earthquake resistance according to current generation seismic codes. The reader is supposed to be fairly conversant with the fundamentals of Structural Dynamics and their application for the seismic analysis of buildings.

As in Chapters 1 and 2, emphasis is placed on the portfolio of seismic analysis methods provided in Parts 1 and 3 of EN-Eurocode 8 and their scope of applicability. Special attention is paid to nonlinear seismic response analysis and to practical modelling of concrete members and buildings for its purposes. Examples of nonlinear modelling of concrete members and buildings and nonlinear dynamic analysis are presented.

4.1 Scope of Analysis in Codified Seismic Design or Assessment

4.1.1 Analysis for the Purposes of Seismic Design

As pointed out in Section 1.2 and elsewhere in Chapter 1, seismic design of new buildings according to current codes is force-based. Its prime workhorse is linear-elastic analysis, based on the 5%-damped elastic spectrum divided by a factor that accounts mainly for ductility and energy dissipation capacity, but also for overstrength (see Section 4.2.2). In Europe this factor is denoted by q and called "behaviour factor". In North America it is termed "Force reduction factor" or "Response modification factor" and denoted by R.

M.N. Fardis, *Seismic Design, Assessment and Retrofitting of Concrete Buildings*, Geotechnical, Geological, and Earthquake Engineering 8, DOI 10.1007/978-1-4020-9842-0_4,

Most current generation codes for the seismic design of new buildings include two alternative methods of linear-elastic seismic analysis:

(a) Linear static analysis, termed "lateral force" method of analysis in Eurocode 8 (CEN 2004a) and in certain US codes (SEAOC 1999), or "equivalent lateral force" procedure in other US codes (BSSC 2003), but known also in practice as "equivalent static" analysis.
(b) Modal response spectrum analysis, as called in Eurocode 8 (CEN 2004a); US codes use the term "response spectrum" procedure (BSSC 2003) or "dynamic lateral force" (SEAOC 1999) procedure.

Differences between codes are not limited to terminology but extend to the general attitude towards the method of analysis. Most codes allow application of the "modal response spectrum" analysis for the design of all new buildings and make it mandatory for new buildings that are irregular in elevation, or tall and/or flexible (i.e., in which higher modes are important). Only Eurocode 8 adopts it as the reference method for the design of new buildings and fully respects its rules and results. US codes essentially consider the linear static ("equivalent lateral force") procedure as the reference method and adapt the results and rules of application of "modal" analysis to conform to it. Their reasoning is that linear analysis is of limited relevance and value in the framework of seismic design, as its results apply only for ground motions less than a small fraction ($1/q$ or $1/R$) of the design seismic action. It makes little sense therefore, according to that point of view, to apply a sophisticated, complex and computationally demanding analysis method, liable to misuse, misinterpretation or errors due to lack of experience and expertise. It makes more sense, instead, to select the structural layout so that the structure lies well within the scope of the time-tested and almost fool-proof linear static analysis procedure.

This concept of the role of analysis is reflected in the common view that the value of the "modal response spectrum" procedure is limited:

1. to furnishing a heightwise pattern of lateral inertia forces in buildings with heightwise irregular geometry, mass, stiffness or strength, or dominated by higher modes which is more representative of the expected dynamic response; and
2. to better accounting for the coupling of torsional and translational vibrations in buildings with strong irregularity in plan.

Consistent with point (1) above, some codes with this attitude suggest applying "modal response spectrum" analysis not directly (i.e., computing modal contributions to the seismic action effects from the mode shapes themselves and combining them according to the appropriate rules, see Section 4.4.3), but indirectly: by deriving storey modal lateral forces through modal analysis, applying them as static lateral loads and computing via linear static analysis the modal seismic action effects of interest. Moreover, in SEAOC (1999) all modal lateral forces are scaled

up so that their resultant (the base shear) matches fully the value computed from the design spectrum at the fundamental period, if the building is irregular, or 90% of that value, if it is regular. In BSSC (2003) scaling of these modal lateral forces aims at matching 85% of the base shear obtained from the design spectrum at a period of 1.4 to 1.7 times an empirical period estimate, depending on the magnitude of the design ground acceleration.

If both the lateral force method and modal response spectrum analysis are applicable to the design of a given new building, modal response spectrum analysis gives on average a slightly more even distribution of peak internal forces at different critical sections (e.g. at the two ends of the same beam or column), translated to some material savings. If its results are used for member dimensioning, the overall inelastic performance of the structure would be expected to be better, as peak inelastic deformations normally agree better with its predictions than to those of linear static analysis (see Section 4.11.2).

As its use is not subject to any constraints of applicability, the modal response spectrum method can be adopted as the single analysis tool for seismic design of new buildings in 3D, provided that the designer masters the method. It is more sound (e.g., unlike the linear static method, its results for concurrent application of the two horizontal seismic action components are independent of the choice of the directions, X and Y, of these components) and offers a better overall balance of safety and economy. Its predictions for displacements and deformations are closer to those of a nonlinear dynamic analysis (see Section 4.11.2), while, for the same column or beam shears it gives a more even balance of column or beam seismic moments on opposite faces of joints, which are anyway covered by the same longitudinal reinforcement. So, with today's availability of reliable and efficient computer programs for modal response spectrum analysis in 3D, and the establishment of Structural Dynamics as a main subject in structural engineering curricula in seismic regions, it is expected that the application of modal response spectrum analysis for the design of new buildings will grow and prevail in the long run. Even then, though, the intuitively appealing, practical and conceptually simple lateral force method is expected to stay in codes as an option for the seismic design of new buildings.

In the framework of Part 1 of Eurocode 8 (CEN 2004a):

i. nonlinear static analysis (commonly known as "pushover" analysis), and
ii. nonlinear dynamic (time-history or response-history) analysis.

have a certain role for the design of new buildings. This role is limited to:

- detailed evaluation of the expected seismic performance of a building that has been designed using linear analysis (including confirmation of the intended plastic mechanism and of the distribution and extent of damage);
- the design of buildings with seismic isolation, for which nonlinear analysis is the reference method and linear analysis is allowed only under certain very restrictive conditions.

Specifically for the nonlinear static method of analysis, Part 1 of Eurocode 8 (CEN 2004a) defines two additional possible uses in the framework of the design of new buildings:

- To verify or revise the value of the factor α_u/α_1 incorporated in the basic or reference value of the behaviour factor, q_o, of concrete etc. buildings, to account for overstrength due to redundancy of the structural system (see Section 1.4.3.1 and Fig. 1.12).
- To design buildings on the basis of a nonlinear static analysis followed by deformation-based verification of its ductile members, in lieu of force-based design with linear elastic analysis and a design spectrum incorporating the behaviour factor q. The use of "pushover" analysis for the direct design of new buildings is a novelty of Part 1 of Eurocode 8 without precedent in codified seismic design.

Internal forces for dimensioning are taken equal to those estimated from the linear analysis for the design response spectrum (i.e. the 5%-damped elastic spectrum divided by the behaviour factor q). Consistent with the equal displacement rule and the concept and use of the behaviour factor, displacements due to the seismic action are taken in Part 1 of Eurocode 8 as equal to those derived from the linear analysis times the behaviour factor q. By contrast, when nonlinear analysis is used, all seismic action effects (internal forces, displacements and deformations) are those derived from the nonlinear analysis.

4.1.2 Analysis for Seismic Assessment and Retrofitting

Unlike seismic design of new buildings, which is still (mainly) force-based, seismic assessment or retrofitting of existing ones is nowadays fully displacement-based. The underlying reason is practical: Force-based approaches entail capacity-demand comparisons in terms of internal forces, with seismic internal force demands computed from a design response spectrum incorporating a global behaviour or force reduction factor, q or R. Values of this factor given in seismic design codes for new buildings go hand-in-hand with a corresponding set of prescriptive rules or restrictions (on structural layout, member detailing, capacity design, etc.). For an existing building to be entitled a q-factor larger than the value attributed to overstrength alone ($q = 1.5$ in Eurocode 8), the structure as a whole, as well as every single member considered to contribute to earthquake resistance (a "primary seismic" one, in Eurocode 8 terminology, see Section 4.12) should meet all the rules pertaining to one of the discrete ductility classes for which (higher) values of q are given in the code for new buildings (e.g., in Eurocode 8 for at least DC Medium). As the building most likely violates these rules in one way or another, it will be assigned at the end the value of the q-factor attributed to overstrength alone. In all likelihood, the force capacity of some members considered to contribute to earthquake resistance

will be less than the force demand resulting from such a low q-factor value. In this way any old concrete building, possibly except low-rise ones with large walls, will be assessed as seismically inadequate and will need retrofitting. Moreover, if it is decided to retrofit the building and the designer wants to use the (higher) q value of one of the discrete ductility classes in a code for new buildings, every single member considered to contribute to earthquake resistance should be retrofitted to meet all detailing, capacity design, etc. rules of that ductility class. This may increase the cost of retrofitting so much, that demolition or the "do-nothing" alternative may be the most likely outcome.

The only way out of the predicament created by the prescriptive rules of current force-based seismic design codes for new buildings, is to abandon the concept of a global q-factor that reduces the overall elastic seismic forces. Instead, each member should be assessed and retrofitted individually, on the basis of its own capacity determined by its own features and peculiarities. The capacity which is important for a member's seismic performance (including failure) is not its force-, but its deformation-capacity. One should keep in mind that, unlike gravity or wind actions, the seismic action is not a set of given forces to be resisted by the structure, but a given dynamic displacement or energy input to be accommodated. Therefore structural displacements and their derivatives, i.e., member deformations, should be the basis of seismic assessment, instead of forces. After all, structures collapse not because of the seismic lateral loads per se, but owing to gravity loads acting through the lateral displacements induced by the earthquake (P-Δ effects).

The prime objective of an analysis for the purposes of displacement-based seismic assessment or retrofitting is the calculation of deformation demands in structural members. Codes or standards that have recently emerged for (displacement-based) seismic assessment and retrofitting of buildings (ASCE 2007, CEN 2005a) provide to this end the full menu of analysis options mentioned in Section 4.1.1:

- the two linear-elastic options: (a) linear static analysis and (b) modal response spectrum analysis, and
- the two nonlinear ones: (i) nonlinear static or "pushover" analysis and (ii) nonlinear dynamic analysis.

Unlike linear analysis carried out for design purposes, which uses the design response spectrum, incorporating the behaviour factor q, linear analysis for displacement-based assessment and retrofitting employs the 5%-damped elastic response spectrum. Member inelastic deformation demands (e.g., chord-rotations) may be derived directly from such an analysis, essentially employing the equal-displacement rule at the member level. Of course, this simplification can be made only when the estimated chord-rotation ductility demands meet certain fairly restrictive conditions. In ASCE (2007) these conditions comprise upper limits on the absolute magnitude of these demands, as well as on their difference between storeys or at opposite sides of the building. By contrast, in CEN (2005a) only non-uniformity of the chord-rotation ductility ratio demands throughout the building restricts the

application of linear analysis for the estimation of member inelastic deformation demands. If the applicability conditions of linear-elastic analysis are not met, one should resort to nonlinear analysis. So, nonlinear analysis, being always applicable, is the reference method for displacement-based seismic assessment and retrofitting. Note that in seismic assessment all information necessary for the calculation of the yield moment, the secant stiffness to the yield-point, and all other member properties needed as input to nonlinear analysis, is readily available. In design of new structures, by contrast, the reinforcement is not known a-priori and (several) cycles of design-analysis iterations are needed, at the expense of design effort and convenience.

To be assessed on the basis of inelastic deformations, members (or, in general, mechanisms of behaviour) should have a minimum of ductility. As brittle mechanisms of behaviour, such as shear in concrete members, exhibit practically no ductility, they are more conveniently and reliably assessed on the basis of forces. Linear-elastic analysis is of no use for the estimation of internal force demands in the inelastic regime, even when its applicability conditions for the estimation of member inelastic deformation demands are met. When these conditions are met and member inelastic deformation demands are indeed estimated for simplicity from linear analysis, one has to resort to other means (notably, to capacity design calculations) to establish the internal force demands on members entering in the inelastic range.

4.2 The Seismic Action for the Analysis

4.2.1 Elastic Spectra

4.2.1.1 Elastic Response Spectra and Peak Ground Accelerations

The most common representation of the seismic action in codes is through the response spectrum of an elastic Single-Degree-of-Freedom (SDOF) oscillator with 5% viscous damping ratio. Any other alternative representation of the seismic action (e.g. in the form of acceleration time-histories) should conform to the 5%-damped elastic response spectrum.

Because:

- earthquake ground motions are traditionally recorded as acceleration time-histories, and
- seismic design is still based on forces, conveniently derived from accelerations,

the pseudo-acceleration response spectrum, $S_a(T)$, is normally used. If spectral displacements, $S_d(T)$, are of interest (notably for displacement-based assessment or design), they can be obtained from $S_a(T)$ assuming simple harmonic oscillation: $S_d(T) = (T/2\pi)^2 S_a(T)$. Spectral pseudo-velocities can also be obtained from $S_a(T)$ as $S_v(T) = (T/2\pi)S_a(T)$. Note that pseudo-values do not correspond to the real peak

spectral velocity or acceleration. For damping ratio up to 10% and for natural period T between 0.2 and 1.0 s, the pseudo-velocity spectrum closely approximates the actual relative velocity spectrum.

The Eurocode 8 spectra include ranges of:

- constant spectral pseudo-acceleration for natural periods between T_B and T_C;
- constant spectral pseudo-velocity between periods T_C and T_D; and
- constant spectral displacement, for periods longer than T_D.

In Eurocode 8 the elastic response spectrum is taken as proportional ("anchored") to the peak acceleration of the ground:

- the horizontal peak acceleration, a_g, for the horizontal component(s) of the seismic action, or
- the vertical peak acceleration, a_{vg}, for the vertical component.

The basis of the seismic design of new structures in Eurocode 8 is the "design seismic action", for which the no-(local-)collapse requirement should be met. It is specified through the "design ground acceleration" in the horizontal direction, a_g, which is equal to the "reference peak ground acceleration" on rock from national zonation maps,[1] times the importance factor, γ_I, of the building (see Section 1.1.1); for ordinary importance, by definition $\gamma_I = 1.0$. The "reference peak ground acceleration" corresponds to the reference return period, T_{NCR}, of the "design seismic action" for structures of ordinary importance.[2] Values of the importance factor greater or shorter than 1.0 correspond to mean return periods longer or shorter, respectively, than T_{NCR}. It is in the authority of each country to select the value of T_{NCR} that gives the appropriate trade-off between economy and public safety in its territory, as well as the importance factors for building other than ordinary, taking into account the specific regional features of the seismic hazard. Part 1 of Eurocode 8 (CEN 2004a) recommends the value T_{NCR}.= 475 years.

Eurocode 8 adopts the same spectral shape for the different seismic actions to be used for different performance levels or Limit States. The difference in the hazard level is reflected only through the peak ground acceleration to which the spectrum is anchored. Recall from Section 1.1.3 that Part 1 of Eurocode 8 recommends for the "damage limitation seismic action" of new buildings one having probability 10% of being exceeded in 10 years (i.e., mean return period: 95 years). Recall

[1] Data from Europe available at the time of drafting Eurocode 8 could not support dependence of the elastic spectrum on additional parameters.

[2] Under the Poisson assumption of earthquake occurrence (i.e. that the number of earthquakes in an interval of time depends only on the length of the interval in a time-invariant way), the return period, T_R, of seismic events exceeding a certain threshold is related to the probability this threshold will be exceeded, P, in T_L years as: $T_R = -T_L/\ln(1-P)$. So, for given T_L (e.g., the conventional design life of $T_L = 50$ years) the seismic action may equivalently be specified either via its mean return period, T_R, or its probability of exceedance in T_L years, P_R.

also from Section 1.1.3 that Part 3 of Eurocode 8 does not make a recommendation to countries or owners/designers for the hazard levels associated with the three "Limit States" ("Damage Limitation", "Significant Damage" and "Near Collapse") in performance-based seismic assessment and retrofitting.

The mean return period, $T_R(a_g)$, of a peak ground acceleration exceeding a value a_g is the inverse of the annual rate, $\lambda_a(a_g)$, of exceedance of this acceleration level: $T_R(a_g) = 1/\lambda_a(a_g)$. A functional form commonly used for $\lambda_a(a_g)$ is: $\lambda_a(a_g) = K_o(a_g)^{-k}$. If the exponent k (: slope of the "hazard curve" $\lambda_a(a_g)$ in a log-log plot) is about constant, two peak ground acceleration levels a_{g1}, a_{g2}, corresponding to two different mean return periods, $T_R(a_{g1})$, $T_R(a_{g2})$, are related as:

$$\frac{a_{g1}}{a_{g2}} = \left(\frac{T_R(a_{g1})}{T_R(a_{g2})}\right)^{1/k} \tag{4.1}$$

The value of k characterises the seismicity of the site. Regions where the difference in peak ground acceleration of frequent and very rare seismic excitations is very large, have low k values (around 2). For such regions full performance-based design or assessment at several performance levels with widely different hazard levels is very meaningful. Large values of k ($k > 4$) are typical of regions where high ground acceleration levels are almost as frequent as smaller ones. One performance level (normally the one associated with the lowest among the hazard levels) would always govern there; performance-based design or assessment at the other levels may be redundant.

For buildings Eurocode 8 does not have provisions for near-source effects on the seismic action. It provides, though, for topographic amplification (ridge effect, etc.) of the seismic action for all types of structures. Such effects have been identified in past earthquakes in Italy (Faccioli et al. 2002, Paolluci 2002, 2006) and along the Chelidonou ravine during the 1999 Athens earthquake. According to Eurocode 8, topographic amplification is mandatory for structures of importance above ordinary. An Informative Annex in Part 5 of Eurocode 8 (CEN 2004c) recommends amplification factors of the seismic action equal to 1.2 over isolated cliffs or long ridges with slope (to the horizontal) less than 30°, or to 1.4 at ridges steeper than 30°.

4.2.1.2 Elastic Spectra of the Horizontal Components in Eurocode 8

The elastic response spectral acceleration for the horizontal components of the seismic action in Eurocode 8 is described by the following expressions (Fig. 4.1):

$$0 \le T \le T_B \; : S_a(T) = a_g S \left[1 + \frac{T}{T_B}(2.5\eta - 1)\right] \tag{4.2a}$$

Constant spectral pseudo-acceleration range:

$$T_B \le T \le T_C \; : S_a(T) = a_g S \cdot 2.5\eta \tag{4.2b}$$

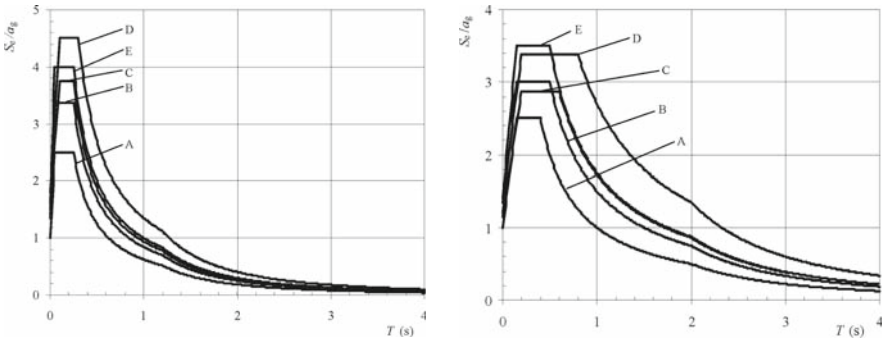

Fig. 4.1 Elastic response spectra of Type 1 (*left*) and 2 (*right*) recommended in EC8, for PGA on rock equal to 1 g and for 5% damping

Constant spectral pseudo-velocity range:

$$T_C \leq T \leq T_D \; : S_a(T) = a_g S \cdot 2.5\eta \left[\frac{T_C}{T} \right] \tag{4.2c}$$

Constant spectral displacement range:

$$T_D \leq T \leq 4 \; sec : S_a(T) = a_g S \cdot 2.5\eta \left[\frac{T_C T_D}{T^2} \right] \tag{4.2d}$$

where:

a_g is the design ground acceleration on rock;
S is the "soil factor";
$\eta = \sqrt{10/(5+\zeta)} \geq 0.55$ is a correction factor for viscous damping ratio, ζ, other than the reference value of 5% (Bommer and Elnashai 1999).

Witness the uniform amplification of the entire spectrum by the "soil factor" S over the spectrum for rock. By definition $S = 1$ over rock. The value $a_g S$ plays the role of "effective ground acceleration", as the spectral acceleration at the constant spectral acceleration plateau is always equal to $2.5 a_g S$.

The values of the periods T_B, T_C and T_D (i.e., the extent of the ranges of constant spectral pseudo-acceleration, pseudo-velocity and displacement) and of the soil factor, S, are taken to depend mainly on "ground type". In the Eurocodes the term ground includes any type of soil and rock. Eurocode 8 recognises five standard ground types, over which it recommends values for T_B, T_C, T_D and S, and two special ones, as listed in Table 4.1. The characterisation of the ground is based on the average value of shear wave velocity, $v_{s,30}$, at the top 30 m:

Table 4.1 Ground types in Eurocode 8 for the definition of the seismic action

	Description	$v_{s,30}$ (m/s)	N_{SPT}	c_u (kPa)
A	Rock outcrop, with less than 5 m cover of weaker material	>800	–	–
B	Very dense sand or gravel, or very stiff clay, several tens of metres deep; mechanical properties gradually increase with depth	360–800	>50	>250
C	Dense to medium-dense sand or gravel, or stiff clay, several tens to many hundreds metres deep	180–360	15–50	70–250
D	Loose-to-medium sand or gravel, or soft-to-firm clay	<180	<15	<70
E	5–20 m surface alluvium layer with $v_s < 360$ m/s underlain by rock (with $v_s > 800$ m/s)			
S_1	≥10 m thick soft clay or silt with plasticity index > 40 and high water content	<100	–	10–20
S_2	Liquefiable soils; sensitive clays; any soil not of type A to E or S_1			

$$v_{s,30} = \frac{30}{\sum_{i=1,N} \frac{h_i}{v_i}} \tag{4.3}$$

where h_i and v_i are the thickness (in m) and the shear wave velocity at small shear strains (less than 10^{-6}) of the i-th layer in N layers. If the value of $v_{s,30}$ is not known, the SPT (Standard Penetration Test) blow-count number may be used for soil types B, C or D, according to the correspondence of SPT to $v_{s,30}$ in Ohta and Goto (1976). If neither the SPT nor $v_{s,30}$ are available, the undrained cohesive resistance (c_u) may used to characterise the soil.

The two special ground types, S1 and S2, deserve carrying out special site-specific studies to define the seismic action. For ground type S1 the special study should take into account the thickness and the v_s-value of the soft clay or silt layer and the difference with the underlying materials and should quantify their effects on the elastic response spectrum. Note that soils of type S1 may have low internal damping and exhibit linear behaviour over a large range of strains, producing peculiar amplification of the bedrock motion and unusual or abnormal soil-structure interaction effects. The scope of the site-specific study should also address the possibility of soil failure under the design seismic action (especially at ground type S2 deposits with liquefiable soils or sensitive clays).

The values of T_B, T_C, T_D and S for the five standard ground types A to E, are meant to be defined by each country in the National Annex to Eurocode 8, depending on the magnitude of earthquakes contributing most to the hazard. The geological conditions at the site may also be taken into account in addition to determine these values. In principle, S factors may be introduced that decrease with increasing spectral value because of the soil nonlinearity effect. Instead of spectral amplification factors that decrease with increasing design acceleration (spectral or ground) as in US codes, e.g., BSSC (2003) and ASCE (2007), the non-binding recommendation of a note in Eurocode 8 is for two types of spectra:

Table 4.2 Recommended parameter values for the standard horizontal elastic response spectra in Eurocode 8 (Fig. 4.1)

Ground type	Spectrum type 1				Spectrum type 2			
	S	T_B (s)	T_C (s)	T_D (s)	S	T_B (s)	T_C (s)	T_D (s)
A	1.00	0.15	0.4	2.0	1.0	0.05	0.25	1.2
B	1.20	0.15	0.5	2.0	1.35	0.05	0.25	1.2
C	1.15	0.20	0.6	2.0	1.50	0.10	0.25	1.2
D	1.35	0.20	0.8	2.0	1.80	0.10	0.30	1.2
E	1.40	0.15	0.5	2.0	1.60	0.05	0.25	1.2

- Type 1: for moderate to large magnitude earthquakes;
- Type 2: for low magnitude ones (e.g. with surface magnitude less than 5.5) at close distance, producing over soft soils motions rich in high frequencies.

The values of T_B, T_C, T_D and S recommended in a non-binding note of Eurocode 8 for the five standard ground types A to E are given in Table 4.2. They are based on Rey et al. (2002) and European strong motion data. There are certain regions in Europe (e.g., where the hazard is contributed mainly by strong, intermediate depth earthquakes, as in the part of the eastern Balkans affected by the Vrancea region) where the two recommended spectral shapes may not be suitable. The lower S-values of Type 1 spectra are due to the larger soil non-linearity in the stronger ground motions produced by moderate to large magnitude earthquakes. The recommended values of the period T_D at the outset of the constant spectral displacement region seems rather low. For flexible structures (e.g., those with seismic isolation) they may not lead to safe-sided designs. A safeguard against the rapid decay of the elastic spectrum for $T > T_D$, is provided by the lower bound of 20% of $a_g S$ recommended in Eurocode 8 for the design spectral accelerations (see Eqs. (4.5c) and (4.5d) in Section 4.2.2).

4.2.1.3 Elastic Spectra of the Vertical Component

The vertical component of the seismic action needs to be taken into account in design only in few very well prescribed situations (see Section 4.5.1). Therefore, the practical importance of the vertical spectrum is limited. Eurocode 8 gives nevertheless a fairly detailed description of the vertical elastic response spectrum:

$$0 \le T \le T_B \; : \; S_{a,vert}(T) = a_{vg}\left[1 + \frac{T}{T_B}(3\eta - 1)\right] \tag{4.4a}$$

$$T_B \le T \le T_C \; : S_{a,vert}(T) = a_{vg} \cdot 3\eta \tag{4.4b}$$

$$T_C \le T \le T_D \; : S_{a,vert}(T) = a_{vg} \cdot 3\eta \left[\frac{T_C}{T}\right] \tag{4.4c}$$

$$T_{\mathrm{D}} \leq T \leq 4\,\mathrm{sec} \; : S_{\mathrm{a,vert}}(T) = a_{\mathrm{vg}} \cdot 3\eta \left[\frac{T_{\mathrm{C}} T_{\mathrm{D}}}{T^2} \right] \tag{4.4d}$$

The main differences between the horizontal and the vertical spectra lie:

- in the value of the amplification factor in the constant spectral pseudo-acceleration plateau, which is 3 instead of 2.5, and
- in the lack of a uniform amplification of the entire spectrum due to the type of soil.

Eurocode 8 recommends in a note the following non-binding values of T_{B}, T_{C}, T_{D} and of the design ground acceleration in the vertical direction, a_{vg}:

- $T_{\mathrm{B}} = 0.05$ s.
- $T_{\mathrm{C}} = 0.15$ s.
- $T_{\mathrm{D}} = 1.0$ s.
- $a_{\mathrm{vg}} = 0.9 a_{\mathrm{g}}$, if the Type 1 spectrum is considered as appropriate for the site;
- $a_{\mathrm{vg}} = 0.45 a_{\mathrm{g}}$, if the Type 2 spectrum is chosen.

The vertical response spectrum recommended in Eurocode 8 is based on work and data specific to Europe (Ambraseys and Simpson 1996, Elnashai and Papazoglou 1997). The ratio $a_{\mathrm{vg}}/a_{\mathrm{g}}$ is known to be higher at short distances (epicentral or to causative fault). However, as distance does not enter as a parameter in the definition of the seismic action in Eurocode 8, the type of spectrum has been chosen as the parameter determining this ratio, on the basis of the finding that $a_{\mathrm{vg}}/a_{\mathrm{g}}$ increases also with Magnitude (Ambraseys and Simpson 1996, Abrahamson and Litehiser 1989), which in turn determines the selection of the type of spectrum.

4.2.2 Design Spectrum for Forced-Based Design with Linear Analysis

For the horizontal components of the seismic action the design spectrum in Eurocode 8 for force-based design of new buildings is:

$$0 \leq T \leq T_B \; : \; S_{a,d}(T) = a_g S \left[\frac{2}{3} + \frac{T}{T_B} \left(\frac{2.5}{q} - \frac{2}{3} \right) \right] \tag{4.5a}$$

$$T_B \leq T \leq T_C \; : \; S_{a,d}(T) = a_g S \frac{2.5}{q} \tag{4.5b}$$

$$T_C \leq T \leq T_D \; : \; S_{a,d}(T) = a_g S \frac{2.5}{q} \left[\frac{T_C}{T} \right], \; S_{a,d}(T) \geq \beta a_g \tag{4.5c}$$

$$T_D \leq T : \; S_{a,d}(T) = a_g S \frac{2.5}{q} \left[\frac{T_C T_D}{T^2} \right], \; S_{a,d}(T) \geq \beta a_g \tag{4.5d}$$

The value 2/3 in Eq. (4.5a) is the inverse of the overstrength factor of 1.5 considered by Eurocode 8 to always be available even without any design measures for ductility and energy dissipation. Factor β in Eqs. (4.5c) and (4.5d) gives a lower bound for the horizontal design spectrum, acting as a safeguard against excessive reduction of the design forces due to flexibility of the system (real or presumed in the design). Its recommended value in Eurocode 8 is 0.2. Its practical implications may be particularly important, in view of the relatively low values recommended by Eurocode 8 for the corner period T_D at the outset of the constant spectral displacement range.

The design spectrum in the vertical direction is obtained by substituting in Eqs. (4.5) the design ground acceleration in the vertical direction, a_{vg}, for the "effective ground acceleration" $a_g S$. There is no clear, well-known energy dissipation mechanism for the response in the vertical direction. So, the "behaviour factor" q in that direction is attributed to overstrength alone and taken equal to 1.5, unless a higher value is supported by special studies and analyses.

4.3 Linear Static Analysis

4.3.1 Fundamentals and Conditions of Applicability

Linear static analysis is carried out under lateral forces applied separately in two orthogonal horizontal directions, X and Y. These forces are meant to simulate the peak inertia loads induced by the horizontal component of the seismic action in these directions, with the structure vibrating in its fundamental mode in the corresponding direction. As designers are familiar and conversant with elastic analysis for static loads (due to gravity or wind actions, etc.), this analysis is the workhorse of practical seismic design.

The fundamental assumptions of the method are:

1. The fundamental translational mode in the direction of the applied lateral forces governs the response.
2. The shape of the fundamental translational mode is known, without solving the eigenvalue problem.

Accordingly, design codes limit the application of this method to buildings with a heightwise distribution of mass and stiffness which is sufficiently regular for assumption 2 to be made with some confidence. Most codes, especially those adopting a standard 1st mode drift pattern independent of the value of the 1st natural period, e.g. (CEN 2004a), do not allow application of the method to tall flexible structures where higher modes dominate the response. Eurocode 8 in particular, allows applying linear static analysis only if both conditions (a) and (b) are met:

(a) The building is regular in elevation, according to the criteria in Section 2.1.7 which can be checked by inspection of the framing and the architectural drawings, without any structural calculations. The rationale for the exclusion of

heightwise irregular buildings is that their 1st mode shape may be far from the simple approximation assumed in linear static analysis. Moreover, higher mode effects may be locally significant (notably, around discontinuities or abrupt changes along the height), even though they may not be important for the global response (e.g., for the base shear and overturning moment).

(b) The fundamental period of the building is not longer than 2 s or four times the corner period T_C between the constant-spectral-pseudoacceleration and constant-spectral-pseudovelocity ranges of the elastic spectrum. Recall that at periods above 2 s or $4T_C$ spectral pseudoaccelerations are low and that, if the 1st mode is in that range, the 2nd and/or 3rd modes may be at, or close to, the range where spectral pseudo-accelerations are constant and highest. So, their contribution to the response may be comparable to that of the 1st mode, notwithstanding their normally lower participation mass and factors.

Conditions (a) and (b) should be met in both horizontal directions for linear static analysis to be applicable, as it is impractical to carry out this analysis in one horizontal direction and modal response spectrum analysis in the orthogonal one.

US codes (BSSC 2003, SEAOC 1999) allow using linear static analysis for low to moderate seismicity and ordinary importance of the building (notably, for "Seismic Design Categories" A to C in BSSC (2003), see Section 1.4.2.2), i.e., irrespective of its structural features. These aspects aside, the counterpart of regularity condition (a) of Eurocode 8 for the application of linear static analysis comprise all of the following:

i. regularity in plan: the maximum storey drift under the design seismic action should not exceed by 20% or more the mean drift of the storey;
ii. vertical regularity of mass: storey mass not exceeding by more than 50% that of an adjacent storey;
iii. vertical regularity of stiffness: storey stiffness not less than 70% of the storey above or 80% of the average stiffness of the three storeys above;
iv. vertical regularity of geometry: plan dimension of lateral-force-resisting system does not exceed by 30% or more the parallel dimension of an adjacent storey.

The counterpart of the Eurocode's flexibility condition (b) above for the applicability of linear static analysis is:

– In BSSC (2003): Fundamental period shorter than 3.5 times the transition period T_C between the constant-spectral-pseudoacceleration and constant-spectral-pseudovelocity ranges.
– In SEAOC (1999): Height less than 240 ft (73 m) for regular buildings meeting all criteria (i)–(iv) above, or less than 65 ft (20 m) or five storeys for irregular ones, according to any of the criteria (i)–(iv) above.

4.3.2 Fundamental Period and Base Shear

Linear static analysis is applied in Eurocode 8 in a way that gives similar results for storey shears – considered as the most important seismic action effect – as modal response spectrum analysis, at least for the type of buildings where both methods are applicable.

The seismic shear above the foundation or the top of a rigid basement ("base shear"), V_b, is determined separately in horizontal directions X and Y, on the basis of the 1st translational mode period, T_1, in the direction of interest:

$$V_b = m_{eff,1} S_{a,d}(T_1) \tag{4.6}$$

where $S_{a,d}(T_1)$ is the value of the design response spectrum from Eqs. (4.5) at the 1st mode and $m_{eff,1}$ is an estimate of the effective modal mass of that mode. Normally $m_{eff,1}$ is taken equal to the total mass, m, of the building above the foundation or the top of a rigid basement (BSSC 2003, SEAOC 1999). Eurocode 8 (CEN 2004a) allows a reduction to: $m_{eff,1} = 0.85m$, in buildings with more than two storeys above the foundation or the top of a rigid basement and a period $T_1 < 2T_C$ (where T_C is the corner period between the constant-spectral-acceleration and the constant-spectral-pseudovelocity ranges). This value is, on average, representative of heigthwise regular buildings with at least three storeys, while if $T_1 < 2T_C$ the 2nd and higher modes are normally below the plateau where spectral pseudo-accelerations are constant and highest. US codes (BSSC 2003, SEAOC 1999) take $m_{eff,1} = m$ but allow a reduction of the overturning moment (see last paragraph in Section 4.3.3).

Eurocode 8 promotes calculation of T_1 on the basis of mechanics, notably from the Rayleigh quotient:

$$T_1 = 2\pi \sqrt{\frac{\sum_i m_i \delta_i^2}{\sum F_i \delta_i}} \tag{4.7}$$

where:

- i indexes all the degrees-of-freedom (DoF) of the system in the horizontal direction, X or Y, where T_1 is calculated;
- m_i is the (translational) mass associated with degree-of-freedom i;
- F_i is the lateral force applied to degree-of-freedom i; and
- δ_i is the displacement of degree-of-freedom i, obtained from an elastic analysis of the structure for the set of lateral forces F_i.

For given relative magnitudes of the forces F_i (i.e., pattern over the DoFs i), the displacements δ_i are proportional to F_i. So, the value of T_1 from Eq. (4.7) does not depend on the absolute magnitudes of F_i. It is also rather insensitive to the relative magnitudes of F_i: any reasonable distribution of F_i to the DoFs i may be

adopted. It is very convenient and also quite accurate to use as F_i lateral forces proportional to the postulated distribution of V_b to the DoFs i in linear static analysis (see Eq. (4.8) in Section 4.3.3). Note that at the stage of the calculation of T_1 through Eq. (4.7) the base shear, V_b, is still unknown: the lateral forces F_i can be chosen such that their resultant is equal to the total weight of the structure (i.e., with $S_{a,d}(T_1) = 1.0$ g). Then a single linear static analysis per horizontal direction, X or Y, suffices in order both:

- to estimate T_1 from Eq. (4.7), and
- to determine the effects, E_X or E_Y, of the seismic action component in direction X or Y, as the seismic action effects from this analysis just need to be multiplied by $m_{eff,1}S_{a,d}(T_1)/m$, with $S_{a,d}(T_1)$ derived from the design spectrum at the – now known – value of T_1.

Codes (CEN 2004a, BSSC 2003, SEAOC 1999) give also empirical expressions for T_1, representing lower bounds (mean minus standard deviation) from measurements on buildings in California in moderate earthquakes. Such measurements reflect also the influence of non-structural elements on the response. So, the empirical expressions underestimate the period compared to Eq. (4.7). The empirical expressions may give values for T_1 that lie in the constant spectral acceleration region even for flexible buildings. So, they are sometimes used to obtain a safe-side estimate of $S_{a,d}(T_1)$ for force-based design. In the light of the upcoming displacement-based design and assessment, where realistic estimation of displacement demands is of prime importance, the empirical expressions for T_1 are not just inaccurate and misleading, but unsafe as well. So, given that Eq. (4.7) gives accurate estimates of T_1 at no additional effort, further use of the empirical period formulas in seismic design seems unwarranted.

Unlike Eurocode 8, which tries to emulate in linear static analysis a modal response spectrum one through a mechanics-based value of T_1 (e.g., from Eq. (4.7)) and a value of $m_{eff,1}$ in Eq. (4.6) which – under certain conditions – is less than the total mass m, US codes (BSSC 2003, SEAOC 1999) seem to have more confidence in the empirical expressions for T_1 than in Eq. (4.7). So, if the designer applies Eq. (4.7) or any alternative mechanics-based approach, he/she should respect a lower limit on the pseudo-acceleration $S_{a,d}(T_1)$ from the design spectrum. In SEAOC (1999) the limit is 80% of the $S_{a,d}(T_1)$ value determined from the spectrum at the empirical T_1-value. In BSSC (2003) a lower limit is set to the value of T_1 from Eq. (4.7) or other mechanics-based expressions: the T_1-value to be used cannot exceed the empirical period times 1.4–1.7.[3]

[3]Low values of the multiplicative factor are applied for high values of the design ground acceleration and large ones for lower design ground accelerations.

4.3.3 Pattern of Lateral Forces

The base shear of Eq. (4.6) is considered to be the resultant of a set of concurrent peak inertia forces on the masses m_i associated with DoF i in the horizontal direction of the component of the seismic action. In a single mode of vibration (in this case the 1st mode in the direction of the horizontal component) the peak lateral inertia force on DoF i is proportional to $\Phi_i m_i$, where Φ_i is the value of the 1st eigenmode at that DoF. Then, the base shear from Eq. (4.6) is distributed to the DoFs as:

$$F_i = V_b \frac{\Phi_i m_i}{\sum_j \Phi_j m_j} \tag{4.8}$$

with the summation in the denominator extending over all DoFs i.

If the building has rigid diaphragms, masses are often lumped there (at the floor centres of mass). Then the general formulation above, applying for any arrangement of masses and DoFs in space, is simplified to refer just to floors or storeys, with $i = 1$ at the lowest floor above the foundation or the top of a rigid basement and $i = n_{st}$ at the roof. The lateral forces F_i are then applied at the floor centres of mass.

Within the field of application of linear static analysis (regularity in elevation, higher modes unimportant), Eurocode 8 takes for simplicity the 1st mode shape as proportional to the elevation, z, from the base or above the top of a rigid basement: i.e. $\Phi_i = az_i$. Then Eq. (4.8) is commonly termed "inverted triangular" pattern of lateral forces, although it is only the assumed peak response accelerations that have "inverted triangular" distribution, while the force pattern depends also on the distribution of masses, m_i.

As US codes are more liberal than Eurocode 8 on the applicability of linear static analysis to taller, more flexible structures, their lateral force patterns attempt to capture higher-mode effects. So, for structures with $T_1 > 0.7$ s SEAOC (1999) assigns a fraction of the base shear equal to $0.07T_1$(s), but not exceeding one-quarter, to a concentrated force at the roof level and distributes the rest according to Eq. (4.8) with $\Phi_i = az_i$. In BSSC (2003) Φ_i is taken proportional to $z_i{}^k$ with $k = 0.75 + 0.5T_1 \leq 2$ and $k \geq 1$, giving $k = 1$ and $\Phi_i = az_i$ for $T_1 < 0.5$ s.

Interesting is the approach in AIJ (1992). The seismic shear at storey i is given directly as a fraction of the total building weight at storey i and above, a_i; the proportionality constant is equal to $1 + 2(1/\sqrt{a_i} - a_i)/(3 + 1/T_1)$ and empirically reflects higher-mode effects on long-period structures. For uniform distribution of the total weight to n_{st} levels, a_i is equal to $(1–(i+1)/n_{st})$ with $i = 1$ at the lowest storey. For flexible structures this dependence of seismic shears on storey level amount to a very nonlinear distribution of storey lateral loads with height and a strong concentration of lateral loads near the top.

Note that the lateral forces of Eq. (4.8) are meant to produce (by equilibrium) safe-side envelopes of storey seismic shears. Overturning moments, calculated also by equilibrium from these lateral forces, may significantly overestimate the actual peak values at some storeys. Accordingly, BSSC (2003) allows reducing by 25%

the overturning moment at the foundation level computed by equilibrium from the lateral forces of Eq. (4.8).

4.4 Modal Response Spectrum Analysis

4.4.1 Modal Analysis and Its Results

As a first step in a modal response spectrum analysis, the modal shapes (eigenmodes) in 3D and the natural frequencies (eigenvalues) are computed. Note that, even when the building may be sufficiently regular in plan for separate planar (2D) analyses to be allowed in two vertical planes, XZ and YZ, modal response spectrum analysis should be done on a full 3D structural model. Then, each modal shape, represented by vector $\boldsymbol{\Phi}_n$ for mode n, will in general have displacements and rotations in all three directions, X, Y and Z for all nodes i of the structural model (unless the solution of the eigenvalue problem is based on few DoFs, with the rest condensed out, see "indirect" approach at the end of this section).

An eigenmode-eigenvalue analysis gives for each normal mode, n:

1. The natural period, T_n , and the corresponding circular frequency, $\omega_n = 2\pi/T_n$.
2. The mode shape vector $\boldsymbol{\Phi}_n$.
3. Factors of modal participation to the response to the seismic action component in direction X, Y or Z, denoted as Γ_{Xn}, Γ_{Yn}, Γ_{Zn} and calculated as: $\Gamma_{Xn} = \boldsymbol{\Phi}_n{}^T\mathbf{M}\boldsymbol{I}_X/\boldsymbol{\Phi}_n{}^T\mathbf{M}\boldsymbol{\Phi}_n = \Sigma_i\varphi_{Xi,n}m_{Xi}/\Sigma_i(\varphi^2{}_{Xi,n}m_{Xi}+ \varphi^2{}_{Yi,n}m_{Yi}+\varphi^2{}_{Zi,n}m_{Zi})$, where i denotes nodes associated with dynamic DoFs, $\mathbf{M}$ is the mass matrix, $\boldsymbol{I}_X$ is a vector with elements equal to 1 for the translational DoFs parallel to direction X and all other elements equal to 0, $\varphi_{Xi,n}$ is the element of $\boldsymbol{\Phi}_n$ corresponding to the translational DoF of node i parallel to X and m_{Xi} the associated element of the mass matrix. Similarly for $\varphi_{Yi,n}$, $\varphi_{Zi,n}$, m_{Yi} and m_{Zi}. If $\mathbf{M}$ contains rotational mass moments of inertia, $I_{\theta Xi,n}$, $I_{\theta Yi,n}$, $I_{\theta Zi,n}$, the associated terms are included in the sum at the denominator of Γ_{Xn}. The definitions of Γ_{Yn}, Γ_{Zn} are similar.
4. The (base-shear-)effective modal masses in directions X, Y and Z, M_{Xn}, M_{Yn}, and M_{Zn}, respectively: $M_{Xn} = (\boldsymbol{\Phi}_n{}^T\mathbf{M}\boldsymbol{I}_X)^2/\boldsymbol{\Phi}_n{}^T\mathbf{M}\boldsymbol{\Phi}_n = (\Sigma_i\varphi_{Xi,n}m_{Xi})^2/\Sigma_i(\varphi^2{}_{Xi,n}m_{Xi}+ \varphi^2{}_{Yi,n}m_{Yi}+\varphi^2{}_{Zi,n}m_{Zi})$, and similarly for M_{Yn}, $M_{Zn.}$ They are important because they give the peak force resultants in mode n along direction X, Y or Z: $V_{bX,n} = S_a(T_n)M_{Xn}$, $V_{bY,n} = S_a(T_n)M_{Yn}$, $V_{bZ,n} = S_a(T_n)M_{Zn}$, respectively. The sum of the effective modal masses in X, Y or Z over all modes of the structure is equal to its total mass.

Participation factors and effective modal masses convey a certain physical meaning, essential for the understanding of the nature and relative importance of each mode. For example:

– the relative magnitude of the modal participation factors determines the predominant direction of the mode: its inclination to horizontal direction X is Γ_{Yn}/Γ_{Xn}, etc.;

- the predominant direction of the mode with the largest modal base shear is a good choice, together with the orthogonal direction, as a "principal" or "main" direction of the structure in plan, along which the horizontal seismic action components are taken to act.
- a good measure of the regularity in plan (irrespective of the qualitative criteria for regularity) is the lack of significant rotation about the vertical (and of global reaction torque with respect to that axis) in the (few) lower most modes.

Unfortunately, the presence and potential dominance of torsion about the vertical in a mode can only be detected from participation factors and modal masses for rotation about Z, normally not reported in computer output.[4] The importance of torsion in a mode can also be appreciated on the basis of modal reaction forces and moments.

Peak modal seismic action effects in the response to the seismic action component in direction X, Y or Z may be computed as follows:

I. For each normal mode n the spectral displacement, $S_{\mathrm{dX}}(T_{\mathrm{n}})$, is calculated from the pseudo-acceleration spectrum of the seismic action component, let's say X, as $S_{\mathrm{dX}}(T_{\mathrm{n}}) = (T_{\mathrm{n}}/2\pi)^2 S_{\mathrm{aX}}(T_{\mathrm{n}})$.
II. The nodal displacement vector of the structure in mode n due to the seismic action component of interest, let's say in direction X, $\boldsymbol{U}_{\mathrm{Xn}}$, is computed as: $\boldsymbol{U}_{\mathrm{Xn}} = S_{\mathrm{dX}}(T_{\mathrm{n}})\Gamma_{\mathrm{Xn}}\boldsymbol{\Phi}_{\mathrm{n}}$.
III. Peak modal values of the effects of the seismic action component of interest are computed from the modal displacement vector of Step II. Member modal deformations (e.g., chord rotations) or modal interstorey drifts are obtained directly from the nodal displacement vector of mode n. Modal member (end) forces are computed by multiplying the member modal deformations by the member stiffness matrix and modal storey shears, overturning moments, etc. by equilibrium from modal member shears, moments, axial forces, etc.

The so-computed peak modal responses are exact. However, they occur at different instances in the response and can be combined only approximately. Section 4.4.3 presents combination rules for peak modal responses. Rules to take into account in approximation the simultaneous occurrence of the seismic action components are given in Section 4.7.

Condensation of degrees of freedom (DoFs) is sometimes applied to buildings with rigid diaphragms to reduce the number of static DoFs into just three dynamic ones per floor (two horizontal translations, one rotation about the vertical). This is possible only if the vertical seismic action component, Z, is of no interest or importance. Dynamic condensation profits from the fact that horizontal seismic action components normally induce negligible vertical nodal inertia forces or nodal inertia

[4]The commonly reported modal participation factors and effective modal masses along X, Y and Z are not so informative about torsion about the vertical.

moments about the X and Y axes. This allows expressing nodal translations in Z and nodal rotations about X and Y in terms of the dynamic DoFs[5] and eliminating them from the equation of motion. If a diaphragm is rigid, the three in-plane DoFs (two horizontal translations and the rotation about the vertical axis) of each one of its nodes can be expressed through a kinematic constraint in terms of the corresponding DoFs of a single node of the diaphragm, termed master node. The master node is often taken to coincide with the storey centre of mass, where the storey's full translational mass, $m_{\mathrm{Xi}} = m_{\mathrm{Yi}}$, and floor rotational mass moment of inertia, $I_{\theta\mathrm{i}}$, are lumped. The reduced dynamic model has just $3n_{\mathrm{st}}$ modes in 3D (n_{st}: number of storeys). For each mode n the response spectrum in entered with the natural period T_{n} of the mode to read the spectral acceleration $S_{\mathrm{a}}(T_{\mathrm{n}})$. Then, for each one of the two horizontal components of the seismic action two horizontal forces and one torque with respect to the vertical are computed for mode n at each floor level i: $F_{\mathrm{Xi,n}}$, $F_{\mathrm{Yi,n}}$ and $M_{\mathrm{i,n}}$, where indexes X and Y denote now the direction of the two forces and not that of the seismic action component (which may be either X or Y). These forces and moments are computed as $S_{\mathrm{a}}(T_{\mathrm{n}})$ times:

- the participation factor of mode n to the response to the seismic action component of interest, let's say Γ_{Xn} for the one in direction X;
- the mass associated with the corresponding floor DoFs: floor mass $m_{\mathrm{Xi}} = m_{\mathrm{Yi}}$ and floor rotational mass moment of inertia, $I_{\theta\mathrm{i}}$; and
- the corresponding component of the modal eigenvector, $\varphi_{\mathrm{Xi,n}}$, $\varphi_{\mathrm{Yi,n}}$, $\varphi_{\theta\mathrm{i,n}}$.

For each mode n and separately for the two horizontal components of the seismic action, a static analysis of the full structural model in 3D is carried out then, under static forces and moments $F_{\mathrm{Xi,n}}$, $F_{\mathrm{Yi,n}}$ and $M_{\mathrm{i,n}}$, applied to the corresponding dynamic DoFs of each floor i. Peak modal response quantities (nodal displacements, member internal forces or deformations, e.g. chord rotations, interstorey drifts, etc.) are computed separately for each mode and combined for all modes according to the rules in Section 4.4.3 for each horizontal component X or Y of the seismic action.

As the "indirect" approach above computes internal forces and other response quantities by static analysis for specified (modal) forces at floor levels, resembling external loads, it is more intuitive and appealing to designers who are familiar with analysis for static actions, such as wind or gravity, but maybe not so conversant with modal response spectrum analysis. For this reason, despite its lack of generality and limitations in its use (rigid diaphragms, no vertical seismic action component) some codes (BSSC 2003) do suggest the "indirect" procedure for the calculation of peak dynamic response quantities in the framework of modal response spectrum analysis.

[5]Dynamic DoFs are those contributing to the equation of motion with inertia terms.

4.4.2 Minimum Number of Modes

Modal response spectrum analysis should take into account all modes contributing significantly to any response quantity of interest. This is difficult to achieve in practice, because the number of modes to be considered should be specified as input to the eigenvalue analysis. Codes (CEN 2004a, BSSC 2003, SEAOC 1999) focus on base shears as the prime response quantities of interest and use as a criterion the relevant measure(s) from the eigenvalue analysis. They require the N considered modes to provide together a total effective modal mass along any individual seismic action component, X, Y, or even Z, at least 90% of the total mass.

If the above criterion is hard to satisfy, Eurocode 8 (CEN 2004a) allows as alternative to take into account all modes which individually have effective modal mass along any one of the seismic action components, X, Y or Z, considered in design, at least 5% of the total mass. This criterion refers to modes that may have not been captured so far in the eigenvalue analysis; so it is difficult to apply. As a third alternative in case meeting any of the two criteria above is unfeasible (e.g. when torsional modes are important, or when the vertical seismic action component should be considered in design), Eurocode 8 is content if the eigenvalue analysis captures at least $3\sqrt{n_{st}}$ modes (where n_{st} is the number of storeys above the foundation or the top of a rigid basement) and at least one natural periods below 0.2 s.

The 1st and most commonly used of the above criteria (that of the sum of effective modal masses captured) addresses only the base shear reflected in the computed modes, and even that only partly. As modal shears are equal to the effective modal mass times the spectral acceleration at the mode's period, if the 1st mode period is fairly long and higher mode periods are in the constant spectral acceleration plateau, the effective modal mass alone underestimates the contribution of higher modes to base shear. Other global response quantities, such as the overturning moment at the base and the top displacement, are less sensitive to the number of modes than the base shear. However, response quantities used in local verifications (interstorey drifts, member chord rotations or internal forces, etc.) may be more sensitive to the number of modes included. So, these modes would preferably account for much more than 90% of the total mass (close to 100%), to approximate well the peak values of these quantities.

There exist techniques to approximately account for the missing mass due to truncation of higher modes (e.g. by adding static response). However, Eurocode 8 does not require such measures for buildings.

Modal overturning moments from modal analysis reflect realistically the distribution of modal inertia forces along the height. So, their final combination via the rules of Section 4.4.3 into peak dynamic storey overturning moments can be considered as free of the conservatism associated with calculation of storey "static" or "equivalent lateral" forces by equilibrium. BSSC (2003) allows up to 10% reduction of the value of the overturning moment at the foundation level as computed from modal contributions according to Section 4.4.3.

4.4.3 Combination of Modal Results

In modal response spectrum analysis it is convenient to take the elastic response to two different modes as independent of each other. In reality this is just an approximation. The magnitude of the actual correlation between modes *i* and *j* is estimated through a correlation coefficient of the two modes, ρ_{ij}. The following approximation has been proposed in (Rosenblueth and Elorduy 1969):

$$\rho_{ij} = \frac{\zeta^2(1+\lambda)^2}{(1-\lambda)^2 + 4\zeta^2\lambda} \tag{4.9a}$$

Nowadays the approximation proposed in Wilson et al. (1981) and Der Kiureghian (1981) is more widely accepted and used:

$$\rho_{ij} = \frac{8\sqrt{\zeta_i\zeta_j}(\zeta_i + \lambda\zeta_j)\lambda^{3/2}}{(1-\lambda^2)^2 + 4\zeta_i\zeta_j\lambda(1+\lambda^2) + 4(\zeta_i^2 + \zeta_j^2)\lambda^2} \tag{4.9b}$$

In Eqs. (4.9) ζ_i, ζ_j are the viscous damping ratios in modes *i* and *j*, respectively (taken as equal in Eq. (4.9a) and denoted by ζ), while $\lambda = T_i/T_j$. If two modes have closely spaced natural periods ($\lambda \approx 1.0$), ρ_{ij} is close to 1.0 and the responses in the two modes cannot be considered independent of each other. For buildings Eurocode 8 (CEN 2004a) considers that modes *i* and *j* cannot be taken as independent, if λ is between 0.9 and 1/0.9. At the two extremes of this range of λ and for $\zeta_i = \zeta_j = 0.05$, Eq. (4.9b) gives $\rho_{ij} = 0.47$. Part 2 of Eurocode 8 for bridges (CEN 2005b) is more restrictive, considering that modes *i* and *j* are not independent if λ is between $[0.1 + \sqrt{(\zeta_i\zeta_j)}]$ and $0.1/[0.1 + \sqrt{(\zeta_i\zeta_j)}]$; if $\zeta_i = \zeta_j = 0.05$ and λ is equal to these limit values, Eq. (4.9b) gives indeed a low value: $\rho_{ij} = 0.05$. Note that buildings with about the same lateral stiffness in horizontal directions X and Y have pairs of modes with very similar periods at about right angles in plan (albeit not necessarily in the two direction, X and Y). The modes of each pair are closely correlated.

When all relevant modal responses can be taken as independent of each other, random vibration theory gives the expected value of the maximum, E_E, of a seismic action effect as the Square Root of the Sum of Squares of the modal responses – SRSS rule (Rosenblueth 1951):

$$E_E = \sqrt{\sum_N E_{Ei}^2} \tag{4.10}$$

where the summation extends over the *N* modes taken into account and E_{Ei} is the peak value of the seismic action effect in mode *i*. If the response in any two vibration modes *i* and *j* cannot be taken as independent of each other, the SRSS rule is unconservative. Then more accurate procedures for the combination of peak modal responses should be used (CEN 2004a). Random vibration theory gives

the Complete Quadratic Combination – CQC rule (Wilson et al. 1981) quoted in Eurocode 8 for the expected value of the maximum, E_{E}, of a seismic action effect due to correlated modes:

$$E_E = \sqrt{\sum_{i=1}^{N} \sum_{j=1}^{N} \rho_{\mathrm{ij}} E_{Ei} E_{Ej}} \tag{4.11}$$

In Eq. (4.11) E_{Ei}, E_{Ej} are the peak values of the seismic action effect in modes i and j. The correlation coefficient of modes i and j, ρ_{ij}, may be taken from the approximation of Eqs. (4.9). Comparison with the results of response-history analyses has demonstrated good average accuracy of the CQC rule. Note that the CQC includes the SRSS rule, Eq. (4.10), as a special case for $\rho_{\mathrm{ij}} = 0$ if $i \neq j$ (for $i = j$ we have $\rho_{\mathrm{ij}} = 1$).

The SRSS and the CQC give only the absolute value of the peak response estimate, which should be considered and combined with non-seismic action effects (e.g., due to gravity loads) as both negative and positive. So, although modal internal forces satisfy equilibrium at any level, member end force values from the SRSS or CQC rules do not satisfy equilibrium at the level of the individual member or node. So, envelopes of moments along members cannot be constructed from the member end forces and equilibrium. They may be constructed, instead, point-by-point, by SRSS or CQC combination of the modal moments at the generic point x along the member. Such envelopes do not have a point of inflection and do not show whether the member is in single or in double curvature bending when its peak end moments take place. This can be judged from the peak shear forces computed through the same mode combination rules. The member may be considered to be in double or single curvature; if the product of the member's peak shear force and the member length is closer to the sum of the (positive) member end moments, or to their difference, respectively.

4.5 Linear Analysis for the Vertical Seismic Action Component

4.5.1 When is the Vertical Component Important and Should Be Taken Into Account?

In buildings the vertical seismic action component may in general be neglected, because:

- its effects are normally covered by the design for factored gravity loads;
- except in buildings having long span beams with significant mass distributed along them, the fundamental period of the building in the vertical direction is governed by the axial stiffness of vertical members and is very short; so, spectral amplification of the vertical ground motion is low.

Seismic design codes require to take into account the vertical seismic action component only when its effects are likely to be significant (in view of the arguments above). Eurocode 8 considers this to be the case only if the design ground acceleration in the vertical direction, a_{vg}, exceeds 0.25 g, and even then only in the following cases:

- in base-isolated buildings; or
- for (nearly) horizontal members (beams, girders, or slabs) which:
  - have a span of at least 20 m; or
  - cantilever over at least 5 m; or
  - support directly columns; or
  - are prestressed.

4.5.2 Special Linear Static Analysis Approach for the Vertical Component

The analysis provisions of current seismic design codes pertain primarily (essentially only) to the horizontal components of the seismic action. At most they include very limited special guidance for the analysis under the vertical component. The modal response spectrum and the nonlinear dynamic methods of analysis are, of course, applicable for the analysis of the response to the vertical component, provided that floor masses are not lumped only at nodes of vertical and horizontal elements, but at several intermediate points of the horizontal elements as well. However, a very large number of modes may need to be determined in modal analysis to capture 90% of the participating mass in the vertical direction, or, in general, to accurately estimate the seismic action effects due to the vertical component.

Although not described in codes, an "equivalent static" linear analysis can be used for the vertical component. This is a modification of the "lateral force procedure" to address the vertical direction instead of the horizontal. For convenience, it may employ the same structural model as the analysis for the horizontal components. In this approach the fundamental period of vibration in the vertical direction, T_1, may be estimated via Eq. (4.7), using as F_i the weights of the masses m_i and as δ_i the vertical nodal displacements from the analysis for the loads F_i. As these forces are the gravity loads concurrent with the design seismic action, a linear static analysis for them is done anyway and its results are already available. A total vertical seismic force can then be computed from Eq. (4.6) with $m_{eff,1} = m$, on the basis of the spectral acceleration, $S_{av}(T_1)$, derived from the vertical design spectrum (see last paragraph in Section 4.2.2). For the purposes of the static analysis for the vertical seismic action component, this total vertical force can be distributed to all nodes of the structure in proportion to the product of their mass, m_i, times their vertical displacement, δ_i, under the weights of the masses m_i.

In those horizontal members for which the vertical component needs to be taken into account, the relevant dynamic response is often of local nature. It involves these members and their immediately adjacent or supporting ones, but not the entire structure. So, Eurocode 8 considers sufficient to carry out an analysis on a partial structural model capturing the important aspects of the response in the vertical direction, without irrelevant and unimportant influences that may confuse or obscure the important results. The partial model includes fully the horizontal members on which the vertical component is considered to act, as well as the elements (or systems of elements) directly supporting them. All other adjacent elements (e.g. adjacent spans) may be included only with their stiffness. More specifically:

(a) the partial structural model should include all (nearly) horizontal members for which the vertical component needs to be taken into account, each discretised into a few (e.g. about five) beam elements with masses lumped at the intermediate nodes;
(b) directly supporting elements or systems of elements may also be included, up to their supports by the ground or at another vertically stiff element or system of elements; for example, columns directly supporting the members on which the vertical component is taken to act may be included with their full length down to the foundation;
(c) adjacent spans continuous to the member(s) on which the vertical component is taken to act may be included up to their next support, with appropriate boundary conditions there (e.g. pinned or fixed against rotation, fixed vertically, etc.);
(d) the partial structural model should include those beams, girders or other horizontal elements which are connected at an angle (often at right angles) to the members on which the vertical component is taken to act; these transverse or oblique elements should be included in the model with their full connectivity and the appropriate boundary conditions at their supports, but without intermediate nodes for lumped masses;

The members on which the vertical component is considered to act (those listed in (a) above) and their directly associated supporting elements or systems of elements (e.g. those listed in (b) or (d)) are the only ones to be dimensioned on the basis of the computed action effects of the vertical component.

The designer may find it inconvenient to develop the partial structural model just for the purposes of the analysis for the vertical component. He/she may prefer to keep instead the overall structural model of the analysis for gravity loads and the horizontal components of the seismic action, but use a partial model only to calculate T_1 from Eq. (4.7) and distribute to the individual masses the total vertical seismic force derived from T_1 and from the vertical design spectrum. Such a partial model may be developed from the overall structural model, by considering all nodes of vertical elements as fixed against vertical displacement. These vertical DoFs are released in the subsequent static analysis for the calculation of the effects of the

vertical seismic action component. This latter analysis is carried out on the overall structural model under vertical nodal loads proportional to $m_i\delta_i$ and applied only to the vertically active DoFs of the partial structural model. In this way the action effects of the vertical component, E_Z, can be realistically computed, not only in the horizontal members included in the partial model, but also in their supporting or adjacent elements and the whole structure.

4.6 Nonlinear Analysis

4.6.1 Nonlinear Static ("Pushover") Analysis

4.6.1.1 Introduction

The prime use of nonlinear analysis is for assessment of existing or retrofitted buildings, for which, as pointed out in Section 4.1.3, nonlinear analysis is the reference method, or for evaluation of the seismic performance of new designs.

Unlike linear analysis, which has long been the basis of practical seismic design of new buildings, and nonlinear dynamic analysis, which has been extensively used since the 1970s for research, code-calibration or other special tasks, nonlinear static analysis (commonly called "pushover" analysis) was not widely known or used until the first new-generation guidelines for seismic rehabilitation of existing buildings (ATC 1997) adopted it as the reference method. Since then, its appealing simplicity and intuitiveness and the wide availability of reliable and user-friendly analysis software have made it the analysis method of choice for seismic assessment and retrofitting of buildings.

"Pushover" analysis is essentially the extension of the "lateral force procedure" of static analysis into the nonlinear regime. It is carried out under constant gravity loads and monotonically increasing lateral loading applied on the masses of the structural model. This loading is meant to simulate inertia forces due to a horizontal component of the seismic action (the vertical component is not addressed). While the applied lateral forces increase in the course of the analysis, the engineer can follow the gradual emergence of plastic hinges, the evolution of the plastic mechanism and damage, as a function of the magnitude of the imposed lateral loads and of the resulting displacements.

4.6.1.2 Lateral Load Vector

Pushover analysis was initially developed, and still mainly applied, for 2D analyses. Even when applied on 3D structural models the lateral loading simulates the inertia due to a single horizontal seismic action component. In the fundamental and most commonly used version of the method, the forces F_i incrementally applied on the masses m_i remain proportional to an invariant pattern of horizontal displacements Φ_i:

$$F_i = \alpha m_i \Phi_i \tag{4.12}$$

as if the entire response were in a single invariant mode with horizontal modal displacements Φ_i.

According to Eurocode 8 (CEN 2004a, 2005a), pushover analyses should be applied to buildings using both of the following lateral load patterns:

1. A "modal pattern", simulating the inertia forces of the 1st mode in the horizontal direction in which the analysis is carried out. This pattern is meant to apply in the elastic regime and during the initial stages of the plastic mechanism development, as well as in a full-fledged beam-sway mechanism (see Fig. 1.3(b)–(e)). The precise pattern depends on the type of linear analysis applicable:
   - If the building meets the applicability conditions of linear static analysis, an "inverted triangular" unidirectional lateral load pattern is applied, like the one used in a linear static analysis (i.e. with $\Phi_i = z_i$ in Eq. (4.12));
   - When the building does not fulfil the conditions for the application of linear static analysis, Φ_i in Eq. (4.12) is the 1st mode shape from modal analysis. If the 1st mode is not purely translational, the patterns of Φ_i and F_i are not unidirectional: they may have horizontal components orthogonal to that of the seismic action component in question.
2. A "uniform pattern", corresponding to uniform unidirectional lateral accelerations, i.e. to $\Phi_i = 1$ in Eq. (4.12). It attempts to simulate the inertia forces in a potential soft-storey mechanism, limited in all likelihood to the bottom storey, with the lateral drifts concentrated there and the storeys above moving laterally almost as a rigid body (Fig. 1.3(a)).

The most unfavourable result of the pushover analyses with the two standard lateral force patterns, 1 or 2, should be used. Unless the structure is symmetric about an axis at right angles to the seismic action component considered, the lateral forces should be applied in both the positive and the negative direction (sense).

More sophisticated versions of pushover analysis (Bracci et al. 1997, Elnashai 2001, Gupta and Kunnath 2000) do not use a fixed pattern of applied lateral loads, Eq. (4.12), but "adapt" it to the evolution of nonlinearity, as this affects the dynamic properties of the structure. However, any increase in accuracy is at the expense of the most attractive feature of pushover analysis, namely its simplicity. So, here we stay with the original and simplest version of pushover analysis, as in the N2 procedure (Fajfar 2000) adopted in Eurocode 8 (CEN 2004a, 2005a).

4.6.1.3 Capacity Curve and Equivalent SDOF System

It is convenient and common to present the results of a "pushover" analysis in the form of a nonlinear force-displacement curve (Fig. 4.2). Although it depicts a certain aspect of the building's nonlinear response and has little to do with its capacity

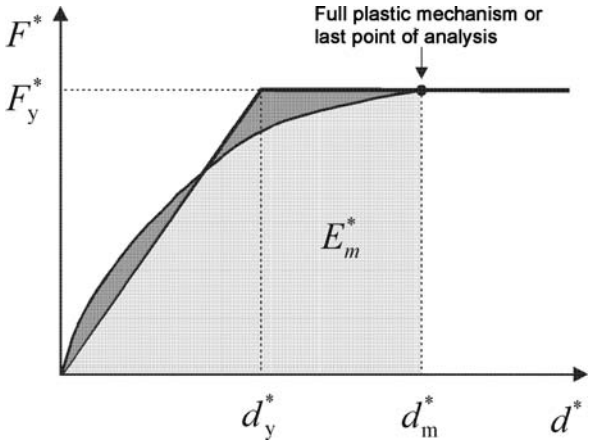

Fig. 4.2 Elastic-perfectly plastic idealisation of capacity curve of equivalent SDOF system in pushover analysis (Fajfar 2000, CEN 2004a)

to withstand the seismic action, the curve is commonly referred to as "capacity curve". This differentiates it from the "demand" curve, which relates the spectral displacement to the product of the mass and the spectral acceleration (Acceleration-Displacement-Response-Spectrum, ADRS, Fig. 4.3). The proximity of the "capacity curve" to the results of a series of nonlinear dynamic (response-history) analysis, considered as the benchmark, is often taken as a measure of the accuracy of a "pushover" analysis.

An obvious force quantity for the vertical axis of the "capacity curve" is the base shear, V_b, as it represents the total force resistance in the horizontal direction considered at an instant of the displacement response. The lateral displacement on the horizontal axis, d_n, is often taken at a certain node n of the structural model, termed "control node". That node is normally at the centre of mass of the roof. A mathematically better choice, relating very well to the definition of the seismic demand in terms of spectral quantities, are the lateral force and displacement of an equivalent Single-Degree-of-Freedom (SDOF) system. In the N2 procedure (Fajfar 2000) adopted in Eurocode 8 the equivalent SDOF system is defined as follows:

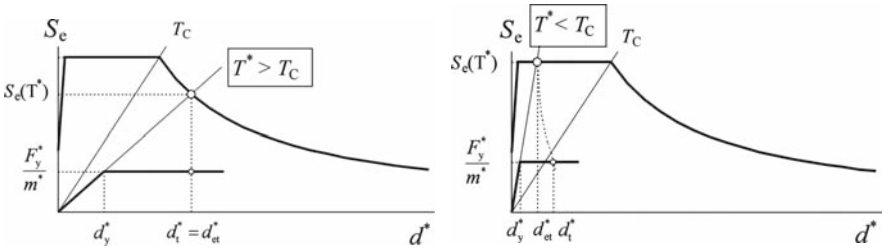

Fig. 4.3 "Target displacement" of equivalent SDOF system in "pushover" analysis (Fajfar 2000, CEN 2004a): (**a**) long and intermediate period ranges; (**b**) short period range

- The horizontal displacements Φ_i in Eq. (4.12) are normalised so that $\Phi_n = 1$ at the control node.
- The mass of the equivalent SDOF system m^* is:

$$m^* = \sum m_i \Phi_i \tag{4.13}$$

- Its force, F^* and displacement d^* are:

$$F^* = \frac{V_b}{\Gamma},\ d^* = \frac{d_n}{\Gamma} \tag{4.14}$$

where:

$$\Gamma = \frac{m^*}{\sum m_i \Phi_i^2} \tag{4.15}$$

Note that in the "modal pattern" of lateral loads, where Φ_i emulates a mode shape, Γ is the participation factor of that mode in the direction of the lateral forces (point 3 in Section 4.4.1).

To determine the seismic demand (see Section 4.6.1.4) we need to estimate the period T^* of the equivalent SDOF system. According to Fajfar (2000) and CEN (2004a) T^* can be determined on the basis of the mass from Eq. (4.13) and of the elastic stiffness of an elastic-perfectly plastic idealisation of the "capacity curve" of the SDOF system. The yield force, $F_y{}^*$, of the elastic-perfectly plastic curve, taken as the ultimate strength of the SDOF system, is the value of F^* when a complete plastic mechanism forms (or at the terminal point of the "capacity curve", if a full plastic mechanism does not develop by then). The yield displacement, $d_y{}^*$, is chosen so that the deformation energy of the elastic-perfectly plastic idealisation at the displacement of the equivalent SDOF system when the plastic mechanism forms or at the terminal point, $d_m{}^*$, is equal to that of the actual "capacity curve" at the same point, $E_m{}^*$ (Fig. 4.2):

$$d_y^* = 2\left(d_m^* - \frac{E_m^*}{F_y^*}\right) \tag{4.16}$$

The elastic stiffness of the SDOF system is $F_y{}^*/d_y{}^*$ and its period T^* is (Fajfar 2000, CEN 2004a):

$$T^* = 2\pi\sqrt{\frac{m^* d_y^*}{F_y^*}} \tag{4.17}$$

If the structure is almost linear until the "yield point" of the elastic-perfectly plastic SDOF system, the period from Eq. (4.17) is the same as the one computed

from Eq. (4.7) on the basis of the results of a linear analysis under lateral forces with the pattern of Eq. (4.12).

4.6.1.4 Definition of the Seismic Demand Through the "Target Displacement"

Unlike linear or nonlinear dynamic analysis, which both give directly all peak seismic demands under a given earthquake, a pushover analysis per se gives only the "capacity curve". The demand is estimated separately. This is normally done in terms of the maximum displacement induced by the earthquake, either to the equivalent SDOF system or at the "control node" of the full structure. This is called "target displacement". In the N2 method (Fajfar 2000, CEN 2004a) the "target displacement" is determined on the basis of the "equal displacement rule", modified for short period systems according to Eqs. (1.1) and (1.2) (Vidic et al. 1994). As shown in Fig. 4.3, if T^* is longer than the transition period, T_C, between the constant pseudo-acceleration and the constant pseudo-velocity parts of the elastic spectrum, the target displacement of the equivalent SDOF system is taken equal to the spectral displacement from the 5%-damped elastic spectrum at period T^*:

$$d_t^* = S_d(T^*) = \left[\frac{T^*}{2\pi}\right]^2 S_a(T^*) \qquad \text{if } T \geq T_C \tag{4.18a}$$

Otherwise, the spectral displacement is corrected according to the q-μ-T relation in (Vidic et al. 1994):

$$d_t^* = \frac{S_d(T^*)}{q_u}\left(1 + (q_u - 1)\frac{T_C}{T^*}\right) \geq S_d(T^*) \qquad \text{if } T < T_C \tag{4.18b}$$

where $q_u = m^* S_a(T^*)/F_y{}^*$. Equation (4.14) can then be inverted for the displacement at the control node, d_n, corresponding to the "target displacement" of the SDOF system.

The "target displacement" may be determined more accurately (especially if the seismic action is given in terms of one or more acceleration time-histories instead of a smooth, 5%-damped elastic spectrum) as the peak displacement from a nonlinear dynamic analysis of a SDOF system with the mass m^* of the equivalent SDOF system and an elastic-perfectly plastic force-deformation monotonic law with the yield force, $F_y{}^*$, and the yield displacement, $d_y{}^*$, of the equivalent SDOF system of Section 4.6.1.3. This analysis may be carried out according to Section 4.6.2, using a hysteresis model, such those in Section 4.10.1.6.

The demands at the local level (inelastic deformations and forces) due to the horizontal component of the seismic action in the direction of the pushover analysis are those corresponding to the "target displacement". Codes (ATC 1997, CEN 2004a, 2005a, ASCE 2007) require carrying out the pushover until a terminal point at 1.5 times the "target displacement".

4.6.1.5 Torsional Effects

The original development of pushover analysis and the N2 method (Fajfar 2000) are for 2D analysis under a single component of the seismic action. The question arises to what extent the standard pushover analysis may be applied, if the response is significantly affected by torsion in 3D and what corrections may be needed in that case.

If the 1st mode along, or close to, each one of the two orthogonal horizontal directions in which the pushover analysis is carried out includes a significant torsional component, the "modal pattern" of lateral loads should be applied to individual nodes (not to the floor centres of mass), with the displacements Φ_i in Eq. (4.12) taken according to the shape of the corresponding 1st mode in 3D. However, if the 1st or 2nd mode in one of the two orthogonal horizontal directions is primarily torsional, such a pushover analysis may overestimate horizontal displacements on the flexible/weak side in plan (the one developing larger horizontal displacements along the direction of lateral forces than the opposite side), i.e., is on the safe side and the difference may be ignored. By contrast, the displacements of the stiff/strong side are underestimated. This difference in the prediction is on the unsafe side and should be taken into account (CEN 2004a). This may be done as follows (Peruš and Fajfar 2005, Marušić and Fajfar 2005, Fajfar et al. 2004, 2005):

1. The standard pushover analysis is carried out on the 3D structure, with the unidirectional pattern of lateral forces, "uniform" or "modal", applied to the floor centres of mass.
2. The equivalent SDOF system is established, along with the elastic-perfectly plastic idealisation of its "capacity curve". Its "target displacement" is determined and translated to a displacement at the control node n at the centre of mass of the roof by inverting Eq. (4.14).
3. A modal response spectrum analysis of the same 3D structural model is carried out. The displacement in the horizontal direction of the pushover analysis is computed at all nodes of the roof (including the control node at the centre of mass) through the CQC rule, Eq. (4.11) and divided by the corresponding value of the control node at the centre of mass, to give an "amplification factor" reflecting the effect of torsion on roof displacements.
4. At all points where the "amplification factor" derived in 3 above is greater than 1.0, it multiplies the displacements of all nodes along the same vertical line, as these are obtained from the standard pushover analysis in 1 and 2 above. These products are taken as the outcome of the analysis, reflecting on one hand the global inelastic response and its heightwise distribution as captured by standard pushover analysis, and on the other the effect of global torsion on the planwise distribution of inelasticity. Eurocode 8 limits the "amplification factor" to values not less than 1.0 and does not allow de-amplification due to the effects of torsion.

Nonlinear dynamic analyses show that the larger the extent and magnitude of inelasticity, the less are the effects of torsion on local response.

4.6.1.6 Higher Mode Effects

Pushover analysis with a force pattern from Eq. (4.12) captures only the effects of a single mode, and, as a matter of fact, only to the extent that the modal shape is fairly well approximated by the displacement pattern(s) used in Eq. (4.12). To capture the effects of higher modes, "Modal Pushover Analysis" has been proposed in Chopra and Goel (2002, 2004). In it a pushover analysis is fully carried out separately for each mode of interest, with gravity loads considered concurrently with every single mode. The horizontal displacement pattern Φ_i in Eq. (4.12) follows the modal shape. For each mode an equivalent SDOF system is defined through Eqs. (4.13), (4.14), (4.15), (4.16) and (4.17) and the seismic demand is determined from Eqs. (4.18) in terms of a "target displacement". A pushover analysis is carried out for each mode up to its own "target displacement"; modal displacements (accounting for the modal participation factors) at the modal target displacement are combined, e.g., via the CQC rule, Eq. (4.11). Recognising that in most cases inelasticity is limited to the 1st mode, a "Modified Modal Pushover Analysis" has been proposed in Chopra et al. (2004), in which higher mode contributions are considered as elastic.

Application of the method to flexible multistorey steel frames, regular or not, suggests that three modes may provide good agreement with the peak storey displacements from nonlinear dynamic analysis. However, element deformations (e.g., plastic hinge or chord rotations) are not estimated equally well. So, they are determined not by combining modal deformations via the CQC rule but from the computed global displacements, using case-dependent transformations from them to local deformations (e.g. via interstorey drifts). Element forces are computed in the end from local element deformations, via the element's nonlinear constitutive relation used in the pushover analysis.

Part 3 of Eurocode 8 limits the application of pushover analysis with the two standard lateral force patterns of Section 4.6.1.2 to buildings meeting condition (b) in Section 4.3.1 for the applicability of linear static analysis (1st mode period not longer than 2 s or four times the transition period T_C between the constant-spectral-acceleration and the constant-spectral-pseudovelocity regions of the spectrum). For buildings violating this condition, reference is made to either "modal pushover" or nonlinear dynamic analysis.

4.6.2 Nonlinear Dynamic (Response- or Time-History) Analysis

4.6.2.1 Scope of Application

Nonlinear dynamic analysis was developed as a method in the 1970s for research, code-calibration, or special applications. Since then, with the availability of several reliable and numerically stable computer codes with nonlinear dynamic analysis capabilities, it has gained its place in engineering practice for the evaluation of structural designs carried out using other approaches (e.g., by conventional force-based design with the q-factor and linear analysis) or cycles of analysis and design evaluation. Its application in design is greatest in buildings with base isolation, as their

response is governed by a few elements (the isolation devices) with strongly nonlinear force-deformation law that depends on the specific devices and does not follow a standard pattern. Moreover, as isolation normally shields the superstructure from seismic damage, residual displacements of the isolation system are of great interest. They can be estimated only through nonlinear dynamic analysis.

The main practical application of nonlinear dynamic analysis, currently and in the foreseeable future, is for seismic assessment of existing structures, where, as pointed out in Section 4.1.3, nonlinear analysis is the reference method. Professionals practicing seismic assessment and retrofitting are fewer and more specialised than in every-day seismic design. So they often master nonlinear dynamic analysis and its special software tools.

4.6.2.2 The Seismic Input Motions

If the analysis is linear or nonlinear static, the seismic action can be defined through its 5%-damped elastic response spectrum. For a nonlinear dynamic (response-history) analysis, time-histories of the ground motion are needed. These time-histories should conform on average with the 5%-damped elastic response spectrum defining the seismic action.

Current seismic codes (CEN 2004a, BSSC 2003, SEAOC 1999, ASCE 2007) require as input for a response-history analysis an ensemble of at least three records (or pairs or triplets of different records, for analysis under two or three concurrent components of the action). Eurocode 8 accepts artificial, historic or simulated records, but US codes (BSSC 2003, SEAOC 1999) only recorded, or simulated ones. Artificial (or "synthetic") records can be mathematically produced using random vibration theory to match almost perfectly the response spectrum defining the seismic action (Gasparini and Vanmarcke 1976). It is fairly straightforward to adjust the phases of the various sinusoidal components of the artificial waveform, as well as the time-evolution of their amplitudes ("envelope function"), so that the artificial record resembles a specific recorded motion. Note, however, that records which are equally rich in all frequencies are not realistic. Moreover, an excitation with a smooth response spectrum without peaks or troughs introduces a conservative bias in the response, as it does not let inelastic response help the structure escape from a spectral peak to a trough at a longer period. Therefore, historic records are favoured also in CEN (2004a). Records simulated from mathematical source models, including rupture, propagation of the motion through the bedrock to the site and, finally, through the subsoil to the surface, are also preferred over artificial ones (CEN 2004a), as the final records resemble natural ones and are physically appealing. Obviously, an equally good average fitting of the target spectrum requires more – appropriately selected – historic or simulated records than artificial ones. Individual recorded or simulated records should be "adequately qualified with regard to the seismogenetic features of the sources and to the soil conditions appropriate to the site" (CEN 2004a). In more plain language, they should come from events with magnitude, fault distance and mechanism of rupture at the source consistent with those of the design seismic action (BSSC 2003, SEAOC 1999, ASCE 2007). The travel

path and the subsoil conditions should preferably resemble those of the site. These requirements are not only hard to meet, but may also conflict with conformity (in the mean) to the target spectrum of the design seismic action. The requirement of CEN (2004a) to scale individual historic or simulated records so that their peak ground acceleration (PGA) matches on average the value of $a_g S$ of the design seismic action may also be considered against physical reality. It is more meaningful, instead, to use individual historic or simulated records with PGA values already conforming to the target value of $a_g S$. Note also that the PGA alone may be artificially increased or reduced, without affecting at all the structural response. So, it is more meaningful to select the records on the basis of conformity of spectral values alone, as described below.

If pairs or triplets of different records are used as input for analysis under two or three concurrent seismic action components, conformity to the target 5%-damped elastic response spectrum may be achieved by scaling the amplitude of the individual records as follows:

- For each earthquake consisting of a triplet of translational components, the records of horizontal components are checked for conformity separately from the vertical one (CEN 2005b).
- The records of the vertical component, if considereded, are scaled so that the average 5%-damped elastic spectra of their ensemble is at least 90% of the 5%-damped vertical spectrum at all periods between $0.2T_v$ and $2T_v$, where T_v is the period of the lowest mode with participation factor of the vertical component higher than those of both horizontal ones (CEN 2005b).
- For analysis in 3D under both horizontal components, the 5%-damped elastic spectra of the two horizontal components in each pair are combined by applying the SRSS rule at each period value. The average of the "SRSS spectra" of the two horizontal components of the individual earthquakes in the ensemble should be at least $0.9\sqrt{2} \approx 1.3$ times ($\sqrt{2} \approx 1.4$ times in (SEAOC 1999, ASCE 2007)) the target 5%-damped horizontal elastic spectrum at all periods from $0.2T_1$ up to $2T_1$ in CEN (2004a) or $1.5T_1$ in BSSC (2003), SEAOC (1999) and ASCE (2007), where T_1 is the lowest natural period of the structure in any horizontal direction. If it isn't, all individual horizontal components are scaled up, so that their final average "SRSS spectrum" exceeds by a factor of 1.3 (or 1.4 in (SEAOC 1999, ASCE 2007)) the target 5%-damped horizontal elastic spectrum everywhere between $0.2T_1$ and $2T_1$ in CEN (2004a) or $1.5T_1$ in BSSC (2003), SEAOC (1999) and ASCE (2007).

For analysis under a single horizontal component, Eurocode 8 (CEN 2004a) requires the mean 5%-damped elastic spectrum of the applied motions not to fall below 90% of that of the design seismic action at any period from $0.2T_1$ to $2T_1$. In BSSC (2003) the lower limit is 100% of the spectrum of the design seismic action at all periods from $0.2T_1$ to $1.5T_1$ (T_1 is the fundamental period in the horizontal direction along which the motion is applied).

If the response is obtained from at least seven nonlinear time-history analyses with (triplets or pairs of) ground motions chosen in accordance with the previous paragraphs, the relevant verifications may use the average of the response quantities from all these analyses as action effect. Otherwise, is should use the most unfavourable value of the response quantity among the analyses.

4.6.2.3 Damping

If the response is indeed elastic, nonlinear and linear response-history analysis should give identical results, even when they are carried out using different algorithms and software tools. Linear response-history analysis should, in turn, produce the same peak SDOF response as given by the elastic response spectrum, normally associated in design codes with viscous damping ratio 5% of critical. Therefore, for consistency across methods as well as with the elastic spectrum to which the input time-histories conform, nonlinear dynamic analysis should have a built-in 5% viscous damping ratio associated with elastic response. Recall that in a design context the upper limit of the elastic regime is defined by yielding of members. So, the 5% viscous damping ratio is considered to encompass all sources of damping up to member yielding, including any structural damping of hysteretic nature, e.g., due to cracking of concrete members and energy dissipation during pre-yield cycles. Hysteretic damping after member yielding should be reflected just by the nonlinear force-deformation laws describing the post-yield behaviour of members in cyclic loading.

Recall that the forces due to viscous damping enter in the equations of motion as $\mathbf{C}\dot{\boldsymbol{U}}$. For convenience of the numerical integration of the nonlinear equations of motion, the damping matrix, $\mathbf{C}$, is typically taken to be of the Rayleigh type,

$$\mathbf{C} = \alpha_{\mathrm{o}}\mathbf{M} + \alpha_1\mathbf{K} \tag{4.19}$$

Rayleigh damping gives a viscous damping ratio ζ at a circular frequency ω equal to:

$$\zeta = \frac{1}{2}\left(\frac{\alpha_o}{\omega} + \alpha_1\omega\right) \tag{4.20}$$

So, the mass-proportional part damps out lower-frequency components and the stiffness-proportional part high-frequency ones. To achieve values of the damping ratio as close as possible to the target value $\zeta = \zeta_{\mathrm{o}} = 0.05$ within the predominant frequency range of the response, one may specify $\zeta = \zeta_{\mathrm{o}}$ at two circular frequencies, ω_1 and ω_2, straddling that range and solve for α_{o} and α_1 to get:

$$\zeta = \frac{\zeta_o}{\omega_1 + \omega_2}\left(\frac{\omega_1\omega_2}{\omega} + \omega\right) \tag{4.20a}$$

For analysis under a single component of the seismic action a good choice for ω_1 is the circular frequency of the mode with the highest modal base shear in the

elastic structure.[6] For concurrent application of the two horizontal components, the average circular frequency in the two modes with the highest modal base shears in two nearly orthogonal horizontal directions may be appropriate. The value of ω_2 may be chosen two to three times ω_1, bracketing the range of the 1st and 2nd modes in both horizontal directions. The resulting viscous damping ratio is lower than $\zeta = \zeta_o = 0.05$ at frequencies between ω_1 and ω_2 and higher outside that range (Chopra 2007). The further away the values of ω_1 and ω_2, the larger is the dip in damping ratio in-between. The minimum damping occurs at $\omega_{min} = \sqrt{(\omega_1 \omega_2)}$ and is equal to $\zeta_{min} = 2\zeta_o \omega_{min}/(\omega_1 + \omega_2)$. However, the closer together ω_1 and ω_2 are, the steeper the increase of damping at higher frequencies.

Hysteretic damping depends on the unloading and reloading rules ("hysteresis rules") adopted for the behaviour of the members after their yielding (see Section 4.10.1.7).

4.6.2.4 Numerical Integration of the Equation of Motion

Nonlinear response-history analysis entails numerical integration of the equation of motion:

$$\boldsymbol{M}\left(\ddot{\boldsymbol{U}} + \sum_j \alpha_{gj} \boldsymbol{e}_j\right) + \boldsymbol{C}\dot{\boldsymbol{U}} + \boldsymbol{F_R} = 0 \tag{4.21}$$

where **M** is the mass matrix (usually diagonal, with masses lumped at the nodes), $\boldsymbol{U}$ is the vector of nodal DoFs relative to the ground, a_{gj} are the acceleration time-histories in the three directions, with $j = 1, 2, 3$ denoting translation along directions X, Y, Z, **C** is the damping matrix, $\boldsymbol{F}_{\mathbf{R}}$ is the vector of resisting forces and vectors $\boldsymbol{e}_j$ have the value 1 at DoF j of each node and 0 at all others. Usually the time-step for the numerical integration, $\Delta t = t_{i+1} - t_i$, is chosen the same as the discretisation interval of the ground acceleration $a_{gj}(t)$ (typically 0.01 s), or one-half of it. Only implicit integration schemes, which are unconditionally stable for linear systems, are appropriate for such a long Δt. For the same stability performance the simpler and computationally efficient explicit schemes, like the central difference method, require a much shorter time-step. They are more appropriate for the analysis of fast transients or wave propagation problems, whose accurate description requires anyway a very short Δt.

Although the engine for the integration of the equation of motion is normally a black box for the user of nonlinear analysis software, the choice among numerical integration schemes and/or of their parameters is often left to him/her. As numerical instabilities in nonlinear response-history analyses are not rare (especially when the number of DoFs is very large and the analysis is carried out for many

[6] An eigenvalue analysis of the elastic structure should precede the nonlinear dynamic one anyway, for insight into the predominant features of the expected response.

ground motions), the user should pay special attention to the choice of numerical integration scheme.

Two widely used schemes, both unconditionally stable for linear systems, are (Chopra 2007):

- Newmark's average acceleration method (Newmark 1959), and
- Wilson's ϑ method.

In Newmark's average acceleration method $\ddot{\boldsymbol{U}}$ is taken constant within Δt : $\ddot{\boldsymbol{U}} = \ddot{\boldsymbol{U}}_{\mathrm{i}} + 0.5\Delta\ddot{\boldsymbol{U}}_{\mathrm{i}}$ giving velocity and displacement at $t_{\mathrm{i+1}}$: $\dot{\boldsymbol{U}}_{i+1} = \dot{\boldsymbol{U}}_i + (\ddot{\boldsymbol{U}}_i + 0.5\Delta\ddot{\boldsymbol{U}}_i)\Delta\boldsymbol{t}$, $\boldsymbol{U}_{i+1} = \boldsymbol{U}_i + (\dot{\boldsymbol{U}}_i + 0.5(\ddot{\boldsymbol{U}}_i + 0.5\Delta\dot{\boldsymbol{U}}_i)\Delta\boldsymbol{t})\Delta\boldsymbol{t}$. Substituting in the incremental equation of motion between t_{i} and $t_{\mathrm{i+1}}$, one obtains for $\Delta\boldsymbol{U}_{\mathrm{i}} = \boldsymbol{U}_{\mathrm{i+1}} - \boldsymbol{U}_{\mathrm{i}}$:

$$\mathbf{K}_{\mathrm{i}}^{*}\Delta\boldsymbol{U}_{\mathrm{i}} = \Delta\boldsymbol{F}_{\mathrm{i}}^{*} \tag{4.22}$$

with:

$$\boldsymbol{K}_i^{*} = \boldsymbol{K}_i + \frac{2}{\Delta\boldsymbol{t}}\left(\boldsymbol{C} + 2\frac{\boldsymbol{M}}{\Delta\boldsymbol{t}}\right),\ \Delta\boldsymbol{F}_i^{*} = 2\left(\boldsymbol{C} + 2\frac{\boldsymbol{M}}{\Delta\boldsymbol{t}}\right)\dot{\boldsymbol{U}}_i + 2\boldsymbol{M}\ddot{\boldsymbol{U}}_i - \boldsymbol{M}\sum_j \Delta\alpha_{gj}\boldsymbol{e}_j \tag{4.23a}$$

where $\mathbf{K}_{\mathrm{i}}$ is the tangent stiffness matrix at time t_{i}. Equation (4.22) is solved with equilibrium iterations, until the unbalanced load vector (i.e., the difference between the generalised external nodal forces and the internal ones calculated from member deformations) becomes less than a specified tolerance. During iterations and after convergence $\boldsymbol{U}_{\mathrm{i+1}}$, $\dot{\boldsymbol{U}}_{i+1}$ and $\ddot{\boldsymbol{U}}_{\mathrm{i+1}}$ are computed (for use in the next step) by adding $\Delta\boldsymbol{U}_{\mathrm{i}}$, $\Delta\dot{\boldsymbol{U}}_i = 2(\Delta\boldsymbol{U}_i/\Delta\boldsymbol{t} - \dot{\boldsymbol{U}}_i)$, $\Delta\ddot{\boldsymbol{U}}_{i+1} = 2\left(2\left(\Delta\boldsymbol{U}_i/\Delta\boldsymbol{t} - \dot{\boldsymbol{U}}_i\right)/\Delta\boldsymbol{t} - \ddot{\boldsymbol{U}}_i\right)$ to $\boldsymbol{U}_{\mathrm{i}}$, $\dot{\boldsymbol{U}}_i$ and $\ddot{\boldsymbol{U}}_{\mathrm{i}}$, respectively.

In Wilson's ϑ-method the nodal acceleration, $\Delta\ddot{\boldsymbol{U}} = \ddot{\boldsymbol{U}} - \ddot{\boldsymbol{U}}_{\mathrm{i+1}}$ and the input accelerations, $\Delta a_{\mathrm{gj}}(t)$ are taken linear functions of $t - t_{\mathrm{i}}$ up to time $t_{\mathrm{i}} + \vartheta\Delta t > t_{\mathrm{i+1}}$ (with $\vartheta > 1$). Then $\mathbf{K}_{\mathrm{i}}{}^{*}$ and $\delta\boldsymbol{F}_{\mathrm{i}}{}^{*}$ (which refers to $\delta\boldsymbol{U}_{\mathrm{i}}$, from t_{i} to $t_{\mathrm{i}} + \vartheta\Delta t$) become:

$$\begin{aligned}
&\boldsymbol{K}_i^{*} = \boldsymbol{K}_i + \frac{3}{\vartheta\Delta\boldsymbol{t}}\left(\boldsymbol{C} + 2\frac{\boldsymbol{M}}{\vartheta\Delta\boldsymbol{t}}\right),\\
&\delta\boldsymbol{F}_i^{*} = 3\left(\boldsymbol{C} + 2\frac{\boldsymbol{M}}{\vartheta\Delta\boldsymbol{t}}\right)\dot{\boldsymbol{U}}_i + \left(3\boldsymbol{M} + \frac{\vartheta\Delta\boldsymbol{t}}{2}\boldsymbol{C}\right)\ddot{\boldsymbol{U}}_i - \vartheta\boldsymbol{M}\sum_j \Delta\ddot{\boldsymbol{u}}_{gj}\alpha_j
\end{aligned} \tag{4.23b}$$

After solving $\mathbf{K}_{\mathrm{i}}{}^{*}\delta\boldsymbol{U}_{\mathrm{i}} = \delta\boldsymbol{F}_{\mathrm{i}}{}^{*}$ for $\delta\boldsymbol{U}_{\mathrm{i}}$, the expression for $\delta\boldsymbol{U}_{\mathrm{i}}$ in terms of $\delta\ddot{\boldsymbol{U}}_{\mathrm{i}}$ is solved for $\delta\ddot{\boldsymbol{U}}_i = 6(\delta\boldsymbol{U}_i/\vartheta\Delta\boldsymbol{t} - \dot{\boldsymbol{U}})/\vartheta\Delta\boldsymbol{t} - 3\ddot{\boldsymbol{U}}_i$, giving $\Delta\ddot{\boldsymbol{U}}_{\mathrm{i}} = \delta\ddot{\boldsymbol{U}}_{\mathrm{i}}/\vartheta$, and then $\Delta\dot{\boldsymbol{U}}_i = (\ddot{\boldsymbol{U}}_i + 0.5\Delta\ddot{\boldsymbol{U}}_i)\Delta t$, $\Delta\boldsymbol{U}_i = (\dot{\boldsymbol{U}}_i + 0.5(\ddot{\boldsymbol{U}}_i + \Delta\ddot{\boldsymbol{U}}_i/3)\Delta\boldsymbol{t})\Delta\boldsymbol{t}$, to be used to compute $\boldsymbol{U}_{\mathrm{i+1}}$, $\dot{\boldsymbol{U}}_{i+1}$, $\ddot{\boldsymbol{U}}_{\mathrm{i+1}}$.

Wilson's method introduces numerical damping which eliminates spurious high frequency response. For $\vartheta \geq 1.37$ it is unconditionally stable for linear systems and for $\vartheta = 1.42$ it gives optimal accuracy for them.

4.6.3 Concluding Remarks on the Nonlinear Analysis Methods

Thanks to its simplicity and intuitiveness and the wide availability of reliable and user-friendly analysis software, the standard form of pushover analysis, as described in Sections 4.6.1.2, 4.6.1.3 and 4.6.1.4 and in Fajfar (2000) (i.e., without the "adaptive" options for the lateral load pattern or higher mode and torsional effects, not even as highlighted in Sections 4.6.1.5 and 4.6.1.6), has become the workhorse of practical nonlinear seismic response analysis. It should be kept in mind, though, that it has been developed for 2D analysis under a single horizontal component of the seismic action and applies under such conditions alone, and even then only when the effects of higher modes are unimportant. This restricts its application to height-wise regular low-rise buildings, almost fully symmetric about an axis parallel to the seismic action component considered. The ways proposed to take into account 3D and torsional effects or higher modes, e.g., according to Sections 4.6.1.5 and 4.6.1.6, respectively, have not been sufficiently validated so far and are not widely accepted yet. The same applies for the concurrent application of both horizontal components of the seismic action (see last paragraph of Section 4.7.1). Last, but not least, there is certain ambiguity in the determination of the seismic demand. The approach in Section 4.6.1.3, Eqs. (4.18), is just one way to determine the "target displacement" for given elastic spectrum. There other approaches that may yield very different answers.

Unlike the static method of nonlinear analysis, the dynamic one does not require approximate a-priori determination of the global nonlinear seismic demand (like the "target displacement" of pushover analysis). Global displacement demands are determined in the course of the analysis of the response and are free of ambiguities, such as that about the "target displacement" in pushover analysis. Torsional, 3D and higher mode effects are fully accounted for, as well as concurrent application of two or three seismic action components. Note, also, that, unlike the modal response spectrum analysis, which provides only (statistically) best estimates of the peak response (via the SRSS or CQC rules), peak response quantities determined via nonlinear dynamic analysis are exact, even under concurrent seismic action components (within, of course, the limits of nonlinear modelling and of its capability to represent well the structure). Last, but not least, nonlinear dynamic analysis provides estimates not only of peak deformations, which are important for the overall safety and integrity of the structure, but of residual ones as well, which are the most meaningful measure of damage and, hence, very important for performance-based design or assessment.

Limitations of nonlinear dynamic analysis are:

- its sophistication and lack of familiarity among practitioners;
- the lack of simple and numerically stable, yet fairly accurate, models for vertical members in 3D analysis (see Section 4.10.1.8); and,
- certain sensitivity of the outcome to the choice of input ground motions, which is at the absolute discretion of the engineer.

The second drawback plagues static and dynamic nonlinear analysis alike (only that static nonlinear analysis does not apply well under 3D conditions, anyway). However, continuous progress in the state of the art and practice will reduce with time the importance of this and of the first drawback. The third limitation often raises doubts about the outcome of nonlinear dynamic analysis. It is possible (although not very likely, unless there is intention) to arrive at one conclusion using one ensemble of input motions meeting the requirements set out by codes and standards (see Section 4.6.2.2) and to another with a different set of equally legitimate motions. Standardisation of motions to resolve this question is too rigid a straitjacket, running, among others, against the continuous evolution of scientific knowledge and information on ground motion.

Despite its current limitations, nonlinear dynamic analysis is bound to become in the long run the technique of choice for practical nonlinear analysis, eclipsing the static version, which may end up being remembered as just an interlude that paved the way of nonlinear dynamic analysis into everyday practice.

4.7 Combination of the Maximum Effects of the Individual Seismic Action Components

4.7.1 The Two Options: The SRSS and the Linear Approximation

The two horizontal components of the seismic action, as well as the vertical component (when taken into account), are considered to act concurrently on the structure.

In planwise regular buildings with completely independent lateral-force-resisting systems along two orthogonal horizontal directions, the seismic action component in each one of these directions does not produce (significant) seismic action effects in the lateral-force-resisting systems of the orthogonal direction. For this reason, if in such buildings the independent lateral-force-resisting systems in the two horizontal directions consist solely of walls, Eurocode 8 (CEN 2004a) does not require combining the effects of the two horizontal components of the seismic action.

Simultaneous occurrence of more than one component can be handled rigourously only in time-history analysis (which is normally nonlinear). Such an analysis is carried out with the two horizontal components (and the vertical one, if taken into account) acting simultaneously. All other methods of analysis (i.e., the two linear approaches and nonlinear static analysis) give only estimates of the peak value of seismic action effects during the response to a single component. These estimates are denoted here as E_X and E_Y for the two horizontal components (considered to include also the effect of the associated accidental eccentricities, see Section 4.8) and E_Z for the vertical component. The peak values of the seismic action effects do not take place simultaneously. So, a combination of the type: $E = E_X + E_Y + E_Z$ is overly conservative for the expected value of the peak seismic action effect, E, under

three concurrent components. Design codes adopt more representative, probability-based combination rules for the estimation of E.

The reference rule for the combination of the peak values of seismic action effects, E_X, E_Y, E_Z, computed for separate action of the individual components is the SRSS rule in (Smebby and Der Kiureghian 1985):

$$E = \pm\sqrt{E_X^2 + E_Y^2 + E_Z^2} \tag{4.24}$$

If E_X, E_Y, E_Z are computed via the modal response spectrum method by combining modal contributions to each one of them via the CQC rule, Eq. (4.11), and, besides, the seismic action components in directions X, Y, Z are statistically independent, the outcome of Eq. (4.24) in an elastic structure is indeed the expected value of the peak seismic action effect, E, under concurrent seismic action components. Under these conditions, the result from Eq. (4.24) is also independent of the choice of horizontal directions X and Y. In other words, if a single modal response spectrum analysis is carried out covering all three components, X, Y, Z, at the same time and modal contributions for each component are combined via the CQC rule, Eq. (4.24) gives the expected value of the peak elastic seismic action effect, E, for all members of the structure, no matter the choice of directions X and Y. In this simple way Eq. (4.24) automatically fulfils an – at first sight – onerous requirement of Eurocode 8 for buildings with resisting elements not in two perpendicular directions (hence with no obvious choice for the two directions X and Y as main or principal ones): to apply the two horizontal components along all relevant horizontal directions, X, and the orthogonal direction, Y.

Eurocode 8 (CEN 2004a) adopts the combination rule of Eq. (4.24) as the reference, not only under the conditions for which it has been developed as an exact rule (namely for modal response spectrum analysis with modal contributions combined via the CQC rule), but also for linear static analysis (the lateral force method of Section 4.3 for the horizontal components and the method in Section 4.5.2 for the vertical component, if considered), modal response spectrum analysis with modal contributions combined via the SRSS rule, or even pushover analysis.

US codes (BSSC 2003, SEAOC 1999) have opted for the linear superposition rule:

$$E = \pm\{E_X + \lambda E_Y + \lambda E_Z\} \tag{4.25a}$$

$$E = \pm\{\lambda E_X + E_Y + \lambda E_Z\} \tag{4.25b}$$

$$E = \pm\{\lambda E_X + \lambda E_Y + E_Z\} \tag{4.25c}$$

A value $\lambda \approx 0.275$ provides the best average agreement with the result of Eq. (4.24) in the range of possible positive values of E_X, E_Y, E_Z. This optimal value has been rounded to $\lambda = 0.3$ in BSSC (2003) and SEAOC (1999). Equations (4.25)

may underestimate the result of Eq. (4.24) by less than 9% (when E_X, E_Y, E_Z are about equal) and may overestimate it by not more than 8% (when two of the three seismic action effects are an order of magnitude less than the third).

Eurocode 8 (CEN 2004a) accepts Eq. (4.25) with $\lambda = 0.3$ as alternative to the reference rule of Eq. (4.24).

If dimensioning is based on a single, one-component stress resultant, as, e.g., for beams in bending or shear, the outcome of Eq. (4.24), or the maximum value among the three alternatives in Eq. (4.25) should be added to, or subtracted from, the action effect of the gravity loads which are concurrent with the design seismic action. Then Eqs. (4.24) and (4.25) give approximately the same design.

Equations (4.24) and (4.25) can be applied also in nonlinear static (pushover) analysis, but only to combine peak displacement and deformation results due to the two horizontal components (the vertical component is irrelevant in that case). Peak internal forces may be combined in the same way only if they are still in the elastic range of the corresponding force-deformation relation. Otherwise, this relation should be used to determine the peak internal forces due to the two horizontal components from the corresponding peak deformation estimated through Eq. (4.24) or (4.25).

4.7.2 Combination of the Effects of the Seismic Action Components in Dimensioning for Vectorial Action Effects

Often dimensioning of a member section or region is carried out for two or three concurrent stress-resultants. Vertical members, for instance, are dimensioned for uniaxial or biaxial bending with axial force and for uniaxial shear with axial force (possibly depending also on the bending moment through the moment-to-shear ratio). It is convenient to consider the seismic action effects that enter such dimensioning as arranged in a vector (array) of dimension 3 for biaxial bending with axial force, 2 for shear with axial force or uniaxial bending with axial force, etc. One of the stress-resultants in that vector should be chosen as the main one, with the others considered as accompanying. For instance, when dimensioning in shear, the shear force may be the main stress-resultant and the axial force and the bending moment the accompanying ones. For uniaxial bending with axial force, the main component is always the moment. In columns under biaxial bending with axial force, the main component is one of the two components of bending moment, chosen as follows: the bending moments are normalised to a measure of the section's moment resistance so that they become independent of it size (e.g., to $A_c h$ with A_c being the cross-sectional area and h its depth for the bending moment considered); then the bending moment with the largest normalised value is the main component.

In dimensioning for multi-component action effects the application of Eqs. (4.24) and Eq. (4.25) may not be so straightforward and may lead to markedly different designs, depending on how the issues of signs and of simultaneity of peak values of

different stress-resultants are addressed. The following sections elaborate different cases and options for the application of Eqs. (4.24) or (4.25) in that case. The implications of the different options are exemplified at the end of each section for a column with centroidal axes y and z parallel to the horizontal components of the seismic action, X and Y, assuming that these components excite exclusively the 1st translational mode in each direction. To eliminate the effect of differences due to the analysis method and focus on the combination rule, it is also assumed that any analysis method produces the same values for the action effects and that we have nearly uniaxial bending, i.e.: $E_X = [M_{y,X}, M_{z,X}, N_X]^T$ with $M_{y,X} >> M_{z,X}$, $E_Y = [M_{y,Y}, M_{z,Y}, N_Y]^T$ with $M_{y,Y} << M_{z,Y}$. The vertical effect of the component of the seismic action is neglected in this illustration: $E_Z \approx [0, 0, 0]^T$.

4.7.2.1 The Linear Approximation with Linear Static Analysis

In each one of the three alternatives of Eq. (4.25), e.g. in $E_X + \lambda E_Y + \lambda E_Z$ for Eq. (4.25a), the seismic action components Y and Z are taken with a sense of action (positive or negative) such that, when component X acts in the positive sense, the contributions of λE_Y and λE_Z to the main component in the vector have the same sign as that of E_X. The signs of the three terms E_X, λE_Y, λE_Z in the sum $E_X + \lambda E_Y + \lambda E_Z$ for the accompanying components (elements of the vector) are controlled by the sense (positive or negative) of the corresponding component, X, Y, or Z, of the seismic action, as this sense is determined from the sign of E_X in the main component of the vector of seismic action effects. As a result, the vector of seismic action effects for $E_X + \lambda E_Y + \lambda E_Z$ assumes only two equal and opposite values. The same applies for Eqs. (4.25b) and (4.25c).

If the main component is the same in all three multi-component action effect vectors of the three versions of Eq. (4.25) (e.g., in dimensioning for shear with axial force and bending moment, or for uniaxial bending with axial force), then the vector to be used as E is normally the one of the three with the largest (absolute) value of the main component. So, there are just two cases for E. If the main component has about equally large values in two of the vectors, both of them are considered as potentially critical and we should consider $2 \times 2 = 4$ cases for E. If it has about equally large values in all three vectors, there are $2 \times 3 = 6$ cases for E.

If the main component is not the same in all three vectors of the three alternatives in Eq. (4.25) (e.g. in biaxial bending with axial force), then the two vectors where each of these two different main components clearly assumes its largest (absolute) value should be considered as potentially critical. Then we have $2 \times 2 = 4$ cases for E. If the choice is not clear, all three vectors of the three alternatives in Eq. (4.25) are potentially critical and there are $2 \times 3 = 6$ cases for E. If in a single one of the three vectors both of the two main components are clearly (absolutely) larger than in the two other vectors, that vector is the single possible choice for E and just two different cases are considered for E.

In the example case of the column, such an application of Eq. (4.25) gives the following four vectors $\boldsymbol{E}$:

$$\pm\,[M_{y,X} + \text{sign}(M_{y,X}M_{y,Y})\lambda M_{y,Y},\quad M_{z,X} + \text{sign}(M_{y,X}M_{y,Y})\lambda M_{z,Y},$$
$$N_X + \text{sign}(M_{y,X}M_{y,Y})\lambda N_Y]^T,$$

$$\pm\,[M_{y,Y} + \text{sign}(M_{z,X}M_{z,Y})\lambda M_{y,X},\quad M_{z,Y} + \text{sign}(M_{z,X}M_{z,Y})\lambda M_{z,X},$$
$$N_Y + \text{sign}(M_{z,X}M_{z,Y})\lambda N_X]^T,$$

where "sign($M_{y,X}M_{y,Y}$)" is the sign of the product of $M_{y,X}$ and $M_{y,Y}$ (similarly for "sign($M_{z,X}M_{z,Y}$)").

4.7.2.2 The Linear Approximation with Modal Response Spectrum Analysis

Modal response spectrum analysis gives positive peak values for all seismic action effects, without any correspondence between the peak value of a seismic action stress resultant and the concurrent values of the other two. The only possible way to combine these stress resultants is to consider their peak values as concurrent and combine them with the same sign in each one of the three alternatives of Eq. (4.25) – because that's how Eq. (4.25) is an approximation to Eq. (4.24) for $\lambda = 0.3$. This gives $3 \times 2^3 = 24$ combinations of signs for the three stress resultants in the vector $\boldsymbol{E}$, namely the following, for biaxial bending with normal force:

$$M_y = \pm\left(|M_{y,X}| + \lambda|M_{y,Y}| + \lambda|M_{y,Z}|\right),\ M_z = \pm\left(|M_{z,X}| + \lambda|M_{z,Y}| + \lambda|M_{z,Z}|\right),$$
$$N = \pm\left(|N_X| + \lambda|N_Y| + \lambda|N_Z|\right) \tag{4.26a}$$

$$M_y = \pm\left(\lambda|M_{y,X}| + |M_{y,Y}| + \lambda|M_{y,Z}|\right),\ M_z = \pm\left(\lambda|M_{z,X}| + |M_{z,Y}| + \lambda|M_{z,Z}|\right),$$
$$N = \pm\left(\lambda|N_X| + |N_Y| + \lambda|N_Z|\right) \tag{4.26b}$$

$$M_y = \pm\left(\lambda|M_{y,X}| + \lambda|M_{y,Y}| + |M_{y,Z}|\right),\ M_z = \pm\left(\lambda|M_{z,X}| + \lambda|M_{z,Y}| + |M_{z,Z}|\right),$$
$$N = \pm\left(\lambda|N_X| + \lambda|N_Y| + |N_Z|\right) \tag{4.26c}$$

For the example of the column this way of applying Eq. (4.25) gives the following 16 vectors $\boldsymbol{E}$:

$$[\pm(|M_{y,X}| + \lambda|M_{y,Y}|),\quad \pm(|M_{z,X}| + \lambda|M_{z,Y}|),\quad \pm(|N_X| + \lambda|N_Y|)]^T,$$
$$[\pm(|M_{y,Y}| + \lambda|M_{y,X}|),\quad \pm(|M_{z,Y}| + \lambda|M_{z,X}|),\quad \pm(|N_Y| + \lambda|N_X|)]^T.$$

The main difference with the approach in Section 4.7.2.1 is that we lose the correspondence between the signs of different stress resultants, notably of bending moments and axial forces in the same element or of the axial forces in different elements (see Sections 5.7.3.5 and 5.7.4.1 for the implications). This may be a more serious handicap of Eq. (4.25) when used with modal response spectrum analysis,

than the large number of different vectors taken in the dimensioning in order to consider all possible combinations of signs.

4.7.2.3 SRSS Rule with Modal Response Spectrum Analysis

When applied for the calculation of each stress-resultant in the vector of seismic action effects for the dimensioning of a member section or region, Eq. (4.24) gives the expected value of the peak stress-resultant during the response to the (three) simultaneous components of the seismic action. The peak values of the individual stress resultants do not take place concurrently. If it is assumed they do, the design is safe-sided but probably too conservative.

Eurocode 8 allows using more accurate rules for the estimation of the most probable value of the seismic action effect that takes place concurrently with the expected value of the maximum of each one of the two (or more) stress-resultants that enter the dimensioning of a member section or region. A rule of this type is described in this section, with reference to biaxial bending with moments M_y and M_z (defined with respect to the local axes y and z of the cross-section) and axial force N. This is a fairly general case, not only as far as the dimension of the vector of stress-resultants is concerned, but also in that either M_y or M_z may be the "main component" of this vector, depending on their (normalised) magnitude. Uniaxial bending with axial force, M_y-N, and uniaxial shear, V_y, with axial force and bending moment, N and M_z, are special cases, with only one of the stress-resultants (V_y and M_z, respectively) being the "main component" of the vector.

Equation (4.24), should be applied at the lowest possible level at which the verification is carried out. For biaxial bending with axial force, this means to the strains of the extreme concrete fibres in the section. This is not feasible, as seismic action effects are calculated through modal response spectrum analysis separately from the nonlinear plane-section analysis. So, extreme combinations of M_y, M_z and N should be sought (rather than extreme but separate values of M_y, M_z, N) which lead, in good approximation, to the SRSS result at the final, e.g., fibre strain, level. It has been shown in Gupta and Singh (1977) that, if the seismic action effect of interest is a scalar which is a linear function of M_y, M_z and N, then the M_y-M_z-N combinations that lead to the expected peak value of this effect under the (three) concurrent components of the seismic action satisfy the condition:

$$\mathbf{E}^{\mathbf{T}}\mathbf{C}^{-1}\,\mathbf{E} = \mathbf{I} \tag{4.27}$$

In Eq. (4.27) $\mathbf{I}$ is the identity matrix, $\boldsymbol{E}$ is the vector $[M_y\ M_z\ N\ ]^T$ and $\mathbf{C}$ is its covariance matrix:

$$\mathbf{C} = \begin{bmatrix} M_{y,\max}^2 & \mathrm{cov}(M_y, M_z) & \mathrm{cov}(M_y, N) \\ & M_{z,\max}^2 & \mathrm{cov}(M_z, N) \\ symmetric & & N_{\max}^2 \end{bmatrix} \tag{4.28}$$

with:

$$M_{y,\max}^2 = \sum_i \sum_j \rho_{ij}(M_{y,iX}M_{y,jX} + M_{y,iY}M_{y,jY} + M_{y,iZ}M_{y,jZ}) = M_{y,X}^2 + M_{y,Y}^2 + M_{y,Z}^2 \tag{4.29}$$

$$M_{z,\max}^2 = \sum_i \sum_j \rho_{ij}(M_{z,iX}M_{z,jX} + M_{z,iY}M_{z,jY} + M_{z,iZ}M_{z,jZ}) = M_{z,X}^2 + M_{z,Y}^2 + M_{z,Z}^2 \tag{4.30}$$

$$N_{\max}^2 = \sum_i \sum_j \rho_{ij}(N_{iX}N_{jX} + N_{iY}N_{jY} + N_{iZ}N_{jZ}) = N_X^2 + N_Y^2 + N_Z^2 \tag{4.31}$$

$$\operatorname{cov}(M_y, M_z) = \sum_i \sum_j \rho_{ij}(M_{y,iX}M_{z,jX} + M_{y,iY}M_{z,jY} + M_{y,iZ}M_{z,jZ}) \tag{4.32}$$

$$\operatorname{cov}(M_y, N) = \sum_i \sum_j \rho_{ij}(M_{y,iX}N_{jX} + M_{y,iY}N_{jY} + M_{y,iZ}N_{jZ}) \tag{4.33}$$

$$\operatorname{cov}(M_z, N) = \sum_i \sum_j \rho_{ij}(N_{iX}M_{z,jX} + N_{iY}M_{z,jY} + N_{iZ}M_{z,jZ}) \tag{4.34}$$

In Eqs. (4.29), (4.30), (4.31), (4.32), (4.33) and (4.34) X, Y or Z index the effects due to the seismic action component X, Y, or Z, respectively, i and j index normal modes, while ρ_{ij} is their correlation coefficient, as given, e.g. from Eqs. (4.9). Modal seismic effects $M_{y,iX}$, etc., are computed as the product of the participation factor of mode i for the seismic action component in direction X, times the stress resultant M_y in mode i from the eigenvector of the mode scaled to the corresponding spectral displacement. $M_{y,\max}$, $M_{z,\max}$ and $N_{\max}$ from Eqs. (4.29), (4.30) and (4.31) are the expected values of the peak stress resultants under the three-component seismic action according to Eq. (4.24).

Values of the vector $[M_y\ M_z\ N]^T$ satisfying Eq. (4.27) lie on an ellipsoidal surface in the space M_y-M_z-N. It is usually sufficient to consider only the six points on this surface corresponding to algebraically maximum and minimum values of one of the stress resultants, M_y, M_z, N, and to the corresponding concurrent values of the two others. With $M_{y,\max}$, $M_{z,\max}$ and $N_{\max}$ taken positive, these six triplets are:

$$\pm\left(M_{y,\max} = \sqrt{M_{y,X}^2 + M_{y,Y}^2 + M_{y,Z}^2},\ \frac{\operatorname{cov}(M_y, M_z)}{M_{y,\max}},\ \frac{\operatorname{cov}(M_y, N)}{M_{y,\max}}\right) \tag{4.35}$$

$$\pm\left(\frac{\operatorname{cov}(M_y, M_z)}{M_{z,\max}},\ M_{z,\max} = \sqrt{M_{z,X}^2 + M_{z,Y}^2 + M_{z,Y}^2},\ \frac{\operatorname{cov}(M_z, N)}{M_{z,\max}}\right) \tag{4.36}$$

$$\pm\left(\frac{\operatorname{cov}(M_y, N)}{N_{\max}},\ \frac{\operatorname{cov}(M_z, N)}{N_{\max}},\ N_{\max} = \sqrt{N_X^2 + N_Y^2 + N_Z^2}\right) \tag{4.37}$$

As $\operatorname{cov}(M_y, M_z)$, $\operatorname{cov}(M_y, N)$, and $\operatorname{cov}(M_z, N)$ have signs, the two stress resultants which take place concurrently with the maximum of the third one also have signs.

If:

- only the two bending moments, M_y and M_z, are taken as main components of $[M_y\ M_z\ N]^T$, and
- only the cases when the absolute value of a main component is maximum are of interest,

then only the four different values from Eqs. (4.35) and (4.36) need to be considered as the values of E from Eq. (4.24). This is the case in the column example, where this way of applying Eq. (4.24) gives the following four vectors $\boldsymbol{E}$:

$$\begin{aligned}
&\pm [\sqrt{(M_{y,X}^2 + M_{y,Y}^2)}, (M_{y,X}M_{z,X} + M_{y,Y}M_{z,Y})/\sqrt{(M_{y,X}^2 + M_{y,Y}^2)},\\
&\quad (M_{y,X}N_X + M_{y,Y}N_Y)/\sqrt{(M_{y,X}^2 + M_{y,Y}^2)}]^T\\
&\pm [(M_{y,X}M_{z,X} + M_{y,Y}M_{z,Y})/\sqrt{(M_{z,X}^2 + M_{z,Y}^2)}, \sqrt{(M_{z,X}^2 + M_{z,Y}^2)},\\
&\quad (M_{z,X}N_X + M_{z,Y}N_Y)/\sqrt{(M_{z,X}^2 + M_{z,Y}^2)}]^T
\end{aligned}$$

4.7.2.4 SRSS Rule with Linear Static Analysis

Calculation of E_X, E_Y, E_Z by linear static analysis corresponds to taking a single normal mode for each component of the seismic action, i.e. to using in Eqs. (4.29), (4.30), (4.31), (4.32), (4.33) and (4.34) i=1, j=2, ρ_{11}=1, ρ_{22}=1, ρ_{12}=0. Then Eqs. (4.35), (4.36) and (4.37) give the following six triplets (M_y, M_z, N):

$$\pm \left(M_{y,\max} = \sqrt{M_{y,X}^2 + M_{y,Z}^2 + M_{y,Z}^2},\ M_z = \frac{M_{y,X}M_{z,X} + M_{y,Y}M_{z,Y} + M_{y,Z}M_{z,Z}}{M_{y,\max}},\ N = \frac{M_{y,X}N_X + M_{y,Y}N_Y + M_{y,Z}N_Z}{M_{y,\max}} \right) \tag{4.38}$$

$$\pm \left(M_y = \frac{M_{y,X}M_{z,X} + M_{y,Y}M_{z,Y} + M_{y,Z}M_{z,Z}}{M_{z,\max}},\ M_{z,\max} = \sqrt{M_{z,X}^2 + M_{z,,Y}^2 + M_{z,Y}^2},\ N = \frac{M_{z,X}N_X + M_{z,Y}N_Y + M_{z,Z}N_Z}{M_{z,\max}} \right) \tag{4.39}$$

$$\pm \left(M_y = \frac{M_{y,X}N_X + M_{y,Y}N_Y + M_{y,Z}N_Z}{N_{\max}},\ M_z = \frac{M_{z,X}N_X + M_{z,Y}N_Y + M_{z,Z}N_Z}{N_{\max}},\ N_{\max} = \sqrt{N_X^2 + N_Y^2 + N_Z^2} \right) \tag{4.40}$$

If only M_y and M_z are taken as main components and just the cases where the absolute value of a main component is maximum are of interest, only the four triplets from Eqs. (4.38), (4.39) will be considered as values of $\boldsymbol{E}$ from Eq. (4.24).

In the column example Section 4.7.2.4 gives the same result as 4.7.2.3, if there are no differences due to the analysis method.

4.7.2.5 Concluding Remarks

The different values of $\boldsymbol{E}$ from any one of the four approaches above should be superimposed to the vector of stress-resultants due to gravity loads considered concurrent with the design seismic action. This gives the vector of stress-resultants for dimensioning. Apart from any difference between the seismic effects from a modal response spectrum analysis or a linear static one, the four approaches in Sections 4.7.2.1, 4.7.2.2, 4.7.2.3 and 4.7.2.4 do not lead normally to very different designs. So, the criteria for selecting which one to apply should be their computational convenience and soundness from the theoretical point of view.

If a modal response spectrum analysis is used, application of Eq. (4.24) the way proposed in Section 4.7.2.3 (which also entails combining modal responses through the CQC rule) is the most sound and computationally convenient approach and leads to economic designs. For this method of analysis, the straightforward application of Eq. (4.25) according to Section 4.7.2.2 is less sound. Besides, it gives many more combinations of stress resultants for dimensioning, some of which are physically meaningless. So, it is computationally inconvenient and may lead to less economic designs.

If linear static analysis is used, application of Eq. (4.24) according to Section 4.7.2.4 is sound and computationally convenient and leads to economic designs. Application of Eq. (4.25) as proposed in Section 4.7.2.1 is a plausible, computationally convenient and economic alternative. It is also physically appealing, as it preserves the correspondence of signs of stress resultants and retains the notion of separate seismic action components, with $E_X + \lambda E_Y + \lambda E_Z$ considered as governed by the horizontal component in direction X, $\lambda E_X + E_Y + \lambda E_Z$ by that in Y and $\lambda E_X + \lambda E_Y + E_Z$ by the vertical component.

The combination of the seismic action effects of the different components according to Section 4.7.2.3 should be integrated in the modal response spectrum analysis. In all other cases these seismic action effects may also be combined after the analysis, just before their use for member dimensioning or verification. This is very convenient, as it can be done with a post-processing module, independently of the analysis software.

The – unfortunately not uncommon in practice – application of Eq. (4.24) to all stress resultants, taking the computed peak response estimates as simultaneous, is overly conservative. For the case of column biaxial bending with normal force addressed in Sections 4.7.2.1, 4.7.2.2, 4.7.2.3 and 4.7.2.4, this would give the following eight values of $\boldsymbol{E}$:

$$\left(\pm M_{y,\max} = \pm\sqrt{M_{y,X}^2 + M_{y,Z}^2 + M_{y,Z}^2}, \pm M_{z,\max} = \pm\sqrt{M_{z,X}^2 + M_{z,Y}^2 + M_{z,Y}^2},\right.$$
$$\left.\pm N_{\max} = \pm\sqrt{N_X^2 + N_Y^2 + N_Z^2}\right)$$

with the individual seismic action effects computed by either a linear static or a modal response spectrum analysis. Such an approach is irrational – despite its presumption of soundness – and leads to very uneconomic designs.

4.8 Analysis for Accidental Torsional Effects

4.8.1 Accidental Eccentricity

When the planwise distribution of stiffness or mass is asymmetric, the response to the horizontal components of the seismic action includes torsional-translational coupling. Analysis in 3D for the horizontal components takes this coupling into account in a satisfactory way, especially in modal response spectrum or nonlinear dynamic analysis.

Some seismic design codes attempt to take into account amplification or de-amplification of the static or "natural" eccentricity between the centres of mass and stiffness during the dynamic response (see Figs. 2.22, 4.14 and 4.19 for examples of this eccentricity). This is very inconvenient for the analysis, as normally the storey stiffness centre cannot be uniquely defined (see Section 2.1.5). Locating a conventionally defined storey stiffness centre is not worth the effort of the tedious additional analyses required to achieve the accuracy and sophistication consistent with a dynamic amplification of static eccentricities.

In a building with full planwise symmetry of stiffness and nominal masses the analysis for the horizontal components of the seismic action produces no torsional response at all. However, a conventional seismic response analysis cannot capture possible variations in the stiffness or mass distribution from the nominal one, or a possible torsional component of the ground motion about the vertical. Such effects may produce torsional response even for a nominally fully symmetric building. To ensure a minimum of torsional resistance and stiffness and limit the consequences of unforeseen torsional response, most seismic design codes introduce accidental torsional effects by shifting the masses with respect to their nominal positions by an "accidental eccentricity". Examples of factors for which the "accidental eccentricity" attempts to account are:

- A planwise distribution of any "imposed" ("live" loads) present at the instant the earthquake occurs that differs from the uniform one assumed in design.
- Infill walls – considered as nonstructural elements and neglected in design calculations – with a distribution in plan that does not follow that of the elements of the lateral-load-resisting system.
- A planwise distribution of the effective stiffness of structural members different from that of the nominal ones used in design (based on the geometry of the cross-section alone, no matter the reinforcement). Recall that in design of new buildings the analysis is based on nominal member rigidities, $(EI)_n$, taken for convenience as a fixed fraction of the rigidity of the gross uncracked section, $(EI)_c$, e.g. $(EI)_n =$

$0.5(EI)_c$ (see Section 4.9.2). As pointed out in Section 3.2.3.3, for given cross-sectional dimensions the effective member rigidity after cracking, e.g. the secant rigidity to yield-point, $(EI)_{eff}$, depends on the shear span ratio and axial stress of the member, as well as on the amount and layout of reinforcement. So, the actual distribution in plan of structural stiffness may significantly differ from the nominal one considered in design.

The "accidental eccentricity" of each horizontal seismic action component is specified in codes as a fraction of the dimension of the storey at right angles to that of the seismic action component. In most codes (CEN 2004a, BSSC 2003, SEAOC 1999) this fraction is one-twentieth (5%). Eurocode 8 doubles that fraction to one-tenth (10%), if the effects of the "accidental eccentricity" are taken into account in the simplified way of Section 4.8.4 on a separate 2D model for each horizontal component of the seismic action,[7] instead of a full 3D model. Moreover, if there are masonry infills with a moderately irregular and asymmetric distribution in plan,[8] the "accidental eccentricity" is doubled further in Eurocode 8 (i.e., to 10% of the storey orthogonal dimension in the baseline case, or 20% if accidental torsional effects are evaluated in a simplified way when using two separate 2D models).

The "accidental eccentricity" is taken in both the positive and the negative sense along any horizontal direction, but practically along the two orthogonal directions of the horizontal seismic action components. It is taken also in the same horizontal direction and in the same sense (positive or negative) for the whole building at a time, which is simple and safe-sided for the global seismic action effects (but not always for local ones).

In a dynamic analysis (modal response spectrum analysis or nonlinear dynamic), the masses may be shifted from their nominal location by the "accidental eccentricity". This produces four dynamic models in total, with different dynamic characteristics (natural periods and mode shapes) and entails using the envelope of the seismic action effects from the four analyses. This is at the expense not only of convenience and computational effort, but also of our understanding of the dynamic response. So, it is done only in the framework of nonlinear analysis (dynamic and often for static, as well) for the assessment of existing buildings, but very rarely in modal response spectrum analysis for design. Seismic design codes normally allow replacing the "accidental eccentricity" of the masses from their nominal positions, by an "accidental eccentricity" of the horizontal seismic components with respect to the nominal position of the masses. The effects of the "accidental eccentricity" are determined then through static approaches (see Section 4.8.2).

In SEAOC (1999) and BSSC (2003) as well – but only for "Seismic Design Category" C and above, as defined in Section 1.4.2.2 – the "accidental eccentricity"

[7]This is allowed in Eurocode 8 for structures regular in plan. Note than in a 2D model all nodes of a floor that may belong to different 2D frames have the same horizontal displacement, regardless of any static eccentricity between the floor centres of stiffness and mass.

[8]Strongly irregular arrangements, such as infills mainly along two adjacent faces of the building, cannot be taken into account in this simplified way, see Section 2.1.13.2.

of 5% of the perpendicular floor plan dimension is multiplied by the following factor at each floor level i, to take into account dynamic amplification:

$$A_{xi} = \left(\frac{\delta_{\max,i}}{0.6(\delta_{\max,i} + \delta_{\min,i})} \right)^2 \tag{4.41}$$

In Eq. (4.41) $\delta_{\max,i}$ and $\delta_{\min,i}$ are the maximum and minimum, over the plan, lateral displacements in the direction of the horizontal seismic action component in question, under the combination of this component and its accidental eccentricity, which is taken initially as 5% of the perpendicular floor plan dimension, but then multiplied by A_{xi}. The accidental eccentricity of each horizontal component should be taken both in the positive and in the negative sense, giving two values of A_{xi}. If the maximum of these two values is greater than 1.0 in at least one floor level i, the analysis should be repeated, using the corresponding value of A_i (but not greater than 3.0) as amplification factor of the accidental eccentricity at the corresponding level(s). Values of A_{xi} for this horizontal seismic direction and sense (sign) of the corresponding eccentricities are recomputed, the analyses repeated, etc., until convergence of all values of A_{xi} which are greater than 1.0. However, considering the semi-empirical nature of the amplification factor A_{xi} and the arbitrary choice of the initial accidental eccentricity value as 5% of the structure's plan dimension, the iterative calculation may not be worthy. A single cycle of analysis under the combination of this horizontal component and its accidental eccentricity at 5% of the perpendicular floor plan dimension would seem sufficient for the calculation of A_{xi}. Note that each sense of action of the accidental eccentricity, positive or negative, is in principle associated with different values of A_{xi}, and should normally be considered as a different load case, uniquely associated to the corresponding direction and sense of action of the horizontal seismic action component.

4.8.2 Estimation of the Effects of Accidental Eccentricity Through Linear Static Analysis

In linear static analysis the action effects of the "accidental eccentricity" alone of a horizontal seismic action component are computed through a linear static analysis of a 3D structural model under storey torques about the vertical axis, taken all with the same sign and equal to the storey lateral loads due to the horizontal component in question times its "accidental eccentricity" at the storey. The lateral loads are those of Eq. (4.8) in Section 4.3.3. In the context of linear static analysis this is equivalent to shifting the masses, and hence exact. By analogy, if the modal response spectrum method is used in the analysis for the horizontal seismic action components, the static storey torques may be computed as: (a) the storey "accidental eccentricity" times (b) the floor mass times (c) the floor response acceleration in the direction of the considered horizontal component of the seismic action, from the CQC combination of modal contributions to floor response accelerations. Eurocode

8 allows taking, instead, the storey torques as the storey lateral loads of the linear static analysis from Eq. (4.8) times the "accidental eccentricity" at the storey. This is computationally simpler, especially if in both horizontal directions the storey "accidental eccentricity" is constant at all levels (i.e., if all floors have the same plan dimensions). Then it suffices to carry out a single static analysis for storey torques proportional to the storey lateral loads from Eq. (4.8) for $V_b = 1.0$. The effects of the "accidental eccentricity" of each horizontal seismic action component can be obtained then by multiplying the results of this single analysis by the base shear V_b from Eq. (4.6) corresponding to the 1st mode period in the horizontal direction of interest and by the (constant at all floors) eccentricity of this component of the seismic action.

If the floors are taken as rigid diaphragms, the total storey torque may be applied to a single floor node of the storey (the "master node"). If a diaphragm may not be considered as rigid and its in-plane flexibility is taken into account in the 3D structural model, it is more meaningful to replace the storey torque with nodal torques at each nodal mass m_i, equal to the product of the "accidental eccentricity" and that mass's lateral force from Eq. (4.8).

Action effects of "accidental eccentricities" produced from static analysis have signs. As the "accidental eccentricity" is meant to be taken in both the positive and the negative sense along the two directions of the horizontal seismic action components in order to produce the most unfavourable value for the seismic action effect of interest, the action effect of the accidental eccentricity of horizontal component X, symbolised here as e_X, is taken to have the same sign as that due to the horizontal component X itself and superimposed to it. The outcome is the total seismic action effect of horizontal component X, symbolised here as E_X. Note that it is these latter total 1st-order action effects that should be multiplied by $1/(1–\theta_i)$ to include a-posteriori P-Δ effects according to the approximate procedure of Section 4.9.7. The exact approaches of the three last paragraphs of Section 4.9.7 for 2nd-order effects apply to both analyses: for the horizontal component X itself and for its accidental eccentricity, if carried out separately. When the "accidental eccentricities" are modelled by shifting the masses from their nominal location, as often done in nonlinear dynamic analysis, 2nd-order effects are taken into account once and for all.

4.8.3 Combination of Accidental Eccentricity Effects Due to the Two Horizontal Components of the Seismic Action for Linear Analysis

An accidental eccentricity is associated to each direction of application of the translational component, X or Y, of the seismic action. The total action effect of horizontal component X, including the effect of accidental eccentricity e_X, is considered as E_X. It is this total effect that is combined according to Section 4.7 with the total action effect of horizontal component Y, E_Y, (that includes the effect of accidental eccentricity e_Y) and sometimes with the action effect of the vertical component Z.

If the action effects of the components X, Y, Z are combined linearly through Eq. (4.25) (cf. Sections 4.7.2.1 and 4.7.2.2), the action effects of the accidental eccentricity e_X of component X and those of the translational component X itself are added with the same sign. Similarly for horizontal component Y and e_Y. It is computationally straightforward to incorporate the effect of e_X or e_Y, into the total effect of horizontal component X or Y, respectively, as the combination of seismic action effects anyway takes place after the analysis for the individual seismic action components.

When action effects are computed through separate analyses for each components X, Y or Z and combined via the rigorous approach of Eq. (4.24) as in Sections 4.7.2.3 and 4.7.2.4, those due to the accidental eccentricity e_X from linear static analysis may be added (with the same sign) to the action effects of the horizontal component X, no matter whether the latter is computed by linear static or modal response spectrum analysis. Similarly for component Y and e_Y. These individual "sums" are considered as E_X and E_Y, respectively, and enter as such in Eq. (4.24). When, by contrast, the action effects due to the translational components X and Y are computed via a single modal response spectrum analysis for all three components, with an extension of the CQC combination module to include expressions like Eqs. (4.29)–(4.37) in Section 4.7.2.3, it is computationally inconvenient to include the effects of e_X or e_Y in the total effect of horizontal components X or Y through such an "addition". Moreover, such an "addition" destroys the beauty and rigour of the approach of Section 4.7.2.3 for the combination of the three seismic action components in a single step. A procedure like the following would be more consistent with the rigorous approach of Eq. (4.24):

1. Combine separately, via Eq. (4.24), and in a single-step the action effects of the translational components X, Y, (Z) from modal response spectrum analysis.
2. Carry out one static analysis to determine the effect of accidental eccentricity e_X, and another one to determine that of e_Y and combine their results using Eq. (4.24). It is convenient to substitute for these analyses a single one, with storey torques equal to the SRSS of those representing e_X and e_Y at that storey.
3. Add together the (positive) outcomes of the two calculations 1 and 2.

As a matter of fact, the outcome of this procedure is generally more safe-sided than the option given at the beginning of the previous paragraph, where the action effects of the accidental eccentricity of each component are "added" to those due to the horizontal component itself, and the two sums (for X and Y) combined via Eq. (4.24) in the end.

4.8.4 Simplified Estimation of Accidental Eccentricity Effects in Eurocode 8 for Planwise Symmetric Lateral Stiffness and Mass

In the spirit of simplification associated with linear static analysis, Eurocode 8 allows it to account for the effects of "accidental eccentricities" in buildings with

planwise symmetric distribution of lateral stiffness and mass in a way simpler than that in Sections 4.8.2 and 4.8.3. This may be done by amplifying the results of linear static analysis for each translational component of the seismic action by $(1 + 0.6x/L)$, where x is the distance of the member in question to the mass centre in plan and L is the plan dimension, both at right angles to the horizontal component of the seismic action. This factor is derived assuming that:

- torsional effects are fully resisted by the stiffness of the structural elements in the direction of the horizontal component in question, without any contribution from any element stiffness in the orthogonal horizontal direction; and
- the stiffness of the members resisting the torsional effects is uniformly distributed in plan.

As a matter of fact, the term $0.6/L$ is equal to the storey torque due to the "accidental eccentricity" of $0.05L$ acting on the storey seismic shear, V, divided by the moment of inertia of a uniform lateral stiffness, k_B, per unit floor area parallel to side B in plan, $k_B BL^3/12$, and further divided by the normalised storey shear, $V/(k_B BL)$. Normally there is also lateral stiffness, $k_L \approx k_B$, per unit floor area parallel to side L in plan and $k_L LB^3/12$ should be added to $k_B BL^3/12$ before it divides the storey torque $0.05LV$. The contribution of k_L is neglected and therefore the term $0.6x/L$ is safe-sided by an average factor of 2. If this additional conservatism is too high a price for the simplicity, the general approach of Sections 4.8.2 and 4.8.3 may always be used.

The general approach of Sections 4.8.2 and 4.8.3 can only be applied with a full 3D structural model. It does not apply if a separate 2D analysis is carried out for each horizontal component, as allowed by Eurocode 8 for buildings meeting the criteria in Sections 2.1.5 and 2.1.6 for regularity in plan. If such separate 2D analyses are made, the effects of the accidental eccentricity can only be estimated through the simplified approach of this section. As these analyses neglect any static eccentricity between the storey centres of mass and stiffness, the amplification factor of the simplified approach becomes in that case $(1+1.2x/L)$, to cover the effect of the neglected static eccentricity, no matter whether there is actually one.

4.8.5 Accidental Eccentricity in Nonlinear Analysis

In nonlinear dynamic analysis masses are shifted from their nominal location by the "accidental eccentricity". The shifting is in the same direction at all storeys. For analysis in 3D this gives four dynamic models to be subjected to each (in general bi-directional) input motion. If the analysis is carried out for unidirectional ground motions, masses are shifted only at right angles to the excitation and there are two models to be analysed for each ground motion. Although this sounds inconvenient and computationally demanding, it is consistent with the sophistication and complexity of nonlinear dynamic analysis.

The same approach should be followed for nonlinear static analysis, which is normally carried out separately for each horizontal component of the seismic action, giving two models to be analysed with the seismic action component applied in the positive and negative sense. The torsional effects due to each eccentrically acting horizontal component should then be calculated according to Section 4.6.1.5.

The envelope of seismic action effects from the two or four sets of analyses for unidirectional or bidirectional seismic action, respectively, is used in the design or assessment.

This approach cannot be followed unless a full 3D structural model is analysed. If a separate 2D model is used for each horizontal component of the seismic action, as allowed by Eurocode 8 for buildings meeting the criteria for regularity in plan (see Sections 2.1.5 and 2.1.6), the effects of the accidental eccentricity can only be estimated through the simplified approach described in the last paragraph of Section 4.8.4.

4.9 Modeling of Buildings for Linear Analysis

4.9.1 The Level of Discretisation

The selection of the appropriate mathematical model of the physical structure depends not only on the action(s) and the method of analysis, but also on the intended use of its results. The objective of a structural model for the purposes of seismic design or assessment is not to serve the analysis per se but the ultimate phase of member detailed design, assessment or retrofitting. The only purpose of modelling and analysis is to provide the data for that phase. Rules for practical dimensioning and detailing or assessment of members against cyclic inelastic deformations are sufficiently developed mainly – if not only – for prismatic members. Corresponding rules for 2D members are available only for special elements with a specific structural role, e.g. low-shear-ratio coupling beams in skew symmetric bending, interior or exterior beam-column joints, etc. Dimensioning or assessment of generic 2D concrete elements for strength can be done using Strut-and-Tie models, which are still developing and have not penetrated yet everyday practice. Moreover, rules for detailing for ductility elements dimensioned on the basis of the Strut-and-Tie approach are not well-developed yet. So, the structural model should employ mainly 3D beam elements.

According to codes the structural model for linear analysis should represent well the distribution of stiffness and mass. This may not be sufficient in design or assessment. The model and the discretisation of the structure should correspond closely to its layout in 3D, to provide the seismic action effects for the dimensioning and detailing or assessing members and sections. For instance, a stick model, with all members of a storey lumped into a single mathematical element connecting adjacent floors with only 3 DoFs per storey (for analysis in 3D) is insufficient. At the other extreme, a very detailed Finite Element (FE) discretisation, providing

very "accurate" predictions of elastic displacements and stresses at a point-by-point basis, may be practically useless. Reliable and almost equally accurate predictions of the "average" seismic action effects needed for member dimensioning or assessment, such as stress resultants or chord rotations at member ends, can be directly obtained from an appropriate space frame model of the structure. Moreover, certain fine effects captured by a detailed FE analysis, such as those of non-planar distribution of strains in the cross-section of deep members, or shear lag in members with composite cross-section, etc., lose their relevance during inelastic seismic response or are anyway neglected in ULS calculations and member verifications. Note also that the connectivity of:

- a 2D element or region modelled via 2D FEs, with
- 3D beam elements in the plane of the 2D FEs,

requires special treatment, as even in shell FEs the rotation DoFs about the normal to the shell surface do not possess stiffness and cannot be directly connected to 3D beam elements in the plane of the 2D FE.[9] For all these reasons, the analysis model appropriate for seismic design or assessment is a member-by-member type of model, where every beam, column or part of a wall between floors is represented as a 3D beam element, with the 3 translations and the 3 rotations at each node between such elements considered as DoFs. Masses may also be lumped at these nodes and associated in general with all six DoFs there. If the vertical component of the seismic action is considered, lumped masses should be included at intermediate points of long-span girders or at the ends of cantilevers. This requires nodes with 6 DoFs at these points, even when no other element frames into these nodes.

4.9.2 Effective Elastic Stiffness of Concrete Members

Section 3.2.3.3 has pointed out that the elastic stiffness in an analysis for seismic design should correspond to the elastic branch of a bilinear force-deformation behaviour. Accordingly, current seismic design codes, e.g. CEN (2004a), BSSC (2003) and SEAOC (1999) require that design of concrete buildings be based on an analysis in which member stiffness takes into account the effect of cracking.[10]

---

[9] One way to achieve a non-pinned connection of a region modelled with 2D FEs to a 3D beam element in the same plane, is to provide the end of the 3D beam element with an almost rigid extension into the region modelled with 2D FEs, connecting the node at the physical end of the beam element with any FE node inside the 2D FE region.

[10] As a matter of fact, in the context of US codes (BSSC 2003, SEAOC 1999) a realistic stiffness for concrete members has little practical implication for strength-based member design, as the design base shear is not allowed to be less than 80% of the value computed from the design spectrum on the basis of empirical period formulas (SEAOC 1999), or less than that given by the design spectrum at a multiple between 1.4 and 1.7 of the empirical period (BSSC 2003). The reduction in lateral force demands due to concrete cracking may account partly for the high values of the force

Eurocode 8, in particular, specifies the stiffness at incipient yielding of the reinforcement. A default stiffness value equal to 50% of that of the uncracked member neglecting the effect of the reinforcement is normally accepted by seismic design codes – including Part 1 of Eurocode 8 (CEN 2004a) in case the cracked member is not modelled more accurately. This default value is much higher than the experimental secant stiffness at incipient yielding, including the effect of bar slippage from the joints (see Section 3.2.3.3). So, it is considered as safe-sided for force- and strength-based design of new buildings, because it underestimates the period and increases the design spectral acceleration and the design forces. However, it leads to underestimation of storey drifts and P-Δ effects, which is not safe-sided.

Although torsion does develop in beams and columns of concrete buildings during the seismic response, it is almost immaterial for their earthquake resistance. Cracking reduces the torsional rigidity much more than the shear- or flexural-rigidity. So, considering that overestimation of member torsional moments may be at the expense of their bending moments and shears, which are more important for earthquake resistance, and that torsional moments due to deformation compatibility drop with the large reduction of torsional rigidity upon cracking, the effective torsional rigidity, $G_c C_{ef}$, of concrete members should be assigned a very small value (close to zero). This should not be done by reducing the concrete shear modulus, G_c, as this will also reduce the effective shear stiffness and unduly increase member shear deformations. In the special case of using the torsional rigidity of a supporting beam to model the restraining effect of the slab on the bending of another element (e.g. of a staircase supported on that beam), the effective torsional rigidity of at least part of the length of the beam should be assigned an artificially high value. Torsional rigidity may also be important in U-shaped structural walls subjected to large torques (see Section 4.9.4).

4.9.3 Modelling of Beams and Columns

Beams and columns are normally modelled as prismatic 3D beam elements. Their parameters for linear analysis are the cross-sectional area, A, the moments of inertia, I_y and I_z, with respect to the principal axes y and z of the section, the shear areas A_y and A_z along these local axes (for shear flexibility, which is important in members with low shear span ratio) and the torsional moment of inertia, C or I_x for St. Venant torsion about the centroidal axis x.

Members with cross-section comprising more than one rectangular parts (L-, T-, C-sections, etc.) are normally dimensioned or assessed for action effects (moments, shears, curvatures or chord rotations) defined with respect to axes parallel to the section sides. So, the analysis should provide action effects referring to such axes. In columns or walls without double symmetry of the section (L-, T-sections, etc.),

---

reduction factors R of US codes. The stiffness used for concrete members has implications mainly for the calculated interstorey drifts.

such axes normally are not principal ones. When the deviation is large and, in addition, the flexural rigidity differs significantly between the two actual principal directions (as, e.g., in an L-shaped section), it may be desirable to have this difference reflected in the action effects from the analysis (e.g. for consistency of the relative magnitude of the bending moment demands with that of flexural capacities in these two directions). Then, the product of inertia I_{yz} with respect to centroidal axes y and z parallel to the sides of the section, should also be specified together with the moments of inertia about these axes (alternatively, the principal moments of inertia and the orientation of the principal axes with respect to the global coordinate system should be given). Shear areas of such sections along their sides may be taken equal to the full area of the rectangle(s) having the long side parallel to the direction in question. These shear areas may then be projected onto the principal centroidal axes, to compute the shear areas in the principal directions, A_y and A_z.

Concrete beams integral with a floor slab are considered to have T- or L-, etc., section, with a constant effective flange width throughout their span. The effective width of the slab on each side of the web, taken in design for convenience the same as for gravity loads, is normally specified in design codes as the sum of a fraction of the distance between adjacent points of inflection of the beam (10% in Eurocode 2) plus another fraction (again 10% in Eurocode 2) of the clear distance to the adjacent parallel beam. More realistic estimates of the effective slab width are proposed in Section 4.10.5.1 for nonlinear analysis. In a long girder providing support (at intermediate points) to secondary joist beams or to vertically interrupted ("floating") columns, intermediate nodes are normally introduced along the span and the girder is modelled as a series of short beams, all with the same effective flange width, as determined from the overall span of the girder between supports on vertical elements. By contrast, the effective flange width of the secondary joist beams depends on their shorter spans between girders.

What has been said above for members of non-doubly symmetric section notwithstanding, beams integral with a floor slab should be assigned local y and z axes normal and parallel to the plane of the slab, respectively, even when their web is not at right angles to the slab (as, e.g., in a horizontal beam supporting a sloping roof).[11] The moment of inertia I_z is computed for the T- or L-section on the basis of the effective flange width. The shear area A_y is that of the beam web alone. If the slab is considered as a rigid diaphragm, the values of A, I_y and A_z are immaterial. If it isn't, they may have to be determined so that the flexibility of the diaphragm is included in the model, e.g., according to Section 4.9.5.

[11] The beam is dimensioned for the ULS in bending, or assessed on the basis of its ultimate deformation, for action effects about an axis parallel to the slab, using as beam depth the projection, $h\sin\beta$, of the actual depth h on the normal to the slab and as web width the value $b_w/\sin\beta$ (β is the angle of the web to the plane of the slab). Assessment of the beam and of its transverse reinforcement in shear can be based on the actual depth and width of the web, h and b_w, but with a shear force equal to the shear V_y from the analysis or capacity design in the direction of the normal to the slab, divided by $\sin\beta$.

The model should account for the effect of sizeable joints between members to the stiffness of these members and of the structure as a whole. The length of the 3D beam element falling in the physical region of its joints with another member is often considered as rigid. If this is done for every member framing into a joint, the global stiffness is overestimated, even when slippage and pull-through of longitudinal bars from the joint is indirectly taken into account as an apparent increase in the flexibility of these members, because the shear deformation of the joint panel zone is neglected. It is preferable to consider as rigid just the parts within the physical joint that belong to the less bulky and stiff among the elements framing in it (normally of the beams).

There are two options for modelling the end region(s) of a member as rigid:

1. To consider the clear length of the member as its real "elastic" length and use a (6×6) transfer matrix to express the kinematic constraint between the DoFs at the real end of the member at the face of the joint and the ones of the mathematical node, where the elements of the model are interconnected.
2. To insert a fictitious almost rigid short element between the real end of the "elastic" member and the mathematical node.

Apart from the increase in computational burden brought about by the additional elements and nodes, approach No. 2 may produce ill-conditioning, because of the large difference in stiffness between the connected elements, real and fictitious. If this approach is used owing to lack of computational tools for approach No. 1, the sensitivity of the analysis results to the stiffness of the fictitious members should be checked, e.g. by ensuring that results are almost the same when the stiffness of a fictitious element changes by an order of magnitude.

If the member end region within a joint is modelled as rigid, stress resultants or chord rotations at member ends, routinely given as output of the analysis, can be used directly for dimensioning or assessing the member at its end section at the joint face. When such rigid ends are not employed, unless the stress resultant or chord rotation at the joint face is separately calculated on the basis of the joint dimensions, a safe-sided member dimensioning or assessment may be carried out assuming that the stress resultants or chord rotations at the mathematical nodes apply at the face of the joint.

Often the centroidal axes of connected members do not intersect. Then the mathematical node is placed on the centroidal axis of one of the connected members, typically a vertical one, with the ends of the other members connected to that node at an eccentricity. This eccentricity can easily be incorporated in the modelling of the member end region within the joint as rigid: the rigid end will be at an angle to the member axis.

Distributed gravity loads on members with rigid ends are often considered by the analysis program to act only on the "elastic" element between the rigid ends. Any gravity load unaccounted for, as falling outside the "elastic" element length, should be specified separately as a concentrated nodal force.

4.9.4 Special Modelling Aspects for Walls

The part of a wall between successive floors and/or substantial openings should be modelled as a single 3D beam element. Such a modelling is often called "wide-column-analogy". Elastic displacements and stress resultants predicted by the "wide-column-analogy" in the wall itself and the rest of the system compare well with those of detailed FE analysis, provided that shear deformations in the wall are accounted for through a finite shear area.

Code rules regarding the amount and detailing of their horizontal reinforcement ensure that walls with composite section, consisting of connected or intersecting rectangular segments (L-, T-, U-, H-shaped, etc.), work as a single integral unit. So, no matter how they are modelled for the analysis, such walls are dimensioned or verified in flexure with axial force and in shear along and normal to the long sides of their constituent rectangles. For each of the two directions of bending considered, the part of the section parallel to the shear force and normal to the moment vector is taken as the web and the parts orthogonal to it are the flanges. The Eurocode 8 rules for the confinement reinforcement of such walls also presume a single integral section. So, it is most convenient for the subsequent phases of dimensioning and detailing or assessment to model walls of any section using storey-tall 3D beam elements with the cross-sectional properties of the entire section. The only question regarding this approach may concern the modelling of torsion in walls with section other than (nearly) rectangular, as detailed below.

Except possibly in walls with semi-closed channel-section addressed later in this section, compatibility torsion is not an important component of the seismic resistance of walls. So, accurate estimation of torsion-induced shear for the design or assessment of the wall itself is unimportant. The main relevant issue is whether potentially unrealistic modelling of the torsional stiffness and response of a wall with section other than (nearly) rectangular, has a significant effect on the seismic action effects calculated for other structural members. If storey-tall 3D-beam elements are used with the cross-sectional properties of the entire section, the accuracy of the prediction of seismic action effects in other members is improved if the axis of the 3D beam element modelling the wall passes through the shear centre of its cross-section, instead of its centroid. For L- or T-shaped sections this is very convenient, as the shear centre is near the intersection of the two rectangular parts of the section, through which the axis of the beams framing into the wall often pass. The offset from the centroid to the shear centre introduces some error in the calculation of the vertical displacement of the end of a beam eccentrically connected to that node of the wall. Another issue is that the torsional rigidity, $G_c C$, of the section estimated for pure St. Venant torsion – i.e. as $G_c \sum (l_w b_w{}^3/3)$, with l_w and b_w denoting the length and thickness of each rectangular part of the section - does not account for the resistance of the wall to torsion-induced warping of the section. When evaluating these questions, though, we should keep in mind the large uncertainty regarding the reduction of torsional rigidity due to concrete cracking (see last paragraph of Section 4.9.2).

An alternative to the single-element modelling of walls with a section consisting of connected or intersecting rectangular segments is to use a separate 3D beam element at the centroidal axis of each such segment of the section. To dimension and detail the entire section in bending with axial force, computed bending moments and axial forces of the individual 3D beam elements need to be composed into a single M_y, a single M_z and a single N for the entire section. If these elements are connected at floor levels to a common mathematical node (e.g. via rigid horizontal arms or equivalent kinematic constraints), the model is fully equivalent to a single 3D beam element along the centroidal axis of the full section. According to Xenidis et al. (1993) the overall torsional behaviour is better represented if the constituent elements of the section are not connected to a common mathematical node at each floor, but to individual end nodes at the centroid of each segment of the wall section. The connection between the individual elements may best be effected through arms within the plane of the section, connected to each other at the intersection of adjacent segments of the section. These arms should be rigid in bending, shear or axial extension, but should have finite torsional rigidity: $G_c C = G_c H_{st} b_w{}^3/3$ (where H_{st} is the storey height and b_w the thickness of the web of the corresponding wall segment). Then the individual 3D beam elements of the wall may bend relatively independently of each other in the vertical plane of their length dimension, developing, through their in-plane shear forces, a torque with respect to the centroid of the composite section. This multiple vertical 3D element model with connection through horizontal arms meeting at the corner(s) of the section has one drawback: the replacement of the continuous shear stress distribution along the vertical connection of the individual wall segments by a discrete vertical force at the node where the horizontal arms meet induces fictitious counterflexure moments in the individual elements (Stafford-Smith and Girgis 1986, Kwan 1993). The counterflexure decreases the shear stiffness of individual wall segments and hence the apparent torsional rigidity of the wall. More important, the fictitious moments have maximum value at the two ends of the element, i.e. at storey levels, and distort most the calculated moments at the most critical cross-sections of the wall. To remove the effect of parasitic counterflexure on these end moments, Kwan (1993) suggested introducing another set of nodes at storey mid-height and use two sets of elements per storey, in lieu of one. Then the "real" end moments at storey levels can be estimated by linear extrapolation from the moments at storey quarter-height, as these are estimated by averaging the end moments of the half-storey individual elements.

Channel-shaped walls with openings regularly spaced vertically and separated by deep spandrel beams are semi-closed sections. Their torsion is dominated by circulatory shear flow. So, they can be modelled with a single element at the centroid or shear centre of the full section, with torsional rigidity according to Bredt's formula for closed sections: $GC = 4G_c A_m{}^2/\int \mathrm{d}s/t$. In this formula A_m is the area enclosed by the centreline of the closed thin-walled section at the spandrel beam level. The integral all along the perimeter is calculated with an equivalent thickness of the spandrel beam, smeared over the storey height H_{st} (Rutenberg et al. 1986):

$$t_{\mathrm{eq}} = \frac{H_{\mathrm{st}}}{h_{\mathrm{b}}} \frac{12 E_{\mathrm{c}} I_{\mathrm{b}}}{l_{\mathrm{b}}^3 \left[G_{\mathrm{c}} + E_{\mathrm{c}} \left(\frac{h_{\mathrm{b}}}{l_{\mathrm{b}}} \right)^2 \right]} \tag{4.42}$$

In Eq. (4.42) I_{b} and h_{b} denote the moment of inertia and the depth of the spandrel beam and l_{b} its span. If the spandrel beam is very flexible, or if just the slab plays that role, the wall section is closer to an open one. In that case, if the torsional stiffness of the wall itself is an important component of the total torsional rigidity of the structure and, moreover, the overall structural layout is such that torsion is an important component of the response to the horizontal seismic action components, it may be better to use the multiple vertical 3D element model connected at the corner(s) of the section through horizontal arms which are rigid except for their finite torsional rigidity: $G_{\mathrm{c}}C = G_{\mathrm{c}}H_{\mathrm{st}}{b_{\mathrm{w}}}^3/3$, as outlined in the previous paragraph. The individual vertical elements will always suffer from torsion-induced parasitic counterflexure. In this case, however, parasitic moments at opposite sides of the wall section cancel each other, when the moments and axial forces of the individual wall elements are assembled into a resultant moment at the centroid of the full section for the dimensioning of the wall in bending with axial force.

Recall from Fig. 1.7 in Section 1.3.5 that in Eurocode 8 (CEN 2004a) design of new walls using linear analysis employs heightwise linear envelopes of wall elastic moments from the analysis (see also Section 5.7.4.1). So, bending moment values from the analysis at any level other than the base and the top of the wall are not relevant for design according to Eurocode 8.

Beams framing into a wall at floor levels, etc., should be connected to the mathematical node at the axis of the wall. An eccentricity between this node and the real end of the beam should be modelled with a rigid connection. If eccentrically framing beams are at right angles to the plane of the wall (i.e. in its weak direction), it is more accurate to give to this rigid connection a finite torsional rigidity, $G_{\mathrm{c}}C = G_{\mathrm{c}}H_{\mathrm{st}}{b_{\mathrm{w}}}^3/3$ (where H_{st} is the storey height and b_{w} the thickness of the web of the wall. Note also that less than the full length of a rectangular (part of a) wall section works effectively in out-of-plane frame action with beams connected to the wall at right angles to its plane. The fully effective width of the wall in that direction may be taken to extend up to about twice the wall thickness on each side of the beam. To take into account the anyway small contribution of the weak direction of a rectangular wall to frame action, its cross-sectional moment of inertia may be conservatively computed using a depth of b_{w} and a width of $4b_{\mathrm{w}}$.

4.9.5 Modelling of Floor Diaphragms

4.9.5.1 Rigid Diaphragms

The in-plane stiffness of floor slabs acting as diaphragms should be properly recognised and reflected by the model for the seismic analysis. Floor diaphragms are commonly assumed and modelled as rigid. The most convenient way to model a

diaphragm as rigid is by introducing at each floor level an additional node ("master" node) close to the centre of mass of the floor and preferably not coinciding with anyone of the floor nodes modelling physical connection of members. This node has only 3 DoFs: two translations in the plane of the diaphragm and a rotation about the normal to that plane. The corresponding DoFs of all floor nodes (called in this respect "slaves") are related to those of their "master" through a 3×3 transfer matrix, expressing the rigid-body kinematic constraint. If the diaphragm is horizontal, the "master" and "slave" DoFs refer to the global coordinate system and the "slave" DoFs can be condensed out of the global equations of equilibrium or motion, where only the "master" DoFs remain. If the floor is at an inclination to the horizontal, the kinematic constraints between translations in the plane of the floor and rotations about the normal to it can be introduced as linear constraints between global DoFs, after appropriate rotation transformations. The same end can be achieved in a more general way, by considering rigid 3D elements between the "master" node and the physical end of all elements with nodes on the floor in question. At the "master" node the mass of the two translational DoFs is equal to the sum of the corresponding masses of all its "slaves". The rotational mass moment of inertia about the vertical axis at the "master" is the sum of those of its "slaves" (normally neglected as small), plus the sum over all the "slave" nodes of the product of that node's mass, m_i, times the square of its distance to the "master": $m_i[(X_i–X_m)^2 + (Y_i–Y_m)^2]$.

If the analysis program has neither one of the above computational capabilities or an equivalent alternative to express kinematic constraints between the floor nodes, the floor diaphragm can be included in the model as non-rigid but with high in-plane stiffness, e.g., using the modelling approach of the next section.

4.9.5.2 Flexible Diaphragms

In-plane flexibility of floor diaphragms should be realistically modelled, if:

1. the layout in plan of the floor diaphragm and of some lateral-force-resisting elements is such that the distribution of seismic action effects in these elements may deviate significantly from the result of the rigid diaphragm assumption; or
2. if in-plane seismic action effects of the floor diaphragm, needed for its verification, cannot be accurately computed on the basis of the rigid diaphragm assumption; or
3. the floor itself and/or some of its beams are post-tensioned, and the flexible floor diaphragm model of the floor-frame system is anyway necessary for a reliable calculation of the in-plane action effects due to post-tensioning.

If diaphragm flexibility is included in the model for reason No. 1, a FE model of the diaphragm within its plane is not the best option. Combining FE with 3D beam elements in the same model is fairly expensive and tricky. One FE for each panel of the floor between beams is not sufficient. To use several FEs for a panel, each surrounding beam should be broken up in several 3D beam elements with intermediate nodes, increasing computational demands and unduly complicating the

subsequent phases of beam dimensioning/detailing or assessment. Shell FEs should preferably be used, and not 2D FEs with just in-plane translational DoFs.

Unless there is compelling need to use FEs for the diaphragm, its in-plane flexibility can be approximated through the value of the moment of inertia I_y of its beams about the normal to the plane of the diaphragm, with or without X-bracing added to the model of each slab panel. For a diaphragm with thickness h, plan dimensions l_x and l_z (with direction y reserved for the normal to the diaphragm, as in the local coordinate system of the beams), Young's Modulus E and a Poisson ratio value of 1/3, the stiffness for in-plane extension or shear is essentially reproduced if the panel is modelled as a horizontal frame with X- bracing having the following properties (Yettram and Husain 1966):

– Frame members with length l_x are assigned:
  - a flexural rigidity about the normal to the diaphragm:

$$(EI)_y = \frac{Eh}{60} l_x^2 l_z \tag{4.43a}$$

  - an axial stiffness:

$$(EA) = \frac{Ehl_z}{2}\left[1 - 0.2\left(\frac{l_x}{l_z}\right)^2\right] \tag{4.43b}$$

– X-diagonals have only axial stiffness:

$$(EA)_d = \frac{Eh}{10}\frac{(l_x^2 + l_z^2)^{3/2}}{l_x l_z} \tag{4.43c}$$

For frame members parallel to l_z subscript x replaces z and vice-versa. Since the 3D beam elements around the diaphragm panel are already in the model with out-of-plane flexural properties EI_z and GA_y, only X-bracing elements need to be added.

The above modelling approach works well if the aspect ratio l_x/l_z of each diaphragm panel is not far from 1.0. For panels with $l_x >> l_z$ Eq. (4.43b) may give negative stiffness, which does not make sense. A simpler and more reasonable, but generally less accurate, alternative is to omit the 2nd term in brackets in Eq. (4.43b) and the X-bracing, and increase instead by a factor of 4 the flexural stiffness of the frame members in Eq. (4.43a). The new expressions for the in-plane parameters of the beams of length l_x are then as follows, including the effects of diaphragm panels (possibly) on both sides of a beam (Fardis 1997):

$$(EI)_y \approx \frac{Eh}{15} l_x^2 \sum l_z \tag{4.44a}$$

$$(EA) \approx \frac{Eh}{2}\sum l_z + Eb_w(h_b - h) \tag{4.44b}$$

The 2nd term in Eq. (4.44b) is the contribution of the web of beams to their axial stiffness. For the beams which are parallel to side l_z subscript z replaces x and vice-versa.

Eurocode 8 states in a note that the diaphragm flexibility may be neglected, if it increases horizontal displacements by more than 10%. To apply this conventional definition of a rigid diaphragm, two analyses are unfortunately needed, one neglecting and the other considering the diaphragm's in-plane flexibility.

4.9.6 A Special Case in Modelling: Concrete Staircases

If the lateral-load-resisting system itself is flexible, as e.g. in low-rise frame structures, and/or if the location of the staircase in plan is such that the torsional rigidity and response of the building is significantly affected (as, e.g., in the case of Fig. 2.13(b) and (c)), the designer may want to include the staircase in the structural model. In this way the effect of the staircase on the seismic action effects in the rest of the structure can be determined, and even the staircase could be designed or assessed under its own seismic action effects.

A staircase may be modelled as a series of prismatic 3D beam elements along its axis, inclined to the horizontal. The sectional properties (including shear areas) of these elements should be those of the full-width solid part beneath the steps. A curved axis may be modelled as multilinear. For staircases supported only at the ends, having a helical axis or one consisting of a combination of straight segments and quarter- or semi-circular segments, the 12×12 stiffness matrix of the entire stair between its ends is given in Skouteropoulou et al. (1986, 1987) and Fardis et al. (1987). Inclined beams supporting the staircase and supported, in turn, by elements of the lateral-load-resisting system, should be similarly and appropriately included in the model. Only integral connections of the staircase and/or its supporting beams to the rest of the structure should be included in the model as nodes between elements. Connections without properly detailed and anchored reinforcement will, in all likelihood, break loose in an earthquake. They cannot be relied upon under seismic actions and the designer should not only omit them from the model, but also avoid them altogether in new buildings.

At floor levels a stair is typically supported on beams. Its partial fixity there in bending and torsion is provided by its continuation into a floor slab on the other side of the supporting beam. As this slab is not included in the model of the lateral-load-resisting system, the partial fixity of the stair against rotations at its support node on the beam should be modelled either:

- by connecting the node supporting the stair to the nearest floor node in a direction close to the extension of the stair axis in plan, through a fictitious horizontal member having cross-sectional properties about the same as the stair; or
- by assigning a very large torsional rigidity to the segment of the supporting beam between the support node of the stair on the beam and the nearest common node of the supporting beam with a transverse frame.

If this is not done, the stair in the model will be almost hinged for rotation about the supporting beam.

Examples of staircases included in the model are presented in Section 4.10.5.3.

4.9.7 2nd-Order (P-Δ) Effects

It has been pointed out in Section 1.2.1 that collapse of structures during an earthquake is caused not by the seismic lateral forces per se but by the seismic lateral displacements, Δ, acting with the structure's weight to generate (P-Δ) moments in vertical elements. To appreciate the importance of P-Δ effects, think of a situation in which the P-Δ moment alone, $M = N\delta$, produced at the base of a single column by its axial force, N, and the interstorey displacement, δ, reaches the column's moment resistance, M_R. As the support of gravity loads is force-controlled, the column may collapse, no matter its ductility. Normalising M_R into $\mu_R \equiv M_R/(bh^2 f_c)$ and N into $\nu \equiv N/(bhf_c)$, column collapse may occur when the interstorey drift ratio, δ/H (equal to the sum of the average column chord rotations and beam chord rotations around a frame bay plus the average shear distortion of the joint panels, see Fig. 3.30) exceeds the value of $(\mu_R/\nu)/(H/h)$, where H/h is the column slenderness (i.e., length-to-depth) ratio. Slender columns, lightly reinforced and under high axial load (i.e., with low μ_R/ν values) might then collapse at relatively moderate interstorey drift ratios. Hence the importance of computing and limiting P-Δ effects.

All seismic design codes require taking into account 2nd-order (P-Δ) effects in buildings, whenever at any storey the aggregate 2nd-order (P-Δ) effects in vertical members exceed 10% of the 1st-order ones. The criterion is the interstorey drift sensitivity coefficient, θ, defined for storey i as the ratio of the total 2nd-order moment in storey i, to the change in the 1st-order overturning moment within that storey:

$$\theta_i = \frac{N_{\text{tot},i}\,\Delta d_i}{V_{\text{tot},i}\,H_i} \tag{4.45}$$

where:

- $N_{\text{tot,i}}$ is the total gravity load concurrent with the seismic action at and above storey i.
- $V_{\text{tot,i}}$ is the total seismic shear at storey i.
- H_i is the height of storey i.
- Δd_i is the interstorey drift at storey i, i.e., the difference of the lateral displacements at the top and bottom of the storey, d_i and d_{i-1}, at the floor centre of mass, or at the floor "master" node. In Eurocode 8 (CEN 2004a) it is the inelastic drift, estimated via the equal displacement rule according to the 2nd paragraph of Section 4.11.1 (for all practical purposes by back-multiplying by the behaviour factor q the values of d_i, d_{i-1} from the linear analysis for the design spectrum). US codes (BSSC 2003, SEAOC 1999) take for this purpose d_i and d_{i-1} directly from the analysis for the design spectrum, underestimating them by a factor of R

(where R is the force reduction factor incorporated in the design spectrum); the estimated P–Δ effects are very much on the low side.

Second-order effects may be neglected, if the value of θ_i does not exceed 0.1 at any storey. They should be taken into account for the entire structure, if at any storey θ_i exceeds 0.1. If θ_i does not exceed 0.2 at any storey, seismic design codes, such as Eurocode 8 (CEN 2004a), allow taking P–Δ effects into account without a 2nd-order analysis, but in approximation: by multiplying a-posteriori all 1st-order action effects due to the horizontal component of the seismic action by $1/(1–\theta_i)$. For given lateral forces, this approximation gives seismic action effects in fairly good agreement, on average, to those of an exact 2nd-order analysis carried out as described below. The simplified approach fails to capture, though, the global effect of the lengthening of the natural periods due to the 2nd-order effects. Note that, although it is the value θ_i of the individual storeys that can be used in this amplification, it is safe-sided to use for the entire the building the maximum value of θ_i in all storeys. It also respects equilibrium in the framework of 1st-order analysis.

In the very unlikely for RC buildings case that θ_i exceeds 0.2 at any storey, an exact 2nd-order analysis is required (CEN 2004a). This analysis may be performed with the modelling described below.

If the vertical members connect floors which are considered as rigid diaphragms, the P-Δ effects can be calculated exactly as highlighted in the next paragraph. If there are no such floors, or if they may not be taken as rigid diaphragms, P-Δ effects may be considered at an individual column basis, by subtracting from the column elastic stiffness matrix its linearised geometric stiffness matrix. If the analysis is elastic using the design spectrum, the linearised geometric stiffness matrix of each column should be multiplied by the displacement amplification factor for conversion of elastic displacement estimates from the analysis into inelastic ones (as pointed out in the definition of Δd_i in connection with Eq. (4.45)). In the context of elastic analysis, axial forces in the geometric stiffness matrix of the column may be taken constant and equal to the value due to the gravity loads alone.

If diaphragms can be considered as rigid, P–Δ effects may be accounted for exactly in the analysis without subtracting the linearised geometric stiffness matrix of each individual vertical element from the corresponding elastic stiffness matrix. It has been proposed in Rutenberg (1982) to introduce instead a fictitious vertical element between adjacent floors i and i–1, with negligible axial stiffness EA and flexural rigidities EI_y, EI_z, but with negative shear areas: $GA_y = GA_z = -q(\sum N)_i$ and negative torsional rigidity: $GC = -q(\sum Nr^2)_i$, where N and r denote respectively the axial force in the individual columns of storey i and their distance from the centroid of the axial forces in all the columns. These fictitious vertical elements should be connected (through horizontal rigid elements or rigid-body kinematic constraints in the horizontal plane) to the centroids of the axial forces in all columns, $(\sum N)_i$, of storeys i and i–1. These centroids differ from the storey centres of mass, as the axial forces include contributions from all storeys above. P–Δ effects can thus be introduced in a direct and exact way in computer codes that lack the element geometric stiffness facility.

4.9.8 Modelling of Masonry Infills

Before any guidance for linear modelling of infills, a few words are in order about its scope.

Modelling for linear analysis is primarily of interest for the seismic design of new buildings. The provisions of Eurocode 8 for the design of new frame buildings having masonry infills are outlined in Sections 2.1.13 (regarding the global aspects) and 5.7.3.6 (for the potential adverse local effects on columns). Their underlying concept is to prevent any adverse effect of the infills, while not profiting explicitly from the beneficial ones to reduce the seismic action effects in structural members. In this context, analysis of a 3D structural model explicitly including the infills is required by Eurocode 8 (CEN 2004a) only for new buildings with a severely irregular layout of the infills in plan. It can be argued that this approach is neither rational nor cost-effective, as it does not explicitly account for an effect (that of the infills) which is generally important and normally beneficial. Note that, to account rationally for this influence, individual infill panels should be:

(a) explicitly included in the model for the seismic analysis of the building, and
(b) considered as structural elements and verified for the seismic action demands computed for them from the analysis for the seismic action.

In the verifications under (b) above the resistance of the infills should be expressed in terms of design values of their strength properties. This implies that, at the design stage, nominal (lower characteristic) values of these properties are specified and sampling of infill materials (masonry units, mortar, etc.) for testing takes place during execution, exactly as in masonry buildings designed according to Eurocodes 6 and 8. It also implies that modifications of infill panels or of their openings is not allowed at a later stage, without re-visiting the seismic design of the building and assessing the impact on the seismic safety of the entire system and all its elements. This would be a major change in the current practice of design, execution and maintenance of masonry-infilled buildings. Moreover, the costs incurred for the additional design effort and the quality assurance for masonry infills may outweigh any savings in the members of the structural system. So, no matter the rationality of a design approach that explicitly accounts for all individual infill panels, the one adopted by Eurocode 8 seems to provide a good balance of simplicity in design and execution, overall construction cost and seismic safety.

In the light of the above, what follows regarding linear modelling of masonry infills is meant to be used primarily for new buildings with a strongly irregular layout of the infills in plan, required by Eurocode 8 to be analysed including the infills explicitly. It also serves as a prelude to Section 4.10.2, dealing with nonlinear modelling of masonry infills primarily for the purposes of assessment and retrofitting of existing new buildings.

A solid infill panel can be conveniently modelled as a strut along its compressed diagonal (see Fig. 4.4). A widely-known strut model is based on the beam-on-elastic-foundation analogy for the estimation of the strut width (Mainstone 1971).

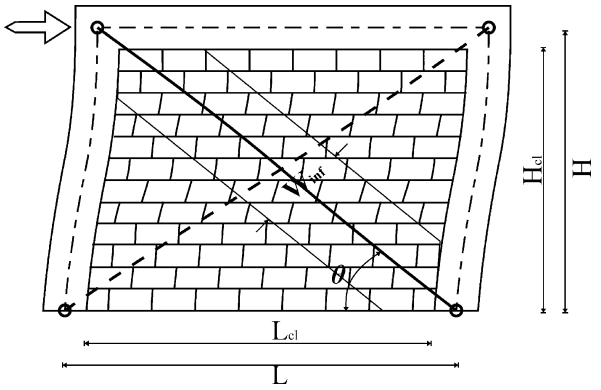

Fig. 4.4 Modelling of solid infill panel with strut along the compressed diagonal

According to that model, the strut has the same thickness as the infill wall, t_w, and width in the plane of the infill, w_{inf}:

$$w_{inf} = \frac{0.175 L_{cl}}{\cos\theta\,(\lambda H)^{0.4}} \tag{4.46a}$$

where:

$$\lambda = \left(\frac{E_w t_w \sin 2\theta}{4 E_c I_c H_{cl}}\right)^{\frac{1}{4}} \tag{4.46b}$$

- L_{cl} : clear horizontal dimension of the infill panel;
- θ : arctan(H_{cl}/L_{cl}) = inclination of the diagonal to the horizontal;
- H, H_{cl} : theoretical and clear column height, respectively;
- E_c, E_w, : Elastic modulus of the column concrete and of infill masonry (ranging according to Eurocode 6 from 500 to 1000 times the masonry compressive strength), respectively;
- t_w : infill wall thickness;
- I_c : moment of inertia of the column section about the normal to the infill panel.

As an alternative to Eq. (4.46a), Eurocode 8 (CEN 2004a) allows a strut width equal to a fraction of the clear length of the panel diagonal, $L_{cl}/\cos\theta$. A strut width around 10–15% of the length of the diagonal is a good approximation, at least for new buildings designed for Life Safety performance ("Significant Damage" in Part 3 of Eurocode 8 (CEN 2005a)) under the design seismic action. For lower level response – e.g., that normally associated with Immediate Occupancy performance ("Damage Limitation" Limit State in Part 3 of Eurocode 8) – a value around 20% of the length of the diagonal is more appropriate. Whenever the integrity of frame members is questionable or of interest (notably at the Near Collapse performance level), it is preferable to assume that the diagonal strut has disintegrated and does not contribute anymore to the global lateral strength and stiffness. Of course, infill

panels having clearly adverse effects on the seismic performance of the structural frame, locally or globally, should be retained in the model with their Life Safety performance width. This may be the case of infills with a strongly irregular heightwise distribution that may have "open-storey" and "soft-storey" effects, or of partial-height infills that produce captive columns, etc. In that latter case the strut which models the infill should run not along the diagonal of the frame panel, but along that of the infill itself, i.e., between an intermediate node introduced in the column at the level of the top of the partial-height infill (i.e., at that of the sill) and the diagonally opposite node at the bottom of the column.

In linear analysis a solid infill panel may be modelled as an elastic strut along the compressed diagonal, with cross-sectional area equal to t_w times w_{inf} and modulus equal to E_w (taken, e.g., according to Eurocode 6). This is realistic for the estimation of both the panel's local effects on the surrounding frame members, as well as of its effects on the global response. A strut only along the compressed diagonal is, however, a nonlinear modelling feature. The only difference that a strut along the tension diagonal would make on the response is in the sign of the axial forces in the columns bordering the panel. Unlike the axial forces due to the overturning moment, those associated with the action of infills are all tensile and nearly uniformly distributed in the columns of the entire plan (except in the columns of the "lee-ward" side, where no axial force is induced in columns by the infills). The resultant of all these axial forces is equal and opposite to the vertical resultant of all strut forces in the infills. In static analysis – linear with the lateral force procedure or nonlinear "pushover" – the diagonal of the panel where the strut is placed can be chosen according to the perceived sense of deformation of the panel. In frames (about) parallel to the horizontal seismic action component, it is easy to identify the diagonal where the strut should be placed. By contrast, in frames at (about) right angles to this direction the choice of panel diagonal for the strut relies on intuition, judgement or – possibly – iterations. As modal response spectrum analysis gives results without signs, it is almost immaterial whether the struts modelling the infills are placed along one diagonal or the other. However, unlike other seismic action effects from modal analysis that are taken both positive and negative, strut forces should always be taken compressive (and double its value from the modal response spectrum analysis, if struts are placed along both diagonals of a panel), while axial forces induced in columns by the infills should be tensile. It is not easy, however, to identify which part of a column's axial force is due to the infills.

The most challenging open issue for modelling infills is the influence of openings. A panel with openings may be modelled with multiple struts starting at opposite corners of the panel, passing near the corners of the openings and ending at intermediate points along the members framing the panel. A simpler way to take into account the effect of infill openings on the global response is through reduction factors on the infill stiffness. The value of these factors depends on the shape, size and location of the opening(s) within the infill panel, and – in panels with asymmetric openings – the direction of loading. They should be established through systematic parametric analyses of infilled RC frame panels with openings, using detailed FE models for the infill and its interaction with the surrounding frame. Figure 4.5 gives such reduction factors, λ, on the stiffness of the solid infill panel, as derived

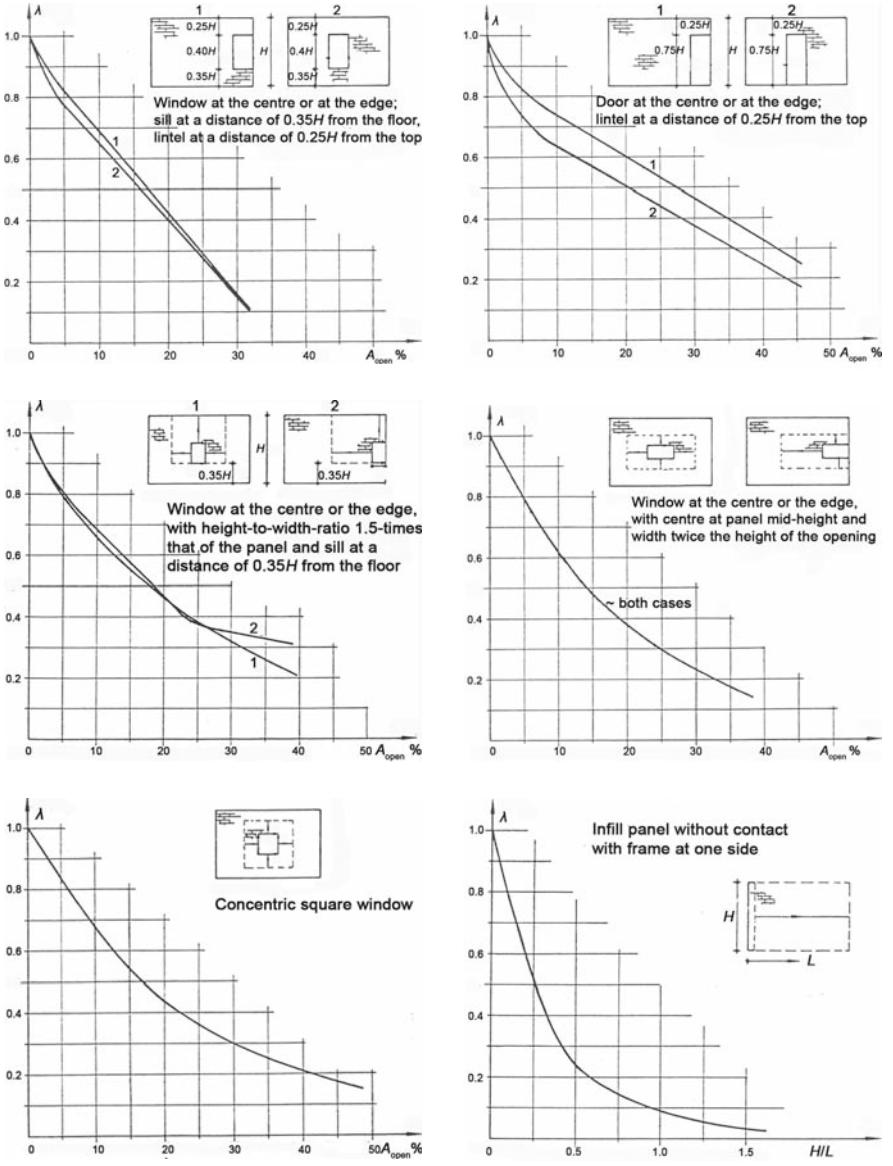

Fig. 4.5 Reduction factor on solid infill stiffness, in terms of fraction of panel area in elevation taken up by opening. *Bottom-right*: reduction factor on panel stiffness, for no contact with frame on one side, as a function of panel height-to-width-ratio (Giannakas et al. 1987)

from elastic FE analyses of single panels with openings. If there are more than one openings in the panel, the overall reduction factor is bounded by the sum of the individual λ_i's minus 1.0 and by their product (Giannakas et al. 1987). Note that Eurocode 8 (CEN 2004a) instructs the designer to neglect in the model infill panels

with two or more significant openings. Models, especially those for nonlinear analysis (see Section 4.10.2) should be validated or calibrated on the basis of the few available cyclic test results on infills with an opening, such as those given in CEB (1996a) and Kakaletsis and Karayannis (2008).

4.9.9 Modelling of Foundation Elements and of Soil Compliance

4.9.9.1 Introduction

No matter whether we are talking about seismic design or design just for other, non-seismic actions, in order to use analysis results to design or assess piles or elements of shallow foundations, such as tie- or foundation-beams or a raft (mat) foundation, we should include these elements in the model and take into account the compliance of the ground.

The superstructure, especially if founded on two-way deep foundation beams, as in the box-type systems of Section 2.3.3.3, is sometimes analysed separately from the foundation, considered fixed at the top of the foundation system. The so-computed stress resultants at the base of the vertical elements are taken as external actions for the foundation system, which is in turn analysed accounting for the compliance of the soil, in order to compute the action effects in foundation elements, necessary for their dimensioning or verification. There are many examples of the limited accuracy of this uncoupled approach: (1) if the walls of a dual system are assumed fixed at the base, their contribution to lateral strength and stiffness is overestimated, especially at the lower storeys; (2) if a column is taken fixed at the foundation, seismic moments are overestimated at its base and underestimated at the top of the storey; (3) fixity of vertical elements at the base leads to underestimation of lateral drifts and of P–Δ effects, etc. Note, though, that, if soil compliance does not change the magnitude of storey seismic shears and overturning moments, neglecting it in a linear seismic response analysis does not adversely affect the overall earthquake resistance of a ductile structure. Such a structure can redistribute internal forces from where they have been underestimated in the analysis to adjacent regions where they were overestimated.

Uncoupled modelling and analysis of the superstructure and the foundation system is also computationally inconvenient. It requires setting up two different structural models and transferring the (reaction) output from the analysis of the superstructure as input to the foundation, for several load cases and their combinations.

Today's computational capabilities allow including the superstructure, the foundation system and the soil into a single, coupled linear model for seismic response analysis. Such a model reflects much better the seismic response of the lateral-load-resisting system, as affected by the degree of fixity of the vertical elements at the base.

Codes and standards do not seem ready yet to consider full-fledged soil-structure-interaction in seismic design, especially as its effects are mostly favourable. BSSC

(2003) has taken the bold step to allow a (up to 30%) reduction of the base shear computed for rigid ground and full fixity of the structural elements to it, if the lengthening of the 1st mode period due to the horizontal and rotational (rocking) deformation of the ground and the additional material and radiation damping in the soil are explicitly and separately accounted for as specified there. Practically all codes for everyday seismic design of ordinary buildings derive the seismic action effects implicitly assuming that the structure as a whole is fixed to the ground. For instance, the global displacement ductility factor implicit in the values of the behaviour factor, q, or force reduction factor, R, specified by a code refers to a global yield displacement of the structure fully fixed to the ground, without any contributions from the compliance of the soil. So, when working in the framework of these codes, incorporation of the effects of soil compliance in the design should not violate this key point, either by increasing the effective damping, or by overly reducing lateral force demands. In other words, soil-structure-interaction phenomena to be considered should have mainly "internal" effects on the structure, notably redistributing internally seismic action effects, without reducing the overall seismic demands from the "outside".

4.9.9.2 Elastic Support Conditions

A convenient way to take into account soil compliance in linear analysis is through elastic support conditions at support nodes, normally at the bottom of foundation elements. These nodes should be connected to nodes at the physical ends of structural elements (walls, columns, tie- or foundation beams) either via rigid connecting elements, or (preferably) through kinematic constraints expressing rigid-body connection.

Not all 6 DoFs of a support node need to be elastically supported. In a sound conceptual design of a building for earthquake resistance the base of all foundation elements is at the same level and all foundation elements are tied together in both horizontal directions, so that the foundation system moves almost as a rigid body (see Section 2.3.2). Then both horizontal translations and the rotation about the vertical axis can be fully constrained at all foundation nodes. The main effect of elastic supports in these directions would had been a horizontal rigid-body-component dominant in the lowest three modes and a significant lengthening of their periods (in all likelihood reducing the corresponding base shears), without a significant and physically meaningful effect on the distribution of seismic forces and deformations in the structure. Moreover, there is significant uncertainty about the elastic constants for soil compliance in the horizontal direction(s), mainly due to the effect of embedment.

The displacements of the foundation in a horizontal plane can be fixed only if all foundation nodes are at the same horizontal level. As pointed out in Section 2.3.2, if foundation nodes are elastically supported in the vertical direction and against rotation about the two horizontal axes and, in addition, support nodes placed at different horizontal levels are horizontally constrained, the full overturning moment will be taken by horizontal reactions at these latter fixed supports, rather than by

nonuniform vertical reactions. In other words, rocking of the structure will be prevented by an artificial horizontal support condition that distorts the distribution of seismic action effects in the elements of the foundation and those it supports. Note that, if there are support nodes at different horizontal levels but only those at the lowest level are horizontally constrained, no horizontal reactions develop at the other support nodes and the vertical elements supported there will have zero seismic shears. So, modelling considerations lead to the same end as a sound conceptual design: a strong horizontal connection of all foundation elements that maybe at different horizontal levels, through stiff tie-beams or foundation walls, so that the entire foundation is almost rigid in both horizontal directions. Then, only support nodes at the lowest level may be constrained in both horizontal directions and about the vertical, without fictitious effects on the seismic shears and axial forces of vertical structural elements.

When it is meaningful to include elastic support conditions in the horizontal direction, as e.g., in structures supported on piles (see Section 4.9.9.5), horizontal elastic supports may be placed at different horizontal levels, as needed.

Note that, if soil compliance in the vertical or horizontal direction is taken into account, this should be done at all support nodes; translational constraint of just a few of them may change drastically the pattern of action effects in the foundation. Constraint of rotations about the horizontal will totally distort the effect of vertically elastic supports, but not vice-versa.

For foundation on spread footings with tie-beams or on piles, the distribution of seismic internal forces in the superstructure and in the foundation system is mainly influenced by the rotational elastic supports and relatively little by the translational ones. In raft (mat) foundations and foundation beams, the effect of vertical elastic supports on the distribution of seismic internal forces is at least as much as that of the rotational ones.

Elastic support "constants" are in general function of the frequency of vibration. In view of the uncertainty of soil parameters on which these "constants" depend, the effect of frequency is normally neglected and the (larger) static stiffness is used. This is safe-sided for internal forces, but not always for deformations.

If there are no elastic supports in the library of the analysis software, the designer can introduce fictitious elements between the support node and a fictitious one below at an arbitrary vertical distance h and with all its six DoFs fully restrained. The axial stiffness of the fictitious element, EA/h, is set equal to the target vertical impedance at the support node, K_z. With the support node restrained in both horizontal directions, the fictitious element's flexural rigidities, EI_x, EI_y, are chosen so that $4EI_x/h$ and $4EI_y/h$ match the target rotational impedances, $K_{\varphi x}$ and $K_{\varphi y}$, respectively.

4.9.9.3 Foundation Beams and Raft Foundations

Soil compliance under foundation beams or raft (mat) foundations is almost always modelled using the subgrade reaction modulus (or Winkler spring) approach, which assumes that a soil pressure p applied at a point of the soil-structure interface causes an absolute displacement of that point, y_s, which is proportional to p:

$$p = k_s y_s \tag{4.47}$$

The constant k_s is the subgrade modulus (or Winkler constant). Note that Eq. (4.47) entails lack of coupling between different points at the soil-structure interface, as if the soil were a system of independent vertical springs, each with spring constant (vertical impedance):

$$K_z = k_s A_f \tag{4.48}$$

where A_f is the tributary area of the spring.

Foundation beams should be modelled by special-purpose beam-on-elastic-foundation elements connecting two adjacent physical joints of the beam with other structural elements (walls, columns, foundation beams). The stiffness matrix of this type of element is a function not only of the properties of the beam, but of k_s as well. Shear deformations should always be accounted for, if the depth of the foundation beam is large.

If the library of the analysis software used does not include the special-purpose beam-on-elastic-foundation element, recourse to a "poor-man's" alternative may be necessary, that is less accurate, but computationally more demanding and inconvenient to apply. In this option the length of the foundation beam between two adjacent physical joints with other structural elements is broken up, via intermediate nodes, into a string of conventional 3D beam elements. The intermediate nodes, as well as those corresponding to physical joints of the beam with other structural elements, are elastically supported in the vertical direction. The vertical impedance at these supports may be taken from Eq. (4.48), with A_f being the tributary area of the node at the soil-foundation beam interface. An average soil pressure may be estimated at each support node, as the vertical reaction there divided by the tributary area, A_f. The shear force diagram along the foundation beam is discontinuous at the support nodes (as only self-weight acts between them), each discontinuity being equal to the vertical reaction there. The bending moment diagram is multilinear. Note the inconvenience for dimensioning and detailing of a so-modelled foundation beam, as the bending moment and shear force diagrams of the subelements along its length should be assembled into a single moment- or shear-diagram for the whole beam.

Rotational DoFs about the horizontal axes can be taken as completely free at all support nodes along the foundation beam, unless its bottom flange is asymmetric with respect to the web and the so-induced torsion needs to be taken into account, along with the restraining of the twisting by the subgrade. In that case, an impedance K_φ against rotation about the longitudinal axis x of the foundation beam should be assigned to each support node:

$$K_\varphi = k_s \frac{A_f b_f^2}{5.75} \tag{4.49}$$

where b_f is the width of the bottom flange.[12] The x axis of the foundation beam should pass then through the shear centre of the flanged beam section at the intersection of the web and the flange, instead of its centroid. This reflects the horizontal eccentricity between the web, which takes the torsion, and mid-flange, where the support nodes are placed.

Raft (mat) foundations, integral with beams connecting the bases of adjacent vertical elements, are sometimes modelled as a two-way system of foundation beams, each with a flange between panel mid-spans on either side of the beam. This computationally convenient approximation is fairly good for the calculation of the global response, but gives insufficient information for the design of the raft slab itself. If the raft is an inverted flat plate with no beams except at the perimeter, its approximation as a grid of strip-like "foundation beams" between adjacent vertical elements is not good enough. A finer two-way grid of intersecting "beams" is certainly an improvement. However, the best and only accurate model of such a raft is by plate FEs,[13] with each panel of the slab between adjacent vertical elements discretised into a (fair) number of FEs. All nodes of these elements should be elastically supported vertically, with elastic constant from Eq. (4.48), using as A_f the tributary area of the node. Such a model can depict well the distribution and magnitude of soil pressures and is sufficiently accurate for the internal forces in the slab (including around column bases) to be used in its dimensioning. Beams along the perimeter, as well as any beams connecting the base of adjacent vertical elements, should be modelled as a string of conventional 3D beam elements following the discretisation of the slab. The elastically supported nodes for the plate FEs render the use of special beam-on-elastic-foundation elements for these beams not only meaningless, but also wrong. Note that 4-node plate elements for the slab, having as nodal DoFs the displacement normal to the mid-plane and the two rotations about axes within that plane, fit well with the DoFs of the 3D beam elements used for the beams. Note also that, a rigid-body connection between a raft slab modelled with "shell" FEs (i.e., with plate elements possessing active DoFs and stiffness in-plane, in addition to out-of-plane) and the eccentric centroidal axis of a beam's web induces coupling of the beam bending with the in-plane deformations of the slab. This is an effective flange effect in the beam. However, it is questionable if the results would reflect realistically the composite action of the beam in bending with the slab. Note also that, unless judiciously placed so that they don't obstruct any deformation of the raft's slab within its plane, constraints of the horizontal DoFs of the slab's "shell" elements will obstruct or even suppress any bending of those beams that have rigid-body connection of their eccentric centroidal axis to the slab's nodes. It is therefore preferable and computationally simpler to specify an effective flange width for the beam and employ for the slab plate FEs (not "shell"), without active in-plane DoFs and stiffness. Alternatively, the centroidal axis of the beam elements could be shifted

[12] Equation (4.49) approximates the rotational impedance of a strip footing about its longitudinal axis from Eq. (4.53b), using Eq (4.54) for k_s.

[13] If the slab is thick, thick-plate FEs, e.g. of the Midlin type, should preferably be used.

to the mid-plane of the slab. But this may not be meaningful for very deep beams, e.g., perimeter walls.

4.9.9.4 Footings

According to a common rule-of-thumb, a footing may be considered as rigid, if it does not protrude in plan from the vertical element it supports by more than twice the footing depth.

When the footing is considered rigid, the impedance of the underling soil may be lumped at the centroid of the footing in plan, in 3 uncoupled springs: one vertical (z) and two rotational about the centroidal horizontal axes x and y of the footing. Expressions for these impedances have been developed on the basis of analytical or FE studies of footings embedded in elastic soil and in full contact with it. For instance, Kausel and Roesset (1975) and Elsabee et al. (1977) developed Eqs. (4.50) and (4.51) for footings with effective embedment depth d[14] in an elastic stratum having depth D_s above rigid bedrock. The impedance in the vertical direction is:

$$K_z = \frac{4Gr_a}{1-\nu}\left(1 + 0.4\frac{d}{r_a}\right) \tag{4.50}$$

and for rotation about the x or y axis:

$$\begin{aligned} K_{\varphi x} &\approx \frac{8Gr_{mx}^3}{3(1-\nu)}\left(1+\frac{2d}{r_{mx}}\right)\left(1+\frac{0.7d}{D_s}\right)\left(1+\frac{r_{mx}}{6D_s}\right), \\ K_{\varphi y} &\approx \frac{8Gr_{my}^3}{3(1-\nu)}\left(1+\frac{2d}{r_{my}}\right)\left(1+\frac{0.7d}{D_s}\right)\left(1+\frac{r_{my}}{6D_s}\right) \end{aligned} \tag{4.51}$$

In these expressions $r_a = \sqrt{(A_f/\pi)}$, $r_{mx} = (4I_x/\pi)^{1/4}$ and $r_{my} = (4I_y/\pi)^{1/4}$ are the radii of a circular footing with the same area or moment of inertia, respectively. G is the secant shear modulus of the soil at the expected shear strain level at a depth of $2r_a$ for K_z, or of $0.75r_{mx}$ or $0.75r_{my}$ for $K_{\varphi x}$, $K_{\varphi y}$, respectively. Part 5 of Eurocode 8 (CEN 2004c) gives indicative values of G equal to 80, 50 or 36% of its value at small strains ($<10^{-5}$), if the peak ground acceleration, a_gS, is 0.1, 0.2 or 0.3 g, respectively. The soil's Poisson ratio, ν, may be taken equal to 0.4 for stiff clays, 0.45 for soft clays or 0.33 for clean sands and gravels.

The fitting of Eqs. (4.50) and (4.51) to FE results applies if r_a, r_{mx}, r_{my} are all less than 50% of the stratum depth, D_s, but greater than the effective embedment depth, d.

More general and recent FE-based alternatives to Eqs. (4.50) and (4.51) are given in (ASCE 2007):

[14] Full lateral contact should develop over the effective embedment depth, capable of both sidewall friction and passive earth pressure. So, d cannot be more than the thickness of the footing and normally is less.

$$K_z = \frac{G_s\, b_x}{1-\nu}\left[1.55\left(\frac{b_y}{b_x}\right)^{\frac{3}{4}} + 0.8\right]\left[1 + \frac{2}{21}\frac{t}{b_x}\left(1 + 1.3\frac{b_x}{b_y}\right)\right]\left[1 + 0.32\left(\frac{d\,(b_y + b_y)}{b_x\, b_y}\right)^{\frac{2}{3}}\right] \tag{4.52}$$

$$K_{\varphi x} = \frac{G_s\, b_x^3}{1-\nu}\left[0.47\left(\frac{b_y}{b_x}\right)^{2.4} + 0.034\right]\left[1 + 1.4\left(\frac{d}{b_y}\right)^{0.6}\left(1.5 + 3.7\frac{\left(\frac{d}{b_y}\right)^{1.9}}{\left(\frac{d}{t}\right)^{0.6}}\right)\right] \tag{4.53a}$$

$$K_{\varphi y} = \frac{G_s\, b_x^3}{1-\nu}\left[0.4\frac{b_y}{b_x} + 0.1\right]\left[1 + 2.5\frac{d}{b_x}\left(1 + \frac{\frac{2d}{\sqrt{b_x\, b_y}}}{\left(\frac{d}{t}\right)^{0.2}}\right)\right] \tag{4.53b}$$

In these expressions b_x always denotes the smaller of the two plan dimensions of the footing and b_y the larger one ($b_x < b_y$); the x-axis is normal to b_x and the y-axis normal to b_y; d is again the effective embedment depth defined for Eqs. (4.50) and (4.51) and t the soil depth from the surface to the underside of the footing. The results of Eqs. (4.52) and (4.53) are consistent with those of Eqs. (4.50) and (4.51).

Sometimes, the elastic constants for the compliance of the soil under the footing are expressed in terms of k_s, for consistency with the subgrade reaction modulus approach followed for foundation beams and rafts. In that case, if Eq. (4.48) is retained for the soil's impedance in the vertical direction with $A_f = b_x b_y$, the following value of k_s should be used for consistent results with Eqs. (4.49) and (4.51) in approximately square footings:

$$k_s \approx \frac{2.3G}{b_x(1-\nu)} \tag{4.54}$$

where b_x is the smaller of the two plan dimensions of the footing. Note that Eq. (4.54) gives values about 75% higher than the expression normally used for k_s (Horvath 1983):

$$k_s \approx \frac{1.3G}{b_x(1-\nu)} \tag{4.54a}$$

The rotational impedances should then be computed from Eqs. (4.51) or (4.53), using in them a value of G obtained by inverting Eq. (4.54) for G in terms of k_s.

If the footing cannot be considered as rigid, the underlying soil should be modelled via Winkler springs spread out over the underside of the footing, having only vertical impedance. To better reflect the rotational impedance, the springs should be concentrated close to the edges of the footing in plan. The simplest layout would employ just four springs, each one close to a corner of the footing. The constant

of the springs should be chosen to reproduce the total vertical impedance of a rigid footing from Eqs. (4.50) or (4.52). With the so-determined spring constant, their distance in x and y should be chosen so that the rotational impedances from Eqs. (4.51) or (4.53) is reproduced. All this is arduous enough to dissuade the designer from choosing flexible footings. As pointed out at the beginning of this section, a thickness not less half the largest outhang of the footing from the vertical element it supports is commonly considered sufficient for a footing to be considered rigid.

4.9.9.5 Pile Foundations

When piles are used for the foundation of a building elastic supports in the horizontal directions are worth including, provided that this is done at all foundation elements, regardless of whether they are at the same horizontal level or not.

Groups of piles can be replaced by elastic supports at the group's centroid at the underside of the pile-cap. The group vertical or horizontal impedance is the sum of those of the individual piles, k_{zi}, k_{xi}, k_{yi}. Its rotational impedances about the horizontal axes are:

$$K_{\varphi x} = \sum_i (y_i^2 k_{zi} + k_{\varphi xi}), \quad K_{\varphi y} = \sum_i (x_i^2 k_{zi} + k_{\varphi yi}) \tag{4.55}$$

where x_i and y_i are measured from the centroid of the pile group. Point bearing is usually taken for a pile and the pile-head vertical stiffness, k_{zi}, is taken equal to the pile full axial stiffness, $E_c A/L$. The impedance of an individual pile in the horizontal directions, $k_x = k_y$, the rotational impedance, $k_{\varphi x} = k_{\varphi y}$, and the coupling stiffness, $k_{\varphi x,y} = k_{\varphi y,x}$, between the force along one axis and the rotation about the other, or the moment about one axis and the translation along the other, may be taken from the expressions given in Part 5 of Eurocode 8 (CEN 2004c) in terms of the pile diameter and Modulus of Elasticity, D and E_c:

– If the Modulus of Elasticity of the soil, E_s, is taken constant with depth:

$$\begin{aligned} k_x = k_y &= 1.08 D E_s \left(\frac{E_c}{E_s}\right)^{0.21} \quad k_{\varphi x} = k_{\varphi y} = 0.16 D^3 E_s \left(\frac{E_c}{E_s}\right)^{0.75} \\ k_{\varphi x-y} &= k_{\varphi y-x} = -0.22 D^2 E_s \left(\frac{E_c}{E_s}\right)^{0.5} \end{aligned} \tag{4.56a}$$

– If the soil Modulus is proportional to depth, with value E_s at a depth equal to the pile diameter:

$$\begin{aligned} k_x = k_y &= 0.6 D E_s \left(\frac{E_c}{E_s}\right)^{0.35} \quad k_{\varphi x} = k_{\varphi y} = 0.14 D^3 E_s \left(\frac{E_c}{E_s}\right)^{0.8} \\ k_{\varphi x-y} &= k_{\varphi y-x} = -0.17 D^2 E_s \left(\frac{E_c}{E_s}\right)^{0.6} \end{aligned} \tag{4.56b}$$

For soil Modulus proportional to the square root of depth, the coefficients and exponents in the applicable expressions assume average values between those in Eqs. (4.56a) and (4.56b).

4.9.9.6 Separating the Rigid-Body Motion from Seismic Analysis Results with Soil Compliance

It has been pointed out in Section 4.9.9.1 that, unless a rigid, box-type foundation system is provided for the entire structure, a representative picture of the distribution of seismic demands in the lateral load resisting system cannot be obtained, unless the model includes the compliance of the ground. This is also essential for the calculation of the action effects, seismic or not, which are necessary for the design or assessment of any tie-beams, foundation beams or a raft foundation.

If the soil compliance is recognised in the model by providing throughout the foundation elastic supports in the vertical direction and for rotation about the two horizontal axes, the inertial soil-structure-interaction effect of rocking is fully reflected in the 1st translational mode in each horizontal direction. Although, at least for elastic response, the ensuing reduction in the base shear and internal forces corresponds to physical reality, it might in some cases be beyond what is allowed by the code, or felt by the designer to be safe-sided. In such cases, most of (if not all) the favourable effects of soil-structure interaction on the period(s) and base shear(s) could be removed, without adversely affecting the accuracy of the distribution of internal forces in the structure. Measures to this end are outlined below.

Rigid body rocking of the structure is made possible, and affected, mainly by the vertical elastic supports, and less by the rotational ones about the two horizontal axes. The effect of rocking is normally confined in the 1st predominantly translational mode in each horizontal direction. Dunkerley's rule allows removing it from the value of the 1st period in direction X, T_{1X}, computed including soil compliance in the model:

$$T_{1X}^{*} = \sqrt{T_{1X}^{2} - T_{\varphi X}^{2}} \tag{4.57}$$

where T^{*}_{1X} is the estimate of the 1st mode period of the structure fixed to the ground and $T_{\varphi X}$ is the period of its rigid-body rocking in the vertical plane through direction X:

$$T_{\varphi X} = 2\pi \sqrt{\frac{\sum_{i} m_i (x_i^2 + z_i^2)}{\sum_{j} (K_{zj} x_j^2 + K_{\varphi yj})}} \tag{4.58}$$

In Eq. (4.58) i indexes the masses of the entire structure and j the support nodes at the foundation. Heights z are measured from the level of the foundation, while x is horizontal distance from the centroid in plan of the vertical impedence:

$$\sum_j K_{zi} x_j = 0 \tag{4.59}$$

The (modal) spectral acceleration can then be read from the response spectrum using the value of the period from Eq. (4.57). Similarly for direction Y.

Rigid-body rocking induces no internal forces. If desired, the influence of rocking on the 1st mode response in each horizontal direction can be essentially removed, not only from the internal forces, but also from the modal participation factor, the modal mass and the displacements that determine interstorey drifts and are of interest for the control of damage in nonstructural elements. Rigid-body rotation in the 1st mode within vertical plane XZ (positive when it is in the +Y direction) can be estimated from the ratio of the 1st mode overturning moment at the level of the foundation to the corresponding rotational stiffness:

$$\Phi_X \approx \frac{\sum_j (R_{zj} x_j - M_{yj})}{\sum_j (K_{zj} x_j^2 + K_{\varphi yj})} \tag{4.60a}$$

where j indexes again the support nodes, R_{zj} is the modal vertical reaction force (positive when it acts upwards on the structure) and M_{yj} is the modal reaction moment about axis Y (positive when its vector on the structure is in the +Y direction). To remove the effect of rocking from this mode, its eigenvector is modified by:

- subtracting Φ_X from all nodal rotations about the positive Y-axis;
- subtracting $\Phi_X z_i$ from all nodal displacements in direction X; and
- adding $\Phi_X x_i$ to all nodal vertical displacements (taken positive upwards).

where i indexes nodes on the structure. Modal internal forces obtained from the revised mode shape do not incorporate the effect of rocking (i.e., they refer to a structure fixed to the ground) and will be the same as from a model that includes soil compliance. The modal participation factor, the modal mass and the modal displacements will be different, though.

The rigid-body rotation in vertical plane YZ, Φ_Y, (positive when it is in the +X direction) is estimated as:

$$\Phi_Y \approx -\frac{\sum_j (R_{zj} y_j + M_{xj})}{\sum_j (K_{zj} y_j^2 + K_{\varphi xj})} \tag{4.60b}$$

where M_{xj} is modal reaction moment about axis X (positive when its vector on the structure is in the +X direction).The eigenvector of this mode is modified by:

- subtracting Φ_Y from all nodal rotations about the positive X-axis,
- subtracting $\Phi_Y z_i$ from all nodal displacements in direction Y, and
- adding $\Phi_Y y_i$ to the nodal displacements in direction Z.

Note that P–Δ effects include the contribution of rigid-body rocking on lateral drifts and should be computed before removing it.

If design for the vertical component of the seismic action uses the results of an elastic analysis of the full structure including vertical compliance of the soil, the effect of the latter should be removed from the calculated dynamic characteristics of the structure. Dunkerley's rule can be applied to the computed period, T_{1Z}, of the mode with the largest modal mass in direction Z:

$$T_{1Z}^{*} = \sqrt{T_{1Z}^{2} - T_{Z}^{2}} \tag{4.57a}$$

with the period of rigid-body vertical vibration of the structure on flexible soil computed as:

$$T_z = 2\pi \sqrt{\frac{\sum\limits_i M_i}{\sum\limits_j K_{zj}}} \tag{4.61}$$

To remove the contribution of rigid-body vertical vibration from the shape of this mode, a vertical displacement:

$$\delta_z = \sum_j R_{zj} / \sum_j K_{zj} \tag{4.62}$$

should be added to the modal vertical displacements (taken positive if upwards) of all nodes *i*. This changes the modal participation factor and the modal mass, but not the modal internal forces.

4.10 Modelling of Buildings for Nonlinear Analysis

4.10.1 Nonlinear Models for Concrete Members

4.10.1.1 The Level of Discretisation

Concrete structures are often discretised for nonlinear static analysis under monotonically increasing non-seismic loads at a point-by-point basis and modelled at the material level. A large number of FEs in 2D or 3D is used, with different Elements for the concrete and for the reinforcing steel and possibly for their interaction through bond. Such (micro-)modelling allows us, in principle, reproduce even minor details in the geometry of the members and follow the history of stresses and strains at every point. There has been immense progress in constitutive modelling of plain or reinforced concrete under generalised multiaxial loading (including reversals), in

mesh-independent FE representation of crack initiation and propagation and of the behaviour of crack interfaces, etc. (CEB 1996b, *fib* 2008). These advances notwithstanding, computational and memory requirements confine point-by-point nonlinear modelling to the analysis of the seismic response of individual members (especially shear walls) or subassemblies of members (e.g. beam-column joints, along with the beams and columns framing into them) and hamper its application to entire structures in 3D.

Practical nonlinear seismic response analysis, static or dynamic, of full RC structures is normally carried out using less sophisticated member-by-member modelling, with one-to-one correspondence between elements of the model and members of the structure. A single element is used for a beam, a column, the part of a wall between two floors, a panel of a floor-diaphragm between adjacent frames, etc. Although this does not account for every minute detail in the geometry and the reinforcement of a member, it allows a sufficiently close representation of the key features of its behaviour. Furthermore, it is capable of describing the distribution of inelasticity and damage among and within members with reasonable computational requirements even for large 3D structures. So, macro- or member-by-member modelling has been established as the main workhorse for practical nonlinear seismic response analysis of concrete structures and will remain so in the foreseeable future. Accordingly, only this modelling approach is covered here.

The starting point of the overview of member models is Fibre modelling. Fibre models fall in-between micro- and macro-modelling. They resemble macro-models in using member models as their building block. To develop the member model, though, the detailed σ-ε response at a large number of points over several cross-sections of the member is traced during the entire multi-step response analysis. Therefore, Fibre models may be considered as an application of the FE method to the one-dimensional continuum of a prismatic member, using the Bernoulli assumption of plane sections as a kinematic constraint to express the DoFs of the various points of a cross-section in terms of the three deformation measures of the section. They are the most fundamental, physically-based approach, capable of treating the general case of biaxial flexure and varying axial load, a special case of which is uniaxial bending with constant axial force. Fibre models are also closer to point-by-point FE modelling in what concerns their requirements in computer time and memory. Simpler member models are also derived in Sections 4.10.1.3 and 4.10.1.4 as simplifications of the fundamental Fibre approach.

If no member yields during the seismic response, nonlinear analysis degenerates into a linear one. Therefore, the models used in nonlinear analysis and their parameters should be such that linear-elastic behaviour can be described as a special case, without major discrepancies from the results of an ordinary linear analysis. This does not mean that the level of discretisation should be identical in the two types of analysis. Nonlinear analysis models may well be more refined, using at the member level, e.g., Fibre models, provided that they give about the same elastic stiffness as the simple member models used in linear analysis.

Before entering the description of the various modelling approaches and models, it is worth recalling that at each (time-)step *i* of a nonlinear seismic response analysis:

- the element tangent stiffness matrix, $\mathbf{K}_m{}^t$, is computed, to be assembled in the global stiffness matrix $\mathbf{K}_i$ in Eqs. (4.23),
- the vector of element internal nodal forces, $\boldsymbol{F}_m$, should be derived from the current deformation state of the element, to be assembled in the global internal force vector; and
- the difference between $\boldsymbol{F}_i$ in Eqs. (4.23) and the global internal force vector is equilibrated by iterations within the current step of the analysis, before proceeding to the next one.

4.10.1.2 Fibre Models

The most general, fundamental and powerful model for one-dimensional members is the Fibre model. It is also best suited for inhomogeneous materials, like RC (CEB 1996a). In a Fibre model the member is discretised both longitudinally, into segments represented by discrete cross-sections or slices, and at the cross-sectional level, into finite regions. If bending takes place within a single plane (uniaxial), the discretisation is into strips or "fibres" normal to this plane (e.g. Aziz 1976, Mark 1976). If bending is biaxial, the cross-section is divided into a number of rectangular finite regions, with sides parallel to the cross-sectional axes, y and z, see Fig. 4.6 (e.g. Menegotto and Pinto 1973, Aktan et al. 1974, Zeris and Mahin 1984). The generic fibre comprises concrete and/or reinforcing steel, lumped at the fibre centroid. The nonlinear uniaxial σ-ε laws of these two materials are

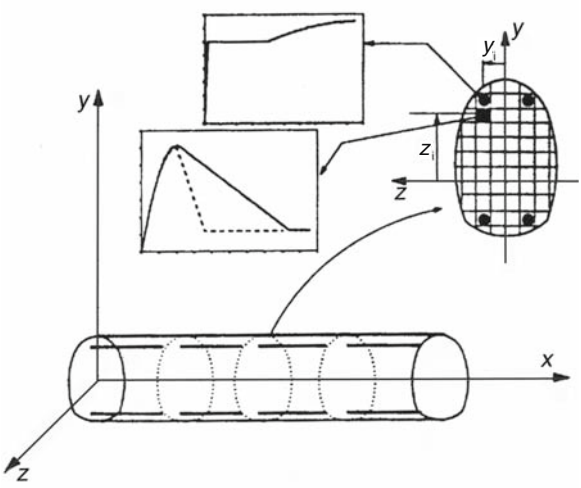

Fig. 4.6 Monitored sections and section subdivision in a Fibre model, adapted from CEB (1996a)

employed at that level. They take into account, in principle, stress reversals, concrete cracking, tension-stiffening and confinement, buckling of discrete reinforcing bars, etc.

In a Fibre model the normal strain at a point (y, z) of the member section at x along its axis is related to the section deformation vector[15]:

$$\boldsymbol{\varepsilon}_{\mathrm{s}}(x) = [\varphi_{\mathrm{y}}(x), \varphi_{\mathrm{z}}(x), \varepsilon_{\mathrm{o}}(x)]^{\mathrm{T}} \tag{4.63}$$

on the basis of the plane-sections assumption:

$$\varepsilon(x, y, z) = \boldsymbol{B}_{\mathrm{s}}(y, z)\boldsymbol{\varepsilon}_{\mathrm{s}}(x) \tag{4.64}$$

where:

$$\boldsymbol{B}_{\mathrm{s}}(y, z) \equiv [z, -y, 1] \tag{4.65}$$

The section force vector:

$$\boldsymbol{S}_{\mathrm{s}}(x) \equiv [M_{\mathrm{y}}(x), M_{\mathrm{z}}(x), N(x)]^{\mathrm{T}} \tag{4.66}$$

is derived from the normal stresses, $\sigma(y, z)$, over the section A as:

$$\boldsymbol{S}_{\mathrm{s}}(x) = \int_{\mathrm{A}} \boldsymbol{B}_{\mathrm{s}}{}^{\mathrm{T}}\sigma(x, y, z)\mathrm{d}A \tag{4.67}$$

It is incrementally related to $\boldsymbol{\varepsilon}_{\mathrm{s}}$ as:

$$\mathrm{d}\boldsymbol{S}_{\mathrm{s}}(x) = \mathbf{K}_{\mathrm{s}}{}^{\mathrm{t}}(x)\mathrm{d}\boldsymbol{\varepsilon}_{\mathrm{s}}(x) \tag{4.68}$$

where the section tangent stiffness matrix is:

$$\mathbf{K}_{\mathrm{s}}{}^{\mathrm{t}}(x) = \int_{\mathrm{A}} E^{\mathrm{t}}(x, y, z)\boldsymbol{B}_{\mathrm{s}}{}^{\mathrm{T}}\boldsymbol{B}_{\mathrm{s}}\mathrm{d}A \tag{4.69}$$

The tangent modulus $E^{\mathrm{t}}(x, y, z)$ is the ratio of $\mathrm{d}\sigma$ to $\mathrm{d}\varepsilon$ at point (y, z) of section x. It depends on the type of material at that point (i.e., whether it is steel or concrete), as well as on its previous σ- and ε-history, through the material cyclic σ-ε law.

The element nodal force vector at member end nodes A and B:

$$\boldsymbol{S}_{\mathrm{m}} \equiv [M_{\mathrm{y}}{}^{\mathrm{A}}, M_{\mathrm{z}}{}^{\mathrm{A}}, M_{\mathrm{y}}{}^{\mathrm{B}}, M_{\mathrm{z}}{}^{\mathrm{B}}, N, T]^{\mathrm{T}} \tag{4.70}$$

---

[15] In Eq. (4.63) φ_{y} denotes the curvature from the analysis and index y signifies the cross-sectional axis about which φ_{y} is defined. In this case index y has nothing to do with yielding.

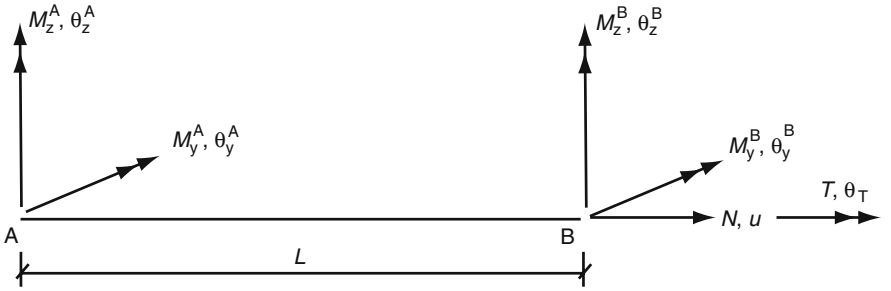

Fig. 4.7 Internal forces and element deformations at member ends

is incrementally related to the corresponding element deformation vector:

$$\boldsymbol{v}_{\mathrm{m}} \equiv [\theta_{\mathrm{y}}{}^{\mathrm{A}}, \theta_{\mathrm{z}}{}^{\mathrm{A}}, \theta_{\mathrm{y}}{}^{\mathrm{B}}, \theta_{\mathrm{z}}{}^{\mathrm{B}}, N, T]^{\mathrm{T}} \tag{4.71}$$

where θ_{y}, θ_{z} are the chord rotations at nodes A and B[16] and u, θ_{T} the relative displacement and the twist of these two nodes along and about the member axis x (see Fig. 4.7):

$$\mathrm{d}\boldsymbol{S}_{\mathrm{m}} = \mathbf{K}_{\mathrm{m}}{}^{\mathrm{t}}\mathrm{d}\boldsymbol{v}_{\mathrm{m}} \tag{4.72}$$

$\mathbf{K}_{\mathrm{m}}{}^{\mathrm{t}}$ in Eq. (4.72) is the element tangent stiffness matrix.

Following the classical elastic FE formulation, early Fibre models adopted for the construction of the element stiffness matrix a "stiffness-based" approach (Aktan et al. 1974). They postulate an invariant interpolation function matrix $\mathbf{B}_{\mathrm{m}}(x)$ for element deformations such that[17]:

$$\mathrm{d}\boldsymbol{\varepsilon}_{\mathrm{s}}(\mathrm{x}) = \mathbf{B}_{\mathrm{m}}(x)^{\mathrm{T}}\mathrm{d}\boldsymbol{v}_{\mathrm{m}} \tag{4.73}$$

Then, the principle of virtual displacements is invoked, to compute $\mathbf{K}_{\mathrm{m}}{}^{\mathrm{t}}$ as:

$$\mathbf{K}_{\mathrm{m}}{}^{\mathrm{t}} = \int_{\mathrm{L}} \mathbf{B}_{\mathrm{m}}(x)^{\mathrm{T}}\mathbf{K}_{\mathrm{s}}{}^{\mathrm{t}}(x)\mathbf{B}_{\mathrm{m}}(x)\mathrm{d}x \tag{4.74}$$

[16]In this section M^{A} and θ^{A} denote the moment and the chord rotation from the analysis at member end node A. Index y signifies the cross-sectional axis about which $M_{\mathrm{y}}{}^{\mathrm{A}}$ and $\theta_{\mathrm{y}}{}^{\mathrm{A}}$ are defined and has nothing to do with yielding.

[17]Note that the distribution of inelasticity along the member changes during the response. After plastic hinging, further flexural deformations take place mainly in the vicinity of the yielding end(s), spreading thereafter over the rest of the length with further loading. So, an interpolation function matrix $\mathbf{B}_{\mathrm{m}}(x)$ which is invariant during the response is against this physical reality.

as well as the increment of the internal nodal force vector:

$$\mathrm{d}\boldsymbol{F}_{\mathrm{m}} = \int_{\mathrm{L}} \mathbf{B}_{\mathrm{m}}(x)^{\mathrm{T}} \mathrm{d}\boldsymbol{S}_{\mathrm{s}}(x)\mathrm{d}x \tag{4.75}$$

with $\mathrm{d}\boldsymbol{S}_{\mathrm{s}}(\mathrm{x})$ from Eq. (4.68), etc.

For the integrations over its area, A, the cross-section at x is discretised into "fibres" or "filaments" of surface area $\mathrm{d}A$. For the calculation of $\mathrm{d}\sigma$ at point (x, y, z) and of $E^{\mathrm{t}}(x, y, z) = \mathrm{d}\sigma/\mathrm{d}\varepsilon$, the value of $\mathrm{d}\varepsilon$ calculated at the current step from Eqs. (4.64) and (4.73) and the cyclic σ-ε law of the material are not sufficient. Any other past-history information required by this law should be kept in memory at the section fibre level.

Integration over x along the member length L is in principle performed numerically. Integration stations may be equidistant, if the trapezoidal rule is used, or at irregular intervals more closely spaced near the ends, if a more elaborate but efficient scheme is adopted, such as Gauss or Gauss-Lobatto (with integration stations at each end and at three to seven sections in-between). Serious problems sometimes arise from the numerical integration. Once inelasticity develops at member ends, the variation of $\boldsymbol{\varepsilon}_{\mathrm{s}}(\mathrm{x})$ with x deviates significantly from that imposed by the use in Eq. (4.73) of an invariant $\mathbf{B}_{\mathrm{m}}(x)$ matrix (typically based on cubic Hermitian polynomials as in elastic FEs). This may cause, e.g., a spurious variation with x of the internal axial force $N(\mathrm{x}) = \int_{\mathrm{A}} \sigma(x, y, z)\mathrm{d}A$, which cannot be corrected through equilibrium iterations (CEB 1996a). A more serious problem can arise when the analysis proceeds beyond the ultimate strength at an end section. Then, if the end section continues loading on the post-ultimate strength softening branch, intermediate sections will unload elastically (CEB 1996a, Zeris and Mahin 1984). If post-ultimate strength softening is included in the model, this behaviour cannot be reflected by an invariant $\mathbf{B}_{\mathrm{m}}(x)$ matrix and causes numerical problems.

Nonlinear analysis programs with "stiffness-based" Fibre models sometimes attempt to by-pass the problems above by providing intermediate nodes between member ends, at a number sufficient to capture the distribution of inelasticity along the member even when using an invariant $\mathbf{B}_{\mathrm{m}}(x)$ matrix between the intermediate nodes (Izzuddin and Elnashai 1989, Millard 1993). Some programs even have the capability of automatically generating such internal nodes when member inelasticity develops and subsequently refine the mesh with the progression of inelasticity (Izzuddin and Elnashai 1989). To reduce computations for the solution of Eq. (4.22), all DoFs of these intermediate nodes may be condensed out statically, provided that there are no lumped masses there. Even without condensation, intermediate nodes do not overly increase the computational demands, as these are determined mainly from the need to keep track of fibre stresses and strains at the monitored sections and to perform the integration over the section.

"Flexibility-based" fibre models (Zeris and Mahin 1984, Kaba and Mahin 1984) tackle the problems above, but not fully. In them the section tangent flexibility matrix, $\mathbf{F}_{\mathrm{s}}{}^{\mathrm{t}}(x)$, obtained by inverting $\mathbf{K}_{\mathrm{s}}{}^{\mathrm{t}}(x)$, is integrated to give the element tangent flexibility matrix, $\mathbf{F}_{\mathrm{m}}{}^{\mathrm{t}}$:

$$\mathbf{F}_{\mathrm{m}}{}^{\mathrm{t}} = \int_{\mathrm{L}} \mathbf{e}(x)^{\mathrm{T}} \mathbf{F}_{\mathrm{s}}{}^{\mathrm{t}}(x) \mathbf{e}(x) \mathrm{d}x \tag{4.76}$$

The element equilibrium matrix, $\mathbf{e}$(x), relating $\boldsymbol{S}_{\mathrm{s}}(x)$ to $\boldsymbol{S}_{\mathrm{m}}$ as:

$$\boldsymbol{S}_{\mathrm{s}}(x) = \mathbf{e}(x) \boldsymbol{S}_{\mathrm{m}} \tag{4.77}$$

is exact irrespective of the distribution of inelasticity along the member, if no loads are applied between its two ends. As $\mathrm{d}\boldsymbol{\varepsilon}_{\mathrm{s}}(x) = \mathbf{F}_{\mathrm{s}}{}^{\mathrm{t}}(x)\mathrm{d}\boldsymbol{S}_{\mathrm{s}}(x) = \mathbf{F}_{\mathrm{s}}{}^{\mathrm{t}}(x)\mathbf{e}(x)\mathrm{d}\boldsymbol{S}_{\mathrm{m}} = \mathbf{F}_{\mathrm{s}}{}^{\mathrm{t}}(x)\mathbf{e}(x)\mathbf{K}_{\mathrm{m}}{}^{\mathrm{t}}\mathrm{d}\boldsymbol{v}_{\mathrm{m}}$, incremental internal nodal forces, $\mathrm{d}\boldsymbol{F}_{\mathrm{m}} = \int_{\mathrm{L}} \mathbf{B}_{\mathrm{m}}(x)^{\mathrm{T}} \mathrm{d}\boldsymbol{S}_{\mathrm{s}}(x)\mathrm{d}x$, can be calculated using a non-invariant flexibility-dependent matrix $\mathbf{B}_{\mathrm{m}}(x)$, continuously updated during the analysis as: $\mathbf{B}_{\mathrm{m}}(x) = \mathbf{F}_{\mathrm{s}}{}^{\mathrm{t}}(x)\mathbf{e}(x)\mathbf{K}_{\mathrm{m}}{}^{\mathrm{t}}$ while the internal nonlinearities vary (Mahasuverachai and Powell 1982). An inconsistency persists regardless, this time between the section forces $\boldsymbol{S}_{\mathrm{s}}(x)$ computed at the section level from Eq. (4.67) and those derived from nodal forces through Eq. (4.77). So do most numerical and physical problems associated with the "stiffness-based" approach. To solve them without introducing intermediate nodes, more complex mixed two-field models (with assumed force and deformation distributions) have been proposed (Taucer et al. 1991).

Although Fibre models are based on the plane-sections assumption, they can account for nonlinear shear deformations of the member. A shear strain, γ, that depends on the element shear force $V = (M^{\mathrm{A}} + M^{\mathrm{B}})/L$ through the nodal moments M^{A}, M^{B}, may be considered as a fictitious chord rotation and added to the flexural ones at member ends (CEB 1996a). However, the possibility of shear failure cannot be detected and accounted for in this way.

Fixed-end rotation at the end section of the member due to slippage of longitudinal bars from the joint region beyond that end may be taken into account by introducing a nonlinear rotational spring at that end, similar to those of the one-component point-hinge model in Sections 4.10.1.4 and Fig. 4.9. The tangent flexibility of such a rotational spring at end A or B within one of the two orthogonal planes of bending, xy or xz, is denoted here by f_{A} or f_{B}, respectively. These terms are added to the diagonal ones, f_{AA} and f_{BB}, relating the increments of inelastic chord rotations, $\mathrm{d}\theta_{\mathrm{A}}$, $\mathrm{d}\theta_{\mathrm{B}}$, with respect to chord AB to those of the end moments, $\mathrm{d}M_{\mathrm{A}}$, $\mathrm{d}M_{\mathrm{B}}$, in the Fibre model's element tangent flexibility matrix, $\mathbf{F}_{\mathrm{m}}{}^{\mathrm{t}}$ (obtained from Eq. (4.76) in the "flexibility-based" approach, or by inverting the element tangent flexibility matrix $\mathbf{K}_{\mathrm{m}}{}^{\mathrm{t}}$ of Eq. (4.74) in the "stiffness-based" one):

$$F_{\mathrm{m,total}}{}^{t} = \begin{bmatrix} f_{\mathrm{AA}} + f_{\mathrm{A}} & f_{\mathrm{AB}} \\ f_{\mathrm{AB}} & f_{\mathrm{BB}} + f_{\mathrm{B}} \end{bmatrix} \tag{4.78}$$

The total element tangent flexibility matrix, $\mathbf{F}_{\mathrm{m,total}}{}^{\mathrm{t}}$, obtained by adding diagonal flexibility terms, f_{A}, f_{B}, within each one of the two orthogonal planes of bending, xy or xz, is then inverted to give the tangent stiffness matrix of the element. At each end, let's say A, and within the corresponding plane of bending, this

term may be approximated as $f_A = \theta_{y,slip}/M_y$ before flexural yielding and as $f_A = \Delta\theta_{u,slip}/(M_u\text{-}M_y)$ afterwards; $\theta_{y,slip}$ and $\Delta\theta_{u,slip}$ may be estimated from Eqs. (3.42) in Section 3.2.2.3 and (3.63) in Section 3.2.2.9, respectively, while M_y, M_u can be obtained as $\int_A \sigma y_{cg} dA$ from the fibre discretisation of the end section, or according to Sections 3.2.2.2 and 3.2.2.5, respectively (with the effects of any lap-splicing, FRP-wrapping or prestressing taken into account on the basis of Sections 3.2.3.9, 3.2.3.10 or 3.2.3.11, respectively). As shown in Fig. 3.45(d), the hysteresis loops of the fixed-end rotation due to bond-slip are narrow, with inverted-S shape. This type of behaviour may be captured by the hysteresis rules of models with pinching (Roufaiel and Meyer 1987, Costa and Costa 1987, Park et al. 1987, Reinhorn et al. 1988, Coelho and Carvalho 1990) in Section 4.10.1.6 and Table 4.4, if the pinching parameters are judiciously chosen.

Fibre models account for the details of the geometry of the cross-section and of the distribution of the reinforcement, can follow the spreading of inelasticity along the member and reproduce realistically pinching of moment-curvature hysteresis loops. As they use directly realistic σ-ε laws of the individual materials (possibly including confinement of concrete, strength and stiffness degradation due to low-cycle fatigue, buckling of bars, etc.) Fibre models are "fundamental" models. In principle, they can take into account the effects of biaxial bending (see Sections 3.2.3.7 and 3.2.3.8), the coupling between bending and the axial direction (Section 3.2.3.6), as well as the effects of a varying axial load (see Section 3.2.2.8). The simplified member-type models described in the following, by contrast, try to capture the complex overall behaviour of the member through phenomenological rules and semi-empirical hysteresis relations between moment and curvature or moment and plastic hinge rotation (see Sections 4.10.1.5 and 4.10.1.6). Notwithstanding their power and rationality, Fibre models require at each step of the analysis lengthy computations to construct the member tangent stiffness matrix and calculate stresses and strains at the fibre level at each slice, as well as tracing all the σ- and ε-history information of each fibre which is necessary for the calculation of the tangent modulus and the stress at the current strain. So, Fibre models are far more demanding in computer time and storage than the simplified member-type models described in Sections 4.10.1.3, 4.10.1.4, 4.10.15 and 4.10.1.6. Note that the larger the number of nonlinear operations required by a computational scheme, the higher is the likelihood of a local numerical instability spreading throughout the structure. Last, but not least, the input properties and parameters of Fibre models should be carefully tuned, to reproduce the experimental behaviour of the member, including its connections. Such tuning requires specialised knowledge and experience, beyond current capabilities of design professionals. All things considered, it is not at all certain that the power and rationality of Fibre models warrant their generalised practical use.

To avoid the large computational requirements of Fibre models while retaining their main strength, namely their ability to capture biaxial effects and axial-flexural coupling, it has been proposed to replace discretisation of the section and monitoring of the σ-ε history at the fibre level with incremental relations between the section force and deformation vectors, $\boldsymbol{\varepsilon}_s(x)$ and $\boldsymbol{S}_s(x)$, or between the nodal force and deformation vectors, $\boldsymbol{S}_m$ and $\boldsymbol{v}_m$. Such models are overviewed in Fardis

(1991) and CEB (1996a). Some of them use forms of Plasticity Theory in 3D (e.g. Sfakianakis and Fardis 1991a, b, Bousias and Fardis 1994, Bousias et al. 2002). They may suffer though from similar or even worse numerical problems than Fibre models. Besides they do not enjoy their generality. So, they do not seem to be viable alternatives.

The unique advantage of Fibre models is their ability to take into account the effects of biaxial bending and the coupling between bending and the axial direction. When bending is essentially in a single plane and axial-flexural coupling is of no interest (e.g. in beams) there may be little point in using a Fibre model instead of the simpler alternatives described in Sections 4.10.1.3, 4.10.1.4, 4.10.15 and 4.10.1.6. When using a Fibre model in such cases, tinkering with its axial DoFs or with those associated with out-of-plane bending should be avoided. For example, if the cross-section is asymmetric with respect to what is considered as a single plane of bending, restraining its out-of-plane rotation will have a parasitic (normally stiffening) effect on the computed in-plane flexure. By the same token, constraining the nodal displacements at the two ends of the element to be the same introduces a fictitious axial force in the element and changes its inelastic flexural behaviour. If we want to restrain or constrain such DoFs for reasons of computational efficiency, we would better use a simple model for uniaxial bending without axial-flexural coupling, of the type described in Sections 4.10.1.3 or 4.10.1.4.

4.10.1.3 Spread Inelasticity Models with Phenomenological M-φ Relations for Uniaxial Bending Without Axial-Flexural Coupling

In beams bending is uniaxial while axial-flexural coupling is commonly considered as irrelevant.[18] For walls, only inelastic flexure in their strong direction of bending is of interest, while axial-flexural coupling, although important (see Section 2.2.2.4), is often ignored. In columns, as we will see in Section 4.10.1.4, the inelastic flexural response is often treated independently in the two directions of bending for simplicity, while only few aspects of axial-flexural coupling are considered in each direction. Therefore, uniaxial bending with axial-flexural coupling ignored or treated in a simplified way, is of prime practical importance.

For uniaxial bending the tangent flexibility matrix of section x, $\mathbf{F}_s{}^t(x)$, degenerates into a scalar section flexibility, $f_s{}^t(x) = \mathrm{d}\varphi\,/\mathrm{d}M$ and its tangent stiffness matrix into the section rigidity, $k_s{}^t(x) = \mathrm{d}M/\mathrm{d}\varphi$. The element tangent stiffness matrix, $\mathbf{K}_m{}^t$, is of dimension 2×2 and relates the nodal moment increments vector, $[\mathrm{d}M^A, \mathrm{d}M^B]^T$, to the chord rotations increments vector, $[\theta^A, \theta^B]^T$. The spreading of flexural inelasticity along the member renders meaningless the constant elastic interpolation vector, $\boldsymbol{b}_m(x) = (2/L)[(3x/L–2), (3x/L–1)]$, into which the elastic interpolation function matrix $\mathbf{B}_m(x)$ of Eq. (4.73) degenerates (see footnote to Eq. (4.73)). So, it makes more sense physically to adopt the flexibility approach and compute the 2×2 member tangent flexibility matrix $\mathbf{F}_m{}^t$ of Eq. (4.76), using $f_s{}^t(x) = \mathrm{d}\varphi\,/\mathrm{d}M$ for $\mathbf{F}_s{}^t(x)$ and $\mathbf{e}(x) = [(x/L\text{-}1), x/L]$ as the equilibrium matrix.

[18] It is also very uncertain and difficult to model, as it very much depends on the width of the slab which is effective as a flange of the beam.

In the present case the prime strength of Fibre modelling at the section level, namely their ability to capture biaxial effects and axial-flexural coupling, is irrelevant. So, to determine the tangent rigidity of the section it is not necessary to discretise the generic cross-section into fibres, monitor the σ-ε response there and perform the integration in Eq. (4.69). Instead, a hysteretic relation between moment and (smeared) curvature may be adopted, describing phenomenologically the experimental behaviour or the one analytically derived, e.g., from a fibre model used once to fit the phenomenological one. The *M*-φ relation may be chosen among the models presented in Section 4.10.1.6. This is the first simplification advanced here.

The second step for the reduction of the large computational demands of the fundamental fibre approach and bypassing some of its problems, is to construct the member tangent flexibility matrix without calculating the tangent flexibility at various intermediate control sections of the member and numerically integrating Eq. (4.76). Instead, Eq. (4.76) is integrated analytically, using control sections only at the ends, but still accounting for the actual distribution of inelasticity along the member ("spread inelasticity" models). In this way the inconsistency between the section forces $\boldsymbol{S}_s(x)$ from Eq. (4.67) and those from Eq. (4.77) is bypassed.

If the instantaneous bending moment diagram due to the combination of the seismic and the gravity actions is approximately linear near each member end, plastification extends up to a distance (normalised to the member length, *L*) from end A or B, respectively, equal to:

$$\lambda_A = (M_A - M_y^A)/(V_A L) \geq 0, \qquad \lambda_B = (M_B - M_y^B)/(V_B L) \geq 0 \tag{4.79}$$

with the yield moment, $M_y{}^A$ or $M_y{}^B$, taken constant throughout each plastic zone. If the phenomenological *M*-φ relation adopted is multi-linear, having elastic rigidity *EI* before yielding and tangent rigidities in primary loading, unloading or reloading expressed through their piece-wise constant ratios to *EI*, φ will also vary linearly along each dimensionless length λ_A and λ_B. Then, the element tangent flexibility matrix $\mathbf{F}_m{}^t$ of Eq. (4.76) may be analytically computed, using $f_s{}^t(x) = d\varphi/dM$ for $\mathbf{F}_s{}^t(x)$ and $\mathbf{e}(x) = [(x/L–1), x/L]$ for the equilibrium matrix (Filippou and Issa 1988):

$$\mathbf{F}_m{}^t = \begin{bmatrix} f_{AA} & f_{AB} \\ f_{AB} & f_{BB} \end{bmatrix} \tag{4.80}$$

where:

$$f_{AA} = \frac{1 + \dfrac{1-(1-\lambda_A)^3}{p_A} + \dfrac{\lambda_B^3}{p_B}}{3EI/L}, \; f_{AB} = -\frac{1 + \dfrac{\lambda_A^2\left(3-2\lambda_A\right)}{p_A} + \dfrac{\lambda_B^2\left(3-2\lambda_B\right)}{p_B}}{6EI/L},$$
$$f_{BB} = \frac{1 + \dfrac{1-(1-\lambda_B)^3}{p_B} + \dfrac{\lambda_A^3}{p_A}}{3EI/L} \tag{4.81}$$

In Eq. (4.81) p_A and p_B denote the ratios of the effective tangent rigidity within the plastic zone near end A or B, respectively, to the difference of that rigidity from *EI*. It is assumed that when the end section unloads, reloads or is in primary loading, the full length of the corresponding plastic zone does the same. If the plastic zone near end A is in primary loading, all its sections have the same tangent rigidity, *pEI*, where *p* is the hardening ratio in primary loading. Then $p_A = p/(1–p)$. If it unloads or reloads, the tangent section rigidity is not constant anymore along its length. It has its minimum value, EI_A, at the end section, which unloads or reloads from the maximum curvature in the zone, while it is equal to *EI* at a distance $\lambda_A L$ from A, where the section is elastic. If the effective tangent rigidity of the plastic zone corresponds to the average tangent flexibility along $\lambda_A L$, i.e., to $(1/EI+1/EI_A)/2$, then $p_A = 2EI_A/(EI–EI_A)$ (which gives $1/p_A = 0$ in Eq. (4.81) for unloading parallel to the elastic branch). Similarly for the plastic zone near end B and p_B (Filippou and Issa 1988).

The values of λ_A, λ_B in Eq. (4.81) are non-decreasing, giving the maximum ever length of plastification at the corresponding end. The flexibility matrix evolves owing to changes in the state of the two plastic zones from loading (or reloading) to unloading, or vice-versa, or to an increase in their length.

The elastic rigidity, *EI*, to be used in Eq. (4.81) and as the basis for p_A and p_B may be taken equal to M_y/φ_y, with M_y and φ_y computed according to Section 3.2.2.2. For *primary loading* p_A or p_B may be taken equal to:

$$p_A(or\ p_B) = \frac{\left(M_u - M_y\right) / \left(\varphi_u - \varphi_y\right)}{M_y/\varphi_y - \left(M_u - M_y\right) / \left(\varphi_u - \varphi_y\right)} \tag{4.82}$$

with M_u and φ_u determined according to Sections 3.2.2.5 and 3.2.2.4, respectively. The effects of any lap-splicing, FRP-wrapping or prestressing on M_u, M_y, φ_u, φ_y, may be taken into account on the basis of Sections 3.2.3.9, 3.2.3.10 or 3.2.3.11, respectively, as relevant. Different values of unloading or reloading rigidity $EI_A = dM/d\varphi$ applies at A for each unloading or reloading branch and a different value of p_A is derived from it as $p_A = 2EI_A/(EI–EI_A)$ (similarly for end B and p_B). The phenomenological hysteretic M-φ model determines how the unloading rigidity depends, in general, on the point of (M and φ) reversal where unloading starts and how the reloading rigidity depends on the value of φ where reloading starts and on the M-φ point where it is heading at, etc. (see Section 4.10.1.6).

Strictly speaking the value of $EI = M_y/\varphi_y$ in Eq. (4.81) for loading that induces tension at one side of the section at A and at the opposite side at B (i.e., hogging moment at A and sagging at B) is different from the *EI*-value applying for loading that induces compression at these two sides (sagging moment at A, hogging at B). This is very inconvenient, as the *EI* values of members determine the global dynamic characteristics of the elastic structure (natural periods and mode shapes), which are considered as independent of the direction of loading. So, we should use in Eq. (4.81) the average *EI* value of the two ends (also average value for positive and negative bending, if the section is asymmetrically reinforced). Different values

of p_A and p_B can be used at A and B (and for positive or negative bending for asymmetrically reinforced sections).

Spread inelasticity models with phenomenological M-φ relations account only for flexural deformations within the clear length of the member. Fixed-end rotations at the end sections due to slippage of longitudinal bars from the joint region beyond the end may be taken into account as in Fibre models, i.e., via nonlinear rotational springs at the ends as described in Section 4.10.1.2 in conjunction with Eq. (4.78).

Spread inelasticity models cannot, in principle, account for coupling of the two directions of bending, and between them and the axial forces and deformations. If used for columns, they are commonly in the form of two uncoupled uniaxial models, one for each of the two orthogonal directions of bending. Although the two twin elements representing the column share its axial force and each has 50% of its full axial stiffness, the full value of the axial force should be used for the calculation of the properties of each one of the two twin elements. The value of the elastic stiffness, EI, should be fixed during the response and calculated from the values of M_y, φ_y due to the axial force for gravity loads alone. It is fairly simple, though, and normally does not create numerical problems, to update the yield moment, M_y, and (with it) the maximum-ever values of λ_A and λ_B from Eq. (4.79), and the hardening ratios p_A, p_B from Eq. (4.82) using the current axial force value. This will make a difference in exterior columns of medium- or high-rise buildings and in piers of coupled walls, where the axial force varies a lot during the response. The value of M_y, and the post-elastic primary loading branch derived from it through Eq. (4.82), may be considered constant during further primary loading. After reversal, by contrast, and while reloading in the reverse direction, the value of M_y in that direction should be updated according to the evolution of the axial force. By the same token, the value of the uniaxial yield moment signalling plastification of the end section may be taken to decrease with increasing current moment component in the orthogonal direction (see Sections 3.2.3.7 and 3.2.3.8). This is computationally more cumbersome, though, than tracing the axial load and accounting for it, not only owing to the complications associated with biaxial moment interaction diagrammes, but also because each one of the two uncoupled uniaxial elements used for the column normally is unaware of the current state of bending in its companion. All in all, the returns in accuracy from attempts to emulate Fibre models may not warrant the sacrifice in simplicity they entail.

4.10.1.4 "Point-Hinge" or "Lumped Inelasticity" Models

Under lateral actions flexural inelastic deformations are concentrated at and near member ends, since it is there that bending moments have maximum values. So in the early inelastic beam models inelasticity was taken to be concentrated ("lumped") at the ends of the member in zero-length "point hinges".

In the earliest inelastic model, the *two-component element* (Clough et al. 1965), the member is considered as a system of two components *in parallel* (Fig. 4.8):

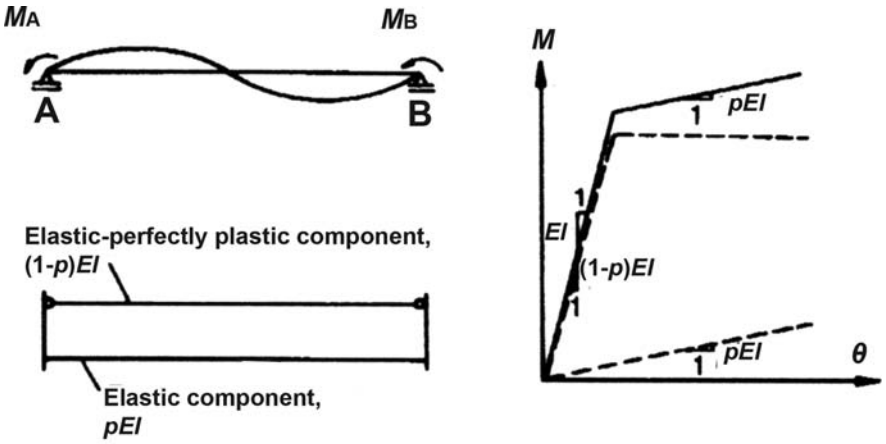

Fig. 4.8 Two-component element model

- The first component is an elastic-perfectly plastic beam and represents yielding. Before yielding at the beam's ends, it is an elastic beam element. After the moment reaches the yield value at an end, the tangent stiffness matrix becomes that of an elastic member with a moment release there. If the yield moment is reached at the other end as well, the tangent stiffness matrix is that of a member with moment releases at both ends.
- The second component is an elastic beam and represents post-yield hardening. Its section rigidity is a small fraction, p, of the elastic rigidity, EI, of the member.

The tangent stiffness matrices of the two components are added and the composite member exhibits a bilinear (elastic-linearly strain hardening) moment-rotation behaviour with a hardening rigidity of pEI. In order for the sum of the elastic section rigidities of the two components to give that of the member, EI, the elastic rigidity of the elastic-perfectly plastic component is equal to $(1–p)EI$.

The hysteretic behaviour of the two-component model is bilinear, with unloading and reloading branches parallel to those in primary (virgin) loading. Such a cyclic behaviour may fit well steel members with stable hysteresis loops exhibiting a moderate Bauschinger effect. It does not represent well the degradation of unloading and reloading stiffness and the narrow hysteresis loops of concrete members. So, it is appropriate only when there is essentially a single inelastic excursion of the member and we are interested only in the magnitude of the peak inelastic deformation. The two-component model significantly overestimates energy dissipation when the member goes through several inelastic cycles. It has been included regardless in the libraries of widely used general purpose nonlinear dynamic analysis software, because in some cases it has certain advantages over the equally simple alternatives represented by the one-component model described next.

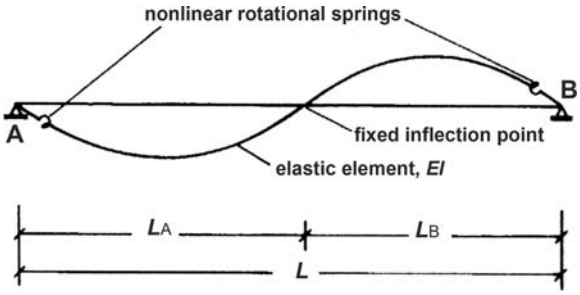

Fig. 4.9 One-component element model

To avoid the bilinear hysteresis inherent in the two-component model, a *one-component element* has been proposed in Giberson (1967). It is a *series model* of an elastic element and nonlinear rotational springs at its ends (Fig. 4.9). All inelastic deformations are lumped at the two end springs. The two nonlinear end springs are taken to contribute to the tangent flexibility matrix of the member with diagonal terms f_A, f_B alone, as in Eq. (4.78). For uniaxial bending $\mathbf{F}_m{}^t$ is:

$$\mathbf{F}_m{}^t = \frac{L}{6EI}\begin{bmatrix} 2 + a_A / p_A & -1 \\ -1 & 2 + a_B / p_B \end{bmatrix} \tag{4.83}$$

where:

- a_A and a_B are zero-one variables for plastic hinging at the end sections:
  - $a_A = 0$ before plastic hinging at end A, i.e., so long as $M^A < M_y{}^A$;
  - $a_A = 1$ after plastic hinging there, i.e., for $M^A \geq M_y{}^A$;

  and similarly for a_B at end B;
- $p_A = (L/(6EI))/f_A$, $p_B = (L/(6EI))/f_B$ are the current tangent stiffnesses of the rotational springs, as a fraction of the elastic stiffness of the member in skew-symmetric bending, $6EI/L$.[19] During the course of cyclic loading or response, piece-wise constant values of f_A, f_B are derived from the multilinear rules in Section 4.10.1.5 for primary loading and Section 4.10.1.6 for unloading-reloading.

$\mathbf{F}_m{}^t$ is inverted to give the member's tangent stiffness matrix, $\mathbf{K}_m{}^t$. For uniaxial bending $\mathbf{K}_m{}^t$ is:

$$\mathbf{K}_m{}^t = \frac{6EI/L}{3 + 2\,(a_A/p_A + a_B/p_B) + (a_A/p_A)\,(a_B/p_B)}\begin{bmatrix} 2 + a_B/p_B & 1 \\ 1 & 2 + a_A/p_A \end{bmatrix} \tag{4.84}$$

[19] Unlike the two-component element, which turns into a fully elastic model if $p = 1$, the one-component element can reproduce elastic overall behaviour only through very large values of the yield moments, $M_y{}^A$, $M_y{}^B$, at which the point hinges at the ends A and B are activated. As the rotational springs are in series with the elastic element in-between, setting $p_A = p_B = 1$ for them just increases the overall flexibility of the element (doubles it for skew-symmetric bending).

In the two- or the one-component element the rigidity of the member section, EI, may be taken equal to the secant-to-yield-point stiffness, EI_{eff}, from Section 3.2.3.3, Eq. (3.68). Fixed-end rotations due to slippage of longitudinal bars from the joint region beyond the member ends can then be reflected in EI_{eff}, through the term involving a_{sl} in Eq. (3.66). If the longitudinal reinforcement is different at the two end sections of the member, Eq. (3.68) gives two different values of EI_{eff} there. Moreover, if the end sections are asymmetrically reinforced (as in beams with different reinforcement at top and bottom), the value of EI_{eff} is different for each sense of bending (positive or negative). According to the reasoning at the 2nd paragraph from the end of Section 4.10.1.3, the average value of EI_{eff} over the two ends and the two senses of bending is used then as rigidity of the member section, EI, in the two- or the one-component model.

The calculated nonlinear seismic response does not depend heavily on the exact value of the single hardening ratio in primary loading, p, of the two-component model, or of the two hardening ratios, p_{A}, p_{B}, of the one-component one in the individual members. So, default constant values, such as 0.05, 0.1, or even sometimes zero, are often used for *primary loading*. More representative values may be estimated from the member properties:

$$p = \frac{\left(M_u - M_y\right) / \left(\theta_u - \theta_y\right)}{M_y/\theta_y - \left(M_u - M_y\right) / \left(\theta_u - \theta_y\right)} \tag{4.85}$$

For the purposes of Eq. (4.85) M_{u}, M_{y} may be computed according to Sections 3.2.2.5 and 3.2.2.2, respectively. Sections 3.2.3.5 (or 3.2.3.4) and 3.2.3.2, may be used for the calculation of the chord rotations θ_{u} and θ_{y}, respectively. The effects of any lap-splicing or FRP-wrapping may be taken into account on the basis of Sections 3.2.3.9 and 3.2.3.10, respectively. Note that hardening ratios for primary loading have higher values in terms of chord rotations (i.e. from Eq. (4.85)) than curvatures (from Eq. (4.82)), often by a factor of 2 to 3. A single hardening ratio, p, is used in the two-component model, namely the average over the two ends and for positive and negative bending. The one-component model can use different values of p_{A} and p_{B} at A and B (and for positive or negative bending for asymmetrically reinforced sections, although an average value is also acceptable).

Implicit in the use of the secant stiffness to the yield-point from Section 3.2.3.3, Eq. (3.68), as EI_{eff} in the one- or two-component model is the assumption of constant values of the member axial load and of the shear span, L_{s}, at each end. The same for the estimation of the hardening ratio in primary loading from Eq. (4.85). For all practical purposes the axial load may be taken equal to the value due to gravity loads alone. The choice of a constant value for the shear span (i.e, the distance of an end section where plastic hinging may take place under lateral loading to the inflection point) is less clear cut. For a frame member, especially a beam, the natural choice is to assume that plastic hinges will develop in skew symmetric bending at both sections where the member frames into transverse ones within the plane of bending. Then, the shear span is half the clear length from one beam-column joint to the next

within the plane of bending: $L_s = L_{cl}/2$.[20] Plastic hinging in walls takes place only at the storey's bottom section and indeed with an imaginary point of inflection well above that storey. As pointed out in Section 2.2.2.2, the shear span of the entire part of a wall between floors, defined as the moment-to-shear ratio at the storey's bottom section, is about 50% of the height from that section to the top of the wall, $L_s = H_{tot}/2$.

An inflection point that stays steady after the first excursion of the member into the inelastic range is also a necessary condition for the inelastic part of the one-component model's tangent flexibility matrix to be diagonal, i.e., with diagonal terms f_A, f_B alone, without coupling between the two ends. Establishing the values of the hardening ratios, p_A, p_B, of this model on the basis of a fixed shear span value at the corresponding end implies that a steady inflection point has indeed been assumed.

A point-hinge or lumped inelasticity member model is intentionally very simple. So, it does not, and cannot, aspire to account for coupling of the two directions of bending, and between them and the axial forces and deformations. It can be used for columns as two separate and uncoupled uniaxial models, one for each of the two orthogonal directions of bending, sharing the axial force and the column's full axial stiffness. As pointed out in the last paragraph of Section 4.10.1.3, any plastic hinge property in each one of the two twin elements should be calculated on the basis of the full axial force of the column. The value of EI_{eff} should be considered fixed during the response, as calculated from the values of M_y, θ_y due to the axial force for gravity loads alone. It is fairly simple, though, and normally does not give rise to numerical problems, to activate a hinge when the end moment reaches the current yield moment, M_y, as determined from the current value of the axial force. The value of M_y and the post-elastic primary loading branch derived from it may be considered constant during further primary loading. After reversal and during reloading in the opposite direction, the value of M_y in that direction should be updated according to the evolution of the axial force. The plastic hinge will be activated in the reverse direction when this updated value of M_y, or the post-elastic primary loading branch derived from it, are reached. Finally, as pointed out in the last paragraph of Section 4.10.1.3, in principle a non-zero concurrent moment component in the orthogonal direction may be taken into account to reduce the value of the uniaxial yield moment for activation/re-activation of a plastic hinge (see Section 3.2.3.8). However, with the same reasoning as at the end of Section 4.10.1.3, any gains in accuracy are not worth sacrificing the inherent simplicity of the one-component point-hinge model.

---

[20] In a beam indirectly supported on another beam at one end, plastic hinging can take place only at the other end and the beam's shear span may be taken equal to the beam full clear span. In girders connected at intermediate points with cross-beams or girders, plastic hinging will develop only at the girder's connection with vertical members. Then the shear span is determined on the basis of the girder clear span between columns into which the girder frames. Although the parts of a girder between joints with cross-beams may be modelled as individual beam elements, their effective elastic stiffness and hardening ratios should be taken the same, as established from the clear span of the overall girder.

Notwithstanding its lack of generality and inherent limitations, the lumped inelasticity one-component model has become the workhorse for practical nonlinear – especially dynamic – seismic response analysis. Obvious incentives for the user are its flexibility, intuitive appeal, simple computational implementation and use, minimal computational requirements and superior numerical robustness. There are good technical reasons as well for its practical application:

- The most common form of the one-component point-hinge model works directly with chord rotations, which encompass shear deformations of the member and fixed-end rotations due to bond-slip of longitudinal bars from their anchorage zones. So, compared with Fibre or spread inelasticity models based on curvatures, it lends itself better to fitting or calibrating model parameters using directly the wealth of member test results, typically given as force-deflection (i.e., -chord rotation) hysteretic loops, without differentiating between flexural and shear deformations or bond-slip effects of longitudinal bars from the anchorage. As a matter of fact, most (if not all) empirical hysteresis rules of Section 4.10.1.6 have been empirically developed from such test data and suit better models that use chord rotations. For the same reason, the portfolio of tools offered in Chapter 3 for the derivation of model parameters in terms of chord rotations are wider in scope and more robust (i.e., associated with smaller scatter or bias) than those for curvatures.
- The material σ-ε behaviour traced in Fibre models, including yielding, rupture or even buckling of bars and local crushing of concrete, cannot be directly translated into loss of member lateral- or axial-load resistance. By contrast, member ultimate conditions, conventionally identified with permanent loss of peak lateral load resistance, are most conveniently described by response variables at the member level, notably by chord rotations or shear forces for ultimate condition due to flexure or shear, respectively.

All things considered, the one-component point-hinge model seems to provide at present the best option for practical nonlinear seismic response analysis, static or dynamic, of concrete buildings with realistic size and complexity in 3D, either for evaluation of the performance of a new design or for assessment and retrofitting of an existing building. The rationality, power and generality of Fibre models can best be used in the realm of research.

4.10.1.5 The Uniaxial M-φ or M-θ Curve for Monotonic or Primary Loading

To be consistent with the linear analysis into which it degenerates if no member yields during the seismic response, nonlinear analysis should use about the same pre-yield stiffness as a usual linear analysis. As emphasised in Sections 3.2.3.3 and 4.9.2, the elastic stiffness of the monotonic force-deformation relation of members should be the secant stiffness to the yield-point, so that the global elastic stiffness corresponds to the elastic branch of a bilinear monotonic global force-deformation relation. It has also been pointed out there that, if a default elastic

stiffness of one-half the uncracked gross section stiffness is used, e.g., for consistency with linear analysis, deformation demands are seriously underestimated. This may ruin the very end of nonlinear analysis, namely the estimation of seismic deformation demands to be compared to the corresponding capacities, be it for assessment (and/or retrofitting) of existing buildings or for performance evaluation of new designs. Normally, realistic values are used for the capacities, as, e.g., given in Chapter 3 and in Annex A of CEN (2005a). Therefore, the estimates of the demands should also be realistic. This can indeed be achieved if the effective elastic stiffness of members is taken equal to their secant stiffness to the yield-point from Eq. (3.68), as Annex A of CEN (2005a) recommends doing in assessment and retrofitting of concrete buildings on the basis of nonlinear or linear analysis.

A realistic value of the elastic stiffness up to the yield point of all members is more vital for nonlinear dynamic than for static analysis, because important contributions of higher modes to inelastic response often entail post-yield excursions in members which may stay in the elastic range under the fundamental mode alone. In pushover analysis it is primarily (if not only) the "target displacement" that is affected by the global stiffness of an effective elasto-plastic system normally fitted to the capacity curve on the basis of equal deformation energy (equal areas, see Fig. 4.2). This stiffness is in turn not seriously affected by a fictitiously high early stiffness of certain members.

The corner point of a bilinear force-deformation relation in primary loading is the yield point of the member, as governed by the member's most critical (i.e. weakest) mechanism of force transfer, in flexure, brittle shear or bond of longitudinal bars. Brittle shear failure before plastic hinging is catastrophic and once it occurs lateral load resistance is considered to be lost. The M-φ or M-θ relation in monotonic or primary loading stops then at a value of the end moment $M = V_R L_s < M_y$ where V_R is the resistance in brittle shear and L_s and M_y are the shear span and the yield moment at the end in question. By contrast, ductile shear failure occurs in a flexural plastic hinge, after the hinge forms. The yield point is still at the yield moment.

In addition to the elastic stiffness and the yield strength, a main parameter of a bilinear monotonic force-deformation relation is the post-elastic stiffness. A meaningfully long post-elastic branch is due to flexural inelastic deformations and normally exhibits strain hardening. A constant hardening ratio (: post- to pre-yield stiffness) is given by Eq. (4.82) or (4.85) in M-φ or M-θ terms, respectively. Recall, however, that the monotonic (also called primary) M-φ or M-θ curve serves as skeleton to the hysteresis loops in cyclic loading, which may entail significant strength decay when ultimate deformation is approached.[21] So, to make room for post-elastic strength degradation, positive strain hardening in flexure may be neglected for simplicity and zero post-yield stiffness may be used, as Eurocode 8 allows doing.

The end point of the primary loading curve is the ultimate deformation. If governed by flexure, it is the ultimate curvature, φ_u, or chord rotation, θ_u, in M-φ or M-θ terms, respectively. Sections 3.2.2.4 and 3.2.3.5 (or 3.2.3.4) may be used to compute φ_u and θ_u, respectively, with the effect of any lap-splicing, FRP-wrapping or

[21] Recall, in this connection, that the ultimate deformation is conventionally identified with a drop in peak force resistance after ultimate strength equal to 20% of the ultimate strength value.

prestressing taken into account on the basis of Sections 3.2.3.9, 3.2.3.10 or 3.2.3.11, respectively, as relevant. For cyclic loading the primary loading curve may end at the point where the acting shear force in the plastic hinge is found to exceed the cyclic resistance against ductile shear failure according to Sections 3.2.4.3, 3.2.4.5 or 3.2.5.4, at a value of the chord rotation less than θ_u.

A residual post-ultimate moment resistance may be retained in the model afterwards. However, there is no solid technical support for the selection of its level. Note, though, that the question of residual resistance is academic. For the performance of a structure to be verified as acceptable in practical applications, every single member (new, retrofitted, or existing and non-retrofitted) should be verified in the end to have ultimate deformation well above the seismic demand (see Section 6.5.6 and Table 6.1). So, there is no real need to introduce an abrupt drop in resistance after the ultimate deformation.

Unlike the elastic stiffness, which should be the same, all other parameters of the primary loading curve may be different for positive and negative loading, depending on how symmetric the geometry and the reinforcement of the section is.

Eurocode 8 requires as a minimum a bilinear primary loading curve in nonlinear member models. It allows, though, using instead a trilinear curve, as, e.g., in Takeda et al. (1970), Park et al. (1987), Reinhorn et al. (1988) and Costa and Costa (1987) to take into account the difference between pre- and post-cracking stiffness. If used as skeleton curve for cyclic loading, such a trilinear curve produces certain hysteretic damping before yielding, which increases from zero at cracking to a maximum value at yielding. Moreover, from cracking to yielding the secant stiffness of the trilinear model does not have a unique value. This ambiguity does not allow direct comparisons with the elastic response spectrum predictions, let alone conformity with linear analysis in the pre-yielding stage. So, it is strongly recommended to use in nonlinear dynamic analysis member models with bilinear force-deformation relationship in primary loading.[22] After all, by the time of a strong earthquake concrete members most likely will be cracked owing to gravity loads, thermal strains and drying shrinkage, or even previous shocks. In nonlinear static analysis a trilinear monotonic force-deformation relationship for members affects only the initial part of the "capacity curve", without the problems and ambiguities it causes in nonlinear dynamic analysis.

4.10.1.6 Phenomenological Models for the Cyclic Uniaxial M-φ or M-θ Behaviour

The M-φ or M-θ curve in primary loading suffices for nonlinear static analysis and serves as skeleton curve in nonlinear response-history analysis. It is supplemented there with hysteresis rules for post-elastic unloading-reloading cycles.

The main objective of nonlinear response-history analysis in practical applications is the estimation of member peak seismic deformation demands, to be compared to the corresponding capacities. Estimates of member peak deformation demands depend on the hysteretic energy dissipation inherent in

[22] By the same token, the tensile strength of concrete should be neglected in Fibre models.

unloading-reloading rules, but are little affected by their precise shape and other details.[23] For this reason, the only requirement posed by Eurocode 8 on hysteretic models is to realistically reflect energy dissipation within the range of displacement amplitudes induced in members by the seismic action used for the analysis. Moreover, as the predictions of nonlinear dynamic analysis for peak response are not highly sensitive to the hysteresis rules, a more essential feature of the hysteretic model for applications is its numerical robustness under any potential response history. This is of utmost importance, as any numerical weakness of the model will certainly show up during at least one of the ground motions for which a system with hundreds of members is analysed in thousands of time-steps, possibly with a few iterations in each step. Numerical problems at the member level might spread and develop into global ones, preventing convergence. Even when the stabilising effect of inertia forces and damping salvages global stability, local numerical problems may lead to errors in member demands, which an inexperienced eye cannot detect. Simple and clear hysteretic models, using few rules to describe the response under any (small or large, full or partial) cycle of unloading and reloading, are less prone to numerical problems than elaborate and presumptuous ones, especially when complexity obscures certain unlikely possibilities with dangerous outcomes.

Multilinear unloading and reloading from and to the skeleton curve or to a reloading branch (Fig. 4.10) is simple and computationally efficient. Using δ as the generic symbol for deformation (φ or θ), unloading from a maximum ever value of $\delta = \mu\delta_y$ on the primary loading branch is typically taken linear down to a residual deformation on the δ-axis, $\delta_{res} = \varepsilon\delta_y$, which is different in different hysteretic models according to Table 4.3. Note that the models in Park et al. (1987), Reinhorn et al. (1988) and Costa and Costa (1987) have trilinear monotonic or primary loading curve, using its pre-cracking branch to define the unloading slope. This definition may be retained even when a bilinear model is used, with the first two branches

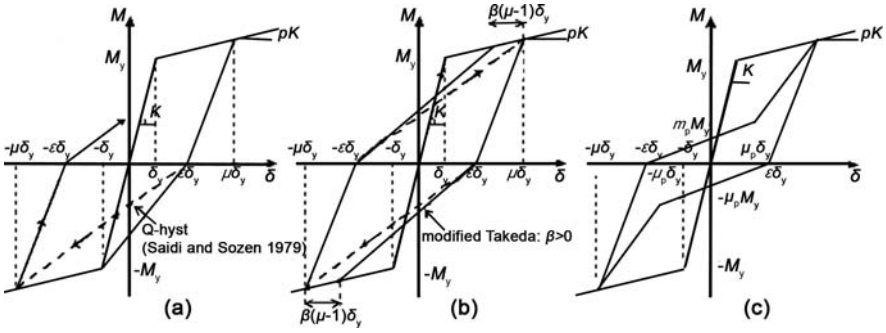

Fig. 4.10 Multilinear hysteretic models: (**a**) straight reloading to past peak point; (**b**) straight reloading to point before past peak (Otani 1974, Litton 1975); (**c**) with pinching

[23]Residual deformations are very much affected by the details of the hysteresis rules. However, their estimation is even more influenced by the details of the ground motion. So, if estimation of residual deformations is indeed of interest, current rules about the minimum number of input motions and their conformity to 5%-damped elastic response spectrum should be revisited.

Table 4.3 Residual deformation after unloading from deformation $\delta = \mu\delta_y$ on primary loading curve ($\mu > 1$, p: hardening ratio of post-yield primary loading branch)

Hysteresis model	Unloading rule	Residual deformation $\delta_{res}=\varepsilon\delta_y$
Takeda et al. (1970), and Clough and Johnston (1966)	Unloading stiffness = elastic stiffness	$\varepsilon = (1-p)(\mu-1)$
Saiidi and Sozen (1979), Coelho and Carvalho (1990), Anagnostopoulos (1972), and Costa and Costa (1987)	Unloading stiffness = μ^{-a} times the elastic stiffness ($a \approx 0.5$ or from Eq. (4.90))	$\varepsilon = \mu - (1 + p(\mu-1))\mu^{a}$
Otani (1974), and Litton (1975)	Unloading to residual deformation (1–α) times that in elastic unloading ($\alpha \approx 0.3$ or from Eq. (4.91))	$\varepsilon = (1-\alpha)(1-p)(\mu-1)$
Park et al. (1987), and Reinhorn et al. (1988)	Extension of unloading passes through point on opposite direction's pre-cracking elastic branch where $M = aM_y$ ($a \approx 2$)	$\varepsilon = \dfrac{a(1-p)(\mu-1)}{a+1+p(\mu-1)}$
Roufaiel and Meyer (1987)		$\varepsilon = \dfrac{(1-p)(\mu-1)}{1+2p(\mu-1)}$

replaced by a single one to yielding, as suggested here. The models in Otani (1974), Litton (1975), Clough and Johnston (1966), Saiidi and Sozen (1979), Roufaiel and Meyer (1987), Park et al. (1987), Reinhorn et al. (1988), Coelho and Carvalho (1990) and Costa and Costa (1987) include degradation of unloading stiffness (see point 2 in Section 3.2.2.6).

If unloading to the δ-axis continues into first-time loading in the reverse direction, it heads linearly towards the yield point of the primary loading curve in that direction and follows its post-elastic branch thereafter. If the reverse direction has been revisited before, we have reloading. It is in reloading that the model accounts or not for pinching of the hysteresis loops. If it doesn't, then the extreme point ever reached on the primary loading curve in that direction normally becomes an effective yield point to which reloading linearly heads[24] (Fig. 4.10). In (Otani 1974, Litton 1975) this straight reloading branch is directed towards a point on the primary loading curve before the previous peak, at a deformation of $[\mu-\beta(\mu-1)]\delta_y$ instead of $\mu\delta_y$ ($0 < \beta < 1$). Models without pinching (Takeda et al. 1970, Otani 1974, Litton 1975, Clough and Johnston 1966, Saiidi and Sozen 1979) are more suitable for the M-φ behaviour.

[24]Except in Saiidi and Sozen (1979), where this branch always heads towards the point on the primary loading at the maximum deformation ever reached in any of the two directions, even when this is first-time loading or real reloading.

Table 4.4 Moment and deformation at corner of bilinear reloading for models with pinching

Model	Reloading branch from (–) to (+) starting at residual deformation $-\varepsilon_{-}\delta_y^{-}$	m_p for $M_p = m_p M_y$, and μ_p for $\delta_p = \mu_p \delta_y$
Park et al. (1987)	Reloading heads first toward point where $M = \gamma M_y$ ($\gamma \approx 0.5$) on extreme branch of past unloading in (+) direction from peak past deformation $\delta^+ = \mu_+ \delta_y{}^+$ on primary loading branch to residual deformation $\delta_{res}{}^+ = \varepsilon_+ \delta_y$. It stiffens towards δ^+ on primary loading branch when $\delta_{res}{}^+$ is reached	$m_p^+ = \dfrac{(\varepsilon_+ + \varepsilon_-)\,\gamma\left[1 + p_+(\mu_+ - 1)\right]}{(\varepsilon_+ + \varepsilon_-)\left[1 + p_+(\mu_+ - 1)\right] + \gamma(\mu_+ - \varepsilon_+)}$ $\mu_p^+ = \varepsilon_+$ For reloading from (+) to (–) $m_p^- = \dfrac{(\varepsilon_+ + \varepsilon_-)\,\gamma\left[1 + p_-(\mu_- - 1)\right]}{(\varepsilon_+ + \varepsilon_-)\left[1 + p_-(\mu_- - 1)\right] + \gamma(\mu_- - \varepsilon_-)}$ $\mu_p^- = \varepsilon_-$
Reinhorn et al. (1988)	Reloading heads first toward point where $M = \gamma M_y$ ($\gamma \approx 0.5$) on pre-cracking elastic branch in (+) direction. It stiffens towards past peak point on primary loading branch when peak residual deformation $\delta_{res}{}^+ = \varepsilon_+ \delta_y$ is reached	$m_p^+ = \dfrac{(\varepsilon_+ + \varepsilon_-)\,\gamma}{\gamma + \varepsilon_-}$, $\mu_p^+ = \varepsilon_+$ For reloading from (+) to (–): $m_p^- = \dfrac{(\varepsilon_+ + \varepsilon_-)\,\gamma}{\gamma + \varepsilon_+}$, $\mu_p^- = \varepsilon_-$
Roufaiel and Meyer (1987)	Reloading to point on elastic branch where $M = mM_y$ ($m = \min[1; (0.4L_s/h – 0.6)] \geq 0$). It stiffens then towards peak past deformation on primary loading branch	$m_p = m$, $\mu_p = m$
Coelho and Carvalho (1990)	Reloading has stiffness m-times that of reloading to the peak past deformation $\delta^+ = \mu_+ \delta_y{}^+$ on primary loading branch. It stiffens towards peak past point on primary loading branch when M-axis is reached ($m < 1$).	$m_p^+ = \dfrac{m\varepsilon_-\left[1 + p_+(\mu_+ - 1)\right]}{\mu_+ + \varepsilon_-}$, $\mu_p = 0$ For reloading from (+) to (–): $m_p^- = \dfrac{m\varepsilon_+\left[1 + p_-(\mu_- - 1)\right]}{\mu_- + \varepsilon_+}$, $\mu_p = 0$
Costa and Costa (1987)	Reloading first has stiffness $\mu_+{}^{-\beta}$-times that of reloading to the peak past deformation $\delta^+ = \mu_+ \delta_y{}^+$ on primary loading branch ($\beta > 0$). It stiffens towards peak past point on primary loading branch when secant from origin to that point is reached.	$\mu_p^+ = \dfrac{\varepsilon_-\left[1 + p_+(\mu_+ - 1)\right]}{\mu_+\left(\varepsilon_-\mu_+^{\beta-1} + \mu_+^{\beta} - 1\right)}$ $m_p^+ = \dfrac{\varepsilon_-}{\varepsilon_-\mu_+^{\beta-1} + \mu_+^{\beta} - 1}$ For reloading from (+) to (–): $\mu_p^- = \dfrac{\varepsilon_+\left[1 + p_-(\mu_- - 1)\right]}{\mu_-(\varepsilon_+\mu_-^{\beta-1} - 1 + \mu_-^{\beta})}$ $m_p^- = \dfrac{\varepsilon_+}{\varepsilon_+\mu_-^{\beta-1} + \mu_-^{\beta} - 1}$

To include pinching, reloading heads first towards a corner point where the moment is denoted by $M_p = m_p M_y$ ($m_p < 1$) and the deformation by $\delta_p = \mu_p \delta_y$. It turns then towards the extreme point ever reached on the primary loading curve in the current direction of reloading (Fig. 4.10). Table 4.4 gives the values of m_p and μ_p for different hysteretic models that include pinching (Roufaiel and Meyer 1987, Park et al. 1987, Reinhorn et al. 1988, Coelho and Carvalho 1990, Costa and Costa 1987). Such models are more suitable for the overall M-θ behaviour that includes the effects of shear deformations and fixed-end rotation.[25] With appropriately chosen pinching parameters they may also describe the flexibility of nonlinear rotational springs added at ends A and B of a Fibre model, to account separately for the fixed-end rotations due to slippage of longitudinal bars from the joint region beyond that end (terms f_A, f_B in Eq. (4.78)).

Reloading after partial unloading (i.e., before the horizontal axis is reached) follows the unloading path toward the point of last reversal. If unloading resumes before that point is reached, it continues along the same unloading branch towards the δ-axis. If reloading turns into unloading before reaching its destination, i.e., the extreme past point on the primary loading curve in the current reloading direction, the unloading stiffness is the one corresponding to the original destination of reloading.

In some models (Park et al. 1987, Reinhorn et al. 1988, Coelho and Carvalho 1990, Costa and Costa 1987) reloading is directed to a point below (i.e. with lower peak resistance) than the extreme past point on the primary loading curve of that direction. In new buildings with detailing of members for ductility, degradation of strength with cycling is negligible. Besides, in general cyclic strength decay has small effect on the computed response. For given primary loading curve, the response is more sensitive to the amount of hysteretic energy dissipation, an issue addressed in the next section.

4.10.1.7 Hysteretic Damping Ratio in Cyclic Uniaxial Models

The hysteretic energy dissipation in post-yield cycles of given amplitude may be conveniently expressed as an equivalent hysteretic damping ratio, ζ, of a linearly-damped oscillator with the same natural period, that dissipates the same amount of energy per cycle as the nonlinear one:

$$\zeta = \frac{E_h}{4\pi E_{el}} \tag{4.86}$$

where E_h is the energy dissipated in a full cycle of loading-unloading-reloading and E_{el} is the elastic strain energy, $F_{max}\delta_{max}/2$, at the peak force and displacement of the cycle.

With ε according to Table 4.3, the *first full cycle* of loading-unloading-reloading to peak ductility ratio $\pm\mu$ gives the following hysteretic damping ratio (Fardis and Panagiotakos 1996):

[25] The pinching parameters of the model in Roufaiel and Meyer (1987) depend indeed on the shear span ratio, to reflect the more pronounced pinching of squat members.

$$\zeta_{n=1} = \frac{2(\mu-1)(1-p+\varepsilon p)+3\varepsilon}{4\pi\mu(1+p(\mu-1))} \tag{4.87}$$

except for the Q-hyst model in Saiidi and Sozen (1979), which gives:

$$\zeta_{n=1,Q} = \frac{(\mu-1)(1-p+3\varepsilon p)+3\varepsilon}{4\pi\mu(1+p(\mu-1))} \tag{4.87a}$$

Models without pinching (Takeda et al. 1970, Clough and Johnston 1966, Saiidi and Sozen 1979) or strength decay (Fig. 4.10a) produce the following hysteretic damping ratio in a *full subsequent cycle* of unloading-reloading to peak ductility ratio $\pm\mu$ (Fardis and Panagiotakos 1996):

$$\zeta_{n>1,no-pinching} = \frac{\varepsilon}{\pi\mu} \tag{4.88}$$

except in Otani (1974) and Litton (1975), where reloading towards a point on the primary loading curve at deformation $[\mu\text{-}\beta(\mu\text{-}1)]\delta_y$ instead of $\mu\delta_y$ (Fig. 4.10b) gives a hysteretic damping ratio in a full subsequent cycle (Fardis and Panagiotakos 1996):

$$\zeta_{n>1,\boldsymbol{Otani}} = \frac{\varepsilon}{\pi\mu}\left(1+\frac{\beta(1-p-p\varepsilon)}{2(1-\alpha)(1+p(\mu-1))}\right) \tag{4.88a}$$

If strength decay is neglected, models with pinching (Roufaiel and Meyer 1987, Park et al. 1987, Reinhorn et al. 1988, Coelho and Carvalho 1990, Costa and Costa 1987) according to Fig. 4.10c and with m_p and μ_p from Table 4.4 produce the following hysteretic damping ratio in a subsequent full cycle of unloading-reloading to peak ductility ratio $\pm\mu$ (Fardis and Panagiotakos 1996):

$$\zeta_{n>1,pinching} = \frac{1}{2\pi\mu}\left(\varepsilon-\mu_p+\frac{m_p(\varepsilon+\mu)}{1+p(\mu-1)}\right) \tag{4.89}$$

Note that the equivalent damping given by Eqs. (4.87), (4.88), (4.88a) and (4.89) as a function of ductility ratio $\pm\mu$ refers to the energy dissipation in a single cycle to that ductility ratio, at the same period of oscillation as the linear system. If applied using the peak ductility ratio, μ, that takes place in a seismic response history having cycles of varying amplitude, Eqs. (4.87), (4.88), (4.88a) and (4.89) significantly overestimate the average damping ratio of a linear system with the same period of oscillation. They can only be used to evaluate a model's ability to reflect the hysteretic energy dissipation in members, as derived through Eq. (4.86) from the experimental response. On this basis, Fardis and Panagiotakos (1996) used about 190 cyclic uniaxial tests with several cycles of pre- and post-yield loading to derive through Eq. (4.86) experimental pairs of μ and ζ for RC members. The large scatter of individual data, even within a family of specimens with the same geometric and mechanical properties or even in a single test, obscures the difference between

the first post-yield cycle and subsequent ones reflected by Eqs. (4.87) and (4.88). For given value of $\mu > 1$, ζ on average increases with increasing shear span ratio, L_s/h, decreasing axial load ratio, ν, increasing ratio of confining steel and decreasing ratio of longitudinal reinforcement. However, only the dependence on L_s/h is statistically strong. Statistical fitting with a presumed hardening ratio p=0.02 has given the following expressions for certain model parameters (Fardis and Panagiotakos 1996):

– exponent a for unloading in (Saiidi and Sozen 1979, Coelho and Carvalho 1990, Anagnostopoulos 1972, Costa and Costa 1987):

$$a = 0.84 - 0.09\frac{L_s}{h} \tag{4.90}$$

– coefficient α for unloading in (Otani 1974, Litton 1975):

$$\alpha = 0.75 - 0.095\frac{L_s}{h} \tag{4.91}$$

– pinching parameter m in (Roufaiel and Meyer 1987):

$$m = 0.465 \tag{4.92}$$

The data suggest significant energy dissipation in post-cracking, pre-yield load cycles, equivalent to a damping ratio of about 8%, almost independently of the amplitude of loading and of specimen characteristics. This may mean that, if a bilinear model is used, it may be physically more appropriate to use a damping value higher than 5% in the damping matrix **C** characterising elastic response. However, this will bring about inconsistencies with the default, conventional value of 5% associated with elastic response spectra in codes.[26]

4.10.1.8 Concluding Remarks on Concrete Member Models for 3D Analyses

It is natural to expect that a nonlinear seismic response analysis is at least as good as a linear one in tackling general design situations in their full complexity. However, the nonlinear static analysis method has been developed for analysis of the seismic response in 2D (no matter whether the structural model is in 3D) and its applicability for truly 3D response is still questionable. The nonlinear dynamic method can, in principle, be applied for seismic response analysis in 3D, although it has been developed primarily for 2D analysis. Application of nonlinear seismic response analysis

[26] As a matter of fact, the universal value of 5% damping associated in codes with elastic response spectra is just a compromise between the lower values acknowledged for prestressed concrete and structural steel with bolted or welded connections on one hand and the higher ones for cracked concrete members.

in 3D presumes that appropriate member models under 3D loading are available. As emphasised is Section 4.10.1.2, Fibre models serve well this end. However, their large requirements in computer time and memory, the exponential increase of the risk of numerical problems with the amount of calculations and the specialised knowledge and experience needed to tune Fibre models to the experimental behaviour, limit currently their applicability in practical design and assessment. Point hinge models cannot represent well the post-elastic behaviour of members in two orthogonal directions without sacrificing the simplicity, flexibility and reliability/numerical stability that make them the model of choice for practical nonlinear analysis in 2D. The currently common use of one independent and uncoupled point hinge model in each horizontal direction is acceptable, when the nonlinear response is primarily in one of the two directions of bending, as is often the case in fairly symmetric buildings under a single horizontal seismic action component. However, it may be insufficient – and as a matter of fact unconservative – for two concurrent horizontal components and/or for strongly torsional response due to irregularity in plan. All in all, the lack of reliable, yet simple and inexpensive models for the inelastic cyclic behaviour of vertical members in two transverse directions is still the single most serious challenge for full-fledged nonlinear seismic response analysis in 3D, static or dynamic.

4.10.2 Nonlinear Modelling of Masonry Infills

4.10.2.1 Modelling of the Cyclic Behaviour

As the main features of the cyclic behaviour of infills have not been presented elsewhere in the book, they are highlighted here, together with their modelling.

The macroscopic behaviour of an infill panel may be described in terms of either:

1. the total infill shear force, V, and the relative horizontal displacement between top and bottom of the panel, δ; the ratio of δ to the clear infill panel height, H_{cl}, gives the smeared shear strain of the panel, $\gamma = \delta/H_{\mathrm{cl}}$, which is essentially the interstorey drift ratio of the surrounding frame; or
2. the axial force in the compressed diagonal (the equivalent strut), F, and the corresponding shortening of the diagonal, or, equivalently, the compressive strain along the diagonal, ε.

The panel shear strain, γ, and the diagonal compressive strain, ε, are related as: $\gamma = 2\varepsilon/\sin 2\theta$. The infill shear force, V, is the horizontal projection of the diagonal strut's axial force, F: $V = F\cos\theta$, where θ is the angle between the horizontal and the panel diagonal: $\theta = \arctan(H_{\mathrm{cl}}/L_{\mathrm{cl}})$. So the pairs V-γ and F-ε are interchangeable. With this in mind, the infill panel behaviour is described and modelled in what follows in generic force-deformation terms, F-δ.

The response of an infill panel to monotonic or primary loading may be approximated as a multilinear curve (dashed line $\mathrm{OA_oU_oR_o}$ in Fig. 4.11). A minor change in stiffness at the first separation of the infill from the frame may be neglected and

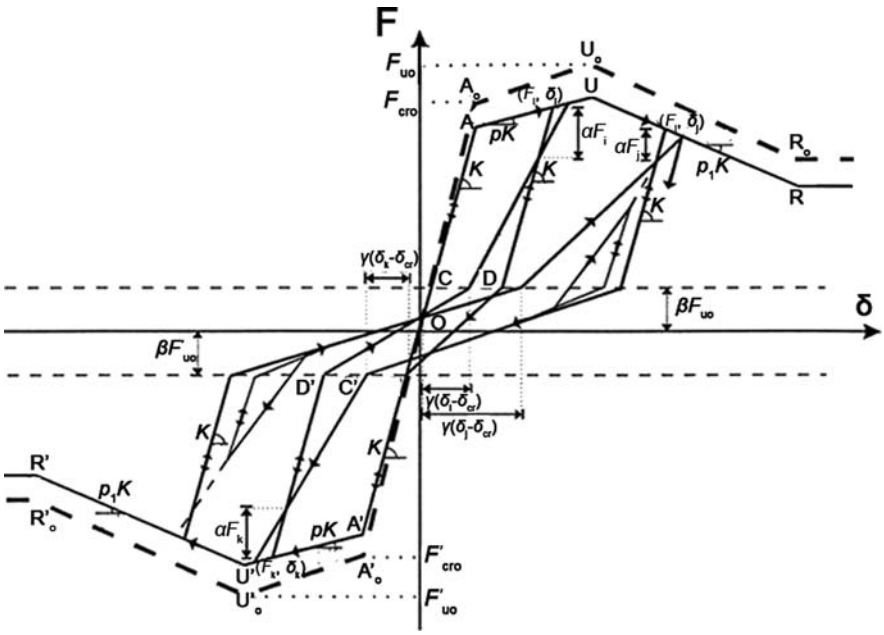

Fig. 4.11 Cyclic force-deformation model of infill panel in Panagiotakos and Fardis (1994) and Fardis and Panagiotakos (1997a)

the first change in slope at point A_o may be taken to correspond to the first visible cracking of the panel. The peak point, U_o, is at ultimate strength. The post-ultimate-strength branch may also be taken linear, leading to the horizontal residual strength branch. If there are asymmetric openings, the virgin loading curve in the opposite direction, $OA_o'U_o'R_o'$, may not be a mirror image of $OA_oU_oR_o$ with respect to O.

Under cyclic loading the primary loading curve is the skeleton and envelope for reloading. In the model described here (Panagiotakos and Fardis 1994, Fardis and Panagiotakos 1997a), which is a refinement and extension of Tassios (1984), the primary loading curve, OAUR in Fig. 4.11 gradually degrades with cyclic deformations. Specifically, if in a post-cracking half-cycle i, a maximum ever peak deformation is reached, δ_i, for positive, δ_i', for negative, then the ordinates of the corner points of the primary curve decrease as:

$$F_j = F_{jo}\, e^{-a\frac{\sum_i \delta_i}{\delta_{cr}} - a'\frac{\sum_i \delta'_i}{\delta'_{cr}}} \tag{4.93}$$

where j denotes points A (or cr), U (or u) and R, j' points A′, U′, and R′ in the reverse direction, $\delta_{cr} = F_{cro}/K_o$ is the cracking displacement, (with δ_{cr}' defined similarly in the reverse direction) and a, a' are parameters.

Before the infill cracks, unloading and reloading takes place along the non-degraded first branch of the virgin loading curve with the initial elastic stiffness

K_o (respectively K'_o). After cracking, unloading from the skeleton curve, e.g., from (F_i, δ_i), takes place initially with a slope equal to the degraded (by cycling) elastic stiffness, $K = F_{cr}/\delta_{cr}$, until the force is reduced to a fraction α of the non-degraded value of the ultimate force, F_{uo}. Unloading below that force level and continuation into first loading or reloading in the opposite direction after the δ-axis is reached are softer, as cracks open in the direction of reloading and contact with the frame is lost. This takes place before full closure of the cracks and re-instatement of contact in the past (opposite) direction of loading. The softer unloading-reloading branch heads towards point D′, where cracks and interfaces in the previous loading direction do close and cracking and loss of contact in the new loading direction stabilises. Point D is at a force $-\beta F_{uo}'$ and at a horizontal distance $\gamma(\delta_k - \delta_{cr}')$ from point C′, which is also at a force $-\beta F_{uo}'$ but on the elastic branch. $\delta_k - \delta_{cr}'$ is the maximum past post-cracking excursion in the current direction of reloading and $\gamma < 1.0$ is a parameter. If cracking has not taken place in a previous cycle in the direction of reloading, point D′ coincides with C′. Then, after reaching C′ reloading turns into primary loading in that direction. If, instead, there has been in the past a post-cracking excursion to a peak point (F_k, δ_k) on the degraded skeleton curve beyond A′, reloading from D′ heads straight to a point on the unloading branch from (F_k, δ_k) at a force level $(1-\alpha)F_k$. Reloading past that point continues to the degraded skeleton curve OA′U′R′, beyond which it follows the skeleton curve as in primary loading.

Reversal during the initial, stiffer part of an unloading branch, e.g., the one starting at (F_i, δ_i) on the degraded skeleton curve takes place along that same branch until its starting point (F_i, δ_i). From there on it follows the primary loading branch from where the unloading had started. A reversal from the subsequent, softer unloading-reloading branch starts renewed loading towards a point on the unloading branch from the most extreme deformation in this direction, δ_i, but at a lower force level, $(1-\alpha)F_i$. Reversal during the subsequent, stiffer reloading branch produces unloading with the degraded elastic stiffness, $K = F_{cr}/\delta_{cr}$, until the nearest force level at $\pm\beta F_{uo}$ is reached and the softer branch of unloading-reloading begins.

For a full cycle to a peak deformation $\mu\delta_{cr}$ in each direction, the above hysteretic model gives the following equivalent viscous damping ratio:

– in the *first full cycle* in each direction:

  - if the deformation $\mu\delta_{cr}$ is less than that at ultimate strength, $\mu\delta_{cr}$, i.e., if $\mu < \mu_u = \delta_u/\delta_{cr}$:

$$\zeta_{n=1,\,\mathrm{pre-ult}} = \frac{1-\mathrm{p}}{2\pi}\left(\frac{\mu-1}{\mu}\right)\frac{2+\mathrm{p}(\mu-1)+0.5\beta}{1+\mathrm{p}(\mu-1)} \tag{4.94a}$$

  - if the deformation $\mu\delta_{cr}$ exceeds that at ultimate strength, $\mu > \mu_u = \delta_u/\delta_{cr}$:

$$\zeta_{n=1,\,\mathrm{post-ult}} = \frac{(\mu-1)(1+\mathrm{p}(\mu_u-1))+\mu_u(\mathrm{p}_1(\mu-\mu_u)-\mathrm{p}(\mu_u-1))+(\mu-1-\mathrm{p}(\mu_u-1)+\mathrm{p}_1(\mu-\mu_u))(1+\mathrm{p}(\mu_u-1)-\mathrm{p}_1(\mu-\mu_u)+0.5\beta)}{2\pi\,\mu(1+\mathrm{p}(\mu_u-1)-\mathrm{p}_1(\mu-\mu_u))} \tag{4.94b}$$

– in a *full unloading-reloading cycle after the first*:

- if the ultimate strength is not exceeded, i.e., if $\mu < \mu_u$:

$$\zeta_{n>1,\,\text{pre-ult}} = \frac{(1-\text{p})(\mu-1)}{2\pi\mu}\,\frac{2\beta+(1-\alpha)(1-\gamma)\,(1+\text{p}(\mu-1))}{1+\text{p}(\mu-1)} \quad (4.95a)$$

- if the ultimate strength is exceeded, $\mu > \mu_u$:

$$\zeta_{n>1,\,\text{post-ult}} = \frac{\mu-1-\text{p}(\mu_u-1)+\text{p}_1(\mu-\mu_u)}{2\pi\mu}\,\frac{2\beta+(1-\alpha)(1-\gamma)\,(1+\text{p}(\mu_u-1)-\text{p}_1(\mu-\mu_u))}{1+\text{p}(\mu_u-1)-\text{p}_1(\mu-\mu_u)} \quad (4.95b)$$

In Eqs. (4.94) and (4.95) p is the hardening ratio of the post-cracking primary branch and $p_1{=}K_2/K_o$ the post-ultimate softening ratio.

For nonlinear static (pushover) analysis, the force-deformation response of solid infill panels may be simplified to the multilinear curve of Fig. 4.12.

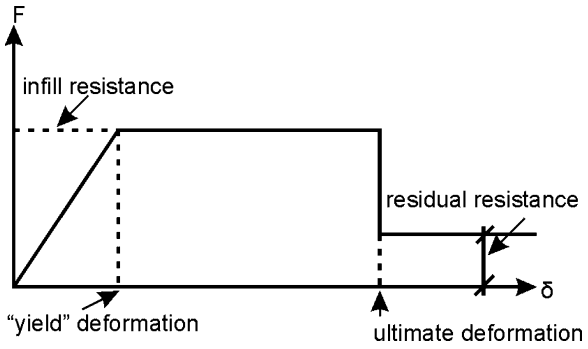

Fig. 4.12 Simplified force-deformation curve of infill panel for nonlinear static analysis

4.10.2.2 Model Parameters

Any multilinear infill model for monotonic loading with corner points at infill (visible) cracking, ultimate strength and post-ultimate residual strength is parametrised through the force and deformation values at these points. One of these values may be replaced by the slope to that point, secant from the origin or tangent to an adjacent corner of the curve. The values of these parameters should be determined on the basis of the geometry of the infill panel and of the material properties of the masonry, especially in the direction of the diagonal of the infill panel.[27] Rules for the calculation of these parameters should be developed or calibrated on the basis

[27] As there is coupling between the infill and the frame, these parameters cannot be given as if the infill panel were a stand-alone component, but depend in principle on the properties and sizes of the surrounding frame members.

of (cyclic) test results. This is, however, hampered by insufficient information on the material properties of the masonry of the tested infilled frames in the diagonal direction. Rare cases where such information has been reported are Stylianidis (1985) and Pires (1990). So, they have been used in Panagiotakos and Fardis (1994) to develop such rules, as highlighted below for the case when the force F is taken as the total infill shear force, V, and the displacement, δ, as the relative horizontal displacement between top and bottom of the panel (case 1 in Section 4.10.2.1).

1. The corner point at infill (visible) cracking (A_o in Fig. 4.11) can be specified through the shear force at cracking in monotonic loading, F_{cro}, and the initial stiffness to panel cracking, $K_o = F_{cro}/\delta_{cr}$. Among various (simple) alternatives examined in Panagiotakos and Fardis (1994), the best agreement with the test results in Stylianidis (1985) and Pires (1990) is given by:
   - an infill initial cracking strength equal to:

$$F_{cro} = \tau_{cr} A \tag{4.96}$$

   - an initial stiffness to panel cracking of:

$$K_o = G_w A / H_{cl} \tag{4.97}$$

where:

- $A = L_{cl} t_w$ and H_{cl} denote the horizontal cross-sectional area of the infill and its clear height, respectively, and
- τ_{cr} and G_w are the diagonal cracking strength and the shear modulus, respectively, of the masonry as determined from wallette diagonal compression tests (e.g., according to ASTM E519-81).

2. The ultimate strength point of the infill (U_o in Fig. 4.11) can be specified through the ultimate shear force in monotonic loading, F_{uo}, and the secant stiffness to that point from the origin. Among various (simple) alternatives examined in Panagiotakos and Fardis (1994), the best agreement with the test results in Stylianidis (1985) and Pires (1990) is given by:
   - a secant stiffness to ultimate strength, $K_u = F_{uo}/\delta_u$, obtained from that of the elastic diagonal strut given in Section 4.9.8 for linear analysis:

$$K_u = E_w (w_{inf} t_w) \cos^3 \theta / L_{cl} \tag{4.98}$$

where:

- the strut width, w_{inf}, is given from Eqs. (4.46) in Sect. 4.9.8 and
- the elastic modulus, E_w, is in the panel diagonal direction, or as close to it as possible, if the value along the diagonal is not available (e.g., in the horizontal direction if $L_{cl} > H_{cl}$, or in the vertical if $L_{cl} < H_{cl}$);

– an ultimate strength 1.3 times the cracking strength:

$$F_{uo} = 1.3\, F_{uo} \tag{4.99}$$

Alternatively F_{uo} may be taken equal to either:

- the horizontal cross-sectional area of the infill $A = L_{cl} t_w$, times the shear strength of bed joints, or
- the resistance of the diagonal strut in compression (i.e, its cross-sectional area, $w_{inf} t_w$, times the diagonal compressive strength of the masonry) projected on the horizontal direction.

3. The onset of the residual strength branch (R_o in Fig. 4.11) can be obtained from the ultimate strength point (U_o in Fig. 4.11), the residual strength and the tangent stiffness of the post-ultimate-strength softening branch in monotonic loading, K_2, expressed as the post-ultimate softening ratio, $-p_1$, times the initial stiffness to cracking, K_o. These parameters are hard to quantify from test results, but are for practical purposes less important than those in 1 and 2 above. For solid panels well confined by the surrounding frame a value of 0.05 for p_1 and of 50% of the ultimate strength, F_{uo}, for the residual strength seem to be supported by test results.

All the above refer to virgin, monotonic loading. Parameters a and a' determine according to Eq. (4.93) the cyclic decay of the monotonic curve when it serves as envelope to the hysteresis loops. If the degradation of the envelope in one direction is independent of previous infill damage in the opposite direction, then $a' = 0$. If cyclic deformations in either direction affect the same the response degradation in both directions, parameters a and a' may be about equal. The test results in Zarnic and Tomazevic (1985) and Stylianidis (1985) suggest $a + a' \approx 0.05$.

The value of the damping ratio under cyclic loading is affected by those of parameters:

– α : percentage-drop in peak force in repeated full unloading-reloading half-cycles to or beyond the peak past displacement in the same direction of loading,
– β: force at the transition from the initial stiffer unloading to the softer stage of unloading-reloading, or from this latter stage back to a subsequent stiffer reloading, as a fraction of the initial ultimate strength, F_{uo} and
– γ, which determines the displacement at the transition between the initial softer stage of reloading and the subsequent stiffer one, as a fraction of the maximum previous post-cracking excursion in the current reloading direction.

The outcome of Eqs. (4.94) for the damping ratio in the first full cycle is independent of α and γ and rather insensitive to the value of β. It is around 15% in the 1st cycle to $\mu = 2$, in good agreement with the test results in Stylianidis (1985) and Zarnic and Tomazevic (1985); if the 1st cycle takes place at larger values of μ, the damping ratio from Eqs. (4.94) increases to about 30%, but there are no 1st cycle

data at so large μ values for confirmation. For subsequent cycles the damping ratio from Eqs. (4.95) is nearly proportional to (1-α) and fairly sensitive to the values of β and γ, increasing slightly with increasing β and with decreasing γ. Values $\alpha \approx 0.15$, $\beta \approx 0.1$ and $\gamma \approx 0.8$ give fairly good overall agreement with the test results in Stylianidis (1985) and Zarnic and Tomazevic (1985).

4.10.3 Modelling of Foundation Uplift

Nonlinearities in ground compliance during the seismic response normally derive more from the no-tension feature of the soil and its interface with foundation elements, than from the behaviour of the soil itself in shear or compression. This shows up mostly as uplift of the foundation element from the ground. Uplift of rafts or long foundation beams is not so extensive and normally can be ignored. To take it into account, one should model ground compliance with springs of the no-tension type. The same modelling should be used under flexible footings.

Normally footings may be considered as rigid. The three conventional springs of Section 4.9.9.4 (the vertical one and one rotational spring per horizontal direction) at the node at the centre of the underside of a rigid footing have constant stiffness based on full contact at the footing-ground interface. So, they are sufficient for linear analysis and before any significant uplift takes place. After the onset of uplift the linear springs do not reflect:

- the significant reduction of rotational compliance (softening), due to loss of contact area;
- the (usually upward) displacement at the centre of the footing due to rotation about an axis which does not pass through the centre of the footing in plan;
- the different magnitude (normally larger) of the absolute vertical displacements of the ends of tie-beams connecting to the uplifting part of the footing perimeter, relative to those connected to the down-going part.

Such effects may be captured by using a pair of nonlinear vertical springs at opposite ends of the footing that account for uplifting. The spring at the uplifting end has lower stiffness than that at the down-going end. Such springs may be derived from the dependence of the rotation, θ, and vertical displacement at the centre of the footing, δ_o, on the applied moment M fitted in Crémer (2001) to results of nonlinear 2D FE analyses of uplifting strip footings on elastic or inelastic soil. According to Crémer (2001), if B is the width of a footing in the plane of M, the relations giving θ and δ_o in terms of a monotonically increasing M are:

$$\theta \approx \frac{\theta_o}{2 - \frac{M}{M_o}} \tag{4.100}$$

$$\delta_o \approx \frac{B\theta_o}{2}\left[\frac{\frac{M}{M_o} - 1}{2 - \frac{M}{M_o}} + \ln\left(2 - \frac{M}{M_o}\right)\right] \tag{4.101}$$

In Eqs. (4.100) and (4.101) M_o denotes the moment at the onset of uplift and $\theta_o = M_o/K_{\theta o}$ the associated (elastic) rotation derived from the elastic rotational impedance $K_{\theta o}$ of a footing in full contact with elastic soil. According to Crémer (2001), if the vertical load N at the base of the wall is very much lower than the bearing capacity of the (concentric) footing, N_u, the value of M_o on elastic soil may be taken approximately equal to:

$$M_o \approx 0.25BN \tag{4.102}$$

Note that the outcome of Eq. (4.102), fitted to the results of 2D FE analyses of elastic soil, exceeds by 50% the value of $BN/6$ predicted for a rigid footing by the subgrade reaction modulus approach. For higher values of N a more accurate approximation is (Crémer 2001):

$$M_o \approx 0.25BN \exp\left(-2.5\frac{N}{N_u}\right) \tag{4.102a}$$

The secant relation between the force $F = M/B$ at two nonlinear vertical springs introduced at the ends of the footing to model uplift and the associated vertical displacements are:

– at the uplifting edge ($\delta_1 > 0$):

$$\delta_1 = \frac{B\theta_o}{2}\left(\frac{\frac{FB}{M_o}}{2-\frac{FB}{M_o}} + \ln\left(2-\frac{FB}{M_o}\right)\right) \tag{4.103a}$$

– at the down-going opposite edge ($\delta_2 > 0$):

$$\delta_2 = \frac{B\theta_o}{2}\left(1-\ln\left(2-\frac{FB}{M_o}\right)\right) \tag{4.103b}$$

giving tangent stiffnesses:

$$\frac{dF}{d\delta_1} = \frac{2K_{\theta o}}{B^2}\frac{\left(2-\frac{FB}{M_o}\right)^2}{\frac{FB}{M_o}} \tag{4.104a}$$

$$\frac{dF}{d\delta_2} = \frac{2K_{\theta o}}{B^2}\left(2-\frac{FB}{M_o}\right) \tag{4.104b}$$

If the axial load N is low compared to N_u, there is very little hysteresis in cyclic loading, i.e. the cyclic M-θ and F-θ relations are nonlinear-elastic, recentring to approximately zero displacement for zero moment or force and dissipating very little energy. Then Eqs. (4.104) may be applied also for nonlinear response-history analysis, considering the springs as nonlinear elastic.

Column footings may uplift and rock in both orthogonal horizontal directions. Then, a different pair of nonlinear springs based on Eqs. (4.104) should be used in each horizontal direction, in a cross-like arrangement around the centre of the footing.

This procedure is exemplified in Section 6.9.2.2 for the pushover analysis of a plane frame with a shear wall at its central bay.

4.10.4 Special Provisions of Eurocode 8 for Nonlinear Analysis

Gravity loads concurrent with the seismic action should be applied on the relevant elements of the model in the course of the nonlinear analysis, as separate analyses and superposition cannot be used. Eurocode 8 (CEN 2004a) implicitly allows neglecting the effect of the variation of axial force of vertical elements during the seismic response and determining (the parameters of) their force-deformation relations on the basis of the axial force due to gravity loads alone. As we have seen in Sections 4.10.1.2, 4.10.1.3 and 4.10.1.4, however, most element models can take into account – be it approximately – the effect of this variation on the force-deformation relations of vertical elements .

For simplicity, Eurocode 8 (CEN 2004a) allows neglecting in nonlinear analysis bending moments in vertical members due to gravity loads, unless they are significant with respect to the yield moment. Note, however, that including such moments and starting the nonlinear seismic response analysis from a non-zero initial force state presents no special difficulty.

The parameters of force-deformation models for nonlinear analysis should use the best-estimate (mean) values of material strengths, which are higher than the nominal or design values.[28] For existing buildings the best-estimate of the strength of a material is the one inferred from in-situ measurements, lab tests of samples or any other relevant source of information (e.g., in the absence of hard data, from literature and judgment). Regarding the mean strength of materials to be incorporated in future, the mean strength of concrete is normally taken as 8 MPa greater than the characteristic strength, f_{ck} (CEN 2004b). For the reinforcing steel, the locally applicable data should be used, if known (e.g., from test reports of the same type of steel produced in about the same period). Statistics drawn from the widest available survey of ductile steels of the type used in the seismic regions of Europe in the early 1990s are summarised in Table 3.2. Notwithstanding the fairly large inter-country variation of the ratio of the mean yield strength, f_{ym}, to the nominal, f_{yk}, the average f_{ym}/f_{yk} ratio of the five columns of Table 3.2 is exactly equal to the commonly used default value of 1.15.

[28] Recall that, even in linear analysis, the Elastic Modulus of concrete is derived from the best-estimate (mean) value of concrete strength, f_{cm}, and not from the nominal one, f_{ck} (CEN 2004b).

4.10.5 Example Applications of Nonlinear Analysis in 3D and Comparison with Measured Dynamic Response

4.10.5.1 Computational Modelling for Seismic Response Analysis, Assessment and Retrofitting

A computational capability has been developed at the Structures Laboratory of the University of Patras for modelling and seismic response analysis of concrete buildings, as well as for their seismic assessment and retrofit design according to the relevant provisions of Eurocode 8, Part 1 (CEN 2004a) and Part 3 (CEN 2005a). It has been incorporated in computer program ANSRuop, a significantly improved and expanded version of the ANSR-I program (Mondkar and Powel 1975). All types of seismic response analysis in Eurocode 8 are covered, always in 3D. The modelling approach may be considered as the simplest one allowed in Eurocode 8, Parts 1 and 3. Yet, it represents fairly well the inelastic behaviour of members and the structure as a whole.

The key points of the nonlinear modelling approach adopted and illustrated in the present applications are the following:

1. Prismatic beam elements in 3D are used for all members (see Section 4.10.1.1). A point hinge model is adopted for them (see Section 4.10.1.4) with bilinear M-θ curve for primary loading (see Section 4.10.1.5). Nonlinear dynamic analysis uses modified-Takeda-type hysteresis rules (Otani 1974, Litton 1975) (see Section 4.10.1.6 and Table 4.3), with unloading parameter $\alpha = 0.3$ (see Table 4.3) and reloading parameter $\beta = 0$ (cf. definition of β in Section 4.10.1.7 in relation to Eq. (4.88a)).
2. The element elastic stiffness is the secant stiffness to yield-point, $(EI)_{\text{eff}}$, from Eq. (3.68) and Section 3.2.3.3. Its calculation is based on the member axial force due to gravity loads alone and on the values of the shear span at the yielding end(s) of the member suggested in Section 4.10.1.4: for beams or columns, half the clear length from one beam-column joint to the next within the plane of bending; for walls, 50% of the height from the bottom section in a storey to the top of the wall. The average secant-to-yield-point stiffness at the two end sections, in positive or negative bending is used (see Section 4.10.1.4). For beams that end at an indirect support on another beam (e.g., for beams B3, B7 and B9 in Fig. 4.14(a)) the shear span is taken equal to the beam full clear span. For girders connected at intermediate points with cross-beams or girders, the shear span is determined on the basis of the girder clear span between adjacent columns into which the girder frames (see Fig. 4.18-right for several such girders, two of which are indirectly supported at one end by another girder). Although the parts of the length of a girder between joints with cross-beams are modelled as individual beam elements, their elastic stiffness is taken the same all along the girder and equal to the value established from the secant-to-yield-point stiffness at the (two) end section(s) and the clear span of the overall girder. The effective flange width, in tension or compression, of T- or L-beams

on either side of their web is taken as 50% of the beam shear span or of the distance to the adjacent parallel beam (whichever is shorter). Slab bars parallel to such a beam and falling within this width are considered fully effective as longitudinal reinforcement of the beam's end section.

3. The strength, stiffness and behaviour of vertical members are considered independent in the two orthogonal planes of bending. The yield moment of each element is determined from the current value of its axial force, but considered constant during further primary loading. After reversal and during reloading in the reverse direction, the value of M_y is updated according to the evolution of the axial force (see last paragraph of Section 4.10.1.3 and further discussion in Section 4.10.1.4). Walls with non-rectangular section (e.g., the U-shaped wall around the elevator shaft in Fig. 2.21 and the two large walls with L-section at the corners of the right-hand side of the building in Fig. 4.18) are modelled with a single prismatic element per storey at the shear centre of the section.
4. Joints are considered as rigid, but slippage of longitudinal bars through or from a joint is accounted for, by including the effect of the resulting fixed-end rotation of member end sections on the secant-to-yield-point stiffness of Eq. (3.68) and the ultimate chord rotation (i.e., by setting $a_{sl} = 1$ in Eqs. (3.42) and (3.78), etc.).
5. Eccentricities in the connections between members are modelled through rigid elements.
6. The in-plane flexibility of floor diaphragms is included at the level of individual panels in plan, by considering the beams at the boundary of a panel (including the balconies) as prismatic elements in 3D with moment of inertia about an axis normal to the floor plane and cross-sectional area according to Eqs. (4.44) in Section 4.9.5.2.
7. Staircases are included in the model. Landings between floors, along with their supporting beams, are modelled in-plane according to point 6 above. Flights are modelled according to points 1–5 as oblique column elements (i.e. with strength and stiffness in both transverse directions) between the two nodes belonging to vertical elements closest to the axis of the flight at the two horizontal levels it connects.
8. P-Δ effects are included.
9. Masses are lumped at the nearest node of the model.
10. Rayleigh damping is used, with 5% damping ratio at the average period of the two modes with the highest modal base shears in two orthogonal horizontal directions and at half that value.
11. Damage is evaluated at member ends, using as index the ratio of the demand from the analysis to the corresponding capacity. Flexural damage is evaluated in terms of chord rotations, using as capacity the empirical ultimate chord rotation from Eqs. (3.78) in Section 3.2.3.5, with modifications due to lack of detailing for earthquake resistance, lap-splicing of vertical bars in plastic hinge zones, jacketing with FRP, etc., according to Sections 3.2.3.9 and 3.2.3.10. Shear damage is evaluated in terms of forces, using capacities for failure due to diagonal tension after yielding from Eqs. (3.114) in Section 3.2.4.3 and for shear

failure by diagonal compression before or after yielding from Eq. (3.115) in Section 3.2.4.5 or Eq. (3.127) in Section 3.2.5.4, as relevant. Demand-capacity-ratios of vertical members in the two orthogonal planes of bending are combined via the SRSS rule (see Eq. (3.84) in Section 3.2.3.8). In the calculation of the damage ratio (demand-to-capacity) both demand and capacity are updated during the response-history. The most adverse (i.e., the maximum) value of the damage index during the entire response is reported in the end. Values of this index near 1.0 signify likely or incipient failure.

The seismic response analysis and assessment capability has been applied to three concrete buildings, all designed with codes and practices applying in Greece from the 1950s to the 1970s, having various types and degrees of irregularity in plan that induce torsional response. The results of three Pseudo-Dynamic (PsD) tests of the first of these buildings provide, indeed, the basis for validation of the computational capability for seismic response analysis and member assessment, as well as of the modelling adopted here.

4.10.5.2 Verification of Modelling, Analysis and Assessment on the Basis of Pseudo-Dynamic (PsD) Test Results

The 3-storey full-scale building of Figs. 4.13 and 4.14 has been subjected to PsD testing under bi-directional excitation at the ELSA facility of the JRC in the framework of the SPEAR project. It has been designed in (Kosmopoulos et al. 2003) simulating practices of the 1950s in Greece (Fig. 4.14(a)). It was PsD-tested at ELSA (Molina et al. 2005) in three different versions (Mola and Negro 2005):

- As unretrofitted (Figs. 4.13(a) and 4.14(a));
- Retrofitted with FRPs as follows: All 0.25 m-columns were wrapped with unidirectional Glass FRP (GFRP) over a length of 0.6 m from each end section,

(a) (b)

Fig. 4.13 SPEAR test structure (**a**) unretrofitted: (**b**) retrofitted with FRP jackets

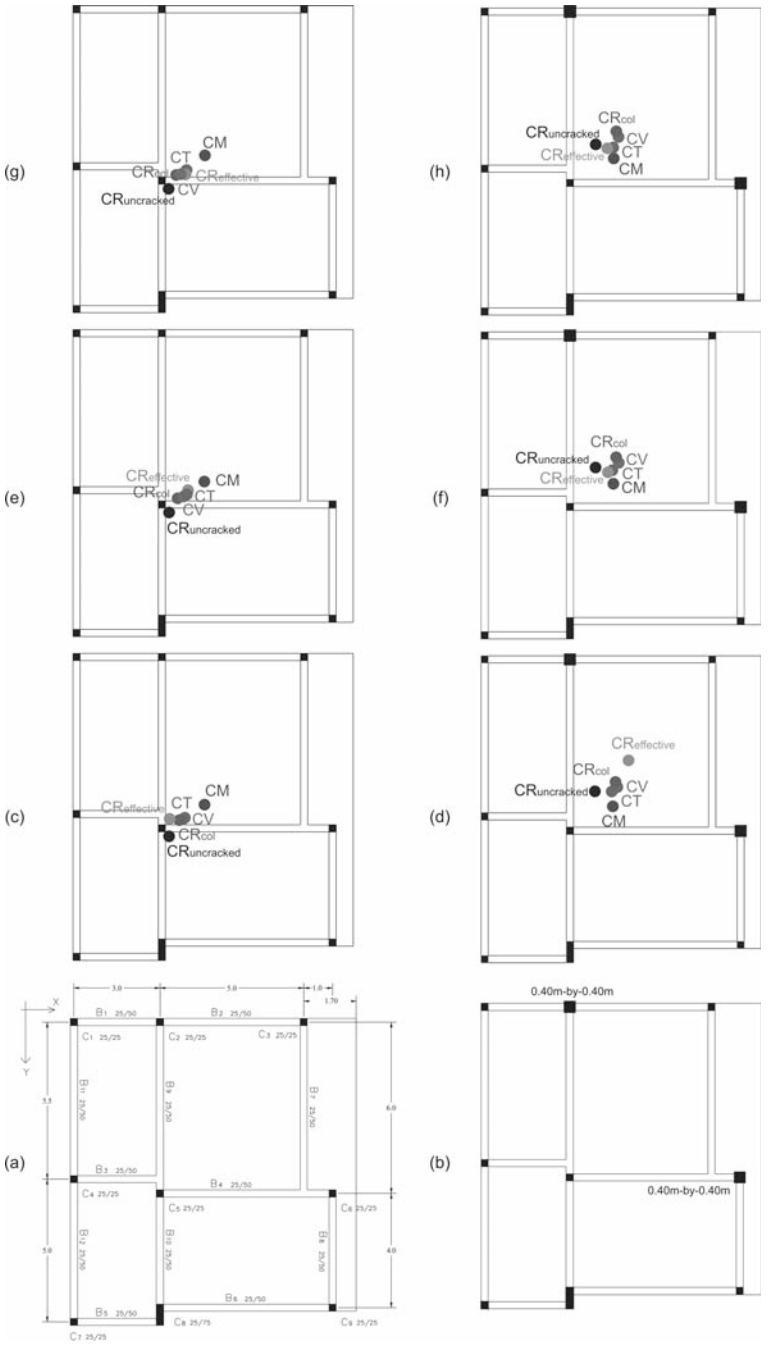

Fig. 4.14 SPEAR test structure: (**a**) framing plan of unretrofitted building: (**b**) framing plan with RC jackets at columns C2, C6; (**c**)–(**h**) centres of mass (CM), rigidity (CR), strength CV) and twist (CT) of 1st, 2nd and 3rd storey (from *bottom up*) – (*left*) unretrofitted structure; (*right*) with jacketed-columns (Kosmopoulos and Fardis 2008)

for confinement and clamping of short lap-splices (Fig. 4.13(b)). For the same purpose, but also for shear strengthening, column C8 in Fig. 4.14(a) (with 0.25 m-by-0.75 m section) was wrapped with bidirectional GFRP over its full height. Finally, the exterior faces of corner joints were strengthened in shear with bidirectional GFRP, not continued into the columns (Fig. 4.13(b)).

- In the 2nd phase the FRPs were removed and the central columns of the two "flexible" sides (C2 and C6 in Fig. 4.14(a)) were concrete-jacketed from 0.25 to 0.4 m square (Fig. 4.14(b)), to mitigate the torsional imbalance.

Further details about the retrofitting are given in Section 6.10.1.

In both its retrofitted or unretrofitted versions the building is torsionally flexible. The radius of gyration of overlying masses exceeds at every floor the torsional radius of the frame with respect to the centre of overlying masses in horizontal direction Y, violating therefore Eq. (2.4) in Section 2.1.6. To quantify further the irregularity in plan of the building, this centre, CM, is shown in Fig. 4.14(c) and (d) along with the following points:

(a) CR-uncracked: centroid of the gross section rigidity, $(EI)_c$, of storey vertical members, from Eqs. (2.2) in Section 2.1.5;
(b) CR-col: centroid of the secant stiffness of the storey vertical members at yielding, $(EI)_{eff}$, from Eq. (3.68) and according to the modelling in point 2 of Section 4.10.5.1;
(c) CR-effective: the storey centre of rigidity defined and determined as in Cheung and Tso (1986) and Tso (1990) (see Section 2.1.5);
(d) CV: centroid of resistances of storey vertical members, as controlled by shear or flexure – whichever is most critical.
(e) CT: pivoting point of the floor under storey torques with an inverted triangular heightwise pattern (see Section 2.1.5), as obtained from elastic analysis with member stiffness equal to their secant-to-yield-point stiffness from Eq. (3.68).

The nonlinear dynamic analysis follows the general modelling approach highlighted in Section 4.10.5.1, points 1–11. An additional assumption is introduced, to emulate the very tight fixing of the building's stiff and strong foundation to the laboratory's strong floor:

12. Vertical members are considered fixed at their connection with the foundation.

The bidirectional input motion applied at the PsD test and in the nonlinear analyses consists of the two Herzeg Novi records in the Montenegro 1979 earthquake, modified to simulate EC8-spectra-compatible ground motions for ground type C. Pre-test nonlinear response-history simulations have been carried out for the following PsD tests at ELSA (Kosmopoulos and Fardis 2004, Fardis et al. 2005):

- The unretrofitted structure under bidirectional motion scaled to a peak ground acceleration (PGA) of 0.15 g (Fig. 4.15, top);
- The same bidirectional motions, but scaled to a PGA of 0.2 g, applied to the test structure after its retrofitting with FRPs (Fig. 4.15, middle);

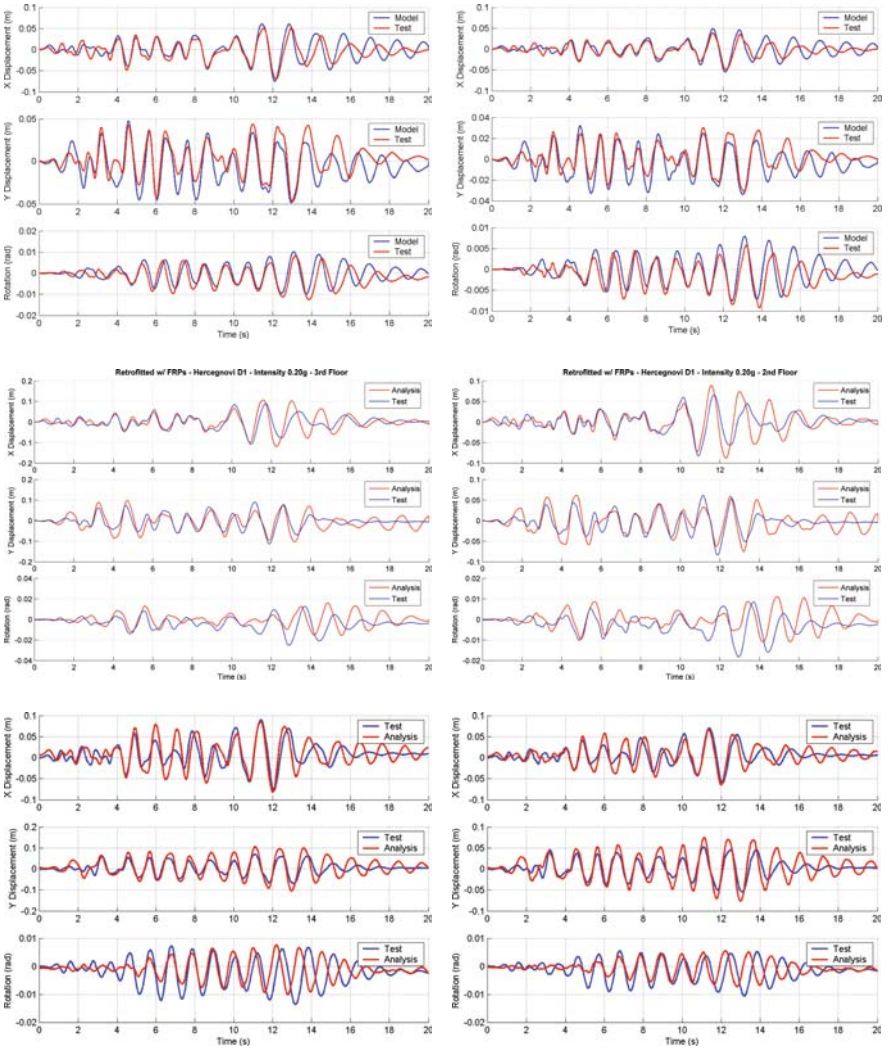

Fig. 4.15 Translation and twist histories, 3rd (*left*) and 2nd (*right*) floor in PsD test or analysis: (*top*) unretrofitted SPEAR building; (*middle*) with FRP-wraps; (*bottom*) with RC jackets (Kosmopoulos and Fardis 2004) (See also Colour Plate 11 on page 725)

- The same motions scaled to a 0.2 g PGA, applied to the test structure without FRPs but with columns C2 and C6 concrete-jacketed (Fig. 4.15, bottom).

Figure 4.15 compares the predictions of floor translation and twist time-histories for the bidirectional input ground motions applied in the PsD tests to the measured ones (Kosmopoulos and Fardis 2004, Fardis et al. 2005). Overall agreement is good, confirming the modelling assumptions above, including the use of the secant

stiffness to yield-point, Eq. (3.68). Witness, though, the initial overestimation of the dominant period of the response and of the displacements in the test of the unretrofitted building (top part of Fig. 4.15), until the time (at ~3 s) when cracking took place. From that point on the effective stiffness used in the analysis (from Eq. (3.68)) was indeed consistent with the actual member stiffness. As the peak member deformations induced by this test at ~13 s inflicted significant damage (see predicted flexural damage index at the top part of Fig. 4.16), members seem to have entered the strength degradation range of their moment-rotation relationship, not reflected in the bilinear model used in the analyses. So, the model fails to capture the ensuing lengthening of the dominant period of the measured response and the associated increase in displacement amplitudes. The pre-cracking and post-ultimate strength mismatch between predictions and test does not appear in the retrofitted versions, which were cracked from the outset and did not come as close to generalised member failure as the unretrofiited building. Witness also that analysis undershoots the twisting measured in all three tests, owing to the lack of inelastic coupling between the two directions of bending in the model used for columns. The softening and strength reduction induced by this coupling seem to have a measurable effect.

Figure 4.16 shows the maximum values of the computed damage index by the end of the dynamic response, separately for flexure and shear. Values near 1.0 signify likely or incipient failure. Failure is considered almost certain if the damage index exceeds 1 (numerals in bold in Fig. 4.16). Section 6.10.1 comments on how the predicted damage patterns for the two retrofitted versions of the SPEAR structure in Fig. 4.16 compare with the observed one.

4.10.5.3 Seismic Assessment of Two Real Buildings on the Basis of Nonlinear Dynamic Analysis

Section 2.4.2 and Figs. 2.21, 2.22 and 2.23 have presented the L-shaped building (with 5-storeys plus basement and penthouse), whose wing (to the right of the elevator shaft and of the column across the floor in Fig. 2.21) collapsed during the Athens 1999 earthquake. To identify the mechanism that led to collapse, a series of nonlinear response-history analyses have been carried out (Kosmopoulos and Fardis 2006), for six ground motions that had been derived as "most likely" at the site on the basis of several ground motion records in the Athens area and of the detailed subsoil conditions at the recording stations and at the building site.

The seismic response analyses were in accordance with the relevant rules and guidance of Eurocode 8 and followed the modelling approach highlighted in Section 4.10.5.1 under points 1–11, as well as assumption no. 12 in Section 4.10.5.2 for the SPEAR building, namely that vertical members, in this case all of them at the perimeter of the building, are fixed at their connection with the stiff, storey-high perimeter wall of the basement, which provides the foundation. An analysis has been carried out with each one of the six ground motions applied in one horizontal direction and any other one applied at right angles, giving in total 30 bidirectional motions. The displacement time-histories for each individual bidirectional motion and the natural periods and modes of the elastic structure show that the response

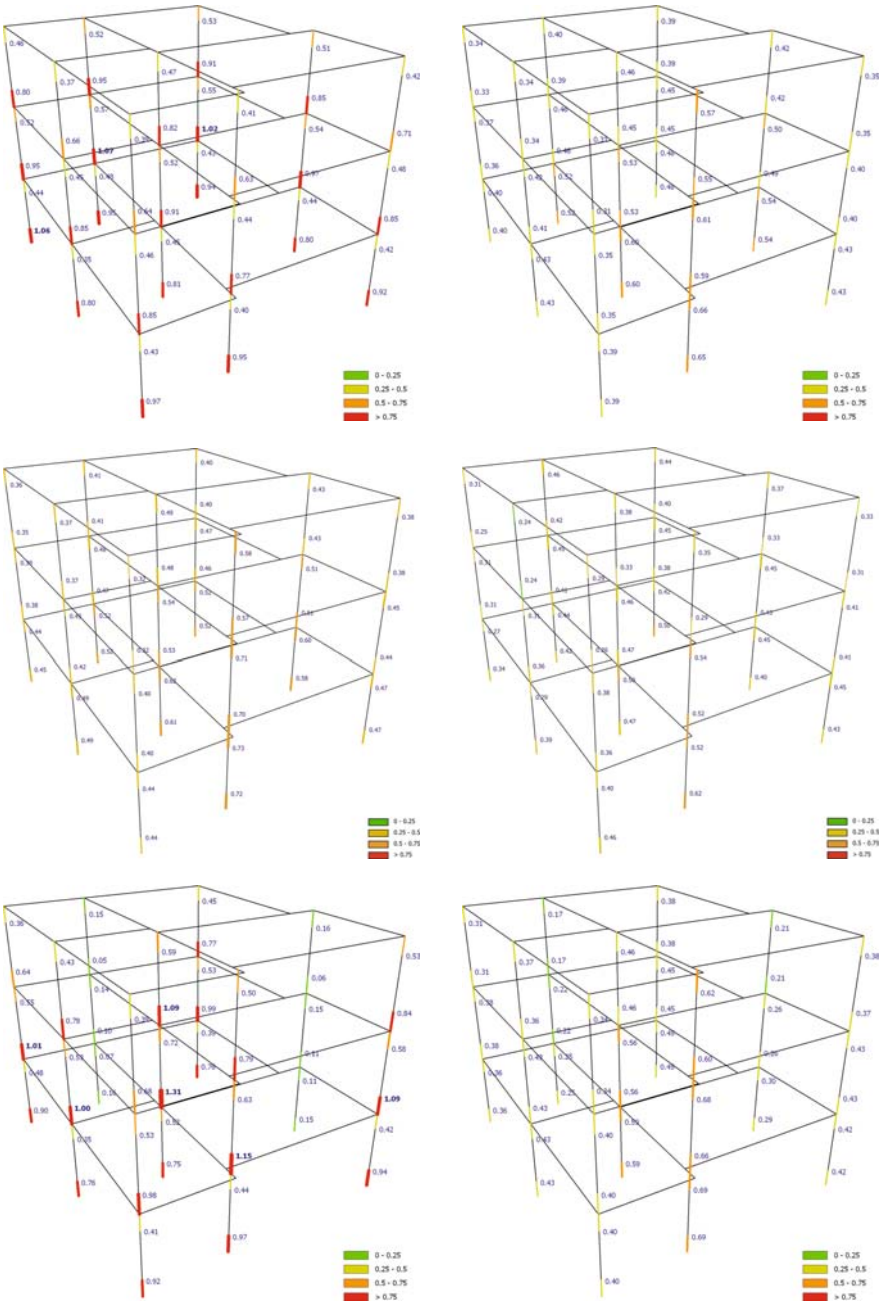

Fig. 4.16 Column damage index in flexure (*left*) or shear (*right*): (*top*) unretrofitted SPEAR building, 0.15 g PGA; (*middle*) 0.2 g PGA with FRP-wraps; (*bottom*) ibid, with RC jackets (See also Colour Plate 12 on page 726)

was controlled by higher modes. Moreover, due to the non-rigid connection of the floors to the stiff elevator shaft and to the staircase next to it, higher mode response generally entails out-of-phase twisting of the shaft/staircase and of the rest of the floor. The demand-to-capacity ratios (damage indices) in Fig. 4.17 show how close to its cyclic flexure-controlled ultimate deformation or to its cyclic shear resistance each member came. These results suggest that most critical in the building were the penthouse above the 5th floor and several columns in the upper storeys of the right-hand wing. Figure 4.17 shows also that the penthouse columns are near-critical in biaxial bending and certainly in shear. Critical in shear are also at least five of the other columns in the upper storeys, as well as the base of the elevator shaft wall. This supports the scenario advanced in Section 2.4.2 as most likely for the collapse: that it started with shear failures of columns at the penthouse and in the upper storeys of the part of the building to the right of the elevator shaft. Floor diaphragms, being almost unreinforced in their secondary direction, were unable to transfer forces from the deficient right-hand-side wing to the more resistant wing on the left of the elevator shaft. So, they teared off along a line next to the shaft, extending to the opposite side in plan.

The last case addressed here is a building constructed on the highly seismic island of Kephalonia (GR) in the early 1970s to house a theatre. As shown in Figs. 4.18 and 4.19, it consists of two structurally independent units, separated by an expansion joint that runs through the foundation. Both units are torsionally stiff, in the sense that Eq. (2.4) in Section 2.1.6 is met at all floors. Extensive vertical cracking had been observed at perimeter vertical members, owing to severe reinforcement corrosion.

The structure, designed according to codes of the 1950s for a base shear coefficient of 0.17 without detailing for ductility (corresponding to a peak ground acceleration – PGA – of about 0.1 g), is grossly inadequate against the 475 year return period earthquake with a PGA of 0.36 g specified for ordinary buildings at the site in the post-1995 seismic design code.

On the occasion of the rehabilitation of those members that suffer from reinforcement corrosion, it was decided to upgrade the entire structure to survive the design earthquake of the present-day seismic code. The seismic assessment and the retrofit design were the first application of Eurocode 8 Part 3 (CEN 2005a) to a real building.

The two parts of the as-built structure have been subjected to nonlinear dynamic analysis under semi-artificial bidirectional (two component) ground motions. Each motion emulates the two components of seven historic earthquakes, with each component modified to fit the 5%-damped Type 1 elastic spectrum recommended in Eurocode 8 for soil type C.[29] The two components of each bidirectional motion are normalised to a PGA of 0.1 g and interchanged between horizontal directions X and Y. Owing to certain asymmetry of the framing plan, each component of the

[29]One of these bidirectional motions was used in all PsD tests of the SPEAR building and in the analyses of Sect. 4.10.5.2, but scaled to a different PGA.

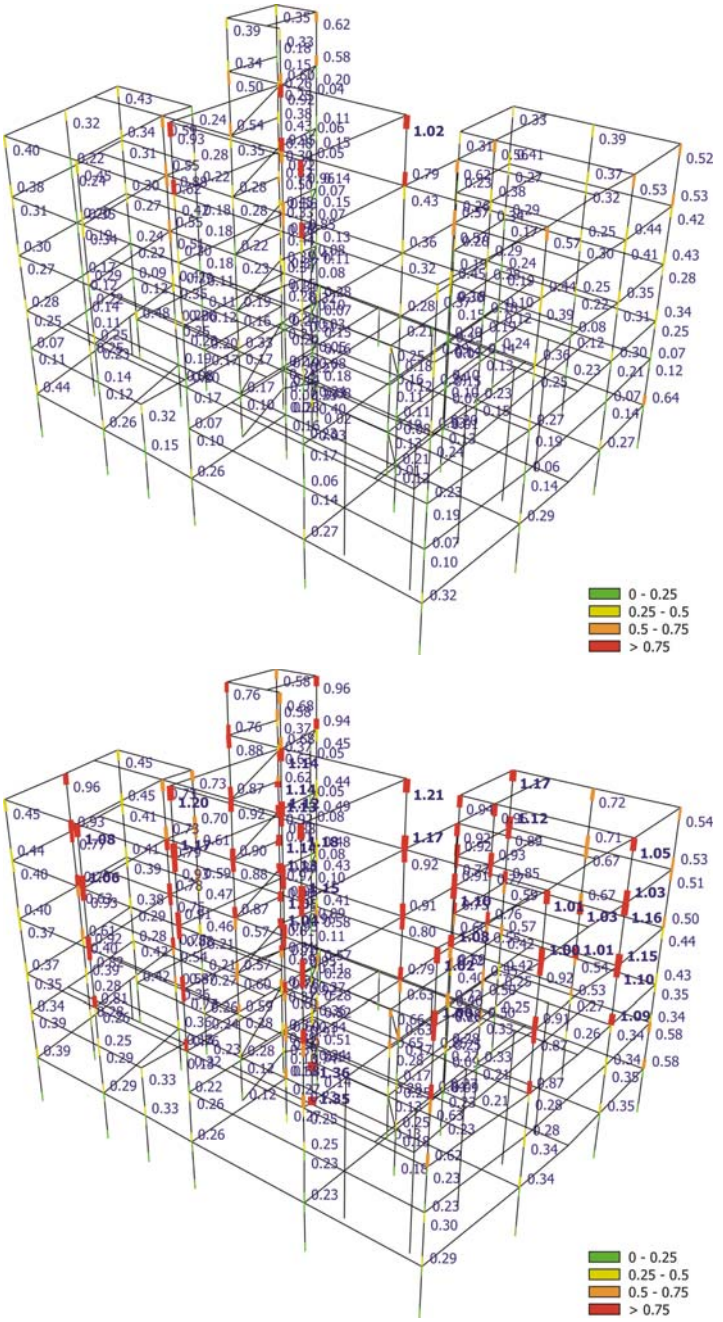

Fig. 4.17 Column damage index (demand-capacity ratio) in flexure (*top*) or shear (*bottom*); mean values from seismic response analyses of the 6-storey building subjected to the 30 "most likely" bidirectional ground motions at the site in the Athens 1999 earthquake (Kosmopoulos and Fardis 2006) (See also Colour Plate 13 on page 727)

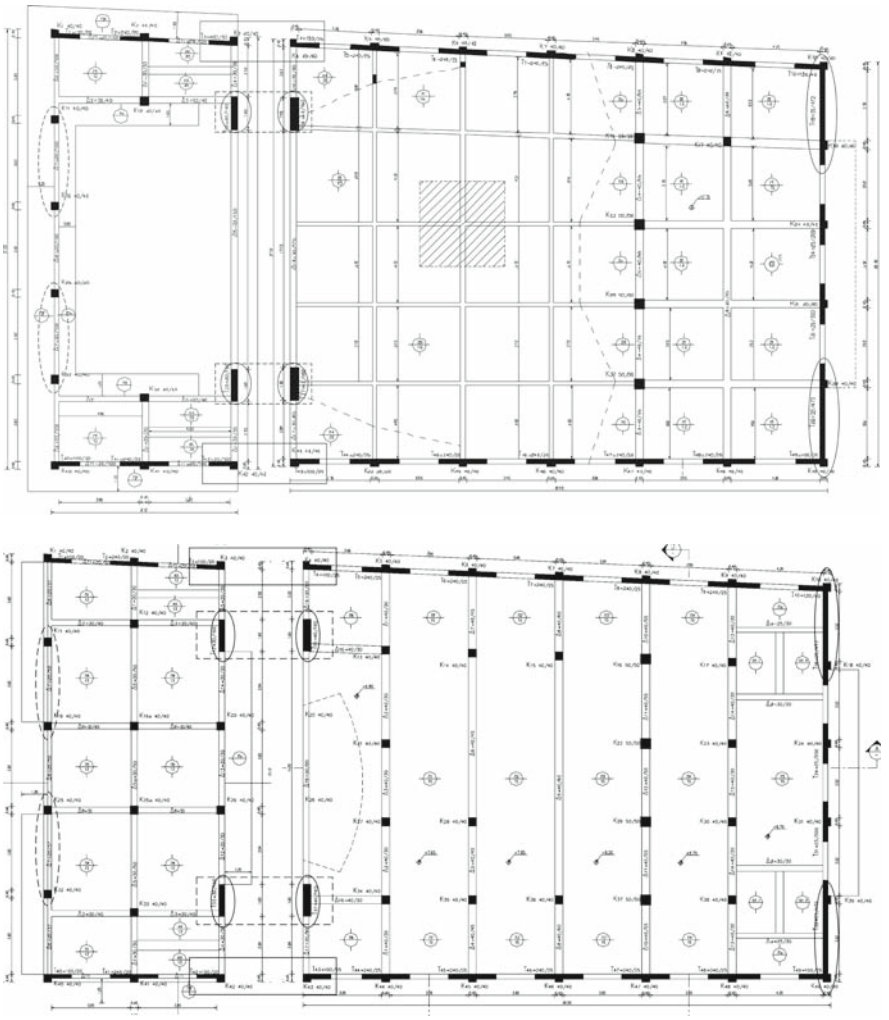

Fig. 4.18 Framing plan of the two-parts of the theatre facility. *Top*: roof; *bottom*: ground floor. *Left*: Stage part. *Right*: Theatre part (*Continuous-line ovals*: retrofitting with one-sided FRP; *dashed-line ovals*: added walls; *continuous-line rectangles*: jacketing into single wall across joint; *broken-line rectangles*: walls connceted with steel rods across joint; see Section 6.10.2)

motion is applied in the positive or in the negative sense, giving 8 orientations of the components of each bidirectional motion. So $7 \times 8 = 56$ nonlinear analyses have been carried out. The PGA level of 0.1 g has been chosen for the assessment of the as-built structure on the basis of pushover analyses with inverted triangular and 1st mode force patterns, which show that a seismic action with a PGA of 0.1 g in any of the two horizontal directions would cause violation of the limits specified in

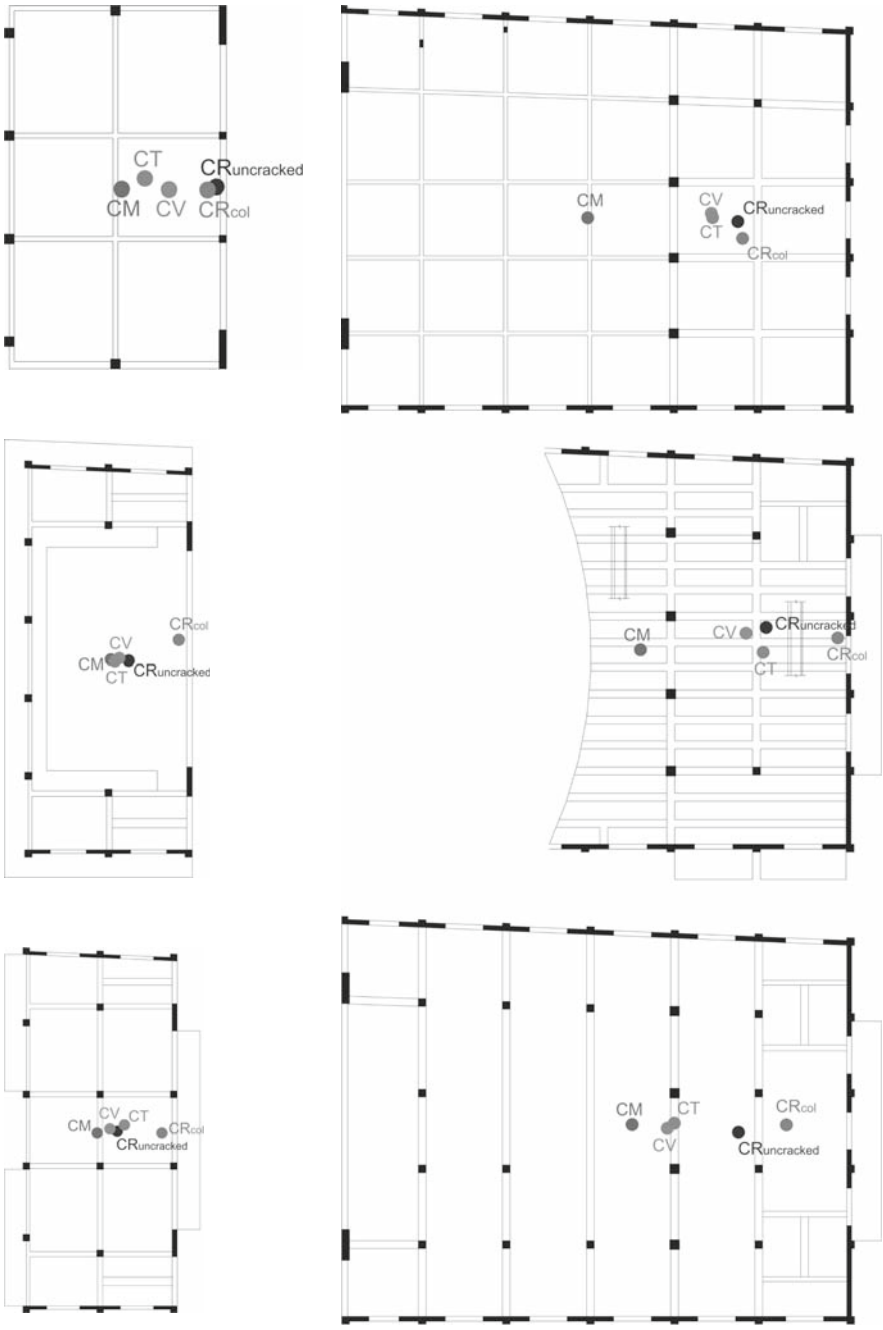

Fig. 4.19 Centres of mass (CM), stiffness (CR) or resistance (CV) and centre of twist (CT) at three levels of the stage (*left*) and the theatre (*right*) part of the theatre facility (Kosmopoulos and Fardis 2007)

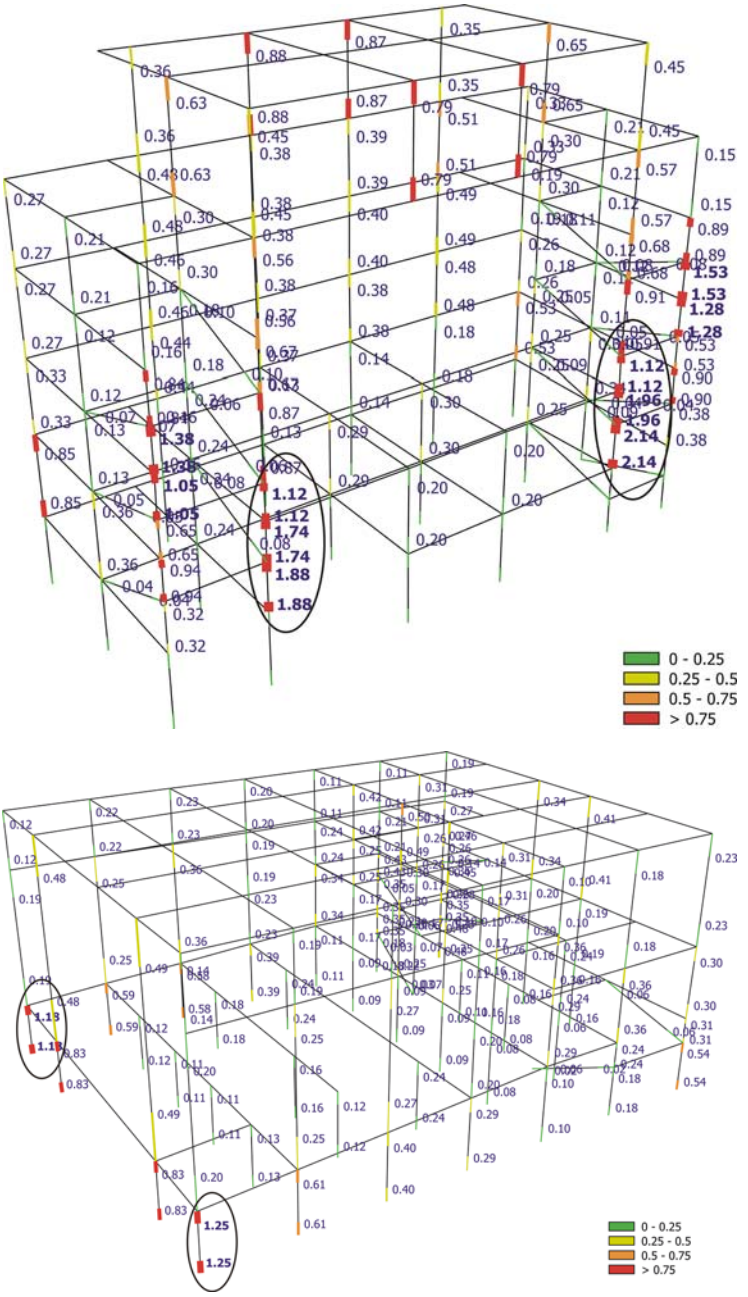

Fig. 4.20 Shear force demand-capacity-ratio (damage index) in vertical members of stage (*top*) and theatre (*bottom*) of as-built theatre facility (mean value over 56 bidirectional ground motions at PGA 0.1 g) (Kosmopoulos et al. 2007) (See also Colour Plate 14 on page 728)

Eurocode 8-Part 3 for Life Safety or Near Collapse in few members of both parts of the structure (Kosmopoulos et al. 2007).

The seismic response analyses follow the general modelling approach, points 1–11, of Section 4.10.5.1. Assumption no. 12 in Section 4.10.5.2 is also made. Vertical members are considered fixed at their connection with the foundation of the building (a two-way system of deep and heavy foundation beams for the theatre part, a basement-deep perimeter wall plus heavy two-way interior foundation beams at the stage part). Pounding between the two parts of the building at the vertical joint between them is neglected.

The shear force demand-capacity ratios (damage index) in Fig. 4.20 show that indeed a seismic action with a PGA of 0.1 g causes shear failures in two pairs of shear walls adjoining the expansion joint between the two parts of the building. The critical walls of the stage part are the two interior ones parallel to the joint. In the theatre part, critical are the two exterior walls at right angles to the joint. Twisting about a vertical axis near the side of the building opposite to the joint is one of the causes of shear failure at these locations. It is induced by the large eccentricity between the centres of stiffness (CR) or resistance (CV) or the centre of twist (CT) and the centre of overlying masses in the theatre part of the facility (Fig. 4.19, right).

Section 6.10.2 highlights the retrofitting of the building and the seismic response of the retrofitted structure.

4.11 Calculation of Displacement and Deformation Demands

4.11.1 Estimation of Inelastic Displacements and Deformations Through Linear Analysis

The prime role of seismic analysis for current force-based seismic design of new buildings is the estimation of seismic action effects in terms of internal forces, for use in force-based dimensioning or verification of members. As pointed out in Sections 1.2 and 4.1.2, linear-analysis, based on a 5%-damped elastic spectrum divided by the "behaviour factor" q of European codes or the "Force reduction" or "Response modification" factor R of US codes, is presently considered to serve well this end. Seismic displacement and deformation demands enter in member dimensioning and detailing only in an average sense and indirectly, via the ductility ratio, global or local, that determines the value of q (or R) for the estimation of seismic internal forces or the member detailing requirements, respectively. Their absolute magnitude is needed only for the calculation of P-Δ effects (see Section 4.9.7), the checks of interstorey drifts limits (e.g., for Eurocode 8 those listed in Section 1.1.3 under (i)–(iii)) and of the clearance between adjacent structures to avoid pounding, etc. These aspects are of secondary importance in force-based design of new buildings. So, an approximate estimation of seismic displacement demands seems sufficient.

In Eurocode 8 (CEN 2004a) the equal displacement rule suffices for the estimation of seismic displacements in the design of new buildings. In the period range where the design spectrum is not inversely proportional to q (notably up to the first corner period T_B, see Eq. (4.5a) in Section 4.2.2) the computed displacements are the elastic ones, as obtained from the elastic spectrum. For longer periods, displacement results of linear analysis for the 5%-damped elastic spectrum divided by the q-factor are back-multiplied by q. Eurocode 8 (CEN 2004a) allows National Annexes to refine the displacement calculation rules, e.g., through a q-μ-T relation, such as that of Eqs. (1.1) and (1.2) in Section 1.2.

In US codes for the design of new buildings displacements are calculated by back-multiplying the results of a linear analysis with the 5%-damped elastic spectrum divided by R, not by the full value of R but by $0.7R$ (SEAOC 1999), or by a value between about $0.7R$ (for systems with high R-values) and R (for low R-values) (BSSC 2003).[30]

The equal displacement rule, with variants such as Eqs. (1.1) and (1.2) in Section 1.2, is a well established approximation of the global displacement demand in a bilinear SDOF system, be it an equivalent one in the sense of Section 4.6.1.3 and Eqs. (4.13), (4.14) and (4.15) therein. However, its universal extension down to the level of nodal displacements and member deformations, just on grounds of their secondary importance in the context of force-based seismic design, may not be warranted. Implicit in this extension is the presumption of inelastic deformation demands spreading throughout the structural system. Indeed, codes for the seismic design of new buildings make every effort to prevent concentration of these demands in few members or locations (notably in a single "soft" storey): by providing a stiff and strong vertical spine over the full height of the building, by controlling the location of plastic hinges and the inelastic response mechanism through an imposed hierarchy of strengths and by guiding the designer towards a favourable structural layout. One of the returns is the permission to apply the equal displacement rule at the level of nodal displacements and member deformations. Indeed its applicability has been confirmed in Panagiotakos and Fardis (1999a) on the basis of over one thousand nonlinear dynamic response analyses of several planwise symmetric multistorey buildings designed in full accordance with the ENV-Eurocode 8.

The situation is very different in seismic assessment of existing substandard buildings. These buildings do not have an engineered hierarchy of strengths to spread inelastic deformation demands throughout the structure. Instead, their structural layout often promotes concentration of these demands in few members or locations. Moreover, in seismic assessment and retrofitting, which is nowadays fully displacement-based, member deformation demands are not anymore 2nd-class outcomes of the analysis but have the prime role in member verifications. So, they

[30]Except in the calculation of P-Δ effects, for which US codes use the displacements from the linear analysis with the 5%-damped elastic spectrum divided by R, without removing at all the effect of R (see Section 4.9.7).

should be estimated as reliably and accurately as practically feasible. For these reasons, recent codes for seismic assessment and retrofitting (ASCE 2007, CEN 2005a) are more prudent than those for new designs. They allow estimation of inelastic member deformation demands through linear analysis only when their variation between different members or locations is within certain limits:

- According to Part 3 of Eurocode 8 (CEN 2005a), linear analysis is applicable for the estimation of deformation demands in structural members, if the distribution of ductility demands over the *entire structure* is fairly uniform. A conveniently computed measure of the local ductility demand is employed: the demand-to-capacity ratio, D/C, in *flexure*, where D is the bending moment at the end of a member due to the seismic action and the concurrent gravity loads from elastic analysis and C the corresponding moment resistance. Note that, if the equal displacement rule indeed applies, D/C is about equal to the demand value of the chord-rotation ductility ratio, μ_θ. For linear analysis to be applicable, the maximum D/C-ratio in all "primary seismic" elements (defined and discussed in Section 4.12) should not exceed by more than a factor of about 2.5 its minimum value over those having $D/C > 1$.[31] D/C is taken not to exceed 1 (elastic response) at those sections around beam-column joints where the comparison of the sum of beam moment resistances, ΣM_{Rb}, to that of the columns, ΣM_{Rc}, precludes plastic hinging. No limit is set on the absolute magnitude of D/C for the applicability of linear analysis. However, there will always be an end section or two in the whole structure where plastic hinging will marginally be predicted, with a value of D/C a little over 1.0. So, the relative limit on the value of D/C is essentially an absolute one. In this respect the limitation on the basis of the D/C-ratio is quite restrictive for those Limit States where inelastic response is allowed. However, we will see in Section 4.11.2 that this restriction is not fully supported by hard evidence. Anyway, if this criterion is met (CEN 2005a) allows estimation of nodal displacements and member deformations through linear analysis with the 5%-damped elastic spectrum. If, in addition, both conditions (a) and (b) in Section 4.3.1 are met (CEN 2005a) allows using linear static analysis ("lateral force" procedure), instead of modal response spectrum analysis.
- The US Standard for seismic rehabilitation (ASCE 2007) uses as a criterion the maximum value of the elastic *internal force* demand (due to the seismic action and the concurrent gravity loads) to the corresponding capacity, *DCR*, throughout an "element". In this case an "element" is not just a single structural member, but a subsystem of the lateral-force resisting structure, such as a wall or plane frame. Estimation of deformation demands from linear analysis with the 5%-damped elastic spectrum is allowed, if the nonlinearity of the response is

[31] As a matter of fact, the value of this factor may be determined nationally within the range 2 to 3, as a Nationally Determined Parameter. 2.5 is the value recommended in Eurocode 8 (CEN 2005a).

either limited overall, or uniformly distributed throughout the structure. More specifically, either one of the following two conditions should be met:

(a) the maximum *DCR* value over the entire structure does not exceed 2.0, or
(b) all three of the following conditions are met:

1. all "primary" walls and plane frames of the building continue throughout its height, without out-of-plane offsets;
2. the weighted-average *DCR* of the "elements" in a storey, using as weight the (seismic) shear force of the "element", does not differ by more than 25% from that of an adjacent storey (to avoid a weak storey);
3. the "element" *DCR* does not increase from one side of the storey's centre of resistance to the other by more than 50% (for torsionally balanced strength).

The criteria in ASCE (2007) are harder to check or meet than those in CEN (2005a), as they use the demand-to-capacity ratio in the most critical internal force of a subsystem, which assumes more extreme values than the corresponding ratio in flexure alone.

4.11.2 Evaluation of the Capability of Linear Analysis to Predict Inelastic Deformation Demands

Panagiotakos and Fardis (1999a) have confirmed that linear analysis with the 5%-damped elastic spectrum provides indeed an acceptable approximation of inelastic chord rotation demands in planwise symmetric multistorey (and in most cases very regular in elevation) concrete buildings designed to the ENV-Eurocode 8, under unidirectional ground motions up to twice the design seimic action. However, what is at issue is the applicability of linear analysis for the prediction of inelastic deformation demands in existing buildings with poor structural layout, including strong irregularities in plan and/or elevation and subjected to bidirectional ground motions. This question has been addressed in Kosmopoulos and Fardis (2007) and Fardis and Kosmopoulos (2007), using as testcases the substandard and irregular buildings of Section 4.10.5, including as separate cases the unretrofitted and the partly concrete-jacketed versions of the SPEAR building and the two parts of the theatre facility. Like those in Panagiotakos and Fardis (1999a), these buildings are typical of multistorey concrete ones in that their 1st and 2nd mode periods are in the velocity-controlled part of the spectrum, $T_C < T < T_D$, where the equal displacement rule is considered to apply well for SDOF systems (see Eq. (1.1)). Nonlinear response-history analyses of these buildings have been carried out under the suite of 56 bidirectional ground motions described in Section 4.10.5.3 in connection with the theatre facility, with each component comforming to the smooth 5%-damped elastic response spectrum in Eurocode 8 for soil type C. The PGA of the motions

applied to the two versions of the SPEAR building increased from 0.15 to 0.3 g in steps of 0.05 g, to study the effect of motion intensity. The motions applied to the "Athens" building of Sections 2.4.2 and 4.10.5.3 and Figs. 2.21, 2.22 and 2.23 and to both parts of the theatre facility of Section 4.10.5.3 and Fig. 4.18 have a PGA of 0.15 and 0.1 g, respectively.

The results of the nonlinear response-history analyses of these buildings were compared to those of:

- linear static analysis according to Section 4.3, except that in Eq. (4.6) $m_{\text{eff},1}$ was taken equal to the full mass, m, and not reduced to $0.85m$, as allowed in CEN (2004a, 2005a), and
- modal response spectrum analysis in 3D according to Section 4.4, with CQC combination of peak modal responses (Eq. (4.11)).

Member stiffness in the linear analyses was equal to the corresponding elastic stiffness in the nonlinear ones (i.e., from Eq. (3.68)). The smooth 5%-damped Eurocode 8 elastic spectrum, to which the individual components of the suite of 56 bidirectional ground motions of the nonlinear response-history analysis are compatible, has been applied separately in horizontal directions X and Y. Member chord rotations from the separate analyses in X and Y were combined via the rigorous SRSS rule, Eq. (4.24). The oucome was added or subtracted from that due to the concurrent gravity loads, giving an elastic estimate of the chord rotation, θ_{el}, to be compared to the average over the 56 nonlinear response-history analyses of the peak inelastic chord rotation at the same member end, θ_{inel}. The conclusions of the comparison are the following:

- For elastic chord rotations estimated through modal response spectrum analysis, the average $\theta_{\text{inel}}/\theta_{\text{el}}$ ratio is overall very close to 1.0. When linear static analysis is used, the building-average $\theta_{\text{inel}}/\theta_{\text{el}}$ ratio is systematically less than 1.0; from a few percent to one-third in the different building cases, but giving an overall average value of 0.835 for $\theta_{\text{inel}}/\theta_{\text{el}}$ (very close to the factor of 0.85 given by CEN (2004a) for $m_{\text{eff},1}/m$ in Eq. (4.6), with only slight upwards deviations in the two out of the five buildings that indeed violated the Eurocode 8 condition of $T_1 < 2T_C$ for $m_{\text{eff},1}/m = 0.85$, see Section 4.3.2). Note, however, that the average $\theta_{\text{inel}}/\theta_{\text{el}}$ ratio in the various regular and fully symmetric multistorey buildings in Panagiotakos and Fardis (1999a) under unidirectional ground motions was equal to 1.07, both for modal response spectrum and linear static analysis. Provided, therefore, that the outcomes of separate linear analyses in X and Y are combined through the SRSS rule, Eq. (4.24), peak inelastic chord rotations are overall better estimated by their linear counterparts in real situations of geometry and loading in 3D than in rather idealised cases of near-perfectly regular and symmetric buildings under one-component seismic actions.

- The building-average inelastic-to-elastic-chord-rotation-ratio decreases with increasing PGA, despite the spreading of inelasticity and the increase of its magnitude, but the scatter of individual results increases.
- The storey-average $\theta_{inel}/\theta_{el}$ ratio does not systematically depend on elevation in the building. If elastic chord rotations are estimated via static analysis, there is a weak tendency of the storey-mean to increase on average from the base to the roof; but when modal response spectrum analysis is used instead, this tendency is weakened further or sometimes reversed.
- Linear static analysis does not produce as heightwise uniform a value of $\theta_{inel}/\theta_{el}$ as modal response spectrum analysis, especially when higher modes are important, as in the "Athens" building of Sections 2.4.2 and 4.10.5.3 and Figs. 2.21, 2.22 and 2.23. However, it gives more consistent results (i.e., with lower scatter within a storey) than modal response spectrum analysis for the beams and the two different axes of column bending. Only in the "Athens" building, for which higher modes are important, did modal response spectrum analysis produce lower scatter of individual $\theta_{inel}/\theta_{el}$ ratios in a storey than linear static analysis. In all other buildings linear static analysis gave much more uniform $\theta_{inel}/\theta_{el}$ ratios within a storey than modal response spectrum analysis. Note that this latter method is the only type of linear analysis allowed by Eurocode 8 for the "Athens" building and the two parts of the theatre facility, owing to their heightwise irregularity and for the "Athens" building to its long 1st and 2nd mode periods as well.
- Column $\theta_{inel}/\theta_{el}$ ratios are very consistent between top and bottom of the storey for the same axis of bending, regardless of the type of linear analysis.
- The pattern of deviations of individual $\theta_{inel}/\theta_{el}$ ratios in the various member types of each building, with respect to the storey-average for that member type, suggests a tendency of linear static analysis to overestimate inelastic torsional effects at the flexible side(s) and the central part of the torsionally flexible buildings (i.e., those violating Eq. (2.6)) and underestimate them at the stiff side(s). There is no clear trend in this respect for the torsionally stiff buildings. By contrast, the tendency of modal response spectrum analysis is to overestimate inelastic torsional effects at the stiff side(s) and the central part of the torsionally stiff buildings and underestimate them somewhat at the flexible side(s). This trend is less clear in the torsionally flexible buildings.
- In every single case the *D*/*C* (or *DCR*) values (with elastic demands, *D*, from the separate analyses in X and Y combined via the SRSS rule, Eq. (424)) violate the applicability criteria of ASCE (2007) or CEN (2005a) for the estimation of inelastic deformation demands at member ends through 5%-damped linear analysis.

The overall conclusion of the comparative analyses is that elastic modal response spectrum analysis with 5% damping gives on average unbiased and fairly accurate (within a few percent) estimates of member inelastic chord rotation demands

in multistorey concrete buildings typical of existing substandard construction. This might be taken to mean that there is room for revisiting and possibly relaxing the relevant criteria in ASCE (2007) or CEN (2005a), in order to allow wider use of 5%-damped elastic analysis for estimation of member inelastic chord rotation demands.

4.12 "Primary" V "Secondary Members" for Earthquake Resistance

4.12.1 Definition and Role of "Primary" and "Secondary Members"

Most current seismic codes recognise that certain structural members may have a secondary role and contribution to earthquake resistance. The main goal of the distinction of these "secondary members" from the rest, termed "primary", is to allow a certain simplification of the seismic design, assessment or retrofitting:

- In the design of new buildings, the contribution of "secondary members" to stiffness and resistance against seismic actions is not included in the structural model for the seismic analysis. The building structure is taken in design to rely for its earthquake resistance only on its "primary members". Only them are designed and detailed for earthquake resistance, in accordance with all the relevant rules in the seismic design code. "Secondary members" are fully considered and designed for the non-seismic actions and are subject to special verifications under the design seismic action and the concurrent gravity loads (see Section 4.12.3).
- In seismic assessment and retrofitting of existing buildings we accept more severe seismic damage in "secondary members", as they are less important for the performance and safety of the whole. Accordingly, their verification criteria for the seismic action are relaxed compared to those of "primary members". According to Eurocode 8 (CEN 2005a) in existing or retrofitted buildings the contribution of "secondary members" to stiffness and resistance against seismic actions should be neglected in the model for linear seismic analysis, like in new buildings, but should be included in a nonlinear analysis model.[32] Note, however, that, unless "secondary members" are fully included in the model for the seismic actions, it is not easy to check whether they meet their (relaxed) compliance criteria (see Section 4.12.5).

The classification of members into "primary" and "secondary" (as they are called in CEN 2004a, 2005a, ASCE 2007) is equivalent to the old-time distinction in US

[32] According to (ASCE 2007), cyclic degradation of strength and stiffness shoud be accounted for in the model of "secondary members" for a nonlinear analysis, while it may be disregarded for "primary members".

seismic design codes for new buildings (BSSC 2003, SEAOC 1999) of members which are part of the lateral- (or seismic) force-resisting system from those that are not. In Eurocode 8 (CEN 2004a, 2005a) the qualification "seismic" has been added to "primary" or "secondary", to make it clear that the differentiation applies only for the seismic action.

4.12.2 Constraints on the Designation of Members as "Secondary"

Besides the vague feature that it is not part of the lateral-load-resisting system, there is no precise definition of a "secondary member". It is up to the designer to decide which members, if any, he/she may consider as "secondary". To establish a limit to the discretion of the designer of a new building, Part 1 of Eurocode 8 (CEN 2004a) gives three conditions to be met:

1. The total contribution to lateral stiffness of all "secondary members" should not exceed 15% of that of all "primary" ones. Unless it is obvious that this condition is met (e.g., through back-of-the-envelope calculations on the basis of moments of inertia of vertical elements, or when the "secondary members" are few and/or truly secondary), to check it the designer should carry out two analyses per horizontal component of the seismic action. One including and another neglecting the contribution of "secondary members" to lateral stiffness (see Section 4.12.5). For the condition to be met, storey drifts computed from the latter analysis should be less than 1.15 times those from the first one.
2. The characterisation of some of the structural members as "secondary" should not change the classification of the structure from irregular to regular. As outlined in Sections 2.1.5, 2.1.6, 2.1.7 and 2.1.8, most Eurocode 8 regularity criteria – both in plan and in elevation – are qualitative and can be checked by inspection without analysis of the structural system for the seismic action. As far as regularity in elevation is concerned, this condition implies that (see Sections 2.1.7 and 2.1.8):

   (i). if a frame, column or wall does not continue throughout the full height of the relevant part of the building, it cannot be classified as "secondary"; and
   (ii). if in a frame buildings there is an abrupt change in the storey overstrength – as measured by the ratio of the sum of lateral force capacities of vertical elements and of masonry infills to the design storey shear – the overstrength variation cannot be smoothened out by classifying some vertical elements as "secondary".

As far as regularity in plan is concerned, this condition implies that, classification of some vertical elements as "secondary":

(i). does not reduce the eccentricity between any storey's centres of mass and stiffness from more than 30% of the storey torsional radius to less (see Section 2.1.5), and

(ii). will not increase the torsional radius in any direction from less than the radius of gyration of the masses to more (see Section 2.1.6).

3. "Secondary members" should meet the special requirements applying to them (see Section 4.12.3).

According to Part 3 of Eurocode 8 (CEN 2005a), seismic assessment and retrofitting of *existing buildings* is still subjected to the 2nd condition above, but not to the 1st one. Moreover, instead of the special requirements of Section 4.12.3, "secondary members" should meet the same verification criteria as "primary" ones, albeit with less conservative estimates of their capacities (see Section 6.5.6).

4.12.3 Special Design Requirements for "Secondary Members" in New Buildings

"Secondary members" of new buildings do not have to meet the rules and requirements of seismic design codes for dimensioning and detailing of structural members for earthquake resistance through energy dissipation and ductility. They only need to satisfy code rules for design for non-seismic actions and the additional requirement to maintain support of gravity loads under the most adverse displacements and deformations induced by the design seismic action applied together with the concurrent gravity loads. These seismic deformation demands are determined according to the equal displacement rule, on the basis of the results of normally two linear analyses per horizontal component of the design seismic action:

1. one neglecting the contribution of "secondary members" to lateral stiffness (see Section 4.12.5.1 for guidance), and
2. another including it.

The effect of the behaviour factor, q, is removed then according to Section 4.11.1 from the seismic deformations resulting from analysis no. 2 and the outcome is multiplied by the ratio of the interstorey drifts in the storey from analysis no. 1 to those of no. 2, to give our estimate for the seismic deformation demands in the "secondary members" when their contribution to lateral stiffness is ignored. If the value of the sensitivity ratio θ (from Eq. (4.45) in Section 4.9.7) exceeds 0.1, the 1st-order values should be divided by $(1–\theta)$ to account for 2nd-order (P–Δ) effects

According to Part 1 Eurocode 8 (CEN 2004a), internal forces (bending moments and shears) in "secondary members" calculated from their cracked stiffness (taken equal to the default value of 50% the gross, uncracked section stiffness) and the deformations induced by the design seismic action and computed according to the previous paragraph, should not exceed the design value of their flexural and shear resistance, M_{Rd} and V_{Rd}, respectively, when applied together with the concurrent gravity loads. This severely penalises "secondary members", as it requires them to remain elastic under the design seismic action. It amounts to an overstrength factor

of q in "secondary members" relative to the "primary" ones, if the strength of both is governed by the design seismic action and the concurrent gravity loads. Verification of "secondary members" on the basis of these requirements may not be feasible, unless:

- the global stiffness of the system of "primary members" and its connectivity to the "secondary" ones is such that seismic deformations imposed on the latter are low; or
- the lateral stiffness of "secondary members" is indeed very low.

4.12.4 Guidance on the Use of the Facility of "Secondary Members"

4.12.4.1 Seismic Design of New Buildings

A prime reason for the designer to consider as "secondary" some of the members of a new building designed for ductility, is when they are not within the scope of the rules for seismic design based on energy dissipation and ductility. For instance, flat slab frames and post-tensioned girders are not covered by seismic design codes. So, when using them, the designer may have to resist the full seismic action with walls or strong frames (usually at the perimeter), designating the flat slabs, the post-tensioned girders, as well as their supporting columns, as "secondary members". In a frame or frame-equivalent dual system, the columns supporting post-tensioned girders would better be taken as "secondary" anyway, because normally the large size of prestressed girders makes it unfeasible to satisfy Eq. (1.4). Moreover, such columns should have as small a cross-section as necessary for the support of gravity loads, to reduce the "parasitic" shears developing in them during post-tensioning at the expense of the axial force in the girder.

The designer may also want to consider as "secondary" those members of a new building that – owing to architectural constraints – cannot be made to conform to the seismic design rules for geometry, dimensioning or detailing for energy dissipation and ductility. Examples in DC M or H buildings designed according to Part 1 of Eurocode 8 (CEN 2004a) are beams which:

- are connected to a column at an eccentricity of the centroidal axes more than 25% of the largest cross-sectional dimension of the column at right angles to the beam, b_c, which is the limit specified in CEN (2004a);
- are supported on a column with cross-sectional depth, h_c, in the direction of the beam axis that cannot be made to satisfy the Eurocode 8 rule for bond and maximum diameter of the top bars of the beam within the joint (see Sections 3.3.2 and 5.4.1);
- have a width, b_w, greater than b_c plus the minimum of b_c or the depth of the beam, h_w, violating the relevant restriction in CEN (2004a);

– have top reinforcement (as governed by the combination of factored gravity loads) that cannot comply with the maximum allowed reinforcement ratio (see Section 5.3.2);
– connect two closely spaced columns, having a capacity-design shear from Eq. (1.9a) in Section 1.3.6.2 which is so large owing to the small clear span, L_{cl}, that the beam cannot be verified against the shear resistance for diagonal compression in the web, $V_{Rd,max}$; or, in a DC H building, the value of the ratio ζ_i in Eq. (1.10) of Section 1.3.6.2 is so close to –1, that the diagonal reinforcement required in the beam is too much to place.

Unlike the cases which are outside the scope of design rules for energy dissipation and ductility, those of the type above should preferably be accommodated through proper selection of the local structural layout, instead of resorting to the facility of "secondary members". There are two good reasons for doing so:

– The earthquake "sees" the structure as built, neither "knowing" much, nor "caring" about the considerations and assumptions made in its design calculations. So, the "primary members" may perform well thanks to their ductility, but the "secondary" ones may suffer serious damage.
– A structural system that cannot be utilised in its entirety for the engineered earthquake resistance of the building is a waste of resources. This is more so, given the conservatism of the special design requirements for "secondary members" (see Section 4.12.3).

That said, the option of designing the entire structural system for strength, instead of ductility (see Section 1.4.1) could be considered. In the framework of Eurocode 8, this means selecting DC L (Low) and $q = 1.5$. Then a distinction between "secondary" and "primary" members does not need to be made, as all members can be designed and detailed according to Eurocode 2 for non-seismic actions, without any regard to the special detailing and dimensioning rules of Eurocode 8 (CEN 2004a) for energy dissipation and ductility.

4.12.4.2 Seismic Assessment or Retrofitting

Unlike in the design of new buildings, where it may create more problems than it solves, the facility of "secondary members" can be used to advantage in seismic assessment and retrofitting of existing buildings. The designer may designate at the outset of the assessment (almost) all members as "primary" and, depending on the outcome of the verifications, consider whether few elements that (marginally) violate the verification criteria for "primary members" have reduced importance for seismic safety and performance to justify downgrading them to "secondary members", so that they can be checked with the relaxed pertinent criteria. In the framework of Part 3 of Eurocode 8 (CEN 2005a), the designer can do so free of constraints on the contribution of "secondary members" to the overall lateral stiffness (i.e., of condition no. 1 in Section 4.12.2, which applies only to new buildings). Besides, if

the structural model used from the outset is retained, there is no need to re-do the analysis with a new model either of the structure as a whole, or with its "primary members" alone.

The facility of "secondary members" is even more convenient for the retrofitting. It can be used to retrofit the structure by upgrading the earthquake resistance of only certain major existing elements and/or by adding a few new but large ones (e.g., concrete walls). The upgraded and/or the new elements may then be designed to take almost the full seismic action. They will be verified with the stricter criteria applying to "primary members", while the rest will be allowed to stay with their substandard detailing and poor earthquake resistance, if they meet the lax criteria for "secondary members". This may turn out to be a very cost-effective retrofitting strategy, as it allows limiting the disruption, including collection of information about the material properties and reinforcement of the as-built structure, to a small part of the building where the intervention takes place.

4.12.5 Modelling of "Secondary Members" in the Analysis

4.12.5.1 Modelling for the Design of New Buildings

In seismic design of new buildings based on linear analysis the strength and stiffness of "secondary members" against lateral loads is neglected in the analysis for the seismic action, but it may be considered in that for all other actions (e.g. gravity loads). Then, two different structural models may be used for the linear analysis (see also analysis types no. 1 and 2 in Section 4.12.3):

1. A model that completely neglects the contribution of "secondary members" to lateral stiffness.
2. Another which includes fully the "secondary members".

As pointed out in Section 4.12.3, the seismic deformation demands in the "secondary members" may then be obtained in a two-step procedure:

I. The elastic deformation demands in the "secondary members" due to the design seismic action are estimated from a linear seismic analysis using Model no. 2 (with the design spectrum, but removing afterwards the effect of the behaviour factor, q, from displacements and deformations according to Section 4.11.1).
II. The outcome of the Step I for storey i is multiplied by the ratio of interstorey drifts in that storey using Model no. 1 in the linear analysis for the design seismic action to those using Model no. 2.

Using two different structural models is not convenient, especially if linear analysis and design take place in an integrated computational environment. Among other problems, we have to use in the verifications:

- seismic action effects from an analysis with Model no. 1 (with seismic deformation demands in "secondary members" modified according to the paragraph above) and
- action effects of the concurrent gravity loads coming from an analysis with Model no. 2.

If we don't need to design the building for another lateral action, e.g., wind, it may be possible to use in some cases a single structural model for the seismic action and for gravity loads, namely one in which "secondary members" are included only with those properties that are essential for their gravity-load-bearing function. In such a model "secondary" columns and walls may be considered only with their axial stiffness and with zero flexural rigidity, or with moment releases (i.e., hinges) introduced between their ends and the joint they frame into. Such an approximation is acceptable, so long as the bending moments and shears induced in these members by gravity loads are negligible and their axial forces due to the seismic action also small. This precludes vertical elements on the perimeter of the building from such treatment. It is not good practice, anyway, to consider such members as "secondary".

If a single model is used for the seismic action and gravity loads according to the previous paragraph, "secondary" beams cannot in general be modelled with zero flexural rigidity or moment releases at the nodes, because this rigidity and the continuity of their spans are essential for their gravity-load bearing function. If they are not directly supported on vertical elements at all (e.g., when they are supported on girders), their seismic action effects will be negligible anyway, even when they are included in the model with their full flexural stiffness and connectivity. "Secondary" beams which are directly supported on vertical elements and continuous over two or more spans should be modelled with their full flexural stiffness. Their connectivity with the vertical elements depends on whether the latter are also "secondary" or not. If they are, zero flexural rigidity of these "secondary" vertical members, or moment releases at their connections with the beam-column joint are satisfactory also for the "secondary" beams they support. If the vertical elements are "primary", then two separate nodes can be introduced at the beam-column joint with pin connection between them: one node for the beam and another for the vertical element. The beam and the vertical element that continue past the joint will resist with their full flexural stiffness the gravity loads or the seismic action, respectively.

Note that, if a single structural model is used for the seismic action and for gravity loads along the lines of the two paragraphs above, internal forces in "secondary members"due to their seismic deformation demands can be estimated only by ad-hoc and approximate procedures for the verifications according to Section 4.12.3. For example, for a frame of "secondary" beams and/or columns, one may use the seismic interstorey drifts in the plane of the frame computed from the single model, remove from them the effect of the q-factor according to Section 4.11.1, use the corrected values as $\Delta\delta_i$ in Eq. (2.8) and solve for the column average seismic shear in that storey. If the columns of the frame have different moments of inertia, the total storey seismic shear in the frame is computed from the column average shear (with a weight of 0.5 on exterior columns) and back-distributed to the frame columns

in proportion to their moment of inertia. Individual column shears may then be multiplied by the clear column height to estimate the column end moments. The sum of these column seismic moments above and below a joint may then be distributed to the ends of the beams framing into the joint in inverse proportion to their span. The whole thing is as onerous as it sounds, especially as it is difficult to set it in a computational framework and most calculations may have to be done by hand or with spreadsheets.

It may be argued that, for damage limitation checks on the basis of interstorey drifts the contribution of "secondary members" to lateral stiffness may be considered in the linear analysis, as it is very unlikely that seismic deformations under the damage limitation seismic action will jeopardise their lateral stiffness and strength. However, seismic design codes do not differentiate the structural model to be applied in the analysis for the damage limitation seismic action from the one used for the design seismic action. Besides, for the designer's convenience, normally a single linear analysis is required for both levels of the seismic action. Analysis results for the damage limitation action are computed then by multiplying those for the design seismic action by the ratio of peak ground accelerations of the two actions. So, the contribution of "secondary members" to lateral stiffness should be neglected also at the damage limitation verifications.

4.12.5.2 Modelling for Seismic Assessment or Retrofitting

There is no real requirement to differentiate the modelling approach for "secondary members" from the normal one used for "primary" in seismic assessment and retrofitting. First of all, an analysis that neglects their contribution to stiffness against lateral loads (as Part 3 of Eurocode 8 allows doing for linear analysis) cannot determine the seismic deformation demands against which the capacities of "secondary members" should be verified (see Section 6.5.6). If the cyclic degradation of strength and stiffness is thought to be indeed much larger in "secondary members" than in "primary" ones,[33] it can be included in a nonlinear model. This can be done through a post-yield branch of the force-deformation curve in primary loading that is descending (with negative slope), instead of hardening or horizontal. If nonlinear dynamic analysis is used, the hysteresis rules may include degradation of strength with cycling, as in Park et al. (1987), Reinhorn et al. (1988), Coelho and Carvalho (1990), and Costa and Costa (1987).

[33]Note that, unless they are retrofitted, even the "primary members" of an existing substandard structure have larger cyclic degradation of strength and stiffness than a new member well designed and detailed for ductility.

Chapter 5
Detailing and Dimensioning of New Buildings in Eurocode 8

Like Chapter 2, this chapter is devoted solely to new concrete buildings. Moreover, Chapter 5 is the only one in the book referring exclusively to EN-Eurocode 8, notably to the rules in its Part 1 for the dimensioning and detailing of the members of new concrete buildings for earthquake resistance. It starts with an overview of Eurocode 8's detailing rules, deriving the most important of them from fist principles and from background information presented in Chapters 3 (mainly) and 1. It then presents Eurocode 8's special dimensioning rules in shear for various types of concrete components, relating them to the Eurocode 2 rules for non-seimic loading and documenting them – to the extent possible – on the basis of background information from Chapter 3. It proceeds then with proposals on how to implement in practice the Eurocode 8 dimensioning and detailing rules, appropriately sequencing them for the purposes of cost-effective detailed design.

The second half of Chapter 5 is devoted to two examples of detailed design according to Part 1 of Eurocode 8, including design of the foundation. The design of the superstructure in these two examples is just application of what has been said in Chapters 1, 4 and 5, while the design of the foundation gives the only opportunity in the book to present (and apply) expressions and rules for the verification of the foundation system (both for the soil and for the concrete elements). The two examples have been chosen so that, with certain simplifications for the analysis, calculations can be done by hand and presented in detail.

Overall, Chapter 5 serves as a justification document for the rules in Part 1 of EN-Eurocode 8 for dimensioning and detailing new concrete members for earthquake resistance and as a guide for the application of this part of EN-Eurocode 8 for practical seismic design of buildings.

5.1 Introduction

5.1.1 "Critical Regions" in Ductile Elements

The overview in Section 3.1 of the cyclic behaviour of concrete and reinforcing steel has concluded that RC members can dissipate energy only in bending (see

M.N. Fardis, *Seismic Design, Assessment and Retrofitting of Concrete Buildings*, Geotechnical, Geological, and Earthquake Engineering 8, DOI 10.1007/978-1-4020-9842-0_5,

Section 3.1.4). Usually energy dissipation takes place by alternate positive and negative bending in flexural plastic hinges at member ends.[1] Part 1 of Eurocode 8 (CEN 2004a) calls the zones where energy is dissipated "critical regions", a term with a more conventional connotation than the term "dissipative zone" used in CEN (2004a) for the part of a concrete, steel, composite or timber member or connection where energy dissipation takes place by design. In concrete members a "critical region" is a conventionally defined part of a "primary member", up to a certain distance from an end section – or in beams from the section of maximum positive (hogging) moment under the combination of the design seismic action and the concurrent gravity loads.

Part 1 of Eurocode 8 (CEN 2004a) prescribes the length of "critical regions" and special detailing rules for them, depending on the type of "primary member" and on the Ductility Class (DC) of the building. In buildings designed for energy dissipation (i.e., for DC Medium and High) a "critical region" is defined at an end of a "primary" column or beam framing into a beam or vertical element, respectively, no matter whether the relative magnitude of the moment resistances of the cross-sections around the joint suggests that a plastic hinge at that end is likely. Framing action and large seismic moments cannot develop at the end of a beam supported on another one at certain distance from a joint of that latter beam with a vertical member. The same applies at the end(s) of a cantilevering beam, unless that beam is explicitly designed against the vertical seismic action component (see Section 4.5.1). So, we can preclude plastic hinging at such beam ends and we don't need to consider a "critical region" there.

5.1.2 Geometry, Detailing and Special Dimensioning Rules in Eurocode 8: An Overview

Tables 5.1, 5.2 and 5.3 give a comprehensive overview of the detailing and dimensioning rules in CEN (2004a) for beams, columns and walls, respectively, for the three DCs. Some detailing rules are prescriptive and originate from the tradition of earthquake resistant design in different seismic regions of Europe. The most important among the detailing and special dimensioning rules, though, have a rational basis, explained in the individual sections of this Chapter.

Prescriptive detailing rules are overall slightly stricter in Eurocode 8 than in US codes (BSSC 2003, SEAOC 1999, ACI 2008) for the corresponding DC (with "Intermediate" being the counterpart of DC M and "Special" of DC H). Rules for anchorage of beam bars at or through beam-column joints in particular are much more detailed and demanding than in US codes.

[1] One-sided plastic hinges may form under positive (sagging) moments at some distance from the end section(s) of long span beams with significant gravity loading.

Table 5.1 EC8 rules for detailing and dimensioning of primary beams (secondary beams: as in DCL)

	DCH	DCM	DCL
"Critical region" length	$1.5\,h_w$	h_w	
Longitudinal bars (L)			
ρ_{min}, tension side	$0.5 f_{ctm}/f_{yk}$		$0.26 f_{ctm}/f_{yk}$, 0.13%[1]
ρ_{max}, critical regions[2]	$\rho' + 0.0018 f_{cd}/(\mu_\phi \varepsilon_{sy,d} f_{yd})$[2]		0.04
$A_{s,min}$, top and bottom	$2\Phi 14$ (308 mm^2)	–	
$A_{s,min}$, top-span	$A_{s,top\text{-}supports}/4$	–	
$A_{s,min}$, critical regions bottom	$0.5 A_{s,top}$[3]		–
$A_{s,min}$, supports bottom		$A_{s,bottom\text{-}span}/4$[1]	
d_{bL}/h_c – bar crossing interior joint[4]	$\leq \dfrac{6.25(1+0.8\nu_d)}{\left(1+0.75\dfrac{\rho'}{\rho_{max}}\right)}\dfrac{f_{ctm}}{f_{yd}}$	$\leq \dfrac{7.5(1+0.8\nu_d)}{\left(1+0.5\dfrac{\rho'}{\rho_{max}}\right)}\dfrac{f_{ctm}}{f_{yd}}$	–
d_{bL}/h_c – bar anchored at exterior joint[4]	$\leq 6.25(1+0.8\nu_d)\dfrac{f_{ctm}}{f_{yd}}$	$\leq 7.5(1+0.8\nu_d)\dfrac{f_{ctm}}{f_{yd}}$	–
Transverse bars (w)			
(i) outside critical regions			
Spacing $s_w \leq$		0.75d	
$\rho_w \geq$		$0.08\sqrt{(f_{ck}(\text{MPa})/f_{yk}(\text{MPa}))}$[1]	
(ii) in critical regions			
$d_{bw} \geq$		6 mm	
Spacing $s_w \leq$	$6d_{bL}$, $\dfrac{h_w}{4}$, $24d_{bw}$, 175 mm	$8d_{bL}$, $\dfrac{h_w}{4}$, $24d_{bw}$, 225 mm	–

Table 5.1 (continued)

	DC H	DCM	DCL
Shear design			
V_{Ed}, seismic[5]	$1.2\frac{\sum M_{Rb}}{l_{cl}} \pm V_{o,g+\psi_2 q}$ [5]	$\frac{\sum M_{Rb}}{l_{cl}} \pm V_{o,g+\psi_2 q}$ [5]	From analysis for design seismic action plus gravity
$V_{Rd,max}$ seismic[6]		As in EC2: $V_{Rd,max}=0.3(1-f_{ck}(MPa)/250)b_{wo}zf_{cd}$ sin 2δ[6], $1\leq$ cot $\delta\leq 2.5$	
$V_{Rd,s}$, outside critical regions[6]		As in EC2: $V_{Rd,s}=b_w z\rho_w f_{ywd}cot\delta$[6], $1\leq$ cot $\delta\leq 2.5$	
$V_{Rd,s}$, critical regions[6]	$V_{Rd,s}=b_w z\rho_w f_{ywd}$ ($\delta=45°$)	As in EC2: $V_{Rd,s}=b_w z\rho_w f_{ywd}$cot δ, $1\leq$ cot $\delta\leq 2.5$	
If $\zeta\equiv V_{Emin}/V_{Emax}$[7] < -0.5: inclined bars at angle $\pm\alpha$ to beam axis, with cross-section A_s/direction	If $V_{Emax}>(2+\zeta)f_{ctd}b_w d$ $A_s=0.5\ V_{Emax}/f_{yd}$sin α and stirrups for 0.5 V_{Emax}	–	

[1]NDP (Nationally Determined Parameter) according to Eurocode 2. The Table gives the value recommended in Eurocode 2.
[2]μ_ϕ is the value of the curvature ductility factor that corresponds to the basic value, q_o, of the behaviour factor used in the design (Eqs. (5.2)).
[3]The minimum area of bottom steel, $A_{s,min}$, is in addition to any compression steel that may be needed for the verification of the end section for the ULS in bending under the (absolutely) maximum negative (hogging) moment from the analysis for the design seismic action plus concurrent gravity, M_{Ed}.
[4]h_c is the column depth in the direction of the bar, $\nu_d = N_{Ed}/A_c f_{cd}$ is the column axial load ratio, for the algebraically minimum value of the axial load due to the design seismic action plus concurrent gravity (compression: positive).
[5]At a member end where the moment capacities around the joint satisfy: $\sum M_{Rb} > \sum M_{Rc}$, M_{Rb} is replaced in the calculation of the design shear force, V_{Ed}, by $M_{Rb}(\sum M_{Rc}/\sum M_{Rb})$.
[6]z is the internal lever arm, taken equal to 0.9d or to the distance between the tension and the compression reinforcement, $d-d_1$.
[7]V_{Emax}, $V_{E,min}$ are the algebraically maximum and minimum values of V_{Ed} resulting from the $\pm$ sign; V_{Emax} is the absolutely largest of the two values, and is taken positive in the calculation of ζ; the sign of V_{Emin} is determined according to whether it is the same as that of V_{Emax} or not.

Table 5.2 EC8 rules for detailing and dimensioning of primary columns (secondary columns as in DCL)

	DCH	DCM	DCL
Cross-section sides, h_c, $b_c \geq$	0.25m; $h_v/10$ if $\theta = P\delta/Vh > 0.1$[1]	–	
"Critical region" length [1] $\geq$	$1.5h_c$, $1.5b_c$, 0.6 m, $l_c/5$	h_c, b_c, 0.45 m, $l_c/5$	h_c, b_c
Longitudinal bars (L)			
ρ_{min}	1%		0.1 $N_d/A_c f_{yd}$, 0.2%[2]
ρ_{max}	4%		4%[2]
$d_{bL} \geq$		8 mm	
Bars per side $\geq$	3		2
Spacing between restrained bars	$\leq$150 mm	$\leq$200 mm	–
Distance of unrestrained bar from nearest restrained bar		$\leq$150 mm	
Transverse bars (w)			
Outside critical regions			
$d_{bw} \geq$		6 mm, $d_{bL}/4$	
Spacing $s_w \leq$	$20d_{bL}$, h_c, b_c, 400 mm		$12d_{bL}$, $0.6h_c$, $0.6b_c$, 240 mm
At lap splices, if $d_{bL} > 14$ mm: $s_w \leq$		$12d_{bL}$, $0.6h_c$, $0.6b_c$, 240 mm	
Within critical regions[3]			
$d_{bw} \geq$ [4]	6 mm, $0.4(f_{yd}/f_{ywd})^{1/2} d_{bL}$	6 mm, $d_{bL}/4$	
$s_w \leq$ [4],[5]	$6d_{bL}$, $b_o/3$, 125 mm	$8d_{bL}$, $b_o/2$, 175 mm	–
$\omega_{wd} \geq$ [6]	0.08	–	
$a\omega_{wd} \geq$ [5],[6],[7],[8]	$30\mu_\phi^* \nu_d \varepsilon_{sy,d} b_c/b_o - 0.035$	–	
In critical region at column base			
$\omega_{wd} \geq$	0.12	0.08	–
$a\omega_{wd} \geq$ [5],[6],[7],[9],[10]	$30\mu_\phi \nu_d \varepsilon_{sy,d} b_c/b_o - 0.035$		–
Capacity design check at beam-column joints[11]	$1.3 \sum M_{Rb} \leq \sum M_{Rc}$		
	No moment in transverse direction of column		–
Verification for M_x-M_y-N	Truly biaxial, or uniaxial with (M_z/0.7, N), (M_y/0.7, N)		
Axial load ratio $\nu_d = N_{Ed}/A_c f_{cd}$	$\leq$ 0.55	$\leq$ 0.65	–

Table 5.2 (continued)

	DCH	DCM	DCL
Shear design			
V_{Ed} seismic[12]	$1.3\frac{\sum M_{Rc}^{ends(12)}}{l_{cl}}$	$1.1\frac{\sum M_{Rc}^{ends(11)}}{l_{cl}}$	From analysis for design seismic action plus gravity
$V_{Rd,max}$ seismic[13] $V_{Rd,s}$ seismic [13),(14),(15)]	As in EC2: $V_{Rd,max}=0.3(1-f_{ck}(MPa)/250)b_{wo}zf_{cd}\sin 2\delta$, $1\leq \cot\delta\leq 2.5$ As in EC2: $V_{Rd,s}=b_w z\rho_w f_{ywd}\cot\delta+N_{Ed}(h-x)/l_{cl}$, $1\leq \cot\delta\leq 2.5$		

[1] h_v is the distance of the inflection point to the column end further away, for bending within a plane parallel to the side of interest; l_c is the column clear length.
[2] Note (1) of Table 5.1 applies.
[3] For DCM: if a value of q not greater than 2 is used for the design, the transverse reinforcement in critical regions of columns with axial load ratio ν_d not greater than 0.2 may just follow the rules applying to DCL columns.
[4] For DCH: In the two lower storeys of the building, the requirements on d_{bw}, s_w apply over a distance from the end section not less than 1.5 times the critical region length.
[5] Index c denotes the full concrete section and index o the confined core to the centreline of the perimeter hoop; b_o is the smaller side of this core.
[6] ω_{wd} is the ratio of the volume of confining hoops to that of the confined core to the centreline of the perimeter hoop, times f_{yd}/f_{cd}.
[7] a is the "confinement effectiveness" factor, computed as $a = a_s a_n$; where: $a_s= (1-s/2b_o)(1-s/2h_o)$ for hoops and $a_s= (1-s/2b_o)$ for spirals; $a_n= 1$ for circular hoops and $a_n=1-\{b_o/((n_h-1)h_o)+h_o/((n_b-1)b_o)\}/3$ for rectangular hoops with n_b legs parallel to the side of the core with length b_o and n_h legs parallel to the one with length h_o.
[8] For DCH: at column ends protected from plastic hinging through the capacity design check at beam-column joints, $\mu_\phi{}^*$ is the value of the curvature ductility factor that corresponds to 2/3 of the basic value, q_o, of the behaviour factor used in the design (see Eqs. (5.2)); at the ends of columns where plastic hinging is not prevented because of the exemptions listed in Note (11) below, $\mu_\phi{}^*$ is taken equal to μ_ϕ defined in Note (2) of Table 5.1 (see also Note (10) below); $\varepsilon_{sy,d}= f_{yd}/E_s$.
[9] Note (2) of Table 5.1 applies.
[10] For DCH: The requirement applies also in the critical regions at the ends of columns where plastic hinging is not prevented, as falling within the exemptions in Note (11) below.
[11] The capacity design check does not need to be fulfilled at beam-column joints: (a) of the top floor, (b) of the ground storey in two-storey buildings with axial load ratio ν_d not greater than 0.3 in all columns, (c) if shear walls resist at least 50% of the base shear parallel to the plane of the frame (wall buildings or wall-equivalent dual buildings), and (d) in one-out-of-four columns of plane frames with columns of similar size.
[12] At a member end where the moment capacities around the joint satisfy: $\sum M_{Rb}< \sum M_{Rc}$, M_{Rc} is replaced by $M_{Rc}(\sum M_{Rb}/\sum M_{Rc})$.
[13] z is the internal lever arm, taken equal to 0.9d or to the distance between the tension and the compression reinforcement, $d-d_1$.
[14] The axial load, N_{Ed}, and its normalised value, ν_d, are taken with their most unfavourable values for the shear verification under the design seismic action plus concurrent gravity (considering both the demand, V_{Ed}, and the capacity, V_{Rd}).
[15] x is the neutral axis depth at the end section in the ULS of bending with axial load.

Table 5.3 EC8 rules for the detailing and dimensioning of ductile walls

	DCH	DCM	DCL
Web thickness, $b_{wo} \geq$	$\max(150\text{ mm}, h_{storey}/20)$		–
Critical region length, h_{cr}	$\geq \max(l_w, H_w/6)$[1] $\leq \min(2\,l_w, h_{storey})$ if wall $\leq$ 6 storeys $\leq \min(2\,l_w, 2h_{storey})$ if wall $>$ 6 storeys		–
Boundary elements			
(a) in critical region			
– Length l_c from edge $\geq$	$0.15l_w$, $1.5b_w$, length over which $\varepsilon_c > 0.0035$		–
–Thickness b_w over $l_c \geq$	200 mm; $h_{st}/15$ if $l_c \leq \max(2b_w, l_w/5)$, $h_{st}/10$ if $l_c > \max(2b_w, l_w/5)$		–
–Vertical reinforcement:			
ρ_{min} over $A_c = l_c b_w$	0.5%		0.2%[2]
ρ_{max} over A_c		4%[2]	
– Confining hoops (w)[3]:			
$d_{bw} \geq$	8 mm	In the part of the section where $\rho_L > 2\%$: as over the rest of the wall (case c, below)	
spacing $s_w \leq$[4]	$\min(25d_{bh}, 250\text{ mm})$		
$\omega_{wd} \geq$[3]	0.12	0.08	–
$a\omega_{wd} \geq$[4],[5]	$30\mu_\phi(\nu_d+\omega_v)\varepsilon_{sy,d}b_w/b_o - 0.035$		–
(b) Storey above critical region	As in critical region, but $a\omega_{wd}$ and ω_{wd}: 50% of the ones required in critical region	As over the rest of the wall (case c, below)	

Table 5.3 (continued)

	DCH	DCM	DCL
(c) Over the rest of the wall height	In parts of the section where $\rho_L > 2\%$: – Distance of unrestrained bar in compression zone from nearest restrained bar $\leq$150 mm; – hoops with $d_{bw} \geq \max(6\text{ mm}, d_{bL}/4)$ and spacing $s_w \leq \min(12d_{bL}, 0.6b_{wo}, 240\text{ mm})^{(2)}$ up to a distance of $4b_w$ above or below floor beams or slabs, or $s_w \leq \min(20d_{bL}, b_{wo}, 400\text{ mm})^{(2)}$ beyond that distance		
Web			
–Vertical bars (v):			
$\rho_{v,min}$	Wherever $\varepsilon_c > 0.2\%$: 0.5%; elsewhere 0.2%		$0.2\%^{(2)}$
$\rho_{v,max}$	4%		
$d_{bv} \geq$	8 mm	–	
$d_{bv} \leq$	$b_{wo}/8$	–	
Spacing $s_v \leq$	$\min(25d_{bv}, 250\text{ mm})$	$\min(3b_{wo}, 400\text{ mm})$	
–Horizontal bars:			
$\rho_{h,min}$	0.2%	$\max(0.1\%, 0.25\rho_v)^{(2)}$	
$d_{bh} \geq$	8 mm	–	
$d_{bh} \leq$	$b_{wo}/8$	–	
Spacing $s_h \leq$	$\min(25d_{bh}, 250\text{ mm})$	400 mm	
Axial load ratio $\nu_d = N_{Ed}/A_c f_{cd}$	$\leq$0.35	$\leq$0.4	–
Design moments M_{Ed}	If $H_w/l_w \geq 2$, the design moments from linear envelope of maximum moments M_{Ed} from analysis for the "seismic design situation", are shifted up by the "tension shift" a_l		From analysis for design seismic action and gravity

Table 5.3 (continued)

	DCH	DCM	DCL
Shear design			
Design shear force V_{Ed} = shear force V'_{Ed} from the analysis for the design seismic action, times factor ε	If $H_w/l_w \le 2$[6]: ε=1.2 $M_{Rdo}/M_{Edo} \le q$ if $H_w/l_w > 2$[6],[7]: $\varepsilon = \sqrt{\left(1.2\frac{M_{Rdo}}{M_{Edo}}\right)^2 + 0.1\left(q\frac{S_e(T_C)}{S_e(T_1)}\right)^2} \le q$	ε=1.5	ε=1.0
Design shear force in walls of dual systems with $H_w/l_w > 2$, for z between $H_w/3$ and H_w[8]	$V_{Ed}(z) = \left(\frac{0.75z}{H_w} - \frac{1}{4}\right)\varepsilon V_{Ed}(0) + \left(1.5 - \frac{1.5z}{H_w}\right)\varepsilon V_{Ed}\left(\frac{H_w}{3}\right)$		From analysis for design seismic action and gravity
$V_{Rd,max}$ outside critical region	As in EC2: $V_{Rd,max} = 0.3(1 - f_{ck}(\text{MPa})/250) b_{wo}(0.8\, l_w) f_{cd} \sin 2\delta$, with $1 \le \cot\delta \le 2.5$		
$V_{Rd,max}$ in critical region	40% of EC2 value	As in EC2	
$V_{Rd,s}$ outside critical region	As in EC2: $V_{Rd,s} = b_{wo}(0.8\, l_w)\rho_h f_{ywd} \cot\delta$, $1 \le \cot\delta \le 2.5$		
$V_{Rd,s}$ in critical region; web reinforcement ratios: ρ_h, ρ_v			
(i) if $\alpha_s = M_{Ed}/V_{Ed} l_w \ge 2$: $\rho_v = \rho_{v,min}$, ρ_h from $V_{Rd,s}$:	As in EC2: $V_{Rd,s} = b_{wo}(0.8\, l_w)\rho_h f_{ywd} \cot\delta$, $1 \le \cot\delta \le 2.5$		
(ii) if $\alpha_s < 2$: ρ_h from $V_{Rd,s}$:[9]	$V_{Rd,s} = V_{Rd,c} + b_{wo}\alpha_s(0.75\, l_w)\rho_h f_{yhd}$	As in EC2: $V_{Rd,s} = b_{wo}(0.8\, l_w)\rho_h f_{ywd} \cot\delta$, $1 \le \cot\delta \le 2.5$	
ρ_v from:[10]	$\rho_v f_{yvd} \ge \rho_h f_{yhd} - N_{Ed}/(0.8\, l_w b_{wo})$		
Resistance to sliding shear: via bars with total area A_{si} at angle ±α to the horizontal [11]	$V_{Rd,s} = A_{si} f_{yd} \cos\alpha + A_{sv} \min(0.25 f_{yd}, 1.3\sqrt{(f_{yd} f_{cd})}) + 0.3(1 - f_{ck}(\text{MPa})/250) b_{wo} x f_{cd}$		

Table 5.3 (continued)

	DCH	DCM	DCL
$\rho_{v,min}$ at construction joints [10),(12)]	$0.0025, \dfrac{1.3 f_{ctd} - \dfrac{N_{Ed}}{A_c}}{f_{yd} + 1.5\sqrt{f_{cd} f_{yd}}}$	–	

[1)] l_w is the long side of the rectangular wall section or rectangular part thereof; H_w is the total height of the wall; h_{storey} is the storey height.

[2)] Notes (1) and (2) of Tables 5.1 or 5.2 apply.

[3)] For DC M: If, under the maximum axial force in the wall from the analysis for the design seismic action plus concurrent gravity the wall axial load ratio $\nu_d = N_{Ed}/A_c f_{cd}$ satisfies $\nu_d \leq 0.15$, the DCL rules may be applied for the confining reinforcement of boundary elements; these DCL rules apply also if this value of the wall axial load ratio is $\nu_d \leq 0.2$ but the value of q used in the design of the building is not greater than 85% of the q-value allowed when the DC M confining reinforcement is used in boundary elements.

[4)] Notes (5), (6), (7) of Table 5.2 apply for the confined core of boundary elements.

[5)] μ_ϕ is the value of the curvature ductility factor that corresponds through Eqs. (5.2) to the product of the basic value q_o of the behaviour factor times the value of the ratio M_{Edo}/M_{Rdo} at the base of the wall (see Note (6)); $\varepsilon_{sy,d} = f_{yd}/E_s$, ω_{vd} is the mechanical ratio of the vertical web reinforcement.

[6)] M_{Edo} is the moment at the wall base from the analysis for the design seismic action plus concurrent gravity; M_{Rdo} is the design value of the moment resistance at the wall base for the axial force N_{Ed} from the same analysis (design seismic action plus concurrent gravity).

[7)] $S_e(T_1)$ is the value of the elastic spectral acceleration at the period of the fundamental mode in the horizontal direction (closest to that) of the wall shear force multiplied by ε; $S_e(T_c)$ is the spectral acceleration at the corner period T_C of the elastic spectrum.

[8)] A dual structural system is one in which walls resist between 35 and 65% of the seismic base shear in the direction of the wall shear force considered; z is distance from the base of the wall.

[9)] For b_w and d in m, f_{cd} in MPa, ρ_L denoting the tensile reinforcement ratio, N_{Ed} in kN, $V_{Rd,c}$ (in kN) is given by:

$$V_{Rd,c} = \left\{ \max \left[180(100\rho_1)^{1/3},\ 35\sqrt{1 + \sqrt{\frac{0.2}{d}}}\, f_{cd}^{1/6} \right] \left(1 + \sqrt{\frac{0.2}{d}}\right) f_{cd}^{1/3} + 0.15 \frac{N_{Ed}}{A_c} \right\} b_w d$$

N_{Ed} is positive for compression; its minimum value from the analysis for the design seismic action plus concurrent gravity is used; if the minimum value is negative (tension), $V_{Rd,c} = 0$.

[10)] N_{Ed} is positive for compression; its minimum value from the analysis for the design seismic action plus concurrent gravity is used.

[11)] A_{sv} is the total area of web vertical bars and of any additional vertical bars placed in boundary elements against shear sliding; x is the depth of the compression zone.

[12)] $f_{ctd} = f_{ctk,0.05}/\gamma_c$ is the design value of the (5%-fractile) tensile strength of concrete.

5.2 Curvature Ductility Requirements According to Eurocode 8

It has been repeatedly pointed out (notably in Sections 1.3.6.1, 3.1.4 and 5.1.1) that the only reliable mechanism of force transfer that allows using to advantage the fundamental ductility of steel in tension and effectively enhancing the ductility of concrete and of the compression bars through lateral restraint, is in flexural "plastic hinges" that develop at member ends. The plastic hinge regions are then detailed for the inelastic deformation demands expected to develop there under the design seismic action.

Eurocode 8 pursues linking the local displacement and deformation demands on plastic hinges to the value of the behaviour factor q used in the design. Note that, unlike the discrete values of the force reduction R of US codes (BSSC 2003, SEAOC 1999), a q-factor which is proportional to the system overstrength factor α_u/α_1 assumes continuous values. So, the link between q and the local displacement and deformation demands should be algebraic. The link is provided via the global displacement ductility factor, μ_δ, related to q through Eqs. (1.1) and (1.2). Recall that an overstrength factor of 1.5 (for materials and elements) is already built in the q-factor values for buildings of DC M or H (see Table 1.1). So, normally Eqs. (1.1) and (1.2) should be applied using in the right-hand-side the value q/1.5 that corresponds to inelastic action and ductility. As the full q-value is used instead, a safety margin of 1.5 is hidden in the resulting value of μ_δ.

The link between local deformation demands on plastic hinges and the global displacement ductility factor, μ_δ, is based on the kinematics of the beam-sway mechanism, ensured by the walls of the structural system, or by the fulfillment of Eq . (1.4) around almost every beam-column joint. If the intended pattern of distributed plastic hinging in such a mechanism (shown in Figs. 1.3b–e of Section 1.3.2) occurs simultaneously throughout the structure, the demand value of the local ductility factor of the chord rotation at all member ends where plastic hinges form, μ_θ, is about equal to the demand value of the global displacement ductility factor, μ_δ.[2] The demand value of μ_θ is linked, in turn, to that of the curvature ductility factor at the end section, μ_φ, via Eq. (3.71).

Part 1 of Eurocode 8 (CEN 2004a) has followed Eurocode 2 (CEN 2004b) in adopting the confinement model in the CEB/FIP Model Code 90 (CEB 1991), given by Eqs. (3.8), (3.9), and (3.13) in Section 3.1.2.2. So, the curvature ductility requirements in CEN (2004a) are based on that model. Annex A in Part 3 of Eurocode 8 (CEN 2005a) gives the values of steel strain at rupture, ε_{su}, mentioned in Section 3.2.2.10 as case a(ii), for use together with the confinement model in CEB (1991) to calculate the ultimate curvatures in cyclic loading. If φ_u is computed that way, then, according to Annex A of CEN (2005a), the value of L_{pl} to be used in Eq. (3.70a) is that from Eq. (3.76) in Section 3.2.3.4. As pointed out in Section 3.2.3.4-Case

[2]Normally plastic hinges form sequentially, starting at the lower part of the building and never extending throughout their full intended pattern. So the maximum value of μ_θ in the building is about double its ideal value of μ_δ: $\mu_\theta \approx 2\mu_\delta$. Plastic hinges form essentially simultaneously only in wall systems having walls of similar size fixed at the base. In these walls $\mu_\theta \approx \mu_\delta$.

I(ii), the set of Eqs. (3.70a) and (3.76) and of the values of ε_{su}, ε_{cu} specified in CEN (2005a) or CEB (1991), respectively, underestimates, on average, by about 20% the currently available cyclic test results on member chord-rotation at flexure-controlled failure.

For the range of parameters L_s, h, d_{bL}, f_y and f_c commonly found in structural members of buildings, the value of L_{pl} from Eq. (3.76) ranges from $0.35L_s$ to $0.45L_s$ for columns (mean value $0.4L_s$), from 0.25 to $0.35L_s$ in beams (mean value $0.3L_s$) and from 0.18 to $0.24L_s$ in walls (mean value $0.21L_s$). These values are on the high side, because ε_{cu} (and hence $\mu_\varphi = \varphi_u/\varphi_y$ too) is underestimated by the confinement model in CEB (1991), adopted in Eurocode 2 and used in Eurocode 8 to implement the required curvature ductility through confinement (see Fig. 3.11c). In principle, for the value of $\mu_\theta = \mu_\delta$ that corresponds through Eqs. (1.1) and (1.2) to the value of q used in the design, the demand value of the curvature ductility factor of the end section, μ_φ, can be computed for each member from Eq. (3.71), using the particular value of L_{pl} from Eq. (3.76). Eurocode 8, instead, has opted for a single relation between μ_φ and q,based on a conservative approximation of Eq. (3.71) as: $\mu_\theta = 1 + 0.5(\mu_\varphi - 1)$:

$$\mu_\varphi = 2\mu_\theta - 1 \tag{5.1}$$

Presuming that the full value of q corresponds to inelastic action and ductility, within the full range of values of q for DC M and H buildings and the usual ranges of L_{pl} for the three types of concrete members, Eq. (5.1) gives a mean safety factor of about 1.65 for columns, about 1.35 for beams and about 1.1 for ductile walls, with respect to the more realistic values provided by inverting Eq. (3.71). If we take into account that inelastic deformations and ductility demands correspond to a value of just $q/1.5$, the average safety factor implicit in the demand value of μ_φ becomes 2.45 for columns, 1.9 for beams and 1.2 for ductile walls. This safety factor increases further, when the value of μ_φ is used for the calculation of the confining reinforcement in the "critical regions" of columns (see Section 5.3.3 and Table 5.2) and the boundary elements of the "critical region" of ductile walls (see Section 5.3.3 and Table 5.3), or of the compression reinforcement in beam end sections (see Section 5.3.2 and Table 5.1).

Eurocode 8 gives the demand value of μ_φ in terms of the basic value of the behaviour factor, q_o, by combining Eq. (5.1) with Eqs. (1.1) and (1.2) and with $\mu_\theta \approx \mu_\delta$

$$\mu_\varphi = 2q_o - 1 \quad \text{if } T \geq T_C \tag{5.2a}$$

$$\mu_\varphi = 1 + 2(q_o - 1)\frac{T_C}{T} \quad \text{if } T < T_C \tag{5.2b}$$

where T and T_C are as in Eqs. (1.1) and (1.2) and q_o, T refer to the vertical plane in which bending of the member being detailed takes place. Note that the

basic value q_o of the behaviour factor is used in Eqs. (5.2), instead of the final value q that may be lower than q_o owing to irregularity in elevation or to walls with low aspect ratio. Such features are considered to reduce the global ductility capacity for given local ductility capacities (e.g., because of non-uniform distribution of ductility and deformation demand in heightwise irregular buildings). Note that, by the same token, in torsionally flexible systems a q-factor value higher than the one used to reduce the elastic spectrum should had been specified for use in Eqs. (5.2), as their perimeter elements may be subjected to higher ductility and deformation demands than the rest. As this is not done in Eurocode 8, the designer is advised to detail the perimeter elements of torsionally flexible systems with additional caution and conservatism. This is not necessary in buildings considered as inverted pendulum systems, because, with their already very low q_o values, such systems will respond elastically to the design seismic action.

Recall that the values of q_o in Table 1.1 (and the final q-factor value derived from them after reductions for heightwise irregularity or wall aspect ratio) are upper limits of q for the derivation of the design response spectrum from the elastic one. Even if the designer uses a lower q value than the upper limit for the ductility class of a particular building, the required curvature ductility factor from Eqs. (5.2), or the prescriptive detailing rules for elements are not relaxed.

In ductile walls designed according to Eurocode 8 the lateral force resistance – i.e., the quantity directly related to the q-factor – depends only on the moment capacity of the base section. The wall overstrength is the ratio M_{Rd}/M_{Ed} – where M_{Ed} is the bending moment at the base from the analysis for the design seismic action and M_{Rd} the design value of moment resistance under the corresponding axial force from the analysis. Eurocode 8 allows computing μ_φ at the base of individual ductile walls using in Eqs. (5.2) the value of q_o divided by the minimum value of the wall M_{Rd}/M_{Ed}–ratio among all combinations of the design seismic action with the concurrent gravity loads. It would had been more representative – albeit less convenient – to use instead the ratio $\Sigma M_{Rd}/\Sigma M_{Ed}$, with both summations extending to all the walls in the system. Note that the plastic hinge at a wall base controls the lateral force resistance of the entire wall, which in turn may be an important contributor to the global lateral force capacity. By contrast, a frame system's lateral force resistance depends little on the moment resistance of individual beams or columns. So, there is no one-to-one correspondence between the deformation demands on a beam or column plastic hinge and its flexural overstrength, to support a simple rule for reduction of the local demand value of μ_φ in critical regions of beams or columns thanks to their overstrength.

Recognising the possible reduction of member flexural ductility when less ductile steel is used as longitudinal reinforcement (see Eqs. (3.1) and (3.2) in Section 3.1.1.4 and Eqs. (3.64) in Section 3.2.2.10), if steel of class B in Eurocode 2 (CEN 2004b) is used in the "critical region" of a primary element (as allowed in buildings of DC M, see Table 3.1) Eurocode 8 uses for its detailing a value of μ_φ increased by 50% over

that given by Eqs. (5.2). Note that the resulting value of μ_φ is used for the detailing of the compression reinforcement and of the confinement of the compression zone. So, the increase will not make up directly for the possible reduction in ductility due to the more brittle steel. It may have an indirect impact, though, by alerting the designer on the effects of such steels and encouraging the use of steel class C (or choosing DC L, instead, where design does not rely on ductility and there is no penalty for using steel class B).

5.3 Detailing Rules for Local Ductility of Concrete Members

5.3.1 Minimum Longitudinal Reinforcement Throughout a Beam

Concrete cracking may be considered as brittle fracture, releasing significant deformation energy when it happens. If a beam's cross-sectional area is large, its longitudinal reinforcement may fracture too upon beam cracking, if it is not sufficient to resist the cracking moment without yielding. So, the amount of longitudinal reinforcement should ensure that the yield moment exceeds the cracking moment. Because the magnitude and the distribution of seismic moments in a beam are very uncertain, all sections of a beam should meet this requirement, for both signs of the bending moment. More specifically, the minimum reinforcement area, $A_{s,\min}$, should be enough to sustain, with its yield force, $A_{s,\min} f_y$, the full tensile force released when concrete cracks. For linear stress distribution across the beam section, this force is equal to $0.5 f_{ct} b h_t$, where b and h_t are the width and the depth of the tension zone, respectively, before cracking. Beams commonly have a T- or L-section and when their flange is in compression the neutral axis is very close to it (also before cracking). So, it can be conservatively assumed that: $h_t \approx 0.9h \approx d$. If the flange is in tension, the depth and width of the tension zone are quite uncertain. It may be assumed again that $bh_t \approx bd$, where b and d are the width and effective depth of the rectangular web of the beam. Then the minimum ratio of reinforcement with respect to bd is:

$$\rho_{\min} = \frac{A_{s,\min}}{bd} = \frac{0.5 f_{ct} b h_t}{bd f_{yk}} \approx 0.5 \frac{f_{ctm}}{f_{yk}} \tag{5.3}$$

where the (28-day) mean value, f_{ctm}, is used for the tensile strength of concrete, f_{ct}, and the characteristic or nominal value, f_{yk}, for the yield stress of the longitudinal reinforcement. Note that the margin between the steel tensile strength, f_t, and the nominal yield stress, f_{yk}, is in the order of 25%, providing a safety margin against fracture due to overstrength of the concrete in tension (the 95%-fractile of f_{ct} exceeds f_{ctm} by about 30% and, unlike the compressive strength of concrete, its tensile strength does not increase significantly over time).

5.3.2 Maximum Longitudinal Reinforcement Ratio in "Critical Regions" of Beams

The value of μ_φ at plastic hinges of beams from Eqs. (5.2) is provided through an upper limit on the tension longitudinal reinforcement ratio in beam "critical regions", $\rho_{1,\max} = A_{s1,\max}/bd$. The value of $\rho_{1,\max}$ is derived as follows.

If the tension reinforcement is less than the compression reinforcement, $A_{s1} < A_{s2}$, the ultimate deformation at the end of the beam takes place when the effective ultimate strain of the tension reinforcement, ε_{su}, is exhausted. The requirements for the steel class in DC M or H buildings posed by Eurocode 8 (see Table 3.1 in Section 3.1.1.4) and the penalty on μ_φ if class B steel is used in DC M buildings (see last paragraph of Section 5.2) prevent fracture of tension reinforcement before the beam end reaches its ultimate flexural deformation by failure of the compression zone with the larger of the two reinforcement in tension: $A_{s1} > A_{s2}$. The limit on $\rho_{1,\max}$ refers to that situation. Therefore, Eq. (3.44) in the part *Definitions and Assumptions* of Section 3.2.2.4 applies for φ_u in $\mu_\varphi = \varphi_u/\varphi_y$, and not Eq. (3.43). In Eq. (3.44) ε_{cu} is taken equal to the ultimate strain of unconfined concrete in Eurocode 2: $\varepsilon_{cu2} = 0.0035$, because beams do not rely for ductility on confinement of their compression zone. For this value of ε_{cu} the right-hand-side of Eq. (3.50a) is about equal to 1/6 and the condition of Eq. (3.50a) is normally met by the beam. Moreover, for their usual parameter values (including $\omega_v = 0$ and $0.5\ \omega_1 \le \omega_2 \le \omega_1$) and with no axial load, beams satisfy Eq. (3.51) in the part *Curvature at Spalling of the Concrete Cover* of Section 3.2.2.4. Then Eq. (3.52) applies for the dimensionless neutral axis depth $\xi_{cu} = x_{cu}/d$. The conventional value, $\varepsilon_{c2} = 0.002$, can be used there for ε_{co}. Using in $\mu_\varphi = \varphi_u/\varphi_y$ the semi-empirical value $\varphi_y = 1.54\varepsilon_y/d$ from tests of beams or columns (see Eq. (3.40a) in the part *Comparison with Experimental Results and Empirical Expressions for the Curvature* of Section 3.2.2.2), the following upper limit comes out for the beam's tension reinforcement ratio, ρ_1:

$$\rho_{1,\max} = \frac{A_{s,\max}}{bd} \approx \rho_2 + \frac{0.0018}{\varepsilon_y \mu_\phi} \frac{f_c}{f_y} \tag{5.4a}$$

where $\rho_2 = A_{s2}/bd$ is the ratio of compression reinforcement. Both ρ_1 and ρ_2 are normalised to the width b of the compression flange, not of the web. In Eurocode 8 the design values of concrete and steel strengths, $f_{cd} = f_{ck}/\gamma_c$, $f_{yd} = f_{yk}/\gamma_s$ and the value $\varepsilon_{yd} = f_{yd}/E_s$ of $\varepsilon_y = f_y/E_s$ are used in Eq. (5.4a):

$$\rho_{1,\max} = \rho_2 + \frac{0.0018}{\varepsilon_{yd} \mu_\varphi} \frac{f_{cd}}{f_{yd}} \tag{5.4b}$$

As noted in Section 5.2 just before Eq. (5.1), for the value $L_{pl}/L_s = 0.3$ representative of typical beams in buildings, application of Eq. (5.2) gives a safety factor of about 1.35 with respect to the more realistic values provided by inverting Eq. (3.71) – or to 1.9, if it is recognised that the value of q includes a material (and member) overstrength factor of 1.5, hence only a value of $q/1.5$ produces ductility

demands. The safety factor on μ_φ becomes $1.35 \times 1.5/(1.15)^2 \approx 1.55$ if the values $\gamma_c = 1.5$, $\gamma_s = 1.15$ recommended in Eurocode 2 for ULS dimensioning under factored non-seismic actions are used, or just 1.35, if the values $\gamma_c = 1.0$, $\gamma_s = 1.0$ recommended in Eurocode 2 for the ULS under accidental actions are used instead. The ratio between these implicit safety factors is: $1.55/1.35 \approx 1.15$, i.e. equal to the partial factor of steel recommended for the ULS under factored non-seismic actions. This is consistent with adopting or not this safety factor for seismic design as well. This "theoretical" safety factor has been compared in Fardis (2004) to the ratio of:

1. the "demand" value of μ_φ from Eq. (5.1) using there the value of μ_θ at the ultimate deflection of beams cyclically tested to flexural failure; to
2. the "supply" value of μ_φ from inverting Eq. (5.4b) at the value of $(\rho_1 - \rho_2)$ in the tested beam.

The median value of this ratio in 52 cyclic tests of beams is 0.76 for γ_c=1, γ_s=1, or 0.82 for γ_c=1.5, γ_s=1.15. Being less than 1.0, these values suggest that Eq. (5.4b) is unsafe. If, however, the value of μ_θ is determined not as the ratio of the beam ultimate deflection to the experimental yield deflection, but to the value $M_y L_s/3(0.5\, E_c I_c)$ corresponding to the effective elastic stiffness of $0.5\, E_c I_c$ specified in CEN (2004a), the median ratio in the 52 beam tests is 2.65 for γ_c=1, γ_s=1, or 3.0 for γ_c=1.5, γ_s=1.15, well above the "theoretical" safety factors of 1.35 or 1.55 calculated here.

Equation (5.4b) is very restrictive for the top reinforcement at beam supports, especially for high values of μ_φ (e.g. in DC H buildings with high q_o values). To accommodate the top reinforcement needed to satisfy the ULS in bending at beam supports for the design seismic action together with the concurrent gravity loads without unduly increasing the beam section, the bottom reinforcement ratio, ρ_2, may be increased above the value of ρ_{min} of Eq. (5.3) and the prescriptive lower limit of $0.5\rho_1$ for the bottom reinforcement in beam "critical regions" (cf. Table 5.1).

5.3.3 Confining Reinforcement in "Critical Regions" of Primary Columns and Ductile Walls

The longitudinal reinforcement of columns and walls is normally symmetric: $\rho_1 = \rho_2$. So, the value of μ_φ in plastic hinges from Eqs. (5.2) cannot be achieved in the same way as in beams, notably through a compression reinforcement ratio, ρ_2, close enough to the tension reinforcement ratio, ρ_1, to keep the extreme concrete fibres below their ultimate strain (see Eq. (5.4b)). In columns and walls the extreme concrete fibres are allowed to reach their ultimate strain and spall. We rely thereafter on the enhanced ultimate strain of the confined concrete core to the centreline of the hoops and we provide the required value of μ_φ through confinement. The amount of confinement reinforcement required to this end is derived as follows.

For the same reason as in beams (see 2nd paragraph of Section 5.3.2), φ_u is taken from Eq. (3.44), this time applied to the section of the confined core inside the centreline of the hoops, i.e., with:

- depth: $h_o = h_c - 2(c + d_{bh}/2)$,
- width: $b_o = b_c - 2(c + d_{bh}/2)$ and
- effective depth: $d_o = d - 2(c + d_{bh}/2)$,

where (see Fig. 5.1):

c is the concrete cover to the outside of the hoops,
h_c, b_c are the external dimensions of the original unspalled concrete section and
d_{bh} is the hoop diameter.

The strain at the extreme fibres of the confined core, ε^*_{cu}, is taken equal to the ultimate strain of confined concrete, $\varepsilon_{cu2,c}$, according to Eurocode 2, i.e., from Eqs. (3.13) and (3.25). Recall that in Eurocode 2 confinement enhances the concrete strength and the corresponding strain according to Eqs. (3.8), (3.9) and (3.25). Using in $\mu_\varphi = \varphi_u/\varphi_y$ the semi-empirical value $\varphi_y = \lambda\varepsilon_y/h$, with $\lambda = 1.75$ for columns and $\lambda = 1.44$ for walls (see Eqs. (3.41b) and (3.41c) in the part *Comparison with Experimental Results and Empirical Expressions for the Curvature* of Section 3.2.2.2), the strain at the extreme fibres of the confined core, ε^*_{cu}, required for the target value of μ_φ is:

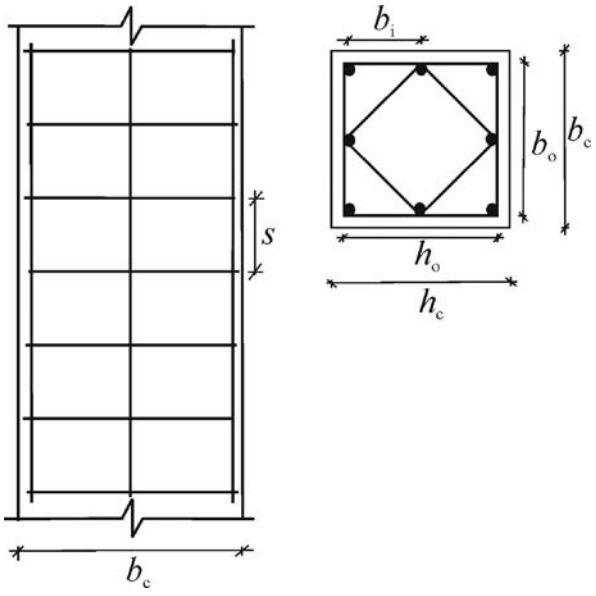

Fig. 5.1 Geometric terms for concrete confinement in columns (CEN 2004a)

$$\varepsilon^*_{cu} = \lambda \mu_\varphi \varepsilon_y \xi^*_{cu} \frac{h_o}{h_c} \tag{5.5}$$

As in Flow Chart 3.2 and in Section 3.2.2.4, variables with an asterisk or subscript "o" refer to the confined core, while h_c is the depth of the original column section. Note that in the confined core the compression reinforcement is so close to the extreme compression fibres[3] that Eq. (3.50a) is always met. For the same reason, with $\omega^*{}_1 = \omega^*{}_2$ the left-hand-side of Eq. (3.51) is negative, while, thanks to the increase of ε_{cu} by confinement, the value of its right-hand-side is positive and high. So, the dimensionless axial force in the confined core, $\nu^* = N/(b_o h_o f^*{}_c)$, being low thanks to the increase of $f^*{}_c$ by confinement and the large size of primary columns,[4] satisfies Eq. (3.51) in the part *Curvature at Spalling of the Concrete Cover* of Section 3.2.2.4. The physical meaning is that confinement delays crushing of the extreme fibres in the confined core till after both the tension and the compression bars yield. Then, Eq. (3.52) applies for the neutral axis depth of the confined core (normalised to h_o as $\xi^*{}_{cu}$), giving (for $\omega^*{}_1 = \omega^*{}_2$ and $\delta_1 \approx 0$):

$$\xi^*_{cu} \approx \frac{\nu^* + \omega^*_\nu}{\left(1 - \dfrac{\varepsilon^*{}_{co}}{3\varepsilon^*{}_{cu}}\right) + 2\omega^*_\nu} \approx \frac{\nu + \omega_\nu}{\left(1 - \dfrac{\varepsilon^*{}_{co}}{3\varepsilon^*{}_{cu}}\right) \dfrac{f^*{}_c}{f_c} \dfrac{b_o h_o}{b_c h_c} + 2\omega_\nu} \tag{5.6}$$

where $\omega^*{}_v = A_{sv} f_y / b_o h_o f^*{}_c$ is the mechanical reinforcement ratio of vertical bars between the extreme tension and compression bars in the confined core and $\omega_v = A_{sv} f_y / h_c b_c f_c$, is the corresponding ratio in the unspalled section. After substituting $\xi^*{}_{cu}$ from Eq. (5.6) into Eq. (5.5), setting $\varepsilon^*{}_{cu}$ equal to the value from Eqs. (3.13) and (3.25), substituting the values of $f^*{}_c$, $\varepsilon^*{}_{co}$ from Eqs. (3.8) and (3.9) and neglecting 2nd-order terms, the following result is obtained for the effective mechanical (volumetric) ratio of confining reinforcement, $a\omega_w$:

$$a\omega_w \approx 10\lambda \mu_\varphi \varepsilon_y (\nu + \omega_\nu) \frac{b_c}{b_o} - 0.0285 \tag{5.7a}$$

or, after multiplying both sides by $(f_{yd}/f_y)(f_c/f_{cd}) = \gamma_c/\gamma_s$:

$$a\omega_{wd} \approx 10\lambda \mu_\varphi \varepsilon_{yd} (\nu_d + \gamma_s \omega_{vd}) \frac{b_c}{b_o} - 0.0285 \gamma_c/\gamma_s \tag{5.7b}$$

In lieu of Eq. (5.7b), Eurocode 8 adopts the following expression:

---

[3] $\delta_1 = (h_o - d_o)/h_o = (d_{bL} + d_{bh})/2h_o \approx 0$

[4] Primary columns designed for DC H or M according to Eurocode 8 are large, not so much to satisfy Eq. (1.4) or the prescriptive upper limits on the dimensionless axial load ratio, ν_d, (see Table 5.2), but thanks to the upper limit on the ratio of beam longitudinal bar diameter to column depth at beam-column joints (see Section 5.4.1 and Table 5.1)

$$a\omega_{wd} = 30\mu_{\varphi}\varepsilon_{yd}\,(\nu_d + \omega_{\nu d})\,\frac{b_c}{b_o} - 0.035 \tag{5.8}$$

Moreover, in columns Eurocode 8 neglects ω_{vd}, as small compared to ν_{d}. The difference between 10λ and the adopted value of 30 for the coefficient provides a safety margin on the value of μ_{φ} achieved for given value of $a\omega_{\mathrm{wd}}$. Regarding the last term in Eqs. (5.7b) and (5.8), note that for the values of γ_{c}, γ_{s} recommended in Eurocode 2 for ULS design against non-seismic actions $0.0285\gamma_{\mathrm{c}}/\gamma_{\mathrm{s}}$ is equal to 0.037, i.e. larger than 0.035 and the difference is on the safe side. However, the same term is equal to 0.0285 for the values of γ_{c}, γ_{s} recommended for ULS design against accidental actions and the difference is on the unsafe side. Overall, for the usual amounts of confining reinforcement the difference of the final confinement requirements from Eqs. (5.7b) and (5.8) corresponds to the difference in the γ_{s} values ($\gamma_{\mathrm{s}} = 1.15$ v $\gamma_{\mathrm{s}} = 1.0$).

Recall from the paragraph of Section 5.2 before Eq. (5.1) that:

- for the usual values of $L_{\mathrm{pl}}/L_{\mathrm{s}}$ in typical building columns, Eq. (5.1) gives an average safety factor of about 1.65 with respect to more realistic values obtained by inverting Eq. (3.71); if it is considered that q includes an overstrength factor of 1.5 and only a value of $q/1.5$ produces ductility demands, this safety factor increases to 2.45;
- for the values of $L_{\mathrm{pl}}/L_{\mathrm{s}}$ representative of typical ductile walls in buildings, Eq. (5.1) gives an average safety factor of about 1.1 with respect to the values obtained by inverting Eq. (3.71), or of 1.2 when it is taken into account that only $q/1.5$ gives rise to ductility demands.

The end result is an average safety factor on μ_{φ} of:

- $1.65 \times 30/(10 \times 1.75) \approx 2.8$ for columns, or
- $1.1 \times 30/(10 \times 1.44) \approx 2.3$ for walls.

Such values of the safety factor on μ_{φ} are fully justified for vertical elements, in view of:

- their crucial importance for the integrity of the whole, and
- the large scatter of experimental results about the correspondence between μ_{φ} and μ_{θ} and the associated uncertainty.

In view of this uncertainty, the "theoretical" safety factor has been compared to the ratio of:

1. the "demand" value of μ_{φ} from Eq. (5.1) using there the value of μ_{θ} at the ultimate deformation of columns or walls cyclically tested to flexural failure, to
2. the "supply" value of μ_{φ} from inverting Eq. (5.8) for the value of $a\omega_{\mathrm{wd}}$+0.035 in the test specimens.

The median value of the ratio in about 640 cyclic tests of columns with non-zero axial load is 0.82 for γ_c=1, γ_s=1, or 0.85 if γ_c =1.5, γ_s =1.15. The corresponding median values in about 50 cyclic tests on flexure-controlled walls is 0.9 for γ_c=1, γ_s=1, or 1.02 for γ_c=1.5, γ_s=1.15. Values less than 1.0 suggest that Eq. (5.8) is unsafe. If, however, the value of μ_θ is determined as the ratio of the member ultimate drift not to the experimental yield drift but to the value $M_y L_s/3(0.5E_cI_c)$ corresponding to the effective elastic stiffness of $0.5E_cI_c$ specified in Eurocode 8 for the analysis of concrete buildings, the median ratio becomes (Fardis 2004):

- 1.85 for γ_c =1, γ_s =1, or 2.0 for γ_c =1.5, γ_s =1.15 in the column tests, and
- 2.9 for γ_c =1, γ_s =1, or 3.3 for γ_c=1.5, γ_s=1.15 in the wall tests,

compared to the "theoretical" safety factors of 2.8 or 2.3 quoted above.

If Eq. (5.8) gives a negative outcome when applied with b_o=b_c, the target value of μ_φ can be achieved by the unspalled section without confinement. Then stirrups in the "critical region" may just follow the prescriptive detailing rules of the corresponding DC (cf. Tables 5.2 and 5.3).

The confinement reinforcement from Eq. (5.8) is not required by Eurocode 8 at all column "critical regions" indiscriminately, but only where plastic hinges may develop by design. These are the "critical regions" at the base of DC M or H columns (at the connection to the foundation). In all other "critical regions" of DC M columns, only the prescriptive detailing rules of Table 5.2 – e.g. against buckling of bars, etc. – do apply. In DC H buildings, however, the confining reinforcement from Eq. (5.8) is required by Eurocode 8 in the "critical regions" at the ends of all columns not checked for fulfilment of Eq. (1.4) (those falling in the exemptions allowed by Eurocode 8 and listed in Section 1.3.4). Besides, some confining reinforcement is also required even in the "critical regions" at the ends of DC H columns which are protected from plastic hinging by meeting Eq. (1.4) in both horizontal directions. In that case it is computed from Eq. (5.8) for the value of μ_φ obtained from Eqs. (5.2) for two-thirds of the basic q-factor value, q_o, used in the design, instead of the full value.

In columns Eq. (5.8) should be applied separately in the two directions of bending, using the values of q_o (and hence of μ_φ) applying to the structural system in these two directions and the most unfavourable (i.e., maximum) value of the axial force from the analysis for the seismic action and the concurrent gravity loads. The largest outcome of Eq. (5.8) from these two separate applications should be used for ω_{wd}. It should be implemented as sum of mechanical reinforcement ratios in both transverse directions, $(\rho_x+\rho_y)f_{ywd}/f_{cd}$, providing, however, about equal transverse reinforcement ratios in both directions: $\rho_x \approx \rho_y$. The layout of confining reinforcement in walls, rectangular or not, is the subject of the next section.

Wall or column sections often consist of several rectangular parts: sections with T-, L-, double-tee, U-, or even Z-shape, hollow rectangular sections, walls with "barbells" at the edges of the section, etc. For such sections ω_{wd} should be determined separately for each rectangular part of the section that may serve as compression flange under any direction of the seismic action. Eq. (5.8) should first be applied

taking as width b_c the external width of the compression flange at the extreme compression fibres. This applies also to the normalisation of the axial force, N_{Ed}, and of the area of vertical reinforcement between the tension and compression flanges, A_{sv}, as $\nu_d = N_{Ed}/(h_c b_c f_{cd})$, $\omega_{vd} = A_{sv}/(h_c b_c) f_{yd}/f_{cd}$, with h_c denoting the maximum dimension of the unspalled section at right angles to b_c (as if the section were rectangular, with width b_c and depth h_c). For this to apply the compression zone should be limited within the compression flange with width b_c. To check this, the neutral axis depth at the ultimate curvature after the concrete cover spalls at the compression flange is calculated as[5]:

$$x_u = (\nu_d + \omega_{vd}) \frac{h_c b_c}{b_o} \tag{5.9}$$

The outcome of Eq. (5.9) for x_u is then compared to the dimension of the rectangular compression flange at right angles to b_c (i.e., parallel to h_c), after reducing it by $(c+d_{bh}/2)$ for spalling. If this reduced dimension exceeds x_u, the outcome of Eq. (5.8) for ω_{wd} is implemented with stirrups in the compression flange in question. Again about equal stirrup ratios should preferably be provided in both directions of this compression flange: $\rho_x \approx \rho_y$. However, what mainly counts in this case is the steel ratio of the stirrup legs at right angles to b_c.

If the value of x_u from Eq. (5.9) appreciably exceeds the dimension of the compression flange at right angles to b_c reduced by $(c+d_{bh}/2)$, there are three alternatives:

1. The difficult one: Eurocode 8 recommends the cumbersome and tricky option of generalising the rigorous approach highlighted above in the derivation of Eqs. (5.7) and (5.8), notably by:

- defining μ_φ as $\mu_\varphi = \varphi_u/\varphi_y$,
- calculating φ_u as $\varphi_u = \varepsilon^*_{cu}/x_{cu}$ and φ_y as $\varphi_y = \varepsilon_y/(d-x_y)$,
- estimating the neutral axis depths x_u and x_y from equilibrium over the section, and
- using Eqs. (3.8), (3.9), (3.13) and (3.25) for the properties of the confined concrete.

In principle this can be done using the iterative algorithms mentioned in Section 5.7.3.1 for the ULS verification of sections with any shape and layout of reinforcement for any M_y-M_z-N combination, provided that the properties of confined concrete from Eqs. (3.8), (3.9), (3.13) and (3.25) are used in its parabolic-rectangular σ-ε law. Confinement reinforcement should be calculated both for the compression flange of width b_c and the adjoining rectangular part of the section at right angles to it (the "web"). It should provide the same safety margin on the value of μ_φ as given by Eq. (5.8) over Eq. (5.7) (i.e., it should achieve the safety margin provided by Eq. (5.8) for rectangular sections).

[5] Equation (5.9) is an approximation of Eq. (5.6).

2. The easy option. To physically increase the dimension of the rectangular compression flange at right angles to b_c, so that, after been reduced by $(c+d_{bh}/2)$ because of spalling, it exceeds the value of x_u from Eq. (5.9).
3. The intermediate option: To provide confinement over the rectangular part of the section at right angles to the compression flange (the "web"), instead of the compression flange itself. This option is meaningful only if the compression flange for which the neutral axis depth has first been calculated from Eq. (5.9) is shallow and not much wider than the "web". Eq. (5.8) should be applied then with width b_c the thickness of the "web" (also in the normalisation of N_{Ed} and A_{sv} into ν_d, ω_{vd}). The value of ω_{wd} from Eq. (5.8) should be implemented through stirrups in the "web". It is consistent with this to sacrifice the compression flange by placing in its parts that protrude from the "web" transverse reinforcement meeting only the prescriptive rules of the corresponding DC for stirrup spacing and diameter, without any confinement requirements. It is more prudent, though, to place in them the same confining reinforcement as in the "web".

Note that, although the approach above covers also columns with composite section, Eurocode 8 specifies it (with option 1) only for walls. Then h_c is the length of the wall section, l_w. The only difference of walls from columns in this respect is in the extent of the confinement in the direction of the length, l_w, as described in the following section.

5.3.4 Boundary Elements at Section Edges in "Critical Regions" of Ductile Walls

As noted in the definition of walls in Section 2.2.2.1, a wall differs from a column in its design and detailing as a concrete member. The wall's moment resistance is assigned to the "tension and compression chords" or "flanges" at the edges of its section and its shear resistance to the "web" in-between them. The wall vertical reinforcement is concentrated in "boundary elements" at the two edges of the section. Confinement of the concrete is also limited there (Fig. 5.2).

Confined boundary elements may be limited to the part of the section where at ultimate deformation the concrete strain exceeds the ultimate strain of unconfined concrete according to Eurocode 2, $\varepsilon_{cu} = 0.0035$. The hoop enclosing a boundary element should have a (centreline) length of $x_u(1-\varepsilon_{cu}/\varepsilon^*_{cu})$ in the direction of the wall length, l_w. In this calculation the neutral axis depth after concrete spalling, x_u, is estimated from Eq. (5.9) with h_c equal to l_w. ε^*_{cu} is estimated as $\varepsilon^*_{cu} = 0.0035+0.1a\omega_{wd}$ (cf. Eqs. (3.13) and (3.25)) using the actual value of $a\omega_{wd}$ in the boundary element. The overall length of the confined boundary element, including the concrete cover of its perimeter hoop, $l_c \geq x_u(1-\varepsilon_{cu2}/\varepsilon^*_{cu})+2(c+d_{bh}/2)$, should respect the minimum value in Table 5.3.

According to Eurocode 8, boundary elements with confinement as specified above are required only in the "critical region" at the base of ductile walls of DC M

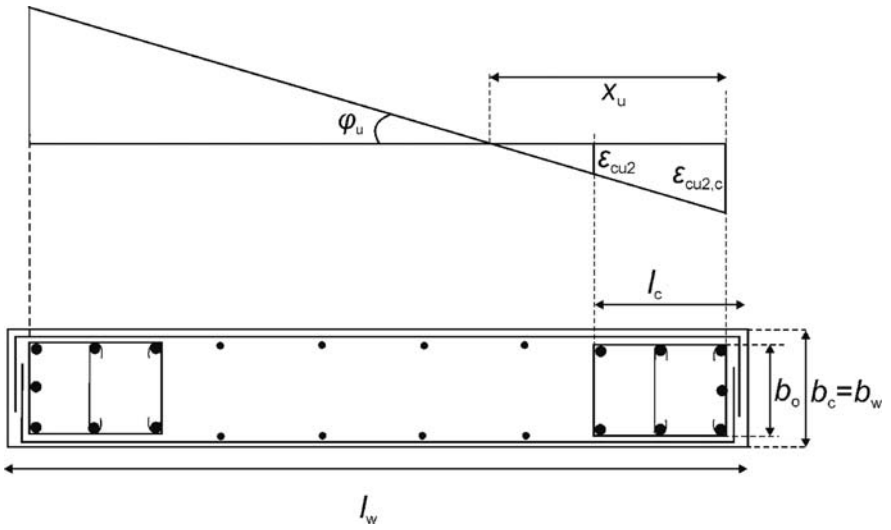

Fig. 5.2 Boundary elements in rectangular wall and strain distribution at ultimate curvature (CEN 2004a)

and H. In DC H walls, boundary elements should be provided for one more storey above the "critical region", with half the confining reinforcement required in the "critical region" below. Although it is not required by Eurocode 8, it is advisable to provide boundary elements over the full height of a ductile wall, with their minimum length and reinforcement. This is particularly important in "barbelled" walls, as the "barbells" should be detailed anyway as column-like elements.

5.4 Detailing and Dimensioning of Beam-Column Joints

5.4.1 Maximum Diameter of Longitudinal Beam Bars Crossing or Anchored at Beam-Column Joints

Shear forces are introduced in beam-column joints primarily via bond stresses along the beam and column bars around the joint core. Cyclic degradation of bond and slippage of these bars along their length within the joint increases the apparent flexibility of the joint and the interstorey drifts. It might even prevent development of the member's moment resistance at the face of the joint. Although the global consequences of such phenomena are not dramatic, loss of bond along these bars in a joint would better be avoided through appropriate verifications. Section 3.3.2 mentioned that an upper limit is obtained for the ratio d_{bL}/h_c of beam bars passing through interior beam-column joints or anchored at exterior ones, by setting the bond stress in Eq. (3.133) equal to the ultimate bond stress. The d_{bL}/h_c-limits set in Eurocode 8

have been chosen as follows, before the relevant recent advances in the State-of-the-Art (Cairns 2006, Eligehausen and Lettow 2007).

As pointed out in Section 3.1.3.2, the design value of the ultimate bond stress in Eurocode 2 is $2.25f_{ctd}$ for "good" bond conditions, or 70% of that value for "poor" conditions. The design value of the concrete tensile strength is $f_{ctd} = f_{ctk,0.05}/\gamma_c = 0.7f_{ctm}/\gamma_c$. As the consequences of bar pull-out from the joint core are not catastrophic, if the design bond strength is based on the 5%-fractile of the tensile strength of concrete, it is too conservative to divide it further by the partial factor for concrete. So, this partial factor may not be applied in this particular case. As bond outside the confined joint core is neglected, the positive effects of confinement by the joint stirrups, the top bars of the transverse beam and the large volume of the surrounding concrete may be taken into account. This may be done according to CEB (1991), by doubling the design value of the ultimate bond stress, instead of dividing it by 0.7 according to Eurocode 2. The factor of 2.0 is consistent with the upper limit value on the confinement terms (the 1st and the 2nd one inside the brackets) in Eq. (3.31), for the pull-out (or -through) mode of failure. This gives an ultimate bond stress for the top bars ("poor" bond conditions) of $2.0 \times [0.7 \times 2.25 \times (0.7f_{ctm})] = 2.2f_{ctm}$. This value may be further increased by the friction due to the normal stress on the bar-concrete interface, $\sigma\cos^2\varphi$, produced by the mean vertical compressive stress in the column above the joint, $\sigma = N_{Ed}/A_c = \nu_d f_{cd}$. When averaged around the bar perimeter, this bond strength enhancement becomes $0.5\,\mu\nu_d f_{cd}$, where μ is the friction coefficient. For the design value $\mu = 0.5$ specified in Eurocode 2 at an interface with roughness similar to that of the bar surface, friction enhances the design value of bond strength to $2.2f_{ctm}+0.5 \times 0.5\nu_d f_{cd} \approx 2.2f_{ctm}(1+0.8\nu_d)$.[6] The factor 0.8 in the parenthesis incorporates a value of 10.5 for the ratio of $f_{ck} = 1.5f_{cd}$ to f_{ctm}.[7] By setting τ_b from Eq. (3.133) equal to this design value of bond strength along the top bars, the following condition is derived for the diameter of beam longitudinal bars in beam-column joints, d_{bL}:

– in interior beam-column joints:

$$\frac{d_{bL}}{h_c} \le \frac{7.5 f_{ctm}}{\gamma_{Rd} f_{yd}} \cdot \frac{1 + 0.8\nu_d}{1 + k\frac{\rho_2}{\rho_{1,max}}} \tag{5.10a}$$

–in beam-column joints which are exterior in the direction of the beam:

$$\frac{d_{bL}}{h_c} \le \frac{7.5 f_{ctm}}{\gamma_{Rd} f_{yd}} \cdot (1 + 0.8\nu_d) \tag{5.10b}$$

–where the overstrength coefficient for the beam bars, γ_{Rd}, is taken as:

[6] The value $0.25\nu_d f_{cd}$ used here is 25% higher than the value $0.5p = 0.2\nu_d f_{cd}$ of the corresponding term in Eq. (3.31) (the 3rd one inside the brackets).

[7] The ratio f_{ck}/f_{ctm} varies between 9 and 11.8 for f_{ck} from 20 to 45 MPa. The value 10.5 corresponds to f_{ck}= 30 MPa.

– $\gamma_{Rd} = 1.0$ for DC M and
– $\gamma_{Rd} = 1.2$ for DC H.

Coefficient k in Eq. (5.10a), standing for $(1–\xi_{eff}/\omega)$ in Eq. (3.133), is taken equal to:

– $k = 0.5$ for DC M and
– $k = 0.75$ for DC H.

In exterior beam-column joints we have $\sigma_{s2} = 0$, which is equivalent to $k = 0$, giving Eq. (5.10b).

The value of $\nu_d = N_{Ed}/f_{cd}A_c$ to be used in Eqs. (5.10) should be the minimum value among all combinations of the design seismic action with the concurrent gravity loads. Eurocode 8 does not give any instructions for tensile net axial forces (that may occur in exterior columns of medium- or high-rise buildings). It is clear from the derivation of Eqs. (5.10) that in that case $\nu_d = 0$.

It is most convenient to apply Eqs. (5.10) during the initial sizing of columns, with a target maximum value of the beam bar diameter. This can be done on the basis of a rough estimate of the minimum axial load N_{Ed} in any combination of the design seismic action with the concurrent gravity loads, $\min N_d$ in Eq. (2.13) of Section 2.2.1.5. At that stage the final value of the top reinforcement ratio ρ_1 in Eq. (5.10a) is not known. So in Eq. (5.10a) the value of ρ_1 in Eq. (3.133) has been taken equal to the maximum value allowed, $\rho_{1,max}$, from Eq. (5.4b). At the same stage the bottom steel ratio ρ_2 may be taken equal to the minimum value from Eq. (5.3), or to $0.5\rho_{1,max}$. Although these convenient choices for ρ_2 and $\rho_{1,max}$ are favourable (not safe-sided) for d_{bL}, it should be kept in mind that Eq. (5.10a) is over-demanding for the size of interior columns. For common values of the axial load ($\nu_d \sim 0.2$) and of the steel nominal yield stress (500 MPa) and a relatively low concrete grade ($f_{ck} = 20$ MPa), a column size h_c of about $40d_{bL}$ is required for DC H (i.e. h_c more than 0.6 m for $d_{bL} = 14$ mm, or about 0.8 m if $d_{bL} = 20$ mm)! The required size is relaxed to about $30d_{bL}$ for medium-high axial loads and higher concrete grades. If DC M is chosen, the required column size is reduced by about 25%.

Although onerous, the restrictions of Eqs. (5.10) are justified by the cyclic test results in Fig. 3.46 (Kaku and Asakusa 1991). These results show that the cyclic response of a beam-column subassembly with $h_c = 18.75d_{bL}$ is governed by bond-slip of the beam bars within the joint and exhibits low energy dissipation and rapid stiffness decay. A column size of $h_c = 37.5d_{bL}$ is needed in Fig. 3.46 for the cyclic behaviour of the subassembly to be governed by flexure in the beam and exhibit stable hysteresis loops with high energy dissipation. Subassemblies with $h_c = 28d_{bL}$ gave mediocre results. According to Kitayama et al. (1991), the energy dissipated by subassemblies with $h_c = 20d_{bL}$ cycled to a storey drift ratio of 2% corresponds to an effective global damping ratio of only 8%.

Eurocode 8 allows applying Eq. (5.10a), derived for the top bars, also to the bottom bars of the beam. For them the denominator in the 2nd term of Eq. (5.10a) should have been replaced by 2 and term $7.5f_{ctm}$ in the numerator divided by 0.7 to account for the "good" bond conditions. As the end result would be about the same

as that of Eq. (5.10a), for simplicity the same expression is used for the bottom bars as well. Note, though, that for bottom bars at exterior joints Eq. (5.10b) is conservative by a factor of about 0.7 on the required column depth h_c, thanks to the "good" bond conditions there.

For exterior joints Eq. (5.10b) is safe-sided for both top and bottom bars for another reason: although at the exterior face of such joints top beam bars are normally bent down and bottom bars up, Eq. (5.10b) takes into account the bond only along the horizontal part of these bars and discounts completely the contribution of the 90°-hook or bend. Behind this assumption is the letter of Eurocode 2, which says that only the straight part of the bar counts toward anchorage in compression. Prevention of push-out of 90°-hooks or bends, if the straight part of the bar is not sufficient to transfer the full yield force of the bar to the joint, is another goal behind the adoption of the letter of Eurocode 2 in this respect. However, the dense horizontal stirrups placed in an exterior joint between a 90°-hook or bend and the exterior surface prevents push-out of the hook or bend – as well as its opening up and kick-out of the concrete cover when the bar is in tension. Moreover, top bars are normally protected from yielding in compression thanks to the overstrength of the top flange over the tensile capacity of its bottom counterpart. So, only the bottom bars may yield in compression at an exterior joint. The margin of about 0.7 on h_c mentioned at the end of the previous paragraph is available for them. The same margin of about 0.7 on h_c is available according to the Eurocode 2 rules for anchorage of top bars in tension with a 90° standard hook or a bend near the exterior face of the joint. On these grounds, the value of h_c at exterior joints from Eq. (5.10b) may be reduced by as much as 30%, without reducing their safety margin below that offered by Eq. (5.10a) for interior joints.

5.4.2 Verification of Beam-Column Joints in Shear

To simplify the design process and on the basis of the fairly good field performance of beam-column joints in shear, Eurocode 8 exempts DC M buildings from explicit shear verification of beam-column joints on the basis of their shear force. Prescriptive detailing rules are given for them, instead. These rules have proved quite effective in protecting joints in past earthquakes. So, the shear verification of beam-column joints according to the present section applies only to DC H buildings.

The nominal shear stress in the concrete core of the joint is the same, no matter whether it is computed from the horizontal shear force, V_{jh}, or the vertical one, V_{jv}. In new buildings the beams normally yield before the columns, even when they do not meet Eq. (1.4). So, from the capacity-design point of view, it is more convenient to compute the shear stress in the joint from V_{jh}, using the forces transferred via bond along the top bars of the beam (cf. Eq. (3.134)). This is on the safe side for the joint, even when columns yield before the beams. So, the design value of the horizontal shear force in the joint is taken from an expression resulting from Eq. (3.134), using

there an overstrength value, $\gamma_{\mathrm{Rd}} f_{\mathrm{yd}}$ (with $\gamma_{\mathrm{Rd}} = 1.2$) for the design yield stress of beam bars:

$$V_{jhd} = \gamma_{Rd} \left(A_{sb1} + A_{sb2}\right) f_{yd} - V_c \tag{5.11}$$

The shear force V_{c} in the column above may be taken equal to the value from the analysis for the design seismic action. The shear stress in the joint core is then computed from Eq. (3.135), using the value of V_{jhd} from Eq. (5.11).

$$v_j = \frac{V_{jhd}}{b_j h_{jc}} \tag{5.12}$$

The verification criterion of interior joints against diagonal compression failure results from Eq. (3.144), using design values:

$$V_{\mathrm{jhd}} \leq n f_{\mathrm{cd}} \sqrt{1 - \frac{\nu_{\mathrm{d}}}{n}} b_{\mathrm{j}} h_{\mathrm{jc}} \tag{5.13a}$$

At joints which are exterior in the direction of the beam, Eurocode 8 relies on just 80% of the value from Eq. (5.13a):

$$V_{\mathrm{jhd}} \leq 0.8 n f_{\mathrm{cd}} \sqrt{1 - \frac{\nu_{\mathrm{d}}}{n}} b_{\mathrm{j}} h_{\mathrm{jc}} \tag{5.13b}$$

In Eqs. (5.13) ν_{d} is computed from the maximum axial force in the column below the joint, under any combination of the design seismic action with the concurrent gravity loads.

Eurocode 8 uses Eq. (3.143) to calculate the required total area, A_{sh}, of horizontal legs of hoops within the joint between the top and bottom reinforcement of the beam horizontal reinforcement, using design values for the strengths (including $f_{\mathrm{ctd}} = f_{\mathrm{ctk},0.05}/\gamma_{\mathrm{c}} = 0.7 f_{\mathrm{ctm}}/\gamma_{\mathrm{c}}$):

$$\frac{A_{\mathrm{sh}} f_{\mathrm{ywd}}}{b_{\mathrm{j}} h_{\mathrm{jw}}} \geq \frac{\left(\dfrac{V_{\mathrm{jhd}}}{b_{\mathrm{j}} h_{\mathrm{jc}}}\right)^2}{f_{\mathrm{ctd}} + \nu_{\mathrm{d}} f_{\mathrm{cd}}} - f_{\mathrm{ctd}} \tag{5.14}$$

Equations (3.142) are accepted in Eurocode 8 as an alternative for the calculation of the total area, A_{sh}, of horizontal reinforcement within joints. In terms of design values, including $\nu_{\mathrm{d}} = \gamma_{\mathrm{c}} \nu$ for the recommended value of $\gamma_{\mathrm{c}} = 1.5$, Eq. (3.142a) gives for interior joints:

$$A_{\mathrm{sh}} f_{\mathrm{ywd}} \geq \gamma_{Rd} \left(A_{sb1} + A_{sb2}\right) f_{yd} \left(1 - 0.8 \nu_d\right) \tag{5.15a}$$

At exterior joints Eq. (3.142b) gives:

$$A_{\mathrm{sh}} f_{\mathrm{ywd}} \geq \gamma_{Rd} A_{sb2} f_{yd} (1 - 0.8 \nu_d) \tag{5.15b}$$

In Eqs. (5.15) $\gamma_{\mathrm{Rd}} = 1.2$, as in Eq.(5.11). In Eqs. (5.14) and (5.15a) ν_{d} is computed from the minimum axial force in the column above the joint (negative for tension) among the combinations of the design seismic action with the concurrent gravity loads. The only difference in Eq. (5.15b) is that ν_{d} is from the column below the joint.

The two options allowed by Eurocode 8, Eqs. (5.14) or (5.15), give very different results. The amount of reinforcement from Eqs. (5.14) is very sensitive to the values of ν_{d} and ν_{j} (implying that the shear resisted by the diagonal tension mechanism is insensitive to the amount of horizontal reinforcement). By contrast, the joint reinforcement from Eqs. (5.15) is proportional to ν_{j} and fairly insensitive to ν_{d}. For medium-high values of ν_{d} (around 0.3) Eq. (5.14) requires much less joint reinforcement than Eqs. (5.15). For low values of ν_{d} (around 0.15) it gives less horizontal reinforcement than Eqs. (5.15) if $\nu_{\mathrm{j}} < 0.3 f_{\mathrm{cd}}$ but the other way around if $\nu_{\mathrm{j}}. > 0.3 f_{\mathrm{cd}}$. When ν_{d} is close to zero Eq. (5.14) gives much more joint reinforcement than Eqs. (5.15), especially for high values of ν_{j}. If such differences are disturbing, even less reassuring is the discrepancy between the predictions of both options and the experimental strength values in Fig. 3.48 (Kitayama et al. 1991). The only case of acceptable agreement with test results is that of Eq. (5.14) for medium-high values of ν_{d} (around 0.3). At any rate, the least among the steel requirements of Eqs. (5.14) or (5.15) may be used with some confidence.

One of the strength components in the truss mechanism underlying Eqs. (3.142) and (5.15) is the vertical reinforcement in the joint core. It provides a vertical tensile field equilibrating the vertical component of the concrete diagonal compression field. Intermediate bars between the corner ones, arranged along the sides of the column with depth h_{c}, can play this role, while contributing also to the moment resistance of the end sections of the column above and below the joint. According to Table 5.2, such bars should be provided along the perimeter at a spacing of not more than 150 mm for DC H or 200 mm for DC M, to improve the effectiveness of concrete confinement. For the purposes of the joint, Eurocode 8 requires at least one intermediate bar between the corner ones, even on short column sides.

In DC H buildings Eurocode 8 requires a total area of column intermediate bars between the corner ones, $A_{\mathrm{sv,i}}$, as vertical joint reinforcement:

$$A_{\mathrm{sv,i}} \geq (2/3)\, A_{\mathrm{sh}} \left(h_{\mathrm{jc}} / h_{\mathrm{jw}} \right) \tag{5.16}$$

The factor 2/3 in Eq. (5.11) accounts for the inclination of the strut and of the truss compression field to the horizontal, which is normally steeper than the diagonal of the joint core. It also limits the effect on the vertical reinforcement of the overestimation of A_{sh} by Eqs. (5.14) or (5.15).

As pointed out at the outset of the present section, beam-column joints are required by Eurocode 8 to be verificied in shear by calculation on the basis of Eqs. (5.11), (5.12), (5.13), (5.14), and (5.15) only in DC H buildings. For DC M ones, the detailing prescribed in CEN (2004a) for both DC H and M joints suffices.

According to it, the transverse reinforcement in the "critical regions" of the column above or below the joint (whichever is more) should also be placed within the joint, unless beams with width at least 75% of the parallel cross-sectional dimension of the column frame into all four sides of the joint. In that case, the horizontal reinforcement in the joint is placed at double the spacing in the columns above and below, but not more than 150 mm.

To appreciate better what the prescriptive rules above imply for the minimum horizontal reinforcement in a joint, note that for DC H the "critical regions" of columns above the base of the building have (a design value of) mechanical volumetric ratio of transverse reinforcement, ω_{wd}, at least equal to 0.08 (see Table 5.2). For S500 steel and $f_{ck} = 30$ MPa, this value corresponds to $\rho_{jh} = 0.185\%$ per horizontal direction, if the partial factors for steel and concrete are equal to their recommended values for ULS design against non-seismic actions, or to $\rho_{jh} = 0.24\%$, if these partial factors are equal to 1.0 as recommended for accidental actions. For other concrete grades the minimum value of ρ_{jh} is proportional to f_{ck}. Of course, other constraints on the column transverse reinforcement in critical regions (e.g. on the diameter and spacing of transverse reinforcement: $d_{bh} \geq \max(6\text{ mm}; 0.4d_{bL})$, $s_w \leq \min(6d_{bL}; b_o/3; 125\text{ mm})$, see Table 5.2, or on the minimum value of μ_φ) may govern. Note, though, that the ρ_{jh} values above are much less than the value of 0.4% marking the limit of the contribution of horizontal reinforcement to the shear resistance of the joint according to Kitayama et al. (1991). Eurocode 8 has no lower limit on ω_{wd} in the "critical regions" of DC M columns, but only bounds on the hoop diameter: $d_{bh} \geq \max(6\text{ mm}; d_{bL}/4)$, and spacing: $s_w \leq \min(8d_{bL}; b_o/2; 175\text{ mm})$, see Table 5.2. These limit values give low horizontal reinforcement ratio in the joint. Considering that the practical minimum for DC M is 8 mm hoops at 125 mm vertically and with horizontal spacing of legs 200 mm, the resulting steel ratio in the joint is $\rho_{jh} = 0.2\%$ per horizontal direction.

5.5 Special Dimensioning Rules for Shear

5.5.1 Dimensioning of Shear Reinforcement in "Critical Regions" of Beams or Columns

As Tables 5.1 and 5.2 show, the design value of shear resistance for beams or columns is computed according to the rules of Eurocode 2 for monotonic loading, both when transverse reinforcement controls the shear resistance (denoted in that case as $V_{Rd,s}$) and when diagonal compression in the member's web does (denoted then as $V_{Rd,max}$). The special rules described below for the values of $V_{Rd,s}$ and $V_{Rd,max}$ in "critical regions" of beams of DC H are an exception.

In the "critical regions" of DC H beams the strut inclination, δ, in Eqs. (3.94), (3.95), (3.97) and (3.104) of the part *The Variable Strut Inclination Truss of the CEB/FIP Model Code 90 and Eurocode 2* of Section 3.2.4.2 is taken equal to 45° ($\tan\delta = 1$). This is equivalent to a classical Mörsch-Ritter 45°-truss without

a concrete contribution term. The underlying reason is the reduction of $V_{R,s}$ with increasing inelastic cyclic deformations (see Sections 3.2.4.3, 3.2.4.4 and Fig. 3.41) in plastic hinges, which by design take place in beams and in DC H are subjected to significant chord rotation ductility demands, $\mu_\theta \approx \mu_\delta$. For simplicity, the reduction of $V_{R,s}$ with inelastic cyclic deformations is neglected in DC M beams, as the lower q-factor of DC M design gives, through Eqs. (1.1) and (1.2), lower chord rotation ductility demands, $\mu_\theta \approx \mu_\delta$.

In columns of new buildings designed to Eurocode 8 for DC M or H, plastic hinging under the design seismic action is the exception. If it does take place, it will normally lead to lower chord rotation ductility demands and hence less reduction of the value of $V_{R,s}$ than in beams. It is expected that, if such a reduction does happen, its effects on safety will be offset by the γ_{Rd} factor of 1.1 for DC M and of 1.3 for DC H employed in the capacity-design calculation of shear force demands (cf. Eqs. (1.11) and (1.12) and Table 5.2). So, Eurocode 8 neglects the reduction of shear resistance in "critical regions" of columns and applies the normal expressions for shear resistance from Eurocode 2, Eqs. (3.94), (3.95), (3.96a), (3.97), (3.98), (3.104a), etc.

5.5.2 *Inclined Reinforcement Against Sliding Shear in "Critical Regions" of DC H Beams*

Another aspect where shear design in "critical regions" of DC H beams deviates from the Eurocode 2 rules is the use of inclined bars, at an angle $\pm\alpha$ to the axis, against shear sliding at the end section of the beam (see bottom row in Table 5.1). Such sliding may occur at an instant in the response when the end section is cracked throughout its depth and the shear force demand is high. This may happen if the shear force has a large reversal and a high peak value. Eurocode 8 requires inclined bars against sliding shear, if both of the following criteria are met:

$$-1 \leq \zeta < -0.5 \tag{5.17}$$

as the criterion for a large shear reversal, with ζ from Eq. (1.10) in Section 1.3.6.2; and

$$\max V_{i,d} > (2 + \zeta) f_{ctd} b_w d \tag{5.18}$$

where max $V_{i,d}$ is the maximum design shear force from Eq. (1.9a) of Section 1.3.6.2, at the end section of the beam "critical region" at end i. The limit shear value of Eq. (5.18) is between one-third to one-half of the value of $V_{Rd,max}$ for $\delta = 45^\circ$.

As no stirrups cross a section liable to shear sliding, inclined bars with total cross-sectional area A_s, should cross that section if both limits in Eqs. (5.17) and (5.18) are exceeded. They should resist, through the vertical components $A_s f_{yd} \sin\alpha$ of their

yield force – in tension and compression – at least 50% of max $V_{i,d}$ from Eq. (1.9a), respecting the recommendation of Eurocode 2 to resist at least 50% of the design shear force through shear links:

$$A_s f_{yd} \sin\alpha \geq 0.5 \max V_{i,d} \tag{5.19}$$

If the beam is short, inclined bars are most conveniently placed along its two diagonals in elevation (see coupling beam of Fig. 3.44). Then $\tan\alpha \approx (d–d_1)/L_{cl}$. If the beam is not short, the inclination of its diagonals to the beam axis is small and the effectiveness of inclined bars placed along them low. Two series of shear links, one at an angle $\alpha = 45^\circ$ to the beam axis and the other at $\alpha = –45^\circ$, are more cost-effective then. However, constructability and reinforcement congestion hamper this option. Normally there is neither risk from sliding shear, nor need for inclined reinforcement, if the layout of the framing is selected as suggested in Section 2.2.1, notably avoiding beams that are both short and not loaded with significant gravity loads concurrent with the design seismic action (i.e., beams with small value of the 1st term and large value of the 2nd term in the right-hand-side of Eqs. (1.9) in Section 1.3.6.2).

Plastic hinges in columns are subjected to an almost full reversal of shear ($\zeta \approx –1$). Moreover Eq. (1.13) normally gives a large design shear force for them. Inclined bars are not required in columns, nonetheless, because their axial force and the low magnitude of plastic strains in the vertical bars prevent through-depth cracking of the end section. Sliding is also resisted by clamping and dowel action in the large diameter intermediate bars between the corner bars, which remain elastic at the instant of peak positive or negative shear force.

5.5.3 Shear Verification of Ductile Walls of DC H

As shown in Table 5.3, like in beams and columns, the design value of the shear resistance of ductile walls, as controlled by the transverse reinforcement, $V_{Rd,s}$, or diagonal compression in the web, $V_{Rd,max}$, is computed according to the rules of Eurocode 2 for monotonic loading, except in the "critical region" of DC H walls. There, the design value of cyclic shear resistance, as controlled by diagonal compression in the web, $V_{Rd,max}$, is taken as 40% of the value given by Eurocode 2 for monotonic loading. The reason is clear from Fig. 3.42. For the sake of simplicity, ductile walls of DC M are spared from this reduction, but this is certainly not safe-sided.

Unlike columns, ductile walls of DC H are required to be verified for sliding shear, as their axial load level is low and the web bars are of smaller diameter and more sparse than in columns. As an outcome of this verification, inclined bars may be placed at the wall base (Table 5.3, 2nd row from the bottom). An important practical difference with columns in this respect is that, thanks to their large size, less dense transverse and vertical reinforcement and one-directional cross-sectional shape and function, walls lend themselves better to placing inclined bars.

The shear design of DC H walls deviates from the general Eurocode 2 rules also in the calculation of web reinforcement ratios, horizontal ρ_h, and vertical ρ_v, at those storeys where the maximum shear span ratio in the storey (normally at the base of the storey), $L_s/h = M_{Ed}/(V_{Ed}l_w)$ is less than 2. Note that most tested walls with $L_s/h < 2$ have failed in diagonal compression and are included in the 50 specimens with $L_s/h \leq 2.5$ behind Eq. (3.115) and depicted in Fig. 3.42 of Section 3.2.4.5. By contrast, only four out of 32 tested walls (rectangular or not) that failed in shear by diagonal tension after flexural yielding and support Eqs. (3.114) in Section 3.2.4.3 have $L_s/h < 2$. So, there is certain lack of knowledge of the propensity of squat walls to failure in cyclic diagonal tension. In view of this, for DC H walls Eurocode 8 adopted a safe-side modification of the Eurocode 2 rule for members with $0.5 < L_s/h < 2$ under monotonic loading: the resistance in diagonal tension at those storeys where $\max M_{Ed}/(V_{Ed}l_w) < 2$ is:

$$V_{Rd,s} = V_{Rd,c} + \rho_h b_{wo} \left(0.75 \frac{\max M_{Ed}}{V_{Ed}}\right) f_{yh,d} \tag{5.20}$$

In Eq. (5.20) ρ_h is the ratio of horizontal reinforcement, normalised to the web thickness, b_{wo}, and $f_{yh,d}$ is its design yield strength. The $V_{Rd,c}$ term is the design shear resistance of concrete members without shear reinforcement according to Eurocode 2, from Eq. (3.67) in Section 3.2.3.2 but using the web thickness as b_w and design values of concrete strength. Specially in the "critical region of the wall", it is taken $V_{Rd,c} = 0$ if N_d is tensile (negative). The vertical web reinforcement ratio, ρ_v, is then dimensioned to provide a 45° inclination of the concrete strut in the web, when acting together with the horizontal reinforcement and the vertical compression due to the minimum axial force for the design seismic action plus concurrent gravity loads, min N_{Ed}. Note that M_{Ed} in $M_{Ed}/(V_{Ed}l_w)$ is from the M-envelope of Fig. 1.7 in Section 1.3.5, which does not exhibit inflection points in any storey, and V_{Ed} is the magnified shear according to Eqs. (1.14) and (1.15) in Section 1.3.6.4 (and the envelope in Fig. 1.11, for the walls of dual, frame-wall systems). So, the value of $M_{Ed}/(V_{Ed}l_w)$ may turn out to be less than 2 at upper storeys of walls with large l_w. At such storeys the Eurocode 8 rule, being safe-sided owing to insufficient knowledge, may give unduly large web reinforcement.

5.6 Systems of "Large Lightly Reinforced Walls" in Eurocode 8

5.6.1 Definitions

As pointed out in Section 2.2.2.4, Eurocode 8 has special design provisions for systems consisting of several large but lightly reinforced RC walls, sustaining seismic demands not by dissipating seismic energy through hysteresis in plastic hinges, but by converting part of it into potential energy of the masses due to upward displacements and returning another part to the ground by radiation from their foundation.

This is a special feature of Eurocode 8, based on the experience of the application of similar rules in the seismic region of the south of France. To qualify for Eurocode 8's special design provisions for "systems of large lightly reinforced walls", a building should have:

1. fundamental period in each horizontal direction not longer than 0.5 s, under presumed fixity at the base of all vertical elements against rotation. This promotes walls with low aspect ratio and/or large total cross-sectional area as a percentage of the total floor plan area and takes better into account the effect of potential openings in the wall than a mere geometric criterion.
2. Primary seismic walls in each horizontal direction qualifying as "large walls", by:

   (a) having length of the cross-section l_w at least 4 m, or 2/3 of the total height of buildings shorter than 6 m (see Fig. 5.3 for examples);
   (b) resisting together at least 65% of the seismic base shear in the direction of their length; and
   (c) supporting together at least 20% of the total gravity load (i.e. at least 40% in total for the walls of both directions); this ensures that rocking of the walls increases the potential energy of at least 20% of the total mass of the building; and

3. At least two primary walls fulfilling conditions 2(a)–(c) above in each horizontal direction (for redundancy and torsional resistance). Just one primary "large wall" meeting these conditions may suffice in one of the two horizontal directions, if there are at least two of them in the orthogonal direction and conditions 1 and 2 above are met in both directions. In that case the q-factor in the direction having just one "large wall" is reduced by one-third.

If the structural system meets all conditions 1–3, Eurocode 8 allows all its walls qualifying as "large" by meeting condition 2(a), to be designed and detailed in a very economic way, according to the special rules for "large lightly reinforced walls" in Sections 5.6.2, 5.6.3, and 5.6.4.

(a) (b) (c) (d)

Fig. 5.3 Examples of walls with dimensions qualifying them as "large", in what may qualify as systems of "large lightly reinforced walls" according to Eurocode 8

A "system of large lightly reinforced walls" can only be in DC M. Although designed and detailed to much less demanding rules, it enjoys the same q-factors as wall systems of uncoupled ductile walls of DC M: a basic q-factor of 3 (or 2, if there is only one "large wall" in the horizontal direction in question), to be multiplied by $(1+\alpha_o)/3$ if the mean aspect ratio of the walls, α_o, is less than 2. Normally such systems are not heightwise irregular; so their q-factor is not reduced any further.

If a "system of large lightly reinforced walls" includes one or more primary walls not meeting condition 2(a) above (i.e., less than 4 m-long), these walls are designed and detailed according to the rules for ductile walls of DC M. Conversely, if the building as a whole does not qualify as a "system of large lightly reinforced walls" by failing to meet one of the conditions 1 to 3 above, all its primary walls should be designed as ductile walls of the corresponding DC, no matter whether themselves do qualify as "large" by meeting some of these conditions.

5.6.2 Dimensioning of "Large Lightly Reinforced Walls" for the ULS in Bending and Axial Force

"Large walls" in "systems of large lightly reinforced walls" are dimensioned for the ULS in flexure without any increase of their design moments over the results of the analysis for the design seismic action (in other words, the linear moment envelope of Fig. 1.7 in Section 1.3.5 is not applied). Their vertical reinforcement should be tailored to the requirements of the ULS in flexure with axial force, without excess reinforcement area and with less minimum vertical reinforcement than in ductile walls. The objective is to spread wall flexural yielding to several floors and not limit it to the base of the wall. This increases the overall lateral deflection of the wall and mobilises better, by uplift, the contribution to earthquake resistance of masses and transverse beams supported on the wall at intermediate floors. Minimisation of flexural overstrength reduces shear force demands and helps avoid pre-emptive shear distress.

The small thickness of "large walls" compared to their length increases the risk of out-of-plane instability. Eurocode 8 requires limiting the magnitude of compression stresses due to bending with axial force, to avoid out-of-plane instability. It does not give detailed guidance for that, but refers to the pertinent Eurocode 2 rules:

1. The rules for 2nd-order effects in plain (unreinforced) or lightly reinforced walls:

   – The compressive strength of concrete is multiplied by $\varphi=\min\{[1.14(1-2e/b_{wo})-0.02l_o/b_{wo}]; [1-2e/b_{wo}]\} < 1.0$, where e is the eccentricity of loading along the wall thickness, b_{wo}, having default value $e = l_o/400$, and l_o the unbraced length of the wall, taken equal to the clear storey height, h_{st}. If the wall is connected at one or both ends of its length, l_w, to a transverse wall with length at least $h_{st}/5$ and thickness at least $b_{wo}/2$, this unbraced length is further divided by $[1+(h_{st}/3l_w)^2]$, or $[1+(h_{st}/l_w)^2]$, respectively.

- (Only for cast-in-situ walls) The thickness of the wall, b_{wo}, should be at least 4% of its unbraced length, l_o.

2. The rule against lateral instability of laterally unrestrained compression flanges of beams[8]:
   - $(h_{st}/b_{wo})(l_w/b_{wo})^{1/3} < 70$.

The seismic response of "large walls" entails rigid-body rocking on the ground if they are on footings, or bending as a stack of storey-high rigid blocks. Such a response causes hard impact(s) of the uplifting footing to the ground or upon closure of horizontal cracks at floor levels. The hard impact excites high-frequency vertical vibrations of the entire wall, or of certain storeys. Although high-frequency vibrations die out fast and do not have significant global effects, they cause a fluctuation of the axial force in the wall itself. As these local phenomena are very uncertain and complex, Eurocode 8 is content with a simplified, safe-sided treatment: a design axial force of the wall equal to the value due to the concurrent gravity loads increased or reduced by 50%. The vertical reinforcement is conditioned by the minimum axial load. By contrast, the maximum compressive axial force is more critical for the concrete and the wall's lateral instability. This increase or decrease of axial force may be neglected, if a q-factor of 2.0 or less is used in the design.

Owing to the high frequency of the vertical vibrations, the ULS verification for flexure with axial load may use an increased ultimate strain of unconfined concrete: $\varepsilon_{cu} = 0.005$. The beneficial effect of confinement may be taken into account according to Eqs. (3.13) and (3.25), but unconfined concrete is considered to spall if its strain exceeds 0.005. Because of this, and as the (effectively) confined part of a thin wall section is normally quite small, it may not be worthwhile to consider the effect of confinement, as it may not increase the moment resistance of the section.

5.6.3 Dimensioning of "Large Lightly Reinforced Walls" for the ULS in Shear

To preclude shear failure, "large walls" are dimensioned for a shear force, V_{Ed}, obtained by multiplying the value from the analysis for the design seismic action, V'_{Ed}, by a factor ε:

$$\varepsilon = \frac{V_{Ed}}{V'_{Ed}} = \frac{q+1}{2} \tag{5.21}$$

For the usual value of $q = 3$ applying to "systems of large lightly reinforced walls", $\varepsilon = 2.0$, above the value $\varepsilon = 1.5$ for ductile walls of DC M (see Eq. (1.16)). Moreover, as:

[8] A 2nd rule in Eurocode 2: $l_w < 3.5 b_{wo}$, is meaningless for walls.

- the dimensioning rules for the vertical reinforcement explicitly request minimising the flexural overstrength at the base of the wall, M_{Rd}/M_{Ed}, and
- the fundamental period in the direction of the length of the wall, T_1, is normally not (much) longer than the corner period of the spectrum, T_C,

the value of ε from Eq. (5.21) exceeds that from Eq. (1.14) for squat ductile walls of DC H and is similar to the outcome of Eq. (1.15) for slender ductile walls of DC H. So, the design shear of "large lightly reinforced walls" is quite safe-sided. For this reason, and also because flexure, with its overstrength minimised by design, governs the inelastic response, Eurocode 8 allows omitting altogether the minimum smeared horizontal reinforcement in "large lightly reinforced walls" whose design shear force, $V_{Ed} = \varepsilon V'_{Ed}$, is less than the design shear resistance without shear reinforcement, $V_{Rd,c}$, according to Eurocode 2 (see Eq. (3.67)). Although relaxing a requirement that applies according to Eurocode 2 even to walls designed for non-seismic actions sounds weird, it does make sense, because:

- Even if inclined cracks do form despite fulfillment of the verification: $V_{Ed} \leq V_{Rd,c}$, their width will not grow uncontrolled as in walls without horizontal reinforcement under force-controlled actions (e.g. wind). Such cracks will close, when the transient and deformation-controlled seismic response reverses.
- Thanks to the large horizontal dimension of the wall, l_w, any inclined crack will intersect a floor slab and mobilise in shear the horizontal ties placed at its intersection with the wall, as well as slab reinforcement parallel to l_w and close to the wall.

If $V_{Ed} > V_{Rd,c}$, horizontal reinforcement will be calculated according to Eurocode 2, using:

1. either the variable-strut-inclination model of shear resistance in the part of Section 3.2.4.2 on *The Variable Strut Inclination Truss of the CEB/FIP Model Code 90 and Eurocode 2*, with strut inclination to the vertical, δ, between 22 and 45° (see Eq. (3.104a), or
2. a Strut-and-Tie model (for walls with openings).

When using the variable-strut-inclination model according to Eurocode 2, constant horizontal reinforcement may be dimensioned within lengths of $z \cot \delta$ up the wall (with the internal lever arm normally taken as $z = 0.8 l_w$) from the minimum value of V_{Ed} in each length. Experimental and field evidence suggests, however, that in a large wall the struts follow a fan pattern up to a distance z from the base. From there up they are at an inclination $\delta \approx 45°$, intersecting the floors and mobilising them as ties. The implication is that wall horizontal reinforcement should better be calculated with $\delta = 45°$, starting with the value of V_{Ed} at a distance of $z = 0.8 l_w$ from the base and possibly counting in the shear reinforcement any steel ties at intersections of the wall and the floors.

Strut-and-Tie models (see Fig. 5.4) should include the floors as ties. If the openings are asymmetric with respect to the wall centreline, a different model should be

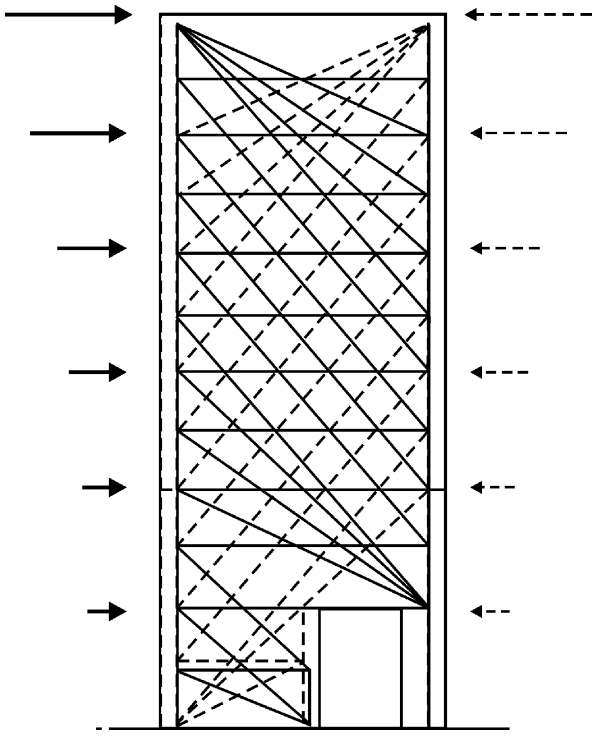

Fig. 5.4 Example of a Strut-and-Tie model for a wall with openings

constructed for each sense of the seismic action parallel to the wall (positive or negative). Struts should have width not more than $0.25l_w$ or $4b_{wo}$ (whichever is smaller) and stay clear of openings.

At construction joints at floor levels the shear force $V_{Ed} = \varepsilon V'_{Ed}$ should be verified against the sliding shear resistance at the interface owing to cohesion and friction according to Eurocode 2:

$$V_{Rdi} = \left[0.35 f_{ctd} + 0.6\left(\frac{N_{Ed}}{A_c} + \rho_v f_{yd}\right)\right] z b_{wo} \tag{5.22}$$

where:

- $f_{ctd} = f_{ctk,0.05}/\gamma_c = 0.7 f_{ctm}/\gamma_c$ is the design value of the tensile strength of concrete;
- N_{Ed} is the minimum axial force from the analysis for the design seismic action and the concurrent gravity loads (positive for compression), without the 50% increase or decrease of axial force due to the high-frequency vertical vibrations induced by hard impact;
- ρ_v is the ratio of wall vertical reinforcement providing clamping at the interface.

The coefficient values of 0.35 and 0.6 for cohesion and friction, respectively, refer to a naturally rough, untreated interface between concretes cast at different times. If the surface cast first is artificially roughened by raking and exposure of aggregates to an average 3 mm of roughness every about 40 mm, the coefficient values may be increased to 0.45 and 0.7, respectively. According to Eurocode 8, the anchorage length of the clamping bars included in ρ_v is increased by 50% over the normal value required in Eurocode 2. This requirement applies only to those vertical bars crossing the interface that need to be included in ρ_v so that $V_{Ed} \leq V_{Rdi}$.

5.6.4 Detailing of the Reinforcement in "Large Lightly Reinforced Walls"

As pointed out in Section 5.6.3, wherever the design shear force V_{Ed} can be resisted without horizontal reinforcement, the "large lightly reinforced walls" may be constructed without such reinforcement. Minimum horizontal reinforcement has to be placed only where the wall needs horizontal reinforcement to resist V_{Ed}. This minimum is a Nationally Determined Parameter, with recommended value equal to the minimum horizontal reinforcement required by Eurocode 2 for walls under non-seismic actions (at maximum spacing vertically of 0.4 m and at a minimum ratio which is a Nationally Determined Parameter, with a recommended value of 0.1% or equal to that of the web vertical reinforcement ratio, whichever is larger).

There is no specific mention of minimum vertical reinforcement in Eurocode 8. So, the pertinent rules of Eurocode 2 apply: smeared web reinforcement at maximum bar spacing of 400 mm or 3 times the web thickness, b_{wo}, in two layers, one near each face of the wall. The minimum vertical reinforcement ratio is a Nationally Determined Parameter, with a recommended value of 0.2%. Both the smeared web reinforcement and the vertical bars placed at the edges of the cross-section for ULS resistance in flexure with axial force, count into the total vertical reinforcement to meet the minimum ratio.

The vertical bars supplementing the minimum smeared reinforcement in order to provide the ULS resistance in flexure with axial force should be concentrated at boundary elements, one at each edge of the section (Fig. 5.5). The length, l_c, of each boundary element in the direction of the length l_w of the wall should be at least b_{wo} times the maximum of 1.0 or $3\sigma_{cm}/f_{cd}$, where σ_{cm} is the average concrete stress in the compression zone at the ULS in flexure with axial force. If the parabolic-rectangular σ-ε diagram is used in this ULS verification, then $\sigma_{cm}/f_{cd} = \varphi(1–\varepsilon_{co}/3\varepsilon_{cu})$, with $\varepsilon_{co} = 0.002$ and $\varepsilon_{cu} = 0.005$, when the additional force due to the vertical vibration of the wall is downwards (compressive), or $\varepsilon_{cu} = 0.0035$ otherwise; $\varphi < 1$ is the reduction factor for 2nd-order out-of-plane effects (see point 1 in Section 5.6.2). At the bottom storey of the wall and at any storey where the wall length l_w is reduced with respect to the storey below by

Fig. 5.5 Hoops around boundary elements and cross-ties engaging vertical bars in "large lightly reinforced wall"

more than one-third of the storey height, h_{st}, the vertical bars in the boundary elements should be at least 12 mm in diameter. Everywhere else, a 10 mm diameter suffices.

All vertical bars should be laterally restrained at the corner of a hoop or the hook of a cross-tie. The boundary elements at the edges should be enclosed by hoops engaging the four corner bars. Intermediate vertical bars in the boundary elements, as well as vertical bars placed between the two boundary elements as minimum vertical reinforcement, may just be engaged by cross-ties across the thickness of the wall. Such hoops or cross-ties should have a minimum diameter of 6 mm or one

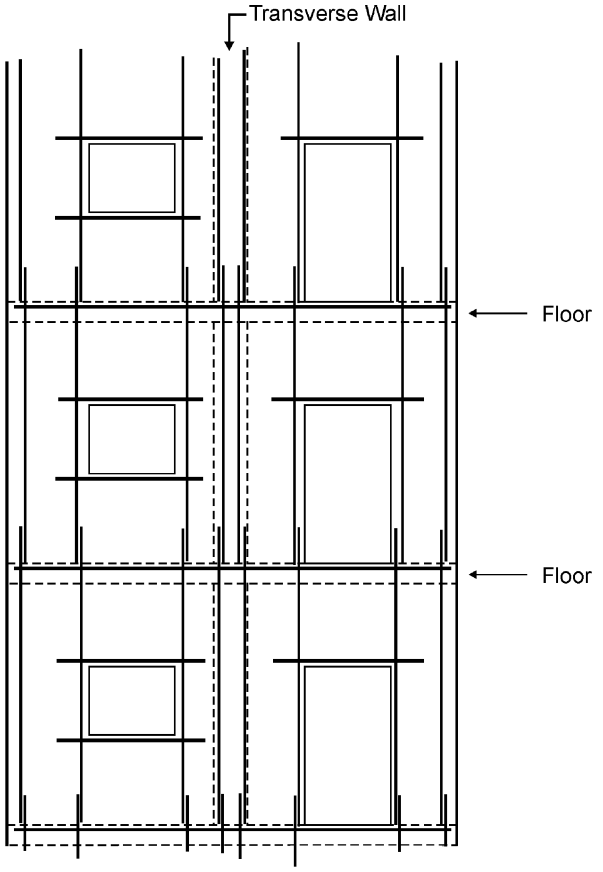

Fig. 5.6 Horizontal and vertical steel ties in large lightly reinforced walls with openings

third of the vertical bar diameter, d_{bL}, whichever is larger, and a maximum vertical spacing of 100 mm or $8d_{bL}$, whichever is less.

A continuous horizontal steel tie should be placed along each intersection of a "large wall" with a floor, extending into the floor beyond the edge of the wall at a length sufficient for anchorage and collection of inertia forces from the floor diaphragm and transfer to the wall. Vertical steel ties are required at any intersection of the wall with transverse ones or with wall flanges and along the vertical edges of wall openings. Vertical ties should continue from storey to storey through the floor, by lapping. When openings are not staggered at different storeys but have the same width and location, vertical steel ties along their edges should also be made continuous through lapping (see Fig. 5.6). Horizontal ties should be placed at the lintels above openings, but do not need to be continuous from one opening to the next. Specific rules for the dimensions and the capacity of the ties are not given, but reference to Eurocode 2 is made.

5.7 Implementation of Detailed Design of a Building Structure

5.7.1 The Sequence of Operations in Detailed Design for Ductility

Especially in frames, capacity design introduces strong interdependence between various phases of a building's detailed seismic design for ductility, within or between members:

- dimensioning a column in flexure depends on the amount and layout of the longitudinal reinforcement of the beams it is connected to in any horizontal direction;
- dimensioning of a column or a beam in shear depends on the amount and detailing of its own longitudinal reinforcement, as well as of the members framing into it at either end;
- verification of the foundation soil and design of foundation elements (especially of individual footings and their tie-beams) depends on the amount and layout of the longitudinal reinforcement of the vertical elements they support, etc.
- dimensioning any storey of a shear wall in shear depends on the amount and detailing of vertical reinforcement at the base of the bottom storey; etc.

The detailed design operations should follow a certain sequence, so that information necessary at a step is already available. More important, if detailed design takes place within an integrated computational environment (as is not only common, but also essential nowadays), this information should be appropriately transferred between the various modules of the system.

Flow Charts 5.1 and 5.2 depict the interdependence of the various components of a detailed design process. A sequence is suggested there (with roman numerals) for their execution, with specific reference to equations, sections or tables in this or previous chapters. Step IVa in Flow Chart 5.1 may be carried out before IVb

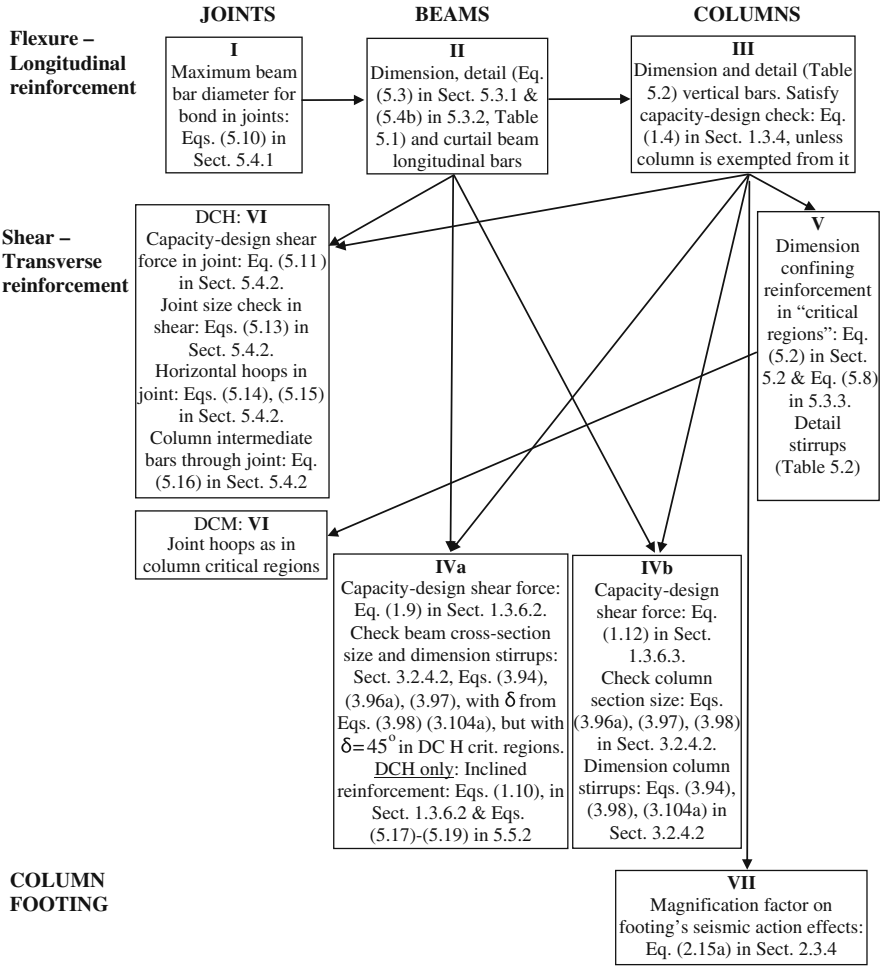

Flow Chart 5.1 Steps and interdependencies in dimensioning and detailing frame members in DC M or DC H

or vice-versa; while Steps V to VII can be executed at any sequence after II and III, even before IVa and IVb. The same applies to Step IV in Flow Chart 5.2, with respect to II and III there.

5.7.2 Detailed Design of Beam and Joints

5.7.2.1 Detailed Design of Beam Longitudinal Reinforcement

The maximum size of beam bars passing through joints or anchored there depends on the size of the column. So, as shown at Step I in Flow Chart 5.1, the detailed seismic design of a building structure for ductility starts from its joints. The maximum

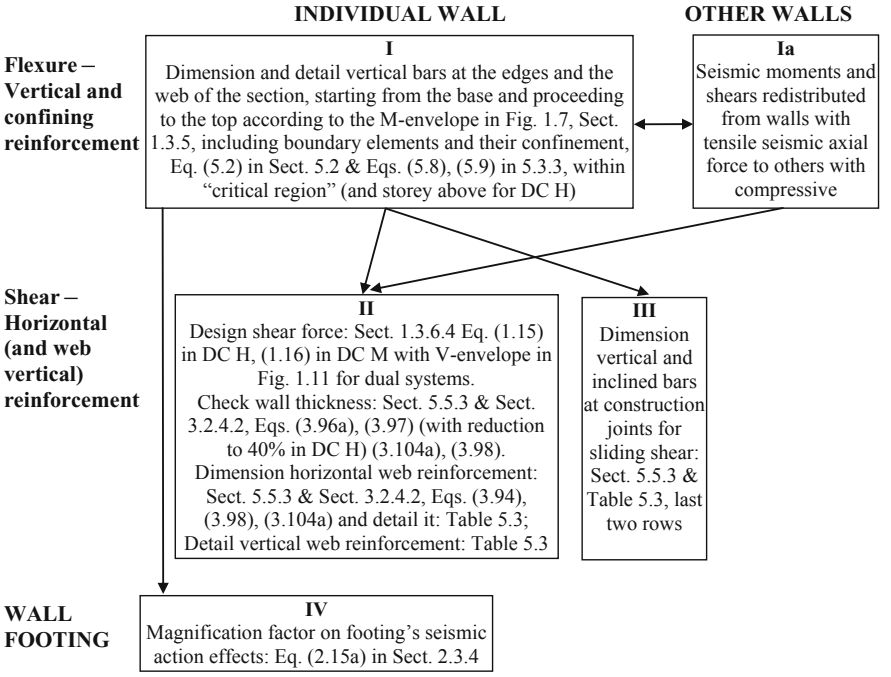

Flow Chart 5.2 Steps and interdependencies in dimensioning and detailing slender ductile walls of DC M or DC H

diameter of beam bars often controls the size of columns, especially in low-rise buildings (see Section 2.2.1.5).

Beams are dimensioned in bending (Step II in Flow Chart 5.1) on the basis of the moment envelope in Eq. (2.9), i.e. from:

(a) the combination of factored gravity loads, $\gamma_g G+\gamma_q Q$, and
(b) the design seismic action, separately in the plus and minus directions, and the quasi-permanent gravity loads, $G+\psi_2 Q$, acting with it.

The moment due to the design seismic action, M_{Eb}, is obtained from Eq. (4.24) or (4.25) in Section 4.7.1. The action effects of the horizontal components, E_X, $E_{Y,}$ include the effect of their accidental eccentricities. Note that, this is one of the very few cases in the entire structure where detailed design is based exclusively on results of the analysis. Besides, the so-dimensioned beam longitudinal reinforcement controls through capacity design:

– the vertical reinforcement of columns designed to meet Eq. (1.4) (Step III in Flow Chart 5.1),
– the design shears in the beam itself and the columns connected to it (Steps IVa and IVb), and
– (at least in DC H buildings) the shear design of the joints.

The beam longitudinal reinforcement is dimensioned at the beam sections where the moment envelope exhibits extreme positive or negative values:

1. the top bars of each end region are determined at the column face under hogging moments;
2. the bottom bars at an end region are dimensioned at the column face or a section nearby, but for sagging moment; and
3. the beam's main bottom reinforcement, from a section near mid-span, under sagging moments.

To reduce reinforcement of type 1 above, beam elastic moments may be redistributed around interior joints according to Section 5.7.2.2. This normally entails a reduction of peak hogging moments at column faces, increasing the sagging moments there and at mid-span, but not necessarily the bottom reinforcement of types 2 and 3 above, which may be governed by minimum requirements or by the maximum sagging moment due to factored gravity loads, $\gamma_g G+\gamma_q Q$.

Beam reinforcement is typically dimensioned in uniaxial bending without axial force. If there is no rigid floor diaphragm, or if the diaphragm has been modelled as flexible (see Section 4.9.5.2), the axial force from the analysis may also be taken into account and the beams may be dimensioned in bending with axial force, provided that:

- the model uses realistic values of the axial stiffness of the beams, consistent with the effective flange width in tension used in the dimensioning (i.e., the slab reinforcement within that width should also count as beam top reinforcement) and
- masses are lumped at floor nodes according to the tributary areas of the nodes or to the difference in the vertical component of the nodal force vector due to gravity loads above and below floor joints.

In the end, bars are curtailed and anchored according to the positive and negative moment envelope and the shift rule. Needless to say, the entire string of beams ("continuous beam") in a frame should be designed in bending together. Then, beam reinforcement requirements can be combined across joints. It is also good practice to combine different top or bottom bars into continuous ones, if their ends come close or overlap. To this end, few bar sizes (even a single size) should be used all along each string of beams.

At the end of Step II, the design values of the moment resistance at the beam end sections are computed from the final cross-sectional areas of the top and bottom reinforcement, A_{s1}, A_{s2}, respectively. The design value of the moment resistance in hogging (negative) or sagging (positive) bending, respectively, may be estimated as:

$$M^{-}_{Rd,b} = \min\left(A_{s1},\ A_{s2}\right) f_{yd}\left(d - d_2\right) + \max\left[0,\ \left(A_{s1} - A_{s2}\right)\right] f_{yd}\left[d - 0.5\left(A_{s1} - A_{s2}\right) f_{yd}/\left(b_w f_{cd}\right)\right] \tag{5.23a}$$

$$M^{+}_{Rd,b} = A_{s2} f_{yd} \max\left[\left(d - 0.5 A_{s2} f_{yd} / \left(b_{eff} f_{cd}\right)\right),\ (d - d_1)\right] \qquad (5.23b)$$

where:

- d is the effective depth of the section,
- d_2 is the distance of the centre of A_{s2} from the bottom of the beam,
- d_1 is the distance of the centre of A_{s1} from the top of the section,
- b_w is the effective width of the bottom flange in compression (normally that of the web),
- b_{eff} is the effective width of the top flange in compression, and
- f_{yd}, f_{cd} are the design strengths of steel and concrete, respectively.

The values of $M_{Rd,b}$ are used then for the capacity design of columns designed to meet Eq. (1.4) of Section 1.3.4 (Step III in Flow Chart 5.1) and for the design shears in the beam itself and the columns connected to it (Steps IVa and IVb in Flow Chart 5.1).

5.7.2.2 Redistribution of Beam Elastic Moments Around a Joint

Eurocodes 2 and 8 allow redistribution of beam moments from elastic analysis, under conditions which are commonly met by earthquake resistant beams (including those of DC L):

- use of steel class B or C; and
- ratios of adjacent span lengths not larger than 2.0.

Unless the plastic rotation capacity of the beam is explicitly checked, the percent reduction of a beam's elastic moment by redistribution should not exceed 54–125ξ, where ξ is the dimensionless neutral axis depth at the beam design moment resistance, i.e., when its extreme compression fibres reach the conventional ultimate strain of concrete, $\varepsilon_{cu} = 0.0035$. Eq. (3.52) gives $\xi = 0.81(\omega_1 - \omega_2) = 0.81(\rho_1 - \rho_2) f_{yd}/f_{cd}$. The top reinforcement limit in Eq. (5.4b) gives: $\xi \leq 290/(\mu_\varphi f_{yd}(\text{MPa}))$, which is a small value and allows a large percent reduction of a beam's moments by redistribution. The most serious restriction comes from the limitation of redistribution only among different interior joints of the same continuous beam or around them, but not from beams to columns.

Redistribution of elastic moments from one section to others can take place only within the same combination of actions, listed in Section 5.7.2.1 as (a) and (b). So to profit from redistribution, we need the moment diagrams for each combination, not just their envelope.

Redistribution of beam elastic moments can be used to advantage, in order to:

a. Reduce the total amount and the congestion of reinforcement, by (nearly) equalising design moments with the same sign across the joint, so that they can be serviced by the same bars.

b. Respect the maximum tension steel ratio allowed at beam ends by Eq. (5.4b) in Section 5.3.2, without increasing the beam cross-sectional dimensions and re-doing the analysis.
c. Prevent minimum reinforcement requirements from controlling the beam moment resistance, M_{Rb}, and, therefore, the column flexural capacities (via Eq. (1.4)) and the capacity-design shears in beams (Eq. (1.9) in Section 1.3.6.2) or columns (Eq. (1.12) in Section 1.3.6.3).
d. Prevent the combination of factored gravity loads (combination (a) in Section 5.7.2.1) from governing the beam moment resistance at column faces, and, therefore, the capacity-design effects listed in (c) above. Redistribution of moments from this combination takes place not just around interior joints (as in combinations of the design seismic action with concurrent gravity loads, (b) in Section 5.7.2.1), but mainly from beam interior supports to mid-span.

To see how redistribution of beam elastic moments around an interior joint can serve those aims, let's introduce the following quantities:

- $M_{G+\psi 2Q,i}$, $M_{G+\psi 2Q,j}$ are the beam elastic moments due to the quasi-permanent gravity loads at face *i* and *j* of a joint, respectively, positive if hogging (tension at the top); their difference is denoted as: $\Delta M_g = M_{G+\psi 2Q,i} - M_{G+\psi 2Q,j}$
- $M_{E,i}$, $M_{E,j}$ denote the magnitude of the corresponding elastic moments due to the design seismic action, taken always positive; their sum is : $\sum M_E = M_{E,i} + M_{E,j}$,
- M_i^t, M_j^t are the final hogging moments (tension at the top) for the design of the beam at faces *i* and *j* of the joint, respectively, after the redistribution, taken always positive;
- M_i^b, M_j^b are the final sagging moments (tension at the bottom) for the design of the beam at faces *i* and *j* of the joint, respectively, after the redistribution, taken positive for sagging;
- L_i, L_j are the lengths of the beams on side *i* or *j* of the joint, respectively, and x_i, x_j, denote the distance of a beam section from the corresponding face of the joint along them.

Redistribution normally entails reduction of the peak hogging moments at the column faces:

- by superimposing to the moments in the combination inducing hogging moments next to face *i* and sagging ones next to face *j*, a sagging moment diagram equal to $\Delta M_i(1-x_i/L_i)$ along the beam at side *i* and to $\Delta M_i(1-x_j/L_j)$ along that at side *j*; and
- by superimposing to the moments in the combination inducing sagging moments next to face *i* and hogging ones next to face *j*, a sagging moment diagram equal to $\Delta M_j(1-x_i/L_i)$ along the beam at side *i* and to $\Delta M_j(1-x_j/L_j)$ along that at side *j*.

The redistribution is specified through the reductions in hogging moments, ΔM_{i} and ΔM_{j}.[9]

1. Suppose that the objective of the redistribution is:

$$M_{\mathrm{i}}^{\mathrm{t}} = r_{\mathrm{i}} M_{\mathrm{i}}^{\mathrm{b}}, \qquad M_{\mathrm{j}}^{\mathrm{b}} = r_{\mathrm{j}} M_{\mathrm{j}}^{\mathrm{t}} \tag{5.24}$$

with:

$$1 \geq r_{\mathrm{i}},\ r_{\mathrm{j}} \geq 0.5 \tag{5.25}$$

(0.5: minimum value according to Eurocode 8, see Table 5.1)
This leads to the following final hogging moments:

$$M_i^t = \frac{\left(1 - r_j\right) \sum M_E + \left(1 + r_j\right) \Delta M_g}{1 - r_i r_j},\ M_j^t = \frac{\left(1 - r_i\right) \sum M_E - \left(1 + r_i\right) \Delta M_g}{1 - r_i r_j} \tag{5.26}$$

The reductions in hogging moments are:

$$\Delta M_i = \frac{M_{G+\psi 2Q,j} - M_{E,j} + r_j \left(\sum M_E - \Delta M_g\right) - r_i r_j \left(M_{G+\psi 2Q,i} + M_{E,i}\right)}{1 - r_i r_j} \tag{5.27a}$$

$$\Delta M_j = \frac{M_{G+\psi 2Q,i} - M_{E,i} + r_i \left(\sum M_E + \Delta M_g\right) - r_i r_j \left(M_{G+\psi 2Q,j} + M_{E,j}\right)}{1 - r_i r_j} \tag{5.27b}$$

One aspect to be checked is whether the resulting sagging moment resistances exceed at both sides i and j of the joint the minimum values, $M_{\mathrm{i,o}}{}^{\mathrm{b}}$, $M_{\mathrm{j,o}}{}^{\mathrm{b}}$, respectively, governed by minimum bottom reinforcement, not as a fraction $r = 0.5$ of the top reinforcement, but in absolute terms (in that case: $M_{\mathrm{i,o}}{}^{\mathrm{b}} = M_{\mathrm{j,o}}{}^{\mathrm{b}}$). They do, if:

$$\begin{aligned} r_i M_i^t &= r_i \frac{\left(1 - r_j\right) \sum M_E + \left(1 + r_j\right) \Delta M_g}{1 - r_i r_j} \geq M_{i,o}^b, \\ r_j M_j^t &= r_j \frac{\left(1 - r_i\right) \sum M_E - \left(1 + r_i\right) \Delta M_g}{1 - r_i r_j} \geq M_{j,o}^b \end{aligned} \tag{5.28}$$

2. Let's extend now the above redistribution objective, expressed by Eqs. (5.24), (5.25), (5.26), (5.27), and (5.28), to achieving the same top reinforcement at both sides of the joint:

[9] To avoid the explicit check of the plastic rotation capacity of the beam required by Eurocode 2, the moment reduction, ΔM_{i} and ΔM_{j}, should be not more than (0.54–1.25ξ) times the unreduced pertinent hogging moment, $M_{\mathrm{E,i}}$+$M_{\mathrm{G+\psi 2Q,i}}$ or $M_{\mathrm{E,j}}$+$M_{\mathrm{G+\psi 2Q,j}}$. Any "critical region" of a beam detailed for ductility would meet such a check without difficulty, but carrying out the check is a nuisance, regardless.

$$M_{\mathrm{i}}^{\mathrm{t}} = M_{\mathrm{j}}^{\mathrm{t}} \tag{5.29}$$

This brings about the following condition:

$$r_i = \frac{r_j \left(\sum M_E - \Delta M_g\right) - 2\Delta M_g}{\sum M_E + \Delta M_g} \tag{5.30}$$

and it is $r_{\mathrm{i}} > r_{\mathrm{j}}$ if $\Delta M_{\mathrm{g}} < 0$, i.e., $M_{\mathrm{G}+\psi 2\mathrm{Q,j}} > M_{\mathrm{G}+\psi 2\mathrm{Q,i}}$. In other words, if we have in the end the same top reinforcement across the joint, the side subjected to the larger hogging moment owing to quasi-permanent gravity loads has the smaller bottom reinforcement of the two. We can have $r_{\mathrm{i}} = r_{\mathrm{j}}$, i.e., equalise the reinforcement across the joint both at top and bottom, only if $M_{\mathrm{G}+\psi 2\mathrm{Q,i}} = M_{\mathrm{G}+\psi 2\mathrm{Q,j}}$.

3. Let's replace now redistribution objective no. 2 above, Eq. (5.29), with that of equal bottom reinforcement across the joint:

$$M_{\mathrm{i}}^{\mathrm{b}} = M_{\mathrm{j}}^{\mathrm{b}} \tag{5.31}$$

This gives the condition:

$$r_j = \frac{r_i \left(\sum M_E + \Delta M_g\right)}{\sum M_E - (1 + 2r_i)\,\Delta M_g} \tag{5.32}$$

Again, $r_{\mathrm{i}} > r_{\mathrm{j}}$ if $\Delta M_{\mathrm{g}} < 0$, i.e., $M_{\mathrm{G}+\psi 2\mathrm{Q,j}} > M_{\mathrm{G}+\psi 2\mathrm{Q,i}}$. In this case, for the same bottom reinforcement in the end across the joint, the side subjected to the larger hogging moment due to quasi-permanent gravity loads ends up with the larger top reinforcement of the two. Only if $M_{\mathrm{G}+\psi 2\mathrm{Q,i}} = M_{\mathrm{G}+\psi 2\mathrm{Q,j}}$, can one equalise the reinforcement across the joint both at top and bottom. In that case, with $r_{\mathrm{i}} = r_{\mathrm{j}} = r$, $M_{\mathrm{i}}^{\mathrm{t}} = M_{\mathrm{j}}^{\mathrm{t}} = \sum M_{\mathrm{E}}/(1+r)$ and $M_{\mathrm{i}}^{\mathrm{b}} = M_{\mathrm{j}}^{\mathrm{b}} = r\sum M_{\mathrm{E}}/(1+r)$.

4. Let's see now the case when the target of the redistribution is to match the value of the hogging moment resistance at one or both faces i and j of the joint, $M_{\mathrm{i.o}}{}^{\mathrm{t}}$, $M_{\mathrm{j.o}}{}^{\mathrm{t}}$, respectively, as governed by another consideration (e.g. by factored gravity loads, $\gamma_{\mathrm{g}}\mathrm{G}+\gamma_{\mathrm{q}}\mathrm{Q}$, when redistribution of their moments from beam supports to mid-span had not prevented them from governing at column faces):

$$M_{\mathrm{i}}^{\mathrm{t}} = M_{\mathrm{i,o}}{}^{\mathrm{t}}, \qquad M_{\mathrm{j}}^{\mathrm{t}} = M_{\mathrm{j,o}}{}^{\mathrm{t}} \tag{5.33}$$

The reduction in hogging moment required to match $M_{\mathrm{i.o}}{}^{\mathrm{t}}$, at side i and/or $M_{\mathrm{j.o}}{}^{\mathrm{t}}$ at side j is:

$$\Delta M_{\mathrm{i}} = M_{\mathrm{E,i}} + M_{\mathrm{G}+\psi 2\mathrm{Q,i}} - M_{\mathrm{i,o}}{}^{\mathrm{t}}, \qquad \Delta M_{\mathrm{j}} = M_{\mathrm{E,j}} + M_{\mathrm{G}+\psi 2\mathrm{Q,j}} - M_{\mathrm{j,o}}{}^{\mathrm{t}} \tag{5.34}$$

respectively, giving final sagging moments at the sides of the joint:

$$M_{\mathrm{j}}^{\mathrm{b}} = \sum M_{\mathrm{E}} + \Delta M_{\mathrm{g}} - M_{\mathrm{i,o}}{}^{\mathrm{t}}, \qquad M_{\mathrm{i}}^{\mathrm{b}} = \sum M_{\mathrm{E}} - \Delta M_{\mathrm{g}} - M_{\mathrm{j,o}}{}^{\mathrm{t}} \tag{5.35}$$

One aspect to be checked is whether the values of $r_i = M_i{}^b/M_{i,o}{}^t$ and $r_j = M_j{}^b/M_{j,o}{}^t$ respect the lower limit $r = 0.5$ set by Eurocode 8. They do, if:

$$\sum M_E - \Delta M_g \geq M_{j,o}{}^t + r M_{i,o}{}^t, \quad \sum M_E + \Delta M_g \geq M_{i,o}{}^t + r M_{j,o}{}^t \quad (\text{with } r = 0.5) \tag{5.36}$$

5. As companion to case 4 above, we target now matching the value of the sagging moment resistance at one or both faces i and j of the joint, $M_{i,o}{}^b$, $M_{j,o}{}^b$, respectively, as governed, e.g. by minimum bottom reinforcement, not as a fraction $r = 0.5$ of the top reinforcement, but in absolute terms (in that case: $M_{i,o}{}^b = M_{j,o}{}^b$):

$$M_i^b = M_{i,o}{}^b, \quad M_j^b = M_{j,o}{}^b \tag{5.37}$$

The increase in sagging moment required to match $M_{i,o}{}^b$ at side i and/or $M_{j,o}{}^b$ at side j is:

$$\Delta M_i = M_{G+\psi 2Q,i} - M_{E,i} + M_{i,o}{}^b, \quad \Delta M_j = M_{G+\psi 2Q,j} - M_{E,j} + M_{j,o}{}^b \tag{5.38}$$

respectively, giving final hogging moments at the sides of the joint:

$$M_j^t = \sum M_E - \Delta M_g - M_{i,o}{}^b, \quad M_i{}^t = \Delta M_E + \Delta M_g - M_{j,o}{}^b \tag{5.39}$$

The values of $r_i = M_{i,o}{}^b/M_i{}^t$ and $r_j = M_{j,o}{}^b/M_j{}^t$ respect the lower limit $r = 0.5$ in Eurocode 8, if:

$$(1/r)M_{j,o}{}^b + M_{i,o}{}^b \geq \sum M_E - \Delta M_g, (1/r)M_{i,o}{}^b + M_{j,o}{}^b \geq \sum M_E + \Delta M_g, \quad (\text{with } r = 0.5) \tag{5.40}$$

If redistribution takes place according to case 1 and Eqs. (5.24), (5.25), (5.26), (5.27), and (5.28), extended or not to cases 2 or 3, Eqs. (5.29), (5.30), (5.31), and (5.32), the sums of beam moment resistances diagonally across the joint, $\sum M_{Rb}$, entering in the capacity design calculations of Eqs. (1.4), (1.9) and (1.12), become:

For sagging next to face i and hogging next to face j:

$$\sum M_{Rb}{}^+ = M_j^t + M_j^b = \sum M_E - \Delta M_g \tag{5.41a}$$

For hogging next to face i and sagging next to face j:

$$\sum M_{Rb}{}^- = M_i^t + M_j^b = \sum M_E + \Delta M_g \tag{5.41b}$$

The same holds if the redistribution is according to cases 4, Eqs. (5.33), (5.34), (5.35), and (5.36), or 5, Eqs. (5.37), (5.38), (5.39), and (5.40), Therefore, by

matching the overall elastic moment demands with the minimum requirements of the code, the redistributions above reduce as much as possible the demands placed by the beams, through capacity design, on columns designed to meet Eq. (1.4) of Section 1.3.4 and on the design shears in the beams themselves and in the columns connected to them (and in DC H buildings on the design of joints in shear).

5.7.2.3 Capacity Design of Beams and Joints in Shear

Unless all the columns to which a beam is connected are capacity-designed in flexure to meet Eq. (1.4) of Section 1.3.4, shear design of beams (Step IVa in Flow Chart 5.1) should take place after dimensioning and detailing of the vertical steel is complete for all columns framing into the beam(s) in question. Then, for the calculation of the capacity-design shear from Eq. (1.9) in Section 1.3.6.2 we know not only the values of $M_{\mathrm{Rd,b}}{}^{-}$, $M_{\mathrm{Rd,b}}{}^{+}$ at the two ends of the beam and of $\sum M_{\mathrm{Rd,b}}$ around the joints there, but also the sum of column moment resistances around the joints, $\sum M_{\mathrm{Rd,c}}$, for bending in the vertical plane of the beam. These $M_{\mathrm{Rd,c}}$ values should be the maximum possible in all combinations of the design seismic action with the concurrent gravity loads. To this end, the value of $M_{\mathrm{Rd,c}}$ should correspond to the minimum among the two column forces:

1. The maximum compressive axial load in all combinations of the design seismic action with the concurrent gravity loads. This maximum value is addressed further in Section 5.7.3.5.
2. The "balance load", where the extreme compression fibres reach the ultimate strain of concrete, $\varepsilon_{\mathrm{cu}} = 0.0035$, at the same time the tension reinforcement yields. Normally Eq. (3.50a) in the part *Curvature at Spalling of the Concrete Cover* of Section 3.2.2.4 is satisfied and the balance load in dimensionless terms is equal to $\nu_{\mathrm{c,y1}}$ at the right-hand-side of Eq. (3.51). Then the moment resistance, M_{Rc}, is computed from Eq. (3.60) in Section 3.2.2.5, with the value of ξ_{cu} from Eq. (3.52). All these calculations use the conventional values: $\varepsilon_{\mathrm{co}} = 0.002$, $\varepsilon_{\mathrm{cu}} = 0.0035$ and the design values f_{yd}, f_{cd} for f_{y}, f_{c}.

Joints are typically two-way. So, the horizontal dimensions of DC H joints should be verified in shear in Step VI in Flow Chart 5.1 and their horizontal reinforcement dimensioned, after all beams framing in them in any horizontal direction have been fully designed.

5.7.3 Detailed Design of Columns

5.7.3.1 Dimensioning of Column Vertical Reinforcement for Action Effects from the Analysis

Columns exempted from the capacity-design check of Eq. (1.4) in Section 1.3.4, as well as the base section of the bottom storey of a column (at the connection to the

foundation), are dimensioned for the ULS in biaxial flexure with axial force, using triplets M_y-M_z-N from the analyses for:

(a) the combination of factored gravity loads, $\gamma_g G+\gamma_q Q$, and
(b) the design seismic action and the quasi-permanent gravity loads, $G+\psi_2 Q$, acting with it.

Combination (a) is normally not critical in primary columns and may even be ignored in their dimensioning. At any rate, it is not addressed here. The vertical component of the seismic action is also not considered in this discussion, as it rarely affects the dimensioning of columns.

Normally, the column sections right above and right below a beam-column joint are served by the same vertical reinforcement. Besides, as pointed out in Section 2.2.1.5, it is good practice to avoid changing the column section from storey to storey. Therefore, these two sections are dimensioned as a single one, for all M_y-M_z-N triplets that the analysis yields for them in the combinations of type (b) above. According to Section 4.7.2, in general there are 4 different seismic triplets M_y-M_z-N for a column section, to be superimposed to the single triplet due to the gravity loads concurrent with the design seismic action. As an exception, if the effects of the two horizontal seismic action components are combined through the linear approximation, Eq. (4.25), and a modal response spectrum analysis is used, the number of seismic triplets M_y-M_z-N to be considered at each section increases from 4 to 16 (see Section 4.7.2.2). Most critical among all the (4 or 16) triplets is the one giving the largest amount of reinforcement in one of the two sections. Unfortunately, it is not easy to screen out non-critical M_y-M_z-N triplets. The only general criterion is that, for the usual range of values of the dimensionless axial load, most critical among triplets with similar biaxial moments, M_y, M_z, is the one with the lowest axial compression, N.

There are various iterative algorithms for the ULS verification of sections with any shape and amount and layout of reinforcement, for any M_y-M_z-N combination. They use plane section analysis and the σ-ε laws of steel and concrete (normally taken in design as elastic-perfectly plastic and parabolic-rectangular, respectively) to find a strain distribution satisfying equilibrium. It is checked then whether the conventional ultimate strain of concrete, $\varepsilon_{cu} = 0.0035$, is exceeded at (any corner of) the section. By contrast, there is no general algorithm for direct dimensioning of a section, i.e., calculation of its reinforcement for a given M_y-M_z-N combination. The traditional manual approach with design charts is not practical when the designer is faced with many columns in a real 3D building. Besides, it is quite restrictive in its choice of parameters, notably of bar layouts in the section and steel grade. So, a feasible fully computational approach is proposed here for direct dimensioning of symmetric reinforcement in rectangular sections under a set of M_y-M_z-N combinations:

1. The amount of steel along each pair of opposite sides of the section is computed in uniaxial bending with axial force, neglecting the moment component with

vector at right angles to these sides. To this end, the expressions in Sections 3.2.2.4 and 3.2.2.5 may be applied:

- considering symmetric reinforcement, $\omega_2 = \omega_1$, and no intermediate bars between them, $\omega_v = 0$;
- using the material σ-ε laws and criteria adopted in ULS verifications for bending:
  - elastic-perfectly plastic for steel, with f_{yd} as yield stress and unlimited strain capacity;
  - parabolic-rectangular σ-ε law for concrete, with strength f_{cd} at strain $\varepsilon_{co} = 0.002$ and ultimate strain $\varepsilon_{cu} = 0.0035$;
- assuming that Eq. (3.50a) in the part *Curvature at Spalling of the Concrete Cover* of Section 3.2.2.4 is met, which is quite normal for column sizes typical of buildings designed for earthquake resistance;
- assuming that ν_d is less than the limit value $\nu_{c,y1}$ at the right-hand-side of Eq. (3.51), which is also normal for the usual range of dimensionless axial load in seismic design;

Under these conditions, there are two possible cases:

(i) The dimensionless axial load, ν_d, satisfies the version of Eq. (3.51) applicable in this case:

$$\delta_1 \frac{\varepsilon_{cu} - \frac{\varepsilon_{co}}{3}}{\varepsilon_{cu} - \varepsilon_{y2d}} \equiv \nu_{c,y2} \leq \nu_d \leq \nu_{c,y1} \equiv \frac{\varepsilon_{cu} - \frac{\varepsilon_{co}}{3}}{\varepsilon_{cu} + \varepsilon_{y1d}} \tag{5.42}$$

The version of Eq. (3.52) applying here gives then a ξ-value independent of the amount of reinforcement:

$$\xi = \frac{\nu_d}{1 - \frac{\varepsilon_{co}}{3\varepsilon_{cu}}} \tag{5.43}$$

to be substituted in terms of ν_d in the applicable version of the expression for moment resistance, Eq. (3.60), and solve directly for the amount of reinforcement:

$$(1 - \delta_1)\,\omega_1 = \frac{M}{bd^2 f_{cd}} - \xi \left[\frac{1 - \xi}{2} - \frac{\varepsilon_{co}}{3\varepsilon_{cu}} \left(\frac{1}{2} - \xi + \frac{\varepsilon_{co}}{4\varepsilon_{cu}} \xi \right) \right] \tag{5.44}$$

(ii) The dimensionless axial load, ν_d, is less than $\nu_{c,y2}$ at the left-hand-side of Eq. (5.42): $\nu_d < \nu_{c,y2}$; then the value of ξ is the positive root of the version of Eq. (3.54) applying here:

$$\left[1 - \frac{\varepsilon_{co}}{3\varepsilon_{cu}} \right] \xi^2 - \left[\nu_d + \omega_1 \left(1 - \frac{\varepsilon_{cu}}{\varepsilon_{yd}} \right) \right] \xi - \omega_1 \frac{\varepsilon_{cu} \delta_1}{\varepsilon_{yd}} = 0 \tag{5.45}$$

The version of the expression for moment resistance, Eq. (3.59), applicable in this case can be used to express ω_1 in terms of ξ and the moment:

$$\omega_1 \frac{(1-\delta_1)}{2}\left(1+\frac{\xi-\delta_1}{\xi}\frac{\varepsilon_{cu}}{\varepsilon_{yd}}\right)=\frac{M}{bd^2 f_{cd}} - \xi\left[\frac{1-\xi}{2}-\frac{\varepsilon_{co}}{3\varepsilon_{cu}}\left(\frac{1}{2}-\xi+\frac{\varepsilon_{co}}{4\varepsilon_{cu}}\xi\right)\right] \tag{5.46}$$

and replace ω_1 in Eq. (5.45). The resulting equation is highly nonlinear in ξ and can be solved only iteratively; ω_1 is then determined from Eq. (5.46).

2. The procedure in 1 above is applied first with all M_y-N pairs in the set of M_y-M_z-N combinations, using as b the side length parallel to the vector of M_y and as d and d_1 dimensions at right angles to it. The most critical pair will give the total area of reinforcement, A_{sy}, along each side which is parallel to the vector of M_y. This is repeated with all M_z-N pairs and the roles reversed, to find the total area of reinforcement, A_{sz}, along each one of the two other sides (those parallel to the M_z-vector). No matter which one among the four options in Section 4.7.2 has been adopted, the M_y-N pair from which A_{sy} derives will most likely not belong in the same M_y-M_z-N combination as the pair M_z-N that gives A_{sz}. So, these reinforcement requirements are superimposed on the section and translated into a bar layout satisfying the detailing rules for column vertical reinforcement, with the corner bars counting to both sides.
3. If available, an iterative algorithm is used in the end to verify that the section with the selected layout of reinforcement does not violate the conventional ultimate strain of concrete, $\varepsilon_{cu} = 0.0035$ under any one of the M_y-M_z-N combinations. If it does, one bar may be added to each side, till the section fulfils the verification criteria.

The procedure above can be applied to sections consisting of two or more rectangular parts orthogonal to each other (L-, T-, U-shaped, etc.). In Step 1 above such a section is taken as rectangular with the cross-sectional area of the actual one and the same effective depth at right angles to the vector of uniaxial bending moment considered. The reinforcement areas, A_{sy} and A_{sz}, coming out of this exercise are distributed along the corresponding extreme tension and compression fibres of the section, meeting the detailing rules for column vertical reinforcement. If Step 3 above is carried out, it is for the actual cross-sectional shape and the final bar layout.

To avoid the onerous verification of sections in biaxial bending with axial force, Eurocode 8 allows replacing it for columns of DC M or L buildings with separate uniaxial verifications, but with moments increased by 43%, i.e. under pairs (M_y/0.7)–N and (M_z/0.7)–N. In its effort to cover also the case of about equal moment components, this simplified verification is often overly conservative, especially if the seismic action effects derive from Eq. (4.25) according to Sections 4.7.2.1 or 4.7.2.2. So, if the computational capability of a truly biaxial verification

is available anyway for use in DC H structures, there is no need to resort to the uniaxial approximation.

5.7.3.2 Practical Dimensioning of Columns to Satisfy Eq. (1.4)

Wherever Eq. (1.4) needs to be fulfilled, it may well be checked after the vertical reinforcement crossing both column sections right above and below the joint has been dimensioned for the ULS in biaxial bending on the basis of the analysis results for all combinations of the design seismic action with the concurrent gravity loads (e.g. according to Section 5.7.3.1) and detailed to meet the relevant rules for the DC of the building (see Table 5.2). Note, however, that Eq. (1.4) normally governs over the ULS verification for these analysis results. So, it makes sense to defer dimensioning of the column vertical reinforcement until checking Eq. (1.4). At that stage about half of the value of $\gamma_{\mathrm{Rd}}\sum M_{\mathrm{Rd,b}}$ may be assigned to the column section right above and the rest to the section right below the joint. The vertical reinforcement serving both these sections may be dimensioned for these two uniaxial bending moments, acting together with the corresponding minimum value of the column axial force for the combination(s) of the design seismic action with the concurrent gravity loads (determined, e.g., according to Section 5.7.3.5). Recall that the moment resistance of a concrete section normally increases with increasing compressive axial force. So, it makes sense to assign a little less than half of $\gamma_{\mathrm{Rd}}\sum M_{\mathrm{Rd,b}}$ to the column section right above the joint. The most cost-effective apportioning is the one that gives the same amount of vertical reinforcement in these two sections. An about 45–55% split is normally appropriate. The approach in Step 1 of Section 5.7.3.1 may be used to directly dimension the column for these uniaxial moment demands. If the column belongs in a two-way frame and Eq. (1.4) needs to be met in both horizontal directions, the two-way dimensioning may be carried out as in Step 2 of Section 5.7.3.1.

Replacing a ULS verification for biaxial bending and axial force with a simplified, normally safe-sided, uniaxial one, as described at the end of Section 5.7.3.1 and allowed by Eurocode 8 for DC M columns, gives $\sum M_{\mathrm{Rd,c}} > 1.43\ \max(\sum M_{\mathrm{E}}+\Delta M_{\mathrm{g}})$, where $\sum M_{\mathrm{Rd,c}}$ is the total column moment resistance around the joint under the minimum compressive (or maximum tensile) column axial force over all combinations of the seismic action with the concurrent gravity loads, and $\sum M_{\mathrm{E}}+\Delta M_{\mathrm{g}}$ is the maximum sum of elastic moments from the analysis, which, owing to moment equilibrium at the joint, is the same as in the beams (see Eqs. (5.41) in Section 5.7.2.2). If redistribution of beam elastic moments according to Section 5.7.2.2 has produced the slimmest possible design for the beams, Eqs. (5.41) show that DC M columns subjected to the simplified uniaxial ULS verification of Eurocode 8 fulfil Eq. (1.4) with a 10% margin. So, checking Eq. (1.4) is redundant. On the other hand, in practice the outcome of the dimensioning of beams never meets exactly Eqs. (5.41). Rounding up of the reinforcement and the minimum steel requirements (especially at the bottom) produce beam designs with at least 10% margin over the right-hand-side of Eqs. (5.41). Therefore, fulfilment of Eq. (1.4) provides, on average, at least the same safety as the simplified uniaxial ULS verification allowed by Eurocode 8.

So, given that this simplified verification is admittedly safe-sided compared to a truly biaxial one for the results of the analysis, such a ULS verification is redundant if Eq. (1.4) is satisfied with $\gamma_{Rd} = 1.3$. The second implication is that, unless the beams have large overstrengths over the elastic action effects in the right-hand-side of Eqs. (5.41), Eq. (1.4) does not over-penalise the column vertical reinforcement compared to a ULS verification for the analysis results. So, in frames with little excess beam strength over the requirements of the analysis, exemptions from the application of Eq. (1.4) do not offer a real benefit for the economy of the structure (except, of course, at top-storey columns). Moroever, contrary to conventional wisdom, such exemptions do not simplify the design process either. Straightforward dimensioning of the column to satisfy Eq. (1.4) following the instructions in the first part of the present section is less tedious than ULS verification of the columns on the basis of the analysis results for the combinations of the seismic action with the concurrent gravity loads, even when this is done with the simplified uniaxial verification permitted by Eurocode 8 for DC M columns. If nothing else, it has to be done once in two horizontal directions (i.e., along the two orthogonal cross-sectional axes of the column) along which Eq. (1.4) is checked. By contrast, owing to the combination of the seismic action components according to Section 4.7.2 and the need to account for the effects of accidental eccentricity, ULS verification of columns for the analysis results should be done for normally 4, but possibly 16 (in the case of Section 4.7.2.2) combinations of moments with axial force.

Note that the vertical reinforcement at the base section of the bottom storey of a column (at the connection to the foundation) is dimensioned for the ULS in bending with axial force under the action effects from the analysis for the combination(s) of the seismic action and the concurrent gravity loads, without capacity design considerations. It is good practice to place there at least the same vertical reinforcement as at the top section of the bottom storey. Indeed, this is required by Eurocode 8 for DC H buildings, where seismic action effects computed from the analysis with fairly large q-factor values may have relatively low values. This practice ensures that, after the plastic hinge develops at the base of the column, the moment at the top section will not increase to (much) larger values than at the bottom. Such an increase would unduly reduce the value of the shear span at the plastic hinge, $L_s = M/V$, relative to its value at yielding at the base, decreasing therefore the plastic rotation capacity of the very crucial plastic hinge at the column base.

5.7.3.3 Moment Resistances in the Beam-Column Capacity Design Check, Eq. (1.4)

The design values of beam moment resistances for use in Eq. (1.4) are calculated from Eqs. (5.23) in Section 5.7.2.1. Section 5.7.3.2 has been pointed out that, at interior beam-column joints, which are more critical for Eq. (1.4) as two beams contribute to $\sum M_{Rd,b}$, redistribution of beam elastic moments in full accordance with Section 5.7.2.2 gives the minimum possible values of $\sum {M_{Rd,b}}^{+}$ and $\sum {M_{Rd,b}}^{-}$. These values are given in Eqs. (5.41) and are independent of the amount of beam reinforcement.

The rest of this section addresses the column moment resistances, $M_{Rd,c}$, for use in Eq. (1.4). Normally Eq. (1.4) is checked within the vertical plane of each frame, as defined by the beams. If the column cross-sectional axis with respect to which the moment resistance is computed is at an angle ψ to this plane, $M_{Rd,c}$ should enter Eq. (1.4) multiplied by $\sin \psi$.

Building columns are commonly square or rectangular and $M_{Rd,c}$ is computed with respect to centroidal axes parallel to the sides. Section 3.2.2.5 can be applied for the calculation of $M_{Rd,c}$ with the pertinent value of ξ from Section 3.2.2.4. In this calculation the conventional values $\varepsilon_{co} = 0.002$ (for f_{ck} up to 50 MPa) and $\varepsilon_{cu} = 0.0035$ from Eurocode 2 are used for concrete, the σ-ε diagram of steel is taken elastic-perfectly plastic with unlimited strain capacity and the design strengths of steel and concrete, f_{yd}, f_{cd}, respectively, are used for f_y, f_c. The width b is the length of the side parallel to the vector of $M_{Rd,c}$ of interest, while the depth h and dimensions d and d_1 are at right angles to it. The tension and compression reinforcement along the sides with length b is commonly symmetric ($A_{s1} = A_{s2}$). For the purposes of Sections 3.2.2.4 and 3.2.2.5, any intermediate bars between the tension and compression reinforcement are taken as uniformly distributed along the length (h–$2d_1$) of the depth h,[10] with cross-sectional area A_{sv}.

If the cross-section consists of more than one rectangular parts in two orthogonal directions (as in L-, T- or U-sections), the beams framing into the column are parallel or normal to the sides of these parts. So, it is convenient to compute the moment resistance, $M_{Rd,c}$ with respect to centroidal axes parallel to the two orthogonal directions of the sides, no matter whether they are indeed principal directions. If an iterative algorithm of the type mentioned in Section 5.7.3.1 (e.g., at Step 3) is available for the ULS verification of sections with any shape and reinforcement layout under any M_y-M_z-N combination, it can be used for the calculation of $M_{Rd,c}$, by setting the strain all-along the extreme fibres of the compression flange equal to $\varepsilon_{cu} = 0.0035$ and searching for a neutral axis depth that equilibrates the axial load N. As pointed out in the last paragraph of Section 3.2.2.4 under *Definitions and Assumptions*, if such an algorithm is not available, $M_{Rd,c}$ may be estimated considering the section as rectangular, with width b that of the compression flange. This is acceptable, if the width of the compression zone is constant between the neutral axis and the extreme compression fibres (i.e., the compression zone lies within a single one of the rectangular parts of the section).

The value of the column axial force, N, to be used in the calculation of $M_{Rd,c}$ should be the most safe-sided for the fulfillment of Eq. (1.4), notably the minimum compressive or maximum tensile force in the range of values derived from the analysis for the combination(s) of the design seismic action and the concurrent gravity loads, which is physically consistent with the sense of action (sign) of $M_{Rd,c}$. Section 5.7.3.5 addresses this issue in more detail.

[10] A_{s1} or A_{s2} are taken to include just one-half of each corner bar. The other half counts as part of A_{sv}.

5.7.3.4 Capacity Design of Columns in Shear

The moment resistances of beams and columns that enter in the calculation of capacity design shears of columns through Eq. (1.12) in Section 1.3.6.3 have been discussed in Sections 5.7.2.3 and 5.7.3.3. The only question is about the value of the column axial load to be used in the calculation of the column moment resistance, $M_{Rd,c}$. That value should be safe-sided, but also consistent with the verification in shear.

For the usual range of dimensionless axial load in the seismic design of columns, their shear resistance increases with increasing axial compression (both the shear resistance controlled by transverse reinforcement, $V_{Rd,s}$, and the one controlled by diagonal compression in the web of the member, $V_{Rd,max}$, see Sections 3.2.4.3 and 3.2.4.5 and Table 5.2). In addition, the capacity-design shear force from Eq. (1.12) increases with increasing moment resistance, $M_{Rd,c}$, which increases as the axial load increases till the balance load (see point 2 of Section 5.7.2.3). So, both of the following two cases should be considered as potentially critical for the shear verification:

1. The minimum compressive or maximum tensile force from the analysis, among all combinations of the design seismic action with the concurrent gravity loads. This value is also of interest for the strong column-weak beam capacity design of Eq. (1.4) in Section 5.7.3.2.
2. That value of axial load, within its range of variation for the combinations of the design seismic action with the concurrent gravity loads, at which $M_{Rd,c}$ becomes maximum. This value is also of interest for the capacity design shear of beams in Section 5.7.2.3 and is the minimum of the two values listed under points 1 and 2 in that section.

5.7.3.5 Column Axial Force Values for Capacity Design Calculations

A key question in the calculation of the column moment resistance, $M_{Rd,c}$, for capacity-design purposes is what value to choose for the column axial force, N, within the range derived from the analysis for the combination(s) of the design seismic action and the concurrent gravity loads. The choice should be meaningful but also safe-sided for the specific capacity design calculation:

1. For the capacity design shear of beams, we are interested in the maximum compressive column axial force (see Section 5.7.2.3).
2. For the strong column-weak beam capacity design of Eq. (1.4), we should use the minimum compressive or maximum tensile force in the column (see Section 5.7.3.3).
3. For the capacity design shear of the column itself, both the maximum compressive and the maximum tensile (or minimum compressive) force in the column are of interest (see Section 5.7.3.4).

4. For the capacity design of the foundation system and the bearing capacity verification of the soil, both the maximum compressive and the maximum tensile (or minimum compressive) force in the column are of interest (see Section 2.3.4 and the design of the foundation in Section 5.8.1).

The maximum or minimum compressive axial force for the combination of the design seismic action with the concurrent gravity loads derive from the maximum compressive and maximum tensile axial force, respectively, from the analysis for the seismic action.

In principle, the value used for N should be consistent with the sense of action (sign) of $M_{\mathrm{Rd,c}}$.[11] Note that:

(i) The column or beam moment resistances enter as sums, $\sum M_{\mathrm{Rd,c}}$, $\sum M_{\mathrm{Rd,b}}$:

- on opposite sides of the joint, in all three types of capacity design calculations;
- at the top and base of a storey, in calculations of type 3 above;
- of a hogging moment at one end of the beam and a sagging one at the opposite end, in type 1 calculations;

(ii) The sums of column moment resistances, $\sum M_{\mathrm{Rd,c}}$, are normally (about) the same for the two opposite senses of uniaxial bending, owing to symmetry of the section and its reinforcement;

(iii) By contrast, unless the beam reinforcement is symmetric (top and bottom) in each one of the two sections involved or the same in both, the beam moment resistance sums, $\sum M_{\mathrm{Rd,b}}$, are normally different for the two opposite senses of bending. Then, the sense (sign) of bending moments (and, therefore, of the seismic response) makes a difference.

The value of the maximum compressive or tensile seismic axial force in the column depends on how the effects of the seismic action components are combined according to Section 4.7.2 and which analysis method is used for them. This is elaborated further below for the four different cases in Section 4.7.2, taking as main component of $[M_{\mathrm{y}}\ M_{\mathrm{z}}\ N]$ the bending moment for which a plastic hinge forms, let's say M_{y}. The other moment component is not relevant. With the moment resistance, $M_{\mathrm{Rd,c}}$, conventionally taken as positive, M_{y} is considered positive if it has the same sense of action as $M_{\mathrm{Rd,c}}$. The axial force N is considered positive if compressive.

[11] For example, when the response is dominated by the 1st translational mode in a given horizontal direction, flexural plastic hinges at the base of columns normally have tension on the "windward" side of the column and compression on the "leeward" one. The opposite normally happens in plastic hinges at column tops. On the other hand, the 1st mode dominated response induces tensile axial forces at top and bottom of the exterior columns of the "windward" side and compressive ones in those of the "leeward" side.

1. *E_X, E_Y are combined through Eq. (4.25).* If E_X, E_Y are computed separately by lateral force analysis, direct application of Section 4.7.2.1 leads to a maximum compressive force in the column equal to the algebraically maximum of the two values:

   – $\text{sign}(M_{y,X}N_X)N_X + \text{sign}(M_{y,Y}N_Y)\lambda N_Y$,
   – $\text{sign}(M_{y,Y}N_Y)N_Y + \text{sign}(M_{y,X}N_X)\lambda N_X$

   and to a maximum tensile (or minimum compressive) one equal to the algebraically minimum of them. These are the values to be used, if the sense (sign) of bending moments and of the seismic response makes a difference for the value of $\sum M_{Rd,b}$ according to (iii) above. If it doesn't, the maximum compressive force in the column is the maximum of:
   – $|N_X| + \lambda|N_Y|$,
   – $|N_Y| + \lambda|N_X|$

   The maximum tensile one is its opposite. These same values come out from the direct application of Section 4.7.7.2, when E_X, E_Y are computed separately by modal response spectrum analysis, regardless of whether the sense (sign) of bending moments and of the seismic response makes a difference or not for the value of $\sum M_{Rd,b}$ according to (iii) above.
   It is physically more meaningful and less conservative to use as N the axial force due to the seismic action component giving the largest column moment in the direction of $M_{Rd,c}$, with the same sign as the axial force in the mode with the largest contribution to this moment when that contribution has the same sense (sign) as $M_{Rd,c}$. The axial force due to the orthogonal horizontal component of the seismic action is added with the same sign as the extreme axial force we are after (tensile or compressive).

2. *E_X, E_Y are combined via Eq. (4.24):* Direct application of Sections 4.7.2.3 and 4.7.2.4 (3rd term of Eqs. (4.37) or (4.40), respectively) gives a maximum compressive or tensile seismic force: $N = \pm\sqrt{(N_X{}^2+N_Y{}^2)}$. These values apply if the sense (sign) of bending moments and of the seismic response doesn't make a difference for the value of $\sum M_{Rd,b}$ according to (iii) above. If it does, recalling that the main component in $[M_y\ M_z\ N]$ is M_y and that the only other component of interest is N, we compute a single axial force value:

   – If E_X, E_Y are computed separately through modal response spectrum analysis, the 3rd term of Eq. (4.35) is modified as $N = [\text{cov}(M_yN)/M_{y,max}][M_{Rd,c}/M_{y,max}]$. Another physically meaningful alternative is to take the magnitude of N as $\sqrt{(N_X{}^2+N_Y{}^2)}$ and use the sign of the axial force in the mode with the largest contribution to the moment in the direction of $M_{Rd,c}$ when that contribution has the same sense (sign) as $M_{Rd,c}$.
   – If E_X, E_Y are computed separately by lateral force analysis, the 3rd term of Eq. (4.38) is modified as $N = [(M_{y,X}N_X+M_{y,Y}N_Y)/M_{y,max}][M_{Rd,c}/M_{y,max}]$ with $M_{y,max} = \sqrt{(M_{y,X}{}^2+M_{y,Y}{}^2)}$.

In every case the column axial forces due to the accidental eccentricities of both horizontal components are added with the same sign as the extreme axial force we are after (tensile for minimum N, compressive for maximum N).

So far this section has sought the extreme values of the column axial force within the range derived from the analysis for all combinations of the design seismic action with the concurrent gravity loads. Without restricting the seismic action to be the design one, one can estimate extreme values of column axial loads in a full-fledged beam-sway plastic mechanism, where plastic hinges develop at both ends of the beams framing in the column in the overlying floors:

$$\max N \approx \sum_{\text{overlying floors}} \left(R_{G+\psi_2 Q} + \Delta V_E\right);\ \min N \approx \sum_{\text{overlying floors}} \left(R_{G+\psi_2 Q} - \Delta V_E\right) \tag{5.47a}$$

$$\Delta V_E = \sum_{\text{adj. spans}} \max\left[\left(\frac{M^+_{Rd,bi} + M^-_{Rd,bj}}{L_{cl}}\right)_r - \left(\frac{M^+_{Rd,bi} + M^-_{Rd,bj}}{L_{cl}}\right)_l;\ \left(\frac{M^-_{Rd,bi} + M^+_{Rd,bj}}{L_{cl}}\right)_l - \left(\frac{M^-_{Rd,bi} + M^+_{Rd,bj}}{L_{cl}}\right)_r\right] \tag{5.47b}$$

where symbols are as in the preliminary design parallel of Eqs. (5.47) in Section 2.2.1.5, namely Eqs. (2.13) and (2.14), except $R_{G+\psi 2Q}$, which is the total reaction due to the concurrent gravity loads, G+ψ_2Q, delivered at a floor to the column by all beams framing in it from all directions.

5.7.3.6 Design of Columns Against Adverse Local Effects of Non-Structural Infills

According to Section 2.1.13.4, non-structural infills have two types of potential adverse local effects on adjoining columns:

1. A stiff and strong infill may shear-off weak columns, especially for unbalanced (i.e., one-sided) contact (see Fig. 2.11 in Section 2.1.13.4).
2. A "captive" column, laterally restrained by the infill(s) over part of its full height, is subjected to higher chord rotation demands and, more important, to larger shears. It may fail in flexure-shear or by pure shear, notably by diagonal compression (see Fig. 2.12 for examples).

Eurocode 8 has the following rules to protect concrete buildings from these two types of adverse local effects. They apply to buildings designed for DC H or M (not for L), no matter the structural system (wall or frame).

To prevent failure of type 1, the length of the column against which the diagonal strut bears should be verified in shear for the smallest of the following design shear forces:

(a) the horizontal component of the strut force of the infill, taken equal to the horizontal shear strength of the panel estimated from the shear resistance of bed joints (shear strength of bed joints times the wall thickness, t_w, times the clear length of the infill panel, L_{cl}); or
(b) the shear force computed from Eq. (1.12), taking the clear length of the column, H_{cl}, as equal to the contact length, l_c, and the parenthesis in the numerator equal to twice the design value of the column flexural capacity, $2M_{Rd,c}$ (see Fig. 5.7 for the rationale).

In case (b), the contact length should be taken equal to the full vertical width of the diagonal strut of the infill, $w_{inf}/\cos\theta$, where θ is the angle between the horizontal and the panel diagonal: $\theta = \arctan(H_{cl}/L_{cl})$.[12] This contact length is consistent with the calculation in case (a), which conservatively assumes that the full strut force is applied to the column. It is also closer to reality at the top of the column, as there the joint between the top of the infill and the soffit of the beam may already be open due to creep of the masonry or concrete infill.

Section 2.1.13.4 has listed several architectural or conceptual design solutions to the captive column problem. If none of them is feasible or effective, we can only use the dimensioning and detailing options provided by Eurocode 8 for captive columns. According to them, the design shear force of the "captive" column should be calculated according to Eq. (1.12), with:

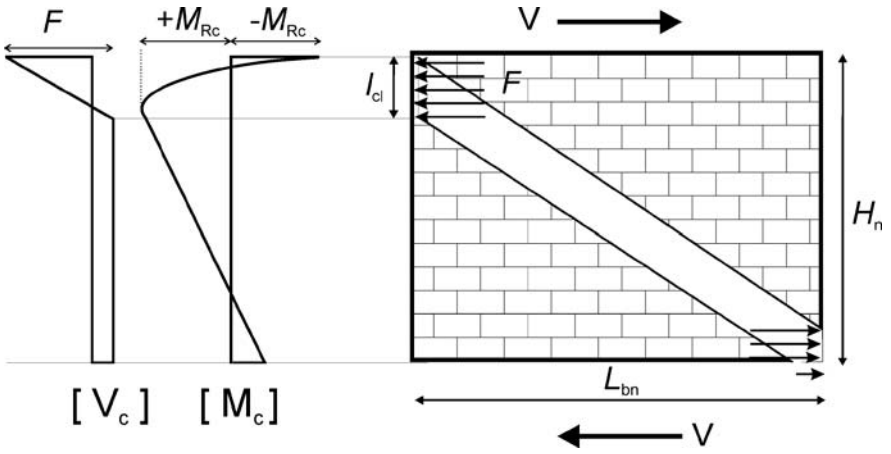

Fig. 5.7 Shear loading of column by the strut force of the infill

[12] Strictly speaking, in the present case where the strut is conservatively taken to bear fully on the columns, θ is the angle between the horizontal and the strut centreline, $\theta = \arctan[(H_{cl}-l_c)/L_{cl}]$. In Eqs. (4.46), though, θ is indeed the angle between the horizontal and the panel diagonal.

1. the clear length of the column, H_{cl}, taken equal to its free length not in contact with the infill (i.e., the clear height of the opening), and
2. the term min[. . .] taken equal to 1.0 at the column section at the far end of the column within the length of contact with the infill.

Behind this calculation is the presumption that the lateral restraint of the captive column by the infill is sufficient to induce a column plastic hinge at the level of the sill of the opening, rather than at the bottom of the column within the contact length with the infill or in weaker (than the column) beams framing into that end. Moreover, because:

– the clear height of the captive column may be short, and
– the exact location and extent of the potential plastic hinge around the level of the opening's sill is not clear and may well extend into the length of the column in contact with the infill,

Eurocode 8 imposes the following detailing on captive columns:

1. placing transverse reinforcement as required for resistance against the design shear force not just over the free length of the column, H_{cl}, but also along the part of the column in contact with the infill and within a length equal to the column depth in the plane of the infill, h_c, and
2. applying the special detailing and confinement requirements for column critical regions over the full height of the column in the storey.

The transverse reinforcement resulting from 2 above increases the nominal shear resistance of the captive column over its full height beyond the design shear force for which it has been verified and enhances its deformation capacity for any potential location of the plastic hinges. This may partly compensate for the lack of a special rule in Eurocode 8 for the calculation of the nominal shear resistance of columns with low shear span ratio (squat columns), regardless of their reduced flexural resistance owing to flexure-shear interaction (see Section 3.2.5.2) and their lower shear resistance for concrete failure along the diagonal(s) of the column in elevation (see Section 3.2.5.4).

If the free length of the column, H_{cl}, (i.e., the clear height of the opening) is short, the design shear force may come out of Eq. (1.12) so large that it may not be feasibe to verify the column for it, especially if shear resistance is governed by shear compression (see Eq. (3.127) in Section 3.2.5.4) and cannot be increased further through transverse reinforcement. Although designating the column as "secondary" may seem as a convenient way out of the deadlock, it is more sensible to solve the problem by reducing (instead of increasing) the size of the column. This may work, as:

1. if the shear span ratio, $H_{cl}/(2h_c)$, of the column increases to values above 2 (or, preferably, above 2.5) its behaviour in cyclic shear will not exhibit the special vulnerability and low dissipation capacity characterising short columns; and
2. the decrease in the cross-sectional dimensions will reduce the design shear force from Eq. (1.12) by reducing the moment resistance of the column, $M_{Rdc,i}$, ($i=$, 2) more than its nominal shear resistance.

Another option is to place reinforcing bars along both diagonals of the clear length of the captive column within the plane of the infill. Such bars, supplementing or replacing the conventional transverse reinforcement of the column, are very effective for energy dissipation and deformation capacity (see Section 3.2.5.5). They may be dimensioned to resist at the same time the design shear force from Eq. (1.12), as well as the design bending moments at the end sections of the short column, in accordance with the relevant rules for coupling beams of coupled walls. According to Eurocode 8, placing such reinforcement and dimensioning it to resist the full value of the design shear force is mandatory, if the free length of the column, H_{cl}, is less than $1.5h_c$ (corresponding to a value of the shear span ratio, $H_{cl}/(2h_c)$, less than 0.75).

5.7.4 Detailed Design of Ductile Walls

5.7.4.1 Dimensioning of Wall Vertical Reinforcement

As we have seen in Flow Chart 5.1 and Sections 5.7.2 and 5.7.3, seismic design of frame members for ductility entails significant interdependencies between phases of detailed design of different members. By contrast, the detailed design of a ductile wall does not depend on that of any other element. The only exception is when the designer uses the facility offered by Eurocode 8 to redistribute up to 30% of the seismic moment and shear of a wall with tensile seismic axial force to others with compressive.[13] Such redistribution should take place separately for each sense of action of the horizontal seismic components. It is meaningful only when the analysis method and the combination of the effects of the two horizontal components of the seismic action maintain the correspondence of signs between seismic action effects in the same or different elements. So, redistribution is not meaningful if the maximum effects of seismic action components computed by modal response spectrum analysis are combined via the linear approximation, Eq. (4.25), according to Section 4.7.2.2. The redistribution facility can be used to advantage to equalise the vertical reinforcement required when the wall is under seismic axial tension or compression and prevent large flexural overstrengths at the base from penalising the shear force demand in DC H walls (see Eqs. (1.14) and (1.15) in Section 1.3.6.4). Note, however, that this facility is worth using only if large axial forces are induced in the wall by the seismic response along its strong direction. This is not very common, as walls are normally placed between opposite sides in plan in their weak direction

[13] Axial tension is taxing for the ULS in bending with axial force, while compression is favourable.

(see, Fig. 2.2a in Section 2.1.6). By design, seismic axial forces are high in the piers of coupled walls. Redistribution between two symmetric piers is very easy: the pier elastic seismic moment and shear is reduced by up to 30% when its seismic axial force is tensile and increased by the same amount when it is compressive. The exact amount of redistribution should be chosen so that the pier vertical reinforcement just suffices under seismic axial tension, without producing flexural overstrength when in compression. Unless this is achieved, it is very hard to verify a coupled wall of DC H against the magnified shears of Eqs. (1.14) and (1.15).

Detailed design of ductile walls starts from dimensioning the vertical bars at the base section and proceeds to the top following the M-envelope in Fig. 1.7, Section 1.3.5. The vertical reinforcement of rectangular walls (even with barbells or narrow but symmetric flanges) is concentrated near the two far edges of the section and governed by the (essentially) uniaxial moment with axial force induced by the seismic response in the strong direction of the wall. Normally the minimum web vertical reinforcement is placed,[14] giving mechanical reinforcement ratio $\omega_v = \min \rho_v f_{yv}/f_c$. This value is used in the version of Eq. (3.51) applying in this case[15]:

$$\begin{aligned} \frac{\omega_v}{1-\delta_1}\left(\delta_1 \frac{\varepsilon_{cu}+\varepsilon_{y2d}}{\varepsilon_{cu}-\varepsilon_{y2d}} - 1\right) + \delta_1 \frac{\varepsilon_{cu} - \dfrac{\varepsilon_{co}}{3}}{\varepsilon_{cu}-\varepsilon_{y2d}} &\le \nu_d \\ &\le \frac{\omega_v}{1-\delta_1}\left(\frac{\varepsilon_{cu}-\varepsilon_{y1d}}{\varepsilon_{cu}+\varepsilon_{y1d}} - \delta_1\right) + \frac{\varepsilon_{cu} - \dfrac{\varepsilon_{co}}{3}}{\varepsilon_{cu}+\varepsilon_{y1d}} \end{aligned} \tag{5.42a}$$

If Eq. (5.42a) is satisfied, then the version of Eqs. (3.52) and (3.60) applicable here are used to find the symmetric edge reinforcement, $\omega_2 = \omega_1$ (cf. Step 1(i) in Section 5.7.3.1):

$$\xi = \frac{(1-\delta_1)\,\nu_d + (1+\delta_1)\,\omega_v}{(1-\delta_1)\left(1 - \dfrac{\varepsilon_{co}}{3\varepsilon_{cu}}\right) + 2\omega_v} \tag{5.43a}$$

$$\begin{aligned} (1-\delta_1)\,\omega_1 = \frac{M}{bd^2 f_{cd}} &- \xi\left[\frac{1-\xi}{2} - \frac{\varepsilon_{co}}{3\varepsilon_{cu}}\left(\frac{1}{2} - \xi + \frac{\varepsilon_{co}}{4\varepsilon_{cu}}\xi\right)\right] \\ &- \frac{\omega_v}{1-\delta_1}\left[(\xi-\delta_1)(1-\xi) - \frac{1}{3}\left(\frac{\xi\varepsilon_{yvd}}{\varepsilon_{cu}}\right)^2\right] \end{aligned} \tag{5.44a}$$

Often, however, the wall axial load, ν_d, is less than the limit of the left-hand-side in Eq. (5.42a), implying that the compression reinforcement, ω_2, is elastic. Then the value of ξ is the positive root of the version of Eq. (3.54) applying here:

---

[14] In the present context it is safe-sided and expedient to assume the minimum vertical web reinforcement, even when more is finally placed.

[15] As in Step 1 of Section 5.7.3.1, the design values f_{yd}, f_{cd}, $\varepsilon_{co} = 0.002$, $\varepsilon_{cu} = 0.0035$ are used in all these calculations.

$$\left[1-\frac{\varepsilon_{co}}{3\varepsilon_{cu}}+\frac{\omega_v}{2(1-\delta_1)}\frac{\left(\varepsilon_{cu}+\varepsilon_{yvd}\right)^2}{\varepsilon_{cu}\varepsilon_{yvd}}\right]\xi^2-\left[\nu+\omega_1\left(1-\frac{\varepsilon_{cu}}{\varepsilon_{yd}}\right)+\frac{\omega_v}{1-\delta_1}\left(1+\frac{\varepsilon_{cu}\delta_1}{\varepsilon_{yvd}}\right)\right]\xi$$
$$-\left[\frac{\omega_1}{\varepsilon_{yd}}-\frac{\omega_v\delta_1}{2\left(1-\delta_1\right)\varepsilon_{yvd}}\right]\varepsilon_{cu}\delta_1=0 \tag{5.45a}$$

The version of the expression for moment resistance, Eq. (3.59), applicable here may be used to express ω_1 in terms of ξ and the moment:

$$\omega_1\frac{(1-\delta_1)}{2}\left(1+\frac{\xi-\delta_1}{\xi}\frac{\varepsilon_{cu}}{\varepsilon_{yd}}\right)=\frac{M}{bd^2f_{cd}}-\xi\left[\frac{1-\xi}{2}-\frac{\varepsilon_{co}}{3\varepsilon_{cu}}\left(\frac{1}{2}-\xi+\frac{\varepsilon_{co}}{4\varepsilon_{cu}}\xi\right)\right]-$$
$$\frac{\omega_v}{4(1-\delta_1)}\left[\xi\left(1+\frac{\varepsilon_{yvd}}{\varepsilon_{cu}}\right)-\delta_1\right]\left[1+\frac{\varepsilon_{cu}}{\varepsilon_{yvd}}\left(\frac{\xi-\delta_1}{\xi}\right)\right]\left[1-\frac{\delta_1}{3}-\frac{2}{3}\xi\left(1+\frac{\varepsilon_{yvd}}{\varepsilon_{cu}}\right)\right] \tag{5.46a}$$

and replace ω_1 in Eq. (5.45a). The resulting equation is highly nonlinear in ξ and is solved iteratively; ω_1 is then determined from Eq. (5.46a).

The edge reinforcement from Eqs. (5.44a) or (5.46a) is implemented into a number of bars near the edge of the section, normally spread over a certain distance, l_c, from it (e.g., along a boundary element, see Fig. 5.2 in Section 5.3.4). The distance of this reinforcement from the section edge, normalised to d as δ_1, refers to the centroid of these bars. Note that A_{sv} and ω_v are considered uniformly distributed between the centroids of ω_2 and ω_1; a fraction $(l_c/d–\delta_1)/(1–\delta_1)$ of A_{sv} falls within the distance l_c over which the edge reinforcement is spread and should be added to the area from Eqs. (5.44a) or (5.46a) before translating it into edge reinforcement area.

In the piers of coupled walls there is a clear correspondence between the sign of the seismic axial force and the sense of the acting bending moment, even when it does not come out of the analysis (e.g., when the linear approximation, Eq. (4.25), is used to combine maximum effects of seismic action components computed by modal response spectrum analysis according to Section 4.7.2.2). They are such that they both put the exterior edge of each pier either in tension or in compression. The designer may decide then to place more reinforcement at that edge of the pier, let's say with mechanical ratio ω_2, than at the opposite one (towards the coupling beam), let's say with mechanical ratio $\omega_1 < \omega_2$. Normally the vertical reinforcement of the web is known, let's say ω_v. In principle the values of ω_1 and ω_2 can be determined using for each pier one of the expressions in Section 3.2.2.4 for the (unknown) neutral axis depth, ξ, and another one from Section 3.2.2.5 for the moment resistance (set equal to the design moment of the pier), both in terms of the unknown ω_1 and ω_2 but with the roles of ω_1 and ω_2 reversed in the two piers (in one pier the tension reinforcement is ω_2 and in the other ω_1). However, owing to the multitude of expressions in Sections 3.2.2.4 and 3.2.2.5, there is no clear-cut iterative solution, let alone a closed-form one. A practical possible procedure to determine ω_1 and ω_2 is the following.

We start from the pier where the seismic axial force is compressive. There ω_2 is indeed the compression reinforcement ratio and ω_1 that of tension reinforcement. To prevent the extreme compression fibres from crushing before the tension reinforcement yields (balance point), ξ is set equal to $\varepsilon_{cu}/(\varepsilon_{cu}+\varepsilon_{y1})$. Then for that pier ν_d is equal to the limit value $\nu_{c,y1}$ defined at the right-hand-side of Eq. (3.51):

$$\omega_2 - \omega_1 = \nu_d - \frac{\omega_v}{1-\delta_1}\left(\frac{\varepsilon_{cu}-\varepsilon_{y1}}{\varepsilon_{cu}+\varepsilon_{y1}} - \delta_1\right) - \frac{\varepsilon_{cu} - \dfrac{\varepsilon_{co}}{3}}{\varepsilon_{cu}+\varepsilon_{y1}} \tag{5.48a}$$

The second expression is obtained by inverting Eq. (3.60):

$$\omega_1 + \omega_2 = \frac{2\dfrac{M_d}{bd^2 f_c} - \xi\left[\dfrac{1-\xi}{2} - \dfrac{\varepsilon_{co}}{3\varepsilon_{cu}}\left(\frac{1}{2} - \xi + \dfrac{\varepsilon_{co}}{4\varepsilon_{cu}}\xi\right)\right] - \dfrac{\omega_v}{1-\delta_1}\left[(\xi-\delta_1)(1-\xi) - \frac{1}{3}\left(\dfrac{\xi\varepsilon_{yv}}{\varepsilon_{cu}}\right)^2\right]}{1-\delta_1} \tag{5.48b}$$

and using there $\xi = \varepsilon_{cu}/(\varepsilon_{cu}+\varepsilon_{y1})$. The pier where the seismic axial force is tensile is considered next. Depending on its net axial force (most likely tensile), the expressions for ξ in Section 3.2.2.4 are used with ω_1 and ω_2 known but with reversed roles. Those in Section 3.2.2.5 give the resulting moment resistance, to be compared with the design moment entrusted to this pier. If there is a shortfall, the moment redistributed to the other pier is increased and the calculation repeated. Conversely for a moment surplus.

Strictly speaking, a wall, being a vertical element, is under biaxial bending with axial force, M_y-M_z-N. So, after the vertical reinforcement is estimated, e.g., as in the above paragraph, and placed in the section according to the pertinent detailing rules, the section should be verified for the ULS in bending with axial force for all M_y-M_z-N combinations from the analysis for the design seismic action and the concurrent gravity loads (see Section 4.7.2 for these combinations and Section 5.7.3.1 for the iterative algorithms available for the ULS verification of sections with any shape and layout of reinforcement for any M_y-M_z-N combination). The moment in the strong direction of the wall, let's say M_y, is obtained from the linear M-envelope in Fig. 1.7 of Section 1.3.5. The value of M_z is that from the analysis. Its value is maximum at storey tops and bottoms. So, the ULS verification of the wall for M_y-M_z-N may take place at the base section of each storey. Wall flanges longer than 4-times their thickness qualify themselves as walls in the orthogonal direction. Then the M_z values are obtained from the linear M-envelope of Fig. 1.7 in that direction and not directly from the analysis. This raises the issue of non-rectangular walls discussed in the paragraph immediately following.

Wall sections not consisting of a single elongated rectangle but of several ones at right angles to each other (T-, L-, U-sections, etc.) should be verified in flexure as a whole for the M_y-M_z-N triplet of the entire composite section, assuming that it

remains plane. If the composite section is modelled in the analysis as an assemblage of (quasi-rigidly connected) rectangular parts (see Section 4.9.4), this separation should not be retained during its dimensioning and verification in flexure. The non-linearities in a section analysis at the ULS may lead to a distribution of strains and stresses in the actual composite section which is vastly different from that in the artificially articulated section under the M_y-M_z-N triplets of its individual parts. So, these triplets should be composed into a single one for the entire wall section. Note that the linear M-envelopes of Fig. 1.7 are used then both for M_y and M_z. Their values from the analysis at any level other than the base and the top of the wall are only of academic interest, whatever that may mean for the intricacies of elastic modelling of non-rectangular walls (see Section 4.9.4).

A safe-side estimate of the vertical reinforcement near the extreme tension and compression fibres of a non-rectangular wall section may be obtained via the 3-step procedure of Section 5.7.3.1 for the dimensioning of column vertical reinforcement under M_y-M_z-N, notably with the extension proposed there for non-rectangular columns. The full vertical reinforcement placed over the section should also meet the detailing rules for boundary elements, web minimum reinforcement, etc. Note that the size of any boundary elements needed around the non-rectangular section may be estimated from the strain profile(s) obtained in the course of Step 3 of the procedure, namely through the iterative algorithm for the ULS verification of sections with any shape and layout of reinforcement for any combination M_y-M_z-N.

5.7.4.2 Dimensioning of DC H Walls in Shear

It is hard to verify in shear the "critical region" of DC H walls. Its cyclic shear resistance for diagonal compression, $V_{Rd,max}$, is reduced to just 40% of the Eurocode 2 value for monotonic loading (see Section 5.5.3 and Fig. 3.42 in Section 3.2.4.5). The reduced resistance should exceed the shear forces from the analysis multiplied by the ε-factor of Eqs. (1.14) and (1.15) in Section 1.3.6.4, which normally is much larger than 1.0. If the verification fails, an increase of the web thickness, b_{wo}, is normally not very effective. It will increase proportionally the value of $V_{Rd,max}$, but it will also increase, albeit less than proportionally, the seismic shear force from the elastic analysis.[16] Keeping the flexural overstrength ratio at the wall base, $M_{Rd,o}/M_{Ed,o}$, to a minimum (equal to 1.0, if at all possible) may be much more effective. To this end, the wall thickness should not be so large that the vertical reinforcement is controlled by minimum requirements. The most important overstrength, however, comes from the variation of the wall axial force when the design seismic action changes sign. The vertical reinforcement is governed by the axial tension situation and provides large flexural overstrength, $M_{Rd,o}/M_{Ed,o}$, under equal and opposite acting moments, $M_{Ed,o}$, but in axial compression. Recourse should be

[16] The elastic stiffness is proportional to b_{wo} in rectangular walls and less than proportional to it in non-rectangular ones. The wall's elastic seismic action effects, in turn, are less than proportional to its elastic stiffness, especially if the wall has a major contribution to the global lateral stiffness.

made to the redistribution facility described in the first paragraph of Section 5.7.4.1, in order to equalise the vertical reinforcement requirements for the wall under axial tension or compression and achieve always: $M_{Rd,o} \approx M_{Ed,o}$.

The value of $M_{Rd,o}$ for the purposes of Eqs. (1.14) and (1.15) should be computed as outlined for columns in Section 5.7.3.3. If the wall is rectangular Section 3.2.2.5 applies, using the pertinent value of ξ from Section 3.2.2.4. If it is non-rectangular, an iterative algorithm of the type mentioned in Section 5.7.3.1 (at Step 3) may be used. Alternatively, the section may be taken as rectangular with width b that of the compression flange, provided that in the end the compression zone lies fully within a single rectangular part of the section.

In coupled walls the redistribution of $M_{Ed,o}$ from the pier in tension to that in compression may not be sufficient to keep $M_{Rd,o}$ close to $M_{Ed,o}$. If it is difficult to verify the piers in shear, the values of $M_{Rd,o}$ and $M_{Ed,o}$ for the ratio $M_{Rd,o}/M_{Ed,o}$ may be computed considering the two piers as a single section. Then the couple, $N_E l$, where l is the axial distance between the pies and N_E the seismic axial force in them for the seismic action combination of interest, should be added both to the sum of $M_{Rd,o}$'s of the piers and to that of their $M_{Ed,o}$'s. The shear forces of the piers from the analysis, as modified by the redistribution, are then amplified by a common ε -factor according to Eqs. (1.14) and (1.15).

5.8 Application Examples

5.8.1 3-Storey Frame Building on Spread Footings

A 3-storey RC frame building has rectangular plan with dimensions $L_x = 10$ m in horizontal direction X and $L_y = 25$ m in horizontal direction Y. It consists of:

- six frames in direction X, each having two bays with bay length $L = 5$ m (see Fig. 5.8) and
- three five-bay frames in direction Y, with constant bay length $L = 5$ m.

The storey height is $H = 3$ m. The columns are square, with side:

- $h_{c,int} = 0.4$ m for interior columns,
- $h_{c,ext} = 0.35$ m for the exterior ones, and
- $h_{c,corner} = 0.3$ m for the four corner ones.

All beams have width $b_w = 0.3$ m and flange (i.e. slab) thickness 0.15 m; their depth is:

- $h_b = 0.5$ m for interior beams, and
- $h_b = 0.45$ m for exterior ones.

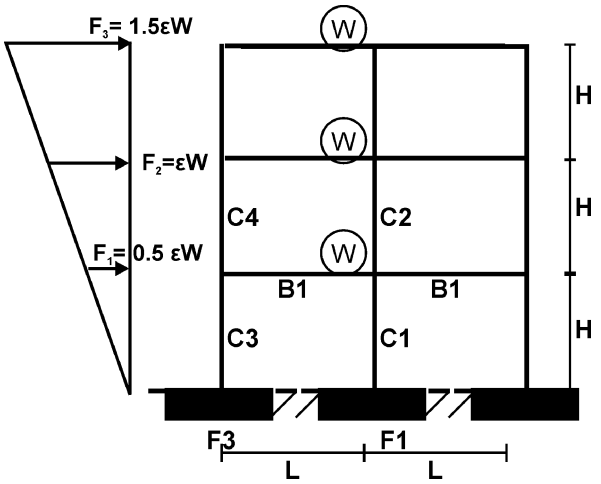

Fig. 5.8 Interior 3-storey frame in direction X with heightwise linear lateral forces

Global aspects covered in the design of the frame building are limited to what is required for the determination of seismic action effects (behaviour factor, fundamental periods, base shear, 2nd-order effects, etc.). Global verifications include checking of drifts under the damage limitation seismic action and detailed design (including capacity design) of:

- the 1st interior 2-bay frame in direction X (at distance $y = 7.5$ m from the mass centre), and
- the interior columns and beam spans in all 5-bay frames in direction Y,

with emphasis on the ground storey and the foundation.

Design specifications

- Storey quasi-permanent gravity load concurrent with the earthquake: 9 kN/m^2, corresponding to uniform transverse load on interior beams B1: $g+\psi_2 q$=20 kN/m and on exterior ones: $g+\psi_2 q$ =15 kN/m.
- Permanent load g =18 kN/m on interior beams, g =14 kN/m on exterior ones.
- For factored gravity loads (persistent and transient design situation), γ_gG+γ_qQ: uniform transverse load q_d=35 kN/m on interior beams, q_d=24 kN/m on exterior ones.
- Reference Peak Ground Acceleration on type A ground (rock) a_{gR}=0.23 g.
- EC8 Type 1 recommended spectrum on ground type E (see Table 4.2 for the parameters),
- Importance Class III; importance factor $\gamma_I = 1.2$.
- Ductility Class (DC) Medium (M).

- Concrete C30/37; Steel S500; concrete cover to reinforcement: $c = 25$ mm.
- Soil: clay with design value of undrained shear strength $c_{ud} = 100$ kPa and unit weight $\gamma_{soil} = 19$ kN/m^3.
- The top of the footing is at ground surface (no surcharge due to overburden of footing by soil).

Simplifying assumptions for the analysis

- Columns are considered fixed at the top of the footing.
- The points of inflection of columns under lateral loading are assumed at storey mid-height; then seismic bending moments at column ends may be taken equal to the shear force of the column, times one-half of its clear height, $H_{cl}=H-h_b$:
  - $M_{Ec1}=\pm 0.5 V_{Ec,1} H_{cl}$ in column C1 (at the ground storey),
  - $M_{Ec2}=\pm 0.5 V_{Ec,2} H_{cl}$ in column C2 (storey 2), etc.
- Interior columns may be considered to have twice the moment of inertia of exterior ones. Similarly for exterior columns v the corner ones. Then (cf. 2nd paragraph of Section 2.2.1.3):
  - Interior columns may be considered to take twice the seismic shear compared to exterior ones, which in turn take twice the seismic shear compared to corner columns;
  - All beam points of inflection under lateral loading may be taken at mid-span;
  - Seismic axial forces in columns which are interior in the direction of the seismic action are zero. The seismic overturning moment is taken by axial forces only in the columns which are exterior in the direction of the seismic action.
  - Interstorey drifts due to lateral loading, from midheight of storey i to mid-height of storey $i+1$, may be calculated from Eq. (2.8a) in Section 2.2.1.3, giving storey drifts:
    - at the ground storey ($i=1$):

$$\delta_1 = \frac{1}{24} H_{cl}^3 \left[\frac{V_{Ec,1}}{(EI)_{c,1}} \right] + \Delta\delta_1/2$$

    - at storey $i>1$: $\delta_i = \delta_{i-1} + (\Delta\delta_i + \Delta\delta_{i-1})/2$
    - of the top storey ($i = n$):

$$\delta_n = \Delta\delta_{n-1}/2 + \delta_{n-1} + \frac{1}{24} V_{Ec,n} \left[\frac{H_{cl}^3}{(EI)_{c,n}} \left(1 + 1.5 \frac{h_{b,n}}{H_{cl}} \right) + \frac{L_{cl}^3}{(EI)_{b,n}} \left(\frac{H}{L} \right)^2 \left(1 + 1.5 \frac{h_{c,n}}{L_{cl}} \right) \right]$$

- At the sections of beam B1 in an interior 2-bay frame in direction X at the support on the central column, C1:

- the top reinforcement is dimensioned for the maximum of the following moments:

  (1) $M_{\gamma gG+\gamma qQ} = q_d L_{cl}^2/8$, with:

  - L_{cl} = beam clear span = L–0.5($h_{c,ext}$+$h_{c,int}$);

  (2) $M_{g+\psi 2q}$+(|$M_{Ec1,yX}$|+|$M_{Ec2,yX}$|)/2, with:

  - $M_{g+\psi 2q}$=($g + \psi_2 q$)L_{cl}^2/8 and
  - $M_{Ec1,yX}$, $M_{Ec2,yX}$: seismic bending moments in 1st and 2nd storey central columns, C1 and C2, respectively, due to the horizontal seismic action component in direction X, about the local axis y of the column which is normal to direction X and to the vertical plane of the interior frame;

- the bottom reinforcement is dimensioned for moment: (|$M_{Ec1,yX}$|+|$M_{Ec2,yX}$|) /2-$M_{g+\psi 2q} \geq 0$.

- The section of beam B1 of an interior 2-bay frame in direction X at the support by the exterior column C3 is dimensioned for moment: ±(|$M_{Ec3,yX}$|+|$M_{Ec4,yX}$|), with $M_{Ec3,yX}$, $M_{Ec4,yX}$ defined like $M_{Ec1,yX}$, $M_{Ec2,yX}$ but for the exterior columns C3 and C4, respectively.
- At the sections of any interior beam of a 5-bay frame in direction Y at the supports to the interior columns of these frames:

  - the top reinforcement is dimensioned for the maximum of the following moments:

    (3) $M_{\gamma gG+\gamma qQ} = (q_d/9 - g/36)L_{cl}^2$, with:

    - L_{cl}=L –h_c (h_c=$h_{c,ext}$ for exterior 5-bay frames and h_c=$h_{c,int}$ for interior ones);

    (4) $M_{g+\psi 2q}$+(|$M_{Ec1,zY}$|+|$M_{Ec2,zY}$|)/2, with:

    - $M_{g+\psi 2q}$=($g + \psi_2 q$)L_{cl}^2/12 and
    - $M_{Ec1,zY}$, $M_{Ec2,zY}$: seismic bending moments in 1st and 2nd storey columns (C1 and C2, respectively, for interior 5-bay frame, or C3 and C4, respectively, for the exterior one) due to the horizontal seismic action component in direction Y, about local axis z of the column normal to direction Y and to the vertical plane of the interior 5-bay frame;

  - the bottom reinforcement is dimensioned for moment: (|$M_{Ec1,zY}$|+|$M_{Ec2,zY}$|)/ 2-$M_{g+\psi 2q} \geq 0$.

- Interior columns support 125% of the gravity loads within their tributary area, while exterior ones support 75% of the gravity loads in theirs.
- Column bending moments due to gravity loads are neglected.

(a) Material parameters

$$f_{cd} = 30/1.5 = 20\,\text{MPa};\ f_{ctm} = 2.9\,\text{MPa},\ E_c = 33000\,\text{MPa};$$
$$f_{yd} = 500/1.15\,\text{MPa};\ \varepsilon_{yd} = 500/(1.15 \times 200000) = 0.217\%;$$

Distance of centre of longitudinal bars from nearest concrete surface: $d_1 = c + d_{bh} + d_{bL}/2 \sim 0.025 + 0.008 + 0.018/2 \sim 0.04$ m.

(b) Geometric parameters

Effective flange width (according to Eurocode 2) and moment of inertia of beams:
Interior T-beams: $b_{eff} = 2 \times 0.2 \times 0.85L + b_w = 0.34 \times 5 + 0.3 = 2$ m,

- Cross-sectional area: $A = 1.7 \times 0.15 + 0.5 \times 0.3 = 0.405\ \text{m}^2$
- Distance of centroid from top: $y_t = (1.7 \times 0.15 \times 0.075 + 0.5 \times 0.3 \times 0.25)/0.405 = 0.1398$ m,
- Moment of inertia: $I_b = (1.7 \times 0.15^3 + 0.3 \times 0.5^3)/3 - 0.405 \times 0.1398^2 = 0.0065\ \text{m}^4$

Exterior L-beams: $b_{eff} = 0.2 \times 0.85L + b_w = 0.17 \times 5 + 0.3 = 1.15$ m,

- Cross-sectional area: $A = 0.85 \times 0.15 + 0.45 \times 0.3 = 0.2625\ \text{m}^2$
- Distance of centroid from top: $y_t = (0.85 \times 0.15^2/2 + 0.3 \times 0.45^2/2)/0.2625 = 0.15215$ m,
- Moment of inertia: $I_b = (0.85 \times 0.15^3 + 0.3 \times 0.45^3)/3 - 0.2625 \times 0.15215^2 = 0.004\ \text{m}^4$

Moment of inertia of interior columns: $I_{c,int} = 0.4^4/12 = 0.00214\ \text{m}^4$
Moment of inertia of exterior columns: $I_{c,ext} = 0.35^4/12 = 0.00125\ \text{m}^4$
Moment of inertia of corner columns: $I_{c,corner} = 0.3^4/12 = 0.000675\ \text{m}^4$

(c) Check of storey torsional radii versus radius of gyration of floor mass

Storey torsional radii from Eq. (2.3) and the moments of inertia of the column sections:

$$\sum \left(x^2 I_y + y^2 I_x\right) = 2 \times \{5^2(4 \times 0.00125 + 2 \times 0.000675) + 12.5^2(2 \times 0.000675 + 0.00125) + (7.5^2 + 2.5^2)(2 \times 0.00125 + 0.00214)\} = 1.71\,\text{m}^6,$$

$$\sum \left(I_y\right) = \sum (I_x) = 10 \times 0.00125 + 4 \times 0.000675 + 4 \times 0.00214 = 0.02376\,\text{m}^4,$$

$$r_x = r_y = \sqrt{\frac{1.71}{0.02376}} = 8.48\,\text{m}$$

As the mass is uniformly distributed over the rectangular floor area, the radius of gyration of the floor mass in plan, l_s, is: $l_s = \sqrt{(L_x^2 + L_y^2)/12} = \sqrt{(25^2 + 10^2)/12} = 7.77$ m

So, the frame system has sufficient torsional rigidity to ensure that the fundamental translational periods in the two horizontal directions are longer than the twisting

period. This condition is only marginally met, just thanks to the fact that the moment of inertia of exterior columns is slightly more than 50% (namely, 58%) of that of interior ones, and that of corner columns is slightly higher than 50% (namely, 54%) of the moment of inertia of interior columns. If the ratio of these moments of inertia were exactly 50%, then the distribution of stiffness in plan would had been as uniform as that of mass and the storey torsional radii would had been equal to the radius of gyration of the floor mass in plan, l_s. Note also that the moment of inertia of the exterior beams is also slightly higher than 50% (namely, 59%) of that of interior ones. Should the effect of the beams on storey lateral and torsional stiffness had been taken into account, the conclusion regarding the relative magnitude of the storey torsional radii and the radius of gyration of the floor mass in plan would not had changed.

(d) Member rigidities

As $I_{c,int} \sim 2I_{c,ext}$, for simplicity of the calculations the interior columns may be considered to have twice the moment of inertia of exterior ones, so that they can be considered to take twice the seismic shear of exterior columns. Similarly for exterior columns v the corner ones, as $I_{c,ext} \sim 2I_{c,corner}$. Then, all beam points of inflection under lateral loading may be taken to be at mid-span.

- If the interior columns are taken with exactly twice the moment of inertia of exterior ones and the exterior columns with exactly twice the moment of inertia of corner ones, interior columns have moment of inertia:

$$I_c = (10 \times 0.00125 + 4 \times 0.000675 + 4 \times 0.00214)/(10 \times 0.5 + 4 \times 0.25 + 4 \times 1) = 0.002376\,\text{m}^4.$$

- In the interior two-bay frames in direction X, the moment of inertia of the beams may be taken equal to $I_b = (4 \times 0.0065 + 2 \times 0.004)/5 = 0.0068\ \text{m}^4$.
- In the 5-bay frames in direction Y, the two exterior frames are taken as the basis. For them the moment of inertia of beams may be taken equal to $I_b = (0.0065 + 2 \times 0.004)/4 = 0.00363\ \text{m}^4$ and that of columns equal to that of exterior ones: $I_c = 0.002376/2 = 0.001188\ \text{m}^4$.

Effective rigidity:
(Interior) frames in direction X:

- Central column: $(EI)_c = 0.5 \times 33000000 \times 0.002376 = 39200\ \text{kNm}^2$;
- Beams: $(EI)_b = 0.5 \times 33000000 \times 0.0068 = 112200\ \text{kNm}^2$.

(Exterior) frames in direction Y:

- Interior columns: $(EI)_c = 0.5 \times 33000000 \times 0.001188 = 19600\ \text{kNm}^2$.
- Beams: $(EI)_b = 0.5 \times 33000000 \times 0.00363 = 59900\ \text{kNm}^2$.

(e) Seismic action effects for a design spectral acceleration of 1 g

Thanks to the building's regularity and apparently relatively short natural period ($T_1 < 4T_C$, 2 s), the lateral force analysis procedure may be used. As all storeys have the same mass, the seismic lateral forces have heightwise linear distribution (see Fig. 5.8). The seismic shear in storey 1 (ground storey) is V_{E1}=F_1+F_2+F_3, in storey 2: V_{E2} =F_2+F_3 and in storey 3: $V_{E3} = F_3$.
Seismic action in horizontal direction X (E_X) – on the basis of an interior frame.
Tributary weight of interior frame: $W = 5 \times 10 \times 9$=450 kN/per storey.
Storey seismic shears:

- Ground storey: V_{E1}=$3 \times 450 = 1350$ N
- 2nd storey: V_{E2}=$2.5 \times 450 = 1125$ kN
- 3rd storey: V_{E3}=$1.5 \times 450 = 675$ kN

Seismic shear forces in interior column:

- Ground storey: V_{Ec1}=0.5×1350=675 kN
- 2nd storey: V_{Ec2}=0.5×1125=562.5 kN
- 3rd storey: V_{Ec3}=0.5×675=337.5 kN

Interstorey drift, midheight of storey 1 to midheight of storey 2:

$$\Delta\delta_1 = \frac{675 + 562.5}{24}\left[\frac{2.5^3}{39200}\left(1 + 1.5\frac{0.5}{2.5}\right) + \frac{4.6^3}{112200}\left(\frac{3}{5}\right)^2\left(1 + 1.5\frac{0.4}{4.6}\right)\right]$$
$$= 0.0449\,\text{m}$$

Interstorey drift, storey 2 to storey 3: $\Delta\delta_2$=$0.0449 \times$ (562.5+337.5)/(675+562.5)= 0.0328 m
Storey drifts:

- Ground storey (i=1): δ_1=(2.5^3/24)(675/39200)+0.0449 / 2 = 0.0336 m
- 2nd storey (i=2): $\delta_2 = \delta_1$+($\Delta\delta_1 + \Delta\delta_2$)/2=0.0336+(0.0449+0.0328) / 2 = 0.0724 m
- Top storey (i=3): δ_3 = 0.0724+0.0328/2+$0.0449 \times$ 337.5 / (675+562.5) = 0.101 m

Seismic action in horizontal direction Y (E_Y) – on the basis of an exterior frame.
Tributary weight of exterior frame: $W = 2.5 \times 25 \times 9 = 562.5$ kN/per storey.
Seismic shear forces, interior column:

- Ground storey: $V_{Ec1} = (3 \times 562.5)/5 = 337.5$ kN
- 2nd storey: $V_{Ec2} = (2.5 \times 562.5)/5 = 281.25$ kN
- 3rd storey: $V_{Ec3} = (1.5 \times 562.5)/5 = 168.75$ kN

Interstorey drift, midheight of storey 1 to midheight of storey 2:

$$\Delta\delta_1 = \frac{337.5 + 281.25}{24}\left[\frac{2.55^3}{19600}\left(1 + 1.5\frac{0.45}{2.55}\right) + \frac{4.65^3}{59900}\left(\frac{3}{5}\right)^2\left(1 + 1.5\frac{0.35}{4.65}\right)\right]$$
$$= 0.0449\,\text{m}$$

Interstorey drift, storey 2 to storey 3: $\Delta\delta_2$=0.0449 × (337.5+168.75)/(337.5+281.25) = 0.0328 m
Storey drifts:

- Ground storey (i=1): $\delta_1 = (2.55^3/24)(337.5/19600)+0.0449/2 = 0.0343$ m
- 2nd storey (i=2): $\delta_2 = \delta_1+(\Delta\delta_1+ \Delta\delta_2)/2 = 0.0343+(0.0449+0.0328)/2 = 0.0731$ m
- Top storey (i=3): $\delta_3 = 0.0731+0.0328/2+0.0449 \times 168.75/(337.5+281.25) = 0.1017$ m

(f) Estimation of the fundamental period from the Rayleigh quotient, Eq. (4.7)

Seismic action in horizontal direction X (E_X):

- Ground storey: $F_1 = 0.5 \times 450 = 225$ kN
- 2nd storey: $F_2 = (1.0 \times 450) = 450$ kN
- 3rd storey: $F_3 = (1.5 \times 450) = 675$ kN

For m_1=m_2=m_3 = 450/g = 45.8 kN/(m/s^2), the values of F_i above and storey drifts δ_i in (e) for a design spectral acceleration of 1 g, the fundamental period in direction X is: T_X~0.525 s.

Seismic action in horizontal direction Y (E_Y):

- Ground storey: $F_1 = 0.5 \times 562.5 = 281.25$ kN
- 2nd storey: $F_2 = 1.0 \times 562.5 = 562.5$ kN
- 3rd storey: $F_3 = 1.5 \times 562.5 = 843.75$ kN

For m_1=m_2=m_3 = 562.5/g = 57.3 kN/(m/s^2), the values of F_i above and storey drifts δ_i in (e) for a design spectral acceleration of 1 g, the fundamental period in direction Y is: T_Y=0.527 s

(g) Estimation of design spectral acceleration

Design ground acceleration on type A ground: a_g=$\gamma_I a_{gR} = 0.276$ g.
Behaviour factor: q =$q_o = 3 \times 1.3 = 3.9$.
Seismic action in horizontal direction X (E_X). For $T_X = 0.525\,\text{s} > T_C$, Eq. (4.5c) gives:

$S_d(\text{T}) = 0.276 \times 1.4 \times (2.5/3.9) \times (0.5/0.525) = 0.236\,\text{g} > 0.2 \times 0.276\,\text{g} = 0.055\,\text{g}.$

Seismic action in horizontal direction Y (E_Y): For $T_Y = 0.527\,\text{s} > T_C$, Eq. (4.5c) gives:

$$S_d(\text{T}) = 0.276 \times 1.4 \times (2.5/3.9) \times (0.5/0.527) = 0.235\,\text{g} > 0.2 \times 0.276\,\text{g}.$$

As $T_1 < 2T_C = 1.0$ s, we may reduce the base shear by 15% in the lateral force analysis:

- Design spectral acceleration in horizontal direction X (E_X): 0.85 × 0.237 g∼0.201 g.
- Design spectral acceleration in horizontal direction Y (E_Y): 0.85 × 0.235 g∼0.20 g.

For $T \geq T_C$: $\mu_\varphi = 2\, q_o - 1 = 6.8$.

(h) Estimation of action effects due to the accidental eccentricity

Storey lateral forces due to the seismic action in horizontal direction X, $F_{X,i}$, are applied at an accidental eccentricity to the mass centre, $e_{y,i} = 0.05 L_{y,i}$. Those due to the horizontal component in direction Y, $F_{Y,i}$, are applied at an accidental eccentricity $e_{x,i} = 0.05 L_{x,i}$.

As the structure is fully symmetric in both horizontal directions and $e_{y,i}$ is constant in all storeys, the accidental eccentricity of the seismic action in direction X has the following effects on an element at a distance y to the centre of mass in direction Y and x in direction X:

- for bending in a vertical plane parallel to X, it increases the seismic moments and shears due to the horizontal component in direction X applied at the mass centre by a factor of $\left(1 + \frac{e_y}{r_y}\frac{|y|}{r_y}\right)$;
- for bending in a vertical plane parallel to Y, it induces seismic moments and shears similar to those induced by the horizontal component in direction Y, applied at the centre of mass, times a factor of $\frac{V_X}{V_Y}\frac{e_y}{r_x}\frac{|x|}{r_x}$, where V_X and V_Y are the storey shears at that level due to the horizontal seismic action components in directions X and Y, respectively.

Similarly, the accidental eccentricity of the component in direction Y, e_x=0.05L_x:

- for bending in a vertical plane parallel to Y, it increases seismic moments and shears due to the horizontal component in direction Y applied at the mass centre by a factor of $\left(1 + \frac{e_x}{r_x}\frac{|x|}{r_x}\right)$;
- for bending in a vertical plane parallel to X, it induces seismic moments and shears similar to those induced by the horizontal component in direction X applied at the centre of mass, times $\frac{V_y}{V_x}\frac{e_x}{r_y}\frac{|y|}{r_y}$.

Combination of the peak effects of the two horizontal components, E_X and E_Y, according to Eq. (4.25) gives the following effects of the accidental eccentricities (for $e_x/e_y = L_x/L_y = 0.4$, $V_X/V_Y = 1.005$, $r_x = r_y = 8.48$ m, $e_x/r_y = e_x/r_x = 0.05 L_x/r_y = 0.05 \times 10/8.48 = 0.059$, $e_y/r_y = e_y/r_x = 0.05 L_y/r_y = 0.05 \times 25/8.48 = 0.1475$):

- Seismic moments and shears for bending in a vertical plane parallel to X are those due to the horizontal component in direction X through the centre of mass,

times $\left(1+\frac{e_y}{r_y}\frac{|y|}{r_y}\right) = \left(1+0.148\frac{|y|}{r_y}\right)$. The same horizontal component induces seismic moments and shears in the orthogonal direction (bending in a vertical plane parallel to Y) equal to those induced in that direction of bending by the direction Y component applied at the centre of mass, times $\frac{V_X}{V_Y}\frac{e_y}{r_x}\frac{|x|}{r_x} = 0.148\frac{|x|}{r_x}$.
- Seismic moments and shears for bending in a vertical plane parallel to Y are those due to the direction Y component through the mass centre, times $\left(1+\frac{e_x}{r_x}\frac{|x|}{r_x}\right) = \left(1+0.059\frac{|x|}{r_x}\right)$. Concurrent seismic moments and shears in the orthogonal direction (bending in a vertical plane parallel to X) are equal to those induced in that direction by the horizontal component in direction X applied at the centre of mass, times $\frac{V_Y}{V_X}\frac{e_x}{r_y}\frac{|y|}{r_y} = 0.059\frac{|y|}{r_y}$.

(i) Interstorey drift check against limit (i) in Section 1.1.3 under the damage limitation seismic action

The damage limitation seismic action is equal to the design seismic action times a reduction factor ν, which for Importance Class III is $\nu = 0.4$. Interstorey drift ratios are computed at the storey centre of mass, and hence are not affected by the accidental eccentricity. They are equal to:

- the difference of storey drifts calculated above for a design spectral acceleration of 1 g divided by the storey height $H = 3.0$ m, times
- the final design spectral acceleration in g's: ~0.2, times
- the reduction factor $\nu = 0.4$, and times
- the behaviour factor $q = 3.9$.

They are computed and checked here only for the seismic action component in direction X:

- Ground storey (i=1): $\Delta\delta_1 = 0.0336 \times 0.201 \times 0.4 \times 3.9 / 3.0 = 0.00351 < 0.005 \rightarrow$OK
- 2nd storey (i=2): $\Delta\delta_2 = (0.0724–0.0336) \times 0.201 \times 0.4 \times 3.9 / 3.0 = 0.00406 < 0.005 \rightarrow$OK
- Top storey (i=3): $\Delta\delta_3 = (0.101–0.0724) \times 0.201 \times 0.4 \times 3.9 / 3.0 = 0.003 < 0.005 \rightarrow$OK

(j) Estimation and check of 2nd-order effects through the sensitivity coefficient θ

The sensitivity coefficient θ is computed from Eq. (4.45) only for the component in direction X:

- Ground storey (i=1): $\theta_1 = (0.00351/0.4) \times (3 \times 450) / (0.201 \times 3 \times 450) = 0.0441 < 0.10 \rightarrow$OK
- 2nd storey (i=2): $\theta_2 = (0.00406/0.4) \times (2 \times 450) / (0.201 \times 2.5 \times 450) = 0.0406 < 0.10 \rightarrow$OK
- Top storey (i=3): $\theta_3 = (0.003/0.4) \times 450 / (0.201 \times 1.5 \times 450) = 0.025 < 0.10 \rightarrow$OK

(k) Gravity action effects in interior and exterior columns

Axial forces in the interior and exterior columns due to gravity loads, $G+\psi_2 Q$. Considering the beam of any interior frame in the X direction as a two-span continuous beam supported on columns that do not exert any rotational restraint (simple supports):

- Column C1: $N_{1,g+\psi 2q} = 1.25 \times 3 \times (9 \times 5 \times 5) = 843.8$ kN
- Column C2: $N_{2,g+\psi 2q} = 1.25 \times 2 \times (9 \times 5 \times 5) = 562.5$ kN
- Column C3: $N_{3,g+\psi 2q} = 0.75 \times 3 \times (9 \times 2.5 \times 5) = 253.1$ kN
- Column C4: $N_{4,g+\psi 2q} = 0.75 \times 2 \times (9 \times 2.5 \times 5) = 168.8$ kN

These values are close to those from an elastic analysis of the full structural system in 3D.

(l) Seismic bending moments in columns of 1st interior 2-bay frame in direction X (at distance $y = 7.5$ m from mass centre) and in interior columns of the 5-bay frames in direction Y

Seismic bending moments in the columns for the final value of design spectral accelerations in X or Y:

- The horizontal seismic action component in direction X induces the following moments to any interior 2-bay frame in direction X, for bending within a vertical plane parallel to X (about the local y axis of the column, which is parallel to direction Y and normal to the vertical plane of the interior frame), without the effect of accidental eccentricity:

$$M_{\mathrm{Ec1,yX}} = V_{\mathrm{Ec,1X}} H_{\mathrm{cl}}/2 = (0.201 \times 3 \times 450/2) \times 2.5/2 = 169.6\,\mathrm{kNm}$$
$$M_{\mathrm{Ec3,yX}} = M_{\mathrm{Ec1,yX}}/2 = 169.6/2 = 84.8\,\mathrm{kNm}$$
$$M_{\mathrm{Ec2,yX}} = M_{\mathrm{Ec1,yX}}(V_{\mathrm{Ec,2X}}/V_{\mathrm{Ec,1X}}) = 169.6 \times 2.5/3 = 141.3\,\mathrm{kNm}$$
$$M_{\mathrm{Ec4,yX}} = M_{\mathrm{Ec2,yX}}/2 = 141.3/2 = 70.7\,\mathrm{kNm}.$$

  These values are not far from those obtained through an elastic analysis of the full structural system in 3D.
  Including the effect of the accidental eccentricity of the horizontal component in direction X (see (h) above), the seismic moments in the columns of the 1st interior 2-bay frame in direction X are:

$$M_{\mathrm{Ec1,yX}} = (1 + 0.148 y/r_{\mathrm{y}}) V_{\mathrm{Ec,1X}} H_{\mathrm{cl}}/2 = (1 + 0.148 \times 7.5/8.48) \times 169.6/2 = 191.8\,\mathrm{kNm}$$
$$M_{\mathrm{Ec3,yX}} = M_{\mathrm{Ec1,yX}}/2 = 191.8/2 = 95.9\,\mathrm{kNm}$$
$$M_{\mathrm{Ec2,yX}} = M_{\mathrm{Ec1,yX}}(V_{Ec,2X}/V_{Ec,1X}) = 191.8 \times 2.5/3 = 159.8\,\mathrm{kNm}$$
$$M_{\mathrm{Ec4,yX}} = M_{\mathrm{Ec2,yX}}/2 = 159.8/2 = 79.9\,\mathrm{kNm},$$

Because of the torsional response due to the accidental eccentricity these moments act concurrently with a bending moment component in the orthogonal direction of bending (about the local axis z of the column, which is parallel to direction X and to the vertical plane of the interior frame), equal to:

$$M_{\mathrm{Ec1,zX}} = (0.148x/r_x)[V_{\mathrm{Ec,1Y}} H_{\mathrm{cl}}/2] = 0$$
$$M_{\mathrm{Ec3,zX}} = (0.148x/r_x)[0.5V_{\mathrm{Ec,1Y}} H_{\mathrm{cl}}/2] = (0.148 \times 5/8.48) \times (0.2 \times 3 \times 450/4) \times 2.55/2 = 7.5\,\mathrm{kNm}$$
$$M_{\mathrm{Ec2,zX}} = M_{\mathrm{Ec1,zX}}(V_{\mathrm{Ec,2Y}}/V_{\mathrm{Ec,1Y}}) = 0$$
$$M_{\mathrm{Ec4,zX}} = M_{\mathrm{Ec3,zX}}(V_{\mathrm{Ec,2Y}}/V_{\mathrm{Ec,1Y}}) = 7.5 \times 2.5/3 = 6.2\,\mathrm{kNm}.$$

– The horizontal seismic action component in direction Y induces the following moments to the columns of the interior and exterior 5-bay frames in direction Y, for bending in a vertical plane parallel to Y (about the local z axis of the column, parallel to direction X and to the vertical plane of the interior frame), without the effect of accidental eccentricity:

$$M_{\mathrm{Ec1,zY}} = V_{\mathrm{Ec,1Y}} H_{\mathrm{cl}}/2 = (0.2 \times 3 \times 450/2) \times 2.5/2 = 168.75\,\mathrm{kNm}$$
$$M_{\mathrm{Ec3,zY}} = V_{\mathrm{Ec,3Y}} H_{\mathrm{cl}}/2 = (0.2 \times 3 \times 450/4) \times 2.55/2 = 86.1\,\mathrm{kNm}$$
$$M_{\mathrm{Ec2,zY}} = M_{\mathrm{Ec1,zY}}(V_{\mathrm{Ec,2Y}}/V_{\mathrm{Ec,1Y}}) = 168.75 \times 2.5/3 = 140.6\,\mathrm{kNm}$$
$$M_{\mathrm{Ec4,zY}} = M_{\mathrm{Ec3,zY}}(V_{\mathrm{Ec,2Y}}/V_{\mathrm{Ec,1Y}}) = 86.1 \times 2.5/3 = 74.2\,\mathrm{kNm}.$$

These values are close to those from an elastic analysis of the full structural system in 3D.
Including the effect of the accidental eccentricity of the horizontal component in direction Y:

$$M_{\mathrm{Ec1,zY}} = (1 + 0.059x/r_x)V_{\mathrm{Ec,1Y}} H_{\mathrm{cl}}/2 = 168.75\,\mathrm{kNm}$$
$$M_{\mathrm{Ec3,zY}} = (1 + 0.059x/r_x)V_{\mathrm{Ec,\,3Y}} H_{\mathrm{cl}}/2 = (1 + 0.059 \times 5/8.48) \times 86.1 = 89\,\mathrm{kNm}$$
$$M_{\mathrm{Ec2,zY}} = M_{\mathrm{Ec1,\,zY}}(V_{\mathrm{Ec,\,2Y}}/V_{\mathrm{Ec,\,1Y}}) = 168.75 \times 2.5/3 = 140.6\,\mathrm{kNm}$$
$$M_{\mathrm{Ec4,zY}} = M_{\mathrm{Ec3,zY}}(V_{\mathrm{Ec,2Y}}/V_{\mathrm{Ec,1Y}}) = 89 \times 2.5/3 = 74.2\,\mathrm{kNm}$$

Due to the torsion induced by the accidental eccentricity, these moments act concurrently with a moment component in the orthogonal direction of bending (about the column local axis y, parallel to direction Y and normal to the vertical plane of the interior frame), equal to:

$$M_{\mathrm{Ec1,yY}} = (0.059y/r_{\mathrm{y}})[V_{\mathrm{Ec,1X}}H_{\mathrm{cl}}/2] = (0.059 \times 7.5/8.48) \times (0.201 \times 3 \times 450/2) \times 2.5/2 = 8.8\,\mathrm{kNm}$$

$$M_{\mathrm{Ec3,yY}} = (0.059y/r_{\mathrm{y}})[V_{\mathrm{Ec,1X}}H_{\mathrm{cl}}/4] = (0.059 \times 7.5/8.48) \times (0.201 \times 3 \times 450/4) \times 2.5/2 = 4.4\,\mathrm{kNm}$$

$$M_{\mathrm{Ec2,yY}} = M_{\mathrm{Ec1,yY}}(V_{\mathrm{Ec,2X}}/V_{\mathrm{Ec,1X}}) = 8.8 \times 2.5/3 = 7.3\,\mathrm{kNm}$$

$$M_{\mathrm{Ec4,yY}} = M_{\mathrm{Ec3,yY}}(V_{\mathrm{Ec,2X}}/V_{\mathrm{Ec,1X}}) = 4.4 \times 2.5/3 = 3.7\,\mathrm{kNm}.$$

(m) Seismic axial forces in the columns of interior 2-bay frames in direction X and in interior columns of the 5-bay frames in direction Y

Seismic axial forces are induced in the columns of the interior 2-bay frames in direction X only by the horizontal component in direction X ($\mathrm{E_X}$) and still only in exterior columns. They are calculated from the seismic overturning moment at the level where the column seismic moment is zero (at storey mid-height):

– Overturning moment at the ground storey:

$$M_1 = (2.5H + h_{\mathrm{b}}/2)F_3 + (1.5H + h_{\mathrm{b}}/2)F_2 + (0.5H + h_{\mathrm{b}}/2)F_1 = (7.75 \times 1.5\,W + 4.75\,W + 1.75 \times 0.5\,W) \times 0.201 = 17.25 \times 450 \times 0.201 = 1560\,\mathrm{kNm}$$

– Overturning moment at the 2nd storey:

$$M_2 = 4.75F_3 + 1.75F_2 = (4.75 \times 1.5\,W + 1.75\,W) \times 0.201 = 802\,\mathrm{kNm}.$$

The exterior columns take the seismic overturning moment with a lever arm equal to their distance, $2L_{\mathrm{x}}$:

– Column C3 (ground storey): $N_{3,\mathrm{EX}} = 1560/(2 \times 5) = 156$ kN
– Column C4 (2nd storey): $N_{4,\mathrm{EX}} = 802/(2 \times 5) = 80.2$ kN.

No seismic axial forces are induced in the interior columns of the 5-bay frames in direction Y by the seismic action component in that direction ($\mathrm{E_Y}$).

The above values are close to the seismic axial forces from elastic analysis of the full structure in 3D.

(n) Combination of seismic action effects of the two horizontal components in columns

Table 5.4 gives the maximum effects of the individual horizontal components, as computed above for the columns, as well as the likely peak action effects of the two concurrent components, computed either applying Eq. (4.24), i.e., from Eqs. (4.38) and (4.39) in Section 4.7.2.4, or Eq. (4.25).

Table 5.4 Bending moment components and axial forces at the ends of the columns for simultaneous horizontal components of the seismic action, from the analysis

Seismic action component	Bending moment components (kNm) and axial force (kN)	C1	C3	C2	C4
E_X= X+acc. ecc.	$M_{y,X}$	191.7	95.9	159.8	79.9
e_x	$M_{z,X}$	0	7.5	0	6.2
	N_X	0	156	0	80.2
E_Y= Y+acc. ecc.	$M_{y,Y}$	8.8	4.4	7.3	3.7
e_y	$M_{z,Y}$	168.75	89	140.6	74.2
	N_Y	0	0	0	0
Eq. (4.24)	max $M_{y,SRSS\text{-}X\text{-}Y}$	191.9	96	160	80
$\sqrt{(E_X^2+E_Y^2)}$	$M_{z,SRSS\text{-}X\text{-}Y}$concurrent with max$M_{y,SRSS\text{-}X\text{-}Y}$	7.7	7.5	6.4	9.6
	$N_{SRSS\text{-}X\text{-}Y}$ concurrent with max M_y	0	155.8	0	80.1
	max $M_{z,SRSS\text{-}X\text{-}Y}$	168.75	89	140.6	74.5
	$M_{y,SRSS\text{-}X\text{-}Y}$ concurrent with max $M_{z,SRSS\text{-}X\text{-}Y}$	8.8	12.5	7.3	10.3
	$N_{SRSS\text{-}X\text{-}Y}$ concurrent with max $M_{z,SRSS\text{-}X\text{-}Y}$	0	13.1	0	6.7
Eq. (4.25)	$M_{y,X+0.3Y}$	194.3	97.2	162	81
E_X+0.3E_Y	$M_{z,X+0.3Y}$	50.6	26.7	49.7	28.5
	$N_{X+0.3Y}$	0	156	0	80.2
Eq. (4.25)	$M_{y,Y+0.3X}$	66.3	33.2	55.2	24.6
E_Y+0.3E_X	$M_{z,Y+0.3X}$	168.75	89	142.8	76.1
	$N_{Y+0.3X}$	0	46.8	0	24.1

When they are non-zero, the seismic axial forces are combined with those due to the concurrent gravity loads, G+ψ_2Q, to give the following extreme values of axial load.

- For G+ψ_2Q+SRSS in the combination that gives the likely maximum value of M_y:

  Column C3 (ground storey): min $N_{3,G+\psi 2Q+SRSS\text{-}X\text{-}Y}$ = 253.1–155.8=97.3 kN
  Column C4 (2nd storey): min $N_{4,G+\psi 2Q+SRSS\text{-}X\text{-}Y}$ = 168.8–80.1=88.7 kN
  Column C3 (ground storey): max $N_{3,G+\psi 2Q+SRSS\text{-}X\text{-}Y}$=253.1+155.8=408.9 kN
  Column C4 (2nd storey): max $N_{4,G+\psi 2Q+SRSS\text{-}X\text{-}Y}$ = 168.8+80.1=248.9 kN

- For G+ψ_2Q+SRSS in the combination that gives the likely maximum value of M_z:

  Column C3 (ground storey): min $N_{3,G+\psi 2Q+SRSS\text{-}X\text{-}Y}$=253.1–13.1=240 kN
  Column C4 (2nd storey): min $N_{4,G+\psi 2Q+SRSS\text{-}X\text{-}Y}$ =168.8–6.7=162.1 kN
  Column C3 (ground storey): max $N_{3,G+\psi 2Q+SRSS\text{-}X\text{-}Y}$=253.1+13.1=266.2 kN
  Column C4 (2nd storey): max $N_{4,G+\psi 2Q+SRSS\text{-}X\text{-}Y}$=168.8+6.7=175.5 kN

- For G+ψ_2Q+E_X+0.3E_Y, which gives the estimated likely maximum value of M_y:

  Column C3 (ground storey): min $N_{3,G+\psi 2Q+X+0.3Y}$ =253.1–156=97.1 kN
  Column C4 (2nd storey): min $N_{4,G+\psi 2Q+X+0.3Y}$ =168.8–80.2=88.6 kN

Column C3 (ground storey): max $N_{3,G+\psi 2Q+X+0.3Y}$ =253.1+156=409.1 kN
Column C4 (2nd storey): max $N_{4,G+\psi 2Q+X+0.3Y}$ =168.8+80.2=249 kN.

– For $G+\psi_2 Q+E_Y+0.3E_X$, which gives the estimated likely maximum value of M_z:
Column C3 (ground storey): min $N_{3,G+\psi 2Q+Y+0.3EX}$ =253.1–46.8=206.3 kN
Column C4 (2nd storey): min $N_{4,G+\psi 2Q+Y+0.3EX}$ =168.8–24.1=144.7 kN
Column C3 (ground storey): max $N_{3,G+\psi 2Q+Y+0.3EX}$ =253.1+46.8=299.9 kN
Column C4 (2nd storey): max $N_{4,G+\psi 2Q+Y+0.3EX}$ =168.8+24.1=192.9 kN.

Witness the slightly lower estimates of likely peak values of the various seismic action effects from the SRSS approach, Eq. (4.24), compared to the linear approximation in Eq. (4.25) and the significantly lower values of the other components concurrently acting with the maximum values. At least in the present case, the linear approximation, Eq. (4.25) is safe-sided.

In the dimensioning and verifications that follow, the results of the SRSS estimation will be used, as more accurate and more economic.

(o) Design bending moments in the beams for the final value of the design spectral acceleration

Beams B1 of 1st interior 2-bay frame (at distance y =7.5 m from centre of mass) in direction X.

– Beam section at the support on C1:

$$M_{\gamma^{gG}+\gamma^{qQ}} = 35 \times 4.625^2/8 = 93.6\,\text{kNm},$$
$$M_{g+\psi 2q} = (20/35) \times 93.6 = 53.5\,\text{kNm}$$

– Hogging design moment for the top reinforcement:

$$M_{d1} = \max[M_{\gamma^{gG}+\gamma^{qQ}}; M_{g+\psi 2q} + (|\max M_{Ec1,y}| + |\max M_{Ec2,y}|)/2]$$
$$= \max[93.6; 53.5 + (191.9 + 160)/2] = 229.5\,\text{kNm}$$

– Sagging design moment for the bottom reinforcement:

$$M_{d2} = (191.9 + 160)/2 - 53.5 = 122.5\,\text{kNm}$$

– Beam section at the support on C3:
– Sagging and hogging design moments, for the top and bottom reinforcement:

$$M_d = 96 + 80 = 176\,\text{kNm}.$$

Interior spans of interior 5-bay frame in direction Y (at distance x =0 from centre of mass).

– Beam sections at the support by interior columns:

$$M_{\gamma^{gG}+\gamma^{qQ}} = (q_d/9 - g/36)L_{cl}^2 = (35/9 - 18/36) \times 4.6^2 = 71.7\,\text{kNm},$$
$$M_{g+\psi 2q} = 20 \times 4.6^2/12 = 35.3\,\text{kNm}$$

– Hogging design moment for the top reinforcement:

$$M_{d1} = \max[M_{\gamma^{gG}+\gamma^{qQ}};\ M_{g+\psi 2q} + (|\max M_{Ec1,z}| + |\max M_{Ec2,z}|)/2]$$
$$= \max[71.7; 35.3 + (168.75 + 140.6)/2] = 190\,\text{kNm}$$

– Sagging design moment for the bottom reinforcement:

$$M_{d2} = (168.75 + 140.6)/2 - 35.3 = 119.4\,\text{kNm}$$

Interior spans of exterior 5-bay frames in direction Y (at distance $x = 5$ m from centre of mass).

– Beam sections at the support on columns:

$$M_{\gamma^{gG}+\gamma^{qQ}} = (q_d/9 - g/36)L_{cl}^2 = (24/9 - 14/36) \times 4.65^2 = 49.3\,\text{kNm},$$
$$M_{g+\psi 2q} = 15 \times 4.65^2/12 = 27\,\text{kNm}$$

– Hogging design moment for the top reinforcement:

$$M_{d1} = \max[M_{\gamma^{gG}+\gamma^{qG}}; M_{g+\psi 2q} + (|\max M_{Ec3,z}| + |\max M_{Ec4,z}|)/2]$$
$$= \max[49.3; 27 + (89 + 74.5)/2] = 108.8\,\text{kNm}$$

– Sagging design moment for the bottom reinforcement:

$$M_{d2} = (89 + 74.5)/2 - 27 = 54.8\,\text{kNm}.$$

The approximate values above for the beam moments due to gravity loads, $g+\psi_2 q$, are derived with the beams considered as continuous, supported on columns not exerting any rotational restraint (simple supports). They are not far from the values obtained via an elastic analysis of the full structure in 3D.

(p) Beam longitudinal reinforcement (as $A_s = M_d/zf_{yd}$, with $z = d - d_1$):
From Eq. (5.3): $\rho_{min} = 0.5f_{ctm}/f_{yk} = 0.5 \times 2.9/500 = 0.0029$
Maximum diameter of bars, d_{bL}:
Beams B1 of 1st interior 2-bay frame in direction X at the support on the exterior column:
From Eq. (5.10b) with $\nu_d = \min(\min N_{3,X}, \min N_{4,X})/(0.35^2 \times 20000)) = 0.03935$:

$$d_{bL}/h_{c,ext} \le 7.5 \times 1.0315 \times 2.9/(1 \times 500/1.15) = 0.0516,\ d_{bL} \le 18\,\text{mm}$$

Interior beams (B1 of interior 2-bay frames in direction X or interior spans of interior 5-bay frame in direction Y) at the support on the central column:

From Eq. (5.10a) with ν_d=min($N_{1,g+\psi 2q}$, $N_{2,g+\psi 2q}$)/($0.4^2 \times 20000$)=0.176.

$$\text{If } \rho' = 0.5\rho_{max} : d_{bL}/h_{c,int} \leq 7.5 \times 1.141 \times 2.9/(500/1.15)/1.25$$
$$= 0.0457,\ d_{bL} \leq 18\,\text{mm}$$

Interior spans of exterior 5-bay frames in direction Y, at the support on the exterior column:

From Eq. (5.10a) with ν_d=min($N_{3,Y}$, $N_{4,Y}$)/($0.35^2 \times 20000$)=0.06.

$$\text{If } \rho' = 0.5\rho_{max} : d_{bL}/h_{c,ext} \leq 7.5 \times 1.048 \times 2.9/(500/1.15)/1.25$$
$$= 0.0524,\ d_{bL} \leq 18\,\text{mm}$$

Dimensioning of beam B1 of interior 2-bay frames in direction X:

$$d = 0.46\,\text{m},\ z = 0.46 - 0.04 = 0.42\,\text{m},\ A_{s,min} = 0.0029 \times 300 \times 460$$
$$= 400\,\text{mm}^2 (2\Phi 16 - 402\,\text{mm}^2)$$

Longitudinal reinforcement at the support on C1:

- Top reinforcement: $A_{s1} = M_d/zf_{yd} = 229.5 \times 10^3/(0.42 \times 500/1.15)$= 1257 mm^2: 5Φ16+1Φ18 (1260 mm^2), ρ =1257/(460 × 300)=0.0091
- Bottom reinforcement: A_{s2} =M_d/zf_{yd}=122.5 × 1257/229.5=671 mm^2: 4Φ16 (804 mm^2> 1260/2=630 mm^2), ρ '=804/(460 × 300)=0.0058,

From Eq. (5.4b): ρ_{max}=ρ'+$0.0018 f_{cd}/(\mu_\varphi \varepsilon_{yd} f_{yd})$=0.0058+0.0018 × 20/(6.8 × 0.00217 × 500/1.15)= 0.0114, $\rho_{max} > \rho$ =0.0091

$$M_{Rb}{}^- = 1260 \times 0.42 \times (500/1.15)/10^3 = 230\,\text{kNm},\ M_{Rb}{}^+ = 802 \times 0.42 \times$$
$$(500/1.15)/10^3 = 146.5\,\text{kNm}$$

Longitudinal reinforcement at the support on C3:

- Top and bottom reinforcement: A_{s1}=A_{s2}=176 × 1257/229.5=964 mm^2: 5Φ16 (1005 mm^2)> $A_{s,min}$=400 mm^2

$$M_{Rb}{}^+ = M_{Rb}{}^- = 1005 \times 0.42 \times 500/1.15/10^3 = 183.5\,\text{kNm}$$

Dimensioning of interior beams of interior 5-bay frame in direction Y:

$$d = 0.46\,\text{m},\ z = 0.46 - 0.04 = 0.42\,\text{m},\ A_{s,\,min} = 0.0029 \times 300 \times 460$$
$$= 400\,\text{mm}^2 (2\Phi 16 - 402\,\text{mm}^2).$$

- Top reinforcement: A_{s1}=190 × 10^3/(0.42 × 500/1.15)=1040 mm^2: 4Φ16+1Φ18 (1058 mm^2), ρ =1058/(460 × 300)=0.0077
- Bottom reinforcement: A_{s2}=119.4 × 1040/190=654 mm^2: 2Φ16+1Φ18 (656 mm^2 >1058/2 =529 mm^2), ρ '=656/(460 × 300)=0.0048,

$$\begin{aligned}\rho_{max} &= 0.0048 + 0.0018 \times 20/(6.8 \times 0.00217 \times 500/1.15)\\ &= 0.0104 > \rho = 0.0077.\\ M_{Rb}{}^{-} &= 1058 \times 0.42 \times (500/1.15)/10^3 = 193.3\,\text{kNm},\ M_{Rb}{}^{+}\\ &= 656 \times 0.42 \times (500/1.15)/10^3 = 119.8\,\text{kNm}.\end{aligned}$$

Dimensioning of interior beams of exterior 5-bay frames in direction Y:

$$d = 0.41\,\text{m},\ z = 0.41 - 0.04 = 0.37\,\text{m},\ A_{s,min} = 0.0029 \times 300 \times 370 = 322\,mm^2 (2\Phi16 - 402\,mm^2).$$

- Top reinforcement: A_{s1}=108.8 × 10^3/(0.37 × 500/1.15)=676 mm^2: 4Φ16 (804 mm^2), ρ = 804/(410 × 300)=0.0065
- Bottom reinforcement: A_{s2}=54.8 × 676/108.8=340 mm^2: 2Φ16 (402 mm^2 = 804/2 = 402 mm^2), ρ '=402/(410 × 300)=0.0033,

$$\begin{aligned}\rho_{max} &= 0.0033 + 0.0018 \times 20/(6.8 \times 0.00217 \times 500/1.15)\\ &= 0.0089 > \rho = 0.0065.\\ M_{Rb}{}^{-} &= 804 \times 0.37 \times (500/1.15)/10^3 = 129.5 \quad \text{kNm},\\ M_{Rb}^{+} &= 402 \times 0.42 \times (500/1.15)/10^3 = 64.8\,\text{kNm}.\end{aligned}$$

(q) Dimensioning of columns and capacity design check in flexure

The likely peak values of the column bending moments from the analysis are listed in Table 5.5 along with the likely concurrent axial force and bending moment in the orthogonal direction of bending. The table lists also the required moment resistance of the columns to fulfill Eq. (1.4), with the value of $\Sigma M_{Rc} > 1.3 \times \Sigma M_{Rb}$ split between the column sections above and below the joint (e.g., top section of C1 and base section of C2). If the axial load is somewhat smaller at the column section above the joint than below, it is assumed that the section below the joint has about 10% more required moment resistance than the section above for the same amount of required vertical reinforcement at these two sections.

- At the joint at the top of C1 and the base of C2:
  - For bending within a vertical plane parallel to X (about the local axis y of the column, which is parallel to direction Y and normal to the vertical plane of the interior frame):

$$\Sigma M_{Rc,y} > 1.3 \times \Sigma M_{Rb} = 1.3 \times (230 + 146.5) = 489.5\,\text{kNm}$$

Table 5.5 Bending moments and axial forces at column ends for column dimensioning – including capacity design, Eq. (1.4)

	Bending moments and axial force for column dimensioning	Top of C1	Base of C2	Top of C3	Base of C4
Bending moments (kNm) and axial force (kN) from the analysis for $G+\psi_2 Q+$(SRSS of E_X, E_Y)	max M_y	191.9	160	96	80
	M_z concurrent with maxM_y	7.7	6.4	7.5	9.6
	min$N$ concurrent with maxM_y	843.8	562.5	97.3	88.7
	max M_z	168.75	140.6	89	74.5
	M_y concurrent with max M_z	8.8	7.3	12.5	10.3
	min N concurrent with max M_z	843.8	562.5	240	162.1
Moment resistance for capacity design. Upper and lower column share $\Sigma M_{Rc} > 1.3 \times \Sigma M_{Rb}$ depending on their axial force N: – Equally, if N's ~same; – Otherwise, lower column takes ~10% more than upper one.	$M_{Rc,y} \geq$	*257*	*232.5*	*119.3*	*119.3*
	M_z concurrent with $M_{Rc,y}$	*0*	*0*	*0*	*0*
	N concurrent with $M_{Rc,y}$: min N_{EX}	*843.8*	*562.5*	*97.3*	*88.7*
	$M_{Rc,z} \geq$	213.7	193.3	132.6	120
	M_y concurrent with $M_{Rc,z}$	0	0	0	0
	N concurrent with $M_{Rc,z}$: min N_{EY}	843.8	562.5	240	162.8

– For bending within a vertical plane parallel to Y (about the local axis z of the column, which is parallel to direction X and to the vertical plane of the interior frame):

$$\Sigma M_{Rc,z} > 1.3 \times \Sigma M_{Rb} = 1.3 \times (193.3 + 119.8) = 407\,\text{kNm}.$$

– At the joint at the top of C3 and the base of C4:

– For bending within a vertical plane parallel to X (about the local axis y of the column, which is parallel to direction Y and normal to the vertical plane of the interior frame):

$$\Sigma M_{Rc,y} > 1.3 \times \Sigma M_{Rb} = 1.3 \times 183.5 = 238.6\,\text{kNm}.$$

– For bending within a vertical plane parallel to Y (about the local axis z of the column, which is parallel to direction X and to the vertical plane of the interior frame):

$$\Sigma M_{Rc,z} > 1.3 \times \Sigma M_{Rb} = 1.3 \times (129.5 + 64.8) = 252.6\,\text{kNm}$$

The capacity design rule turns out to be more demanding for the moment resistance of the column than the seismic moments from the analysis, despite the fact that the latter are biaxial. The larger of the two biaxial bending moments from the

analysis exceeds the smaller of the two so much, that the latter is almost insignificant for the dimensioning of the column. Moreover, at least in this case, the Eurocode 8 rule that allows neglecting biaxial bending if dimensioning is done uniaxially for a bending moment equal to the larger of the two biaxial ones divided by 0.7, gives about the same requirements for moment resistance of the column as the capacity design rule. Note also that the column axial forces considered in the capacity design rule verification are the most safe-sided ones for it, notably the minimum N for the direction of the seismic action that causes beam plastic hinging within the pertinent plane of bending.

On the basis of the above and the fact that columns are square and face similar moment demands in the two transverse directions y and z (hence, they can have the same amount of reinforcement in the two pairs of opposite sides), it suffices to dimension them only for the combinations of bending moments and axial force shown in italics in Table 5.5 (arising from the capacity design rule within a plane of bending parallel to direction X).

For columns C1 and C2 (d_1/h =40/400=0.1): Axial forces and moments normalised to bhf_{cd} and $bh\,^2f_{cd}$:

- Column C1: ν_{d1}=843.8/(0.4^2 × 20000)=0.264, μ_{d1}=257/(0.4^3 × 20000)= 0.201, giving total mechanical ratio of vertical reinforcement, uniformly distributed along the perimeter of the section: ω_{tot} ~0.46.
- Column C2: ν_{d2}=562.5/(0.4^2 × 20000)=0.176, μ_{d2}=232.5/(0.4^3 × 20000)= 0.182, giving ω_{tot} ~0.40.
  We use ω_{tot}~0.43, giving $A_{s,tot}$=0.43 × 400^2 × 20/(500/1.15)=3165 mm^2. We place 16Φ16 (3216 mm^2), i.e. 5Φ16 per side, giving: ρ=3216/(400 × 400)= 0.0201>ρ_{min}=0.01. The same reinforcement is placed at the bottom of C1 (at the connection to the foundation).

For columns C3 and C4 (d_1/h =40/360=0.11): Axial forces and moments normalised to bhf_{cd} and $bh\,^2f_{cd}$

- ν_d=0.5 × (97.3+88.7)/(0.35^2 × 20000)=0.038, μ_d=119.3/(0.35^3 × 20000)= 0.139, giving total mechanical ratio of vertical reinforcement, uniformly distributed along the perimeter of the section: ω_{tot} ~0.34,
  $A_{s,tot}$=0.34 × 350^2 × 20/(500/1.15)=1916 mm^2. We choose 8Φ18, i.e., 3Φ18 along each side (2036 mm^2), giving ρ =2036/(350 × 350)=0.0166> ρ_{min}=0.01. The same reinforcement is placed at the base of C3 (at the connection to the foundation).

The resulting moment resistance of the columns for the maximum and the minimum value of their axial force are calculated next on the basis of Sections 3.2.2.4 and 3.2.2.5:

- Columns C1, C2:
  ω_1=ω_2=0.25 × 3216/(400 × 360) × (500/1.15)/20=0.1214, ω_v=2ω_1=0.2428, δ_1=40/360=1/9, satisfying Eq. (3.50a): δ_1< 0.235.
  The axial load of both columns is always equal to that due to gravity loads alone:
  - for C1: ν =0.8438/(0.4 × 0.36 × 20)=0.293,
  - for C2: ν =0.5625/(0.4 × 0.36 × 20)=0.195.

Eq. (3.52) is met: $0.094 \leq \nu_d \leq 0.533$ at both columns; so from Eqs. (3.52) and (3.60):

- Column C1: $\xi = 0.440$, $M_{Rc1,y} = M_{Rc1,z} = 0.2645 \times 0.4 \times 0.36^2 \times 20000 = 274$ kNm;
- Column C2: $\xi = 0.368$, $M_{Rc2,y} = M_{Rc2,z} = 0.2225 \times 0.4 \times 0.36^2 \times 20000 = 231$ kNm.

  - For bending within a vertical plane parallel to X (about the local axis y of the column, which is parallel to direction Y and normal to the vertical plane of the interior frame):

$$\Sigma M_{Rc,y} = 274 + 231 = 505\,\text{kNm} >$$
$$1.3 \times \Sigma M_{Rb} = 1.3 \times (230 + 146.5) = 489.5\,\text{kNm}.$$

  - For bending within a vertical plane parallel to Y (about the local axis z of the column, which is parallel to direction X and to the vertical plane of the interior frame):

$$\Sigma M_{Rc,z} = 274 + 231 = 505\text{kNm} >$$
$$1.3 \times \Sigma M_{Rb} = 1.3 \times (193.3 + 119.8) = 407\,\text{kNm}.$$

- Columns C3, C4:
  $\omega_1 = \omega_2 = 0.25 \times 2036/(350 \times 308) \times (500/1.15)/20 = 0.1026$, $\omega_v = 2\omega_1 = 0.2053$, $\delta_1 = 42/308 = 0.136$, and Eq. (3.52) above on ν_d is: $0.191 \leq \nu_d \leq 0.523$.

  The axial load of both columns depends on the direction of bending.

- For bending within a vertical plane parallel to X (about the local axis y of the column, which is parallel to direction Y and normal to the vertical plane of the interior frame):

  - min $N_3 \sim \text{min}N_4 \sim (97.3+88.7)/2 = 93$ kN, $\nu_d = 0.093/(0.35 \times 0.308 \times 20) = 0.0431$.
    ν_d is less than the limit value $\nu_{c,y2}$ defined at the left-hand-side of Eq. (3.51): $\nu_d \leq 0.191$. Then from Eq. (3.54): $\xi = 0.2611$ and from Eq. (3.59): $\text{min}M_{Rc3,y} = \text{min}M_{Rc4,y} = 0.1816 \times 0.35 \times 0.308^2 \times 20000 = 120.6$ kNm;

$$\Sigma M_{Rc,y} = 241.2\,\text{kNm} > 1.3 \times \Sigma M_{Rb} = 238.6\,\text{kNm}$$

  - max $N_3 = 408.9$ kN, $\nu_d = 0.4089/(0.35 \times 0.308 \times 20) = 0.19$.
    Eq. (3.52) gives: $0.191 \leq \nu_d \leq 0.523$ and is marginally not met. Then from Eq. (3.54): $\xi = 0.358$ and from Eq. (3.59): $\text{max}M_{Rc3,y} = 0.22 \times 0.35 \times 0.308^2 \times 20000 = 146$ kNm;
  - max $N_4 = 249$ kN, $\nu_d = 0.249/(0.35 \times 0.308 \times 20) = 0.115$.

ν_d is less than the limit value $\nu_{c,y2}$ defined at the left-hand-side of Eq. (3.51): $\nu_d \leq 0.191$. Then from Eq. (3.54): $\xi = 0.28$ and from Eq. (3.59): $\max M_{Rc4,y} = 0.190 \times 0.35 \times 0.308^2 \times 20000 = 126.5$ kNm.

- For bending within a vertical plane parallel to Y (about the local axis z of the column, parallel to direction X and to the vertical plane of the interior frame), the axial force from the analysis varies little. As the cross-section is square and its reinforcement is equally shared by the two pairs of opposite sides, the moment resistance is the same for bending within vertical planes parallel or normal to direction X: $M_{Rc,y} = M_{Rc,z}$. Therefore, the calculation of $M_{Rc,z}$ for the limited variation of the column axial force for bending within a vertical plane parallel to Y is based on linear interpolation between the values of $M_{Rc,y}$ computed above for the range of variation of the column axial force for bending within a vertical plane parallel to X (namely: $M_{Rc,y} = 120.6$ kNm for $N = 92.9$ kN, $M_{Rc,y} = 126.5$ kNm for $N = 249$ kN and $M_{Rc,y} = 146$ kNm for $N = 408.9$ kN).
  - for $\min N_3 = 240$ kN, $\min M_{Rc3,z} = 126.2$ kNm and for $\min N_4 = 162.8$ kN, $\min M_{Rc4,z} = 123.3$ kNm. $\Sigma M_{Rc,z} = 123.3 + 126.2 = 249.5$ kNm $\approx 1.3 \times \Sigma M_{Rb} = 252.6$ kNm.
  - for $\max N_3 = 266.2$ kN, $\max M_{Rc3,z} = 128.6$ kNm.
  - for $\max N_4 = 174.8$ kN, $\max M_{Rc4,z} = 123.7$ kNm.

(r) Design of transverse reinforcement of interior beams (with capacity design in shear)

As $\Sigma M_{Rc} > 1.3 \times \Sigma M_{Rb}$ at any beam-column joint of the beams of interest, the capacity design shear of all three types of interior beams is found considering plastic hinges at both beam ends.

According to Eurocode 2, calculation of shear reinforcement may start at a distance d from the face of the support. Besides, within segments of the beam of length $z \cot \delta = 0.9d \cot \delta$, the shear reinforcement may be constant and equal to that calculated from the minimum design shear force, V_{Ed}, in the segment. According to Eurocode 8, in "critical regions" of DC M beams, i.e., up to a distance h from the face of the support on a column, the maximum stirrup spacing is $\max s_w = \min\{8d_{bL}; h/4; 24d_{bw}; 225 \text{ mm}\}$ with d_{bL}: longitudinal bar diameter and d_{bw}: stirrup diameter (see Table 5.1). This is less than the maximum stirrup spacing of $0.75d$ applying outside "critical regions" according to Eurocode 2. So, the stirrups in a "critical region" are calculated from the design shear force at a distance h from that support.

Beam B1 of interior 2-bay frames in direction X:

- Capacity design seismic shear for the part of the beam closer to the support on column C1:

$$V_{CD,1} = (230 + 183.5)/4.625 = 89.4\,\text{kN}$$

- Capacity design seismic shear for the part of the beam closer to the support on column C3:

$$V_{CD,3} = (146.5 + 183.5)/4.625 = 71.4\,\text{kN}$$

– Shear verification at the end section at the support on column C1 (x =0):
For the factored gravity loads (persistent and transient design situation) γ_gG+γ_qQ:

$$V_{Ed}(0) = 35 \times 4.625/2 = 80.94\,\text{kN}$$

For the seismic action and concurrent gravity loads, G+ψ_2Q+E:

$$V_{Ed}(0) = V_{CD,1} + 20 \times 4.625/2 = 135.65\,\text{kN}$$

The shear resistance at the face of the support for shear compression in the web is according to Eurocode 2 (see Table 5.1):

$$V_{Rd,max} = 0.3(1 - f_{ck}(\text{MPa})/250)b_w z f_{cd} \sin 2\delta \text{ with } 1 \leq \cot\delta \leq 2.5.$$

$V_{Rd,max} = 0.3 \times (1-30/250) \times 0.3 \times 0.9 \times 0.46 \times 20000 \sin 2\delta = 655.8 \sin 2\delta$
$\geq V_{Ed}(0) = 135.65\,\text{kN} \rightarrow$
$\sin 2\delta > 0.207 \rightarrow \delta > 6^\circ$. OK if $\cot\delta = 2.5$, i.e. $\delta = 21.8^\circ$
over the length of the beam closer to column C1.

– Shear verification at the end section at the support on column C3 (x =4.625 m):

$V_{CD,3} = (146.5 + 183.5)/4.625 = 71.4\,\text{kN} < V_{CD,1} = 89.4\,\text{kN} \rightarrow$ OK if $\cot\delta = 2.5$, i.e.
$\delta = 21.8^\circ$over the length of the beam closer to column C3.

– Shear reinforcement in the "critical regions" of the beam next to the column faces:
Design shear force at a distance h =0.5 m from the support on column C1:

$$V_{Ed}(0.5\,\text{m}) = V_{CD,1} + 20 \times (4.625/2 - 0.5) = 125.65\,\text{kN}$$

For $V_{Rd,s}$=$b_w z \rho_w f_{ywd}$ cot δ=0.3 × 0.9 × 0.46 × (500000/1.15) × 2.5ρ_w= 135000ρ_w>125.65 kN → ρ_w> 0.000931, i.e. slightly over the minimum stirrup ratio required by Eurocode 2: min ρ_w=0.08f_{ck}(MPa)/f_{yk}(MPa)= 0.000876. In the present case: d_{bL} =16 mm, d_{bw} = 8 mm and max s_w=128 mm. So, 8 mm-diameter stirrups at 125 mm centres are chosen for the "critical region" next to column C1, giving ρ_w=2 × 50.25/(125 × 300)= 0.00268>0.000931. According to Eurocode 8, the 1st stirrup is not further than 50 mm from the face of the column; so the five 8 mm-dia. stirrups @ 125 mm centres extend up to 550 mm from the face of column C1.

As $V_{CD,1} > V_{CD,3}$, similar stirrup reinforcement (8 mm stirrups @ 125 mm centres) suffices in the "critical region" next to column C3 as well.

- Shear reinforcement between the "critical regions" at the two ends of the beam: The length of the beam outside the "critical regions" is: 4.625–2 × 0.55=3.525 m. There, the maximum stirrup spacing according to Eurocode 2 is $0.75d$ =0.75 × 460=345 mm. Ten 8 mm-dia. stirrups @ 320 mm centres cover that length, giving ρ_w=2 × 50.25/(320 × 300)=0.00105> minρ_w =0.000876 and providing shear resistance: $V_{Rd,s}$= 135000ρ_w=137 kN that exceeds the maximum design shear V_{Ed}(0.5 m)=125.65 kN at the end of the "critical regions". As a matter of fact, the stirrups there may be dimensioned for the design shear at a distance z cot δ=0.9d cot δ=0.9 × 0.46 × 2.5=1.035 m from the end of the "critical regions":

$$V_{Ed}(1.585\,\text{m}) = V_{CD,1} + 20 \times (4.625/2 - 1.585) = 104\,\text{kN}.$$

Interior beams of interior 5-bay frame in direction Y:

- Capacity design seismic shear:
  Because both ends of the beam have the same longitudinal reinforcement, there is no difference in the shear design of the two halves of the beam length. So:

$$V_{CD} = (193.3 + 119.8)/4.6 = 68.1\,\text{kN}.$$

- At the end section at face of column C1 (x =0):
  For the factored gravity loads (persistent and transient design situation), γ_gG+γ_qQ:

$$V_{Ed}(0) = 35 \times 4.6/2 = 80.5\,\text{kN}$$

  For the seismic action and concurrent gravity loads, G+ψ_2Q+E:

$$V_{Ed}(0) = V_{CD} + 20 \times 4.6/2 = 114.1\,\text{kN}.$$

  As the beam has the same cross-section as beam B1 of the interior 2-bay frames in direction X and the seismic design shear is smaller, the shear verification for shear compression in the web according to Eurocode 2 is met also for this beam with cot δ=2.5.
- Shear reinforcement in the "critical regions" of the beam and between them:
  As the beam cross-sectional dimensions are the same as in beam B1 of the interior 2-bay frames in direction X while the seismic design shear is smaller, the same transverse reinforcement is placed as in beam B1:
  - up to 540 mm from the face of each column: five 8 mm-dia. stirrups @ 125 mm centres, with the 1st one at 40 mm from the face of the column;
  - over the 3.52 m-long rest of the beam: ten 8 mm-dia. stirrups @ 320 mm centres.

Interior beams of exterior 5-bay frames in direction Y:

– Capacity design seismic shear:
Because both ends of the beam have the same longitudinal reinforcement, there is no difference in the shear design of the two halves of the beam length. So:

$$V_{CD} = (129.5 + 64.8)/4.65 = 41.8\,\text{kN}.$$

– Shear verification at the end section at face of columns C3 (x=0):
For the factored gravity loads (persistent and transient design situation), γ_gG+γ_qQ:

$$V_{Ed}(0) = 24 \times 4.65/2 = 55.8\,\text{kN}.$$

For the seismic action and concurrent gravity loads, G+ψ_2Q+E:

$$V_{Ed}(0) = V_{CD} + 15 \times 4.65/2 = 76.7\,\text{kN}.$$

$$V_{Rd,max} = 0.3 \times (1 - 30/250) \times 0.3 \times 0.9 \times 0.41 \times 20000 \sin 2\delta$$
$$= 584.5 \sin 2\delta > V_{Ed}(0) = 76.7\,\text{kN} \rightarrow \sin 2\delta > 0.1312 \rightarrow \delta \geq 3.8^\circ.$$

OK if $\cot\delta = 2.5$, i.e. $\delta = 21.8^\circ$ over the entire beam.

– Shear reinforcement in the "critical regions" of the beam and between them: The stirrups in the "critical region", i.e., up to a distance h=0.45 m from the face of the support on column C3, are calculated on the basis of the design shear force at distance h=0.45 m to that support:

$$V_{Ed}(0.45\,\text{m}) = V_{CD} + 15 \times (4.65/2 - 0.45) = 69.9\,\text{kN}$$

For $V_{Rd,s} = b_w z \rho_w f_{ywd} \cot\delta$=0.3 × 0.9 × 0.41 × (500000/1.15) × 2.5ρ_w = 120325ρ_w >69.9 kN → ρ_w> 0.000581, less than the minimum stirrup ratio in Eurocode 2: minρ_w= 0.000876.
Also in this beam max s_w=128 mm; so, 8 mm-dia. stirrups at 125 mm centres in the "critical region" next to the columns, give ρ_w=2 × 50.25/(125 × 300)=0.00268> minρ_w=0.000876.
The maximum stirrup spacing according to Eurocode 2: 0.75d=0.75 × 410= 307.5 mm applies outside the "critical regions". Eleven 8 mm-dia. stirrups @ 300 mm centres cover a length of 12 × 0.3=3.6 m between the "critical regions", giving ρ_w=2 × 50.25/(300 × 300)=0.00112> minρ_w=0.000876 and providing shear resistance: $V_{Rd,s}$= 120325ρ_w=134.4 kN exceeding the maximum design shear V_{Ed}(0.45 m)=69.9 k N between the "critical regions". So, the shear reinforcement in the interior beams of the two exterior 5-bay frames in direction Y is:

- up to 525 mm from the face of each column: five 8 mm-dia. stirrups @ 125 mm centres, with the 1st one at 25 mm from the face of the column;
- over the 3.6 m-long rest of the beam: Eleven 8 mm-dia. stirrups @ 300 mm centres.

(s) Design of transverse reinforcement of the columns (with capacity design in shear)

As the columns are square, the maximum capacity design shear in the two horizontal directions is used for the dimensioning of their transverse reinforcement.

Because the columns were designed so that $\Sigma M_{\mathrm{Rc}} > 1.3 \times \Sigma M_{\mathrm{Rb}}$ at any beam-column joint of the ground floor, the capacity design shear of the columns is computed considering plastic hinging in the beams at the top and in the column at the connection to the foundation. In this calculation the value of the column moment at the face of a beam-column joint (here at the top of the column) is essentially independent of the columns' axial force, as it is proportional to $M_{\mathrm{Rc,i}}/\Sigma M_{\mathrm{Rc}}$. However, in the same calculation the column moment resistance at the base depends on the column axial force, increasing with increasing axial force, as does the column shear resistance. Therefore, wherever the value of the column axial force changes with the sense of action of the lateral loading, the column capacity design shear is calculated and checked against the corresponding shear resistance both for the maximum and for the minimum values of the column axial force.

According to Eurocode 8 and Table 5.2, in "critical regions" of DC M columns, i.e., up to a distance $\max\{h_{\mathrm{c}}; b_{\mathrm{c}}; 0.45\ \mathrm{m}, H_{\mathrm{cl}}/5\}$ from the end sections of the column (h_{c}, b_{c}: cross-sectional dimensions, H_{cl}: clear height of the column), the maximum stirrup spacing is $\max s_{\mathrm{w}} = \min\{8d_{\mathrm{bL}}; b_{\mathrm{o}}; 175\ \mathrm{mm}\}$ (d_{bL} : vertical bar diameter, b_{o}: minimum dimension of confined core). Outside the "critical regions", the maximum stirrup spacing in Eurocode 2 applies: $\max s_{\mathrm{w}} = \min\{20d_{\mathrm{bL}}; h_{\mathrm{c}}; b_{\mathrm{c}}; 400\ \mathrm{mm}\}$, or $0.6\ \min\{20d_{\mathrm{bL}}; h_{\mathrm{c}}; b_{\mathrm{c}}; 400\ \mathrm{mm}\}$, if vertical bars are lap-spliced there (as is commonly the case).

According to Eurocode 8, along the perimeter of DC M columns vertical bars laterally restrained by a stirrup corner or cross-tie should not be further apart than 200 mm. The implication for the present columns is that the vertical bar at the centre of each side should be laterally restrained. This can be achieved either:

- with two interior cross-ties, each extending from one side of the section to the opposite and engaging the two vertical bars at the centre of the two sides, or
- with a single internal diamond-shaped tie engaging all four central bars of the four sides.

The 2nd option is adopted here. The diamond-shaped internal tie, with cross-sectional area A_{sw}, contributes to the shear reinforcement in each direction with cross-sectional area $A_{\mathrm{sw}}\sqrt{2}$.

According to Eurocode 8 the "critical region" at the base (i.e., at the connection to the foundation) of DC M columns meeting the weak beam/strong column capacity design rule should have volumetric mechanical ratio of confinement reinforcement $\omega_{\mathrm{wd}} \geq 0.08$, as well as such that Eq. (5.8) is met with $\omega_{\mathrm{vd}} = 0$: $a\omega_{\mathrm{wd}} \geq$

$30\mu_\varphi \nu_d \varepsilon_{yd} b_c/b_o$–0.035. For rectangular hoops with n_b or n_h vertical bars laterally restrained by a stirrup corner or cross-tie along the side of the core with length b_o or h_o, respectively, the "confinement effectiveness" factor is a=(1–0.5s_w/b_o) (1–0.5s_w/h_o)[1–{b_o/((n_b–1)h_o)+h_o/((n_h–1)b_o)}/3].

Column C1:

– Confinement reinforcement in the "critical region" at the base of the column:
For confinement reinforcement consisting of a perimeter hoop and a diamond-shaped internal tie around the central bars of the sides:

$$\omega_{wd}=A_{sw}[2(b_o+h_o)+\sqrt{2}(b_o^2+h_o^2)]/(b_o h_o s_w) f_{yd}/f_{cd}$$
$$=2A_{sw}[2+\sqrt{2}]/(b_o s_w) f_{yd}/f_{cd}, \text{ if } b_o = h_o.$$

$$a=(1-0.5s_w/b_o)(1-0.5s_w/h_o)[1-\{b_o/((n_b-1)h_o)+h_o/((n_h-1)b_o)\}/3]$$
$$=(1-0.5s_w/b_o)^2/1.5, \text{ if } \quad n_b = n_h = 3 \text{ and } b_o = h_o.$$

$$\text{For } \nu_d = 843.8/(0.42 \times 20000) = 0.264:$$

$$a\,\omega_{wd} \geq 30\mu_\phi \nu_d\, \varepsilon_{yd} b_c/b_o - 0.035 = 30 \times 6.8 \times 0.264 \times 0.00217 \times 0.4/$$
$$(0.4 - 2 \times 0.029) - 0.035 = 0.102 \rightarrow s_w \leq 103 \text{ mm for 8 mm-dia. hoops.}$$
$$\omega_{wd} \leq 0.08 \rightarrow s_w \leq 272 \text{ mm.}$$

In the "critical region" at the base of column C1: 8 mm-dia. hoops @100 mm centres.

– Capacity design shears:
The seismic axial forces in columns C1, C2 are zero, no matter the direction and sense of action of lateral loading. Besides, the section is square with reinforcement equally shared by the two pairs of opposite sides. Therefore, the moment resistance of the columns is the same for bending within vertical planes parallel or normal to direction X: $M_{Rc,y}$=$M_{Rc,z}$. So, as the clear height of the column is the same in both horizontal directions, the largest capacity design shear is found in the vertical plane where the beams framing into the top of column C1 have the largest value of ΣM_{Rb}: in the plane parallel to direction X: ΣM_{Rb}= 230+146.5=376.5 kNm, exceeding that parallel to direction Y: ΣM_{Rb}=193.3+119.8= 313.1 kNm. So, only the capacity design shear parallel to direction X is calculated.

  – At the joint at the top of column C1: M_{Rc1}=274 kNm, ΣM_{Rc}=274+231=505 kNm.
  – At the base of column C1: M_{Rc1}=274 kNm.
  $V_{CD,1}$ =1.1 × (274+274 × 376.5/505)/2.5=210.4 kN.
  The maximum shear in the column from the analysis may be calculated from its maximum end moments estimated in (m) above:

$$\max M_{y,SRSS-X-Y} = 191.9 \quad \text{kNm} \rightarrow \max V_{Ec1,SRSS-X-Y} = 2 \times 191.9/2.5$$
$$= 153.5\,\text{kN} \leq V_{CD,1} = 210.4\,\text{kN}$$
$$(M_{y,X+0.3Y} = 194.3\,\text{kNm} \rightarrow \max\ V_{Ec1,X+0.3Y} = 2 \times 194.3/2.5$$
$$= 155.4\,\text{kN} \leq V_{CD,1} = 210.4\,\text{kN}).$$

– Verification of shear resistance of the column, for shear compression in the web: Shear resistance for shear compression, according to Eurocode 2:

$$V_{Rd,max} = 0.3(1 - f_{ck}(\text{MPa})/250)b_w z f_{cd}\ \sin 2\,\delta\ (1 \leq \cot\delta \leq 2.5).$$
$$V_{Rd,max} = 0.3 \times (1 - 30/250) \times 1.25 \times 0.4 \times 0.9 \times 0.36 \times 20000\ \sin 2\,\delta$$
$$= 684.3\ \sin 2\,\delta$$
$$V_{Rd,max} = 684.3\ \sin 2\,\delta \geq V_{CD,1} = 210.4.3\,\text{kN} \rightarrow \sin 2\,\delta \geq 0.308.\ \text{OK if}\ \cot\delta$$
$$= 2.5,\ \text{i.e.}\ \delta = 21.8^\circ$$

– Shear reinforcement of the column:
$V_{Rd,s} = b_w z \rho_w f_{ywd} \cot\delta + N_{Ed}(h–x)/H_{cl}$, where the neutral axis depth, $x=\xi d$, may be (conservatively) estimated from the value $\xi=0.44$ associated with the moment resistance of the column, $M_{Rc1,y}$, under $N_{Ed} = 843.8$ kN (see (q) above).

$$V_{Rd,\,s} = 0.4 \times 0.9 \times 0.36 \times (500000/1.15) \times 2.5\rho_w + 843.8$$
$$\times (0.4 - 0.44 \times 0.36)/2.5 = 140870\rho_w + 81.5 \geq V_{CD,1}$$
$$= 210.4\,\text{kN} \rightarrow \rho_w > 0.000915.$$

The maximum stirrup spacing is:

– max s_w=min{$8d_{bL}$; b_o; 175 mm}=128 mm in the 0.45 m-long "critical regions" of the two ends,
– max s_w=0.6 min{$20d_{bL}$; h_c; b_c; 400 mm}=192 mm, in the 1.6 m-long central part of the column height, between the "critical regions".

Taking into account the requirement above for confinement reinforcement with $s_w < 100$ mm at the "critical region" of the base, a 8 mm-dia. perimeter tie and a 8 mm-dia. diamond-shaped internal tie engaging the four central bars of the four sides are provided, as follows:

– up to 440 mm from the bottom section of the column: five stirrups @ 100 mm, with the 1st one 40 mm from the bottom section; they provide: $\rho_w = (2+\sqrt{2}) \times 50.25/(100 \times 400)=0.00429 > 0.000915$;
– over the top 440 mm of the column: four stirrups @ 125 mm centres, with the 1st one 65 mm from the top section; they provide: $\rho_w(2+\sqrt{2}) \times 50.25/(125 \times 400)=0.00343 > 0.000915$;
– over the 1.62 m-long central part of the column height: eight stirrups @ 180 mm centres; they provide: $\rho_w = (2 + \sqrt{2}) \times 50.25/(180 \times 400) = 0.00238 > 0.000915$.

Column C3:

– Confinement reinforcement in the "critical region" at the base of the column:

$$\text{For } \max N_3 = 408.9\,\text{kN} : \nu_\text{d} = 408.9/(0.35^2 \times 20000) = 0.167.$$

$$a\ \omega_\text{wd} \geq 30\mu_\phi\ \nu_\text{d}\ \varepsilon_\text{yd} b_\text{c}/b_\text{o} - 0.035 = 30 \times 6.8 \times 0.167 \times 0.00217 \times 0.35/(0.35 - 2 \times 0.029) - 0.035 = 0.0538$$

$$\rightarrow s_\text{w} \leq 110\,\text{mm for 8 mm-dia. hoops. } \omega_\text{wd} \leq 0.08 \rightarrow s_\text{w} \leq 250\,\text{mm}.$$

In the "critical region" at the base of column C3: 8 mm-dia. hoops @110 mm centres.

– Capacity design shears:

The seismic axial forces in columns C3, C4 vary much more if bending is within a vertical plane parallel to X instead of within an orthogonal plane. So, this is the direction of prime interest for the calculation of the capacity design shear. Besides, for bending within a vertical plane parallel to X the clear height of the column is slightly shorter than for bending within an orthogonal plane (2.5 m vs 2.55 m), suggesting that the capacity design shear would be more critical. However, the moment input to the top of the column from the beams is higher for bending within a vertical plane parallel to X:

  – in the plane parallel to direction X: ΣM_Rb=183.5 kNm,
  – in the plane parallel to direction Y: ΣM_Rb=129.5+64.8=194.3 kNm.

  For completeness the capacity design shears are computed in both transverse directions of column C3:

  – For bending within a vertical plane parallel to X (about the local axis y of the column, which is parallel to direction Y and normal to the plane of the interior 2-bay frame):

    • for min *N*:

      – at the top of C3: min $M_\text{Rc3,y}$=120.6 kNm, Σ min $M_\text{Rc,y}$= 120.6+120.6= 241.2 kNm,
      – at the base of C3: min $M_\text{Rc3,y}$=120.6 kNm,
      – min $V_\text{CD3,z}$ =1.1 × (120.6+120.6 × 183.5/241.2)/2.5=93.3 kN.

    • for max *N*:

      – at the top of C3: max $M_\text{Rc3,y}$ = 146 kNm, Σ max $M_\text{MRc,y}$ = 146+126.5 = 272.5 kNm,
      – at the base of C3: max $M_\text{Rc3,y}$ = 146 kNm,
      – max $V_\text{CD,3z}$ = 1.1 × (146+146 × 183.5/272.5)/2.5 = 107.4 kN.

  The maximum shear force in the column from the analysis is independent of the sense of action of lateral loading. So, it does not relate to the maximum or minimum of the column axial force (it applies for either one). It may be found from the column maximum end moments from (m) above:

$$\max\ M_{y,\mathrm{SRSS-X-Y}} = 96\,\mathrm{kNm} \rightarrow \max V_{\mathrm{Ec3,SRSS-X-Y}} = 2 \times 96/2.5$$
$$= 76.8\,\mathrm{kN} \geq \min V_{\mathrm{CD,3z}} = 93.3\,\mathrm{kN},$$
$$(M_{y,\mathrm{X+0.3Y}} = 97.2\,\mathrm{kNm} \rightarrow \max V_{\mathrm{Ec3,X+0.3Y}} = 2 \times 97.2/2.5$$
$$= 77.8\,\mathrm{kN} \leq V_{\mathrm{CD,3z}} = 93.3\,\mathrm{kN}).$$

– For bending within a vertical plane parallel to Y (about the local axis z of the column, which is parallel to direction X and to the plane of the interior 2-bay frame):

- for min N:
  - at the top of C3: min $M_{\mathrm{Rc3,z}}$=126.2 kNm, Σ min $M_{\mathrm{Rc,y}}$=249.5 kNm,
  - at the base of C3: min $M_{\mathrm{Rc3,z}}$=126.2 kNm,
  - min $V_{\mathrm{CD3,y}}$ =1.1 × (126.2+126.2 × 194.3/249.5)/2.55=96.8 kN.
- for max N:
  - at the top of C3: max $M_{\mathrm{Rc3,z}}$ =128.6 kNm, Σ max $M_{\mathrm{Rc,z}}$ = 252.3 kNm,
  - at the base of C3: max $M_{\mathrm{Rc3,z}}$ =128.6 kNm,
  - max $V_{\mathrm{CD,3y}}$ = 1.1 × (128.6+128.6 × 194.3/252.3)/2.55=98.2 kN.

Maximum column shear force from the analysis:

- max $M_{\mathrm{z,SRSS\text{-}X\text{-}Y}} = M_{\mathrm{z,X+0.3Y}} = 89\,\mathrm{kNm}\rightarrow$

$$\max V_{\mathrm{Ec3,SRSS-X-Y}} = \max V_{\mathrm{Ec3,X+0.3Y}} = 2 \times 89/2.55 = 69.8\,\mathrm{kN}$$
$$\leq V_{\mathrm{CD,3z}}$$

– Verification of the shear resistance of the column, for shear compression in the web:

$$V_{\mathrm{Rd,max}} = 0.3 \times (1 - 30/250) \times 0.35 \times 0.9 \times 0.31 \times 20000\ \sin 2\,\delta = 515.4\ \sin 2\,\delta$$

– For bending within a vertical plane parallel to X (about the local axis y of the column, which is parallel to direction Y and normal to the plane of the interior 2-bay frame):

$$\text{For}\ \max N_3 = 408.9\,\mathrm{kN} : V_{\mathrm{CD,3z}} = 107.4\,\mathrm{kN} :$$

– For bending within a vertical plane parallel to Y (about the local axis z of the column, which is parallel to direction X and to the plane of the interior 2-bay frame):
For max N_3=266.2 kN: $V_{\mathrm{CD,3y}}$ =98.2 kN:

$$V_{\mathrm{Rd,max}}=515.4\ \sin 2\,\delta \geq V_{\mathrm{CD3,z}} = 107.4\,\mathrm{kN} \rightarrow \sin 2\,\delta \geq 0.21.\ \text{OK if}$$
$$\cot \delta = 2.5,\ \text{i.e.}\ \delta = 21.8^{\circ}.$$

– Shear reinforcement of the column:

– For bending within a vertical plane parallel to X (about the local axis y of the column, which is parallel to direction Y and normal to the plane of the interior 2-bay frame):

- for min N_3=97.3 kN and $V_{CD3,z}$ =93.3 kN:

  The neutral axis depth, $x=\xi d$, may be found from the value ξ =0.2611 associated with the moment resistance of the column, min$M_{Rc3,y}$ for minN_3 =97.3 kN (see (q) above).

$$V_{Rd,s} = 0.35 \times 0.9 \times 0.31 \times (500000/1.15) \times 2.5\rho_w + 97.3 \times (0.35 - 0.2611 \times 0.31)/2.5 = 106140\rho_w + 10.4 \geq V_{CD3,z} = 93.3\,\text{kN} \rightarrow \rho_w \geq 0.000787.$$

- for max N_3=408.9 kN and $V_{CD,3z}$ =107.4 kN:

  The neutral axis depth, $x=\xi d$, may be estimated from the value ξ=0.358 associated with the moment resistance of the column, max $M_{Rc3,y}$ for max N_3 =408.9 kN (see (q) above).

$$V_{Rd,s} = 0.35 \times 0.9 \times 0.31 \times (500000/1.15) \times 2.5\rho_w + 408.9 \times (0.35 - 0.358 \times 0.31)/2.5 = 106140\rho_w + 39.1 \geq V_{CD3,z} = 107.4\,\text{kN} \rightarrow \rho_w > 0.00064.$$

– For bending within a vertical plane parallel to Y (about the local axis z of the column, which is parallel to direction X and to the plane of the interior 2-bay frame):
Because the axial force does not vary appreciably and the outcome is not very sensitive to the value of N, the average of minN_3 and maxN_3 is used in the dimensioning: N_3=253.1 kN, along with the corresponding average shear force: $V_{CD,3y}$= (96.8+98.2)/2=97.5 kN
As the axial force, N_3=253.1 kN, is the average of min N_3, max N_3 for bending in a vertical plane parallel to X, the neutral axis depth, $x=\xi d$, may be found accordingly as ξ=(0.2611+0.358)/2=0.31.

$$V_{Rd,s} = 0.35 \times 0.9 \times 0.31 \times (500000/1.15) \times 2.5\rho_w + 253.1 \times (0.35 - 0.31 \times 0.31)/2.55 = 106140\rho_w + 25.2 \geq V_{CD3,z} = 97.5\,\text{kN} \rightarrow \rho_w \geq 0.00068.$$

The three cases above gave very similar results, with the one corresponding to the minimum axial force being slightly more critical.
The maximum stirrup spacing is:

– max s_w=min{8d_{bL}; b_o; 175 mm}=144 mm in the 0.45 m-long "critical regions" of the two ends,

– max s_w=0.6 min{20d_{bL}; h_c; b_c; 400 mm}=210 mm, in the 1.6 m-long central part of the column height between the "critical regions".

Taking into account the requirement above for confinement reinforcement with $s_w <$ 110 mm at the "critical region" of the base, a 8 mm-dia. perimeter tie and a 8 mm-dia. diamond-shaped internal tie engaging the four central bars of the four sides are provided, as follows:

– up to 450 mm from the bottom section of the column: five stirrups @ 110 mm, with the 1st one 10 mm from the bottom section; they provide: $\rho_w = (2+\sqrt{2}) \times 50.25/(110 \times 350)=0.00446 > 0.00081$;
– over the top 450 mm of the column: four stirrups @ 140 mm centres, with the 1st one 30 mm from the top section; they provide: $\rho_w = (2+\sqrt{2}) \times 50.25/(140 \times 350) = 0.0035 > 0.000785$;
– over the 1.6 m-long central part of the column: seven stirrups @ 200 mm centres; they provide: $\rho_w = (2+\sqrt{2}) \times 50.25/(200 \times 350)=0.00245 > 0.00081$.

(t) Design of footings, F1, F3

Table 5.6 lists the seismic action effects at the base of columns C1, C3 from the analysis of the superstructure. From them, the seismic action effects at the base of the footing can be obtained. The moment is the sum of that at the base of the column plus the shear force times the height of the footing, while the shear and axial force are retained the same. The capacity magnification factor to be applied on them is computed from Eq. (2.15a): $a_{CD} = 1.2$ min($M_{Rc,y}/M_{Ec,y}$; $M_{Rc,z}/M_{Ec,z}$). Although the outcome of the linear approximation of the likely maximum action effects of the two concurrent components of the seismic action, Eq. (4.25), is also included in Table 5.6, only the results of the SRSS estimation, Eq. (4.24), are used in the dimensioning and verifications of the footings, as more accurate and more economic. They are slightly lower for the likely maximum values of the various seismic action effects, but significantly lower for the other components concurrently acting with these maximum values.

The values of the column moment resistance at its base, $M_{Rc,y}$, $M_{Rc,z}$, are also listed in Table 5.6, separately for the cases when the seismic axial force concurrent with the maximum likely values of M_y or M_z, from the analysis is added to that due to gravity loads as tensile or as compressive.

The most critical condition for a footing is normally when the seismic axial force in the column is tensile and the total axial force is minimum.

Each footing is dimensioned/verified for the action effects associated with the maximum moments about the local axis y and z at the base of the column, max $M_{y,SRSS\text{-}X\text{-}Y}$ and max $M_{z,SRSS\text{-}X\text{-}Y}$, respectively.

Footing F1
The depth of the footing is chosen: $h = 0.7$ m

– Dimensioning of the footing in plan for the action effects associated with the maximum bending moment about the local axis y of the column (: parallel to

Table 5.6 Bending moments and axial forces at the base of columns from the analysis and column moment resistances there, with the seismic axial force concurrent with the likely maximum moment values taken tensile or compressive

Combination of seismic action components	Bending moments (kNm), corresponding shears and axial forces (kN) at column base	C1	C3
$\sqrt{(E_X^2 + E_Y^2)}$	max $M_{y,SRSS\text{-}X\text{-}Y}$	191.9	96
	$V_{z,SRSS\text{-}X\text{-}Y}$ concurrent with maxM_y	153.5	76.8
	$M_{z,SRSS\text{-}X\text{-}Y}$ concurrent with maxM_y	7.7	7.5
	$V_{y,SRSS\text{-}X\text{-}Y}$ concurrent with maxM_y	6.2	5.9
	$N_{SRSS\text{-}X\text{-}Y}$ concurrent with maxM_y	0	155.8
	$M_{Rc,y}$ for $N_{G+\psi 2Q}$–$N_{SRSS\text{-}X\text{-}Y}$ concurrent with maxM_y	274	120.6
	$M_{Rc,y}$ for $N_{G+\psi 2Q}$+$N_{SRSS\text{-}X\text{-}Y}$ concurrent with maxM_y	274	146
	max $M_{z,SRSS\text{-}X\text{-}Y}$	168.75	89
	$V_{y,SRSS\text{-}X\text{-}Y}$ concurrent with max M_z	135	69.8
	$M_{y,SRSS\text{-}X\text{-}Y}$ concurrent with max M_z	8.8	12.5
	$V_{z,SRSS\text{-}X\text{-}Y}$ concurrent with max M_z	7.0	10.0
	$N_{SRSS\text{-}X\text{-}Y}$ concurrent with max M_z	0	13.1
	$M_{Rc,z}$ for $N_{G+\psi 2Q}$-$N_{SRSS\text{-}X\text{-}Y}$ concurrent with max M_y	274	126.2
	$M_{Rc,z}$ for $N_{G+\psi 2Q}$+$N_{SRSS\text{-}X\text{-}Y}$ concurrent with max M_y	274	128.6
E_X+0.3E_Y	$M_{y,X+0.3Y}$	194.3	97.2
	$M_{z,X+0.3Y}$	50.6	26.7
	$N_{X+0.3Y}$	0	156
E_Y+0.3E_X	$M_{y,Y+0.3X}$	66.3	33.2
	$M_{z,Y+0.3X}$	168.75	89
	$N_{Y+0.3X}$	0	46.8

direction Y, normal to the plane of the interior 2-bay frame), arising from bending of the column in a vertical plane parallel to X.

$$\begin{aligned} a_{CD} &= 1.2 \times \min(M_{Rc1,y}/M_{Ec1,y};\ \text{concurrent } M_{Rc1,z}/M_{Ec1,z}) \\ &= 1.2 \times \min(274/191.9; 274/7.7) = 1.713. \end{aligned}$$

Design horizontal reactions (shears) at the base of the footing:

$$V_z = a_{CD} V_{Ez} = 1.713 \times 153.5 = 263\,\text{kN},\ V_y = a_{CD} V_{Ey} = 1.713 \times 6.2 = 10.6\,\text{kN}$$

Design moments at the base of the footing:

$$\begin{aligned} M_y &= a_{CD} M_{Ey} = 1.713 \times (191.9 + 0.7 \times 153.5) = 512.8\,\text{kNm}, \\ M_z &= a_{CD} M_{Ez} = 1.713 \times (7.7 + 0.7 \times 6.2) = 20.6\,\text{kNm} \end{aligned}$$

The axial force is due to gravity loads alone: $N = N_1 = 843.8$ kN

Consider a square footing with plan dimension b. The total vertical load at its base is:

$$N_{\text{tot}} = N + \gamma_{\text{concrete}} h b^2 = 843.8 + 25 \times 0.7 b^2 = 843.8 + 17.5 b^2$$

A lower bound to the size of the footing is that needed for an effective footing area greater than zero, i.e. for an eccentricity $e_y = M_y/N_{\text{tot}} = 512.8/(843.8 + 12.5b^2)$ inside the footing area in plan:
$e_y = 512.8/(843.8 + 17.5b^2) \leq b/2$. This gives (through iterations) $b > 1.2$ m.
The design value of the bearing capacity of the ground is computed on the basis of the design value of the undrained shear strength, $c_{\text{ud}} = 100$ kPa, and for an effective footing area:

$$A'_{\text{f}} = (b - 2e_y)(b - 2e_z) \tag{5.49}$$

$$A'_{\text{f}} = [b - 2M_y/(N + 17.5b^2)][b - 2M_z/(N + 17.5b^2)] =$$
$$[b - 2 \times 512.8/(843.8 + 17.5b^2)][b - 2 \times 20.6/(843.8 + 17.5b^2)]$$

The uniform normal stress on the contact area between the effective footing and the ground is:

$$\sigma = \frac{N + 17.5b^2}{A'_{\text{f}}} = \frac{843.8 + 17.5b^2}{b^2 \left(1 - \frac{1025.6}{b(843.8+17.5b^2)}\right)\left(1 - \frac{41.2}{b(843.8+17.5b^2)}\right)}.$$

It should be less than the design value of the bearing capacity according to Eurocode 7 (CEN 2003):

$$q_{\text{ud}} = q + (\pi + 2) c_{\text{ud}} [1 + 0.2(b - 2e_y)/(b - 2e_z)] i_c \tag{5.50}$$

with $q = h\gamma_{\text{soil}} = 0.7 \times 19 = 13.3$ kN/m^2 and

$$i_c = \frac{1}{2}\left(1 + \frac{\tan^{-1}\left(\frac{V_y}{V_z}\right)}{\pi/2}\sqrt{1 - \frac{V_y}{A'_f c_u}} + \left(1 - \frac{\tan^{-1}\left(\frac{V_y}{V_z}\right)}{\pi/2}\right)\sqrt{1 - \frac{V_z}{A'_f c_u}}\right) \tag{5.51}$$

Therefore:

$$q_{\text{ud}} = 13.3 + \frac{100(\pi + 2)}{2}\left(1 + 0.2.\frac{1 - \frac{1025.6}{b(843.8+17.5b^2)}}{1 - \frac{41.2}{b(843.8+17.5b^2)}}\right).$$

$$\left(1+\frac{\tan^{-1}\left(\frac{263}{10.6}\right)}{\pi/2}\sqrt{1-\frac{263}{100b^2\left(1-\frac{1025.6}{b(843.8+17.5b^2)}\right)\left(1-\frac{41.2}{b(843.8+17.5b^2)}\right)}}+\left(1-\frac{\tan^{-1}\left(\frac{263}{10.6}\right)}{\pi/2}\right)\sqrt{1-\frac{10.6}{100b^2\left(1-\frac{1025.6}{b(843.8+17.5b^2)}\right)\left(1-\frac{41.2}{b(843.8+17.5b^2)}\right)}}\right)$$

The requirement $\sigma \leq q_{ud}$ gives through iterations: $b = 2.3$ m. A footing of this size nearly exhausts the shear resistance of the contact area between the effective footing and the ground under the acting shear force V_z alone (corresponding to a negative value for the quantity under the 1st square root in the i_c factor and the bearing capacity expression). For $b = 2.3$ m the acting uniform normal stress at the interface is $\sigma = 344.5$ kPa and the design value of bearing capacity is $q_{ud} = 354$ kPa.

– Dimensioning of the footing in plan for the action effects associated with the maximum moment about the local axis z of the column (: parallel to direction X and to the plane of the interior 2-bay frame), arising from bending of the column in a vertical plane parallel to Y.

$$\begin{aligned} a_{CD} &= 1.2\min(M_{Rcl,z}/M_{Ecl,z};\ \text{concurrent}\ M_{Rcl,y}/M_{Ecl,y}) \\ &= 1.2\min(274/168.75; 274/8.8) = 1.948. \end{aligned}$$

Design shears at the base of the footing:

$$V_y = a_{CD}V_{Ey} = 1.948 \times 135 = 263\,\text{kN},\ V_z = a_{CD}V_{Ez} = 1.948 \times 7 = 13.65\,\text{N}$$

Design moments at the base of the footing:

$$\begin{aligned} M_z &= a_{CD}M_{Ez} = 1.948 \times (168.75 + 0.7 \times 135) = 512.8\,\text{kNm}, \\ M_y &= a_{CD}M_{Ey} = 1.948 \times (8.8 + 0.7 \times 7) = 26.7\,\text{kNm}. \end{aligned}$$

It is notable that the design value of the maximum moment component at the base of the footing and of the associated shear force are exactly the same as in the previous loading case (i.e., for the action effects associated with the maximum bending moment about the local y axis of the column). In both cases the footing is designed for development at the base of the column of a moment equal to 1.2 times its design moment resistance, first in one of the two directions of bending and then in the other. So, as the column has the same moment resistance and the same shear span (moment-shear-ratio) in both directions, the design value of the maximum bending moment component at the base of the footing is also the same. Note, though, that the design values of the smaller bending moment concurrently acting in the orthogonal direction at the base of the footing and of the associated shear force are slightly larger in the present, second, loading case than in the first

one, although at the level of seismic action effects from the analysis this loading case is less critical than the first. This may presage a more critical condition for the dimensions of the footing than in the previous loading case.

The axial force is again due to gravity loads alone, $N = 843.8$ kN, and (for a square footing with side b) the total vertical load at the base of the footing is again: $N_{\text{tot}} = 843.8+17.5b^2$

The effective footing area from Eq. (5.49) is:

$$A'_{\text{f}}=[b - 2M_{\text{y}}/(N + 17.5b^2)][b - 2M_{\text{z}}/(N + 17.5b^2)]$$
$$=[b - 2 \times 26.7/(843.8 + 17.5b^2)][b - 2 \times 512.8/(843.8 + 17.5b^2)]$$

The uniform normal stress on the contact area between the effective footing and the ground is:

$$\sigma = \frac{N + 17.5b^2}{A'_{\text{f}}} = \frac{843.8 + 17.5b^2}{b^2\left(1 - \frac{1025.6}{b(843.8+17.5b^2)}\right)\left(1 - \frac{53.4}{b(843.8+17.5b^2)}\right)},$$

It should be less than the design value of bearing capacity from Eqs. (5.50) and (5.51):

$$q_{\text{ud}} = 13.3 + \frac{100(\pi + 2)}{2}\left(1 + 0.2 \cdot \frac{1 - \frac{1025.6}{b(843.8+17.5b^2)}}{1 - \frac{53.4}{b(843.8+17.5b^2)}}\right) \cdot$$
$$\left(1 + \frac{\tan^{-1}\left(\frac{263}{13.65}\right)}{\pi/2}\sqrt{1 - \frac{263}{100b^2\left(1 - \frac{1025.6}{b(843.8+17.5b^2)}\right)\left(1 - \frac{53.4}{b(843.8+17.5b^2)}\right)}} + \right.$$
$$\left.\left(1 - \frac{\tan^{-1}\left(\frac{263}{13.65}\right)}{\pi/2}\right)\sqrt{1 - \frac{13.65}{100b^2\left(1 - \frac{1025.6}{b(843.8+17.5b^2)}\right)\left(1 - \frac{53.4}{b(843.8+17.5b^2)}\right)}}\right)$$

For the previously selected footing size, $b = 2.3$ m, the acting uniform normal stress at the interface is $\sigma = 346.5$ kPa and the design value of the bearing capacity is $q_{\text{ud}} = 352.3$ Pa. The verification of this second loading case is indeed slightly more critical, but not to the point of requiring a larger footing.

– Verification of the depth of the footing in shear and punching shear.

The depth of the footing should be chosen so that the footing does not require shear reinforcement. The acting shear force should be calculated at vertical sections through the footing at distance d from the face of the column and compared to the design shear resistance of concrete members without shear reinforcement according to Eurocode 2, $V_{\text{Rd,c}}$, from Eq. (3.67) in Section 3.2.3.2, but with the design values of concrete strength.

Acting shear forces are calculated at two vertical sections through the footing normal to direction X and to the plane of the interior 2-bay frame (i.e., parallel to the local axis y of the column), at a distance d from two opposite faces of the column:

1. One on the same side with respect to the centre of the footing as the eccentricity $e_y = M_y/N_{tot}$, with distance from the centre of the footing denoted by s_y and taken positive;
2. A 2nd one on the opposite side with respect to the column, with distance from the centre of the footing denoted by s'_y and taken positive if it is on the same side with respect to the centre of the footing as the eccentricity $e_y = M_y/N_{tot}$ (normally it is not, and s'_y is negative).

The acting shear forces at these sections are calculated assuming that the vertical soil stresses exerted over the contact area at the underside of the footing vary linearly along the two horizontal directions, y and z. This is consistent with:

- the presumed rigidity of the footing, compared to the underlying soil, and
- the sizing of the plan area of the footing so that the design value of the soil bearing capacity (calculated using design values of the soil strength parameters, that involve material partial factors) is not attained, implying that vertical stresses over the contact area of the footing and the soil are in the linear-elastic range of soil behaviour.

If b_y denotes the plan dimension of the footing parallel to the eccentricity $e_y = M_y/N_{tot}$, then, for contact stresses linear in y and z the acting shear force at the 1st control section (at a distance from the centre of the footing s_y) is:

$$V_{Ed,y} = N_{tot}\left(1 + \frac{3|e_y|}{b_y}\left(1 + \frac{2s_y}{b_y}\right)\right)\left(0.5 - \frac{s_y}{b_y}\right) - (N_{tot} - N)\left(0.5 - \frac{s_y}{b_y}\right) \quad \text{if} \quad \frac{6|e_y|}{b_y} \le 1 \tag{5.52a}$$

$$V_{Ed,y} = \frac{N_{tot}}{9}\frac{\left(2.5 - \frac{6|e_y|}{b_y} + \frac{s_y}{b_y}\right)\left(0.5 - \frac{s_y}{b_y}\right)}{\left(0.5 - \frac{e_y}{b_y}\right)^2} - (N_{tot} - N)\left(0.5 - \frac{s_y}{b_y}\right) \quad \text{if} \quad \frac{6|e_y|}{b_y} > 1 \tag{5.52b}$$

The shear force acting at the 2nd control section (at a distance from the centre of the footing s'_y) is:

$$V'_{Ed,y} = N_{tot}\left(1 - \frac{3|e_y|}{b_y}\left(1 - \frac{2s'_y}{b_y}\right)\right)\left(0.5 + \frac{s'_y}{b_y}\right) - (N_{tot} - N)\left(0.5 + \frac{s'_y}{b_y}\right) \quad \text{if} \quad \frac{6|e_y|}{b_y} \le 1 \tag{5.53a}$$

$$V'_{Ed,y} = \frac{N_{tot}}{9}\left(\frac{\max\left(0;\ 1-\frac{3|e_y|}{b_y}+\frac{s'_y}{b_y}\right)}{0.5-\frac{e_y}{b_y}}\right)^2 - (N_{tot}-N)\left(0.5+\frac{s'_y}{b_y}\right)$$
$$\text{if} \quad \frac{6|e_y|}{b_y} > 1 \tag{5.53b}$$

The maximum of the two acting shear forces from the expressions above should be less than the shear resistance without shear reinforcement, $V_{\mathrm{Rd,c}}$, calculated with b_{w} equal to the plan dimension of the footing normal to the eccentricity e_{y}, denoted here by b_{z}.

The expressions above are applied when the maximum bending moment M_{y} takes place at the base of the footing and the corresponding eccentricity $e_{\mathrm{y}} = M_{\mathrm{y}}/N_{\mathrm{tot}}$. It is exact to neglect in this calculation the contribution of the moment M_{z} concurrently acting in the transverse direction, z, if $6e_{\mathrm{y}}/b_{\mathrm{y}} \leq 1$. If $6e_{\mathrm{y}}/b_{\mathrm{y}} > 1$, it is a very good approximation. For the occurrence of the maximum bending moment M_{z} at the base of the footing and the corresponding eccentricity $e_{\mathrm{z}} = M_{\mathrm{z}}/N_{\mathrm{tot}}$, a similar calculation with index y replaced by z and vice-versa gives the shear forces acting at two vertical sections through the footing normal to direction Y and parallel to the plane of the interior 2-bay frame (i.e., parallel to the local axis z of the column).

For a footing concentric with a column having cross-sectional dimensions c_{y} and c_{z} parallel to local axes y and z, the control sections for the acting bending moments are at distances to the centre of the footing: $s_{\mathrm{y}} = d+c_{\mathrm{y}}/2$, $s'_{\mathrm{y}} = -s_{\mathrm{y}}$, $s_{\mathrm{z}} = d+c_{\mathrm{z}}/2$, $s'_{\mathrm{z}} = -s_{\mathrm{z}}$. For the present square column and footing: $s_{\mathrm{y}} = s_{\mathrm{z}} = d+c/2 = 0.65+0.4/2 = 0.85$m, $s'_{\mathrm{y}} = s'_{\mathrm{z}} = -0.85$m, $b_{\mathrm{y}} = b_{\mathrm{z}} = b = 2.3$m, $N_{\mathrm{tot}} = N+\gamma_{\mathrm{concrete}}hb^2 = 843.8+17.5 \times 2.3^2 = 936.4$ kN, $N_{\mathrm{tot}}-N = 92.6$ kN, e_{y} (for the maximum moment M_{y} at the base of the footing) $= 512.8/936.4 = 0.548$ m and e_{z} (for the maximum moment M_{z} at the base of the footing) $= 512.8/936.4 = 0.548$ m. Note that $e_{\mathrm{y}} = e_{\mathrm{z}}$ and $e_{\mathrm{y}} > b_{\mathrm{y}}/6 = 0.383$m, $e_{\mathrm{z}} > b_{\mathrm{z}}/6 = 0.383$m. So, from Eqs. (5.52b) and (5.53b):

$$V_{Ed,y}=V_{Ed,z} = \frac{936.4}{9}\frac{\left(2.5-\frac{6\cdot 0.548}{2.3}+\frac{0.85}{2.3}\right)\left(0.5-\frac{0.85}{2.3}\right)}{\left(0.5-\frac{0.548}{2.3}\right)^2} - 92.6\left(0.5-\frac{0.85}{2.3}\right)$$
$$= 240.6\,\mathrm{kN}$$
$$V'_{Ed,y}=V'_{Ed,z} = \frac{936.4}{9}\frac{\left(\max\left(0;\ 1-\frac{3\cdot 0.548}{2.3}-\frac{0.85}{2.3}\right)\right)^2}{\left(0.5-\frac{0.548}{2.3}\right)^2} - 92.6\left(0.5-\frac{0.85}{2.3}\right)$$
$$= -12.1\,\mathrm{kN}$$

For the calculation of the shear resistance of the footing without shear reinforcement, $V_{\mathrm{Rd,c}}$, the tensile reinforcement ratio, ρ_1, should be known. The minimum reinforcement ratio required by Eurocode 2 for slabs is considered to apply

to footings: $0.26 f_{ctm}/f_{yk} = 0.0013$, normalised to bd. This gives $A_s \geq (0.26 \times 2.9/500) \times 650 \times 1000 = 980.2$ mm^2/m$\rightarrow$ 14 mm-dia. bars @ 150 mm centres (1026 mm^2/m), i.e. $\rho_1 = 1026/(650 \times 1000) = 0.00158$. So, from Eq. (3.67) in Section 3.2.3.2:

$$V_{Rd,c} = \max \left[180\,(100 \cdot 0.00158)^{1/3},\ 35\sqrt{1 + \sqrt{\frac{0.2}{0.65}}}\,20^{1/6} \right]$$

$$\left(1 + \sqrt{\frac{0.2}{0.65}}\right) 20^{1/3} \cdot 2.3 \cdot 0.65 = 614\text{kN}$$

Indeed $V_{Rd,c} > \max[V_{Ed,y};\ |V'_{Ed,y}|;\ V_{Ed,z};\ |V'_{Ed,z}|]$; so no shear reinforcement is needed, despite the slender footing.

The critical section for punching shear is at a distance from the perimeter of the column between $d = 0.65$ m and $2d = 1.3$ m, i.e. 0.85–1.5 m from its centre. So, it is close to, or falls outside, the perimeter of the footing plan. Given the fairly large eccentricity of the shear force, verification in punching shear will not be more critical than in shear.

– Dimensioning of the footing reinforcement.

Due to the slenderness of the footing, the footing reinforcement is dimensioned on the basis of flexural considerations, rather than with a Strut-and-Tie model.

The bending moment for dimensioning the footing reinforcement which is parallel to direction X and side b_z of the footing is the one acting at vertical sections through the footing at the two column faces which are normal to direction X and to the plane of the interior 2-bay frame (i.e., parallel to the local axis y of the column). They coincide with the vertical planes through two opposite column faces:

1. One on the same side with respect to the centre of the footing as the eccentricity $e_y = M_y/N_{tot}$, with distance from the centre of the footing denoted by s_y and taken positive;
2. A 2nd one on the opposite side with respect to the column, with distance from the centre of the footing denoted by s'_y and taken positive if it is on the same side with respect to the centre of the footing as the eccentricity $e_y = M_y/N_{tot}$ (normally it is not, and s'_y is negative).

Similarly to the acting shear forces in the shear verifications and for the same reasons, the bending moments acting at these sections are computed assuming that the vertical soil stresses exerted over the contact area at the underside of the footing vary linearly along the two horizontal directions, y and z. Then, if b_y is the plan dimension of the footing parallel to the eccentricity $e_y = M_y/N_{tot}$, the bending moment acting at the 1st control section (at a distance s_y from the centre of the footing) is:

$$M_{Ed,y}=\frac{N_{tot}b_y}{2}\left(1+\frac{4|e_y|}{b_y}\left(1+\frac{s_y}{b_y}\right)\right)\left(0.5-\frac{s_y}{b_y}\right)^2 - \frac{(N_{tot}-N)\,b_y}{2}\left(0.5-\frac{s_y}{b_y}\right)^2 \quad \text{if} \quad \frac{6|e_y|}{b_y}\le 1 \tag{5.54a}$$

$$M_{Ed,y}=\frac{N_{tot}b_y}{27}\frac{\left(4-\frac{9|e_y|}{b_y}+\frac{s_y}{b_y}\right)\left(0.5-\frac{s_y}{b_y}\right)^2}{\left(0.5-\frac{e_y}{b_y}\right)^2} - \frac{(N_{tot}-N)\,b_y}{2}\left(0.5-\frac{s_y}{b_y}\right)^2 \quad \text{if} \quad \frac{6|e_y|}{b_y}>1 \tag{5.54b}$$

The bending moment acting at the 2nd control section (at a distance s'_y from the footing's centre) is:

$$M'_{Ed,y}=\frac{N_{tot}b_y}{2}\left(1-\frac{4|e_y|}{b_y}\left(1-\frac{s'_y}{b_y}\right)\right)\left(0.5+\frac{s'_y}{b_y}\right)^2 - \frac{(N_{tot}-N)\,b_y}{2}\left(0.5+\frac{s'_y}{b_y}\right)^2 \quad \text{if} \quad \frac{6|e_y|}{b_y}\le 1 \tag{5.55a}$$

$$M'_{Ed,y}=\frac{N_{tot}b_y}{27}\frac{\left(\max\left(0;1-\frac{3|e_y|}{b_y}+\frac{s'_y}{b_y}\right)\right)^3}{\left(0.5-\frac{e_y}{b_y}\right)^2} - \frac{(N_{tot}-N)\,b_y}{2}\left(0.5+\frac{s'_y}{b_y}\right)^2 \quad \text{if} \quad \frac{6|e_y|}{b_y}>1 \tag{5.55b}$$

The expressions above should be applied for the eccentricity $e_y=M_y/N_{tot}$ resulting from the maximum bending moment M_y in the column, in order to dimension the footing reinforcement parallel to side b_y and global direction X. It is exact to neglect in this calculation the effect of the moment M_z concurrently acting in the transverse direction z, if $6e_y/b_y \le 1$. It is a very good approximation if $6e_y/b_y > 1$.

The footing reinforcement parallel to side b_z and global direction Y is found from the bending moments acting at two vertical sections through the footing normal to direction Y and parallel to the plane of the interior 2-bay frame (i.e., parallel to the local axis z of the column), via a similar calculation with index y replaced by z and vice-versa.

If the footing is concentric with a column having cross-sectional dimensions c_y and c_z parallel to local axes y and z, the control sections for the calculation of the acting bending moments are at distances from the centre of the footing: $s_y=c_y/2$, $s'_y=-s_y$, $s_z=c_z/2$, $s'_z=-s_z$. For the present square column and footing, we have $s_y=s_z=c/2=0.4/2=0.2$ m, $s'_y=s'_z=-0.2$ m, $b_y=b_z=b=2.3$ m, $N_{tot}=936.4$ kN,

N_{tot}–N= 92.6 kN, e_y (for the maximum moment M_y at the base of the footing) =512.8/936.4=0.548 m and e_z (for the maximum moment M_z at the base of the footing) =512.8/936.4=0.548 m. Note that e_y=e_z and e_y>b_y/6=0.383 m, e_z>b_z/6=0.383 m. So, from Eqs. (5.54b) and (5.55b):

$$M_{Ed,y}=M_{Ed,z}=\frac{936.4\cdot 2.3}{27}\frac{\left(4-\frac{9\cdot 0.383}{2.3}+\frac{0.2}{2.3}\right)\left(0.5-\frac{0.2}{2.3}\right)^2}{\left(0.5-\frac{0.383}{2.3}\right)^2}$$
$$-\frac{92.6\cdot 2.3}{2}\left(0.5-\frac{0.2}{2.3}\right)^2=298.6\,\text{kNm}$$
$$M'_{Ed,y}=M'_{Ed,z}=\frac{936.4\cdot 2.3}{27}\frac{\left(\max\left(0;1-\frac{3\cdot 0.383}{2.3}-\frac{0.2}{2.3}\right)\right)^3}{\left(0.5-\frac{0.383}{2.3}\right)^2}$$
$$-\frac{92.6\cdot 2.3}{2}\left(0.5-\frac{0.2}{2.3}\right)^2=32.5\,\text{kNm}$$

A_{sy}=A_{sy}=$M_{Ed,y}/zf_{yd}$=298.6 × 10^3/(0.9 × 0.65 × 500/1.15)=1174 mm^2, i.e. 1174/2.3=510 mm^2/m. The minimum reinforcement of 14 mm-dia. bars @ 150 mm centres (1026 mm^2/m) suffices.

Footing of column C3:
The depth of this footing is also chosen: $h = 0.7$ m

– Dimensioning of the footing in plan for the action effects associated with the maximum bending moment about the local axis y of the column (: parallel to direction Y, normal to the plane of the interior 2-bay frame), arising from bending of the column in a vertical plane parallel to X.
The most critical condition for the footing is when the seismic axial force in the column is tensile and the total vertical load is minimum, $N_{G+\psi 2Q}$–$N_{SRSS\text{-}X\text{-}Y}$, giving $M_{Rc3,y}$=120.6 kNm.

$$a_{CD}=1.2\,\min(M_{Rc3,y}/M_{Ec3,y};\ \text{concurrent}\ M_{Rc3,z}/M_{Ec3,z})$$
$$=1.2\ \min(120.6/96;120.6/7.5)=1.51.$$

Design shears at the base of the footing:

$$V_z=a_{CD}V_{Ez}=1.51\times 76.8=116\,\text{kN},V_y=a_{CD}V_{Ey}=1.51\times 5.9=8.9\,\text{kN}$$

Design moments at the base of the footing:

$$M_y=a_{CD}M_{Ey}=1.51\times(96+0.7\times 76.8)=226\,\text{kNm},\ M_z=a_{CD}M_{Ez}$$
$$=1.51\times(7.5+0.7\times 5.9)=17.6\,\text{kNm}$$

Vertical seismic load on the footing (the increase due to the overturning moment is included in the seismic moment at the base of the footing): $N_E = 155.8$ kN
Vertical load due to gravity loads from the superstructure: $N = N_3 = 253.1$ kN
Minimum design vertical load at the top of the footing: min $N = 253.1–1.51 \times 155.8 = 17.1$ kN
For a square footing with side b, the total axial force at the base of the footing is:

$$N_{tot} = N + \gamma_{concrete} h b^2 = 17.1 + 25 \times 0.7 b^2 = 17.1 + 17.5 b^2$$

The footing size necessary in order for the eccentricity $e_y = M_y/N_{tot} = 226/(17.1+17.5b^2)$ to fall inside the plan area of the footing, so that the effective (reduced) footing area is greater than zero, is obtained from the condition: $e_y = 226/(17.1+17.5b^2) \leq b/2$, which gives (through iterations) $b > 2.85$ m.
The effective footing area from Eq. (5.49) is:

$$A'_f = [b - 2M_y/(N + 17.5b^2)][b - 2M_z/(N + 17.5b^2)] = [b - 2 \times 226/(17.1 + 17.5b^2)][b - 2 \times 17.6/(17.1 + 17.5b^2)]$$

The uniform normal stress on the contact area between the effective footing and the ground is:

$$\sigma = \frac{N + 17.5b^2}{A'_f} = \frac{17.1 + 17.5b^2}{b^2 \left(1 - \frac{452}{b(17.1+17.5b^2)}\right)\left(1 - \frac{35.2}{b(17.1+17.5b^2)}\right)}.$$

It should be less than the design value of bearing capacity from Eqs. (5.50) and (5.51):

$$q_{ud} = 13.3 + \frac{100(\pi + 2)}{2}\left(1 + 0.2 \cdot \frac{1 - \frac{452}{b(17.1+17.5b^2)}}{1 - \frac{35.2}{b(17.1+17.5b^2)}}\right) \cdot \left(1 + \frac{\tan^{-1}\left(\frac{116}{8.9}\right)}{\pi/2}\sqrt{1 - \frac{116}{100b^2\left(1 - \frac{452}{b(17.1+17.5b^2)}\right)\left(1 - \frac{35.2}{b(17.1+17.5b^2)}\right)}} + \left(1 - \frac{\tan^{-1}\left(\frac{116}{8.9}\right)}{\pi/2}\right)\sqrt{1 - \frac{8.9}{100b^2\left(1 - \frac{452}{b(17.1+17.5b^2)}\right)\left(1 - \frac{35.2}{b(17.1+17.5b^2)}\right)}}\right)$$

The requirement $\sigma \leq q_{ud}$ gives, through iterations: $b = 3.1$ m. This size of footing nearly exhausts the shear resistance of the contact area between the effective footing and the ground under the acting shear force V_z alone (corresponding to a negative value for the quantity under the 1st square root in the i_c factor and the bearing capacity expression). For $b = 3.1$ m the acting uniform normal stress at

the interface is just σ =96.4 kPa, while the design value of the bearing capacity is q_{ud} =456 kPa. Despite the apparently wide margin against the bearing capacity, a lower value, e.g. b=3 m, is not feasible, due to failure under the acting shear force V_z alone.

For completeness we also consider the case when the seismic axial force in the column is compressive and the total vertical load is maximum, $N_{G+\psi 2Q}+N_{SRSS\text{-}X\text{-}Y}$, giving M_{Rcy}= max M_{Rc3}=146 kNm and

$$\begin{aligned} a_{CD} &= 1.2\min(M_{Rc3,y}/M_{Ec3,y};\ \text{concurrent } M_{Rc3,z}M_{Ec3,z}) \\ &= 1.2\min(146/96; 146/7.5) = 1.825. \end{aligned}$$

Design shears at the base of the footing:

$$V_z = a_{CD}V_{Ez} = 1.825{\times}76.8 = 140.15\,\text{kN}, V_y = a_{CD}V_{Ey} = 1.825{\times}6 = 10.95\,\text{kN}$$

Design moments at the base of the footing:

$$\begin{aligned} M_y{=}a_{CD}M_{Ey} &= 1.825 \times (96 + 0.7 \times 76.8) = 273.3\,\text{kNm}, \\ M_z &= a_{CD}M_{Ez} = 1.825 \times (7.5 + 0.7 \times 6) = 21.35\,\text{kNm} \end{aligned}$$

Vertical seismic load on the footing (the increase due to the overturning moment is included in the seismic moment at the base of the footing): N_E=155.8 kN
Vertical load due to gravity loads from the superstructure: $N = N_3$ = 253.1 kN
Maximum design vertical load at the top of the footing: max$N$=253.1+1.825 × 155.8 = 537.5 kN
Total vertical load at the base of the footing: N_{tot}=N+$\gamma_{concrete}hb^2$=537.5+17.5b^2
Effective footing area from Eq. (5.49):

$$\begin{aligned} A'_f &= [b - 2M_y/(N + 17.5b^2)][b - 2M_z/(N + 17.5b^2)] = \\ &[b - 2 \times 273.3/(537.5 + 17.5\text{b}^2)][b - 2 \times 21.35/(537.5 + 17.5b^2)] \end{aligned}$$

Uniform normal stress on the contact area between the effective footing and the ground:

$$\sigma = \frac{N + 17.5b^2}{A'_f} = \frac{537.5 + 17.5b^2}{b^2\left(1 - \frac{546.6}{b(537.5+17.5b^2)}\right)\left(1 - \frac{42.7}{b(537.5+17.5b^2)}\right)}.$$

Design value of bearing capacity from Eqs. (5.50) and (5.51):

$$q_{\mathrm{ud}} = 13.3 + \frac{100(\pi+2)}{2}\left(1 + 0.2 \cdot \frac{1 - \frac{546.6}{b(537.5+17.5b^2)}}{1 - \frac{42.7}{b(537.5+17.5b^2)}}\right) \cdot$$
$$\left(1 + \frac{\tan^{-1}\left(\frac{140.15}{10.95}\right)}{\pi/2}\sqrt{1 - \frac{140.15}{100b^2\left(1 - \frac{546.6}{b(537.5+17.5b^2)}\right)\left(1 - \frac{42.7}{b(537.5+17.5b^2)}\right)}} + \right.$$
$$\left.\left(1 - \frac{\tan^{-1}\left(\frac{140.15}{10.95}\right)}{\pi/2}\right)\sqrt{1 - \frac{10.95}{100b^2\left(1 - \frac{546.6}{b(537.5+17.5b^2)}\right)\left(1 - \frac{42.7}{b(537.5+17.5b^2)}\right)}}\right)$$

For the previously selected footing size, b=3.1 m, the acting uniform normal stress at the interface is σ =99.8 kPa and the design value of the bearing capacity is q_{ud} =608 kPa. Indeed, most critical for the footing is when the seismic axial force in the column is tensile and the total axial force is minimum.

– Dimensioning of the footing in plan for the action effects associated with the maximum bending moment about the local axis z of the column (: parallel to direction X and to the plane of the interior 2-bay frame), arising from bending of the column in a vertical plane parallel to Y.

Only the case when the seismic axial force in the column is tensile and the total axial force is minimum, $N_{\mathrm{G+\psi 2Q}}$–$N_{\mathrm{SRSS\text{-}X\text{-}Y}}$, is considered as potentially critical for the bearing capacity, giving $M_{\mathrm{Rc,z}}$=126.2 kNm.

$$\begin{aligned} a_{\mathrm{CD}} &= 1.2\,\min(M_{\mathrm{Rc3,z}}/M_{\mathrm{Ec3,z}};\ \text{concurrent}\ M_{\mathrm{Rc3,y}}/M_{\mathrm{Ec3,y}}) \\ &= 1.2\,\min(126.2/89; 126.2/12.5) = 1.7. \end{aligned}$$

Design shears at the base of the footing:

$$V_{\mathrm{y}} = a_{\mathrm{CD}} V_{\mathrm{Ey}} = 1.7 \times 69.8 = 119\,\mathrm{kN},\ V_{\mathrm{z}} = a_{\mathrm{CD}} V_{\mathrm{Ez}} = 1.7 \times 10 = 17\,\mathrm{N}$$

Design moments at the base of the footing:

$$\begin{aligned} M_{\mathrm{z}} &= a_{\mathrm{CD}} M_{\mathrm{Ez}} = 1.7 \times (89 + 0.7 \times 69.8) = 234\,\mathrm{kNm}, \\ M_{\mathrm{y}} &= a_{\mathrm{CD}} M_{\mathrm{Ey}} = 1.7 \times (12.5 + 0.7 \times 10) = 33\,\mathrm{kNm}. \end{aligned}$$

Minimum design vertical load at the top of the footing: min$N$ = 253.1 – 1.7 × 13.1 = 231 kN

The design value of the maximum bending moment at the base of the footing is less than in the previous loading case (i.e., for the action effects associated with the maximum bending moment about the local y axis of the column), while the design shear force is slightly larger in this loading case. However, the minimum design axial load at the top of the footing is much higher than in the previous loading case, presaging a much larger effective footing area and a less critical condition for the dimensions of the footing. So, the verification of the footing in

plan for the action effects associated with the maximum bending moment about the local y axis of the column is not pursued any further.

– Verification of the depth of the footing in shear and punching shear.
In the present case of square column and footing: $s_y=s_z=d+c/2=0.65+0.35/2=0.825$ m, $s'_y=s'_z=-0.825$ m, $b_y=b_z=b=3.1$ m, $N_{tot}-N=17.5b^2=168.2$ kN.

The action effects associated with the maximum bending moment about the column's local axis y (normal to the plane of the interior 2-bay frame, parallel to direction Y), arising from bending of the column in a vertical plane parallel to X, give the extreme variation of vertical load at the footing's base.

For the combination of minimum design axial load $N_{tot}=17.1+168.2=185.3$ kN and the corresponding maximum moment $M_y=226$ kNm at the base of the footing: $e_y=226/185.3=1.22$ m$>b_y/6=0.517$ m. So, from Eqs. (5.52b) and (5.53b):

$$V_{Ed,y}=\frac{185.3}{9}\frac{\left(2.5-\frac{6\cdot 1.22}{3.12}+\frac{0.825}{3.1}\right)\left(0.5-\frac{0.825}{3.1}\right)}{\left(0.5-\frac{1.22}{3.1}\right)^2}-168.2\left(0.5-\frac{0.825}{3.1}\right)$$
$$=132.7\,\text{kN}$$
$$V'_{Ed,y}=\frac{185.3}{9}\frac{\left(\max\left(0;1-\frac{3\cdot 1.22}{3.1}-\frac{0.825}{3.1}\right)\right)^2}{\left(0.5-\frac{1.22}{3.1}\right)^2}-168.2\left(0.5-\frac{0.825}{3.1}\right)$$
$$=-39.3\,\text{kN}$$

For the combination of maximum design vertical load $N_{tot}=537.5+168.2=705.7$ kN and the corresponding maximum moment $M_y=273.3$ kNm at the base of the footing: $e_y=273.3/705.7=0.387$ m $< b_y/6=0.517$ m. Therefore, from Eqs. (5.52a) and (5.53a):

$$V_{Ed,y}=705.7\left(1+\frac{3\cdot 0.387}{3.1}\left(1+\frac{2\cdot 0.825}{3.1}\right)\right)\left(0.5-\frac{0.825}{3.1}\right)$$
$$-168.2\left(0.5-\frac{0.825}{3.1}\right)=220.2\text{kN}$$
$$V'_{Ed,y}=705.7\left(1-\frac{3\cdot 0.387}{3.1}\left(1-\frac{2\cdot 0.825}{3.1}\right)\right)\left(0.5-\frac{0.825}{3.1}\right)$$
$$-168.2\left(0.5-\frac{0.825}{3.1}\right)=97\text{kN}$$

Note that the combination of the maximum design vertical load and of the corresponding maximum bending moment M_y at the base of the footing is more critical for shear than the minimum design vertical load with the corresponding maximum bending moment M_y, which was found to govern the bearing capacity verification and the size of the footing in plan.

On the basis of this last conclusion, the verification of the footing in shear for the action effects associated with the maximum bending moment about the local

axis z of the column (: parallel to direction X and to the plane of the interior 2-bay frame), that arise from bending of the column in a vertical plane parallel to Y, considers only the case when the seismic axial force in the column is compressive and the total vertical load is maximum, $N_{G+\psi 2Q}+N_{SRSS\text{-}X\text{-}Y}$, giving $M_{Rc,z}$=128.6 kNm.

$$\begin{aligned} a_{CD} &= 1.2 \min\left(M_{Rc3,z}/M_{Ec3,z};\ \text{concurrent } M_{Rc3,y}/M_{Ec3,y}\right) \\ &= 1.2 \min\left(128.6/89; 128.6/12.5\right) = 1.73. \end{aligned}$$

Design moment at the base of the footing: $M_z = a_{CD}M_{Ez}$=1.73 × (89+0.7 × 69.8)=238 kNm.

Maximum design vertical load at the top of the footing: max N = 253.1+1.73 × 13.1=276 kN.

$$\begin{aligned} N_{tot} &= 276 + 168.2 = 444.2\,\text{kN},\ e_y = 238/444.2 = 0.536\,\text{m} > b_y/6 \\ &= 0.517\,\text{m. So, from Eqs. (5.52b) and (5.53b) :} \end{aligned}$$

$$\begin{aligned} V_{Ed,y} &= \frac{444.2}{9}\frac{\left(2.5 - \frac{6\cdot 0.536}{3.1} + \frac{0.825}{3.1}\right)\left(0.5 - \frac{0.825}{3.1}\right)}{\left(0.5 - \frac{0.536}{3.1}\right)^2} - 168.2\left(0.5 - \frac{0.825}{3.1}\right) \\ &= 147.2\,\text{kN} \\ V'_{Ed,y} &= \frac{444.2}{9}\frac{\left(\max\left(0; 1 - \frac{3\cdot 0.536}{3.1} - \frac{0.825}{3.1}\right)\right)^2}{\left(0.5 - \frac{0.536}{3.1}\right)^2} - 168.2\left(0.5 - \frac{0.825}{3.1}\right) \\ &= -18\,\text{kN} \end{aligned}$$

So, more critical for the verification of the footing in shear is the loading and direction of bending of the column which produces the most extreme variation of vertical load on the footing.

Using as tensile reinforcement 14 mm-dia. bars @ 150 mm centres (1026 mm^2/m), giving ρ_1=0.00158 and meeting the minimum Eurocode 2 reinforcement ratio for slabs ($A_s \geq$ (0.26 × 2.9/500) × 650 × 1000= 980.2 mm^2/m), the shear resistance of the footing without shear reinforcement is:

$$V_{R,c} = \max\left[180(100 \cdot 0.00158)^{1/3}, 35\sqrt{1 + \sqrt{\frac{0.2}{0.65}}}20^{1/6}\right]$$
$$\left(1 + \sqrt{\frac{0.2}{0.65}}\right)20^{1/3} \cdot 3.1 \cdot 0.65 = 827\,kN$$

Indeed $V_{Rc} > \max[V_{Ed,y}; |V'_{Ed,y}|; V_{Ed,z}; |V'_{Ed,z}|]$ and no shear reinforcement is needed, despite the slenderness of the footing, which is at the limit of considering it as rigid relative to the ground.

The critical section for punching shear is at a distance from the perimeter of the column between d=0.65 m and 2d=1.3 m, i.e. 0.825–1.475 m from its centre. So,

it is close to the perimeter of the footing plan. Given the very large eccentricity of the seismic shear force in the footing, verification in punching shear is not expected to be more critical than in shear.

– Dimensioning of footing reinforcement.

In this case: $s_y=s_z=c/2=0.35/2=0.175$ m, $s'_y=s'_z=-0.175$ m, $b_y=b_z=b=3.1$ m, N_{tot}-N=168.2 kN.

Only the combination of the maximum design vertical load with the corresponding maximum moment M_y at the footing's base is considered, found above to be more critical for the footing in shear. For that combination we have N_{tot}=705.7 kN and corresponding maximum moment M_y=273.3 kNm at the footing's base, giving: $e_y=273.3/705.7=0.387$ m$< b_y/6=0.517$ m. So, from Eqs. (5.54a) and (5.55a):

$$M_{Ed,y} = \frac{705.7 \cdot 3.1}{2}\left(1+\frac{4 \cdot 0.387}{3.1}\left(1+\frac{0.175}{3.1}\right)\right)\left(0.5-\frac{0.175}{3.1}\right)^2 - \frac{168.2 \cdot 3.1}{2}\left(0.5-\frac{0.175}{3.1}\right)^2 = 277.4\,\text{kNm}$$

$$M'_{Ed,y} = \frac{705.7 \cdot 3.1}{2}\left(1-\frac{4 \cdot 0.387}{3.1}\left(1-\frac{0.175}{3.1}\right)\right)\left(0.5-\frac{0.175}{3.1}\right)^2 - \frac{168.2 \cdot 3.1}{2}\left(0.5-\frac{0.175}{3.1}\right)^2 = 53.2\,\text{kNm}$$

$A_{sy}=A_{sy}=M_{Ed,y}/zf_{yd}=277.4 \times 10^3/(0.9 \times 0.65 \times 500/1.15)=1089$ mm^2, i.e. 1089/3.1=351 mm^2/m. The minimum reinforcement of 14 mm-dia. bars @ 150 mm centres (1026 mm^2/m) is sufficient.

5.8.2 7-Storey Wall Building with Box Foundation and Flat Slab Frames Taken as Secondary Elements

A building has square plan with dimensions $L_x=L_y=25$ m, 7 storeys above ground, 2.8 m-high each, and a basement with a total height of 5 m from the top of its roof slab to the base of the foundation. It has 5 m-long, 0.3 m-thick concrete walls, W1 and W2, at the centre of each side of the perimeter and 28 square columns at a 5 m-grid in each horizontal direction (Fig. 5.9). The column side is:

– $h_{c,int}$=0.6 m for the 16 interior columns,
– $h_{c,edge}$=0.5 m for the eight edge columns, and
– $h_{c,corner}$=0.4 m for the four corner ones,

The floors consist of a flat slab without drop panels around the columns.
There is a box-type foundation, comprising:

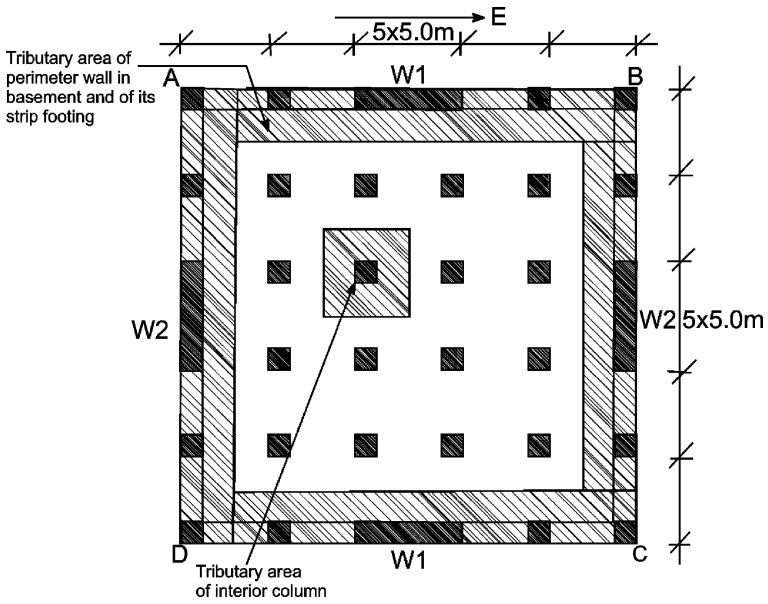

Fig. 5.9 Plan of 7-storey building

- a 200 mm-thick basement wall with a strip footing all along the perimeter, transferring the seismic action effects to the ground acting as a deep foundation beam;
- a 150 mm-thick concrete slab at the level of the top of the basement wall, serving as basement roof;
- spread footings, connected to each other and to the strip footing of the perimeter wall through a two-way system of tie-beams at the level of the bottom of the perimeter foundation beams.

Design specifications

- Permanent loads due to floor finishings, etc.: 0.92 kN/m^2.
- Permanent loads on roof due to finishings and equipment: 4.45 kN/m^2.
- Permanent loads due to partition walls: 1.5 kN/m^2.
- Live load (residential use): q=2 kN/m^2.
- Coefficient ψ_2 for quasi-permanent part of live loads in storeys other than the roof: ψ_2=0.3; on the roof: ψ_2=0.
- Reduction factor on live loads for independently occupied storeys φ=0.8.
- Reference Peak Ground Acceleration on type A ground (rock) a_{gR}=0.25 g.
- EC8 Type 1 recommended spectrum on ground type C (see Table 4.2 for the parameters).
- Importance Class II (importance factor $\gamma_I = 1.0$).
- Ductility Class (DC) Medium (M).
- Concrete C35/45; Steel S500.

- Exposure class related to environmental conditions in accordance with EN 206-1: XC3 (Concrete inside buildings with moderate or high air humidity; external concrete sheltered from rain; concrete surface not exposed to chlorides).
- Foundation above the water table on medium-dense sand, with weight density γ_{soil}=20 kN/m^3, angle of shearing resistance ϕ'_k=36° (characteristic value), no cohesion, friction angle at the interface of the base and the soil (characteristic value), $\delta = \phi'_k$. Depth of overburden at the base of the foundation (average value for the two sides of the footings): 2.5 m.

Simplifying assumptions for the analysis

- Vertical members collect gravity load from tributary areas defined by the mid-distance to the adjacent vertical elements.
- Flat slab frames, consisting of the flat slab and their supporting columns or walls (in the weak direction of bending), may be considered as secondary seismic elements if their total contribution to the lateral stiffness of the building is less than 15% of the total lateral stiffness of primary elements.
- To determine the lateral stiffness of flat slab frames the following assumptions may be made:
  - The two walls which are parallel to the considered horizontal seismic action component are subjected to the full inertia loads of all floors due to that seismic action component and to a concentrated force at the top in a sense opposite to that of floor lateral loads. The flat slab frames are overall subjected to a concentrated force at the top in the same sense as the floor inertia loads, but to no floor lateral loads (hence their seismic shear is constant in all storeys).
  - A strip of the flat slab with width equal to 25% of the bay length on each side of the centreline between columns is considered as the horizontal member (effective beam) of the flat slab frame.[17]
  - For lateral loading the points of inflection of the columns of the flat slab frames are at storey mid-height. Those of the horizontal members (effective beams) are at mid-span.
  - Because interior columns have about twice the moment of inertia of the edge ones and edge columns about twice the moment of inertia of corner ones, interior columns may be considered to take twice the seismic shear relative to edge ones, which in turn take twice the seismic shear compared to corner columns.
  - The storey drifts of the flat slab frames under to lateral loading may be calculated as in the Example of Section 5.9.1, including the use of Eq. (2.8a) in Section 2.2.1.3 for interstorey drifts.

[17]This slab effective width is on the high side. Therefore it is conservative for checking the Eurocode 8 condition for secondary seismic elements, as the contribution of the flat slab frame to lateral stiffness is overestimated.

– According to Eurocode 8 the combination of the two horizontal components of the seismic action may be neglected in regular in plan buildings with walls in the two main horizontal directions as the only primary seismic elements (see 2nd paragraph of Section 4.7.1). So, the seismic action may be assumed to act separately along the two main orthogonal horizontal axes, X and Y.

(a) Material parameters

f_{cd}=35/1.5 MPa; E_c=34000 MPa;
f_{yd}=500/1.15 MPa; ε_{yd}=500/(1.15 × 200000)=0.217%;
Minimum cover of reinforcement for exposure class XC3 according to Eurocode2: c=20 mm (c=15 mm for slabs).

(b) Geometric parameters

Moment of inertia of effective beam with width 0.5 × 5.0=2.5 m: $I_b=2.5 \times 0.15^3/12=0.0007\ m^4$

Moment of inertia of interior columns:	$I_{c,int}=0.6^4/12=0.0108\ m^4$
Moment of inertia of edge columns:	$I_{c,edge}=0.5^4/12=0.0052\ m^4=0.48I_{c,int}$
Moment of inertia of corner columns:	$I_{c,corner}=0.4^4/12=0.00215\ m^4=0.41I_{c,edge}$
Moment of inertia of wall – strong direction (major axis):	$I_w=0.3 \times 5^3/12=3.125\ m^4$
Moment of inertia of wall – weak direction (minor axis):	$I_{w,weak}=5 \times 0.3^3/12=0.01125\ m^4$

Note that a single wall in its weak direction has about the same moment of inertia as the two exterior columns it replaces on the perimeter.

If one interior column, or a wall in its weak direction, are considered equivalent to two edge columns and one edge column as equivalent to two corner ones, all columns in the system and two walls in their weak direction are equivalent to 16+8/2+4/4+2=23 interior columns with an average moment of inertia:

$$I_c = (16 \times 0.0108 + 8 \times 0.0052 + 4 \times 0.00215 + 2 \times 3.125 + 2 \times 0.01125)/23 = 0.01067\,m^4$$

(c) Check of storey torsional radii versus radius of gyration of floor mass

The calculation of the storey torsional radii for the regularity classification of the building should be based on the moments of inertia of all the elements, primary seismic (walls) and secondary seismic (columns of flat slab frames):

$$\Sigma\left(x^2 I_y + y^2 I_x\right) = 4 \times \{12.5^2(3.125 + 2 \times 0.0052 + 2 \times 0.00215) + (7.5^2 + 2.5^2)(4 \times 0.0108 + 2 \times 0.0052)\} = 1953.13\,\mathrm{m}^6,$$

$$\Sigma\left(I_y\right) = \Sigma(I_x) = 16 \times 0.0108 + 8 \times 0.0052 + 4 \times 0.00215 + 2 \times 3.125 + 2 \times 0.01125 = 6.4955\,\mathrm{m}^4,$$

$$r_x = r_y = \sqrt{\frac{1953.13}{6.4955}} = 17.34\,\mathrm{m}.$$

As the mass is uniformly distributed over the rectangular floor area, the radius of gyration of the floor mass in plan, l_s, is: $l_s = \sqrt{(L_x^2 + L_y^2)/12} = \sqrt{2 \cdot 25^2/12} = 10.21\,\mathrm{m} \leq r_x = r_y = 17.34\,\mathrm{m}$.

If only the primary seismic elements are considered, then: $r_x = r_y = L_x/\sqrt{2} = 17.68$ m.

So, the frame system has sufficient torsional rigidity to ensure fundamental translational periods in the two horizontal directions longer than the twisting period and to justify classification of the structural system as planwise regular, no matter the classification of the flat slab frames as secondary elements.

(d) Estimation of the contribution of flat slab frames to the lateral stiffness of the building

The contribution of all flat slab frames to the lateral stiffness of the building, as a fraction of the total lateral stiffness, may be estimated as the ratio of the fraction of the base shear borne by all flat slab frames together, to the total base shear, V_b, when the flat slab frames and the shear walls have the same lateral displacement, either at the roof, or at the level where the resultant lateral force is applied, i.e., at two-thirds of the building height above the top of the basement, H_{tot}.

The top deflection of a vertical cantilever (the two walls, with total moment of inertia $I_w = 2 \times 3.125 = 6.25\ \mathrm{m}^4$) is:

- due to lateral loading with a continuous inverted triangular heightwise distribution (about the same as a set of concentrated forces at floor levels) having force resultant V_b (: base shear):

$$\delta_{w,Vb,top} = \frac{11}{60}\frac{V_b H_{tot}^3}{(EI)_w}$$

- due to a concentrated force F at the top:

$$\delta_{w,F,top} = \frac{1}{3}\frac{F H_{tot}^3}{(EI)_w}$$

The top deflection of a frame system consisting of $m=23$ equivalent interior columns each with moment of inertia $I_c = 0.01067\ \mathrm{m}^4$, connected via beams with moment of inertia $I_b = 0.0007\ \mathrm{m}^4$ and subjected to a concentrated force F at the top that produces a constant storey shear, $V_i = V_{i+1} = F$, is:

$$\delta_{f,F,top} = \frac{1}{12}\frac{F}{m}H^2\left[\frac{H_{tot}}{(EI)_c} + \frac{H_{tot} - H/2}{(EI)_b}\frac{L}{H}\right]$$

The condition: $\delta_{w,Vb,top} - \delta_{w,F,top} = \delta_{f,F,top}$ gives:

$$F = V_b \frac{11/20}{1 + \frac{1}{4}\frac{(EI)_w}{m}\frac{H^2}{H_{tot}^2}\left[\frac{1}{(EI)_c} + \frac{1 - H/(2H_{tot})}{(EI)_b}\frac{L}{H}\right]} = 0.129V_b$$

Therefore, all flat slab frames and the walls in their weak direction may be considered as secondary seismic elements, without their total contribution to lateral stiffness exceeding 15% of that of the primary seismic elements (i.e. 15/115=13.1% of the total lateral stiffness, which is more than the 12.9% share of the frame force F in the base shear). Note that an elastic analysis of the full structural system in 3D, with the in-plane flexibility of the diaphragm taken into account and the flat slab considered as an effective beam with a width of 2.5 m at the interior of the plan or 1.25 m at the perimeter, confirms this result: the total contribution of flat slab frames and of the walls in their weak direction to lateral stiffness is 13.9% of that of the walls in their strong direction. It gives also the following total shear force of all flat slab frames and of the walls in their weak direction as fraction of the base shear:

at the top storey: $0.216V_b$,
at the 6th storey: $0.170V_b$,
at the 5th storey: $0.169V_b$,
at the 4th storey: $0.165V_b$,
at the 3rd storey: $0.147V_b$,
at the 2nd storey: $0.114V_b$,
at the 1st storey: $0.122V_b$.

This confirms the assumption made for the estimation of F: that the total shear force of all flat slab frames and of the walls in the weak direction is (about) constant in all storeys. In fact, it has a tendency to decrease from top to bottom.

Flat slab frames are outside the scope of Eurocode 8. They, as well as the walls in the weak direction, are taken as secondary seismic elements. The full seismic action is resisted by the walls in their strong direction.

(e) Calculation of quasi-permanent gravity loads (per floor and total)

Storeys other than the top one:

- Weight of slab: $25 \times 0.15 = 3.75$ kN/m^2
- Weight of vertical members: $25 \times 2.65 \times (16 \times 0.6^2 + 8 \times 0.5^2 + 4 \times 0.45^2 + 4 \times 5 \times 0.3)/25^2 = 1.55$ kN/m^2
- Floor finishings, etc.: 0.92 kN/m^2
- Partition walls: 1.50 kN/m^2

- Quasi-permanent part of live loads: $0.3 \times 0.8 \times 2 = 0.48$ kN/m^2
- Total: 8.20 kN/m^2
- Storey weight: 8.20×25^2=5125 kN.

Top storey:

- Weight of roof slab: 25×0.15=3.75 kN/m^2
- Roof finishings, etc.: 4.45 kN/m^2
- Quasi-permanent part of live loads: $0 \times 1.0 \times 2 = 0$
- Total: 8.20 kN/m^2
- Storey weight: 8.20×25^2=5125 kN.

Total weight of the superstructure: W=7×5125=35875 kN

(f) Fundamental period.

Thanks to the building's regularity and apparently relatively short natural period ($T_1 < 4T_C$, 2 s), the lateral force analysis procedure may be used. As all storeys have the same mass, the heightwise distribution of seismic lateral loads is linear. Their resultant is applied at two-thirds of the height from the top of the basement. The stiffness of a SDOF system consisting of the two cantilever walls with a total moment of inertia I_w=2×3.125=6.25 m^4 may be taken as equal to the ratio of the force resultant V_b (base shear), to the deflection at two-thirds of the height from the base due to lateral loading with a continuous inverted triangular heightwise distribution (instead of a set of concentrated forces at floor levels):

$$\delta_{w,Vb,2/3} = \frac{368}{3645}\frac{V_b H_{tot}^3}{(EI)_w} \rightarrow K = \frac{V_b}{\delta_{w,Vb,2/3}} = \frac{3645}{368}\frac{(EI)_w}{H_{tot}^3} \rightarrow$$

$$T_1 = 2\pi\sqrt{\frac{M}{K}} = 2\pi\sqrt{\frac{35875/9.81}{\frac{3645}{368}\frac{0.5 \cdot 34000000 \cdot 6.25}{(7 \cdot 2.8)^3}}} = 1.015s$$

Note that the fundamental period of the full structural system in 3D, with the in-plane flexibility of the diaphragm taken into account and neglecting the flexural and shear stiffness of the columns and the walls in their weak direction, is 1.035 s. This is very close to the value estimated above for a SDOF system with all its mass concentrated at the point of application of the lateral force resultant.

(g) Design spectral acceleration

Design ground acceleration on type A ground: a_g=$\gamma_1 a_{gR}$=1.0×0.25=0.25 g.
Behaviour factor: $q = q_o$=3.
For T_1=1.015 s>T_C=0.6 s, Eq. (4.5c) gives for the design spectral acceleration:

$$S_d(T) = 0.25 \times 1.15 \times (2.5/3) \times (0.6/1.015) = 0.1416\,g\ (> 0.2 \times 0.25\,g).$$

As $T_1 < 2T_C = 1.2$ s, we can reduce the base shear by 15% in the lateral force analysis. So, the design spectral acceleration is 0.85×0.1416 g=0.1204 g. For a weight of the superstructure W=35875 kN, the seismic base shear is: V_b=0.1204×35875=4320 kN.

(h) Estimation of the action effects due to the accidental eccentricity

Because the structure is fully symmetric in plan and identical in the two horizontal directions, an accidental eccentricity of a horizontal component of the seismic action, let's say in direction X, e=$0.05L_x$ which is constant in all storeys i, has the following effects on an element at a distance from the centre of mass equal to y in direction Y and to x in direction X:

- for bending in a vertical plane parallel to X, it increases the seismic moments and shears due to the horizontal component in direction X applied at the mass centre, by a factor of

$$1 + \frac{e}{r_y}\frac{|y|}{r_y} = 1 + 0.1\frac{|y|}{L_x};$$

- for bending in a vertical plane parallel to Y, it induces seismic moments and shears similar to those induced by the horizontal component in direction Y applied at the mass centre times

$$\frac{e}{r_x}\frac{|x|}{r_x} = 0.1\frac{|x|}{L_x}.$$

The two walls at the centre of the sides of the perimeter have: $x = L_y/2$, y=0, or x=0, y=$L_x/2$. Then, these factors are equal to 1.05 and to 0.05, respectively.

(i) Interstorey drift ratio check, for the damage limitation seismic action

The interstorey drift ratio at the storey centre of mass is controlled by the deflection of the walls as vertical cantilevers under inverted triangular lateral loading. It attains its maximum value at the top storey, where the axis of the wall rotates most with respect to the vertical. It is equal to the elastic interstorey drift ratio under the design lateral loading (considered for simplicity with a continuous inverted triangular distribution, instead of concentrated forces at floor levels), times the reduction factor ν for the damage limitation seismic action (ν =0.5 for Importance Class II) times the behaviour factor q=3:

$$\frac{\Delta\delta_7}{H} \approx \nu q \frac{1}{28}\frac{V_b H_{tot}^3}{(EI)_w H} = 0.5 \cdot 3 \cdot \frac{1}{28} \cdot \frac{4320 \cdot (7 \cdot 2.8)^3}{(0.5 \cdot 34000000 \cdot 6.25) \cdot 2.8} = 0.00586$$

So the interstorey drift ratio at the top storey exceeds the Eurocode 8 limit of 0.5% for damage limitation of brittle infill walls, but is acceptable for ductile partitions (see Section 1.1.3). An exceedance by about 12% may be considered tolerable,

in view of the fact that the contribution of the flat slab frames to lateral stiffness has been neglected, although it is be available under the damage limitation seismic action and indeed is quite large at the top storey.

An elastic analysis of the full structural system in 3D, with the in-plane flexibility of the diaphragm taken into account but the flexural and shear stiffness of the columns and the walls in their weak direction neglected, gives the following interstorey drift ratios under the damage limitation seismic action:

at the top storey: 0.00627,
at the 6th storey: 0.00619,
at the 5th storey: 0.00591,
at the 4th storey: 0.00534,
at the 3rd storey: 0.00440,
at the 2nd storey: 0.00305,
at the 1st storey: 0.00125.

These values refer to the storey centre and are larger than at the location of the walls, owing to the in-plane flexibility of the diaphragm considered in the analysis.

(j) Estimation and check of 2nd-order (P-Δ) effects through the sensitivity coefficient θ

The sensitivity coefficient θ (Eq. (4.45)) is equal to the interstorey drift ratio under the design seismic action, times the total weight overlying the storey, divided by the storey seismic shear. As in a wall system the reduction of the interstorey drift ratio from the roof to the base is much faster than the increase of the ratio of total weight overlying a storey to the storey seismic shear, θ is largest at the top storey:

$$\theta_7 \approx q\frac{1}{28}\frac{V_b H_{tot}^3}{(EI)_w H}\cdot\frac{W/n_{st}}{2V_b/(n_{st}+1)} = \frac{qW(n_{st}+1)H_{tot}^2}{56(EI)_w}$$
$$= \frac{3\cdot 4320\cdot 8\cdot(7\cdot 2.8)^2}{56\cdot(0.5\cdot 34000000\cdot 6.25)} = 0.0067 \ll 0.1 \rightarrow \text{OK}$$

For comparison, at the ground storey:

$$\theta_1 \approx q\frac{5}{792}\frac{V_b H_{tot}^3}{(EI)_w H}\cdot\frac{W}{V_b} = \frac{5qWn_{st}H_{tot}^2}{792(EI)_w}$$
$$= \frac{5\cdot 3\cdot 4320\cdot 7\cdot(7\cdot 2.8)^2}{792\cdot(0.5\cdot 34000000\cdot 6.25)} = 0.0021.$$

(k) Verification of secondary seismic columns for the deformation-induced seismic action effects

Bending moments and shears in secondary seismic elements are calculated from their cracked stiffness and the deformations imposed on them by the design seismic

action, as obtained from an analysis where the contribution of secondary seismic elements to lateral stiffness is neglected and primary seismic elements are modelled with their cracked stiffness. These moments and shears should be less than the design flexural and shear resistance M_{Rd} and V_{Rd}, respectively, determined according to Eurocode 2.

According to (j) above, the interstorey displacement due to the design seismic action is maximum at the top storey:

$$\Delta\delta_7 \approx q\frac{1}{28}\frac{V_b H_{tot}^3}{(EI)_w} = 3\cdot\frac{1}{28}\cdot\frac{4320\cdot(7\cdot 2.8)^3}{0.5\cdot 34000000\cdot 6.25} = 0.033\,\mathrm{m}$$

At the ground storey, by contrast:

$$\delta_1 \approx q\frac{5}{792}\frac{V_b H_{tot}^3}{(EI)_w} = 3\cdot\frac{5\cdot 4320\cdot(7\cdot 2.8)^3}{792\cdot(0.5\cdot 34000000\cdot 6.25)} = 0.0058\,\mathrm{m}$$

If $V_{\mathrm{Ec,n}}$ is the (discounted) seismic shear of an interior column at the top storey ($i=n$), the interstorey deflection of that column is:

$$\Delta\delta_7 \approx \frac{V_{Ec,n}H^2}{12}\left[\frac{H}{(EI)_{c,}} + \frac{L}{(EI)_b}\right]$$

where for the column: EI_{c}=0.5 × 34000000 × 0.01067 kNm^2 and for the equivalent beam of the flat slab: EI_{b}=0.5 × 34000000 × 0.0007 kNm^2

If the interstorey deflection of an interior top storey column is equal to the value of 0.033 m imposed by the wall deformation, $V_{\mathrm{Ec,n}}$=116 kN is obtained, for which the end moments is: $M_{\mathrm{Ec,n}}$=116 × 2.65/2=153.6 kNm.

In a real design case, the elastic moments and shears in secondary seismic elements induced by the deformations imposed on them by the design earthquake acting on the system of primary elements alone, may be estimated from an elastic analysis of the full structural system in 3D (in this case with all columns and the flat slab included) under lateral forces that produce in the primary seismic elements in total the full design seismic base shear, V_{b}, multiplied by the q-factor. So, elastic moments and shears in the secondary elements from the elastic analysis of the full structural system in 3D, performed above to verify that the total contribution of secondary elements to lateral stiffness is less than 15% of that of primary elements, should be multiplied by q and divided by the fraction of the base shear taken by the primary seismic elements. In this case that analysis gave a total base shear in all flat slab frames and the weak direction of the walls 12.2% of the total base shear (see end of Section (d) above). So, the multiplicative factor is: $qV_{\mathrm{b}}/(V_{\mathrm{b}}–0.122V_{\mathrm{b}})$=3.42. This exercise gives an elastic seismic shear in the top storey of a column near the centre in plan equal to 136 kN and corresponding end moments 236 and 125 kNm at the top and bottom section of that column, respectively. The maximum bending moment estimate in an interior column is 369 kNm and happens at the ground

storey, because that column has a point of inflection near the level of the 1st floor. To seek a hand-calculation approximation of that result, the 1st floor deflection of the system of primary seismic elements, estimated above as 0.0058 m, is set equal to the tip deflection of a ground storey column considered as a cantilever over the full storey height:

$$\delta_1 \approx \frac{V_{Ec,1} H^3}{3(EI)_c}$$

This gives: $V_{\mathrm{Ec},1}$=144 kN and a moment at the bottom section of 144 × 2.65=381 kNm.

– Check of interior columns in flexure:

  - The minimum vertical reinforcement ratio of secondary columns is, according to Eurocode 2, 0.2%. For an interior column, eight 14 mm-dia. bars (1230 mm^2), engaged at a corner of either the perimeter hoop or of a diamond-shaped tie around the mid-side bars, give ρ=0.342%, d_1=0.035 m, d=0.6–0.035=0.565 m, δ_1=0.035/0.565=0.062. Then for the tension and the compression reinforcement: $\omega_1=\omega_2=$ 0.25 × 1230 × (500/1.15)/(565 × 600 × 35/1.5)=0.0169 and for the web reinforcement: $\omega_\mathrm{v}=2\omega_1$ =0.0338.
  - At the top storey the axial load is N=5 × 5 × 8.2=205 kN, giving $\nu_\mathrm{d}=N/bdf_\mathrm{cd}=$ 205/(0.565 × 0.6 × 35000/1.5)=0.0259, i.e., less than the value of 0.106 of the left-hand-side of Eq. (3.51). Then Eq. (3.54) applies, giving ξ=0.084 and the design value of moment resistance from Eq. (3.59) is: $M_{\mathrm{Rdc,n}}$=346 kNm>$M_{\mathrm{Ec,n}}$.
  - At the ground storey we have N=7 × 205=1435 kN, giving ν_d=7 × 0.0259=0.181 which meets Eq. (3.52): 0.106≤ν_d≤0.506. So from Eq. (3.52) we get ξ=0.249 and Eq. (3.60) gives a design value of the moment resistance $M_{\mathrm{Rdc},1}$=795 kNm>$M_{\mathrm{Ec},1}$.

– Check of interior columns in shear:

  - Maximum stirrup spacing according to Eurocode 2:
    – max s_w=min{20d_bL; h_c; b_c; 400 mm}, or
    – max s_w=0.6 min{20d_bL; h_c; b_c; 400 mm} at lap-splices of vertical bars.
    In this case, a 8 mm-dia. perimeter hoop and diamond-shaped ties engaging the mid-side vertical bars, both @ 165 mm centres, fulfil the 2nd and more stringent maximum spacing, providing $\rho_\mathrm{w}=$ (2+$\sqrt{2}$) × 50.25/(165 × 600)=0.00173.

  - Shear resistance of the column for shear compression according to Eurocode 2:

$$V_{\mathrm{Rd,max}} = 0.3(1 - f_{\mathrm{ck}}(\mathrm{MPa})/250) b_\mathrm{w} z f_\mathrm{cd} \ \sin 2\,\delta \ (1 \le \cot\delta \le 2.5).$$

$$V_{\mathrm{Rd,max}} = 0.3 \times (1 - 35/250) \times 0.6 \times 0.9 \times 0.565 \times (35000/1.5)\ \sin 2\,\delta$$
$$= 1269\,\mathrm{kN}, \text{ for } \cot\delta = 2.5.$$

- Shear resistance of the column due to the shear reinforcement, according to Eurocode 2:
  $V_{\mathrm{Rd,s}}=b_{\mathrm{w}}z\rho_{\mathrm{w}}f_{\mathrm{ywd}}$ cot $\delta+N_{\mathrm{Ed}}(h–x)/H_{\mathrm{cl}}$, where the neutral axis depth, $x=\xi d$, may be taken equal to that at the moment resistance of the column.
  - Top storey: $V_{\mathrm{Rd,s}}=0.6 \times 0.9 \times 0.565 \times 0.00173 \times (500000/1.15) \times 2.5+205 \times (0.6–0.084 \times 0.565)/2.65 = 616.5$ kN.
  - Ground storey: $V_{\mathrm{Rd,s}}=0.6 \times 0.9 \times 0.565 \times 0.00173 \times (500000/1.15) \times 2.5+1435 \times (0.6–0.249 \times 0.565)/2.65 =822.5$ kN.

  There is ample safety margin in shear.

(l) Design bending moments of the shear walls

The seismic base shear is shared equally by the two walls which are parallel to the horizontal seismic action component, producing at the base of each wall:

- a bending moment equal to $(2/3) \times (7 \times 2.8) \times 4320/2=28225$ kNm,
- increased for the accidental eccentricity to $M_{\mathrm{Ed,o}}=1.05 \times 28225=29635$ kNm.

The design envelope of seismic bending moments increases linearly from zero at roof level to the maximum value, $M_{\mathrm{Ed,o}}$, at the base. It is then displaced upwards by the tension shift length, a_{l}, which should be consistent with the strut inclination taken in the ULS verification for shear. The Eurocode 2 approximation is to take a_{l} as 50% of the internal lever arm of the wall, $\sim 0.8l_{\mathrm{w}}$, times the strut inclination taken in the ULS verification for shear, cot δ: $a_{\mathrm{l}}=0.5 \times 0.8l_{\mathrm{w}}$ cot $\delta=2$ cot δ (in m). So the design moment at a height z above the base of the wall is:

$$M_{\mathrm{d}}(\mathrm{z}) = M_{\mathrm{Ed,o}}[1 - \max(0; z - 2\cot\delta)/H_{\mathrm{tot}}].$$

(m) Dimensioning of vertical reinforcement at the base section of the walls for the ULS in flexure

At its base each wall W1 has collected from its tributary floor area gravity loads equal to $N_{\mathrm{d}}=7 \times 2.5 \times 10 \times 8.2= 1435$ kN. The vertical reinforcement at the base of the wall may be estimated as follows.

The web reinforcement is chosen first: 14 mm-dia. bars @ 200 mm centres, are placed near each face of the web, giving 1540 mm^2/m and $\rho=1540/(300 \times 1000)=0.51\%$, i.e. above the minimum required of 0.2%. In walls the internal lever arm of the section is commonly taken equal to $z=0.8l_{\mathrm{w}}$, giving:

- effective depth $d=4.5$ m;
- distance of compression reinforcement from extreme fibres $d_1=0.5$ m and $\delta_1=0.5/4.5=0.111$;

– mechanical ratio of web reinforcement: $\omega_v = 1540 \times 4 \times (500/1.15)/(4500 \times 300 \times 35/1.5) = 0.085$.

At the base section we have $\nu_d = N/bdf_{cd} = 1435/(4.5 \times 0.3 \times 35000/1.5) = 0.0456$, i.e., less than the limit value of 0.187 at the left-hand-side of Eq. (5.42a). Solving the nonlinear system of Eqs. (5.45a) and (5.46a), we estimate $\xi \approx 0.2$ and $\omega_1 = \omega_2 \approx 0.18$, which gives:

$$A_{s1} \approx 0.18 \times 4500 \times 300 \times (35/1.5)/(500/1.15) \approx 13000\,\text{mm}^2.$$

This reinforcement area should be placed in a boundary element near each edge of the section. Because the web reinforcement of 1540 mm^2/m is considered above to extend up to the centroid of the tension reinforcement, i.e. to a distance $(l_w\text{-}z)/2 = 0.1l_w = 0.5$ m from the edge of the section, the corresponding reinforcement area of $1540 \times 0.5 = 770$ mm^2 should be added to the $\sim$13000 mm^2 of tension reinforcement area estimated above, giving a total of $\sim$13770 mm^2.

Twenty-eight 25 mm-dia bars (13740 mm^2) are placed in each boundary element near the section edge. For transverse reinforcement between these bars and the concrete surface with 12 mm diameter, the centre of the 25 mm-dia bars is: $c + d_{bh} + d_{bL}/2 \sim 0.02 + 0.012 + 0.025/2 \sim 0.045$ m from the nearest concrete surface.

The length of a boundary element corresponding to the maximum allowable steel ratio of 0.04 in each boundary element is about $13740/(0.04 \times 300) = 1145$ mm. This exceeds the minimum required length of $\max(0.15l_w, 1.5b_w) = 0.75$ m. Four out of the 28 bars are arranged closest to the extreme fibres of the section, in a row parallel to the short side of the wall and at a distance of 45 mm from it. The remaining 24 bars are placed at a distance of 45 mm from the surface of the long sides of the section, at 85 mm centres (see section at the bottom of Fig. 5.10(a)). This gives a total length of the boundary element: $l_c = 2 \times 0.045 + 12 \times 0.085 = 1.11$ m and reinforcement ratio in each boundary element equal to: $\rho = 13740/(1110 \times 300) = 4.125\%$, slightly over the maximum of 4%.

If $l_c > \max(2b_w, l_w/5) = 1.0$ m, the thickness of the boundary element, b_w, should be at least 200 mm and at least 10% of the storey height, $H = 2.8$ m, i.e. at least 280 mm. In this case $b_w = 300$ mm is sufficient.

Within the length of $5 - 2 \times 1.11 = 2.78$ m between the boundary elements at the opposite edges of the section, thirteen 14 mm-dia. bars @ 200 mm centres are provided near each face of the web. For the boundary element reinforcement arranged within a length $l_c = 1.11$ m from the edge of the section, about $0.61 \times 1540 = 940$ mm^2 out of the 13740 mm^2 of vertical steel in the boundary element belongs to the web reinforcement of 1540 mm^2/m, considered to extend up to the centroid of the tension reinforcement of the section. The balance of $13740 - 940 = 12800$ mm^2 is the actual additional reinforcement of the boundary element. Its centroid is at a distance from the short side of the section equal to: $[490.9 \times (2 \times 45 + 26 \times 1110/2) - 940 \times (500 + (1110 - 500)/2)]/12800 \approx 500$ mm. This confirms the values $d = 4.5$ m and $d_1 = 0.5$ m adopted so far on the basis of the internal lever arm value of $0.8l_w = 4.0$ m.

For: δ_1=0.5/4.5=0.111; $\omega_1=\omega_2$= 12800 × (500/1.15)/(4500 × 300 × 35/1.5)= 0.1767; ω_v=0.085; ν_d=0.0456; Eqs. (3.54) and (3.59) give a moment resistance at the base section $M_{Rd,o}=M_{Rd}(0)$=29900 kNm≈$M_{Rd,o}$.

(n) Design shear forces of walls W1

The inverted triangular lateral forces that approximate the seismic loading at storey i:

$$F_i = 2V_b i/n_{st}(n_{st}+1),$$

produce storey shears:

$$V_i = V_b(n_{st}+i)(n_{st}+1-i)/n_{st}(n_{st}+1)$$

shared equally by the two walls W1 which are parallel to the horizontal seismic action component. The design storey shear of each wall from the analysis is further multiplied by 1.05 for the accidental eccentricity. The seismic base shear is V_b=0.1204 × 35875=4320 kN. Taking into account the amplification factor ε=1.5 of Eq. (1.16) on the storey shears of each wall from the analysis, V'_{Ed}, the design storey shear of each wall W1 at storey i is (in kN):

$$\begin{aligned} V_{Ed}(i) &= 0.5 \times 1.05\varepsilon V_b(n_{st}+i)(n_{st}+1-i)/n_{st}(n_{st}+1) \\ &= 3402(n_{st}+i)(n_{st}+1-i)/n_{st}(n_{st}+1). \end{aligned}$$

Note that Eq. (1.15) gives an amplification factor ε for DC H (for M_{Rdo}=29900 kNm, M_{Edo}=29635 kNm, T_1=1.015 s>T_C=0.6 s and for q=4 in DC H) ε=2.46. Therefore, for DC H and taking into account the higher value of the behaviour factor (q=4, in lieu of q=3), the design storey shear of each wall W1 at storey i would had been 23% higher.

(o) Verification of walls W1 for the ULS in shear and dimensioning of their shear reinforcement

The "critical region" of the wall extends up to a height from the base: $h_{cr}\geq\max(l_w, H_{tot}/6)$=5 m, which is less than the upper limit of $\min(2l_w, 2H)$=5.6 m from the base for walls with more than 6 storeys.

The shear resistance of DC M walls for diagonal compression is as specified in Eurocode 2 for non-seismic actions: $V_{Rd,max}=0.3(1-f_{ck}(\text{MPa})/250)b_w z f_{cd} \sin 2\delta$ ($1\leq\cot\delta\leq 2.5$).

$$\begin{aligned} \text{For } \cot\delta = 1:\ V_{Rd,max} &= 0.3(1-35/250)\times 0.3\times 0.8\times 5\times(35000/1.5) \\ &= 7220\,\text{kN} \geq V_{Ed}(1) = 3402\,\text{kN}. \end{aligned}$$

Note that with the reduction by 60% of $V_{Rd,max}$ in the critical region of DC H walls, we would have $V_{Rd,max}$=0.4 × 7220=2888 kN for DC H, which is less than the design shear of 1.23 × 3402=4185 kN for DC H. Because of the large

shortfall of shear resistance if the wall had been designed for DC H, it is prudent not to increase the value of cot δ above the lower limit of cot δ=1, notwithstanding the large margin between $V_{Rd,max}$ = 7220 kN and $V_{Ed}(1)$ =3402 kN in the design for DC M. This margin would had allowed reducing the strut inclination so that sin2δ=3402/7220=0.47, which nominally corresponds to cot δ=4. So, the upper limit value cot δ=2.5 could have been employed in the critical region of the DC M wall design.

The horizontal reinforcement ratio $\rho_h=A_{sw}/(b_w s_h)$ of slender walls is as in Eurocode 2, i.e. for a design resisting shear of: $V_{Rd,s}=b_w z \rho_w f_{ywd}$ cot δ, $1 \le \cot \delta \le 2.5$. Table 5.7 shows the outcome of its calculation for the limit values of cot δ. Recall that we have opted for the safe-sided value cot δ=1 in the critical region, i.e. in the 1st and 2nd storey. So, the 1st and 2nd storey results for cot δ=2.5 are shown in parentheses, as they will not be applied.

Design with cot δ =2.5 gives total savings of 600 kg in horizontal reinforcement. The implications of the two alternative values of cot δ on the curtailment of vertical reinforcement are considered below.

(p) Dimensioning and curtailment of wall vertical reinforcement above the base for the ULS in flexure

The axial force in wall W1 (in kN) has a stepwise reduction at storey floors. In storey i (i=1 at the base of the building) it is: $N_d(i)=1435[1-(i-1)/n_{st}]$, where n_{st}=7 is the total number of storeys.

With the design moment decreasing with increasing height z from the base of the wall as: $M_d(z)= M_{Ed,o}[1-\max(0; z-2 \cot \delta)/H_{tot}]$, the vertical reinforcement provided at the base should be continued and anchored beyond the section at a distance from the base z=2 cot δ (in m).

The web reinforcement of 14 mm-dia. bars @ 200 mm centres is continued to the top of the wall. There, a curtain of twenty-five 14 mm-dia. bars @ 200 mm centres is provided near each face of the wall, with the 1st and the last bar at 100 mm from the edge of the section (top of Fig. 5.10(a)). To see if, and up to which level, this reinforcement is sufficient for the design seismic moments of the top storey, the moment resistance, M_{Rd}, provided by this web reinforcement alone is calculated for:

- $\omega_1=\omega_2=0$;
- d=5 m and δ_1=0/5=0 (because the 1st and the last of the 14 mm-dia. bars @ 200 mm centres are at 100 mm from the end of the section while their influence reaches up to bar mid-distance, i.e. for 100 mm on each side of the bar, which is to the extreme fibres of the wall);
- ω_v=1540 × (500/1.15)/(1000 × 300 × 35/1.5)=0.0957 (for web reinforcement of 1540 mm^2/m);
- two values of the axial load ratio:
  - one for cot δ=1, guessing that the level, z, we are looking for is within the 2nd storey from the top: ν_d=2 × 205/(5 × 0.3 × 35000/1.5)=0.0117, and

Table 5.7 Dimensioning of wall horizontal reinforcement for two alternative strut inclinations

		Design for cot $\delta=1$		Design ρ_h for cot $\delta=1$	
Storey($i=1$ at base)	Design at shear V_{Ed}(kN)	ρ_h(%)	Horizontal reinforcement	ρ_h(%)	Horizontal reinforcement
1	3402	0.652	Two 12 mm-dia. @ 115 mm	(0.261)	Two 12 mm-dia. @ 290 mm
2	3280.5	0.629	Two 12 mm-dia. @ 120 mm	(0.252)	Two 12 mm-dia. @ 300 mm
3	3037.5	0.582	Two 12 mm-dia. @ 130 mm	0.233	Two 12 mm-dia. @ 325 mm
4	2673	0.512	Two 12 mm-dia. @ 145 mm	0.205	Two 12 mm-dia. @ 365 mm
5	2187	0.419	Two 12 mm-dia. @ 180 mm	0.168	Two 12 mm-dia. @ 450 mm
6	1579.5	0.303	Two 12 mm-dia. @ 250 mm	0.128[a]	Two 10 mm-dia. @ 400 mm[a]
7	850.5	0.163	Two 10 mm-dia. @ 320 mm	0.128[a]	Two 10 mm-dia. @ 400 mm[a]

[a]Governed by the minimum requirements: $\rho_h \geq \max(0.1\%, 0.25\rho_v)$, $s_h \leq 400$ mm.

- another for cot δ=2.5, guessing that the level, z, we are looking for is in the top storey, where $N_d(i = n_{st})$ =205 kN: ν_d=205/(5 × 0.3 × 35000/1.5)=0.0059.

Eq. (3.51) becomes: –0.0957 < ν_d < 0.5217 and is met by both values of ν_d above (i.e., the extreme bars of the web reinforcement at the tension or the compression side have yielded when the extreme compression fibres reach ε_{cu}=0.0035). So Eq. (3.52) applies for ξ and (3.60) for the moment resistance, M_{Rd}, giving:

- For cot δ=1, ξ=0.1075 and M_{Rd}=8490 kNm. For $M_{Ed,o}$=29635 kNm, $M_d(z)$=$M_{Ed,o}$[1–(z–2 cot δ)/H_{tot}] is equal to M_{Rd}=8490 kNm at z=16 m, and the web reinforcement alone suffices above that level.
- For cot δ=2.5, ξ=0.102 and M_{Rd}=8135 kNm. $M_d(z)$ is equal to M_{Rd}=8490 kNm at z=19.2 m, i.e. just 0.4 m below the top of the building.

Below the z-levels determined above, the web reinforcement should be supplemented with some of the 25 mm-dia. bars placed at lower levels near the edge of the section; let's say, at each edge of the wall with four 25 mm-dia. bars within a vertical plane parallel to the short side of the section (2nd from the top in Fig. 5.10(a)).

The 14 mm-dia. bars of the web need anchorage length $l_b = (f_{yd}/f_{bd})(d_b/4) = (500/1.15)/(2.25 \times 2.2/1.5)d_b/4 = 33d_b = 465$ mm, starting at the bottom surface of the roof slab, i.e. 150 mm below the top of that slab. To accommodate this length, the end of each 14 mm-dia. bar should be bent to a 90°-hook. The axis of the horizontal length of the bent bar should be at least 27 mm below the top surface of the roof slab, to provide at least 20 mm of cover. To avoid damaging a bar when bending it, Eurocode 2 requires a mandrel diameter of at least 4 bar diameters for bars with not more than 16 mm-dia. (mandrel radius 2 × 14 mm=28 mm). According to Eurocode 2, this minumum mandrel diameter can be taken to prevent also damage to the concrete by the high bearing pressures exerted on it by the bent, if

1. the straight length required past the end of the bend for anchorage of the bar is not more than the 5 bar diameters used in "standard hooks"; and
2. the plane of bending is not close to the surface of the concrete face and, besides, there is a cross bar inside the bend with diameter at least equal to that of the bent bar.

If one of these conditions is not met (here the 14 mm-dia. bars do not meet condition 1) then, according to Eurocode 2, to avoid damage to the concrete, the value of the mandrel diameter, d_m, should be not less than $F_{bt}[(1/a_b)+1/(2d_b)]/f_{cd}$ where F_{bt} is the tensile force in the bent bar at the start of the bend and a_b is the distance from the bar centre to the nearest concrete surface parallel to the plane of the bend, or from the mid-point to the closest parallel bent bar (whichever is smaller). In the present case, with the web bars @ 200 mm centres and the 1st and the last one of them at 100 mm from the end of the section we have: a_b=min[200/2; 100]=100 mm. F_{bt} is equal to $f_{yd}\pi d_b^2/4$ times the ratio of the distance of the start of the bend to the end of the bar (total anchorage length reduced by the straight

anchorage length before the bend), to the required anchorage length, l_b. As the axis of a bent 14 mm-dia. bar should be at least 27 mm below the top surface of the roof slab to provide at least 20 mm of cover for its horizontal portion, the bent bar should start 27 mm+d_m/2 below the top surface of the roof slab, providing a straight part of the bar anchorage before the bend equal to (in mm) 150–27–d_m/2. Therefore, with dimensions in mm:

$$d_m \geq [1/a_b + 0.5/d_b][33d_b - (150 - 27 - d_m/2)]f_{yd}\pi d_b^2/(4l_b f_{cd}) = [1/100 + 0.5/14][342 + d_m/2]\pi d_b(500/1.15)/(4 \times 33 \times 35/1.5),$$

giving $d_m \geq$ 113 mm or 8.1d_b. So, the 14 mm-dia. web bars should be bent around a mandrel diameter of 115 mm, starting at a point approximately 85 mm below the top of the roof slab. This provides a straight anchorage length of 65 mm before the bend. A horizontal length of 465–65-(π/4) $\times$ 115=310 mm should be provided after the bend, for full anchorage of the 14 mm-dia. bars.

If cot δ=1 is used, curtailment of the *four outermost 25 mm-dia. bars* (those within a vertical plane parallel to the short side of the wall section and 45 mm from it) at z=16 m (i.e. 0.8 m below the floor of the 7th storey) is followed by a straight anchorage length l_b=33d_b=0.825 m. So, these four bars should continue *up to z=16.8 m, i.e. exactly to the top of the floor of the top storey* (Fig. 5.10(b)).

If cot δ=2.5 is used, the outermost four 25 mm-dia. bars are curtailed at z=19.2 m (i.e., 0.4 m below the roof top, Fig. 5.10(c)). To accommodate the anchorage length of l_b=33d_b=0.825 m above that level, the 25 mm-dia. bars should be bent into a 90°-hook horizontally. To avoid damaging a bar when bending it, Eurocode 2 requires a mandrel diameter of at least 7 bar diameters, for bars of more than 16 mm-dia. (mandrel radius 3.5 $\times$ 25 mm=87.5 mm). Regarding the mandrel diameter needed according to Eurocode 2 to avoid damage to the concrete, as the 25 mm-dia. bars continued to the roof and anchored there are at (300–2 $\times$ 45)/3=70 mm centres, we have: a_b=min[70/2; 45]=35 mm. Regarding the calculation of F_{bt} as $f_{yd}\pi d_b^2/4$ times the ratio of the distance of the start of the bend to the tip of the bar (total anchorage length minus the straight part of it before the bend), to the required anchorage length, l_b, it is noted that the axis of the bent bar should be at least 32.5 mm below the top surface of the roof slab, for at least 20 mm of cover to its horizontal length. So the bent bar should start 32.5 mm+d_m/2 below the top surface of the roof slab, providing a straight anchorage length before the bend of 400–32.5–d_m/2 (in mm). Therefore, with dimensions in mm, we need a mandrel diameter: $d_m \geq [1/a_b+0.5/d_b][33d_b-(400-32.5-d_m/2)]f_{yd}\pi d_b^2/(4l_b f_{cd}) =$ [1/35+0.5/25][457.5+d_m/2]πd_b(500/1.15)/(4 $\times$ 33 $\times$ 35/1.5), giving $d_m \geq$ 335 mm or 13.5d_b. So, the 25 mm-dia. bars should be bent around a mandrel diameter of 335 mm, starting at a point approximately 32.5+d_m/2=200 mm below the top of the roof slab. This provides a straight anchorage length of 200 mm before the bend. Therefore, for full anchorage of the 25 mm-dia. bars a horizontal length of 825–200–(π/4) $\times$ 335=160 mm should be provided after the bend (top of Fig. 5.10(c)).

To determine the level, z, down to which the four 25 mm-dia. bars at a distance d_1=45 mm from the edge of the section, plus the web reinforcement of 14 mm-dia.

bars @ 200 mm centres (with the 1st and the last bar 100 mm from the section's edge) suffice, the design value of moment resistance, M_{Rd}, is calculated with:

- d=5–0.045=4.955 m and δ_1=45/4955=0.009;
- $\omega_1=\omega_2=4 \times 490.9/(4955 \times 300) \times (500/1.15)/(35/1.5)=0.0246$;
- $\omega_v=1540 \times 5/(4955 \times 300) \times (500/1.15)/(35/1.5)=0.0965$;
- two values of the axial load ratio:

  - one for cot δ=1, guessing that the level, z, we are looking for is within the 3rd storey from the top: $\nu_d=3 \times 205/(4.955 \times 0.3 \times 35000/1.5)=0.0177$; then, ξ=0.1155 and M_{Rd}=12975 kNm, which is equal to $M_d(z)=M_{Ed,o}[1-(z-2 \text{ cot } \delta)/H_{tot}]$ at z=13.02 m; including $l_b=33d_b$=0.825 m for anchorage of the bars coming from below, *the four 25 mm-dia. bars next to each edge* of the section, plus the web reinforcement, are *not sufficient below z=13.85 m (0.15 m below the floor of the 2nd storey from the top*, Fig. 5.10(b)).
  - another for cot δ=2.5, guessing that the level, z, we are looking for is within the 2nd storey from the top: $\nu_d=2 \times 205/(4.955 \times 0.3 \times 35000/1.5)=0.0118$; then, ξ=0.11 and M_{Rd}=12630 kNm, which is equal to $M_d(z)=M_{Ed,o}[1-(z-2 \text{ cot } \delta)/H_{tot}]$ at z=16.25 m; with $l_b=33d_b$=0.825 m for anchorage of the bars coming from below, the four 25 mm-dia. bars next to each edge of the section, plus the web reinforcement, are not sufficient below: z=17.1 m, i.e. 0.3 m above the floor of the top storey, Fig. 5.10(c).

The twenty four 25 mm-dia. bars arranged at each far end of the base section parallel to the long sides should be gradually introduced between level $z=2 \text{ cot } \delta$ (plus straight anchorage) on one hand and z=13.85 m for cot δ=1, or z=17.2 m for cot δ=2.5 on the other. The difference between these two levels corresponds to about four storeys. So, these twenty four 25 mm-dia. bars are curtailed in four groups of three pairs of bars each, starting from the pairs closest to the centre of the section and proceeding towards the edge, Fig 5.10(a). We determine next the four levels where each group of three pairs of 25 mm-dia. bars is curtailed.

We start with the search for level, z, down to which it is sufficient to have (a) four 25 mm-dia. bars at a distance of 45 mm from each end of the section, plus (b) three pairs of 25 mm-dia. bars at 85 mm centres parallel to the long side, with the first one at 45+85=130 mm from the end of the wall section, plus (c) the web reinforcement of 14 mm-dia. bars @ 200 mm centres (with the 1st and the last bar 500 mm from the end of the section, see 3rd section from the top in Fig. 5.10(a)). To this end, we calculate the corresponding design value of moment resistance, M_{Rd}. The ten 25 mm-dia. bars near each of the end of the section occupy an end length of the wall section equal to 0.045+3 × 0.085+0.045=0.345 m from the edge of the section. About 0.2×1540=310 mm^2 out of the 4910 mm^2 of the ten 25 mm-dia bars of that end belong to the web reinforcement of 1540 mm^2/m. The balance of 4910–310=4600 mm^2 is the actual additional tension or compression reinforcement of the section. Its centroid is at: $[490.9 \times (2 \times 45+8 \times 345/2)-310 \times (140+(345-140)/2)]/4600 \approx 140$ mm from the section edge. So:

- d_1=0.14 m, d=5–0.14=4.86 m and δ_1=0.14/4.86=0.029;
- $\omega_1=\omega_2$=4600 × (500/1.15)/(4860 × 300 × 35/1.5)=0.0588;
- ω_v=1540 × (4.86–0.14)/(4860 × 300) × (500/1.15)/(35/1.5)=0.0929;
- two values of the axial load ratio are of interest:
  - one for cot δ=1, guessing that the level, z, we are looking for is within the 4th storey from the top: ν_d=4 × 205/(4.86 × 0.3 × 35000/1.5)=0.0241; then, ξ=0.1225 and M_{Rd}=18070 kNm, which is equal to $M_d(z)=M_{Ed,o}[1-(z-2 \cot \delta)/H_{tot}]$ at z=9.65 m; with $l_b=33d_b$=0.825 m for anchorage of the bars coming from below, the *ten outermost 25 mm-dia. bars* near each edge of the section, plus the web reinforcement, *suffice down to z=10.5 m (0.7 m below the floor of the 5th storey,* Fig. 5.10(b)*)*.
  - another for cot δ=2.5, guessing that the level, z, we are looking for is within the 3rd storey from the top: ν_d=3 × 205/(4.86 × 0.3 × 35000/1.5)=0.0181; then, ξ=0.1165 and M_{Rd}=17675 kNm, which is equal to $M_d(z)=M_{Ed,o}[1-(z-2 \cot \delta)/H_{tot}]$ at z=12.9 m; including $l_b=33d_b$=0.825 m for anchorage of the bars coming from below, the ten outermost 25 mm-dia. bars near each edge of the section, plus the web reinforcement, suffice down to z=13.75 m, i.e. 0.25 m below the floor of the 6th storey, Fig. 5.10(c).

Below the z-level established above, another set of three pairs of 25 mm-dia. bars is added near each far end of the wall section, at 85 mm centres parallel to the long sides.

To determine the level, z, down to which it is sufficient to have (see 3rd section from the top in Fig. 5.10(a)): (a) four 25 mm-dia. bars at 45 mm from each far end of the section, plus (b) 6 pairs of 25 mm-dia. bars at 85 mm centres parallel to the long side, with the 1st pair at 45+85=130 mm from the end of the wall section, plus (c) the web reinforcement of 14 mm-dia. bars @ 200 mm centres (with the 1st and the last bar 700 mm from the end of the section), the corresponding design moment resistance, M_{Rd}, is computed. The sixteen 25 mm-dia. bars near each end of the section occupy a length of 0.045+6 × 0.085+0.045=0.6 m from the edge. Then, about 0.35 × 1540=540 mm^2 out of the 7855 mm^2 of the sixteen 25 mm-dia bars of that end belong to the web reinforcement of 1540 mm^2/m and the actual area of the additional tension or compression reinforcement is 7855–540=7315 mm^2. Its centroid is at [490.9 × (2 × 45+14 × 600/2)–540 × (255+(600–255)/2)]/7315≈255 mm from the edge of the section. So,

- d_1=0. 255 m, d=5–0. 255=4.745 m and δ_1=0. 255/4.745=0.054;
- $\omega_1=\omega_2$=7315 × (500/1.15)/(4745 × 300 × 35/1.5)=0.0958;
- ω_v=1540 × (4.745–0.255) × (500/1.15)/(4745 × 300 × 35/1.5)=0.0905;
- two values of the axial load ratio are considered:
  - one for cot δ=1, guessing that the level, z, we are looking for is within the 5th storey from the top: ν_d=5 × 205/(4.745 × 0.3 × 35000/1.5)=0.0309; this value of ν_d is less than that of the left-hand-side of Eq. (3.51); then from Eqs. (3.54) and (3.59): ξ=0.135 and M_{Rd}= 22700 kNm, which is equal to $M_d(z)=M_{Ed,o}[1-(z-2 \cot \delta)/H_{tot}]$ at z=6.6 m; with $l_b=33d_b$= 0.825 m for

anchorage of the bars coming from below, the *sixteen outermost 25 mm-dia. bars* near each edge of the section, plus the web reinforcement, *suffice down to z=7.4 m, i.e. 1.0 m below the floor of the 4th storey*, Fig. 5.10(b).

- another for cot δ=2.5, guessing that the level, z, we are looking for is within the 4th storey from the top: ν_d=4 × 205/(4.745 × 0.3 × 35000/1.5)=0.0247; as above we get ξ=0.135 and M_{Rd}=22320 kNm, which is equal to $M_d(z)=M_{Ed,o}[1-(z-2 \cot \delta)/H_{tot}]$ at z=9.85 m; with $l_b=33d_b$=0.825 m for anchorage of the bars coming from below, the sixteen outermost 25 mm-dia. bars near each edge of the section, plus the web reinforcement, suffice down to z=10.65 m, i.e. 0.55 m below the floor of the 5th storey, Fig. 5.10(c).

Below the z-level established above, another set of three pairs of 25 mm-dia. bars is added at each end of the wall, at 85 mm centres parallel to its long side.

To determine the level, z, down to which it is sufficient to have (see 2nd section from the bottom in Fig. 5.10(a)): (a) four 25 mm-dia. bars at a distance of 45 mm from each end of the section, plus (b) nine pairs of 25 mm-dia. bars at 85 mm centres parallel to the long side, the 1st pair at 45+85=130 mm from the edge of the wall section, plus (c) the web reinforcement of 14 mm-dia. bars @ 200 mm centres (with the 1st and the last bar 900 mm from the edge of the section), the corresponding design moment resistance, M_{Rd}, is computed. If the 22 bars near each end occupy 0.045+9 × 0.085+0.045=0.855 m from the edge, about 0.48 × 1540=740 mm^2 out of the 10800 mm^2 of the twenty-two 25 mm-dia bars of that end belong to the web reinforcement of 1540 mm^2/m. The balance of 10800–740=10060 mm^2 is the actual additional tension or compression reinforcement in the section. Its centroid is at [490.9 × (2 × 45+20 × 855/2)–740 × (375+(855–375)/2)]/10060≈375 mm from the edge. So:

- d_1=0.375 m, d=5–0.375=4.625 m and δ_1=0.375/4.625=0.08;
- $\omega_1=\omega_2$=10060 × (500/1.15)/(4625 × 300 × 35/1.5)=0.1351;
- ω_v=1540 × (4.625–0.375) × (500/1.15)/(4625 × 300 × 35/1.5)=0.0879.
- two values of the axial load ratio are of interest:

  - one for cot δ=1, guessing that the level, z, we are looking for is at the 2nd storey: ν_d= 6 × 205/(4.625 × 0.3 × 35000/1.5)=0.038; then ξ=0.1645 and M_{Rd}=26580 kNm, which is equal to $M_d(z)=M_{Ed,o}[1-(z-2 \cot \delta)/H_{tot}]$ at z=4.03 m; with $l_b=33d_b$=0.825 m for anchorage of the bars coming from below, the *twenty-two outermost 25 mm-dia. bars* near each edge of the section, plus the web reinforcement, *suffice down to z=4.85 m, i.e. 0.75 m below the floor of the 2nd storey*, Fig. 5.10(b).
  - another for cot δ=2.5, guessing that the level, z, we are looking for is within the 5th storey from the top: ν_d=5 × 205/(4.625 × 0.3 × 35000/1.5)=0.0317; then ξ=0.157 and M_{Rd}= 25830 kNm, which is equal to $M_d(z)=M_{Ed,o}[1-(z-2 \cot \delta)/H_{tot}]$ at z=7.5 m; with $l_b=33d_b$= 0.825 m for anchorage of the bars coming from below, the *twenty-two outermost 25 mm-dia. bars* near each edge of the section, plus the web reinforcement, *suffice down to z=8.35 m, i.e. 0.05 m below the floor of the 4th storey*.

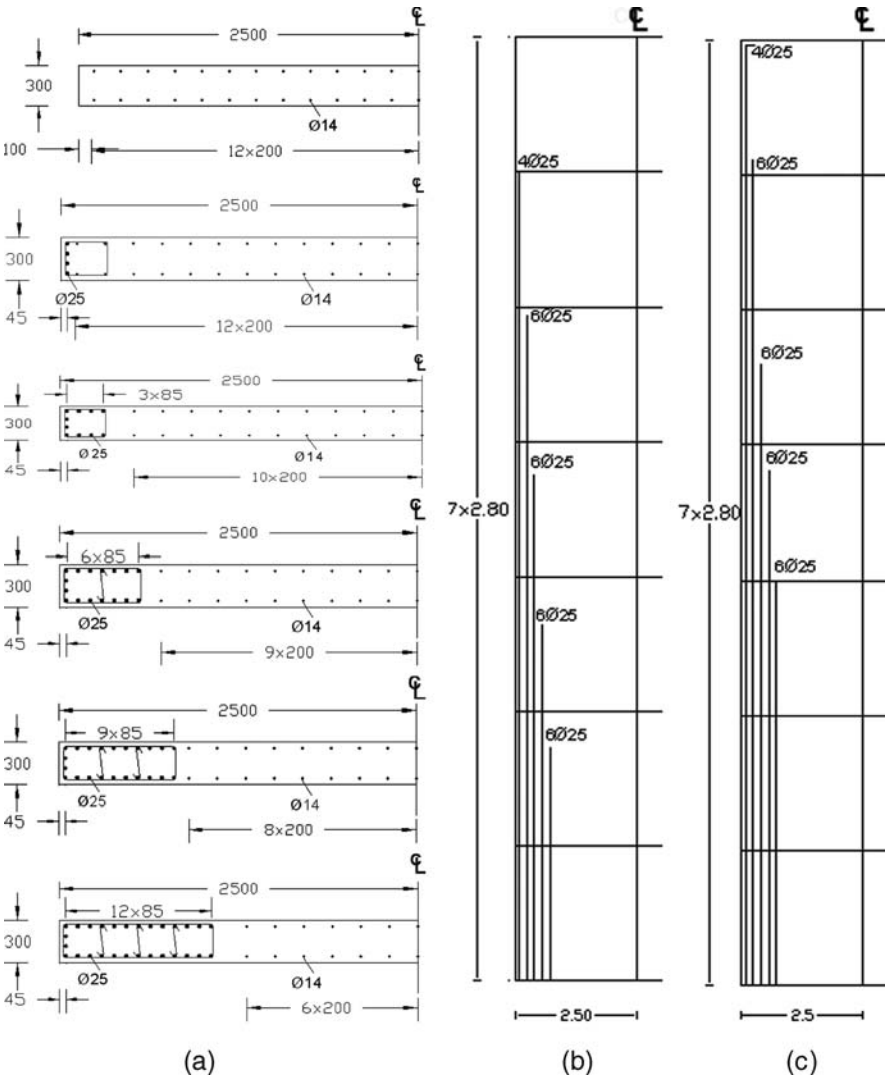

Fig. 5.10 Vertical wall reinforcement in one (symmetric) half of the wall for the two values of cot δ: layout of vertical bars in wall section (a); curtailment of vertical bars for (b) cot $\delta = 1$; (c) cot $\delta = 2.5$

Below the level established above, the full twenty-eight 25 mm-dia. bars are placed at each end of the wall section, at 85 mm centres parallel to its long side (bottom section in Fig. 5.10(a)).

Fig. 5.10 depicts the layout of vertical reinforcement for the two values of cot δ.

Design with cot δ=1 gives savings of 712 kg in the vertical steel compared to cot δ=2.5. The savings exceed the additional 600 kg of horizontal reinforcement required. So, the use of cot δ=1 not only provides better protection against brittle shear failure, but is also more cost-effective.

(q) Confinement and detailing of boundary elements in the "critical region" of walls W1

The "critical region" of walls W1 extends up to a height from the base, $h_{cr} \geq \max(l_w, H_{tot}/6) = 5$ m.

For DC M walls Eurocode 8 allows using for the confining reinforcement of boundary elements in the "critical region" the Eurocode 2 rules alone, if for the maximum value of the wall axial force from the analysis for the design seismic action plus concurrent gravity loads ν_d does not exceed 0.15. The Eurocode 2 requirements, limited to the part of the section where $\rho_L > 2\%$, are as follows:

- laterally unrestrained bars in the compression zone should be not further than 150 mm from a restrained one;
- transverse reinforcement should be provided, with diameter $d_{bw} \geq \max(6\text{ mm}; d_{bL}/4)$ and spacing $s_w \leq \min\{12d_{bL}; 0.6b_{wo}; 240\text{ mm}\}$ up to a distance of $4b_w$ above and below floor beams and slabs, or $s_w \leq \min(20d_{bL}; b_{wo}; 400\text{ mm})$ beyond that distance.

The condition $\nu_d \leq 0.15$ is met in the present case. So, just 8 mm-dia. transverse reinforcement ($d_{bw} \geq d_{bL}/4$) at 180 mm centres ($s_w \leq 0.6b_{wo}$) suffices (the length of the wall where wider spacing is sufficient is just $2.65 - 2 \times 4b_w = 0.25$ m at storey mid-height). It should engage 25 mm-dia. vertical bars at a spacing along the perimeter $3 \times 85 = 265\text{ mm} < 2 \times 150$ mm.

For illustration purposes, the rules for confinement and detailing of boundary elements in the "critical region" of DC M walls holding in the normal case without the exception for $\nu_d \leq 0.15$ are applied. According to them, the detailing provisions of the "critical regions" of DC M columns apply (see Tables 5.2 and 5.3 and Section 5.3.4). They are applied with:

- at the ground storey: $\nu_d = 1435/(5 \times 0.3 \times 35000/1.5) = 0.041$;
- web reinforcement over a length of $d - d_1 = 4$ m: $\omega_v = 1540 \times 4 \times (500/1.15)/(5000 \times 300 \times 35/1.5) = 0.0765$;
- $b_o = b_w - 2c - d_{bw} = 0.3 - 2 \times 0.02 - 0.012 = 0.248$ m, for hoop diameter $d_{bw} = 12$ mm and cover $c = 20$ mm;
- minimum length $\min l_c = 0.15 l_w = 0.75$ m;
- $M_{Rdo} = 29900$ kNm and $M_{Edo} = 29635$ kNm, giving $\mu_\varphi = 2q_o(M_{Edo}/M_{Rdo}) - 1 = 4.95$.

Then: $a\omega_{wd} \geq 30\mu_\phi(\nu_d + \omega_v)\varepsilon_{yd} b_w/b_o - 0.035 = 30 \times 4.95 \times (0.041 + 0.0765) \times 0.00217 \times 0.3/0.248 - 0.035 = -0.03 < 0$, confirming that Eurocode 2 rules may be applied for the confinement of boundary elements if $\nu_d \leq 0.15$.

When the wall base was verified for the ULS in flexure, the total length of the boundary element was chosen as $l_c = 1.11$ m, i.e., larger than the minimum of $0.15 l_w = 0.75$ m. This was to respect the maximum vertical reinforcement ratio of 0.04 in boundary elements. A perimeter tie around the boundary element has centreline dimensions $b_o \text{x} h_o \approx 1055 \times 250$ mm and is supplemented by five cross-ties with centreline length of ~250 mm, each one engaging every 2nd pair of vertical bars on opposite faces of the wall, placed at 85 mm centres along the long side of

the boundary element (bottom section in Fig. 5.10(a)). So, there is indeed a vertical bar engaged by a stirrup corner or cross-tie every ≤200 mm along the perimeter of the boundary element, except along the short side at the edge, where only the corner bars are engaged at a distance of ~210 mm. This gives:

$$\begin{aligned}\omega_{\mathrm{wd}} &= A_{\mathrm{sw}}[2(b_{\mathrm{o}}+h_{\mathrm{o}})+5b_{\mathrm{o}}]/(b_{\mathrm{o}}h_{o}s_{\mathrm{w}})f_{\mathrm{yd}}/f_{\mathrm{cd}}\\ &= (\pi 12^2/4)\times[2\times(1055+250)+5\times 250]\\ &\quad (500/1.15)/(35/1.5)/(1055\times 250s_{\mathrm{w}})\end{aligned}$$

and for $\omega_{\mathrm{wd}}\geq 0.08$ we need: $s_{\mathrm{w}}< 385$ mm. So, in the end the minimum requirement on stirrup spacing governs: $s_{\mathrm{w}}=\min\{8d_{\mathrm{bL}};\ b_{\mathrm{o}};\ 175\ \mathrm{mm}\}=175$ mm, which provides $\omega_{\mathrm{wd}}=0.08\times 385/175=0.176$.

With the chosen arrangement and detailing of the boundary elements, we have: $n_{\mathrm{b}}=2$, $n_{\mathrm{h}}=7$ and:

$$\begin{aligned}a &= (1-0.5\times 175/250)(1-0.5\times 175/1055)[1-\{250/((2-1)\\ &\quad\times 1055)+1055/((7-1)\times 250)\}/3]=0.409,\ a\omega_{\mathrm{wd}}=0.072.\end{aligned}$$

With this available value of $a\omega_{\mathrm{wd}}$, the condition $a\omega_{\mathrm{wd}}=30\mu_{\phi}(\nu_{\mathrm{d}}+\omega_{\nu})\varepsilon_{\mathrm{yd}}b_{\mathrm{w}}/b_{\mathrm{o}}-0.035$ gives an available value of μ_{ϕ}: $\mu_{\phi}=11.5$, which in turn gives a corresponding value of $q_{\mathrm{o}}=(\mu_{\varphi}+1)/(2M_{\mathrm{Edo}}/M_{\mathrm{Rdo}})=6.3$. So, with the confinement reinforcement placed, the wall has ductility and deformation capacity that can support a q-factor value 57.5% higher than that of a DC H wall and a design peak ground acceleration of 0.525 g, instead of the present one of 0.25 g. However, this flexural deformation capacity cannot be exploited in the framework of Eurocode 8 design for DC H, because, with its shear resistance reduced to 40% of the Eurocode 2 value, the wall cannot take the highly amplified design shear forces of a DC H design.

Above the "critical region" (in this case, from the 3rd to the top storey) transverse reinforcement is required around the 25 mm-dia. vertical bars near the edges of the wall section, because there the vertical steel ratio, ρ_{L}, exceeds 2%. Such transverse reinforcement is placed all along the storey height, because the distance of $4b_{\mathrm{w}}=1.2$ m above and below the floor slabs leaves just 250 mm at storey mid-height as the part of the wall where a wider transverse reinforcement spacing suffices.

A 8 mm-dia. ($d_{\mathrm{bw}}\geq d_{\mathrm{bL}}/4$) perimeter tie at 180 mm centres ($s_{\mathrm{w}}\leq 0.6b_{\mathrm{wo}}$) is used around the outermost 25 mm-dia. vertical bars at the level of interest. It is supplemented by cross-ties with centreline length ~250 mm engaging every 3rd pair of 25 mm-dia. vertical bars on opposite faces of the wall in its short direction (so, in the compression zone the distance of laterally unrestrained bars from the nearest restrained one is ≤150 mm). More specifically (see Fig. 5.10(a)):

1. Wherever the full twenty-eight 25 mm-dia. bars are needed near each end of the wall section, the compression zone extends to ~900 mm from the edge of the section and the 8 mm-dia. perimeter tie engaging the four corner 25 mm-dia. bars has centreline dimensions b_{o}x$h_{\mathrm{o}}\approx 1055\times 250$ mm. It is supplemented by three cross-ties with centreline length ~250 mm engaging

every 3rd pair of intermediate 25 mm-dia. vertical bars on opposite faces of the wall (see bottom section in Fig. 5.10(a)).

2. Wherever twenty-two 25 mm-dia. bars are placed near each end of the section, the compression zone extends up to ~760 mm from the section edge and the 8 mm-dia. perimeter tie engaging the four corner 25 mm-dia. bars has centreline dimensions $b_o x h_o \approx 800 \times 250$ mm. It is supplemented by two cross-ties with centreline length ~250 mm engaging every 3rd pair of intermediate 25 mm-dia. vertical bars on opposite faces of the wall (see 2nd section from the bottom in Fig. 5.10(a)).
3. Wherever sixteen 25 mm-dia. bars are needed near each section end, the compression zone extends to ~640 mm from the edge of the section and the 8 mm-dia. perimeter tie engaging the 4 corner bars has centreline dimensions $b_o x h_o \approx 545 \times 250$ mm. It is supplemented by one cross-tie with centreline length ~250 mm engaging only the middle pair of 25 mm-dia. vertical bars on opposite faces of the wall (see 3rd section from the bottom in Fig. 5.10(a)).
4. Wherever ten 25 mm-dia. bars are needed near each end of the wall section, the compression zone extends to ~600 mm from the section edge but the vertical steel ratio, ρ_L, exceeds 2% only over the outermost 340 mm. Only an 8 mm-dia. perimeter tie is placed around the four corner 25 mm-dia. bars, with centreline dimensions $b_o x h_o \approx 290 \times 250$ mm (see 3rd section from the top in Fig. 5.10(a)).
5. Near the top of the wall, where four 25 mm-dia. bars are placed next to the edge of the wall section, the compression zone extends up to ~540 mm from the end of the section, but the steel ratio, ρ_L, of the combination of the four 25 mm-dia. bars and the 14 mm-dia. web bars exceeds 2% only over the outermost ~330 mm. A 8 mm-dia. perimeter tie is placed around the two corner 25 mm-dia. bars and the 2nd pair of 14 mm-dia. web bars, with centreline dimensions $b_o x h_o \approx 285 \times 250$ mm (see 2nd section from the top in Fig. 5.10(a)).

As pointed out at the beginning of this section, because the condition $\nu_d \leq 0.15$ is met, 8 mm-dia. hoops @ 180 mm centres placed all around 25 mm-dia. bars at a distance on the perimeter of 265 mm, are sufficient even in the "critical region", i.e. as in case 1 above. This gives:
$\omega_{wd} = A_{sw}[2(b_o+h_o)+5b_o]/(b_o h_o s_w) f_{yd}/f_{cd} = (\pi \times 8^2/4) \times [2 \times (1055+250)+3 \times 250] \times (500/1.15)/(35/1.5)/(1055 \times 250 \times 180) = 0.066$. With the chosen detailing of reinforcement in boundary elements, we have: $n_b=2$, $n_h=7$ and hence:
$a=(1-0.5 \times 180/250)(1-0.5 \times 180/1055)[1-\{250/((2-1) \times 1055)+1055/((5-1) \times 250)\}/3]=0.333$, $a\omega_{wd} = 0.022$. With this available value of $a\omega_{wd}$ the condition $a\omega_{wd}=30\mu_\phi(\nu_d+\omega_v)\varepsilon_{yd} b_w/b_o-0.035$ gives an available value of μ_ϕ: $\mu_\phi=6.15$, which in turn gives a corresponding value of $q_o = (\mu_\varphi+1)/(2M_{Edo}/M_{Rdo})=3.6$, consistent with DC M design. So, indeed, at least in the present case with $\nu_d = 0.045$, confinement of the "critical region" following just the Eurocode 2 rules is sufficient.

(r) ULS verification of diaphragms

According to Eurocode 8, floor diaphragms should have the in-plane resistance necessary to transfer to the lateral-load-resisting systems the inertia loads that develop

in them from the analysis for the design seismic action, multiplied by an overstrength factor γ_d, with a recommended value of 1.1 for ductile modes of behaviour and failure (those associated with yielding of steel) or of 1.3 for brittle ones (e.g., for concrete in shear). The action-effects in a diaphragm may be estimated by modelling it as a deep beam or plane truss, or with Strut-and-Tie models, considering the lateral-load-resisting system as providing elastic support in the horizontal direction. Strictly speaking, explicit verification of concrete diaphragms is called for in Eurocode 8 only for DC H buildings with recesses, re-entrant corners or other diaphragm irregularities in plan, or irregularities in the distribution of mass or stiffness (e.g., due to set-backs or off-sets in plan), or with basement walls only along part of the perimeter or of the ground floor area. Special mention is made in Eurocode 8 of the need to verify the transfer of horizontal forces from diaphragms to the cores or walls of DC H buildings. To this end, the design shear stress at the interface of the diaphragm and the core or wall should be limited to 1.5 times the design value of concrete tensile strength, f_{ctd}. Besides, the resistance against shear sliding should be verified with a strut inclination of 45°.

Although this building does not fall in one of the cases where explicit verification of diaphragms is required in Eurocode 8, such a verification is included here, not only for illustration, but also because the entire floor inertia loads in each horizontal direction are transferred to just two shear walls at the edges.

According to the analysis, the inertia loads at floor i of a building with n_{st} storeys are equal to the design spectral acceleration (in g's) times $2i/(n_{st}+1)$, times the floor gravity load which is concurrent with the design seismic action.[18] This concurrent gravity load is computed without a reduction on the quasi-permanent part of the live loads for simultaneity of loading at different floors ($\varphi=1$) and does not include the weight of primary seismic vertical members. Normally the most critical diaphragm is either at the roof ($i=n_{st}$) or at the storey below, if it has larger floor weight than the roof. In the present case the design spectral acceleration is 0.1204 g and the floor weight at the roof is 8.2 kN/m^2 and at the storey below is 8.2+0.2 × 0.6–25 × 2.65 × (2 × 5 × 0.3)/25^2 = 8.161 kN/m^2. So, the roof is more critical, with inertia load of q_E=0.1204 × 8.2 × 2 × 7/(7+1) = 1.728 kN/m^2.

The shear force for the ULS verification of the diaphragm in shear and against shear sliding at the interface of the diaphragm and walls W1 is equal to $\gamma_d q_E L_x L_x$=1.3 × 1.728 × 25^2/2= 702 kN.

The diaphragms of this building may be considered to work under the horizontal seismic action component in direction X as deep beams with span L_y=25 m and total depth L_x=25 m, simply supported at mid-depth of the two end sections by the shear walls W1 and subjected to a uniformly distributed in-plane load (q_E = 1.728 kN/m^2 at the roof). The deep beam idealisation is equivalent to a Strut-and-Tie model as a

[18]Nonlinear dynamic seismic response analyses, as well as measurements on buildings, give floor response acceleration values much higher than suggested by a linear elastic analysis with the elastic spectrum reduced by the q-factor. The large difference may be due to higher modes, as well as to the overstrength of the lateral-load-resisting system, which extends the elastic range of response much beyond what is assumed in design.

plane truss over the part of the diaphragm between two parallel lines, at right angles to the horizontal seismic action component in question:

1. the 1st line connects the centres of the two walls W1 which are parallel to the horizontal component of the seismic action and resist the lateral loading;
2. the 2nd line is along the edge in plan on the "windward" side (where the overturning moment due to lateral loading induces tension in the vertical elements of the lateral-load-resisting system).

The Strut-and-Tie model comprises (see Fig. 5.11):

a) a tension chord centred along line 1, with width equal to the length, l_w, of the walls W1 it connects;
b) a polygonal (about semi-circular) compression chord connecting the two ends of the tension chord at the centres of the two walls W1; its apex is near the centre of the orthogonal wall W2 on line 2;
c) a number of closely spaced tension ties parallel to the horizontal component of the seismic action, running from the edge in plan which is parallel and opposite to line 2 above; the ties collect the in-plane load q_E=1.728 kN/m^2 and transfer it to the compression chord.

– Verification of the tension ties in (c) above:

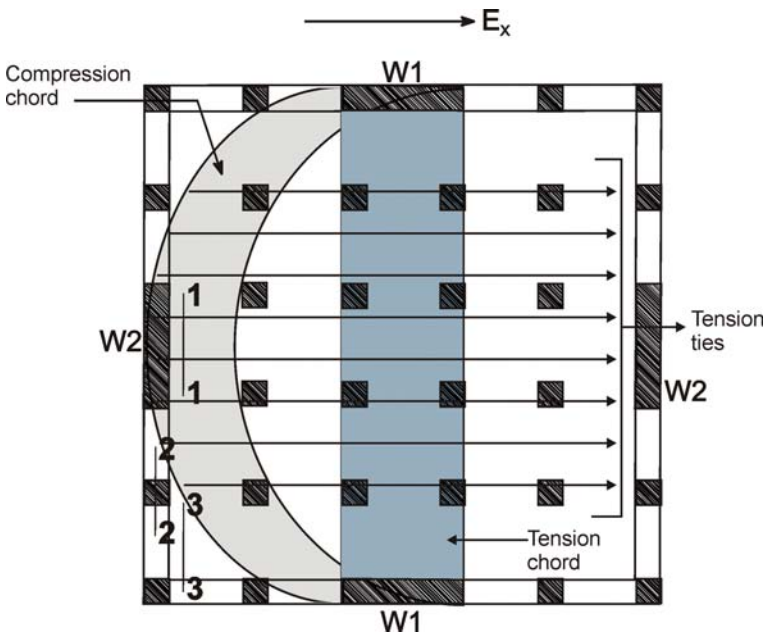

Fig. 5.11 Strut-and-Tie model of diaphragm

The longest tension ties (those close to the apex of the compression chord) collect an in-plane load $q_E = 1.728$ kN/m^2 along the full plan dimension L_x of the building parallel to the horizontal component of the seismic action. For the ULS verification of the ties in tension, any vertical section through the flat slab normal to horizontal direction X should have reinforcement area at least $\gamma_d q_E L_x/f_{yd} = 1.1 \times 1.728 \times 25/(0.5/1.15) = 110$ mm^2/m over and above what is required for the moment resistance of the flat slab for bending due to the floor gravity load which is concurrent with the design seismic action.

The reinforcement of the flat slab is normally dimensioned for ULS resistance in bending for the moments in the flat slab under the factored gravity loads, denoted here as M_d. If $M_{g+\psi 2q}$ is the moment (per linear meter) in the flat slab due to the floor gravity loads which are concurrent with the design seismic action, then the surplus of reinforcement area over and above what is necessary for ULS resistance under this bending moment is $\Delta A_s = \max[A_{s,min}; M_d/(zf_{yd})] - M_{g+\psi 2q}/(zf_{yd})$, where $z \approx 0.9 \times (0.15–0.025) \approx 0.11$ m is the internal lever arm and $A_{s,min}$ the minimum reinforcement in the flat slab according to Eurocode 2. Without crack control requirements, it is: $A_{s,min} = (0.26 f_{ctm}/f_{yk}) bd = (0.26 \times 3.2/500) \times 1000 \times 125 = 208$ mm^2/m. If the factored gravity loads combination is $\gamma_g G + \gamma_q Q = 1.35G + 1.5Q$, it produces a load on the roof slab $q_d = 1.35 \times 8.2 + 1.5 \times 2 = 14.7$ kN/m. The corresponding load due to the gravity loads concurrent with the design seismic action is $g = 8.2$ kN/m. So, $M_{g+\psi 2q} = (8.2/14.7) M_d$. The critical location for ΔA_s is where M_d is minimum.

With the bending of the flat slab fully restrained at the edge by the weak direction of walls W2, the minimum value of M_d along the longest tension ties is the sagging moment at mid-distance between wall W2 and the 1st row of interior columns parallel to W2 (Section 1-1 in Fig. 5.11). According to the direct design method in ACI (2008) this moment is equal to $0.35 M_o$, where $M_o = q_d l_{xn}^2 l_y/8$ is the total static moment in a flat slab panel, $l_{xn} = 5 – 0.6/2 – 0.5/2 = 4.45$ m is the clear span of the exterior panel in the X direction and $l_y = L_y/5$ its centre-to-centre span in the orthogonal direction. The middle strip of the flat slab between column strips, having width $0.5 l_y = 2.5$ m, should resist 40% of the sagging moment $0.35 M_o$. So, the design moment in the middle strip is: $M_d = 0.4 \times (0.35 \times 14.7 \times 4.45^2 \times 5/8)/(2.5) = 10.2$ kNm/m and requires reinforcement area $A_s = 10.2/(0.11 \times 0.5/1.15) = 213$ mm^2/m$> A_{s,min}$. Hence, the surplus of reinforcement area is: $\Delta A_s = (1 – 8.2/14.7) \times 10.2/(0.11 \times 0.5/1.15) = 94.4$ mm^2/m, i.e., less than the required area of 110 mm^2/m. Verification of the tension ties requires increasing the reinforcement area of the flat slab within its middle strips between wall W2 and the 1st parallel row of interior columns, as well as between any rows of interior columns, to $\geq 110 + 213 \times 8.2/14.7 = 229$ mm^2/m.

Another potentially critical location is at the tension ties heading towards the edge column next to wall W2 (Section 2-2 in Fig. 5.11). In flat slabs without edge beams the minimum value of M_d occurs near the edge column restraining the flat slab. According to the direct design method of ACI (2008) the total moment transferred there from the slab to the edge column is 26% of $M_o = q_d l_{xn}^2 l_y/8$. This moment is resisted by reinforcement at right angles to the edge of the flat slab, placed according to Eurocode 2 within a slab width centred at the edge column and equal to

the sum of its cross-sectional dimensions. This gives a design moment: M_d=(0.26 × 14.7 × 4.45^2 × 5/8)/(0.5+0.5)=47.3 kNm/m and a surplus of reinforcement area ΔA_s=(1–8.2/14.7) × 47.3/(0.11 × 0.5/1.15)=438 mm^2/m, i.e., more than the required area of 110 mm^2/m in the tension ties. Outside this slab width the reinforcement at right angles to the edge of the flat slab is just the minimum in Eurocode 2: $A_{s,min}$=208 mm^2/m, which is again more than the area of 110 mm^2/m required for the tension ties.

A final potentially critical location for the tension ties is between the row of columns at the edge of the slab and the 1st parallel row of interior columns (Section 3-3 in Fig. 5.11). According to the direct design method of ACI (2008) the middle strip of the flat slab, having width 0.5l_y=2.5 m, should resist 52% of M_o=$q_d l_{xn}{}^2 l_y$/8. This gives a design moment: M_d=(0.52 × 14.7 × 4.45^2 × 5/8)/2.5= 37.85 kNm/m, producing a surplus of reinforcement area: ΔA_s=(1–8.2/14.7) × 37.85/(0.11 × 0.5/1.15)= 350 mm^2/m, again greater than the minimum tension tie area of 110 mm^2/m. Therefore, it is only at the bottom surface of the flat slab within its middle strips between wall W2 and the 1st parallel row of interior columns, as well as between any rows of interior columns, that the reinforcement area should be increased to a total of 229 mm^2/m (sum at top and bottom surface), to allow the tension ties to transfer the floor inertia loads to the compression chord of the Strut-and-Tie model.

– Verification of the tension chord between the supports of the deep beam by the two walls W1.

The tension force in this chord may be estimated from moment equilibrium between:

- the couple of internal forces in the tension chord connecting the walls W1 on one hand and in the compression chord close to wall W2 on the other, and
- the uniformly distributed in-plane load of 1.728 kN/m^2 and the force reactions to it at walls W1.

This gives an internal lever arm in the deep beam $z \approx L_x/2$ and a force in the tension chord: $(q_E L_x L_y{}^2/8)/(L_x/2) = q_E L_y{}^2/4$. The required reinforcement area is: $A_{s,t\text{-}chord} = \gamma_d q_E L_y{}^2/(4 f_{yd}) = 1.1 \times 1.728 \times 25^2/(4 \times 0.5/1.15)$=683 mm^2, i.e. 683/5=136.5 mm^2/m within the 5 m of the width of the tension chord from one wall W1 to the opposite. The minimum area of reinforcement available in that 5 m-wide strip, over and above what is necessary for ULS resistance against the bending moments in the flat slab due to the floor gravity load concurrent with the design seismic action is $\Delta A_s = \max[A_{s,min}; M_d/(z f_{yd})] - M_{g+\psi 2q}/(z f_{yd})$, computed with the minimum values of M_d and $M_{g+\psi 2q}$= (8.2/14.7)M_d along the strip. With the flat slab fully restrained at the edge by the weak direction of walls W1, the minimum value of M_d in that strip according to the direct design method of ACI (2008) is the sagging moment at mid-distance between W1 and the 1st parallel row of interior columns, or between any two rows of interior columns: M_d=0.35M_o=0.35$q_d l_{yn}{}^2 l_x$/8, where l_{yn}=5–0.6/2–0.5/2= 4.45 m is the clear span

of the exterior panel in the Y direction and $l_x = L_x/5$ its centre-to-centre span in the orthogonal direction. 40% of that moment is resisted by the 2.5 m-wide middle strip between the two column strips centred along the rows of columns defining the tension chord. The sagging design moment in the middle strip is then: $M_d = 0.4 \times (0.35 \times 14.7 \times 4.45^2 \times 5/8)/2.5 = 10.2$ kNm/m, requiring reinforcement area: $10.2/(0.11 \times 0.5/1.15) = 213$ mm^2/m$> A_{s,min}$ and giving surplus reinforcement area $\Delta A_s = (1 - 8.2/14.7) \times 10.2/(0.11 \times 0.5/1.15) = 94.4$ mm^2/m, i.e., less than the required area of 136.5 mm^2/m for the tension chord. So, the reinforcement area neccesary between W1 and the 1st parallel row of interior columns, as well as between any rows of interior columns between the two walls W1, should be increased to at least 136.5 mm^2/m$+M_{g+\psi 2q}/(zf_{yd}) = 136.5 + 8.2/14.7 \times 10.2/(0.11 \times 0.5/1.15) = 255.5$ mm^2/m

Taking into account that the design seismic action is applied separately in horizontal directions X and Y, the conclusions of the Strut-and-Tie verifications of the diaphragm are:

- Within the 5 m-wide strips of the flat slab extending from one wall of the perimeter to its counterpart on the opposite side in plan, the reinforcement area of the flat slab should be at least 255.5 mm^2/m.
- Outside the above 5 m-wide central strips, the reinforcement area should be at least 229 mm^2/m.

(s) Design action effects for the perimeter elements of the box foundation

The perimeter wall of the box foundation collects a gravity load from the tributary area of the perimeter elements of the superstructure and the top slab of the basement equal to:

$$N_{\text{perimeter}} = 2.5 \times (25 + 25 + 20 + 20) \times 8.2 \times 8 = 14760\,\text{kN}$$

The total gravity load at the bottom of the foundation includes the self weight of the basement wall and of its strip footing. Our preliminary estimates of the width of the footing is 1.0 m and of its thickness 0.25 m (to be verified by dimensioning the foundation). Then, the additional weight of the basement wall, etc. is:

$$N_{\text{basement}} = 25 \times 4 \times 25 \times (5.0 \times 0.2 + 0.8 \times 0.25) = 3000\,\text{kN}$$

and the total vertical force at the bottom of the foundation is: $N_{Ed} = 14760 + 3000 = 17760$ kN.

The total seismic action effects at the top of the box foundation from the elastic analysis comprise a horizontal force of 4320 kN and an overturning moment of $4320 \times (2/3) \times 7 \times 2.8 = 56448$ kNm, applied to it through the two superstructure walls which are parallel to the horizontal component of the seismic action. These action effects are not affected by the accidental eccentricity, which increases the shear and overturning moment in one of the walls and decreases them by an equal

and opposite amount at the opposite one. They should be multiplied by the capacity design magnification factor, $a_{CD}=\gamma_{Rd}M_{Rd}/M_{Ed}$ of Eq. (2.15a) in Section 2.3.4, where $M_{Rd}=2 \times 29900$ kNm is the total design moment resistance at the base of the two walls and $M_{Ed}=56448$ kNm is the bending moment in them from the elastic analysis, without the effect of the accidental eccentricity. So, $a_{CD}=1.271$. However, as the box foundation system supports also many secondary seismic elements, notably the 28 columns of the flat slab system and the two walls that are at right angles to the horizontal component of the seismic action and respond in their weak direction, it is prudent to design the foundation with the value $a_{CD}=1.4$ allowed by Eurocode 8 for common foundations of several elements (see Eq. (2.16)). The increased value of a_{CD} provides for the seismic action effects transferred to the foundation by the many secondary seismic elements. No matter how unreliable it is for design purposes, the lateral force resistance of these secondary seismic elements may be significant in magnitude. So, the design values of the seismic action effects are:

– At the top of the box foundation:

  - horizontal force (base shear): $1.4 \times 4320=6050$ kN
  - overturning moment: $1.4 \times 56448=79030$ kNm.

– At the base of the box foundation:

  - horizontal force (base shear): $V_{Ed}=6050$ kN
  - overturning moment: $M_{Ed}=79030+5 \times 6050=109280$ kNm.

The horizontal force is transferred to the ground through shear stresses at the interface between the soil and the underside of the foundation strip of the perimeter wall. The overturning moment, acting together with the total vertical force at the level of the foundation bottom, is transferred via vertical bearing pressures.

(t) Dimensioning of the width of the strip footing on the basis of the ULS of the foundation against sliding or bearing capacity failure

According to Part 5 of Eurocode 8 (CEN 2004c):

– the design normal force N_{Ed} and bending moment M_{Ed} at the foundation can be transferred to the ground by means of the vertical force resultant and bending moment resultant of:
  1. the (design values of) resisting vertical forces acting on the base of the foundation, and
  2. the (design values of) the horizontal and vertical shear resistance between the embedded sides of deep foundations (boxes, piles, caissons) and the soil.

For shallow foundations, only the first of the two mechanisms may be relied upon.

The design horizontal shear force V_{Ed} can be transferred to the ground by the design shear resistance developing between the ground on one hand, and the horizontal base and the vertical sides of the foundation on the other. Up to 30% of the design lateral resistance E_{pd} arising from fully-mobilised passive earth pressures on the sides of the foundation may be added to the design shear resistance, if:

1. the backfill is compacted against the vertical sides of the foundation, or
2. the vertical sides consist of concrete poured directly against a clean, vertical soil face, or
3. the vertical sides belong to vertical walls driven into the soil.

The 2nd or 3rd conditions are not met in this case. For simplicity, we do not rely on the compaction of the backfill against the vertical sides of the box foundation. So, passive earth pressures on the sides of the box foundation will not be taken to contribute to the transfer of the design horizontal force V_{Ed} to the ground.

If the base of the foundation is above the water table (as in the present case), the design shear resistance is the design friction resistance of the horizontal base, calculated as the normal force on the horizontal base times the design value of $\tan\delta$, $\tan\delta/\gamma_{\mathrm{M}}$, where δ is the friction angle of the interface of the base and the soil and γ_{M} the material partial factor, taken equal to that applied on $\tan\phi'$ (the recommended value in Part 5 of Eurocode 8 is: $\gamma_{\phi'}=1.25$).

According to Annex D of Eurocode 7 (CEN 2003), the design value of the bearing capacity of a concentrically-loaded rectangular footing with rough and horizontal base having (effective) dimensions $b_z' \leq b_y'$ and (effective) surface area $A_f'=b_y' b_z'$, on cohesionless soil under drained conditions, is:

$$\frac{R_N}{A_f'} = q N_q \, s_q \, i_q + c' \, N_c \, s_c \, i_c + 0.5\gamma' \, \mathrm{N}_\gamma \, b_x' \, s_\gamma \, i_\gamma \tag{5.56}$$

where:

- q' is the (design) effective overburden pressure (surcharge) at the level of the foundation base;
- c' is the effective cohesion of the soil;
- γ' is the effective weight density of the soil below the foundation level;
- the dimensionless factors for the bearing capacity are:

$$N_q = e^{\pi \tan\phi'} \tan^2\left(45 + \frac{\phi'}{2}\right); N_c = \frac{N_q - 1}{\tan\phi'}; N_\gamma = 2(N_q - 1)\tan\phi' \tag{5.57}$$

with $\phi\prime$: angle of internal friction or shearing resistance (design value);

- the dimensionless shape factors are:

$$s_c = \frac{s_q\, N_q - 1}{N_q - 1}; \quad s_q = 1 + \sin\phi' \frac{b'_z}{b'_y} \quad (b'_z < b'_y); \quad s_\gamma = 1 - 0.3\frac{b'_z}{b'_y} \quad (b'_z < b'_y) \tag{5.58}$$

– the dimensionless factors for the inclination of the vertical load to the horizontal (owing to a horizontal load, with components V_z and V_y) parallel to sides b_z', b_y', respectively, are:

$$i_q = \left(1 - \frac{\sqrt{V_z^2 + V_y^2}}{N_{Ed} + A'_f c' \cot\phi'}\right)^m; \quad i_\gamma = \left(1 - \frac{\sqrt{V_z^2 + V_y^2}}{N_{Ed} + A'_f c' \cot\phi'}\right)^{m+1};$$
$$i_c = \frac{i_q\, N_q - 1}{N_q - 1} \tag{5.59}$$

with:

$$m = \frac{2 + \frac{b'_z}{b'_y}}{1 + \frac{b'_z}{b'_y}} \sin^2\psi + \frac{2 + \frac{b'_y}{b'_z}}{1 + \frac{b'_y}{b'_z}} \cos^2\psi \quad (b'_z < b'_y) \tag{5.60}$$

where ψ=arctan (V_z/V_y) is the direction angle of the resultant of V_z, V_y, with respect to side b_y'.

Recall that the effective dimensions of the footing are derived from the actual ones, b_y, b_z, as:

$$b_y' = b_y - 2e_y; \quad b'_z = b_z - 2e_z, \tag{5.61}$$

where the eccentricities $e_y = M_{Ed,y}/N_{Ed}$, $e_z = M_{Ed,z}/N_{Ed}$ result from the moments, $M_{Ed,y}$, $M_{Ed,z}$ with respect to the centre of the actual footing. $M_{Ed,y}$, $M_{Ed,z}$ act within vertical planes parallel to b_y, b_z, respectively.

In the present case $e_y = M_{Ed,y}/N_{Ed}$=0, $e_z = M_{Ed,z}/N_{Ed} = 109280/17760 = 6.153$ m. The effective footing is a composite one, consisting of the following rectangular parts, with uniform soil pressures developing at the bottom of each one of them (hence each rectangular part is considered as concentrically loaded):

1. A rectangular part at the side BC of the plan where the seismic overturning moment induces (the maximum) compression ("leeward" side), see Fig. 5.9. Its dimensions are $b_y' = b_y = 25$ m, $b'_z = b_z = b$, where b is the width of the strip footing of the perimeter basement wall ($b_z' \le b_y'$)
2. Two rectangular parts at the sides AB and CD of the plan which are parallel to the horizontal component of the seismic action considered. Their dimensions are $b_y' = b_y = X$, $b'_z = b_z = b$ ($b_z' \le b_y'$). Regarding dimension, X:

a. if the effective area of the overall footing extends into the "windward" side AD in plan opposite to the one where the seismic overturning moment induces maximum compression, then: $X = 25$ m;
b. otherwise, X is unknown, to be determined so that the vertical force resultant of the soil bearing pressures on parts 1 and 2 of the footing above coincides with the point of application of the total vertical force at the bottom of the foundation: N_{Ed}=18635 kN.

3. Another part exists at the "windward" side AD of the plan, only if case 2(a) above applies. Then this part is rectangular, with dimensions $b_y' = b_y$=25 m, $b'_z = b_z = xb$ and ($b_z' \leq b_y'$). The unknown fraction x of the width of the strip footing is determined so that the vertical force resultant of the bearing pressures on parts 1, 2 and 3 of the footing has the same point of application as the total vertical force at the bottom of the foundation, N_{Ed}=18635 kN.

If case 2(b) above is taken to apply, and the vertical soil pressure is assumed uniform over the effective area of the base of the composite footing (as in the ULS verification of the bearing capacity of the foundation), then the length X can estimated from the condition that the eccentricity of the soil bearing pressures on parts 1 and 2 of the footing is equal to $e_z = 6.153$ m:

$$2X^2/2/(25 + 2X) = 12.5 - 6.153 = 6.347\,\text{m} \rightarrow X = 20.45\,\text{m} < 25\,\text{m},$$

So, case 2(b) above applies indeed. This means that the sides AB and CD of the plan which are parallel to the considered horizontal component of the seismic action are engaged in the transfer of the seismic action effects to the soil only up to a distance of 20.45 m from the "leeward" side BC. The entire "windward" side AD opposite to BC uplifts and does not participate in the effective footing.

The total bearing capacity of the overall footing is the sum of the individually computed bearing capacities of parts 1, 2 and, in general 3, above. Their parameters are:

- Design value of angle ϕ'_d of shearing resistance: $\phi'_d = \tan^{-1}(\tan\phi'_k/\gamma_{\phi'}) = 30^\circ$ (denoted simply as ϕ'),
  where the value recommended in Part 5 of Eurocode 8 (CEN 2004c): $\gamma_{\phi'} = 1.25$ has been used.
- Mean surcharge due to soil overburden on both sides of the footing: $q = h\gamma_{soil} = 2.5 \times 20 = 50$ kN/m^2
- Effective cohesion $c' = 0$.
- $\gamma = 20$ kN/m^3
- $N_q = 18.4$, $N_c = 30.14$, $N_\gamma = 20.1$.
- All individual rectangular parts of the overall effective footing have very elongated shape. So, their dimensionless shape factors are all approximately equal to 1.0: $s_c \approx s_q \approx s_\gamma \approx 1.0$.

The horizontal force (base shear) V_{Ed}=6050 kN, transferred to the box foundation by the two walls of the superstructure which are parallel to the considered horizontal component of the seismic action, will be transferred to the ground mainly through the base of Part 2 of the composite footing. For simplicity, the safe-sided assumption is made that 100% of this force is transferred to the soil through that part. As it is assumed that there is no transfer of horizontal force to the soil by Part 1 (or 3, in general) of the overall footing, there the dimensionless inclination factors i_q, i_γ are approximately equal to 1.0 (i_c is of no interest, as c'=0).

For Part 2 of the effective footing area, we have $V_y=V_{Ed}$, V_z=0, ψ=arctan(V_z/V_y)=0 and, as b_z'/b_y'=1.0/20.45≈0, Eq. (5.60) gives for Part 2 m≈1. The value of N_{Ed} in Eqs. (5.60) should be taken equal to the part of the full value N_{Ed}=18635 kN attributed to Part 2, i.e. to 17760 × 2 × 20.45/(2 × 20.45+25)=11020 kN. So, for Part 2: i_q=1–6050/11020=0.451, i_γ≈ (1–6050/11020)^2 =0.203 (i_c is not relevant, as c'=0).

The design value of the bearing capacity is:

- for Part 1 of the effective footing: $R_N/(25b)$=50 × 18.4+0.5 × 20 × 20.1=1121 kN/m^2. For R_N>17760–11020 =6740 kN →b>0.24 m;
- for Part 2 of the effective footing: $R_N/(2 \times 20.45b)$=50 × 18.4 × 0.451+0.5 × 20 × 20.1 × 0.203= 455.7 kN/m^2. So, for R_N>11020 kN →b>0.59 m.

Sides AD and BC of the plan, where Part 1 is, become Part 2 of the foundation when the horizontal component Y of the seismic action is considered. So, the value b>0.59 m applies for the full length of the strip footing. The width of the strip footing finally chosen is: *b=1.0 m.* This choice provides an additional safety margin of 1.0/0.59 = 1.7 on the bearing capacity for the part of the strip footing which is parallel to the horizontal component of the seismic action considered and of 1.0/0.24=4.17 for the part orthogonal to it.

The full horizontal force V_{Ed}=6050 kN is transferred to the soil by a 20.45 m-long part of sides AB and CD of the foundation strip which are parallel to the considered horizontal component of the seismic action. This part transfers to the ground a vertical force N_{Ed}=11020 kN. So, the design friction resistance of the horizontal base is:

$$F_{Rd} = N_{Ed} \tan\delta/\gamma_M = N_{Ed} \tan\phi_d' = 11020 \tan(30^\circ) = 6360\,\text{kN} \geq V_{Ed} = 6050\,\text{kN}.$$

Therefore, the ample safety margin of bearing capacity is not matched by the verification against sliding. It is reminded, though, that the contribution of passive earth pressures on the vertical sides of the box foundation to the transfer of the horizontal shear force V_{Ed} to the ground has been neglected, to be on the safe side.

(u) Action effects in the basement wall for its ULS dimensioning

The action effects in the basement wall (bending moments and shear forces) are calculated assuming that the vertical soil pressures applied to the underside of the strip footing vary linearly in the two horizontal directions, X and Y. This is consistent

with the rigidity of the box foundation relative to the underlying soil and with the large safety margin against bearing capacity failure (owing in part to the material partial factors involved in the design values of the soil strength parameters). This safety margin implies that the vertical soil pressures acting on the base of the strip footing are in the elastic range of soil behaviour.

If there is no uplift at the base of the foundation, the distribution of vertical soil pressures at the base of the foundation is:

$$\sigma = \frac{N_{Ed}}{A_f} + \frac{M_{Ed}}{I_f} x \tag{5.62}$$

where:

- $A_f = 2b(L_x + L_y)$ and $I_f = bL_x^2(L_x + L_y/3)/2$ denote the surface area and the moment of inertia, respectively, of the plan of the strip footing around the perimeter of the basement, and
- x is the distance of the centre of the foundation in plan from the point on the centreline of the strip footing where the vertical soil pressure is computed; x is measured in the direction of the horizontal component of the seismic action considered.

For $L_x = L_y = 25$ m, $b = 1.0$ m, $N_{Ed} = 17760$ kN, $M_{Ed} = e_z N_{Ed} = 6.153 N_{Ed}$, Eq. (5.62) gives:

$$\sigma = \frac{N_{Ed}}{A_f}\left(1 + \frac{6e_x}{L_x} \cdot \frac{x}{L_x}\right) = \frac{17760}{4 \cdot 1.0 \cdot 25}\left(1 + \frac{6 \cdot 6.153}{25} \cdot \frac{x}{25}\right)$$

Therefore, at $x = L_x/2$: $\sigma = 308.7$ kN/m^2 and at $x = -L_x/2$: $\sigma = 46.5$ kN/m$^2 > 0$. So, there is indeed no uplift at the base of the foundation and Eq. (5.62) does apply.

In addition to the vertical soil above, acting upwards on the base of the strip footing, the self-weight of the basement wall exerts a uniform load downwards $g_w = 25 \times (5.0 \times 0.2 + 0.8 \times 0.25) = 30$ kN/m or $30/1.0 = 30$ kN/m^2. This load reduces the upwards soil pressures of Eq. (5.62) into a net upwards load (in kN/m):

$$b\sigma - g_w = \frac{17760}{4 \cdot 25}\left(1 + \frac{6 \cdot 6.153}{25} \cdot \frac{x}{25}\right) - 30 = 147.6 + 262.3\frac{x}{25},$$

i.e. to 278.7 kN/m for $x = L_x/2 = 12.5$ m and to 16.5 kN/m for $x = -L_x/2 = -12.5$ m (see Free-Body-Diagrams in Fig. 5.12).

The Free-Body-Diagrams in Fig. 5.12 for sides AD and BC and in Fig. 5.13 for part AB (or CD) of the basement wall show:

- At the bottom of the basement wall:

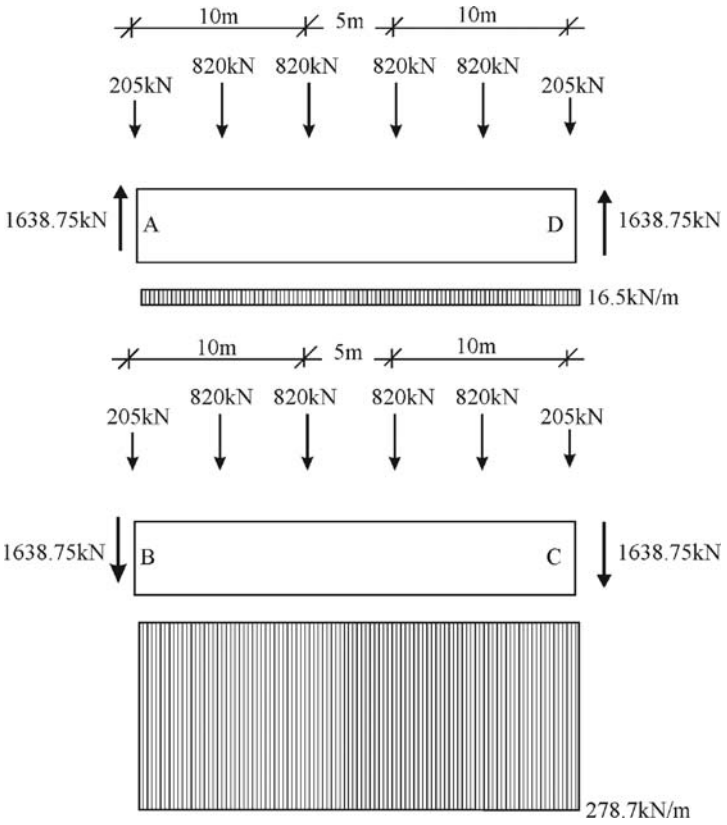

Fig. 5.12 Free-Body-Diagram of sides of basement wall at right angles to the seismic action component: (*top*) "windward" side AD, (*bottom*) "leeward" side BC

- the upwards vertical load due to soil pressure minus the self-weight of the wall, trapezoidally distributed at the top of wall part AB (or CD), or constant for parts AD and BC, and
- the horizontal force (base shear) V_{Ed}=6050/2=3025 kN acting to the left.

– At the top of the basement wall:

- vertical forces equal to 2.5 × 5 × 8 × 8.2=820 kN, due to gravity loads of the seven overlying storeys plus the basement roof, are applied downwards by each one of the two columns on either side of the shear wall; for simplicity, such a vertical force is also taken to be applied at each end of the wall itself;
- each corner column applies a downwards vertical force of (2.5 × 2.5 × 8 × 8.2)/2=205 kN due to gravity loads of the eight storeys (the other half of the total vertical force of the corner column goes to the orthogonal wall); and
- the shear wall applies to the top of wall part AB (or CD) a seismic base moment of 79030/2=39515 kNm and a horizontal force (base shear) V_{Ed}=6050/2=3025 kN to the right.

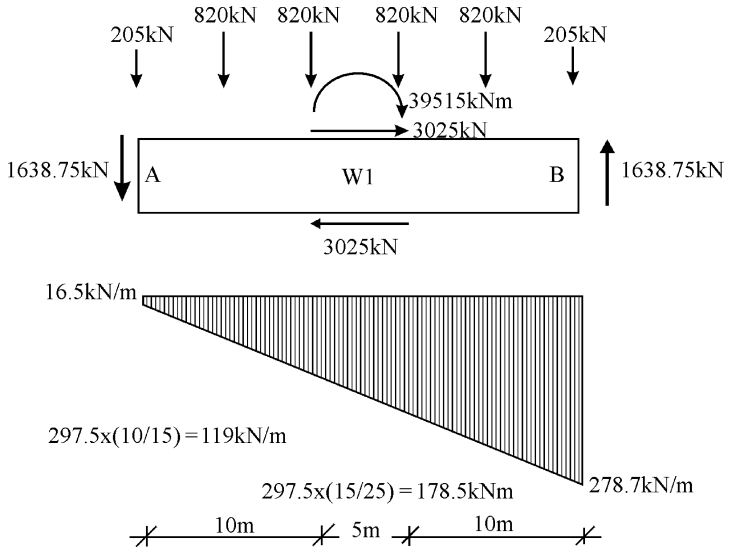

Fig. 5.13 Free-Body-Diagram of sides AB (or CD) of basement wall (parallel to the seismic action component)

– At the left-hand-end A of part AB (or D of part CD) of the basement wall:

  - a vertical force is applied downwards by the orthogonal wall AD, equal to one-half of the difference between:

    - the total gravity load of the eight storeys applied on part AD of the basement wall via the shear wall, the corner columns and the two edge columns of this part of the perimeter: $4 \times 820+2 \times 205=3690$ kN, and
    - the resultant of the vertical soil pressure of the strip footing of part AD of the basement wall, which is $16.5 \times 25=412.5$ kN

  So this downwards vertical force is: (3690–412.5)/2=1638.75 kN. That same force is applied upwards by parts AB and CD at the two ends A and D of the orthogonal wall, AD.

– At the right-hand-end B of part AB (or C of part CD) of the basement wall:

  - a vertical force is applied upwards by the orthogonal wall, BC, equal to one-half of the difference between:

    - the resultant of the vertical soil pressure of the strip footing of part BC of the basement wall, $278.7 \times 25=6967.5$ kN, and
    - the total gravity load of the eight storeys applied on part BC of the basement wall via the shear wall, the corner columns and the two edge columns of this part of the perimeter, 3690 kN.

So, this upwards vertical force is: (6967.5–3690)/2=1638.75 kN. That same force is applied downwards by parts AB and CD to the two ends B and C of the orthogonal wall, BC.

(v) Dimensioning of the basement wall for the ULS in shear

The individual parts, AB, BC, CD or AD of the basement wall are considered as horizontal beam elements, with centroidal axis at mid-depth of the basement wall. Their effective depth is taken to mid-depth of the strip footing: d=5–0.25/2=4.875 m; the internal lever arm is equal to the distance between the mid-depths of the roof slab of the basement and of the strip footing: z≈5–(0.25+0.15)/2=4.8 m.

Parts AB and CD, in particular, may be considered as cantilevering from both sides of the shear wall they support and loaded by transverse loads at both top and bottom: predominantly upwards on the part to the right of the shear wall, inducing tension at the bottom flange (at the strip footing); primarily downwards on the part to the left of the shear wall, inducing tension in the top flange (at the slab of the basement roof). Part BC may be considered as a simply supported beam, loaded primarily by upwards transverse loads at the bottom, causing tension at the bottom flange (at the strip footing). Part AD may be considered as a simply supported beam, loaded predominantly by downwards transverse loads at the top, inducing tension in the top flange (at the slab of the basement roof). The shear forces and bending moments are calculated from the Free-Body-Diagrams in Figs. 5.12 and 5.13.

The shear force in parts BC or AD of the basement wall is maximum right at their end sections and equal to V_E=1638.75+205=1843.75 kN or V_E=1638.75–205=1433.75 kN, respectively.

In part AB of the basement wall, the shear force is:

- just to the right of the 2nd column from the left end A: V_E=1638.75+205+820–16.5 × 5–(5/25) × (278.7–16.5) × 5/2 =2450 kN;
- just to left of the shear wall: V_E=1638.75+205+820–16.5 × 10–(10/25) × (278.7–16.5) × 10/2= 1974.35 kN;
- just to the right of the shear wall: V_E=278.7 × 10–(10/25) × (278.7–16.5) × 10/2+1638.75–820–205= 2876.4 kN, which is the maximum shear force anywhere along part AB of the basement wall.

This last value is the maximum-ever shear force anywhere around the basement wall, to be used in the verification of the wall thickness in shear: V_{Ed}=2876.4 kN.

If foundation elements are dimensioned for seismic action effects obtained by multiplying those from the elastic analysis times the capacity design magnification factor, a_{CD} (in this case a_{CD}=1.4), their dimensioning and detailing follows just the rules of Eurocode 2 for non-seismic actions.

Shear resistance for the ULS verification against diagonal compression (web crushing):

$V_{Rd,max} = 0.3(1 - f_{ck}(\text{MPa})/250)b_w z f_{cd} \sin 2\delta = 0.3(1 - 35/250)$ $\times 0.2 \times 4.8 \times (35000/1.5) \sin 2\delta = 5780 \sin 2\delta(\text{kN}) \geq V_{Ed} = 2876.4\,\text{kN} \rightarrow \sin 2\delta \geq 0.497 \rightarrow \delta > 14.9^\circ$. So, $\delta = 21.8^\circ$ and $\cot\delta = 2.5$.

The shear (i.e. vertical) reinforcement ratio of the basement wall, $\rho_v = A_{sw}/(b_w s_v)$, is calculated from the acting shear force at the section of maximum shear, not at a distance d from it, because the connection of the basement wall to the shear wall of the superstructure is not a direct support of the beam, with the transverse loads being applied to one flange and the reaction to them to an opposite one.

For $\cot\delta = 2.5$, $V_{Rd,s} = b_w z \rho_v f_{ywd} \cot\delta = 0.2 \times 4.8 \times (500000/1.15) \times 2.5\rho_v > V_{Ed} = 2876.4$ kN: $\rho_v > 0.276\%$. A curtain of 12 mm-dia. @ 200 mm centres is placed near each face of the basement wall (1131 mm^2/m, $\rho = 1131/(200 \times 1000) = 0.565\%$). This is sufficient even for shear design with $\cot\delta = 1.22$.

(w) Dimensioning of the basement wall for the ULS in bending

The sagging bending moment, causing *tension at the bottom* flange (at the strip footing) is maximum either:

- at the mid-point of part AD: $M^+ = (1638.75–205) \times 12.5–820 \times 7.5–820 \times 2.5+16.5 \times 12.5^2/2 = 11010$ kNm, or
- in parts AB and CD, just to the right of the shear wall: $M^+ = (1638.75–205) \times 10–820 \times 5+278.7 \times 10^2/2–(10/25) \times (278.7–16.5) \times 10^2/6–(10/25) \times 3025 \times 5/2 \approx$ *19400 kNm* (the last term is due to the fraction of the horizontal force acting on the bottom of parts AB and CD to the right of the shear wall).

The maximum hogging moment (*tension at the top flange*, at the slab of the basement roof) occurs either:

- at the mid-point of part BC: $M^- = (1638.75+205) \times 12.5+820 \times 7.5+820 \times 2.5–278.7 \times 12.5^2/2 = 9475$ kNm, or
- in parts AB and CD, just to the left of the shear wall: $M^- = (1638.75+205) \times 10+820 \times 5–16.5 \times 10^2/2–(10/25) \times (278.7–16.5) \times 10^2/6–(10/25) \times 3025 \times 5/2 =$ *16945 kNm* (the last term is due to the fraction of the horizontal force acting on the bottom of parts AB or CD to the left of the shear wall).

Note that the shear span is equal to:

- 16945/1974.35=8.585 m at the section just to the left of the shear wall; and
- 19400/2876.4=6.745 m at the section just to the right of the shear wall.

and does not exceeds the depth of the wall, h=5 m; so the basement wall does not need to be dimensioned with a Strut-and-Tie model.

A curtain of 12 mm-dia. @ 200 mm centres is placed near each face of the basement wall (1131 mm^2/m, $\rho_h = 1131/(200 \times 1000) = 0.565\%$), as web reinforcement

over the internal lever arm of z=4.8 m. The entire web reinforcement, A_{sh}=4.8 × 1131=5430 mm^2, contributes to the design moment resistance with:

$$M_{Rd,h} \approx 0.5 A_{sh} f_{yd} z = 0.5 \times 5430 \times (0.5/1.15) \times 4.8 = 5670\,\text{kNm}.$$

The difference $\Delta M_{Rd}{}^{+}$=$M_{Ed}{}^{+}$–$M_{Rd,h}$=19400–5670=13730 kNm should be resisted by reinforcement with cross-sectional area: A_{s1}≈$\Delta M_{Rd}{}^{+}/zf_{yd}$=13730/(4.8 × 0.5/1.15)=6580 mm^2. Fourteen 25 mm-dia. bars (6870 mm^2) are placed for that: six 25 mm-dia. bars @ ∼180 mm centres at top and bottom of the longitudinal section of the strip footing, plus an intermediate 25 mm-dia. bar at each one of the two vertical sides of that section.

The difference $\Delta M_{Rd}{}^{-}$=$M_{Ed}{}^{-}$–$M_{Rd,h}$=16945–5670=11275 kNm should be resisted by similar reinforcement at the top: A_{s2}≈$\Delta M_{Rd}{}^{-}/zf_{yd}$=11275/(4.8 × 0.5/1.15)= 5400 mm^2. Eleven 25 mm-dia. bars (5400 mm^2) are placed in the slab of the basement roof: six at the top surface of the slab and five at the bottom one, within a ∼1.0 m-wide strip of the slab parallel to the basement wall (i.e., @ ∼200 mm centres).

For tension at the bottom, the resulting design resisting moment, $M_{Rd}{}^{+}$, is calculated with ν=0; d=5–0.125=4.875 m; d_1=0.15/2=0.075 m (δ_1=75/4875=0.0154); b≈1.0 m; ω_1= 6870/(4875 × 1000) × (500/1.15)/(35/1.5)=0.02626; ω_2=5400/(4875 × 1000) × (500/1.15)/(35/1.5)= 0.02064; ω_v=5430/(4875 × 1000) × (500/1.15)/(35/1.5)=0.02075. The left-hand-side value of Eq. (3.51) is equal to –0.0197 and Eq. (3.51) is satisfied. Eq. (3.52) gives then: ξ=0.0317, so that indeed $x=\xi d$=0.1545 m and essentially it does not exceed the thickness of the slab. Eq. (3.60) gives then: $M_{Rd}{}^{+}$=19900 kNm > $M_{Ed}{}^{+}$=19400 kNm.

For tension at the top, the resulting design resisting moment, $M_{Rd}{}^{-}$, is calculated with: ν=0; d= 5–0.075=4.925 m; d_1=0.25/2=0.125 m (δ_1=125/4925=0.0254); b≈1.0 m; ω_1 = 5400/(4925 × 1000) × (500/1.15)/(35/1.5)=0.02043; ω_2 = 6870/(4925 × 1000) × (500/1.15)/(35/1.5) = 0.026; ω_v = 5430/(4925 × 1000) × (500/1.15)/(35/1.5) = 0.02054. The left-hand-side value of Eq. (3.51) is equal to 0.0415 and Eq. (3.51) is not met. Eq. (3.54) gives then ξ=0.0354 and indeed $x=\xi d$=0.1745 m is less than the depth of the strip footing. M_{Rd} is obtained from Eq. (3.59): $M_{Rd}{}^{-}$=16900 kNm ≈ $M_{Ed}{}^{-}$=16945 kNm.

Taking into account the alternating nature of the seismic action, the top and bottom reinforcement calculated above for the basement walls are placed on both sides of the shear walls W1 and W2. Besides, with the tension shift of 0.5z cot δ =6 m for the value cot δ =2.5 originally considered in the ULS verifications in shear, or 0.5z cot δ =2.95 m for the value cot δ=1.22 which is consistent with the shear reinforcement placed in the basement walls, the top and bottom reinforcement calculated above continue uncurtailed to the end of the corresponding part of the basement wall.

Chapter 6
Seismic Assessment and Retrofitting of Existing Concrete Buildings

This chapter is the only one in the book devoted exclusively to existing concrete buildings. It builds on:

- Chapter 1, for the seismic performance requirements that may be apply to existing buildings and to their upgrading,
- Chapter 2, for the demonstration of the inherent vulnerability of substandard existing buildings,
- Chapter 3 for the quantification of the cyclic force and deformation capacity of concrete members, including the effect of poor detailing or retrofitting, and on
- Chapter 4 for the estimation of the seismic response via (mainly nonlinear) analysis.

The first part of the chapter is mainly devoted to seismic assessment of the as-is building. The rest to its upgrading through appropriate and cost-effective retrofitting. One section, namely Section 6.5, is specific to Part 3 of Eurocode 8. Retrofitting strategies and techniques commonly used today and in the foreseeable future for a concrete building as a whole and for its members, respectively, are described and their scope, pros and cons highlighted. Procedures, rules and expressions are given for practical member retrofit design. Finally, practical retrofitting is illustrated through two real applications.

6.1 Introduction

In many parts of the world, including Europe, design of new buildings for earthquake resistance is a relatively recent development. In those regions, resistance of buildings to lateral forces resulted in the past only from wind considerations. Provisions for seismic design and detailing of members and structures resembling those found in modern seismic codes did not appear before the mid-1970s in US standards, or the mid-1980s in European national codes. So, in the light of our current knowledge, the building inventory of many seismic regions worldwide is by and large substandard and seismically deficient.

M.N. Fardis, *Seismic Design, Assessment and Retrofitting of Concrete Buildings*, Geotechnical, Geological, and Earthquake Engineering 8, DOI 10.1007/978-1-4020-9842-0_6,

Although today and for the years to come the major earthquake threat to human life and property comes from existing substandard buildings, the emphasis of earthquake engineering research, practice and code-writing has been, and still is, on new construction. Policy makers hope that the problem of existing buildings will be solved gradually by attrition (sometimes accelerated by urban renewal and redevelopment). This may be a socio-economically optimal solution for those regions where the rate of occurrence of moderate to strong earthquakes is much lower than the attrition rate of old buildings. Although seismic resistance adds very little to the construction cost of a new building, the cost of seismic upgrading an existing one, including disruption of use, relocation of tenants, removal and replacement of non-structural parts, etc., is normally a large fraction of the building replacement cost and may be prohibitive for private owners or difficult for the local economy to bear.

Regardless of the economics, seismic retrofitting of buildings is effective in mitigating the seismic risk posed by a substandard building stock. The owner, private or public, may take the initiative individually, often on the occasion of a change in use, architectural remodelling or repair of damage due to an earthquake. Besides, in the context of a broader strategy for seismic risk mitigation, national or local authorities may launch "active" or "passive" seismic assessment and retrofitting programmes:

- In "active" programmes owners of certain categories of buildings may be required to complete the seismic assessment and – depending on its outcome – the retrofitting by certain deadlines. The buildings to be targeted may depend on the seismicity and ground conditions, on the importance, occupancy and perceived vulnerability of the building – as influenced by the type of material and structural system, the number of storeys, the time of construction with respect to certain benchmark dates of code enforcement, etc.
- In "passive" programmes seismic assessment – possibly leading to retrofitting – is triggered by events or activities related to the use of the building, such as a change that increases occupancy or importance class, repair of damage after an earthquake, remodelling of a minimum percentage of the floor area or above a certain budget, etc.

The seismic performance requirements to be met by the building as is or after retrofitting – if necessary – may be less stringent in compulsory, "active" programmes than in "passive" ones. In a "passive" programme triggered by remodelling, performance requirements may gradate with the extent and cost of remodelling works.

The need to retrofit or not a specific building and the scope and targets of the retrofitting (in terms of weaknesses and deficiencies to be corrected) normally come out of a detailed seismic assessment (or evaluation) of the building. A technically sound seismic assessment is a challenge. However, even when the need to retrofit is obvious, a detailed seismic assessment is worth carrying out: once a structural model of the building as-is is set up and analysed, it can be used at little extra cost as the basis for studying various retrofitting options and for detailed retrofit

design. Besides, a detailed assessment in principle provides an objective picture of the seismic vulnerability and resistance, independent of any preconceptions of the engineer doing it. So, recent years have seen a dramatic decline in the use and perceived value of empirical rapid screening methods, used in the past to identify whether seismic retrofitting is indeed necessary.

It is nowadays recognised that rapid screening procedures are not reliable and cannot replace detailed seismic assessment of individual buildings. Rapid screening may be considered as a useful guide in "active" seismic assessment and retrofitting programmes for seismic risk mitigation in a certain region or urban area, helping to identify priority buildings or categories thereof. The motivation of rapid screening derives from the fairly good performance of most substandard buildings in earthquakes as strong as in Mexico 1985, Luzon Philippines 1990, Erzincan 1992, Kobe 1995 or Kocaeli 1999. The objective then is to screen out the buildings that can withstand a strong earthquake by virtue of overstrength alone, rather than ductility. The more costly detailed assessment may be reserved for the most vulnerable part of the building stock. The final verdict for the individual buildings identified as most vulnerable has to await the outcome of their detailed seismic assessment.

For the reasons put forward in the previous paragraph, rapid screening procedures are not dealt with in this book beyond broadly defining their features in the rest of Section 6.1.

The archetypal rapid screening procedure is that in ATC (1988). As this procedure is tailored to the building stock of the US, only its basic idea can be transferred elsewhere. Any adaptation to the specific features of the local building stock should be continuously calibrated on the basis of damage data from earthquakes that have hit the area where the procedure is being applied. In general, in a ATC (1988)-type of rapid screening, a single Basic Structural Score (*BSS*) is first assigned to a (concrete) building, depending on the combination of seicmicity zone, structural system (frame, wall or dual), design code(s) applied and special features (e.g., partial or full infilling, squat columns, open storey, etc.) that may or may not have been sufficiently addressed by the design code applicable at the time of construction. A Structural Score *S* is calculated then, as the sum of *BSS* and of a series of Performance Modification Factors (*PMF*s), accounting, e.g., for apparent construction quality and deterioration (e.g., reinforcement corrosion), irregularity of the building in plan and elevation, number of storeys, topography and ground conditions, location in the building block and possibility of mid-floor pounding with adjacent buildings, etc. The seismic vulnerability of the building at the specific site is evaluated on the basis of its final *S*-value.

To bridge the gap between the empirical, narrow-scope rapid screening in ATC (1988) and modern-day detailed seismic assessment, a three-tier assessment approach has been introduced in the US (ASCE 2003). The 3rd tier is a full-fledged detailed seismic assessment of the type in ASCE (2007). The 1st one comprises several checklists requiring trivial calculations and some detailed information on the as-built structure. Under certain conditions of seismicity, number of storeys and target performance level, a positive outcome of the 1st tier may be taken as definite

and make recourse to the 2nd tier (which is a simplified detailed seismic assessment) redundant. The earlier Japanese three-tier approach (JBDPA 1977) is of a similar character.

6.2 Seismic Vulnerability of Existing Concrete Buildings

6.2.1 System and Layout Aspects and Deficiencies

Normally existing substandard buildings have been designed for very low lateral force resistance, if any. So, they are expected to develop significant inelastic action, even under a moderate earthquake. To sustain it, they should have considerable ductility. As emphasised in Chapter 1, this requires ductility at both the local and the global level. As pointed out in the next section, in existing substandard buildings potential plastic hinge regions are not detailed for ductility. Besides, members are not capacity-designed against pre-emptive brittle failure in shear. More important, though, existing substandard buildings seldom have the strong and stiff vertical spine necessary for spreading inelastic deformation demands throughout their height and avoiding a storey mechanism. If they have one in the form of strong walls, it is more by coincidence than by design. Even more important, as a rule their overall structural layout is seismically deficient.

The compelling consideration in conceptual structural design of old buildings was not earthquake resistance but gravity loads and conformity to the architectural layout. Complete two-way frames are the exception rather than the rule, as beams are often indirectly supported on other beams instead of columns (see Figs. 2.13(c), 2.25 and 4.14 for examples), or are mainly in a single horizontal direction to support one-way slabs (as, e.g., in Figs. 2.21 and 2.24). Overall, old buildings have few, if any, of the attributes listed in Section 2.1.2 and analysed in the rest of Section 2.1 as favourable for earthquake resistance. Torsional imbalances of lateral resistance and stiffness are common (see Fig. 2.1), as are vertical irregularities of strength and stiffness (Fig. 2.4) or geometry (Fig. 2.3). Floor diaphragms are sometimes not continuous or strong enough (see Figs. 2.21 and 2.25) or well connected to the lateral load resisting elements (see Figs. 2.6 and 2.7) to tie everything together into an integral system. Buildings with only the ground storey open (for commercial use or parking) are not protected by strong walls from soft-storey collapse (Fig. 2.10) or may develop plastic hinges in strong columns connected with weak beams owing to the effect in Fig. 2.9(b) and (c) (see Fig. 3.27(a) and (b) for examples). Captive columns are quite common for architectural reasons (Fig. 2.12), etc.

As pointed out in Section 2.1.13.5 in connection with Fig. 2.13(a), the contribution of staircases to the storey lateral strength and stiffness sometimes helps flexible buildings. Most of the times, however, depending on its connection to the elements of the lateral load resisting system and/or its location in plan, the staircase does more harm than good (see Fig. 2.13(b) and (c) and case at the bottom left corner of Fig. 3.35).

The systematic deficiencies of old substandard concrete buildings do not necessarily mean that they will do poorly in the event of an earthquake. Quite a few of them have gone unscathed through strong earthquakes thanks to unintended, albeit significant, lateral strength provided by design and construction practices of the past. Examples include closely spaced columns, uniform infilling with strong, good quality masonry having few large openings, or even large concrete walls, be it underreinforced.

6.2.2 Common Deficiencies and Failure Modes of Concrete Members

Owing to their poor structural layout, the lack of a strength hierarchy engineered to control the inelastic response mechanism, deficient or discontinuous load paths, etc., existing substandard buildings may experience certain concentration of seismic deformation demands to few of their elements in the event of a strong earthquake. Unfortunately these elements may be ill-prepared to withstand the increased demands, as they lack detailing for ductility and are not protected from pre-emptive brittle failures.

Non-ductile failures of members or connections due to poor detailing are aplenty in reconnaissance reports. Regarding flexural plastic hinges, Fig. 3.27(b), (c) and (f) depict failed column end regions with little confining reinforcement. In these figures ties not anchored by a 135° hook into the concrete opened up. Figure 3.27(f) is also a case of poor lapping at floor level. Figure 3.29 shows that beam bars (especially bottom ones) may pull-out from corner joints, if not anchored there by a 90°-bend or hook. Figure 3.35 depicts several shear failures of columns or walls having only widely spaced perimeter ties and indeed in some cases poorly closed ones. Obviously, the members in Fig. 3.35 have not been protected from shear failure by capacity design. Finally, the two corner joints in Fig. 3.47(b) and (c) had no horizontal reinforcement.

Columns without engineered earthquake resistance have normally been designed only for gravity compression with a nominal eccentricity. So, they are not only undersized and poorly detailed, but also have low flexural and shear resistance against lateral loads. By contrast, the beams of seismically deficient buildings normally have substantial flexural and shear resistance thanks to their design for factored gravity loads. So, unlike column failures which abound, beam failures are rare. They are mostly limited to bar pull-out of the type of Fig. 3.29, as anchorage of bottom bars at the supports is of little importance for gravity loading. This type of failure reduces the moment resistance of the frame and increases its flexibility, but poses little threat to life safety.

Faced with the poor detailing and obvious lack of engineered earthquake resistance of old concrete members and the deficiencies of the structural layout, the engineer carrying out a seismic evaluation of an existing building will contrast them with current knowledge and design practice for new buildings (including his/her own

practice) and may come to the conclusion that the building is doomed in the event of a strong earthquake. This is human, but it may be premature. Each building has its own personality, reflecting that of the original designer and his/her perceptions, which may be different from the preconceptions of the engineer carrying out the evaluation. He/she should also look for possible sources of overstrength (see last paragraph of Section 6.2.1) that may partly make up for the member and system deficiencies. Although good judgment and experience are of prime importance for the seismic evaluation of an existing building, only a meticulous detailed assessment, e.g., along the lines of Section 6.5, can point out its real deficiencies and overstrengths and guide properly the decisions for its retrofitting.

6.3 The Predicament of Force-Based Seismic Assessment and Retrofitting

In the past detailed seismic assessment of individual buildings was force-based, mimicking design of new buildings. Capacity-demand comparisons were carried out at the member level in terms of forces, with internal force demands and resistances determined according to code provisions for the seismic design of new buildings. A prime example is the ENV version of the relevant part of Eurocode 8 (CEN 1996), according to which assessment had to be carried out by checking whether the provisions of the part of the ENV-Eurocode 8 for the design of new buildings for one of three Ductility Classes (H, M or L) were met. So, all members were first examined for fulfilment of detailing and minimum/maximum reinforcement rules of the three alternative DCs. If all of them satisfied those of one of the two upper DCs, they were also checked for fulfilment of the corresponding capacity design rules. If these rules were met, the value of the q-factor for which the building qualified was determined, according to its structural system and regularity. Otherwise, the engineer would classify the building as DC L and be content with its low q-factor value.[1] With the value of the behaviour factor q known, the design spectrum could be entered and linear analysis, of the lateral force or of the modal response spectrum type was employed to determine the design internal forces, E_d, of members (including P-Δ effects and the applicable capacity-design calculations). Design values of member resistances, R_d, were also determined, according to the relevant rules of Eurocode 2, as modified by Eurocode 8, if DC M or H was applicable. If $E_d > R_d$ was not satisfied, strengthening of the building was required.

Assessment of existing structures by checking compliance with a standard for the design of new ones is neither rational nor practical. An old structure is very unlikely to meet the very stringent requirements of modern codes for structural regularity, ductility at the local level (member detailing) and at the structural level (control of inelastic response through capacity design), continuity of the load path, etc., and

[1]The ENV-Eurocode 8 did not provide for "secondary" members, to allow exempting some elements from full satisfaction of the requirements of DC M or H for detailing, capacity design, etc.

qualify for a Ductility Class that uses ductility and energy dissipation capacity for earthquake resistance. If it doesn't, and unless it is a low-rise building with large concrete walls, it is also very unlikely to have the lateral strength necessary to resist elastically the seismic action (i.e., with $q = 1.5$). In this way all old structures may be found to be inadequate and to need retrofitting. If so, to comply with a code for new structures, practically all structural elements would have to be upgraded to meet all the resistance and detailing requirements of that code. Then the cost of retrofitting would exceed that of replacement. The owner is then very likely to decide to do nothing and continue using (or living in) a building that is now known to be unsafe.

6.4 Seismic Performance Requirements and Criteria for Existing or Retrofitted Buildings

In view of the predicament of conventional force-based approaches, the performance requirements, criteria and procedures adopted now for existing or retrofitted buildings differ from those in current codes for new construction. Recognising the much higher total cost of retrofitting (including the indirect cost of disruption of occupancy) compared to new construction, the new approach adopts more flexible requirements, which address the real intent of the owner and of the code-maker. The new requirements are served by more rational and less conservative criteria, limiting retrofitting to the cases where it is really needed and making it more cost-effective. Note that the pragmatic new attitude does not rely on the presumably shorter remaining service life of an existing building, as on that basis a building could be evaluated as adequate for the lower seismic action corresponding to a remaining life of a few years, after the eventless end of which the positive evaluation might be renewed for another period, etc., which does not make much sense.

The new requirements are fully and explicitly performance-based, in the sense of Section 1.1.2. A multi-level performance menu is provided, for the owner (or the competent authority) to choose the performance objectives that fit not only the importance, use and occupancy of the building, but also his/her means and intent. For example, an owner may be prepared to pay more, to avoid any disruption of the operation of the facility after a rare earthquake. By contrast, another owner may just have the means and the wish to avoid collapse under an occasional earthquake, retaining the option of retrofitting to a higher performance objective if financing conditions improve in future (see Section 1.1.2 for the meaning and definitions of the various performance and hazard levels).

The new criteria serving the performance objectives are also more rational and less conservative than the prescriptive ones associated with the performance requirements of current codes for new buildings:

– Poor detailing combined with low force resistance in many members is not a problem, provided that the system of lateral-load-resisting elements, old, retrofitted or new, assures global stability. Some members may be explicitly

allowed to develop large, permanent post-ultimate-strength deformations, provided that their gravity-load capacity is not impaired. These may be "secondary members", at a number and with a contribution to lateral resistance which are more relaxed compared to new buildings or not capped at all. They may even be "primary" ones, under the condition that the system as a whole meets the performance objectives. This of course entails checking member deformation demands against their capacities.

– Sources of earthquake resistance and energy dissipation in the existing and in the retrofitted structure that are normally neglected in the design of new buildings, are explicitly taken into account. Examples include the positive effects of non-structural elements (e.g. masonry infills) and the redistribution and reduction of seismic demands thanks to nonlinearities in the structural system and the foundation, without artificial limits. This of course entails modelling and analysis at a higher level of sophistication than in the simple, yet conservative, approaches commonly used for new designs.

As these new trends become established through successful application in assessment and retrofitting projects, they will start affecting codes for the design of new structures as well. This represents a reversal over the past tradition, where procedures and codification for existing structures followed and emulated those for new ones.

6.5 Performance- and Displacement-Based Seismic Assessment and Retrofitting in Eurocode 8

6.5.1 Introduction

Part 3 of Eurocode 8 (CEN 2005a) is unique among all EN-Eurocode parts in many respects:

1. It is the only one in the whole set of 58 EN-Eurocode that deals with existing structures.[2]
2. It is essentially the first standard in Europe on seismic assessment and retrofitting. So, as there is no previous experience in European practice with codified seismic assessment and retrofitting, Part 3 of Eurocode 8 is an experiment. It is not sure yet how it will work in engineering practice.
3. Unlike all other EN-Eurocodes, which will eventually apply for all structures within their scope (i.e., to all new structures), Part 3 of EN-Eurocode 8 will not apply to all structures in its scope, i.e., to all existing buildings, but only to those that the owner – or local Authorities – have decided to seismically assess and possibly retrofit. So, this EN-Eurocode addresses only the structural aspects of

[2]As a matter of fact, an effort for an Annex to EN1990: "Basis of Design" on "Assessment and Retrofitting" has been launched in 2008.

seismic assessment and retrofitting and will apply once the requirement or will to assess a particular building has been established. The conditions under which seismic assessment of individual buildings – possibly leading to retrofitting – may be required are beyond the scope of Part 3 of EN-Eurocode 8. The initiative for seismic assessment and retrofitting lies with the owner, unless a national or local programme is undertaken for seismic risk mitigation through seismic assessment and retrofitting.

4. As a consequence of the other peculiarities, the extent and scope of the normative (i.e., mandatory) part of Eurocode 8-Part 3 is limited, covering only the general rules on:

   – the performance requirements and criteria,
   – the applicability conditions of the four analysis methods,
   – the type of verifications for ductile and brittle modes of behaviour and failure, and
   – the collection of information for the assessment and its implications, etc.

   All material-specific aspects and details (including expressions for modelling and verifications) can be found in Informative Annexes, for:

   – concrete structures,
   – steel or composite structures, and
   – masonry buildings.

   The information in these Annexes is not binding. It is up to National Authorities (but not to individual designers or owners) to adopt or not this information or even replace it with reference to other, national, sources of information.

6.5.2 Performance Requirements

Section 1.1.3 has described the three performance levels provided in CEN (2005a), called there Limit States:

1. "Damage Limitation" (DL);
2. "Significant Damage" (SD); and
3. "Near Collapse" (NC).

As pointed out in Section 1.1.3, it is not necessary to fulfil all three Limit States under the corresponding the "hazard level". The country, through its National Annex – or the owner, if the country doesn't make a choice – will decide how many and which of the three should be met. National authorities will also choose the "hazard levels" corresponding to these Limit States, depending on the prevailing level of risk tolerance and the socio-economic conditions. National authorities may well leave the choice open for the owner to make.

It is hoped that national authorities will choose the performance requirements for existing buildings in their territory so that they encourage owners to retrofit their property, while the population of buildings to be retrofitted is acceptable for the society and the national economy. As a matter of fact, the intent of the Eurocode is to let the owner make all these choices (of course after listening to advice from the designer or an engineering consultant), depending on his/her means, priorities and needs. For example, an owner may afford only to upgrade the very poor seismic resistance of his/her residence for collapse prevention in an occasional earthquake, while another may have the interest and means to retrofit his/her facility to be operational even after a rare event.

Unlike its practice for most Nationally Determined Parameters, the Eurocode itself does not a give a recommendation for the "hazard levels" corresponding to the three Limit States. It mentions, instead, in a note that the performance objective recommended as suitable to ordinary new buildings is a 225 year earthquake (20% probability of exceedance in 50 years), a 475 year event (10% probability in 50 years), or a 2475 year one (2% probability of being exceeded in 50 years), for the DL, the SD or the NC "Limit State", respectively. As a matter of fact, countries and owners should avoid adopting blindly this note, because in most seismic regions of Europe the 475 year earthquake is not much stronger than the 225 year one. So, if the 225 year earthquake is indeed chosen for the "Damage Limitation" Limit State, it will govern the whole assessment and/or retrofitting sufficiently to make it at best uneconomical or sometimes unfeasible.

Note that an earthquake with a mean return period of 475 years, mentioned in the above note of Part 3 of Eurocode 8 as suitable for the "Significant Damage" (SD) level in ordinary new buildings, is also the choice recommended in Part 1 of Eurocode 8 for the "local-collapse prevention" level of new designs. It appears, therefore, that these two parts of Eurocode 8 do not recommend any differentiation in the "performance objective" that has to do with Life Safety between new and existing buildings. However, such differentiation is made through the "compliance criteria" specified in these two parts for this single performance level. Although there is no direct correspondence of the criteria, those in Part 3 for existing buildings are less demanding than what Part 1 provides for new ones.

Performance differentiation of essential or large occupancy buildings from ordinary ones is effected as in new buildings, i.e., by multiplying the seismic action with the "importance factor", which has the recommended values given in Part 1 for new buildings (see Section 1.1.1).

6.5.3 Information on the As-Built Geometry, Materials and Reinforcement

A prime prerequisite for the seismic assessment or retrofitting of an individual building through analysis of a fairly detailed structural model is to have all the information needed for setting up the model: the topology of the lateral-load-resisting

system, the cross-sectional dimensions, reinforcement and relevant material properties of its members, the gravity loads acting concurrently with the seismic action and the corresponding masses, etc.. If infill walls play an important role in the seismic response and will be included in the model, their topology, thickness and openings, as well as the masonry properties, should also be known. Ideally, all this information will be available in as-built drawings and material test reports from the time of construction and should be confirmed through spot-checks and lab testing of few samples. However such information is often not available, or turns out to be incomplete or unreliable. In that case, missing information is collected through a survey of the building and a campaign of in-situ measurements and lab tests on samples.

If the building as-is has certain earthquake resistance and is assessed to find out whether retrofitting might be avoided, it is essential to have good knowledge of the amount and detailing of the reinforcement and of the material properties in at least the critical structural and non-structural members. However, it is in such a building that collection of this information through exposure of reinforcement and extracting samples for lab tests is harder, as in all likelihood it is occupied and used at the time. Moreover, any damage to members that will not be retrofitted in the end should be fully redressed and not just patched-up. In other cases it is clear from the outset that the as-is building is doomed unless drastically upgraded, e.g., by adding major new components, such as concrete walls, to provide most of the required earthquake resistance. Then its structural model, although still valuable for identifying the specific deficiencies to be remedied by retrofitting, is mainly used as the basis for studying different retrofitting schemes. In such situations the performance of the retrofitted building is not very sensitive to the amount and detailing of the reinforcement or the material properties in the existing structural and non-structural members. The same applies for (vertical) members suffering from severe reinforcement corrosion and to be concrete-jacketed anyway. Unfortunately, these are also the cases where collection of information is easiest, as the building may be evacuated anyway before the retrofitting and any damage due to exposure of reinforcement and material sampling will be corrected anyway during retrofitting. At any rate, plenty of judgement is needed to adapt the scope and depth of the campaign of destructive in-situ measurements and sampling to the specific conditions and needs of a project. To this end, the in-situ collection of data should be carried out – or at least controlled – by the engineer in charge of the subsequent seismic assessment and retrofit design. It should never be delegated to another team that follows blindly a protocol producing lots of redundant data, while possibly leaving out crucial information.

Needless to say, the more extensive and reliable the information, the smaller is the uncertainty and the closer is the analysis model to reality. The uncertainty is reflected in the values of the partial safety factors, γ_{m}, for the calculation of member capacities and of any model uncertainty factors, γ_{Rd}, involved in the verifications of the existing or of the retrofitted building. So CEN (2005a) distinguishes three different cases, depending on the amount and reliability of the information available for the as-built structure:

1. "Limited knowledge";
2. "Normal knowledge";
3. "Full knowledge".

These three cases are defined as follows:

1. In "limited knowledge" permanent loads and masses, as well as member and infill geometry should be derived either:
   - from drawings of the original construction and of any subsequent modifications, validated in-situ visually and with spot-measurements, or
   - through a full campaign of in-situ measurements of geometrical quantities.

   Original information on the amount and detailing of reinforcement or the materials used is not essential. Indirect information and judgement may be used for them, instead. One can make default assumptions for the materials on the basis of the codes applicable and the practice prevailing at the time of construction (for the steel, after visual identification of its grade among the ones used at that time). These assumptions should to be spot-verified or calibrated in-situ with one material sample per floor for each type of member (column, beam or wall). Past codes and practice may also be the basis for the estimation of the amount and detailing of reinforcement through simulation of the original design. In other words, to figure out the reinforcement the engineer tries to put him/herself in the position of the original designer and contractor. The results of the simulated design should be confirmed or calibrated through spot checks of a small fraction of the total number of structural members of each type, recommended in CEN (2005a) as at least 20%. Needless to say, all this requires good knowledge of past codes and design/construction practice, as well as experience and judgement. For example, attention and spot-checking should focus on the important primary elements (especially those of the most critical storey) and may be more lax for secondary ones or for infills. Spot-checking should be prolonged if it has given large scatter or significant deviations from the default assumptions for materials or from the outcome of the simulated design. Extraction and testing of concrete cores should be supplemented with an extensive campaign of indirect measurements (with concrete hammer or ultrasounds), calibrated against the core test results.
2. "Normal knowledge" is the reference case for the available information. It entails knowledge of structural topology, cross-sectional dimensions, infills and amount and detailing of reinforcement either from:
   - original construction drawings (including any subsequent modifications), confirmed by in-situ checks (as in "limited knowledge"), or
   - (if original construction drawings are unavailable or not confirmed by the spot-checks) a full campaign of in-situ measurements, with exposure of reinforcement in a large fraction of the total number of structural members of each type, recommended in CEN (2005a) as at least 50%.

Material properties are derived either:

- from the original specifications, verified in-situ with few samples (Eurocode 8 recommends one per floor for each type of member), or
- through in-situ sampling and testing of some samples (Eurocode 8 recommends two per floor and member type).

Although masonry infills are not specifically mentioned by Eurocode 8 in this connection, it makes sense to estimate their strength properties and Elastic Modulus from the properties and geometry of the masonry blocks and mortar using semi-empirical expressions (e.g., those in Eurocode 6).

3. For "full knowledge", the engineer should draw information for the permanent loads, the topology of the structural system, the member cross-sectional dimensions, the amount and detailing of reinforcement and the location and geometry of infill walls from detailed original construction drawings, confirmed by checking at least 20% of all members per member type (column, wall, beam or infill). If the outcome of the spot checks does not fully agree with the drawings, then it is as if these drawings were not available. Lacking original drawings, a thorough survey of the structure is carried out, including exposure of reinforcement in almost all structural members of each type ((CEN 2005a) recommends at least 80%). Material properties are inferred either:

   - from test reports at the time of construction, verified by few samples ((CEN 2005a) recommends one per floor and member type), or
   - from in-situ testing, material sampling and lab tests of several samples ((CEN 2005a) recommends three per floor and member type).

   If masonry infills are considered in the assessment, certain sampling and testing for shear and compressive strength and for Elastic Modulus makes sense.

In all cases, whenever the scatter of test results in-situ or in the lab (as measured by the coefficient of variation) is large, or there is evidence that supervision during construction has not been so meticulous, the engineer should use judgment to possibly extend sampling and testing beyond the minimum required.

According to CEN (2005a), the mean value properties of existing materials should be used, as directly obtained from in-situ tests and any additional sources of information, after "correction" with a "confidence factor". The "correction" should always be safe-sided. Mean material properties used in the calculation of a capacity of an existing member (yield moment, shear resistance, chord rotation or curvature at yielding or at ultimate, etc.) to be compared to a demand, are divided by the "confidence factor". By contrast, if these mean material properties are employed for the calculation of a moment resistance from which capacity-design action effects are derived for a brittle mode of failure through equilibrium (see Section 1.3.6), then they are multiplied by the "confidence factor". Similarly, the yield stress considered for existing longitudinal bars at lap splices or bar anchorages is the mean value from in-situ tests and any additional sources of information, multiplied by the "confidence factor".

The values of the "confidence factor" recommended in CEN (2005a) are:

1. For "limited knowledge": 1.35;
2. for "normal knowledge": 1.20;
3. for "full knowledge": 1.00.

No confidence factor is applied on the nominal strength of new materials added for the purposes of retrofitting. If an existing member is modified, e.g., by FRP- or concrete-jacketing, a "confidence factor" is applied only on its old materials. Moreover, although such a distinction is not clear in CEN (2005a), it makes sense to apply to each old material (steel, concrete, or infill masonry) the value of the "confidence factor" corresponding to its own level of knowledge. For instance, member sizes may be well known and concrete may have been thoroughly sampled and lab-tested, while the amount and detailing of reinforcing bars may be rather unknown, or bars of a certain diameter or the infill material have not been sampled and tested at all.

According to CEN (2005a) "limited knowledge" may support only linear analysis. Note that the applicability of an analysis approach does not really depend on the level of knowledge available for the as-built structure. The restriction of the use of nonlinear analysis methods only to the cases of "normal" or "full knowledge" stems mainly from the concept of harmonised accuracy: it does not make much sense to use sophisticated and complex modelling and analysis with poor and highly uncertain input data. The real purpose, though, of the restriction is to motivate engineers who prefer using a more advanced method of analysis as less conservative, to collect also more information about the as-built structure. Note that, if the level of knowledge associated with different aspects of the as-built structure (e.g., the loads, the material strengths, the quantity and detailing of reinforcement, etc.) is different, it is the lowest level of knowledge for any one of these aspects that determines the type of analysis allowed.

6.5.4 Seismic Analysis and Models

6.5.4.1 Seismic Analysis Procedures and Applicability Conditions

As pointed out in Sections 4.1.2 and 4.11.1, the prime (if not only) aim of an analysis for displacement-based seismic assessment or retrofitting is the calculation of the deformation demands in structural members. Part 3 of Eurocode 8 (CEN 2005a) provides to this end the full menu of analysis options described in Chapter 4:

- the two linear options: linear static (Section 4.3) and modal response spectrum analysis (Section 4.4), and
- the two nonlinear ones: nonlinear static or "pushover" analysis (Section 4.6.1) and nonlinear dynamic analysis (Section 4.6.2).

In seismic design of new buildings linear analysis uses the design response spectrum incorporating the behaviour factor q. In displacement-based assessment or

retrofitting, by contrast, linear analysis – when applicable – uses the 5%-damped elastic response spectrum. In CEN (2005a) member inelastic deformation demands (e.g., chord-rotations) are derived directly from such an analysis, applying the equal-displacement rule at the member level. The sole condition for this simplification is to have uniform chord-rotation ductility demands throughout the building. As pointed out in Section 4.11.1, uniformity of inelastic chord-rotation demands over the building is evaluated on the basis of the demand-to-capacity ratio, D/C, in *flexure*, where D is the bending moment at the end of a member due to the seismic action and the concurrent gravity loads from linear analysis and C the corresponding moment resistance,[3] calculated on the basis of the axial force due to gravity loads alone and using mean-value properties of old materials from in-situ tests and any additional source of information, or nominal values for new materials. Linear analysis is not allowed, if the maximum D/C-ratio in all "primary members" exceeds its minimum value over all such elements that have $D/C > 1$ by more than a factor in the range of 2–3 (as a Nationally Determined Parameter) with a recommended value of 2.5. Those sections around beam-column joints where plastic hinging is ruled out on the basis of the sums of beam or column moment resistances, ΣM_{Rb} or ΣM_{Rc}, respectively, are presumed to remain elastic and neglected in the check of the variation of D/C throughout the structure. As noted in Section 4.11.1, although there is no limit on the absolute magnitude of D/C for the applicability of linear analysis, there will always be at least one section in the entire structure where D/C slightly exceeds 1.0, making the relative limit on D/C essentially an absolute one.

If this applicability condition of linear analysis is not met, only nonlinear analysis is permitted. Recall, however, that (CEN 2005a) allows nonlinear analysis only when we have "normal" or "full knowledge" of the as-built structure. So, if only nonlinear analysis turns out to be applicable, or if the engineer wants to include in the structural model the contribution of "secondary members" to the lateral strength and stiffness (see below), he/she has no choice but to collect enough information for at least "normal knowledge".

The rules and procedures for linear or non-linear analysis are those described in Sections 4.3, 4.4 and 4.6 with reference to Part 1 of Eurocode 8 (CEN 2004a).

No matter which method of analysis is applied, we should take into account torsional effects due to the accidental eccentricity and simultaneous seismic action components according to Sections 4.8 and 4.7, respectively.

6.5.4.2 Modelling Aspects

For modelling, the reader is referred to Sections 4.9 and 4.10. Points which are of special importance in the context of an analysis for seismic assessment and retrofitting are highlighted and elaborated further in the present section.

Throughout the structural model mean values of material properties should be used. For old materials, as derived from in-situ tests and any additional sources of

[3] If the equal displacement rule indeed applies, D/C is about equal to the demand value of the chord-rotation ductility ratio, μ_θ.

information without modification by the "confidence factor" of Section 6.5.3. For new materials, as estimated on the basis of the nominal values of their properties.[4]

Part 3 of Eurocode 8 places special emphasis on the effective elastic stiffness of members to be used in linear or nonlinear analysis. It recommends for that purpose the secant stiffness to the yield-point from Eq. (3.68), instead of 50% of the uncracked gross-section stiffness, which is the default for force-based design in Part 1 of Eurocode 8 (see Section 4.9.2). For the purposes of Eq. (3.68) M_y and θ_y may be computed according to Sections 3.2.2.2 and 3.2.3.2, respectively, with the effect of any lap-splicing or FRP-wrapping taken into account on the basis of Sections 3.2.3.9 or 3.2.3.10, respectively, and that of concrete jacketing according to Section 6.8.2.3.

As pointed out in Section 6.5.6, in order to have a successful (i.e., positive) seismic assessment of the as-is building or evaluation of the retrofitted one, every single member in the model, "secondary" or "primary", should meet all relevant verification criteria. Verification criteria for brittle modes of behaviour (i.e., in shear), include a margin against failure (in that case, against significant loss of force resistance). Verification criteria for ductile modes (namely in flexure), also in general entail a certain margin from the expected value of ultimate deformation (conventionally identified with a drop in peak force resistance to less than 80% of the maximum possible capacity). Therefore, there is no real need to incorporate in nonlinear force-deformation models of members any strength decay due to this conventionally defined failure. If indeed failure takes place, the verification criteria will in all likelihood be violated, signalling the need for (more effective) retrofitting. When in the end all verification criteria are met, all members will be at sufficient distance from ultimate conditions (identified with a drop in peak resistance) to justify using a nonlinear force-deformation model with a non-decreasing primary loading branch. For example, Eqs. (4.82) and (4.85) may be used for the constant post-yield hardening ratio of the uniaxial M-φ or M-θ curve in primary loading. In these expressions M_u may be computed according to Section 3.2.2.5, M_y and φ_y from Section 3.2.2.2, θ_u and θ_y according to Sections 3.2.3.5 and 3.2.3.2, respectively, and φ_u from Section 3.2.2.4. Minor differentiations of the information in Annex A of CEN (2005a) from the contents of these latter sections in Chapter 3 have been pointed out: in Section 3.2.2.10 for φ_u, in Section 3.2.3.2 for θ_y and in Section 3.2.3.5 for θ_u. Sections 3.2.3.9, 3.2.3.10 or 6.8.2.3 provide means to take into account the effects of any lap-splicing, FRP-wrapping, or concrete jacketing, respectively, on M_u, M_y, φ_u, φ_y, θ_u and θ_y and point out also any differentiation from the information in Annex A of CEN (2005a).

Except wherever slippage of longitudinal bars from a joint or a foundation element is prevented or restricted through positive means of fixity at the end section or at a short distance inside the joint or the foundation element, model parameters should be determined assuming that such slippage does take place (i.e., using $a_{sl} = 1$ in Eqs. (3.66), (3.72), (3.78), etc.).

---

[4]The value f_{ck} + 8 MPa, from which the elastic modulus of concrete is calculated according to Eurocode 2, is indeed a conventional mean value of the compressive strength of a concrete with nominal strength f_{ck}.

For any one of the simple models mentioned above we need to know the applicable values of the member shear span and axial load. As pointed out in Sections 4.10.1.3 and 4.10.1.4, even in a nonlinear analysis the member effective stiffness should stay constant throughout the course of the analysis. So, it should be based on the member axial force due to the gravity loads concurrent with the seismic action and on a constant value of the shear span at the member end(s) where a plastic hinge might form. Section 4.10.1.4 has suggested and Section 4.10.5.1 adopted (at point 2) the following values of the shear span:

(i) At each end of a beam or column framing into a joint with another element: half the clear length from one such joint to the next within the plane of bending, neglecting any intermediate nodes along this clear length where the beam or the column may be connected to another member lying in a plane at right angles to the plane of bending.
(ii) The shear span of a beam ending at an indirect support on another beam may be taken equal to its full clear span.
(iii) For each wall segment between successive floors: 50% of the height from the bottom section of the storey to the top of the wall in the building.

Because there is a single effective stiffness for each member, the average secant-to-yield-point stiffness at the two end sections in positive or negative bending should be used. Beams or columns connected at intermediate nodes with other members that have no stiffness within the plane of bending (e.g., a girder connected with cross-beams or girders, a column with two-way frame action in certain storeys and one-way action in others, etc.) have a single effective stiffness value throughout the full length between successive nodes where the member in question frames into elements with certain stiffness within the plane of bending. That effective stiffness is determined using in Eq. (3.68) the yield moments at the two end sections of this full length and as shear span 50% of the clear length between them.

During the course of nonlinear analysis any parameter of the member's nonlinear force-deformation relation other than its effective stiffness, such as the yield moment and the post-elastic primary loading branch derived from it, may be taken to vary with the axial force. Model parameters are not overly sensitive to the axial force value, at least for the smooth variation it exhibits even during a response-history analysis. By contrast, the shear span at each member end may vary wildly, depending on the relative magnitude and sign of the end moments and – in beams – on the concurrently acting transverse loads. So, it is strongly recommended to continue basing all parameters of the member nonlinear force-deformation relation on the initially adopted values of the shear span at the two member ends.

Note that the fixed-end moments at beam end sections due to the concurrent transverse loads induce zero chord rotation there. Moreover, the shear span value used in the calculation of the member's single effective stiffness normally differs from the moment-to-shear ratio at an end section at the time it first reaches its yield moment, M_y, during the calculated response. For these two reasons we may have significant disparity between the end's chord rotation at first yielding from the analysis on one hand, and the value of θ_y from Section 3.2.3.2 on the other. To avoid

ambiguities, yielding of an end section should be considered to take place when M_y is attained there, no matter how much the concurrent chord rotation from the analysis, $\theta_{y,act}$, differs from the θ_y-value used in the calculation of the effective stiffness from Eq. (3.68). Plastic deformations are taken to start from that chord rotation. For member assessment the demand value of the plastic chord rotation should be compared with the plastic part of the ultimate chord rotation, ${\theta_u}^{pl}$, i.e., with the part of the ultimate chord rotation, θ_u, in Eqs. (3.72), (3.78) and (3.79) beyond θ_y (as this part is modified for the effect of any lap-splicing or FRP-wrapping according to Sections 3.2.3.9 and 3.2.3.10, respectively). It is also that demand value of plastic chord rotation that should be divided by the value of θ_y from Eqs. (3.66) to give a ${\mu_\theta}^{pl}$-value for use in the verification of the member in cyclic shear through Eqs. (3.114), (3.115) and (3.127). If it is the total ultimate chord rotation, θ_u, from Eqs. (3.72), (3.78), (3.79), (3.80) and (3.84), etc., or a fraction thereof (see Section 6.5.6 and Table 6.1) that is compared to the demand for the purposes of member verification, that demand should be the value from the analysis plus $(\theta_{y,act.} - \theta_y)$, with $\theta_{y,act}$ being the chord rotation from the analysis when M_y is attained there and θ_y the value from Eqs. (3.66).

Unlike in new buildings, the contributions of "secondary members" to strength and stiffness against lateral loads may well be included in the structural model. Part 3 of Eurocode 8 (CEN 2005a) essentially requires including them, if the analysis is nonlinear. If their contributions are neglected, as allowed by CEN (2005a) in linear analysis, we cannot determine the seismic deformation demands against which "secondary members" should be verified (see Section 6.5.6.1 and Table 6.1). In that case, we should carry out two linear analyses per horizontal component of the seismic action, namely those referred to as analysis no. 1 and 2 in Section 4.12.3 (see also models no. 1 and 2 in Section 4.12.5.1). The seismic deformation demands in the "secondary members" of storey *i* from analysis no. 2 (including the "secondary members") is then multiplied by the ratio of interstorey drifts of that storey from analysis no. 1 (neglecting them) to those from no. 2. The outcome may be taken as the seismic deformation demands in the "secondary members" and compared to the corresponding capacities.

As pointed out in Section 4.12.5.2, if the cyclic degradation of strength and stiffness in "secondary members" is thought to be indeed much larger than in "primary" ones, it can be included in a nonlinear model via a descending post-yield branch (with negative slope) of the force-deformation curve in primary loading. In nonlinear dynamic analysis the hysteresis rules may instead include degradation of strength with cycling (see Section 4.10.1.6).

6.5.5 Estimation of Force Demands by Capacity Design In Lieu of Linear Analysis

Brittle mechanisms of behaviour, such as shear, are assessed in terms of forces. Linear analysis is not appropriate for the estimation of internal force demands in the inelastic regime, even when it is applicable for the estimation of member inelastic

deformation demands. When the relevant applicability conditions are met and member inelastic deformation demands are indeed estimated for simplicity from linear analysis, we should resort to capacity design calculations of the internal force demands on members going into the inelastic range.

According to CEN (2005a) any moment resistance involved in the estimation of internal force demands through capacity design may be calculated using the axial force due to gravity loads alone, neglecting the one induced by the seismic action. After all, this latter value is unknown in the framework of linear analysis.

6.5.5.1 Shear Forces in Beams or Columns

Taking into account the possibility that under the seismic action of interest and the concurrent gravity loads plastic hinging in a column may take place at both, or just one, or none of the two end sections, i =1, 2, its shear force is estimated from the following modification of Eq. (1.12):

$$V_{\mathrm{CD,c}} = \frac{M_{\mathrm{c1}} + M_{\mathrm{c2}}}{H_{cl}} \tag{6.1}$$

where:

– if $M_{\mathrm{Ed,ci}} > M_{\mathrm{R,ci}} \min\left(1; \dfrac{\sum M_{\mathrm{R,b}}}{\sum M_{\mathrm{R,c}}}\right)_i$, then $M_{\mathrm{ci}} = M_{\mathrm{Rd,ci}} \min\left(1; \dfrac{\sum M_{\mathrm{R,b}}}{\sum M_{\mathrm{R,c}}}\right)_i$ $(i = 1,2)$ (6.2a)

– if $M_{\mathrm{Ed,ci}} \leq M_{\mathrm{R,ci}} \min\left(1; \dfrac{\sum M_{\mathrm{R,b}}}{\sum M_{\mathrm{R,c}}}\right)_i$, then $M_{\mathrm{ci}} = M_{\mathrm{Ed,ci}}$ $(i = 1,2)$ (6.2b)

$M_{\mathrm{Ed,ci}}$ in Eqs. (6.2) denotes the moment at column end section i (=1, 2) from the linear analysis for the seismic action of interest and the concurrent gravity loads. $M_{\mathrm{R,ci}}$ is the moment resistance there calculated from the mean material properties from in-situ tests and any additional sources of information. $M_{\mathrm{Rd,ci}}$, appearing only in the 2nd part of Eq. (6.2a), is the moment resistance from these mean material properties times the relevant "confidence factor" corresponding to the "knowledge level" applying to this case. The ratios of sums of moment resistances, $\Sigma M_{\mathrm{R,b}}$, $\Sigma M_{\mathrm{R,c}}$, refer to the end sections of those beams and columns, respectively, that frame into the joint at column end i (=1, 2). H_{cl} is the clear height of the column.

By the same token, the shear force at cross-section x along the part of the beam nearest to beam end 1 (the other end denoted as 2) is estimated from a modification of Eq. (1.9a):

$$\max V_{\mathrm{CD,b1}}(x) = \frac{M^-_{\mathrm{b1}} + M^+_{\mathrm{b2}}}{L_{cl}} + V_{\mathrm{g}+\psi\mathrm{q,o}}(x) \tag{6.3}$$

where:

– if
$$M_{\mathrm{Ed,b1}}{}^{-} > M_{\mathrm{R,b1}}{}^{-} \min\left(1; \frac{\sum M_{\mathrm{R,c}}}{\sum M_{\mathrm{R,b}}}\right)_1, \text{ then } M_{\mathrm{b1}}{}^{-} = M_{\mathrm{Rd,b1}}{}^{-} \min\left(1; \frac{\sum M_{\mathrm{R,c}}}{\sum M_{\mathrm{R,b}}}\right)_1 \tag{6.4a}$$

– if $M_{\mathrm{Ed,b1}}{}^{-} \le M_{\mathrm{R,b1}}{}^{-} \min\left(1; \frac{\sum M_{\mathrm{R,c}}}{\sum M_{\mathrm{R,b}}}\right)_1$, then $M_{\mathrm{b1}}{}^{-} = M_{\mathrm{Ed,b1}}{}^{-}$ (6.4b)

– if
$$M_{\mathrm{Ed,b2}}{}^{+} > M_{\mathrm{R,b2}}{}^{+} \min\left(1; \frac{\sum M_{\mathrm{R,c}}}{\sum M_{\mathrm{R,b}}}\right)_2, \text{ then } M_{\mathrm{b2}}{}^{+} = M_{\mathrm{Rd,b2}}{}^{+} \min\left(1; \frac{\sum M_{\mathrm{R,c}}}{\sum M_{\mathrm{R,b}}}\right)_2 \tag{6.5a}$$

– if $M_{\mathrm{Ed,b2}}{}^{+} \le M_{\mathrm{R,b2}}{}^{+} \min\left(1; \frac{\sum M_{\mathrm{R,c}}}{\sum M_{\mathrm{R,b}}}\right)_2$, then $M_{\mathrm{b2}}{}^{+} = M_{\mathrm{Ed,b2}}{}^{+}$ (6.5b)

In Eqs. (6.4) and (6.5) $M_{\mathrm{Ed,bi}}$ (i=1, 2) is the moment at beam end section i (=1, 2) from the linear analysis for the seismic action of interest and the concurrent gravity loads. $M_{\mathrm{R,bi}}$ is the value of moment resistance there from the mean material strengths from in-situ tests and any additional sources of information and $M_{\mathrm{Rd,bi}}$ its value from these mean material properties times the relevant "confidence factor" corresponding to the "knowledge level" applying to this case. Hogging moments (superscript (–), tension at the top flange of the beam) are considered at end section 1 which is closer to the beam cross-section x where the shear force is calculated and sagging ones (tension at the bottom flange, superscript (+)) at the opposite end, 2. All moments enter in these expressions as positive, no matter whether they are hogging or sagging. The same for the shear force $V_{\mathrm{g+\psi q,o}}(x)$ at cross-section x in a simply supported beam subjected to the concurrent gravity loads, $g+\psi q$.

6.5.5.2 Shear Forces in Walls

Capacity-design shears along the height of a multistorey wall cannot be established from the moment resistances of beams framing into it at floor levels, because the (unknown) lateral forces transferred to the wall by the floors enter also into the equilibrium condition. So, for all types of walls, "squat" (with $h_{\mathrm{w}}/l_{\mathrm{w}}$>2) or "slender" ($h_{\mathrm{w}}/l_{\mathrm{w}} > 2$), Part 3 of Eurocode 8 allows calculating capacity design shears from the following modification of Eq. (1.14):

– if $M_{\mathrm{Ed,w}}\ (z=0) > M_{\mathrm{R,w}}\ (z=0)$, then $V_{\mathrm{CD,w}}(z) = \left(\frac{M_{\mathrm{Rd,w}}(z=0)}{M_{\mathrm{Ed,w}}(z=0)}\right) V_{\mathrm{Ed,w}}(z)$ (6.6a)

– if $M_{\mathrm{Ed,w}}\ (z=0) \le M_{\mathrm{R,w}}\ (z=0)$, then $V_{\mathrm{CD,w}}(z) = V_{\mathrm{Ed,w}}(z)$ (6.6b)

where z is elevation above the base, $M_{\mathrm{Ed,w}}(z)$ and $V_{\mathrm{Ed,w}}(z)$ are the moment and the shear from linear analysis for the seismic action of interest and the concurrent gravity loads, $M_{\mathrm{R,w}}(z{=}0)$ is the value of moment resistance at the base section from the mean material properties from in-situ tests and any additional sources of information and $M_{\mathrm{Rd,w}}(z{=}0)$ its value there from mean material properties times the relevant "confidence factor" corresponding to the "knowledge level" applying to that case.

According to the reasoning in Section 1.3.6.4 about Eq. (1.15), Eq. (6.6a) may be seriously on the unsafe side for "slender" walls in the nonlinear response regime, as it neglects higher mode effects on wall shears after yielding at the base. To avoid being on the unsafe side, for "slender" walls (i.e., where $h_{\mathrm{w}}/l_{\mathrm{w}} > 2$) with $M_{\mathrm{Ed,w}}(z) > M_{\mathrm{R,w}}(z{=}0)$, Eq. (6.6a) may be replaced by the following adaptation of Eq. (1.15) to the present conditions:

$$V_{\mathrm{CD,w}}(z) = \sqrt{\left(\frac{M_{\mathrm{Rd,w}}(z=0)}{M_{\mathrm{Ed},w}(z=0)}\right)^2 + 0.1\left(\frac{S_a\,(T_C)}{S_a\,(T_1)}\right)^2}\, V_{\mathrm{Ed},w}(z) \tag{6.7}$$

As in Eq. (1.15), $S_{\mathrm{a}}(T_1)$ and $S_{\mathrm{a}}(T_{\mathrm{C}})$ are the elastic spectral accelerations at the period of the fundamental mode in the horizontal direction closest to that of the wall shear force and at the corner period, T_{C}, of the spectrum, respectively.

6.5.5.3 Shear and Bond in Joints

By referring to the provisions for DC H beams in Part 1 of Eurocode 8, Annex A of Part 3 bases the calculation of shear force demands in joints on plastic hinging in the beams, Eqs. (3.134) and (3.135), discounting the possibility of column hinging. This is safe-sided. It makes more sense, however, to consider both possibilities and use the full set of Eqs. (3.134), (3.135), (3.136), (3.137), (3.138), (3.139) and (3.140) in Section 3.3.3.1 for the shear force and stress demand in a joint. Note that, if the moments from the linear analysis, M_{Eb}, M_{Ec}, are such that $\sum M_{\mathrm{Eb}} < \sum M_{\mathrm{Rb}}$ and $\sum M_{\mathrm{Ec}} < \sum M_{\mathrm{Rc}}$, then the nominal shear stress in the joint, v_{j}, may be estimated either:

– from Eq. (3.135) and a joint horizontal shear force, V_{jh}, calculated using in Eq. (3.134) $\sum M_{\mathrm{Eb}}$ instead of $\sum M_{\mathrm{Rb}}$, or
– from Eq. (3.140) and a joint vertical shear force, V_{jv}, calculated using in Eq. (3.139) $\sum M_{\mathrm{Ec}}$ instead of $\sum M_{\mathrm{Rc}}$.

According to the spirit of Part 3 of Eurocode 8 (CEN 2005a), the value of f_{y} to be used in Eqs. (3.134), (3.136) and (3.138) is the mean yield strength of beam bars estimated from in-situ tests and any additional sources of information times

the relevant "confidence factor" corresponding to the "knowledge level" applying to the case in question. By referring to the rules for DC H beams in Part 1 (CEN 2004a), however, the letter only introduces a multiplicative factor of $\gamma_{\mathrm{Rd}} = 1.2$ on f_{y}, to account for strain-hardening.

CEN (2005a) does not explicitly mention bond along beam bars crossing or anchored at beam-column joints, which is also a force-controlled mechanism. At any rate, Section 5.4.1 and Eqs. (5.10) in particular apply for their maximum diameter. The values $\gamma_{\mathrm{Rd}} = 1.0$ and $k = 0.75$ may be used in these expressions. The mean tensile strength of concrete inferred from in-situ tests and any additional sources of information should be used there, divided by the "confidence factor" corresponding to the "knowledge level" applying to the particular case. The mean yield strength of beam bars from in-situ tests and any additional sources of information times the relevant "confidence factor" should be used there as f_{yd}. By the same token, ν_{d} should be calculated using the mean compressive strength of concrete as estimated from in-situ tests and any additional sources of information times the relevant "confidence factor". Note, however, that in existing buildings beam bars crossing or anchored at beam-column joints are very unlikely to fulfil Eqs. (5.10) applied according to the present paragraph. If they don't, we should keep in mind, first, that the problem cannot be easily fixed by retrofitting and, second, that the consequences of slippage of beam bars through or from joints are not so catastrophic. They amount to an apparent increase of beam flexibility due to fixed-end rotations and to a cap on the moment resistance of beams anchored at a joint without a bend.[5] If we want to take this latter effect into account, we may compute the beam moment resistance on the basis of a steel yield stress multiplied by the ratio of the bar diameter from Eq. (5.10b) to the actual diameter. The effective elastic stiffness of the beam from Eq. (3.68) does not need to be revised. However, the ultimate chord rotation at the beam end framing into such a joint is governed by the uncontrolled fixed-end rotation due to bar pull-out and cannot be computed anymore from Sections 3.2.3.4 or 3.2.3.5.

6.5.5.4 Transfer of Seismic Action Effects to the Ground

CEN (2005a) does not explicitly mention force-controlled mechanisms other than shear in beams, columns, walls or joints. Loss of bearing capacity under (part of) the foundation during an earthquake amounts to permanent deformations of the soil, leading to a permanent tilt and/or settlement of the building. Therefore, in essence it may be considered as a deformation-controlled, "ductile", mode of behaviour and failure. However, procedures for the estimation of permanent soil deformations in an earthquake and displacement-based verifications of the ground in the

[5] A bar passing through an interior joint, even when it slips along its length within the joint, will be stabilised in the beam at the other side of the joint. Beam bars anchored at a joint through a 90° bend or a 180° hook rely on it for ultimate stabilisation against pull-out.

framework of an integrated, fully-coupled seismic design of the superstructure-foundation-soil system are still far away. The transfer of action effects to the ground is still checked as force-controlled and will do so for the foreseeable future.

Tie-beams and foundation beams of an existing building may be treated like the beams of the superstructure, allowed to enter the inelastic range and develop plastic hinges. So, if analysis is linear, these beams may be verified in flexure on the basis of elastically estimated chord-rotation demands[6] and in shear on the basis of forces derived according to Section 6.5.5.1. The bearing capacity of the underlying soil, however, should be checked in terms of forces. As long as we don't discover in the end that there is bearing capacity failure, the foundation soil may be considered elastic. The rules presented in Section 2.3.4 for the capacity design of the foundation may be applied for the calculation of the seismic action effects (forces and moments) transferred to the ground by the foundation system. This entails multiplying all seismic action effects transferred to the ground according to linear analysis by a factor a_{CD}. For individual footings Eq. (2.15a) may be adopted to the present conditions as follows:

$$- \text{ if } M_{R,y} \geq M_{Ed,y} \quad \underline{\text{and}} \quad M_{R,z} \geq M_{Ed,z,} \quad \text{then } a_{CD} = 1 \tag{6.8a}$$

$$- \text{if } M_{R,y} < M_{Ed,y} \quad \underline{\text{or}} \quad M_{R,z} < M_{Ed,z,} \quad \text{then } a_{CD} = \min[(M_{Rd,y}/M_{Ed,y}); (M_{Rd,z}/M_{Ed,z})] \tag{6.8b}$$

where $M_{Ed,y}$, $M_{Ed,z}$ are the two orthogonal moment components at the base of the column or the wall from the linear analysis for the seismic action of interest and the concurrent gravity loads. $M_{R,y}$, $M_{R,z}$ are the values of the corresponding uniaxial moment resistances from the mean material properties from in-situ tests and any additional sources of information, and $M_{Rd,y}$, $M_{Rd,z}$ are those from these mean material properties times the relevant "confidence factor" corresponding to the "knowledge level" applying to the case in question.

For common foundations of $N > 1$ vertical elements (e.g. on a foundation beam, a box-type foundation, a raft, etc.) the simplification allowed in Part 1 of Eurocode 8 (CEN 2005a) for new buildings ($a_{CD} = 1.4$, Eq. (2.16)) is not meaningful, as in the present case the seismic action effects from linear analysis should be de-amplified ($a_{CD} \leq 1$). A sensible option is to determine from Eqs. (6.8) a value of a_{CD} at the base of each one of the jointly-founded vertical elements, indexed by i (i=1, N) and weight-average the individual values, $a_{CD,i}$, into a composite one:

[6]Note that the applicability of the equal displacement rule to buildings considered on compliant elastic ground, and to the elements of the foundation system in particular, has not been confirmed yet.

$$a_{CD} = \frac{\sum_{i=1}^{N} a_{CD,i} M_{Ed,i}}{\sum_{i=1}^{N} M_{Ed,i}} \tag{6.9}$$

where $M_{Ed,i}$ is that moment component $M_{Ed,y}$, $M_{Ed,z}$ from linear analysis for the seismic action of interest and the concurrent gravity loads which gives the minimum ratio $M_{R,y}/M_{Ed,y}$ or $M_{R,z}/M_{Ed,z}$ at the base of vertical element i (hence governs plastic hinging there).

6.5.6 *Verification Criteria for Existing, Retrofitted, or New Members*

6.5.6.1 Overview of the Criteria

For a (as-is or retrofitted) building to meet a given performance level (Limit State) under the corresponding seismic action, all its members, "primary" or "secondary", old, retrofitted or new, should conform to the corresponding verification criteria. As pointed out in Section 4.12.1, different criteria are used for "primary" and "secondary elements", with more safe-sided ones applying to the "primary" ones. It is up to the engineer to evaluate the real importance of certain elements of the existing or retrofitted building for its earthquake resistance and (re-)classify some of them as "secondary", if they meet the criteria for "secondary elements" but not those for "primary" ones.

The criteria follow the general verification format, $E_d \leq R_d$ (cf. Eq. (1.3)), but using for E_d and R_d:

- Deformations in the "ductile" modes of behaviour and failure (i.e., for flexure).
- Forces for the "brittle" ones (i.e., for shear).

The normative text of Part 3 of Eurocode 8 (CEN 2005a) describes these criteria in very general terms:

- At the Damage Limitation (DL) Limit State, structural elements, ductile or brittle, should stay below yielding;
- At the Limit State of Significant Damage (SD), ductile elements should not exceed certain "damage-related deformations" and brittle ones their "conservatively estimated strengths"; and
- At the Near Collapse (NC) Limit State, ductile elements should stay below "appropriately defined ultimate deformations" and brittle ones below their "ultimate strengths".

The information given then in Annex A of CEN (2005a) for concrete members is very specific, as summarised in Table 6.1. Following the proposals in Fardis (1998, 2001) and Fardis et al. (2003), the deformation measure used in

Table 6.1 Compliance criteria for assessment or retrofitting of concrete members in Annex A of CEN (2005a)

Mechanism	Member	Damage limitation – LD	Significant damage – SD	Near collapse – NC
Flexure (ductile)	Primary	$M_E \leq M_y$	$\theta_E \leq 0.75\,\theta_{u,m\text{-}\sigma}$	$\theta_E \leq \theta_{u,m\text{-}\sigma}$
	Secondary	or $\theta_E \leq \theta_{y,act}$	$\theta_E \leq 0.75\,\theta_{um}$	$\theta_E \leq \theta_{um}$
Shear (brittle)	Primary	$V_E \leq V_{Rd,EC2}$ and $V_E \leq V_{Rd,EC8}/1.15$; joints: $V_{CD,j} \leq V_{Rd,j\ EC8}$		
	Secondary	$V_E \leq V_{Rm,EC2}$ and $V_E \leq V_{Rm,EC8}/1.15$; joints: $V_{CD,j} \leq V_{Rm,j\ EC8}$		

these specific criteria is the chord-rotation at member ends The demand and the capacity measures in Table 6.1 are elaborated further in Sections 6.5.6.2 and 6.5.6.3, respectively.

6.5.6.2 The Demand Side of the Verification

The demand and its measures in Table 6.1 are due to the seismic action in question, plus the concurrent gravity loads:

1. The moment, M_E, and the chord-rotation, θ_E, are of interest only at sections where the member frames into others having stiffness within a plane normal to the vector of M_E.
2. The shear force demand V_E at the SD or NC Limit State is obtained from capacity design calculations according to Sections 6.5.5.1 and 6.5.5.2, if linear analysis is used. Otherwise, the analysis results are used.
3. $V_{CD,j}$ is the maximum shear force in the joint from capacity design calculations according to the first paragraph of Section 6.5.5.3.

It is necessary to clarify how θ_E is determined. The chord with respect to which the rotation of member end sections is measured should be fairly consistent with the shear span used for the calculation of the corresponding ultimate chord rotation, θ_u, at the two ends:

– In a member expected to be in counterflexure when it yields at one end, θ_E is measured with respect to the chord connecting its two nodes on either side of the expected point of inflection. More specifically, in beams or columns with end nodes where the member frames into elements with certain stiffness within the plane of bending, θ_E is measured with respect to the chord connecting these two nodes, no matter any intermediate ones with other members having no stiffness in the plane of bending. The length of this chord is twice the shear span determined according to (i) in Section 6.5.4.2.
– If the member is expected to be in single curvature when it yields at one end, θ_E is measured with respect to the chord connecting that end to a node at or near the expected point of inflection. For example, if a beam frames into a column at one end and ends at an indirect support on another beam at the other, θ_E may be

measured with respect to the chord connecting these two ends. In a wall θ_E is of interest at a storey's bottom section and is measured with respect to a chord connecting the node there to one about half-way the distance from the top of the wall. In all these cases the length of the chord is equal to the shear span determined according to (ii) or (iii) in Section 6.5.4.2.

For the implementation of the above in systems beyond full two-way frames in 3D, the post-processor of analysis results for member verifications should allow the user to define for each member the chord with respect to which chord rotations at the nodes of interest are defined within each plane of bending and then calculate θ_E from the nodal rotations and displacements of these nodes in the global co-ordinate system.

6.5.6.3 The Supply or Capacity Side

(1) M_y in Table 6.1 is the yield moment at the end section, as computed, e.g., from Section 3.2.2.2, taking into account FRP-wrapping of the end of the member, short lap splices there or short anchorage beyond the end section, according to Sections 3.2.3.10 and *Effect of Lap-Splicing on the Yield Properties* in Section 3.2.3.9, respectively. For concrete-jacketed members Section 6.8.2.3 applies. Biaxial effects on yielding may be taken into account according to Section 3.2.3.8. As M_y is in this case an indirect measure of a deformation capacity, namely of $\theta_{y,act}$ in (2) below, it is based on mean strengths of old materials divided by the confidence factor applicable and on the nominal strengths of new materials. Because of the confidence factor, it is generally different from the value used in Eq. (3.68) for the effective stiffness.

(2) $\theta_{y,act}$ in Table 6.1 is the chord-rotation demand at the time the value of M_y in (1) above is attained during the analysis. Note that, if the verification is in terms of deformations, Annex A of Part 3 of Eurocode 8 recommends using instead the value of θ_y from Eqs. (3.66) in Section 3.2.3.2 (corrected for FRP-wrapping, short lap splicing or anchorage and biaxial loading according to the sections mentioned in (1) above). As discussed in Section 6.5.4.2, if this suggestion is adopted we may have a mismatch with attainment of M_y and ambiguities about yielding.

(3) θ_{um} in Table 6.1 is the expected value of the ultimate chord-rotation under cyclic loading, calculated using mean strengths for old materials divided by the confidence factor and nominal strengths for new materials. According to Annex A of CEN (2005a) the reference approach for its estimation is via Eqs. (3.78a) or (3.78b), modified for: poor detailing through to Eqs. (3.79), but with coefficient 0.825 instead of $1/1.2 = 0.833$; for lap-splicing of longitudinal bars starting from the end section according to approach (i) in section *Effect of Lap-Splicing on the Flexure-Controlled Ultimate Deformation* in Section 3.2.3.9; for FRP-wrapping of a plastic hinge region via the approaches in Section 3.2.3.10 based on Eq. (3.92) with lap-splicing or (3.89) without. The application of the reference approach to concrete-jacketed members is described in Section 6.8.2.4. The second approach in Eurocode 8 for θ_{um} applies

only to members detailed for earthquake resistance. It does not have extensions for poor detailing, lap-splicing, FRP-wrapping or concrete jacketing. It employs Eq. (3.70a), with the full expression for θ_y from Eqs. (3.66) instead of the flexure-only term, $\varphi_y L_s/3$. It calculates φ_u as described under point (a) at the end of Section 3.2.2.10, giving two confinement options. A different expression for the plastic hinge length, Eq. (3.75) or (3.76) in Section 3.2.3.4, goes with each option.

Section 3.2.3.5 has pointed out that Eq. (3.78c) is an equally good alternative to the reference approach in Annex A of CEN (2005a), Eqs. (3.78a) or (3.78b). Section 3.2.3.10 has added two alternatives to Eq. (3.89) for the estimation of the effect of FRP-wraps over a plastic hinge region without lap-splicing. Section 3.2.3.4 has shown that Eq. (3.72), used with Eq. (3.73) or (3.74) for the plastic hinge length and with φ_u according to Sections 3.2.2.4 and 3.2.2.10, predicts θ_{um} much better than its Eurocode 8 counterpart, albeit worse than the reference one based on Eqs. (3.78). When extended according to approach (ii) in sub-section *Effect of Lap-Splicing on the Flexure-Controlled Ultimate Deformation* for members with lap-spliced longitudinal bars, Eqs. (3.72), (3.73) and (3.74) predict θ_{um} better than approach (i) in sub-section *Effect of Lap-Splicing on the Flexure-Controlled Ultimate Deformation* in Section 3.2.3.9, which is the counterpart of the reference approach. The extension of Eqs. (3.72), (3.73) and (3.74) to members with continuous bars and FRP wrapping according to sub-section *Members with Continuous Bars* in Section 3.2.3.10 is also as successful as the reference approach with Eqs. (3.89), (3.90) and (3.91). As pointed out at the end of sub-section *Members with Lap-Spliced Ribbed Bars* in Section 3.2.3.10, however, this extension is not so good for FRP-wrapped members with lap-spliced bars. Last, but not least, the approach of Section 3.2.3.4, Eqs. (3.72), (3.73) and (3.74), has not been extended to members with continuous bars but poor detailing. All things considered, the extended version of Eqs. (3.72), (3.73) and (3.74) is still not as good or general as the reference approach of Section 3.2.3.5 and its extensions.

As pointed out at the end of Section 3.2.3.8, for biaxial bending both the approach in Section 3.2.3.4 and that of Section 3.2.3.5 may be applied in Eq. (3.84).

(4) $\theta_{u,m\text{-}\sigma}$ in Table 6.1 denotes the mean-minus-standard deviation estimate of the ultimate chord-rotation under cyclic loading. Like θ_{um} above, it is calculated from mean strengths for old materials divided by the confidence factor and from nominal strengths for new materials. Annex A in CEN (2005a) replaces this estimate directly with:

(i) $\theta_{u,m\text{-}\sigma} = \theta_{um}/1.5$, if θ_{um} is obtained from Eq. (3.78a) in Section 3.2.3.5 and its extensions for poor detailing, lap-splicing, FRP-wrapping, etc.;

(ii) $\theta_{u,m\text{-}\sigma} = \theta_y + \theta^{pl}{}_{um}/1.8$, if one uses the value of θ_y from Eq. (3.66) in Section 3.2.3.2 and $\theta^{pl}{}_{um}$ from Eq. (3.78b) in Section 3.2.3.5, with their corresponding extensions for poor detailing, lap-splicing, FRP-wrapping, etc.

(iii) $\theta_{u,m\text{-}\sigma} = \theta_{um}/2$, for θ_{um} from Eq. (3.70a) but with θ_y from Eqs. (3.66) instead of $\theta_y = \varphi_y L_s/3$, with Eq. (3.76) for the plastic hinge length and φ_u calculated according to point (a) at the end of Section 3.2.2.10 with the confinement model in Eurocode 2 and CEB (1991), Eqs. (3.8), (3.9), (3.13) and (3.25);

(iv) $\theta_{u,m\text{-}\sigma} = \theta_{um}/1.7$, if θ_{um} is obtained from Eq. (3.70a) with θ_y as in (iii) above, with Eq. (3.75) for the plastic hinge length and with φ_u calculated according to point (a) in Section 3.2.2.10 with the confinement model of Eqs. (3.4), (3.5), (3.10) and (3.18).

In the light of the test-to-prediction statistics for cyclic loading quoted in Section 3.2.3.5 for unretrofitted members with continuous bars and elsewhere in Section 3.2.3 for members with lap-splices and/or FRP-wrapping, the values in (i) and (ii) above may be considered as close to mean-minus-standard deviation estimates, for the cases when θ_{um} as a whole is obtained from either one of Eqs. (3.78), or ${\theta^{pl}}_{um}$ is estimated from Eqs. (3.78b) and (3.78c), respectively (also for the extensions of Eqs. (3.78) for poor detailing, lap-splicing, FRP-wrapping, etc.). However, the statistics quoted in Section 3.2.3.4 right below Eqs. (3.75) and (3.76) show that the values in (iii) and (iv) above are higher than mean-minus-standard deviation estimates by 50 and 37.5%, respectively. The statistics for cyclic loading quoted in the Section 3.2.3.4 right below Eqs. (3.73) and (3.74) suggest that a mean-minus-standard deviation estimate of θ_u may indeed be obtained as:

(v) $\theta_{u,m\text{-}\sigma} = \theta_{um}/1.8$, for θ_{um} from Eq. (3.72), with a plastic hinge length from Eqs. (3.73) or (3.74) and φ_u according to Sections 3.2.2.4 and 3.2.2.10.

(5) $V_{Rd,EC2}$ in Table 6.1 is the monotonic shear resistance before flexural yielding according to Eurocode 2, as given in detail in sub-section *The Variable Strut Inclination Truss of the CEB/FIP Model Code 90 and Eurocode 2* in Section 3.2.4.2. It is computed using mean strengths of old materials divided by the confidence factor and nominal strengths of new materials, in all cases divided by the partial factor for the material.

(6) $V_{Rd,EC8}$ is the cyclic shear resistance after flexural yielding from Eurocode 8, i.e., from Eqs. (3.114) for cyclic diagonal tension, or Eqs. (3.115) and (3.127), for cyclic diagonal compression in squat walls or columns, respectively. Like $V_{Rd,EC2}$, it is computed from mean strengths of old materials divided by the confidence factor and from nominal strengths of new materials, always divided by the partial factor of the material.

(7) $V_{Rd,jEC8}$ is the cyclic shear resistance of the joint according to Part 1 of Eurocode 8, Eqs. (5.13) and (5.14) in Section 5.4.2 ((3.143), (3.144) in Section 3.3.3.1), from the mean strength of old steel and concrete divided by the confidence factor and from the nominal one for new materials, in both cases divided by the partial factor of the material. Equations (5.15) (or (3.142) in Section 3.3.3.1) may be used as alternative to (5.14) and (3.143), with f_y at the right-hand-side

taken equal to the mean yield strength of beam bars multiplied by the confidence factor and by $\gamma_{Rd} = 1.2$ for strain hardening, without material partial factor.

(8) $V_{Rm,EC2}$, $V_{Rm,EC8}$, $V_{Rm,jEC8}$ in Table 6.1 are the shear resistances as in (5), (6) and (7), respectively, but computed from mean strengths of old materials modified through the confidence factor and from nominal strengths of new materials.

Annex A of CEN (2005a) recommends for (6)–(7) the usual values of partial factors for concrete and steel: 1.5 and 1.15, respectively, and a value of 1.5 for FRP.

The ultimate deformation estimates in (3) and (4) above increase with increasing shear span, L_s, at the end in question and with decreasing axial force, N, in the member. When N increases, a member's shear resistance in (5) or (6) increases, while that of a joint in (8) may increase or decrease. The shear resistance in (6), $V_{Rd,EC8}$, decreases with increasing L_s and with increasing demand value of the chord rotation ductility factor, μ_θ, at the end in question. All these parameters vary during the seismic response. If the analysis is linear, the verifications take place in the end, using the initial values of L_s (e.g., as listed under (i)–(iii) in Section 6.5.4.2) and N (due to gravity loads alone) and the peak value of μ_θ from the analysis. If the analysis is nonlinear, it is preferable to check all verifications at each point during the response, using the instantaneous values of N and μ_θ. For L_s it is normally sufficient to use the current value of M/V only at beam ends and, as a matter of fact, only when they are in hogging bending. This is the most critical condition for the shear and the chord rotation (at least for the usual position of the slab and distribution of longitudinal reinforcement between top and bottom). Conditions are rarely critical at the sagging end, while the variation of M/V there may be such that absurd instantaneous capacity estimates come out. If a nonlinear static ("pushover") analysis is carried out, the value of M/V at column or wall end sections varies smoothly with increasing lateral forces and may be taken as the instantaneous value of L_s in capacity calculations. However, during a nonlinear dynamic response analysis the instantaneous value of M/V at these locations varies wildly and should never be taken as instantaneous value of L_s. For this type of analysis the biaxial failure criterion, Eq. (3.84) in Section 3.2.3.8, should also be checked at each point of the response, with the instantaneous values of the two chord rotation components. For the other methods, a final biaxial check with the peak component values suffices.

The shear verifications in Table 6.1 may be limited to the highest LS being verified, as they will then be met by default at any lower Limit State. Note also that the ratio between the required chord rotation capacities at the Significant Damage (SD) and the Near Collapse (NC) Limit States (LSs) is constant and equal to 0.75. Chord rotation demands estimated via linear analysis are proportional to the Peak Ground Acceleration (PGA) of the seismic action. So, the SD Limit State will govern, if the PGA of the corresponding seismic action is less than 75% of that applying for the NC LS. Conversely, if it exceeds that value. So, checking both LSs is redundant. This conclusion may be extended to the use of nonlinear analysis, provided that the ratio of the PGA values for the SD and NC LSs is not close to 0.75.

6.5.7 Masonry Infills in Assessment and Retrofitting

According to Part 3 of Eurocode 8, wherever there are no specific provisions for masonry infills, the pertinent ones of Part 1 (CEN 2004a) apply. According to one of them, if walls take at least 50% of the base shear from a linear analysis, the interaction of the structure with the masonry infills may be neglected. This may be taken to imply that it is allowed then to disregard the infills in the structural model. However, this is not always a safe assumption. Other implications for the analysis derive from the CEN (2004a) requirements highlighted in Section 2.1.13.2, namely that infills with strongly asymmetric or irregular layout in plan should be included in a 3D structural model and a sensitivity analysis of the effect of the stiffness and position of the infills carried out (e.g., disregarding one out of three or four infill panels per planar frame). If the layout of infills in plan is not so asymmetric or irregular to warrant including them in the analysis model, the requirement in CEN (2004a) to double the accidental eccentricity in an analysis that neglects them applies for existing buildings as well. The provisions in CEN (2004a) about infills with irregular distribution in elevation (see Section 2.1.13.3) address the problem in a fully force-based context. So, they can only guide the decision about including or not in the structural model heightwise irregularly distributed infills. If the value of η from Eq. (2.7) is less than 1.1, their heightwise distribution is not a sufficient reason for including them.

For modelling of masonry infills the reader is referred to Sections 4.9.8 and 4.10.2. Recall the different values proposed in Section 4.9.8 for the effective width of the diagonal strut of solid infill panels at the three Limit States of CEN (2005a).

Masonry infills included in the structural model seem more like "primary elements" than "secondary" ones, as they do not play a role in the support of gravity loads and contribute only to lateral stiffness and strength. Infill panels are naturally classified as "primary members", if engineered into parts of the lateral-force-resisting system for retrofitting, e.g., by adding overlays of shotcrete or strong mortar with curtains of light reinforcement. Moreover, if confined at all four sides by a fairly strong concrete frame, they may exhibit remarkable deformation capacity (but offer little energy dissipation). So, they may well be checked in terms of deformations.

Notwithstanding their effectiveness, CEN (2005a) does not explicitly cover masonry infills engineered to be part of the lateral force resisting system. It only mentions masonry infills in general, in relation to the Damage Limitation (DL) Limit State, stating that at that LS they should be checked on the basis of their interstorey drift capacity. This makes sense for the following reasons:

- At the Near Collapse LS we cannot rely on non-engineered infills. Even when we include them in the model to take into account their potential adverse effects, we will not bother to check their integrity, as falling hazards are accepted at this LS;
- At the Significant Damage LS we may include non-engineered infills in the model to also take into account any benefits derived from their contribution to lateral strength and stiffness. Then we rely on their fairly large deformation capacity

without explicitly checking it, since non-structural elements may be sacrificed at this LS.
– One of the targets of the Damage Limitation LS is to ensure that damage to non-structural components is minor (for infill walls, distributed cracking) and can be easily and economically repaired later. So, masonry infills should be explicitly checked at this LS.

CEN (2005a) does not give specific interstorey drift limits for infills at the Damage Limitation LS. Note, though, that the interstorey drift checks required under the Damage Limitation seismic action in the framework of the "*q*-factor approach" (see Section 6.5.8) include indirect reference to the pertinent provisions of Part 1 for new buildings. It is inferred from this that the target protection of infills in existing buildings under the Damage Limitation seismic action is achieved, if we meet the interstorey drift limits specified in Part 1 of Eurocode 8 for new buildings (listed in Section 1.1.3 under (i) and (ii)). Indeed, limit (i) in Section 1.1.3 is physically reasonable for the onset of damage in ordinary masonry infills. So, infills can be verified for the Damage Limitation LS by checking limits (i) and (ii) in Section 1.1.3. Note that these limits (especially (i)) often govern member sizes in frame buildings designed for earthquake resistance according to CEN (2004a), even though they are checked using the default value of 50% the stiffness of the uncracked gross concrete section. With their smaller member sizes, existing frame buildings will have larger difficulty in meeting these limits under the same Damage Limitation seismic action, especially when the realistic stiffness values from Eq. (3.68) are used. They may very well meet them, however, if the contribution of infills to lateral stiffness is taken into account. So, we should not attempt to verify the interstorey drift limits (i) and (ii) in Section 1.1.3 under the Damage Limitation seismic action, unless the infills are included in the model for this level of seismic action. This is a good practical reason to consider even non-engineered masonry infills as "primary members".

6.5.8 Force-Based Assessment and Retrofitting (the "q-factor Approach")

Part 3 of Eurocode 8 allows also force-based assessment and retrofitting using the *q*-factor. The purpose is two-fold:

– To allow a positive seismic assessment for buildings that may have been (recently) designed in accordance with EN-Eurocode 2 (CEN 2004b) and EN-Eurocode 8 (CEN 2004a) – be it on the basis more of (over)strength than of ductility – and avoid, therefore, embarrassing situations where a structure designed as new on the basis of one part of the suite of EN-Eurocodes is formally rejected by another when considered as an existing one.
– To facilitate retrofitting buildings by adding a new lateral-load-resisting system capable of sustaining the full seismic action. The new system may be designed in full accordance with CEN (2004a), considering all existing elements

as "secondary" even when their total contribution to lateral stiffness might exceed 15% of that of the added system.

Note that, to claim that it is a Eurocode assessment and retrofitting, a force-based one should comply with all relevant design provisions for new buildings in CEN (2004a,b).

The "q-factor approach" is a two-tier seismic assessment and retrofitting similar to a new design according to the EN-Eurocodes. It is based on two Limit States:

1. Damage Limitation, checked exactly as for new buildings, i.e., on the basis of the interstorey drift limits listed in Section 1.1.3 under (i–iii); and
2. Significant Damage, identical to the No-(local-)collapse performance level for new buildings and checked with the criteria and procedures of CEN (2004a).

The parallel with the design requirements for new buildings stops at the definition of the seismic action, as it is not necessary to adopt for Limit States 1 and 2 above the hazard levels specified in the National Annex to CEN (2004a) for the "damage limitation" and the "design" seismic action, respectively. The National Annex to Part 3 (CEN 2005a) applies instead, which may leave to the owner and the designer the choice of these hazard levels.

As in new designs, most demanding is the fulfillment of Limit State 2 above. This entails a linear analysis with the design spectrum in CEN (2004a), Eqs. (4.5) in Section 4.2.2. There we are always entitled to use $q = 1.5$. For this q-factor value safety verifications are limited to checking that in every single "primary element" internal force and moment demands due to the design seismic action plus the concurrent gravity loads do not exceed the corresponding force and moment resistances.[7] These resistances are computed as in new buildings, except that for old materials mean strengths are used divided by the confidence factor. Like the nominal strengths of new materials, they are divided in the end by the material partial factor.

To use a value of q higher than $q = 1.5$, one has to show that the building has the corresponding local and global available ductility according to Part 1 of Eurocode 8:

- For retrofitting with a new lateral-load-resisting system capable of sustaining the full seismic action, one has to choose a Ductility Class from Part 1 of Eurocode 8 (DC M or H) and use the associated q-factor value. The new system and its connection to the old one should meet all the detailing and capacity design requirements for the chosen DC.
- To find out what q-factor value can be used for the existing system as is, possibly with some of its members retrofitted or with certain new elements added, one may first check one-by-one the end sections of all "primary elements" where Part

[7] "Secondary elements" are checked as in new buildings, see Section 4.12.3.

1 of Eurocode 8 would require detailing for ductility and determine the value of the curvature ductility factor, μ_φ, for each one from its detailing. More specifically, at the end sections of each "primary beam" Eq. (5.4b) is inverted for the available value of μ_φ. Equation (5.8) is also inverted for μ_φ at the base section (connection to the foundation) of each "primary column" (taking $\omega_{vd} = 0$) and "primary wall". The minimum of all these so-determined μ_φ-values is used then to invert Eqs. (5.2) for the basic value of the behaviour factor, q_o. This exercise should be carried out separately for each horizontal direction. By going back to Table 1.1 (and the rest of Section 1.4.3.1 for the default value of α_u/α_1), one may find out which DC the building (as is or retrofitted) may claim to belong for the specific lateral-load-resisting system of the horizontal direction considered. If, for example, the q_o-value is between those of DC M and H, the building might qualify for DC M. This preliminary conclusion on a single potential DC for both horizontal directions should be confirmed, by making sure that every single "primary element" and its connections meet the prescriptive detailing rules and the capacity design provisions (Eq. (1.4) if applicable, as well as in shear, etc.) pertaining to this DC (see Tables 5.1, 5.2 and 5.3). It is only after this is confirmed that one can determine the final q-factor value (incorporating any reductions for irregularity in elevation) and calculate the internal force and moment demands due to the design seismic action on the basis of the design spectrum. Needless to say, it is very unlikely that the as-is building or a moderately upgraded version of it will meet all detailing, capacity design and strength verification requirements for DC M buildings (let alone DC H). However, this exercise may point out (hopefully few) "primary members" that need to be modified or downgraded to the class of "secondary", for the building to qualify for a Ductility Class higher than L.

For conformity with Part 1 of Eurocode 8 and the background of Eqs. (5.2), (5.4b) and (5.8), the analyses for the "damage limitation" and the "design" seismic action, should use the default stiffness of 50% of that of the uncracked gross concrete section. Seismic action effects should not be reduced by including non-structural infills in the model.

6.6 Liability Questions in Seismic Assessment and Retrofitting

The designer and the contractor of a building normally share the liability for property damage, injuries or casualties in the event of an earthquake, subject of course to any statute of limitations. The picture is not so clear, once a new engineer assesses the building as adequate, according to the performance targets set by the owner who hired him/her and/or the applicable codes and standards. Besides, if the assessment is followed by retrofitting, the designer and the contractor who carry it out enter the picture as well. At first sight, the new people bear the full liability for the building, especially if the original designer and/or contractor are not available anymore or are

protected by statute of limitations. However, if the original designer has chosen a poor structural layout, its effects on seismic response and performance cannot be fully reversed through retrofitting. Moreover, owing to cost constraints or time pressures, or to limit disturbance and damage to the building for material sampling and exposure of reinforcement, the campaign of in-situ measurements may not reveal potential serious flaws in materials or detailing, for which the original contractor is responsible.

It may be difficult for the owner to find a designer and a contractor prepared to bear the full responsibilty and liability for the actions of others. In some cases, the new engineer of the retrofitting may choose to protect himself from future liabilities by taking a very safe-sided attitude. He/she may recommend retrofitting a building that would normally be assessed as meeting the performance targets, and/or choose a heavy and unduly costly retrofitting strategy. In addition to being a waste of resources, such an attitude does not serve well the cause of seismic risk mitigation through retrofitting of existing buildings, as owners may in the end be discouraged to go ahead with the implementation of a prohibitively expensive retrofit design. Therefore, competent authorities should make sure that the applicable legal framework for liability is perceived by designers and contractors of retrofitting projects as fair and equitable. Targeted programmes for the reduction of seismic risk by retrofitting existing buildings may well include special litigation schemes to resolve potential liability cases for the buildings to be rehabilitated.

6.7 Retrofitting Strategies

6.7.1 General Guidelines

The aim of retrofitting is to modify the seismic demands, E_d, and/or the capacities, so that all relevant elements of the retrofitted building fulfill the general verification inequality, $E_d \leq R_d$, at all performance levels ("Limit States") under the corresponding seismic action (see Sections 6.5.6 and 6.5.7 for Eurocode 8). This goal may be achieved by adopting one of the following approaches or strategies, or even combining them:

1. By reducing the seismic *demands* on members and the structure as a whole;
2. By increasing the member *capacities*.

Each strategy may be implemented using one or more retrofitting techniques (*fib* 2003, Thermou and Elnashai 2006, Thermou et al. 2007b). Techniques serving mainly Strategy no. 2 are described in Section 6.8, while some of those employed for Strategy no. 1 are highlighted in Section 6.9. Each technique has its own advantages and drawbacks, scope and limitations of use and fits better in one of these strategies. The choice of the technique depends on:

a. the locally available materials and technologies;
b. cost considerations;
c. the disruption of use it entails and the duration of the works;
d. architectural, functional and aesthetic considerations or restrictions, etc.

One or more retrofitting technique(s) are normally chosen on the basis of considerations (a–d), etc. This choice and how it is implemented determines which retrofitting strategy is being adopted.

Each retrofitting intervention is a special case, with more than one appropriate solutions. So, generalisation of rules is neither possible nor advisable. With this in mind, there are some general (but not absolute) guidelines to follow, depending on the outcome of the assessment of the as-built structure:

1. If there is general deficiency in the building, retrofitting Strategy no. 1 above is more cost-effective, as it can reduce the seismic demands throughout.
2. If there are capacity deficiencies in just a few scattered members, it is more cost-effective to focus on them and upgrade their capacities with retrofitting Strategy no. 2.
3. If the deficiencies are concentrated in a single or few ("weak") storeys, they may be due to a vertical irregularity. Retrofitting Strategy no. 2 is an option, to upgrade the capacities of the members of these storeys. Retrofitting Strategy no. 1 could be adopted instead, to remove the irregularity by adding strong and stiff new elements from the ground to the weak storey(s) and beyond, or to strengthen and stiffen existing elements there to overshadow the irregularity and suppress storey-sway mechanisms.
4. If the deficiencies are concentrated at a single side of the building, they may be due to a torsional imbalance in plan. It may be chosen to stiffen and strengthen existing elements on that side or add new ones there, to balance the stiffness and strength (retrofitting Strategy no. 1). Alternatively, the deformation capacity and the shear strength of the members of the "flexible side" may be upgraded, to accommodate the larger demands on them (retrofitting Strategy no. 2).

In buildings with a large surface area and strongly irregular and asymmetric structural layout, it may even be chosen to introduce vertical joints at selected locations in plan, converting the building to a number of structurally independent regular units. Vertical elements should be provided in that case at both sides of each joint, for independent support of the corresponding horizontal elements. The width of the joint should be sufficient to prevent pounding, especially if there is large disparity in lateral stiffness between the parts being separated. Conversely, if the building is already separated by vertical joints into a number of structurally independent but asymmetric in plan units, it may be decided to join them into an integral structure, by providing structural continuity across the joints. In this way we avoid pounding between the units during their strongly torsional seismic response. More important, it is easier to come up with a structure with an overall balanced in plan lateral stiffness and strength. An example is given in Section 6.10.2. Note that, by the time

of the retrofitting the joints would have served their primary mission, notably to accommodate the shrinkage of concrete. With shrinkage practically complete, future movements at the joints due to daily or seasonal temperature cycles alone will be minor and, if suppressed, they will not induce high stresses in the horizontal elements of the integral building. Besides, if the connection across a joint takes place at ambient temperatures markedly below the yearly average, these stresses will be compressive most of the time.

Regardless of its type and extent, a retrofitting intervention should in no way impair the safety or capacity of any part of the building, e.g. by introducing irregularities in plan or elevation, by shifting the deformation demands to inadequate components or other failure modes, etc. Upgrading the moment resistance of a member should never make it critical in shear. Strengthening of beams should not shift plastic hinging to columns.

6.7.2 Reduction of Seismic Action Effects Through Retrofitting

In this strategy seismic deformation demands on existing structural or (drift-sensitive) non-structural elements are reduced below the corresponding capacities, which may remain unchanged. Absolute displacements are also reduced, decreasing the likelihood of pounding with adjacent buildings. Shear force demands cannot decrease, unless the member in question is kept in the elastic region.

This strategy lends itself better for a multi-tier performance-based rehabilitation. It can prevent member failures in rare, strong earthquakes, while limiting structural and non-structural damage in frequent, moderate ones.

The most effective and common means for the reduction of seismic deformation demands is by increasing the global lateral stiffness. Normally this brings about an increase in global lateral strength, which, however, should be seen as a by-product and not as the main target of the retrofitting. In order of decreasing effectiveness, global lateral stiffness may be increased by:

1. Adding a whole new lateral-load-resisting system to take almost the full seismic action. This system may consist of steel bracing (see Section 6.9.3), new concrete walls (Section 6.9.2), new moment frames, or combinations thereof. The new elements are normally placed at the perimeter, to facilitate their foundation and to limit disruption of use of the building (under certain conditions, operation may continue during retrofitting). The new system can overshadow completely any irregularities in plan or elevation. Critical elements in this approach are the foundation of the new lateral-load-resisting system and the connection to the existing system for the transfer of inertia forces. This approach lends itself to application of force-based retrofitting according to Section 6.5.8. In that case the new system is designed for ductility in full accordance with a code for new buildings, while the existing elements are considered as “secondary” and verified as such.

2. Adding new elements (new concrete walls, see Section 6.9.2, or steel bracing, Section 6.9.3), to supplement the existing structural system. The new elements may be used to advantage to balance a strongly asymmetric layout in plan, or to eliminate soft/weak storeys. If the contribution of the added elements to lateral stiffness is large, this approach may be considered as a scaled-down version of approach 1. Then what has been said for it above still holds, except the applicability of Section 6.5.8 for force-based retrofitting.
3. Converting non-structural infill walls into structural elements, integrating them with the surrounding frame. The approach has many aspects in common with 3 above, but is not covered at all in this chapter, because there is not sufficient technical basis for the verification of infill walls as "primary" structural elements. Note that, if the overlays added to the infills contain curtains of light reinforcement, detailing aspects (e.g., the connection or anchorage of the reinforcement to the frame and how it affects the behaviour and the verifications; corrosion protection of the reinforcement, in view of the small thickness of the overlay, etc.) become very important.
4. Concrete jacketing, mainly of columns. This is closer to retrofitting for the purposes of increasing the capacities. Only when practically all columns are jacketed (e.g., when architectural reasons do not allow adding new walls or steel bracing, or when there is wide-spread reinforcement corrosion), it might also be considered as part of a strategy to reduce seismic demands, albeit not the most cost-effective and less disruptive one.

Depending on the case, the engineer may use approaches 2, 3 or 4 in the same retrofitting. The stiffening (and strengthening) should not be discontinued vertically at a level below the top, without considering the potential concentration of damage just above that level.

Reduction of mass is another means of reducing deformation and displacement demands, as in the pseudo-velocity controlled region of the spectrum, where the effective fundamental period of concrete buildings normally falls, seismic displacement demands are about proportional to the square root of the total mass. Except in special cases (e.g., when there is a single large mass at the upper floors), this approach is marginally effective by itself, but can be used to advantage in combination with other techniques or approaches. It can be implemented by removing heavy items (e.g., water tanks, heavy pieces of equipment, storage loads), by replacing heavy floor (or roof) finishings, cladding or partitions with lighter ones, or even by demolishing one or more top floors. Demolition of penthouses and upper storey setbacks also removes extreme irregularities in elevation and is sometimes worth considering. If the deficiencies identified in the existing structure are marginal, reduction and removal of masses throughout the building or, in extreme cases, complete removal of the upper storey(s), may make seismic upgrading of the rest unnecessary.

The introduction of base isolation and energy dissipation is also a means to reduce seismic deformation demands. These two techniques are not covered in this book at all, even for new buildings. For seismic upgrading, they are best suited for

bridges, where they often represent by far the best option. However, for existing buildings normally they are not cost-effective. This is more so for base isolation, as inserting the isolation devices is technically challenging: one needs to cut one-by-one the vertical elements at the base, while jacking up the superstructure around them.[8] Base isolation provides not only safety to the building and its occupants under very strong and rare earthquakes, but also protection of building contents under any earthquake event. Therefore, if the facility is required to remain operational during the earthquake or be available for immediate occupancy afterwards, isolation may be the most cost-effective strategy, provided that the building is not slender but stocky (to avoid axial tension on the devices, due to the overturning moment) and the superstructure has large stiffness (to be considered as rigid, compared to the isolation system). At any rate, base isolation is a sophisticated and complex technique and its application requires not only specialised expertise, but also peer review of the design.

For energy dissipation to be effective, significant lateral seismic displacements are necessary. So, it can only be used in flexible structures, as a supplement of another system which does not significantly increase the global stiffness. Dissipation devices can be used together with base isolation, or can be inserted in braces of an added steel bracing system. In this latter case the displacement demands for the activation of the dissipation system are not concentrated at the base (isolation) level but distributed throughout the structure, possibly causing significant damage to existing structural and non-structural components. This technique also is sophisticated, requires specialised expertise and peer review of the design, and is costly, but less so compared to base isolation.

6.7.3 Upgrading of Member Capacities

The deformation capacity and shear strength of individual members may be significantly upgraded by FRP-wrapping, without modifying at all their stiffness. Concrete jackets also improve deformation capacity and shear strength, but increase stiffness as well. So, when applied to many elements they also reduce deformation demands, not only locally but also globally. Improvement of certain details (e.g., of poor connections between the floor diaphragms and the lateral-load-resisting system or within diaphragms, see Section 6.7.4) may also be considered to belong to this retrofitting strategy.

Modification of existing components uses up less floor area and does not require closing openings. So it is, in general, more convenient for the future functionality of the building than the addition of new elements, or of a large concrete volume to existing members to increase stiffness and reduce seismic demands. However, it may entail removal and replacement of finishing materials and often partial

[8] A double foundation, sandwiching the isolation system, would normally be used in a new building.

demolition and reconstruction of partitions, lengthening the work and increasing its cost. Besides, modification of interior elements may disrupt use of the building. So, retrofitting via enhancement of member capacities alone makes more sense when deficiencies are limited to few members or connections or to part of the structure (a storey or one side in plan). It may also be adopted when it is not feasible to add new elements (e.g., because of architectural constraints) and/or provide a proper foundation for them.

Unless very specific and substantial deficiencies are identified in some beams, upgrading of existing members may be limited to vertical elements, possibly including their joints with the beams. Due to the integral connection of the beams with the slabs, upgrading a beam is technically more difficult than upgrading a column or a wall. Besides, experience from past earthquakes shows that damage in beams is far less common than in columns and its impact on global stability minor. Moreover, the design of beams for gravity loads normally provides sufficient top reinforcement at the supports (supplemented by the slab bars within a sizable effective flange width) and substantial shear reinforcement in the form of stirrups which are closed at the critical side (the bottom one). What is missing in such beams is continuity and anchorage of bottom bars over the supports. However, bar pull-out under sagging moments, if it occurs, only increases the lateral deformability of frames. Another weak point is the poor deformation capacity of the bottom flange in compression, in plastic hinges under hogging moments, which however, not always take place. Note that concrete jacketing of the columns into which a beam frames, improves, albeit indirectly, anchorage of its bottom bars and confinement of its bottom flange. Last but not least, the main hazard for existing buildings is posed by too much, rather than by too little, moment resistance of beams with respect to columns.

Existing components may sometimes be modified to improve not their own performance but that of elements they connect to. For example, a weak-beam/strong-column combination may be achieved by cutting beam longitudinal bars at the support by the column, provided that this is acceptable for gravity load resistance. Captive columns may also be set free by severing their connection to spandrel walls.

6.7.4 Completeness of the Load-Path

No matter which retrofitting strategy and technique he/she chooses, the engineer should check carefully the retrofitted structure for continuity of the load path(s). Transfer of inertia forces from the masses to the (primary) elements of the lateral-load-resisting system and from there to the foundation should be ensured. Note that inertia forces that may need to be transferred are proportional to peak floor accelerations, which are increased by global strengthening and stiffening.

Any connection within the floor system, between the floors and the lateral-load-resisting elements and between existing and new members should be checked in terms of forces, for the maximum possible demands that it may be required to transfer. Connectors and fasteners may exhaust their deformation capacity soon after

yielding, as they are called to accommodate within their small size significant relative displacements of the components they connect. So, even though they normally consist of a ductile material (steel), they should be checked in terms of forces and protected from yielding. Connections likely to be subjected to cycles of tension and compression may fracture under forces below their nominal tensile capacity, if they buckle or are severely deformed in a previous compression half-cycle. Welded or bolted connections are inherently brittle. Steel parts in an existing connection that appear adequate in construction documents may have corroded in the mean time.

Connections between prefabricated elements, especially in diaphragms consisting of precast units, are potentially weak links in the load path. Thin and lightly reinforced toppings in precast floors or roofs may already be cracked over seams between the precast units, or may easily crack during the earthquake and break open. It is difficult and not cost-effective to ensure integrity of a precast floor or roof, topped or untopped, through retrofitting. It is better to replace such a floor with a proper cast-in-place concrete floor or roof, integral with the vertical framing elements.

Cast-in-place slabs are normally considered to provide a continuous load path. However, one-way slabs in old buildings may have little reinforcement in their secondary direction. Floors with one-way slabs may break open through the points of inflection of the supporting beams under gravity loads, because in old days beam longitudinal reinforcement was dimensioned without the shift rule and had short anchorage. So, it was curtailed near the inflection point, as this came out from the analysis for gravity loads.

6.8 Retrofitting Techniques for Concrete Members

6.8.1 Repair of Damaged Members

6.8.1.1 Scope of Repair Techniques

For completeness, repair of seismic damage without strengthening is addressed before going in detail in the application and design of various means of modifying existing members. Nowadays seismic damage almost invariably triggers upgrading of the deficient earthquake resistance of a building through global seismic retrofitting. So, the subject of repair is of interest only for those members which are not upgraded, but just restored to their pre-earthquake condition.

Retrofitting enhances one or more properties of a member which are important for its seismic behaviour and performance. By contrast, the target of repair is just to re-instate some original characteristics that may have degraded because of age and/or adverse environmental influences, or owing to an earthquake or other damaging event. When such deterioration or damage is minor to moderate, repair may be sufficient, provided that any necessary global upgrading of earthquake resistance is provided elsewhere or by other means. The effects of severe damage, with disintegration of concrete inside the stirrups and/or buckling or fracture of

the reinforcement, cannot be fully redressed by simple repair. Repair is then usually followed by certain upgrading of the damaged zone (e.g., through jacketing with concrete of FRP), overshadowing any residual effects of the damage.

Repair may comprise one or more of the following:

- Replacement of buckled or fractured bars.
- Injection of cracks with epoxy or sometimes grout.
- Replacement of concrete that is loose, or has spalled, or has been removed to replace bars.

These measures are also applied, as appropriate, to damaged members before retrofitting with concrete or FRP jackets. In such cases it is not essential to inject fine cracks (e.g., less than about 0.3 mm wide), while spalled or removed concrete may be replaced with the cast-in-situ concrete or the shotcrete of the jacket.

Some practical information about these repair measures is given below.

- Replacement of reinforcing bars: Longitudinal bars that have fractured or suffered visible buckling are often replaced over a certain length. After removing the concrete around this length, the old bar is cut and its two ends are butt- or lap-welded to a new piece of bar. This is not a trivial operation and should be undertaken only when the old bar is essential. Otherwise, we just do not rely on it anymore.
- Replacement of concrete: Any loose concrete should be removed. If a bar is broken or has buckled, or has been partially exposed owing to spalling or disintegration of concrete, any still sound concrete around the length affected should also be removed to provide sufficient room for the repair mortar to surround the bar. The replacement material is commonly epoxy- or cement-based nonshrink grout mortar, with sand, pea-gravel or coarser aggregates, depending on the size and depth of the cavity. The mortar is normally trowelled against the substrate or against the previous mortar lifts, without applying an epoxy-based bonding agent as a primer. Formwork is redundant.
- Injection of cracks: If properly carried out, injection fully reinstates the continuity of the material and the tensile strength and cohesion across a crack. A common low-viscosity epoxy can be used to fill cracks wider than about 0.1 mm and up to few (2 or 3) mm. Cracks narrower than 0.2–0.3 mm may not be worth injecting, as the depth of penetration of the epoxy is uncertain and the epoxy is fairly expensive. For crack widths from 2 or 3 mm to 5 or 6 mm, medium-viscosity epoxies are more appropriate. Wider cracks, up to 20 mm, should better be grouted with cement.
- Before injection or grouting, loose material is removed from the trace of the crack on the concrete surface. For epoxy injection, the trace is fully sealed with epoxy paste, leaving only surface-mounted plastic nozzles as injection ports. Ports should be not further apart along the crack than the distance the epoxy can travel before it hardens. This distance depends on the width of the crack and the viscosity of the epoxy at the application temperature. If the member is thicker

than this distance, injection should take place through cracks on opposite faces. The injection starts from the lowest level where a crack appears in the member and continues upwards. It stops when the epoxy bleeds out from another port. The current port is then sealed by bending and tying the nozzle and injection continues from the next port. In the end, after the epoxy fully sets, the ends of the nozzles may be cut flush with the finished surface of the repaired member.

The procedure for cement grouting is similar, but the injection pressure is much lower.

6.8.1.2 Effectiveness of Repair for Strength, Stiffness and Deformation Capacity

There are very few cyclic tests in the literature on RC members repaired and retested without strengthening (Fardis et al. 2005). In these tests repair was limited to replacement of the crushed concrete shell of the plastic hinge with epoxy mortar, non-shrink concrete, fibre-reinforced concrete, etc. Data on 15 such tests on walls and 18 more on columns are given in (Fardis et al. 2005). The expressions in Section 3.2 may be applied to the repaired member, assuming that the strength of the repair concrete used in the shell of the plastic hinge (typically higher than that of the original concrete) applies to the whole element. The test-to-prediction ratio for the yield moment M_y (from Section 3.2.2.2) has median values of 1.005, 1.035 and 1.015, for columns, walls or overall, comparing well to those quoted for virgin members in Section 3.2.2.2 under *Comparison with Experimental Results and Empirical Expressions for the Curvature*, but the coefficient of variation of about 26% is markedly higher. The medians of the test-to-prediction ratio for the chord rotation at yielding θ_y (from Eqs. (3.66)) are 1.26, 1.66 and 1.27 for columns, walls or overall, while the corresponding coefficients of variation are 24, 40.5 and 38%. The test-to-prediction ratio for the secant stiffness to the yield-point (from Eq. (3.68)) has medians of 0.79, 0.54 and 0.725 for columns, walls or overall and coefficients of variation of 32.5, 58.8 and 45%, respectively. For 15 of the repaired columns carried to flexural failure, the test-to-prediction ratio for the ultimate chord rotation, θ_u, has median values of 0.675, 0.72, 0.705 or 0.705 and coefficients of variation of 32.5, 32.5, 32.5 or 54%, for θ_u computed from Eqs. (3.78a), (3.78b), (3.78c) or (3.72), (3.73) and (3.74), respectively. The corresponding medians for the 15 walls are 0.7, 0.695, 0.825 or 0.97 and the coefficients of variation 55%, 58.5%, 53% or 58.5%. For the total of 30 repaired specimens carried to flexural failure, the test-to-prediction ratio for θ_u has median values of 0.69, 0.71, 0.74 or 0.805 and coefficients of variation of 43.5, 45.5, 43 or 57.5%, for θ_u computed from Eqs. (3.78a), (3.78b), (3.78c) or (3.72), (3.73) and (3.74), respectively.

Although based on limited data, the above comparisons show that, even when carried out as carefully as in a research lab, repair re-instates fully only the yield moment (and hence the moment resistance), failing by 25–30% to recover the secant stiffness to the yield-point and the deformation capacity. Interestingly, repaired walls exhibit much larger loss of stiffness than repaired columns, but they fare a little

better than columns at ultimate (although the difference is statistically insignificant). Although the small sample size normally reduces the apparent scatter, the dispersion of test results with respect to predictions is much larger than in virgin specimens, even for the yield moment which is recovered well on average. Apparently, not only the repair process and materials, but also the type and degree of the original damage, introduce significant additional uncertainty.

The final conclusion is that, no matter how carefully it is done, mere repair cannot be considered to fulfil its intent, notably the re-instatement of key properties of the member. It is especially disconcerting in the context of displacement-based assessment and retrofitting that, the repaired members will be subjected to increased seismic displacement and deformation demands than similar virgin ones, owing to their loss of stiffness, while having more difficulty copying with them, given their reduced deformation capacity. So, unless global measures are taken to drastically reduce seismic displacement demands, members that suffered major damage or failed in the first event, will do even worse in a future one, despite the repair.

6.8.2 Concrete Jacketing

6.8.2.1 Introduction: Advantages and Disadvantages of Concrete Jackets

Owing to their cost-effectiveness, concrete jackets are still the method of choice for seismic upgrading of individual concrete members. There are several reasons:

- Every engineer or contractor is familiar with the field application of concrete. Recall in this connection that retrofitting, and especially modification of existing members, does not lend itself to (even partial) prefabrication in shop. So concrete is the prime candidate, as it is the most common structural material for field fabrication and application.
- Concrete jacketing is the most suitable technique for retrofitting severely damaged members, as crushed and removed concrete is replaced while casting or shotcreting the jacket, while buckled or fractured bars do not need to be fully restored if replaced by the new reinforcement of the jacket. This aspect was even more important in the past, as only recent years have seen wide application of seismic retrofitting without seismic damage as the trigger.
- Structural concrete is versatile and can adapt to almost any shape, e.g., in order to fully encapsulate existing members and joints and provide structural continuity between different components (between a joint and the adjoining members, between members in adjacent storeys, etc.).
- A concrete jacket can, through the appropriate reinforcement, have multiple effects. It is the only means to improve at the same time:

  1. stiffness,
  2. shear strength,
  3. deformation capacity,

4. anchorage/continuity of reinforcement in anchorage or splicing zones,
5. moment resistance (even turning a weak-column/strong-beam frame into a strong-column/weak-beam one),
6. shear strength and bond in joints through which the jacket continues, and
7. protection of the old reinforcement from (further) corrosion.

– Stiffness and flexural resistance are enhanced by the increased cross-section and the added longitudinal reinforcement, which – very importantly and unlike for other retrofit techniques of individual components – can easily extend beyond the member end into and through the joint. The main contribution to shear strength, deformation capacity and anchorage or splicing of reinforcement comes from the added transverse reinforcement, which works in shear, against buckling and for confinement. The added concrete is also a factor there. The increased dimensions of a joint when a jacket continues into and past it, provide more length for bond along old bars going through the joint and improve the joint shear strength. They also make room for adding transverse reinforcement in the joint. Finally, if the jacket concrete is of sufficiently low porosity, it can prevent or arrest corrosion of old reinforcement even in carbonated concrete. As a minimum, it reduces markedly the mechanical and aesthetic consequences of any corrosion that may go on.

Concrete jacketing may be considered to serve at the same time both types of retrofitting strategies in Section 6.7. By increasing the stiffness (item no. 1 above) it reduces seismic displacement and deformation demands. Besides, it is very effective in enhancing the force and deformation capacity of the jacketed member (items no. 2–7).

From the technical point of view, the multiple effectiveness of concrete jackets is what mainly distinguishes them from the other seismic retrofitting techniques for individual concrete members, which cannot readily extend beyond the member end and into a joint region. Other techniques mainly enhance some or all of the properties no. 1–4 above, but normally not the flexural strength, the resistance of the joints themselves or the corrosion protection all along the member (items no. 5–7).

RC jackets have certain handicaps, compared to other member modification techniques:

– They considerably increase member cross sectional dimensions. This may be a serious drawback when space, especially floor area, is at a premium.
– They normally cause the largest inconvenience and the lengthiest disruption of occupancy, produce the largest amount of dust and debris (especially if shotcrete is used) and cause the most noise pollution and safety or health hazards for the workers.

As the factors where concrete jackets are at disadvantage to the competition become more and more important, the balance may soon turn against them, notwithstanding their present and future advantage in direct construction cost.

6.8.2.2 Detailing, Technological and Construction Aspects

The concrete overlay of the jacket should be at least 75–100 mm, to provide sufficient cover of the new reinforcement and space for 135°-hooks at tie ends (Fig. 6.1(a)). For this range of thickness shotcrete is more convenient. Thicker overlays are normally cast-in-place.

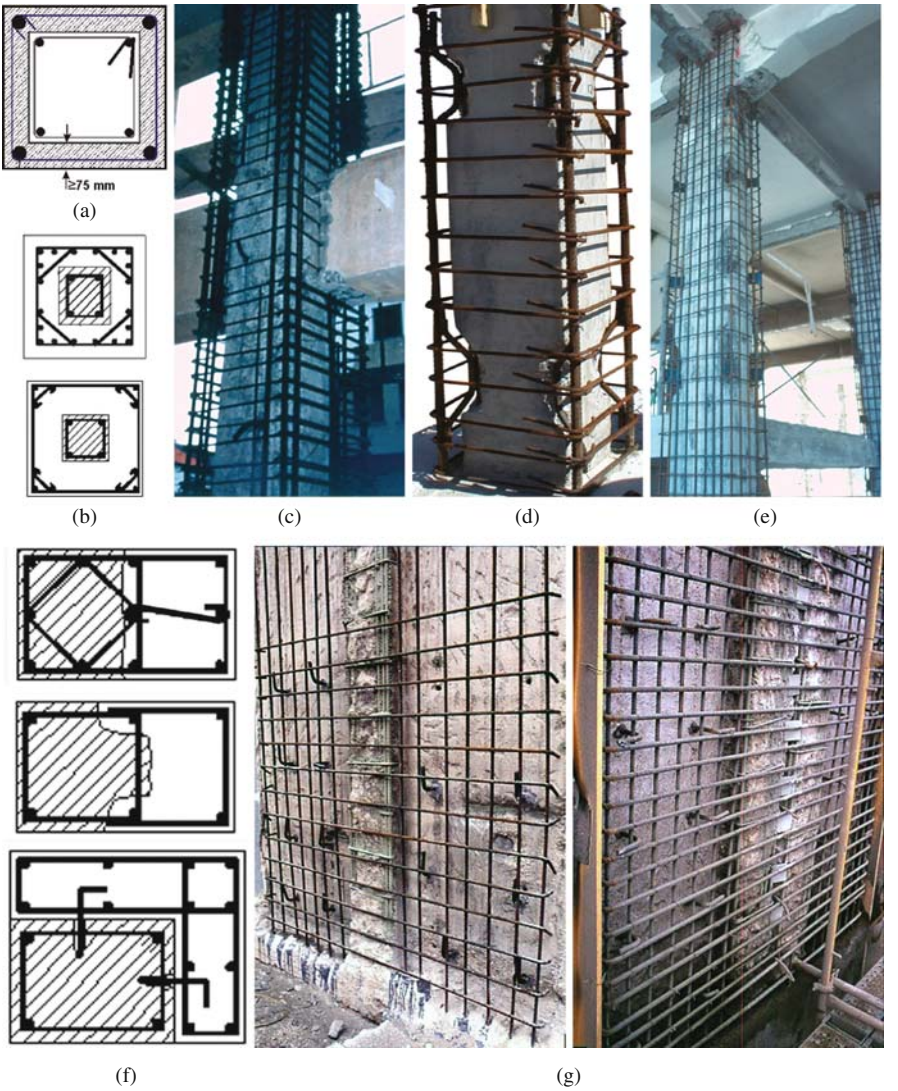

Fig. 6.1 Concrete jackets in columns: (**a**) simplest case; (**b**) jacket bars bundled near corners, engaged by cross-ties or octagonal tie; (**c**) jacket bars bundled at corners, dowels at interface with old column; (**d**) U-bars welded to corner bars; (**e**) steel plates welded to corner bars; (**f**) one- or two-sided jackets; (**g**) one-sided concrete overlay with single curtain of two-way reinforcement at exterior face of perimeter walls (cf. Section 6.10.2)

For the moment resistance of vertical elements to increase, longitudinal reinforcement should be continued to the adjacent storeys through holes or slots in the slab. To avoid perforating the beams on all sides of the cross-section into which a beam frames, jacket bars continuing through the slab should be concentrated near the corners of the new section, often in bundles (Fig. 6.1(b) and (c)). Jacket vertical bars may be anchored into a foundation element either:

- by enlarging the foundation element to accommodate anchorage of the jacket bars in new concrete there (possibly increasing at the same time the capacity of the foundation element to meet the larger moment demands from the jacketed vertical member), or
- by fastening (e.g. through epoxy) starter bars within vertical holes drilled in the foundation element, to be lap-spliced with the jacket vertical bars outside the plastic hinge that may form at the bottom of the retrofitted element.

If the target of the concrete jacket is just to enhance the deformation capacity of the member by offering confinement and anti-buckling action to the old member, to increase the shear strength and to remedy deficient lap splices without increasing the moment resistance, then the jacket does not need to continue past the joint into the next storey for a column or the next span for a beam. A gap of about 10 mm is recommended there, to avoid increasing indirectly the moment resistance of the member and, hence, the shear force demands in the member itself and the joint. Concentration of flexural deformation demands in a few-millimetre-length of the old member is not a concern. The gap serves there as a pre-existing wide crack. Within its length the compression zone in the old member is effectively confined by the concrete beyond the gap. At any rate, FRP jackets lend themselves better than RC ones for shear strengthening, enhancement of deformation capacity and improvement of deficient lap-splices without flexural strengthening.

A closed perimeter tie around the vertical bars of a column jacket restrains them against buckling, adds shear strength and confines the concrete. If we need multiple ties but do not want to drill holes and thread cross-links through the core of the old column, we can supplement the perimeter tie with an octagonal hoop outside the old column, which restrains buckling of any vertical bars close to, but not exactly at the corner. Instead of the octagonal tie, short corner ties at 45° to the perimeter may be used, engaging in 90–135° hooks the two bars adjacent to the corner bar (Fig. 6.1(b)). A diamond-shaped tie can be used only when the side of the jacketed column is at least twice as long as that of the old column. However, it is meaningless unless the jacket has mid-side bars to be restrained.

Confined boundary elements can be added to poorly detailed shear walls by jacketing the edges of the cross section. The ties around the new boundary element can come in two pieces: a straight one driven through a hole drilled in the web of the wall and a U-shaped piece around the edge of the wall, lap-welded to the first. A concrete overlay over one or preferably both sides of the web, with a curtain of horizontal and vertical bars, can provide additional shear strength.

Three-sided jackets are sufficient for beams integral with the slab. However, one-, two-, or three-sided jackets not fully surrounding an old column are much

less effective than full jackets. Besides, their seismic behaviour is little known. If a full jacket around a column is not feasible, the old reinforcement should be exposed and the new ties welded to the old ones or bent around the old vertical bars (Fig. 6.1(f)). One-sided jackets are easy to add to the exterior face of perimeter members in a building. If the member is a wall, a one-sided jacket having full horizontal and vertical reinforcement and well connected to the old wall through dowels may play the role of an appropriately reinforced new wall (Fig. 6.1(g)). The main contributions of the old wall are its concrete and the connection it provides to the rest of the structural system and to the foundation for the transfer of seismic forces.

Past guidance documents for concrete jackets – and past practice alike – include measures for shear connection of the old and the new concrete. Connecting the (corner) bars of the jacket to the (exposed for this purpose) longitudinal bars of the old column, by lap-welding both to Z- or U-shaped steel inserts is commonly recommended and applied (see Fig. 6.1(d) and (e)). Alternatively, the surface of the old element may be roughened and/or dowels may be driven into it (Fig. 6.1(c) and (g)). The dowels are epoxy-grouted in holes drilled into the old element and protrude in the overlay of new concrete for almost its full thickness. As this thickness is usually small, the dowel is often bent at 90° for anchorage in the new concrete.

Welded steel inserts between the new and the old corner bars, as well as epoxy-grouted dowels, were perceived in the 1970–1980s as a means to engage the jacket in sharing the axial force of the column through shear forces in the welded steel inserts and the dowels. The concern about gravity load capacity was motivated by the past use of concrete jackets mainly – if not only – to repair heavily damaged columns, whose core had often partially disintegrated. This concern is reflected in past recommendations to use props, wedges and even jacks under the beams framing into the column, to relieve it from part of its axial load before jacketing. For undamaged or moderately damaged columns these concerns are not warranted. Experimental work has demonstrated that concrete columns subjected to large post-ultimate drifts and heavy damage in the concrete core can retain a large part of their gravity load capacity (Elwood and Moehle 2001).

As we will see in Section 6.8.2.3, welding the new corner bars to the old ones through steel inserts may improve the column cyclic chord rotation capacity (possibly because it delays or prevents bar buckling). However, positive connection of steels of different grade (and composition) may promote corrosion. So, it is not recommended here to connect the old and the new longitudinal bars by welding both to pieces of steel in-between.

Dowels at the interface have a larger beneficial effect on the ultimate chord rotation of the jacketed column and do not seem to have collateral negative effects. If placed, they have a geometric ratio about equal to $0.2 f_{\mathrm{ctm}}/f_{\mathrm{yk}}$, which gives about 18 mm or 20 mm-dia dowels at 500 mm centres. The designer may choose to use dowels or not, taking into account their additional cost and time requirements. He/she may consider cost-effective to rely on friction alone for the shear at the interface, without connecting positively the new and the old concrete.

Friction is enhanced by the compressive stress building up normal to the interface, as the old member restrains shrinkage of the concrete overlay in the radial and

circumferential directions. The restraint induces radial compressive stresses in the old and the new concrete and compressive circumferential ones in the old member and the ties, new or old, but tensile circumferential stresses in the jacket. This amounts to certain "active" confinement of the old element, even before any lateral loading. To get an idea of the magnitude of these stresses and of their dependence on various parameters, we consider for simplicity the old member as circular with radius R_o. A final total (drying plus autogenous) shrinkage strain ε_{cs} in a jacket with thickness t_j induces radial compression normal to the interface (confinement stress for the old member) equal to:

$$\sigma_r = \frac{\varepsilon_{cs}}{\left(1+\nu+\frac{2\left(\frac{R_o}{t_j}\right)^2}{1+2\frac{R_o}{t_j}}\right)\frac{1+\varphi_{\infty,j}}{E_{c,j}}+\frac{1}{\frac{E_{c,o}}{(1-\nu)\left(1+\varphi_{\infty,o}\right)}+\frac{E_s A_{sw}}{s_w R_o}}} \tag{6.10}$$

where $E_{c,o}$ and $E_{c,j}$ denote the Modulus of the old concrete and of the jacket, respectively, $\varphi_{\infty,o}$ and $\varphi_{\infty,j}$ their final creep coefficients[9] and ν the Poisson ratio of concrete. A_{sw}/s_w is the total cross-sectional area (old and new) of transverse steel per linear meter of the member, lumped for simplicity at the interface. Equation (6.10) applies only if the jacket does not crack under the accompanying circumferential tensile stress, which is equal to:

$$\sigma_t = \left(1+\frac{2\left(\frac{R_o}{t_j}\right)^2}{1+2\frac{R_o}{t_j}}\right)\frac{\sigma_r}{1+\frac{(1-\nu)\left(1+\varphi_{\infty,o}\right)}{E_{c,o}}\frac{E_s A_{sw,j}}{s_{w,j} R_o}} \tag{6.11}$$

In this case $A_{sw,j}/s_{w,j}$ refers to the transverse steel of the jacket alone, still taken for simplicity near the interface. In thin jackets around large members the stress from Eq. (6.11) eventually exceeds the jacket tensile strength, $f_{ctm,j}$. Cracks may then start along planes normal to the interface and parallel to the member axis. This will reduce the stress normal to the interface to almost zero. By contrast, for typical parameter values Eq. (6.10) gives normal stresses in the order of 1 MPa, which can markedly improve friction at the interface. A large percentage of transverse reinforcement in the jacket increases the compression from Eq. (6.10) and delays cracking of the jacket in the circumferential direction (see Eq. (6.11)). So, its role is vital for friction.

A rough interface enhances friction. For example, in a 1:1.5 scale two-storey, one-bay frame tested in Stoppenhagen et al. (1995) with sizeable concrete jackets around the heavily damaged columns of the original test specimen the interface

[9]The values of $\varphi_{\infty,o}$ and $\varphi_{\infty,j}$ depend on the age of the old concrete and the jacket, respectively, at the time shrinkage starts. For a cast-in-situ jacket this is the age at stripping of the formwork; for shotcrete it is zero.

was just roughened. The jacketed frame sustained storey drifts of 1.25% (which, if they are due to the columns alone, give a drift ratio of the clear column length of over 4%) without loss of the column force resistance and with apparent monolithic behaviour of the jacketed column. However, as we will see in Section 6.8.2.3, artificial roughening of the old surface is not essential. Monolithic behaviour of the jacketed columns and beams was apparently achieved in the tests in Alcocer (1992) and Alcocer and Jirsa (1993), even though no positive measures were taken to improve the shear capacity of the interface. The excellent performance of these specimens deserves special mention. The tests were carried out on four 1:1.5-scale 3D beam-column subassemblies retrofitted with column jackets (continuous through the joints), or – in one test – with beam and column jackets. The retrofitted subassemblies developed a cyclic lateral force resistance at a storey drift of 4% between 3.5 and 6 times that of the unretrofitted companions. In the retrofitted specimens the beams hinged, with a large part of the slab reinforcement fully contributing to the tension flange of the beam. Joint shear was critical, but did not lead to a drop in resistance even under bi-directional load cycles. No bond problems were observed along the length of beam or column bars within the joint, although it was limited to 18 bar-diameters (or 10 equivalent bar diameters for the bar bundles) in the columns and to 23 bar-diameters in the beams.

6.8.2.3 Strength, Stiffness and Deformation Capacity of Members with Concrete Jackets

The cyclic behaviour of a concrete-jacketed member to and beyond yielding and up to ultimate deformation is fairly complex, because it depends on the conditions at the interface of the jacket and the old member, etc. (Thermou et al. 2007a). This complexity notwithstanding, the dimensioning tools for practical retrofit design should be (almost) as simple as those for the design of new members. The so-called "factors of monolithic behaviour" have long been a popular means to this end (CEN 1996). They are conversion factors applied on the strength, stiffness, etc. of an "equivalent" monolithic member to approximate the corresponding property of the composite jacketed one. Values often used for these factors are based on scant test data, sometimes limited to a single experimental study comparing concrete-jacketed members to a monolithic reference specimen. Moreover, the conversion factor needed for practical retrofit design is not one to be applied on the "real" (i.e., experimental) value of the property of the monolithic member, which is also unknown. It should be a factor that multiplies a monolithic property computed by simple, yet fairly reliable means. The comprehensive portfolio of simple tools presented in Section 3.2 for the estimation of strength, stiffness and deformation capacity of monolithic concrete members may well serve as the reference for these conversion factors. To this end Fardis et al. (2005) and Biskinis and Fardis (2009) have compared the experimental strength, stiffness and deformation capacity of about 55 jacketed columns or walls from the literature (about 35 of which carried to flexure-controlled ultimate conditions) to those of an "equivalent" monolithic member, determined according to the rules in Sections 3.2.2.2, 3.2.3.2, 3.2.3.3 and 3.2.3.5 in accordance with Table 6.2.

Table 6.2 Characteristics of monolithic member considered "equivalent" to the jacketed one

I. Flexural resistance and deformation capacity, deformations at flexural yielding		
Case A: The jacket longitudinal bars are anchored beyond the member end section		
A1	Dimensions	The external dimensions of the section of the "equivalent" member are those of the jacket
A2:	Longitudinal reinforcement	The tension and the compression reinforcement are those of the jacket. The longitudinal bars of the old member are considered at their actual location between the tension and compression bars of the jacket: – they may supplement any longitudinal bars of the jacket between the tension and compression reinforcement and be included in a "web" reinforcement ratio, considered as uniformly distributed between the extreme layers of reinforcement; – in a wall, the tension and compression reinforcement of the jacketed member may be taken to include old vertical bars at the edges, as appropriate. Lap splices in the intermediate old reinforcement may be neglected. Any difference between the yield stress of the new and the old longitudinal reinforcement should be taken into account in all cases.
A3	Concrete strength	The f_c value of the jacket applies over the full section of the monolithic member, except for the 3rd term of Eqs. (3.66), where the f_c value of the concrete into which the longitudinal bars are anchored beyond the end section is used.
A4	Axial load	The full axial load is taken to act on the jacketed column as a whole, although it was originally applied to the old column alone.
A5:	Transverse reinforcement	Only the transverse reinforcement in the jacket is taken into account for confinement.
Case B. The longitudinal bars of the jacket stop at the end section		
B1	Dimensions, longitudinal reinforcement, concrete strength	M_y and φ_y (also in the 1st and 3rd term of Eqs. (3.68)) are calculated using the cross-sectional dimensions, the longitudinal reinforcement and the f_c value of the old member, neglecting any contribution from the jacket. The effect of lap splicing of the old bars is taken into account according to Section 3.2.3.9. The section depth h in the 2nd term of Eqs. (3.68) is that of the jacket.
B2	Transverse reinforcement	The deformation capacity, θ_u, is calculated on the basis of the old column alone, taken as confined by the jacket and its transverse steel. Confinement in Eqs. (3.78) or (3.72), (3.73) and (3.74) is taken into account with an effectiveness factor $a_s = 1.0$ and the value of $\rho_s = A_s/b_w s_h$ calculated using the value of A_s/s_h in the jacket and the width of the old column for b_w.
II. Shear resistance		
Shear resistance (even that without shear reinforcement, $V_{R,c}$, from Eq. (3.67), to determine the value of a_V in the 1st term of Eqs. (3.66)) and anything having to do with shear are calculated on the basis of the external dimensions and the transverse reinforcement of the jacket. The old transverse reinforcement may be considered to contribute to shear resistance only in walls, provided it is well anchored into the (new) boundary elements.		

The idea behind assumptions A3 and A4 in Table 6.2 is that, for common ratios of jacket thickness to depth of the jacketed section, when yielding takes place and a plastic hinge forms at the end section of the member, the compression zone there is almost fully within the jacket, carrying the full axial load. Also, it is the jacket that mainly governs shear resistance and bond along the longitudinal reinforcement of the jacket.

An asterisk is used here to denote a calculated value for the jacketed member, e.g., as M_y^*, θ_y^*, θ_u^*. Values calculated for the monolithic member according to the assumptions in Table 6.2 and Section 3.2 have no asterisk (M_y, θ_y, θ_u^{pl}). Ratios of experimental values of M_y, θ_y, $EI_{eff} = M_y L_s/3\theta_y$ and θ_u for the tested jacketed members to values with the asterisk are shown in Fig. 6.2, separately for different types of jacket-to-old-member connection and for members which had been damaged by testing before been jacketed. Those specimens where the jacket longitudinal reinforcement did not continue past the member end and those with lap-spliced reinforcement in the original member are identified in Fig. 6.2. Other than that, they are lumped together with the specimens having continuous vertical bars in the original member. For tests not reaching ultimate conditions and for the two walls that failed in their unstrengthened storeys, an arrow pointing up signifies a test-to-prediction ratio greater than the value plotted.

The average value and ± standard-deviation estimates of the mean test-to-prediction ratios are shown in Fig. 6.2, separately for various groups of specimens with different types of jacket-to-old-member connection and with or no damage in the original column. The distance from the sample average to a certain reference value (e.g. 1.0), divided by the standard-deviation of the mean, is a criterion to decide whether the jacketed member's property in question may be taken equal to that calculated for the monolithic member according to Table 6.2 times that reference value. On this basis, the following simple rules are proposed for the yield moment, the chord rotation at apparent yielding and the ultimate chord rotation, M_y^*, θ_y^*, or θ_u^*, respectively, of the jacketed member, in terms of the values M_y, θ_y, θ_u^{pl} calculated for the monolithic member according to Table 6.2 (see also Bousias et al. 2007b, Biskinis and Fardis 2009):

$$M_y^* = M_{y,\text{Sect.3.2.2.2}} \tag{6.12}$$

$$\theta_y^* = 1.05\theta_{y,\text{Eq.(3.66)}} \tag{6.13}$$

(the main target being the effective stiffness at incipient yielding, computed from Eq. (3.68) as $EI^*_{eff} = M_y^* L_s/3\theta_y^*$), and

$$\theta_u^* = \theta_y^* + \theta_{u\,\text{Eq.(3.78b) or (3.78c)}}^{pl} \tag{6.14a}$$

$$\theta_u^* = \theta_y^* + \theta_{u\,\text{Eq.(3.72),(3.73)}}^{pl} \tag{6.14b}$$

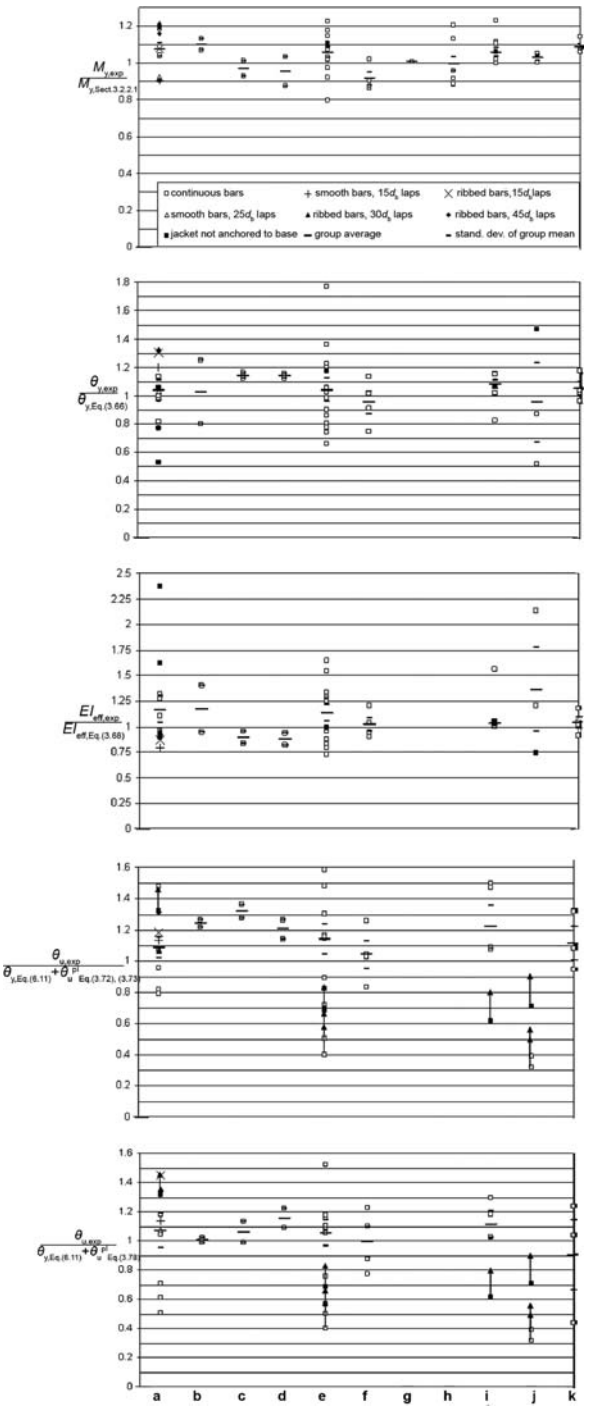

Fig. 6.2 Experimental value of the RC-jacketed member divided by the value calculated for the monolithic member according to Table 6.2 (*Key:*(**a**) no treatment of the interface; (**b**) no interface treatment, pre-damaged member; (**c**) welded U-bars; (**d**) dowels; (**e**) roughened interface; (**f**) roughened interface, member pre-damaged; (**g**) U-bars and roughened interface; (**h**) U-bars and roughened interface, member pre-damaged; (**i**) dowels and roughened interface; (**j**) dowels and roughened interface, member pre-damaged; (**k**) monolithic member)

Note that the value θ_y^* from Eq. (6.13) is used for the calculation of EI_{eff} and of θ_u at the denominator of the three lowermost plots in Fig. 6.2. Note also that the data cannot support a statistically meaningful effect of a pre-damage in the original column. So, Eqs. (6.12), (6.13) and (6.14) are proposed regardless of any such pre-damage. If the jacket longitudinal bars stop at the end section, Eqs. (6.12), (6.13) and (6.14) are used with assumptions B1 and B2 in Table 6.2.

Neglecting the effect of measures taken to enhance shear transfer at the interface of the old and the new concrete and grouping together the data in Fig. 6.2, the ratio of the experimental M_y to the prediction of Eq. (6.12) has a median of 1.035 and a coefficient-of-variation of 10.7%, compared to the values of 1.025 or 1.015 for the median and of 16.3% or 14.8% quoted in Section 3.2.2.2 under *Comparison with Experimental Results and Empirical Expressions for the Curvature* for M_y of monolithic beams/columns or rectangular walls, respectively. The median and the coefficient-of-variation of the ratio of experimental θ_y to the prediction of Eq. (6.13) are 0.99 and 23.5%, respectively, v the values of 1.025 or 0.995 and 32.1% or 33.7% given in Section 3.2.3.2 for the predictions of Eqs. (3.66) for θ_y of monolithic beams/columns or rectangular walls, respectively. Regarding the ratio of experimental EI_{eff} to the value predicted as $EI^*_{eff} = M_y^* L_s/3\theta_y^*$ (for M_y^*, θ_y^* from Eqs. (6.12) and (6.13)), the median and the coefficient-of-variation are 1.005 and 30.5%, to be contrasted to the values of 1.01 or 0.99 and of 32.3% or 47.1% quoted in Section 3.2.3.3 for the application of Eq. (3.68) to the database of monolithic beams/columns or rectangular walls, respectively. The median and the coefficient-of-variation of the experimental θ_u to the outcome of Eq. (6.14a) are 1.145 and 19%, v 1.0 and 42.4% for the predictions of Eqs. (3.78) for monolithic members. They become 1.08 and 24% for Eq. (6.14b), v 1.0 and 51.7% for Eqs. (3.72) and (3.73) and monolithic members. These comparisons show that average agreement with the experimental data is as good as that of the original expressions to the data they have been fitted, except for the ultimate chord rotation, where Eqs. (6.14) (mainly (6.14a)) are on the safe side. The small magnitude of the scatter for the jacketed members, although primarily due to the small sample size, is also re-assuring.

The data in Fig. 6.2 suggest that bonding measures at the interface of the jacket and the old member have a statistically significant effect only on the ultimate chord rotation. Equations (6.14) underestimate the measured θ_u-value of the few specimens with roughening of the interface and/or dowels. U-bars welded to the new and the old vertical bars have a beneficial effect on θ_u according to Eq. (6.14a) (maybe thanks to their anti-buckling action), but not according to (6.14b).[10] Even when no measure is taken to improve the interface between the old and the new concrete or connect the two materials there, Eqs. (6.14) undershoot the ultimate chord rotation of the jacketed member. It is therefore safe-sided for θ_u to use Eqs. (6.14) neglecting any favourable effect of a connection measures at the interface between the old and the new concrete. Interestingly, no systematic positive effect of

[10]Equations (6.14a) and (6.14b) point to opposite directions also about the effect of pre-damage on θ_u for (the just two) specimens without treatment at the interface.

roughening, dowels or welded U-bars on M_y and on the effective stiffness, EI_{eff}, has been found.

Note that slippage between the jacket and the old member is restrained in a real column under double curvature, but not in the cantilever-type specimens used in practically all tests from which the rules above were derived. Therefore, the effect of poor connection between the two layers would be even less in practice than in these tests.

According to Bousias et al. (2007b) there is no bias of Eqs. (6.12), (6.13) and (6.14) with respect to:

- the ratio of f_c or of the cross-sectional area of the jacket to those of the old member;
- the ratio of the mechanical reinforcement ratio in the jacket to that of the old member;
- the axial load, normalised either to the product of the full cross-sectional area of the jacketed section times the f_c-value of the jacket, or to the actual compressive strength of the jacketed section; and
- the ratio of the neutral axis depth at yielding to the thickness of the jacket.

This lack of bias supports assumptions A3 and A4 in Table 6.2, even when the compression zone extends beyond the jacket and into the old column.

None of the jacketed test specimens has shown any shear distress by the time it failed in flexure, which is consistent with the margin of at least 30% found between the shear resistance from Eqs. (3.114) and the maximum shear force applied.

6.8.2.4 Dimensioning and Verification of Jacketed Members According to Eurocode 8

On the basis of an earlier version of the database behind Fig. 6.2 and Eqs. (6.12), (6.13) and (6.14), Annex A in CEN (2005a) has adopted for the jacket the rules in Table 6.2, as well as Eqs. (6.12) and (6.14). However, for θ_y^* and for the effective stiffness at yielding resulting from it as $EI^*_{eff} = M_y^* L_s / 3\theta_y^*$, Eq. (6.13) has been adopted only if the interface between the jacket and the old concrete is roughened. For no treatment of the interface, or for epoxy-grouted dowels alone, or for connection of the jacket bars to the old ones via welded steel inserts, Part 3 of Eurocode 8 adopted a softer response up to yielding:

$$\theta_y^* = 1.2\theta_{y,\text{Eq.(3.66)}} \tag{6.13a}$$

Faced with the scarcity of data on jacketed members failing in shear under cyclic loading, Annex A in CEN (2005a) has again adopted a cautious approach. It accepts for the jacketed member just 90% of the shear resistance computed for the "equivalent monolithic" member according to Eurocodes 2 or 8 (at points (5)–(8) in Section 6.5.6.3).

$$V_R{}^* = 0.9\, V_R \tag{6.15}$$

The values of $M_y{}^*$, $\theta_y{}^*$ and $\theta_u{}^*$ used in the verifications should be based on mean strengths of the old materials divided by the confidence factor and on nominal strengths of the new materials. These strength values enter in the calculation of the shear resistance of "primary elements" further divided by the pertinent partial factors. However, mean values of new or old materials, without a confidence factor, are used to compute $M_y{}^*$, $\theta_y{}^*$ entering in the calculation of $EI^*_{eff} = M_y{}^* L_s/3\theta_y{}^*$, for the analysis.

6.8.3 Jackets of Externally Bonded Fibre Reinforced Polymers (FRP)

6.8.3.1 Scope of Seismic Retrofitting with FRPs

Externally bonded Fibre Reinforced Polymers (FRPs) are used in seismic retrofitting in order to enhance or improve (*fib* 2003, 2006):

a) The deformation capacity of flexural plastic hinges: A FRP jacket, with its fibres mainly along the perimeter of the section, is applied over the full length of the plastic hinge, to confine the concrete and prevent or delay bar buckling.
b) Deficient lap splices: A FRP jacket as in (a) above is applied over at least the full lap length, and
c) Shear resistance: A FRP overlay is applied, with the fibres mainly in the direction in which enhancement of shear strength is pursued.

Unlike concrete jacketing, which reduces through the added stiffness the seismic displacement and deformation demands, externally bonded FRPs only enhance the force and deformation capacities of the retrofitted member, serving therefore only retrofitting Strategy no. 2 in Section 6.7.1.

FRPs do not lend themselves for the enhancement of the moment resistance of members against seismic actions. The reason is that externally bonded FRPs with fibres in the longitudinal direction of a beam, column or wall cannot easily be continued into the joint beyond the member end section where the seismic bending moment is maximum. The moment resistance and the stiffness of a member can easily be enhanced instead through a concrete jacket (see Section 6.8.2), that can readily extend into a joint beyond the end of the member, providing continuity of the retrofitting between the member and the joint and – at the same time – strengthening of the joint itself. So, FRPs lend themselves only for selective modification of concrete members, notably of columns or walls, to improve their performance attributes listed above as (a–c).

Despite their high cost-to-weight ratio, externally bonded FRPs are becoming the material of choice in seismic retrofitting applications, owing to their:

- high strength-to-weight ratio,
- immunity to corrosion,
- easy handling and application (reducing labour costs and minimising disruption of use during installation) and
- very small thickness (minimising the loss in premium floor plan area, when the FRP is externally applied to vertical members).

For cultural heritage or historic buildings, whose architecture should not be altered by the intervention, externally bonded FRPs hold an advantage over any other technique: they can be made to have almost no impact on the external dimensions and appearance of structural elements. Moreover, their application is fully reversible.

That said, we should keep in mind certain drawbacks of the FRPs, such as their sensitivity to temperature and fire.

6.8.3.2 FRP Materials for Seismic Retrofitting

FRPs are relative new materials in seismic retrofitting and engineers are still not very familiar with them. For this reason, they are described in the present section at certain length.

The fibres of FRPs used for strengthening civil engineering structures are made of carbon, glass, or aramid, giving a FRP commonly termed CFRP, GFRP or AFRP, respectively.

Carbon fibres show the best stability under high temperatures and the best resistance to deterioration in acidic, alkalic or organic environments, including marine ones. They have high stiffness (Elastic Modulus) and tensile strength, but higher Modulus normally goes together with lower tensile strength and ultimate tensile strain. However, they are much more expensive than glass or aramid fibres (10–30 times more costly than E-glass fibres (*fib* 2007)).

Glass fibres are classified as (*fib* 2007):

– E-glass, which is popular as less costly;
– AR-glass, which is alkali resistant, but not available yet in sizes compatible with common thermosetting resins; or
– S-glass, which is stronger and stiffer than the other types.

Glass fibres, especially E-glass ones, are less expensive than carbon or aramid fibres. E-glass and S-glass fibres may lose up to 30–100% of their tensile strength in alkaline environments, especially at high temperatures.

Aramid is the term used for polymeric fibres appropriately processed to achieve high tensile strength-to-density ratio. Like E-glass and S-glass, these fibres may also lose up to 25–50% of their tensile strength in alkaline environments, but have good toughness and fatigue characteristics and are more tolerant to damage.

Fibres are linear-elastic up to failure, both in tension and in compression, with strength and Modulus in compression a little less than in tension. Aramid fibres are

Table 6.3 Typical tensile properties of fibres (*fib* 2003, 2006, 2007)

Fibre material		Elastic modulus (GPa)	Strength (GPa)	Ultimate strain (%)
Carbon	High strength	215–240	3.5–4.8	1.1–2.0
	Ultra high strength	215–240	3.5–6.0	1.5–2.3
	High modulus	350–500	2.5–3.1	0.5–0.9
	Ultra high modulus	500–700	2.1–2.4	0.2–0.4
Glass	E	72.5	1.9–3.4	2.5–4.5
	S	85–90	3.5–4.8	3.3–5.5
	AR	70–76	1.8–3.5	2.0–3.0
Aramid	Low modulus	60–80	2.8–4.1	4.3–5.0
	High modulus	115–175	3.4-4.2	1.5–3.5

the exception, being non-linear and ductile in compression with 80% less strength than in tension. Values of important mechanical properties of fibre materials are listed in Table 6.3. They apply for static loading in tension and for fibres not exposed for long to adverse environment. The manufacturer normally gives more representative values than those of Table 6.3, as well as information on their reduction due to adverse environmental exposures and long-term loading (which is not relevant for seismic retrofitting).

The fibres come in the form of flexible sheets (called also fabrics, or textiles), consisting of fibres mainly in one direction, or in two orthogonal ones, or in more directions, including oblique ones. In seismic retrofitting, particularly in buildings, the sheet is impregnated in-situ in a matrix, typically of a thermosetting polymer, that serves also as adhesive to the concrete substrate. The matrix binds the fibres together, transferring loads to them, and protects them in-situ from abrasion and adverse environmental effects. Having much higher – by one to two orders of magnitude – strength and Elastic Modulus than the matrix material, the fibres are the main stress-bearing component. The matrix governs only the shear properties of FRPs having fibres mainly in one or in two orthogonal directions, as well as the transverse modulus and strength of FRPs with fibres primarily in one direction.

The tensile strength and stiffness of the FRP (per linear meter) are typically derived from the corresponding values of the bare fibres (see Table 6.3), by multiplying them by the nominal thickness of the fibre sheet or fabric quoted by the manufacturer (typically a small fraction of a mm) and the number of plies (or layers) of sheets applied. Normally, it is not considered worth accounting for the efficiency of the fibre-matrix system and the sheet or fabric architecture, or for the small increase due to the contribution of the matrix. The FRP tensile strength and stiffness may also be obtained by multiplying the strength and Modulus of the FRP – given by the supplier of the materials for the specific combination of fibre sheet or fabric and matrix material used – by the nominal (and not the actual) thickness of the finished FRP specified by the manufacturer.

FRPs subjected to sustained stresses do creep and may ultimately fail by creep-rupture under stresses well below their short term strength. The time-to-rupture decreases when the temperature or the ratio of sustained stress to short term

strength increase, or when the FRP is subjected to alkaline environment, UV light, or humidity, constant or not. The strength under sustained stresses is, however, of little relevance if the FRP is applied for seismic retrofitting alone. Its low-cycle fatigue behaviour is more important in that case. The structural response to a seismic action of the type considered in retrofitting normally includes an order of ten large cycles of almost constant amplitude. In such a scenario CFRP, AFRP and GFRP may lose about 5–8%, 5–6%, or 10%, respectively, of their short term static strength. The loss about doubles if 100 constant amplitude load cycles are applied (*fib* 2007). The reduction is small enough to be considered as covered by the safety factors applied on the FRP properties in the design of the retrofitting. Anyway, if expressions used for the cyclic capacity of FRP-retrofitted members have been calibrated or derived on the basis of cyclic tests, they are deemed to account for any low-cycle fatigue of the FRP.

The coefficient of thermal expansion of FRPs is dominated by that of the fibres, except in the transverse direction of unidirectional FRPs, where it is governed by the matrix. GFRPs have about the same coefficient of thermal expansion as concrete, except in the transverse direction of unidirectional GFRPs, where this coefficient is about double. CFRP and AFRP have very low but negative coefficients of thermal expansion (they shrink when temperature increases). If they are unidirectional, their coefficient of thermal expansion in the transverse direction is an order of magnitude higher than in concrete. Owing to the way CFRP and AFRP are externally applied to concrete members for seismic retrofitting, such disparities do not cause serious problems during service life.

Thermosetting polymeric matrix materials are epoxy, polyester or vinyl ester resins. Epoxy resins offer good wetting and bonding to the fibres and to various substrates and have rather long open time. They are more costly than polyesters or vinyl esters, but have better mechanical properties, low creep, little shrinkage during curing and good resistance to water, temperature and chemicals. Regarding alkali resistance and water absorption, they rate in-between vinyl ester (which is best) and polyesters (which are worst). Polyester resins have low viscosity. They cure fast but shrink a lot while curing. Vinyl esters have good wetting and bonding to glass fibres, high strength, excellent alkali resistance, low water absorption and – very important – moderate cost. So, they are often the matrix of choice for GFRP.

Polymers, especially polyesters, absorb water from a humid environment, suffering some deterioration of mechanical properties, including, very importantly, debonding between the matrix and the fibres. Temperatures over 60°C exacerbate these adverse effects of moisture (*fib* 2007). Being polymeric, aramid fibres also absorb water, suffering a reversible reduction of tensile strength and Modulus and an irreversible decrease of their fatigue strength. Such reductions can reach 15–25%.

UV radiation inflicts considerable damage to the mechanical properties of polymeric matrices and Aramid fibres. The loss in tensile strength after long exposure to UV light is negligible for CFRP and does not exceed 8% in GFRP. AFRP exhibits larger reductions without a clear limit (*fib* 2007). To avoid losing eventually the matrix, externally bonded FRPs should be shielded from direct sunlight, either through cladding or rendering with plaster, or by means of proprietary protection systems.

CFRPs are almost immune to chloride attack, even under high moisture conditions, but GFRP and AFRP are more vulnerable to chloride-moisture combinations (*fib* 2007). The most important chemical threat comes from alkalis and the alkaline environment of concrete. This threat is negligible for CFRP and GFRP with AR-glass fibres, moderate for AFRP and very serious for GFRP with E-glass and S-glass fibres, especially under high temperatures (*fib* 2007). Note, though, that the surface layer of existing concrete elements would most likely be carbonated (hence, non-alkaline) by the time the FRP is externally bonded to it for seismic retrofitting. This greatly reduces the risk of alkali attack from within.

At their "glass transition temperature" polymers soften from their glassy state to a rubbery one. That temperature ranges between 95 and 175°C for epoxy resins, from 70 to 100°C for polyesters and from 70 to 163°C for vinyl esters (*fib* 2007). In principle, it is prudent to select a matrix material that has glass transition temperature at least 30°C above the maximum expected service temperature (Karbhari et al. 2003). It should be kept in mind, though, that for FRP applied for seismic retrofitting it is the quasi-permanent (average or arbitrary-point-in-time) value of the temperature of the immediate environment of the retrofitted element that should be taken as concurrent with the level of seismic action considered in retrofitting.

The Elastic Modulus of CFRP, AFRP or GFRP decreases when the temperature increases above the glass transition temperature of the matrix. The reduction is reversible, provided that the temperature level causing chemical degradation of the polymer is not reached. The drop in Modulus of CFRP, AFRP or GFRP when the temperature increases from –20 to +60°C is about 10, 25 or 35%, respectively. Being organic, Aramid fibres suffer not only a reduction in Modulus when the temperature increases, but also a drop in tensile strength. However, at 180°C they still retain about 80% of their 20°C strength (*fib* 2007). Carbon fibres can resist temperatures of 800–1000°C with little loss in mechanical properties. Glass fibres do the same up to 300–500°C. However, the polymeric matrix will burn at about 150–200°C, governing the fire resistance of the FRP. This is a serious drawback only if the surface-bonded FRP is applied to strengthen the member just against gravity loads. Then its loss during fire may lead to direct structural failure and collapse. FRPs applied for seismic retrofitting alone can always be replaced if damaged by a fire. The earthquake resistance they originally offered can be fully re-instated for future use.

The specification of the polymeric matrix should include the range of temperatures appropriate for mixing, application and curing. The shelf-life of thermosetting polymers (i.e. the time for which the unmixed resin and the hardener can be stored with no degradation) is limited and depends on the storage temperature. It should be checked that shelf-life has not expired by the time of mixing for in-situ application. The effect of temperature on the resin pot-life (i.e., the time after mixing the resin and the hardener during which the viscosity is low enough for application) and on its open time (in this case, the maximum time available between the resin application to a fibre sheet and the attachment of the sheet to the substrate) should be taken into account.

With the continuous decrease in fibre prices, the polymer is becoming an important factor in the FRP cost. To reduce this cost and bypass the problem of poor fire resistance of polymers, polymer-modified cement-based mortars have been used as binders of the fibres and as adherents to the substrate (Triantafillou et al. 2006, Triantafillou and Papanicolaou 2006, Bousias et al. 2007c). Unlike resins, mortars cannot wet individual fibres. So, continuous fibre sheets need to be replaced by fabric meshes of long woven, knitted or even unwoven fibre rovings in two or more directions (Textile Reinforced Mortars, TRM). The quantity and spacing of rovings per direction can be tailored to the target mechanical properties of the textile and the ability of the mortar to penetrate the textile mesh.

6.8.3.3 Field Application of FRPs

In seismic retrofitting, particularly of buildings, FRPs are typically applied in situ with the "wet lay-up" (or "hand lay-up") method. In this flexible approach, a first coating of adhesive is spread over the appropriately prepared concrete surface. The dry fibre fabric, pre-cut at the desired size, is impregnated in place by pressing into the adhesive usually with a roller (Fig. 6.3(a,b)). The adhesive and air are squeezed out through the fibre sheet, taking care to avoid wrinkles in the FRP and bubbles of entrapped air. The next ply and any subsequent ones are applied in the same way, following fresh application of a layer of adhesive onto the underlying FRP layer. Alternatively, the fibre fabric is impregnated with the adhesive on the floor and then pressed in place against the previously applied layer (Fig. 6.3(c)). For continuous wrapping of the FRP around the concrete member, the adhesive is rolled onto the FRP layer applied last just ahead of the upcoming fibre sheet. A lapping of about 150 mm between the start of a continuous FRP wrapping along the member perimeter and its end is sufficient.

The number of FRP plies should be limited, e.g., to a maximum of five. As mentioned at the end of the part of Section 3.2.3.10 on *Members with Continu-*

(a) (b) (c)

Fig. 6.3 Hand lay-up of FRPs in situ: (**a**), (**b**) dry fabric impregnated in place (courtesy A. Ilki); (**c**) impregnation of the fabric right before placing (See also Colour Plate 15 on page 729)

ous Bars and demonstrated by the last term in Eqs. (3.89), (3.90) and (3.91), the tensile strength of the FRP which is effective in concrete confinement is less than proportional to the total thickness of the FRP provided.

A smooth layer of non-shrink mortar (possibly polymer-modified) is often uniformly applied on the concrete surface. Its purpose is not to act as a bonding agent (polymers bond well to concrete), but to cover any roughness or asperities and provide a smooth, even final surface for the application of the lowermost FRP layer. If earthquake damage or other reasons of deterioration (e.g., reinforcement corrosion) has caused spalling or disintegration of the concrete in the element being retrofitted, the same non-shrink mortar is used to replace the spalled or loose concrete. The surface of the substrate on which the FRP is applied should be absolutely clean and dry. The FRP should not be applied while the substrate has water content more than 4% by weight or its temperature is below 5°C. Below 10°C, hardening of typical polymers stalls.

Before application of the FRP, sharp edges should be chipped off and rounded by applying a layer of non-shrink mortar to a corner radius of 20–30 mm. This is to avoid stress concentrations that may lead to premature FRP rupture and to extend the confining action of the FRP at the corner to a larger concrete volume (see. Eq. (3.28) and Fig. 3.17 in Section 3.1.2.4).

FRP wrapping should start 10–15 mm from the end section of the member (at the connection to a joint or a foundation element). The gap is to prevent bending of the member from causing the FRP to bear against the surface of the element or foundation into which the FRP-wrapped member frames. Such bearing is to be avoided, because it increases the force in the compression zone and the flexural capacity of the member, which in turn increases the shear force demand beyond the capacity design shear (see Sections 6.5.5.1 and 6.5.5.2). An unwrapped length of even 30 mm at the end of the member will not suffer from the lack of direct confinement by FRP, thanks to confinement afforded to it by the FRP-wrapped length of the member on one hand and by the volume of concrete of the transverse member or foundation element into which the member in question frames on the other.

Seepage of water into the FRP-concrete interface at the connection of FRP-wrapped members to the foundation should be prevented through appropriate sealants. If the lateral surface of the member needs to be continuously covered by FRP over its full length (e.g., for shear strengthening), evapouration of moisture should be allowed, e.g. through gaps of 30–50 mm between adjacently wrapped (typically 600 mm-wide) fibre sheets.

6.8.3.4 Material Partial Factor on the Tensile Strength of FRPs

Committee 440 of the American Concrete Institute (ACI 2003) has the equivalent of a material partial factor covering adverse environmental effects on CFRPs, AFRPs and GFRPs, with values of about 1.05, 1.15 and 1.35, respectively. This factor is in addition to (i.e., should multiply) the material partial factor that covers dispersion of the mechanical properties and creep-rupture effects, the value of which, according

to ACI (2003), is between 1.5 and 1.8. The specifications of the Japanese Society of Civil Engineers (JSCE 1997) cover both adverse environmental effects and dispersion of mechanical properties through an overall material partial factor with values of 1.15 for CFRP and AFRP, or 1.3 for GFRP. Annex A to Part 3 of Eurocode 8 provides just a material partial factor against dispersion of mechanical properties, equal to 1.5, as if environmental deterioration would be prevented through appropriate measures.

6.8.3.5 Flexural Strength, Stiffness and Deformation Capacity of Members with FRP-Wrapping

For members wrapped with FRP along the end region where yielding and flexural plastic hinging takes place (to improve the deformation capacity of the plastic hinges and any deficient lap splices, see points (a), (b) in Section 6.8.3.1), Section 3.2.3.10 has presented models for the yield moment, the secant stiffness to the yield-point and the cyclic ultimate chord rotation, as affected by the FRP wrapping. That information is summarised here for convenience:

1. The yield moment of members with continuous bars is somewhat underestimated, if the effect of any FRP wrapping is neglected. The prediction improves if the confined concrete strength, f_c^*, from Eq. (3.27a) in Section 3.1.2.4, is used in this calculation. The same conclusions apply for the moment resistance.
2. In members with continuous bars the secant stiffness to the yield-point may be estimated from Eqs. (3.66), (3.67) and (3.68), neglecting the effect of confinement by the FRP.
3. The ultimate chord rotation of members with continuous bars may be estimated from Eqs. (3.78) in Section 3.2.3.5, provided that either one of the following is added to the exponent of the 2nd term from the end:

   (i) term $a_f \rho_f f_{f,e}$, with $\rho_f = 2t_f/b_w$ being the FRP geometric ratio parallel to the loading direction, a_f the effectiveness factor for confinement by the FRP given by Eq. (3.28) as a_n and $f_{f,e}$ the effective stress of the FRP from Eq. (3.89); or
   (ii) the term given by Eq. (3.90); or
   (iii) the term given by Eq. (3.91).

   Alternatives (ii) and (iii) are more accurate than (i), which is more safe-sided and has been adopted in Annex A of CEN (2005a).

   The so-predicted ultimate chord rotation is on the safe-side by about 5% on average, for members that are intact when retrofitted with FRP. It may be somewhat unconservative for members that had suffered serious damage and were repaired before been wrapped with FRP.
4. The ultimate chord rotation of members with continuous bars may be estimated equally well as in point 3 above, if Eq. (3.72) in Section 3.2.3.4 is used, with L_{pl} from Eq. (3.73) and ultimate curvature, φ_u, from:

- the plane-sections analysis in Section 3.2.2.4 modified to use a parabolic-trapezoidal σ-ε law for FRP-confined concrete, as in Lam and Teng (2003a,b) instead of a parabolic-rectangular one,
- the (Lam and Teng 2003a,b) model for the confined strength, Eq. (3.27a), and
- Eqs. (3.29) and (3.30) for the ultimate strain of FRP-confined concrete under cyclic loading.

5. If ribbed (deformed) longitudinal bars are lap-spliced over a length l_o starting at the end section and the member is wrapped with FRP all along the lapping, then:

   (i) the yield moment, the chord rotation at yielding and the member effective stiffness derived from them may be calculated with:

      a. both bars in any pair of lapped compression bars counting as compression reinforcement and
      b. with a maximum possible stress of the lapped tensile bars:

         I. obtained from Eq. (3.31) in Section 3.1.3.2, using there Eq. (3.32a), or
         II. equal to their yield stress times $l_o/l_{oy,min} \leq 1$, with $l_{oy,min}$ from Eq. (3.85a).

   (ii) the ultimate chord rotation, θ_u, is obtained from Eqs. (3.78b) or (3.78c), with θ_y corrected for the lap-splicing and the FRP-wrapping according to 5(i) above and the last term at the right-hand-side of Eqs. (3.78b) or (3.78c), ${\theta_u}^{pl}$, computed taking into account point 5(i)a above and then multiplied by $l_o/l_{ou,min} \leq 1$, with $l_{ou,min}$ from Eq. (3.92).

6. In members with serious damage (beyond yielding, to nearly ultimate deformation), FRP-wrapping adds very little to the effect of repair carried out according to Section 6.8.1 on yield moment (which is re-instated, anyway) and secant stiffness to the yield-point (which is reduced by previous damage to about three-quarters of the value estimated according to point 2 above). However, unlike mere repair, FRP-wrapping eliminates almost fully the adverse effect of such damage on the member's ultimate chord rotation, which seems to be nearly the same regardless of any damage suffered by the member before been wrapped.

According to Annex A of CEN (2005a) the effect of FRP wrapping on the yield moment, moment resistance and secant stiffness to the yield-point of members with continuous bars may be neglected (see points 1 and 2 above), while that on ultimate chord rotation may be found by applying approach 3(i) above to Eq. (3.78a). If ribbed longitudinal bars are lap-spliced starting at the end section and the member is wrapped with FRP all along this lapping, point 6(i)a and approach II in 6(i)b above apply for the yield moment, the chord rotation at yielding and the member effective stiffness. Point 6(ii) applies for the ultimate chord rotation.

Annex A of CEN (2005a) gives also alternative options for the dimensioning of the FRP for a target value of the curvature ductility factor of the retrofitted member and for clamping of short lap splices. Those alternative approaches, described in detail in *fib* (2003, 2006) have not been validated/calibrated on the basis of test

results, at least to the same extent as the Eurocode 8 options highlighted in the present section and in Section 3.2.3.10.

The values of M_y, θ_y and θ_u used in verifications in the framework of retrofitting according to EN-Eurocode 8 should be based on mean strengths of the old materials divided by the confidence factor and on nominal strengths of the FRP. Mean values of all materials, without confidence factors, are used in the values of M_y, θ_y entering in the calculation of the effective stiffness for the analysis.

6.8.3.6 Cyclic Shear Resistance of FRP-Wrapped Members

Seismic strengthening of beams is easier in shear than in flexure, as it does not require intervention into the joint region or in the top slab. Shear strengthening can be implemented, instead, by side-bonding FRP straps or by U-jacketing with FRP over the three exposed sides of the beam, provided that the individual straps or the open ends of the U-jacket are sufficiently anchored at the beam sides or at their connection with the slab. Normally shear strengthening may be limited to the end regions of the beam where the shear due to the concurrent gravity loads, $g+\psi q$, (cf. 2nd term, $V_{g+\psi q,o}(x)$, in Eq. (6.3)) has large values. Moreover, if the shear force due to gravity is large compared to the seismic shear (1st term in Eq. (6.3)), nearly unidirectional FRP sheets or straps may be used at an angle $\alpha = 45^\circ$ to the beam axis. Such a shear strengthening is dimensioned as for gravity loads (*fib* 2003, 2006, Triantafillou 1998, Monti and Liotta 2005). As a matter of fact, Annex A to CEN (2005a) has adopted the general approach for shear strengthening for gravity loads (Triantafillou 1998, Monti and Liotta 2005) for the dimensioning of FRP straps or sheets that are wrapped around or U-jacket the beam, or are side-bonded to it at any angle to the member axis.

In gravity or seismic load strengthening alike, the contribution of FRP straps or sheets to the member resistance against diagonal tension is taken similar to that of shear reinforcement, except that the FRP cannot be taken to work with its full tensile strength. First, by not being ductile like steel but linear up to failure, the FRP cannot develop its full strength under the variable tensile strains along the diagonal crack. Second, it may exhibit its maximum contribution to shear resistance before the strut inclination rotates sufficiently to maximise that of transverse reinforcement. Third, the variable strut inclination model described in Section 3.2.4.2 under *The Variable Strut Inclination Truss of the CEB/FIP Model Code 90 and Eurocode 2* does not fully apply in this case, as the FRP bridging a diagonal crack may also exhibit a "dowel" type of resistance, instead of mere uniaxial tension. So, when a component due to the FRP is introduced in the variable strut inclination model according to the following generalisation of Eq. (3.94) (*fib* 2003, Triantafillou 1998, Triantafillou and Antonopoulos 2000):

$$V_{R,f} = \rho_f b_w z(\varepsilon_{f,e} E_f)(\cot\delta + \cot\alpha)\sin\alpha \tag{6.16}$$

it should employ an "effective strain", $\varepsilon_{f,e}$, less than the fracture strain of the FRP. In Eq. (6.16) δ and α denote the inclination of the strut and of the main direction of the FRP, respectively, with respect to the member axis, ρ_f is the geometric ratio

of the FRP in its main direction and E_f its Modulus. The value of the "effective strain" $\varepsilon_{f,e}$ depends on whether debonding (especially of side-bonded or U-wrapped FRP) may pre-empt fracture of the FRP in tension. In addition, for a given mode of FRP bonding (U-jacketing, side-bonding or full wrapping), $\varepsilon_{f,e}$ seems to increase with the ratio of the tensile strength of concrete, f_{ct}, that governs debonding, to the extensional stiffness of the FRP, $\rho_f E_f$, which controls the force demands placed on the FRP anchorage (*fib* 2003, Triantafillou 1998, Triantafillou and Antonopoulos 2000). In Triantafillou and Antonopoulos (2000) empirical expressions have been proposed for $\varepsilon_{f,e}$ as a function of $f_{ct}/\rho_f E_f$, of the mode of FRP bonding and of the fracture strain of the FRP. Such an approach has been adopted in ACI (2003) and JSCE (2001) as well.

It is prudent to cap $\varepsilon_{f,e}$, to allow the rest of the shear resisting components to develop their contribution before that of the (brittle) FRP is exhausted. To this end, the following upper limits have been proposed for the design value of $\varepsilon_{f,e}$:

- $\varepsilon_{f,e} \leq 0.007$ in JBDPA (1999);
- $\varepsilon_{f,e} \leq 0.006$ in *fib* (2003).

This also caps the inelastic tensile strain that the transverse reinforcement is allowed to develop and sets a lower limit on the strut inclination δ at exhaustion of the diagonal compression strength of the web. Note that the resistance for diagonal compression (web crushing) does not appreciably increase thanks to enhancement of the diagonal compression strength of concrete by FRP wrapping over the full lateral surface of the member (let alone of just the end regions or of part of the perimeter). Therefore, regardless of any FRP strengthening, the corresponding shear resistance, V_{Rmax}, still has the value given in Section 3.2.4.2 under *The Variable Strut Inclination Truss of the CEB/FIP Model Code 90 and Eurocode 2* for slender members under monotonic or cyclic loading. Then, by setting the value of V_{Rmax} from Eq. (3.97) equal to the sum of $V_{R,s}$ from Eq. (3.94) and $V_{R,f}$ from Eq. (6.16), we obtain the lower limit of δ in slender members with the main direction of the FRP at right angles to their axis, α=90° (cf. Eq. (3.98)):

$$\tan\delta \geq \sqrt{\frac{\dfrac{\rho_w f_w + \rho_f E_f \varepsilon_f}{n f_c}}{1 - \dfrac{\rho_w f_w + \rho_f E_f \varepsilon_f}{n f_c}}} \tag{6.17}$$

At this value of δ the shear resistance is (cf. Eq. (3.99)):

$$V_R = \sqrt{\left(\rho_w f_w + \rho_f E_f \varepsilon_f\right)\left(n f_c - \rho_w f_w - \rho_f E_f \varepsilon_f\right)} b_w z f_c \tag{6.18}$$

Equation (6.18) shows that the gain in shear resistance is less than proportional to the amount of FRP added for shear strengthening, especially as we approach the point of diminishing returns:

$$\rho_f E_f \varepsilon_f = 0.5nf_c - \rho_w f_w \tag{6.19}$$

where the upper limit of shear resistance is reached:

$$V_R = 0.5nb_w z f_c \tag{6.20}$$

A similar approach may be followed if the main direction of the FRP is not at right angles to the member axis, $\alpha < 90^\circ$. The value of V_{Rmax} from Eq. (3.97) is set equal to the sum of $V_{\text{R,s}}$ from Eq. (3.94) and $V_{\text{R,f}}$ from Eq. (6.16), to solve (numerically) for the limit value of δ. Then, the shear resistance of the FRP-retrofitted member is obtained from Eq. (3.97).

The discussion above has mainly beams in mind. As pointed out in Section 6.7.3, the emphasis of Section 6.8 on modification of existing components for seismic retrofitting, is on vertical elements, mainly columns. Unlike beams, columns and walls are subjected to a constant shear force within each storey. So, if indeed shear strengthening is needed, it should be uniform throughout the height of the vertical element in a storey. Moreover, as the shear demand alternates between opposite values, the main direction of the FRP should be horizontal. The end result is a vertical element fully wrapped in (nearly) unidirectional FRP sheets essentially all along its length (see Fig. 6.12(b) for an example). If wrapping all around the element is neither essential (as, e.g., in rectangular walls) nor feasible (e.g., when not all sides are accessible), proper attention should be paid to the anchorage of the FRP near or around the edges of the section (see Section 6.10.2 for such examples). At any rate, the dimensioning of this FRP in shear may be carried out according to the general approach above, or to the more elaborate one in Triantafillou (1998) and Monti and Liotta (2005) adopted in Annex A of CEN (2005a). The focus of the rest of the present section is on the contribution of any FRP wrapping of the plastic hinge region to its resistance against diagonal tension failure ("ductile shear", see Section 3.2.4.3).

FRP-wrapping of a member's end region increases appreciably its cyclic deformation capacity, but does not delay yielding. So, the ductility ratio demand, $\mu_\theta{}^{\text{pl}}$, may increase during inelastic cycling sufficiently for the FRP-wrapped plastic hinge to become critical in shear. Note that FRP-wrapping does not appreciably increase the cyclic shear resistance for diagonal compression failure after flexural yielding, given by Eq. (3.115) for squat walls (with $L_s/h < 2.5$) or Eq. (3.127) for squat columns (with $L_s/h \leq 2.0$). The very few available cyclic tests on FRP-wrapped squat columns failing by diagonal compression after flexural yielding show that Eq. (3.127) is indeed safe-sided. The question is then by how much FRP-wrapping increases the cyclic shear resistance after flexural yielding, over the value given for diagonal tension by Eqs. (3.114).

There are very few (about 10) cyclic tests of concrete members with FRP-wrapped ends that led to diagonal tension failure after flexural yielding. Their results suggest that the resistance to diagonal tension may still be obtained from Eqs. (3.114), provided that a term is added for the FRP contribution. One option is to base this term on the effective, average strength of the FRP all around the column

according to the (Lam and Teng 2003a,b): $f_{\mathrm{fu,L\&T}} = E_{\mathrm{f}}\varepsilon_{\mathrm{fu}}$, with $\varepsilon_{\mathrm{fu}}$ about equal to 60% of the failure strain of tensile coupons (see Sections 3.1.2.4 and *Members with Continuous Bars*):

$$V_{R,FRP} = \frac{h-x}{2L_s}\min\left(N;\, 0.55A_c f_c\right) + \left(1 - 0.05\min(5;\, \mu_\theta^{pl})\right)$$
$$\left[0.16\max(0.5;\, 100\rho_{tot})\left(1 - 0.16\min\left(5;\, \frac{L_s}{h}\right)\right)\sqrt{f_c}A_c + V_w + \rho_f b_w z f_{fu,L\&T}\right] \tag{6.21}$$

This proposal gives a test-to-prediction ratio in the 10 columns tested to ductile shear failure with an average of 0.99 and a coefficient of variation of 14.1%.

A simpler option, proposed in Biskinis (2007) and adopted in Annex A of CEN (2005a), is to add to the right-hand-side of Eqs. (3.114) a term $V_{\mathrm{f}} = 0.5\rho_{\mathrm{f}} b_{\mathrm{w}} z(E_{\mathrm{f}}\varepsilon_{\mathrm{u,f}})$ that does not degrade with inelastic cyclic displacements. In this case $\varepsilon_{\mathrm{u,f}}$ is the failure strain of the FRP from tension coupons and the factor of 0.5 reflects the linear reduction of the FRP stress over the section depth, from the failure strain at the extreme tension fibre to zero at the neutral axis. This simpler alternative gives as good a prediction as Eq. (6.21). The average of the test-to-prediction ratio in the 10 columns is 1.01 and the coefficient of variation is 12.9%.

6.8.4 Steel Jacketing

6.8.4.1 Scope and Construction Aspects

Steel jackets are more expensive than concrete ones. However, their technology is simple, familiar to the construction industry and readily available almost everywhere. So, it is the technique of choice for non-engineered emergency strengthening even hours after a damaging earthquake, to prevent collapse of heavily damaged buildings or give back to use moderately damaged ones during the aftershock period. Detailed assessment and retrofit design may take place afterwards. The steel jackets may be removed when retrofitting is implemented, or incorporated in a concrete jacket (as in Fig. 6.4(a)). Despite this advantage and the long history of surface-bonded steel plates in strengthening of RC members, they are being replaced fast by surface-bonded FRPs, which, although more costly, are much lighter, easier to apply and mechanically more effective.

Thin-walled steel jackets are most efficient and easier to apply around circular columns. There they usually come in two semi-circular halves fitting closely around the column and field-welded along two vertical seems. The gap between the jacket and the column is grouted with non-shrink mortar. Such jackets are considered so efficient, that they have even been proposed for retrofitting square or rectangular columns, using a large quantity of concrete (rather than mortar grout) to fill the gap between the jacket and the column. However, circular or elliptical steel jackets around square or rectangular building columns are neither practical nor aesthetically

(a) (b)

Fig. 6.4 Steel jackets built-up in situ with corner angles and horizontal straps

appealing. For such columns steel jackets are built up of four corner angles, usually epoxy-bonded to the concrete or just in gapless contact to it along the full length. Continuous thin steel plates or thicker horizontal steel straps or batten plates are welded to the corner angles (Fig. 6.4). Within the limitations imposed by the heavy weight of steel segments, continuous thin plates may be shop-welded to the corner angles into larger L-shaped pieces, fitting half the perimeter of the column and fillet-welded in the field. The 10–20 mm gap between the plate and the surface of the column is grouted with non-shrink mortar. Before been welded, straps or batten plates may be pre-heated in the field to 200–400°C, to exert some "active" confinement on the column after they cool down. Most of the benefit is gradually lost owing to concrete creep. So, it is neglected in design. Depending on the intended role of the jacket, the gap between the column and the straps or batten plates may be grouted with non-shrink mortar or left unfilled.

Steel jackets around columns enhance ductility through confinement (see Section 6.8.4.2), increase shear strength (Section 6.8.4.3) and improve deficient lap splices (Section 6.8.4.4). All these effects have to do with the action of the jacket in the transverse direction of the member. But as steel is isotropic, if the jacket consists of a continuous thin plate, it presents significant stiffness and strength in the longitudinal direction as well, which unavoidably affects flexural stiffness and moment resistance. The extent of this influence depends on how the steel jacket is connected to the concrete member and to the ones framing into it. However, steel jackets are normally not intended for flexural strength enhancement. Their continuation beyond the member end, although not so difficult as for FRP jackets, is not easy. Moreover, even though they can transfer forces beyond the member end by bolting or welding to other steel elements through the slab and by bearing against the concrete surface, they are not so effective in resisting cyclic flexure in composite action with the concrete member inside, as their thin walls may buckle. As a result, they are applied

on the concrete surface so that they develop stresses mainly in the circumferential direction, with their effect on member flexural strength and stiffness minimised.

6.8.4.2 Confinement by Steel Jackets

The confinement of a rectangular section by the steel jacket may be calculated from Eqs. (3.23) and (3.25), as if the jacket (continuous or in straps) were internal hoops and ties, using as geometric steel ratio ρ_x or ρ_y in each transverse direction the cross-sectional ratio of the jacket in a vertical section of the column. Unless tied back into the column, thin steel plates or straps welded to the corner angles do not confine the sides of a rectangular section, because, being flexible, they bulge outwards. So, the confinement effectiveness factor within the section, a_n, may be calculated from Eq. (3.28) in Section 3.1.2.4, with the corner radius R replaced by the width, b, of the steel angle (where there is full contact of the angle and the column concrete). If continuous steel plates are welded to the corner angles, the confinement effectiveness factor along the member, a_s, may be taken equal to 1.0. If steel straps or batten plates are welded instead, a_s may be calculated from Eq. (3.20c), using there as b_{xo}, b_{yo} the external dimension of the section and as s the clear spacing, s_{cl}, of straps or batten plates, reduced by twice the corner angle width, b, according to a postulated 45° dispersion of confining action from the strap into the corner angle: $s = s_{cl}$-$2b$ (Dritsos and Pilakoutas 1992).

Friction between the corner angles and the column, owing to the confining forces developed there when the concrete column is approaching ultimate conditions, enhances the composite action of the column with the steel jacket and mobilises the jacket in the longitudinal direction, even when it is not continued into the joint beyond the member end. The resulting increase in stiffness and strength of the jacketed column is uncertain, but forms a second line of defense against loss of axial-load-capacity of the column in the post-ultimate range. Note that an enhancement of the column moment resistance may adversely affect the shear force demand on the column and the joint and the moment and shear input in the foundation. So, a few-mm gap should be provided between the end of the jacket and the end section of the column to prevent the jacket from bearing against the face of the element to which the column is connected and developing compressive forces that enhance the column moment resistance.

The confinement effectiveness of thin-walled steel jackets is further reduced by their Poisson expansion due to any longitudinal compressive stresses that may develop in the jacket through its partial or full composite action with the concrete column inside (see last paragraph). If there is full composite action in the longitudinal direction, the large Poisson ratio of steel will delay confinement until concrete approaches ultimate strength and its Poisson ratio exceeds that of steel. Cages of angles at the corners and welded transverse straps or butten plates do not suffer from reduction of confinement effectiveness due to Poisson effects. Such effects can be minimised also if the continuous thin-walled steel plate is replaced by sheets corrugated in the transverse direction of the member and welded along the corners of the section. Thanks to the very low stiffness of the corrugated sheet for axial

compression in the member, confinement is not reduced by Poisson effects. Moreover, the large out-of-plane rigidity of the corrugated sheet almost eliminates outward bulging of the jacket and enhances confinement. Corrugated steel jacketing has been found to be very effective for the flexural deformation capacity of columns (Ghobarah et al. 1997).

6.8.4.3 Shear Strengthening Through Steel Jackets – Dimensioning According to Eurocode 8

When they aim at enhancement of the column deformation capacity or of deficient lap splices, steel jackets are normally applied only over the plastic hinge or the lap splice region. By contrast, those intended for shear strengthening extend over the full length of the member. The jacket is inactive in shear until a major diagonal crack develops in the concrete member. Relative displacement of the two pieces on either side of such a crack causes the member to bear against the jacket and activate it. From that point on the jacket resists all the additional shear force and controls the width of the original diagonal crack, as well as development of new ones or disintegration of the concrete core due to cyclic shear. To play this role the steel jacket should remain elastic (Aboutaha et al. 1999). The contribution of the jacket to the resistance in diagonal tension is added to that of internal ties and of the concrete.

The analysis of the limited available experimental information on shear critical steel-jacketed columns suggests that the jacket contributes to the resistance in diagonal tension of the jacketed part of the member with the following shear force:

$$V_{R,j} = \eta \frac{2\, t_j\, b}{s} h f_{yj} \cot \delta \tag{6.22}$$

where:

- η is a jacket efficiency factor, with values between 0.4 and 1.0; η seems to have values close to 0.4 for continuous thin plates or corrugated sheets and higher than 0.5 for straps or batten plates welded to corner bars.
- t_j is the thickness of steel straps at right angles to the member axis,
- b is the width of the steel straps,
- s is the centreline spacing of steel straps (with $b/s = 1$ for a continuous steel plate),
- h is the depth of the concrete section in the direction of the shear force,
- δ is the inclination of the compression strut to the member axis,
- f_{yj} is the yield strength of the steel of the jacket.

Annex A of CEN (2005a) adopted Eq. (6.22) with $\eta = 0.5$ (as recommended in Aboutaha et al. 1999) and with the design yield strength of the jacket steel, $f_{yj,d}$ (nominal strength divided by the partial factor for structural steel).

Equation (6.22) applies throughout the length of the member and its outcome should be added to the value of $V_{R,s}$ from Eq. (3.94). In the plastic hinge the value

of $V_{R,j}$ for $\delta = 45^\circ$ from Eq. (6.22) should be added to the right-hand-side of Eqs. (3.114). By remaining elastic the jacket prevents cyclic degradation of the resistance in diagonal tension within the plastic hinge. So, any reduction of V_R with cyclic ductility demand, μ_θ, in Eqs. (3.114) may be neglected.

The steel jacket does not increase markedly the resistance of the member in diagonal compression (against web crushing). Like for FRP-wrapping the corresponding shear resistance, V_{Rmax}, is still as given in Section 3.2.4.2 under *The Variable Strut Inclination Truss of the CEB/FIP Model Code 90 and Eurocode 2* for slender members under monotonic or cyclic loading, or by Eq. (3.127) for squat columns (with $L_s/h \leq 2.0$) in cyclic loading after flexural yielding.

6.8.4.4 Members with Short Lap Splices and Steel Jackets

A steel jacket consisting of a continuous thin plate or corrugated sheet can clamp deficient lap splices in rectangular columns. Its thickness, t_j, may be derived from a friction-based model for the clamping action. The model (Aboutaha et al. 1996a,b) is based on:

1. A postulated shear transfer area along the lap splice, consisting of strips with length equal to the lapping, l_o, and width not more than 1.5 bar-diameters ($1.5d_{bL}$) on either side of each spliced bar. The surface-area of the shear transfer area for one spliced bar is: $A_{sf} = l_o \min(3d_{bL}, s_b)$, where s_b is the spacing between lapped bars.
2. A friction coefficient over the shear transfer area equal to $\mu_f = 1.4$ for clamping by anchor bolts, or $\mu_f = 1.0$ otherwise.
3. Bond stress along the embedment length, l_{ab}, of anchor bolts equal to $v_b = 0.042\sqrt{f_c}$ (units MN, m).
4. Clamping by tie legs which are at right angles to the potential splitting plane and enclose the lap splices, based on the yield force of the tie legs per unit length of the member, $\Sigma A_{st} f_{yt}/s_t$.
5. Clamping by the (two) sides of the steel jacket which are parallel to the tie-legs in point 4 and the anchor bolts of point 3 above, based on the yield stress f_{yj} of the steel jacket.
   The model gives (Aboutaha et al. 1996a,b):

$$2t_j f_{yj} \geq v_{sf} b - \sum \frac{A_{st} f_{yt}}{s_t} - \frac{v_b \pi d_b l_{ab} n_{ab}}{l_o} \tag{6.23}$$

where:

b is the column width parallel to the potential splitting plane, at right angles to the tie legs and the anchor bolts;

A_{st}, s_t are the cross-sectional area and spacing of tie-legs along the member axis;

d_b, n_{ab} are the diameter and the total number of anchor bolts over the entire area of lap splicing, bl_o;

v_{sf} is the shear stress demand over the shear transfer area along the splice length of a single bar:

$$v_{sf} = \frac{\gamma_{Rd} A_{sL} f_{yL}}{\mu_f A_{sf}} \tag{6.24}$$

with A_{sL} and f_{yL} denoting the cross-sectional area and the yield stress of a single lap-spliced bar and γ_{Rd} a model uncertainty factor, accounting for strain hardening in the spliced bars and having a suggested value: $\gamma_{Rd} = 1.25$ (Aboutaha et al. 1996a,b).

According to Aboutaha et al. (1996a,b), unless f_c exceeds 30 MPa, the steel jacket should be back-anchored into the column just above the end of the lap splice and at about one-third of the lap length from the base section where the lapping starts, with two bolts at third-points of the column side at each level. Intermediate (rows of) bolts between these two heights are not necessary for effective clamping of the lap splices.

Test results in Aboutaha et al. (1996a,b) have shown that very high cyclic deformation capacity of retrofitted columns (to drift ratios above 5%) can be achieved with the above rules.

Annex A in CEN (2005a) recognises clamping of deficient lap splices by steel jackets consisting of continuous steel plates, but provides no model for it. It only gives prescriptive guidance, based on the test results and recommendations in (Aboutaha et al. 1996a,b):

- The steel jacket should extend beyond the end of the lapping not less than 50% of the lap length (as extension by just 20% was found insufficient in Aboutaha et al. (1996a,b)).
- The jacket should be anchored to the faces of the column by at least two rows of bolts on column sides at right angles to the direction of loading. If the splicing is at the base of the column, one of these rows of bolts should be near the bottom end of the lapping and another at one-third of its length from the column base.

Note that discrete collars built-up of channel sections fitted around the column and bolted at its corners do not provide as effective a clamping of lap splices as jackets consisting of corner angles and continuous steel plates welded on them.

6.8.4.5 Resistance and Deformations of Steel-Jacketed Members at Yielding and Ultimate

Cyclic test results on steel-jacketed concrete members are limited in the international literature. Their analysis in *fib* (2003) leads to the following conclusions:

- With a 25–50 mm gap between the end of the jacket and the member end, the yield moment and the moment resistance of the jacketed member are equal to those of the end section of the original one.

– The secant-to-yield stiffness of the retrofitted member may be taken equal to that of the original column from Eq. (3.68), neglecting the effect of deficient lap splices that have been remedied according to Section 6.8.4.4.
– The flexure-controlled deformation capacity of the retrofitted member may be taken equal to that of the original one, again neglecting the effect of deficient lap splices corrected by retrofitting according to Section 6.8.4.4. The effect of confinement on the ultimate strain concrete and on the ultimate curvature of the end section may be taken into account according to Section 6.8.4.2, but may also be neglected in view of the limited experimental confirmation. Note, though, that empirical expressions for the plastic hinge length, L_{pl}, fitted to members without retrofitting should be used with caution for steel-jacketed members.

6.9 Stiffening and Strengthening of the Structure as a Whole

6.9.1 Introduction

Interventions at the structure's level to increase global stiffness and reduce seismic deformation demands throughout the system may be more cost-effective than universal upgrading of the capacities of the existing components, if disruption of occupancy and demolition and replacement of partitions, architectural finishes and other interior non-structural components are considered. This is particularly true for flexible buildings. However, they may be less convenient for the future functionality of the building, if they require reducing openings or take up valuable floor area.

6.9.2 Addition of New Concrete Walls

6.9.2.1 Construction of the New Walls and Connection to Existing Members

Adding concrete walls is perhaps the most common technique for seismic retrofitting of buildings. It is very effective for the control of global lateral drifts and the reduction of damage in frames and non-structural elements.

If the system of new walls takes the full seismic action according to Section 6.5.8, with the existing elements verified like "secondary" ones in a new building (see point 1 in Section 6.7.2), then the new walls are designed on the basis of forces and detailed as in new buildings. When retrofitting follows point 2 in Section 6.7.2 and the walls are verified in flexure on the basis of deformations, it is still good practice to detail them as in a new building, i.e. for flexural plastic hinging at the base. To this end, the plastic hinge zone at the base is provided with boundary elements near the edges of the section, well-confined and detailed for flexural ductility. The walls are also capacity-designed in shear throughout the height according to Section 6.5.5.2.

Full continuity of the wall across storeys increases its strength. Good anchorage of the new reinforcement is essential for strength and deformation capacity.

New walls may be conveniently introduced by infilling strategic bays of the existing frame, especially at the perimeter. If the wall takes up the full bay, it can incorporate the beams and also both columns as boundary elements. Then only the web of the wall is totally new. Sometimes it is shotcreted against a partition wall, which is then encapsulated within the core of the web. The new web should be fastened to the existing beams and columns all around the infilled panel through special connectors. The fastening of these connectors to the existing members and their embedment into the new concrete should be capable of fully transferring the web shear and the tensile capacity of the web reinforcement to the frame members. Poor detailing and lack of a proper load-path between the old members and the newly constructed parts of the wall may lead to reduced global ductility or brittle failure of web panels. Moreover, if there is no integral connection between the existing and the new, the behaviour is uncertain and the reliability of modelling and verification of the wall as a single, integral element is in doubt.

For integral behaviour, the new wall should be thick enough to encapsulate the existing beams and columns. In that case holes and slots should be drilled through the slab, for the vertical bars to pass from one storey to the next and for concrete to be cast from the top. The concrete that fills the slots plays the role of shear keys between the new wall and the slab. For fully integral behaviour epoxy-grouted dowels may be placed throughout the interface of the old concrete and the new, at about 0.5 m centres. Even when it does not encapsulate the existing beams, the new wall may have to do so for the columns, to provide the lacking confinement reinforcement, especially if the columns have short lap splices (see Fig. 6.5(a) for an example).

It is essential to ensure the transfer of inertia forces from the floors to the new walls. A wall created by infilling a bay of a frame may be considered as adequately connected to the floor diaphragms if it encapsulates the beams, or if its web panels are well fastened to the surrounding frame members and the floor slab is integral with the beams. Often "collector" elements may need to be added and designed for the transfer of floor inertia loads to the new walls. If the new wall is at the perimeter, a steel tie can be fastened to the side of perimeter beams to collect the floor loads and transfer them to the new wall, where the end of the tie is embedded for anchorage. In the example of Fig. 6.6 the steel tie is fastened by welding on steel plates anchored to the side of the perimeter beam. The collectors and their anchorage to the perimeter beams may be covered with shotcrete for protection. They should be dimensioned for seismic action effects based on capacity-design considerations, accounting also for higher-mode effects. Nonlinear response-history analyses of wall-frame systems show that such effects on peak floor forces are much larger than on storey shears (which are the cumulative effect of floor forces). Equations (1.16) in Section 1.3.6.4 and (6.7) in Section 6.5.5.2 are a good guide for the magnification factor to be applied on the seismic loads transferred from the floor to the new wall according to the analysis for the seismic action.

If it is not feasible to encapsulate the beams and columns of the frame bay, the new wall may be created by fully infilling with RC the space between them. The connection of the new web with the beams and the columns is more critical than when these members are fully encapsulated. Even with very good shear connection,

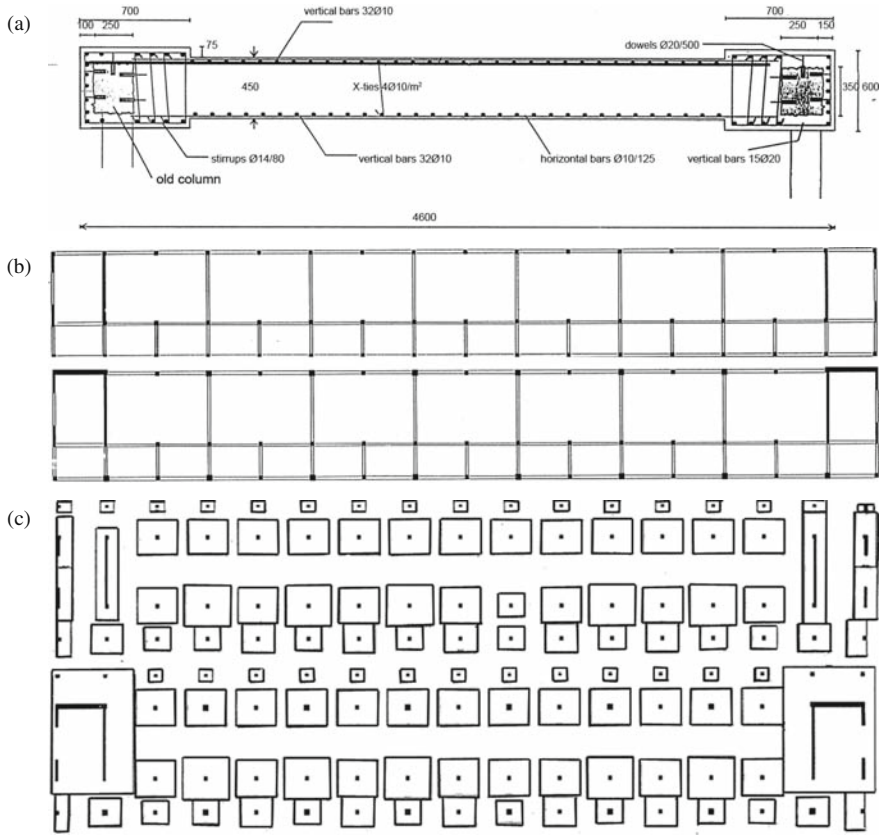

Fig. 6.5 3-storey building strengthened in long direction with two new walls: (**a**) cross-section of added wall; (**b**) plan of framing, before (*top*) and after retrofitting (*bottom*); (**c**) foundation plan, before (*top*) and after retrofitting (*bottom*)

integral behaviour of the old and the new cannot be presumed and the force and moment resistance or the deformation capacity of the system cannot be quantified with any certainty. Very instructive in this respect are the ultimate strength and deformation results of several one-bay, one-storey RC frames converted to walls by infilling them with RC of thickness (about) half the column width at right angles to the plane of the frame (JCI 2007). The infilled frames were invariably predicted to be shear-critical, with the connection of the new web to the surrounding members being the weak link. The force resistance derived from their predicted flexural capacity was always about double the predicted shear resistance. Companion monolithic wall specimens were tested for comparison. Their resistance was also governed by shear, although the margin between the predicted flexure or shear force resistances was narrower, as the connection was not anymore the weak link. In all types of specimens the experimental ultimate strength was always much higher than

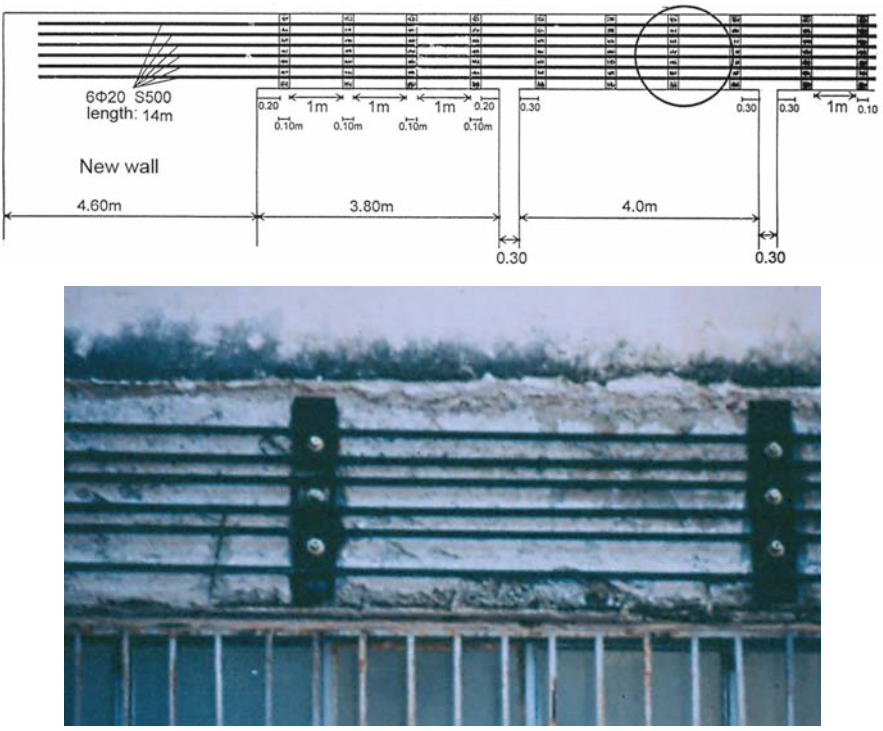

Fig. 6.6 Collector element of the wall in Fig. 6.5, fastened to the side of the perimeter beam (See also Colour Plate 16 on page 729)

the predicted shear resistance and closer to (but less than) the flexure-controlled prediction. The specimens resulting from conversion of a frame to a wall had on average an experimental ultimate strength equal to 92% of that of their monolithic counterparts for dowels connected to the old concrete through adhesive (14 specimens), or 87% for mechanical connection (3 specimens). Two wall specimens resulting from doubling the thickness of a thin web monolithic with the frame had experimental ultimate strength and ultimate deformation 97 and 105%, respectively, of those of their fully monolithic companions. In that case the new thickness of the wall was connected to the frame through dowels with adhesive. In a specimen of the same type but without shear connection other than what was provided by the original monolithic half of the wall thickness, the experimental ultimate strength and ultimate deformation were 83 and 50%, respectively, of those of the fully monolithic ones. Interesting and very important is the experimental ultimate deformation of the specimens resulting from conversion of a frame to a wall. On average it was 175% of that of their monolithic counterparts for shear connection through dowels with adhesive (14 specimens), or 270% for mechanical connection (3 specimens). The deformability of the shear connection seems to increase, therefore, very much the ultimate deformation at little expense of the ultimate strength.

As all the walls in JCI (2007) were shear critical owing to their thin webs and low slenderness (height-to-length ratio), they are not representative of multi-storey frames converted to walls by full-thickness RC-infilling. Their results are more of qualitative value, showing the general trends, the importance of the connection and the uncertainty of the behaviour.

It is not good practice to stop the new wall at a lower storey. For example, a three-storey building with walls added only to the first storey after the 1968 Tokachi-oki earthquake suffered heavy damage at the second storey in another earthquake in 1994 (Nakano 1995).

6.9.2.2 Foundation of New Walls and Impact of its Fixity on Wall Effectiveness

New walls should have proper foundation. As it typically has large cross-section, a new wall is expected to develop high seismic moments at the base. By contrast, its gravity load is low. Unless its foundation element incorporates existing footings (e.g., when the new wall is created by infilling a bay of a frame), its vertical load is not much larger that the self weight of the wall and the foundation element. At any rate, the most serious problem and drawback of the technique is the difficulty to transfer the wall base moment to the ground and the need of a major, costly and disruptive intervention to the foundation.

As emphasised in Section 2.2.2.3, isolated footings of large walls uplift and rock during the earthquake. Uplifting reduces the wall base moment well below the value obtained from constant foundation impedance. Although the rocking wall still acts as a stiff vertical spine and prevents storey mechanisms, rocking increases considerably the lateral drifts at floor levels and the chord rotation demands in beams, especially in those directly framing into the wall within its plane (those chord rotations will be about equal to the rotation of the wall base at the ground). If they are not retrofitted too, these beams may fail under such demands.

If we want the new wall to play its traditional role as a major element of lateral stiffness and strength fixed at the base, we should greatly reduce or even prevent uplifting and rocking. This can be achieved by one or more of the following:

a. by increasing the size of the new footing in plan, to increase its weight and the impedance of the underlying soil and/or to incorporate the footings of adjacent columns and mobilise their vertical load against the uplift (as, e.g., in Fig. 6.5(c));
b. by connecting the new foundation element to neighbouring ones through stiff and strong grade- or tie-beams (see Fig. 6.7 for an example); or
c. by tie-downs of the new foundation element (e.g., micropiles with large tensile strength).

Implementation of these solutions is so disruptive and costly that may discourage adding new walls to buildings not having already a stiff and strong (almost storey-high) foundation beam around the perimeter, to which a new wall could be conveniently anchored.

Fig. 6.7 New wall founded on foundation beam encapsulating footings of nearby columns

A system used by Tsiknias and Pittas (1992) to transfer the base moment of new walls to the soil without large uplifts and base rotations was to construct the new wall over half the bay width L of the frame with its base at the lowermost floor above the foundation and to connect that base to the existing spread footings of the

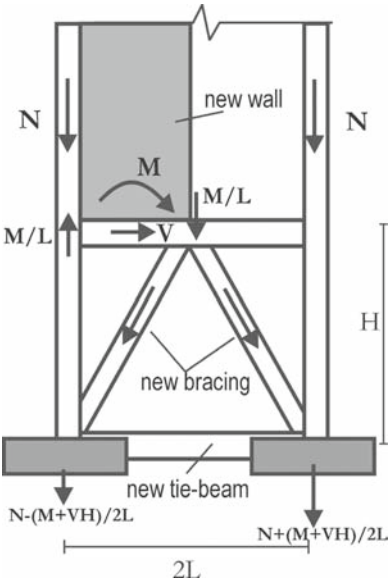

(a)

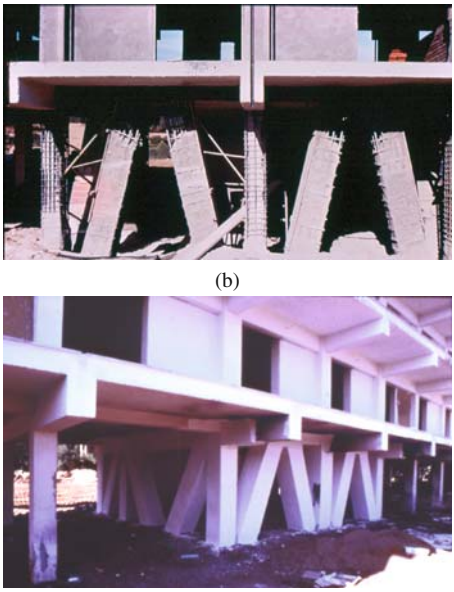

(b) (c)

Fig. 6.8 Foundation of new wall through diagonal concrete bracing: (**a**) transfer of wall forces to the ground; (**b**) shotcreting of braces and of column jackets; (**c**) retrofitting completed

two columns of the bay through Chevron (inverted-V) bracing (Fig. 6.8(a)). The moment M at the base of the new wall just above the Chevron bracing is converted into a couple of vertical forces, $\pm 2M/L$. One of them is applied to the joint of the Chevron bracing at beam mid-span and transferred to the two footings by tension and compression in the two bracings. The other force goes directly to the footing underneath, through the column. The end result is a couple of concentric vertical forces on the existing footings, $\pm M/L$. The axial load N in the existing footing prevents uplift, up to a value of the moment $M=NL$ at the base of the wall, much higher than the uplift resistance of an alternative footing large enough to accommodate the new wall and the existing column. The base rotation is equal to the differential settlement of the two footings divided by L and is low. So, the new wall is very effective in limiting lateral drifts. Implementation of this scheme requires jacketing the ground storey beam and the two columns to connect the Chevron bracing and accommodate the internal forces arising from it, possibly enlarging the footings for the connection to the bracings and the new tie-beam, if one is constructed (Fig. 6.8). The role of the tie beam is just to transfer to the adjacent footing the seismic shear in the event a footing uplifts.

Unless rocking of the base of the new wall is effectively prevented as highlighted above, it should be appropriately modelled in the analysis, to realistically capture its effects on the seismic deformation demands in the superstructure. As emphasised in Section 4.10.3, conventional rotational springs under a footing with constant stiffness, corresponding to full contact of the footing to the ground, are not sufficient. They account neither for the softening of the rotational spring due to uplifting nor for the accompanying vertical displacement of the centre of the footing. Such effects may be captured in nonlinear analysis (static or dynamic) by using a pair of nonlinear vertical springs at opposite ends of the footing that account for uplifting according to Eqs. (4.100), (4.101), (4.102), (4.103) and (4.104) in Section 4.10.3.

To help appreciate the effect of uplifting of the footing of a large wall, the results of a parametric study are presented here (Panagiotakos and Fardis 2001b). A 5-storey frame with five 5 m bays is assumed to be retrofitted by converting its central bay to a wall, incorporating the corresponding beams and columns. Nonlinear static analyses in 2D have been carried out. The one-component point-hinge model of Section 4.10.1.4 has been used and the assumptions in Section 4.10.5.1 relevant to the present case (no. 1–5 and no. 8) are employed for all beams and columns. Unlike the wall, all columns are fixed at the base. Two types of nonlinear models are used for the new wall:

1. A “conventional” one-component point-hinge model according to Section 4.10.1.4 and the relevant assumptions (no. 1–5) in Section 4.10.5.1. Bending takes place about the centroid of the wall section, without axial-flexure interaction.
2. A “new” model which differs from the “conventional” one only in that bending takes place about the current neutral axis. So, flexure induces axial deformations and vertical displacements of the centroid of the section.

For the wall footing, the model of Section 4.10.3, Eqs. (4.100), (4.101), (4.102), (4.103) and (4.104), is used.

Figure 6.9 shows a typical pattern of frame deformation, plastic hinging, etc., at an instant of the response when beam failures take place, using Model no. 2 for

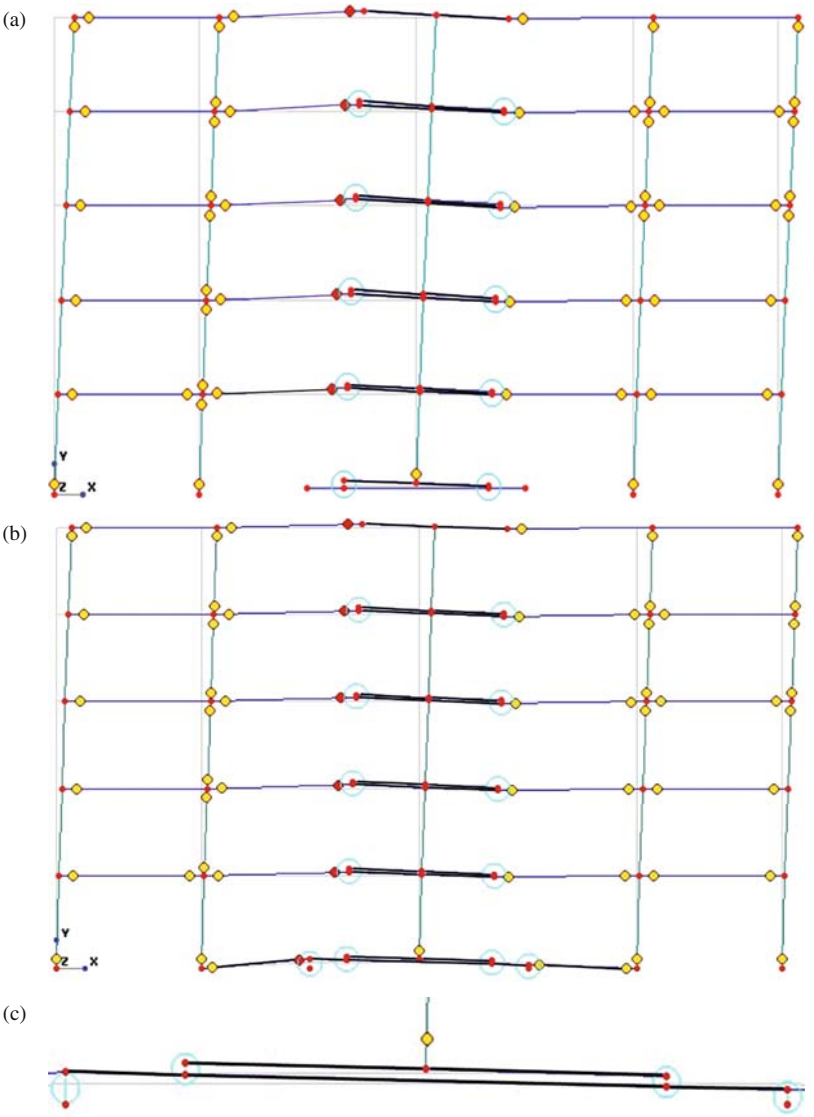

Fig. 6.9 Deformation and plastic hinging in retrofitted frame from nonlinear static analysis: (**a**) wall fixed at the base; (**b**) wall footing connected to tie-beams and uplifting; (**c**) detail of (**b**) at the base of the wall and the footing (*light-coloured circles*: plastic hinges; larger *dark circles*: flexural failure) (See also Colour Plate 17 on page 730)

the wall. When the wall is considered fixed at the foundation (Fig. 6.9(a)) there is a large upward displacement of the ends of beams framing into the "windward" side of the wall owing to the rotation of the wall section about its neutral axis. When the model includes uplifting (Fig. 6.9(b)) these upwards displacements are due to the rotation of the wall footing. In both cases these displacements drive these beam ends (including that of the tie-beam in Fig. 6.9(b)) to ultimate flexural deformation.

Figure 6.10(top), referring to a wall footing without tie-beams, compares:

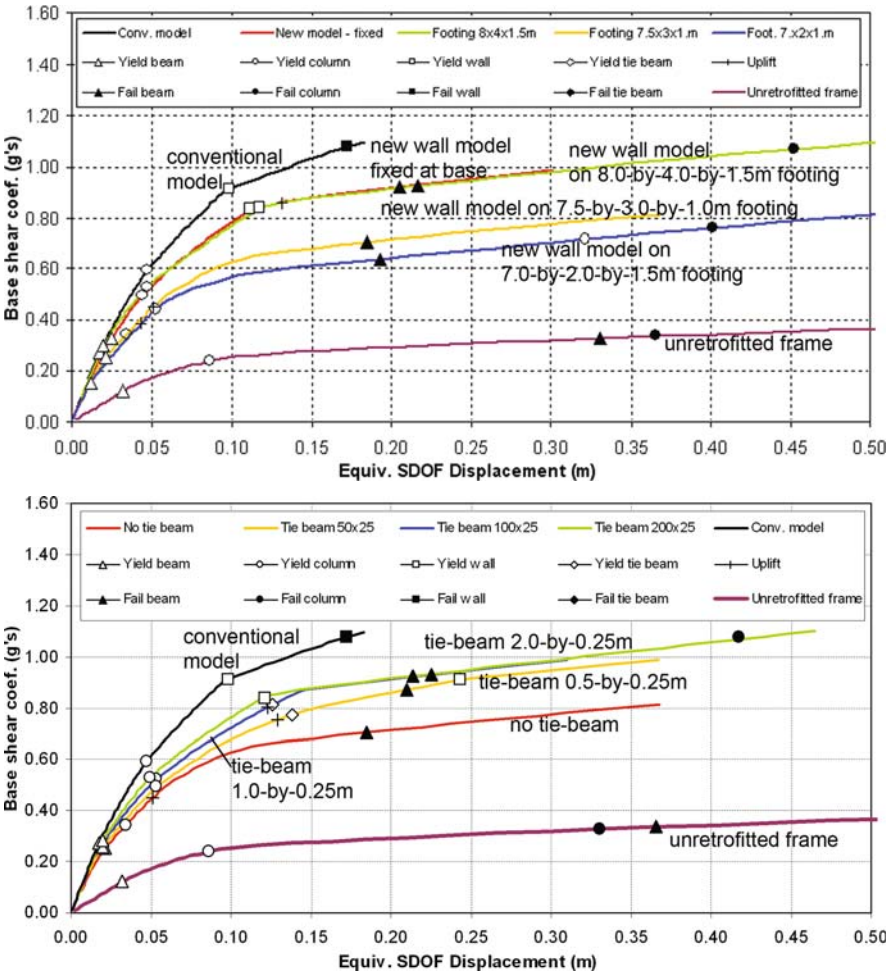

Fig. 6.10 Pushover response of retrofitted frame: (*top*) without tie-beams, using as parameters the model and the size of the footing; (*bottom*) with 1 m deep, 7.5 m-by-3 m footing, using as – parameter the size of the tie-beam (See also Colour Plate 18 on page 731)

– the four "pushover curves" obtained from wall Model no. 2 above and the model of Section 4.10.3, Eqs. (4.100), (4.101), (4.102), (4.103) and (4.104) for the footing, to
– the uppermost "pushover curve" given by Model no. 1 above with the wall fixed at the base, and the lowermost one for the unretrofitted frame.

The "new" wall model by itself produces overall a more flexible response, delaying wall yielding and preventing wall flexure failure (within the range of response considered here). A 1.5 m deep, 8 m-by-4 m footing uplifts shortly after wall yielding, but gives essentially the same overall response as full fixity at the base. Uplifting of the two smaller-size footings considered in Fig. 6.10(top) prevents wall yielding, but causes beam failure(s) a bit earlier.

Figure 6.10(bottom) uses as baseline the moderately-sized 1 m deep, 7 m-by-3 m footing and connects it to those of the adjacent columns via tie-beams of various sizes. A quite small tie-beam (0.5 m-by-0.25 m) is remarkably effective. It delays uplifting but allows yielding at the base of the wall later on (after the first flexural failure of a beam, however). Increasing further the size of the tie-beam delays almost indefinitely yielding at the wall base, but does not affect uplifting very much. Interestingly, in all cases the tie-beam yields right after the footing uplifts. A tie-beam as large as a deep foundation beam (2.0 m-by-0.25 m) provides almost full fixity of the wall, preventing uplift but accelerating yielding at the base of the wall.

The conclusions of this parametric study may be summarised as follows:

– A new wall is very effective for retrofitting a frame building.
– The effectiveness of the wall is grossly overestimated if its sections are assumed to rotate about its centroid in lieu of its neutral axis and/or if uplifting of the footing is neglected.
– A footing heavy enough, or a tie-beam sufficiently stiff, to prevent uplifting until the wall yields, are equivalent to wall fixity at the base.
– A normal-size footing without tie-beams is moderately effective.
– A normal-size footing with tie-beams of moderate or even small size has almost the same overall result as full fixity of the wall at the base.
– The sequence of events (yielding or failure of members, uplifting, etc.) is influenced markedly by the size of key foundation elements. Its prediction is affected very much by how we model the wall and the interaction of its footing with the ground.

6.9.3 Addition of a New Bracing System in Steel

6.9.3.1 Introduction

Adding diagonal bracings to selected bays in all storeys of a frame structure, or to just one or few weak storeys (e.g., to an open storey, see Fig. 6.11(c)), is effective for global strengthening and normally not as disruptive as adding walls. For

convenience and minimal disruption the bracing is usually – but not exclusively – placed at the façades. Architectural constraints and openings may condition the layout of the bracings.

Normally the intervention to the foundation is minimal (see discussion in Section 6.9.2.2 about the concept in Fig. 6.8). The prime challenge in this technique is the connection of the bracings to the existing concrete elements.

Bracings are normally made of structural steel. Steel bracing increases markedly the lateral force resistance of a concrete frame, but not so much its lateral stiffness. Therefore it is not so effective for stiff buildings, such as wall or dual systems and masonry-infilled frames. The overall deformation capacity of flexible, non-ductile concrete frames may be considerably enhanced by steel bracing, provided that we prevent early brittle failures of braces and their connections, or of shear-critical concrete members.

Passive energy dissipation devices may be introduced in the bracing for supplemental damping. These devices normally require large response displacements. So, they may not be cost-effective if the bracing system increases the lateral stiffness considerably.

To design a seismic retrofitting with steel bracings, it is essential to have a good command of seismic design of steel (and composite, steel-concrete) buildings. This subject is outside the scope of this book. So, the following sections focus on aspects specific to seismic retrofitting with steel bracings, without venturing a comprehensive coverage of the subject.

6.9.3.2 Layout and Conceptual Design of Concentric Bracing Systems

Normally, steel bracing systems applied for retrofitting are concentric (see Fig. 6.11 for examples), contributing to lateral-load resistance and stiffness and to energy dissipation through the axial forces in their inclined braces. Their dissipative elements are only the tension braces.

Appropriate (concentric) bracing systems are those with:

1. X-diagonal (“cross-diagonal”) bracings, along both diagonals of the braced bays. This is overall the preferable arrangement.

(a) (b) (c)

Fig. 6.11 Examples of retrofitting with steel bracings (University of Tokyo buildings)

2. Diagonal bracings, with a single diagonal per braced bay. The arrangement of bracings in different bays (or groups of adjacent bays) should give similar lateral resistance and stiffness for the two senses of the seismic action in the plane of bracing. For new braced steel frames, Part 1 of Eurocode 8 (CEN 2004a) restricts the difference of the total horizontal projections of the cross-sectional area of all tension diagonals for the two senses of action to less than 10% of their average value.
3. V-bracings (Fig. 6.11(a)) or inverted-V ones ("Chevron" in US), where a pair of inclined braces is connected to a single point near or at mid-span of a beam. Their advantages include the reduced unbraced length of the braces and the earlier mobilisation of their strength and dissipation capacity.[11] Chevron bracings in particular are most convenient for openings and passage through the braced bay. The horizontal member to which the two braces connect should (be strengthened to) resist a transverse force equal to the difference in the vertical force components of the tension and compression braces. For this purpose, the post-buckling force of the compression brace is normally conservatively taken as 30% of the yield force or one-third of the buckling load.

K-bracings, where the inclined braces are connected to columns at about their mid-height, should be avoided, because the unbalanced force after buckling of the compression brace mentioned above for V-bracings is applied to the columns and may cause them to fail.

If the sense of V-bracings is reversed in adjacent storeys (with an inverted-V in one storey and a V-bracing in the storey above, see Fig. 6.11(b)), the braces in consecutive storeys are almost continuous and there is no unbalanced transverse force on the beam. If the braces are connected to the top and bottom of a beam but, unlike in Fig. 6.11(b), their centrelines do not pass through the same (nodal) point, a concentrated moment is applied on the beam, equal to the sum of the horizontal projections of the tension and compression forces in the braces above or below, times the beam depth.

Composite action with the existing concrete frame and transfer of forces to the bracing are facilitated if the bracings are added within the plane of the frame, with as little eccentricity as possible to the centrelines of the existing beams and columns (Fig. 6.11(a) and (c)). Bracings placed outside the existing frame at the façade (Fig. 6.11(b)) intrude the least with the use of the building and may allow normal operation during retrofitting. However, their connection with the existing frame – usually through (a combination of) post-installed fasteners, grout mortar or even transverse post-tensioning through the concrete beams – is critical and tricky. When the exterior concrete columns are not flush with the beams but protrude from them, it is better to install the bracing between (the protruding parts of) adjacent columns,

[11] Braces yield at an interstorey drift ratio of $2\varepsilon_y/\sin 2\theta$, where ε_y is the yield strain of the brace and θ its inclination to the horizontal. So, the closer to 45° a brace is, the sooner the storey will mobilise its yield force and dissipation capacity.

bearing on them. Attaching in this case the braces to the column through a vertical steel member along its protruding part, helps the connection through interface shear.

Diagonal braces installed fully inside the bays of the existing frame should be supplemented with a frame ("rim") of horizontal and vertical steel members firmly attached to the surrounding concrete members. The rim helps the concrete frame resist the load effects (moments and shears) from any frame action that accompanies the truss action, as well as from the truss action itself (axial forces in the horizontal chords of the truss). Besides, its horizontal members may act as collectors, transferring the inertia forces from the floors to the bracing system. To this end they should be continuously fastened to the corresponding horizontal concrete members. The vertical members of the rim serve as a backup system for gravity loads, in case (some) concrete columns cannot sustain the imposed storey drifts and fail. For this, these members should be made continuous from storey to storey, via threaded rods or other elements passing through the slab.

For convenience of fabrication, the braces may have the same cross-section in several storeys. If their common size is dimensioned on the basis of the upper storeys, the lower storeys will develop the additional lateral force resistance needed through flexural action in the existing frame, possibly with some of its members acting compositely with new horizontal and vertical steel members surrounding the braces. If the braces are dimensioned on the basis of the lower storeys, inelasticity and energy dissipation demands will be concentrated there, owing to the overstrength of the upper storeys. To prevent such situations in new braced steel frames, Part 1 of Eurocode 8 (CEN 2004a) limits the maximum value of the brace overstrength ratio (: ratio of brace force resistance to demand from the analysis) to 1.25 times its minimum value anywhere in the structure.

6.9.3.3 Recommendations for the Design and Detailing of Braces

Experience from past earthquakes shows that steel frames with concentric bracing may fail prematurely by cracking and fracture of the braces and their connections after buckling. The key to good performance of such a system is its ability to withstand post-buckling cyclic deformations without premature fractures, through proper design and detailing of the braces to control the buckling and post-buckling behaviour and the associated adverse effects, like distortion and local buckling, early failure of welds, etc. Such phenomena may jeopardise the full tensile capacity of a brace, after it is straightened back during the next half-cycle of the response. The post-buckling response of braces, particularly of double-channel or double-angle ones, can be improved by welding closely spaced batten plates.

Local buckling in compression bracings precipitates fracture, owing to concentrations of strains or strain accumulation with cycling. To avoid local buckling, "compact" sections should be used, with low width-to-thickness ratios. For braces used in seismic design or retrofitting, the upper limit to this ratio should be considerably lower (e.g. by 50%) than for monotonic loads. For new steel buildings, Part 1 of Eurocode 8 (CEN 2004a) requires using:

– "class" 1 steel sections, if the q-factor 4 or more,
– "class" 1 or 2 sections, for q between 2 and 4, or
– "class" 1, 2 or 3 sections, with q between 1.5 and 2.

These "classes" are defined in EN-Eurocode 3, Part 1, depending on the shape of the section and its width-to-thickness ratio. For bracings in seismic retrofitting it is strongly recommended to avoid "class" 3 sections. If possible, "class" 1 should be used.

No matter whether compression braces are taken into account in the analysis for the retrofit design (as in V-bracings), or neglected (as may be the case in diagonal or X-braced systems, see Section 6.9.3.4), their slenderness should be capped. A sensible upper limit is the value of 2.0 imposed by CEN (2004a) to the non-dimensional slenderness $\bar{\lambda}$ (defined as the square root of the ratio of the member's yield force, $f_y A$, to its critical buckling load, N_{cr}) in new steel structures. CEN (2004a) sets a lower limit of 1.3 on $\bar{\lambda}$ for compression braces which are neglected in a linear analysis for the seismic action. This is to reduce the axial force that will inevitably develop in the (neglected) compression braces during the pre-buckling stage and prevent columns and beams from being overloaded with seismic action effects (much) higher than given by the linear analysis and damaged before the tension diagonals yield. If compression braces are included in a nonlinear analysis, there is little sense in observing a lower limit on $\bar{\lambda}$.

Realistic end restraint assumptions should be made for the effective unbraced length of braces. For X-braces welded to a common gusset plate at their midpoint(s) (ASCE 2007) recommends taking the effective unbraced length equal to half the total (diagonal) length of the brace, including the gusset plates. For other types of braces welded to gusset plates, an effective unbraced length equal to the total length of the brace is recommended for out-of-plane buckling, or 80% (90% for bolted connections) of that length for in-plane buckling.

A gusset plate connected to a brace susceptible to out-of-plane buckling should have clear length at least equal to twice its thickness, to limit restraint of brace plastic rotations in the post-buckling stage (ATC 1997).

6.9.3.4 Seismic Analysis and Design of the Retrofitting

The existing structure is already loaded by the quasi-permanent gravity loads before any steel bracing is added. It continues to support these loads fully, even when the earthquake comes.[12] If the analysis for the seismic action of interest is linear, one analysis should be carried out for the concrete frame alone under the quasi-permanent gravity loads and another for the retrofitted structure under the seismic action. The results are superimposed. If the analysis is nonlinear, quasi-permanent

[12]The seismic action will not cause serious axial distress to the existing vertical members (unless they fail). So, gravity loads will not be redistributed from the existing system to the steel bracing, when the earthquake comes.

gravity loads and the seismic action should be taken to act together. The quasi-permanent gravity loads are applied first, to provide the initial conditions. In that case an artificially high axial stiffness may be used from the outset for the existing vertical members, so that they monopolise the support of gravity loads. Note that, even though by the time the factored gravity loads may be applied the steel bracing will be in place, these loads should be taken to be resisted by the existing concrete frame alone. It is standard (and codified) practice for new steel or composite (steel-concrete) buildings with bracings to design the frame alone for the factored gravity loads and rely on the bracings only for earthquake resistance. V- or inverted-V braces are not taken to provide support to the beams at mid-span under gravity loads.

The most cost-effective approach for the design of the retrofitting with steel bracings is the standard one in Sections 6.5.4, 6.5.5 and 6.5.6, with deformation-based verification of ductile mechanisms in all members, old or new (including the bracing elements intended for energy dissipation) and force-based verification of brittle mechanisms. In this approach all members (including the existing ones, as well as the compression braces) are included in the model. If the analysis is nonlinear (typically static), compression braces may be modelled using an elastic-perfectly plastic force-deformation law in primary loading, with yield force equal to a small fraction of their buckling load – 20% is recommended in ASCE (2007) and ATC (1997). Notwithstanding this low limiting force in compression, the full buckling load should be assumed to develop in these compression braces when checking vertical members connected to these braces.

Table 6.1 still applies for the verification of the members of the concrete frame. All beams and columns around a bay where bracing is added should be considered as "primary elements". Table 6.4 presents the verification criteria for steel braces at the three Limit States (LS) given in Annex B of CEN (2005a) for diagonal braces in existing steel or composite (steel-concrete) buildings. Except at the Damage Limitation LS, the criteria for tension braces are more relaxed than for compression ones.

Table 6.4 Compliance criteria for steel braces in concentric bracing (CEN 2005a)

	Section	Damage limitation	Significant damage	Near collapse
Tension		$\delta_{E,t}$[1] $\leq 0.25\delta_{y,t}$[2]	$\delta_{E,t}$[1] $\leq 7\delta_{y,t}$[2]	$\delta_{E,t}$[1] $\leq 9\delta_{y,t}$[2]
Compression	Class 1	$\delta_{E,c}$[1] $\leq 0.25\delta_{crit}$[3]	$\delta_{E,c}$[1] $\leq 4\delta_{crit}$[3]	$\delta_{E,c}$[1] $\leq 6\delta_{crit}$[3]
	Class 2	$\delta_{E,c}$[1] $\leq 0.25\delta_{crit}$[3]	$\delta_{E,c}$[1] $\leq \delta_{crit}$[3]	$\delta_{E,c}$[1] $\leq 2\delta_{crit}$[3]
		$0.5\ N_{pl,Rd}$[4] $\leq N_{cr}$[5]	$0.5\ N_{pl,Rd}$[4] $\leq N_{cr}$[5]	–
		$N_{E,c}$[6] $\leq 0.8\ N_{pl,Rd}$[4]		

[1] $\delta_{E,t}$, $\delta_{E,c}$ denote the axial deformation of the brace in tension or compression, respectively, from the analysis for the seismic action of interest without gravity loads.
[2] $\delta_{y,t}$ is the axial deformation of the brace at yielding in tension.
[3] δ_{crit} is the axial deformation of the brace at the critical buckling load, N_{cr}.
[4] $N_{pl,Rd}$ is the plastic resistance of the cross-section to normal forces.
[5] N_{cr} the critical buckling load of the brace.
[6] $N_{E,c}$ is the compressive axial force of the brace from the analysis for the seismic action of interest plus the concurrent gravity loads.

So, the limiting deformations of the compression braces normally govern. In reality, if the seismic action is likely to induce more than one half-cycle of large inelastic excursions, we cannot rely too much on the large limiting deformations of tension braces.

Braces yield at an interstorey drift ratio of $2\varepsilon_y/\sin 2\theta$, where ε_y is the yield strain of the brace and θ its inclination to the horizontal. This gives interstorey drifts between 0.4 and 0.6%, which is normally less than what causes storey yielding in a flexible concrete frame. The limit values in Table 6.4 for tension braces at the Significant Damage LS correspond to about 7-times these interstorey drift values, normally beyond what the members of a poorly detailed, deficient concrete frame can take, even when classified as "secondary" ones. By contrast, these members can easily take the interstorey drifts corresponding to the limit values given in Table 6.4 for compression braces at the Significant Damage LS. Another point is that the limit values in Table 6.4 for the Damage Limitation LS correspond to quite low interstorey drifts, namely between 0.1 and 0.15%. All this said, the limits in Table 6.4 derived from values in CEN (2005a) for steel or composite frames, may have to be assessed by applying them to actual retrofitting cases and studying their implications.

The alternative to the above standard approach for the design of the retrofitting with steel bracings is the force-based approach of Section 6.5.8. In that case Part 1 of Eurocode 8 (CEN 2004a), including its Sections on steel buildings (or composite, steel-concrete, wherever relevant), is applied according to Section 6.5.8. Note that, according to CEN (2004a), compression braces should be neglected in the (linear) analysis for the seismic action, except in V-braced systems. Note also that existing beams and columns around a bay where bracing is added cannot be considered as "secondary elements". As a matter of fact, in order to concentrate inelastic action and energy dissipation in the (tension) braces, CEN (2004a) wants some overstrength against the results of the analysis in the frame members. To this end, it requires frame members of new braced steel buildings be dimensioned for the seismic action effects (axial load and bending moment) from the analysis times 110% of the minimum value of the brace overstrength factor (ratio of brace force resistance to demand from the analysis) in all diagonals of the system, plus the action effects of the concurrent gravity loads. If the force-based approach of Section 6.5.8 is adopted, this rule should be applied to the existing members around bays where bracing is added, these members taken as "primary seismic".

6.9.3.5 Construction Issues

Normally there are more construction difficulties in retrofitting with steel bracings, than in construction of new steel or composite buildings.

Prefabrication of large steel subassemblies, as in new construction, is not easy. Most of the welding has to be done in situ and high quality full penetration welds are difficult to achieve. Weldments may end up being the weak link in the retrofitting.

The steel elements may be connected to the surrounding concrete frame through epoxy-grouted fasteners post-installed into the concrete. Normally this is done in phases:

- partial-depth holes are drilled in the concrete using the steel member's annuli as a template;
- the steel member is removed, to finish the drilling and clean the holes;
- the steel member is put back and fixed in place, after grouting the holes with epoxy and inserting the fasteners.

Sometimes interference with reinforcement or with connections between steel members may prevent drilling the holes for some fasteners to full depth. Another location may have to be sought for these fasteners, with new annuli drilled through the steel member's in the field.

In Japan, where retrofitting with steel braces is popular, some of the construction difficulties noted are by-passed using pre-fabricated bracing subassemblies, consisting of a heavy rectangular rim with X-, V- or inverted-V bracings inside. To accommodate variations in the dimensions of the existing bays where the subassemblies are placed, a tolerance of several centimeters is provided around the rim. The subassemblies are connected to the surrounding frame members through a system consisting of:

- closely-spaced headed studs, welded to the outside of the perimeter of the rim and protruding into the gap;
- post-installed fasteners in-between the studs, epoxy-grouted into the interior face of the surrounding frame;
- non-shrink mortar filling the gap between the rim and the frame.

Spiral reinforcement is often inserted along the mortar joint, between the fasteners and the headed studs. Tests in Yamamoto (1993) have shown that one-storey, one-bay frames retrofitted in this way can exhibit a lateral force resistance equal to the sum of the shear capacity of the frame and of the braces (: horizontal projection of the yield force of tension brace and of the buckling load of compression brace) at storey drift ratios over 3%. However, the size and strength of the steel braces could not increase indefinitely, without the horizontal mortar joint becoming the weak link in sliding shear. The horizontal failure plane extends then into the "wind-ward" column, which is in tension and may precipitate a flexure-shear failure of the column on the other side. The lateral force resistance is then the sum of: (a) the resistance of the mortar joint and of the "wind-ward" column in sliding shear, and (b) the shear resistance of the "lee-ward" column. The cyclic drift capacity of this failure mode is smaller, but in the tests in Yamamoto (1993) it was still between 2 and 3%.

An expensive alternative is to fully fill the gap between the steel rim around the bracing and the concrete members with epoxy resin (JCI 2007).

6.10 Application Case Studies

6.10.1 Seismic Retrofitting of SPEAR Test-Structure with RC or FRP Jackets

Section 4.10.5.2 has highlighted the two phases of retrofitting of the 3-storey SPEAR building:

- In the 1st phase, any damage inflicted to the unretrofitted structure was repaired; then:
  - the ends of all 0.25 m columns in all storeys were wrapped with two layers of uni-directional Glass FRP (GFRP) over 0.6 m from the face of the joint, for confinement and clamping of short lap splices (Figs. 4.13(b) and 6.12(a));
  - the full height of the large (0.25 m-by-0.75 m) column C8 was wrapped in two layers of bi-directional GFRP, for confinement and lap splice clamping, but mainly for shear strengthening (Fig. 6.12(b));

(a) (b)

Fig. 6.12 FRP-retrofitted SPEAR test structure: (**a**) column with FRP-wrapped ends during the response; (**b**) large column retrofitted in shear (See also Colour Plate 19 on page 732)

- the exterior faces of corner joints were strengthened in shear with two layers of bi-directional GFRP, without continuity with the FRP wrapping of the columns (Figs. 4.13(b) and 6.12).

- In the 2nd phase:

  - all FRPs were removed, and
  - the central columns of the two "flexible" sides (C2 and C6 in Fig. 4.14(a)) were RC-jacketed from 0.25 to 0.4 m square (Fig. 4.14(b)); the jackets had eight 16 mm-dia. vertical bars (three per side) and a 10 mm-dia. perimeter tie at 100 mm centres; jacketing virtually eliminated the largest of the two eccentricities between the (computed) centres of stiffness or resistance and the centre of mass and reversed the other eccentricity (Fig. 4.14(c) and (d)).

Each retrofitted version of the structure went through a test under a 0.20 g PGA bidirectional motion, for which predicted and measured displacements have been compared in Fig. 4.15 and predicted damage ratios were presented in Fig. 4.16. It was then subjected to a 2nd test with a PGA of 0.30 g. When the FRPs were removed after that test there was no visible damage. This is consistent with the predictions of the analysis in Section 4.10.5.2. The flexural damage ratios in the 0.30 g test are about 1.5-times those at the middle row of Fig. 4.16 (left) and are well below 1.0. The shear damage ratios are only slightly higher than the values at the middle row of Fig. 4.16 (right) and again do not approach 1.0. As shown in Fig. 6.12(a), the large storey drifts of the response took place mainly through fixed end rotations at the column end sections, due to (harmless) slippage of the (smooth) vertical bars from the joints. The performance demonstrates that even light FRP-wrapping of all members improves their deformation capacity sufficiently to enable an originally poorly designed and detailed, flexible and asymmetric structure withstand ground motions with a PGA as high as 0.30 g.

The flexural damage pattern of the version of the structure with the two central columns of the "flexible" sides RC-jacketed, was indeed as predicted in Fig. 4.16 (bottom, left). The jacketed columns went through the test unscathed, but the non-jacketed ones suffered very severe damage; especially the heavily loaded central column and those on the sides of the perimeter opposite to the two jacketed columns. The central column (C5 in Fig. 4.14) failed in flexure at the 2nd storey – as predicted at the bottom row of Fig. 4.16 (left) – as well as at the 1st storey. As a matter of fact, this is the column of Fig. 3.27(c). In the 0.30 g test that followed this column and C4 (the immediately most critical one according to Fig. 4.16) disintegrated completely. Nonetheless, their axial load was redistributed to other ones and the structure did not collapse. Consistently with the shear damage pattern at the right-hand-side of Fig. 4.16, there was no indication of shear effects in the damaged or failed members.

The conclusion of these tests is that in an asymmetric structure it is not sufficient to selectively upgrade the stiffness, strength and deformation capacity of critical columns. This may shift deformation demands to other elements and cause them to fail, if they have not been retrofitted.

The qualitative agreement of damage may be considered as validation of the expressions in Sections 3.2.3.5 and 3.2.4.3 – adopted in Annex A of CEN (2005a) – for the flexure-controlled ultimate cyclic chord rotation and the degradation of shear resistance with cyclic loading.

6.10.2 Seismic Retrofitting of Theatre Building with RC and FRP Jackets and New Walls

The theatre facility presented already in Figs. 4.18 and 4.19 has been retrofitted to remedy the seismic deficiency pointed out in Section 4.10.5.3 as well as the extensive corrosion of the reinforcement in vertical members of the perimeter (Fig. 6.13). The design of the retrofitting (in mid-2005) was the first application of Part 3 of Eurocode 8 to a real building. The performance objective was to fulfil the Significant Damage Limit State (Life Safety performance level) for the 475 year earthquake, with a peak ground acceleration (PGA) of 0.36 g specified for ordinary buildings at the site in the current zonation map.

The seismic assessment of the building under a seismic action with a PGA of 0.10 g has been highlighted in Section 4.10.5.3. The design of the retrofitting and the evaluation of the retrofitted building through nonlinear dynamic seismic response analysis are presented here.

On the basis of the key features of the response of the unretrofitted building and of its assessment under the 0.10 g PGA motions, the following retrofitting measures were chosen (Fig. 6.14):

(a) (b) (c)

Fig. 6.13 Vertical cracks in perimeter members of theatre building (**a**), (**b**), due to reinforcement corrosion (**c**) (See also Colour Plate 20 on page 732)

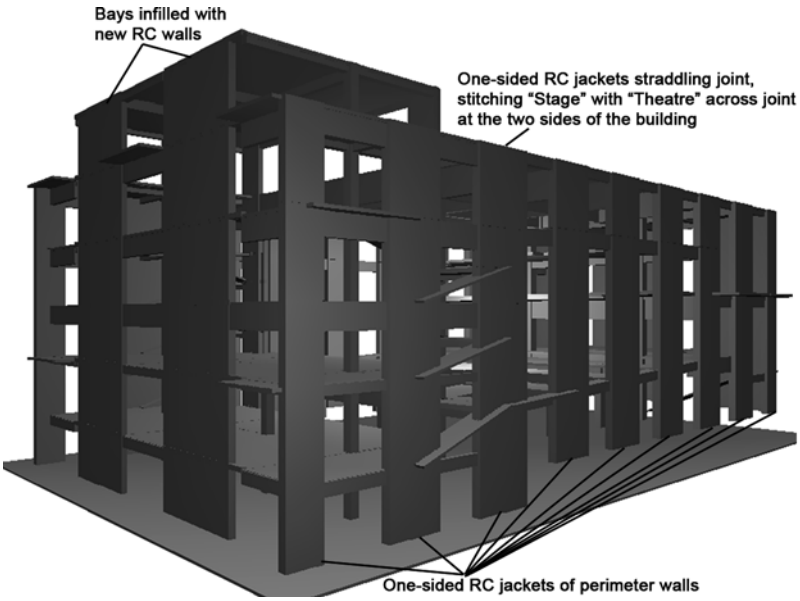

Fig. 6.14 Schematic of RC jackets and new walls in theatre building

1. The two parts of the building across the (practically zero width) expansion joint are connected into an integral structure with planwise balanced stiffness and strength, to avoid twisting of the individual parts and pounding at the joint. This is achieved as follows:

   (i) Each one of the two perimeter walls at the corners of the right-hand-side of the Stage part in Fig. 4.18 (left) is integrated with its counterpart across the expansion joint at the corners of the left-hand-side of the Theatre part in Fig. 4.18 (right), into a single rectangular wall straddling the expansion joint. Pairs of such walls are shown in Fig. 4.18 within continuous-line rectangles. One pair appears also at the right-hand-side of Fig. 6.1(g). The connection is effected through a shotcrete overlay on the exterior face of the two walls, with 18 mm-dia. horizontal bars at 100 mm centres continuous across the joint. Shear connection across the joint is enhanced by batten plates welded to the corner vertical bars of (the barbells of) the individual walls next to the joint.

   (ii) The roof diaphragms of the Stage and the Theatre parts are connected across the expansion joint all along their common length at the roof (i.e., outside the elevated central part – penthouse – of the Stage). This is done with a 0.3 m-deep and 0.8 m-wide RC belt, symmetrically cast over the joint and fastened to the roof slab via epoxy-grouted dowels (Fig. 6.15(a)). It has 14 mm-dia. closed ties across the joint at 100 mm centres and 16 mm bars along it.

   (iii) Each interior wall parallel to the joint at the right-hand-side of the Stage part in Fig. 4.18 (left) is connected to its counterpart across the expansion

Fig. 6.15 Features of the retrofitting of the theatre building: (**a**) RC belt straddling joint at roof level; (**b**) steel rods connecting interior walls across the joint; (**c**) long side of the building with finished wall jackets; (**d**) new bay-long walls at the back

joint at the left-hand-side of the Theatre part in Fig. 4.18 (right). Each pair of such walls is shown in Fig. 4.18 within a dashed-line rectangle. For the connection, two rows of 24 mm-dia. horizontal steel rods at 250 mm centres vertically (Fig. 6.15(b)) are placed in holes drilled through the short direction of the two walls and secured by anchor plates at their accessible vertical faces (i.e., opposite to the faces on the expansion joint). Although the rods act also as dowels across the joint, their main role is to transfer shear forces from one wall of the pair to the other. They have been dimensioned to cover a shear strength shortfall in one of the walls by the surplus in the other, both as obtained from the nonlinear seismic response analyses described later on.

2. The ten exterior shear walls on each one of the two long sides of the integrated building are strengthened and stiffened from the foundation to the roof with an exterior 150 mm-thick shotcrete overlay (see Fig. 6.1(g)). Note that reinforcement corrosion was limited to the perimeter walls or columns. Before applying the overlay, corroded bars were exposed, cleaned from rust and epoxy-coated against future corrosion. The original walls are 250 mm-wide. The ones at the

corners incorporate a 400 mm square column at one end of the cross-section (like a barbell, see Fig. 6.13(a)), while the intermediate ones have the 400 mm square column at mid-length (Fig. 6.13(b)). With the overlay the perimeter walls are converted into 400 mm-wide rectangular ones (compare Figs. 6.13(a) and (b) with 6.15(c)). The overlay is connected to the old wall via epoxy-grouted dowels. It contains one curtain of vertical and horizontal bars, with sufficient cover for corrosion protection in the mid-term and in sufficient quantity for the necessary flexural and shear resistance of the new, integral wall, even after the – at certain points complete – loss of cross-sectional area in the existing horizontal bars due to corrosion. The new vertical bars are epoxy-anchored at the top of underground perimeter walls or of bulky foundation beams. This is easy, as the top of these foundation elements is at about grade level and their exterior face is flush with the added concrete overlay (Figs. 6.1(g) and 6.15(c)).

3. Two new 500 mm-wide concrete walls are added, by infilling the 2nd and the 4th bay of the frame on the left-hand-side of Fig. 4.18, encapsulating existing columns and beams (see dashed-line ovals in Fig. 4.18). The main goal of these walls is to counterbalance the two over-one-bay-long walls at the opposite side of the integrated building. Another purpose is to strengthen the elevated central part – penthouse – of the Stage, to the top of which they continue. The finished walls are shown in Fig. 6.15(d).

Figure 6.16 depicts the average flexural damage ratio in the vertical members of the so-retrofitted building from the analyses under 56 spectrum-compatible bidirectional ground motions with a PGA of 0.36 g. The damage ratio is the maximum ratio of chord rotation demand to the concurrent capacity (as affected by the fluctuating axial load and shear span ratio) at the Near Collapse Limit State according to Part 3 of Eurocode 8. The demand-capacity ratios at the Significant Damage (Life Safety) Limit State may be obtained by multiplying by 4/3 the values in Fig. 6.16. The combination of the retrofitting measures highlighted above is sufficient for essentially all elements at the Significant Damage Limit State. The alarming damage ratios in four columns of the penthouse[13] (especially after the values Fig. 6.16 are multiplied by 4/3) are not a source of concern, because, unlike almost everywhere else in the building, all bays around the penthouse are infilled with strong masonry walls without openings (but a narrow door), which were omitted in the analysis model. The contribution of these infills to the lateral stiffness and resistance of the penthouse is more than enough to prevent the failure of the four columns predicted in Fig. 6.16.

As shown in Fig. 6.17, the measures described so far cannot prevent shear failure of the two large walls of the façade (see Fig. 6.18, one of these walls featuring also in Fig. 6.13(a) – left-hand side) or of the interior walls on either side of the expansion joint (those connected together in the transverse direction through steel

[13]These four columns are all at the three sides of the penthouse which are not retrofitted. The two new walls reaching the top of the penthouse are on the 4th side.

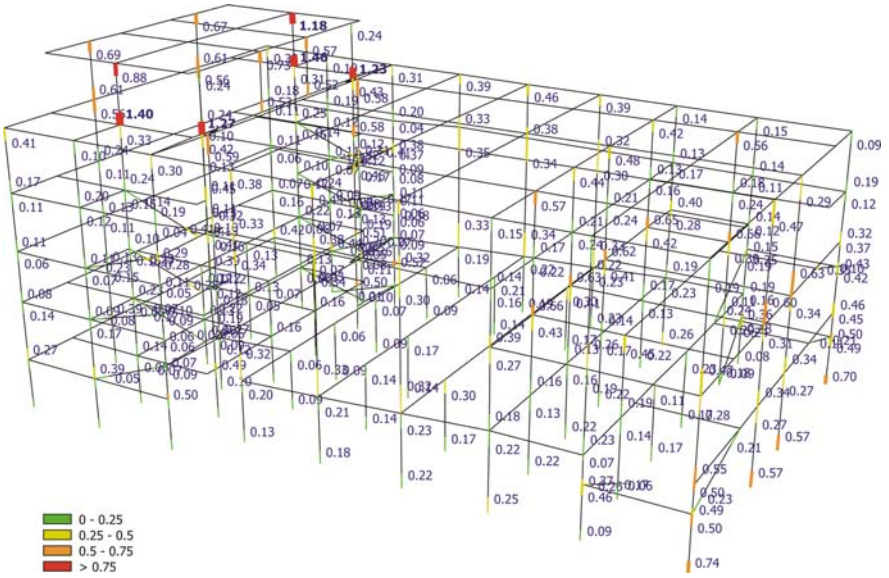

Fig. 6.16 Mean chord rotation demand in vertical members of the retrofitted building from seismic response analyses for 56 bidirectional ground motions at PGA = 0.36 g, divided by the corresponding chord rotation capacity for the Near Collapse Limit State (Kosmopoulos et al. 2007) (See also Colour Plate 21 on page 733)

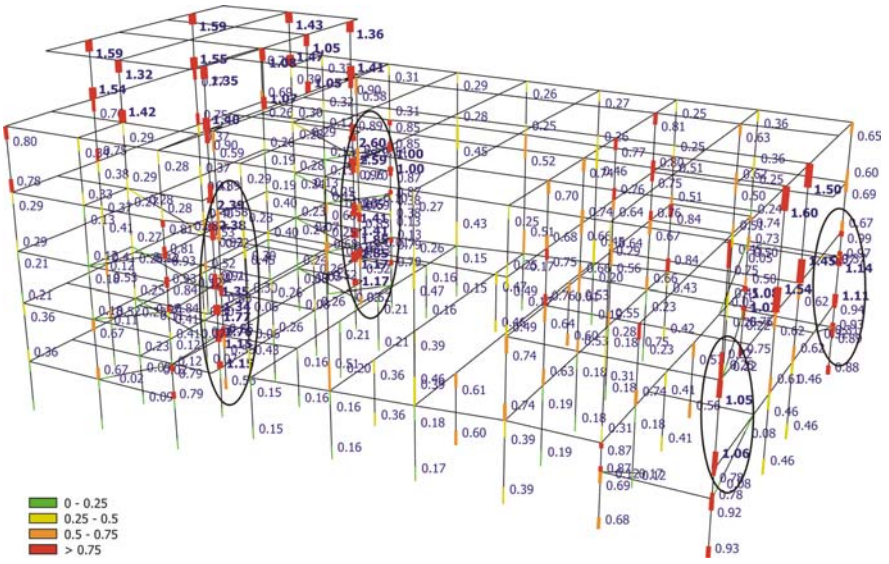

Fig. 6.17 Mean damage ratio in shear in the vertical members of the retrofitted building without the FRPs for 56 bidirectional ground motions at PGA = 0.36 g: shear force demand from the analysis divided by the corresponding capacity for any Limit State (Kosmopoulos et al. 2007) (See also Colour Plate 22 on page 734)

Fig. 6.18 Façade of theatre building with the two walls chosen for strengthening in shear with FRP

rods, see point 1(iii) above and Fig. 6.15(b)). It is not feasible to remedy these shear deficiencies via RC jackets or overlays, like in strengthening measure 1 above, because:

- Adding RC jackets or overlays to the façade is not architecturally acceptable.
- The owner does not welcome the inconvenience and debris produced by casting or shotcreting jackets around the interior walls on either side of the expansion joint.
- It is not feasible to access the foundation at these points in plan and at the façade, in order to connect the RC jacket or overlay and transfer its seismic moments and shears to the ground, without a prohibitively intrusive and costly operation (imagine in Fig. 6.18 the disruption entailed by exposure of the foundation of the walls of the façade);

The shear deficiency of the two large walls of the façade and of the two pairs of interior walls on either side of the expansion joint has been remedied by bonding horizontal Carbon FRP (CFRP) sheets:

- to the exterior face of the two large façade walls, see Fig. 6.19(a), and
- to the surface of the accessible long sides of the two pairs of interior walls (the sides opposite to the ones on the expansion joint), as shown in Fig. 6.19(b).

The six CFRP-retrofitted walls are shown in Fig. 4.18 inside continuous-line ovals.

The total thickness of CFRPs (equivalently, the number of CFRP plies of standard thickness) is dimensioned from the mean deficit of shear strength in the corresponding wall from the seismic response analyses for the 56 bidirectional ground motions with a PGA of 0.36 g, i.e., so that the shear damage ratios in Fig. 6.17 are reduced below 1.0.

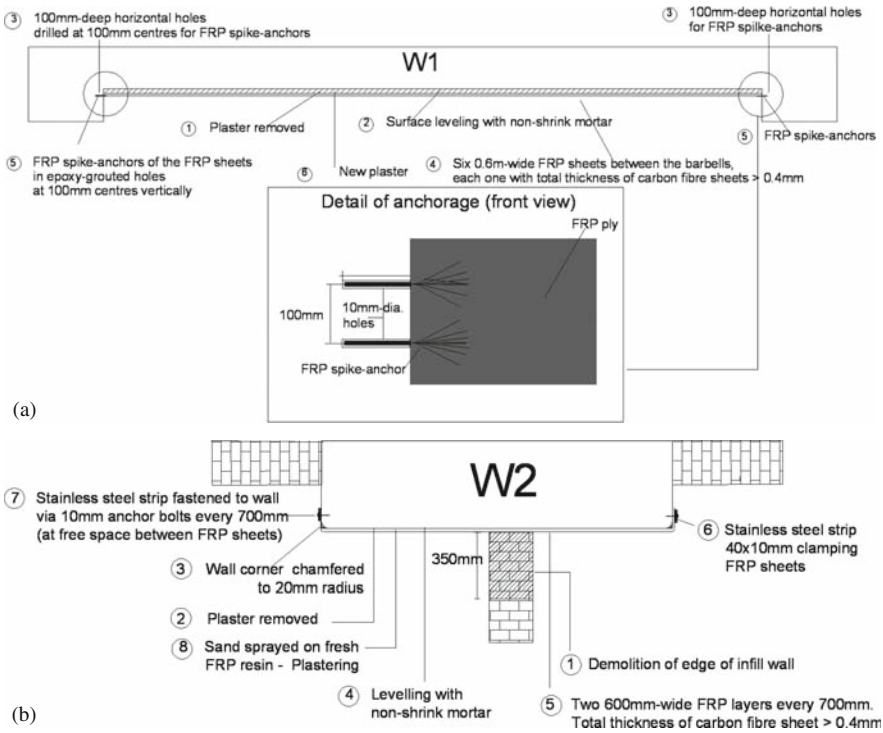

Fig. 6.19 One-sided shear strengthening with surface bonded horizontal CFRP sheets: (**a**) 3.5 m-long part of façade wall; (**b**) 1.6 m-long interior walls next to seismic joint (Kosmopoulos et al. 2007)

Numbers in circles in Fig. 6.19 show the sequence of operations for the application of the FRPs.

Witness in Fig. 6.19(a) the anchorage of the edge of the one-sided FRP sheets at the re-entrant corners of the web of the façade wall with the column-like barbell protruding from it, through 200 mm-long spike FRP anchors placed in 100 mm-deep holes filled with epoxy. The 100 mm-long part of the anchor outside the hole fans out within the epoxy layer between two successive FRP plies, to collect the forces of the FRP sheets and transfer them to the concrete.

Witness also in Fig. 6.19(b) the clamping of the edge of the FRP sheets applied on one side of the four interior walls. The edge is clamped by 40 mm-wide, 10 mm-thick stainless steel straps placed vertically next to the rounded corner of the section and fastened to the short side of the wall via anchor bolts driven into the concrete at the free space between adjacent horizontal FRP sheets.

Because the surface-bonded FRPs applied here for shear strengthening do not affect the stiffness or moment resistance of members, we do not need repeating the (nonlinear) analysis to evaluate their effect on performance. The FRPs can always be dimensioned after the analysis, for the shear strength deficit identified from it.

It is not considered worth remedying the shear deficiency shown in Fig. 6.17 at the two central columns of the façade at the top storey. This could be accomplished by wrapping the entire height of these columns with FRP, dimensioned to resist the deficit in shear strength of the column. That would entail demolishing vertical strips of the brick masonry wall on both sides of these columns (see Fig. 6.18) and restoring these walls after FRP wrapping. The contribution of these masonry piers to the in-plane stiffness and resistance of the façade is sufficient for the protection of these columns from an overstress given by an analysis that neglects the positive contribution of these wall piers.

Epilogue: Some Ideas for Performance- and Displacement-Based Seismic Design of New Buildings

We thus have come to the end of a long development on current-generation seismic design, assessment and retrofitting of concrete buildings. Its emphasis has been on EN-Eurocode 8, scheduled to become the exclusive standard for earthquake resistance in Europe after March 2010. To this point we have focused on the present situation, with the aim to help designers apply the relevant parts of EN-Eurocode 8 correctly and cost-effectively and to familiarise them with their background.

Part 3 of Eurocode 8, and other international codes for seismic assessment and retrofitting of existing buildings, do reflect the current State-of-the-Art and provide a firm basis for codified practice in the foreseeable future. However, this cannot be claimed with much confidence by seismic design standards for new concrete buildings, including Part 1 of Eurocode 8. Indeed, Section 6.4 noted at its closing that, once the new ideas for codified seismic assessment and retrofitting become established through successful application in practice, they are expected to infiltrate codes for seismic design of new buildings as well, marking a reversal of past traditions.

Readers who have followed the long development in this book to its conclusion are invited now to follow it one step further, namely to some ideas for a possible future performance- and deformation-based seismic design of new concrete buildings. Far from being a revolution in the design of concrete buildings for earthquake resistance, these ideas just aspire to introduce there the current State-of-the-Art, as reflected already in codified seismic assessment and retrofitting of existing buildings and in Part 3 of Eurocode 8 in particular. As a matter of fact, it is proposed to venture this in the form of a few measured steps, which preserve or emulate to the largest possible extent current codified design practice.

The ideas presented below have evolved from the early work of Fardis and Panagiotakos (1997c) and Panagiotakos and Fardis (1999, 2001c). According to the new proposal buildings are designed to meet all three performance levels:

- Immediate Occupancy,
- Life Safety and
- Near Collapse

each at the appropriate seismic hazard level, defined through its own 5%-damped elastic spectrum. The proposed compliance criteria for the three performance levels are:

1. Brittle (i.e., shear) failures of members, primary or secondary, and of their connections, should be prevented at all three performance levels.
2. At the Immediate Occupancy level, nominal yielding at potential plastic hinges may be exceeded by a factor with a value around 2, which reflects a presumed overstrength factor of at least 1.5 in materials and members and certain tolerance of flexural yielding at some sections.
3. At the Life Safety level, a safety margin against the ultimate chord rotation at member ends should be provided.
4. At the Near Collapse performance level, member ends should stay below their ultimate chord rotations; indeed primary ones should have a margin for model uncertainty.

The similarity with the Eurocode 8-Part 3 criteria in Table 6.1 for the three Limit States is clear. The safety elements for the checks in 1 above may be those in Table 6.1 for brittle members, primary or secondary. The safety margins in 3 and 4 against ultimate conditions in flexure may also be chosen the same as those in Table 6.1 for primary or secondary ductile members at the Significant Damage and the Near Collapse Limit State, respectively. According to the reasoning in the last paragraph of Section 6.5.3, a constant ratio between the chord rotation limits for Life Safety and Near Collapse (as in Table 6.1) implies that checking them at both these levels is normally redundant. The Near Collapse level will govern, if the spectral values of its own seismic action at the important natural periods of the elastic structure (as determined in Step 5 below with the final effective stiffness values from Step 4) clearly exceed those of the Life Safety seismic action by more than the inverse of the constant ratio of chord rotation limits at these levels. Conversely, if they are clearly less. Besides, the shear verifications are carried out only once. So, in the end the three-tier design normally reduces to single-tier design for shear and a two-tier one for flexure.

The design procedure may comprise the following steps:

Step 1 – Conceptual design and sizing of members: Select the structural layout following as closely as possible the guidance in Sections 2.1.3–2.1.13. Make sure that there is sufficient torsional stiffness to meet Eq. (2.4) in Section 2.1.6, and indeed with a margin. Size the members according to the following, for fruition of Step 7:

- In each one of the two horizontal directions vertical members of the same family (i.e., walls or columns) should have as uniform a cross-sectional depth as possible. If the rotational restraint of members by others in the considered horizontal direction varies among members of the same family, those restrained more by others may be chosen with smaller depth than the rest.
- The beam depth should be uniform all-along any plane frame, but may be smaller in frames with shorter spans than in others with longer ones.

– The beam depth should be gradually reduced from the base to the roof of the building.

Column sections should accommodate the intended beam bar sizes according to the relevant bond criteria, such as Eqs. (5.10) in Section 5.4.1.

Step 2 – Design for non-seismic actions: Dimension the reinforcement of all members on the basis of the Ultimate and the Serviceability Limit States for all pertinent non-seismic actions (gravity loads, wind, etc.), taking into account the minimum reinforcement requirements for structures without earthquake resistance. Redistribute beam ULS moments from supports to mid-span(s) or vice-versa, as appropriate and optimal in design for non-seismic actions.

Step 3 – Capacity Design against storey-sway mechanisms. Unless the walls in a horizontal direction of the building are considered sufficient to preclude a storey-sway mechanism, determine the vertical reinforcement of columns to satisfy Eq. (1.4) in that direction, using there the beam moment resistances resulting from earlier steps.[1] Base this calculation on the axial force due to gravity loads concurrent with the seismic action.

Step 4 – Member effective stiffness: Estimate the member effective stiffness (secant to yield-point) for the seismic action, $(EI)_{eff}$:

– If this is the first time this step is carried out (see Step 8 for the iterations), use empirical expressions independent of the amount and layout of longitudinal reinforcement (e.g., Eq. (3.69) in Section 3.2.3.3). Check the result against the outcome of Eq. (3.68), averaged at the (two) end(s) where a plastic hinge might form and for both directions of bending, using the longitudinal reinforcement from Steps 2 and 3. Adopt the larger of the two $(EI)_{eff}$-values: from Eq. (3.68) or (3.69). In these calculations use a value for the shear span at member ends according to the guidance in Section 4.10.1.4 (summarised also at point 2 of Section 4.10.5.1 and in Section 6.5.4.2). Use judgement to revise upwards the estimates from Eq. (3.69) in those vertical members (especially walls) which are expected to come out of Step 7 with heavy longitudinal reinforcement.

– If the present step is carried out after Step 7 in the context of iterations towards convergence of the stiffness values, calculate $(EI)_{eff}$ only from Eq. (3.68). To accelerate convergence, especially if different walls or columns have different cross-sectional depth, use as shear span, L_s, in Eqs. (3.66), (3.68) the value of the moment-to-shear ratio from the seismic analysis in Step 5 at the end of the member where the moment is largest. Adopt the beam effective flange width suggested in Section 4.10.5.1 and count its bars into the beam top reinforcement.

[1] This step may be revisited in the framework of iterations involving Steps 3–7 (see Step 8).

Use throughout the step the axial force values due to the gravity loads concurrent with the seismic action, as well as mean values of material properties estimated from nominal strengths.

Step 5 – Linear analysis for the Immediate Occupancy seismic action: Carry out a modal response spectrum analysis for the seismic action for which Immediate Occupancy performance is desired, using its 5%-damped elastic spectrum and the estimates of effective stiffness from Step 4. Combine modal contributions through the CQC rule (Eq. (4.11) in Section 4.4.3) and the effects of individual seismic action components through Eq. (4.24) in Section 4.7.1.

Step 6 - Demand-capacity ratios for the Immediate Occupancy seismic action: Calculate the ratio of:

- the elastic moment demand, D, taken equal to the seismic moment from Step 5 plus the one due to the concurrent gravity loads, to
- the corresponding design resistance, C,

at any section where a primary member is connected to another one having stiffness in a plane of bending normal to the vector of the moment in question. Use design values of material strengths (nominal ones divided by the partial factor for the material) for the design value of moment resistance.

Step 7 - Tailoring of flexural capacities to demands for uniformly distributed inelasticity: Increase the longitudinal reinforcement at all locations where plastic hinges are intended to develop, so that their D/C ratios are as uniform as possible:

- within families of such locations, notably:
  - the wall base sections in wall and dual systems,
  - the column base sections in frame and dual systems,
  - the end sections of primary beams connected to stronger columns (i.e., whose sum of moment resistances above and below a joint exceeds the corresponding sum in the beams framing into the joint), and
  - the end sections of primary columns connected to stronger beams (i.e., whose sum of moment resistances across the joint exceeds that of the columns above and below the same joint), as well as
- between different families, as relevant.

According to the compliance criterion for the Immediate Occupancy performance level (criterion no. 2 above), the target D/C-value in each family is (around) 2. However, important plastic hinge locations may have come out of Step 5 with D/C values markedly below this target. If the C-value at such a location is governed by Step 2, it cannot be reduced to increase D/C towards the target value of 2.0. Unless such low D/C values are sporadic and do not cast doubt about the prevailing plastic mechanism, we may go ahead to

achieve the target D/C-value at these locations by raising the seismic action for Immediate Occupancy performance (and of course the capacities at all other locations, so that $D/C \approx 2$ there under the increased seismic hazard level).

Step 8 – Iterations with updated stiffness values. Repeat Steps 3–7, using everywhere the longitudinal reinforcement from Step 7. The change in stiffness may change the demands and partly undo the harmonisation achieved in Step 8. So iterations may be needed through Steps 3–7 until satisfactory convergence. Depending on the progress towards convergence, we may have to overshoot in Step 7 (i.e., increase the low C-values more than required for the target D/C-value), in order to harmonise in the end the D/C values over all potential plastic hinges.

Step 9 – Capacity Design of force-controlled mechanisms: Derive through capacity design calculations (as in Section 6.5.5) the shear force demands in all members or joints, the seismic internal forces in the foundation system and the forces transferred to the ground, using the final longitudinal reinforcement in all relevant members. Verify shear force demands against capacities derived according to the pertinent parts of Chapter 5 (Sections 5.4.2, 5.5, 5.7.2.3, 5.7.3.4 and 5.7.4.2, as relevant), using design values of material properties (nominal strengths divided by partial factor for the material) for primary members and mean values for secondary ones (cf. Table 6.1). Verify the entire foundation system and the ground at the Ultimate Limit State (ULS) for the forces derived in this step via capacity design. Increase member dimensions that turn out to be insufficient (including plan dimensions of foundation elements) and repeat Steps 2–9 as necessary.

Step 10 – Analysis for the Life Safety or/and the Near Collapse seismic actions. Determine the chord rotation demands at all member ends due to simultaneous horizontal components of the Life Safety or the Near Collapse seismic action, whichever seems most critical according to the criteria in the last paragraph before the description of Step 1 above. Thanks to Steps 3, 7 and 9, modal response spectrum analysis may well be used, with the 5%-damped elastic spectrum of the seismic action in question. If this spectrum is proportional to that of the Immediate Occupancy action over the range of natural periods considered, seismic action effects from Step 5 are scaled-up by that proportionality constant and added to those due to the concurrent gravity loads. Alternatively, nonlinear dynamic (response-history) analysis may be carried out both for the Life Safety and the Near Collapse seismic actions, following the guidance in Sections 4.6.2, 4.10.1 and 6.5.4.2, using in the model mean values of material properties estimated from nominal strengths.

Step 11 – Member detailing for the required chord rotation capacities: Upgrade the chord rotation capacities of members to meet the corresponding criteria of Table 6.1. To this end, wherever these criteria are violated:

a. increase the bottom reinforcement, if the member is a beam (see term ω' in Eqs. (3.78)); and/or

b. increase the confining reinforcement ratio, ρ_{sx}, over an appropriate length near the end in question (see exponent of the 2nd term before the last one in Eqs. (3.78)); and/or
c. replace part of any "web" reinforcement distributed between the tension and the compression one with a smaller total amount of tension plus compression reinforcement, to increase ω_2 in Eqs. (3.78) and reduce ω_1 (which is the sum of the tension and "web" reinforcement) while keeping the yield moment, M_y, and the stiffness to yield-point, $(EI)_{eff}$, unchanged; and/or
d. if the member is a column which is squat in a single plane of bending, or a short beam, add diagonal reinforcement (preferably by replacing part of the longitudinal one, to avoid increasing M_y and $(EI)_{eff}$); and/or
e. increase the width of the web, b_w, if it is small compared to the section depth, h (see term involving h/b_w in Eq. (3.78c)); in rectangular sections this will also increase the width of the compression zone, b, and reduce the axial load ratio, ν, which is based on normalisation by bh.

Measures (a) and (e) above unavoidably increase M_y and $(EI)_{eff}$. Normally the increase is minor and does not warrant re-visiting any previous steps, provided that Eq. (1.4) has been met in Step 3 with a margin. The same applies to any other measure involving the longitudinal reinforcement, if care has been taken not to increase M_y and $(EI)_{eff}$. Anyway, such an increase is safe-sided, thanks to co-lateral reductions of the seismic chord rotation demands from Step 10.

Implementation of measures (a)–(e) can best be served by Eqs. (3.78), which reflect in an uncoupled and multiplicative fashion each one of the design parameters that may be changed (ω_2, ω_1, ρ_{sx}, ρ_d, h/b_w), as well as any parameter that varies during the response (notably, the shear span and the axial load, L_s and N). Recall that a nonlinear dynamic analysis carried out for the purposes of Step 10 gives the average and the maximum – across the suite of time-histories – of the largest value of the ratio of chord rotation demand to capacity, as both vary during each response-history at the member end in question (flexural damage ratio).[2] Note also that the terms involving any design parameter to be changed in the framework of measures (a)–(e) above appear separately and multiplicatively in the denominator of the flexural damage ratios and have the same value at the considered member end across the response-histories. By contrast, the terms involving N and L_s have different values in each response-history, namely the ones they assumed when the flexural damage ratio was at its largest. But as the flexural damage ratio includes in the denominator these latter terms also separately and multiplicatively, its average and maximum value in the suite of time-histories

[2] For convenience, demand and capacity may be expressed in terms of the plastic part of chord rotation if Eqs. (3.78b) or (3.78c) are used, or in terms of total chord rotations if Eq. (3.78a) is applied instead.

can be reduced to the desired level by (a combination of) measures (a)–(e) above, without affecting at all the variable terms (those involving N and L_s). So, Step 11 may successfully conclude without re-doing any analysis.

Although it may produce very different designs, the procedure itself differs only at few points from that of today's force-based design with a behaviour factor, q:

1. In conceptual design it includes two explicit goals:
   - The requirement to meet Eq. (2.4), as there is no q-factor anymore to penalise the structural system for torsional sensitivity.
   - The goal of uniform cross-sections among walls or columns and of smooth reduction of beam depths with decreasing average span of the frame and from the base to the roof. This is to promote the most important feature of the design procedure, notably the effort to prevent overstrengths and promote uniform inelastic deformation demands in potential plastic hinges (see point 3 below).
2. In order to realistically estimate seismic displacements and deformations, the analysis uses a secant to yield-point stiffness (from Steps 5 and 8), which is much more representative than the default value of current codified force-based design.
3. Although Steps 5–7 may look like blind force-based design with a force-reduction factor of 2 for the Immediate Occupancy seismic action (i.e. with a q-factor of 2 times the ratio of Life Safety to Immediate Occupancy seismic actions, or, in Eurocode 8 terminology, times the ratio of the design seismic action to the damage limitation one), in reality their goal is to prevent overstrength at potential plastic hinges and ensure uniform distribution of inelastic deformation demands there at all seismic action levels of interest. Steps 5–7 are repeated until this goal is met to a satisfactory degree. Note also that what appears as an effective q-factor of 2 on the Immediate Occupancy seismic action is applied on the sum of its effects to those of the concurrent gravity loads, and not on the Immediate Occupancy action alone.
4. In current force-based seismic design any member end section is dimensioned at the ULS in bending once, for the most adverse effect between those produced from the factored non-seismic actions or from the combination of the design seismic action and the concurrent gravity loads.[3] By contrast, in the above procedure ULS dimensioning in bending is first carried out in Step 2 for the non-seismic actions and then re-visited in Step 7 for the Immediate Occupancy seismic action.
5. Detailing of members for ductility is based not on opaque prescriptions, but on a transparent explicit verification of inelastic deformation demands against capacity limits.

[3] Provided that the same partial factors for materials are used in ULS design for non-seismic and for seismic actions.

References

Aboutaha RS, Engelhardt MD, Jirsa JO, Kreger ME (1996a) Retrofit of concrete columns with inadequate lap splices by the use of rectangular steel jackets. Earthquake Spectra 12(4): 693–714

Aboutaha RS, Engelhardt MD, Jirsa JO, Kreger ME (1996b) Seismic retrofit of R/C columns using steel jackets. In: Sabnis GM et al. (ed) Seismic Rehabilitation of Concrete Structures. ACI-SP160, American Concrete Institute, Detroit, MI, pp. 59–72

Aboutaha RS, Engelhardt MD, Jirsa JO, Kreger ME (1999) Rehabilitation of shear critical concrete columns by use of rectangular steel jackets. ACI Struct J 96(1): 68–78

Abrahamson NA, Litehiser JJ (1989) Attenuation of peak vertical acceleration. Bull Seismolog Soc Am 79: 549–580

Abrams D (1987) Influence of axial force variation on flexural behavior of reinforced concrete columns. ACI Struct J 84(3): 246–254

ACI (2003) ACI 440.IR-03 – Guide for the design and construction of concrete reinforced with FRP bars. ACI Committee 440, American Concrete Institute, Farmington Hills, MI

ACI (2008) Building code requirements for structural concrete and commentary. American Concrete Institute, Farmington Hills, MI

ACI Committee 408 (2001) Splice and development length of high relative rib area reinforcing bars. American Concrete Institute, Farmington Hills, MI

ACI Committee 440 (2002) Guide for the design and construction of externally bonded FRP systems for strengthening concrete structures. American Concrete Institute, Farmington Hills, MI

ACI-ASCE Committee 352 (1988) Recommendations for design of slab-column connections in monotonic reinforced concrete structures. ACI Struct J 85(6): 675–696

AIJ (1992) AIJ standard for structural calculation of reinforced concrete structures, Architectural Institute of Japan, Tokyo

AIJ (1994) AIJ structural design guidelines for reinforced concrete buildings, Architectural Institute of Japan, Tokyo

Aktan A, Pecknold D, Sozen MA (1974) R/C column earthquake response in two dimensions. ASCE J Struct Div 100(ST10): 1999–2015

Alca N, Alexander SDB, MacGregor JG (1997) Effect of size on flexural behavior of high-strength concrete beams. ACI Struct J 94(1): 59–66

Alcocer SM (1992) Rehabilitation of RC frame connections using jacketing. 10th World Conference on Earthquake Engineering, Madrid, Balkema, Rottterdam, pp. 5235–5240

Alcocer SM, Jirsa JO (1993) Strength of reinforced concrete frame connections rehabilitated by jacketing. ACI Struct J 90(3): 249–261

Ambraseys NN, Simpson KA (1996) Prediction of vertical response spectra in Europe. Earthquake Eng Struct Dyn 25(4): 401–412

Anagnostopoulos SA (1972) Nonlinear dynamic response and ductility requirements of building structures subjected to earthquakes. Res. Report R72-54, Department of Civil Engineering, Massachusetts Institute of Technology, Cambridge, MA

ASCE (2003) ASCE/SEI Standard 31-03, Seismic evaluation of existing buildings. American Society of Civil Engineers, Reston, VA

ASCE (2007) ASCE/SEI Standard 41-06, Seismic rehabilitation of existing buildings (including Supplement 1). American Society of Civil Engineers, Reston, VA

Ascheim MA, Moehle JP (1992) Shear strength and deformability of RC bridge columns subjected to inelastic cyclic displacements. Rep. UCB/EERC-92/04, Earthquake Engineering Research Center, University of California, Berkeley, CA

ATC (1988) Rapid visual screening of buildings for potential seismic hazards: A manual. ATC-21 Applied Technology Council for the Federal Emergency Management Agency (FEMA Report 154), Washington, DC

ATC (1997) NEHRP Guidelines for the seismic rehabilitation of buildings. Applied Technology Council for the Building Seismic Safety Council and the Federal Emergency Management Agency (FEMA Reports 273, 274), Washington, DC

ATC (1998) Evaluation of earthquake damaged concrete and masonry wall buildings. Applied Technology Council for the Federal Emergency Management Agency (FEMA Reports 306, 307), Washington, DC

Aziz TS (1976) Inelastic dynamic analysis of building frames. Res. Report R76-37, Department of Civil Engineering, Massachusetts Institute of Technology, Cambridge, MA

Balázs GL (1989) Bond softening under reversed load cycles. Studi e Ricerche, Politecnico di Milano, No. 11, Milano, pp. 503–524

Balázs GL (1991) Fatigue of bond. ACI Mater J 88(6): 620–629

Benjamin JR, Cornell CA (1970) Probability, Statistics and Decision for Civil Engineers. McGraw Hill, New York

Bigaj A, Walraven JC (1993) Size effect on rotational capacity of plastic hinges in reinforced concrete beams. Ductility-Reinforcement, CEB Bulletin d' Information No. 218, pp. 7–23

Biskinis DE (2007) Resistance and deformation capacity of concrete members with or without retrofitting. Doctoral Thesis, Civil Engineering Department, University of Patras, Patras, GR

Biskinis DE, Fardis MN (2004) Cyclic strength and deformation capacity of RC members, including members retrofitted for earthquake resistance. In: Walraven J et al. (ed) 5th International Ph.D Symposium in Civil Engineering, Balkema, Rotterdam, pp. 1125–1133

Biskinis DE, Fardis MN (2007) Effect of lap splices on flexural resistance and cyclic deformation capacity of members. Beton- und Stahlbetonbau, Sonderheft Englisch 102: 51–59

Biskinis DE, Fardis MN (2009) Upgrading of resistance and cyclic deformation capacity of deficient concrete columns. In: Ilki A et al. (ed) Seismic Risk Assessment and Retrofitting, with Special Emphasis on Existing Low Rise Structures, Springer Verlag, Heidelberg

Biskinis DE, Roupakias G, Fardis MN (2004) Degradation of shear strength of RC members with inelastic cyclic displacements. ACI Struct J 101(6): 773–783

Bommer JJ, Elnashai AS (1999) Displacement spectra for seismic design. J Earthquake Eng 3(1): 1–32

Bosco C, Debernardi PG (1993) Influence of some basic parameters on the plastic rotation of reinforced concrete elements. Ductility-Reinforcement, CEB Bulletin d' Information No. 218, pp. 25–44

Bousias SN (1993) Experimental and analytical study of RC columns in cyclic biaxial bending with axial force. Doctoral thesis, Civil Engineering Department, University of Patras, Patras, GR

Bousias SN, Fardis MN (1994) Inelastic R.C. section and member model for general biaxial bending with axial force. In: Mang H et al. (ed) EURO-C 1994, Pineridge Press, Swansea, UK, pp. 795–804

Bousias SN, Panagiotakos TB, Fardis MN (2002) Modelling of RC members under cyclic biaxial flexure and axial force. J Earthquake Eng 6(3): 213–238

Bousias SN, Fardis MN, Biskinis DE (2005a) Retrofitting of RC columns with deficient lap-splices. In: Balazs GL, Borosnyoi A (eds) *fib* Symposium: Keep concrete attractive, Budapest, pp. 885–890

Bousias SN, Spathis L-A, Fardis MN (2007a) Seismic retrofitting of columns with lap-spliced smooth bars through FRP or concrete jackets. J Earthquake Eng 11(5): 653–674

Bousias SN, Verzeletti G, Fardis MN, Magonette G (1992) Reinforced concrete columns in cyclic biaxial bending and axial load. 10th World Conference on Earthquake Engineering, Balkema, Rotterdam, pp. 3041–3049

Bousias SN, Verzeletti G, Fardis MN, Gutierrez E (1995) Load-path effects on column biaxial bending with axial force. ASCE Eng Mech J 121(5): 596–605

Bousias SN, Fardis MN, Spathis L-A, Biskinis DE (2005b) Shotcrete or FRP jacketing of concrete columns for seismic retrofitting. In: Wasti ST, Ozcebe G (eds) Advances in Earthquake Engineering for Urban Risk Reduction, Springer, Dordrecht, NL, pp. 33–46

Bousias SN, Biskinis DE, Fardis MN, Spathis L-A (2007b) Strength, stiffness and cyclic deformation capacity of concrete jacketed members. ACI Struct J 104(5): 521–531

Bousias SN, Spathis L-A, Fardis MN, Papanicolaou CG, Triantafillou TC (2007c) Pseudodynamic tests of non-seismically designed RC structures retrofitted with textile-reinforced mortar. In: Triantafillou TC (ed) 8th International Symposium on Fiber Reinforced Polymer Reinforcement for Concrete Structures (FRPRCS-8), Patras, GR, paper 17-12

Bracci JM, Kunnath SK, Reinhorn AM (1997) Seismic performance and retrofit evaluation for reinforced concrete structures. ASCE J Struct Eng 123(1): 3–10

BSSC (2003) NEHRP recommended provisions for seismic regulations for new buildings and other structures. Building Seismic Safety Council for the Federal Emergency Management Agency (FEMA Rep. 368, 369), Washington, DC

Cairns J (2006) Proposals of *fib* TG4.5 for bond anchorage in the new *fib* Model code. federation internationale du beton, Lausanne

Calvi GM, Grossi V, Magenes G (1994) First report on the characteristics of reinforcing steel available in Italy. Univ. di Pavia contribution to 1st PREC8 Topic 1 annual report, Universita di Pavia, Pavia, IT

Carvalho EC (1995) Prenormative research in support of Eurocode 8. In: Elnashai A (ed) 5th SECED Conference: European Seismic Design Practice – Research and Application, Balkema, Rotterdam, pp. 43–50

Carvalho E, Pipa M (1994) Short note on the characteristics of B400 and B500 Tempcore bars produced in Europe and its comparison with Eurocode 8 requirements – Mechanical characteristics of reinforced steel bars manufactured in Portugal. LNEC contribution to 1st PREC8 Topic 1 annual report, Laboratorio Nacional de Engenharia Civil (LNEC), Lisbon

Carvalho EC, Coelho E (1997) Numerical investigations on the seismic response of R.C. frames designed in accordance with Eurocode 8. ECOEST-PREC8 Rep. 7. Laboratorio Nacional de Engenharia Civil (LNEC), Lisbon

CEB (1970) CEB-FIP International Recommendations for the design and construction of concrete structures: 1 Principles and Recommendations, Bulletin No. 72. Comite Euro-international du Beton, Paris

CEB (1985) CEB Model Code for seismic design of concrete structures, Bulletin No. 165. Comite Euro-International du Beton, Lausanne

CEB (1988a) Concrete structures under impact and impulsive loading, Bull. d' Information No. 187. Comite Euro-International du Beton, Lausanne

CEB (1988b) General principles on reliability of structures: A commentary on ISO 2394, Bulletin No. 191. Comite Euro-International du Beton, Lausanne

CEB (1991) CEB-FIP Model Code 1990, Bull. d' Information No. 203/204/205. Comite Euro-International du Beton, Lausanne

CEB (1996a) RC frames under earthquake loading, T. Telford, London, for Comite Euro-international du Beton, Lausanne

CEB (1996b) RC elements under earthquake loading, T. Telford, London, for Comite Euro-international du Beton, Lausanne

CEN (1996) European prestandard ENV 1998-1-4: Eurocode 8: Design provisions for earthquake resistance of structures, Part 1-4: Strengthening and repair of buildings. Comite Europeen de Normalisation, Brusells

CEN (2002) European Standard EN 1990:2002 Eurocode: Basis of structural design. Comite Europeen de Normalisation, Brusells

CEN (2003) European Standard EN 1997-1:2003 Eurocode 7: Geotechnical design – Part 1: General rules. Comite Europeen de Normalisation, Brusells

CEN (2004a) European Standard EN 1998-1:2004 Eurocode 8: Design of structures for earthquake resistance, Part 1: General rules, seismic actions and rules for buildings. Comite Europeen de Normalisation, Brusells

CEN (2004b) European Standard EN 1992-1-1:2004 Eurocode 2: Design of concrete structures, Part 1-1: General rules and rules for buildings. Comite Europeen de Normalisation, Brusells

CEN (2004c) European Standard EN 1998-5:2004 Eurocode 8: Design of structures for earthquake resistance, Part 5: Foundations, retaining structures, geotechnical aspects. Comite Europeen de Normalisation, Brusells

CEN (2005a) European Standard EN 1998-3:2005 Eurocode 8: Design of structures for earthquake resistance, Part 3: Assessment and retrofitting of buildings. Comite Europeen de Normalisation, Brusells

CEN (2005b). European Standard EN 1998-2:2005 Eurocode 8: Design of structures for earthquake resistance, Part 2: Bridges. Comite Europeen de Normalisation, Brusells

Cheung VW, Tso WK (1986) Eccentricity in irregular multistory buildings. Canadian J Civil Eng 13(1): 46–52

Chopra A (2007) Dynamics of structures. Theory and applications to earthquake engineering. Prentice Hall, Englewood Cliffs, NJ

Chopra AK, Goel RK (2002) A modal pushover analysis procedure for estimating seismic demands for buildings. Earthquake Eng Struct Dyn 31(3): 561–582

Chopra AK, Goel RK (2004) A modal pushover analysis procedure to estimate seismic demands of unsymmetric plan buildings. Earthquake Eng Struct Dyn 33(8): 903–927

Chopra AK, Goel RK, Chintanapakdee C (2004) Evaluation of a modified MPA procedure assuming higher modes as elastic to estimate seismic demands. Earthquake Spectra 20(3): 757–778

Clough R, Johnston S (1966) Effect of stiffness degradation on earthquake ductility requirements. Transactions of Japan Earthquake Engineering Symposium, Tokyo, pp. 195–198

Clough RW, Benuska KL, Wilson EL (1965) Inelastic earthquake response of tall buildings. 3rd World Conference on Earthquake Engineering, Auckland, NZ, V 11

Coelho E, Carvalho EC (1990) Nonlinear seismic behaviour of reinforced concrete structures. 9th European Conference on Earthquake Engineering, Moscow

Costa AC, Costa AG (1987). Hysteretic model of force-displacement relationships for seismic analysis of structures. Res. Report, Laboratorio Nacional de Engenharia Civil, Lisbon

Crémer C (2001) Modélisation du comportement nonlinéaire des fondations superficielles sous séisme. Macro-élément d'interaction sol-structure. Thèse de doctorat, Laboratoire de Mécanique et de Technologie de Cachan. ENS Cachan, Paris

Darwin D, Zuo J, McCabe SL (2002a) Descriptive equations for development and splice strength of straight reinforcing bars. In: Balazs GL et al. (ed) 3rd International Symposium: Bond in Concrete – from Research to Standards, Budapest, pp. 501–508

Darwin D, McCabe SL, Browning J-A, Matamoros A, Zuo J (2002b) Evaluation of development length design expressions. In: Balazs GL et al. (ed) 3rd International Symposium: Bond in Concrete – from Research to Standards, Budapest, pp. 747–754

De Lorenzis L, Tepfers R (2001) A comparative study of models on confinement of concrete cylinders with FRP composites. Publ. No. 01/04, Dept. of Building Materials, Chalmers University of Technology, Göteborg

Der Kiureghian A (1981) A response spectrum method for random vibration analysis of MDF systems. Earthquake Eng Struct Dyn 9: 419–435

Dritsos S, Pilakoutas K (1992) Composite technique for repair-strengthening of RC members. 2nd International Symposium on Composite Materials and Structures, Beijing University Press, Beijing, pp. 958–963

Eibl J, Keintzel E (1988) Seismic shear forces in cantilever shear walls. 9th World Conference in Earthquake Engineering, Tokyo/Kyoto

Eligehausen R, Lettow S (2007) Formulation of Application Rules for Lap Splices in the New *fib* Model Code, federation internationale du beton, Stuttgart

Elnashai AS (1994) Characteristics of reinforcing steel in the United Kingdom. Imperial College contribution to 1st PREC8 Topic 1 annual report, Imperial College of Science, Technology and Medicine, London, UK

Elnashai AS (2001) Advanced inelastic static (pushover) analysis for earthquake applications. Struct Eng Mech 12(1): 51–69

Elnashai AS, Papazoglou AJ (1997) Procedure and spectra for analysis of RC structures subjected to strong vertical earthquake loads. J Earthquake Eng 1(1): 121–155

Elsabee G, Kausel E, Roesset JM (1977) Dynamic stiffness of embedded foundations. ASCE 2nd Annual Engineering Mechanics Division Specialty Conference, pp. 40–43

Elwi AA, Murray DW (1979) A 3D hypoelastic concrete constitutive relationship. ASCE J Eng Mech Div 105(EM4): 623–641

Elwood KJ, Moehle JP (2001) Shake-table tests on the gravity load collapse of reinforced concrete frames. In: Kabeyasawa T, Moehle JP (eds) 3rd US-Japan Workshop on Performance-Based Earthquake Engineering Methodology for Reinforced Concrete Building Structures, PEER-2002/02, Pacific Earthquake Engineering Research Center, University of California, Berkeley, CA

Faccioli E, Vanini M, Frassine L (2002) Complex site effects in earthquake ground motion, including topography. 12th European Conference on Earthquake Engineering, London, paper 844

Fajfar P (2000) A nonlinear analysis method for performance-based seismic design. Earthquake Spectra 16(3): 573–593

Fajfar P, Marušić D, Peruš I (2005) Torsional effects in the pushover-based seismic analysis of buildings. J Earthquake Eng 9: 831–854

Fajfar P, Dolšek M, Marušić D, Peruš I (2004) Extensions of the N2 method – asymmetric buildings, infilled frames and incremental N2. In: Fajfar P, Krawinkler H (eds) Performance-Based Seismic Design Concepts and Implementation, PEER Rep. 2004/05, PEER, University of California, Berkeley, CA, pp. 357–368

Fardis MN (1991) Member-type models for the nonlinear seismic response analysis of reinforced concrete structures. In: Donea J, Jones PM (eds) Experimental and Numerical Methods in Earthquake Engineering, Kluwer Academic Publishers, Dordrecht, NL, pp. 247–280

Fardis MN (1997) Chaper 9: Reinforced concrete structures. In: Beskos D, Anagnostopoulos SA (eds) Computer Analysis and Design of Earthquake Resistant Structures – A Handbook. Computational Mechanics Publications, Southampton, pp. 441–532

Fardis MN (1998) Seismic assessment and retrofit of RC structures. In: Bisch P et al. (ed) Invited Lectures, 11th European Conference on Earthquake Engineering, Paris, Balkema, Rottterdam, pp. 131–150

Fardis MN (2000) Design provisions for masonry-infilled RC frames. 12th World Conference on Earthquake Engineering, Auckland, NZ, paper 2553

Fardis MN (2001) Displacement-based seismic assessment and retrofit of reinforced concrete buildings. In: Bösch K et al. (ed) Seismic Assessment and Upgrading of Existing Structures, 20th European Regional Earthquake Engineering Seminar, European Association of Earthquake Engineering, pp. 67–86

Fardis MN (2004) A European Perspective for Performance-Based Seismic Design, In: Fajfar P, Krawinkler H (eds) Performance-Based Seismic Design Concepts and Implementation, PEER Rep. 2004/05, PEER, University of California, Berkeley, CA, pp. 1–13

Fardis MN, Buyukozturk O (1979) A shear transfer model for reinforced concrete. ASCE J Eng Mech Div 105(EM2): 255-275

Fardis MN, Khalili HH (1981) Concrete encased in fiberglass-reinforced plastic. ACI J 78(6): 440–446

Fardis MN, Khalili HH (1982). FRP-encased concrete as a structural material, Mag Concr Res 34(121): 191–202

Fardis MN, Kosmopoulos A (2007) Practical implementation of seismic assessment method in Eurocode 8 – Part 3, with linear or nonlinear analysis and deformation-based verification using empirical chord rotation capacity expressions. 6th National Conference on Earthquake Engineering, Istanbul, Vol. 3, pp. 69–101

Fardis MN, Panagiotakos TB (1996) Hysteretic damping of reinforced concrete elements, 11th World Conference on Earthquake Engineering, Acapulco, MX, paper 464

Fardis MN, Panagiotakos TB (1997a) Seismic design and response of bare and infilled reinforced concrete buildings – Part I: Bare structures. J Earthquake Eng 1(1): 219–256

Fardis MN, Panagiotakos TB (1997b) Seismic design and response of bare and infilled reinforced concrete buildings – Part II: Infilled structures. J Earthquake Eng 1(3): 473–503

Fardis MN, Panagiotakos TB (1997c) Displacement-based design of RC buildings: Proposed approach and application. In: Fajfar P and Krawinkler H (eds) Seismic Design Methodologies for the Next Generation of Codes, Balkema, Rotterdam, pp. 195–206

Fardis MN, Skouteropoulou A-M, Bousias SN (1987) Stiffness matrix of free-standing helical stairs. ASCE J Struct Eng 113(1): 74–87

Fardis MN, Bousias SN, Franchioni G, Panagiotakos TB (1999a) Seismic response and design of RC structures with plan-eccentric masonry infills. Earthquake Eng Struct Dyn 28: 173–191

Fardis MN, Negro P, Bousias SN, Colombo A (1999b) Seismic design of open-story infilled RC buildings. J Earthquake Eng 3(1): 173–198

Fardis MN, Panagiotakos TB, Biskinis DE, Kosmopoulos A (2003) Seismic assessment of existing RC buildings. In: Wasti ST, Ozcebe G (eds) Seismic Assessment and Rehabilitation of Existing RC Buildings, Kluwer Academic Publishers, Dordrecht, NL, pp. 215–244

Fardis MN, Biskinis DE, Kosmopoulos AJ, Bousias SN, Spathis L-A (2005) Seismic retrofitting techniques for concrete buildings. In: Fardis MN, Negro P (eds) SPEAR Workshop – An Event to Honour the Memory of J Donea. EUR 21768 EN, European Commission, JRC, Ispra, IT, pp. 229–240

fib (2001) Externally bonded FRP reinforcement for RC structures, *fib* Bulletin 14, Lausanne

fib (2003) Seismic assessment and retrofit of RC buildings, *fib* Bulletin 24, Federation Internationale du Beton, Lausanne

fib (2006) Retrofitting of concrete structures through externally bonded FRPs, with emphasis on seismic applications, *fib* Bulletin 35, Federation Internationale du Beton, Lausanne

fib (2007) FRP Reinforcement in RC Structures, *fib* Bulletin 40, Federation Internationale du Beton, Lausanne

fib (2008) A practitioner's guide to computer-based modelling of structural concrete. Bulletin No. 45, Federation Internationale du Beton, Lausanne

Filippou FC, Issa A (1988) Nonlinear analysis of reinforced concrete frames under cyclic load reversals. Rep. UCB/EERC 88-12, Earthquake Engineering Research Center, University of California, Berkeley, CA

Frankel A, Mueller C, Barnhard T, Perkins D, Leyendecker EV, Dickman N, Hanson S, Happer M (1996) National seismic hazard maps: Documentation, USGS Open-file Report 96–532, Denver, CO

Frankel A, Mueller C, Barnhard T, Perkins D, Leyendecker EV, Dickman N, Hanson S, Happer M (1997) Seismic hazard maps for the conterminus United States, USGS Open-file Report 97–131, Denver, CO

French CW, Schultz AE (1991) Minimum available deformation capacity of reinforced concrete beams. In: Ghosh SK (ed) ACI Special Publication SP127, American Concrete Institute, Detroit, MI, pp. 363–410

Fujikake K, Mindess S, Xu H (2004) Analytical model for concrete confined with fiber-reinforced polymer composite. ASCE J Composite Construct 3(3): 143–150

Garstka B (1993) Untersuchungen zum Trag- und Schädigungsverhalten Stabförmiger Stahlbetonbauteile mit Berücksichtigung des Schubeinflusses bei Zyklischer Nichtlinearer Beanspruchung. Dissertation, Ruhr-Universität Bochum, Bochum, DE

Gasparini DA, Vanmarcke EH (1976) Simulated earthquake motions compatible with prescribed response spectra. Res. Report R76-4, Department of Civil Engineering, Massachusetts Institute of Technology, Cambridge, MA

Gazetas G, Anastasopoulos I (2007) Overturning of buildings in Adapazari during the 1999 Kocaeli earthquake. 6th National Earthquake Engineering Conference, Istanbul, Vol. 3, pp. 43–49

Ghobarah A, Biddah A, Mahgoub M (1997) Rehabilitation of reinforced concrete columns using corrugated steel jacketing. J Earthquake Eng 1(4): 651–673

Giannakas A, Patronis D, Fardis MN (1987) Influence of location and size of openings on elastic stiffness of infill walls. 8th Greek Concrete Conference, Kavala, Greece, Vol. II, pp. 49–56

Giberson MF (1967) The response of nonlinear multi-story structures subjected to earthquake excitation. Ph.D. Thesis, California Institute of Technology, Pasadena, CA

Gupta AK, Singh MP (1977) Design of column sections subjected to three components of earthquake. Nucl Eng Des 41: 129–133

Gupta B, Kunnath SK (2000) Adaptive spectra-based pushover procedure for seismic evaluation of structures. Earthquake Spectra 16(2): 367–392

Horvath JS (1983) Modulus of subgrade reaction: new perspective. ASCE J Geotech Eng Div 109(GT12): 1567–1587

Huang Z, Engström B, Magnusson J (1996) Experimental and analytical studies of the bond behaviour of deformed bars in high strength concrete. 4th International Symposium on the Utilization of High Strength/High Performance Concrete, Vol. 3. Laboratories des Ponts et Chaussees, Paris.

ICBO (1997) Uniform Building Code. International Conference of Building Officials, Whitier, CA

ICC (2006) International Building Code. International Code Council, Falls Church, VA

Imai K, Korenaga T, Takiguchi K (2005) Compressive properties of concrete and flexural strength around critical section of reinforced concrete members. AIJ J Struct Construct Eng 587: 189–196

Inoue S, Tanabe A (2006) Seismic performance improvement of reinforced concrete columns by partial prestressing, 2nd *fib* Congress, Napoli, paper 9–35

Izzuddin BA, Elnashai AS (1989) ADAPTIC: A program for the adaptive dynamic analysis of space frames. Rep. ESEE-89/7, Imperial College Imperial College of Science, Technology and Medicine, London, UK

JBDPA (1977) Standard for evaluation of seismic capacity and guidelines for seismic retrofit design of existing reinforced concrete buildings. Japan Building Disaster Prevention Association (revised 1990), Tokyo

JBDPA (1999) Seismic retrofit design and construction guidelines for existing reinforced concrete and steel encased reinforced concrete buildings using continuous fibre reinforcing materials. Japan Building Disaster Prevention Association, Tokyo.

JCI (2007) Seismic rehabilitation of concrete structures. In: Sugano S (ed) International Publication Series IPS-2, American Concrete Institute, Farmington Hills, MI

JPCEA (2002) Seismic design code for prestressed concrete structures. Japan Prestressed Concrete Engineering Association, Tokyo

JSCE (1997) Recommendation for design and construction of concrete structures using continuous fibre reinforcing materials. Research Committee on Continuous Fiber Reinforcing Materials, Japan Society of Civil Engineers, Tokyo

JSCE (2001). Recommendations for upgrading of concrete structures with use of continuous fiber sheets. In: Maruyama K (ed), JSCE 292 Committee on Concrete Structures with Externally Bonded Continuous Fiber Reinforcing Materials, Japan Society of Civil Engineers, Tokyo

Kaba S, Mahin SA (1984) Refined modeling of reinforced concrete columns for seismic analysis. Rep. UCB/EERC 84-3, Earthquake Engineering Research Center, University of California, Berkeley, CA

Kakaletsis DJ, Karayannis CG (2008) Influence of masonry strength and openings on infilled RC frames under cyclic loading. J Earthquake Eng 12(2): 197–221

Kaku T, Asakusa H (1991) Bond and anchorage of bars in reinforced concrete beam-column joints. ACI Special Publication SP123, American Concrete Institute, Detroit, MI pp. 401–424

Karbhari VM, Chin JW, Dunston D, Benmokrane B, Juska T, Morgan R, Lesko JJ, Sorathia U, Reynaud D (2003) Durability gap analysis for fiber-reinforced polymer composites in civil infrastructure. ASCE J Composite Construct 7(3): 238–247

Karsan DI (1968) Behavior of plain concrete under variable load histories. Ph.D. Thesis, Rice University, Houston, TX

Kausel E, Roesset JM (1975) Dynamic stiffness of circular foundations, ASCE J Eng Mech Division l01(EM6): 771–785

Keintzel E (1990) Seismic design shear forces in reinforced concrete cantilever shear wall structures. European J Earthquake Eng 3(1): 7–16

Kitayama K, Otani S, Aoyama H (1991) Development of design criteria for RC interior beam-column joints. ACI Special Publication SP123, American Concrete Institute, Detroit, MI, pp. 97–124.

Kosmopoulos AJ, Fardis MN (2004) Seismic testing of 3-storey full-scale torsionally unbalanced RC structure: Pre-test predictions, design and analyses of retrofitting. In: Walraven J et al. (ed) 5th International Ph.D Symposium in Civil Engineering, Balkema, Rotterdam, pp. 1115–1123

Kosmopoulos AJ, Fardis MN (2006) Seismic evaluation of strongly irregular and torsionally unbalanced concrete buildings, 2nd *fib* Congress, Napoli, paper 9–14

Kosmopoulos AJ, Fardis MN (2007) Estimation of inelastic seismic deformations in asymmetric multistory RC buildings. Earthquake Eng Struct Dyn 36(9): 1209–1234

Kosmopoulos AJ, Fardis MN (2008) Simple models for inelastic seismic analysis of asymmetric multistory RC buildings, J Earthquake Eng, 12(5): 704–727

Kosmopoulos A, Bousias SN, Fardis MN (2003) Design and pre-test assessment of 3-storey torsionally-unbalanced RC test structure, *fib* 2003 Symposium: Concrete Structures in Seismic Regions, Athens, GR, paper 123

Kosmopoulos A, Bousias SN, Fardis MN (2007) Seismic Rehabilitation of a Theater Facility according to Eurocode 8 using CFRPs. In: Triantafillou TC (ed) 8th International Symposium on Fiber Reinforced Polymer Reinforcement for Concrete Structures (FRPRCS-8), Patras, GR, paper 15-8

Kowalsky MJ, Priestley MJN (2000) Improved analytical model for shear strength of circular reinforced concrete columns in seismic regions. ACI Struct J 97(3): 388–396

Kwan AK (1993) Improved wide-column-frame analogy for shear/core wall analysis. ASCE J Struct Eng 119(2): 420–439

Lam L, Teng JG (2003a) Design-oriented stress-strain model for FRP-confined concrete. Construct Build Mater 17(6&7): 471–489

Lam L, Teng JG (2003b) Design-oriented stress-strain model for FRP-confined concrete in rectangular columns. J Reinforc Plast Compos 22(13): 1149–1186

Litton RW (1975) A contribution to the analysis of concrete structures under cyclic loading. Ph.D. Thesis, Department of Civil Engineering, University of California, Berkeley, CA

Ma SM, Bertero VV, Popov EP (1976) Experimental and analytical studies on hysteretic behavior of reinforced concrete rectangular and T-beams. Rep. EERC 76-2, Earthquake Engineering Research Center, University of California, Berkeley, CA

Mahasuverachai M, Powell GH (1982) Inelastic analysis of piping and tubular structures, Rep. UCB/EERC 82-27, Earthquake Engineering Research Center, University of California, Berkeley, CA

Mainstone RJ (1971) On the stiffnesses and strengths of infilled frames. Proceedings of Institution of Civil Engineers v 7360s

Mander JB, Priestley MJN, Park R (1988) Theoretical stress-strain model for confined concrete. ASCE J Struct Eng 114(8): 1804–1826

Mark K (1976) Nonlinear dynamic response of reinforced concrete frames. Res. Report R76-38, Department of Civil Engineering, Massachusetts Institute of Technology, Cambridge, MA

Marušić D, Fajfar P (2005) On the inelastic seismic response of asymmetric buildings under bi-axial excitation. Earthquake Eng Struct Dyn 34(8): 943–963

Menegotto M, Pinto PE (1973) Method of analysis for cyclically loaded RC plane frames including changes in geometry and non-elastic behaviour of elements under combined normal force and bending. Preliminary Report, International Association of Bridge and Structural Engineering, Vol. 13, pp. 15–22

Millard A (1993) CASTEM 2000 Manuel d' utilisation. Rapp. CEA-LAMS No. 93/007, Saclay, FR

Moehle JP (1996) Seismic design considerations for flat-plate construction. ACI Special Publication SP-162, American Concrete Institute, Farmington Hills, MI pp. 1–34
Moehle JP, Kreger ME, Leon R (1988) Background to recommendations for design of reinforced concrete slab-column connections. ACI Struct J 85(6): 636–644
Moehle JP, Lynn A, Elwood K, Sezen H (2001) Gravity load collapse of building frames during earthquakes. PEER Report: 2nd US-Japan Workshop on Performance-based Design Methodology for Reinforced Concrete Building Structures. PEER Center, Richmond, CA
Mola E, Negro P (2005) Full-scale PsD testing of the torsionally unbalanced SPEAR structure in the as-built and retrofitted configurations. In: Fardis MN, Negro P (eds) SPEAR Workshop – An event to honour the memory of J Donea. EUR 21768 EN, European Commission, JRC, Ispra, IT, pp. 139–154
Molina FJ, Buchet P, Magonette GE, Hubert O, Negro P (2005) Full-scale bidirectional PsD testing of the torsionally unbalanced SPEAR structure: Method, algorithm and experimental setup, In: Fardis MN, Negro P (eds) SPEAR Workshop – An event to honour the memory of J Donea. EUR 21768 EN, European Commission, JRC, Ispra, IT, pp. 155–172.
Mondkar DP, Powel GH (1975) ANSR-I General Purpose Program for Analysis of Structural Response. Rep. UCB/EERC 75-37, Earthquake Engineering Research Center, University of California, Berkeley, CA
Monti G, Nuti C (1991) Analytical model of cyclic behaviour of reinforcing bars with inelastic buckling. Rapp. No. 91/06, Università di Roma La Sapienza, Roma
Monti G, Liotta MA (2005) FRP-strengthening in shear: tests and design equations. 7th International Symposium on Fibre-Reinforced Polymer (FRP) Reinforcement for Concrete Structures (FRPRCS-7), Kansas City, MO
Nakano Y (1995) Damage to buildings due to 1994 Sanriku-harukaoki earthquake. Building Disaster 211, Japan Building Disaster Prevention Association, pp. 6–15
Newman K, Newman JB (1971) Failure theories and design criteria for plain concrete. In: Te'eni (ed) Structure, Solid Mechanics and Engineering Design, J. Wiley-Interscience, New York
Newmark NM (1959) A method of computation for structural dynamics, ASCE J Eng Mech Div 85: 67–94
Oh BH, Kim SH (2007) Realistic models for local bond stress-slip of reinforced concrete under repeated loading. ASCE J Struct Eng 133(2): 216–224
Ohta Y, Goto N (1976) Estimation of S-wave velocity in terms of characteristic indices of soil. Butsuri-Tanko 29(4): 34–41
Otani S (1974) Inelastic analysis of R/C frame structures. ASCE J Struct Div 100(ST7): 1433–1449
Pan A, Moehle JP (1989) Lateral displacement ductility of reinforced concrete flat plates. ACI Struct J 86(3): 250–271
Panagiotakos TB, Fardis MN (1994) Proposed nonlinear strut models for infill panels. 1st year progress report of PREC8 project. University of Patras, Patras, GR
Panagiotakos TB, Fardis MN (1998) Effect of column capacity design on earthquake response of reinforced concrete buildings. J Earthquake Eng 2(1): 113–145
Panagiotakos TB, Fardis MN (1999a) Estimation of inelastic deformation demands in multistorey RC buildings. Earthquake Eng Struct Dyn 28: 501–528
Panagiotakos TB, Fardis MN (1999b) Deformation-controlled earthquake resistant design of RC buildings. J Earthquake Eng 3(4): 495–518
Panagiotakos TB, Fardis MN (2001a) Deformations of RC members at yielding and ultimate. ACI Struct J 98(2): 135–148
Panagiotakos TB, Fardis MN (2001b) Nonlinear modelling of wall uplift and rocking. Report to SAFERR project, University of Patras, GR
Panagiotakos TB, Fardis MN (2001c) A displacement-based seismic design procedure of RC buildings and comparison with EC8. Earthquake Eng Struct Dyn 30: 1439–1462
Panagiotakos TB, Fardis MN (2003) Performance of RC frame buildings designed for alternative Ductility Classes according to Eurocode 8 (Final Version, 2003). 5th US-Japan Workshop

on performance-based earthquake engineering methodology for reinforced concrete building structures. Hakone, Japan
Panagiotakos TB, Fardis MN (2004) Seismic performance of RC frame buildings designed to the three Ductility Classes of EN1998 (Eurocode 8) or the Greek Codes 2000. Bull Earthquake Eng 2(2): 221–259
Pantazopoulou SJ (1995) Role of expansion on mechanical behavior of concrete. ASCE J Struct Eng 121(12): 1795–1805
Pantazopoulou SJ (1998) Detailing for reinforcement stability in RC members. ASCE J Struct Eng 124(6): 623–632
Pantazopoulou SJ, Bonacci JF (1994) On earthquake resistant RC frame connections. Canadian J Civil Eng 21(2): 307–328
Paolluci R (2002) Amplification of earthquake ground motion by steep topographic irregularities. Earthquake Eng Struct Dyn 31: 1831–1853
Paolluci R (2006) Numerical investigation of 3D seismic amplification by steep topographic profiles and check of the EC8 topographic amplification coefficients. In: Bouckovalas G (ed) General Report Proceedings of the Athens Workshop, ETC12. Geotechnical Evaluation and Application of the Seismic Eurocode EC8, National Technical University of Athens, pp. 187–191
Park R, Paulay T (1975) Reinforced concrete structures. J. Wiley, New York
Park YJ, Reinhorn AM, Kunnath SK (1987) IDARC: Inelastic damage analysis of reinforced concrete frame-shear-wall structures. Technical Report NCEER-87-0008, National Center for Earthquake Engineering Research, State University of New York, Buffalo, NY
Paulay T, Priestley MJN (1992) Seismic design of reinforced concrete and masonry buildings, J. Wiley, New York
Perdikaris P (1980) Stiffness and strength of biaxially tensioned orthogonally reinforced concrete panels subjected to membrane shear. Ph.D Thesis, Civil Engineering Department, Cornell University, Ithaca, NY
Peruš I, Fajfar P (2005) On the inelastic torsional response of single-storey structures under bi-axial excitation. Earthquake Eng Struct Dyn 34(8): 931–941
Pipa M, Carvalho EC (1994) Reinforcing steel characteristics for earthquake resistant structures. In: Duma G (ed) 10th European Conference on Earthquake Engineering, Balkema, Rotterdam, pp. 2887–2892
Pires FMG (1990) Influencia das paredes de alvbenaria no comportamento de estruturas reticuladas de betao armado sueitas a accoes horizontais. Res. Report, Laboratorio Nacional de Engenharia Civil, Lisbon
Plumier A, Vangelatou O (1995) Synthesis of the statistical data on reinforcing steel collected in Europe and comparison to the Eurocode 8 requirements. Internal PREC8 report No. 4, Universite de Liege, Liege, BE
Priestley MJN (1997) Displacement-based seismic assessment of reinforced concrete buildings. J Earthquake Eng, 1(1): 157–192
Reinhorn AM, Kunnath SK, Panahshahi N (1988) Modelling of RC building structures with flexible floor diaphragms (IDARC 2). Technical Report NCEER-88-0035, National Center for Earthquake Engineering Research, State University of New York, Buffalo, NY
Restrepo-Posada JI, Park R, Buchanan AH (1993) Seismic behaviour of connections between precast concrete elements. Res. Report 93-3, Department of Civil Engineering, University of Canterbury, Christchurch, NZ
Rey J, Faccioli E, Bommer JJ (2002) Derivation of design soil coefficients (S) and response spectral shapes for Eurocode 8 using the European Strong-Motion Database. J Seismology 6(4): 547–555
Richart FE, Brandtzaeg A, Brown RL (1928) A study of the failure of concrete under combined compressive stresses, Bulletin 185. University of Illinois Engineering Experimental Station, Champaign, IL
Rosenblueth E (1951) A basis for aseismic design. Ph.D. Thesis, Department of Civil Engineering, University of Illinois, Urbana, IL

Rosenblueth E, Elorduy J (1969) Response of linear systems to certain transient disturbances, 4th World Conference on Earthquake Engineering, Santiago, Chile, A-1 pp. 185–196
Roufaiel MSL, Meyer C (1987) Analytical modeling of hysteretic behaviour of R/C frames. ASCE J Struct Eng 113(ST3): 429–444
Rowe RE (1970) Current European views on structural safety. ASCE J Struct Div 96(ST3): 461–467
Rutenberg A (1982) Simplified P-Delta analyses for asymmetric structures. ASCE J Struct Div 108(ST9): 1995–2013
Rutenberg A, Shtarkaman M, Eisenberger M (1986) Torsional analysis methods for perforated cores, ASCE J Struct Eng 112(6): 1207–1226
Saadatmanesh H, Ehsani MR, Li MW (1994) Strength and ductility of concrete columns externally reinforced with fiber composite straps. ACI Struct J 91(4): 434–447
Saatcioglou M (1991) Deformability of reinforced concrete columns. In: Ghosh SK (ed) ACI Special Publication SP127, American Concrete Institute, Detroit, MI, pp. 421–452
Saiidi M, Sozen MA (1979) Simple and complex models for nonlinear seismic response of R/C structures. Civil Engineering Studies, Structural Research Series No. 465, University of Illinois, Urbana, IL
Sakai J, Jeong H, Mahin SA (2006) Reinforced concrete bridge columns that re-center following earthquakes. 8th U.S. National Conference on Earthquake Engineering, San Francisco, CA, paper 1421
SEAOC (1995) Performance based seismic engineering of buildings: Vision 2000. Structural Engineers Association of California, Sacramento, CA
SEAOC (1999) Recommended lateral force requirements and commentary. Seismology Committee. Structural Engineers Association of California, Sacramento, CA
Sfakianakis MG, Fardis MN (1991a) Nonlinear finite element for modeling reinforced concrete columns in three-dimensional analysis. Comput Struct 40(6): 1405–1419
Sfakianakis MG, Fardis MN (1991b) RC column model for inelastic seismic response analysis in 3D, ASCE J Eng Mech 117(12): 2770–2787
Sheikh SA, Uzumeri SM (1982) Analytical model for concrete confinement in tied columns. ASCE J Struct Eng 108(ST12): 2703–2722
Shohara R, Kato B (1981) Ultimate strength of reinforced concrete members under combined loading. IABSE Colloquium – Advanced Mechanics of Reinforced Concrete, Delft, NL, pp. 701–716
Skouteropoulou A-M, Bousias SN, Fardis MN (1986) Contribution of curved-in-space free-standing staircases to the lateral stiffness of structures. 8th European Conference on Earthquake Engineering, Lisbon, Vol. 3, 6.6, pp. 41–48
Skouteropoulou A-M, Bousias SN, Fardis MN (1987) Stiffness of free-standing stairs with 180^o turn. ASCE J Struct Eng 113(12): 2415–2438
Smebby W, Der Kiureghian A (1985) Modal combination rules for multicomponent earthquake excitation. Earthquake Eng Struct Dyn 13(1): pp. 1–12
Spoelstra MR, Monti G (1999) FRP-confined concrete model. ASCE J Composite Construct 3(3): 143–150
Stafford-Smith B, Girgis AM (1986) Deficiencies in the wide column analogy for shear wall core analysis. Concr Int 8(4): 58–61
Stanescu D, Plumier A (1993) Types of steel available in Belgium – Statistical data, National Standards. University de Liege contribution to 1st PREC8 Topic 1 annual report, Liege, BE
Stoppenhagen DR, Jirsa JO, Wyllie LA (1995). Seismic repair and strengthening of a severely damaged concrete frame. ACI Struct J 92(2): 177–187
Stylianidis KC (1985) Experimental investigation of the behaviour of the single-storey infilled RC frames under cyclic quasi-static horizontal loading (parametric analysis). Ph.D. Thesis, Department of Civil Engineering, Aristotle University of Thessaloniki, Thessaloniki, GR
Suda K, Murayama Y, Ichinomiya T, Shimbo H (1996) Buckling behavior of longitudinal reinforcing bars in concrete column subjected to reverse lateral loading. 11th World Conference on Earthquake Engineering, Acapulco, paper 1753

Tabbara M, Karam G (2007) Modeling the strength of concrete cylinders with FRP wraps using the Hoek-Brown strength criterion. In: Triantafillou TC (ed) 8th International Symposium on Fiber Reinforced Polymer Reinforcement for Concrete Structures (FRPRCS-8), Patras, GR, paper 6–12

Takeda T, Sozen MA, Nielsen NN (1970) R/C response to simulated earthquakes. ASCE J Struct Div 96(ST12): 2557–2573

Takiguchi K, Imai K, Mizobuchi T (1997) Compressive strength of concrete around critical section of RC column under compression-bending-shear. AIJ J Struct Construct Eng 496: 83–90

Tamužs V, Tepfers R, Valdmanis V, Spārniņš E, Zīle E, Ladnova O (2007). Tests and prediction of the mechanical behaviour of cylindrical concrete specimens confined by composite wrapping. In: Triantafillou TC (ed) 8th International Symposium on Fiber Reinforced Polymer Reinforcement for Concrete Structures (FRPRCS-8), Patras, GR, paper 6-6

Tassios TP (1984) Masonry infill and R/C walls under cyclic actions. CIB Symposium on Wall Structures, Warsaw

Taucer F, Spacone E, Filippou FC (1991) A fiber beam-column element for seismic response analysis of reinforced concrete structures. Rep. UCB/EERC 91-17, Earthquake Engineering Research Center, University of California, Berkeley, CA

Teng JG, Lam L (2004) Behavior and modelling of Fiber Reinforced Polymer-confined concrete. ASCE J Struct Eng 130(11): 1713–1723

Thermou GE, Elnashai AS (2006) Seismic retrofit schemes for RC structures and local-global consequences. J Progr Struct Eng Mater 8(1): 1–15

Thermou GE, Pantazopoulou SJ, Elnashai AS (2007a) Flexural behavior of brittle RC members rehabilitated with concrete jacketing. ASCE J Struct Eng 133(10): 1373–1384

Thermou GE, Pantazopoulou SJ, Elnashai AS (2007b) Design metholodology for seismic upgrading of substandard RC structures. J Earthquake Eng 11(4): 582–606

Toutanji HA, Han M, Matthys S (2007) Axial load behaviour of rectangular concrete columns confined with FRP composites. In: Triantafillou TC (ed) 8th International Symposium on Fiber Reinforced Polymer Reinforcement for Concrete Structures (FRPRCS-8), Patras, GR, paper 6–13

Triantafillou TC (1998) Shear strengthening of reinforced concrete beams using epoxy-bonded FRP composites. ACI Struct J 95(2): 107–115

Triantafillou TC, Antonopoulos CP (2000) Design of concrete flexural members strengthened in shear with FRP. ASCE J Composite Construct 4(4): 198–205

Triantafillou TC, Papanicolaou CG (2006) Shear strengthening of RC members with Textile Reinforced Mortar (TRM) jackets. Mater Struct 39(1): 85–93

Triantafillou TC, Papanicolaou CG, Zisimopoulos P, Laourdekis T (2006) Concrete confinement with Textile Reinforced Mortar (TRM) jackets. ACI Struct J 103(1): 28–37

Tsiknias T, Pittas M (1992) Strengthening of buildings with shotcrete braces. 1st National Conference on Earthquake Engineering and Engineering Seismology, Athens, GR, Vol. B, pp. 349–362

Tso WK (1990) Static eccentricity concept for torsional moment estimations. ASCE J Struct Eng 116(ST5): 1199–1212

Vidic T, Fajfar P, Fischinger M (1994) Consistent inelastic design spectra: strength and displacement. Earthquake Eng Struct Dyn 23: 502–521

Vintzeleou EN (1984) Mechanisms of load transfer along reinforced concrete interfaces under monotonic and cyclic actions. Doctoral Thesis, Civil Engineering Department, National Technical University, Athens, GR

Vintzileou E, Panagiotidou E (2007) An empirical model for predicting the mechanical properties of FRP-confined concrete. In: Triantafillou TC (ed) 8th International Symposium on Fiber Reinforced Polymer Reinforcement for Concrete Structures (FRPRCS-8), Patras, GR, paper 6-4

Viwathanatepa S, Popov E, Bertero VV (1979) Seismic behavior of reinforced concrete beam-column subassemblages. Rep. UCB/EERC-79/14, Earthquake Engineering Research Center, University of California, Berkeley, CA

Walraven JC (2002) Background document for EN 1992-1-1: Eurocode 2: Design of Concrete Structures – Chapter 6.2: Shear, Delft University of Technology, Delft, NL

Wang TY, Bertero VV, Popov EP (1975) Hysteretic behavior of reinforced concrete framed walls. Rep. EERC 75-23, Earthquake Engineering Research Center, University of California, Berkeley, CA

Wilson EL, Der Kiureghian A, Bayo EP (1981) A replacement for the SRSS method in seismic analysis. Earthquake Eng Struct Dyn 9: 187–194

Xenidis E, Athanatopoulou A, Avramidis IE (1993). Modelling of shear wall cores under earthquake loading using equivalent frames. In: Moan T et al. (ed) Structural Dynamics – EURODYN '93, Balkema, Rotterdam, pp. 901–910

Yamamoto Y (1993) Strength and ductility of frames strengthened with steel bracing. In Okada T (ed) Earthquake Resistance of Reinforced Concrete Structures – A Volume Honoring H. Aoyama, Department of Architecture, University of Tokyo, pp. 467–476

Yan Z, Pantelides CP (2006) Fiber-Reinforced Polymer jacketed and shape-modified compression members: II – model. ACI Struct J 103(6): 894–903

Yan Z, Pantelides CP (2007) Design-oriented model for concrete columns confined with bonded FRP jackets or post-tensioned FRP shells. In: Triantafillou TC (ed) 8th International Symposium on Fiber Reinforced Polymer Reinforcement for Concrete Structures (FRPRCS-8), Patras, GR, paper 6-1

Yettram AL, Husain HM (1966) Plain-framework method for plates in extension. ASCE J Eng Mech Div 92(EM1): 157–168

Yoshimura M, Takaine Y, Nakamura T (2004) Collapse drift of R/C columns. In: Kabeyasawa T (ed) Development of Performance-Based Design Methodologies, US-Japan Co-operative Research on Urban Earthquake Disaster Mitigation, Tokyo, pp. 231–242

Zaharia R, Taucer F, Pinto A, Molina J, Vidal V, Coelho E, Candeias P (2004) Earthquake testing of a full-scale RC flat slab building structure. European Laboratory for Structural Assessment (ELSA), Institute for the Protection and Security of the Citizen, JRC, Ispra, IT

Zarnic R, Tomazevic M (1985) Study of the behaviour of masonry infilled reinforced concrete frames subjected to seismic loading – Part II. Rep. ZRMK/lKPl-85/02, Ljubljana, SI

Zeris CA, Mahin SA (1984) Analysis of reinforced concrete beam-columns under uniaxial excitation. ASCE J Struct Eng 114(4): 804–820

Colour Plates

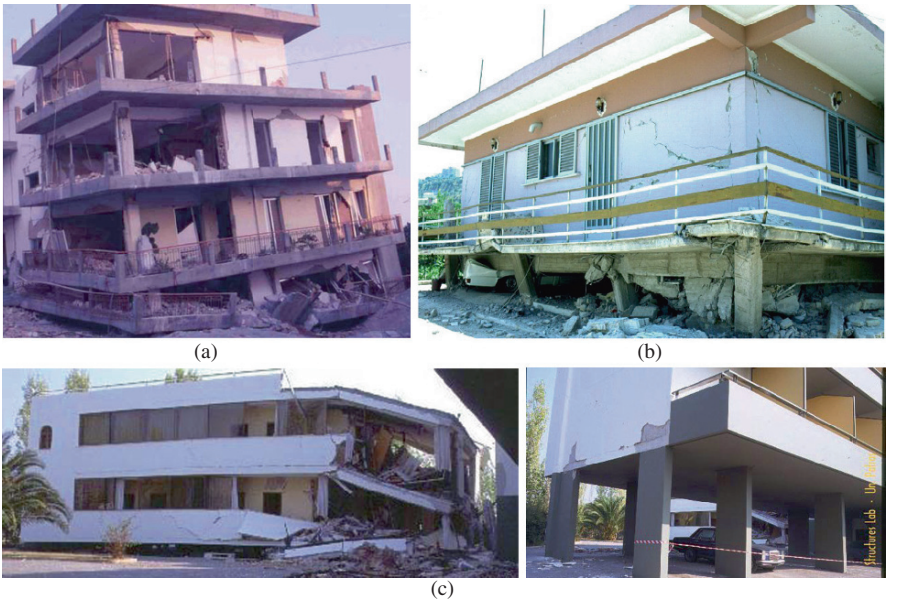

Plate 1 Open ground storey collapses: (**a**) Kalamata, Greece, 1986; (**b**) Aegio, Greece, 1995; (**c**) Athens, 1999 (*Left*: collapsed unit; *Right*: spared similar unit, at right angles to that on the left). (See also Figure 2.10 on page 78)

Plate 2 Examples of shear failure of weak columns interacting with strong infills. (See also Figure 2.11 on page 79)

Plate 3 Examples of captive column failures. (See also Figure 2.12 on page 81)

(a) (b) (c)

Plate 4 (**a**) Stair flight failing in shear as an inclined wall element in its strong direction; (**b**) corner stair in an open ground floor causes damage to the column it is connected to at mid-storey; and (**c**) columns at the diagonally opposite corner of the building failed during torsional response due to the stair in (**b**) – shown near bottom right at the back. (See also Figure 2.13 on page 82)

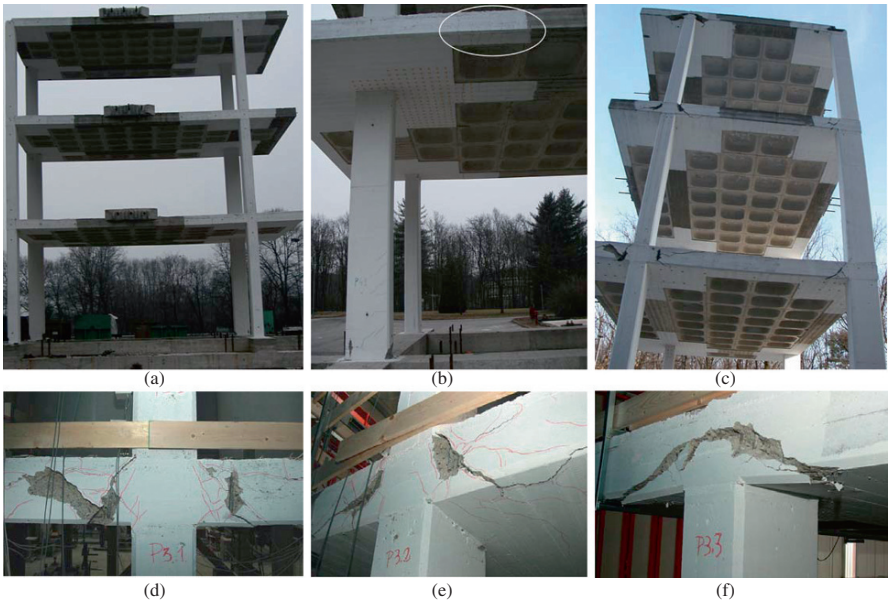

(a) (b) (c)

(d) (e) (f)

Plate 5 Flat slab frame after pseudodynamic test at the ELSA laboratory of the JRC: (**a**) side parallel to loading; (**b**) hinge in slab in positive (sagging) bending and plastic hinges at column base; (**c**) side at right angles to loading, with slab damage around connections; (**d**) edge slab-column connection, 1st floor; (**e**) edge slab-column connection, 2nd floor; (**f**) edge slab-column connection, 3rd floor (pictures (**d**)–(**f**) courtesy F. Taucer, JRC). (See also Figure 2.17 on page 107)

Plate 6 Bearing capacity failures at: (**a**) in Mexico City (1985) (**b**)–(**f**) Adapazari (TR) in the 1999 Kocaeli earthquake (courtesy G. Gazetas, NTUA). (See also Figure 2.18 on page 109)

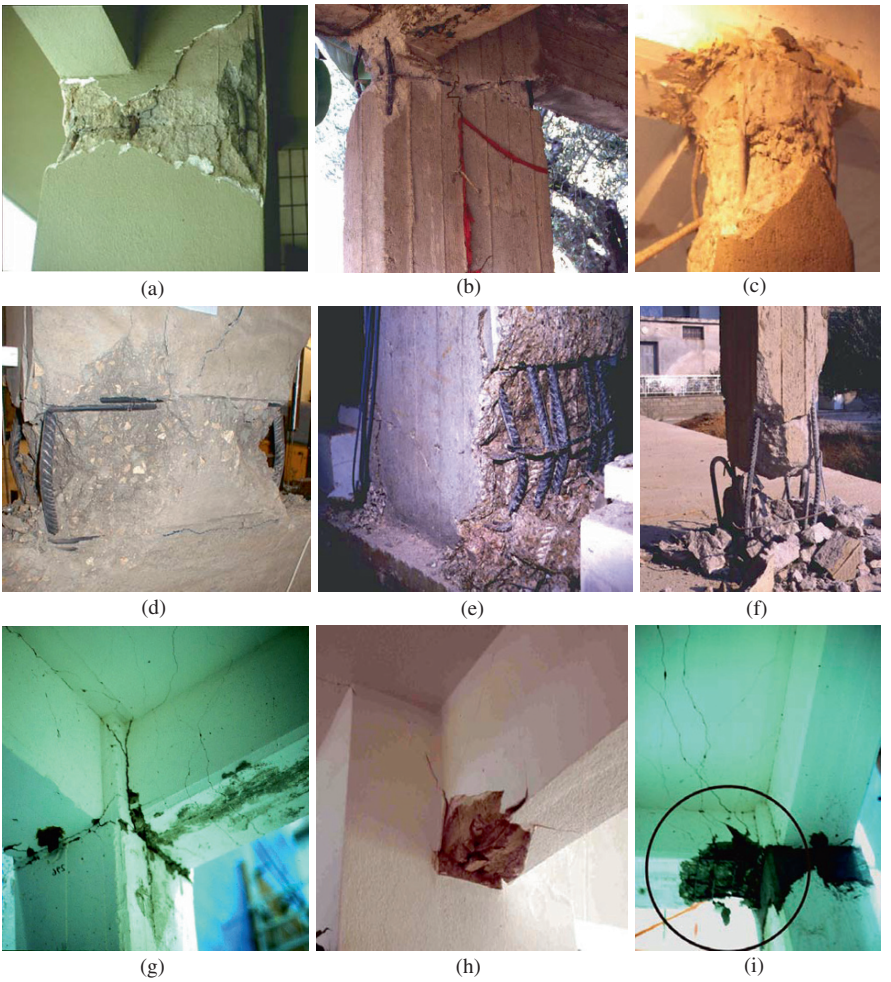

Plate 7 Examples of flexural damage or failure in the lab or in the field: (**a**), (**b**) horizontal crack at column top, concrete spalling at the corners, buckling of corner bars; (**c**) complete loss of cover, partial disintegration of concrete and buckling of bars in horizontal zone near the column top; (**d**) full loss of cover, partial disintegration of concrete and buckling of bars in horizontal zone just above column base; (**e**) loss of cover, partial disintegration of concrete core and bar buckling, with tie opening-up on one side of a column above the base; (**f**) full disintegration of concrete and buckling of bars in a lapping region at floor level; (**g**) through-depth cracking near the support of a T-beam with extension of the cracks into the slab at the top flange; (**h**) local crushing of concrete and bar buckling at the bottom of a T-beam; (**i**) disintegration of concrete and bar buckling at the bottom of a T-beam, with through-depth flexural cracks extending into the slab at the top flange (See also Figure 3.27 on page 204)

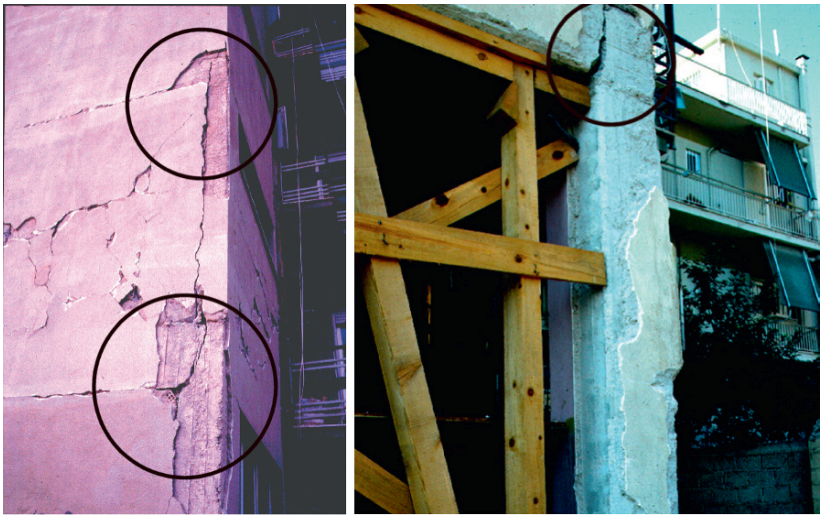

Plate 8 Pull-out of beam bars from short anchorage in corner joint has produced fixed-end rotation during the response and wide residual cracks (See also Figure 3.29 on page 208)

Plate 9 Shear failures of columns or walls (See also Figure 3.35 on page 252)

(a) (b) (c)

Plate 10 Shear failure of exterior joints. (**a**) reinforced joint; (**b**), (**c**): unreinforced joints (See also Figure 3.47 on page 288)

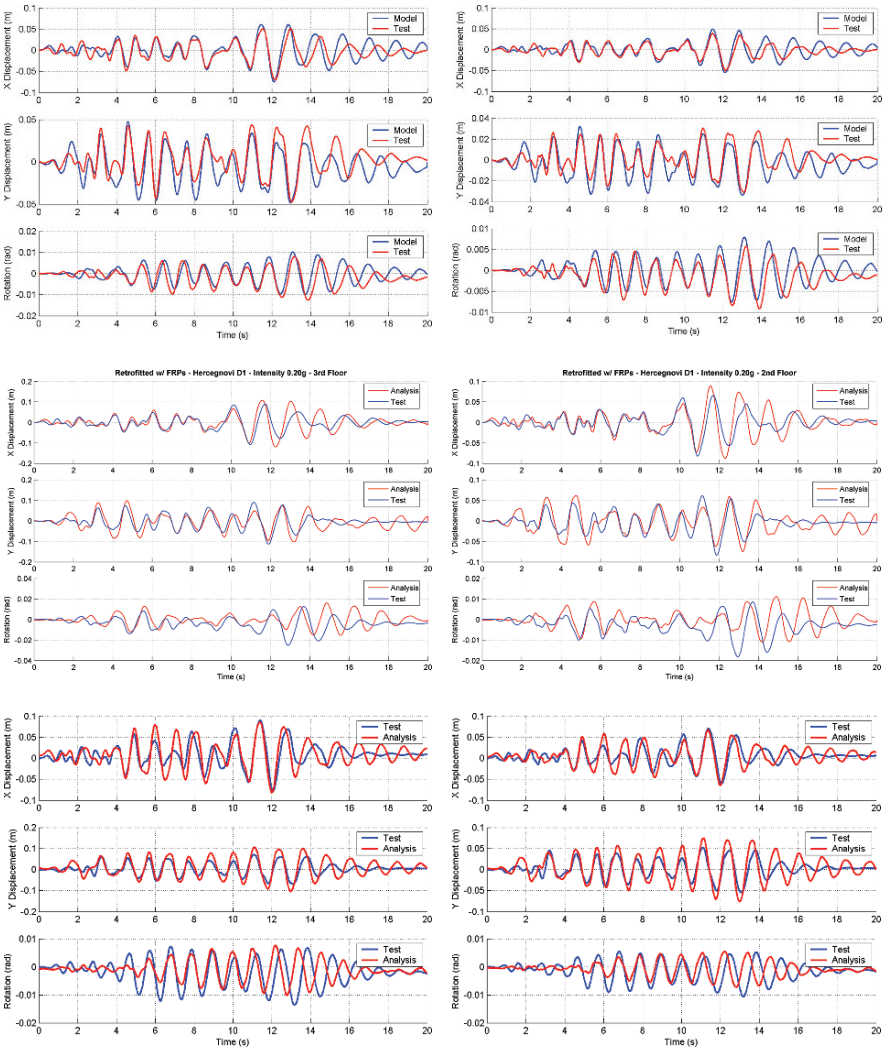

Plate 11 Translation and twist histories, 3rd (*left*) and 2nd (*right*) floor in PsD test or analysis: (*top*) unretrofitted SPEAR building; (*middle*) with FRP-wraps; (*bottom*) with RC jackets (Kosmopoulos and Fardis 2004) (See also Figure 4.15 on page 418)

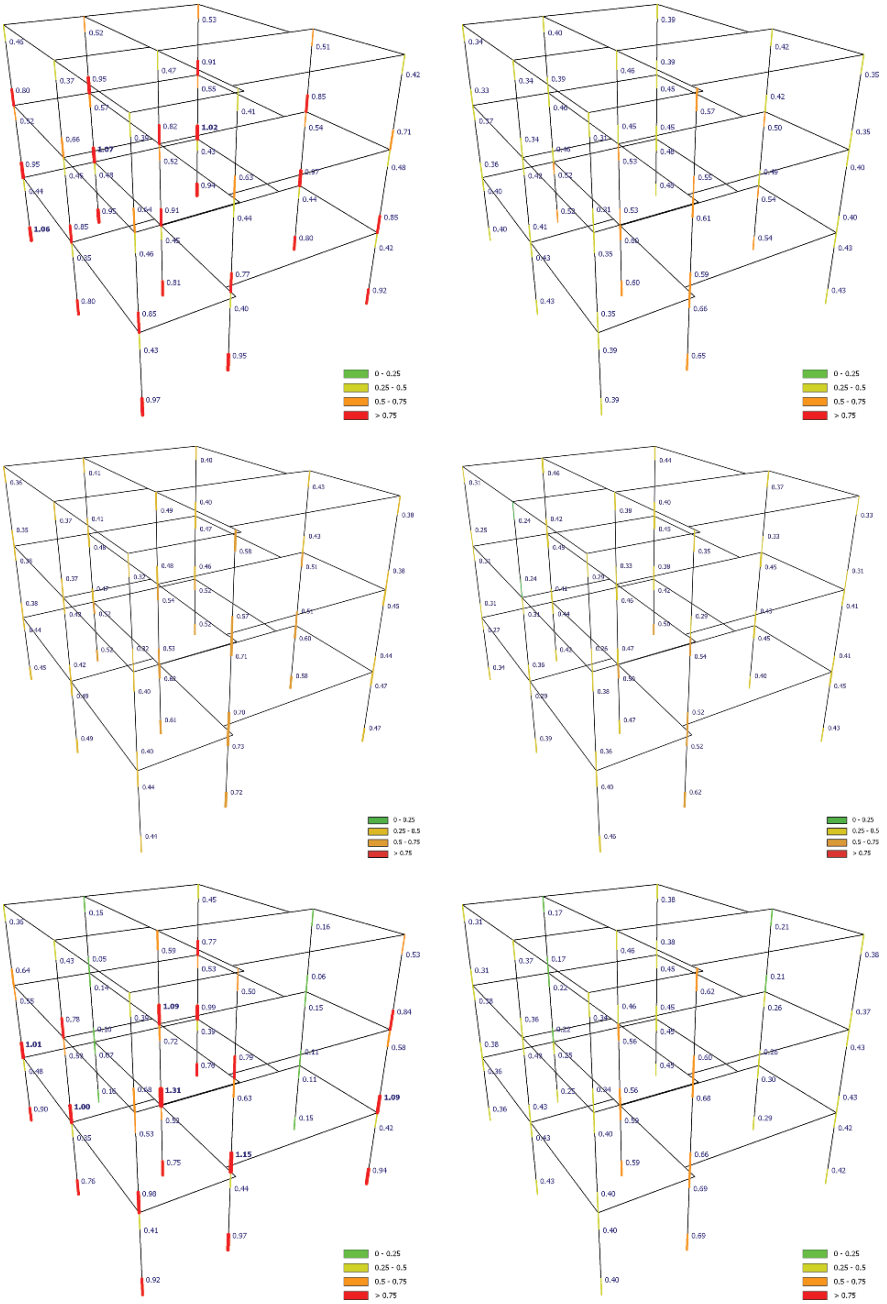

Plate 12 Column damage index in flexure (*left*) or shear (*right*): (*top*) unretrofitted SPEAR building, 0.15 g PGA; (*middle*) 0.2 g PGA with FRP-wraps; (*bottom*) ibid, with RC jackets (See also Figure 4.16 on page 420)

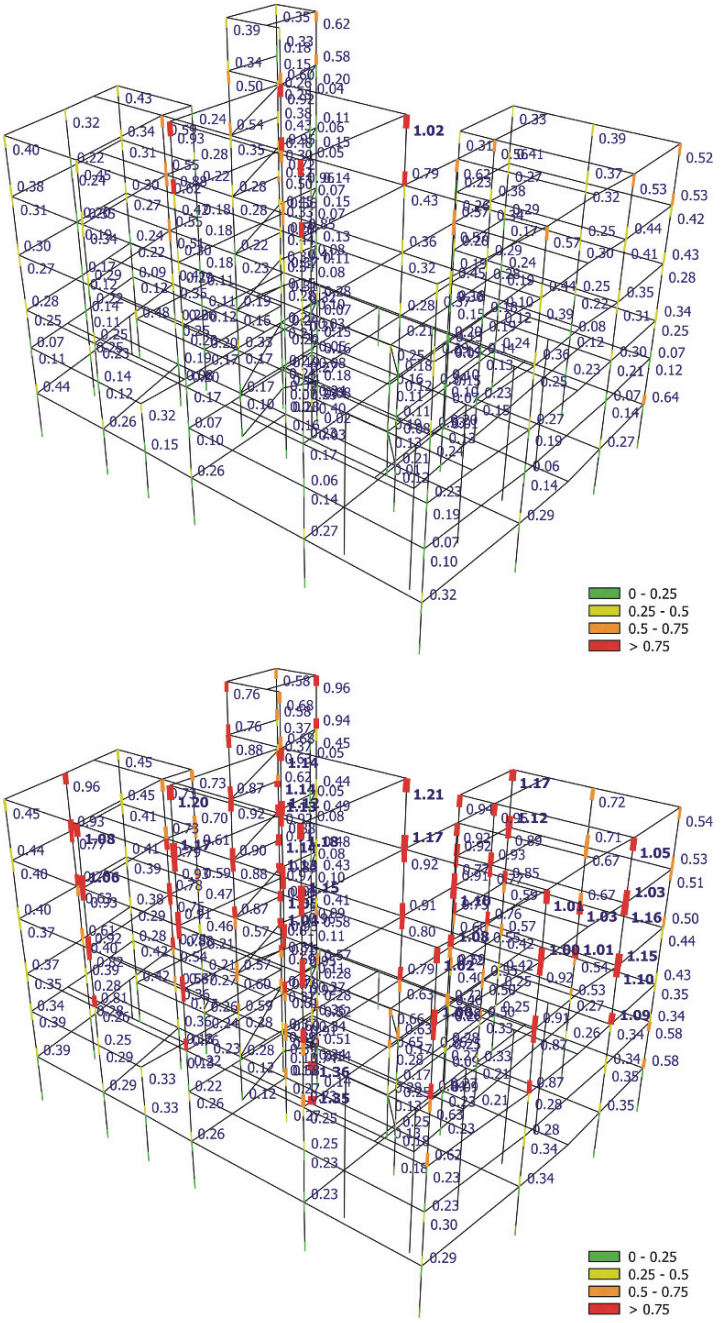

Plate 13 Column damage index (demand-capacity ratio) in flexure (*top*) or shear (*bottom*); mean values from seismic response analyses of the 6-storey building subjected to the 30 "most likely" bidirectional ground motions at the site in the Athens 1999 earthquake (Kosmopoulos and Fardis 2006) (See also Figure 4.17 on page 422)

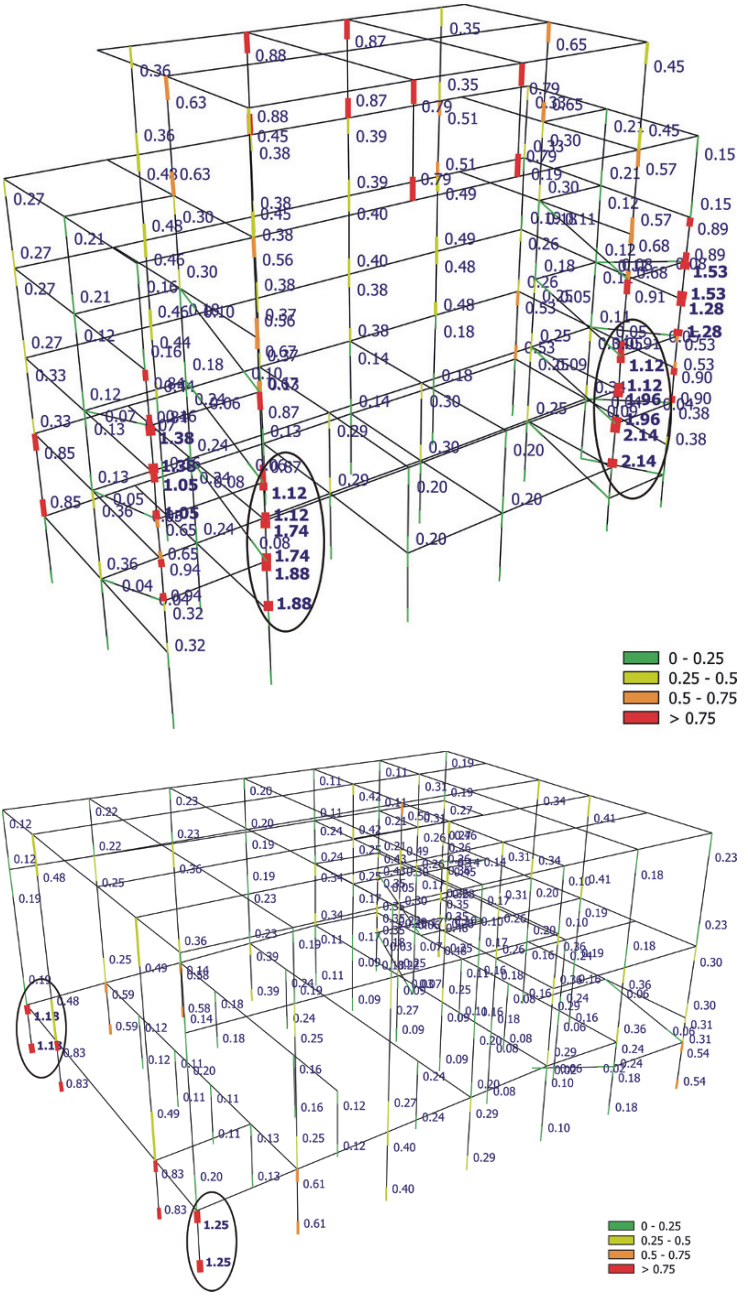

Plate 14 Shear force demand-capacity-ratio (damage index) in vertical members of stage (*top*) and theatre (*bottom*) of as-built theatre facility (mean value over 56 bidirectional ground motions at PGA 0.1 g) (Kosmopoulos et al. 2007) (See also Figure 4.20 on page 425)

(a) (b) (c)

Plate 15 Hand lay-up of FRPs in situ: (**a**), (**b**) dry fabric impregnated in place (courtesy A. Ilki); (**c**) impregnation of the fabric right before placing (See also Figure 6.3 on page 654)

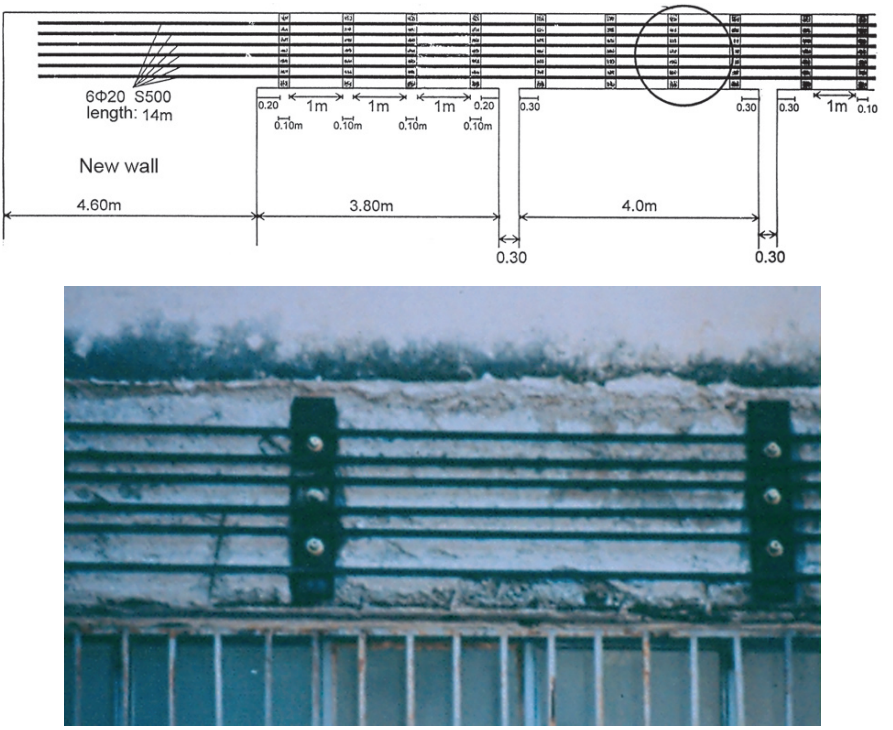

Plate 16 Collector element of the wall in Fig. 6.5, fastened to the side of the perimeter beam (See also Figure 6.6 on page 670)

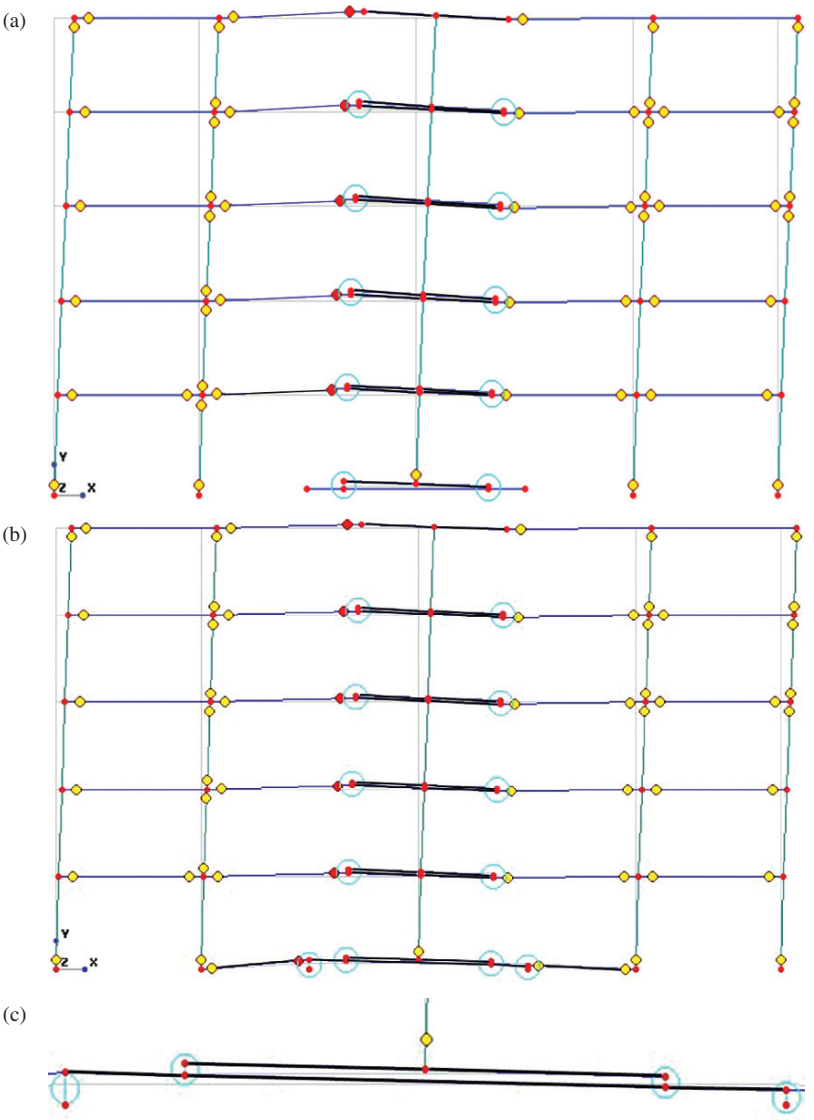

Plate 17 Deformation and plastic hinging in retrofitted frame from nonlinear static analysis: (**a**) wall fixed at the base; (**b**) wall footing connected to tie-beams and uplifting; (**c**) detail of (**b**) at the base of the wall and the footing (*yellow circles*: plastic hinges; larger *red circles*: flexural failure) (See also Figure 6.9 on page 674)

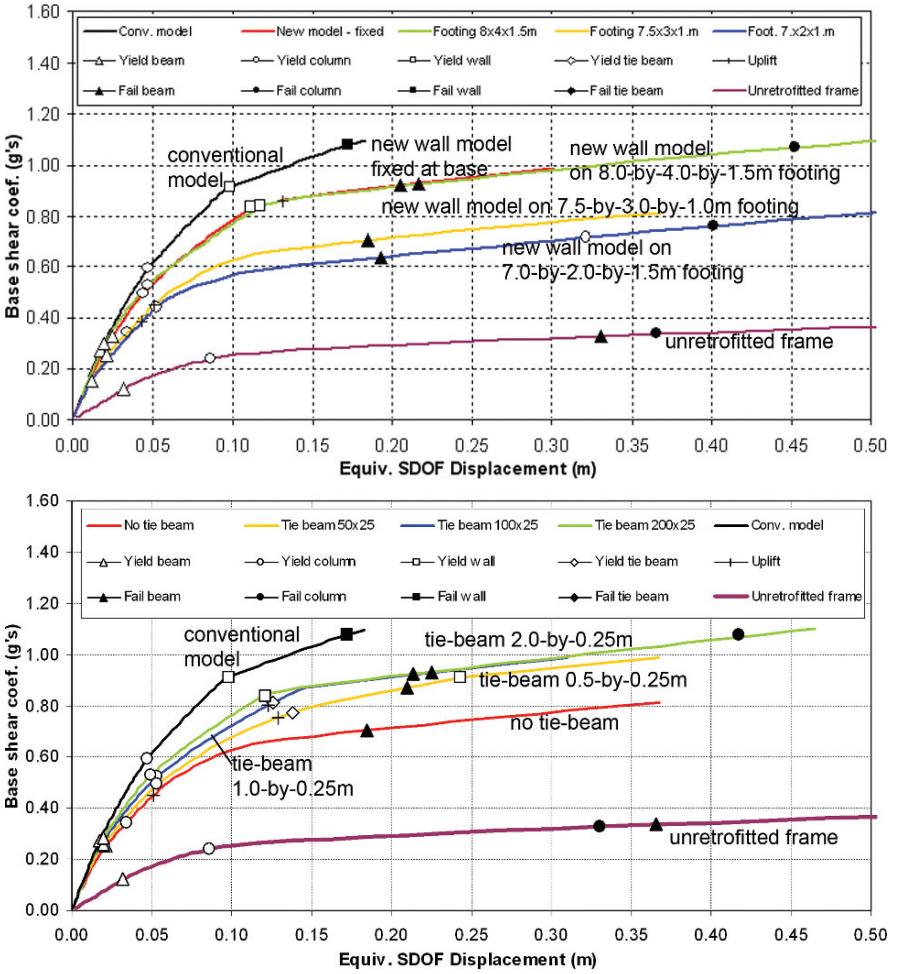

Plate 18 Pushover response of retrofitted frame: (*top*) without tie-beams, using as parameters the model and the size of the footing; (*bottom*) with 1 m deep, 7.5 m-by-3 m footing, using as – parameter the size of the tie-beam (See also Figure 6.10 on page 675)

(a) (b)

Plate 19 FRP-retrofitted SPEAR test structure: (**a**) column with FRP-wrapped ends during the response; (**b**) large column retrofitted in shear (See also Figure 6.12 on page 684)

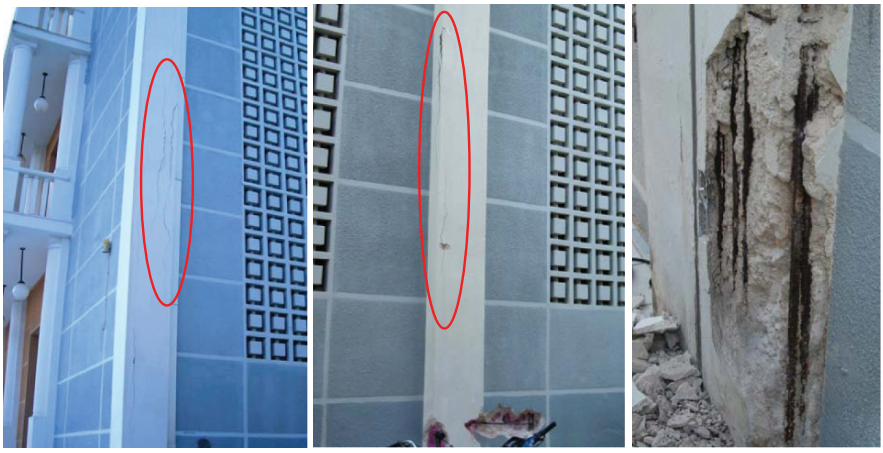

(a) (b) (c)

Plate 20 Vertical cracks in perimeter members of theatre building (**a**), (**b**), due to reinforcement corrosion (**c**) (See also Figure 6.13 on page 686)

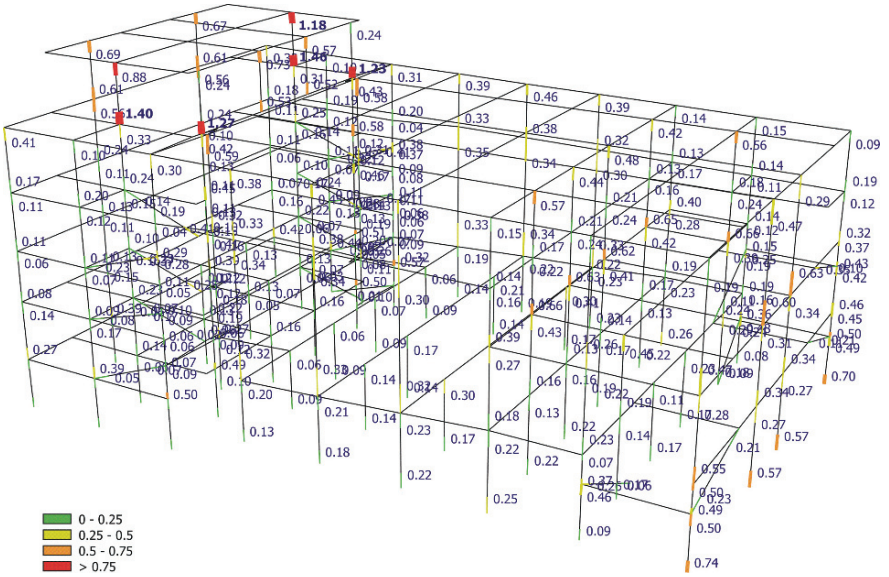

Plate 21 Mean chord rotation demand in vertical members of the retrofitted building from seismic response analyses for 56 bidirectional ground motions at PGA = 0.36 g, divided by the corresponding chord rotation capacity for the Near Collapse Limit State (Kosmopoulos et al. 2007) (See also Figure 6.16 on page 690)

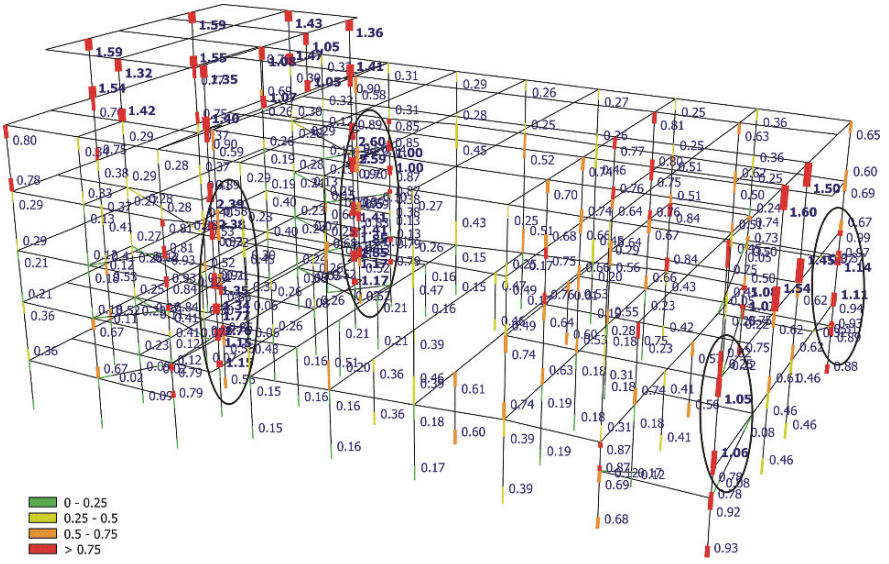

Plate 22 Mean damage ratio in shear in the vertical members of the retrofitted building without the FRPs for 56 bidirectional ground motions at PGA = 0.36 g: shear force demand from the analysis divided by the corresponding capacity for any Limit State (Kosmopoulos et al. 2007) (See also Figure 6.17 on page 690)

Index